Title

Practical Borylation of Alkyl C—H Bonds with Iridium Catalysts: Methodology and Mechanism

Permalink

Author

Yu, Isaac F

Publication Date

2024

Practical Borylation of Alkyl C–H Bonds with Iridium Catalysts: Methodology and Mechanism

by

Isaac Fu-Ray Yu

A dissertation submitted in partial satisfaction of the

requirements for the degree of

Doctor of Philosophy

in

Chemistry

in the

Graduate Division

of the

University of California, Berkeley

Committee in charge:

Professor John F. Hartwig, Chair

Professor F. Dean Toste

Professor Phillip Messersmith

Summer 2024

Abstract

Practical Borylation of Alkyl C–H Bonds with Iridium Catalysts: Methodology and Mechanism

By Isaac Fu-Ray Yu

Doctor of Philosophy in Chemistry

University of California, Berkeley

Professor John F. Hartwig, Chair

The following dissertation discusses the development of iridium catalysts for the undirected borylation of alkyl C–H bonds and includes in-depth studies on the mechanism of these transformations.

Chapter 1 contains a comprehensive review of applications of the borylation of C–H bonds catalyzed by transition metals to the synthesis of complex molecules. This review is subdivided into sections highlighting the state-of-the-art of methodology of the undirected and directed borylation of aryl and alkyl C–H bonds, and focuses on the utility of these reactions for the syntheses of drug precursors, complex bioactive molecules, and optoelectronic materials. Additionally, the review contains a generalized overview of mechanisms by which these reactions occur. Finally, this review provides the author's opinion on future directions for research on the borylation of alkyl C–H bonds.

Chapter 2 describes the development of iridium-catalyzed borylation of the bridgehead, tertiary C–H bonds of bicyclopentanes and bicyclohexanes. Contained is an examination of the scope of the borylation of bicyclopentanes, bicyclohexanes, oxabicyclohexanes, and azabicyclohexanes. Also included are experimental and computational studies that reveal the mechanism of this reaction.

Chapter 3 discusses the development of catalysts that enable the borylation of alkyl C–H bonds to occur at mild temperatures (65 °C). Key to this development was the discovery that catalysts formed from 2-aminophenanthrolines and iridium undergo rapid activation and catalyze the borylation of alkyl C–H bonds at reduced temperatures, maintaining activity even at room temperature. Also included are experimental studies that provide initial information on the identity of the active catalyst species.

Chapter 4 describes the mechanistic study of the origin of improved activation and reaction rates of the borylation of alkyl C–H bonds catalyzed by 2-aminophenanthroline complexes. Experimental studies enabled by a sterically protected aminophenanthroline demonstrate that the *N*-boryl iridium trisboryl complex is the resting state and that the corresponding *N*-boryl iridium bisboryl hydride complex is inactive for the borylation reaction.

Table of Contents

CHAPTER 3

2-Aminophenanthroline Ligands Enable Mild, Undirected, Iridium-Catalyzed Borylation of Alkyl C–H Bonds 333

CHAPTER 4

Mechanism of the Undirected, Iridium-Catalyzed Borylation of Alkyl C–H Bonds with Aminophenanthroline Ligands 494

CHAPTER 1 Overview of Transition-Metal Catalyzed Silylation and Borylation of C–H Bonds for the Synthesis and Functionalization of Complex Molecules

1.1 Introduction

The direct functionalization of C–H bonds, particularly the site-selective functionalization of C–H bonds, has been a longstanding goal of organic chemists.[1] Beyond the fundamental challenge facing the activation of C–H bonds that are non-polar and have high bond dissociation energies, lies the challenge of functionalizing C–H bonds with high site selectivity and high chemoselectivity in molecules ranging from alkanes to complex molecules containing an array of functional groups interspersed with C–H bonds that sit in varying steric environments and possess varying electronic properties. Systems that lead to the functionalization of one C–H bond in alkanes ranging from methane to linear, low-density polyethylene, one C–H bond in a molecule as complex as natural products, medicinally active compounds, or even sophisticated electronic materials would lead to widely applicable, new approaches to the synthesis of organic molecules valuable for a variety of applications.

Because of this challenge and potential application, chemists have developed over the past few decades a series of strategies for the functionalization of C–H bonds, some of which have been applicable to the functionalization of C–H bonds in such complex molecules.[2] The synthetic utility of a particular method for the functionalization of C–H bonds can be demonstrated by the types of complex molecules that can be prepared. The C–H bond functionalization can be applied in the in "late-stage" of a synthetic sequence, or it can be used earlier in the sequence to create building blocks or to install groups that can be diversified later in a synthesis.

Methods for efficient, catalytic functionalization of unactivated C−H bonds with boron reagents are particularly attractive for synthetic chemists because of the versatile reactivity of the boryl functional groups in the products. The boryl groups can serve as temporary functional groups to form products containing a variety of functional groups at the position of the C–B bond. For example, arylboron reagents undergo cross-coupling with carbon-electrophiles in the presence of an appropriate catalyst to form C–C bonds, undergo oxidation by H_2O_2 to form alcohols, undergo halogenations to form aryl halides, and undergo aminations to form a variety of products containing carbon-nitrogen bonds. The mechanism, scope, and applications of these reactions have been presented in several reviews.[3-5] The wide scope, mild conditions, high turnover numbers, and predictable site-selectivity of these reactions, in combination with their value as synthetic intermediates, have caused the widespread adoption of these methods.

Examples of the borylation of C−H bonds can be subdivided into two classes: undirected, intermolecular; and directed, intermolecular. Reactions that occur after binding of the catalyst to a directing group require tethering of the reagent to the substrate, the presence of a suitable directing group on the substrate, or installation of the directing group. Reactions that occur intermolecularly without a directing group typically occur with lower reaction rates, but they do not require the substrate to contain a functional group that can serve as or attach to a directing group.

The most commonly employed catalysts for undirected intermolecular borylation of C–H bonds contain Group 9 metals (Co, Rh, and Ir),[3, 4] although several examples that comprise Group 10 metals,[6-17] Group 8 metals,[18-24] and group 7 metals[25] are known. The borylation of aryl C–H bonds is typically conducted with B_2pin_2 or HBpin as the boron source, and common

catalysts are PNP pincer complexes containing cobalt,[26] and iridium complexes containing bipyridine-type ligands, such as 4,4'-di*tert*-butyl-2,2'-bipyridine (dtbpy)[27] and 3,4,7,8-tetramethyl-1,10-phenanthroline (tmphen).[28, 29] The borylation of alkyl C–H bonds occurs with rhodium piano-stool complexes, such as $Cp*Rh(\eta^6-C_6Me_6)$[30] and iridium complexes containing bipyridine-type ligands (Figure 1.1**Error! Reference source not found.**).

a) catalyst precursors and ligands used for the undirected borylation of arenes

b) catalyst precursors and ligands used for the undirected borylation of alkanes
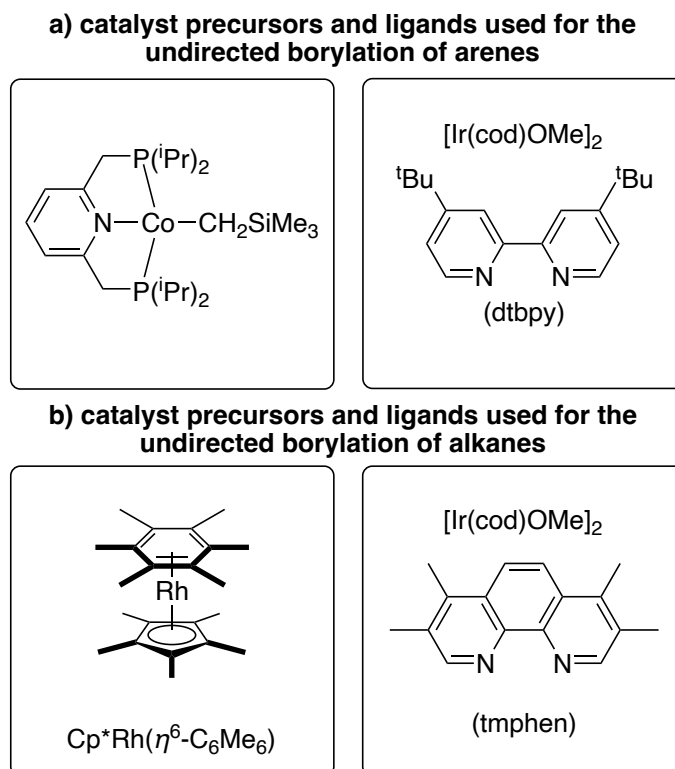
Figure 1.1. Common Group 9 catalyst precursors and ligands for the borylation of C–H bonds.

The borylation of alkyl and aryl C–H bonds are typically run with diboron reagents and generate hydroborane as the byproduct, although there are also many examples in which the reaction was conducted with hydroborane without a hydrogen acceptor.

Mechanistic studies suggest that the borylation of aryl C–H bonds with cobalt pincer complexes occurs by a mechanism comprising a combination of Co(I) and Co(III) intermediates.[26, 31] Mechanistic studies on the borylation of alkyl C–H bonds with rhodium complexes indicate that the reactions occur by mechanisms comprising Rh(I) and Rh(III) intermediates. In stark contrast, the borylation of aryl and alkyl C–H bonds with iridium complexes is accepted to occur by a cycle comprising Ir(III) and Ir(V) intermediates.[27, 29, 32-35] Broadly speaking, however, these reactions occur under the same mechanistic manifold: The C–H bond of the substrate undergoes oxidative addition to the active catalyst $L_2M^{ox}H_mB_n$; L=nitrogen-donor or phosphorus-donor ligand) to generate $L_2M^{ox+2}H_{m+1}B_nR$. The metal-alkyl or metal-aryl intermediate then undergoes reductive elimination to form the C–B bond. Catalyst turnover is achieved by reaction with the main group reagent (Figure 1.2).

a) generalized mechanism of the borylation of C–H bonds

E = B or Si
A = hydrogen acceptor
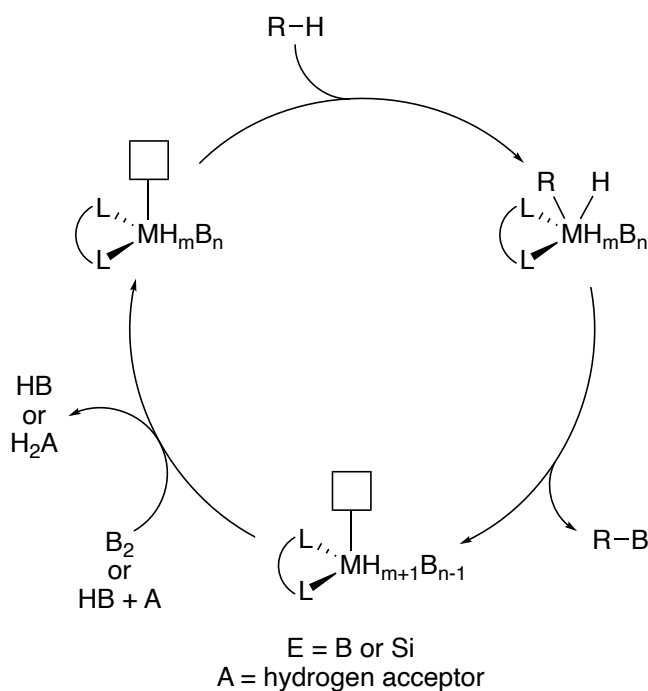
b) intermediates implicated in the borylation of C–H bonds
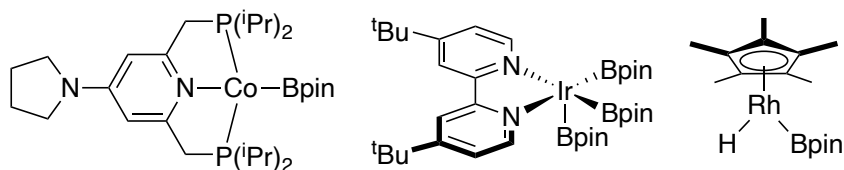
Figure 1.2. Generalized mechanism of transition-metal catalyzed borylation of C–H bonds, and complexes implicated in the reactions.

With these mechanisms in mind, the site-selectivity and strategies for the borylation of C–H bonds can be rationalized. Because these transition metal-catalyzed functionalizations of C–H bonds occur through the formation of an aryl-metal or alkyl-metal intermediate, reactivity trends in the absence of steric factors tend to parallel measures of metal-carbon bond strength or C–H acidity, as have been studied for other metal-catalyzed C–H arylation processes.[36, 37] Undirected borylations tend to favor functionalization of the most acidic heteroaryl C–H bond over aryl C–H bonds, aryl C–H bonds over alkyl C–H bonds, and primary alkyl C–H bonds over secondary or tertiary C–H bonds. Moreover, the pronounced steric bulk around the metal complexes have led to exquisite, sterically driven selectivities for appropriately substituted arenes and heteroarenes, with good *meta*-selectivity. This sterically driven selectivity often overrides electronic factors. Several reviews and models on site selectivity prediction have been published.[38-40] For intermolecular, directed borylations, two coordination sites are needed. The lack of two open coordination sites in the iridium catalysts ligated by chelating dative ligands and the steric bulk of the ancillary ligands in other cases lead to the requirement of alternative types of ligands, including hemilabile ligands, LX ligands, and ligands with charges for ionic interactions. (see below for examples). This review focuses on the application of the

borylation of C–H bonds catalyzed by transition metal catalysts for the synthesis of complex molecules.

Several alternative strategies for the borylation of C–H bonds are emerging, such as those occurring by Friedel-Crafts mechanisms,[41, 42] borylation of alkanes by HAT processes,[43-45] and borylation of heteroarenes by Minisci-type reactions.[46-49] Although some of these reactions contain transition-metal photocatalysts, the bond cleavage and bond formation does not involve a transition metal catalyst and, therefore, are not covered in this review. Also excluded from this review are processes occurring by the combination of lithiation and borylation of the resulting organolithium species.[50]

1.2 Transition-Metal Catalyzed, Borylation of C–H Bonds in Complex Molecules

The use of common reagents, such as HBpin and B_2pin_2, for the borylation of C–H bonds, and the capability of borylated products to undergo some of the reactions most used by synthetic chemists, such as Suzuki couplings, oxidations, and halogenations, has made the borylation of C–H bonds one of the most valuable C–H functionalization reactions.

Among methods for the borylation of C–H bonds, methods for the borylation of aryl C–H bonds are well-established. Those for the borylation of alkyl C–H bonds are evolving. Catalytic systems for the borylation of aryl C–H bonds are highly selective and form aryl and heteroaryl boronates under mild conditions with limiting substrate.

The undirected borylation of the C–H bonds in arenes occurs with regioselectivity controlled by steric factors. For example, 1,3-disubstituted and 1,2,3-trisubstituted arenes undergo selective borylation at the 5-position. For heteroaryl substrates, steric factors are important, but the electronic properties of the heteroarenes can sometimes override the steric preference for the activation of one C–H bond over another or distinguish between reactivity at sterically similar C–H bonds. Guidelines for predicting the selectivity of undirected C–H borylation reactions on heteroarenes are presented in a 2014 paper from our laboratory.[29] Methods for the undirected borylation of aryl C–H bonds have been developed that occur with selectivities that are different from those mentioned above. Such methods achieve complementary selectivity with ligands that can interact with functional groups on the substrate. Additionally, directed methods for the borylation of aryl C–H bonds have been developed to control regioselectivity. All such methods that have been applied to borylation of complex molecules will be reviewed in this section.

It was not until recently that new catalysts were developed with the potential to achieve the borylation of alkyl C–H bonds with the selectivities and mild reaction conditions developed for aryl C–H bonds. The selectivity of such methods was explained in the introduction of this chapter.

Because of the characteristics of this C–H functionalization strategy, the selective introduction of a C–B bond into a highly-functionalized molecule constitutes a powerful strategy to access products that circumvents *de novo* syntheses often required to access complex-molecule derivatives with minor modifications. Therefore, C–H borylation methods are valuable for the

functionalization of complex molecules in drug discovery and natural product synthesis in the early, mid, and late-stage as well as for the functionalization of organic materials and ligand scaffolds. The application of C–H borylation in all these contexts is reviewed in this section.

1.3 Transition-Metal Catalyzed Borylation of C–H Bonds in Precursors to Bioactive Molecules

As noted in the introduction, the borylation of C–H bonds catalyzed by transition metal catalysts occur with high functional group tolerance and with selectivities that can be determined by steric effects or by specific functional groups that direct the transition metal to the site of borylation. Access to these borylated products under mild conditions has spurred the development of synthetic methodologies for the transformation of boronic ester products in a telescoped manner to those containing many functional groups. Taken together, these methods provide a powerful approach to the synthesis of highly decorated building blocks. This section reviews the application of this approach in synthetic campaigns towards biologically active molecules. The examples in this section are subdivided by the reaction that derivatizes the organoboron product of C–H bond functionalization.

1.3.1 Formation of C–C Bonds in Precursors to Bioactive Molecules Enabled by the Borylation of C–H Bonds

The capability of boronic esters and boronic acids to participate in C–C bond-forming reactions, such as Suzuki-Miyaura couplings,[51, 52] makes the borylation of C–H bonds a particularly powerful way to disconnect complex molecules. In one of the earliest examples, Gaunt synthesized rhazinicine by a borylation-cross-coupling sequence of the appropriate pyrrole (Figure 1.3**Error! Reference source not found.**).[53] Under microwave irradiation, the combination of [Ir(cod)Cl]$_2$ and dtbpy catalyzed the borylation of the 3-position of N-Boc-2-trimethylsilylpyrrole. The 3-borylpyrrole product was immediately engaged in a Suzuki-Miyaura cross-coupling reaction. Neier later used a similar strategy for the synthesis of rhazinilam analogues.[54]
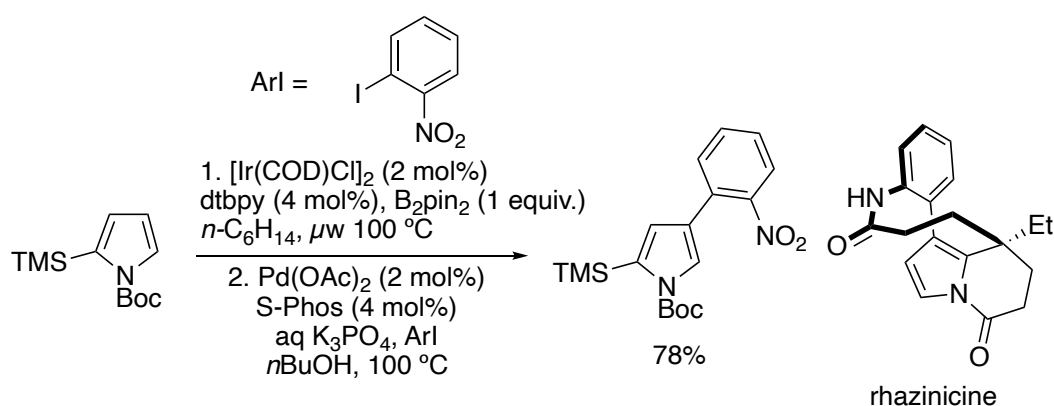
Figure 1.3. Borylation and subsequent cross-coupling of N-Boc-2-trimethylsilylpyrrole en route to rhazinicine.

In 2008, Miyaura disclosed that the combination of dtbpy and iridium catalyzes the borylation of vinyl C–H bonds without deleterious hydroboration of the olefin. The telescoped borylation-cross coupling sequence of enol ethers was applied to the synthesis of key fragments of forskolin and vineomycine B2 methyl ester (Figure 1.4).[55]
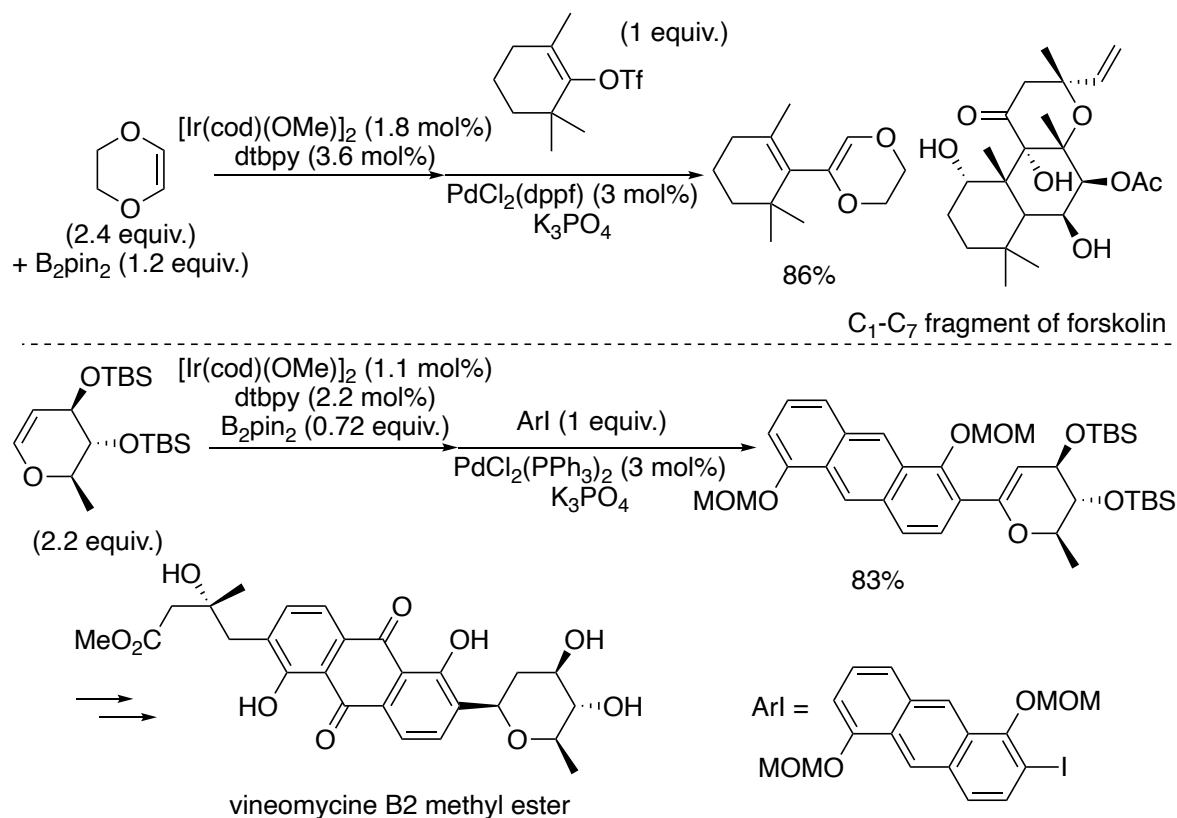
Figure 1.4. Synthesis of forskolin and vineomycine B2 methyl ester enabled by the borylation of vinyl C–H bonds.

Sarpong reported a synthesis of complanadine A that exploited the innate symmetry of the molecule. complanadine A was recognized to be an unsymmetrical dimer of lycodine. Borylation of the pyridine ring of *N*-Boc lycodine, subsequent dimerization with the Lycodine triflate, and global deprotection afforded the desired natural product. Lycopladine F and lycopladine G were also synthesized from the same 3-borylpyridine intermediate (Figure 1.5).[56]

Unprotected indoles lacking a 2-substituent typically react to form 2-boryl indoles. In 2010, our laboratory reported a procedure for the silyl-directed borylation of indoles leading to 7-borylated indoles. Indole was allowed to react with dimethylchlorosilane to install a silylamine directing group. Under iridium catalysis, the silane Si–H oxidatively adds to the iridium center and the 7-C–H bond is cleaved to from a 5-membered metallacycle, leading to the observed site selectivity. This method was used to create a one-pot silylation-borylation-cross-coupling sequence to synthesize Hippadine in good yield (Figure 1.6).[57]
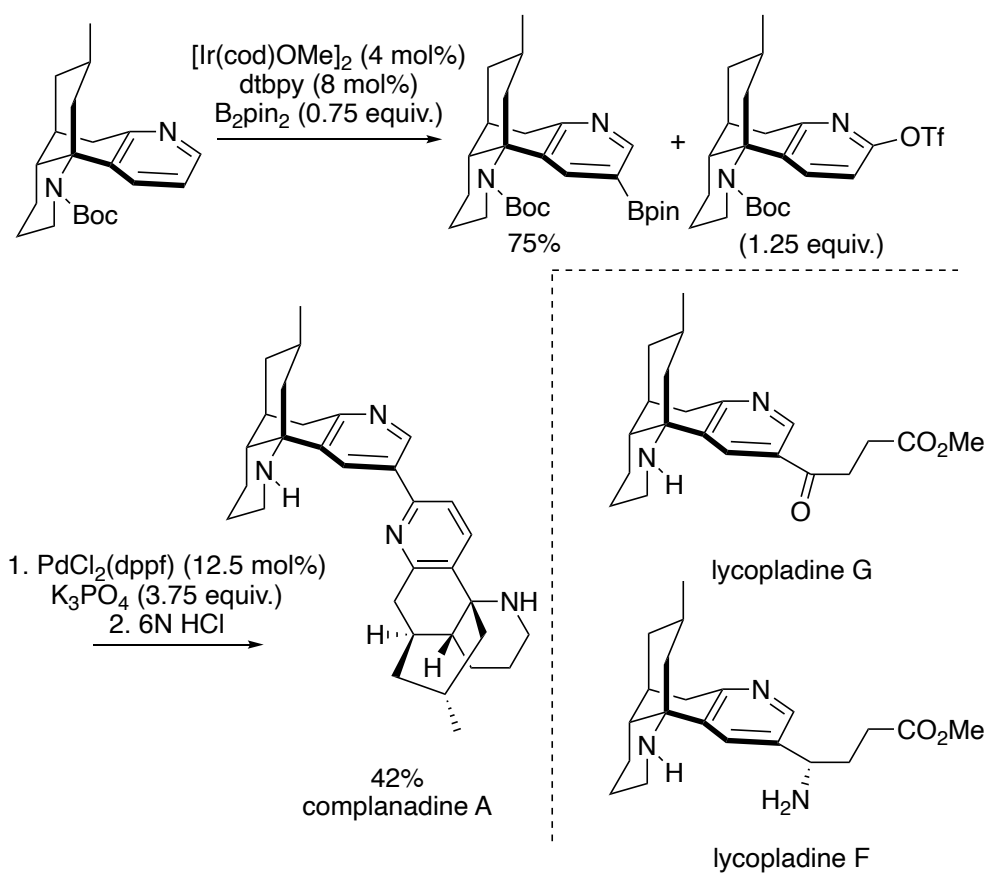
Figure 1.5. *Meta*-selective borylation of lycodine for the preparation of the key intermediate in the synthesis of complanadine A, lycopladine F, and lycopladine G
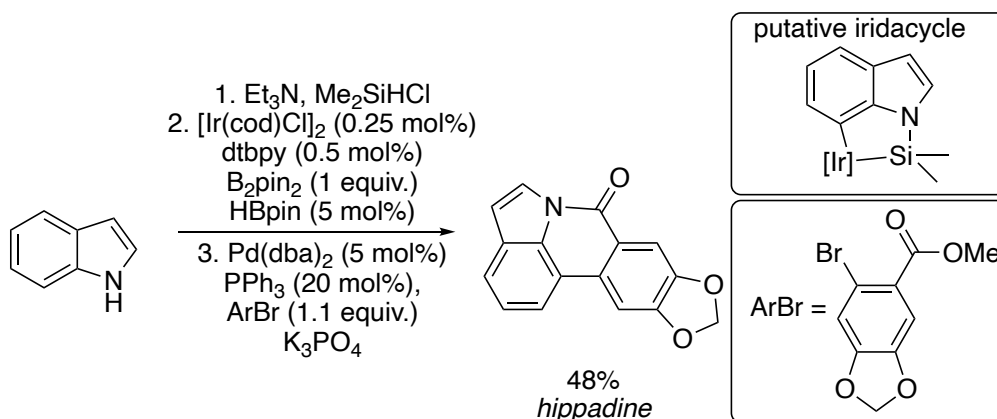
Figure 1.6. Silyl-directed 7-borylation of indoles in the synthesis of hippadine.

In 2010, our laboratory developed copper-mediated conditions for a telescoped borylation-cyanation sequence that enabled the formal C–H cyanation of arenes with zinc cyanide. This method was applied to the synthesis of a key benzonitrile intermediate en route to etravirine (Figure 1.7).[58]
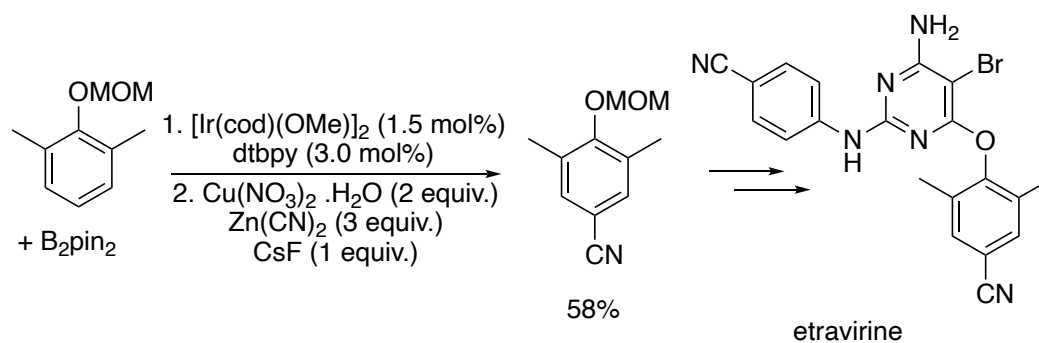
Figure 1.7. Formal cyanation of aryl C–H bonds applied to the synthesis of etravirine.

In 2014, Hosoya developed a route to defucogilvocarcin M that ultilizes silyl-directed ortho borylation of phenols extensively (Figure 1.8). Monobenzylcatechol was silylated and *ortho*-borylated to afford an *ortho*-boryl phenol. The phenol was converted to the corresponding triflate. Addition of *s*-BuLi induced benzyne formation, which in turn was trapped in a [4+2] cycloaddition with 2-methoxyfuran, affording fragment I. The other half of the molecule was also constructed via silyl-directed *ortho*-borylation of creosol. The creosol boronic ester was converted to the corresponding Bdan triflate. Suzuki coupling of the two fragments followed by carbonylation of the boronic acid and finally global deprotection afforded the desired natural product.[59]

Movassaghi reported that the combination of [Ir(cod)OMe]$_2$ and dtbpy catalyze the 2-selective borylation of tryptamine with HBpin. The coupling of the 2-borylindole product and a 2-iodoindole in the presence of Xphos-Pd-G3 and silver phosphate afforded 2,2'-bisindole precursors en route to the synthesis of trigonoliimine A and B (Figure 1.9).[60] Movassaghi again utilized the selective 2-borylation of tryptamine to synthesize 2,5'-bisindole precursors that enabled cyclizations to form bisindole alkaloids (Figure 1.10).[61]
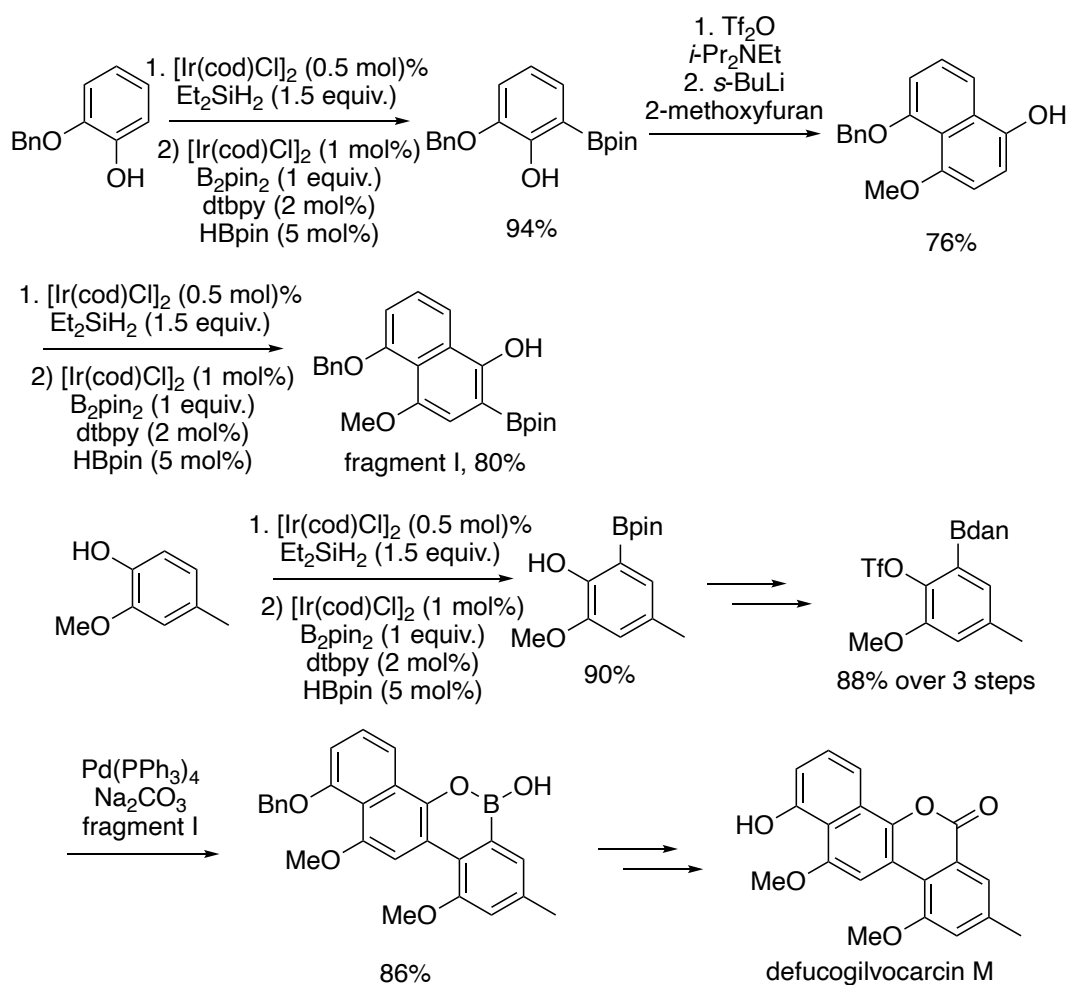
Figure 1.8. Silyl-directed *ortho*-borylation of phenols in the synthesis of defucogilvocarcin M.
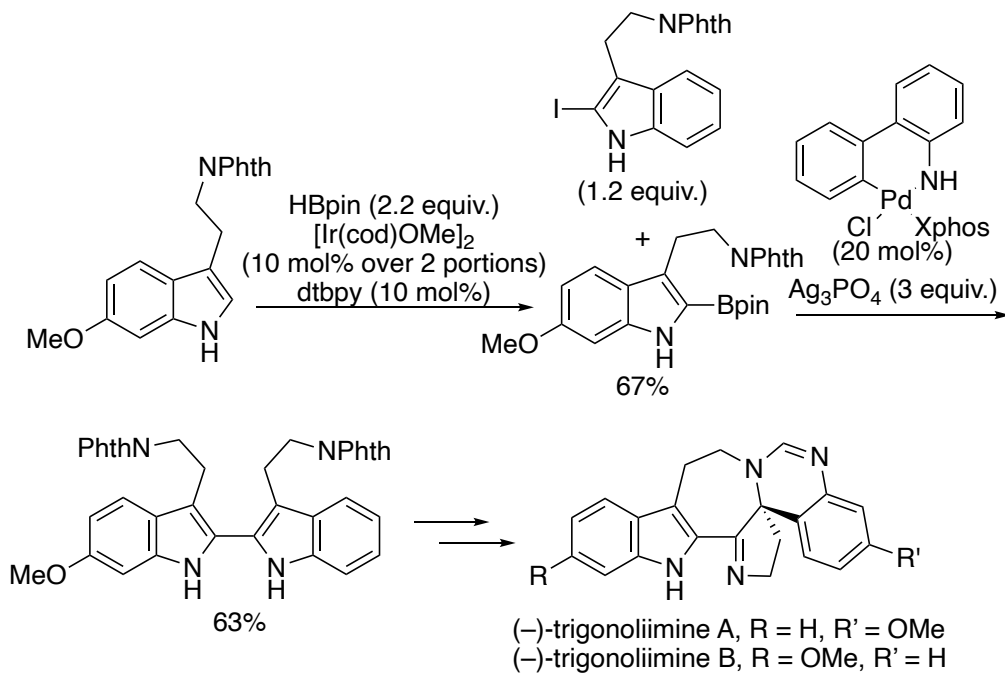
Figure 1.9. Synthesis of trigonoliimine A and B via the 2-selective borylation of tryptamine derivatives.
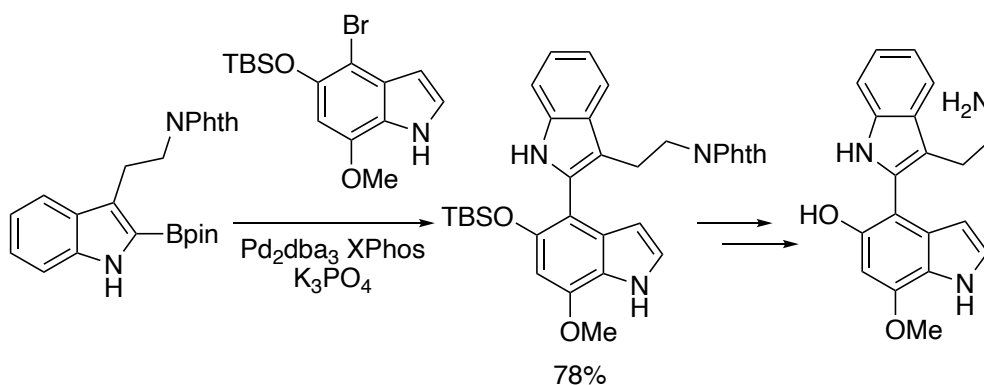
Figure 1.10. Synthesis of 2,5'-bisindoles from the cross-coupling of 5-bromoindoles and 2-borylindole.

Koert reported the synthesis of pestaphthalide A and B by the borylation of a dimethoxyarene to provide the precursor to cross-coupling with a vinyl bromide. A short sequence containing a Jacobsen epoxidation of the olefin and stereodivergent epoxide opening afforded the two natural products (Figure 1.11).[62]

pestaphthalide A   pestaphthalide B
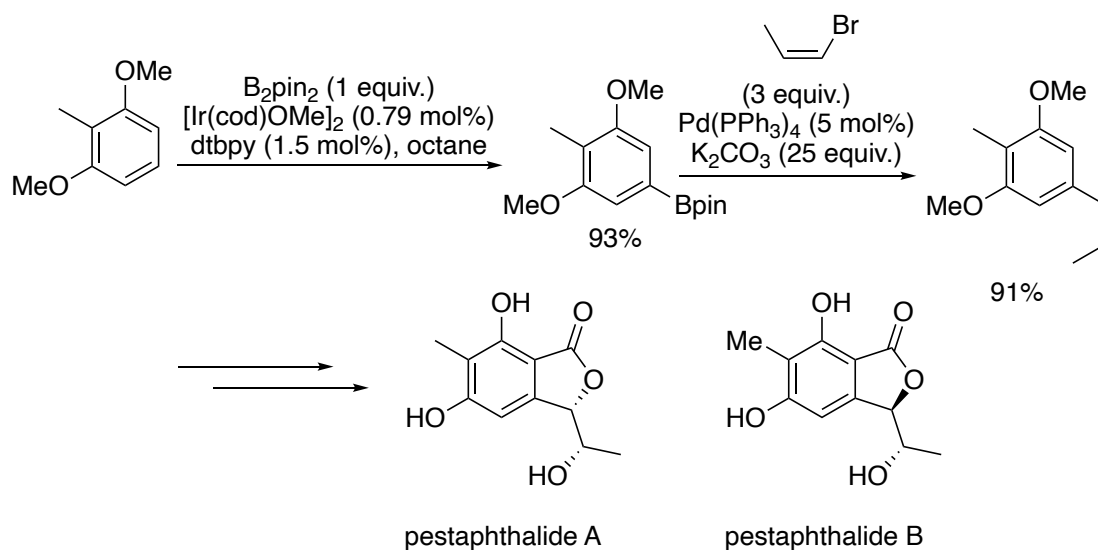
Figure 1.11. Synthesis of pestaphthalide A and B via the *meta*-selective borylation of a dimethyoxyarene.

Koert applied a borylation cross-coupling sequence to the synthesis of the proposed structure of fulicinerine and fulicineroside (Figure 1.12). Comparison of the spectral data obtained from the synthetic material to that of the isolated natural product suggested a structural misassignment in the original isolation report.[63]

In 2012, Lassaletta developed a hemilabile hydrazonepyridine ligand for the *ortho*-selective borylation of aryl hydrazones. The boronic ester products underwent cross-coupling to afford precursors to Sartan drugs (Figure 1.13).[64]
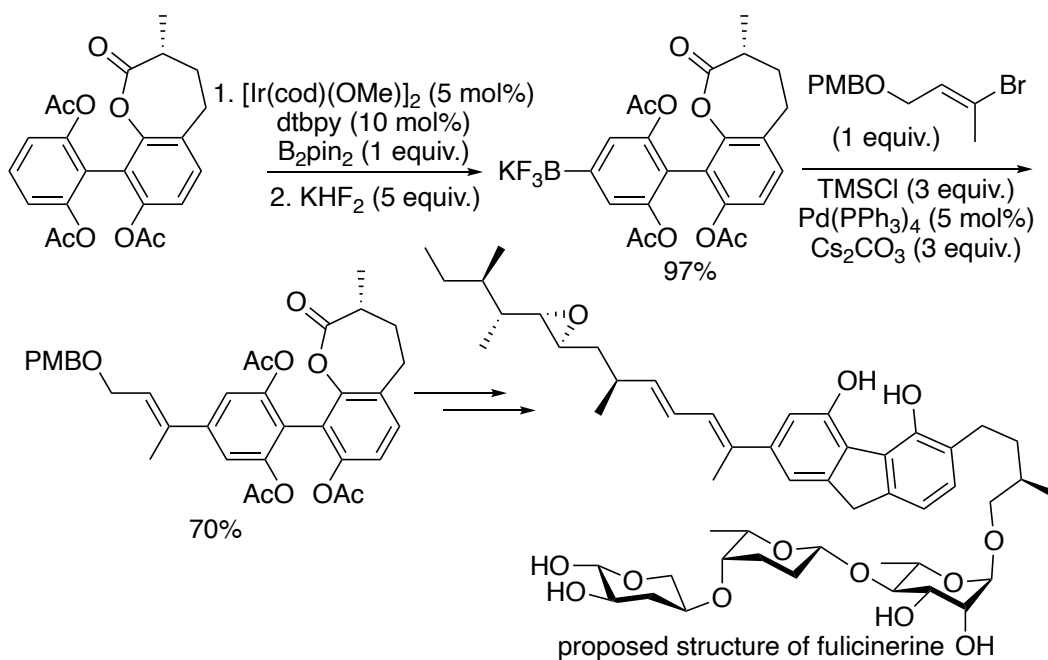
Figure 1.12. Borylation followed by cross-coupling enabled the structural reassignment of fulicinerine.
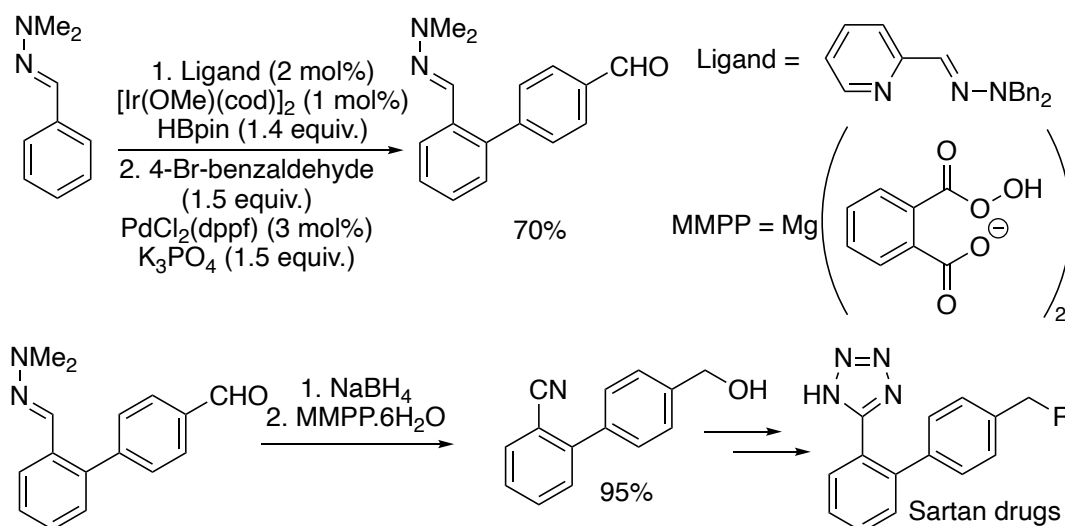
Figure 1.13. Synthesis of Sartan drugs via the *ortho*-selective borylation of aryl hydrazones.

Filipski and coworkers at Pfizer endeavored to conduct donor-acceptor replacement of a heteroarylamide with heteroaryl substitutents as part of a glucokinase activator discovery campaign. The pyrimidone derivative was synthesized by the elaboration of a dialkoxyarene using a borylation-cross-coupling sequence (Figure 1.14).[65]

In 2014, Colacot reported a preligated precatalyst for the borylation of arenes. With this precatalyst, they conducted the borylation of *N*-Boc indole selectively at the 3-position and cross-coupled the product to an aminopyrazine in a concise synthesis of meridianin G (Figure 1.15).[66] The 3-selectivity arises from steric factors and is precedented by the borylation of *N*-Boc indoles with more typical catalyst precursors.[67]
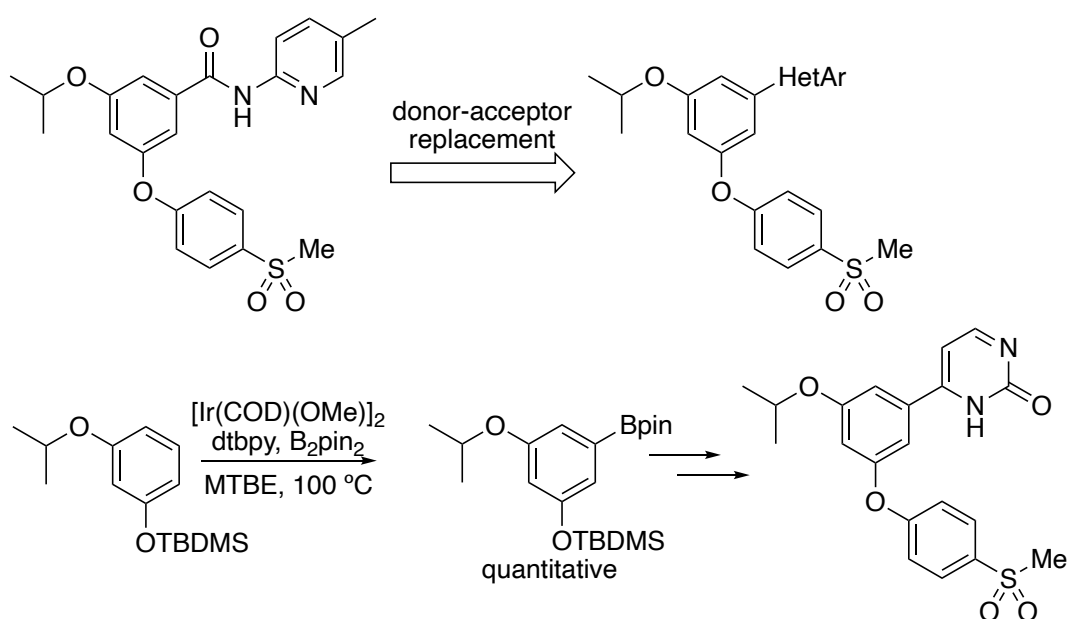
Figure 1.14. Borylation followed by cross-coupling enables the synthesis of glucokinase activators.
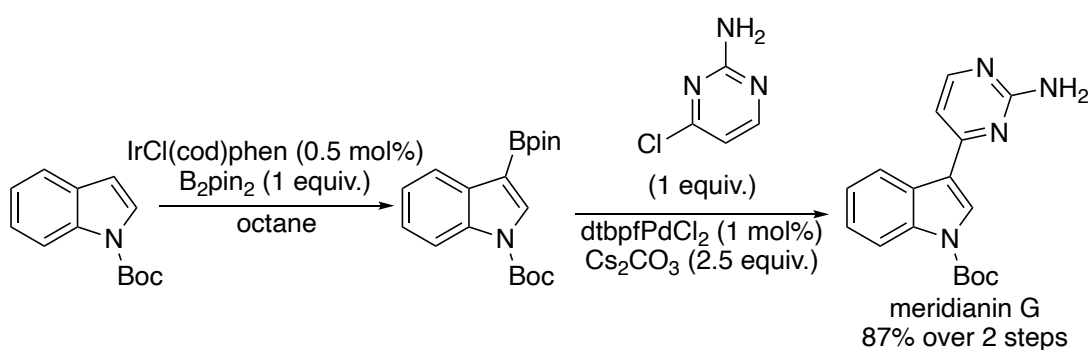
Figure 1.15. Borylation cross-coupling in the synthesis of meridianin G.

In 2014, Stoltz reported the total synthesis of dichroanone and taiwaniaquinone, during which a bromoarene was borylated to afford a key boronic acid. Engagement of this boronic acid with a palladium catalyst containing a chiral PyOx ligand resulted in enantioselective conjugate addition to a cyclohexanone (Figure 1.16). [68]

Gaunt reported a synthesis of dictyodendrin B that included six direct functionalizations of the initial 4-bromo indole. Of the six functionalizations, five were C–H functionalization reactions. Notably, formal C–H arylation of the C-7 position was achieved via a borylation cross-coupling sequence (Figure 1.17).[69]
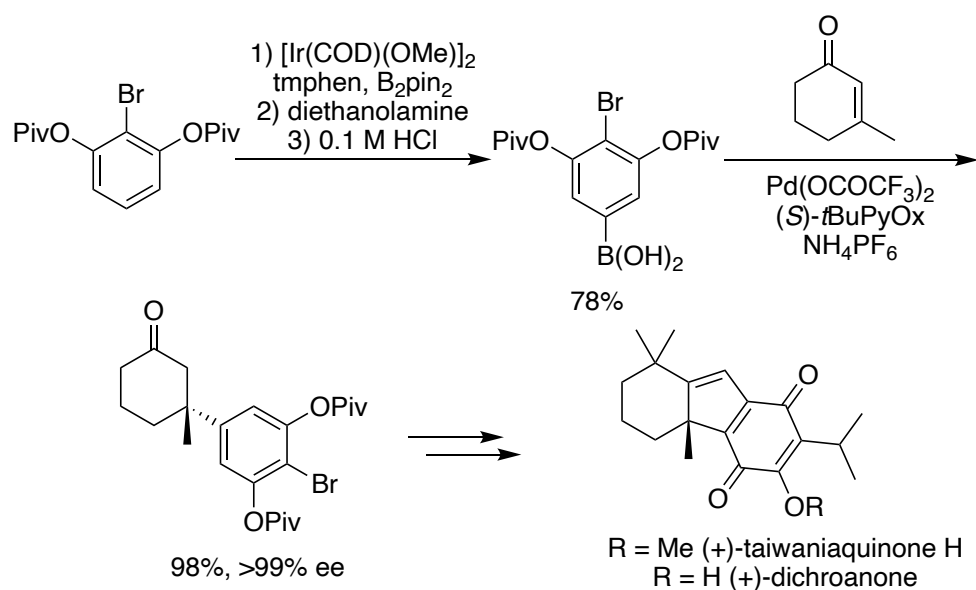
Figure 1.16. Borylation conjugate addition in the synthesis of taiwaniaquinone H and dichroanone.
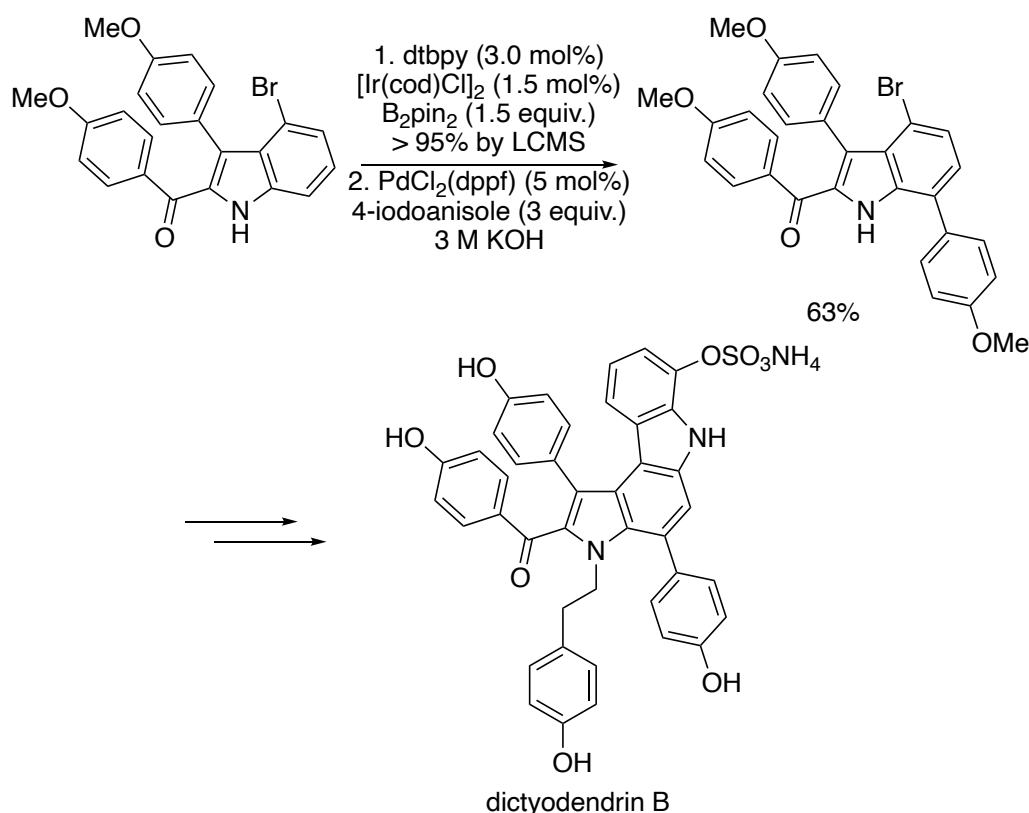
Figure 1.17. Borylation cross-coupling in the synthesis of dictyodendrin B.

In 2017, Kanai reported that catalysts formed from bipyridine ligands containing a boryl substituent catalyze the borylation of thioanisoles with high *ortho*-selectivity. The selectivity was presumed to arise from attractive interactions between the Lewis basic sulfide and the Lewis acidic boryl substitutent on the ligand. This borylation was applied to the synthesis of an intermediate in the preparation of a factor Xa inhibitor (Figure 1.18).[70]
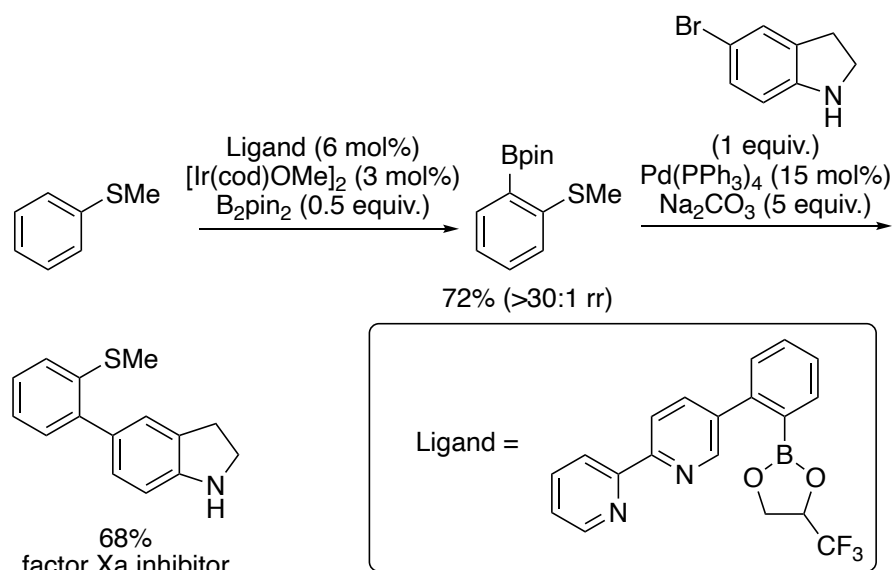
Figure 1.18. *Ortho*-selective borylation of thioanisoles enable the synthesis of a factor Xa inhibitor.

In 2017, Kuninobu reported that catalysts formed from bipyridine ligands containing a trifluorotolyl substituent catalyze the borylation of methylthiomethylethers with *ortho*-selectivity. The protecting group was then cleaved under reductive conditions to reveal a methyl ether. This borylation process was used as part of the synthesis of a calcium receptor modulator (Figure 1.19).[71]
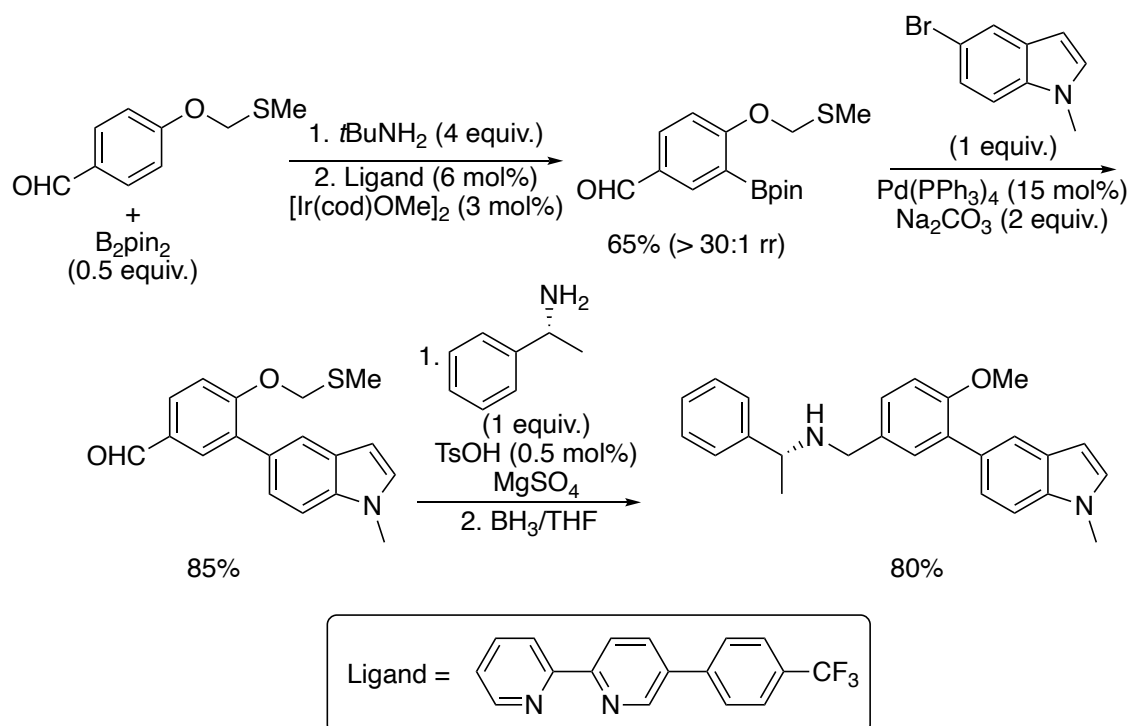
Figure 1.19. *Ortho*-selective borylation of methylthiomethylethers in the synthesis of a calcium receptor moderator.

Chirik has developed a variety of cobalt catalysts that catalyze the borylation of aryl C–H bonds. In 2017, this group reported the PCP-ligated cobalt catalyst shown in Figure 1.20 for the selective *ortho*-borylation of fluoroarenes. The observed *ortho*-selectivity was attributed to the enhanced sensitivity of a first-row metal to electronic factors overriding the greater steric sensitivity typical of the precious metal catalysts. Cross-coupling of the boronic ester product was conducted as part of the synthesis of flurbiprofen.[72]
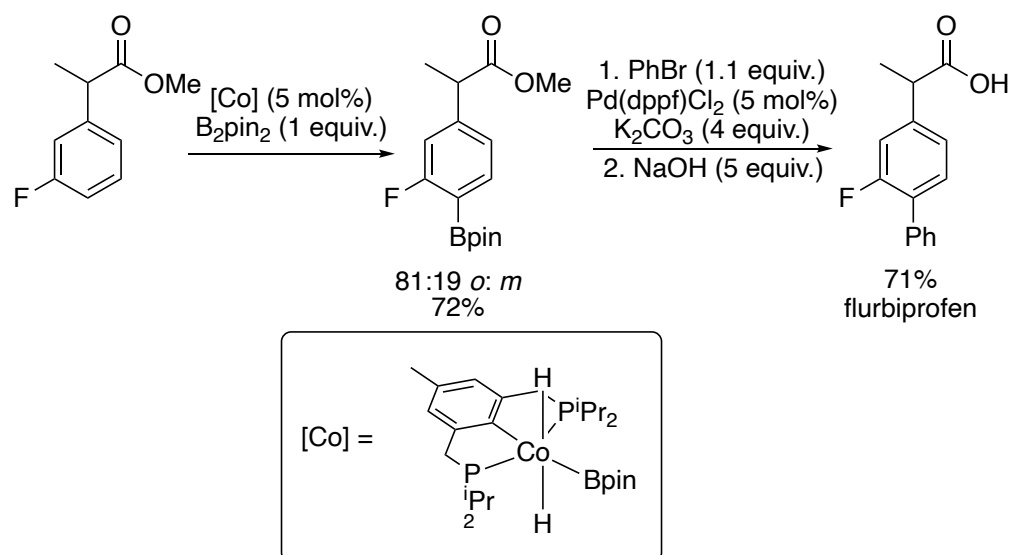
Figure 1.20. Cobalt-catalyzed *ortho*-borylation of fluoroarenes applied to the synthesis of flurbiprofen.

Han reported the synthesis of (−)-hamigeran B and (−)-4-bromohamigeran B, during which a 3-methylanisole was borylated selectively and cross-coupled to a vinyl triflate to afford the key intermediate. Subsequent oxidation and Friedel-Crafts cyclization afforded the core of the molecule (Figure 1.21).[73]

In 2022, Xu reported a chiral boryl ligand that binds to iridium and generates a catalyst for the enantioselective borylation of aminocyclopropanes. The chiral borylpyridine ligand is presumed to bind to iridium in an LX fashion, imparting a chiral environment while maintaining an extra empty site available to interact with directing groups. This reaction was applied to the synthesis of a nematicide candidate (Figure 1.22).[74]

Mascarenas reported that the combination of iridium with a 3-trifluoromethylbipyridine ligand forms a catalyst for the borylation of aryl amides with exclusive *ortho*- selectivity. The selectivity is understood to arise from non-covalent interactions between the amide functionality and the trifluoromethyl substituted ring of the bipyridine. This reaction was applied to a concise synthesis of a fungicide by a borylation and cross-coupling sequence (Figure 1.23).[75]
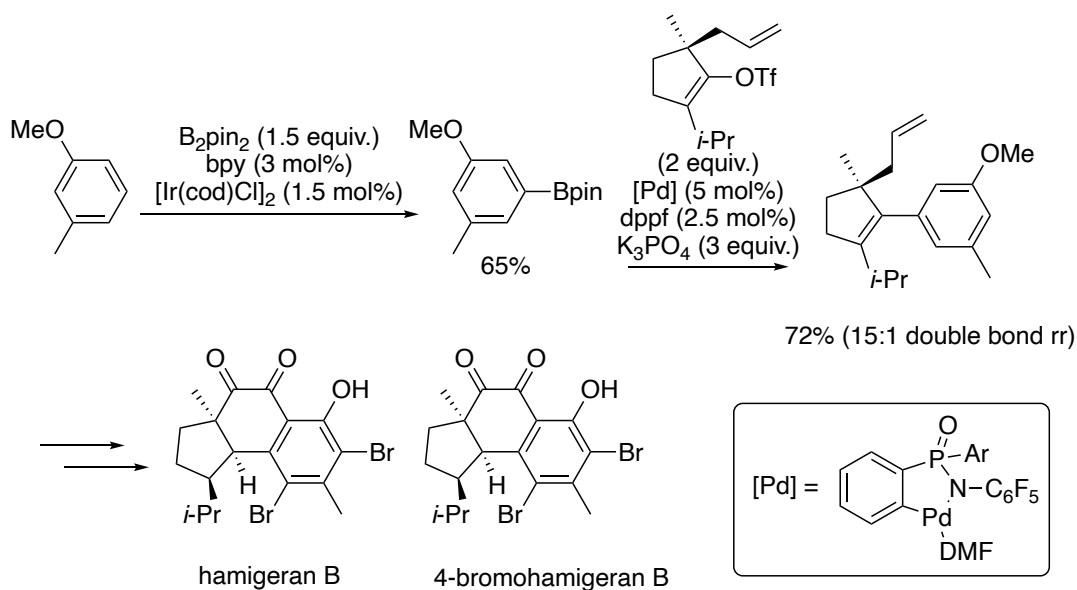
Figure 1.21. Borylation cross-coupling en route to hamigeran B and 4-bromohamigeran B.
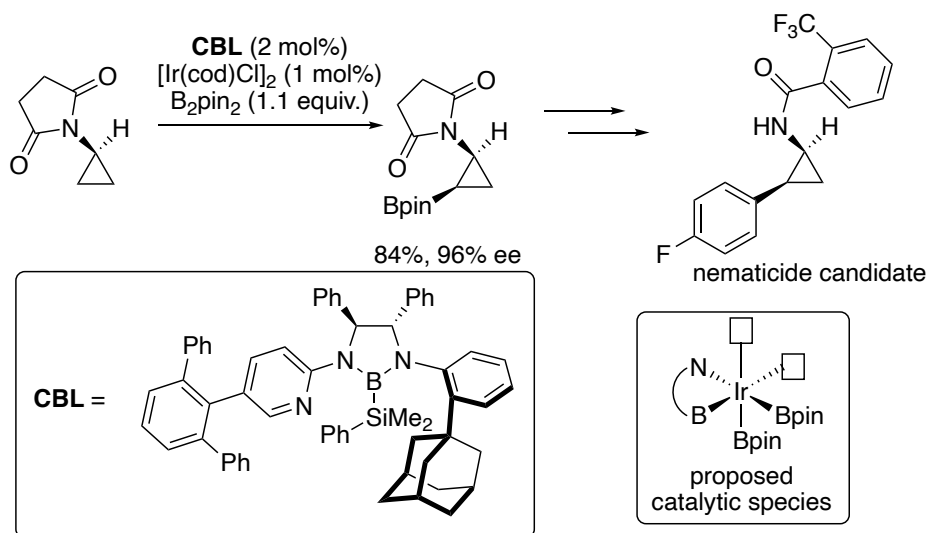
Figure 1.22. Enantioselective borylation of aminocyclopropanes enables the synthesis of a nematicide candidate.
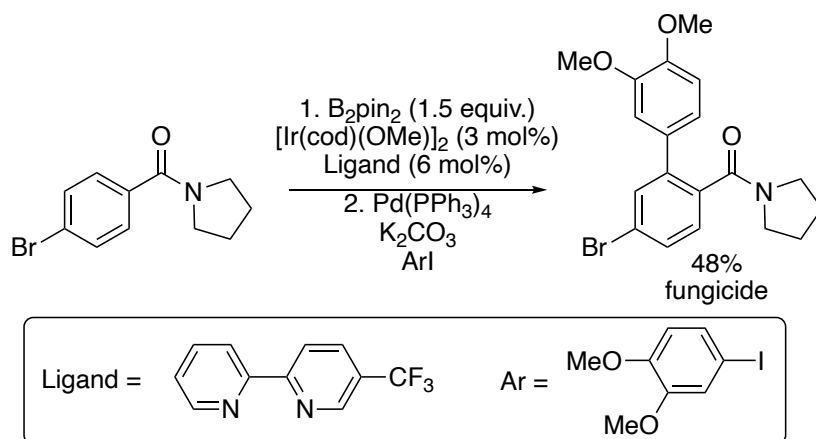
Figure 1.23. *Ortho*-selective borylation of amides in the synthesis of a fungicide.

1.3.2 Transition-Metal Catalyzed Borylation of C–H Bonds in the Synthesis of Precursors to Bioactive Molecules Through Oxidation of the Boronic Ester to the Corresponding Alcohol

The oxidation of boronic esters is one of the oldest transformations of boronic esters. The combination of a *meta*-selective borylation followed by oxidation to the alcohol can be considered a formal *meta*-selective oxidation of arenes.

In 2014, Peat and coworkers from GlaxoSmithKline applied a borylation-oxidation sequence to the synthesis of hepatitis C replication inhibitors (Figure 1.24).[76]
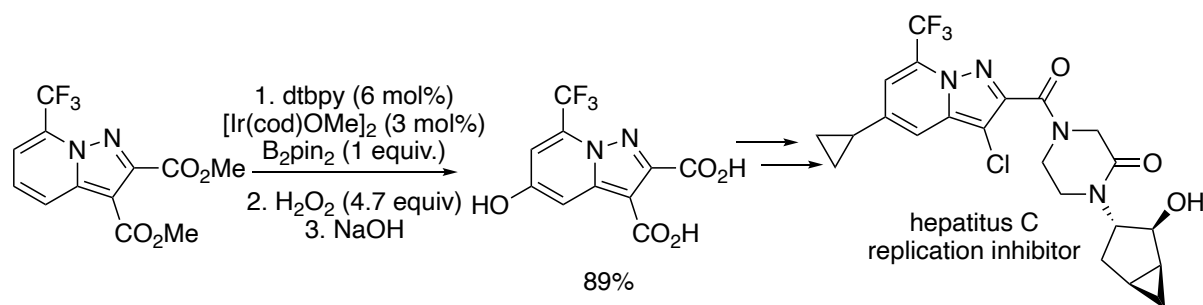
Figure 1.24. Formal oxidation of aryl C–H bonds via borylation-oxidation applied to the synthesis of hepatitis C replication inhibitors.

Campeau and coworkers at Merck reported the synthesis of doravirine by the combination of borylation and oxidation. To deliver the necessary chloroiodophenol intermediate on 75 kg scale, a borylation-oxidation sequence was developed. 2,2'-Bipyridine was chosen as as an economical replacement for the more expensive dtbpy ligand for the borylation. The 3-chloro-5-iodophenol intermediate was then further coupled with cyanide, and the resulting benzonitrile was used in an S$_N$Ar reaction to afford doravirine (Figure 1.25a).[77] In Baran's synthesis of verruculogen and fumitremorgin A, a key 6-methoxyindole intermediate was synthesized by the 6-selective borylation of an *N*-TIPS tryptophan, with the *N*-TIPS protecting group shielding the 2- and 7- positions from undergoing borylation (Figure 1.25b).[78]
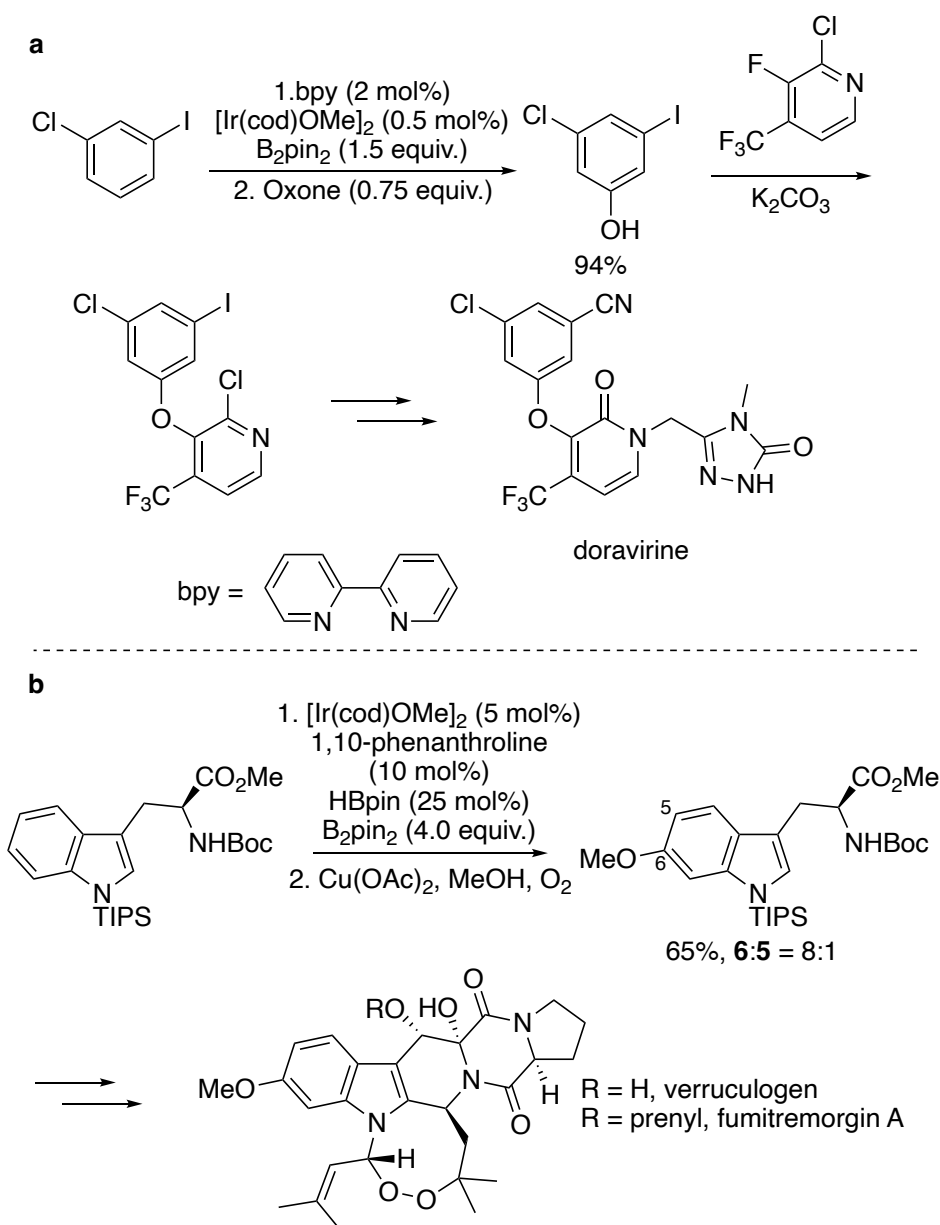
Figure 1.25. Formal oxidation of aryl C–H bonds through borylation-oxidation enabled a synthesis of doravirine on scale and the total synthesis of verruculogen and fumitrimorgin A.

1.3.3 Transition-Metal Catalyzed Borylation of C–H Bonds in the Synthesis of Precursors to Bioactive Molecules Through the Corresponding Halide or Pseudohalide

In 2007, our laboratory developed copper-mediated conditions that transformed aryl boronic esters into the corresponding halide. The reaction sequence was telescoped into a one-pot two-step sequence that affords *meta*-disubstituted aryl bromides. The *meta*-selective borylation of nicotine followed by oxidative bromination afforded 5-bromonicotine, which is an intermediate en route to the synthesis of altinicline (Figure 1.26).[79]
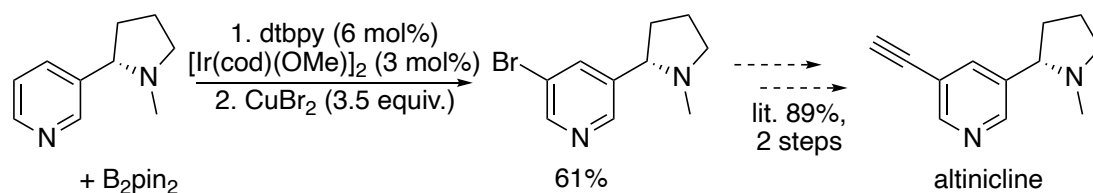
Figure 1.26. Borylation-bromination of the pyridine intermediate en route to altinicline.

Koert used the *meta*-selective borylation, followed by chlorination to synthesize the key chloride intermediate in a synthesis of poipuol. Notably, a tetrasubstituted olefin was tolerated in this sequence (Figure 1.27).[80]
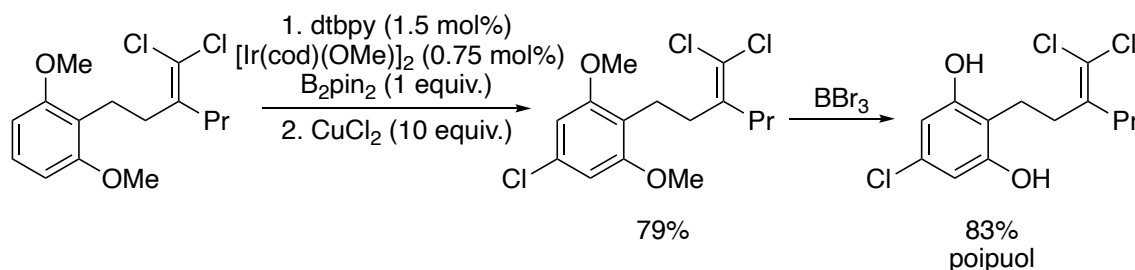
Figure 1.27. Formal chlorination of aryl C–H bonds by the combination of borylation and chlorination in the synthesis of poipuol.

In 2011, our laboratory reported the synthesis of taiwaniaquinone H and taiwaniaquinone B. Ir-Catalyzed, *meta*-selective borylation of a 1,2,3-trisubstituted arene followed by conversion of the boronic ester to the bromide afforded a densely functionalized bromoarene. The bromoarene was a suitable substrate for the Pd-catalyzed, enantioselective α-arylation of a 2-methylcyclohexenone derivative to set a quaternary stereocenter (Figure 1.28).

Hirama reported the synthesis of complanadine A and B. Similar to Sarpong's approach, Hirama's approach included disconnection of the molecules into two lycodine fragments. Selective borylation of the 3-position of the pyridine was achieved in the presence of dtbpy and [Ir(cod)OMe]₂ to generate the desired 3-borylpyridine intermediate. In contrast to Sarpong's approach, the 3-borylpyridine was transformed to the corresponding bromide and engaged in a palladium-catalyzed arylation of a pyridine oxide (Figure 1.29).[81, 82]

Singer and coworkers at Pfizer reported the synthesis of a nicotine hapten on a 10-kilogram scale. They found that the reaction of nicotine with B₂pin₂ with [Ir(cod)Cl]₂ and tmphen as ligand resulted in higher yields of 5-borylnicotine than those containing [Ir(cod)OMe]₂ and dtbpy. Subsequent bromination with CuBr₂ provided the bromide in good yield. Workup with aqueous ammonia and recrystallization with L-DBTA (L-dibenzoyltartaric acid) resulted in nearly complete removal of metal contaminants and avoided the need for chromatographic purification. Further elaboration of the bromide resulted in the desired nicotine hapten (Figure 1.30).[83]
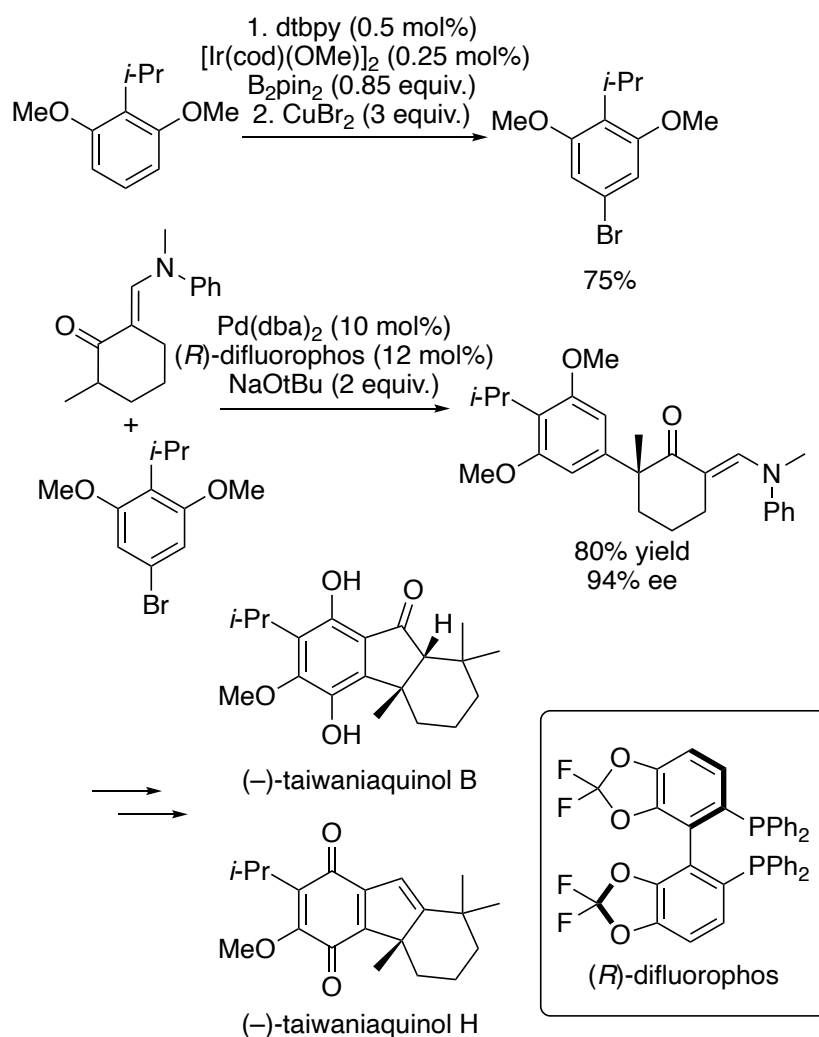
Figure 1.28. Key bromoarene required for the enantioselective synthesis of taiwaniaquinol B and taiwaniaquinol H synthesized by a borylation-bromination sequence.

Nortcliffe reported the borylation of beta-aryl propionic acids catalyzed by the combination of [Ir(cod)OMe]$_2$ and dtbpy. The boryl products underwent subsequent halogenation to the corresponding bromide smoothly. The borylation-bromination sequence did not erode the enantiomeric excess of the beta-aryl propionic acids and was applied to the synthesis of a integrin antagonist (Figure 1.31).[84]
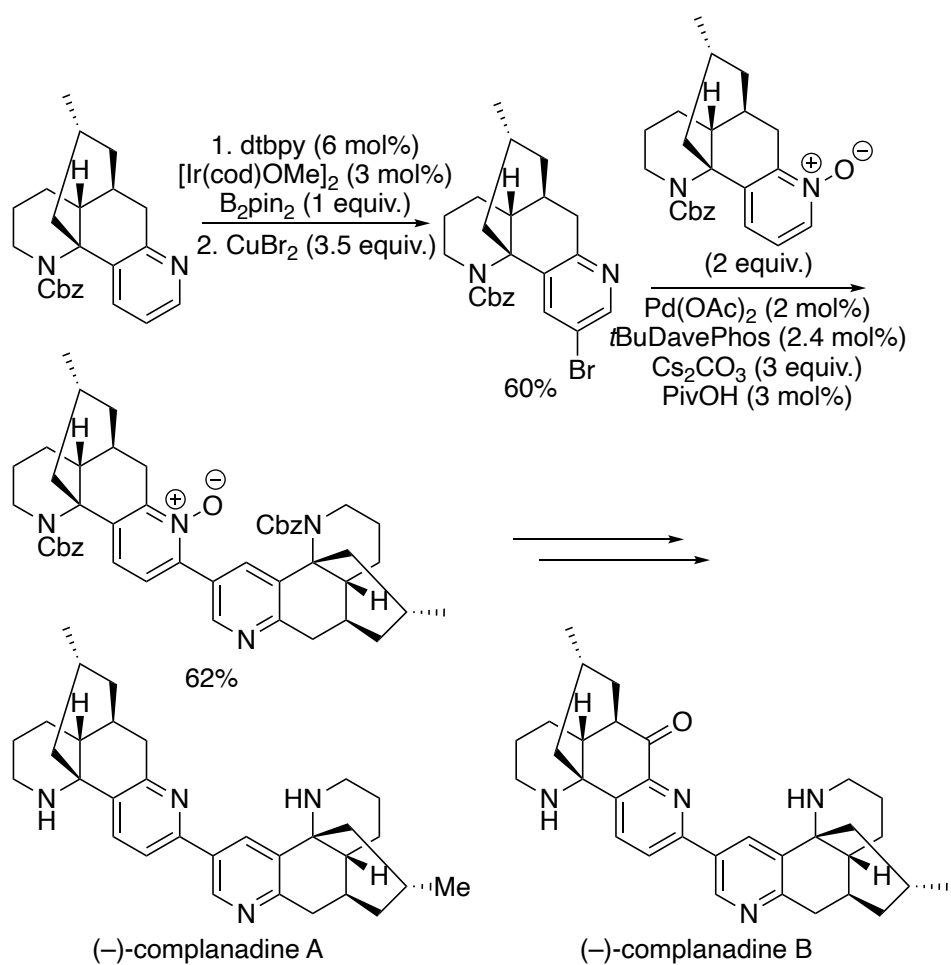
Figure 1.29. Borylation-bromination of lycodine in the synthesis of complanadine A and B.
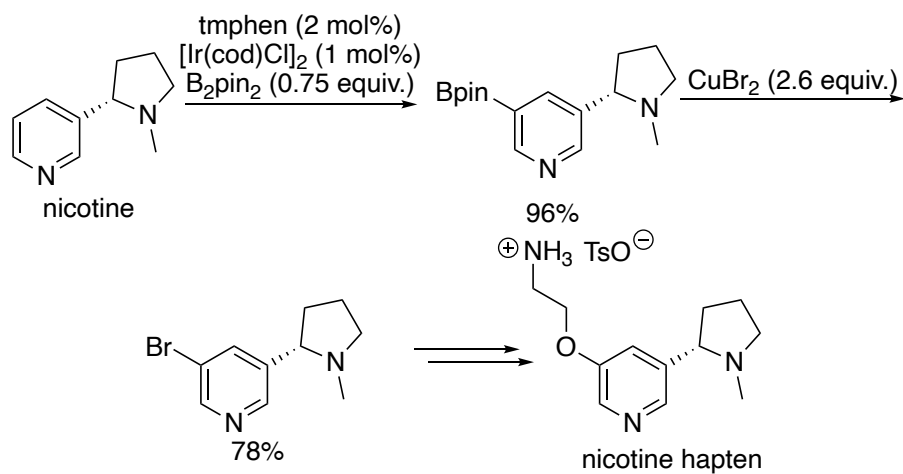
Figure 1.30. Borylation-bromination in the synthesis of nicotine hapten.
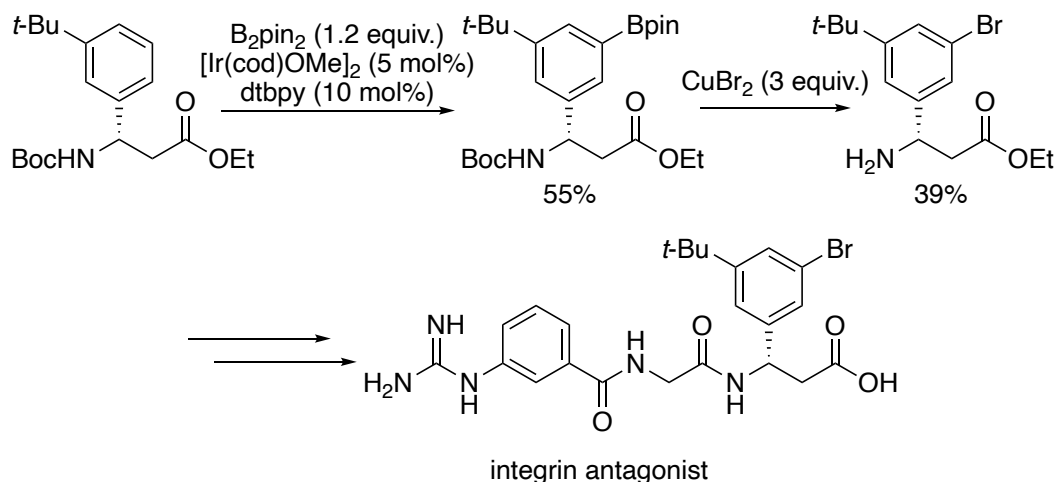
Figure 1.31. Borylation-bromination of beta-aryl propionic acids en route to an integrin antagonist.

1.3.4 Transition-Metal Catalyzed Borylation of C–H Bonds in the Synthesis of Precursors to Bioactive Molecules Through the Formation of C–N Bonds

In 2014, Abell developed conditions for the copper-mediated azidation of aryl boronic esters. The resulting azides were immediately engaged in a Huisgen cycloaddition to form triazoles. The telescoped borylation-azidation sequence was applied to the synthesis of triazole-substituted arenes, including a resveratrol analogue and a nicotine derivative (Figure 1.32).[85]
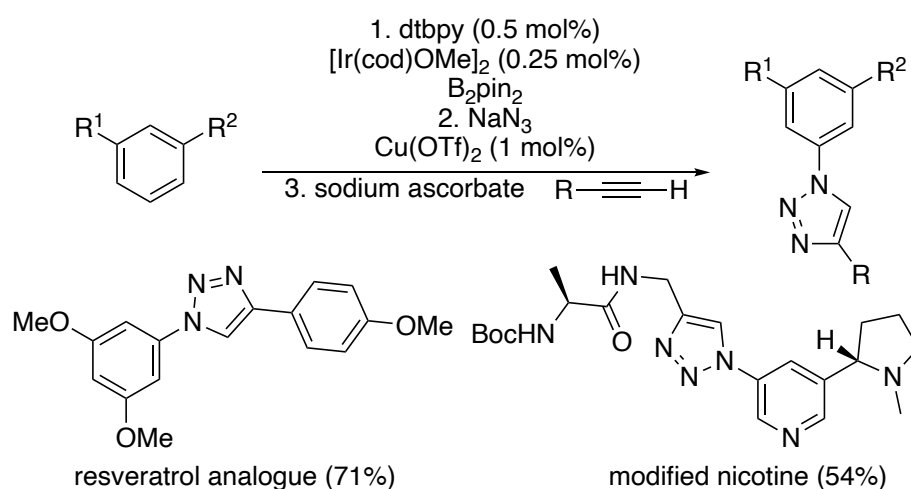
Figure 1.32. Formal azidation of aryl C–H bonds by the combination of borylation and azidation applied to the synthesis of triazole-decorated natural products.

In 2019, Srinivasan developed copper-mediated conditions for the nitration of aryl boronic esters. This enables the rapid synthesis of nitroarenes and the corresponding anilines. The telescoped borylation-nitration protocol was applied to the synthesis of the core of nilotinib (Figure 1.33).[86]
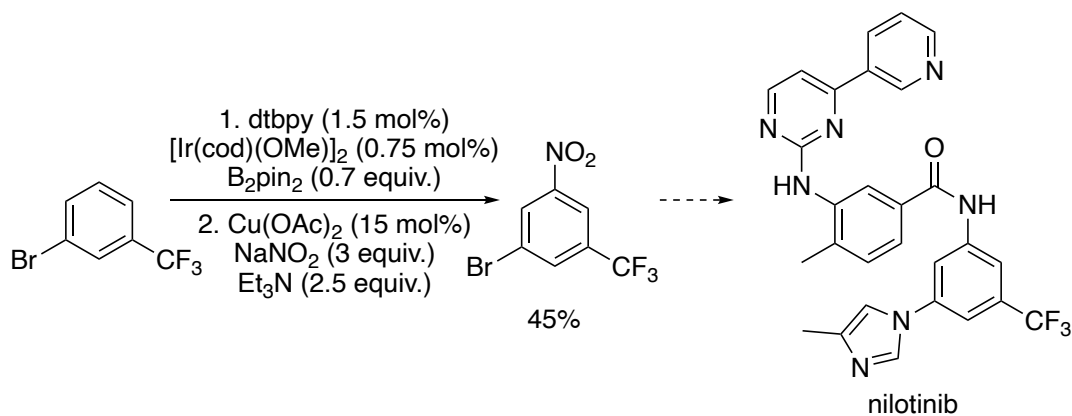
Figure 1.33. Formal amination of aryl C–H bonds by the combination of borylation and nitration applied to the synthesis of nilotinib.

1.4 Transition-Metal Catalyzed, Late-Stage Borylation of C–H Bonds in Complex Molecules

This section of the review provides information on the application of the borylation of C–H bonds to the late-stage functionalization of complex molecules. Examples of the borylation of C–H bonds will be divided into methods that functionalize aryl C–H bonds and methods that functionalize alkyl C–H bonds. Within those categories, the methods will be further divided into undirected examples and directed examples.

1.4.1 Late-Stage Modification of Complex Molecules by the Undirected Borylation of Aryl C–H Bonds

Many applications of the undirected, metal-catalyzed borylations of aryl C–H bonds in complex molecules have been reported. For late-stage functionalization of such compounds, material is often limited and valuable. Thus, it is especially advantageous to achieve high regioselectivity without the requirement of additional synthetic steps to install and remove directing groups.

The general set of conditions for the undirected borylation of aryl C–H bonds that is most used for the late-stage functionalization of complex molecules is a catalyst formed from [Ir(cod)OMe]$_2$ and either 3,4,7,8-tetramethyl-1,10-phenanthroline (tmphen) or 4,4'-di-*tert*-butyl-2,2'-bipyridine (dtbpy) and HBpin or B$_2$pin$_2$ as the boron source. Other ligand systems form catalytic complexes from iridium precatalysts for the directed borylation of aryl C–H bonds on complex molecules, and such systems will be reviewed second in this section.

The catalyst generated from the combination of [Ir(cod)OMe]$_2$ and dtbpy was reported for the C2 borylation of protected tryptophan by Smith and Maleczka in 2009 (Figure 1.34A).[67] In this study, the authors reported that C2 monoborylation occurred alongside competing C2/C7 diborylation. The C2/C7 diborylated product of this reaction has been shown to undergo C2-selective protodeboronation to furnish the C7 monoborylated product when subjected to TFA, as reported by Movassaghi in 2014,[87] or when subjected to catalytic [Ir(cod)OMe]$_2$ in MeOH/CH$_2$Cl$_2$, as reported by Smith and Maleczka in 2015 (Figure 1.34B).[88]

24

In 2010, James published the C–H borylation of 15 a-amino acid derivatives containing aromatic and heteroaromatic side chains with a catalyst generated from [Ir(cod)OMe]$_2$ and dtbpy (Figure 1.35).[89] Substrates with arene side chains in this study were meta substituted and formed 3,5-disubstituted aryl–bpin products. Heteroaryl substrates included thiophene, pyridine, and indole side chains. Late-stage borylation of a-amino acid derivatives is an important strategy for the synthesis of novel therapeutic agents. Methods that modify existing a-amino acid derivatives are attractive because the key a-stereocenter is already present, and the configuration is retained.
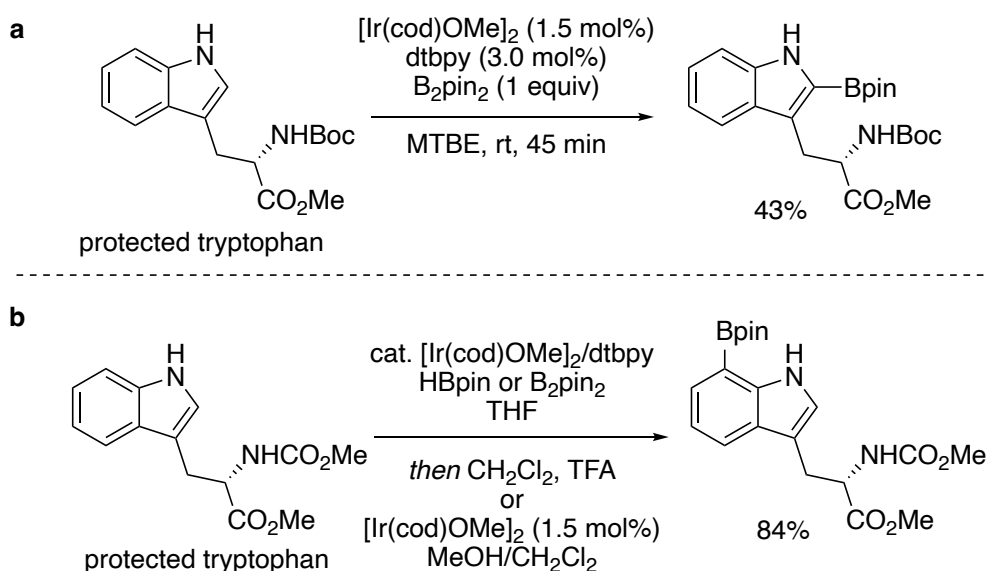
Figure 1.34. C–H borylation of protected tryptophan. (a) C2 monoborylation of protected tryptophan (b) C7 monoborylation of protected tryptophan by diborylation/C2-selective protodeboronation.
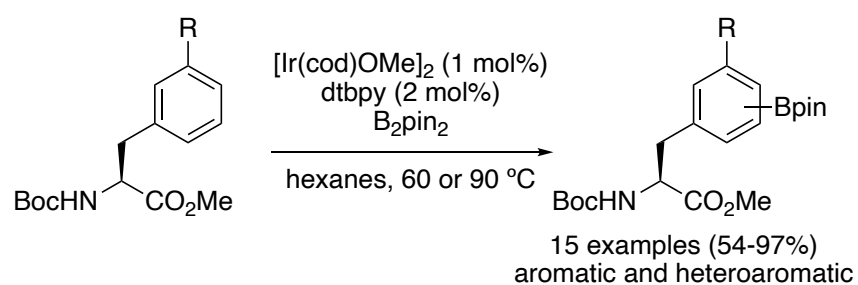
Figure 1.35. The borylation of aryl C–H bonds in α-amino acid derivatives.

A benzoxazole-containing c-Met Kinase Inhibitor that was identified as a potential cancer therapeutic underwent borylation with a catalyst generated from [Ir(cod)OMe]$_2$ and tmphen, as reported by our laboratory in 2014 (Figure 1.36).[29] The selectivity of borylation ortho to oxygen in benzoxazoles is proposed to result from electronic effects.[32] Modification of the substitution pattern on the benzoxazole led to species with high c-Met kinase inhibition, underscoring the importance of methods that can rapidly generate diverse structures in the late-stage.
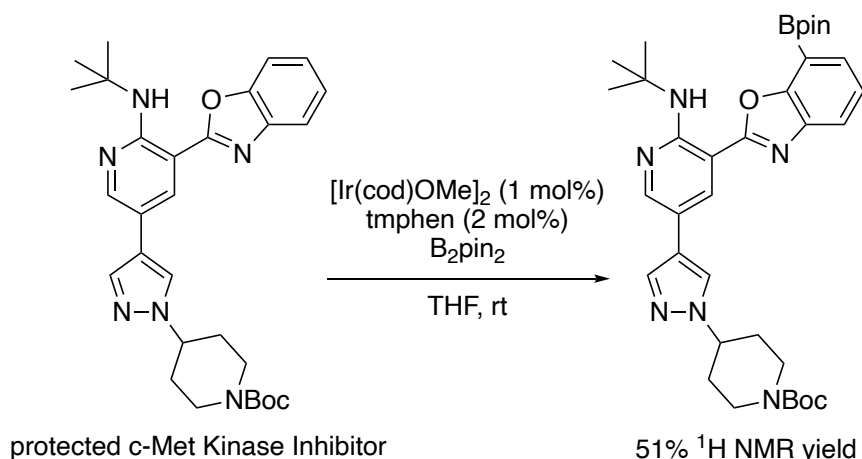
Figure 1.36. Late-stage borylation of a c-Met kinase inhibitor.

The general conditions for the undirected borylation of aryl C–H bonds can be applied to two-step borylation/functionalization sequences on complex molecules, as well as the combination of borylation and protonation of the resulting boronate to enable isotopic labeling at specific positions. Maleczka and Smith used this approach to achieve a net C–H deuteration of clopidogrel, an active ingredient of Plavix. The first step consisted of C–H borylation at the 2-position of a thiophene moiety catalyzed by [Ir(cod)OMe]$_2$ and dtbpy, followed by a deuteriodeborylation catalyzed by [Ir(cod)OMe]$_2$ in CD$_3$OD/CDCl$_3$ to afford 2-deuterioclopidogrel.[88] Deuterium-labeled compounds are widely used for pharmacokinetics and enzyme kinetic studies (Figure 1.37).
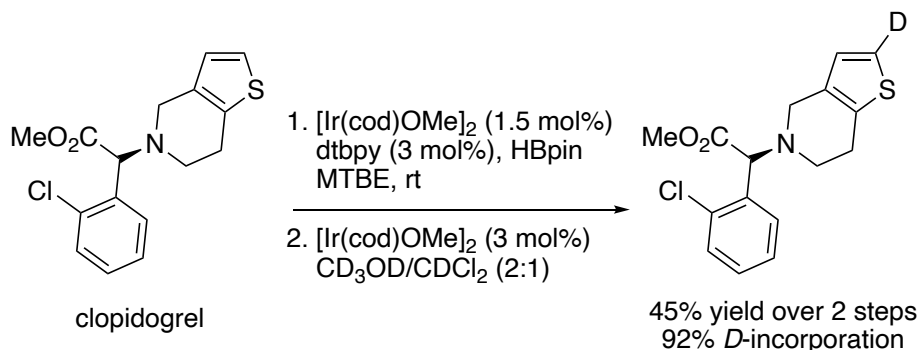
Figure 1.37. Borylation/deuterodeborylation of clopidogrel.

The combination of [Ir(cod)OMe]$_2$ and dtbpy catalyzed the borylation at the 5-position of a 1,2,3-trisubsituted benzene ring in a galactose derivative in a synthesis reported by Shabat in 2016 (Figure 1.38).[90] The resultant boronic ester was used to append a fluorophore to the core structure to generate chemiluminescent probes for sensing and imaging.
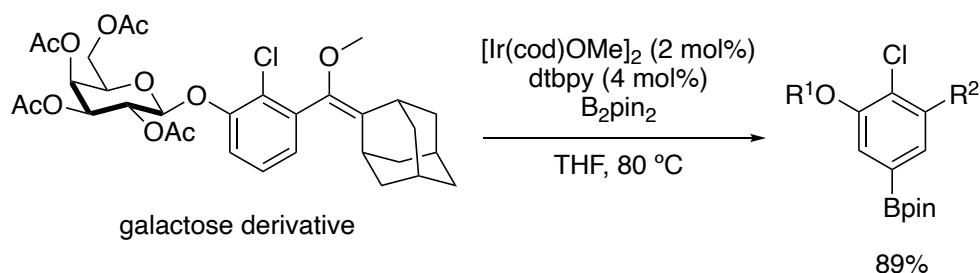
Figure 1.38. C–H borylation of a 1,2,3-trisubstituted benzene on a galactose derivative.

In 2017, Hirano and Miura published C–H borylation of 2-pyridones with a catalyst generated from [Ir(cod)OMe]$_2$ and 2,2'-bipyridine.[91] This catalyst system was applied to the borylation of uracil to produce the C4 and C5-borylated products in a 50:50 ratio and to the borylation of Boc-protected (–)-cytisine, which occurred with perfect site-selectivity (Figure 1.39). 2-Pyridones are frequently occurring substructures in complex molecules, such as ciclopirox, milrinone, camptothecin, fredericamycin, and perampanel. The importance of their borylation is exemplified in Sarpong's total synthesis of complanadine A discussed above (Figure 1.5).[92]
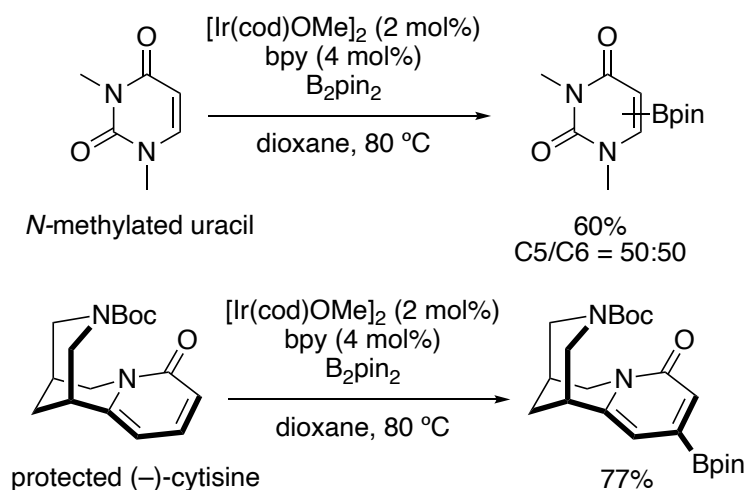
Figure 1.39. C–H borylation of bioactive 2-pyridones.

Movassaghi published the C7 borylation of indole fragments in the core of the aspidosperma family of natural products to produce late-stage intermediates in the synthesis of three different natural products. In a 2018 paper, an iridium complex ligated by dtbpy catalyzed the C7-indole borylation of a polycyclic lactam.[93] After oxidation, the hydroxyindole intermediate generated was converted in three steps to the natural product (–)-vallesine. In a paper they published in 2021, an iridium complex ligated by tmphen catalyzed the C7-indole borylation of a polycyclic intermediate related to the polycyclic lactam used in the synthesis of (–)-vallesine.[94] After oxidation, the hydroxyindole intermediate generated was converted in three steps to (+)-kopsifoline E and in four steps to (–)-kopsifoline A (Figure 1.40).

27
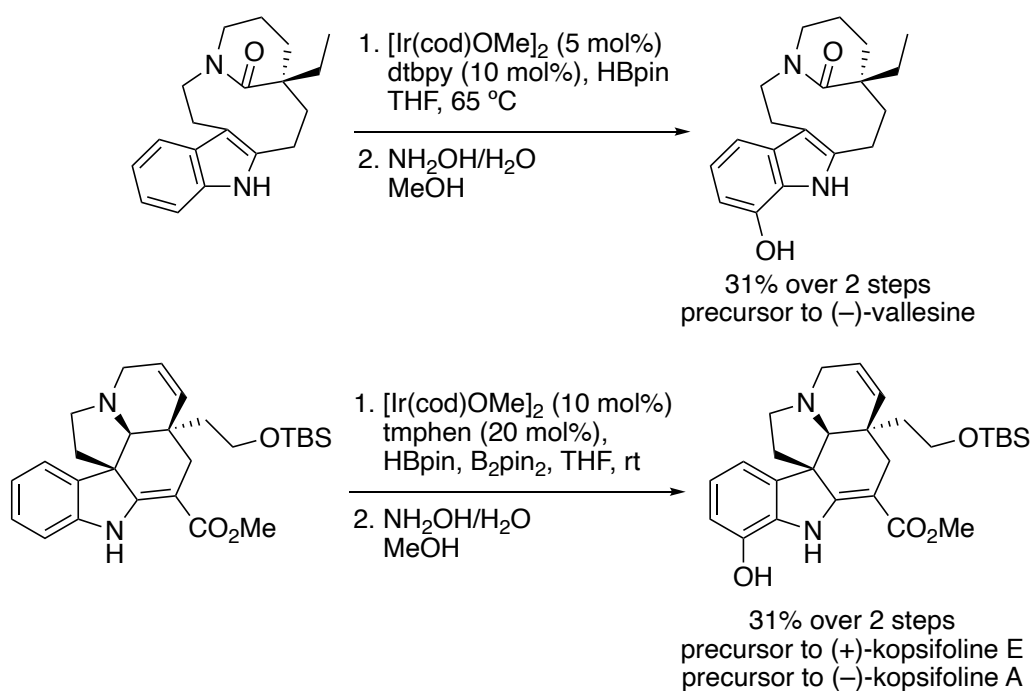
Figure 1.40. C–H borylation on the indole fragment of the aspidosperma family of natural products.

The one-pot, two-step C–H borylation and nitration was presented in section 3.1.4 of this review was applied to the nitration of a-tocopherol nicotinate.[86] First, Ir-catalyzed C–H borylation with dtbpy as ligand installed a boronic ester at the C3 position of the pyridine moiety of α-tocopherol nicotinate. In the same pot, the copper-catalyzed nitration furnished the 3-nitro derivative of a-tocopherol nicotinate (Figure 1.41).
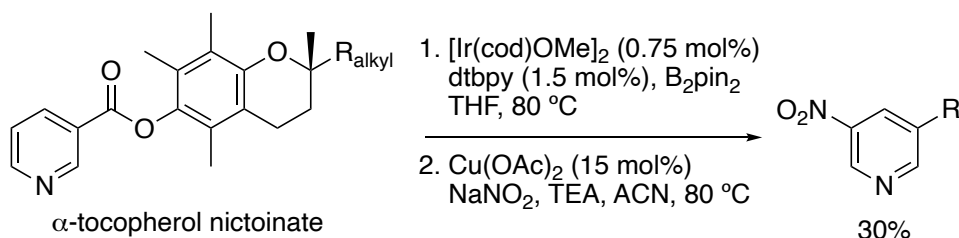
Figure 1.41. One-pot, two-step borylation/nitration of α-tocopherol nicotinate.

A two-step sequence comprising C–H borylation and acylation was published by Szostak in 2020 that was performed without the isolation of the boronic ester intermediate.[95] Various 1,3-disubstituted arenes were borylated at the 5-position with a catalyst generated from [Ir(cod)OMe]$_2$ and dtbpy. The resulting boronic ester was subjected to Pd-catalyzed cross-coupling conditions with a bis(Boc-protected), twisted benzamide as the coupling partner to form a biaryl ketone product. This general method was applied to the acylation of four complex molecules with the boronic ester generated by C–H borylation as the coupling partner (Figure 1.42).
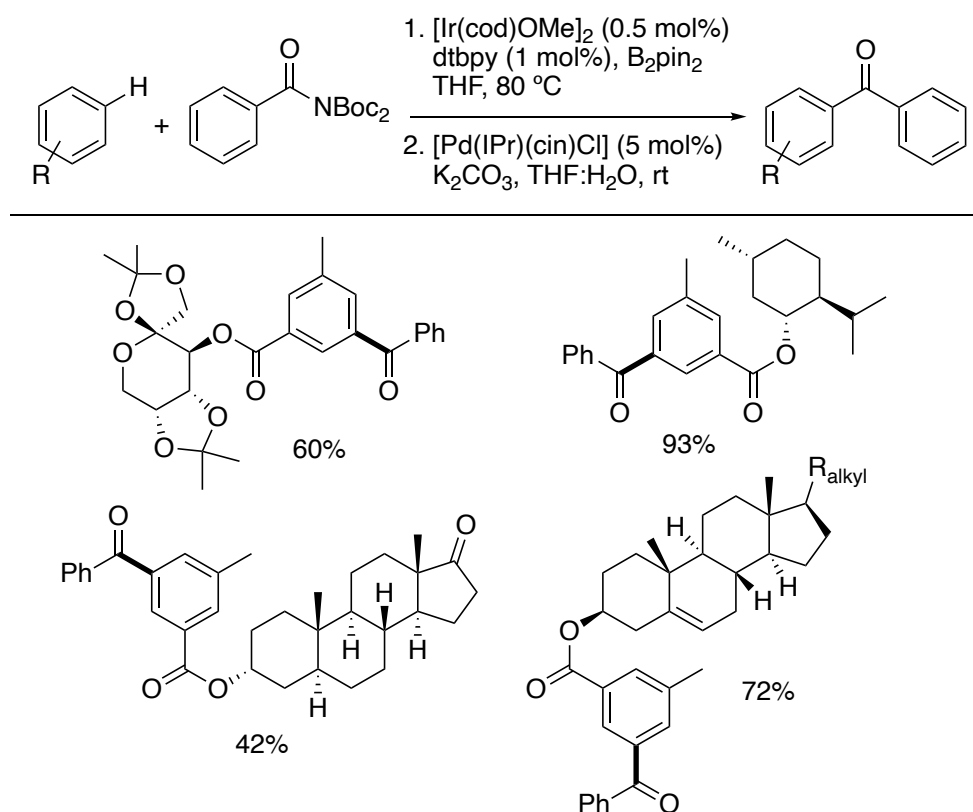
Figure 1.42. Two-step borylation/acylation sequence with complex molecules as the boronic ester coupling partner.

Sanford and Scott published a sequential C–H borylation/radiofluorination method in 2021 that did not require the isolation of the borylated intermediate.[96] C–H borylation catalyzed by a complex generated from [Ir(cod)OMe]$_2$ and tmphen yielded the crude boronic ester intermediate, which was directly subjected to Cu-mediated radiofluorination conditions to forge the C–^{18}F bond. This method was applied to the radiofluorination of lidocaine and a cannabinoid receptor 2 partial agonist, GW405833. PET imaging with radiolabeled compounds is commonly used for the study of disease, highlighting the importance of synthetic methods to access bioactive, radiofluorinationated compounds (Figure 1.43).[97]
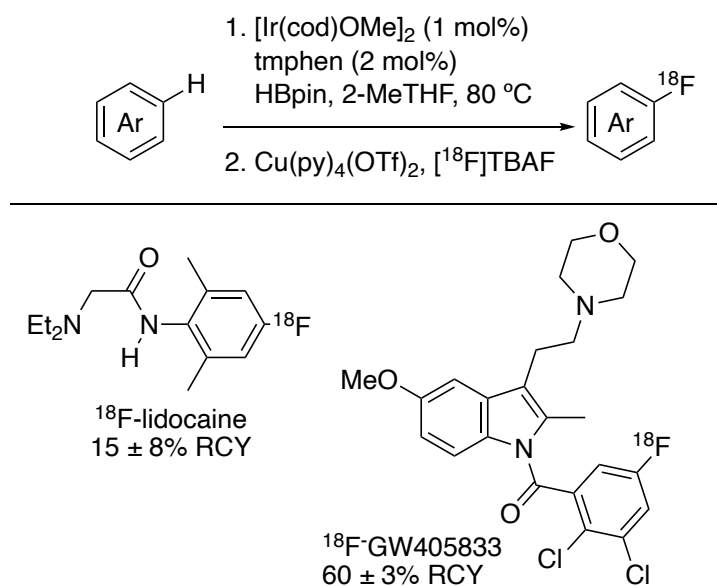
Figure 1.43. C–H borylation/radiofluorination sequence to access radiolabeled, complex molecules.

In a 2020 publication, Taube and Wood applied undirected C–H borylation to generate analogues of staurosporine, a natural product with potent inhibitory properties against a majority of the human kinome.[98] A catalyst generated from [Ir(cod)OMe]$_2$ and 1,10-phenanthroline borylated staurosporine to form five different borylated products, three from mono-borylation and two from diborylation of the indoline moieties (Figure 1.44). Two monoborylated products and the two diborylated products were not separable as boronic esters. However, upon oxidation to the corresponding phenols, the constitutional isomers could be separated.

The cytotoxic activity of the mono-phenol constitutional isomers was evaluated against two tumor-derived cell lines. The study did not reveal increased potency compared to staurosporine. Although the reaction was unselective, the formation of 5 products from a single reaction, all of which could be further diversified, shows how the borylation of C–H bonds is a valuable tool for the rapid generation of complex molecule analogues.

[Ir(cod)OMe]₂ (30 mol%)
1,10-phen (60 mol%)
B₂pin₂

THF, 100 °C

protected staurosporine

4%

31% yield mixture of consitutional isomers

33% yield mixture of consitutional isomers
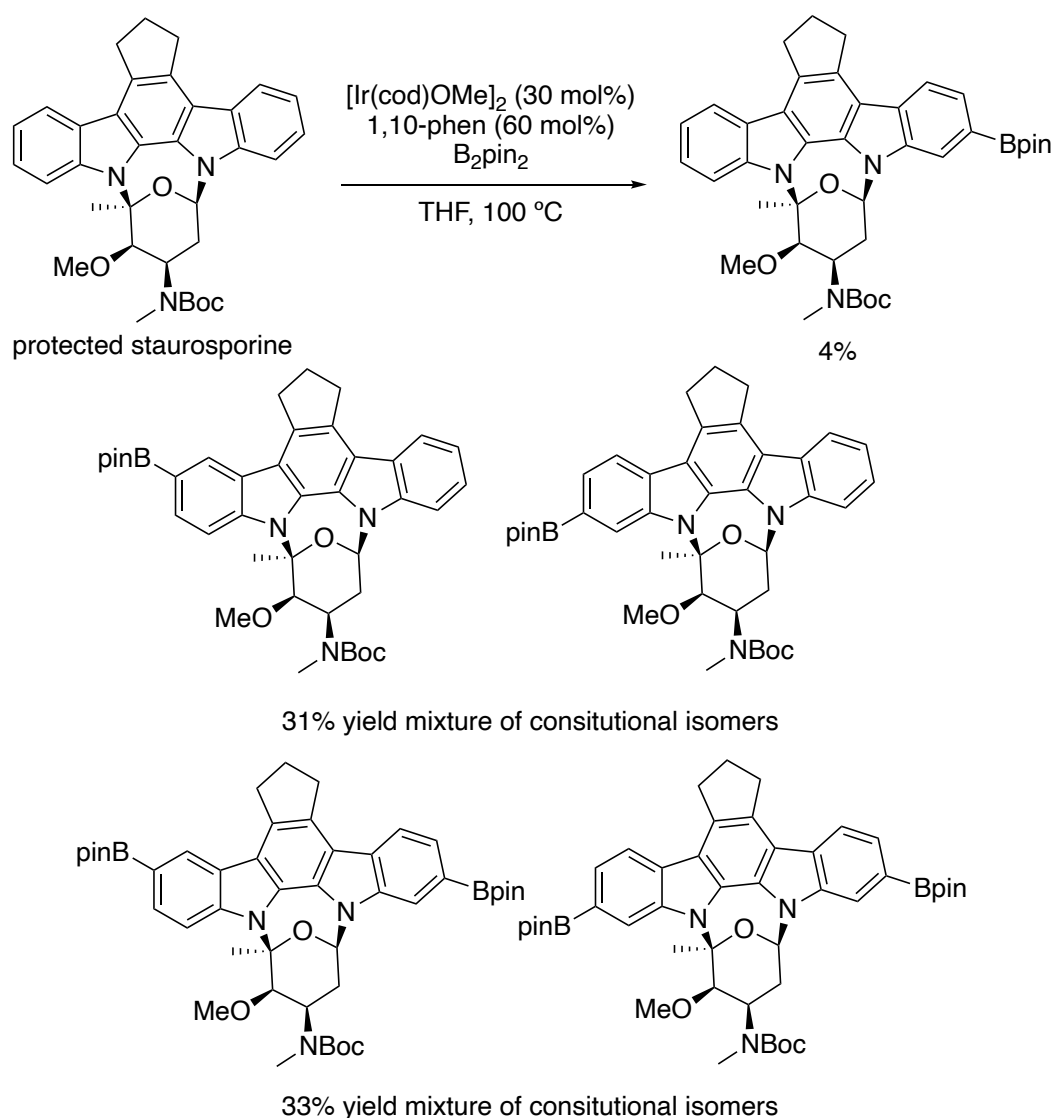
Figure 1.44. The C–H borylation of staurosporine.

The late-stage borylation of aryl C–H bonds in complex molecules has been applied to the large-scale synthesis of pharmaceutical compounds. In 2021, Wheelhouse and Ironmonger from GSK published the borylation of an indazole C–H bond on an advanced intermediate in a route to nemiralisib, a kinase inhibitor in development as a treatment for chronic obstructive pulmonary disease.[99] Diborylation of the complex intermediate on the benzopyrazole ring and the oxazole ring was catalyzed by the combination of [Ir(cod)OMe]₂ and tmphen. The addition of 2-isopropanol led to selective oxazole monodeborylation to reveal a monoborylated intermediate that was transformed to nemiralisib in 2 steps (Figure 1.45). The synthetic route was used to deliver >100 kg of nemiralisib.
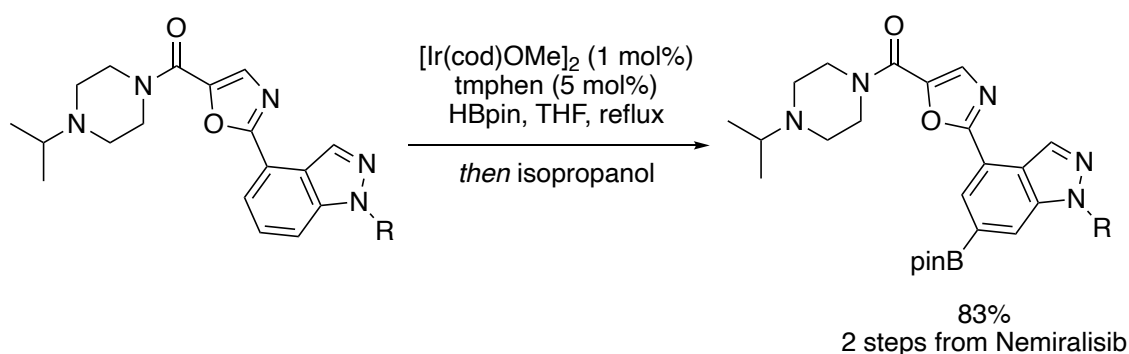
Figure 1.45. The C–H borylation of an advanced intermediate in the synthesis of nemiralisib.

The undirected borylation of C–H bonds on complex molecules can be achieved with iridium catalysts generated from ligands other than tmphen and dtbpy. In 2015, Itami published the *para*-selective borylation of caramiphen by a catalyst generated from [Ir(cod)OH]₂ and OMe-xyl-BIPHEP (Figure 1.46A).[100] Catalysts generated from the OMe-xyl-BIPHEP ligand react with higher *para* selectivity than the iridium catalysts generated from tmphen and dtbpy. The authors suggest that the origin of the higher regioselectivity is a steric interaction between the bulky phosphine ligand and the *para*-substituent on the substrate. In 2020 Itami published the borylation of strychnine, a natural product, and nifedipine, a calcium channel agonist, with a catalyst generated from [Ir(cod)OH]₂ and a related xyl-BIPHEP ligand (Figure 1.46B).[101] In the case of strychnine, olefin isomerization was also observed.
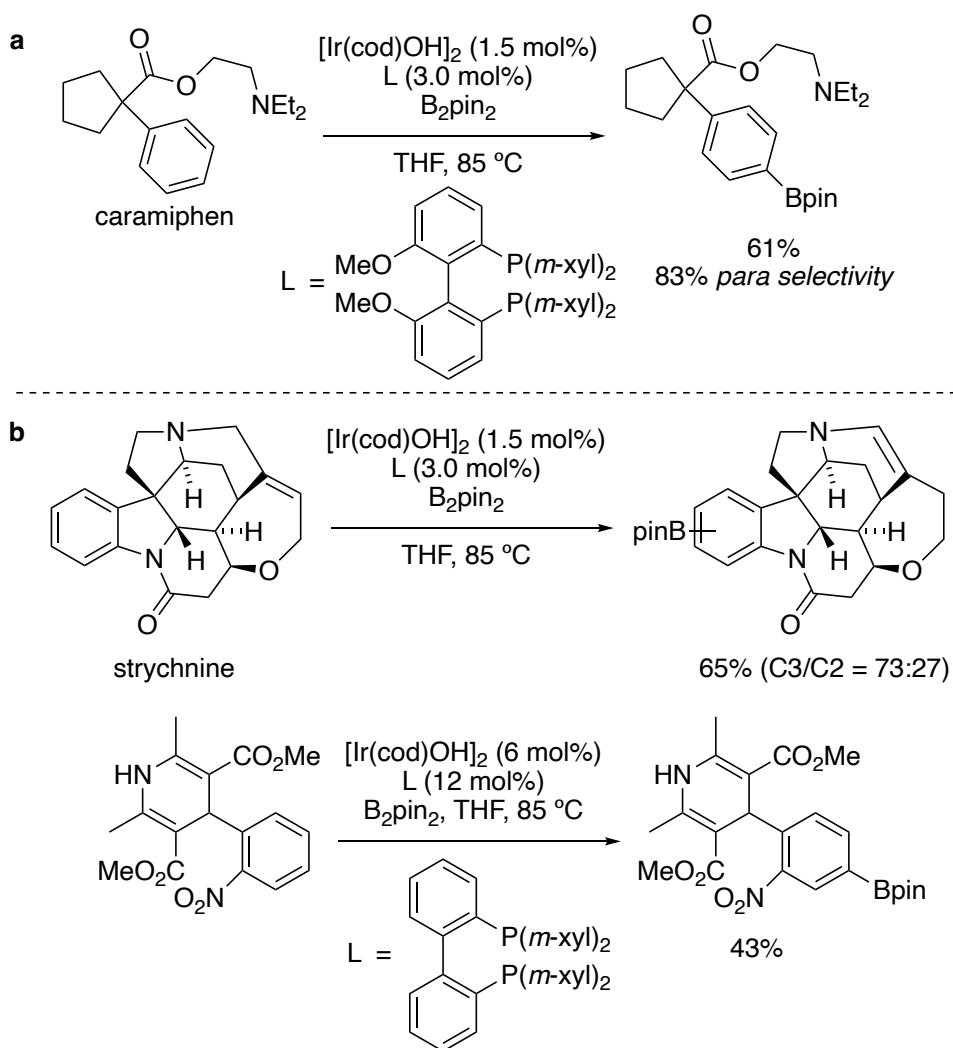
Figure 1.46. *Para*-selective C–H borylation enabled by xyl-BIPHEP ligands.

In 2022, Sunoj and Chattopadhyay published *para*-selective, iridium-catalyzed borylations of aryl C–H bonds on twisted amides catalyzed by iridium and a 4,5-diazafluorene (defa) (Figure 1.47).[102] Computational evidence suggests the intervening methylene on the ligand causes an in-plane distortion, leading to a steric interaction between the ligand and the twisted amide on the substrate. The interaction is minimized by the approach of the substrate at its *para* position. This method was applied to achieve the *para*-selective borylation of two bioactive compounds.
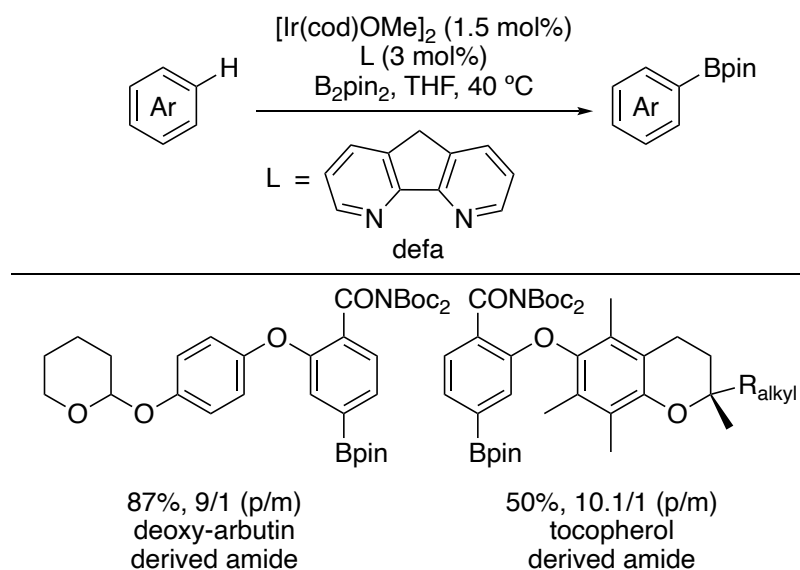
Figure 1.47. *Para*-selective C–H borylation of bioactive compounds enabled by a defa ligand.

A catalytic system formed by the combination of [Ir(cod)OMe]$_2$ and a terpyridine ligand published by Ilies in 2021 enabled C–H borylation *ortho* to fluorine in fluoroarenes.[103] Mechanistic studies suggest that the terpyridine ligand undergoes cyclometalation to generate an *N,N,C*-ligated iridium complex that may undergo reductive elimination to produce a borylated ligand. Computational studies suggested that both the cyclometalated iridium complex and the iridium complex ligated by the borylated ligand increase the energy difference between the transition states for cleavage of the *meta* and *ortho* C–H bonds over the difference with an iridium complex ligated by dtbpy. This method was applied to achieve the *ortho*-borylation of haloperidol (Figure 1.48).
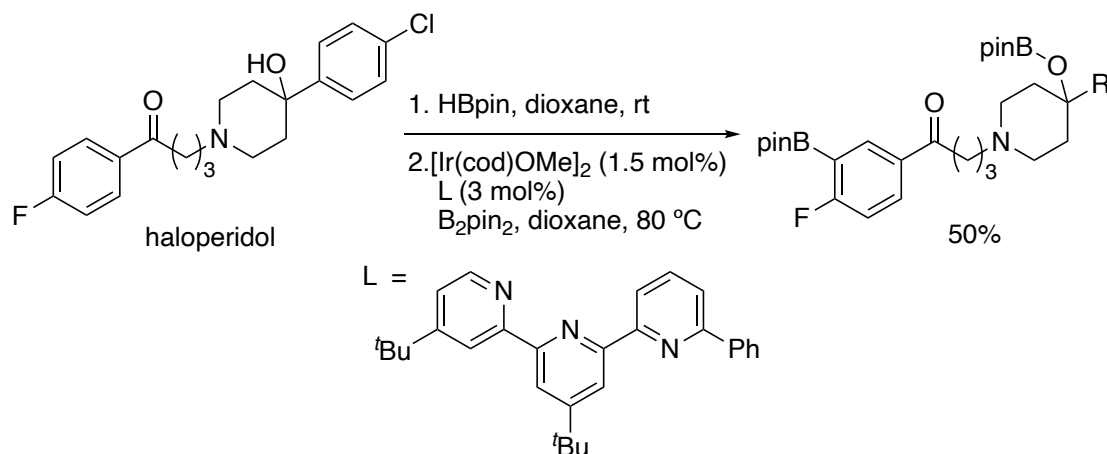
Figure 1.48. *Ortho*-selective borylation of haloperidol.

Ilies and Asaka also published a *meta*-selective borylation of C–H bonds with a catalyst generated from [Ir(cod)OMe]$_2$ and a diborylated, spriopyridine ligand.[104] Computational evidence suggests the roof-like structure of the ligand imposes a steric interaction between the *para* substituent on the substrate and the ligand that leads to a more favorable approach of the *meta*-C–H bond than of the *para*-C–H bond. This method was applied to achieve the *meta*-selective, C–H borylation of 3 active pharmaceutical ingredients (Figure 1.49).
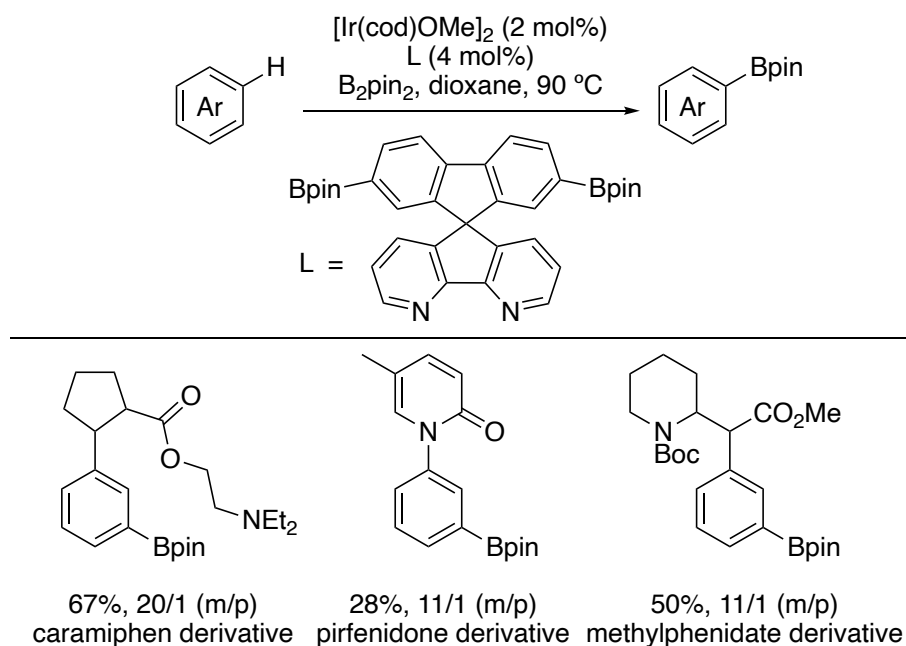
Figure 1.49 *Meta*-selective borylation of bioactive compounds enabled by a functionalized spiropyridine ligand.

In 2023, Jimenez-Oses and Mascarenas published a catalytic system generated from [Ir(cod)OMe]$_2$ and either 5-trifluormethyl-2,2'-bipyrdine or 5,5'-ditrifluormethyl-2'2'-bipyridine for the *ortho*-selective borylation of aromatic amides.[105] Calculations suggest that both complexes undergo the C–H activation step with higher *ortho*-selectivity than does the dtbpy-derived complex, due to enthalpic stabilization from a non-covalent interaction between the benzamide on the substrate and the electron-deficient ring(s) on the ligand. This system catalyzed the borylation the *ortho* position of 3 biologically relevant molecules (Figure 1.50).
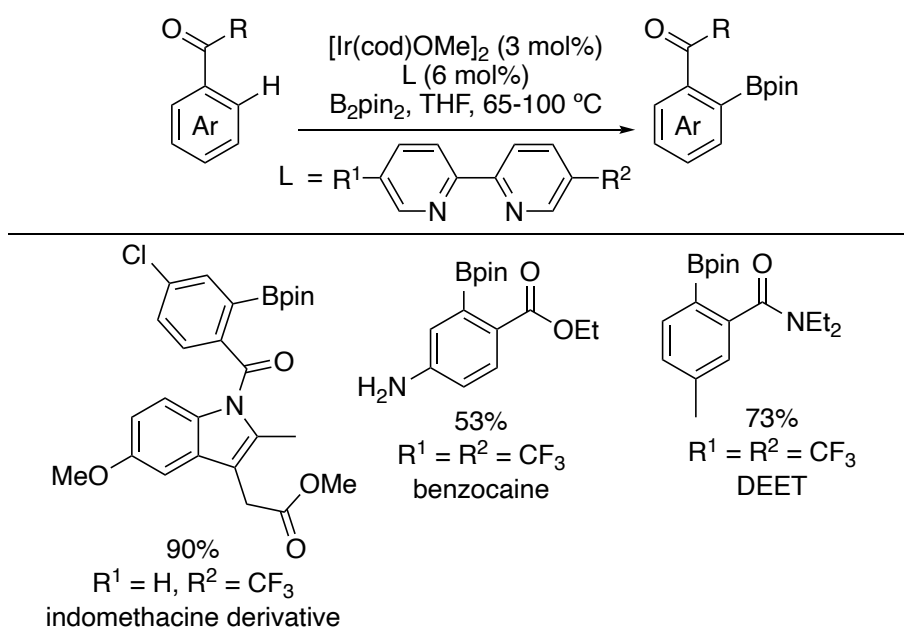
Figure 1.50. *Ortho*-selective borylation of biologically relevant molecules enabled by trifluromethyl-bipyridine ligands.

1.4.2 Late-Stage Modification of Complex Molecules by the Directed Borylation of Aryl C–H Bonds

The directed borylation of aryl C–H bonds occurs when a functional group on the substrate serves as a ligand for a transition-metal complex that activates a specific C–H bond of the substrate. Although directed functionalization often requires the installation and removal of such a functional group, these reactions can occur with regioselectivity that is complementary to that of undirected approaches, making them a valuable tool for the functionalization of complex molecules that contain many potential sites for C–H borylation.

The directed borylation of C–H bonds in complex molecules can occur under ligand-free conditions with [Ir(cod)OMe]₂ as the precatalyst. In 2020, Scott and Moss published the pyridine-directed, C–H borylation of a late-stage intermediate in the synthesis of the clinical candidate AZD9833 using [Ir(cod)OMe]₂ without added ligand (Figure 1.51A).[106] In 2022, Sunoj and Chattopadhyay showed that these ligand-free conditions are compatible with several directing groups and enable the directed borylation of aryl C–H bonds in 26 different complex molecules (Figure 1.51B).[107]
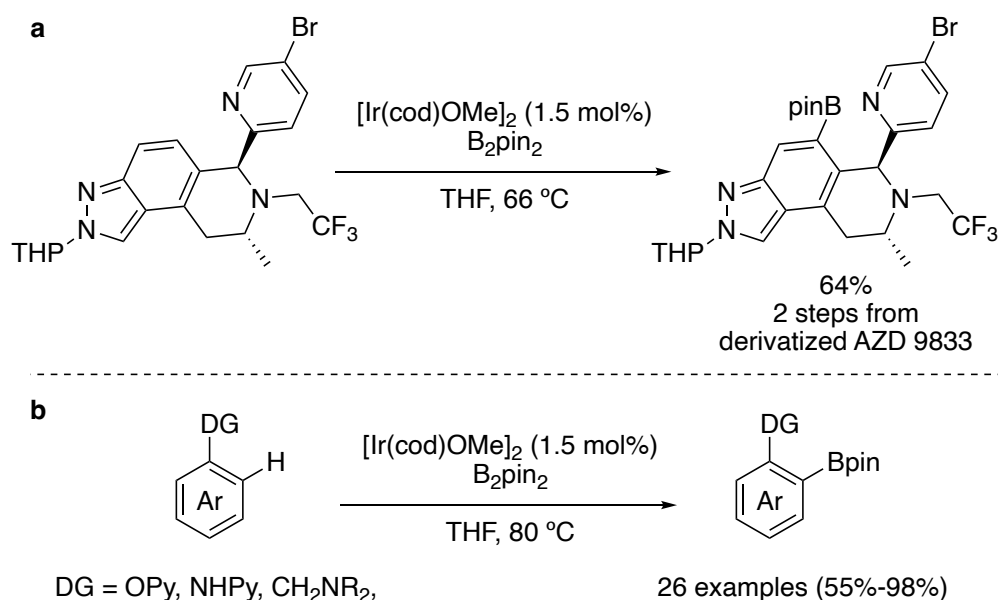
Figure 1.51. Directed C–H borylation under ligand-free conditions. (a) Pyridine-directed C–H borylation of late-stage intermediate in the synthesis of AZD9833. (b) Borylation of complex molecules using various directing groups.

Chattopadhyay has also reported that the combination of [Ir(cod)OMe]₂ and 5-methyl-2-(thiophen-3-yl) pyridine generates a complex that catalyzes the directed borylation of aryl and heteroaryl C–H bonds.[108] As part of this work, they showed six complex molecules undergo C–H borylation with various directing groups (Figure 1.52). The 5-methyl-2-(thiophen-3-yl) pyridine was shown to cyclometalate at the C2 position of the thiophene to form an *N,C*-bound, LX-type ligand, in contrast to the typical *N,N*-bound, LL-ligands used for C–H borylation.
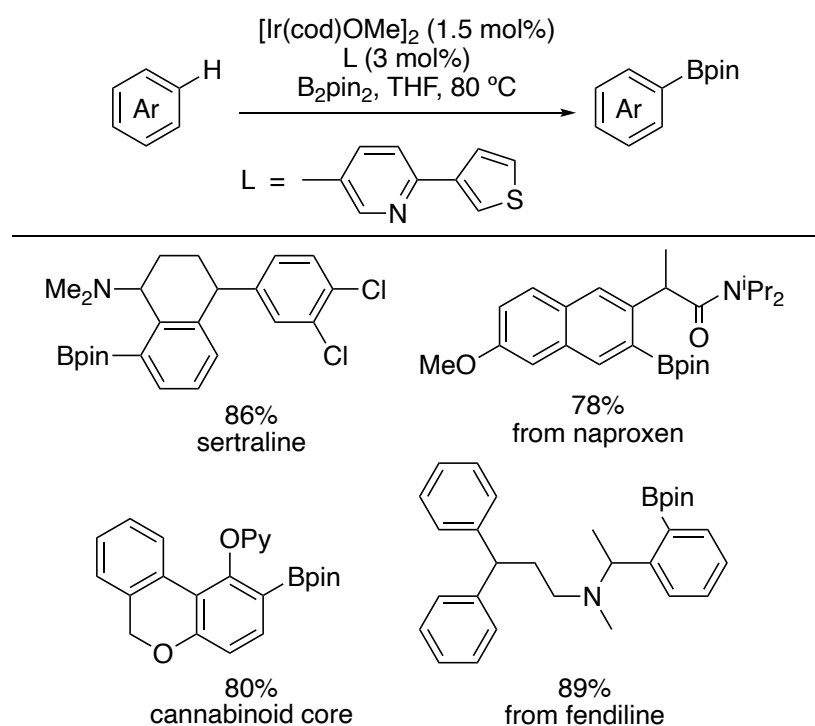
Figure 1.52. Aryl C–H borylation directed by various directing groups using an LX-type ligand system.

1.4.3 Late-Stage Modification of Complex Molecules by the Undirected Borylation of Alkyl C–H Bonds

The development of methods for the practical, catalytic, and selective functionalization of alkyl C–H bonds without the use of directing group is a longstanding goal of synthetic chemistry. The undirected borylation of alkyl C–H bonds is particularly valuable because the application of such methods in the late-stage diversification of complex molecules could potentially enable the installment of a wide array of functionalities in previously inaccessible positions.

There is one example of the application of transition-metal catalyzed, undirected borylation of alkyl C–H bonds that has been applied to a complex molecule. In 2020, our laboratory published the undirected borylation of a primary C–H bond on protected dehydroabietic acid with a catalyst generated from [Ir(cod)OMe]$_2$ and 2-methyl-1,10-phenanthroline (Figure 1.53).[109]
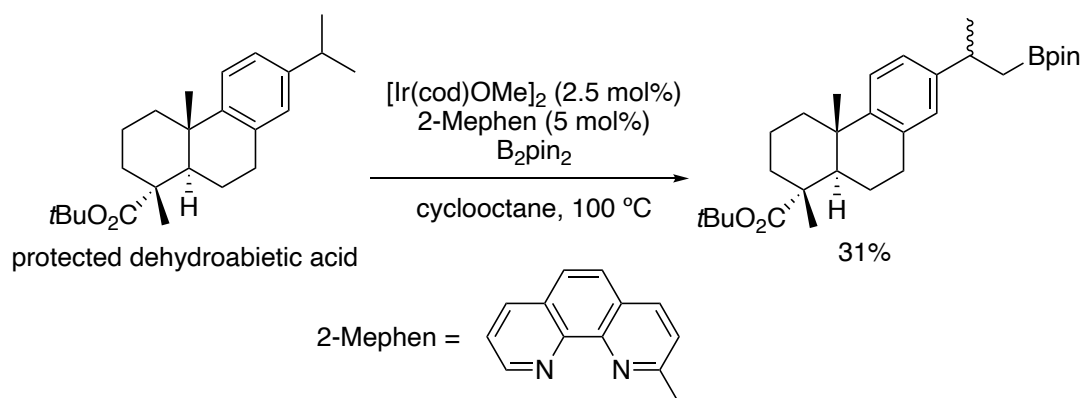
Figure 1.53. The undirected borylation of a primary C–H bond in protected dehydroabietic acid.

1.4.4 Late-Stage Modification of Complex Molecules by the Directed Borylation of Alkyl C–H Bonds

The directed borylation of alkyl C–H bonds is more developed than the undirected borylation of alkyl C–H bonds. Directed approaches can control the site-selectivity of the borylation. Systems that have been applied to the directed borylation of alkyl C–H bonds in complex molecules are based on both palladium and iridium. In this section, examples with palladium systems will be reviewed first, followed by examples with iridium systems.

In 2014, Shi reported the borylation of primary, alkyl C–H bonds with $Pd(OAc)_2$ as precatalyst, diisopropyl sulfide as ligand, and oxygen as the terminal oxidant.[110] A picolinyl directing group was installed on an amine to direct the C–H functionalization. The method was applied to the borylation of 6 amino acids and a derivative of estrone (Figure 1.54). All complex molecules underwent borylation at a C–H bond γ to the directing group.
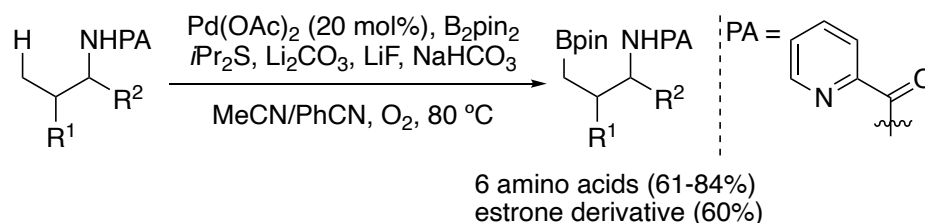
Figure 1.54. Pd-catalyzed borylation of C–H bonds γ to a picolinyl directing group on complex molecules.

In 2021, Ge and Maiti used a picolinyl directing group to achieve the borylation of primary, alkyl C–H bonds δ to the directing group with a catalyst generated from $Pd(OAc)_2$ and 2-hydroxy-6-methylpyridine.[111] These reactions required the γ position of the substrates to be a quaternary center to avoid C–H functionalization at the γ position. This method was applied to three substrates with natural products appended (Figure 1.55).
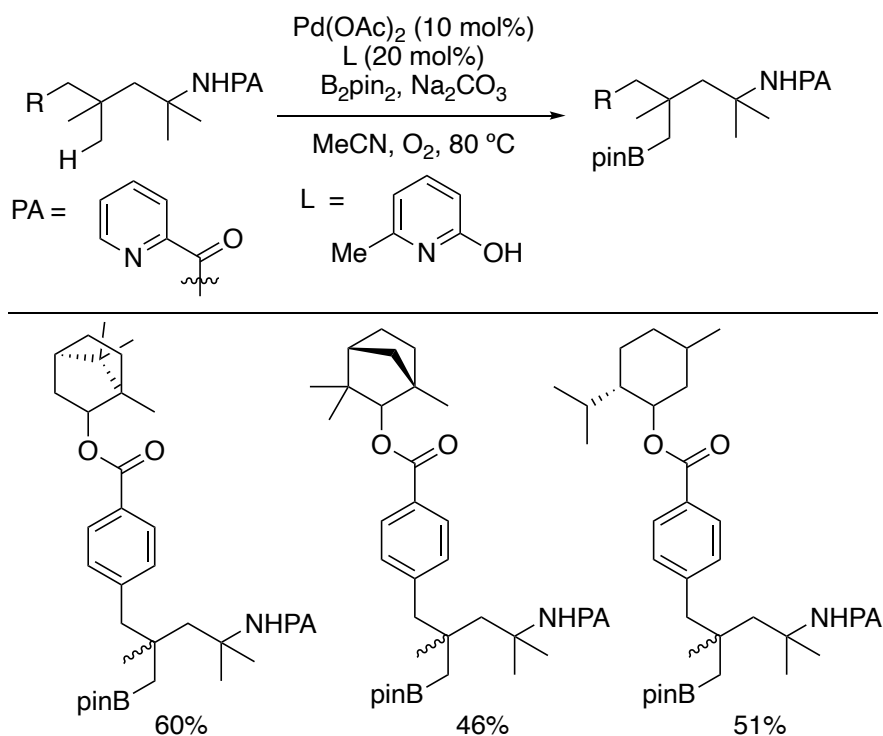
Figure 1.55. Pd-catalyzed borylation of C–H bonds δ to a picolinyl directing group on complex molecules.

Yu showed that a fluorinated, *N*-aryl amide could act as a directing group for the borylation of primary C–H bonds β to the directing amide.[112] A complex generated from Pd(OAc)$_2$ and 2,4-dimethoxyquinoline catalyzed the C–H borylation of a dehydroabietic acid derivative with the fluorinated, *N*-aryl amide directing group appended (Figure 1.56).
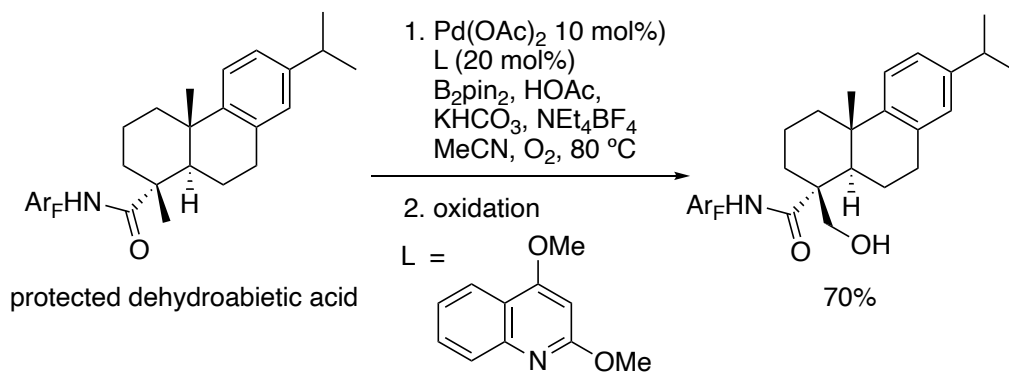
Figure 1.56. Pd-catalyzed borylation of C–H bonds β to an amide directing group on a dehydroabietic acid derivative.

Iridium-catalyzed examples of directed borylation of alkyl C–H bonds on complex molecules have been reported by Xu with a series of chiral, diamino-silylborane ligands that exhibit bidentate, *B,N* binding. These ligands will be reviewed below. Directed reactions with such ligands are successful due to the generation of a chiral, trisboryl iridium complex with two open coordination sites that can bind the directing group and differentiate two prochiral C–H bonds.

Their publication in 2019 disclosed a system generated from [Ir(cod)Cl]₂ and a diamino-boryl ligand with pyridine substitution on one amino group and biaryl substitution on the other that catalyzed an amide-directed borylation of alkyl C–H bonds of cyclopropanes.[113] The catalytic system was applied to the catalyst-controlled, diastereoselective borylation of C–H bonds on cyclopropane rings appended to estradiol and cinacalcet (Figure 1.57).
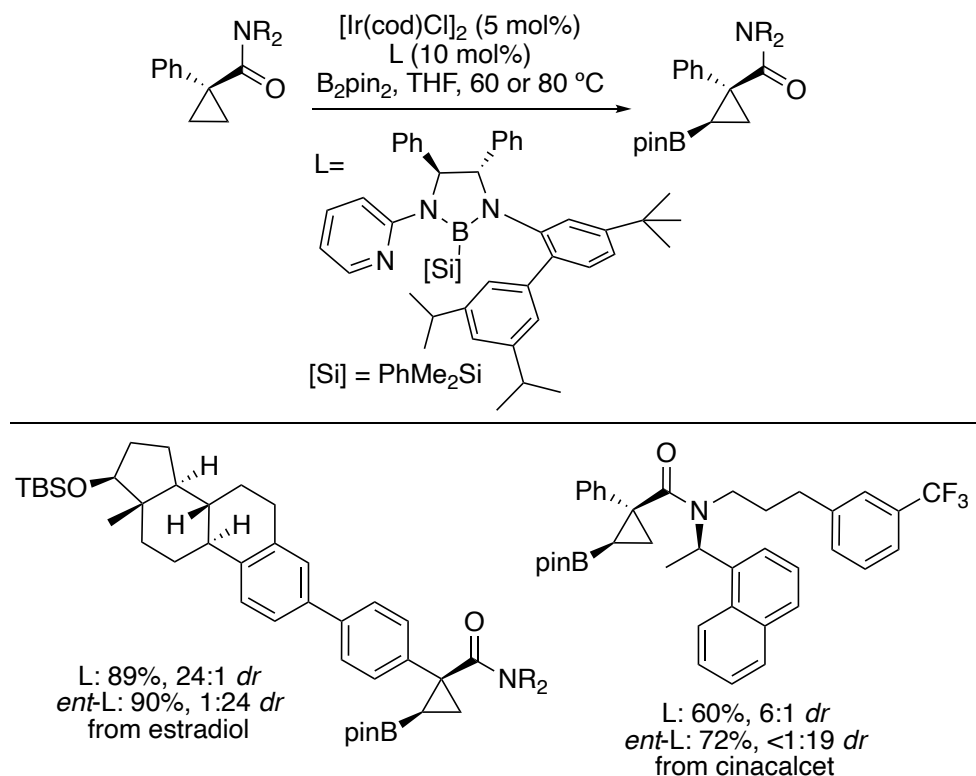
Figure 1.57. Diastereoselective, amide-directed borylation of cyclopropanes with a chiral boryl ligand.

With the same iridium precatalyst and a ligand with a triaryl-substituted pyridine moiety on one amino group and a 2-adamantyl-phenyl substituent on the other, the amide-directed borylation of C–H bonds on cyclopropanols was achieved.[114] Xu and coworkers appended three bioactive molecules to cyclopropanol substrates to exemplify the application of this method in late-stage borylation (Figure 1.58).
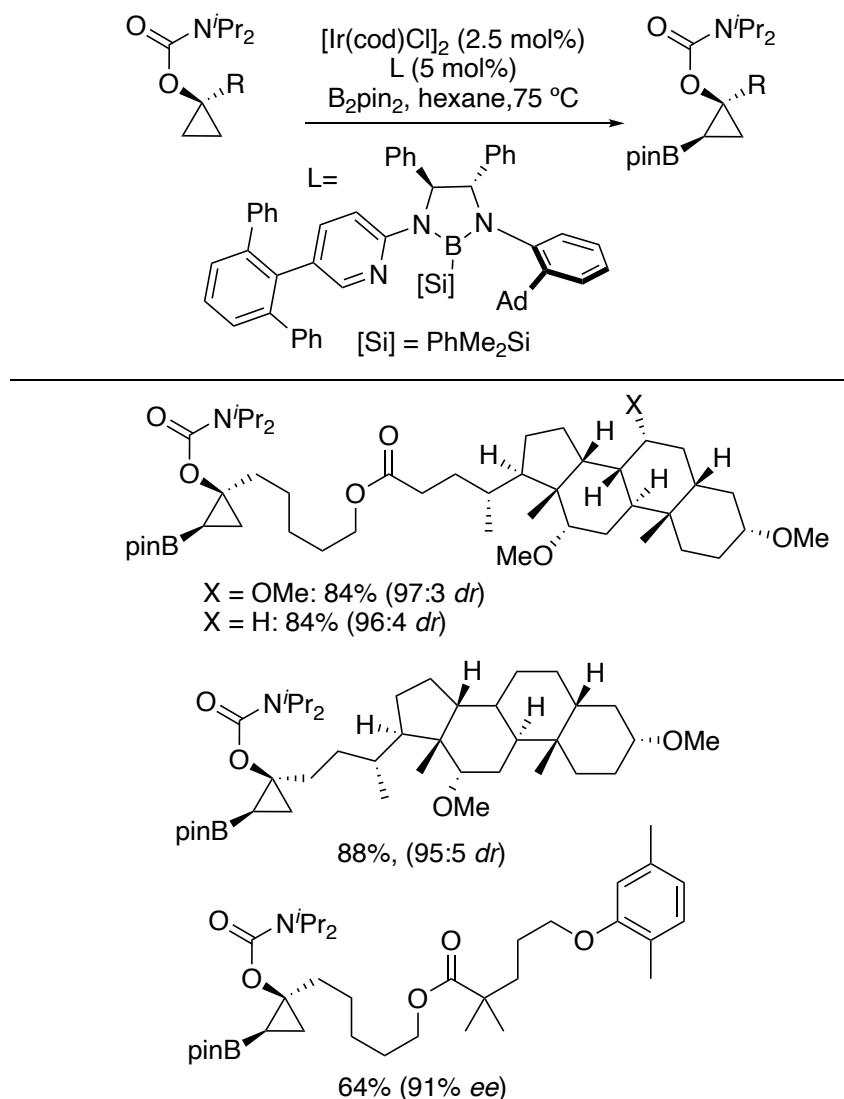
Figure 1.58. Stereoselective, carbamate-directed borylation of cyclopropanols with a chiral boryl ligand.

Xu reported the same catalytic system for the enantioselective borylation of acyclic amides at C–H bonds β to the directing amide.[115] The method was applied to the enantioselective borylation of β-C–H bonds in three fatty acid-derived acyclic amides (Figure 1.59). Such an application exemplifies a valuable method for the conversion of cheap and abundant carboxylic acids to value-added chemicals.
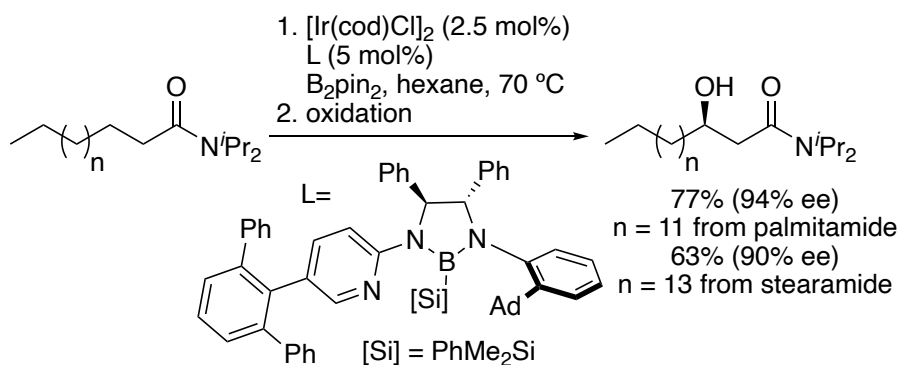
Figure 1.59. Enantioselective, amide-directed borylation of fatty acids with a chiral boryl ligand.

The stereoselective borylation of C–H bonds on carbocycles and azacycles beta to the carbonyl carbon center of amides was reported by Xu in 2020 with a catalyst generated from [Ir(cod)OMe]$_2$ and a ligand with a triaryl-substituted pyridine moiety on one amino group and either 2-cyclohexyl-phenyl substitution or 2,6-diethyl-phenyl substitution on the other.[116] This method was applied to the diastereoselective borylation of C–H bonds in saturated rings on 6 complex molecule-derived substrates (Figure 1.60).
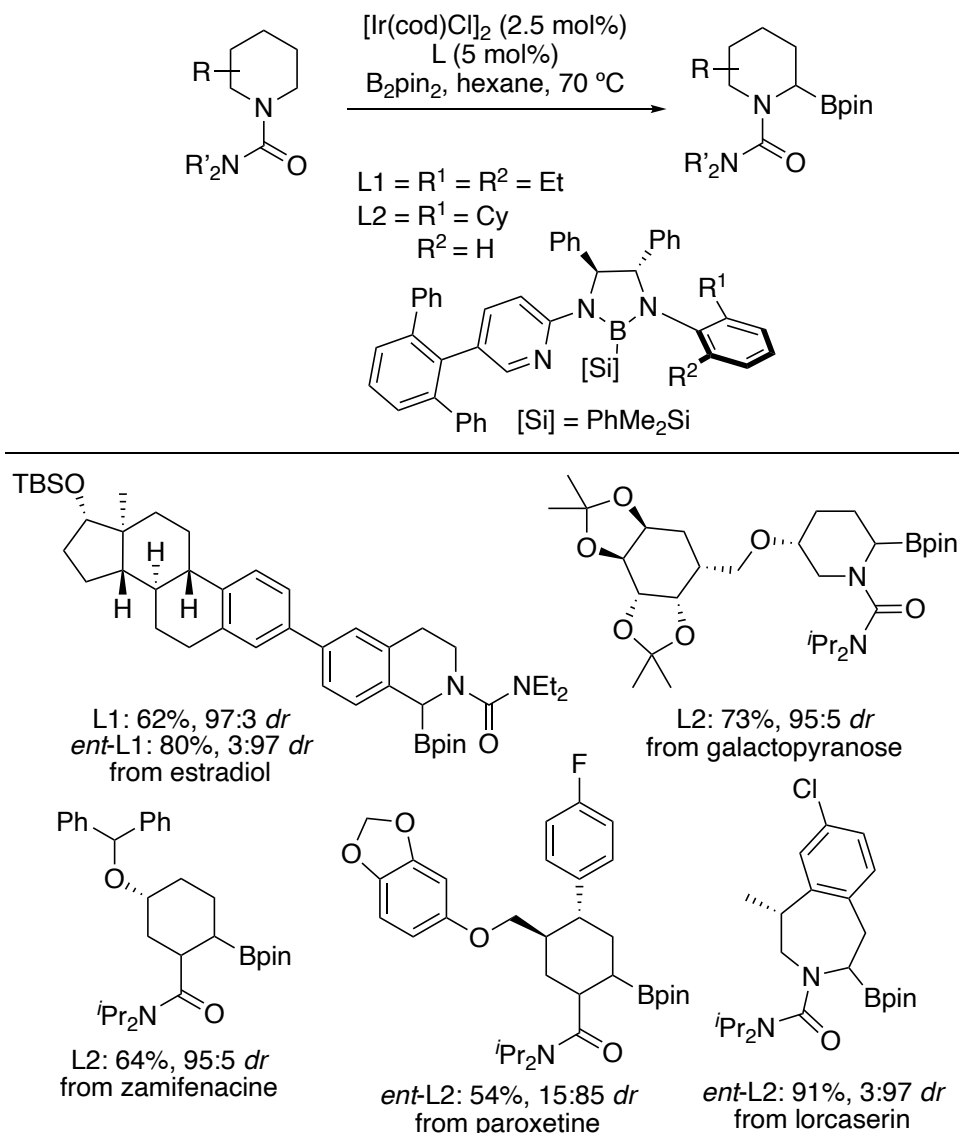
Figure 1.60. Diastereoselective, amide-directed borylation of C–H bonds on carbocycles and azacycles with a chiral boryl ligand.

The stereoselective borylation of C–H bonds b to a directing nitrogen center also was achieved by a catalyst generated from [Ir(cod)OMe]₂ and a ligand with pyridine substitution on one amino group and 2,4,6-tricyclohexylphenyl substitution on the other.[117] The method was applied to the borylation of cholic and deoxycholic acid substituted with a pyrazole group (Figure 1.61).
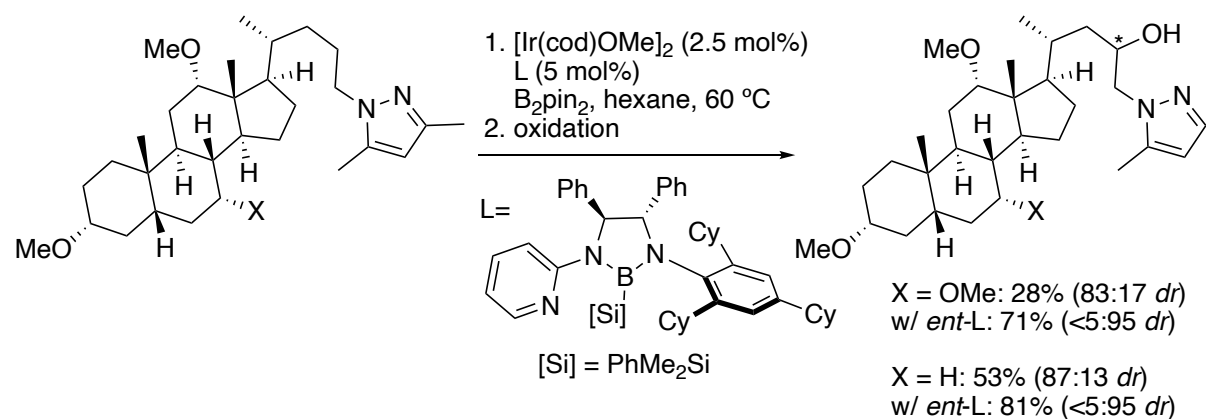
Figure 1.61. Diastereoselective, pyrazole-directed borylation of complex molecule derivatives with a chiral boryl ligand.

In 2022, Xe and Ke published an amide-directed strategy for the dual borylation of ferrocenes at an alkyl and an aryl C–H bond.[118] This reaction is described here because the ligand framework for these reactions is the same as the others in this section for the directed borylation of alkyl C–H bonds. This transformation was achieved with a catalyst generated from [Ir(cod)Cl]₂ and a ligand containing a 4-phenylpyridine moiety on one amino group and 2-aryl-5-methylphenyl substitution on the other. The authors appended three complex molecules to the ferrocene core and conducted the C–H borylation reaction to exemplify the use of this method on ferrocene-labeled complex molecules (Figure 1.62).
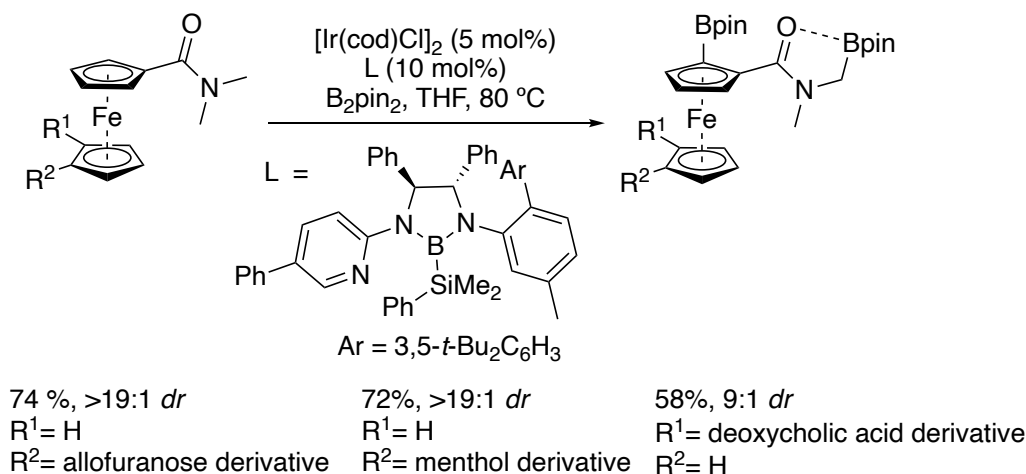
Figure 1.62. Amide-directed, dual alkyl-aryl borylation of complex molecule-derived ferrocenes.

1.5 Transition-Metal Catalyzed, Borylation of C–H Bonds in the Synthesis of Organic Materials

The borylation of C–H bonds catalyzed by transition metal catalysts has been applied extensively to the synthesis of molecules or polymers for applications in materials science, often toward molecules with valuable photophysical properties. Molecules with valuable photophysical properties are often rich in aromatic units, making the borylation of C–H bonds particularly valuable for the modification of these structures. Moreover, transition metal-catalyzed borylations of C–H bonds typically occur at less sterically encumbered positions and with a bias towards electron poor C–H bonds, and this selectivity is complementary to that of methods occurring through electrophilic aromatic substitution. The resultant boronic esters are versatile chemical handles that can be transformed into the desired functional group or substituent.

The distinction between applications in which the borylation has been used to synthesize valuable building blocks and those in which the borylation is used to introduce modifications at a "late-stage" is not always clear. For instance, in 2011 Yamaguchi showed that the borylation of tetrabromobiphenyl occurs cleanly and allows for elaboration of the biphenyl core and ultimately the synthesis of π-extended bis(phosphoryl)biphenyls (**Error! Reference source not found.**)[119] On the other hand, Marder's 2020 synthesis of emissive materials containing biphenyl cores was achieved by using the borylation of simple arenes to generate *meta*-substituted boronic esters that were homocoupled to afford biphenyls and subsequently elaborated to the desired borafluorenes (Figure 1.63).[120] Likewise, Marder used the borylation of dimethoxybenzene during the synthesis of complex donor-acceptor triarylboranes that display thermally-activated delayed fluorescence (TADF). This borylation of a simple arene was used to install the central boron atom (Figure 1.64).[121] They also showed that the borylation of a triarylborane occurs selectively on the less-hindered, electron-poor acceptor fragment to afford modified triarylboranes that display solvent-dependent emission spectra (Figure 1.64).[122] Thus, we have organized the examples of the borylation used to prepare organic materials in this section by structure type and only briefly address whether the borylation reaction was applied to prepare a "building block" or to conduct a "peripheral modification" at the "late stage" of the synthesis of a complex material.
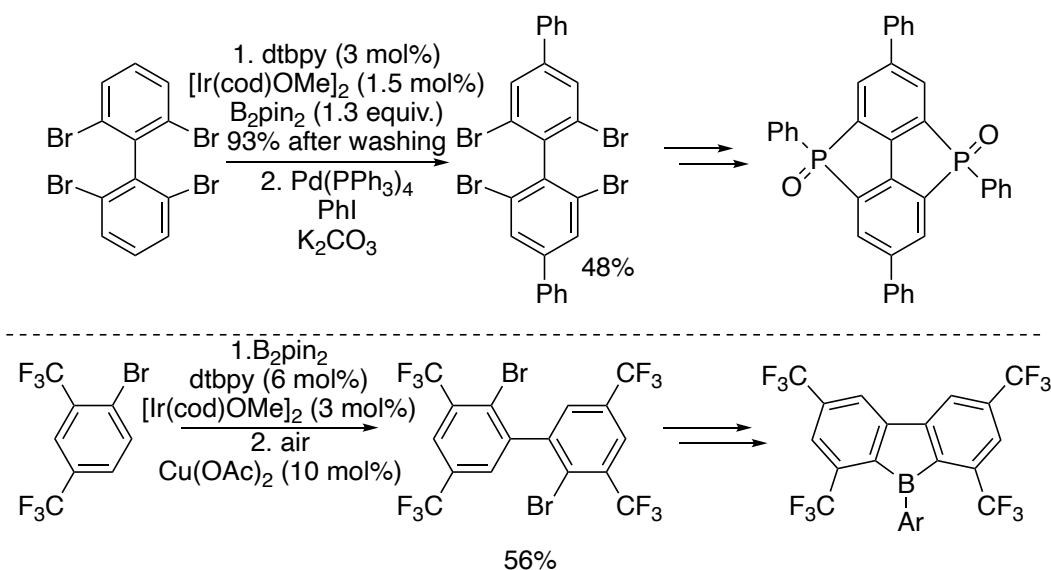
Figure 1.63. Ir-catalyzed borylation of biphenyls and the preparation of biphenyls by homocoupling of arylboronic esters prepared by the borylation of arenes.
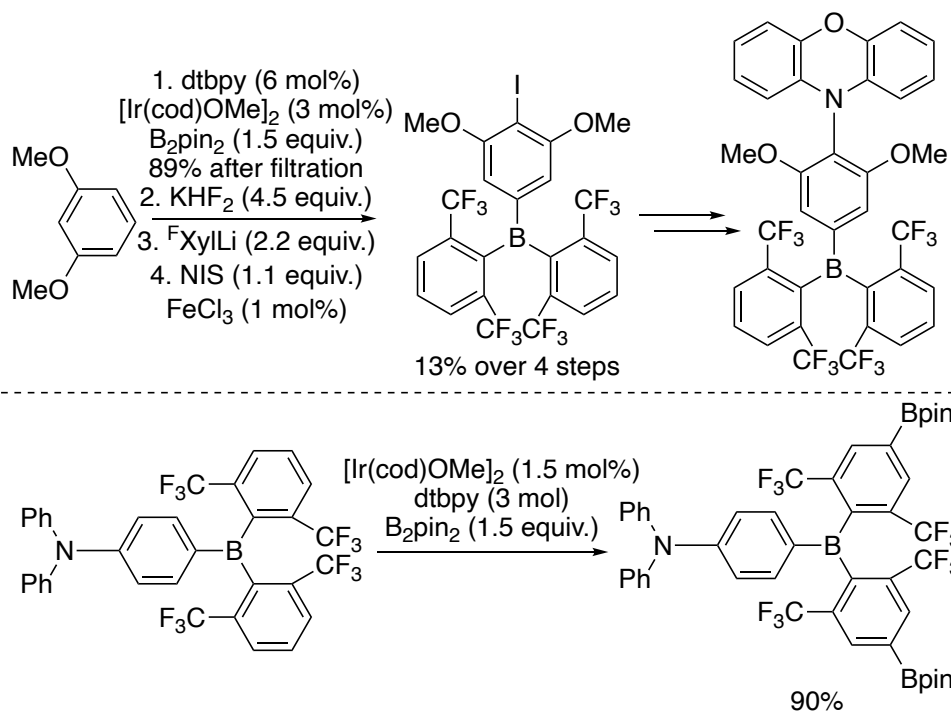
Figure 1.64. Ir-catalyzed, *meta*-selective borylation of and in the synthesis of triarylboranes.

1.5.1 Transition-metal-catalyzed borylation of aryl C–H bonds for the synthesis and modification of polyaromatic hydrocarbons

In 2003 Sugihara reported that the borylation of azulene occurs with good selectivity for the five-membered ring, with 2-borylated azulene being the major product and 1-borylated azulene being the minor product (Figure 1.65). The authors proposed that the selectivity arises from π-complexation of the substrate to the iridium center prior to borylation.[123] It is also possible that the more acute bond angles in five-membered rings cause the distances between the hydrogen atoms to be longer than those in seven-membered rings and the steric hindrance in five-

membered rings to be less, thereby accounting for the observed selectivity. Under more forcing conditions, polyborylation occurred to afford a mixture of products.[124] On the other hand, in 2015, Scott showed that under conditions that facilitate reversible borylation, polyborylation of azulene converges to 1,3,5,7-tetraborylazuluene.[125] This building block was later applied to the synthesis of a hole transporting material (Figure 1.65).[126]

In 2011 and 2017, Kobayashi reported the di-, tri-, and tetra- borylation of anthracenes (Figure 1.66).[127, 128] The borylation of the 2-position is favored over that of the 1-position. Despite this steric preference, efforts to produce polyboryl compounds resulted in statistical mixtures because the A and C rings reacted independent of one another.
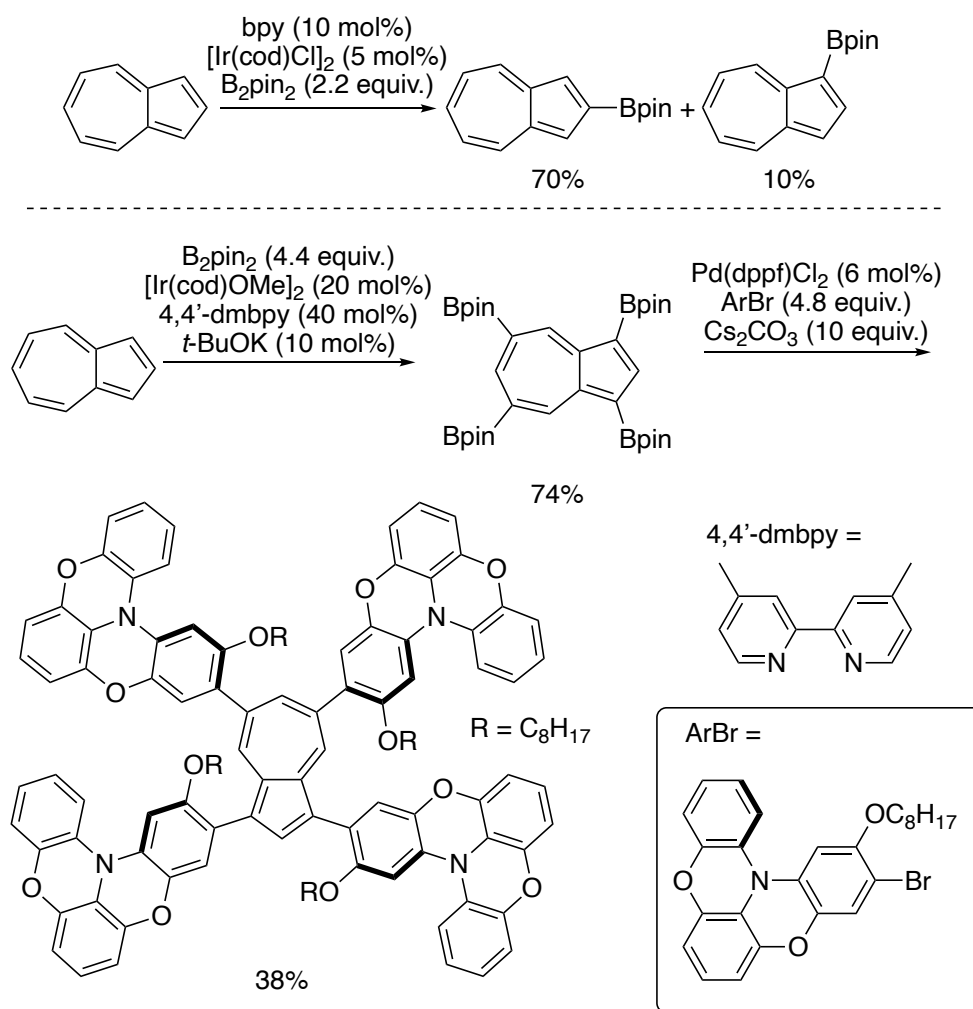
Figure 1.65. Ir-catalyzed borylation of azulenes.

46
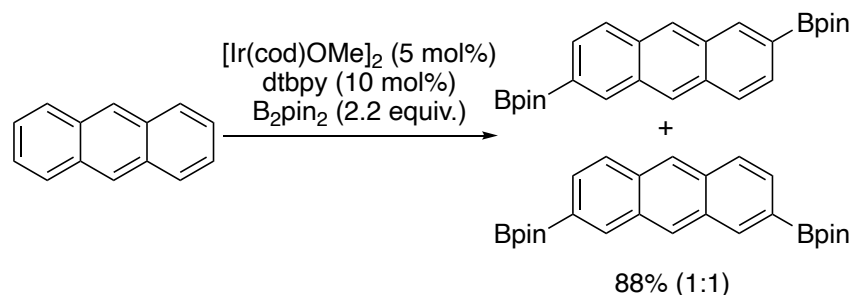
Figure 1.66. Ir-catalyzed borylation of anthracene.

In the same vein, in 2009, Kobayashi reported that the borylation of tetracenes resulted in a 1:1 mixture of 2,8- and 2,9-diborylated products (Figure 1.67). These borylated materials served as valuable building blocks for the synthesis of π-extended tetracenes applied to create organic field-effect transistors (OFETs).[129] Isobe reported the borylation of phenacenes for the modification of single walled carbon nanotubes (SWNTs). Borylation occurs at the edge positions (2-, 3-, 6-, 7- for *n*=3, 2-, 3-, 8-, 9- for *n*=4, 5) with essentially statistical preference. Shown in **Error! Reference source not found.** are the "linear" isomers.[130]

Chemists have had a longstanding interest in pyrenes as chromophores, fluorescent probes, and for organic semiconductor applications.[131] Marder has reported the borylation of pyrene and perylene.[132-134] The borylation of pyrenes occurred with good selectivity at the 2- and 7-positions (Figure 1.68). Under more forcing conditions, borylation also occurred at the 4-position. Yamada and Aratani have reported the borylation of terylene and quaterrylenes (Figure 1.68).[135] (n = 0 = perylene, n = 1 = terylene, n = 2 = quaterrylene)
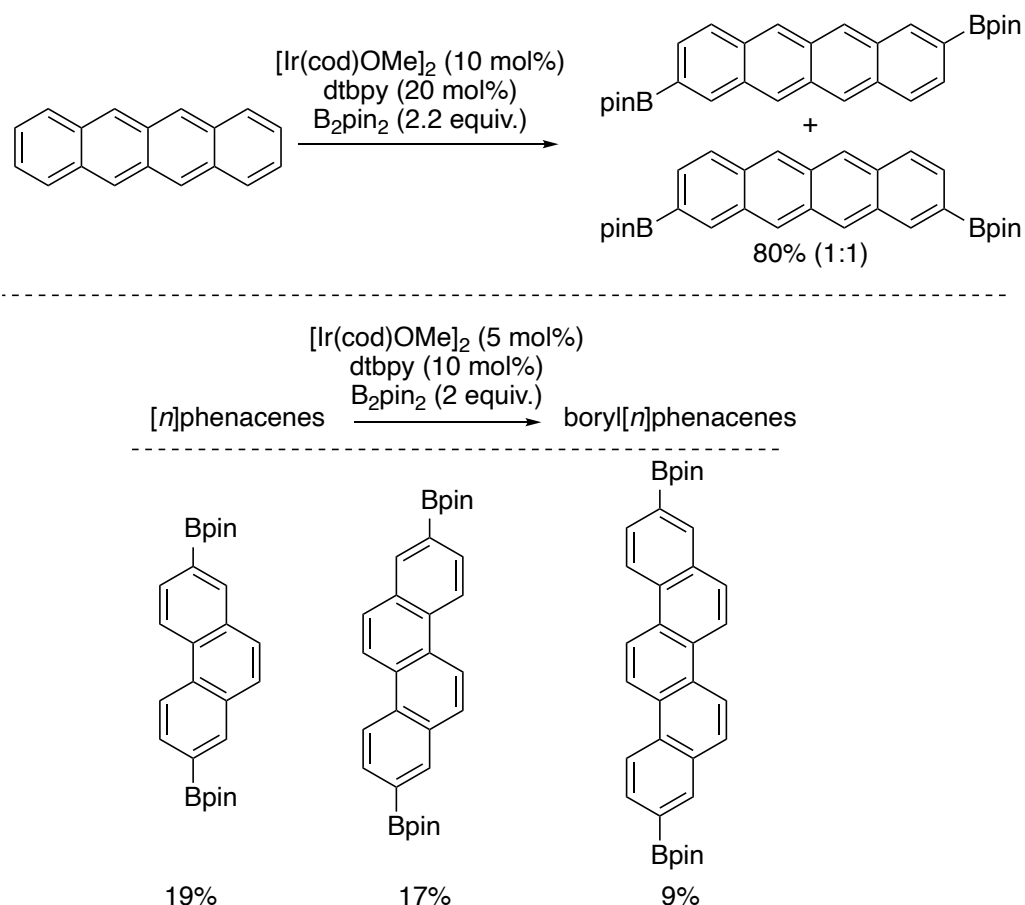
Figure 1.67. Ir-catalyzed borylation of tetracenes and [*n*]-phenacenes.
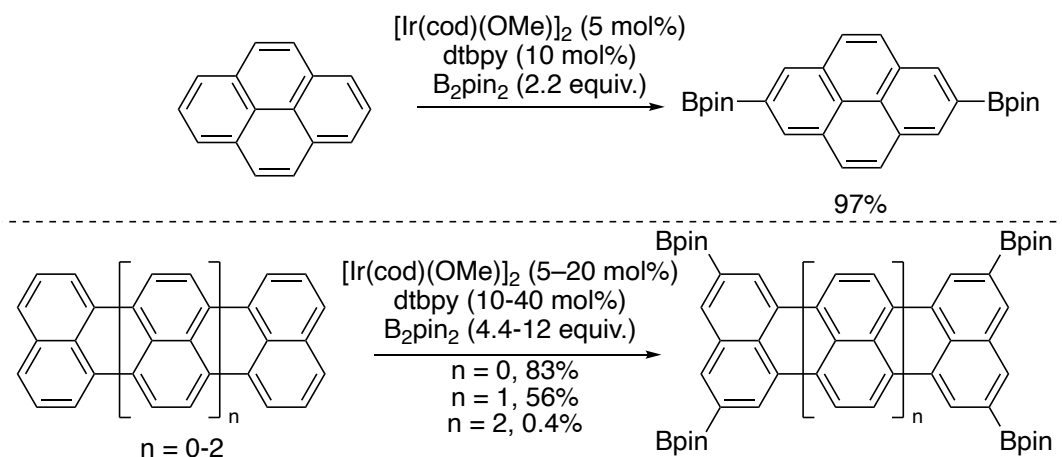
Figure 1.68. Ir-catalyzed borylation of pyrenes, terylenes, and terrylenes.

Mastalertz reported a route to a variety of soluble perylenes that hinges on the regioselective diborylation of a dihydroanthracene. Subsequent Suzuki-Miyaura cross-coupling and cyclization led to the desired perylenes (Figure 1.69).[136] Lin used the borylation of anthraquinone and subsequent oxidation to install the desired alkoxy substituents in their synthesis of highly electron deficient perylene polynitriles (Figure 1.69).[137]

Perylenediimides (PDIs) are valuable chromophores for applications in dye chemistry and organic materials. Traditionally, elaboration of the perylenediimide core has been achieved by halogenation and subsequent downstream functionalization of the 1,6,7, and 12 "bay positions", which tend to twist the ring out of planarity.[138] In 2011, Shinobuko and Müllen disclosed that the iridium- and ruthenium-catalyzed borylations of PDIs occur at the 2,5,8, and 11 "ortho positions" and that subsequent functionalization preserves the planarity of the PDI (Figure 1.70).[139, 140] These building blocks have since enabled the synthesis of π-extended PDIs,[141] including corannulene-decorated PDIs capable of serving as sensors of C_{60}[142] and PDI dimers.[143] The borylation of a nitrogen-bridged naphthalene monoimide dimer also occurred at the position *ortho-* to the amide carbonyl.[144]
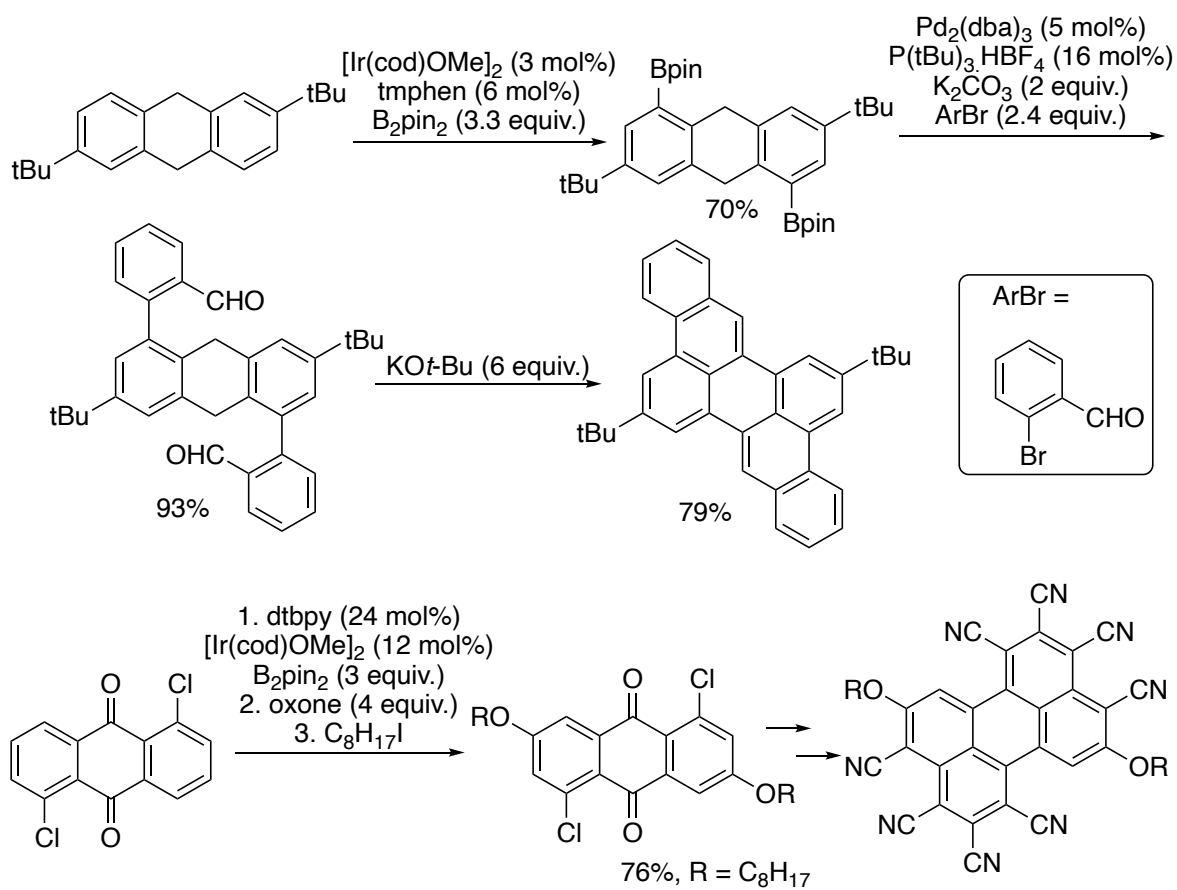
Figure 1.69. Ir-catalyzed borylation of anthracenes and anthraquinones in the synthesis of perylenes.
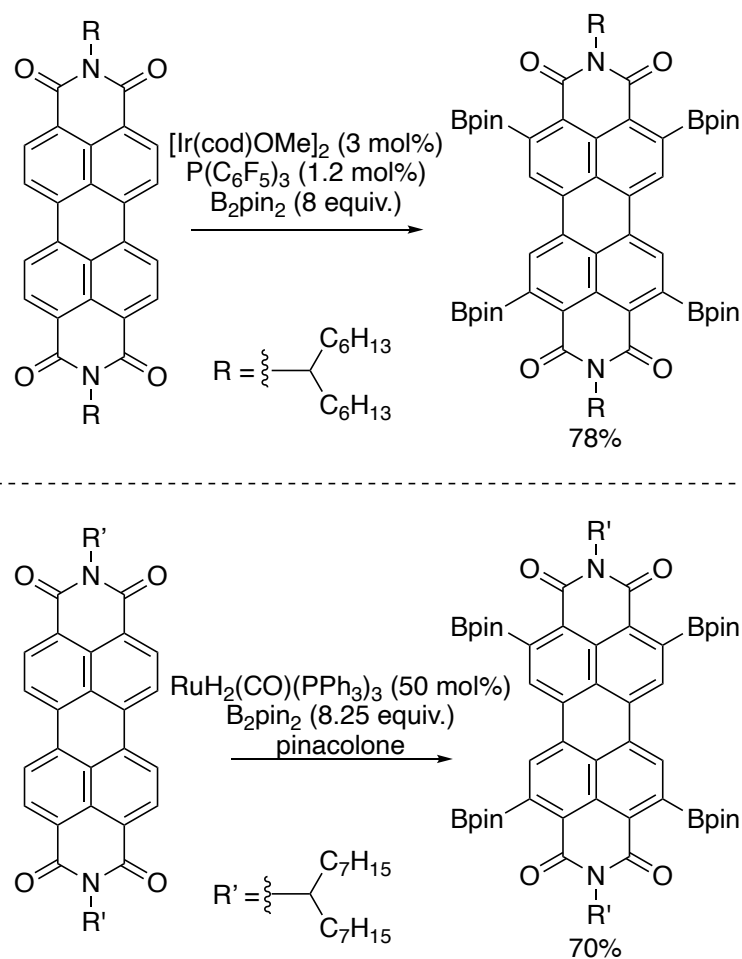
Figure 1.70. Ir-catalyzed and Ru-catalyzed borylation of perylenedimides.

Nečas reported that [4]helicenes and [5]helicenes undergo borylation with regioselectivities controlled by the steric hinderance imparted by the ring on the other end of the molecule in the helical structures (Figure 1.71). The boronic ester products were oxidized to the corresponding alcohols or used in Suzuki-Miyuara cross-coupling reactions.[145, 146] In 2016, Matsuda reported the triple borylation and subsequent cross-coupling of triazatriangulene cations for the late-stage tuning of their emissive properties (Figure 1.71).[147] Lacour further reported that triple borylation of cationic [4]helicenes occur on the periphery and allow for modular modification of these dyes.[148]
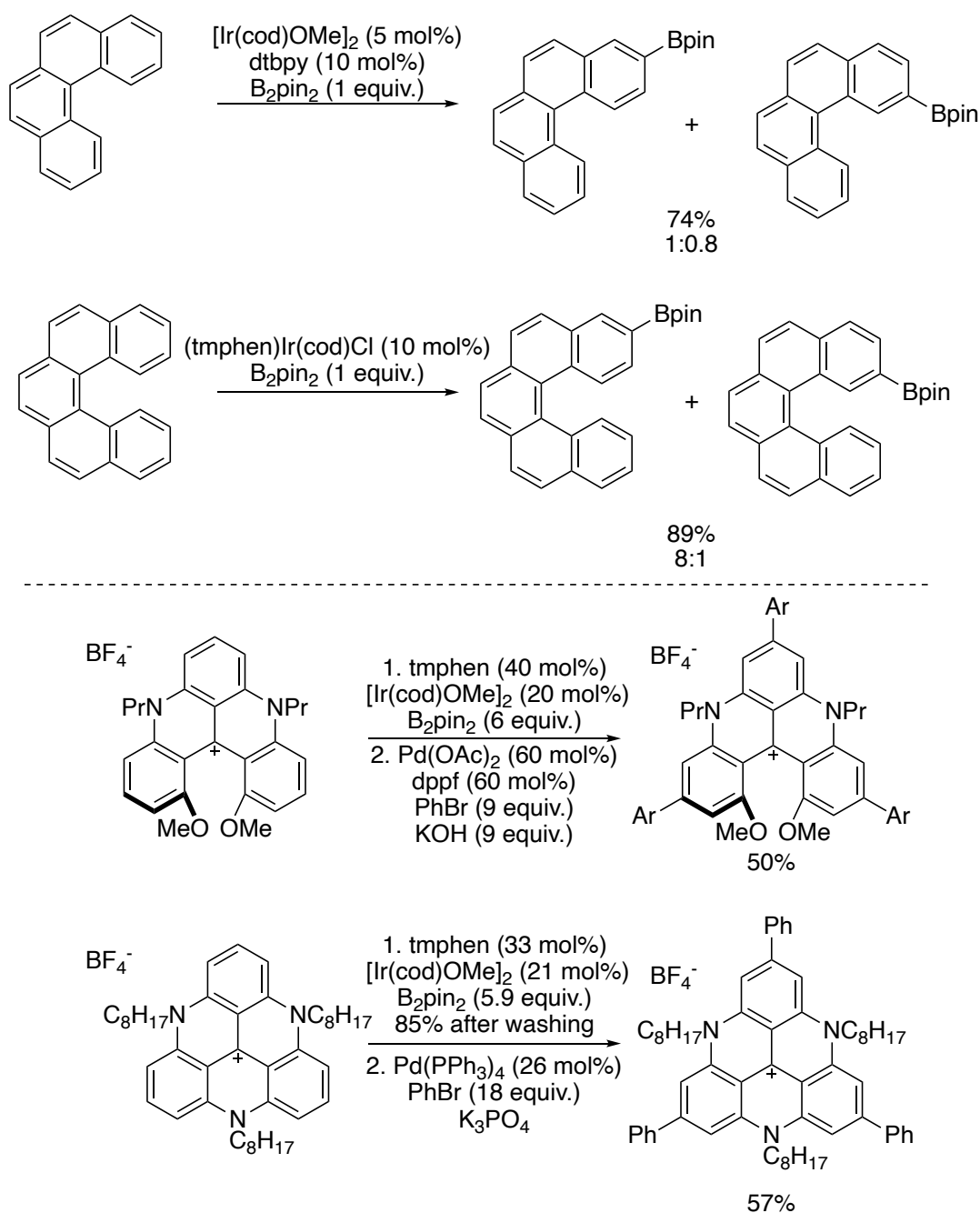
Figure 1.71. Ir-catalyzed borylation of helicenes and triangulene cations.

Iridium-catalyzed borylation has been leveraged further as a synthetic method to construct graphene nanostructures. This strategy is especially powerful for the modification of symmetric structures. In 2018 Sisto reported that triptycene undergoes triple borylation to form a mixture of isomers from a single borylation at each of the three aryl rings (Figure 1.72). The mixture was used directly for a sequence consistenting of cross-coupling and oxidative cyclization to form threefold-symmetric graphene nanoribbons, which were used as the electron-extraction layer in perovskite solar cells. The spoke-like structure is postulated to facilitate interlayer penetration and to lower the contact resistance.[149]
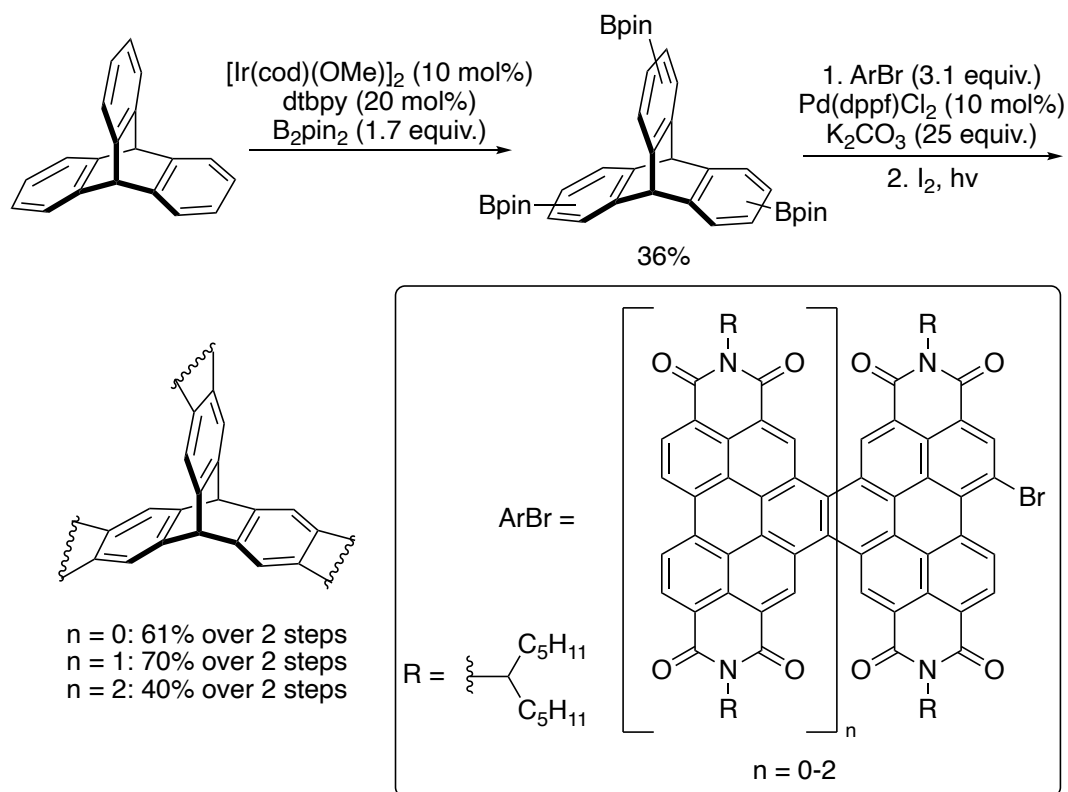
Figure 1.72. Ir-catalyzed borylation of triptycene.

In 2012 and 2013, Scott and Itami reported conditions for the clean and efficient synthesis of five-fold borylated corannulene,[150, 151] and Nozaki reported the five-fold borylation of azapentabenzocorannulenes in 2018.[152] Subsequent cross-coupling and dehydrocoupling led to highly warped graphene nanosheets (Figure 1.73). These warped nanographenes (WNGs) display solubilities and photophysical properties that differ from those of traditional nanographenes, presumably due to differences in crystal packing. Electronic umpolung to access the corresponding pentabromo or pentaiodo derivatives from the pentaboryl corannulene has also been reported.[153] Further regioselective borylation of these WNGs resulted in modification of the periphery.[154, 155]
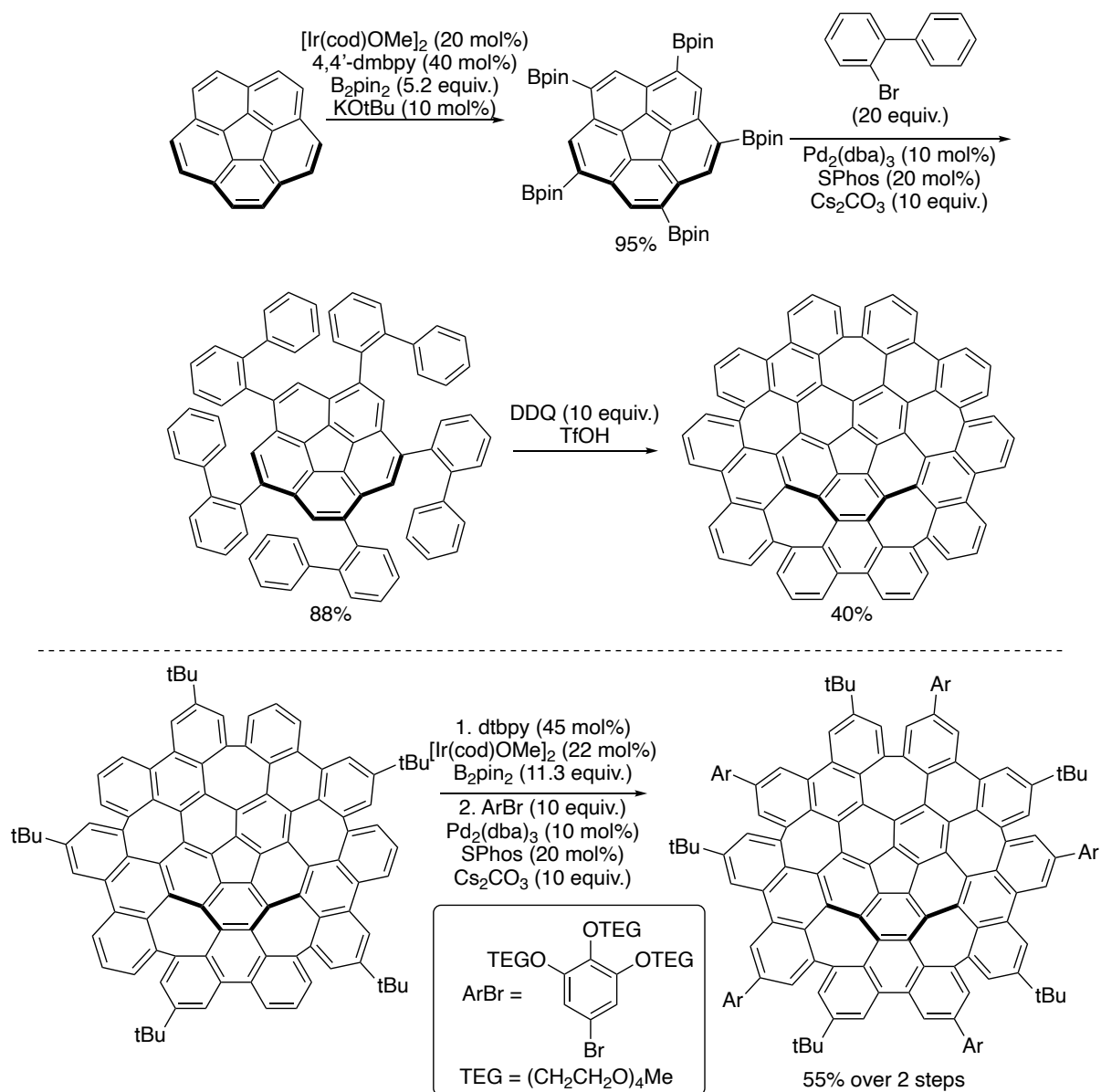
Figure 1.73. Ir-catalyzed five-fold borylation of [5]-circulene and subsequent elaboration to bowl-shaped nanographenes.

Whereas [5]circulenes possess a bowl-shaped topology, [6]circulenes are planar or nearly planar. Nuckolls reported the synthesis of various thiophene boronic esters and applied them to the synthesis of dibenzotetrathienocoronenes, which display solvent dependent structural behavior (Figure 1.74).[156]
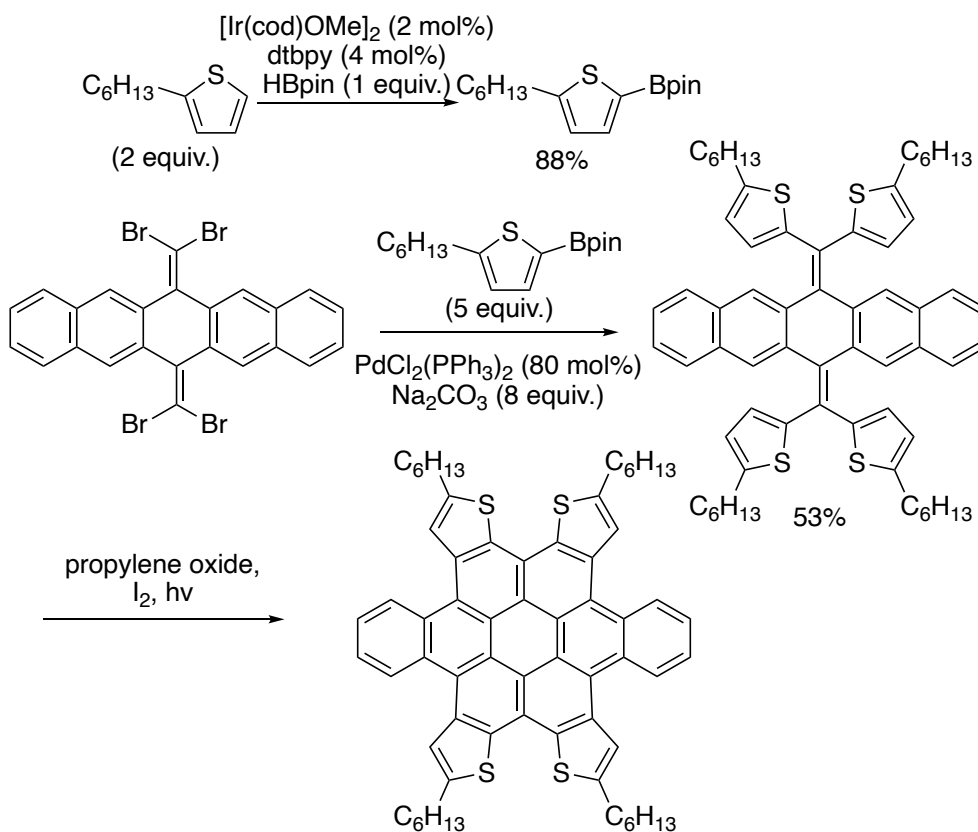
Figure 1.74. Synthesis of [6]-circulenes enabled by Ir-catalyzed borylation of thiophene.

In 2012 and 2013, Shinokubo and Itami first demonstrated that the mono-, di-, tri-, and hexa-borylation of hexabenzocoronenes (HBCs) occur cleanly and provide access to oxidized and arylated HBCs that are difficult to synthesize by Scholl oxidation.[157-160] The peripheral borylation of HBCs also has been applied to the synthesis of oligo-HBCs by Nuckolls (Figure 1.75).[161]
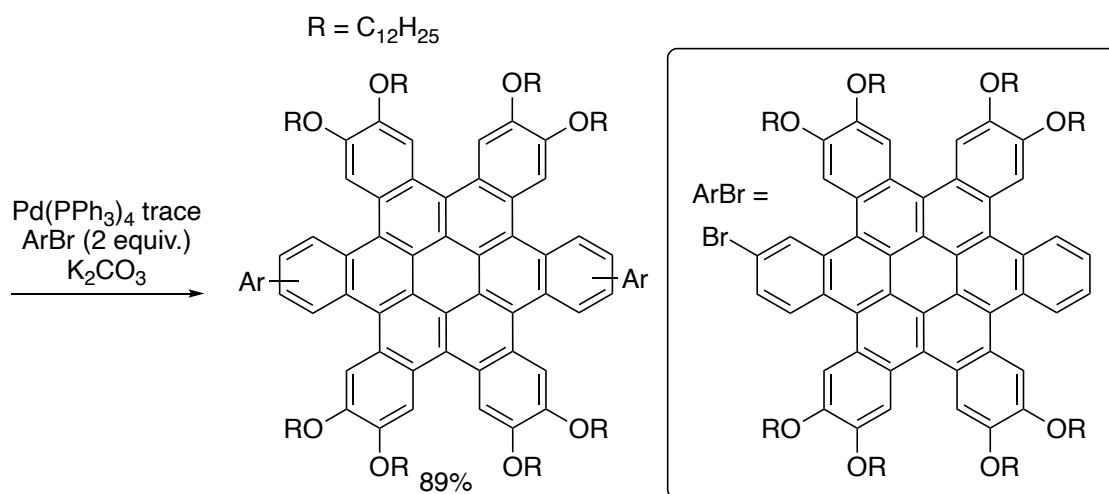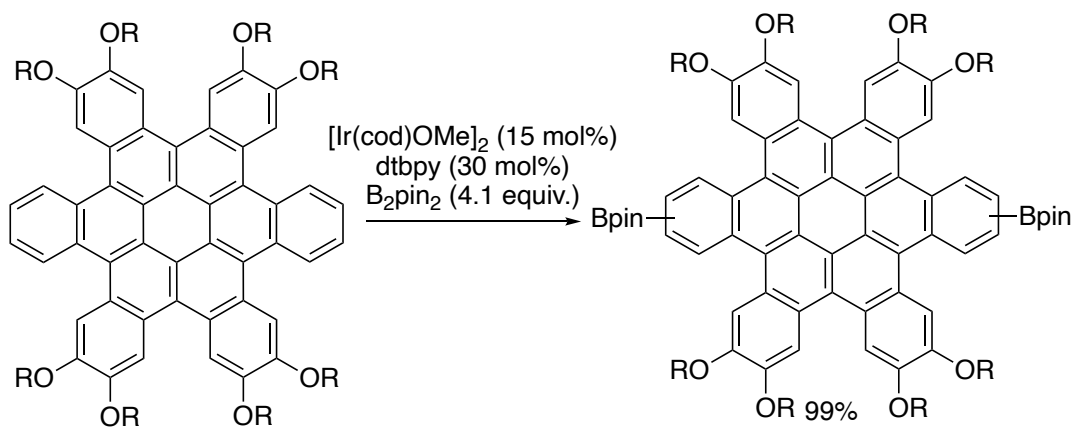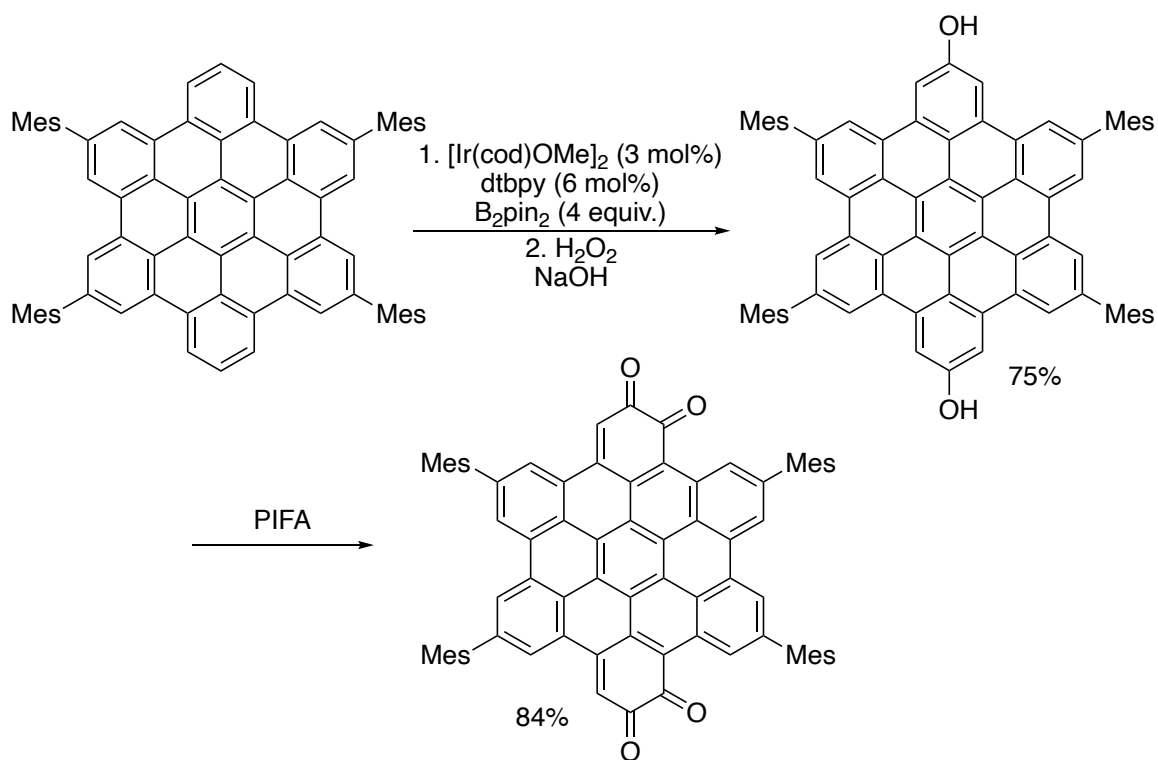
Figure 1.75. Ir-catalyzed borylation of [6]-circulenes.

In 2015, Shinokubo reported the synthesis of tetrathia[8]circulenes from cyclic tetrathiophenes by a sequence comprising borylation and annulation (Figure 1.76).[162] This modular route enabled the study of the relationship between the substitution patterns of the circulene and the aggregation or emission spectra of the molecules.[163]
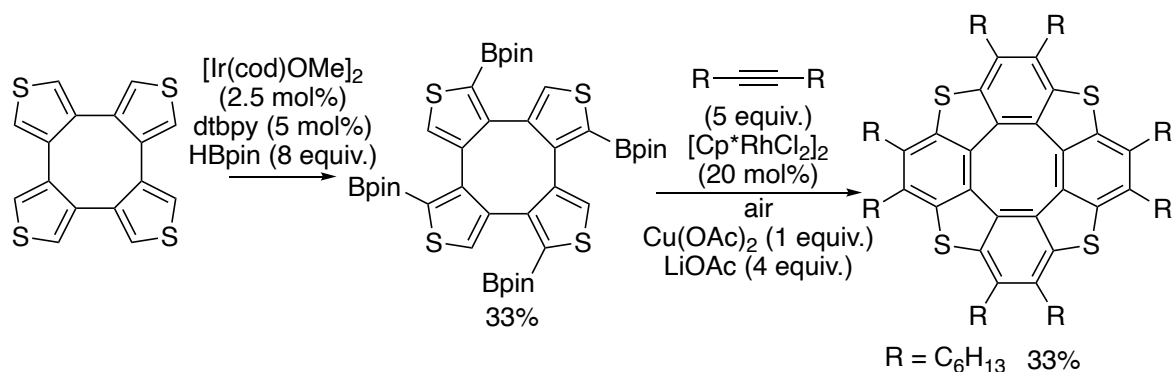
Figure 1.76. Ir-catalyzed borylation of tetrathiophenes enables the synthesis of tetrathia-[8]-circulenes.

The geodesic structures derived from 1,3,5-substituted benzenes (phenines) are topologically related to the corannulenes. Isobe first demonstrated in 2016 that the borylation of cyclo-*meta*-phenylenes (CMPs) occurs in high yield. The five-fold borylated [5]CMP has been used as an intermediate for the modular synthesis of various arylated [5]CMPs, which performed well as components of single-layer OLEDs (Figure 1.77).[164] The borylated [5]CMP, [7]CMP and [8]CMP, and [6]CMP were later found to be valuable building blocks for the synthesis of bowl shaped, saddle shaped, and cylindrical geodesic phenine frameworks (GPFs), respectively (Figure 1.77).[165-168]

[Ir(cod)OMe]₂ (50 mol%)
dtbpy (1 equiv.)
B₂pin₂ (9.9 equiv.)

99%

1. (15 equiv.)
Pd₂(dba)₃ (40 mol%)
SPhos (80 mol%)
Cs₂CO₃ (20 equiv.)

2. Ni(COD)₂ (250 equiv.)
COD (250 equiv.)
2,2'-bpy (250 equiv.)

[5]circulenoidal GPF
18% over 2 steps

[Ir(cod)OMe]₂ (95 mol%)
dtbpy (40 mol%)
B₂pin₂ (4 equiv.)

97%

1. PtCl₂(cod) (1 equiv.)
CsF (10 equiv.)

2. PPh₃ (10 equiv.)

n = 3, 3%
n = 4, 6%
n = 5, 3%

n = 3-5

57
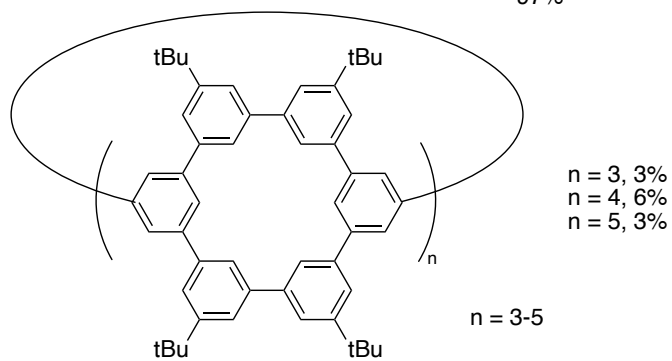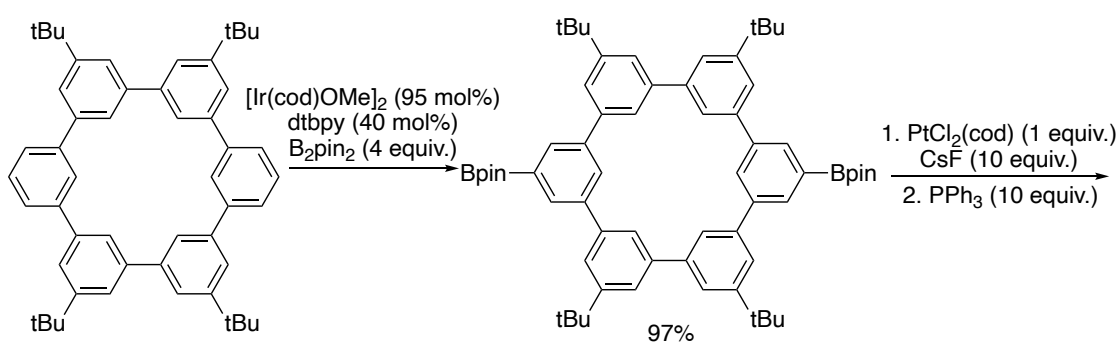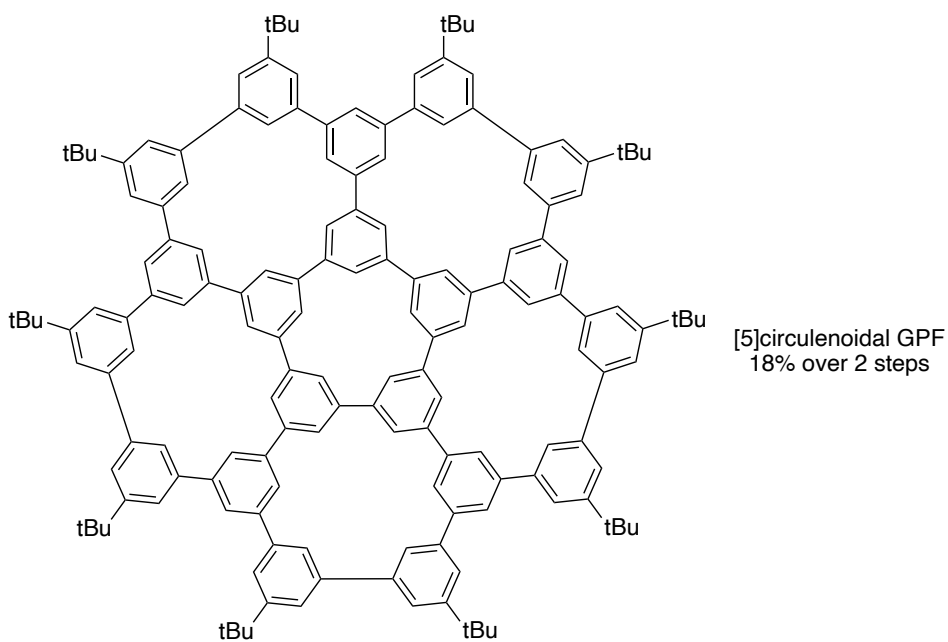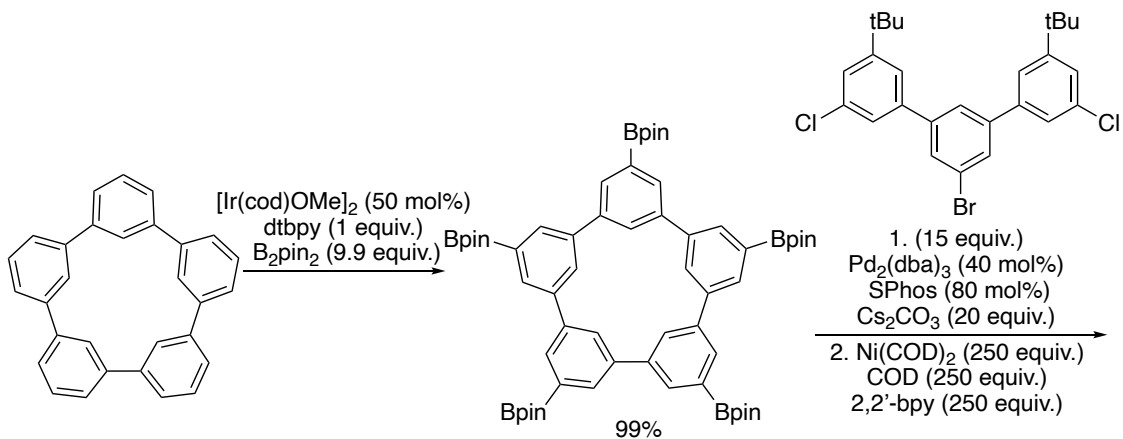
Figure 1.77. Ir-catalyzed borylation of cyclo-*meta*-phenylenes.

Mastalertz reported that the borylation of truxene and tribenzotriquinacene occurs with good selectivity for the C_3-symmetric isomer, which is complementary to selectivities obtained by electrophilic aromatic substitution (Figure 1.78).[169, 170] These curved molecules are valuable as precursors to curved buckybowls.
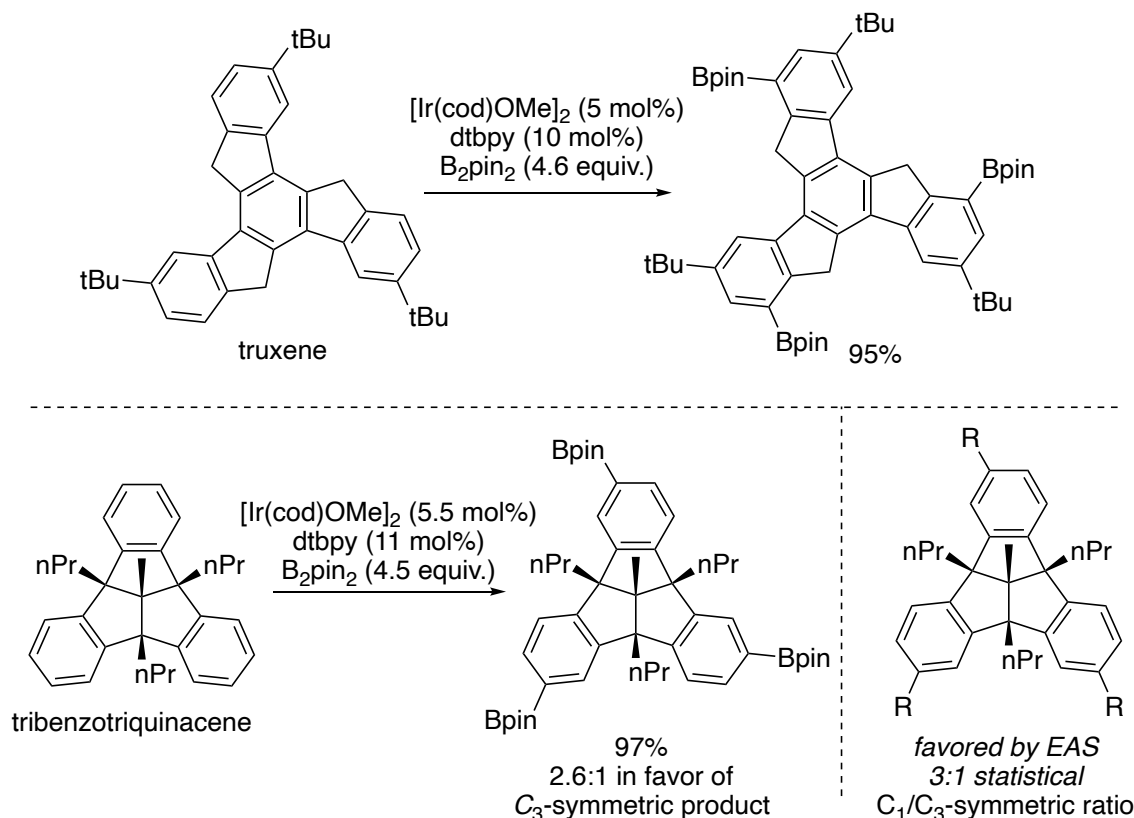
Figure 1.78. Ir-catalyzed borylation of truxenes and tribenzotriquinacenes.

1.5.2 Transition metal catalyzed borylation in the synthesis and modification of dendrimers

Dendrimers are radially symmetric molecules with well-defined and monodisperse structures,[171] and they have received much attention, due to their medicinal, biological, and materials applications.[172] Oligophenylene dendrimers have been investigated for OLED applications.[173] Their synthesis has typically relied on iterative Suzuki-Miyaura couplings of boronic ester building blocks with bifunctional "focal points." These focal points are haloarenes containing masked boronic acids, which then require demasking between the cross-coupling steps. An alternative strategy is to harness the borylation of C–H bonds to introduce the desired boronic ester functionality directly in the appropriate step in the synthesis.

In 2008 and 2009, Moore and Suginome reported that the borylation of *meta*-substituted arenes provides a rapid way to synthesize polyphenylene dendrimers by iterative borylation and cross-coupling of the borylated building blocks (Figure 1.79).[174, 175]

In contrast to coupling borylated arenes to a central "focal point" in a building block approach, Marder and Goto reported that the borylation of the periphery of dendrimers enable the rapid expansion of the dendrimer architecture (Figure 1.80).[176, 177]
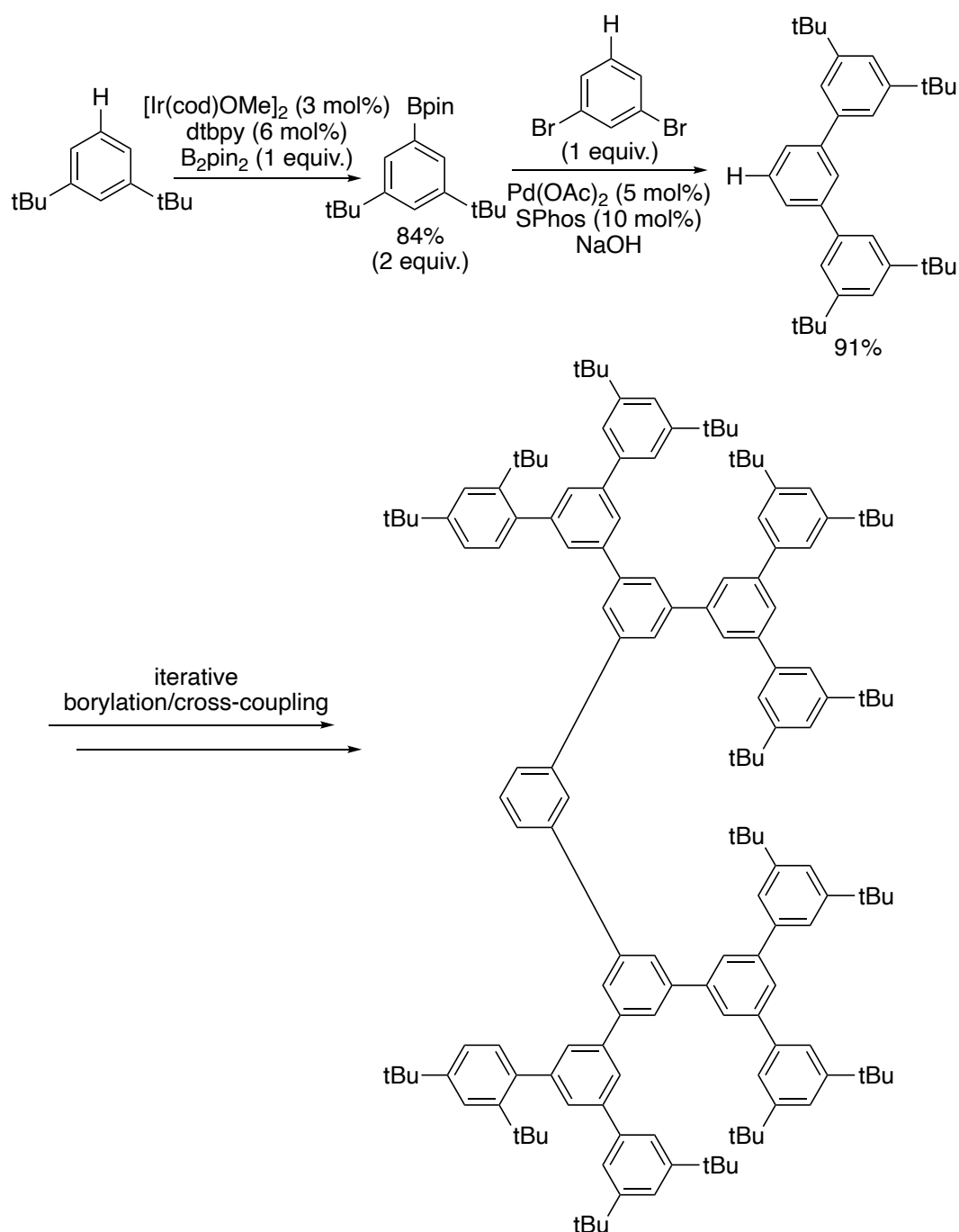
Figure 1.79. Ir-catalyzed borylation of arene building blocks in the synthesis of dendrimers.
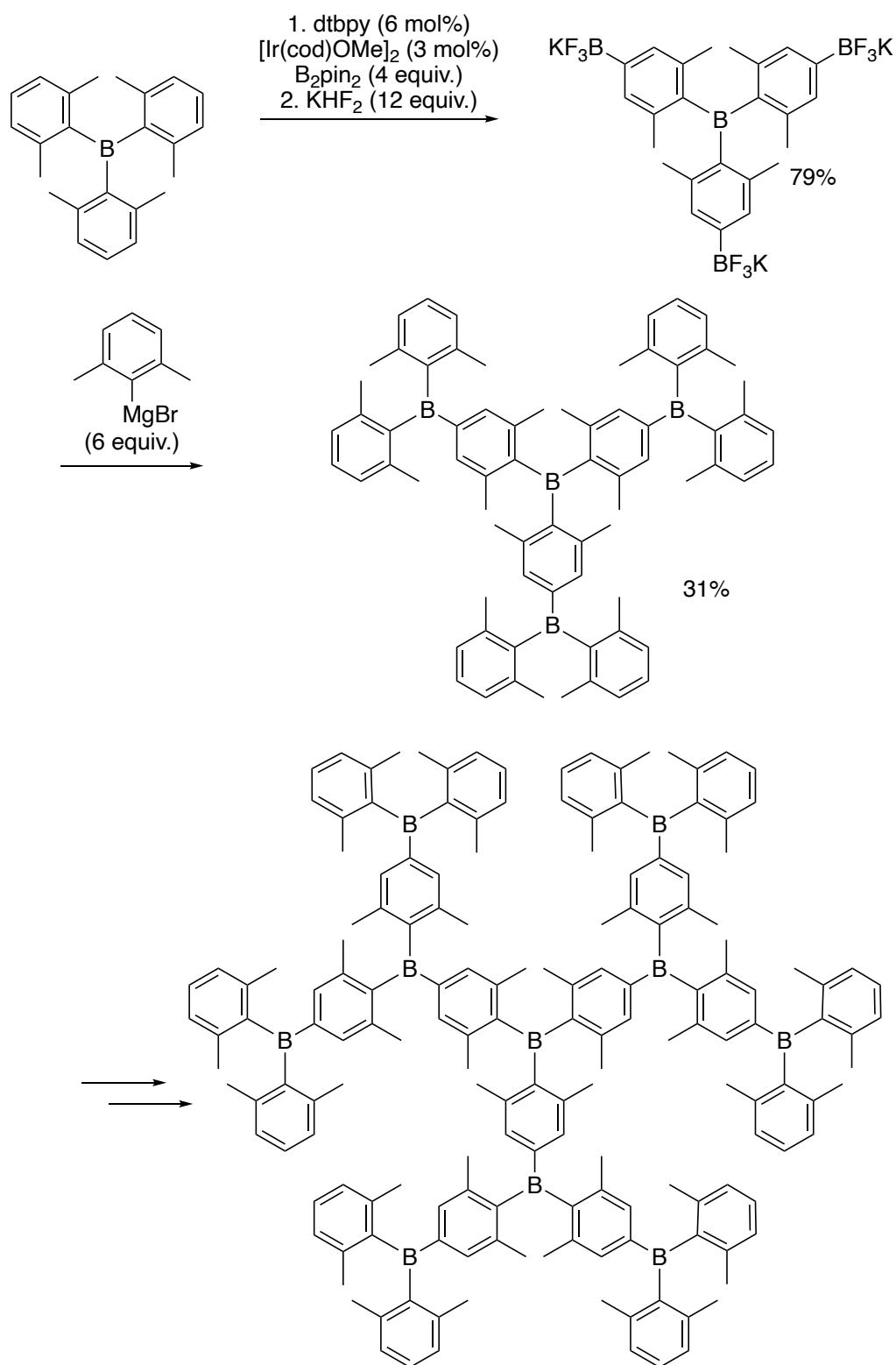
Figure 1.80. Ir-catalyzed peripheral borylation of dendrimers.

1.5.3 Transition metal catalyzed borylation for the post-polymerization modification of polymers

The borylation of C–H bonds also has been applied to the post-polymerization functionalization of polymers. Early efforts focused on the functionalization of polyolefins.

The borylation of polyolefins provides an avenue to access hydroxylated or arylated polyolefins that contain polar functional groups and with high molecular weights, a class of polymers that have been difficult to synthesize through copolymerization strategies.

In 2002, our laboratory in collaboration with Hillmyer's showed the feasibility of this approach in the two-step borylation-hydroxylation of polyethylethylene (PEE).[178] This method was later expanded to achieve the functionalization of linear low density polyethylene (LLDPE) and polypropylene (PP) (Figure 1.81).[179, 180] Bae later reported that isotactic poly(1-butene) and polystyrene undergo borylation in a similar fashion.[181, 182] These functionalized polyolefins were decorated further by functional group manipulations or graft polymerization, and the resulting polymers exhibited changes in crystallinity and the ability to serve as compatibilizers in polymer blends.
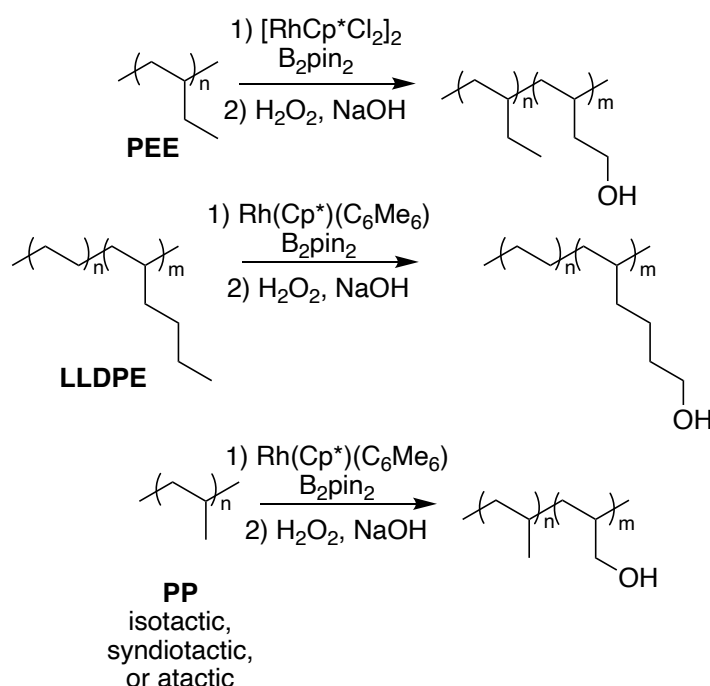
Figure 1.81. Rh-catalyzed borylation of polyolefins.

In 2009 Bae pioneered the application of the borylation of C–H bonds for the modification of aromatic main-chain polymers, in particular to the post-polymerization functionalization of poly(arylene ether sulfone) (Figure 1.82).[183, 184] The reactions occurred cleanly with essentially no cross-linking or chain cleavage, as inferred from the polydispersity index of the resultant polymer. Bielawski leveraged this method to synthesize poly(arylene ether sulfone) polymers decorated by Lewis basic heterocycles as proton exchange membrane materials (Figure 1.82).[185] Scott reported that the borylation of 1,3-bis(3-phenoxyphenoxy)benzene occurs on the ends of the polymer chains and can be applied to the synthesis of polyphenylether-epoxy resin-triamine adhesives.[186]
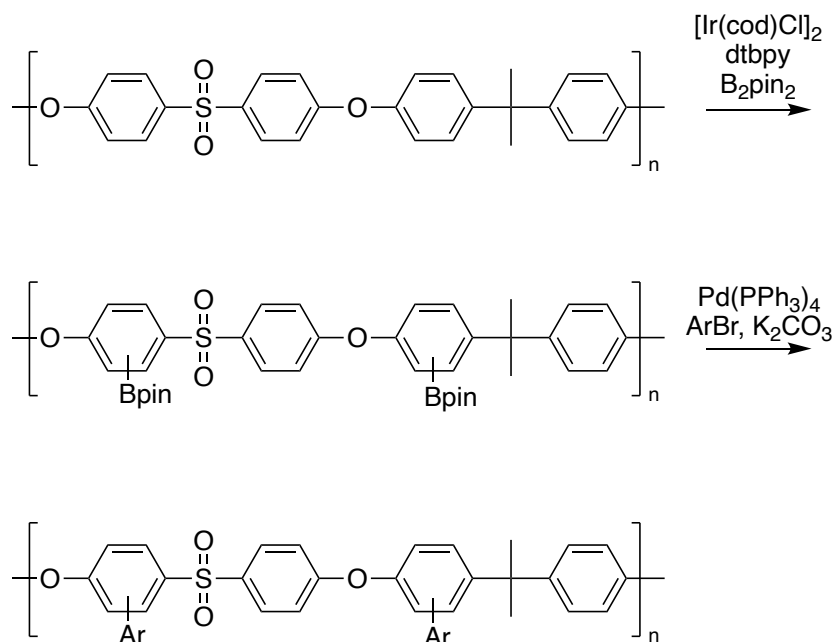
Figure 1.82. Ir-catalyzed borylation of poly(arylene ether sulfones).

1.5.4 Transition metal catalyzed borylation for the synthesis of oligopyrroles, corroles, porphyrins, and porphyrin analogues

The borylation of C–H bonds also has been applied to the synthesis or modification of oligopyrroles, corroles, and porphyrins. 4,4-Difluoro-4-bora-3a,4a-diaza-*s*-indacenes (BODIPYs) are small molecules that exhibit strong fluorescence with sharp peaks.[187, 188] Osuka reported that the borylation of a *meso*-substituted dipyrromethane occurs in high yield and with high α-selectivity, whereas the borylation of a dipyrrin (BODIPY) occurs with moderate yield and β-selectivity (Figure 1.83). This selectivity created complementary approaches to the synthesis of both α- and β- alkenylated BODIPYs.[189]
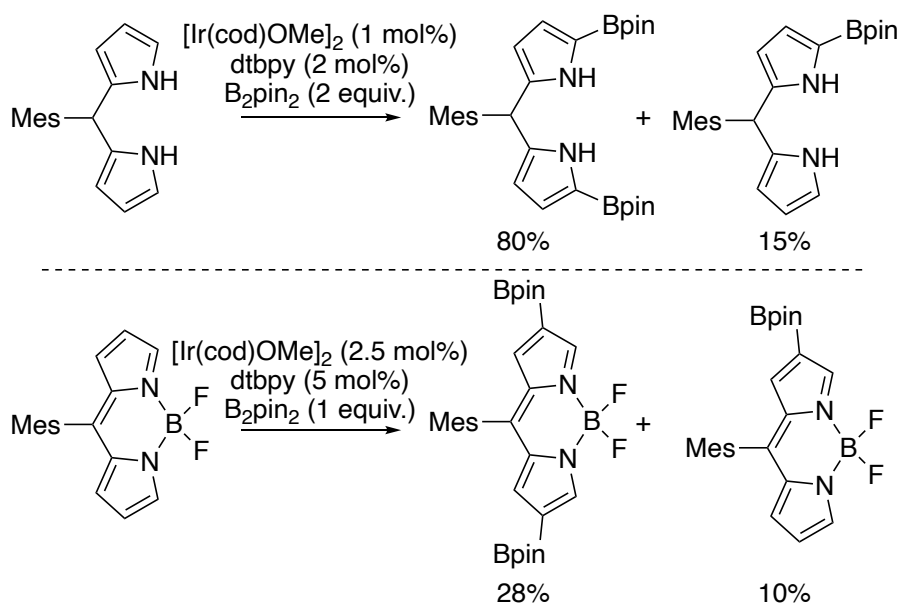
Figure 1.83. Ir-catalyzed borylation of pyrroles and BODIPYs.

Porphyrins are 18π aromatic macrocyclic compounds that are ubiquitous in nature and in organic optoelectronics. Porphyrins have long been studied in fields as varied as photosynthesis, biocatalysis, dyes, information storage, ligand design, and supramolecular chemistry.[190] In 2005 Osuka pioneered the borylation of porphyrins and reported that the direct borylation of porphyrins occurs at the β-position, while other functionalization methods, such as electrophilic aromatic substitution, tend to modify the *meso*-position (Figure 1.84).[191] The borylated porphyrins were further functionalized by Suzuki cross-coupling reactions or Heck-type reactions.[192, 193]
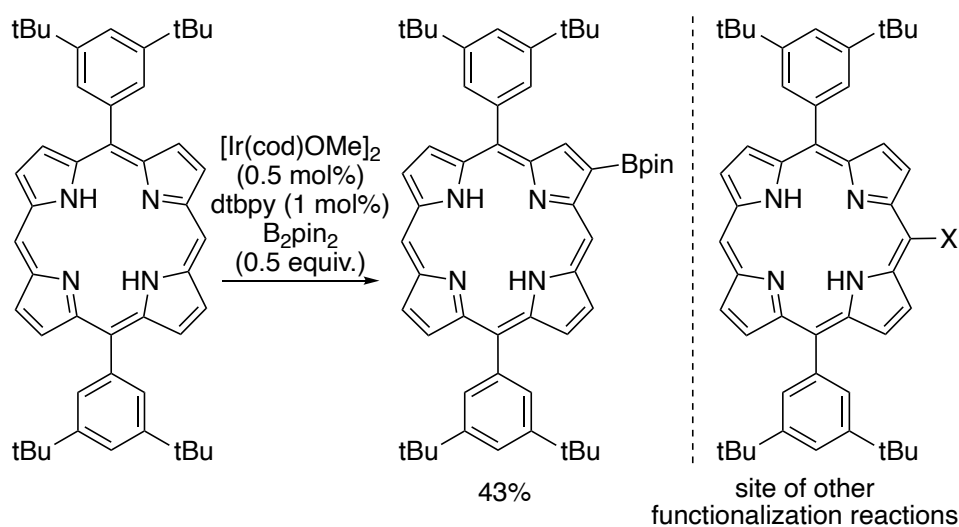
Figure 1.84. Ir-catalyzed, β-selective borylation of porphyrins.

Leveraging the predictable selectivity of C–H borylation, Osuka and others combined appropriate borylated porphyrins with linkers of choice in a "building block" approach to synthesize oligo-porphyrin architectures (Figure 1.85). Many novel porphyrins were synthesized by this approach. For example, doubly 1,3-butadiyne-bridged and 2,5-thienylene-bridged diporphyrins were synthesized from doubly borylated porphyrins, and the two-photon absorption cross sections of the bridged diporphyrins were abnormally large.[194, 195] Other exotic porphyrin oligomers were synthesized with this strategy, such as porphyrin nanobelts,[196-203] cyclometallated porphyrin complexes,[204-210] or cyclophane-like oligoporphyrins.[211]
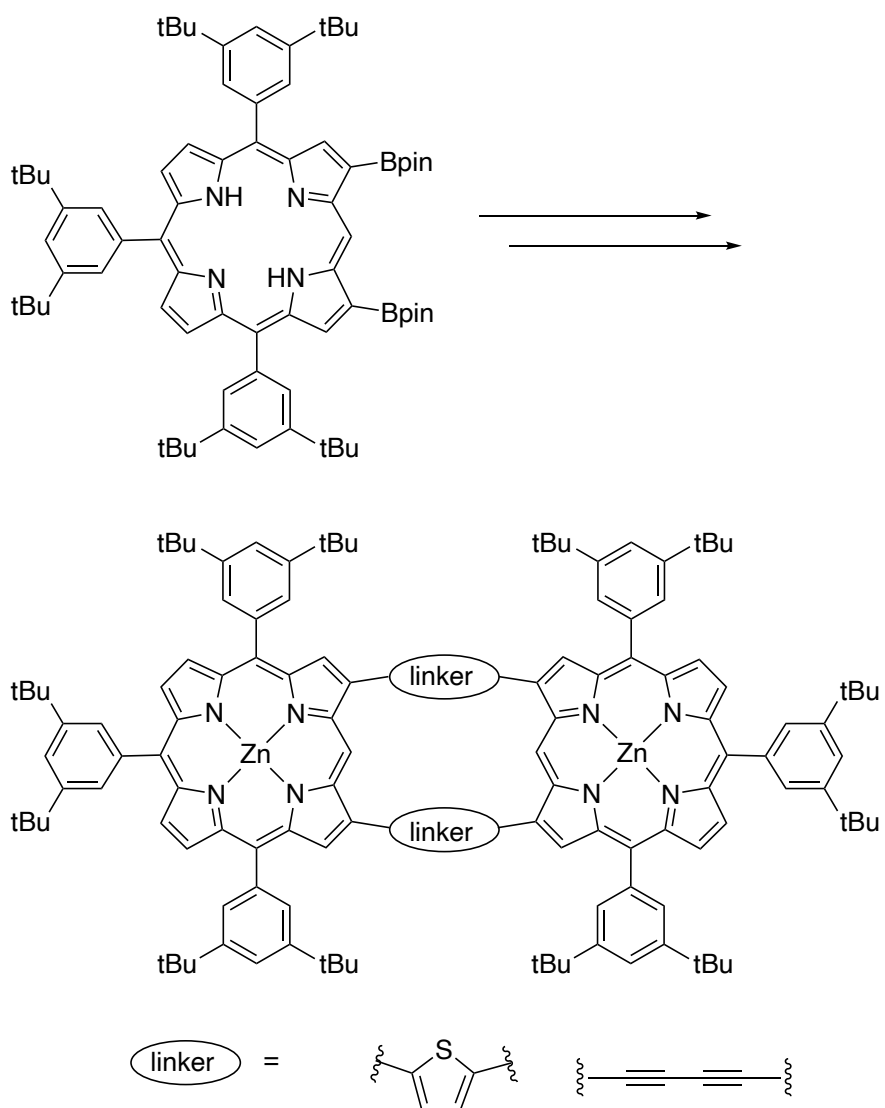
Figure 1.85. β-borylated porphyrins as building blocks for the synthesis of oligoporphyrins.

If the *meso-* and β-positions on the porphyrin ring are sterically hindered and aryl C–H bonds on the distal aryl substituents are sterically accessible, then borylation occurs at the distal aryl C–H bonds. This scenario led to the highly selective terminal borylation of a tetraarylporphyrin (Figure 1.86).[212]
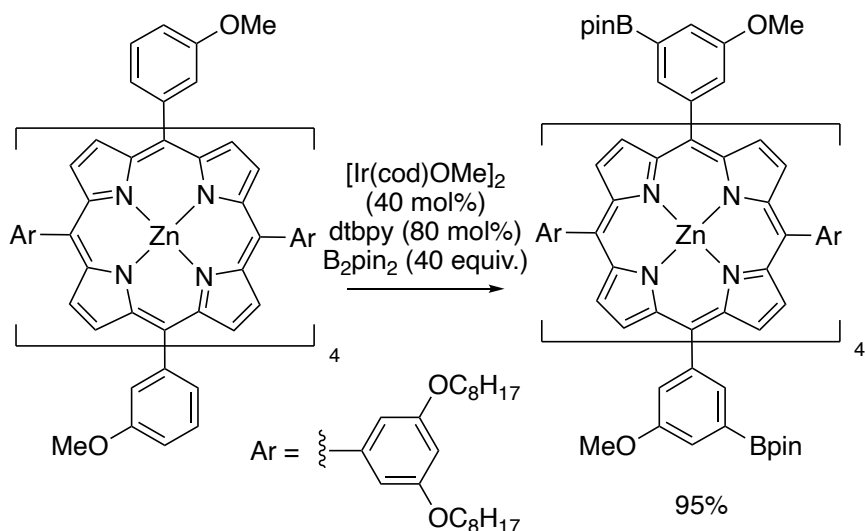
Figure 1.86. Ir-catalyzed peripheral borylation of oligoporphyrins.

Corroles are 18π aromatic tetrapyrrolic compounds that contain a direct pyrrole-pyrrole linkage and are studied for their unique coordination chemistry and optical properties.[213, 214] In 2005, Osuka reported that the borylation of corrole, like the borylation of porphyrins, occurs with β-selectivity. These borylated corroles provided a route to the corrole-porphyrin dimers[215] and doubly-bridged corrole dimers, which possess singlet biradical character (Figure 1.87).[216, 217]
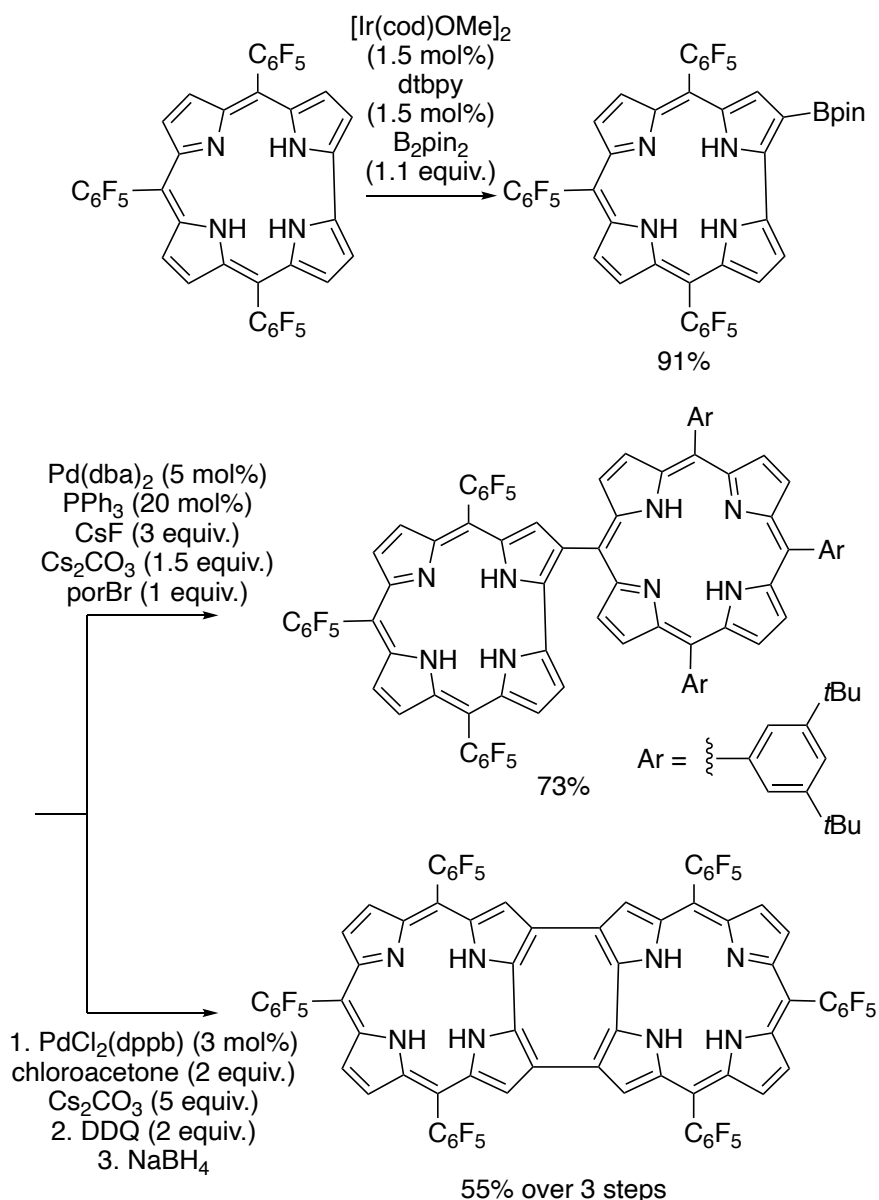
Figure 1.87. Ir-catalyzed, β-selective borylation of corroles.

Subporphyrins are ring-contracted analogues of porphyrins with a 14π aromatic system, a bowl-shaped structure, and often possess non-linear optical properties.[218, 219] In 2015, Osuka reported that subporphyrins undergo clean double borylation at the *meso*-positions (Figure 1.88). The boronic ester products were further elaborated into π-extended subporphyrins and subporphyrin dimers.[220]
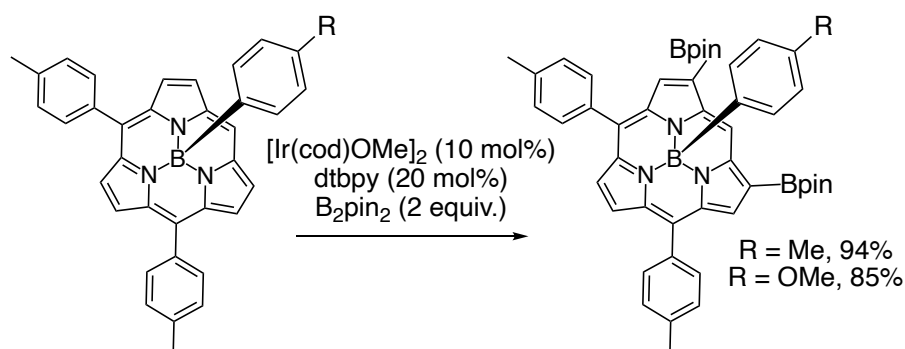
Figure 1.88. Ir-catalyzed borylation of subporphyrins.

In 2021, Tanaka and Osuka used the borylation of phenylene-linked dipyrroles and tripyrroles to provide starting materials for the synthesis of a cyclic oligopyrroles (Figure 1.89).[221] Subsequent oxidation of these oligopyrroles formed the corresponding circulenes.[222, 223]

Song reported that the double borylation of tripyrrins occurred cleanly and applied the diboronic ester products to the synthesis of π-extended "earring" porphyrins (Figure 1.90). The UV-vis spectra of these materials contained bands that are highly red-shifted, relative to the parent porphyrin.[224, 225]
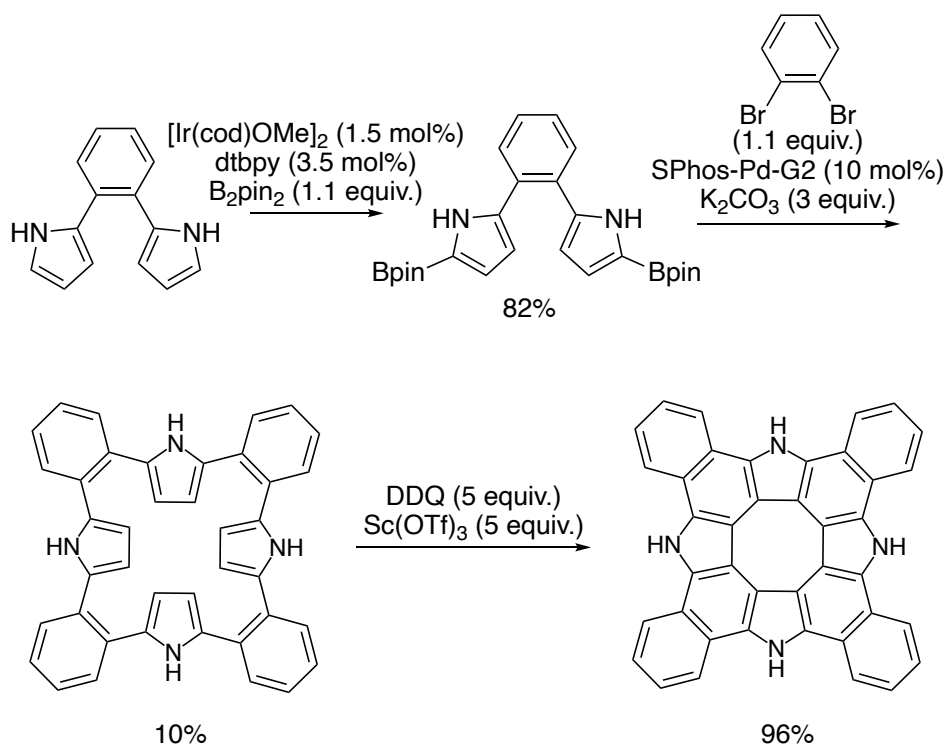
Figure 1.89: Ir-catalyzed borylation of dipyrroles in the synthesis of cyclic oligopyrroles

In a similar fashion, clean six-fold borylation occurred on the distal aryl C–H bonds of a hexaphyrin derivative containing 2,6-substituted aryl groups (Figure 1.91).[226]
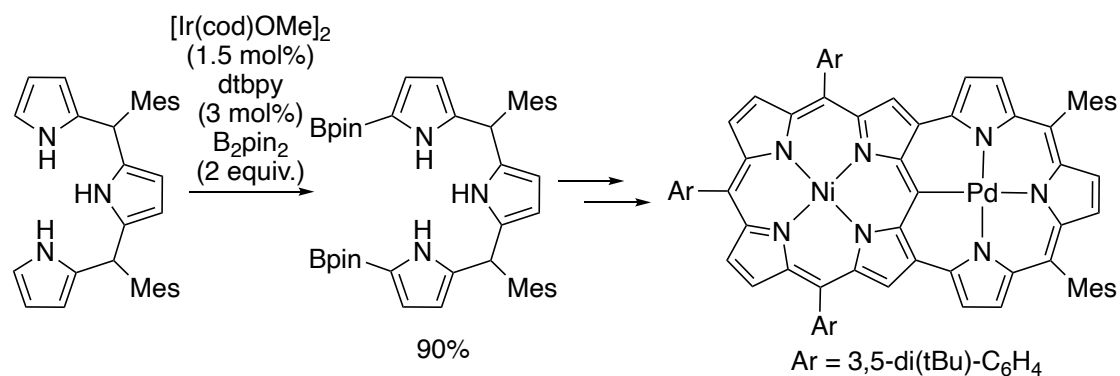
Figure 1.90. Ir-catalyzed borylation of tripyrroles.
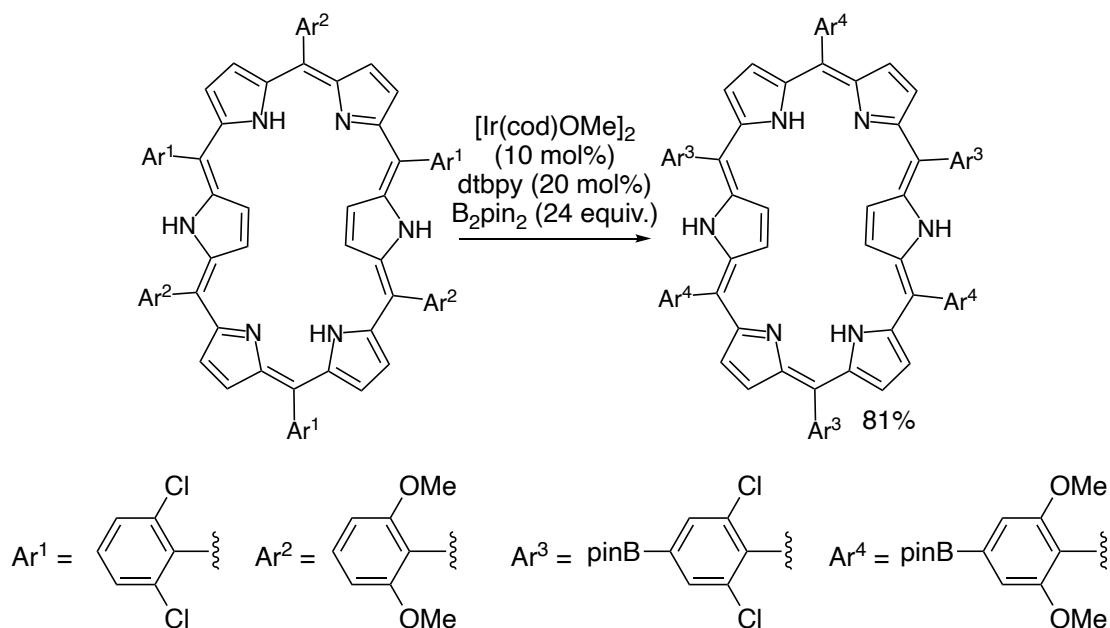
Figure 1.91. Ir-catalyzed borylation of hexaphryns.

Cyclic tetraindoles are considered π-extended porphyrinogen analogs, and they can be transformed into a planar porphyrin-like structure by oxidation. Shinokubo's 2012 route involved the borylation of a bisindole and subsequent dimerization (Figure 1.92).[227] Similar analogs containing benzofuran and benzothiophene units also have been prepared by this route.[228]
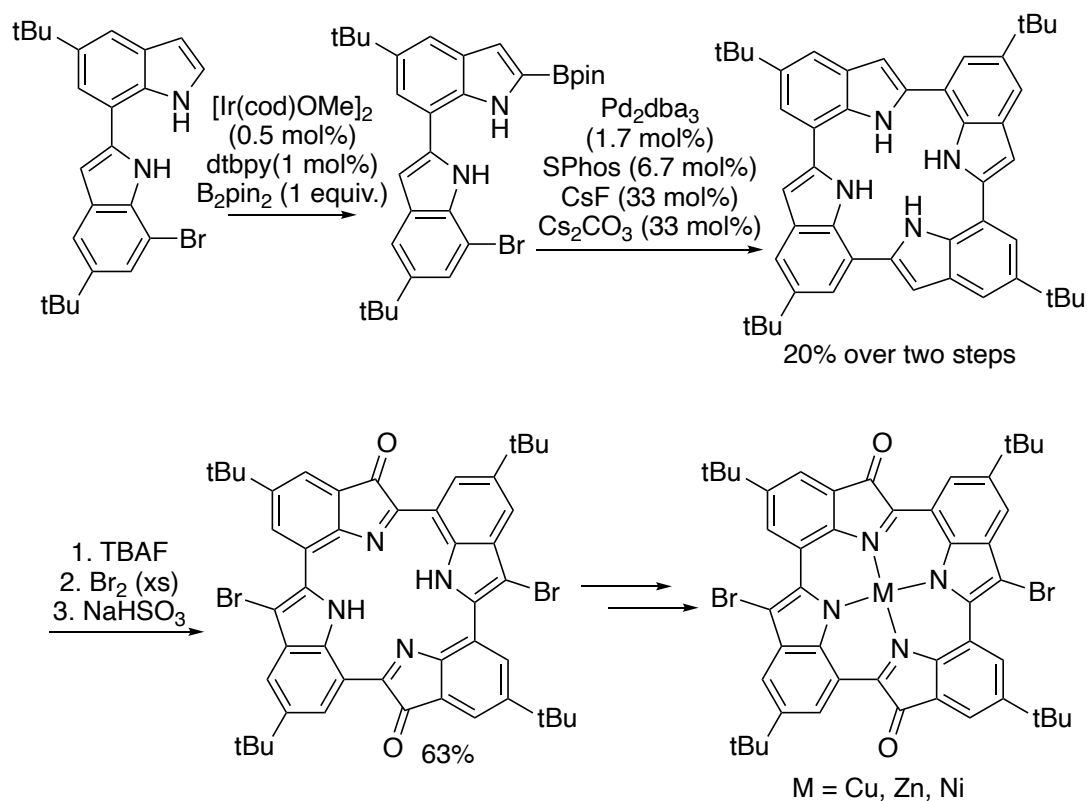
Figure 1.92. Ir-catalyzed borylation of bisindoles in the synthesis of porphyrinogen analogues.

1.5.5 Transition metal catalyzed borylation of arene C–H bonds in the synthesis of chalcophene materials

Due to their solution processability and ability to form stable films, semiconducting polymers are valuable for organic field-effect transistor (OFETs) and organic photovoltaic devices (OPVs). Within this field of research, much effort has been devoted to the exploration of heteroaromatic rings incorporated into the building unit to modulate the electronic properties and structural ordering of the polymers. Thiophene-based building blocks have received particular attention in recent years.[229]

In 2015, Inagaki studied the borylation of various thiophene derivatives with a silica-supported iridium catalyst. In one case, the combination of borylation and cross-coupling resulted in the synthesis of a triarylamine hole transport material in yields that are much higher than those of the prior routes (Figure 1.93).[230]
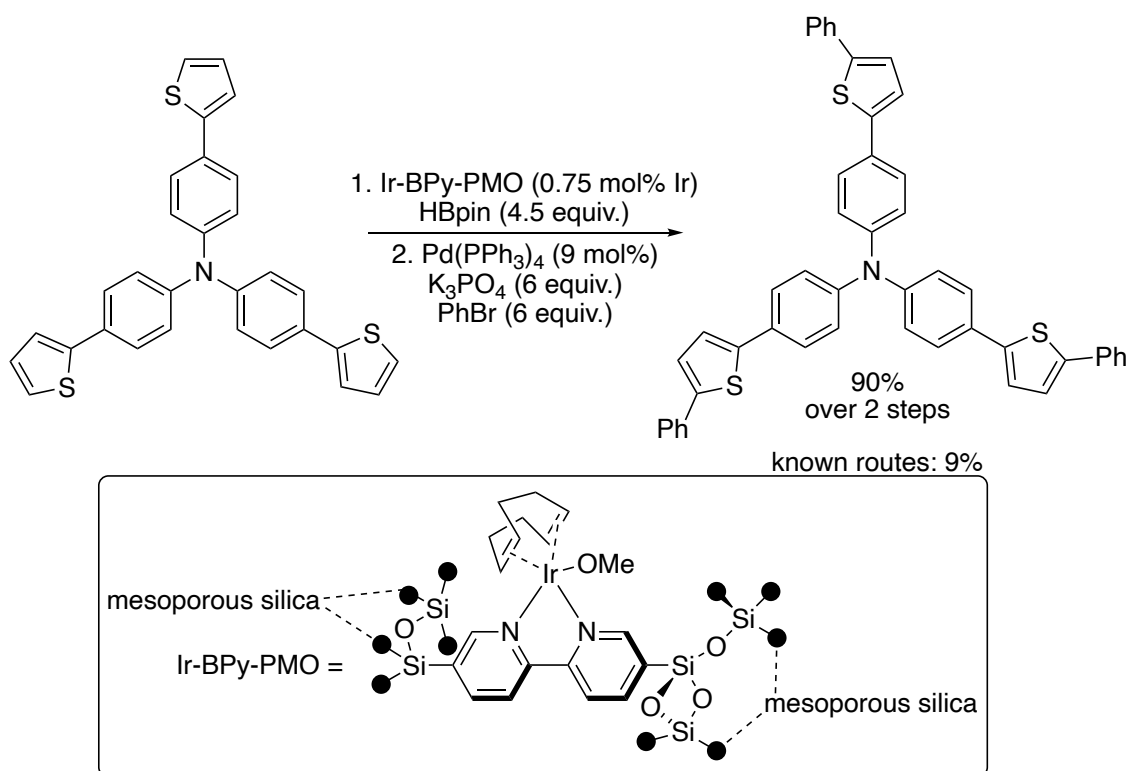
Figure 1.93. Borylation of a trithiophene hole-layer material.

In 2014, Takimiya reported the diborylation of thienothiophene in high yield. Subsequent oxidation formed the corresponding thienothiophenedione, a strong, electron deficient acceptor unit for use in organic semiconductors (Figure 1.94).[231]
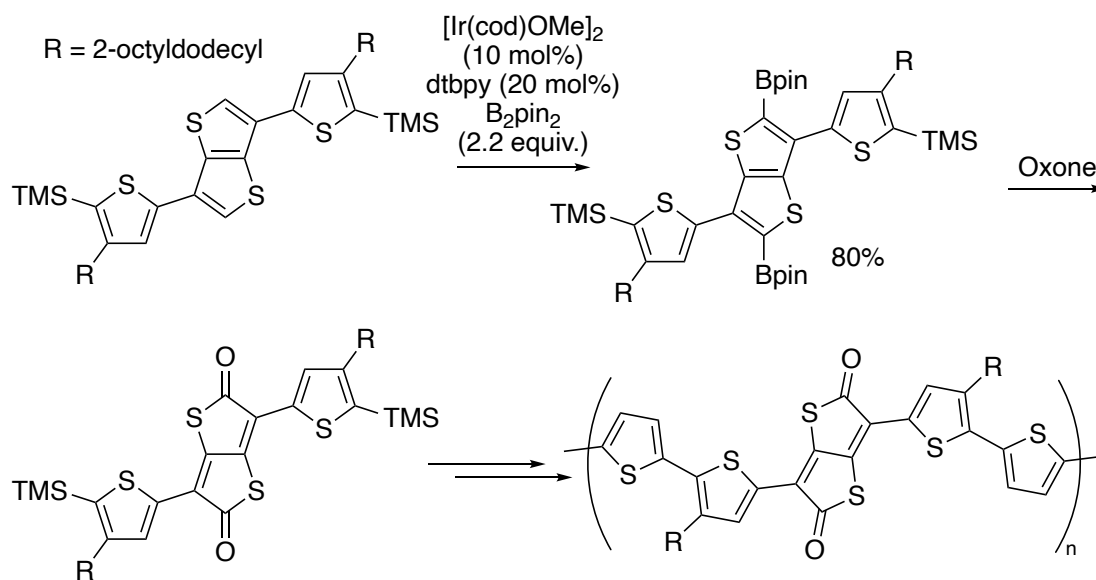
Figure 1.94. Ir-catalyzed borylation of thienothiophene and application to the synthesis of thienothiophenedione.

The borylation of naphthodichalcogenophenes and napthothiadiazoles has been applied to the rapid synthesis of semiconductor materials. For example, in 2012 Takimiya reported the selective 5,10-diborylation of napthodithiophenes and synthesized organic semiconductors for OFET and OPV applications (Figure 1.95). The different charge mobilities of the two polymeric forms shown in Figure 1.95 are attributable to the different levels of twist in the backbone.[232-234]
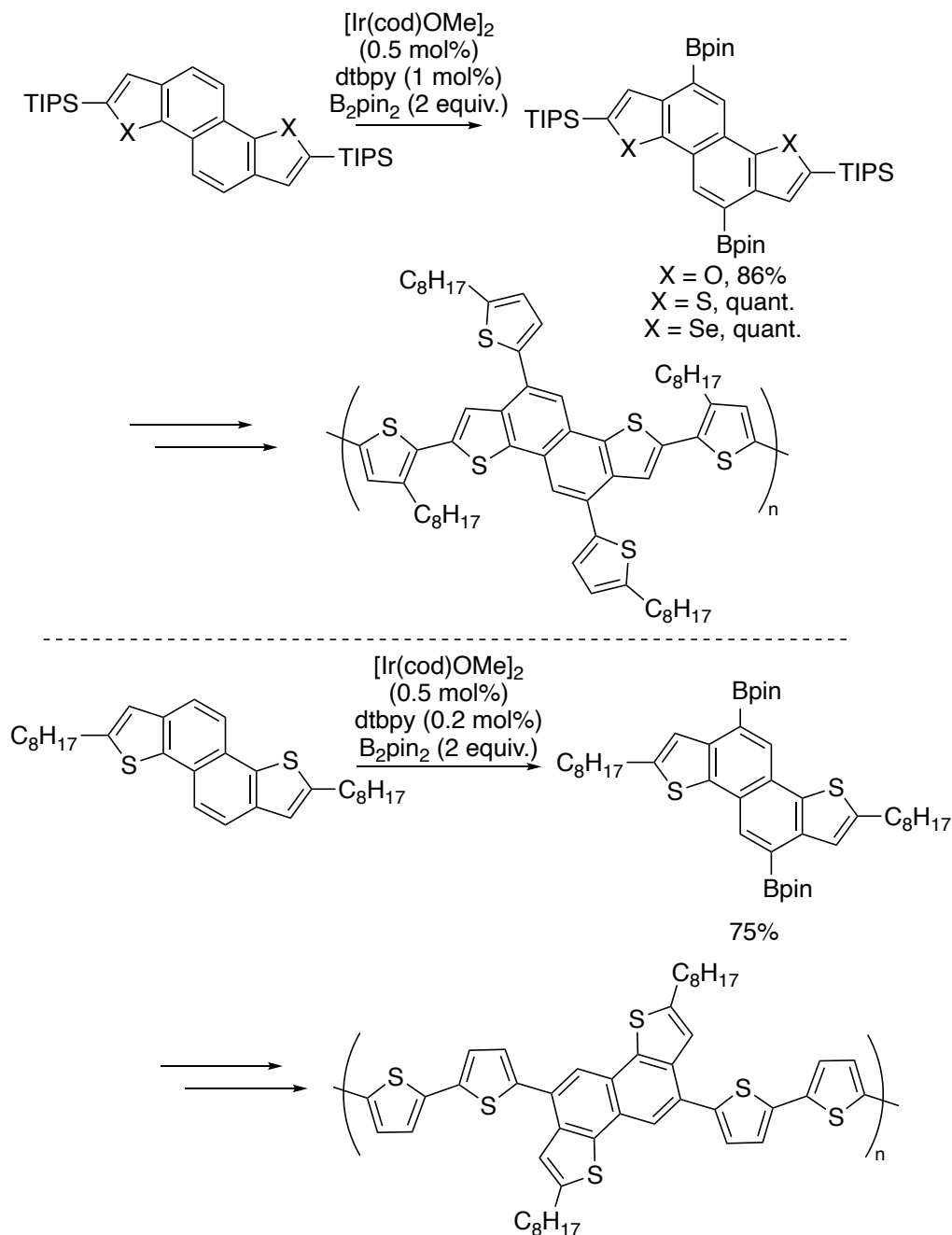
Figure 1.95. Ir-catalyzed borylation of napthodichalcogenophenes.

Naphthothiadiazole units are also valuable as electron deficient units in semiconducting polymers. In 2013, Takimiya reported a convenient route to organic semiconducting polymers containing the napthothiadiazole core by the diborylation of naphthothiadiazole (Figure 1.96).[235, 236]
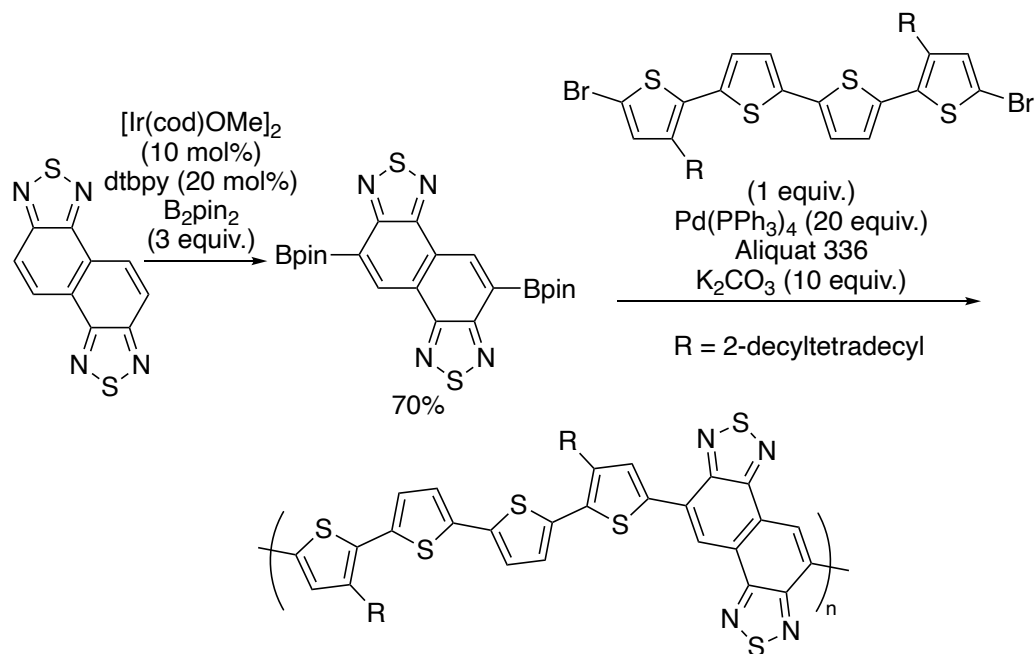
Figure 1.96. Ir-catalyzed borylation of napthothiadiazoles.

In 2021 Okamoto used the borylation of chrysenodithiophene for the synthesis of conjugated polymers containing both chrysenodithiophene and benzothiadiazole units (Figure 1.97).[237]
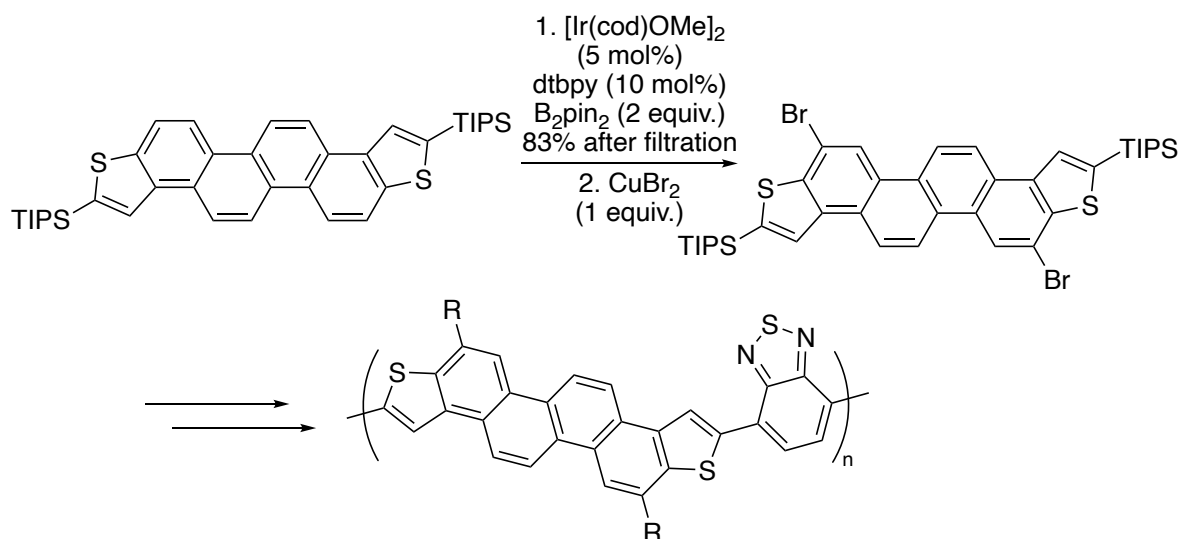
Figure 1.97. Ir-catalyzed borylation of chrysenodithiophenes.

1.6 Transition-Metal Catalyzed, Borylation of C–H Bonds in Synthesis of Ligands

The late-stage modification of ligands for homogeneous catalysis is a final application of the borylation of C–H bonds constituting "late-stage" functionalization. These reactions can be divided into two types of functionalization: 1) the modification of common ligand cores by sequences comprising borylation and functionalization and 2) directed functionalizations in which the coordinating atom of the ligand precursor interacts with the transition metal catalyst and confers the desired site- or stereo- selectivity.

The binaphthalene core is a privileged structural class in enantioselective synthesis. In particular, the chiral binaphthol (BINOL) scaffold has been applied extensively in chiral Brønsted-acid catalysis. Numerous theoretical and experimental studies have shown that aryl substituents at the 3- and 3'- positions strongly influence the selectivities of catalysts formed from these BINOL cores.[238, 239] In 2014 Clark demonstrated that silyl-directed borylation and subsequent Suzuki-Miyaura coupling introduces a wide variety of aryl substitutents at the 3- and 3'- positions (Figure 1.98).[240] Chattopadhy later showed in 2019 that the silyl directing group is not necessary if the diboron reagent is B_2eg_2 (eg = ethylene glycolate) (Figure 1.98). Non-covalent interactions between the phenol and Beg groups appear to direct the borylation to the *ortho*-position.[241]
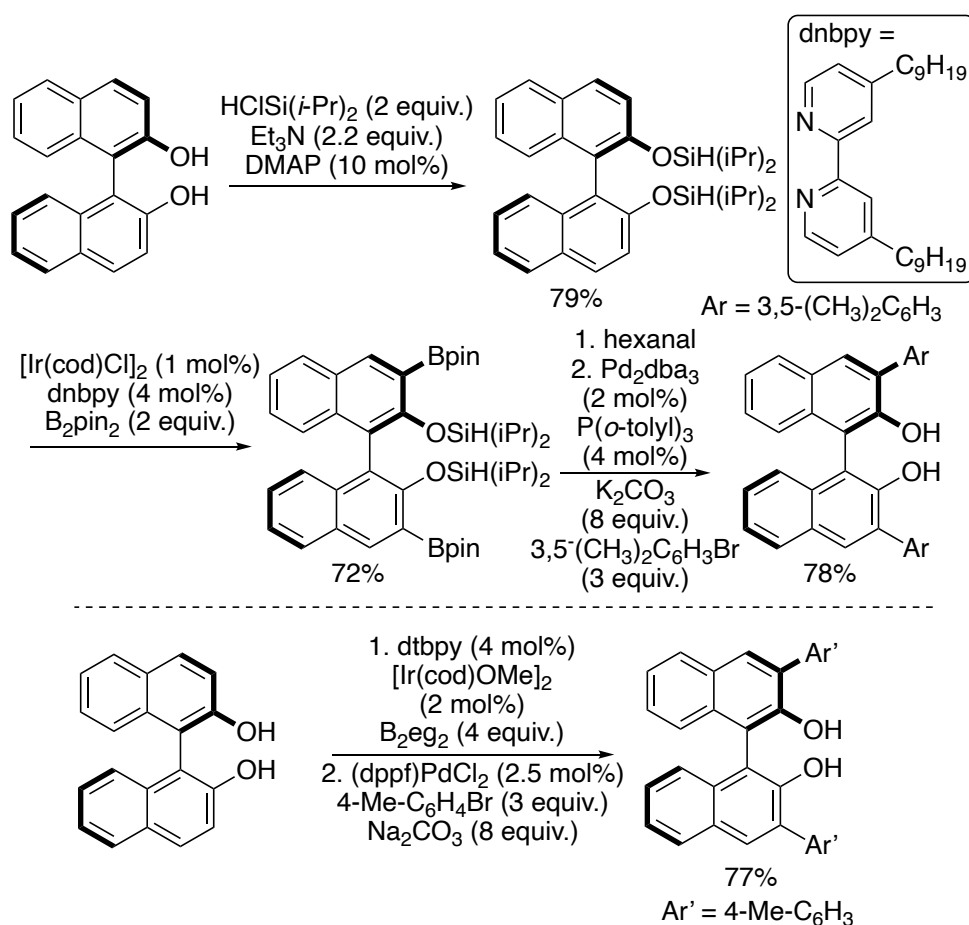
Figure 1.98. Borylation-coupling sequences for the synthesis of 3- and 3'- substituted BINOLs

Ferrocenes are prevalent in ligands for homogenous catalysis. Thus, methods to introduce substituents or even planar chirality to the ferrocene core are valuable for the synthesis of ferrocenyl-based ligands. The undirected borylation of ferrocenes was first investigated by Plenio in 2004, but these reactions occurred in moderate yield.[242] In 2022, Xu developed a chiral bidentate boryl ligand that enabled the enantioselective borylation of ferrocenes containing amide functionality (Figure 1.99). The amide functionality is presumed to interact with a vacant binding site on the iridium catalyst, thereby directing the borylation to the C–H bond located *ortho* to the directing group.[118]
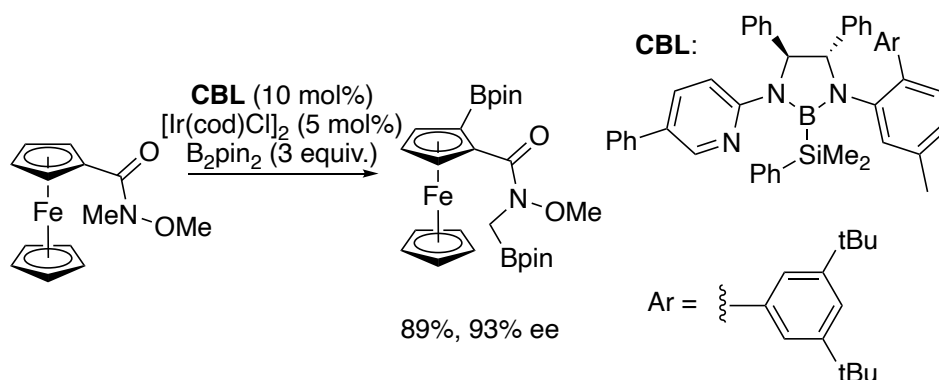
Figure 1.99: Enantioselective borylation of ferrocene enabled by a chiral bidentate boryl ligand.

Phosphines are common supporting ligands in homogenous catalysis. The coordination of phosphines to transition-metal catalysts is a powerful avenue to direct the site of borylation. In 2014, Clark showed that the combination of [Ir(cod)]BF$_4$ and tmphen catalyze the borylation of biaryl phosphines at the distal aryl group (Figure 1.100A). In 2019, Clark further showed that 2-methylaryl phosphines undergo borylation at the benzylic position in the presence of the cationic iridium complex [Ir(cod)]BF$_4$ with tmphen as lignad.[243, 244] Similarly, Takeya showed that aryl phosphines undergo highly *ortho*-selective borylation in the presence of [RuCl$_2$(*p*-cymene)]$_2$ (Figure 1.100B).[245] Shi showed that similar reactivity and selectivity was observed in the presence of [Rh(coe)$_2$Cl]$_2$ and applied the *ortho*-selective borylation to a concise synthesis of CyJohnphos (Figure 1.100C).[246] In all these cases, the selectivity is postulated to arise from coordination of the phosphino group to the metal catalyst.
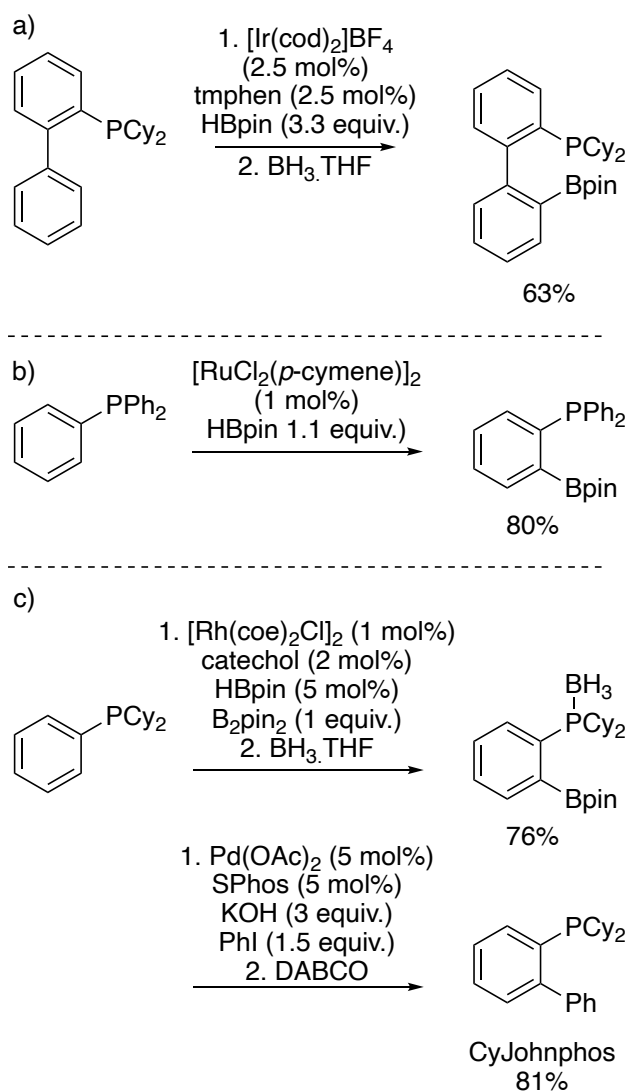
Figure 1.100: Phosphine-directed *ortho-* borylation of arenes.

In 2015, Kanai developed a bipyridine ligand with the capacity to participate in secondary hydrogen bonding interactions with substrates. When combined with [Ir(cod)OMe]$_2$, this ligand forms complexes that catalyze the *meta*-selective borylation of aryl phosphine oxides and phosphonate esters (Figure 1.101).[247, 248]
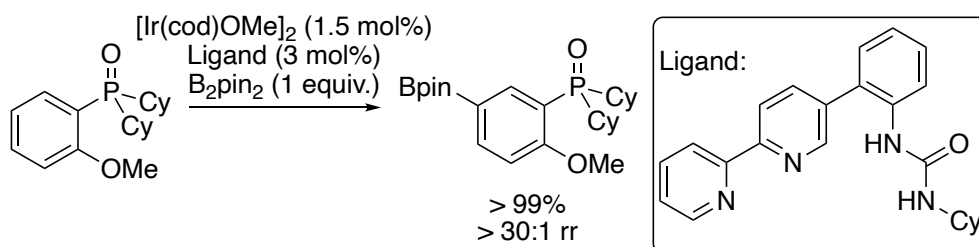
Figure 1.101. *Meta*-selective borylation of phosphine oxides enabled by a hydrogen-bonding ligand.

In 2020 Watson showed that arylphosphonates also undergo *ortho*-selective borylation with cationic iridium catalysts formed from the electron-deficient P[(3,5-CF₃)₂-C₆H₃]₃ ligand and Ir(cod)(acac) (Figure 1.102). The authors noted that similar results were obtained with [Ir(cod)₂]BF₄, but Ir(cod)(acac) was chosen as the precatalyst, due to its bench stability and lower price. The resulting aryl boronic esters were then used in the synthesis of a biarylphosphine ligand.[249]
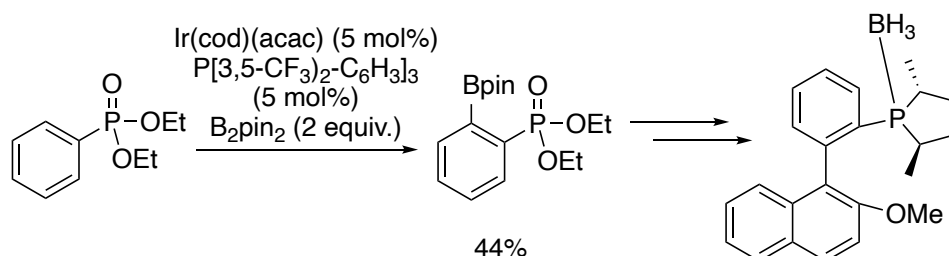
Figure 1.102. *Ortho*-selective borylation of arylphosphonates with cationic iridium catalysts.

In 2020 Phipps reported the desymmetrization of diaryl phosphinamides catalyzed by a complex that interacts with the substrate through an ion pair (Figure 1.103). The phosphinamide is postulated to hydrogen bond to the sulfonate bipyridine, while the chiral cation confers enantioselectivity.[250] In 2021 Xu reported the desymmetrization of diaryl phosphinates to synthesize phosphines in which phosphorus is a stereogenic center (Figure 1.104).[251]
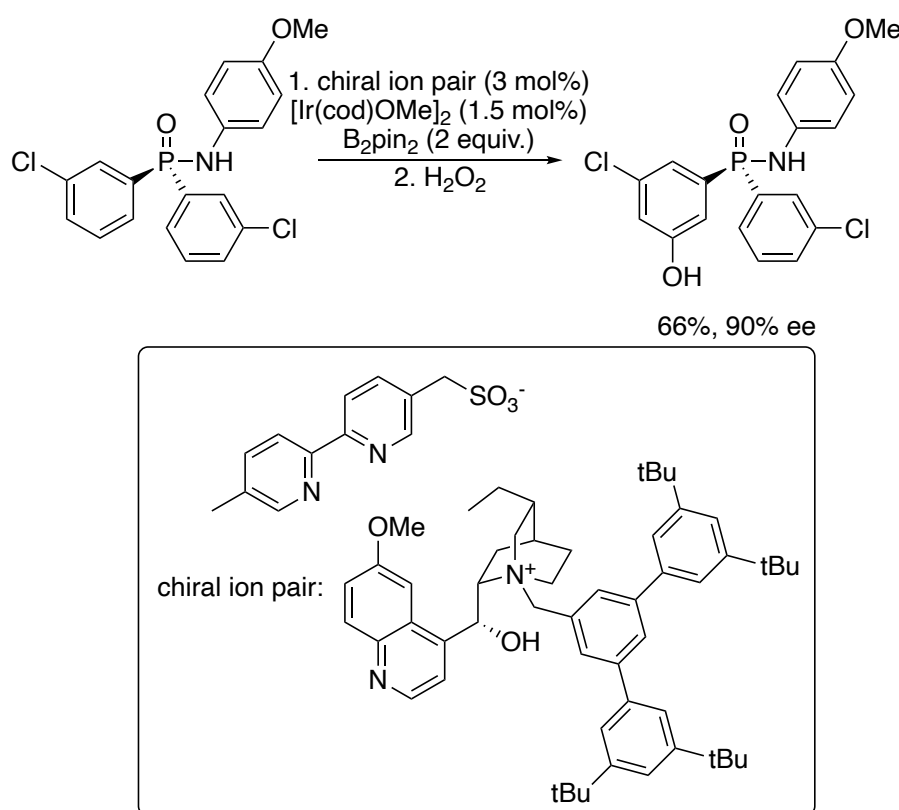
Figure 1.103. Desymmetrization of diaryl phosphinamides by borylation of aryl C–H bonds with a chiral, ion-pairing strategy.
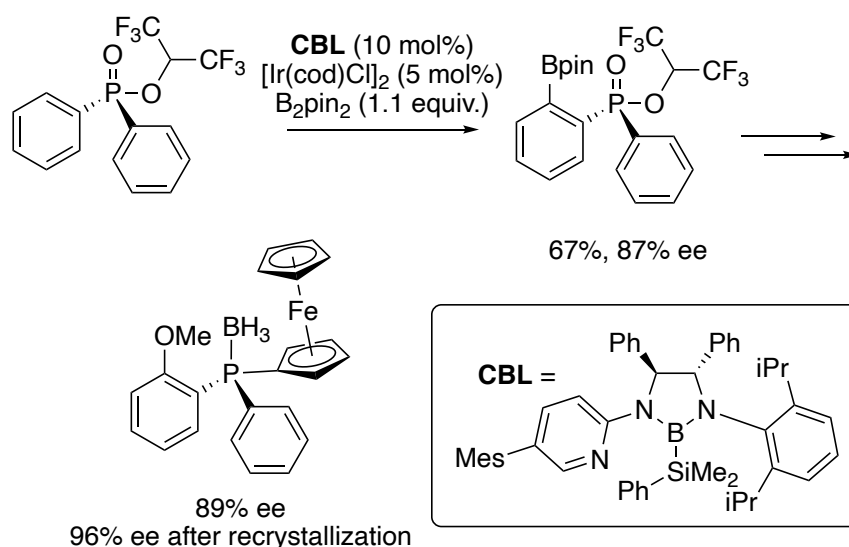
Figure 1.104. Desymmetrization of diaryl phosphinates by borylation with a chiral bidentate boryl ligand.

In 2019 Xu demonstrated that the combination of a chiral bidentate boryl ligand and iridium catalyzes the desymmetrization of diarylaminomethanes. The resulting boronic ester was then used for the synthesis of an aminophosphine ligand (Figure 1.105).[252]
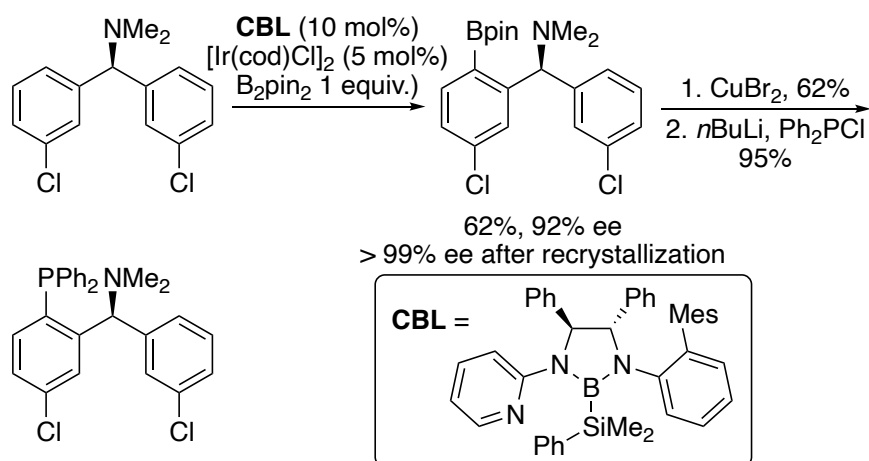
Figure 1.105. Desymmetrization of diaryl aminomethanes by borylation with a chiral bidentate boryl ligand.

Finally, the double borylation of a bipyridine enabled Segawa's 2017 synthesis of a bis-2-pyridylidene palladium complex (Figure 1.106).[253]
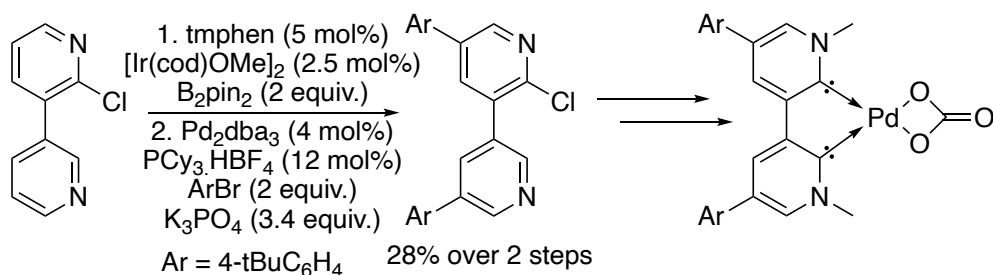
Figure 1.106. Borylation-coupling of a 3,3'-bipyridine enables the synthesis of a bis-2-pyridylidene palladium complex.

1.7 Conclusion and Outlook

C–H functionalization is a fast-growing field that has had and will continue to impact the many research areas of synthetic chemistry. Among methods for C–H functionalization, reactions to functionalize C–H bonds with boron are particularly attractive because they occur with high regioselectivity and form products with boron-based groups that can be transformed into a range of different functional groups. Due to these characteristics, the borylation of C–H bonds have been widely applied to the modification of many classes of complex molecules, including active pharmaceutical ingredients, natural products, precursors in the synthesis of such compounds, organic materials, and ligands. This chapter has outlined such applications.

However, a major goal for future development is the intermolecular borylation of alkyl C–H bonds. Undirected examples of the functionalization of alkyl C–H bonds with boron are the least developed. With the undirected borylation of alkyl C–H bonds reported recently under conditions with the substrate as limiting reagent, it is likely that further catalyst development and reaction designs will enable this class of borylation to occur in a practical fashion.

Although progress has been made toward creating catalysts that react with high activity and site-selectivity, site-selective borylations of C–H bonds in molecules with multiple similarly active C–H bonds is an urgent unmet need. Although directing strategies exist, further developments of methods that exploit existing functionality to control site selectivity and do not require laborious installation and removal of directing groups are needed. More challenging is the development of methods with catalyst-controlled site selectivity. Such methods have the capability to expand the scope of borylation reactions and to enable a broader range of functionalization of complexes molecules at a "late stage."

1.8 References

Parts of this chapter were reprinted with permission from:

"Transition-Metal-Catalyzed Silylation and Borylation of C–H Bonds for the Synthesis and Functionalization of Complex Molecules"

Yu, I.F.; Wilson, J. W.; Hartwig, J.F. *Chem. Rev.* **2023**, *123*, 11619–11663.

1.   Arndtsen, B. A.; Bergman, R. G.; Mobley, T. A.; Peterson, T. H., Selective Intermolecular Carbon-Hydrogen Bond Activation by Synthetic Metal Complexes in Homogeneous Solution. *Acc. Chem. Res.* **1995,** *28*, 154–162.
2.   Cernak, T.; Dykstra, K. D.; Tyagarajan, S.; Vachal, P.; Krska, S. W., The medicinal chemist's toolbox for late stage functionalization of drug-like molecules. *Chem. Soc. Rev.* **2016,** *45*, 546–576.
3.   Mkhalid, I. A. I.; Barnard, J. H.; Marder, T. B.; Murphy, J. M.; Hartwig, J. F., C–H Activation for the Construction of C–B Bonds. *Chem. Rev.* **2010,** *110*, 890–931.
4.   Cheng, C.; Hartwig, J. F., Catalytic Silylation of Unactivated C–H Bonds. *Chem. Rev.* **2015,** *115*, 8946–8975.

5.   Hartwig, J. F., Borylation and Silylation of C–H Bonds: A Platform for Diverse C–H Bond Functionalizations. *Acc. Chem. Res.* **2012,** *45*, 864–873.

6.   Gustavson, W. A.; Epstein, P. S.; Curtis, M. D., Homogeneous Activation of the Carbon-Hydrogen bond. Formation of Phenylsiloxanes from Benzene and Silicon Hydrides. *Organometallics* **1982,** *1*, 884–885.

7.   Ishikawa, M.; Sakamoto, H.; Okazaki, S.; Naka, A., Nickel-Catalyzed Reactions of 3,4-Benzo-1,1,2,2-tetraethyl-1,2-disilacyclobutene. *J. Organomet. Chem.* **1992,** *439*, 19–21.

8.   Uchimaru, Y.; El Sayed, A. M. M.; Tanaka, M., Selective Arylation of a Silicon-Hydrogen Bond in o-Bis(dimethylsilyl)benzene via Carbon-Hydrogen Bond Activation of Arenes. *Organometallics* **1993,** *12*, 2065–2069.

9.   Tatsuo, I.; Kousaku, I.; Jun, T.; Norio, M., Palladium-Catalyzed Benzylic C–H Borylation of Alkylbenzenes with Bis(pinacolato)diboron or Pinacolborane. *Chem. Lett.* **2001,** *30*, 1082–1083.

10.   Tsukada, N.; Hartwig, J. F., Intermolecular and Intramolecular, Platinum-Catalyzed, Acceptorless Dehydrogenative Coupling of Hydrosilanes with Aryl and Aliphatic Methyl C−H Bonds. *J. Am. Chem. Soc.* **2005,** *127*, 5022–5023.

11.   Miki, M.; Naoaki, F.; Jun-ichi, W.; Shinji, W.; Yuzuru, M., Platinum-Catalyzed Aromatic C–H Silylation of Arenes with 1,1,1,3,5,5,5-Heptamethyltrisiloxane. *Chem. Lett.* **2007,** *36*, 910–911.

12.   Ohmura, T.; Kijima, A.; Suginome, M., Synthesis of 1-Borylisoindoles via Palladium-Catalyzed Dehydrogenation/C–H Borylation of Isoindolines. *J. Am. Chem. Soc.* **2009,** *131*, 6070–6071.

13.   Takaya, J.; Ito, S.; Nomoto, H.; Saito, N.; Kirai, N.; Iwasawa, N., Fluorine-Controlled C–H Borylation of Arenes Catalyzed by a PSiN-Pincer Platinum Complex. *Chem. Commun.* **2015,** *51*, 17662–17665.

14.   Furukawa, T.; Tobisu, M.; Chatani, N., C–H Functionalization at Sterically Congested Positions by the Platinum-Catalyzed Borylation of Arenes. *J. Am. Chem. Soc.* **2015,** *137*, 12211–12214.

15.   Furukawa, T.; Tobisu, M.; Chatani, N., Nickel-Catalyzed Borylation of Arenes and Indoles via C–H Bond Cleavage. *Chem. Commun.* **2015,** *51*, 6508–6511.

16.   Zhang, H.; Hagihara, S.; Itami, K., Aromatic C–H Borylation by Nickel Catalysis. *Chem. Lett.* **2015,** *44*, 779–781.

17.   Yoshii, D.; Yatabe, T.; Yabe, T.; Yamaguchi, K., C(sp^3)–H Selective Benzylic Borylation by In Situ Reduced Ultrasmall Ni Species on CeO$_2$. *ACS Catal.* **2021,** *11*, 2150–2155.

18.   Procopio, L. J.; Berry, D. H., Dehydrogenative Coupling of Trialkylsilanes Mediated by Ruthenium Phosphine Complexes: Catalytic Synthesis of Carbosilanes. *J. Am. Chem. Soc.* **1991,** *113*, 4039–4040.

19.   Djurovich, P. I.; Dolich, A. R.; Berry, D. H., Transfer Dehydrogenative Coupling of Triethylsilane Catalysed by Ruthenium and Rhodium Complexes. A New Si–C Bond Forming Process. *J. Chem. Soc. Chem. Commun.* **1994**, 1897–1898.

20.   Ezbiansky, K.; Djurovich, P. I.; LaForest, M.; Sinning, D. J.; Zayes, R.; Berry, D. H., Catalytic C−H Bond Functionalization: Synthesis of Arylsilanes by Dehydrogenative Transfer Coupling of Arenes and Triethylsilane. *Organometallics* **1998,** *17*, 1455–1457.

21.   Murphy, J. M.; Lawrence, J. D.; Kawamura, K.; Incarvito, C.; Hartwig, J. F., Ruthenium-Catalyzed Regiospecific Borylation of Methyl C−H Bonds. *J. Am. Chem. Soc.* **2006,** *128*, 13684–13685.

22.   Mazzacano, T. J.; Mankad, N. P., Base Metal Catalysts for Photochemical C–H Borylation That Utilize Metal–Metal Cooperativity. *J. Am. Chem. Soc.* **2013,** *135*, 17258–17261.

23. Sunada, Y.; Soejima, H.; Nagashima, H., Disilaferracycle Dicarbonyl Complex Containing Weakly Coordinated η^2-(H-Si) Ligands: Application to C–H Functionalization of Indoles and Arenes. *Organometallics* **2014,** *33*, 5936–5939.

24. Dombray, T.; Werncke, C. G.; Jiang, S.; Grellier, M.; Vendier, L.; Bontemps, S.; Sortais, J.-B.; Sabo-Etienne, S.; Darcel, C., Iron-Catalyzed C–H Borylation of Arenes. *J. Am. Chem. Soc.* **2015,** *137*, 4062–4065.

25. Chen, H.; Hartwig, J. F., Catalytic, Regiospecific End-Functionalization of Alkanes: Rhenium-Catalyzed Borylation under Photochemical Conditions. *Angew. Chem. Int. Ed.* **1999,** *38*, 3391–3393.

26. Obligacion, J. V.; Semproni, S. P.; Chirik, P. J., Cobalt-Catalyzed C–H Borylation. *J. Am. Chem. Soc.* **2014,** *136*, 4133–4136.

27. Ishiyama, T.; Takagi, J.; Ishida, K.; Miyaura, N.; Anastasi, N.; Hartwig, J. F., Mild Iridium-Catalyzed Borylation of Arenes. High Turnover Numbers, Room Temperature Reactions, and Isolation of a Potential Intermediate. *J. Am. Chem. Soc.* **2002,** *124*, 390–391.

28. Preshlock, S. M.; Ghaffari, B.; Maligres, P. E.; Krska, S. W.; Maleczka, R. E., Jr.; Smith, M. R., III, High-Throughput Optimization of Ir-Catalyzed C–H Borylation: A Tutorial for Practical Applications. *J. Am. Chem. Soc.* **2013,** *135*, 7572–7582.

29. Larsen, M. A.; Hartwig, J. F., Iridium-Catalyzed C–H Borylation of Heteroarenes: Scope, Regioselectivity, Application to Late-Stage Functionalization, and Mechanism. *J. Am. Chem. Soc.* **2014,** *136*, 4287–4299.

30. Chen, H.; Schlecht, S.; Semple, T. C.; Hartwig, J. F., Thermal, Catalytic, Regiospecific Functionalization of Alkanes. *Science* **2000,** *287*, 1995–1997.

31. Obligacion, J. V.; Semproni, S. P.; Pappas, I.; Chirik, P. J., Cobalt-Catalyzed C(sp^2)-H Borylation: Mechanistic Insights Inspire Catalyst Design. *J. Am. Chem. Soc.* **2016,** *138*, 10645–10653.

32. Boller, T. M.; Murphy, J. M.; Hapke, M.; Ishiyama, T.; Miyaura, N.; Hartwig, J. F., Mechanism of the Mild Functionalization of Arenes by Diboron Reagents Catalyzed by Iridium Complexes. Intermediacy and Chemistry of Bipyridine-Ligated Iridium Tris Boryl Complexes. *J. Am. Chem. Soc.* **2005,** *127*, 14263–14278.

33. Karmel, C.; Hartwig, J. F., Mechanism of the Iridium-Catalyzed Silylation of Aromatic C–H Bonds. *J. Am. Chem. Soc.* **2020,** *142*, 10494–10505.

34. Tamura, H.; Yamazaki, H.; Sato, H.; Sakaki, S., Iridium-Catalyzed Borylation of Benzene with Diboron. Theoretical Elucidation of Catalytic Cycle Including Unusual Iridium(V) Intermediate. *J. Am. Chem. Soc.* **2003,** *125*, 16114–16126.

35. Huang, G.; Kalek, M.; Liao, R.-Z.; Himo, F., Mechanism, Reactivity, and Selectivity of the Iridium-Catalyzed C(sp^3)–H Borylation of Chlorosilanes. *Chem. Sci.* **2015,** *6*, 1735–1746.

36. Clot, E.; Mégret, C.; Eisenstein, O.; Perutz, R. N., Validation of the M−C/H−C Bond Enthalpy Relationship through Application of Density Functional Theory. *J. Am. Chem. Soc.* **2006,** *128*, 8350–8357.

37. Guihaumé, J.; Clot, E.; Eisenstein, O.; Perutz, R. N., Importance of Palladium–Carbon Bond Energies in Direct Arylation of Polyfluorinated Benzenes. *Dalton Trans.* **2010,** *39*, 10510–10519.

38. Tajuddin, H.; Harrisson, P.; Bitterlich, B.; Collings, J. C.; Sim, N.; Batsanov, A. S.; Cheung, M. S.; Kawamorita, S.; Maxwell, A. C.; Shukla, L.; Morris, J.; Lin, Z.; Marder, T. B.; Steel, P. G., Iridium-Catalyzed C–H Borylation of Quinolines and Unsymmetrical 1,2-Disubstituted Benzenes: Insights into Steric and Electronic Effects on Selectivity. *Chem. Sci.* **2012,** *3*, 3505–3515.

39.   Wright, J. S.; Scott, P. J. H.; Steel, P. G., Iridium-Catalysed C−H Borylation of Heteroarenes: Balancing Steric and Electronic Regiocontrol. *Angew. Chem. Int. Ed.* **2021,** *60*, 2796–2821.

40.   Caldeweyher, E.; Elkin, M.; Gheibi, G.; Johansson, M.; Sköld, C.; Norrby, P.-O.; Hartwig, J. F., Hybrid Machine Learning Approach to Predict the Site Selectivity of Iridium-Catalyzed Arene Borylation. *J. Am. Chem. Soc.* **2023,** *145*, 17367–17376.

41.   Rej, S.; Chatani, N., Regioselective Transition-Metal-Free C(sp^2)−H Borylation: A Subject of Practical and Ongoing Interest in Synthetic Organic Chemistry. *Angew. Chem. Int. Ed.* **2022,** *61*, e202209539.

42.   Bähr, S.; Oestreich, M., Electrophilic Aromatic Substitution with Silicon Electrophiles: Catalytic Friedel–Crafts C−H Silylation. *Angew. Chem. Int. Ed.* **2017,** *56*, 52–59.

43.   Shu, C.; Noble, A.; Aggarwal, V. K., Metal-free photoinduced C(sp^3)–H borylation of alkanes. *Nature* **2020,** *586*, 714–719.

44.   Sarkar, S.; Wagulde, S.; Jia, X.; Gevorgyan, V., General and selective metal-free radical α-C–H borylation of aliphatic amines. *Chem* **2022,** *8*, 3096–3108.

45.   Tu, J.-L.; Hu, A.-M.; Guo, L.; Xia, W., Iron-Catalyzed C(sp^3)–H Borylation, Thiolation, and Sulfinylation Enabled by Photoinduced Ligand-to-Metal Charge Transfer. *J. Am. Chem. Soc.* **2023,** *145*, 7600–7611.

46.   Liu, S.; Pan, P.; Fan, H.; Li, H.; Wang, W.; Zhang, Y., Photocatalytic C–H silylation of heteroarenes by using trialkylhydrosilanes. *Chem. Sci.* **2019,** *10*, 3817–3825.

47.   Rammal, F.; Gao, D.; Boujnah, S.; Hussein, A. A.; Lalevée, J.; Gaumont, A.-C.; Morlet-Savary, F.; Lakhdar, S., Photochemical C–H Silylation and Hydroxymethylation of Pyridines and Related Structures: Synthetic Scope and Mechanisms. *ACS Catal.* **2020,** *10*, 13710–13717.

48.   Kim, J. H.; Constantin, T.; Simonetti, M.; Llaveria, J.; Sheikh, N. S.; Leonori, D., A Radical Approach for the Selective C–H Borylation of Azines. *Nature* **2021,** *595*, 677–683.

49.   Du, W.; Kaskar, B.; Blumbergs, P.; Subramanian, P. K.; Curran, D. P., Semisynthesis of DB-67 and other Silatecans from Camptothecin by Thiol-Promoted Addition of Silyl Radicals. *Bioorg. Med. Chem.* **2003,** *11*, 451–458.

50.   Leonori, D.; Aggarwal, V. K., Lithiation–Borylation Methodology and Its Application in Synthesis. *Acc. Chem. Res.* **2014,** *47*, 3174–3183.

51.   Miyaura, N.; Suzuki, A., Palladium-Catalyzed Cross-Coupling Reactions of Organoboron Compounds. *Chem. Rev.* **1995,** *95*, 2457–2483.

52.   Suzuki, A., Cross-Coupling Reactions Of Organoboranes: An Easy Way To Construct C–C Bonds (Nobel Lecture). *Angew. Chem. Int. Ed.* **2011,** *50*, 6722–6737.

53.   Beck, E. M.; Hatley, R.; Gaunt, M. J., Synthesis of Rhazinicine by a Metal-Catalyzed C–H Bond Functionalization Strategy. *Angew. Chem. Int. Ed.* **2008,** *47*, 3004–3007.

54.   Kholod, I.; Vallat, O.; Buciumas, A.-M.; Neels, A.; Neier, R., Synthetic Strategies for the Synthesis and Transformation of Substituted Pyrrolinones as Advanced Intermediates for Rhazinilam Analogues. *Eur. J. Org. Chem.* **2014,** *2014*, 7865–7877.

55.   Kikuchi, T.; Takagi, J.; Isou, H.; Ishiyama, T.; Miyaura, N., Vinylic C–H Borylation of Cyclic Vinyl Ethers with Bis(pinacolato)diboron Catalyzed by an Iridium(I)-dtbpy Complex. *Chem. Asian J.* **2008,** *3*, 2082–2090.

56.   Fischer, D. F.; Sarpong, R., Total Synthesis of (+)-Complanadine A Using an Iridium-Catalyzed Pyridine C−H Functionalization. *J. Am. Chem. Soc.* **2010,** *132*, 5926–5927.

57.   Robbins, D. W.; Boebel, T. A.; Hartwig, J. F., Iridium-Catalyzed, Silyl-Directed Borylation of Nitrogen-Containing Heterocycles. *J. Am. Chem. Soc.* **2010,** *132*, 4068–4069.

58.   Liskey, C. W.; Liao, X. B.; Hartwig, J. F., Cyanation of Arenes via Iridium-Catalyzed Borylation. *J. Am. Chem. Soc.* **2010,** *132*, 11389–11391.

59.   Sumida, Y.; Harada, R.; Kato-Sumida, T.; Johmoto, K.; Uekusa, H.; Hosoya, T., Boron-Selective Biaryl Coupling Approach to Versatile Dibenzoxaborins and Application to Concise Synthesis of Defucogilvocarcin M. *Org. Lett.* **2014,** *16*, 6240–6243.

60.   Han, S.; Movassaghi, M., Concise Total Synthesis and Stereochemical Revision of all (−)-Trigonoliimines. *J. Am. Chem. Soc.* **2011,** *133*, 10768–10771.

61.   Liu, F.; Movassaghi, M., Electrophilic Carbonyl Activation: Competing Condensative Cyclizations of Tryptamine Derivatives. *Tet. Lett.* **2015,** *56*, 2995–3000.

62.   Schwaben, J.; Cordes, J.; Harms, K.; Koert, U., Total Syntheses of (+)-Pestaphthalide A and (-)-Pestaphthalide B. *Synthesis* **2011,** *2011*, 2929–2934.

63.   Bartholomäus, R.; Dommershausen, F.; Thiele, M.; Karanjule, N. S.; Harms, K.; Koert, U., Total Synthesis of the Postulated Structure of Fulicineroside. *Eur. J. Chem.* **2013,** *19*, 7423–7436.

64.   López-Rodríguez, R.; Ros, A.; Fernández, R.; Lassaletta, J. M., Pinacolborane as the Boron Source in Nitrogen-Directed Borylations of Aromatic N,N-Dimethylhydrazones. *J. Org. Chem.* **2012,** *77*, 9915–9920.

65.   Filipski, K. J.; Guzman-Perez, A.; Bian, J.; Perreault, C.; Aspnes, G. E.; Didiuk, M. T.; Dow, R. L.; Hank, R. F.; Jones, C. S.; Maguire, R. J.; Tu, M.; Zeng, D.; Liu, S.; Knafels, J. D.; Litchfield, J.; Atkinson, K.; Derksen, D. R.; Bourbonais, F.; Gajiwala, K. S.; Hickey, M.; Johnson, T. O.; Humphries, P. S.; Pfefferkorn, J. A., Pyrimidone-Based Series of Glucokinase Activators with Alternative Donor–Acceptor Motif. *Bioorg. Med. Chem. Lett.* **2013,** *23*, 4571–4578.

66.   Seechurn, C. C. C. J.; Sivakumar, V.; Satoskar, D.; Colacot, T. J., Iridium-Catalyzed C–H Borylation of Heterocycles Using an Overlooked 1,10-Phenanthroline Ligand: Reinventing the Catalytic Activity by Understanding the Solvent-Assisted Neutral to Cationic Switch. *Organometallics* **2014,** *33*, 3514–3522.

67.   Kallepalli, V. A.; Shi, F.; Paul, S.; Onyeozili, E. N.; Maleczka, R. E.; Smith, M. R. I., Boc Groups as Protectors and Directors for Ir-Catalyzed C–H Borylation of Heterocycles. *J. Org. Chem.* **2009,** *74*, 9199–9201.

68.   Shockley, S. E.; Holder, J. C.; Stoltz, B. M., A Catalytic, Enantioselective Formal Synthesis of (+)-Dichroanone and (+)-Taiwaniaquinone H. *Org. Lett.* **2014,** *16*, 6362–6365.

69.   Pitts, A. K.; O'Hara, F.; Snell, R. H.; Gaunt, M. J., A Concise and Scalable Strategy for the Total Synthesis of Dictyodendrin B Based on Sequential C–H Functionalization. *Angew. Chem. Int. Ed.* **2015,** *54*, 5451–5455.

70.   Li, H. L.; Kuninobu, Y.; Kanai, M., Lewis Acid–Base Interaction-Controlled ortho-Selective C−H Borylation of Aryl Sulfides. *Angew. Chem. Int. Ed.* **2017,** *56*, 1495–1499.

71.   Li, H.-L.; Kanai, M.; Kuninobu, Y., Iridium/Bipyridine-Catalyzed ortho-Selective C–H Borylation of Phenol and Aniline Derivatives. *Org. Lett.* **2017,** *19*, 5944–5947.

72.   Obligacion, J. V.; Bezdek, M. J.; Chirik, P. J., C(sp^2)–H Borylation of Fluorinated Arenes Using an Air-Stable Cobalt Precatalyst: Electronically Enhanced Site Selectivity Enables Synthetic Opportunities. *J. Am. Chem. Soc.* **2017,** *139*, 2825–2832.

73.   Cao, B.-C.; Wu, G.-J.; Yu, F.; He, Y.-P.; Han, F.-S., A Total Synthesis of (−)-Hamigeran B and (−)-4-Bromohamigeran B. *Org. Lett.* **2018,** *20*, 3687–3690.

74.   Shi, Y.; Yang, Y.; Xu, S., Iridium-Catalyzed Enantioselective C(sp^3)−H Borylation of Aminocyclopropanes. *Angew. Chem. Int. Ed.* **2022,** *61*, e202201463.

75.   Marcos-Atanes, D.; Vidal, C.; Navo, C. D.; Peccati, F.; Jiménez-Osés, G.; Mascareñas, J. L., Iridium-Catalyzed ortho-Selective Borylation of Aromatic Amides Enabled by 5-Trifluoromethylated Bipyridine Ligands. *Angew. Chem. Int. Ed. n/a*, e202214510.

76.   Miller, J. F.; Chong, P. Y.; Shotwell, J. B.; Catalano, J. G.; Tai, V. W. F.; Fang, J.; Banka, A. L.; Roberts, C. D.; Youngman, M.; Zhang, H.; Xiong, Z.; Mathis, A.; Pouliot, J. J.; Hamatake, R. K.; Price, D. J.; Seal, J. W., III; Stroup, L. L.; Creech, K. L.; Carballo, L.

H.; Todd, D.; Spaltenstein, A.; Furst, S.; Hong, Z.; Peat, A. J., Hepatitis C Replication Inhibitors That Target the Viral NS4B Protein. *J. Med. Chem.* **2014,** *57*, 2107–2120.

77.   Campeau, L.-C.; Chen, Q.; Gauvreau, D.; Girardin, M.; Belyk, K.; Maligres, P.; Zhou, G.; Gu, C.; Zhang, W.; Tan, L.; O'Shea, P. D., A Robust Kilo-Scale Synthesis of Doravirine. *Org. Process Res. Dev.* **2016,** *20*, 1476–1481.

78.   Feng, Y.; Holte, D.; Zoller, J.; Umemiya, S.; Simke, L. R.; Baran, P. S., Total Synthesis of Verruculogen and Fumitremorgin A Enabled by Ligand-Controlled C–H Borylation. *J. Am. Chem. Soc.* **2015,** *137*, 10160–10163.

79.   Murphy, J. M.; Liao, X.; Hartwig, J. F., Meta Halogenation of 1,3-Disubstituted Arenes via Iridium-Catalyzed Arene Borylation. *J. Am. Chem. Soc.* **2007,** *129*, 15434–15435.

80.   Cordes, J.; Wessel, C.; Harms, K.; Koert, U., meta-Selective Aromatic Borylation as Key Step in the Synthesis of Poipuol. *Synthesis* **2008,** *2008*, 2217–2220.

81.   Zhao, L.; Tsukano, C.; Kwon, E.; Takemoto, Y.; Hirama, M., Total Syntheses of Complanadines A and B. *Angew. Chem. Int. Ed.* **2013,** *52*, 1722–1725.

82.   Zhao, L.; Tsukano, C.; Kwon, E.; Shirakawa, H.; Kaneko, S.; Takemoto, Y.; Hirama, M., Competent Route to Unsymmetric Dimer Architectures: Total Syntheses of (−)-Lycodine and (−)-Complanadines A and B, and Evaluation of Their Neurite Outgrowth Activities. *Eur. J. Chem.* **2017,** *23*, 802–812.

83.   Sieser, J. E.; Maloney, M. T.; Chisowa, E.; Brenek, S. J.; Monfette, S.; Salisbury, J. J.; Do, N. M.; Singer, R. A., Ir-Catalyzed Borylation as an Efficient Route to a Nicotine Hapten. *Org. Process Res. Dev.* **2018,** *22*, 527–534.

84.   Robinson, H.; Stillibrand, J.; Simelis, K.; Macdonald, S. J. F.; Nortcliffe, A., Iridium-catalysed C–H borylation of β-aryl-aminopropionic acids. *Org. Biomol. Chem.* **2020,** *18*, 6696–6701.

85.   Srinivasan, R.; Coyne, A. G.; Abell, C., Regioselective Conversion of Arenes to N-aryl-1,2,3-triazoles Using C–H Borylation. *Eur. J. Chem.* **2014,** *20*, 11680–11684.

86.   Li, X.; Deng, X.; Coyne, A. G.; Srinivasan, R., meta-Nitration of Arenes Bearing ortho/para Directing Group(s) Using C−H Borylation. *Chem. Eur. J.* **2019,** *25*, 8018–8023.

87.   Loach, R. P.; Fenton, O. S.; Amaike, K.; Siegel, D. S.; Ozkal, E.; Movassaghi, M., C7-Derivatization of C3-Alkylindoles Including Tryptophans and Tryptamines. *J. Org. Chem.* **2014,** *79*, 11254–11263.

88.   Kallepalli, V. A.; Gore, K. A.; Shi, F.; Sanchez, L.; Chotana, G. A.; Miller, S. L.; Maleczka, R. E.; Smith, M. R., Harnessing C–H Borylation/Deborylation for Selective Deuteration, Synthesis of Boronate Esters, and Late Stage Functionalization. *J. Org. Chem.* **2015,** *80*, 8341–8353.

89.   Meyer, F.-M.; Liras, S.; Guzman-Perez, A.; Perreault, C.; Bian, J.; James, K., Functionalization of Aromatic Amino Acids via Direct C−H Activation: Generation of Versatile Building Blocks for Accessing Novel Peptide Space. *Org. Lett.* **2010,** *12*, 3870–3873.

90.   Hananya, N.; Eldar Boock, A.; Bauer, C. R.; Satchi-Fainaro, R.; Shabat, D., Remarkable Enhancement of Chemiluminescent Signal by Dioxetane–Fluorophore Conjugates: Turn-ON Chemiluminescence Probes with Color Modulation for Sensing and Imaging. *J. Am. Chem. Soc.* **2016,** *138*, 13438–13446.

91.   Miura, W.; Hirano, K.; Miura, M., Iridium-Catalyzed Site-Selective C–H Borylation of 2-Pyridones. *Synthesis* **2017,** *49*, 4745–4752.

92.   Fischer, D. F.; Sarpong, R., Total Synthesis of (+)-Complanadine A Using an Iridium-Catalyzed Pyridine C–H Functionalization. *J. Am. Chem. Soc.* **2010,** *132*, 5926–5927.

93.   Antropow, A. H.; Garcia, N. R.; White, K. L.; Movassaghi, M., Enantioselective Synthesis of (−)-Vallesine: Late-Stage C17-Oxidation via Complex Indole Boronation. *Org. Lett.* **2018,** *20*, 3647–3650.

94.	Myeong, I.-S.; Avci, N. H.; Movassaghi, M., Total Synthesis of (−)-Kopsifoline A and (+)-Kopsifoline E. *Org. Lett.* **2021,** *23*, 9118–9122.

95.	Gao, P.; Szostak, M., Highly Selective and Divergent Acyl and Aryl Cross-Couplings of Amides via Ir-Catalyzed C–H Borylation/N–C(O) Activation. *Org. Lett.* **2020,** *22*, 6010–6015.

96.	Wright, J. S.; Sharninghausen, L. S.; Preshlock, S.; Brooks, A. F.; Sanford, M. S.; Scott, P. J. H., Sequential Ir/Cu-Mediated Method for the Meta-Selective C–H Radiofluorination of (Hetero)Arenes. *J. Am. Chem. Soc.* **2021,** *143*, 6915–6921.

97.	Brooks, A. F.; Topczewski, J. J.; Ichiishi, N.; Sanford, M. S.; Scott, P. J. H., Late-Stage [18F]Fluorination: New Solutions to Old Problems. *Chem. Sci.* **2014,** *5*, 4545–4553.

98.	Gayler, K. M.; Kong, K.; Reisenauer, K.; Taube, J. H.; Wood, J. L., Staurosporine Analogs Via C–H Borylation. *ACS Med. Chem. Lett.* **2020,** *11*, 2441–2445.

99.	Bream, R. N.; Clark, H.; Edney, D.; Harsanyi, A.; Hayler, J.; Ironmonger, A.; Mc Cleary, N.; Phillips, N.; Priestley, C.; Roberts, A.; Rushworth, P.; Szeto, P.; Webb, M. R.; Wheelhouse, K., Application of C–H Functionalization in the Development of a Concise and Convergent Route to the Phosphatidylinositol-3-kinase Delta Inhibitor Nemiralisib. *Org. Process Res. Dev.* **2021,** *25*, 529–540.

100.	Saito, Y.; Segawa, Y.; Itami, K., para-C–H Borylation of Benzene Derivatives by a Bulky Iridium Catalyst. *J. Am. Chem. Soc.* **2015,** *137*, 5193–5198.

101.	Saito, Y.; Yamanoue, K.; Segawa, Y.; Itami, K., Selective Transformation of Strychnine and 1,2-Disubstituted Benzenes by C–H Borylation. *Chem* **2020,** *6*, 985–993.

102.	Hoque, M. E.; Bisht, R.; Unnikrishnan, A.; Dey, S.; Mahamudul Hassan, M. M.; Guria, S.; Rai, R. N.; Sunoj, R. B.; Chattopadhyay, B., Iridium-Catalyzed Ligand-Controlled Remote para-Selective C−H Activation and Borylation of Twisted Aromatic Amides. *Angew. Chem. Int. Ed.* **2022,** *61*, e202203539.

103.	Kuleshova, O.; Asako, S.; Ilies, L., Ligand-Enabled, Iridium-Catalyzed ortho-Borylation of Fluoroarenes. *ACS Catal.* **2021,** *11*, 5968–5973.

104.	Ramadoss, B.; Jin, Y.; Asako, S.; Ilies, L., Remote Steric Control for Undirected meta-Selective C–H Activation of Arenes. *Science* **2022,** *375*, 658–663.

105.	Marcos-Atanes, D.; Vidal, C.; Navo, C. D.; Peccati, F.; Jiménez-Osés, G.; Mascareñas, J. L., Iridium-Catalyzed ortho-Selective Borylation of Aromatic Amides Enabled by 5-Trifluoromethylated Bipyridine Ligands. *Angew. Chem. Int. Ed.* **2023,** *62*, e202214510.

106.	Scott, J. S.; Moss, T. A.; Barlaam, B.; Davey, P. R. J.; Fairley, G.; Gangl, E. T.; Greenwood, R. D. R.; Hatoum-Mokdad, H.; Lister, A. S.; Longmire, D.; Polanski, R.; Stokes, S.; Tucker, M. J.; Varnes, J. G.; Yang, B., Addition of Fluorine and a Late-Stage Functionalization (LSF) of the Oral SERD AZD9833. *ACS Med. Chem. Lett.* **2020,** *11*, 2519–2525.

107.	Mahamudul Hassan, M. M.; Mondal, B.; Singh, S.; Haldar, C.; Chaturvedi, J.; Bisht, R.; Sunoj, R. B.; Chattopadhyay, B., Ir-Catalyzed Ligand-Free Directed C–H Borylation of Arenes and Pharmaceuticals: Detailed Mechanistic Understanding. *J. Org. Chem.* **2022,** *87*, 4360–4375.

108.	Hoque, M. E.; Hassan, M. M. M.; Chattopadhyay, B., Remarkably Efficient Iridium Catalysts for Directed C(sp²)–H and C(sp³)–H Borylation of Diverse Classes of Substrates. *J. Am. Chem. Soc.* **2021,** *143*, 5022–5037.

109.	Oeschger, R.; Su, B.; Yu, I.; Ehinger, C.; Romero, E.; He, S.; Hartwig, J., Diverse functionalization of strong alkyl C–H bonds by undirected borylation. *Science* **2020,** *368*, 736–741.

110.	Zhang, L. S.; Chen, G. H.; Wang, X.; Guo, Q. Y.; Zhang, X. S.; Pan, F.; Chen, K.; Shi, Z. J., Direct Borylation of Primary C-H Bonds in Functionalized Molecules by Palladium Catalysis. *Angew. Chem. Int. Ed.* **2014,** *53*, 3899–3903.

111.   Chandrashekar, H. B.; Dolui, P.; Li, B.; Mandal, A.; Liu, H.; Guin, S.; Ge, H.; Maiti, D., Ligand-Enabled δ-C(sp^3)−H Borylation of Aliphatic Amines. *Angew. Chem. Int. Ed.* **2021,** *60*, 18194–18200.

112.   He, J.; Jiang, H.; Takise, R.; Zhu, R.-Y.; Chen, G.; Dai, H.-X.; Dhar, T. G. M.; Shi, J.; Zhang, H.; Cheng, P. T. W.; Yu, J.-Q., Ligand-Promoted Borylation of C(sp^3)–H Bonds with Palladium(II) Catalysts. *Angew. Chem. Int. Ed.* **2016,** *55*, 785–789.

113.   Shi, Y.; Gao, Q.; Xu, S., Chiral Bidentate Boryl Ligand Enabled Iridium-Catalyzed Enantioselective C(sp^3)–H Borylation of Cyclopropanes. *J. Am. Chem. Soc.* **2019,** *141*, 10599–10604.

114.   Gao, Q.; Xu, S., Site- and Stereoselective C(sp^3)−H Borylation of Strained (Hetero)Cycloalkanols Enabled by Iridium Catalysis. *Angew. Chem. Int. Ed.* **2023,** *62*, e202218025.

115.   Yang, Y.; Chen, L.; Xu, S., Iridium-Catalyzed Enantioselective Unbiased Methylene C(sp^3)–H Borylation of Acyclic Amides. *Angew. Chem. Int. Ed.* **2021,** *60*, 3524–3528.

116.   Chen, L.; Yang, Y.; Liu, L.; Gao, Q.; Xu, S., Iridium-Catalyzed Enantioselective α-C(sp^3)–H Borylation of Azacycles. *J. Am. Chem. Soc.* **2020,** *142*, 12062–12068.

117.   Du, R.; Liu, L.; Xu, S., Iridium-Catalyzed Regio- and Enantioselective Borylation of Unbiased Methylene C(sp^3)−H Bonds at the Position β to a Nitrogen Center. *Angew. Chem. Int. Ed.* **2021,** *60*, 5843–5847.

118.   Zou, X.; Li, Y.; Ke, Z.; Xu, S., Chiral Bidentate Boryl Ligand-Enabled Iridium-Catalyzed Enantioselective Dual C–H Borylation of Ferrocenes: Reaction Development and Mechanistic Insights. *ACS Catal.* **2022,** *12*, 1830–1840.

119.   Bruch, A.; Fukazawa, A.; Yamaguchi, E.; Yamaguchi, S.; Studer, A., Bis(phosphoryl)-Bridged Biphenyls by Radical Phosphanylation: Synthesis and Photophysical and Electrochemical Properties. *Angew. Chem. Int. Ed.* **2011,** *50*, 12094–12098.

120.   Rauch, F.; Fuchs, S.; Friedrich, A.; Sieh, D.; Krummenacher, I.; Braunschweig, H.; Finze, M.; Marder, T. B., Highly Stable, Readily Reducible, Fluorescent, Trifluoromethylated 9-Borafluorenes. *Eur. J. Chem.* **2020,** *26*, 12794–12808.

121.   Narsaria, A. K.; Rauch, F.; Krebs, J.; Endres, P.; Friedrich, A.; Krummenacher, I.; Braunschweig, H.; Finze, M.; Nitsch, J.; Bickelhaupt, F. M.; Marder, T. B., Computationally Guided Molecular Design to Minimize the LE/CT Gap in D-π-A Fluorinated Triarylboranes for Efficient TADF via D and π-Bridge Tuning. *Adv. Funct. Mater.* **2020,** *30*, 2002064.

122.   Rauch, F.; Krebs, J.; Günther, J.; Friedrich, A.; Hähnel, M.; Krummenacher, I.; Braunschweig, H.; Finze, M.; Marder, T. B., Electronically Driven Regioselective Iridium-Catalyzed C−H Borylation of Donor-π-Acceptor Chromophores Containing Triarylboron Acceptors. *Eur. J. Chem.* **2020,** *26*, 10626–10633.

123.   Kurotobi, K.; Miyauchi, M.; Takakura, K.; Murafuji, T.; Sugihara, Y., Direct Introduction of a Boryl Substituent into the 2-Position of Azulene: Application of the Miyaura and Smith Methods to Azulene. *Eur. J. Org. Chem.* **2003,** *2003*, 3663–3665.

124.   Fujinaga, M.; Murafuji, T.; Kurotobi, K.; Sugihara, Y., Polyborylation of azulenes. *Tetrahedron* **2009,** *65*, 7115–7121.

125.   Nishimura, H.; Eliseeva, M. N.; Wakamiya, A.; Scott, L. T., 1,3,5,7-Tetra(Bpin)azulene by Exhaustive Direct Borylation of Azulene and 5,7-Di(Bpin)azulene by Selective Subsequent Deborylation. *Synlett* **2015,** *26*, 1578–1580.

126.   Nishimura, H.; Ishida, N.; Shimazaki, A.; Wakamiya, A.; Saeki, A.; Scott, L. T.; Murata, Y., Hole-Transporting Materials with a Two-Dimensionally Expanded π-System around an Azulene Core for Efficient Perovskite Solar Cells. *J. Am. Chem. Soc.* **2015,** *137*, 15656–15659.

127.   Ryota, O.; Kenji, Y.; Kenji, K., 2,7-Diborylanthracene as a Useful Building Block for Extended π-Conjugated Aromatics. *Chem. Lett.* **2011,** *40*, 941–943.

128.   Takaki, Y.; Yoza, K.; Kobayashi, K., Fourfold C–H Borylation of Anthracene: 1,3,5,7-Tetraborylanthracene and Its Application to 1,3,5,7-Tetraarylanthracenes. *Chem. Lett.* **2017,** *46*, 655–658.

129.   Kimoto, T.; Tanaka, K.; Sakai, Y.; Ohno, A.; Yoza, K.; Kobayashi, K., 2,8- and 2,9-Diboryltetracenes as Useful Building Blocks for Extended π-Conjugated Tetracenes. *Org. Lett.* **2009,** *11*, 3658–3661.

130.   Hitosugi, S.; Nakamura, Y.; Matsuno, T.; Nakanishi, W.; Isobe, H., Iridium-Catalyzed Direct Borylation of Phenacenes. *Tet. Lett.* **2012,** *53*, 1180–1182.

131.   Figueira-Duarte, T. M.; Müllen, K., Pyrene-Based Materials for Organic Electronics. *Chem. Rev.* **2011,** *111*, 7260–7314.

132.   Coventry, D. N.; Batsanov, A. S.; Goeta, A. E.; Howard, J. A. K.; Marder, T. B.; Perutz, R. N., Selective Ir-Catalysed Borylation of Polycyclic Aromatic Hydrocarbons: Structures of Naphthalene-2,6-bis(boronate), Pyrene-2,7-bis(boronate) and Perylene-2,5,8,11-tetra(boronate) Esters. *Chem. Commun.* **2005**, 2172–2174.

133.   Crawford, A. G.; Liu, Z.; Mkhalid, I. A. I.; Thibault, M.-H.; Schwarz, N.; Alcaraz, G.; Steffen, A.; Collings, J. C.; Batsanov, A. S.; Howard, J. A. K.; Marder, T. B., Synthesis of 2- and 2,7-Functionalized Pyrene Derivatives: An Application of Selective C–H Borylation. *Eur. J. Chem.* **2012,** *18*, 5022–5035.

134.   Ji, L.; Fucke, K.; Bose, S. K.; Marder, T. B., Iridium-Catalyzed Borylation of Pyrene: Irreversibility and the Influence of Ligand on Selectivity. *J. Org. Chem.* **2015,** *80*, 661–665.

135.   Kano, H.; Uehara, K.; Matsuo, K.; Hayashi, H.; Yamada, H.; Aratani, N., Direct borylation of terrylene and quaterrylene. *Beilstein J. Org. Chem.* **2020,** *16*, 621–627.

136.   Zhang, G.; Rominger, F.; Zschieschang, U.; Klauk, H.; Mastalerz, M., Facile Synthetic Approach to a Large Variety of Soluble Diarenoperylenes. *Eur. J. Chem.* **2016,** *22*, 14840–14845.

137.   Li, T.-Y.; Lin, Y.-C.; Song, Y.-H.; Lu, H.-F.; Chao, I.; Lin, C.-H., Synthesis and Physical Study of Perylene and Anthracene Polynitrile as Electron Acceptors. *Org. Lett.* **2019,** *21*, 5397–5401.

138.   Würthner, F., Perylene Bisimide Dyes as Versatile Building Blocks for Functional Supramolecular Architectures. *Chem. Commun.* **2004**, 1564–1579.

139.   Teraoka, T.; Hiroto, S.; Shinokubo, H., Iridium-Catalyzed Direct Tetraborylation of Perylene Bisimides. *Org. Lett.* **2011,** *13*, 2532–2535.

140.   Battagliarin, G.; Li, C.; Enkelmann, V.; Müllen, K., 2,5,8,11-Tetraboronic Ester Perylenediimides: A Next Generation Building Block for Dye-Stuff Synthesis. *Org. Lett.* **2011,** *13*, 3012–3015.

141.   Ito, S.; Hiroto, S.; Shinokubo, H., Facile Synthesis of Nitrogen-containing Polycyclic Aromatic Hydrocarbons from Perylene Bisimides. *Chem. Lett.* **2014,** *43*, 1309–1311.

142.   García-Calvo, V.; Cuevas, J. V.; Barbero, H.; Ferrero, S.; Álvarez, C. M.; González, J. A.; Díaz de Greñu, B.; García-Calvo, J.; Torroba, T., Synthesis of a Tetracorannulene-perylenediimide That Acts as a Selective Receptor for C60 over C70. *Org. Lett.* **2019,** *21*, 5803–5807.

143.   Fan, Y.; Ziabrev, K.; Zhang, S.; Lin, B.; Barlow, S.; Marder, S. R., Comparison of the Optical and Electrochemical Properties of Bi(perylene diimide)s Linked through Ortho and Bay Positions. *ACS Omega* **2017,** *2*, 377–385.

144.   Tajima, K.; Fukui, N.; Shinokubo, H., Aggregation-Induced Emission of Nitrogen-Bridged Naphthalene Monoimide Dimers. *Org. Lett.* **2019,** *21*, 9516–9520.

145.   Kaiser, R. P.; Ulč, J.; Císařová, I.; Nečas, D., Direct regioselective C–H borylation of [5]helicene. *RSC Adv.* **2018,** *8*, 580–583.

146.   Nečas, D.; Kaiser, R. P.; Ulč, J., Selective Borylation of [4]Helicene. *Eur. J. Org. Chem.* **2016,** *2016*, 5647–5652.

147.   Noguchi, H.; Hirose, T.; Yokoyama, S.; Matsuda, K., Fluorescence Behavior of 2,6,10-Trisubstituted 4,8,12-Triazatriangulene Cations in Solution and in the Solid State. *CrystEngComm* **2016,** *18*, 7377–7383.

148.   Frédéric, L.; Fabri, B.; Guénée, L.; Zinna, F.; Di Bari, L.; Lacour, J., Triple Regioselective Functionalization of Cationic [4]Helicenes via Iridium-Catalyzed Borylation and Suzuki Cross-Coupling Reactivity. *Eur. J. Chem.* **2022,** *28*, e202201853.

149.   Peurifoy, S. R.; Castro, E.; Liu, F.; Zhu, X. Y.; Ng, F.; Jockusch, S.; Steigerwald, M. L.; Echegoyen, L.; Nuckolls, C.; Sisto, T. J., Three-Dimensional Graphene Nanostructures. *J. Am. Chem. Soc.* **2018,** *140*, 9341–9345.

150.   Eliseeva, M. N.; Scott, L. T., Pushing the Ir-Catalyzed C–H Polyborylation of Aromatic Compounds to Maximum Capacity by Exploiting Reversibility. *J. Am. Chem. Soc.* **2012,** *134*, 15169–15172.

151.   Kawasumi, K.; Zhang, Q.; Segawa, Y.; Scott, L. T.; Itami, K., A Grossly Warped Nanographene and the Consequences of Multiple Odd-Membered-Ring Defects. *Nat. Chem.* **2013,** *5*, 739–744.

152.   Nagano, T.; Nakamura, K.; Tokimaru, Y.; Ito, S.; Miyajima, D.; Aida, T.; Nozaki, K., Functionalization of Azapentabenzocorannulenes by Fivefold C−H Borylation and Cross-Coupling Arylation: Application to Columnar Liquid-Crystalline Materials. *Eur. J. Chem.* **2018,** *24*, 14075–14078.

153.   Kise, K.; Ooi, S.; Osuka, A.; Tanaka, T., Five-fold-symmetric Pentabromo- and Pentaiodo-corannulenes: Useful Precursors of Heteroatom-substituted Corannulenes. *Asian J. Org. Chem.* **2021,** *10*, 537–540.

154.   Lin, H.-A.; Sato, Y.; Segawa, Y.; Nishihara, T.; Sugimoto, N.; Scott, L. T.; Higashiyama, T.; Itami, K., A Water-Soluble Warped Nanographene: Synthesis and Applications for Photoinduced Cell Death. *Angew. Chem. Int. Ed.* **2018,** *57*, 2874–2878.

155.   Kato, K.; Lin, H.-A.; Kuwayama, M.; Nagase, M.; Segawa, Y.; Scott, L. T.; Itami, K., Two-Step Synthesis of a Red-Emissive Warped Nanographene Eerivative via a Ten-Fold C–H Borylation. *Chem. Sci.* **2019,** *10*, 9038–9041.

156.   Chiu, C.-Y.; Kim, B.; Gorodetsky, A. A.; Sattler, W.; Wei, S.; Sattler, A.; Steigerwald, M.; Nuckolls, C., Shape-shifting in contorted dibenzotetrathienocoronenes. *Chem. Sci.* **2011,** *2*, 1480–1486.

157.   Yamaguchi, R.; Hiroto, S.; Shinokubo, H., Synthesis of Oxygen-Substituted Hexa-peri-hexabenzocoronenes through Ir-Catalyzed Direct Borylation. *Org. Lett.* **2012,** *14*, 2472–2475.

158.   Yamaguchi, R.; Ito, S.; Lee, B. S.; Hiroto, S.; Kim, D.; Shinokubo, H., Functionalization of Hexa-peri-hexabenzocoronenes: Investigation of the Substituent Effects on a Superbenzene. *Chem. Asian J.* **2013,** *8*, 178–190.

159.   Oda, K.; Hiroto, S.; Hisaki, I.; Shinokubo, H., Synthesis of Bright Red-Emissive Dicyanoetheno-Bridged Hexa-Peri-Hexabenzocoronene Dimers. *Org. Biomol. Chem.* **2017,** *15*, 1426–1434.

160.   Nagase, M.; Kato, K.; Yagi, A.; Segawa, Y.; Itami, K., Six-Fold C–H Borylation of Hexa-Peri-Hexabenzocoronene. *Beilstein J. Org. Chem.* **2020,** *16*, 391–397.

161.   Plunkett, K. N.; Godula, K.; Nuckolls, C.; Tremblay, N.; Whalley, A. C.; Xiao, S., Expeditious Synthesis of Contorted Hexabenzocoronenes. *Org. Lett.* **2009,** *11*, 2225–2228.

162.   Kato, S.; Serizawa, Y.; Sakamaki, D.; Seki, S.; Miyake, Y.; Shinokubo, H., Diversity-Oriented Synthesis of Tetrathia[8]circulenes by Sequential C–H Borylation and Annulation. *Chem. Commun.* **2015,** *51*, 16944–16947.

163.   Kato, S.; Akahori, S.; Serizawa, Y.; Lin, X.; Yamauchi, M.; Yagai, S.; Sakurai, T.; Matsuda, W.; Seki, S.; Shinokubo, H.; Miyake, Y., Systematic Synthesis of

Tetrathia[8]circulenes: The Influence of Peripheral Substituents on the Structures and Properties in Solution and Solid States. *J. Org. Chem.* **2020,** *85*, 62–69.

164.   Ikemoto, K.; Yoshii, A.; Izumi, T.; Taka, H.; Kita, H.; Xue, J. Y.; Kobayashi, R.; Sato, S.; Isobe, H., Modular Synthesis of Aromatic Hydrocarbon Macrocycles for Simplified, Single-Layer Organic Light-Emitting Devices. *J. Org. Chem.* **2016,** *81*, 662–666.

165.   Ikemoto, K.; Kobayashi, R.; Sato, S.; Isobe, H., Synthesis and Bowl-in-Bowl Assembly of a Geodesic Phenylene Bowl. *Angew. Chem. Int. Ed.* **2017,** *56*, 6511–6514.

166.   Ikemoto, K.; Lin, J.; Kobayashi, R.; Sato, S.; Isobe, H., Fluctuating Carbonaceous Networks with a Persistent Molecular Shape: A Saddle-Shaped Geodesic Framework of 1,3,5-Trisubstituted Benzene (Phenine). *Angew. Chem. Int. Ed.* **2018,** *57*, 8555–8559.

167.   Sun, Z.; Mio, T.; Ikemoto, K.; Sato, S.; Isobe, H., Synthesis, Structures, and Assembly of Geodesic Phenine Frameworks with Isoreticular Networks of [n]Cyclo-para-phenylenes. *J. Org. Chem.* **2019,** *84*, 3500–3507.

168.   Ikemoto, K.; Akiyoshi, M.; Mio, T.; Nishioka, K.; Sato, S.; Isobe, H., Synthesis of a Negatively Curved Nanocarbon Molecule with an Octagonal Omphalos via Design-of-Experiments Optimizations Supplemented by Machine Learning. *Angew. Chem. Int. Ed.* **2022,** *61*, e202204035.

169.   Zhang, G.; Rominger, F.; Mastalerz, M., Fused π-Extended Truxenes via a Threefold Borylation as the Key Step. *Eur. J. Chem.* **2016,** *22*, 3084–3093.

170.   Wagner, P.; Rominger, F.; Mastalerz, M., Switching the Statistical C3/C1 Ratio in the Threefold Aromatic Substitution of Tribenzotriquinacenes towards the C3 Isomer. *Angew. Chem. Int. Ed.* **2018,** *57*, 11321–11324.

171.   Tomalia, D. A.; Baker, H.; Dewald, J.; Hall, M.; Kallos, G.; Martin, S.; Roeck, J.; Ryder, J.; Smith, P., A New Class of Polymers: Starburst-Dendritic Macromolecules. *Polym. J.* **1985,** *17*, 117–132.

172.   Astruc, D.; Boisselier, E.; Ornelas, C., Dendrimers Designed for Functions: From Physical, Photophysical, and Supramolecular Properties to Applications in Sensing, Catalysis, Molecular Electronics, Photonics, and Nanomedicine. *Chem. Rev.* **2010,** *110*, 1857–1959.

173.   Burn, P. L.; Lo, S.-C.; Samuel, I. D. W., The Development of Light-Emitting Dendrimers for Displays. *Adv. Mater.* **2007,** *19*, 1675–1688.

174.   Finke, A. D.; Moore, J. S., Iterative Synthesis of 1,3,5-Polyphenylene Dendrons via C−H Activation. *Org. Lett.* **2008,** *10*, 4851–4854.

175.   Iwadate, N.; Suginome, M., Synthesis of Masked Haloareneboronic Acids via Iridium-Catalyzed Aromatic C–H Borylation with 1,8-Naphthalenediaminatoborane (danBH). *J. Organomet. Chem.* **2009,** *694*, 1713–1717.

176.   Rauch, F.; Endres, P.; Friedrich, A.; Sieh, D.; Hähnel, M.; Krummenacher, I.; Braunschweig, H.; Finze, M.; Ji, L.; Marder, T. B., An Iterative Divergent Approach to Conjugated Starburst Borane Dendrimers. *Eur. J. Chem.* **2020,** *26*, 12951–12963.

177.   Masuda, R.; Kuwano, S.; Goto, K., Late-Stage Functionalization of the Periphery of Oligophenylene Dendrimers with Various Arene Units via Fourfold C–H Borylation. *J. Org. Chem.* **2021,** *86*, 14433–14443.

178.   Kondo, Y.; García-Cuadrado, D.; Hartwig, J. F.; Boaen, N. K.; Wagner, N. L.; Hillmyer, M. A., Rhodium-Catalyzed, Regiospecific Functionalization of Polyolefins in the Melt. *J. Am. Chem. Soc.* **2002,** *124*, 1164–1165.

179.   Bae, C.; Hartwig, J. F.; Boaen Harris, N. K.; Long, R. O.; Anderson, K. S.; Hillmyer, M. A., Catalytic Hydroxylation of Polypropylenes. *J. Am. Chem. Soc.* **2005,** *127*, 767–776.

180.   Bae, C. S.; Hartwig, J. F.; Chung, H. Y.; Harris, N. K.; Switek, K. A.; Hillmyer, M. A., Regiospecific Side-Chain Functionalization of Linear Low-Density Polyethylene with Polar Groups. *Angew. Chem. Int. Ed.* **2005,** *44*, 6410–6413.

181. Shin, J.; Jensen, S. M.; Ju, J.; Lee, S.; Xue, Z.; Noh, S. K.; Bae, C., Controlled Functionalization of Crystalline Polystyrenes via Activation of Aromatic C−H Bonds. *Macromolecules* **2007,** *40*, 8600–8608.

182. Shin, J.; Chang, A. Y.; Brownell, L. V.; Racoma, I. O.; Ozawa, C. H.; Chung, H.-Y.; Peng, S.; Bae, C., Hydrophilic graft modification of a commercial crystalline polyolefin. *J. Polym. Sci., Part A: Polym. Chem.* **2008,** *46*, 3533–3545.

183. Jo, T. S.; Kim, S. H.; Shin, J.; Bae, C., Highly Efficient Incorporation of Functional Groups into Aromatic Main-Chain Polymer Using Iridium-Catalyzed C−H Activation and Suzuki−Miyaura Reaction. *J. Am. Chem. Soc.* **2009,** *131*, 1656–1657.

184. Chang, Y.; Lee, H. H.; Kim, S. H.; Jo, T. S.; Bae, C., Scope and Regioselectivity of Iridium-Catalyzed C–H Borylation of Aromatic Main-Chain Polymers. *Macromolecules* **2013,** *46*, 1754–1764.

185. Varnado, C. D.; Zhao, X.; Ortiz, M.; Zuo, Z.; Jiang, Z.; Manthiram, A.; Bielawski, C. W., Pyridine- and Pyrimidine-Functionalized Poly(sulfone)s: Performance-Enhancing Crosslinkers for Acid/Base Blend Proton Exchange Membranes Used in Direct Methanol Fuel Cells. *RSC Adv.* **2014,** *4*, 2167–2176.

186. Feng, D.; Mishra, S.; Munyaneza, N. E.; Kundu, S.; Scott, C. N., Facile Transformation of Poly(phenyl ether) by C–H Borylation: A Viable Method to New Aromatic Materials. *Eur. Polym. J.* **2021,** *158*, 110687.

187. Loudet, A.; Burgess, K., BODIPY Dyes and Their Derivatives: Syntheses and Spectroscopic Properties. *Chem. Rev.* **2007,** *107*, 4891–4932.

188. Ulrich, G.; Ziessel, R.; Harriman, A., The Chemistry of Fluorescent Bodipy Dyes: Versatility Unsurpassed. *Angew. Chem. Int. Ed.* **2008,** *47*, 1184–1201.

189. Chen, J.; Mizumura, M.; Shinokubo, H.; Osuka, A., Functionalization of Boron Dipyrrin (BODIPY) Dyes through Iridium and Rhodium Catalysis: A Complementary Approach to α- and β-Substituted BODIPYs. *Eur. J. Chem.* **2009,** *15*, 5942–5949.

190. Kadish, K.; Smith, K. M.; Guilard, R., *The Porphyrin Handbook, Volume 3*. Elsevier: 2000; Vol. 3.

191. Hata, H.; Shinokubo, H.; Osuka, A., Highly Regioselective Ir-Catalyzed β-Borylation of Porphyrins via C−H Bond Activation and Construction of β−β-Linked Diporphyrin. *J. Am. Chem. Soc.* **2005,** *127*, 8264–8265.

192. Baba, H.; Chen, J.; Shinokubo, H.; Osuka, A., Efficient Rhodium-Catalyzed Installation of Unsaturated Ester Functions onto Porphyrins: Site-Specific Heck-Type Addition versus Conjugate Addition. *Eur. J. Chem.* **2008,** *14*, 4256–4262.

193. Chen, J.; Aratani, N.; Shinokubo, H.; Osuka, A., Post-Modification of meso–meso-Linked Porphyrin Arrays by Iridium and Rhodium Catalyses for Tuning of Energy Gap. *Chem. Asian J.* **2009,** *4*, 1126–1133.

194. Hisaki, I.; Hiroto, S.; Kim, K. S.; Noh, S. B.; Kim, D.; Shinokubo, H.; Osuka, A., Synthesis of Doubly β-to-β 1,3-Butadiyne-Bridged Diporphyrins: Enforced Planar Structures and Large Two-Photon Absorption Cross Sections. *Angew. Chem. Int. Ed.* **2007,** *46*, 5125–5128.

195. Song, J.; Jang, S. Y.; Yamaguchi, S.; Sankar, J.; Hiroto, S.; Aratani, N.; Shin, J.-Y.; Easwaramoorthi, S.; Kim, K. S.; Kim, D.; Shinokubo, H.; Osuka, A., 2,5-Thienylene-Bridged Triangular and Linear Porphyrin Trimers. *Angew. Chem. Int. Ed.* **2008,** *47*, 6004–6007.

196. Park, J. K.; Lee, H. R.; Chen, J.; Shinokubo, H.; Osuka, A.; Kim, D., Photoelectrochemical Properties of Doubly β-Functionalized Porphyrin Sensitizers for Dye-Sensitized Nanocrystalline-TiO$_2$ Solar Cells. *J. Phys. Chem. C* **2008,** *112*, 16691–16699.

197. Park, J. K.; Chen, J.; Lee, H. R.; Park, S. W.; Shinokubo, H.; Osuka, A.; Kim, D., Doubly β-Functionalized Meso−Meso Directly Linked Porphyrin Dimer Sensitizers for Photovoltaics. *J. Phys. Chem. C* **2009,** *113*, 21956–21963.

198.   Song, J.; Aratani, N.; Kim, P.; Kim, D.; Shinokubo, H.; Osuka, A., Porphyrin "Lego Block" Strategy To Construct Directly meso–β Doubly Linked Porphyrin Rings. *Angew. Chem. Int. Ed.* **2010,** *49,* 3617–3620.

199.   Song, J.; Kim, P.; Aratani, N.; Kim, D.; Shinokubo, H.; Osuka, A., Strategic Synthesis of 2,6-Pyridylene-Bridged β-to-β Porphyrin Nanorings through Cross-Coupling. *Eur. J. Chem.* **2010,** *16,* 3009–3012.

200.   Song, J.; Aratani, N.; Shinokubo, H.; Osuka, A., A β-to-β 2,5-Thienylene-Bridged Cyclic Porphyrin Tetramer: its Rational Synthesis and 1 : 2 Binding Mode with C60. *Chem. Sci.* **2011,** *2,* 748–751.

201.   Song, J.; Aratani, N.; Shinokubo, H.; Osuka, A., A Porphyrin Nanobarrel That Encapsulates C60. *J. Am. Chem. Soc.* **2010,** *132,* 16356–16357.

202.   Wang, K.; Liu, P.; Zhang, F.; Xu, L.; Zhou, M.; Nakai, A.; Kato, K.; Furukawa, K.; Tanaka, T.; Osuka, A.; Song, J., A Robust Porphyrin-Stabilized Triplet Carbon Diradical. *Angew. Chem. Int. Ed.* **2021,** *60,* 7002–7006.

203.   Fukui, N.; Kim, T.; Kim, D.; Osuka, A., Porphyrin Arch-Tapes: Synthesis, Contorted Structures, and Full Conjugation. *J. Am. Chem. Soc.* **2017,** *139,* 9075–9088.

204.   Yamaguchi, S.; Katoh, T.; Shinokubo, H.; Osuka, A., Porphyrin Pincer Complexes: Peripherally Cyclometalated Porphyrins and Their Catalytic Activities Controlled by Central Metals. *J. Am. Chem. Soc.* **2007,** *129,* 6392–6393.

205.   Song, J.; Aratani, N.; Heo, J. H.; Kim, D.; Shinokubo, H.; Osuka, A., Directly Pd(II)-Bridged Porphyrin Belts with Remarkable Curvatures. *J. Am. Chem. Soc.* **2010,** *132,* 11868–11869.

206.   Yamaguchi, S.; Katoh, T.; Shinokubo, H.; Osuka, A., Pt(II)- and Pt(IV)-Bridged Cofacial Diporphyrins via Carbon−Transition Metal σ-Bonds. *J. Am. Chem. Soc.* **2008,** *130,* 14440–14441.

207.   Yamaguchi, S.; Shinokubo, H.; Osuka, A., Double Cleavage of sp^2 C−H and sp^3 C−H Bonds on One Metal Center: DMF-Appended Cyclometalated Platinum(II) and -(IV) Porphyrins. *Inorg. Chem.* **2009,** *48,* 795–797.

208.   Yamaguchi, S.; Shinokubo, H.; Osuka, A., η2-Porphyrin Ru(II) π Complexes. *J. Am. Chem. Soc.* **2010,** *132,* 9992–9993.

209.   Yoshida, K.; Yamaguchi, S.; Osuka, A.; Shinokubo, H., Platinum(II) and Platinum(IV) Porphyrin Pincer Complexes: Synthesis, Structures, and Reactivity. *Organometallics* **2010,** *29,* 3997–4000.

210.   Yamamoto, J.; Shimizu, T.; Yamaguchi, S.; Aratani, N.; Shinokubo, H.; Osuka, A., Synthesis of a Diimidazolylporphyrin Pincer Palladium Complex. *J. Porphyr. Phthalocyanines* **2011,** *15,* 534–538.

211.   Hiroto, S.; Hisaki, I.; Shinokubo, H.; Osuka, A., Synthesis of Directly and Doubly Linked Dioxoisobacteriochlorin Dimers. *J. Am. Chem. Soc.* **2008,** *130,* 16172–16173.

212.   Hata, H.; Yamaguchi, S.; Mori, G.; Nakazono, S.; Katoh, T.; Takatsu, K.; Hiroto, S.; Shinokubo, H.; Osuka, A., Regioselective Borylation of Porphyrins by C–H Bond Activation under Iridium Catalysis to Afford Useful Building Blocks for Porphyrin Assemblies. *Chem. Asian J.* **2007,** *2,* 849–859.

213.   Ghosh, A.; Steene, E., High-Valent Transition Metal Centers Versus Noninnocent Ligands in Metallocorroles: Insights from Electrochemistry and Implications for High-Valent Heme Protein Intermediates. *J. Inorg. Biochem.* **2002,** *91,* 423–436.

214.   Aviv-Harel, I.; Gross, Z., Aura of Corroles. *Eur. J. Chem.* **2009,** *15,* 8382–8394.

215.   Hiroto, S.; Hisaki, I.; Shinokubo, H.; Osuka, A., Synthesis of Corrole Derivatives through Regioselectgive Ir-Catalyzed Direct Borylation. *Angew. Chem. Int. Ed.* **2005,** *44,* 6763–6766.

216.   Hiroto, S.; Furukawa, K.; Shinokubo, H.; Osuka, A., Synthesis and Biradicaloid Character of Doubly Linked Corrole Dimers. *J. Am. Chem. Soc.* **2006,** *128*, 12380–12381.

217.   Cho, S.; Lim, J. M.; Hiroto, S.; Kim, P.; Shinokubo, H.; Osuka, A.; Kim, D., Unusual Interchromophoric Interactions in β,β′ Directly and Doubly Linked Corrole Dimers: Prohibited Electronic Communication and Abnormal Singlet Ground States. *J. Am. Chem. Soc.* **2009,** *131*, 6412–6420.

218.   Claessens, C. G.; González-Rodríguez, D.; Rodríguez-Morgade, M. S.; Medina, A.; Torres, T., Subphthalocyanines, Subporphyrazines, and Subporphyrins: Singular Nonplanar Aromatic Systems. *Chem. Rev.* **2014,** *114*, 2192–2277.

219.   Shimizu, S., Recent Advances in Subporphyrins and Triphyrin Analogues: Contracted Porphyrins Comprising Three Pyrrole Rings. *Chem. Rev.* **2017,** *117*, 2730–2784.

220.   Kitano, M.; Okuda, Y.; Tsurumaki, E.; Tanaka, T.; Yorimitsu, H.; Osuka, A., β,β-Diborylated Subporphyrinato Boron(III) Complexes as Useful Synthetic Precursors. *Angew. Chem. Int. Ed.* **2015,** *54*, 9275–9279.

221.   Morimoto, Y.; Osuka, A.; Tanaka, T., Synthesis, Properties and Reactivity of an ortho-Phenylene-Cyclopentene-Bridged Tetrapyrrole. *J. Porphyr. Phthalocyanines* **2021,** *25*, 937–943.

222.   Morimoto, Y.; Chen, F.; Matsuo, Y.; Kise, K.; Tanaka, T.; Osuka, A., Improved Synthesis of ortho-Phenylene-bridged Cyclic Tetrapyrroles and Oxidative Fusion Reactions Toward Substituted Tetraaza[8]circulenes. *Chem. Asian J.* **2021,** *16*, 648–655.

223.   Matsuo, Y.; Kise, K.; Morimoto, Y.; Osuka, A.; Tanaka, T., Fold-in Synthesis of a Pentabenzopentaaza[10]circulene. *Angew. Chem. Int. Ed.* **2022,** *61*, e202116789.

224.   Rao, Y.; Kim, T.; Park, K. H.; Peng, F.; Liu, L.; Liu, Y.; Wen, B.; Liu, S.; Kirk, S. R.; Wu, L.; Chen, B.; Ma, M.; Zhou, M.; Yin, B.; Zhang, Y.; Kim, D.; Song, J., π-Extended "Earring" Porphyrins with Multiple Cavities and Near-Infrared Absorption. *Angew. Chem. Int. Ed.* **2016,** *55*, 6438–6442.

225.   Wu, L.; Li, F.; Rao, Y.; Wen, B.; Xu, L.; Zhou, M.; Tanaka, T.; Osuka, A.; Song, J., Synthesis, Structures, and Near-IR Absorption of Heterole-Fused Earring Porphyrins. *Angew. Chem. Int. Ed.* **2019,** *58*, 8124–8128.

226.   Mori, G.; Shinokubo, H.; Osuka, A., Highly Selective Ir-Catalyzed Direct Sixfold Borylation of Peripheral Aromatic Substituents on Hexakisaryl-Substituted [28]Hexaphyrin(1.1.1.1.1.1). *Tet. Lett.* **2008,** *49*, 2170–2172.

227.   Nakamura, S.; Hiroto, S.; Shinokubo, H., Synthesis and oxidation of cyclic tetraindole. *Chem. Sci.* **2012,** *3*, 524–527.

228.   Nakamura, S.; Kondo, T.; Hiroto, S.; Shinokubo, H., Porphyrin Analogues That Consist of Indole, Benzofuran, and Benzothiophene Subunits. *Asian J. Org. Chem.* **2013,** *2*, 312–319.

229.   Perepichka, I. F.; Perepichka, D. F., *Handbook of Thiophene-Based Materials.* 2009.

230.   Maegawa, Y.; Inagaki, S., Iridium–Bipyridine Periodic Mesoporous Organosilica Catalyzed Direct C–H Borylation using a Pinacolborane. *Dalton Trans.* **2015,** *44*, 13007–13016.

231.   Osaka, I.; Abe, T.; Mori, H.; Saito, M.; Takemura, N.; Koganezawa, T.; Takimiya, K., Small band gap polymers incorporating a strong acceptor, thieno[3,2-b]thiophene-2,5-dione, with p-channel and ambipolar charge transport characteristics. *J. Mater. Chem. C* **2014,** *2*, 2307–2312.

232.   Nakano, M.; Shinamura, S.; Sugimoto, R.; Osaka, I.; Miyazaki, E.; Takimiya, K., Borylation on Benzo[1,2-b:4,5-b′]- and Naphtho[1,2-b:5,6-b′]dichalcogenophenes: Different Chalcogen Atom Effects on Borylation Reaction Depending on Fused Ring Structure. *Org. Lett.* **2012,** *14*, 5448–5451.

233. Shinamura, S.; Sugimoto, R.; Yanai, N.; Takemura, N.; Kashiki, T.; Osaka, I.; Miyazaki, E.; Takimiya, K., Orthogonally Functionalized Naphthodithiophenes: Selective Protection and Borylation. *Org. Lett.* **2012,** *14*, 4718–4721.

234. Osaka, I.; Komatsu, K.; Koganezawa, T.; Takimiya, K., 5,10-Linked Naphthodithiophenes as the Building Block for Semiconducting Polymers. *Sci. Technol. Adv. Mater.* **2014,** *15*, 024201.

235. Kawashima, K.; Miyazaki, E.; Shimawaki, M.; Inoue, Y.; Mori, H.; Takemura, N.; Osaka, I.; Takimiya, K., 5,10-Diborylated Naphtho[1,2-c:5,6-c′]bis[1,2,5]thiadiazole: a Ready-to-use Precursor for the Synthesis of High-Performance Semiconducting Polymers. *Polym. Chem.* **2013,** *4*, 5224–5227.

236. Osaka, I.; Takimiya, K., Naphthobischalcogenadiazole Conjugated Polymers: Emerging Materials for Organic Electronics. *Adv. Mater.* **2017,** *29*, 1605218.

237. Kurosawa, T.; Okamoto, T.; Cen, D.; Ikeda, D.; Ishii, H.; Takeya, J., Chrysenodithiophene-Based Conjugated Polymer: An Elongated Fused π-Electronic Backbone with a Unique Orbital Structure Toward Efficient Intermolecular Carrier Transport. *Macromolecules* **2021,** *54*, 2113–2123.

238. Chen, Y.; Yekta, S.; Yudin, A. K., Modified BINOL Ligands in Asymmetric Catalysis. *Chem. Rev.* **2003,** *103*, 3155–3212.

239. Brunel, J. M., BINOL: A Versatile Chiral Reagent. *Chem. Rev.* **2005,** *105*, 857–898.

240. Ahmed, I.; Clark, D. A., Rapid Synthesis of 3,3′ Bis-Arylated BINOL Derivatives Using a C–H Borylation in Situ Suzuki–Miyaura Coupling Sequence. *Org. Lett.* **2014,** *16*, 4332–4335.

241. Bisht, R.; Chaturvedi, J.; Pandey, G.; Chattopadhyay, B., Double-Fold Ortho and Remote C–H Bond Activation/Borylation of BINOL: A Unified Strategy for Arylation of BINOL. *Org. Lett.* **2019,** *21*, 6476–6480.

242. Datta, A.; Köllhofer, A.; Plenio, H., Ir-Catalyzed C–H Activation in the Synthesis of Borylated Ferrocenes and Half-Sandwich Compounds. *Chem. Commun.* **2004**, 1508–1509.

243. Wright, S. E.; Richardson-Solorzano, S.; Stewart, T. N.; Miller, C. D.; Morris, K. C.; Daley, C. J. A.; Clark, T. B., Accessing Ambiphilic Phosphine Boronates through C−H Borylation by an Unforeseen Cationic Iridium Complex. *Angew. Chem. Int. Ed.* **2019,** *58*, 2834–2838.

244. Morris, K. C.; Wright, S. E.; Meyer, G. F.; Clark, T. B., Phosphine-Directed sp³ C–H, C–O, and C–N Borylation. *J. Org. Chem.* **2020,** *85*, 14795–14801.

245. Fukuda, K.; Iwasawa, N.; Takaya, J., Ruthenium-Catalyzed ortho C−H Borylation of Arylphosphines. *Angew. Chem. Int. Ed.* **2019,** *58*, 2850–2853.

246. Wen, J.; Wang, D.; Qian, J.; Wang, D.; Zhu, C.; Zhao, Y.; Shi, Z., Rhodium-Catalyzed PIII-Directed ortho-C−H Borylation of Arylphosphines. *Angew. Chem. Int. Ed.* **2019,** *58*, 2078–2082.

247. Kuninobu, Y.; Ida, H.; Nishi, M.; Kanai, M., A meta-selective C–H borylation directed by a secondary interaction between ligand and substrate. *Nat Chem* **2015,** *7*, 712–717.

248. Wang, J.; Torigoe, T.; Kuninobu, Y., Hydrogen-Bond-Controlled Formal Meta-Selective C–H Transformations and Regioselective Synthesis of Multisubstituted Aromatic Compounds. *Org. Lett.* **2019,** *21*, 1342–1346.

249. Xu, F.; Duke, O. M.; Rojas, D.; Eichelberger, H. M.; Kim, R. S.; Clark, T. B.; Watson, D. A., Arylphosphonate-Directed Ortho C–H Borylation: Rapid Entry into Highly-Substituted Phosphoarenes. *J. Am. Chem. Soc.* **2020,** *142*, 11988–11992.

250. Genov, G. R.; Douthwaite, J. L.; Lahdenperä, A. S. K.; Gibson, D. C.; Phipps, R. J., Enantioselective Remote C–H Activation Directed by a Chiral Cation. *Science* **2020,** *367*, 1246–1251.

251.   Song, S.-Y.;   Li, Y.;   Ke, Z.; Xu, S., Iridium-Catalyzed Enantioselective C–H Borylation of Diarylphosphinates. *ACS Catal.* **2021,** *11*, 13445–13451.

252.   Zou, X.;   Zhao, H.;   Li, Y.;   Gao, Q.;   Ke, Z.; Senmiao, X., Chiral Bidentate Boryl Ligand Enabled Iridium-Catalyzed Asymmetric C(sp^2)–H Borylation of Diarylmethylamines. *J. Am. Chem. Soc.* **2019,** *141*, 5334–5342.

253.   Yoshidomi, T.;   Fukushima, T.;   Itami, K.; Segawa, Y., Synthesis, Structure, and Electrochemical Property of a Bimetallic Bis-2-pyridylidene Palladium Acetate Complex. *Chem. Lett.* **2017,** *46*, 587–590.

CHAPTER 2 Catalytic, undirected borylation of tertiary C–H bonds in bicyclo[1.1.1]pentanes and bicyclo[2.1.1]hexanes

2.1 Introduction

Recent developments in iridium-catalyzed borylation have made the undirected borylation of alkyl C–H bonds an increasingly practical method to access alkyl boronic esters.[1-6] Generally, metal-catalyzed borylation occurs at primary C–H bonds or, in the absence of accessible primary C–H bonds, at secondary C–H bonds activated by ring strain or electron-withdrawing substituents. Even recent radical-based borylations of C–H bonds, which could be expected to occur at tertiary C–H bonds, occurred at primary and secondary over tertiary C–H bonds.[7] The catalytic borylation of tertiary C–H bonds has not been reported, to the best of our knowledge (Figure 2.1a). Our recent discovery of an iridium complex formed from 2-methylphenanthroline (2-mphen) that catalyzes the borylation of primary and secondary alkyl C–H bonds with the alkane as the limiting reagent[5] raised the question of whether the borylation of tertiary C–H bonds could be achieved. For this proposed reaction to occur and to be practical, the C–H functionalization must occur cleanly at a class of C–H bonds typically unreactive toward C–H activation forming metal-carbon bonds, with minimal deleterious C–C bond cleavage, and with the substrate as the limiting reagent.

Since Lovering's seminal paper[8] introducing the concept of "escape from flatland," the synthetic community has become increasingly interested in the incorporation of sp^3-rich fragments into drug candidates. In particular, the highly strained bicyclo[1.1.1]pentane (BCP) motif is being applied as a potential bioisostere to mono- and *para*-disubstituted benzenes,[9-12] internal alkynes,[13] and *tert*-butyl groups.[14, 15] Related bicyclo[2.1.1]hexanes (BCHs) and oxa- and aza-bicyclo[2.1.1]hexanes (XBCHs) have been proposed as possible bioisosteres to *ortho*- and *meta*- disubstituted benzenes[16, 17] and conformationally constrained equivalents of pyrrolidine, respectively.[18, 19] In many cases, bioisosteric substitution of disubstituted benzenes and pyrrolidines for these saturated bicyclic scaffolds imparted greater rigidity, increased solubility, and improved metabolic stability for drug candidates (Figure 2.1b).

The increased demand for functionalized BCPs has led to a surge in the development of methods for the construction of substituted BCPs. Prevailing methods usually involve the manipulation of [1.1.1]propellane. Radical addition to the central bond of [1.1.1]propellane is well-known and is part of radical chain and photoredox pathways to substituted BCPs.[20-30] The addition of organometallic compounds, such as Grignard reagents, to [1.1.1]propellane is also well precedented, and the resulting bicyclo[1.1.1]pentyl organometallic intermediates can be quenched by electrophiles or used as nucleophiles in cross-coupling reactions.[13, 31-37] The insertion of donor-acceptor carbenes into the bridgehead C–H bond of BCPs also has been reported.[38] While these methods allow access to 1,3-disubstituted BCP derivatives, the intermediate bicyclopentyl species are not bench-stable, and the limited scope of reaction partners that are compatible with the harsh reagents and with the conditions to install the second substituent makes rapid diversification of the scaffold difficult. Furthermore, most of these methods are limited to the synthesis of BCP derivatives and cannot be extended to BCHs and (hetero)BCHs (XBCHs).

An alternative and unifying strategy towards the construction of diverse BCP, BCH, and XBCH building blocks is to enlist boronic esters, which are stable synthetic intermediates (Figure 2.1c). The boronic ester motif could be derivatized into a variety of carbo- and heteroatom-based

functional groups through well-established synthetic procedures. In this vein, Aggarwal developed a decarboxylative borylation of redox-active esters, including ester derivatives of BCPs,[39, 40] Uchiyama reported the direct silaboration of propellane,[41] Qin reported a Barluenga−Valdés-inspired cyclization that forges the BCP core from cyclobutanones,[42] and the Anderson, Aggarwal, and Walsh groups demonstrated the feasibility of trapping *in situ*-generated BCP organometallic species with boron electrophiles.[25, 36, 43, 44] Many of these routes rely on the handling of [1.1.1]propellane or the lengthy synthesis of either a prefunctionalized BCP or cyclobutanone scaffold prior to installation of the boryl group, thereby limiting the general applicability of these groups to the preparation of the boronic esters of BCHs and XBCHs (Figure 2.1c). A direct and straightforward strategy to construct these coveted boronic esters would be to repurpose existing, but underutilized, stable and commercially available 1-substituted strained building blocks via the direct functionalization of the bridgehead C–H bond (Figure 2.1d).
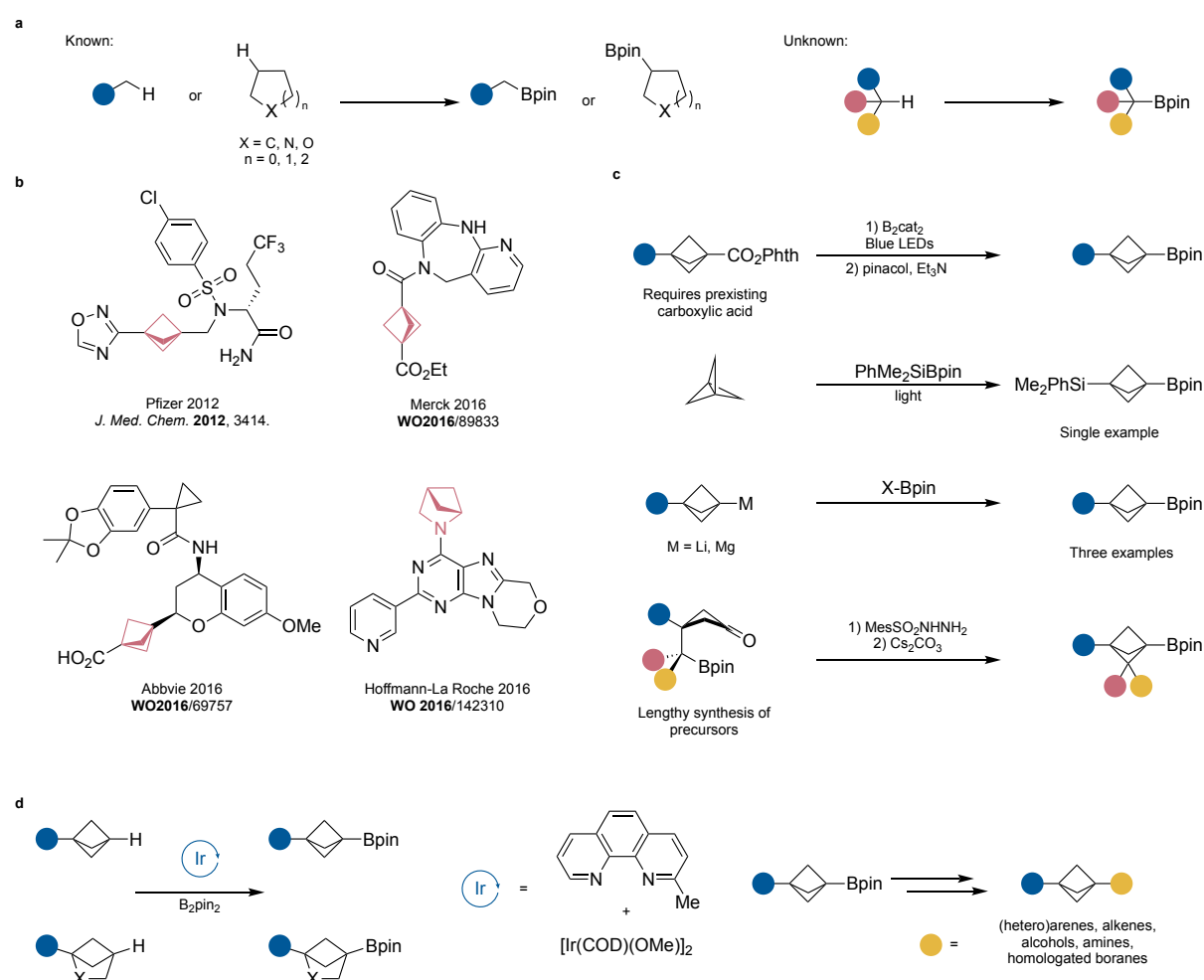
Figure 2.1. State of the borylation of alkyl C–H bonds, applications of BCPs, and routes for their synthesis relevant to this study. (a) The borylation of primary and secondary C–H bonds are known, while the borylation of tertiary C–H bonds is underexplored. (b) Selected examples of drug candidates in which bioisosteric replacement of para-disubstituted benzenes and pyrrolidines with BCPs and (hetero)BCHs has been conducted (c) Existing approaches toward bridgehead-substituted boryl-BCPs. Drawbacks include requirements for prefunctionalization, limitations in scope, and lengthy syntheses. Bridgehead-substituted

96

boryl-BCHs are also underexplored. (d) The direct bridgehead borylation presented in this work occurs with broad scope and provides a complementary avenue to access BCPs and (hetero)BCHs with new substitution patterns.

Herein, we report the iridium-catalyzed borylation of the bridgehead tertiary C–H bonds of BCPs, BCHs and XBCHs. This reaction occurs selectively at this type of tertiary C–H bond over unactivated primary and secondary C–H bonds and tolerates a wide variety of functional groups. This C–H bond reacts with rates that are similar to those observed with cyclopropanes, leading to the broad scope, and the boronic ester products of this method undergo a wide variety of reactions to form 1,3-disubstituted bicyclic building blocks.

2.2 Results and Discussion

2.2.1 Reaction Development of the Borylation of Bridgehead C–H Bonds

We initiated our investigation of the borylation of the bridgehead, tertiary C–H bonds of BCPs by testing reactions of the model substrate 4-*tert*-butylphenylbicyclopentane **1b** in the presence of a series of catalysts reported for the borylation of alkyl C–H bonds (Figure 2.9).[4, 5, 45] Studies on reaction times, stoichiometries and ligands for iridium showed that the iridium system formed from 2-mphen and (mesitylene)Ir(Bpin)$_3$ catalyzed the borylation of **1b** to form **1a** in high yield with the substrate as the limiting reagent and exclusively at the bridgehead tertiary C–H bond. Reactions conducted with 2,9-dimethylphenanthroline (2,9-dmphen, **L1**) also occurred in a high yield, albeit measurably lower than those with 2-mphen, and reactions conducted with 3,4,7,8-tetramethylphenanthroline (tmphen) or 2,2'-((3-fluorophenyl)methylene)dipyridine (**L3**)[4] occurred in moderate to low yields. Reactions conducted with ligands used primarily for the borylation of aromatic C–H bonds, such as 4,4'di-*tert*-butylbipyridine (dtbpy, **L2**)[46] or 5-methyl-2-(thiophen-3-yl)pyridine (**L4**),[45] as ancillary ligands did not form product. Control experiments showed that both the ligand and the iridium precursor are necessary for the formation of the product, and reactions conducted with the commercially available precatalyst [Ir(COD)(OMe)]$_2$ were similar to those with (mesitylene)Ir(Bpin)$_3$. The use of HBpin or alternate diboron reagents in place of B$_2$pin$_2$ as the boron source resulted in lower yields. Although the desired boronic ester was obtained with **L1**, **L3**, or tmphen as ligand, we used 2-mphen as the ligand for further studies on reaction scope because the reaction times could be shorter, and these faster rates would likely reduce competing reactions with auxiliary functional groups and afford the products in superior yields (Figure 2.10).

With conditions for the borylation of model substrate **1b** in hand, we explored the scope of the undirected borylation of monosubstituted BCPs with B$_2$pin$_2$ catalyzed by [Ir(COD)(OMe)]$_2$ and 2-mphen. All substrates underwent borylation exclusively at the bridgehead C–H bond or concomitantly at the bridgehead and at an aryl or acidic primary alkyl C–H bond if those C–H bonds were not sufficiently hindered (Figure 2.2a). Competitive reactions at primary and secondary C–H bonds with fully substituted α-carbons were not observed, presumably due to steric hindrance. Arene, sulfide, stannane, bromide, and ester functionalities did not interfere with borylation at the bridgehead, tertiary C–H bond (**1a-5a**, **8a-10a**). Alcohols were tolerated following an in situ protection procedure (**6a**, **7a**).[5] Reactions of BCPs containing sulfone and

sulfonamide units gave products from borylation at the tertiary C–H bond (**11a-14a**); borylations at the methyl C–H bonds of a methyl sulfone and at the N–H bonds of the primary sulfonamide were observed, but the B–C and B–N bonds at those positions were labile and were selectively hydrolyzed upon workup to afford the product containing a boronic ester solely at the bridgehead position (**11a**, **12a**). Imides, amides and Boc-protected cyclic amines also underwent borylation at the tertiary C–H bond (**15a-18a**). A substrate containing sterically accessible aryl C–H bonds underwent borylation of both the aryl and bridgehead C–H bonds (**19a**). (Figure 2.2b)

The broad functional group compatibility of this method prompted us to apply it to the borylation of medicinally relevant molecules containing the BCP fragment and to test the reaction on larger scale. Exclusive borylation at the bridgehead C–H bond was observed for derivatives of abietic acid and valproic acid (**20a**, **21a**). (Figure 2.2c) The method was easily amenable to syntheses on a gram scale. The borylation of **11b** on a 4.0 mmol scale gave the corresponding boronic ester in 58% yield (631 mg), which was comparable to that of the reaction on smaller scale (0.25 mmol, 64%), and the borylation of **16b** on a 4.0 mmol scale formed the functionalized product in 95% yield (1.89 g), which was also comparable to that of the reaction on smaller scale (0.25 mmol, 94%).
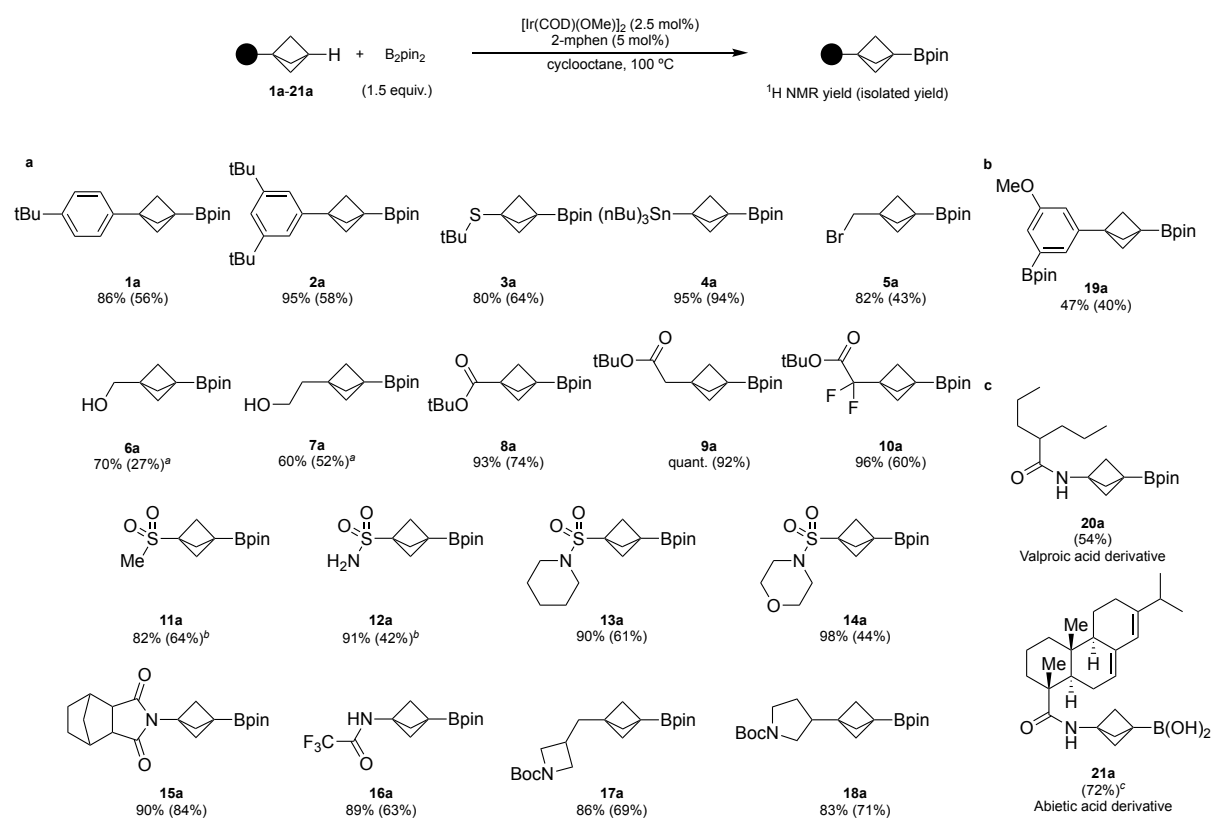
Figure 2.2. Examples of bicyclo-[1.1.1]-pentanes that undergo borylation of the bridgehead C–H bond. (a) Examples of bicyclopentanes containing common functional groups that undergo borylation of the bridgehead C–H bond. (b) Example of an arylbicyclopentane that undergoes borylation of both the aryl and the bridgehead C–H bonds. (c) Examples of medicinally relevant molecules that contain the BCP substructure that undergo exclusive borylation of the bridgehead C–H bond. Reactions were conducted at 0.10-0.25 mmol scale. ^{1}H NMR yields were determined relative to an internal standard of

dibromomethane, and the isolated yields are given in parenthesis. Standard conditions: substrate (0.10-0.25 mmol), B$_2$pin$_2$ (1.5 equiv.), [Ir(COD)(OMe)]$_2$ (2.5 mol%), 2-mphen (5.0 mol%), cyclooctane (100 µL/mmol), 100 ºC. [a] Substrate treated with HBpin (1.3 equiv.) prior to the reaction. [b] Conducted with 3 equivalents of B$_2$pin$_2$. [c] Spontaneous hydrolysis to the corresponding boronic acid upon purification.

This reactivity extended to bridgehead tertiary C–H bonds in additional strained bi- or tri-cyclic systems. The all-carbon bicyclo-[2.1.1]-hexane **22a**, the oxabicyclo-[2.1.1]-hexanes (**23a-26a**), and the azabicyclo-[2.1.1]-hexanes (**27a-38a**) all reacted cleanly at the tertiary C–H bonds to afford the corresponding boronic esters (Figure 2.3). The methylene C–H bonds within the bicyclo-[2.1.1]-hexane cores were unreactive, which we attribute, again, to steric crowding of the methylene hydrogens by the quaternary centers vicinal to this position. Bicyclohexanes possessing esters, alcohols, bromides, and amides underwent borylation at the tertiary C–H bond to afford the corresponding products (**22a-31a**, **33a**, **36a-38a**). The borylations of these bicyclic compounds were also compatible with a tertiary amine (**32a**), a primary amide (**34a**), and a TIPS-protected alkyne (**35a**). Reactions conducted with bicyclo-[1.1.0]-butane and cubane structures gave complicated mixtures, while the less strained bicyclo-[2.2.1]-heptane (norbornane) did not react under our conditions (Figure 2.11).
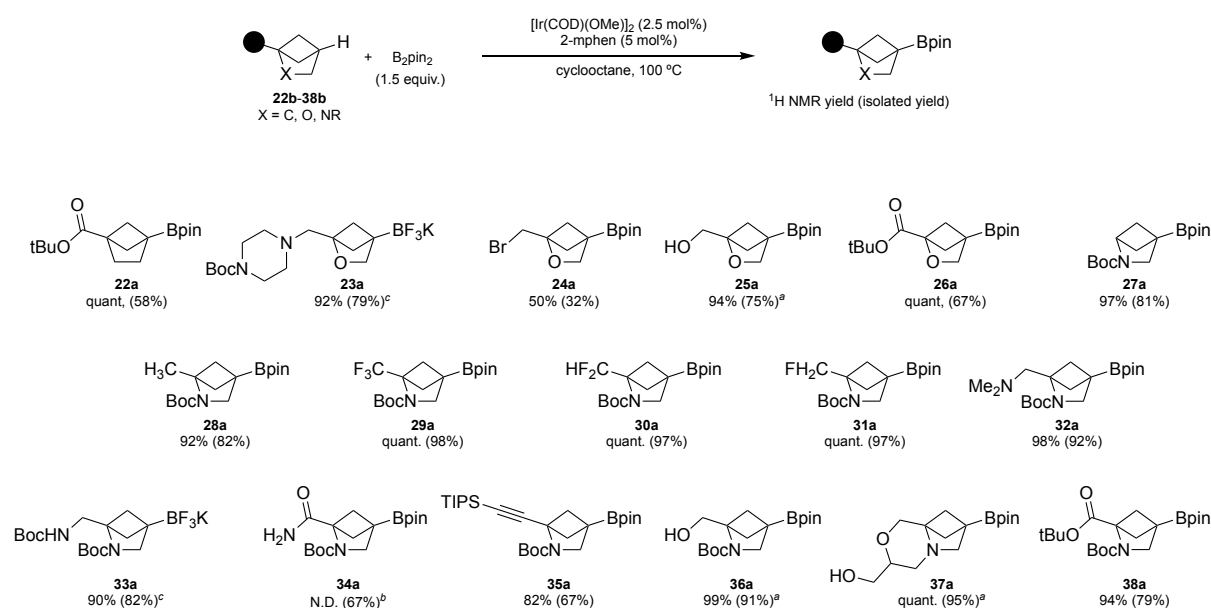
Figure 2.3. Examples of (hetero)bicyclo-[2.1.1]-hexanes that undergo borylation of the bridgehead C–H bond. Reactions were conducted at 0.10-0.25 mmol scale. ^{1}H NMR yields were determined relative to an internal standard of dibromomethane, and the isolated yields are given in parenthesis. Standard conditions: substrate (0.10-0.25 mmol), B$_2$pin$_2$ (1.5 equiv.), [Ir(COD)(OMe)]$_2$ (2.5 mol%), 2-mphen (5.0 mol%), cyclooctane (100 µL/mmol), 100 ºC. [a] Substrate treated with HBpin (1.3 equiv.) prior to the reaction. [b] Conducted with 3 equivalents of B$_2$pin$_2$. [c] Crude reaction mixture treated with 5 equivalents of KHF$_2$ after completion of the borylation reaction.

2.2.2 Derivatization and Applications of the Bridgehead Boronic Esters

The bridgehead pinacol boronic ester fragments in the products of these borylation reactions are primed for conversion to a variety of functional groups (Figure 2.4). The 3-boryl BCPs and 3-boryl BCXHs were readily converted to trifluoroboronates and boronic acids for use when more reactive boron derivatives were needed. Addition of bifluoride formed the corresponding trifluoroborate salts (**1c**, **11c**, **16c**), and addition of methyl boronic acid formed the corresponding boronic acids[47] (**1d**, **11d**, **28c**). This set of 3-boryl BCPs underwent reactions at the B–C bond to form new C–C bonds. Cross-coupling with aryl electrophiles occurred under either metallaphotoredox conditions[40] to form the 3-aryl BCP **1f** from the trifluoroborate **1c** or by activation with *t*-BuLi followed by Pd-catalyzed coupling[41] to form the 3-aryl BCP **1g** from boronic ester **1a**. An intermolecular Barluenga−Valdés coupling[48] afforded **1e** from boronic acid **1d**, Zweifel olefination afforded the 3-vinyl BCP **11e** from boronic ester **11a** and the 3-vinyl BCXH **28c** from boronic ester **28a**, heteroarylation afforded the 3-heteroaryl BCP **13c** from boronic ester **13a**, and Matteson homologation formed the homologated boronic ester **1h** from boronic ester **1a**. The 3-boryl BCPs also underwent reactions to form heteroatom-substituted BCPs. For example, oxidation of boronic ester **16a** occurred with urea hydrogen peroxide to afford the 3-hydroxy BCP **16d**, while oxidation of boronic ester **27a** afforded the 3-hydroxy BCXH **27c**, and amination of the trifluoroborate **16c** occurred under Matteson's conditions[49] to afford the benzyl amine **16e**. C–C and C–N bond formation reactions from 3-boryl BCXHs are under investigation in our laboratories.
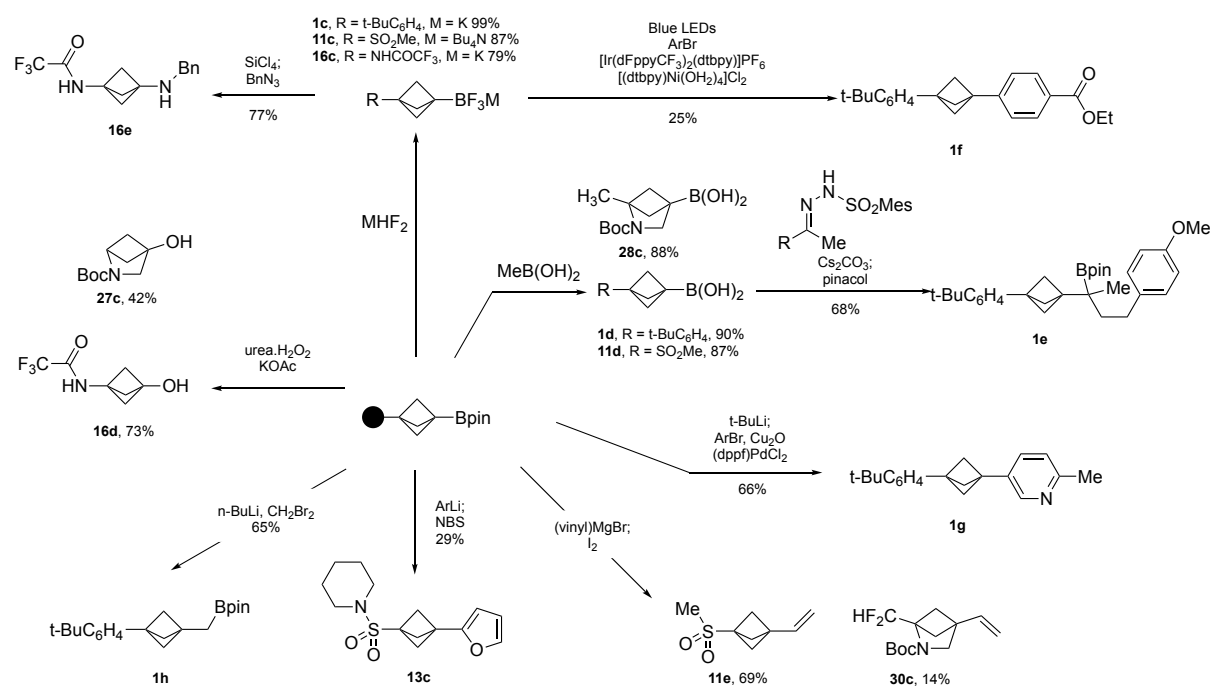
Figure 2.4. Conversion of 3-boryl-bicyclo-[1.1.1]-pentanes and 3-boryl-bicyclo-[2.1.1]-hexanes into various functional groups. The boronic esters were converted to alternative boron species such as trifluoroborate salts or boronic acids. The boryl products reacted to forge C–C bonds through 1,2-metallate rearrangements or cross-coupling. The boryl products also reacted to form C–X bonds through oxidation or aza-1,2-metallate rearrangement reactions. The resultant BCPs and BCHs represent novel building blocks with substitution patterns that are difficult to access.

The examples in Figure 2.4 also showcase the value of our method for medicinal chemistry. For example, **16d**, **16e**, and **27c** are analogs of electron-rich arenes, such as aminophenol or aminoanilines, and **11e**, **13c**, and **30c** represent examples of substitution patterns that would be difficult to access with existing methods.

2.2.3 Investigation of the Mechanism of the Tertiary C–H Borylation

This new borylation presented an opportunity to compare the mechanism of the borylation at tertiary C–H bonds to those at primary C–H bonds and to assess the magnitude of the effect of strain on the borylation of C–H bonds. To obtain preliminary understanding of the functionalization of the tertiary C–H bond in BCPs under our conditions, we compared the relative rates for the borylation the tertiary C–H bond in 4-*tert*-butylphenylbicyclopentane (**1b**) versus sp^2 and other sp^3 C–H bonds through a series of intermolecular competition studies (Figure 2.5a). Because it is not necessary to conduct competition reactions under conditions without an induction period, these experiments were conducted with the most active catalyst, which is generated from [Ir(COD)(OMe)]$_2$ and 2-mphen. The borylation of the bridgehead tertiary C–H bonds of BCP **1b** occurred at a much slower rate than that of the aryl C–H bond of 1,3-dichlorobenzene, at roughly the same rate as that of the strained secondary C–H bonds of *tert*-butyl cyclopropanecarboxylate, at a much higher rate than those of the unactivated secondary C–H bonds of tetrahydrofuran and cyclohexane, and at a much higher rate than that of the unactivated primary C–H bonds of *tert*-butyloctyl ether.
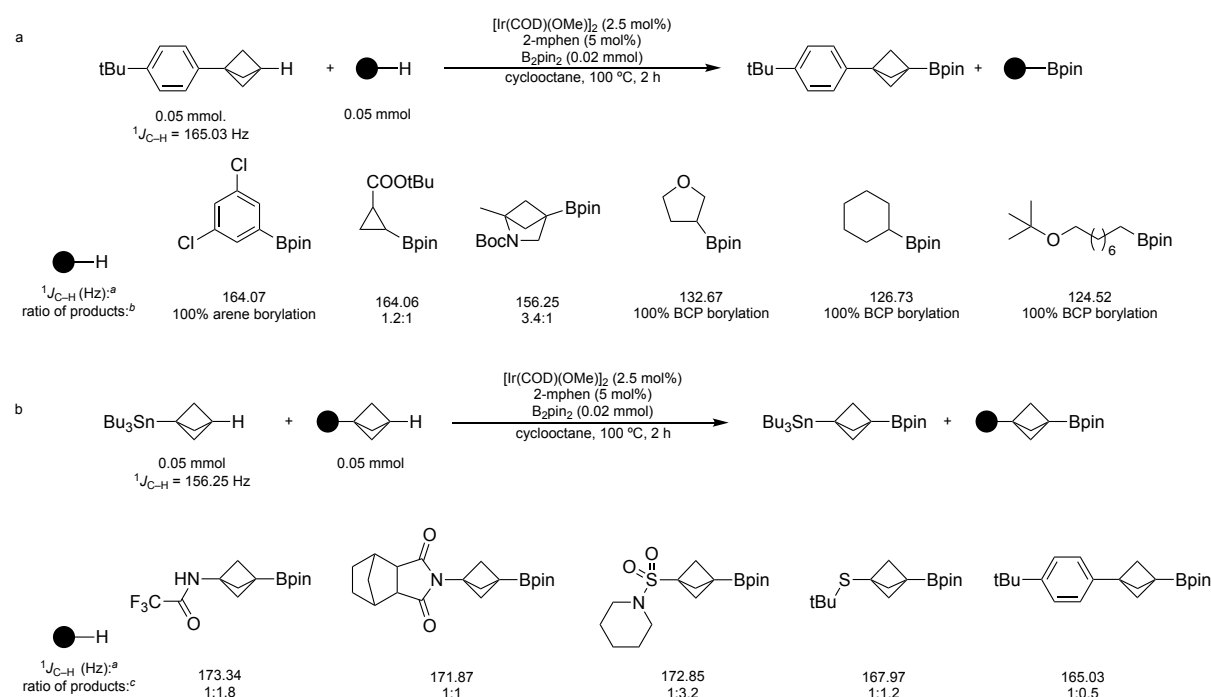
Figure 2.5. Competition experiments and measurement of $^1J_{C–H}$ coupling constants. (a) Competition experiments between BCPs and typical substrates for C–H borylation show that the borylations of BCPs and BCHs occur with comparable rates to that of the borylation of cyclopropanes, is much slower than that of the borylation of arenes, and is much faster than those of the borylation of unactivated alkyl C–H bonds. The relative reactivities correlate well to the $^1J_{C–H}$ coupling constants. (b) Competition experiments between BCP substrates show no apparent correlation between the $^1J_{C–H}$ coupling constant or the electronegativity of the

substituent and the rate of borylation. [a] $^1J_{C-H}$ coupling constant of the C–H bond that underwent borylation. [b] Ratio of products determined by GC analysis. [c] Ratio of products determined by NMR analysis.

We reasoned that the high activity of the BCPs towards borylation could be rationalized by the high degree of *s*-character in the C–H bond, which in turn has been shown to correlate with increased acidity.[50] To investigate the origin of the high levels of activity of the BCP substrates observed for the borylation reaction, relative to the low reactivity of typical tertiary C–H bonds, we measured the $^1J_{C-H}$ coupling constants of various BCPs and non-BCP substrates. We also measured the relative rates of reaction for various BCPs containing different substituents in the 1-position. (Figure 2.5b) Indeed, the measured $^1J_{C-H}$ coupling constants of BCPs and XBCHs were comparable to those of aryl and cyclopropyl C–H bonds. However, no clear correlation was observed between the relative rates of reaction of individual BCPs versus the variation of the $^1J_{C-H}$ coupling constants within the set of BCPs. Thus, the generally high reactivity of these C–H bonds toward undirected borylation can be explained by *s*-character of the C–H bond, but the more precise reactivity of the individual BCPs required a deeper mechanistic evaluation.

Kinetic isotope effect (KIE) data in previous reports on the borylation of aryl and alkyl C–H bonds suggested that cleavage of the C–H bond is likely irreversible and turnover-limiting.[1, 3, 51] Yet, other studies have suggested that reductive elimination to form product or isomerization of an intermediate prior to reductive elimination is turnover-limiting.[52-54] Because we observed no clear trend between the relative rates of reaction and the electronic properties of the substituents on the BCPs and because the steric properties of the BCP substrates are similar, oxidative addition is unlikely to be turnover-limiting.

To test further whether oxidative addition of the C–H bond was turnover-limiting, we measured the kinetic isotope effect (KIE) of the bridgehead C–H bond of the BCP on the reaction. While direct measurements of the rates of reactions initiated with 2-mphen were hampered by a significant induction period, we obtained a KIE value from a pair of competition experiments. In separate flasks, a mixture of 3,5-di(*tert*-butyl)phenylbicyclopentane (**2b**) and either 4-*tert*-butylphenylbicyclopentane (**1b**) or 4-*tert*-butylphenylbicyclopentane-d_1 (**1b-d_1**) was allowed to react in the presence of B_2pin_2, [Ir(COD)OMe]$_2$, and 2-mphen (Figure 2.6a, see section 2.4.7 for details). These experiments yielded a KIE value of 1.8 ± 0.1, which is more consistent with an equilibrium isotope effect than a primary, kinetic isotope effect.

We conducted analogous rate measurements with tmphen as the ligand. The reaction with this ligand on iridium is slower than that with 2-mphen, but it occurred without a significant induction period, thereby enabling us to obtain clear kinetic data. The KIE value obtained from the initial rates of separate reactions initiated with tmphen as the ancillary ligand and either *tert*-butylphenylbicyclopentane (**1b**) or *tert*-butylphenylbicyclopentane-d_1 (**1b-d_1**) was, again, 1.8 ± 0.1 (Figure 2.6b). The reaction with this catalyst was found to be first order in the BCP, first order in the catalyst, and zero order in the diboron reagent (Figure 2.6c). These results imply that the BCP and the iridium catalyst are involved in the turnover-limiting step, but the low KIE value and the lack of correlation between the $^1J_{C-H}$ coupling constants and rate of reaction of the BCPs suggest that oxidative addition is not likely to be turnover-limiting and is likely reversible.
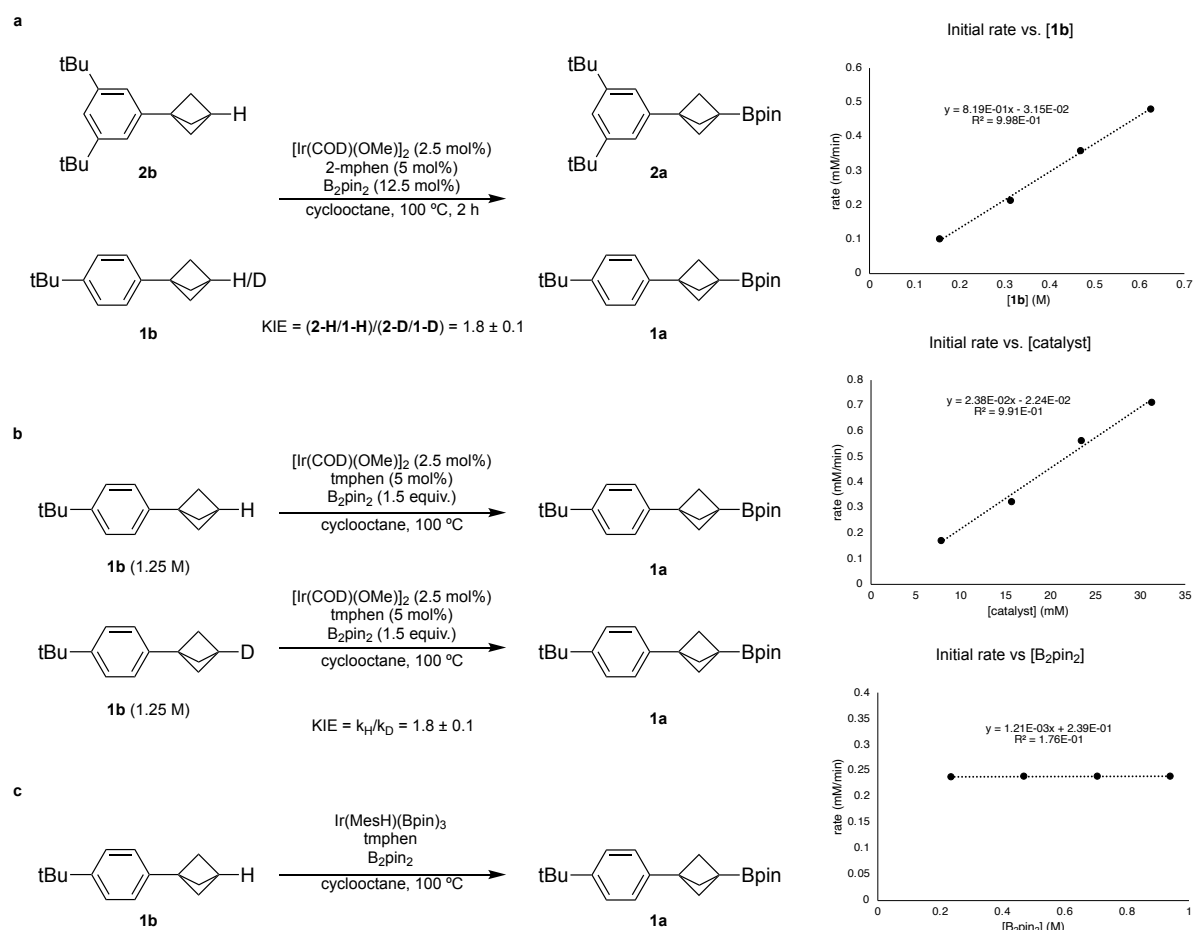
Figure 2.6. Mechanistic Experiments. (a) Kinetic isotope effect obtained by competition experiments with 2-mphen as the ligand. The small magnitude of the KIE implies that C–H cleavage could be reversible. (b) Kinetic isotope effect obtained by measurement of rates in separate vessels with tmphen as the ligand. The small magnitude of the KIE implies that C–H cleavage may not be turnover limiting. (c) Reaction orders were obtained by the method of initial rates. The borylation reaction is first order in substrate, first order in catalyst, and zero order in diboron reagent.

To understand the low KIE value and to determine the turnover limiting step of the C–H borylation process, we conducted density functional theory (DFT) calculations on the borylation of unsubstituted bicyclopentane as a model substrate with tmphen as the ligand on iridium. The computed energy diagram for the reaction process is shown in Figure 2.7. These calculations predict that oxidative addition of bicyclopentane (**R-H**) to the trisboryl species (tmphen)Ir(Bpin)₃ (**[Ir](Bpin)₃**) will be reversible with a barrier of 23.3 kcal/mol to form intermediate **[Ir](Bpin)₃(R)(H)**. This intermediate would then undergo an isomerization with a barrier of 17.9 kcal/mol that lies 30.1 kcal/mol above the starting complex and free substrate to form intermediate ***iso*-[Ir](Bpin)₃(R)(H)**. Reductive elimination from ***iso*-[Ir](Bpin)₃(R)(H)** occurs with a barrier of just 3.6 kcal/mol to afford the product. Turnover with B₂pin₂ then regenerates **[Ir](Bpin)₃**. The KIE value of the reaction by this path was computed to be 2.03 for bicyclopentane as the substrate, which is in good agreement with the experimental value of 1.8 for 4-*tert*-butylphenylbicyclopentane. A discussion of pathways involving Ir(I) species or alternative isomerization pathways is included in section 2.4.8. The higher computed barrier

for isomerization following C–H bond cleavage likely results from the high *s*-character of the bridgehead position leading to more facile oxidative addition of the C–H bond to the iridium center. Because the isomerization step is less sensitive to the identity of the alkyl group, this step becomes turnover limiting. Similar conclusions have been drawn and overall barriers obtained from computational studies on the borylation of chlorosilanes and benzylic C–H bonds.[53, 54]
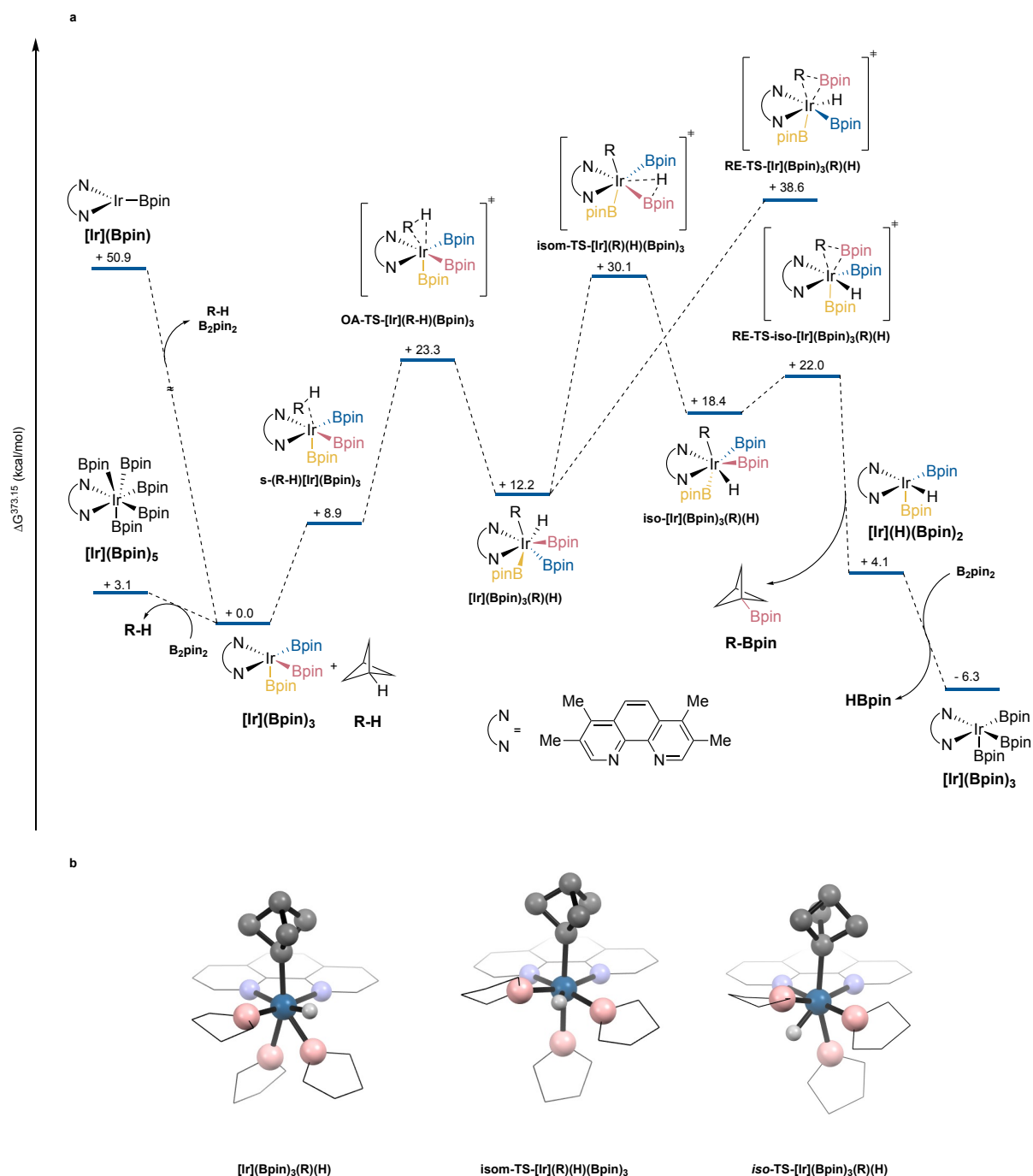
Figure 2.7. DFT studies. (a) Energy diagram obtained by calculations using density functional theory. The resting state of the catalyst, [Ir](Bpin)₃, engages the substrate, which undergoes reversible oxidative addition of the tertiary C–H bond to generate [Ir](Bpin)₃(R)(H). This initial product from oxidative addition undergoes rate-limiting isomerization to afford *iso*-[Ir](Bpin)₃(R)(H). Facile reductive elimination occurs from *iso*-[Ir](Bpin)₃(R)(H) to form the

product. Energies are given in kcal/mol at 373.15 K. See section 8 of the SI for computational details and structures. Boryl groups have been color-coded for clarity. (b) Ball-and-stick structures of the key isomerization process. For clarity, peripheral methyl groups and hydrogen atoms have been omitted, and the phenanthroline ligand and boryl groups are represented as wireframes. The geometry of $[Ir](Bpin)_3(R)(H)$ is roughly pentagonal bipyramidal in which one nitrogen and the boryl ligand that later undergoes reductive elimination occupy axial positions. The geometry of *iso*-$[Ir](Bpin)_3(R)(H)$ is also roughly pentagonal bipyramidal in which the other nitrogen and a boryl ligand now occupy axial positions. The BCP alkyl and the boryl ligand that are poised to undergo reductive elimination lie in the equatorial plane.

Based on our experimental and computational data, we propose that the borylation of BCPs occurs by initial, reversible oxidative addition of the bridgehead C–H bond to **(tmphen)Ir(Bpin)₃** to generate the 7-coordinate Ir(V) species **(tmphen)Ir(R)(H)(Bpin)₃**. Turnover-limiting isomerization of this intermediate leads to the 7-coordinate intermediate ***iso*-(tmphen)Ir(R)(H)(Bpin)₃**, from which facile reductive elimination occurs to afford **(tmphen)Ir(H)(Bpin)₂** and the borylated product. The catalyst is then regenerated by reaction between **(tmphen)Ir(H)(Bpin)₂** and B_2pin_2 with HBpin as the byproduct.

2.3 Conclusion

The undirected borylation of C–H bonds, which is known to occur at aryl, primary alkyl, and some secondary alkyl C–H bonds, now has been shown to occur at a tertiary C–H bond. Although tertiary C–H bonds are typically inert under the conditions for the borylation of C–H bonds, the high strain in BCPs, BCHs and XBCHs and the resulting sp^2 character of these C–H bonds lead to mild activation and functionalization, despite the steric hindrance of a tertiary position. This reactivity enables a new synthesis of BCP and BCH and XBCH structures via the undirected borylation of the bridgehead C–H bonds and provides a direct method to these valuable building blocks from commercial or readily accessible reactants. As a result, this method tolerates a wide variety of functional groups of relevance to drug discovery and can be applied to the late-stage elaboration of complex structures containing these strained units. Mechanistic and computational studies show that the rate of reaction is relatively independent of the electronic properties of substituents on the BCP structures because the turnover-limiting step of the reaction is isomerization of the intermediate, 7-coordinate Ir complex, rather than C–H bond cleavage. Mechanistic insights gained in this study and the demonstration that a tertiary C–H bond can undergo undirected C–H bond functionalization by chemistry known to occur without radical intermediates should help guide future studies at hindered and typically unreactive alkyl C–H bonds.

2.4 Experimental

2.4.1 General Information

Reagents and Solvents

All catalytic reactions were assembled under inert atmosphere in a nitrogen-filled glovebox equipped with oxygen and water sensors (working levels ≤ 1.0 ppm and 0.5 ppm, respectively) and a low temperature refrigeration unit (–35 °C) unless otherwise noted. All other reactions were assembled under inert atmosphere with a Schlenk manifold or a nitrogen glovebox unless otherwise noted. All reagents and solvents were purchased from commercial sources and used as received, unless otherwise noted. All glassware was flame-dried or dried overnight at 120 °C, allowed to cool under vacuum, and stored in a N2-atomsphere drybox until use unless otherwise noted. Tetrahydrofuran, toluene, and diethyl ether were purified by passing the degassed solvents (N_2) through a column of activated alumina (solvent purification system purchased from Innovative Technologies, Newburyport, MA). Cyclooctane was degassed by three freeze-pump-thaw cycles and further dried for a week over activated 4 Å molecular sieves. Deuterated solvents were purchased from Cambridge Isotope Laboratories and used as received. See section 2 for synthesis of reagents and substrates.

Chromatography and Data Analysis

Flash column chromatography was conducted on a Teledyne ISCO Combiflash Rf or Rf+ system, with prepacked RediSep Gold silica gel and C18 columns. All reactions were followed by thin-layer chromatography (TLC) when practical, using Merck Kieselgel 60 F_{254} fluorescent treated silica, which was visualized under UV light when practical, or by staining with a solution of anisaldehyde or phosphomolybdic acid followed by heating.

^{1}H, ^{11}B, ^{13}C, and ^{19}F NMR spectra were recorded on Bruker AV-300, AVQ-400, AVB-400, AV-500, AV-600, NEO-500, and AV-700 spectrometers. Chemical shifts (δ) reported given in parts per million (ppm) relative to the residual solvent signal. Coupling constants (J) are given in Hertz (Hz), rounded to the nearest 0.1 Hz. The ^{1}H NMR spectra are reported as follows: ppm (multiplicity, coupling constants, number of protons). Abbreviations are as follows: s (singlet), d (doublet), t (triplet), q (quartet), m (multiplet), br (broad). The carbon attached to boron is usually not observed.

High-resolution mass spectral (HRMS) data were obtained from the QB3/Chemistry Mass Spectrometry Facility at UC Berkeley.

Gas Chromatography (GC) was performed on an HP 6890 GC system with an Agilent HP-5 column (25 m × 0.200 mm, 0.33 micron).

Naming of Compounds

Compound names were generated by ChemDraw 20.0 software (PerkinElmer), following the IUPAC nomenclature.

2.4.2 Synthesis of reagents and substrates

As shown in Figure 2.8, the bicyclic substrates were obtained from commercial vendors, prepared according to literature procedures, or independently synthesized (see below). A solution of [1.1.1]-propellane in diethyl ether was prepared from 1,1-dibromo-2,2-bis(chloromethyl)cyclopropane and phenyllithium according to a known procedure.[31] Sodium bicyclo[1.1.1]pentanesulfinate was synthesized according to a literature procedure.[55] 2-methylphenanthroline,[56] 2,2'-((3-fluorophenyl)methylene)dipyridine,[4] 5-methyl-2-(thiophen-3-yl)pyridine,[45] 1-(4-(*tert*-butyl)phenyl)bicyclo[1.1.1]pentane,[38] bicyclo[1.1.1]pentan-1-yl(*tert*-butyl)sulfane,[26] bicyclo[1.1.1]pentan-1-yltributylstannane,[57] 1-(methylsulfonyl)bicyclo[1.1.1]pentane,[55] bicyclo[1.1.1]pentane-1-sulfonamide,[55] and *tert*-butyl bicyclo[1.1.0]butane-1-carboxylate[58] were synthesized according to literature precedent. The spectral data of the known compounds were identical to those reported in the literature. All other chemicals were purchased from commercial vendors and used as received unless otherwise noted.

1b
Nat. Catal. **2020**, *3*, 351.

2b
see below

3b
Chem. Eur. J. **2018**, *24*, 1373.

4b
J. Phys. Org. Chem. **1996**, *9*, 168.

5b
commercially available
Enamine
CAS: 161043-38-5

6b
commercially available
Enamine
CAS: 2091785-54-3

7b
commercially available
Enamine
CAS: 22287-3207

8b
commercially available
Enamine
CAS: 117592-90-2

9b
commercially available
Enamine
CAS: 2694745-12-3

10b
commercially available
Enamine
CAS: 2694744-42-6

11b
Chem. Eur. J. **2020**, *26*, 4242.

12b
Chem. Eur. J. **2020**, *26*, 4242.

13b
see below

14b
see below

15b
commercially available
Enamine
CAS: 2680523-03-7

16b
see below

17b
commercially available
Enamine
CAS: 2680542-28-1

18b
commercially available
Enamine
CAS: 2680536-34-7

19b
see below

20b
see below

21b
see below

22b
commercially available
Enamine
CAS: 2648938-91-2

23b
commercially available
Enamine
CAS: 2414430-75-2

24b
commercially available
Enamine
CAS: 2060007-65-8

25b
commercially available
Enamine
CAS: 2253631-03-5

26b
commercially available
Enamine
CAS: 2694734-06-8

27b
commercially available
Enamine
CAS: 467454-33-7

28b
commercially available
Enamine
CAS: 2173473-64-6

29b
commercially available
Enamine
CAS: 2680542-23-6

30b
commercially available
Enamine
CAS: 2680528-57-6

31b
commercially available
Enamine
CAS: 2300307-05-3

32b
commercially available
Enamine
CAS: 2680533-95-1

33b
commercially available
Enamine
CAS: 2680536-37-0

34b
see below

35b
commercially available
Enamine
CAS: 2680531-30-8

36b
commercially available
Enamine
CAS: 467454-51-9

37b
commercially available
Enamine
CAS: 2126159-66-6

38b
commercially available
Enamine
CAS: 2694734-32-0

commercially available
Enamine
CAS: 2680534-60-3

commercially available
Enamine
CAS: 2680528-19-0

commercially available
Enamine
CAS: 1795732-99-8

commercially available
Enamine
CAS: 2416234-57-4

commercially available
Enamine
CAS: 745149-00-3

commercially available
Enamine
CAS: 2680539-61-9

commercially available
Enamine
CAS: 2385077-55-2

commercially available
Enamine
CAS: 2219375-41-2

commercially available
Enamine
CAS: 2089277-63-2

commercially available
Enamine
CAS: 2137722-78-0

commercially available
Sigma-Aldrich
CAS: 279-23-2

commercially available
Enamine
CAS: 134078-23-2

Chem. Sci. **2021**, *12*, 7480.

Figure 2.8. Commercially availability and references for the synthesis of bicyclic substrates.

Sodium bicyclo-[1.1.1]-pentanesulfinate

Prepared according to literature procedures.[55]

¹H NMR (600 MHz, D$_2$O) δ 2.76 (s, 1H), 1.96 (s, 6H). [See spectrum]

¹³C NMR (151 MHz, D$_2$O) δ 69.5, 57.4, 47.4, 37.6, 26.0. [See spectrum]

2-methyl-1,10-phenanthroline
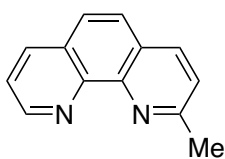
Prepared according to literature procedures.[56]

¹H NMR (300 MHz, CDCl₃) δ 9.37 (dd, J = 4.4, 1.8 Hz, 1H), 8.40 (dd, J = 8.1, 1.8 Hz, 1H), 8.30 (d, J = 8.2 Hz, 1H), 8.00 – 7.84 (m, 2H), 7.78 (dd, J = 8.1, 4.4 Hz, 1H), 7.69 (d, J = 8.2 Hz, 1H), 3.12 (s, 3H). [See spectrum]

¹³C NMR (126 MHz, CDCl₃) δ 159.8, 150.2, 145.8, 145.6, 136.4, 128.9, 126.8, 126.6, 125.6, 123.9, 122.9, 25.9. [See spectrum]

2,2'-((3-fluorophenyl)methylene)dipyridine (L3)
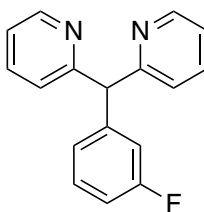
Prepared according to literature procedures.[4]

^{1}H NMR (600 MHz, CDCl$_3$) δ 8.73 (dd, J = 4.9, 1.0 Hz, 2H), 7.77 (td, J = 7.7, 1.9 Hz, 2H), 7.44 – 7.37 (m, 3H), 7.29 (dd, J = 7.5, 4.8 Hz, 2H), 7.19 (d, J = 7.5 Hz, 1H), 7.14 (dt, J = 10.2, 2.2 Hz, 1H), 7.06 (td, J = 8.8, 8.4, 2.4 Hz, 1H), 5.93 (s, 1H). [See spectrum]

^{13}C NMR (151 MHz, CDCl$_3$) δ 163.1 (d, $J_{C–F}$ = 245.7 Hz), 161.6, 149.7, 144.4 (d, $J_{C–F}$ = 7.2 Hz), 136.8, 130.0 (d, $J_{C–H}$ = 8.3 Hz), 125.2 (d, $J_{C–F}$ = 3.0 Hz) , 124.1, 121.9, 116.4 (d, J = 22.1 Hz), 113.8 (d, J = 21.1 Hz), 61.5. [See spectrum]

^{19}F NMR (565 MHz, CDCl$_3$) δ -113.0 (q, J = 8.7 Hz). [See spectrum]

5-methyl-2-(thiophen-3-yl)pyridine (L4)
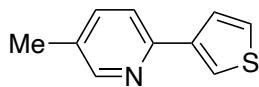
Prepared according to literature procedures.[45]

¹H NMR (600 MHz, CDCl₃) δ 8.49 (s, 1H), 7.88 (dd, *J* = 3.0, 1.3 Hz, 1H), 7.68 (dd, *J* = 5.0, 1.3 Hz, 1H), 7.61 – 7.52 (m, 2H), 7.42 (dd, *J* = 5.0, 3.0 Hz, 1H), 2.39 (s, 3H). [See spectrum]

¹³C NMR (151 MHz, CDCl₃) δ 151.2, 150.1, 142.3, 137.3, 131.4, 126.3, 126.3, 122.8, 119.9, 18.3. [See spectrum]

1-(4-(*tert*-butyl)phenyl)bicyclo[1.1.1]pentane (1b)
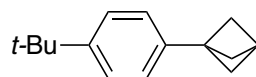
Prepared according to literature procedures.[38]

¹H NMR (500 MHz, CDCl₃) δ 7.47 (d, *J* = 8.3 Hz, 2H), 7.30 (d, *J* = 8.3 Hz, 2H), 2.68 (s, 1H), 2.21 (s, 6H), 1.45 (s, 9H). [See spectrum]

¹³C NMR (126 MHz, CDCl₃) δ 149.3, 138.9, 125.8, 125.1, 52.3, 47.0, 34.6, 31.5, 26.8. [See spectrum]

1-(3,5-di-*tert*-butylphenyl)bicyclo[1.1.1]pentane (2b)
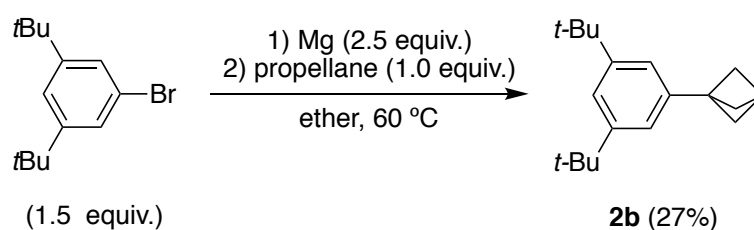
A flame-dried round bottom flask was charged with magnesium turnings (456 mg, 18.8 mmol, 2.50 equiv.), dry THF (1 mL), and a small crystal of iodine in an N_2 atmosphere. The mixture was stirred at room temperature until the solution became milky-white. Then, 1-bromo-3,5-di-*tert*-butylbenzene (3.03 g, 11.2 mmol, 1.50 equiv.) in 10 mL of ether was added dropwise, keeping the solution at a gentle reflux. The resulting solution was further stirred at room temperature for 3 h. Then, a 0.50 M solution of propellane in ether (15.0 mL, 7.50 mmol, 1.00 equiv.) was added. The mixture was heated at 60 ºC for 16 h. The reaction mixture was cooled to room temperature and carefully quenched with an aqueous solution of NH_4Cl (10 mL). The layers were separated, and the aqueous layer further extracted with diethyl ether (25 mL x 2). The combined organic layers were dried over $MgSO_4$, filtered, and concentrated. The crude material was purified by chromatography on silica gel, eluting with pentanes. The fractions were analyzed by GC-MS analysis, and the fractions containing the desired material were collected. The resulting white solid contained substantial amounts of biaryl, and was further purified by sublimation (200 mbar, 80 ºC). The title compound was obtained as a white solid (521 mg, 27%).

TLC: N/A

¹H NMR (500 MHz, CDCl₃) δ 7.33 (t, *J* = 1.9 Hz, 1H), 7.10 (d, *J* = 1.9 Hz, 2H), 2.58 (s, 1H), 2.12 (s, 6H), 1.36 (s, 18H). [See spectrum]

¹³C NMR (126 MHz, CDCl₃) δ 150.6, 140.9, 120.8, 120.1, 52.4, 47.8, 35.0, 31.6, 26.7. [See spectrum]

HRMS (*m/z*): (EI+) calc'd for $C_{19}H_{28}$ [M]⁺: 256.2191, found: 256.2194.

bicyclo[1.1.1]pentan-1-yl(*tert*-butyl)sulfane (3b)

t-BuS —⟨◇⟩
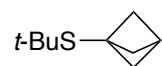
Prepared according to literature procedures.[26]

¹H NMR (500 MHz, CDCl₃) δ 2.75 (s, 1H), 2.13 (s, 6H), 1.41 (s, 9H). [See spectrum]

¹³C NMR (126 MHz, CDCl₃) δ 56.0, 44.7, 44.1, 31.9, 30.6, 14.1. [See spectrum]

bicyclo[1.1.1]pentan-1-yltributylstannane (4b)

$$(n\text{-Bu})_3\text{Sn} - \diamond$$
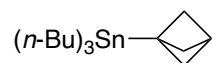
Prepared according to literature procedures.[57]

¹H NMR (500 MHz, CDCl$_3$) δ 2.92 (s, 1H) tin satellites ($J_{\text{H-119Sn}}$ = 179.4 Hz, $J_{\text{H-117Sn}}$ = 171.4 Hz) , 2.01 (s, 6H), 1.60 – 1.42 (m, 6H), 1.38 – 1.27 (m, 6H), 0.93 (t, J = 7.3 Hz, 9H), 0.88 – 0.81 (m, 6H). [See spectrum]

¹³C NMR (126 MHz, CDCl$_3$) δ 56.2, 39.2) tin satellites ($J_{\text{C-Sn}}$ = 117.0 Hz), 37.2, 29.4 tin satellites ($J_{\text{C-Sn}}$ = 20.2 Hz), 27.5 tin satellites ($J_{\text{C-Sn}}$ = 51.3 Hz), 13.9, 9.0 tin satellites ($J_{\text{C-Sn}}$ = 307.6). [See spectrum]

1-(methylsulfonyl)bicyclo[1.1.1]pentane (11b)
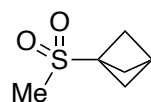
Prepared according to literature procedures.[55]

¹H NMR (600 MHz, CDCl₃) δ 2.86 (s, 3H), 2.84 (s, 1H), 2.30 (s, 6H). [See spectrum]

¹³C NMR (151 MHz, CDCl₃) δ 54.5, 50.7, 37.3, 26.4. [See spectrum]

bicyclo[1.1.1]pentane-1-sulfonamide (12b)
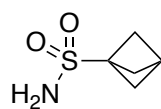
Prepared according to literature procedures.[55]

¹H NMR (700 MHz, Acetone) δ 6.16 (bs, 2H), 2.80 (s, 1H), 2.25 (s, 6H). [See spectrum]

¹³C NMR (176 MHz, Acetone) δ 54.8, 50.4, 25.5. [See spectrum]

1-(bicyclo[1.1.1]pentan-1-ylsulfonyl)piperidine (13b)

13b (82%)
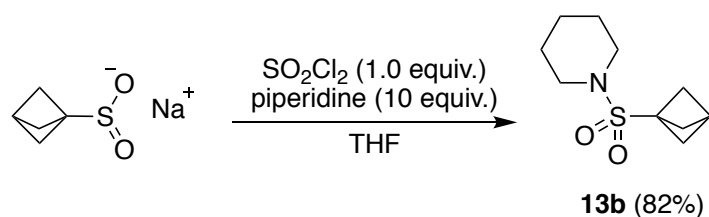
Sodium bicyclo[1.1.1]pentane-1-sulfinate (38.5 mg, 0.250 mmol, 1.00 equiv.) was suspended in THF (3 mL) and cooled to 0 ºC. SO_2Cl_2 (20 µL, 0.25 mmol, 1.0 equiv.) was added dropwise, and the mixture was allowed to warm to room temperature. The mixture was stirred until the complete dissolution of the starting material. Piperidine (247 µL, 2.50 mmol, 10.0 equiv.) was added dropwise, accompanied by the immediate formation of a cloudy white precipitate. The mixture was stirred at ambient temperature for 3 h and quenched carefully with water (5 mL). The biphasic mixture was extracted with ethyl acetate (30 mL x 3), dried over $MgSO_4$, filtered, and concentrated. The crude material was chromatographed on SiO_2, eluting with 33% ethyl acetate in hexanes to afford the title compound as a white powder (44.1 mg, 82%).

TLC: R_f = 0.50 (33% ethyl acetate in hexanes)

^{1}H NMR (500 MHz, CDCl$_3$) δ 3.30 (t, J = 5.2 Hz, 4H), 2.69 (s, 1H), 2.23 (s, 6H), 1.70 – 1.48 (m, 6H). [See spectrum]

^{13}C NMR (126 MHz, CDCl$_3$) δ 53.6, 52.0, 47.2, 27.7, 26.2, 24.1. [See spectrum]

HRMS (*m/z*): (ESI+) calc'd for $C_{10}H_{18}NO_2S$ [M+H]$^+$: 216.1053, found: 216.1056.

4-(bicyclo[1.1.1]pentan-1-ylsulfonyl)morpholine (14b)

14b (75%)
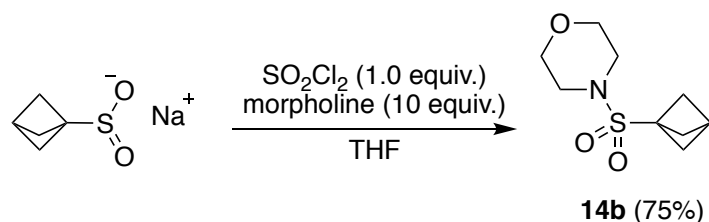
Sodium bicyclo[1.1.1]pentane-1-sulfinate (77.0 mg, 0.500 mmol, 1.00 equiv.) was suspended in THF (5 mL) and cooled to 0 ºC. SO_2Cl_2 (40 µL, 0.50 mmol, 1.0 equiv.) was added dropwise, and the mixture was allowed to warm to room temperature. The mixture was stirred until the starting material had fully dissolved. Morpholine (431 µL, 5.00 mmol, 10.0 equiv.) was added dropwise, accompanied by the immediate formation of a cloudy white precipitate. The mixture was stirred at ambient temperature for 3 h and quenched carefully with water (15 mL). The biphasic mixture was extracted with ethyl acetate (30 mL x 3), dried over $MgSO_4$, filtered, and concentrated. The crude material was chromatographed on SiO_2, eluting with 33% ethyl acetate in hexanes to afford the title compound as a white powder (81.1 mg, 75%).

TLC: R_f = 0.50 (33% ethyl acetate in hexanes)

^{1}H NMR (500 MHz, CDCl$_3$) δ 3.75 – 3.69 (m, 4H), 3.38 – 3.32 (m, 4H), 2.73 (s, 1H), 2.26 (s, 6H). [See spectrum]

^{13}C NMR (126 MHz, CDCl$_3$) δ 67.1, 53.4, 52.2, 46.4, 28.0. [See spectrum]

HRMS (*m/z*): (ESI+) calc'd for $C_9H_{15}NO_3SNa$ [M+Na]$^+$: 240.0665, found: 240.0665.

N-(bicyclo[1.1.1]pentan-1-yl)-2,2,2-trifluoroacetamide (16b)

16b (52%)
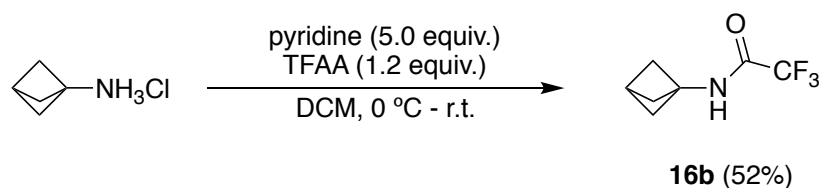
This is a known compound, and it was prepared in a similar manner to that reported in the patent literature.[59] Bicyclo[1.1.1]pentan-1-amine hydrochloride (120 mg, 1.00 mmol, 1.00 equiv.) and pyridine (400 µL, 5.00 mmol, 5.00 equiv.) were dissolved in dry DCM (10 mL). The cloudy mixture was cooled to 0 ºC, and trifluoroacetic anhydride (167 µL, 1.20 mmol, 1.20 equiv.) was added dropwise via syringe. The mixture was allowed to warm to room temperature and stirred overnight. The crude mixture was concentrated and chromatographed over SiO_2 with 10% ethyl acetate in hexanes to afford the title compound as white flakes (94.0 mg, 52%).

TLC: R_f = 0.55 (10% ethyl acetate in hexanes)

^{1}H NMR (500 MHz, CDCl$_3$) δ 6.63 (bs, 1H), 2.53 (s, 1H), 2.17 (s, 6H). [See spectrum]

^{13}C NMR (126 MHz, CDCl$_3$) δ 156.8 (q, $J_{C–F}$ = 37.3 Hz), 115.5 (q, $J_{C–F}$ = 288.6 Hz), 52.7, 47.9, 24.8. [See spectrum]

1-(3-methoxyphenyl)bicyclo[1.1.1]pentane (19b)
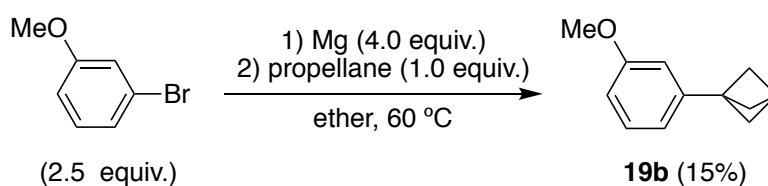
A flame-dried round bottom flask was charged with magnesium turnings (292 mg, 12.0 mmol, 4.00 equiv.), dry THF (1 mL), and a small crystal of iodine. The mixture was stirred at room temperature until the solution became milky-white. Then, 1-bromo-3-methoxybenzene (1.40 g, 7.50 mmol, 2.50 equiv.) in 10 mL of ether was added dropwise, keeping the solution at a gentle reflux. The resulting solution was further stirred at room temperature for 3 h. Then, a 1.00 M solution of propellane in ether (3.00 mL, 3.00 mmol, 1.00 equiv.) was added. The mixture was heated at 60 ºC for 16 h. The reaction mixture was cooled to room temperature, and carefully quenched with an aqueous solution of NH_4Cl (5 mL). The layers were separated, and the aqueous layer further extracted with diethyl ether (10 mL x 2). The combined organic layers were dried over $MgSO_4$, filtered, and concentrated. The crude material was chromatographed on silica gel and eluted with pentanes. The fractions were analyzed by GC-MS analysis, and the fractions containing the desired material were collected. The resulting oil was contaminated with anisole, which was removed by applying vacuum overnight. Some loss of the desired material occurred under vacuum, and the title compound was obtained as a colorless oil (78.0 mg, 15%).

TLC: N/A

^{1}H NMR (400 MHz, CDCl$_3$) δ 7.26 – 7.17 (m, 1H), 6.85 – 6.79 (m, 1H), 6.79 – 6.72 (m, 2H), 3.81 (s, 3H), 2.54 (s, 1H), 2.07 (s, 6H). [See spectrum]

^{13}C NMR (126 MHz, CDCl$_3$) δ 159.7, 143.5, 129.3, 118.5, 111.9, 111.8, 55.3, 52.3, 47.2, 26.7. [See spectrum]

HRMS (*m/z*): (EI+) calc'd for $C_{12}H_{14}O$ [M]$^+$: 174.1045, found: 174.1045.

N-(bicyclo[1.1.1]pentan-1-yl)-2-propylpentanamide (20b)
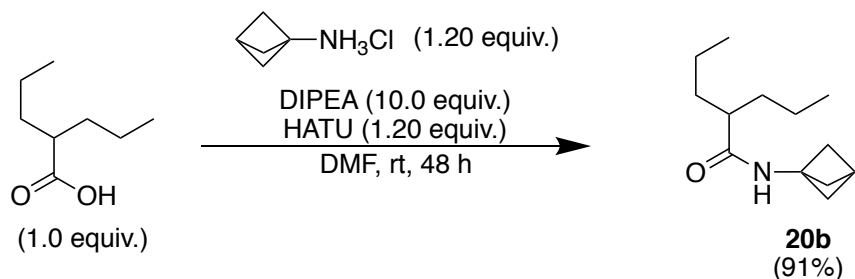
DIPEA (1.78 mL, 10.4 mmol, 10.0 equiv.) was added to a stirred mixture of 2-propylpentanoic acid (150 mg, 1.04 mmol, 1.00 equiv.), bicyclo[1.1.1]pentan-1-amine hydrochloride (149 mg, 1.25 mmol, 1.20 equiv.) and HATU (478 mg, 1.26 mmol, 1.20 equiv.) in DMF (6 mL). The mixture was stirred at room temperature for 48 h. Water (10 mL) was added, and the reaction extracted with EtOAc (3x20 mL). The organic layers were separated, dried (Na$_2$SO$_4$), filtered, and the solvents evaporated in vacuo. The crude material was purified by flash column chromatography (silica, EtOAc in Heptane 0/100 to 30/70). The desired fractions were collected and concentrated in vacuo to give N-(bicyclo[1.1.1]pentan-1-yl)-2-propylpentanamide (198 mg, 0.95 mmol, 91%) as white solid.

^{1}H NMR (400 MHz, CDCl$_3$) δ ppm 5.85 (br s, 1 H), 2.44 (s, 1 H), 2.10 (s, 6 H), 1.90 (dq, J=9.22, 4.56 Hz, 1 H), 1.49 - 1.65 (m, 2 H), 1.22 - 1.40 (m, 6 H), 0.85 - 0.97 (m, 6 H). [See spectrum]

^{13}C NMR (101 MHz, CDCl$_3$) δ ppm 176.4 (s, 1 C), 52.7 (s, 4 C), 47.8 (s, 1 C), 35.2 (s, 2 C), 24.7 (s, 1 C), 20.8 (s, 2 C), 14.2 (s, 2 C). [See spectrum]

HRMS (ESI-TOF) Calculated for C$_{13}$H$_{24}$NO [M+H]$^+$: 210.1780; Found: 210.1856.

(1*R*,4a*R*,4b*R*,10a*R*)-*N*-(bicyclo[1.1.1]pentan-1-yl)-7-isopropyl-1,4a-dimethyl-1,2,3,4,4a,4b,5,6,10,10a-decahydrophenanthrene-1-carboxamide (21b)
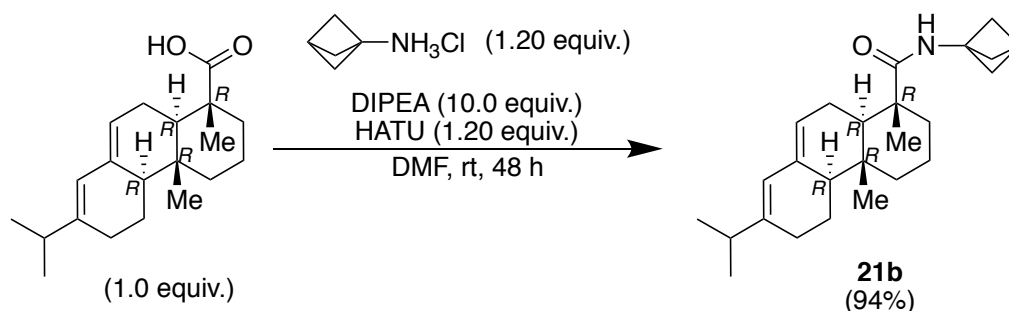
DIPEA (1.7 mL, 9.9 mmol, 10 equiv.) was added to a stirred mixture of abietic acid (300 mg, 0.99 mmol, 1.0 equiv.), bicyclo[1.1.1]pentan-1-amine hydrochloride (247 mg, 2.07 mmol, 1.20 equiv.) and HATU (456 mg, 1.2 mmol, 1.2 equiv.) in DMF (7.6 mL). The mixture was stirred at room temperature for 48 h. Water (10 mL) was added, and the reaction extracted with EtOAc (3x20 mL). The organic layers were separated, dried (Na$_2$SO$_4$), filtered and the solvents evaporated in vacuo. The crude material was purified by flash column chromatography (silica, EtOAc in Heptane 0/100 to 30/70). The desired fractions were collected and concentrated in vacuo to give (1*R*,4a*R*,4b*R*,10a*R*)-*N*-(bicyclo[1.1.1]pentan-1-yl)-7-isopropyl-1,4a-dimethyl-1,2,3,4,4a,4b,5,6,10,10a-decahydrophenanthrene-1-carboxamide (342 mg, 0.93 mmol, 94 %) as white solid.

¹H NMR (500 MHz, DMSO-*d$_6$*) δ ppm 7.92 (s, 1 H) 5.70 (s, 1 H) 5.30 (br d, *J*=4.50 Hz, 1 H) 2.36 (s, 1 H) 2.18 (dt, *J*=13.54, 6.80 Hz, 1 H) 1.97 - 2.10 (m, 2 H) 1.93 (s, 6 H) 1.29 - 1.90 (m, 10 H) 1.05 - 1.16 (m, 5 H) 0.96 (d, *J*=6.75 Hz, 3 H) 0.95 (d, *J*=6.88 Hz, 3 H) 0.72 (s, 3 H). [See spectrum]

¹³C NMR (101 MHz, DMSO-*d$_6$*) δ ppm 178.0 (s, 1 C) 144.3 (s, 1 C) 134.9 (s, 1 C) 122.5 (s, 1 C) 120.8 (s, 1 C) 52.2 (s, 3 C) 50.4 (s, 1 C) 49.3 (s, 1 C) 45.6 (s, 1 C) 44.7 (s, 1 C) 37.6 (s, 1 C) 34.3 (s, 1 C) 34.2 (s, 1 C) 27.0 (s, 1 C) 24.8 (s, 1 C) 24.5 (s, 1 C) 22.0 (s, 1 C) 21.4 (s, 1 C) 20.8 (s, 1 C) 18.1 (s, 1 C) 16.8 (s, 1 C) 13.9 (s, 1 C). [See spectrum]

HRMS (ESI-TOF) Calculated for C$_{25}$H$_{38}$NO [M+H]$^+$: 368.2875; Found: 368.2950.

tert-butyl 4-((triisopropylsilyl)ethynyl)-2-azabicyclo[2.1.1]hexane-2-carboxylate (34b)

34b
75%
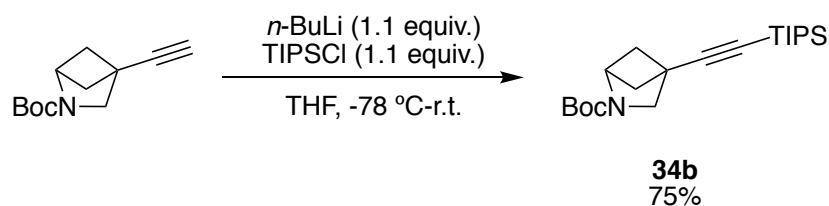
tert-butyl 4-ethynyl-2-azabicyclo[2.1.1]hexane-2-carboxylate (51.8 mg, 0.250 mmol, 1.00 equiv.) was dissolved in dry THF (1.0 mL) and cooled to -78 ºC. _n_-BuLi in hexanes (2.5 M, 0.110 mL, 0.275 mmol, 1.10 equiv.) was added dropwise, and the resultant mixture was stirred for 15 min. Then, TIPSCl (58.8 µL, 0.275 mmol, 1.10 equiv.) was added dropwise to the reaction mixture at -78 ºC. The mixture was warmed to ambient temperature and stirred for 1 h. Then, sat. NaHCO$_3$ was added (2 mL) and the mixture extracted with ethyl acetate (10 mL x 3). The combined organic layers were dried over MgSO$_4$, filtered, and concentrated. The crude material was chromatographed on NEt$_3$-treated SiO$_2$ with 0→15% ethyl acetate in hexanes to afford the title compound as a clear oil (68.0 mg, 75%).

TLC: R_f = 0.65 (20% ethyl acetate in hexanes)

^{1}H NMR (500 MHz, CDCl$_3$) δ 3.42 (s, 2H), 2.73 – 2.67 (m, 1H), 2.17 – 2.08 (m, 2H), 1.85 – 1.77 (m, 2H), 1.53 (s, 9H), 1.22 – 1.07 (m, 21H). [See spectrum]

^{13}C NMR (126 MHz, CDCl$_3$) δ 157.1, 104.4, 88.2, 80.2, 61.4, 52.0, 47.4, 35.4, 28.6, 18.8, 11.4. [See spectrum]

HRMS (_m/z_): (ESI+) calc'd for C$_{21}$H$_{37}$NO$_2$SiNa [M+Na]$^+$:386.2491, found:386.2492.

tert-butyl bicyclo-[1.1.0]-butane-1-carboxylate
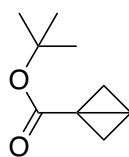
Prepared according to literature procedures.[58]

^{1}H NMR (600 MHz, CDCl$_3$) δ 2.33 (d, J = 3.5 Hz, 2H), 2.08 – 1.98 (m, 1H), 1.49 (s, 9H), 1.13 – 1.07 (m, 1H). [See spectrum]

^{13}C NMR (151 MHz, CDCl$_3$) δ 172.5, 80.4, 35.5, 28.2, 15.8, 10.2. [See spectrum]

2.4.3 Evaluation of Conditions for the Borylation of Bridgehead C–H Bonds.

Evaluation of ligands and boron reagents.

In a nitrogen glovebox, a 4 mL vial was sequentially charged with the appropriate ligand (12.5 µmol, 5.00 mol%), [Ir] source (5.00 mol% iridium), adamantane (17.0 mg, 0.125 mmol, 0.500 equiv.), 4-*tert*butylphenylbicyclopentane (**1b**) (50.1 mg, 0.250 mmol, 1.00 equiv.), and boron reagent (0.375 mmol, 1.50 equiv.). A magnetic stir bar and 0.2 mL of cyclooctane were added to the vial, and the vial was tightly sealed with a Teflon lined cap. The vial was removed from the glovebox and heated at 100 ºC in a preheated aluminum heating block for the specified time. After cooling to ambient temperature, an aliquot was taken and subjected to GC analysis.
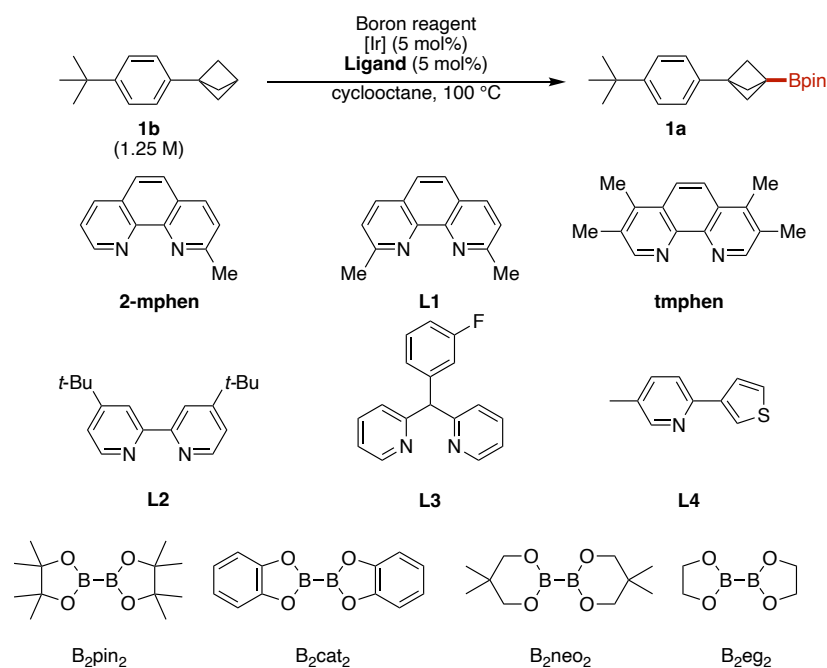
Entry	Ligand	Ir precatalyst	Boron reagent	Reaction time	GC yield (%)
1	2-mphen	(mesitylene)Ir(Bpin)$_3$	B$_2$pin$_2$ (3 equiv.)	24 h	89
2	2-mphen	(mesitylene)Ir(Bpin)$_3$	B$_2$pin$_2$ (3 equiv.)	2 h	92
3	2-mphen	(mesitylene)Ir(Bpin)$_3$	B$_2$pin$_2$ (1.5 equiv.)	2 h	89
4	2-mphen	[Ir(COD)(OMe)]$_2$	B$_2$pin$_2$ (1.5 equiv.)	2 h	90
5	2-mphen	[Ir(COD)(OMe)]$_2$	HBpin (1.5 equiv.)	2 h	19
6	2-mphen	[Ir(COD)(OMe)]$_2$	B$_2$cat$_2$ (1.5 equiv.)	2 h	0
7	2-mphen	[Ir(COD)(OMe)]$_2$	B$_2$neo$_2$ (1.5 equiv.)	2 h	0
8	2-mphen	[Ir(COD)(OMe)]$_2$	B$_2$eg$_2$ (1.5 equiv.)	2 h	0
9	L1	[Ir(COD)(OMe)]$_2$	B$_2$pin$_2$ (1.5 equiv.)	2 h	73
10	tmphen	[Ir(COD)(OMe)]$_2$	B$_2$pin$_2$ (1.5 equiv.)	2 h	4
11	L2	[Ir(COD)(OMe)]$_2$	B$_2$pin$_2$ (1.5 equiv.)	2 h	0
12	L3	[Ir(COD)(OMe)]$_2$	B$_2$pin$_2$ (1.5 equiv.)	2 h	20
13	L4	[Ir(COD)(OMe)]$_2$	B$_2$pin$_2$ (1.5 equiv.)	2 h	0
14	-	[Ir(COD)(OMe)]$_2$	B$_2$pin$_2$ (1.5 equiv.)	2 h	0
15	2-mphen	-	B$_2$pin$_2$ (1.5 equiv.)	2 h	0

Figure 2.9. Evaluation of ligands and boron reagents for the borylation of tertiary C–H bonds.

3.2 Evaluation of the effect of prolonged reaction times.

In a nitrogen glovebox, a 4 mL vial was sequentially charged with the appropriate ligand (12.5 μmol, 5.00 mol%), [Ir(COD)(OMe)]$_2$ (4.14 mg, 6.25 μmol, 2.50 mol%), substrate (0.250 mmol, 1.00 equiv.), and boron reagent (0.375 mmol, 1.50 equiv.). A magnetic stir bar and 0.2 mL of cyclooctane were added to the vial, and the vial was tightly sealed with a Teflon lined cap. The vial was removed from the glovebox and heated at 100 ºC in a preheated aluminum heating block for the specified time. After cooling to ambient temperature, CDCl$_3$ and CH$_2$Br$_2$ (internal standard) were added to the vial, and an aliquot was analyzed by ^{1}H NMR spectroscopy.
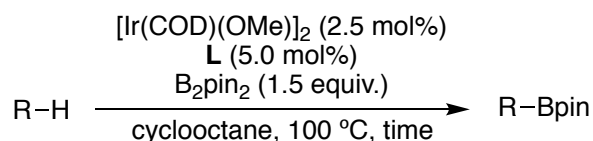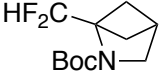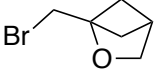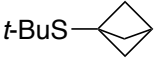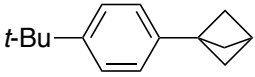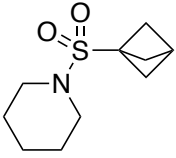
Entry	Substrate	L = 2-mphen, time = 2 h	L = tmphen, time = 24 h
1	HF$_2$C— (ring), BocN—	quant.	quant.
2	Br— (ring), O	50%	trace
3	t-BuS— (ring)	80%	67%
4	t-Bu—(phenyl)—(ring)	86%	73%
5	O=S=O, N (piperidine)—(ring)	90%	83%

Figure 2.10. Comparison of yields obtained with tmphen, 24 h of heating versus those observed under the standard conditions.

2.4.4 General procedures

General Conditions A: Catalytic borylation of bridgehead C–H bonds

In a nitrogen glovebox, a 4 mL vial was sequentially charged with 2-mphen (2.43 mg, 12.5 μmol, 5.00 mol%), [Ir(COD)(OMe)]$_2$ (6.25 μmol, 2.50 mol%), substrate (0.250 mmol, 1.00 equiv.), and B$_2$pin$_2$ (95.2 mg, 0.375 mmol, 1.50 equiv.) (If the substrate was a liquid, it was added last.). A magnetic stir bar and 0.2 mL of cyclooctane were added to the vial, and the vial was tightly sealed with a Teflon lined cap. The vial was removed from the glovebox and heated at 100 ºC in a preheated aluminum heating block for the specified time. After cooling to ambient temperature, CDCl$_3$ and CH$_2$Br$_2$ (internal standard) were added to the vial, and a sample was taken and analyzed by ^{1}H NMR spectroscopy to quantify the conversion. The mixture was then co-evaporated with MeOH (5 mL x 3) at 45 ºC (Caution: vigorous gas evolution upon addition of MeOH!). The crude residue was purified by flash column chromatography (silica or C18 reverse phase) to give the borylated product.

General Conditions B: In situ protection followed by catalytic borylation

In a nitrogen glovebox, a 4 mL vial was charged with substrate (0.250 mmol, 1.00 equiv.) and HBpin (0.325 mmol, 1.30 equiv.), and the vial was tightly sealed with a Teflon lined cap. The vial was removed from the glovebox and heated at 100 ºC in a preheated aluminum heating block for 45 min. The vial was then sent into the glovebox and sequentially charged with 2-mphen (2.43 mg, 12.5 μmol, 5.00 mol%), [Ir(COD)(OMe)]$_2$ (6.25 μmol, 2.50 mol%), and B$_2$pin$_2$ (95.2 mg, 0.375 mmol, 1.50 equiv.). A magnetic stir bar and 0.2 mL of cyclooctane were added to the vial, and the vial was again tightly sealed with a Teflon lined cap. The vial was removed from the glovebox and heated at 100 ºC in a preheated aluminum heating block for the specified time. After cooling to ambient temperature, CDCl$_3$ and CH$_2$Br$_2$ (internal standard) were added to the vial, and a sample was taken and analyzed by ^{1}H NMR spectroscopy to quantify conversion. The mixture was then co-evaporated with MeOH (5 mL x 3) at 45 ºC (Caution: vigorous gas evolution upon addition of MeOH!). The crude residue was purified by flash column chromatography (silica or C18 reverse phase) to give the borylated product.

General Conditions C: Catalytic borylation followed by treatment by KHF$_2$

In a nitrogen glovebox, a 4 mL vial was sequentially charged with 2-mphen (2.43 mg, 12.5 μmol, 5.00 mol%), [Ir(COD)(OMe)]$_2$ (6.25 μmol, 2.50 mol%), substrate (0.250 mmol, 1.00 equiv.), and B$_2$pin$_2$ (95.2 mg, 0.375 mmol, 1.50 equiv.) (If the substrate was a liquid, it was added last.). A magnetic stir bar and 0.2 mL of cyclooctane were added to the vial, and the vial was tightly sealed with a Teflon lined cap. The vial was removed from the glovebox and heated at 100 ºC in a preheated aluminum heating block for the specified time. After cooling to ambient temperature, the crude reaction mixture was passed through a thin pad of C18 reverse phase silica and eluted with acetonitrile. All volatile materials were removed, and the crude residue was dissolved in a mixture of MeOH (0.4 mL) and THF (0.8 mL). Then, KHF$_2$ (97.6 mg, 1.25 mmol, 5.00 equiv.) in water (0.4 mL) was added, and the resulting biphasic mixture stirred overnight at room temperature. The resulting mixture was co-evaporated with a 1:1 mixture of MeOH and water (2 mL x 5) at 45 ºC to remove pinacol and boron byproducts. The residue was extracted with acetone, filtered, and the filtrate concentrated to dryness in

vacuo. The resulting solids were washed with diethyl ether or pentane as appropriate to afford the desired trifluoroborate salt.

General tips for work up and purification of the bridgehead boronic esters

The progress of the reaction is most easily monitored by GC-MS analysis or ^{1}H NMR spectroscopy. One ion commonly seen for these compounds is the $[M-15]^+$ peak resulting from the loss of a methyl of the Bpin moiety.

In general, the bridgehead boronic esters are stable to ambient moisture and air. Prolonged manipulation or storage under ambient conditions is still not recommended because oxidation has been observed in select cases. We generally observed no decomposition when the product boronic esters were stored in a -20 °C freezer under air.

The bridgehead boronic esters are stable towards water and methanol. Co-evaporation with methanol at 45 °C is a convenient method to remove the HOBpin byproduct or to selectively protodeboronate more labile boronic esters.

Most of the BCP-Bpin compounds can be purified by column chromatography on silica, but protodeboronation occurs in select cases. In those cases, purification via column chromatography on C-18 reverse phase silica is recommended.

The BCP-Bpin compounds can generally be visualized on TLC plates with a *p*-anisaldehyde stain (Prepared by mixing 135 mL of absolute ethanol, 5 mL of concentrated sulfuric acid, 1.5 mL of glacial acetic acid, and 3.7 mL of *p*-anisaldehyde). Permanganate or phosphomolybdic acid stains are also occasionally useful, but less general, because the BCP-Bpin compounds do not always stain well with them. Note that pinacol, HOBpin, and B_2pin_2 tend to stain very strongly with all three stains, if present.

2.4.5 Scope of the catalytic borylation of bridgehead C–H bonds

Unsuccessful Substrates
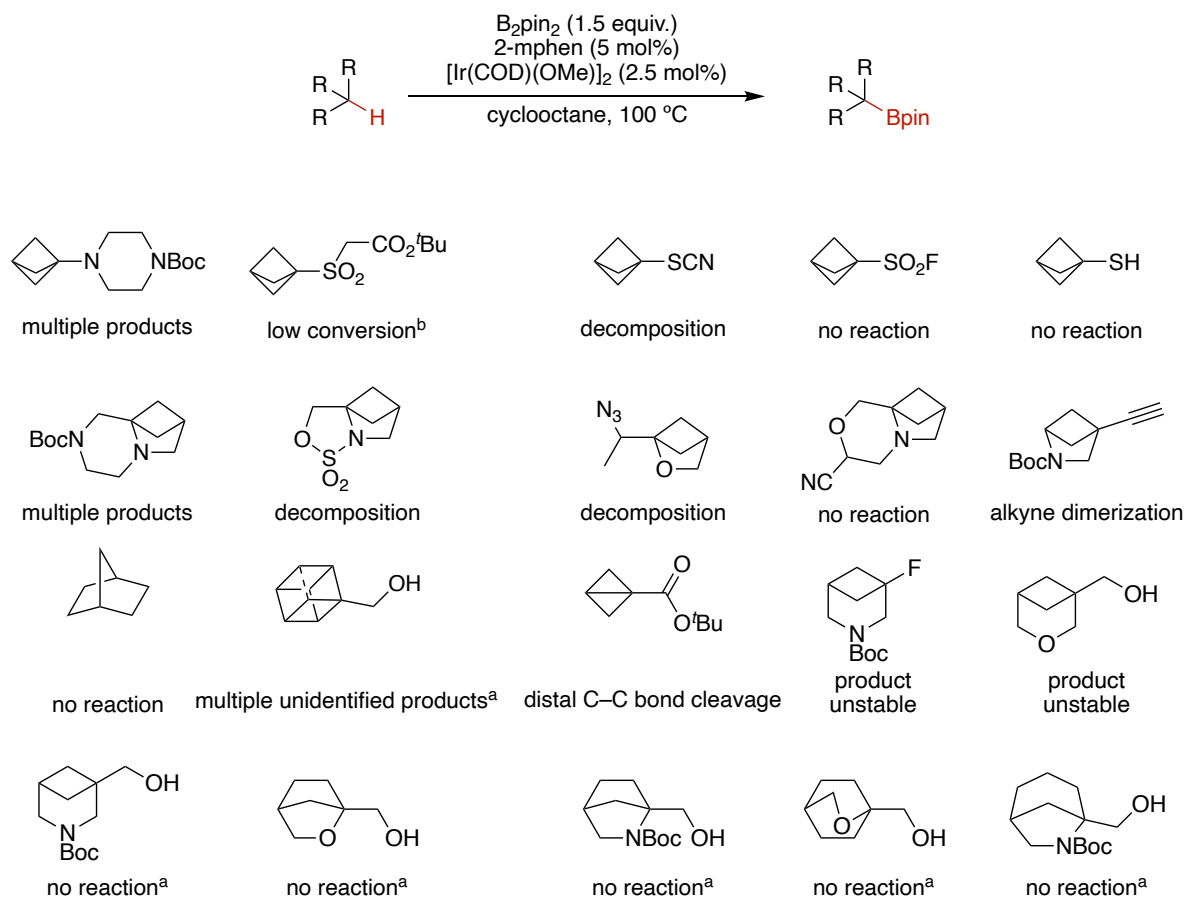
a Substrate treated with 1.3 eq. of HBpin. b with 3 equiv. of B$_2$pin$_2$

Figure 2.11. Substrates that did not undergo borylation of tertiary C–H bonds.

Bicyclo[1.1.1]pentane Substrates

2-(3-(4-(*tert*-butyl)phenyl)bicyclo[1.1.1]pentan-1-yl)-4,4,5,5-tetramethyl-1,3,2-dioxaborolane (1a)
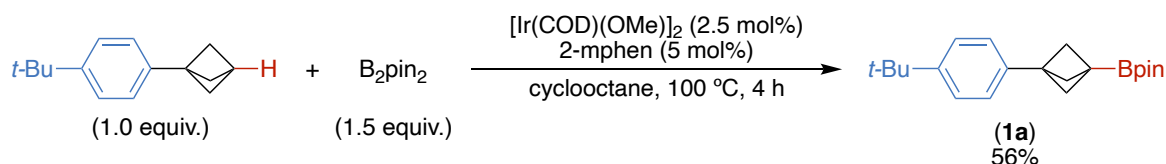
Prepared according to General Procedure A on a 0.25 mmol scale. The reaction mixture was heated for 4 h instead of the usual 2 h. The crude reaction mixture was eluted on SiO_2 with 10% ethyl acetate in hexanes as the eluent to afford 45.0 mg (56%) of the title compound as a white powder.

**TLC:** $R_f = 0.42$ (10% ethyl acetate in hexanes)

^{1}H NMR (500 MHz, CDCl$_3$) δ 7.34 (d, $J = 8.3$ Hz, 2H), 7.17 (d, $J = 8.3$ Hz, 2H), 2.17 (s, 6H), 1.31 (s, 9H), 1.28 (s, 12H). [See spectrum]

^{13}C NMR (126 MHz, CDCl$_3$) δ 149.3, 139.4, 125.6, 125.1, 83.5, 53.2, 47.3, 34.6, 31.5, 24.9. [See spectrum]

^{11}B NMR (160 MHz, CDCl$_3$) δ 30.8. [See spectrum]

HRMS (*m/z*): (EI+) calc'd for $C_{21}H_{31}BO_2$ [M]$^+$: 326.2417, found: 326.2419.

2-(3-(3,5-di-*tert*-butylphenyl)bicyclo[1.1.1]pentan-1-yl)-4,4,5,5-tetramethyl-1,3,2-dioxaborolane (2a)
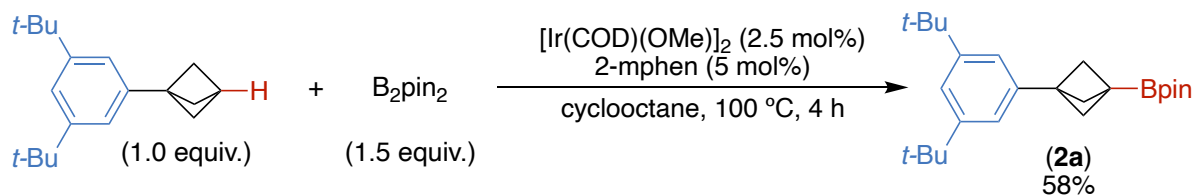
Prepared according to General Procedure A for borylation on a on a 0.40 mmol scale. The reaction mixture was heated for 4 h instead of the usual 2 h. The crude reaction mixture was eluted on SiO$_2$ with 10% ethyl acetate in hexanes as the eluent to afford 88.0 mg (58%) of the title compound as a white powder.

TLC: R_f = 0.52 (10% ethyl acetate in hexanes)

^{1}H NMR (600 MHz, CDCl$_3$) δ 7.29 (t, J = 1.9 Hz, 1H), 7.05 (d, J = 1.9 Hz, 2H), 2.17 (s, 6H), 1.32 (s, 18H), 1.27 (s, 12H). [See spectrum]

^{13}C NMR (151 MHz, CDCl$_3$) δ 150.6, 141.4, 120.8, 119.8, 83.5, 53.3, 48.0, 35.0, 31.6, 24.9. [See spectrum]

^{11}B NMR (193 MHz, CDCl$_3$) δ 30.8. [See spectrum]

HRMS (*m/z*): (EI+) calc'd for C$_{25}$H$_{39}$BO$_2$ [M]$^+$: 382.3043, found: 382.3047.

2-(3-(*tert*-butylthio)bicyclo[1.1.1]pentan-1-yl)-4,4,5,5-tetramethyl-1,3,2-dioxaborolane (3a)
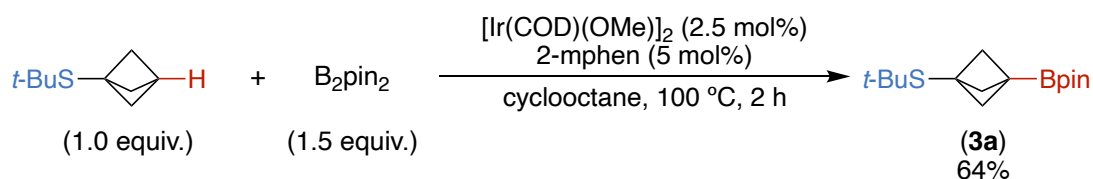
Prepared according to General Procedure A on a 0.25 mmol scale. The crude reaction mixture was eluted on SiO_2 with 10% ethyl acetate in hexanes as the eluent to afford 45.0 mg (64%) of the title compound as a yellow oil that solidified upon standing.

TLC: R_f = 0.48 (10% ethyl acetate in hexanes)

^{1}H NMR (500 MHz, CDCl$_3$) δ 2.18 (s, 6H), 1.36 (s, 9H), 1.23 (s, 12H). [See spectrum]

^{13}C NMR (126 MHz, CDCl$_3$) δ 83.5, 57.0, 44.8, 44.4, 31.9, 24.7. [See spectrum]

^{11}B NMR (160 MHz, CDCl$_3$) δ 29.7. [See spectrum]

HRMS (*m/z*): (EI+) calc'd for $C_{13}H_{17}NO_4$ [M]$^+$: 282.1825, found: 282.1824.

tributyl(3-(4,4,5,5-tetramethyl-1,3,2-dioxaborolan-2-yl)bicyclo[1.1.1]pentan-1-yl)stannane (4a)
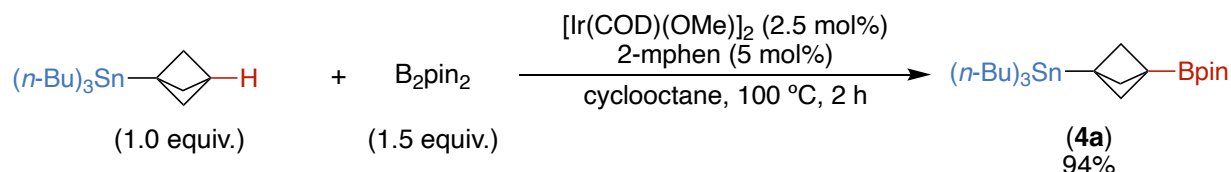
Prepared according to General Procedure A on a 0.25 mmol scale. The crude reaction mixture was eluted on fully endcapped reverse phase silica with 10% dichloromethane in acetonitrile as the eluent. Fractions containing the desired compound were collected and concentrated under vacuum. The residue was co-evaporated with methanol at 45 °C twice (5 mL each), diluted with pentane, and filtered through a glass fibre plug to afford 114 mg (94%) of the title compound as a viscous brown oil.

TLC: R_f = 0.70 (10% dichloromethane in acetonitrile)

^{1}H NMR (600 MHz, CDCl$_3$) δ 2.11 (s, 6H), 1.51 – 1.41 (m, 6H), 1.33 – 1.23 (m, 6H), 1.21 (s, 12H), 0.88 (t, J = 7.3 Hz, 9H), 0.82 – 0.73 (m, with tin magnetic isotope satellites, $J(^{119}Sn^1H)$ = 24.7 Hz, $J(^{117}Sn^1H)$ = 23.8 Hz, 6H). [See spectrum]

^{13}C NMR (151 MHz, CDCl$_3$) δ 83.1, 57.0, 39.0, 29.3 (with tin magnetic isotope satellites, J_{Sn-C} = 10.2 Hz), 27.4 (with tin magnetic isotope satellites, J_{Sn-C} = 24.2 Hz), 24.7, 13.8, 8.8 (with tin magnetic isotope satellites, $J(^{119}Sn^{13}C)$ = 153.5 Hz, $J(^{117}Sn^{13}C)$ = 147.2 Hz). [See spectrum]

^{11}B NMR (160 MHz, CDCl$_3$) δ 27.57. [See spectrum]

^{119}Sn NMR (224 MHz, CDCl$_3$) δ -71.27. [See spectrum]

HRMS (*m/z*): (EI+) calc'd for C$_{19}$H$_{36}$BO$_2$Sn [M-Bu]$^+$ 427.1830 , found: 427.1830.

2-(3-(bromomethyl)bicyclo[1.1.1]pentan-1-yl)-4,4,5,5-tetramethyl-1,3,2-dioxaborolane (5a)
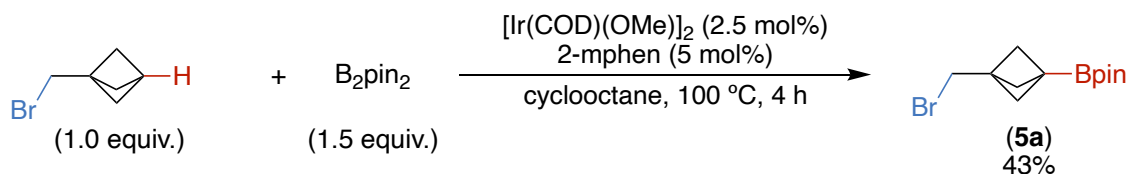
Prepared according to General Procedure A on a 0.25 mmol scale. The reaction mixture was heated for 4 h instead of the usual 2 h. The crude reaction mixture was eluted on SiO$_2$ with 0% → 20% ethyl acetate in hexanes as the eluent to afford 30.5 mg (43%) of the title compound as a white powder.

TLC: R_f = 0.45 (10% ethyl acetate in hexanes)

^{1}H NMR (500 MHz, CDCl$_3$) δ 3.30 (s, 2H), 1.84 (s, 6H), 1.23 (s, 12H). [See spectrum]

^{13}C NMR (126 MHz, CDCl$_3$) δ 83.6, 50.9, 44.5, 35.1, 24.9. [See spectrum]

^{11}B NMR (160 MHz, CDCl$_3$) δ 30.4. [See spectrum]

HRMS (*m/z*): (EI+) calc'd for C$_{11}$H$_{17}$BBrO$_2$ [M-Me]$^+$: 271.0505, found: 271.0504.

(3-(4,4,5,5-tetramethyl-1,3,2-dioxaborolan-2-yl)bicyclo[1.1.1]pentan-1-yl)methanol (6a)
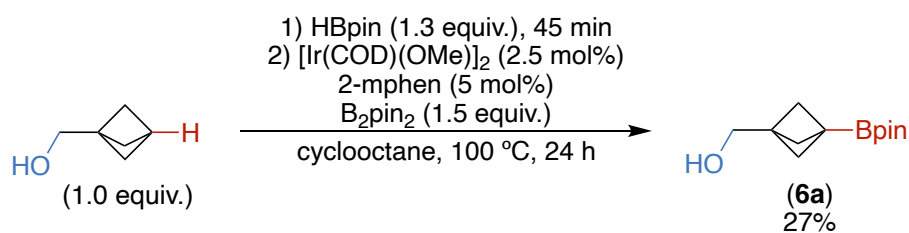
Prepared according to General Procedure B on a 0.10 mmol scale. The crude reaction mixture was eluted on SiO$_2$ with 20% → 30% ethyl acetate in hexanes as the eluent to afford 6.0 mg (27%) of the title compound as a white powder.

TLC: R_f = 0.70 (10% dichloromethane in acetonitrile)

^{1}H NMR (500 MHz, CDCl$_3$) δ 3.46 (s, 2H), 1.82 (s, 6H), 1.24 (s, 12H). [See spectrum]

^{13}C NMR (126 MHz, CDCl$_3$) δ 83.5, 64.2, 49.9, 46.0, 24.9. [See spectrum]

^{11}B NMR (160 MHz, CDCl$_3$) δ 30.4. [See spectrum]

HRMS (*m/z*): (ESI-) calc'd for C$_{12}$H$_{20}$BO$_3$ [M-H]$^-$: 223.1511, found: 223.1512.

2-(3-(4,4,5,5-tetramethyl-1,3,2-dioxaborolan-2-yl)bicyclo[1.1.1]pentan-1-yl)ethan-1-ol) (7a)
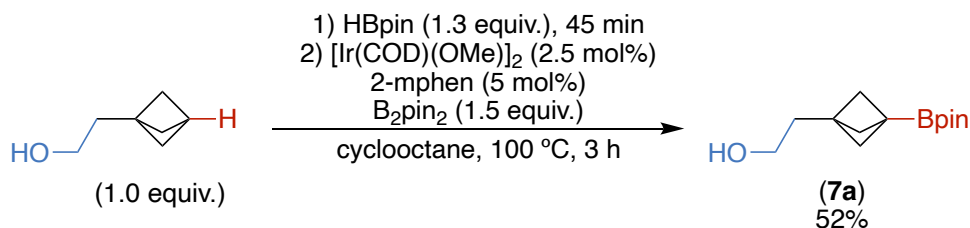
Prepared according to General Procedure B on a 0.10 mmol scale. The crude reaction mixture was eluted on SiO$_2$ with 0% → 50% ethyl acetate in hexanes as the eluent to afford 12.3 mg (52%) of the title compound as a clear oil.

TLC: R_f = 0.48 (50% ethyl acetate in hexanes)

^{1}H NMR (600 MHz, CDCl$_3$) δ 3.64 (t, J = 6.8 Hz, 2H), 1.81 (s, 6H), 1.63 (t, J = 6.8 Hz, 2H), 1.22 (s, 12H). [See spectrum]

^{13}C NMR (151 MHz, CDCl$_3$) δ 83.4, 61.2, 52.2, 43.9, 36.2, 24.9. [See spectrum]

^{11}B NMR (193 MHz, CDCl$_3$) δ 30.4. [See spectrum]

HRMS (*m/z*): (ESI+) calc'd for [M+H]$^+$: 239.1819, found: 239.1817.

tert-butyl 3-(4,4,5,5-tetramethyl-1,3,2-dioxaborolan-2-yl)bicyclo[1.1.1]pentane-1-carboxylate) (8a)
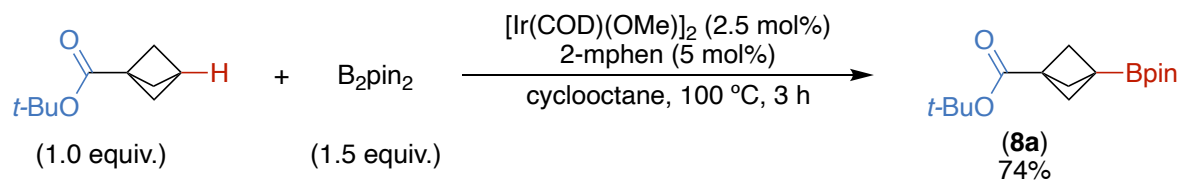
Prepared according to General Procedure A on a 0.25 mmol scale. The crude reaction mixture was eluted on SiO$_2$ with 10% → 35% ethyl acetate in hexanes as the eluent to afford 52.2 mg (71%) of the title compound as a white powder.

TLC: R_f = 0.32 (10 % ethyl acetate in hexanes)

^{1}H NMR (600 MHz, CDCl$_3$) δ 2.05 (s, 6H), 1.40 (s, 9H), 1.21 (s, 12H) [See spectrum]

^{13}C NMR (151 MHz, CDCl$_3$) δ 169.5, 83.6, 80.2, 52.3, 44.1, 28.1, 24.8. [See spectrum]

^{11}B NMR (193 MHz, CDCl$_3$) δ 30.6 [See spectrum]

HRMS (m/z): (ESI+) calc'd for [M+H]$^+$: 295.2081, found: 295.2083.

tert-butyl 2-(3-(4,4,5,5-tetramethyl-1,3,2-dioxaborolan-2-yl)bicyclo[1.1.1]pentan-1-yl)acetate (9a)
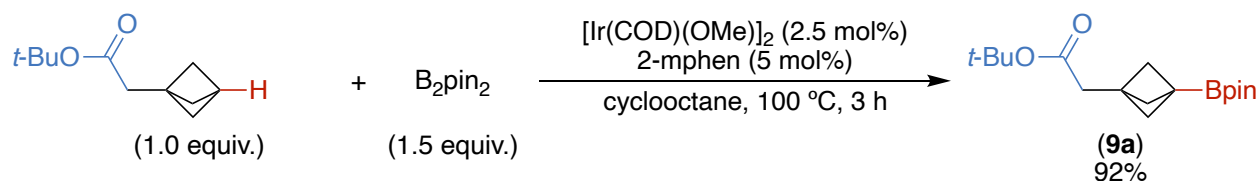
Prepared according to General Procedure A on a 0.15 mmol scale. The reaction mixture was heated for 3 h instead of the usual 2 h. The crude reaction mixture was eluted on SiO_2 with 0% → 20% ethyl acetate in hexanes as the eluent to afford 42.9 mg (92%) of the title compound as a colorless oil.

TLC: R_f = 0.47 (10% ethyl acetate in hexanes)

¹H NMR (500 MHz, CDCl₃) δ 2.28 (s, 2H), 1.85 (s, 6H), 1.42 (s, 9H), 1.22 (s, 12H). [See spectrum]

¹³C NMR (126 MHz, CDCl₃) δ 170.8, 83.4, 80.2, 52.4, 41.9, 41.0, 28.3, 24.9. [See spectrum]

¹¹B NMR ¹¹B NMR (160 MHz, CDCl₃) δ 30.2. [See spectrum]

HRMS (m/z): (ESI+) calc'd for $C_{17}H_{29}BO_4$ [M+H]⁺: 309.2232, found: 309.2231.

tert-butyl 2,2-difluoro-2-(3-(4,4,5,5-tetramethyl-1,3,2-dioxaborolan-2-yl)bicyclo[1.1.1]pentan-1-yl)acetate (10a)
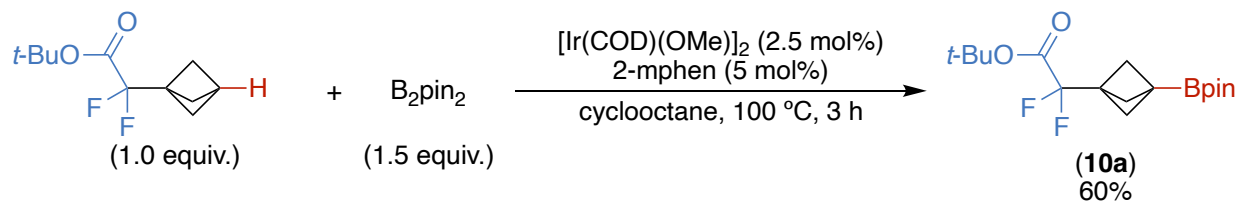
Prepared according to General Procedure A on a 0.15 mmol scale. The reaction mixture was heated for 3 h instead of the usual 2 h. The crude reaction mixture was eluted on SiO_2 with 0% → 20% ethyl acetate in hexanes as the eluent to afford 31.0 mg (60%) of the title compound as a white powder.

TLC: R_f = 0.41 (10% ethyl acetate in hexanes)

¹H NMR (500 MHz, CDCl$_3$) δ 1.99 (s, 6H), 1.51 (s, 9H), 1.23 (s, 12H). [See spectrum]

¹³C NMR (126 MHz, CDCl$_3$) δ 162.4 (t, J_{C-F} = 32.4 Hz) 112.9, 110.9 (t, J_{C-F} = 250.1 Hz), 109.0, 84.4, 83.8, 49.5, 43.6, 43.4 (t, J_{C-F} = 31.1 Hz), 43.2, 28.0, 24.9. [See spectrum]

¹¹B NMR (160 MHz, CDCl$_3$) δ 30.3. [See spectrum]

¹⁹F NMR (470 MHz, CDCl$_3$) δ -113.4. [See spectrum]

HRMS (m/z): (ESI+) calc'd for $C_{17}H_{27}BF_2O_4Na$ [M+Na]$^+$: 367.1863, found: 367.1862.

4,4,5,5-tetramethyl-2-(3-(methylsulfonyl)bicyclo[1.1.1]pentan-1-yl)-1,3,2-dioxaborolane (11a)
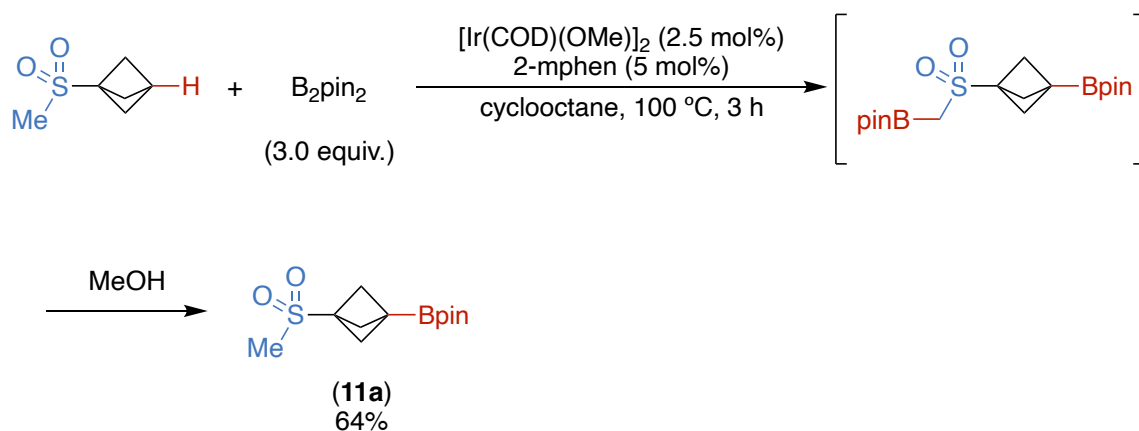
(11a)
64%

Prepared according to General Procedure A on a 0.25 mmol scale with 3 equiv. of B_2pin_2, instead of the usual 1.5 equiv. The reaction mixture was heated for 3 h, rather than the usual 2 h. The crude material was co-evaporated with methanol at 45 °C (10 mL x 4). The residue was dissolved in a minimal amount of CH_2Cl_2, layered with pentane, and stored at -20 °C overnight. The resulting brown powder, which precipitated overnight, was collected and washed with pentane, affording 43.8 mg (64%) of the title compound as a brown solid.

TLC: N/A

¹H NMR (500 MHz, CDCl$_3$) δ 2.76 (s, 3H), 2.26 (s, 6H), 1.23 (s, 12H). [See spectrum]

¹³C NMR (126 MHz, CDCl$_3$) δ 84.3, 54.5, 51.4, 36.8, 25.0, 24.8. [See spectrum]

¹¹B NMR (160 MHz, CDCl$_3$) δ 29.9. [See spectrum]

HRMS (*m/z*): (EI+) calc'd for $C_{12}H_{21}BO_4SNa$ [M+Na]$^+$: 295.1146, found: 295.1150.

3-(4,4,5,5-tetramethyl-1,3,2-dioxaborolan-2-yl)bicyclo[1.1.1]pentane-1-sulfonamide (12a)
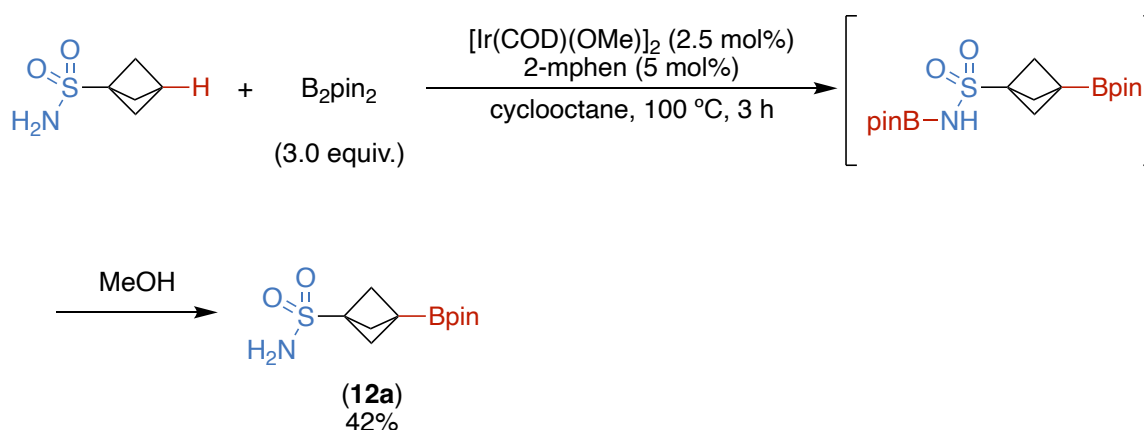
(12a)
42%

Prepared according to General Procedure A on a 0.25 mmol scale with 3 equiv. of B$_2$pin$_2$, instead of the usual 1.5 equiv. The reaction mixture was heated for 3 h, rather than the usual 2 h. The crude material was co-evaporated with methanol at 45 °C (30 mL x 2), then stirred with CH$_2$Cl$_2$ (30 mL) for 1 h. The suspension was filtered over a frit, and the solids were redissolved in methanol and concentrated to yield 28.7 mg (42%) of the title compound as a light brown solid.

TLC: N/A

^{1}H NMR (500 MHz, DMSO) δ 6.69 (s, 1H), 2.02 (s, 6H), 1.18 (s, 12H). [See spectrum]

^{13}C NMR (126 MHz, DMSO) δ 83.5, 54.3, 50.9, 39.4, 24.5. [See spectrum]

^{11}B NMR (160 MHz, DMSO) δ 29.5. [See spectrum]

HRMS (*m/z*): (ESI+) calc'd for C$_{11}$H$_{20}$BNO$_4$SNa [M+Na]$^+$: 296.1098, found: 296.1100.

1-((3-(4,4,5,5-tetramethyl-1,3,2-dioxaborolan-2-yl)bicyclo[1.1.1]pentan-1-yl)sulfonyl)piperidine (13a)

Prepared according to General Procedure A on a 0.10 mmol scale. The crude material was co-evaporated with methanol at 45 °C (10 mL x 3). The residue was dissolved in a minimal amount of CH_2Cl_2, layered with pentane, and stored at -20 ºC overnight. The resulting needles were collected and washed with pentane, affording 20.9 mg (61%) of the title compound as a beige solid.

TLC: N/A

^{1}H NMR (500 MHz, $CDCl_3$) δ 3.29 (t, J = 5.2 Hz, 4H), 2.26 (s, 6H), 1.67 – 1.48 (m, 6H), 1.23 (s, 12H). [See spectrum]

^{13}C NMR (126 MHz, $CDCl_3$) δ 84.1, 53.8, 52.8, 47.1, 26.2, 24.9, 24.1. [See spectrum]

^{11}B NMR (160 MHz, $CDCl_3$) δ 30.0. [See spectrum]

HRMS (*m/z*): (ESI+) calc'd for $C_{16}H_{28}BNO_4SNa$ [M+Na]$^+$: 364.1724, found: 364.1729.

4-((3-(4,4,5,5-tetramethyl-1,3,2-dioxaborolan-2-yl)bicyclo[1.1.1]pentan-1-yl)sulfonyl)morpholine (14a)
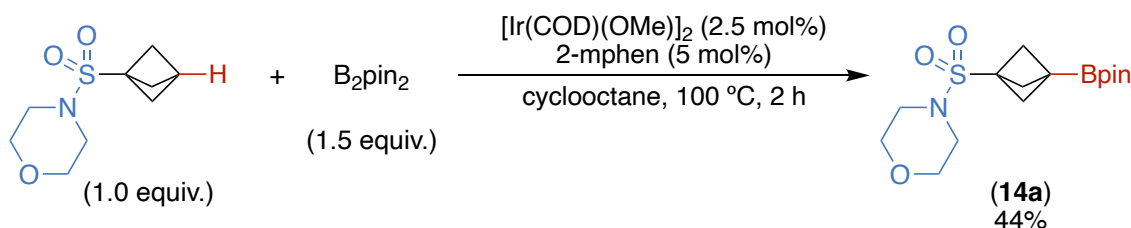
Prepared according to General Procedure A on a 0.10 mmol scale. The crude material was co-evaporated with methanol at 45 °C (10 mL x 3). The residue was dissolved in a minimal amount of CH_2Cl_2, layered with pentane, and stored at -20 ºC overnight. The resulting needles were collected and washed with pentane, affording 15.0 mg (44%) of the title compound as a brown solid.

TLC: N/A

^{1}H NMR (500 MHz, CDCl$_3$) δ 3.73 – 3.66 (m, 4H), 3.36 – 3.31 (m, 4H), 2.29 (s, 6H), 1.24 (s, 12H). [See spectrum]

^{13}C NMR (126 MHz, CDCl$_3$) δ 84.2, 67.1, 53.6, 53.0, 46.4, 24.9. [See spectrum]

^{11}B NMR ^{11}B NMR (160 MHz, CDCl$_3$) δ 29.8. [See spectrum]

HRMS (*m/z*): (ESI+) calc'd for $C_{15}H_{26}BNO_5SNa$ [M+Na]$^+$: 366.1517, found: 366.1515.

2-(3-(4,4,5,5-tetramethyl-1,3,2-dioxaborolan-2-yl)bicyclo[1.1.1]pentan-1-yl)hexahydro-1*H*-4,7-methanoisoindole-1,3(2*H*)-dione (15a)
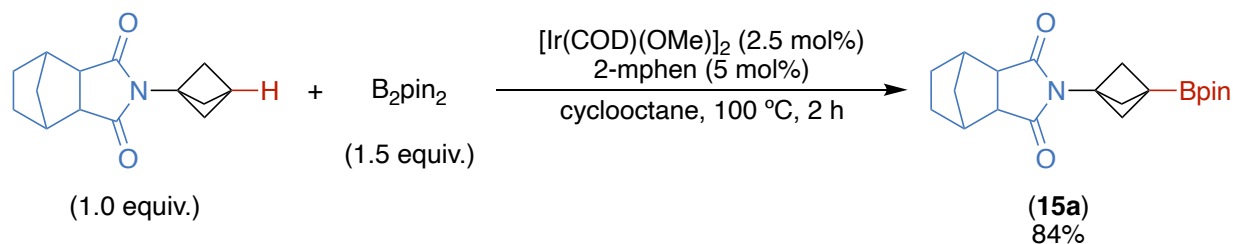
Prepared according to General Procedure A on a 0.25 mmol scale. The crude reaction mixture was eluted on SiO_2 with 20% → 35% ethyl acetate in hexanes as the eluent to afford 75.2 mg (84%) of the title compound as a white powder.

TLC: R_f = 0.35 (25% ethyl acetate in hexanes)

¹H NMR (500 MHz, CDCl₃) δ 2.94 (t, *J* = 2.7 Hz, 2H), 2.70 (p, *J* = 2.1 Hz, 2H), 2.39 (d, *J* = 2.0 Hz, 6H), 1.58 – 1.50 (m, 4H), 1.32 – 1.11 (m, 14H). [See spectrum]

¹³C NMR (126 MHz, CDCl₃) δ 178.7, 83.7, 54.6, 48.8, 48.8, 47.6, 42.0, 39.5, 24.8. [See spectrum]

¹¹B NMR (160 MHz, CDCl₃) δ 30.7. [See spectrum]

HRMS (*m/z*): (ESI+) calc'd for $C_{20}H_{28}BNO_4$ [M+Na]⁺: 380.2004, found: 380.2010.

2,2,2-trifluoro-*N*-(3-(4,4,5,5-tetramethyl-1,3,2-dioxaborolan-2-yl)bicyclo[1.1.1]pentan-1-yl)acetamide (16a)
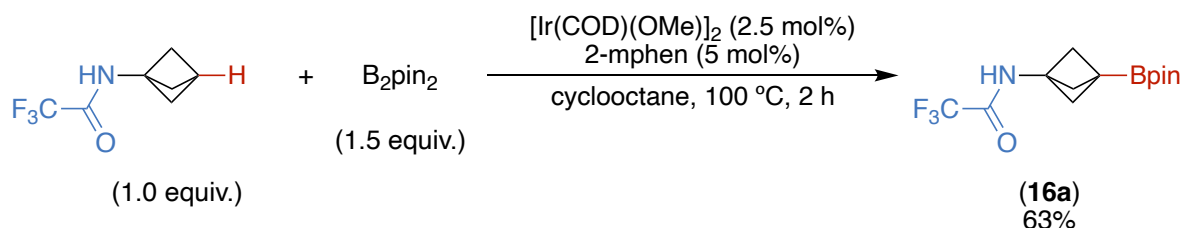
Prepared according to General Procedure A on a 0.15 mmol scale. The crude reaction mixture was eluted on SiO$_2$ with 10% → 35% ethyl acetate in hexanes as the eluent to afford 28.9 mg (63%) of the title compound as a white powder.

TLC: R_f = 0.23 (20% ethyl acetate in hexanes)

^{1}H NMR (500 MHz, CDCl$_3$) δ 6.53 (s, 1H), 2.23 (s, 6H), 1.25 (s, 12H). [See spectrum]

^{13}C NMR (151 MHz, CDCl$_3$) δ 156.7 (q, J_{C-F} = 36.8 Hz), 115.5 (q, J_{C-F} = 285.4 Hz), 83.8, 54.0, 47.5, 24.7. [See spectrum]

^{11}B NMR (160 MHz, CDCl$_3$) δ 30.7. [See spectrum]

^{19}F NMR (470 MHz, CDCl$_3$) δ -76.3. [See spectrum]

HRMS (*m/z*): (EI+) calc'd for C$_{13}$H$_{19}$BF$_3$NO$_3$ [M]$^+$: 305.1410, found: 305.1406.

***tert*-butyl 3-((3-(4,4,5,5-tetramethyl-1,3,2-dioxaborolan-2-yl)bicyclo[1.1.1]pentan-1-yl)methyl)-azetidine-1-carboxylate (17a)**
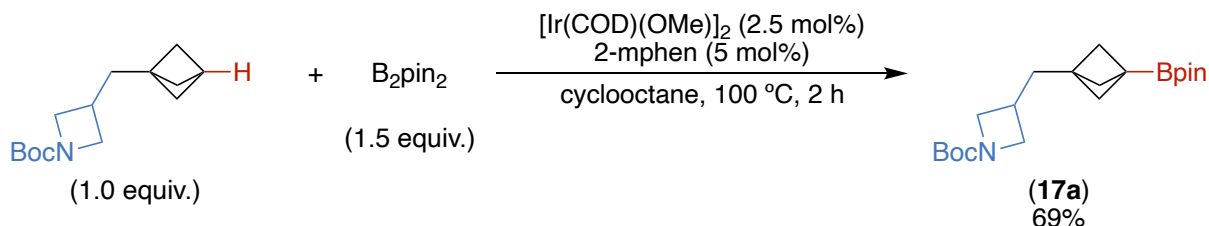
Prepared according to General Procedure A on a 0.10 mmol scale. The crude reaction mixture was eluted on reverse phase silica with 40% → 100% acetonitrile in water as the eluent. Fractions containing the desired compound were collected and concentrated under vacuum to afford 25.0 mg (69%) of the title compound as a white solid.

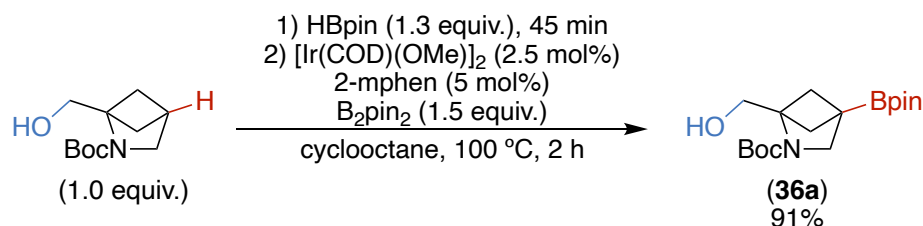**TLC:** R_f = 0.8 (50% acetonitrile in water)

¹H NMR (500 MHz, CDCl₃) δ 3.97 (t, *J* = 8.4 Hz, 2H), 3.51 (dd, *J* = 8.5, 5.7 Hz, 2H), 2.50 (tt, *J* = 8.1, 5.7 Hz, 1H), 1.72 (s, 6H), 1.62 (d, *J* = 7.8 Hz, 2H), 1.42 (s, 9H), 1.22 (s, 12H). [See spectrum]

¹³C NMR (126 MHz, CDCl₃) δ 156.5, 83.4, 79.2, 55.0, 51.8, 50.0, 44.7, 37.9, 28.6, 26.8, 24.9. [See spectrum]

¹¹B NMR (160 MHz, CDCl₃) δ 30.4. [See spectrum]

HRMS (*m/z*): (ESI+) calc'd for $C_{20}H_{35}BNO_4$ [M+H]⁺: 364.2654, found: 364.2652.

tert-butyl 3-(3-(4,4,5,5-tetramethyl-1,3,2-dioxaborolan-2-yl)bicyclo[1.1.1]pentan-1-yl)pyrrolidine-1-carboxylate (18a)
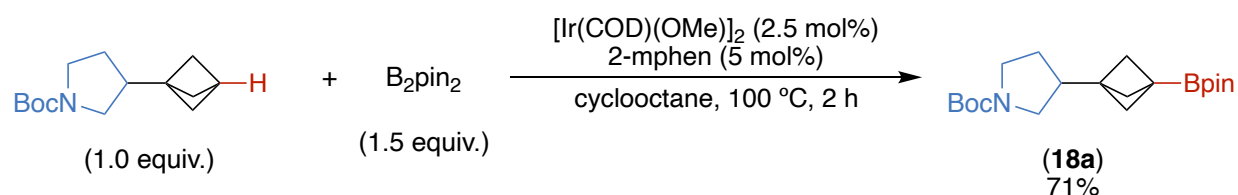
Prepared according to General Procedure A on a 0.10 mmol scale. The crude reaction mixture was eluted on reverse phase silica with 40% → 100% acetonitrile in water as the eluent. Fractions containing the desired compound were collected and concentrated under vacuum to afford 25.8 mg (71%) of the title compound as a white powder.

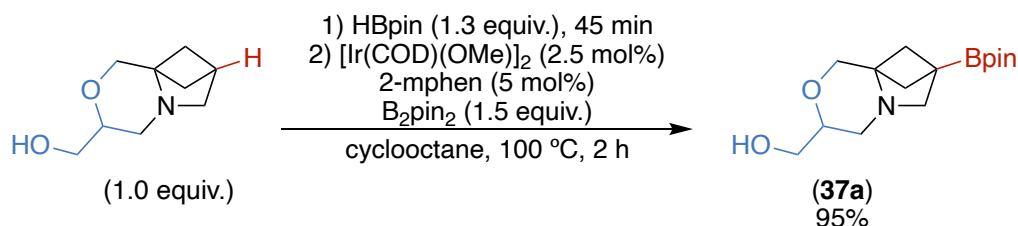**TLC:** R_f = 0.8 (50% acetonitrile in water)

¹H NMR (700 MHz, CDCl$_3$) δ 3.36 (br, 2H), 3.22 (br, 1H), 3.01 (br, 1H), 2.09 (p, J = 7.6 Hz, 1H), 1.79 (dt, J = 12.1, 6.1 Hz, 1H), 1.77 – 1.69 (m, 6H), 1.63 – 1.54 (m, 1H), 1.44 (s, 9H), 1.22 (s, 12H). [See spectrum]

¹³C NMR (151 MHz, CDCl$_3$) δ 154.7, 83.4, 79.0, 50.0, 48.1, 46.5, 45.9, 40.8, 40.0, 28.7, 28.4, 27.7, 24.9. [See spectrum]

¹¹B NMR (160 MHz, CDCl$_3$) (193 MHz, CDCl$_3$) δ 30.8. [See spectrum]

HRMS (_m/z_): (ESI+) calc'd for C$_{20}$H$_{34}$BNO$_4$Na [M+Na]$^+$: 386.2473, found: 386.2472.

2-(3-methoxy-5-(3-(4,4,5,5-tetramethyl-1,3,2-dioxaborolan-2-yl)bicyclo[1.1.1]pentan-1-yl)phenyl)-4,4,5,5-tetramethyl-1,3,2-dioxaborolane (19a)
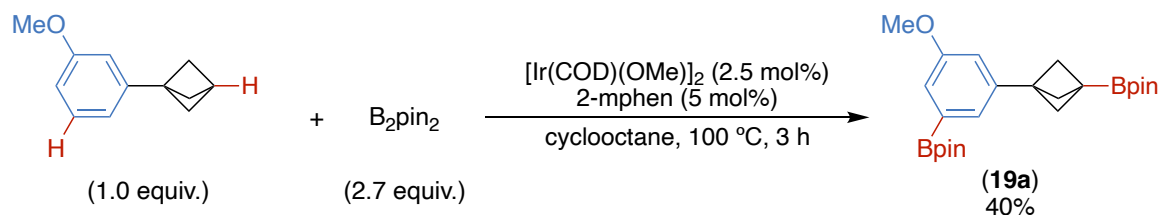
Prepared according to General Procedure A on a 0.1 mmol scale with 2.7 equiv. of B_2pin_2. The reaction mixture was heated for 3 h, rather than the usual 2 h. The crude reaction mixture was eluted on SiO_2 with 10% → 80% ethyl acetate in hexanes as the eluent to afford 17.1 mg (40%) of the title compound as a white powder.

TLC: $R_f = 0.5$ (10% ethyl acetate in hexanes)

^{1}H NMR (600 MHz, CDCl$_3$) δ 7.23 (d, $J = 1.4$ Hz, 1H), 7.17 (d, $J = 2.6$ Hz, 1H), 6.83 (d, $J = 1.2$ Hz, 1H), 3.82 (s, 3H), 2.15 (s, 6H), 1.34 (s, 12H), 1.26 (s, 12H) [See spectrum]

^{13}C NMR (151 MHz, CDCl$_3$) δ 159.2, 143.4, 124.6, 116.7, 115.8, 84.0, 83.5, 55.4, 53.2, 47.4, 25.0, 24.9, 24.9. [See spectrum]

^{11}B NMR (193 MHz, CDCl$_3$) δ 31.5. [See spectrum]

HRMS (*m/z*): (ESI+) calc'd for $C_{24}H_{36}B_2O_5$ [M+H]$^+$: 427.2822, found: 427.2821.

2-propyl-*N*-(3-(4,4,5,5-tetramethyl-1,3,2-dioxaborolan-2-yl)bicyclo[1.1.1]pentan-1-yl)pentanamide (20a)
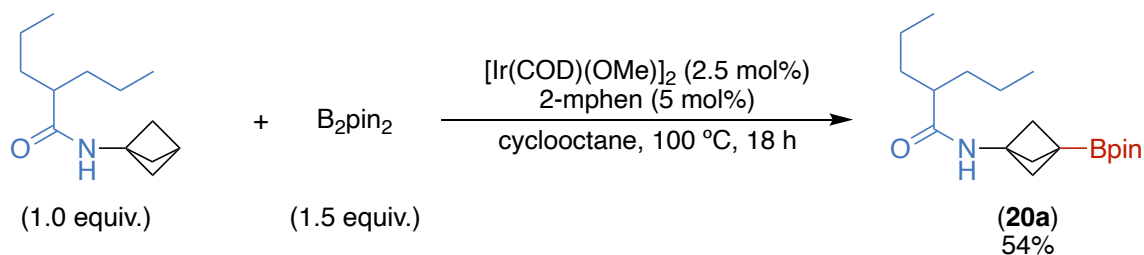
Prepared according to General Procedure A on a 0.48 mmol scale and a reaction time of 18 h. The crude reaction mixture was eluted on SiO_2 with 0% → 40% ethyl acetate in heptanes as the eluent to afford 87.0 mg (54%) of the title compound as a white powder.

¹H NMR (400 MHz, CDCl₃) δ 5.67 (br s, 1 H), 2.15 (s, 6 H), 1.81 - 1.93 (m, 1 H), 1.49 - 1.62 (m, 4 H), 1.28 - 1.32 (m, 4 H), 1.24 (s, 12 H), 0.88 (t, J=7.17 Hz, 6 H). [See spectrum]

¹³C NMR (101 MHz, CDCl₃) δ 176.3 (s, 1 C), 83.4 (s, 2 C), 54.1 (s, 3 C), 48.3 (s, 1 C), 47.7 (s, 1 C), 35.1 (s, 2 C), 24.7 (s, 4 C), 21.3 (br s, 1 C), 20.8 (s, 2 C), 14.1 (s, 2 C). [See spectrum]

HRMS (ESI-TOF) Calculated for $C_{19}H_{35}BNO_3$ [M+H]⁺: 336.2631; Found: 336.2713.

(3-((1R,4aR,4bR,10aR)-7-isopropyl-1,4a-dimethyl-1,2,3,4,4a,4b,5,6,10,10a-decahydrophenanthrene-1-carboxamido)bicyclo[1.1.1]pentan-1-yl)boronic acid (21a)
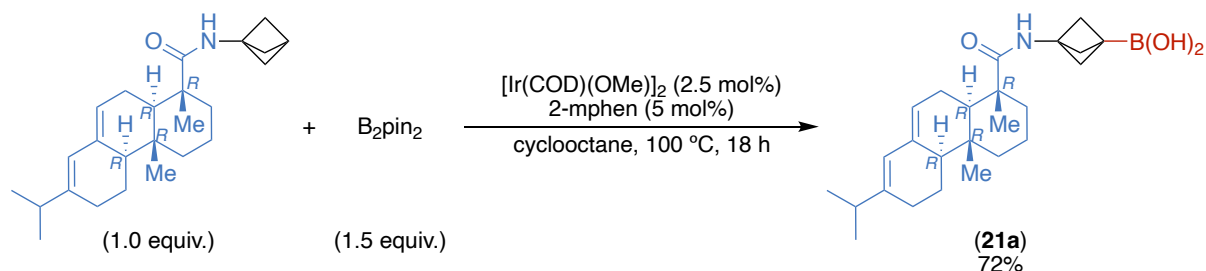
Prepared according to General Procedure A on a 0.27 mmol scale. The crude reaction mixture was eluted on SiO_2 with 0% → 10% methanol in dichloromethane as the eluent. The desired fractions were collected, and the solvents evaporated in vacuo. The crude material was further purified by RP HPLC (Stationary phase: C18 XBridge 30 x 100 mm 5 µm), Mobile phase: Gradient from 90% NH_4HCO_3 0.25% solution in Water, 10% CH_3CN to 10% NH_4HCO_3 0.25% solution in Water, 90% CH_3CN) to afford 81.0 mg (72%) of the title compound as a white powder.

¹H NMR (400 MHz, CDCl₃) δ ppm 5.93 - 6.21 (m, 1 H) 5.76 (s, 1 H) 5.07 - 5.58 (m, 2 H) 2.18 - 2.26 (m, 1 H) 2.13 (s, 6 H) 1.65 - 2.10 (m, 9 H) 1.46 - 1.63 (m, 3 H) 1.09 - 1.25 (m, 5 H) 1.01 (br d, J=6.70 Hz, 3 H) 1.00 (d, J=6.90 Hz, 3 H) 0.81 (s, 3 H). [See spectrum]

¹³C NMR (126 MHz, CDCl₃) δ ppm 178.6 (s, 1 C), 145.4 (s, 1 C), 135.5 (s, 1 C), 122.3 (s, 1 C), 120.7 (s, 1 C), 54.0 (s, 1 C), 53.7 (s, 1 C), 51.0 (s, 1 C), 46.0 (s, 1 C), 41.0 (s, 1 C), 38.4 (s, 1 C), 37.4 (s, 1 C), 34.9 (s, 1 C), 34.7 (s, 1 C), 27.5 (s, 1 C), 25.3 (s, 1 C), 24.8 (s, 1 C), 22.5 (s, 1 C), 21.4 (s, 1 C), 20.9 (s, 1 C), 18.4 (s, 1 C), 16.9 (s, 1 C), 14.1 (s, 1 C). [See spectrum]

HRMS (ESI-TOF) Calculated for $C_{25}H_{38}BNO_3$ [M+H]⁺: 412.2944; Found: 412.3024.

Bicyclo[2.1.1]hexane Substrates

***tert*-butyl 4-(4,4,5,5-tetramethyl-1,3,2-dioxaborolan-2-yl)bicyclo[2.1.1]hexane-1-carboxylate (22a)**
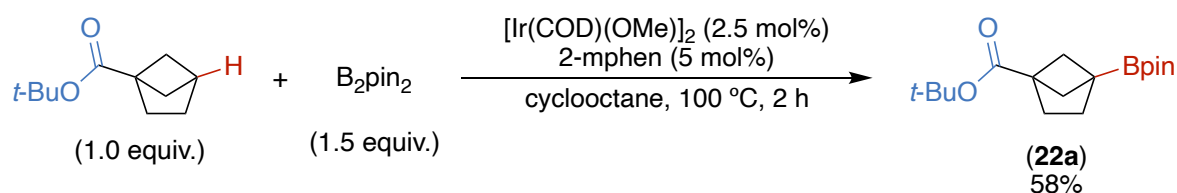
Prepared according to General Procedure A on a 0.10 mmol scale. The crude reaction mixture was eluted on reverse phase silica with 40% → 100% acetonitrile in water as the eluent. Fractions containing the desired compound were collected and concentrated under vacuum to afford 17.9 mg (58%) of the title compound as an off-white solid.

TLC: R_f = 0.68 (50% acetonitrile in water)

^{1}H NMR (500 MHz, CDCl$_3$) δ 1.86 (ddd, J = 7.2, 4.0, 1.6 Hz, 4H), 1.83 – 1.77 (m, 2H), 1.43 (s, 9H), 1.34 (dd, J = 4.3, 2.0 Hz, 2H), 1.23 (s, 12H) [See spectrum]

^{13}C NMR (126 MHz, CDCl$_3$) δ 173.6, 83.3, 79.8, 54.7, 43.7, 30.2, 30.0, 28.2, 24.9. [See spectrum]

^{11}B NMR (160 MHz, CDCl$_3$) δ 32.3. [See spectrum]

HRMS (*m/z*): (EI+) calc'd for C$_{16}$H$_{26}$BO$_4$ [M-Me]$^+$: 293.1924, found: 293.1921.

tert-butyl 4-((4-(trifluoro-λ4-boraneyl)-2-oxabicyclo[2.1.1]hexan-1-yl)methyl)piperazine-1-carboxylate, potassium salt (23a)
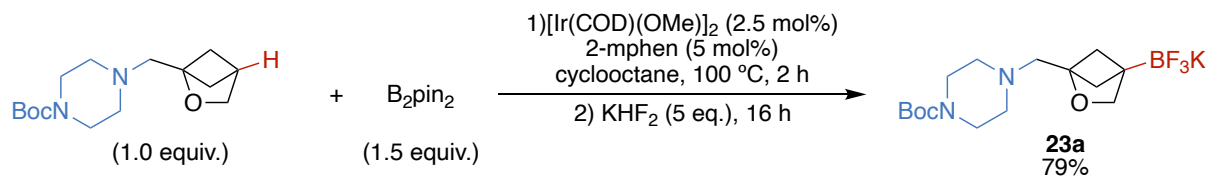
Prepared according to General Procedure C on a 0.10 mmol scale. After washing with pentanes, 30.7 mg (79%) of the title compound was isolated as an off-white powder.

TLC: R_f = N/A

^{1}H NMR (600 MHz, Acetone) δ 3.57 (s, 2H), 3.37 – 3.29 (m, 4H), 2.55 (s, 2H), 2.46 – 2.41 (m, 4H), 1.50 – 1.46 (m, 2H), 1.42 (s, 9H), 1.20 – 1.16 (m, 2H). [See spectrum]

^{13}C NMR (151 MHz, Acetone) δ 155.1, 88.8, 79.4, 74.2, 60.9, 55.0, 43.8, 28.6. [See spectrum]

^{11}B NMR (193 MHz, Acetone) δ 2.6. [See spectrum]

^{19}F NMR (565 MHz, Acetone) δ -146.9. [See spectrum]

HRMS (_m/z_): (ESI-) calc'd for $C_{15}H_{25}BF_3N_2O_3$ [M-K]$^-$: 349.1916, found: 349.1915.

2-(1-(bromomethyl)-2-oxabicyclo[2.1.1]hexan-4-yl)-4,4,5,5-tetramethyl-1,3,2-dioxaborolane (24a)
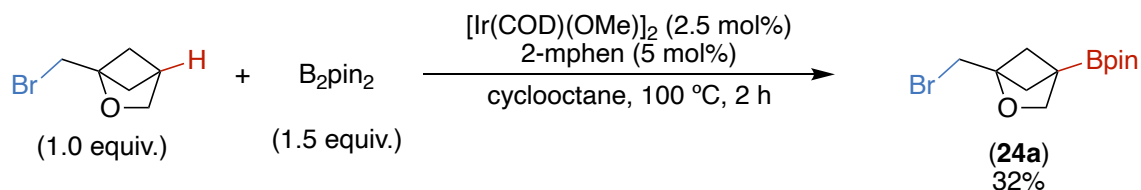
$[Ir(COD)(OMe)]_2$ (2.5 mol%)
2-mphen (5 mol%)
cyclooctane, 100 °C, 2 h

(1.0 equiv.) B_2pin_2 (1.5 equiv.)

(24a)
32%

Prepared according to General Procedure A on a 0.10 mmol scale. The crude reaction mixture was eluted on reverse phase silica with 40% → 100% acetonitrile in water as the eluent. Fractions containing the desired compound were collected and concentrated under vacuum to afford 9.8 mg (32%) of the title compound as an off-white solid.

TLC: R_f = 0.56 (50% acetonitrile in water)

¹H NMR (600 MHz, CDCl$_3$) δ 3.91 (s, 2H), 3.60 (s, 2H), 1.89 (dd, J = 4.7, 1.9 Hz, 2H), 1.63 – 1.59 (m, 2H), 1.25 (s, 12H). [See spectrum]

¹³C NMR (151 MHz, CDCl$_3$) δ 88.0, 83.8, 72.8, 43.5, 31.5, 24.9. [See spectrum]

¹¹B NMR (193 MHz, CDCl$_3$) δ 31.9. [See spectrum]

HRMS (m/z): (EI+) calc'd for C$_{11}$H$_{17}$BBrO$_3$ [M-Me]$^+$: 289.0434, found: 289.0436.

(4-(4,4,5,5-tetramethyl-1,3,2-dioxaborolan-2-yl)-2-oxabicyclo[2.1.1]hexan-1-yl)methanol (25a)
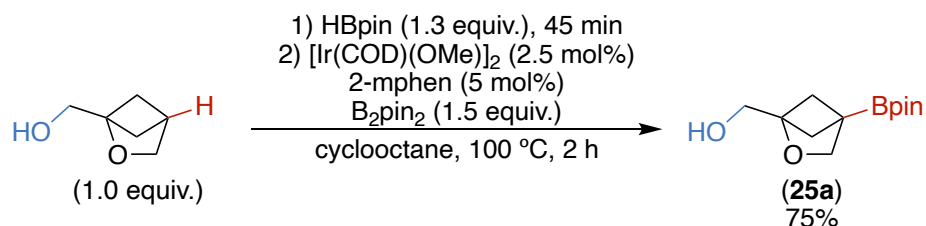
Prepared according to General Procedure B on a 0.10 mmol scale. The crude reaction mixture was eluted on reverse phase silica with 40% → 100% acetonitrile in water as the eluent. Fractions containing the desired compound were collected and concentrated under vacuum to afford 18.0 mg (75%) of the title compound as a clear oil.

TLC: R_f = 0.9 (50% acetonitrile in water)

^{1}H NMR (500 MHz, CDCl$_3$) δ 3.86 (s, 2H), 3.80 (d, J = 5.7 Hz, 2H), 1.92 (t, J = 6.1 Hz, 1H), 1.82 (dd, J = 4.7, 1.9 Hz, 2H), 1.57 (dd, J = 4.7, 1.9 Hz, 2H), 1.25 (s, 12H). [See spectrum]

^{13}C NMR (126 MHz, CDCl$_3$) δ 156.5, 83.4, 79.2, 55.0, 51.8, 50.0, 44.7, 37.9, 28.6, 26.8, 24.9. [See spectrum]

^{11}B NMR (160 MHz, CDCl$_3$) δ 31.6. [See spectrum]

HRMS (*m/z*): (ESI+) calc'd for C$_{12}$H$_{21}$BO$_4$Na [M+Na]$^+$: 263.1425, found: 263.1425.

tert-butyl 4-(4,4,5,5-tetramethyl-1,3,2-dioxaborolan-2-yl)-2-oxabicyclo[2.1.1]hexane-1-carboxylate (26a)
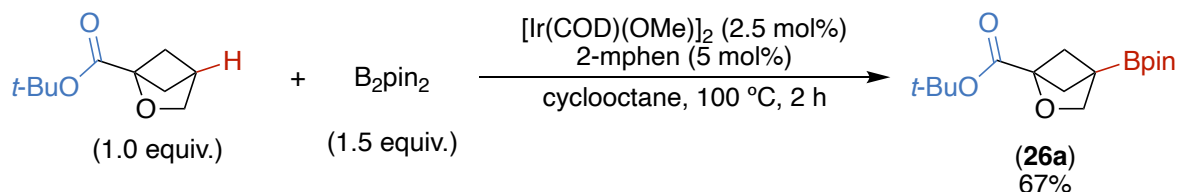
Prepared according to General Procedure A on a 0.10 mmol scale. The crude reaction mixture was eluted on reverse phase silica with 40% → 100% acetonitrile in water as the eluent. Fractions containing the desired compound were collected and concentrated under vacuum to afford 20.9 mg (67%) of the title compound as an off-white solid.

TLC: R_f = 0.56 (50% acetonitrile in water)

^{1}H NMR (600 MHz, CDCl$_3$) δ 3.94 (s, 2H), 2.20 (dd, J = 4.6, 1.8 Hz, 2H), 1.76 (dd, J = 4.7, 1.8 Hz, 2H), 1.48 (s, 9H), 1.25 (s, 12H). [See spectrum]

^{13}C NMR (151 MHz, CDCl$_3$) δ 167.7, 87.2, 83.9, 81.9, 72.5, 44.5, 28.2, 28.0, 24.9. [See spectrum]

^{11}B NMR (193 MHz, CDCl$_3$) δ 31.8. [See spectrum]

HRMS (_m/z_): (ESI+) calc'd for C$_{16}$H$_{27}$BO$_5$Na [M+Na]$^+$: 333.1844, found: 333.1841.

tert-butyl 4-(4,4,5,5-tetramethyl-1,3,2-dioxaborolan-2-yl)-2-azabicyclo[2.1.1]hexane-2-carboxylate (27a)
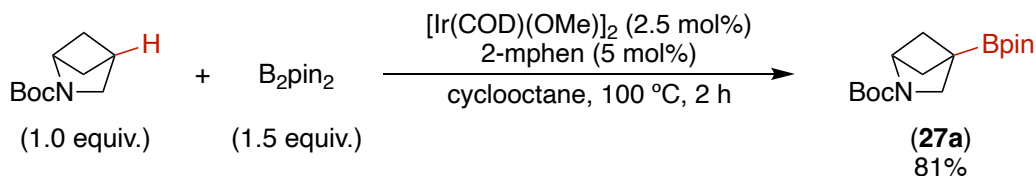
Prepared according to General Procedure A on a 0.10 mmol scale. The crude reaction mixture was eluted on reverse phase silica with 40% → 100% acetonitrile in water as the eluent. Fractions containing the desired compound were collected and concentrated under vacuum to afford 25.1 mg (87%) of the title compound as an off-white solid.

TLC: R_f = 0.52 (50% acetonitrile in water)

^{1}H NMR (500 MHz, CDCl$_3$) δ 4.36 (s, 1H), 3.36 (s, 2H), 2.00 – 1.92 (m, 2H), 1.45 (s, 9H), 1.43 – 1.37 (m, 2H), 1.24 (s, 12H). [See spectrum]

^{13}C NMR (126 MHz, CDCl$_3$) δ 155.2, 82.6, 78.0, 60.8, 50.3, 41.3, 28.7, 27.5, 27.5, 23.7. [See spectrum]

^{11}B NMR (160 MHz, CDCl$_3$) δ 31.5. [See spectrum]

HRMS (m/z): (ESI+) calc'd for C$_{16}$H$_{28}$BNO$_4$ [M+Na]$^+$: 332.2004, found: 332.1997.

tert-butyl 1-methyl-4-(4,4,5,5-tetramethyl-1,3,2-dioxaborolan-2-yl)-2-azabicyclo[2.1.1]hexane-2-carboxylate (28a)
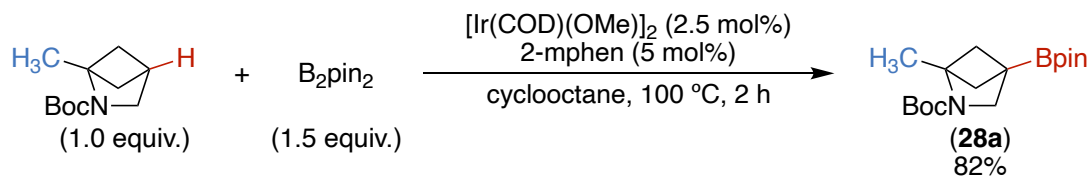
Prepared according to General Procedure A on a 0.10 mmol scale. The crude reaction mixture was eluted on reverse phase silica with 40% → 100% acetonitrile in water as the eluent. Fractions containing the desired compound were collected and concentrated under vacuum to afford 26.6 mg (82%) of the title compound as a white powder.

TLC: R_f = 0.50 (50% acetonitrile in water)

¹H NMR (600 MHz, CDCl₃) δ 3.42 (s, 2H), 1.79 – 1.72 (m, 2H), 1.66 (s, 3H), 1.55 – 1.48 (m, 2H), 1.44 (s, 9H), 1.24 (s, 12H). [See spectrum]

¹³C NMR (126 MHz, CDCl₃) δ 156.5, 83.4, 79.2, 55.0, 51.8, 50.0, 44.7, 37.9, 28.6, 26.8, 24.9. [See spectrum]

¹¹B NMR (193 MHz, CDCl₃) δ 32.0. [See spectrum]

HRMS (_m/z_): (ESI+) calc'd for $C_{17}H_{31}BNO_4$ [M+H]⁺: 324.2341, found: 324.2337.

***tert*-butyl** **4-(4,4,5,5-tetramethyl-1,3,2-dioxaborolan-2-yl)-1-(trifluoromethyl)-2-azabicyclo[2.1.1]hexane-2-carboxylate (29a)**
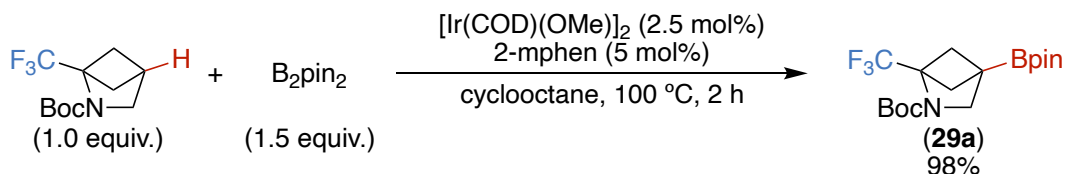
Prepared according to General Procedure A on a 0.10 mmol scale. The crude reaction mixture was eluted on reverse phase silica with 40% → 100% acetonitrile in water as the eluent. Fractions containing the desired compound were collected and concentrated under vacuum to afford 37.0 mg (98%) of the title compound as an off-white solid.

TLC: $R_f = 0.50$ (50% acetonitrile in water)

¹H NMR (600 MHz, CDCl₃) δ 3.54 (s, 2H), 2.26 – 2.19 (m, 2H), 1.73 – 1.69 (m, 2H), 1.46 (s, 9H), 1.25 (s, 12H). [See spectrum]

¹³C NMR (151 MHz, CDCl₃) δ 154.5, 122.8 (q, $J_{C–F}$ = 275.2 Hz), 84.2, 80.4, 70.8 (q, $J_{C–F}$ = 36.9 Hz), 54.7, 42.5, 28.4, 24.9. [See spectrum]

¹¹B NMR (193 MHz, CDCl₃) δ 31.4. [See spectrum]

¹⁹F NMR (565 MHz, CDCl₃) δ -68.6. [See spectrum]

HRMS (*m/z*): (ESI+) calc'd for $C_{17}H_{27}BF_3NO_4Na$ [M+Na]⁺: 400.1877, found:400.1876.

tert-butyl 1-(difluoromethyl)-4-(4,4,5,5-tetramethyl-1,3,2-dioxaborolan-2-yl)-2-azabicyclo[2.1.1]hexane-2-carboxylate (30a)
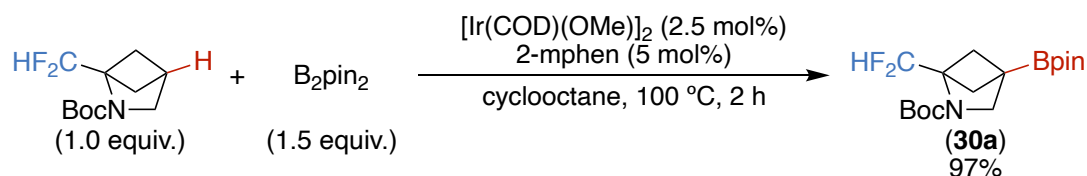
Prepared according to General Procedure A on a 0.10 mmol scale. The crude reaction mixture was eluted on reverse phase silica with 40% → 100% acetonitrile in water as the eluent. Fractions containing the desired compound were collected and concentrated under vacuum to afford 34.8 mg (97%) of the title compound as an off-white solid.

TLC: R_f = 0.4 (50% acetonitrile in water)

^{1}H NMR (500 MHz, CDCl$_3$) δ 6.68 (t, J_{F-H} = 56.1 Hz, 1H), 3.49 (s, 2H), 2.18 – 2.10 (m, 2H), 1.60 – 1.53 (m, 2H), 1.46 (s, 9H), 1.26 (s, 12H). [See spectrum]

^{13}C NMR (151 MHz, CDCl$_3$) δ 155.9, 112.48 (t, J_{C-F} = 236.9 Hz), 84.0, 80.3, 72.6 (t, J_{C-F} = 31.0 Hz), 54.7, 41.0, 28.6, 24.9. [See spectrum]

^{11}B NMR (193 MHz, CDCl$_3$) δ 31.8. [See spectrum]

^{19}F NMR (565 MHz, CDCl$_3$) δ -124.8. [See spectrum]

HRMS (m/z): (ESI+) calc'd for C$_{17}$H$_{28}$BF$_2$NO$_4$Na [M+Na]$^+$: 382.1972, found: 382.1970.

***tert*-butyl 1-(fluoromethyl)-4-(4,4,5,5-tetramethyl-1,3,2-dioxaborolan-2-yl)-2-azabicyclo[2.1.1]hexane-2-carboxylate (31a)**
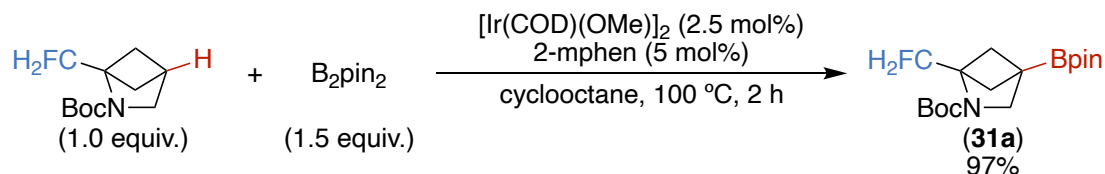
Prepared according to General Procedure A on a 0.10 mmol scale. The crude reaction mixture was eluted on reverse phase silica with 40% → 100% acetonitrile in water as the eluent. Fractions containing the desired compound were collected and concentrated under vacuum to afford 33.0 mg (97%) of the title compound as an off-white solid.

TLC: R_f = 0.45 (50% acetonitrile in water)

^{1}H NMR (600 MHz, CDCl$_3$) δ 4.90 (d, J_{F-H} = 47.9 Hz, 2H), 3.46 (s, 2H), 2.30 – 2.04 (m, 2H), 1.50 – 1.46 (m, 2H), 1.44 (s, 9H), 1.25 (s, 12H). [See spectrum]

^{13}C NMR (151 MHz, CDCl$_3$) δ 155.8, 83.8, 82.0 (d, J_{C-F} = 161.0 Hz), 79.7, 72.5 (d, J_{C-F} = 28.7 Hz), 54.5, 42.6, 28.6, 24.9. [See spectrum]

^{11}B NMR (193 MHz, CDCl$_3$) δ 31.8. [See spectrum]

^{19}F NMR (565 MHz, CDCl$_3$) δ -220.1. [See spectrum]

HRMS (*m/z*): (ESI+) calc'd for C$_{17}$H$_{29}$BFNO$_4$Na [M+Na]$^+$: 364.2066, found: 364.2058.

tert-butyl 1-((dimethylamino)methyl)-4-(4,4,5,5-tetramethyl-1,3,2-dioxaborolan-2-yl)-2-azabicyclo[2.1.1]hexane-2-carboxylate (32a)
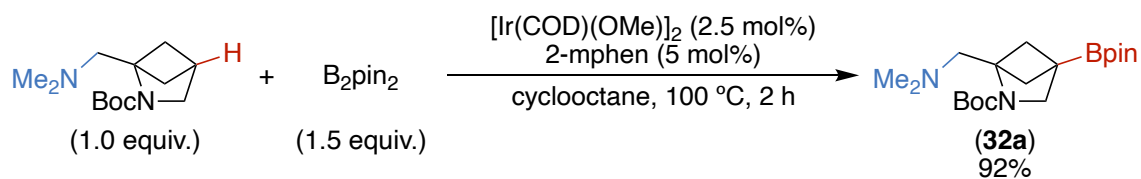
Prepared according to General Procedure A on a 0.10 mmol scale. The crude reaction mixture was eluted on reverse phase silica with 40% → 100% acetonitrile in water as the eluent. Fractions containing the desired compound were collected and concentrated under vacuum to afford 33.6 mg (92%) of the title compound as a brown solid.

**TLC:** R_f = 0.8 (50% acetonitrile in water)

¹H NMR (600 MHz, CDCl$_3$) δ 3.43 (s, 2H), 3.01 (s, 2H), 2.28 (s, 6H), 2.07 – 2.03 (m, 2H), 1.56 – 1.45 (m, 2H), 1.44 (s, 9H), 1.23 (s, 12H). [See spectrum]

¹³C NMR (151 MHz, CDCl$_3$) δ 156.4, 83.6, 79.0, 75.1, 60.1, 55.2, 47.6, 43.8, 28.8, 24.9. [See spectrum]

¹¹B NMR (193 MHz, CDCl$_3$) δ 32.1. [See spectrum]

HRMS (m/z): (ESI+) calc'd for C$_{19}$H$_{36}$BN$_2$O$_4$ [M+H]$^+$: 367.2763, found: 367.2760.

tert-butyl **1-(((tert-butoxycarbonyl)amino)methyl)-4-(trifluoro-λ4-boraneyl)-2-azabicyclo[2.1.1]hexane-2-carboxylate, potassium salt (33a)**
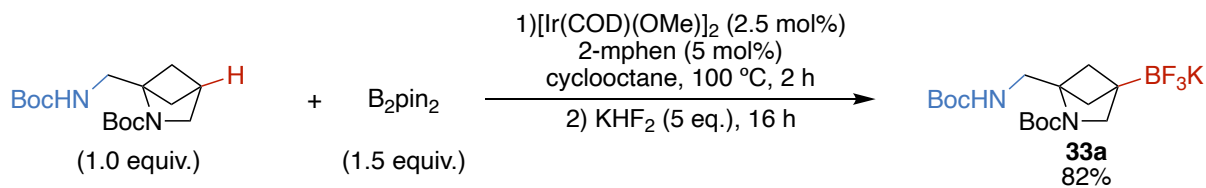
Prepared according to General Procedure C on a 0.10 mmol scale. After washing with pentanes, 34.5 mg (82%) of the title compound was obtained as an off-white solid.

TLC: R_f = N/A

¹H NMR (500 MHz, Acetone) δ 5.89 (s, 1H), 3.59 – 3.54 (m, 2H), 3.19 (s, 2H), 1.57 – 1.50 (m, 2H), 1.43 (s, 9H), 1.39 (s, 9H), 1.20 – 1.11 (m, 2H). [See spectrum]

¹³C NMR (126 MHz, Acetone) δ 156.6, 156.1, 78.4, 78.3, 73.8, 56.9, 43.6, 42.6, 28.9, 28.6. [See spectrum]

¹¹B NMR (160 MHz, Acetone) δ 3.6. [See spectrum]

¹⁹F NMR (470 MHz, Acetone) δ -147.7. [See spectrum]

HRMS (m/z): (ESI-) calc'd for $C_{16}H_{27}BF_3N_2O_4$ [M-K]⁻: 379.2021, found: 379.2017.

tert-butyl 1-carbamoyl-4-(4,4,5,5-tetramethyl-1,3,2-dioxaborolan-2-yl)-2-azabicyclo[2.1.1]hexane-2-carboxylate (34a)
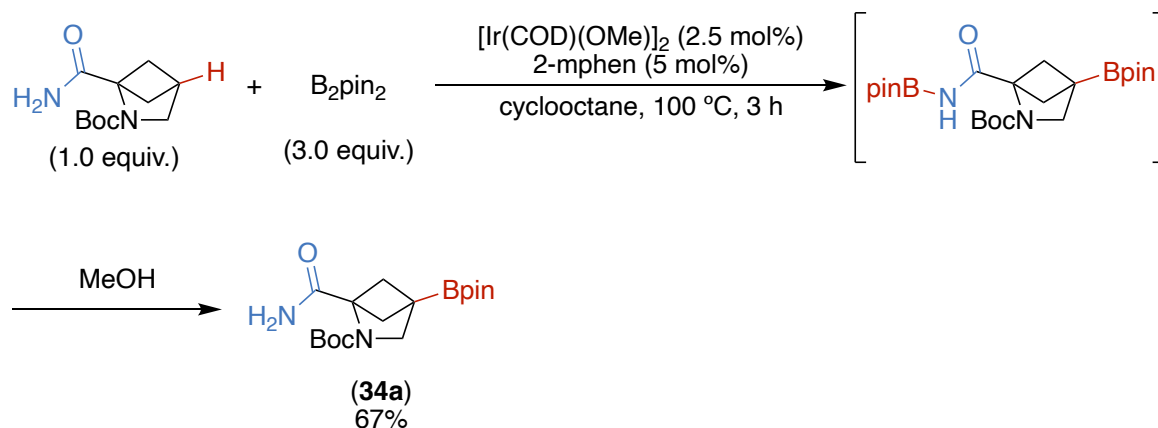
Prepared according to General Procedure A on a 0.10 mmol scale with 3 equiv. of B_2pin_2 instead of the usual 1.5 equiv. The crude material was co-evaporated with methanol at 45 °C (30 mL x 2). The residue was washed repeatedly with pentane to afford 23.6 mg (67%) of the title compound as a brown solid.

TLC: R_f = N/A

^{1}H NMR (600 MHz, CDCl$_3$) δ 5.85 (br s, 1H), 5.66 (br s, 1H), 3.53 (s, 2H), 2.24 – 2.17 (m, 2H), 1.69 – 1.65 (m, 2H), 1.43 (s, 9H), 1.24 (s, 12H). [See spectrum]

^{13}C NMR (151 MHz, CDCl$_3$) δ 171.4, 158.3, 84.0, 81.1, 73.0, 55.6, 44.2, 28.4, 24.9. [See spectrum]

^{11}B NMR (193 MHz, CDCl$_3$) δ 31.7. [See spectrum]

HRMS (m/z): (ESI+) calc'd for $C_{17}H_{30}BN_2O_5$ [M+H]$^+$: 353.2242, found: 353.2238.

tert-butyl 4-(4,4,5,5-tetramethyl-1,3,2-dioxaborolan-2-yl)-1-((triisopropylsilyl)ethynyl)-2-azabicyclo[2.1.1]hexane-2-carboxylate (35a)
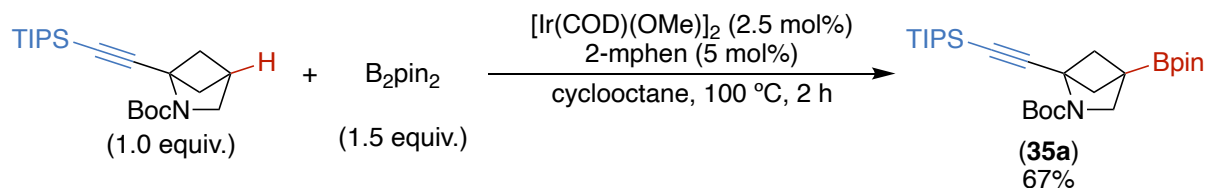
Prepared according to General Procedure A on a 0.05 mmol scale. The crude reaction mixture was eluted on reverse phase silica with 50% → 100% acetonitrile in water as the eluent. Fractions containing the desired compound were collected and concentrated under vacuum to afford 16.3 mg (67%) of the title compound as an off-white solid.

TLC: R_f = 0.68 (50% acetonitrile in water)

^{1}H NMR (600 MHz, CDCl$_3$) δ 3.44 (s, 2H), 2.14 (dd, J = 4.8, 1.8 Hz, 2H), 1.78 (dd, J = 4.6, 2.0 Hz, 2H), 1.47 (s, 9H), 1.24 (s, 12H), 1.07 (m, J = 3.9 Hz, 21H). [See spectrum]

^{13}C NMR (151 MHz, CDCl$_3$) δ 157.2, 104.6, 88.1, 83.9, 80.0, 62.3, 54.2, 48.8, 28.6, 24.9, 18.8, 11.4. [See spectrum]

^{11}B NMR (193 MHz, CDCl$_3$) δ 32.1. [See spectrum]

HRMS (m/z): (ESI+) calc'd for C$_{27}$H$_{49}$BNO$_4$Si [M+H]$^+$: 490.3518, found: 490.3517.

tert-butyl 1-(hydroxymethyl)-4-(4,4,5,5-tetramethyl-1,3,2-dioxaborolan-2-yl)-2-azabicyclo[2.1.1]hexane-2-carboxylate (36a)

Prepared according to General Procedure B on a 0.10 mmol scale. The crude reaction mixture was eluted on reverse phase silica with 40% → 100% acetonitrile in water as the eluent. Fractions containing the desired compound were collected and concentrated under vacuum to afford 30.8 mg (91%) of the title compound as an off-white solid.

TLC: R_f = 0.9 (50% acetonitrile in water)

^{1}H NMR (600 MHz, CDCl$_3$) δ 4.92 (br s, 1H), 3.88 (d, J = 6.4 Hz, 2H), 3.43 (s, 2H), 1.86 – 1.78 (m, 2H), 1.60 – 1.56 (m, 2H), 1.46 (s, 9H), 1.25 (s, 12H). [See spectrum]

^{13}C NMR (151 MHz, CDCl$_3$) δ 155.8, 83.8, 79.9, 75.3, 61.9, 54.4, 43.5, 28.7, 24.9. [See spectrum]

^{11}B NMR (193 MHz, CDCl$_3$) δ 32.0. [See spectrum]

HRMS (_m/z_): (ESI+) calc'd for C$_{17}$H$_{31}$BNO$_5$ [M+H]$^+$: 340.2290, found: 340.2290.

(7-(4,4,5,5-tetramethyl-1,3,2-dioxaborolan-2-yl)tetrahydro-1*H*,6*H*-7,8a-methanopyrrolo[2,1-*c*][1,4]oxazin-3-yl)methanol (37a)

Prepared according to General Procedure B on a 0.10 mmol scale. The crude reaction mixture was eluted on reverse phase silica with 40% → 100% acetonitrile in water as the eluent. Fractions containing the desired compound were collected and concentrated under vacuum to afford 28.0 mg (95%) of the title compound as an off-white solid.

TLC: R_f = 0.9 (50% acetonitrile in water)

¹H NMR (500 MHz, CDCl₃) δ 3.94 (d, *J* = 11.8 Hz, 1H), 3.76 – 3.68 (m, 2H), 3.67 – 3.54 (m, 2H), 3.24 (d, *J* = 8.2 Hz, 1H), 2.90 (dd, *J* = 11.1, 2.3 Hz, 1H), 2.44 – 2.40 (m, 3H), 1.77 (dd, *J* = 10.2, 7.6 Hz, 1H), 1.72 (d, *J* = 6.9 Hz, 1H), 1.54 (d, *J* = 7.5 Hz, 1H), 1.42 (dd, *J* = 10.2, 7.0 Hz, 1H), 1.24 (s, 12H). [See spectrum]

¹³C NMR (126 MHz, CDCl₃) δ 83.6, 69.4, 68.3, 64.3, 59.3, 52.8, 42.2, 37.3, 24.9. [See spectrum]

¹¹B NMR (160 MHz, CDCl₃) δ 32.0. [See spectrum]

HRMS (*m/z*): (ESI+) calc'd for C₁₅H₂₇BNO₄ [M+H]⁺: 296.2028, found: 296.2027.

di-*tert*-butyl 4-(4,4,5,5-tetramethyl-1,3,2-dioxaborolan-2-yl)-2-azabicyclo[2.1.1]hexane-1,2-dicarboxylate (38a)
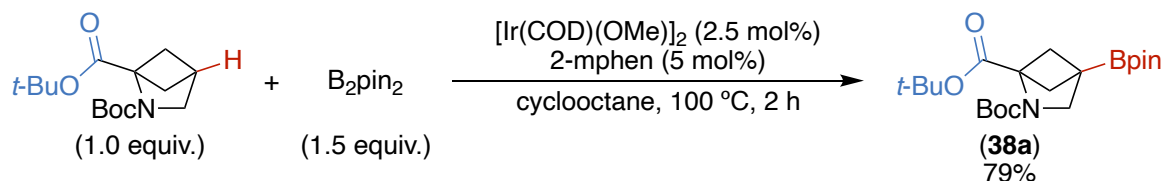
Prepared according to General Procedure A on a 0.10 mmol scale. The crude reaction mixture was eluted on reverse phase silica with 40% → 100% acetonitrile in water as the eluent. Fractions containing the desired compound were collected and concentrated under vacuum to afford 32.5 mg (79%) of the title compound as a colorless oil.

TLC: R_f = 0.8 (50% acetonitrile in water)

^{1}H NMR (600 MHz, CDCl$_3$) δ 3.47 (s, 2H), 2.14 – 2.07 (m, 2H), 1.67 – 1.61 (m, 2H), 1.47 (s, 9H), 1.44 (s, 9H), 1.24 (s, 12H). [See spectrum]

^{13}C NMR (151 MHz, CDCl$_3$) δ 168.0, 158.0, 83.9, 81.0, 80.3, 71.9, 55.1, 44.1, 28.5, 28.2, 24.9. [See spectrum]

^{11}B NMR (193 MHz, CDCl$_3$) δ 31.9. [See spectrum]

HRMS (*m/z*): (ESI+) calc'd for C$_{21}$H$_{37}$BNO$_6$ [M+H]$^+$: 410.2708, found: 410.2703.

2.4.6 Transformations of bridgehead C–Bpin bonds

(3-(4-(*tert*-butyl)phenyl)bicyclo[1.1.1]pentan-1-yl)trifluoro-λ^4-borane, potassium salt (1c)
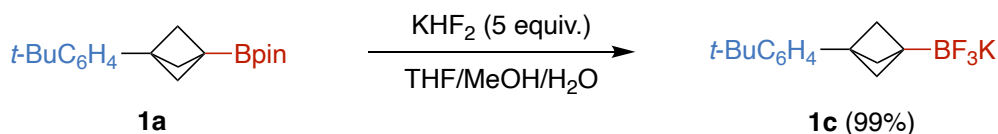
1a (70.0 mg, 0.215 mmol) was dissolved in a mixture of MeOH (0.6 mL) and THF (0.3 mL). Then, KHF$_2$ (84.0 mg, 1.08 mmol, 5.00 equiv.) in water (0.3 mL) was added with vigorous stirring. The resulting mixture was stirred at room temperature overnight. The reaction mixture was co-evaporated with 1:1 methanol:water repeatedly (2 mL x 5) to remove pinacol. The solid residue was extracted with acetone, filtered, and the filtrate concentrated. The resulting solids were washed with pentane to afford 66.2 mg (99%) of the title compound as an off-white powder.

TLC: N/A

^{1}H NMR (600 MHz, Acetone) δ 7.27 (d, *J* = 8.2 Hz, 2H), 7.09 (d, *J* = 8.3 Hz, 2H), 1.74 (s, 6H), 1.27 (s, 9H). [See spectrum]

^{13}C NMR (151 MHz, Acetone) δ 148.6, 142.7, 126.1, 125.4, 52.2, 52.1, 45.0, 34.8, 31.7. [See spectrum]

^{11}B NMR (193 MHz, Acetone) δ 1.6. [See spectrum]

^{19}F NMR (565 MHz, Acetone) δ -147.6. [See spectrum]

HRMS (*m/z*): (ESI-) calc'd for C$_{15}$H$_{19}$BF$_3$ [M-K]$^+$: 267.1537, found: 267.1537.

(3-(methylsulfonyl)bicyclo[1.1.1]pentan-1-yl)trifluoro-λ^4-borane, tetrabutylammonium salt (11c)
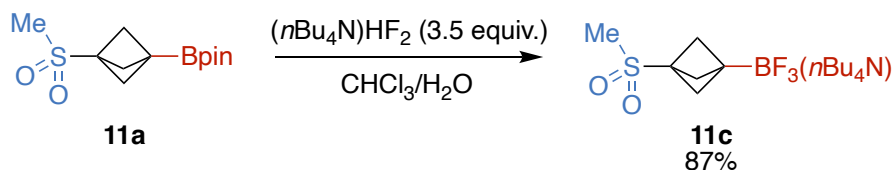
11a (204 mg, 0.750 mmol) and (nBu$_4$N)HF$_2$ (739 mg, 2.62 mmol, 3.50 equiv.) were mixed and chloroform (5.0 mL) and water (10.0 mL) was added. The biphasic mixture with stirred vigorously for 16 h. The layers were separated, and the aqueous layer was further extracted with chloroform (10 mL x 2). The combined organic layers were dried with MgSO$_4$, filtered, and concentrated to afford 298 mg (87%) of the title compound as a colorless oil that solidified upon standing.

TLC: N/A

^{1}H NMR (500 MHz, CDCl$_3$) δ 3.26 – 3.19 (m, 8H), 2.72 (s, 3H), 1.99 (s, 6H), 1.62 (p, J = 7.7 Hz, 8H), 1.43 (h, J = 7.4 Hz, 8H), 1.00 (t, J = 7.3 Hz, 12H). [See spectrum]

^{13}C NMR (126 MHz, CDCl$_3$) δ 58.9, 49.7, 49.7, 36.5, 25.0, 24.1, 19.8, 13.8. [See spectrum]

^{11}B NMR (160 MHz, CDCl$_3$) δ 2.3. [See spectrum]

^{19}F NMR (470 MHz, CDCl$_3$) δ -147.05. [See spectrum]

HRMS (*m/z*): (ESI-) calc'd for C$_6$H$_9$BF$_3$O$_2$S [M-nBu$_4$N]$^+$: 213.0374, found: 213.0373.

2,2,2-trifluoro-*N*-(3-(trifluoro-λ⁴-boraneyl)bicyclo[1.1.1]pentan-1-yl)acetamide, potassium salt (16c)
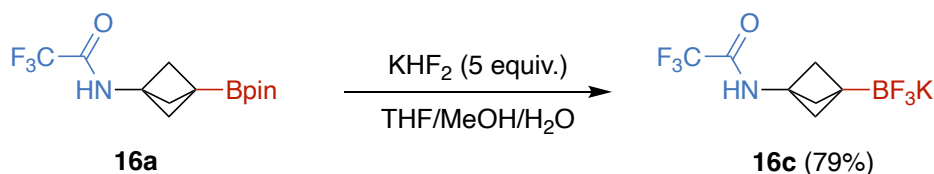
16a (30.5 mg, 0.100 mmol) was dissolved in a mixture of MeOH (0.3 mL) and THF (0.15 mL). Then, KHF₂ (39.1 mg, 0.50 mmol, 5.00 equiv.) in water (0.15 mL) was added with vigorous stirring. The resulting mixture was stirred at room temperature overnight. The reaction mixture was co-evaporated with 1:1 methanol:water repeatedly (1 mL x 5) to remove pinacol. The solid residue was extracted with acetone, filtered, and the filtrate concentrated. The resulting solids were washed with pentane to afford the title compound as an off-white powder (22.6 mg, 79%)

TLC: N/A

¹H NMR (500 MHz, Acetone) δ 8.51 (bs, 1H), 1.78 (s, 6H). [See spectrum]

¹³C NMR (151 MHz, Acetone) δ 156.90 (q, $J_{C–F}$ = 35.5 Hz), 117.00 (q, $J_{C–F}$ = 288.8 Hz), 54.3, 52.8, 47.2. [See spectrum]

¹¹B NMR (160 MHz, Acetone) δ 1.9. [See spectrum]

¹⁹F NMR (470 MHz, Acetone) δ -77.7, -146.9. [See spectrum]

HRMS (*m/z*): (ESI-) calc'd for $C_7H_7BF_6KNO$ [M-K]⁺: 246.0530, found: 246.0529.

(3-(4-(*tert*-butyl)phenyl)bicyclo[1.1.1]pentan-1-yl)boronic acid (1d)

$t\text{-BuC}_6\text{H}_4$ ⎯⟨⟩⎯ Bpin $\xrightarrow[\text{acetone/0.2 N HCl (1:1)}]{\text{MeB(OH)}_2\text{ (5.0 equiv.)}}$ $t\text{-BuC}_6\text{H}_4$ ⎯⟨⟩⎯ $B(OH)_2$

1d
90%
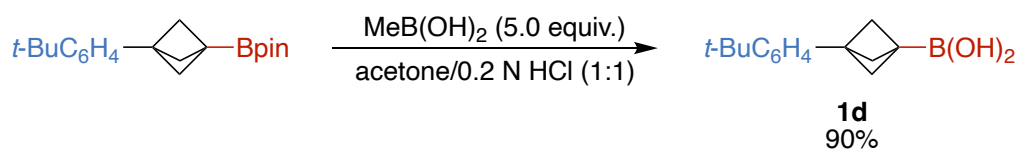
A 20 mL vial was charged with **1a** (42.4 mg, 0.130 mmol, 1.00 equiv.) and methyl boronic acid (38.9 mg, 0.650 mmol, 5.00 equiv.). Acetone (2 mL) and 0.2 N HCl (aq) (2 mL) were added in a 1:1 ratio. The vial was capped under ambient atmosphere and the reaction was stirred at room temperature for 16 h. The reaction mixture was concentrated to dryness, redissolved in acetone, and dried *in vacuo*. The residue was washed with pentanes and dried *in vacuo* to obtain the title compound as an off-white powder (28.5 mg, 90%).

TLC: N/A

^{1}H NMR (600 MHz, Acetone) δ 7.36 – 7.28 (m, 2H), 7.16 – 7.07 (m, 2H), 2.07 (s, 6H), 1.28 (s, 9H). [See spectrum]

^{13}C NMR (151 MHz, Acetone) δ 148.8, 139.6, 125.2, 124.8, 52.5, 45.8, 34.0, 30.8. [See spectrum]

^{11}B NMR (193 MHz, Acetone) δ 28.4. [See spectrum]

HRMS (*m/z*): (ESI-) calc'd for $C_{15}H_{20}BO_2$ [M-H]$^-$: 243.1562, found: 243.1560.

(3-(methylsulfonyl)bicyclo[1.1.1]pentan-1-yl)boronic acid (11d)

MeO$_2$S—◇—Bpin $\xrightarrow[\text{acetone/0.2 N HCl (1:1)}]{\text{MeB(OH)}_2 \text{ (5.0 equiv.)}}$ MeO$_2$S—◇—B(OH)$_2$

11d
87%
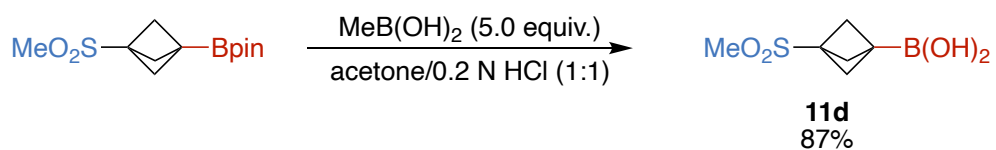
A 20 mL vial was charged with **11a** (81.6 mg, 0.300 mmol, 1.00 equiv.) and methyl boronic acid (89.8 mg, 1.50 mmol, 5.00 equiv.). Acetone (4 mL) and 0.2 N HCl (aq) (4 mL) were added in a 1:1 ratio. The vial was capped under ambient atmosphere, and the reaction was stirred at room temperature for 16 h. The reaction mixture was concentrated to dryness, redissolved in acetone, and dried *in vacuo*. The residue was washed with ether and dried *in vacuo* to obtain the title compound as an off-white powder (49.6 mg, 87%).

TLC: N/A

^{1}H NMR (500 MHz, Acetone) δ 2.77 (s, 3H), 2.17 (s, 6H). [See spectrum]

^{13}C NMR (151 MHz, Acetone) δ 54.5, 51.4, 36.9. [See spectrum]

^{11}B NMR (193 MHz, Acetone) δ 28.7. [See spectrum]

HRMS (*m/z*): (ESI-) calc'd for C$_6$H$_{10}$BO$_4$S [M-H]$^-$: 189.0398, found: 189.0397.

(1-methyl-2-azabicyclo[2.1.1]hexan-4-yl)boronic acid (28c)
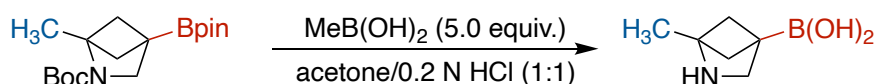
A 20 mL vial was charged with **28a** (18 mg, 0.077 mmol, 1.0 equiv.) and methyl boronic acid (22 mg, 0.77 mmol, 10 equiv.). Acetone (1 mL) and 0.2 N HCl (aq) (1 mL) were added in a 1:1 ratio. The vial was capped under ambient atmosphere, and the reaction was stirred at room temperature for 22 h. The reaction mixture was concentrated to dryness, redissolved in acetone, and dried *in vacuo*. The residue was washed with pentane and dried *in vacuo* to obtain the title compound as a pale-yellow powder (9.6 mg, 88%).

TLC: N/A

¹H NMR (600 MHz, Acetone) δ 3.63 (s, 2H), 2.13 – 2.06 (m, 2H), 1.94 – 1.86 (m, 2H), 1.73 (s, 3H).

¹³C NMR (151 MHz, Acetone) δ 71.5, 51.7, 43.2, 15.8.

¹¹B NMR (193 MHz, Acetone) δ 28.5, 19.2.

HRMS (*m/z*): (ESI+) calc'd for $C_{12}H_{24}B_2N_2O_4K$ [2M+K]⁺: 321.1554, found: 321.1563.

2-(2-(3-(4-(*tert*-butyl)phenyl)bicyclo[1.1.1]pentan-1-yl)-4-(4-methoxyphenyl)butan-2-yl)-4,4,5,5-tetramethyl-1,3,2-dioxaborolane (1e)
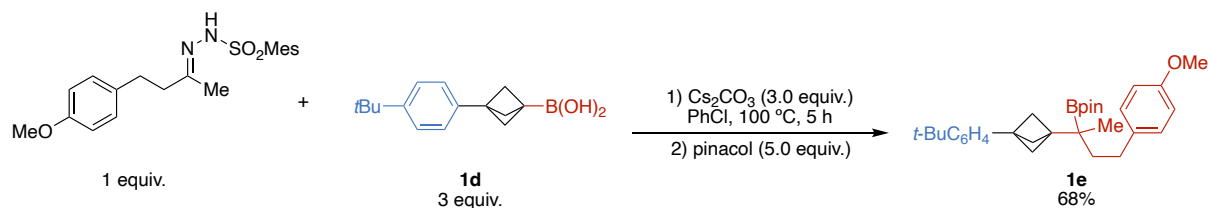
The reaction was conducted following Qin's procedure.[48] A 4 mL vial was charged with N'-(4-(4-methoxyphenyl)butan-2-ylidene)-2,4,6-trimethylbenzenesulfonohydrazide (mixture of isomers, 18.7 mg, 0.0500 mmol, 1.00 equiv.), **1d** (36.6 mg, 0.150 mmol, 3.00 equiv.), and cesium carbonate (48.9 mg, 0.150 mmol, 3.00 equiv.) and brought into the glovebox. Chlorobenzene (0.5 mL) and a stir bar were added, the vial was capped with a Teflon-lined cap, removed from the glovebox, and heated at 100 °C in a preheated aluminum heating block for 5 h. The vial was cooled to room temperature, and pinacol (29.5 mg, 0.250 mmol, 5.00 equiv.) was added as a solid. The mixture was again heated at 100 °C in an aluminum heating block for 1 h. The crude reaction mixture was chromatographed twice on silica gel (0 → 10% ethyl acetate in hexanes, then again with 2 → 3% ethyl acetate in hexanes) to afford the title compound as a white powder (15.5 mg, 63%).

TLC: R_f = 0.6 (10% ethyl acetate in hexanes)

^{1}H NMR (600 MHz, CDCl$_3$) δ 7.32 (d, J = 8.3 Hz, 2H), 7.16 (d, J = 8.3 Hz, 2H), 7.14 (d, J = 8.5 Hz, 2H), 6.84 (d, J = 8.6 Hz, 2H), 3.79 (s, 3H), 2.56 (td, J = 13.0, 5.0 Hz, 1H), 2.45 (td, J = 13.0, 4.4 Hz, 1H), 1.91 – 1.82 (m, 6H), 1.30 (s, 9H), 1.28 (s, 12H). [See spectrum]

^{13}C NMR (151 MHz, CDCl$_3$) δ 157.8, 149.1, 139.0, 136.0, 129.4, 125.9, 125.1, 113.9, 83.4, 55.4, 50.0, 44.6, 40.4, 38.9, 34.6, 32.7, 31.5, 25.3, 25.1, 18.0. [See spectrum]

^{11}B NMR (193 MHz, CDCl$_3$) δ 34.6. [See spectrum]

HRMS (*m/z*): (ESI+) calc'd for C$_{32}$H$_{46}$BO$_3$ [M+H]$^+$: 489.3535, found: 489.3529.

ethyl 4-(3-(4-(*tert*-butyl)phenyl)bicyclo[1.1.1]pentan-1-yl)benzoate (1f)
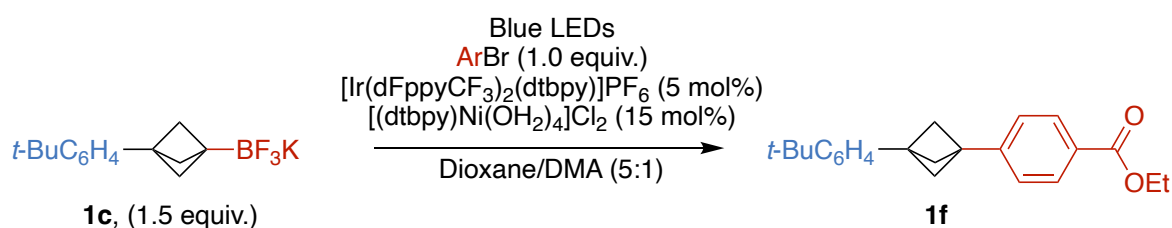
A slightly modified version of VanHeyst's procedure was followed.[40] A 4 mL vial was charged with **1c** (23.0 mg, 75.0 µmol, 1.5 equiv.) and Na$_2$CO$_3$ (10.6 mg, 0.100 mmol, 2.00 equiv.). The vial was then brought into a nitrogen glovebox. [(dtbpy)Ni(OH$_2$)$_4$]Cl$_2$ (3.53 mg, 7.50 µmol, 15.0 mol%), [Ir(dFppyCF$_3$)(dtbpy)]PF$_6$ (2.80 mg, 2.50 µmol, 5.00 mol%), ethyl 4-bromobenzoate (8.16 µL, 50.0 µmol, 1.00 equiv.), and a stir bar were added. Then, 0.5 mL of a 5:1 mixture of dioxane and DMA was added. The vial was tightly capped and removed from the glovebox. The vial was placed in a Merck Photoreactor (450 nm light source, 100% intensity, 1000 rpm stirring and 10000 rpm fan speed) for 16 h. The reaction mixture was diluted with water (5 mL) and extracted with ethyl acetate (5 mL x 3). The combined organic extracts were washed with water (2 mL) and brine (2 mL), dried over MgSO$_4$, filtered, and concentrated. The crude material was chromatographed on silica with 0 → 20% ethyl acetate in hexanes) to afford the title compound as an off-white solid (4.3 mg, 25%).

TLC: R_f = 0.50 (5% ethyl acetate in hexanes)

^{1}H NMR (600 MHz, CDCl$_3$) δ 8.02 (d, J = 8.2 Hz, 2H), 7.40 (d, J = 8.2 Hz, 2H), 7.36 (d, J = 8.2 Hz, 2H), 7.28 (d, J = 4.5 Hz, 2H), 4.40 (q, J = 7.1 Hz, 2H), 2.36 (s, 6H), 1.42 (t, J = 7.1 Hz, 3H), 1.35 (s, 9H). [See spectrum]

^{13}C NMR (151 MHz, CDCl$_3$) δ 166.8, 149.7, 146.2, 137.8, 129.7, 128.8, 126.3, 126.0, 125.3, 61.0, 54.2, 41.0, 40.9, 34.6, 31.5, 14.5. [See spectrum]

HRMS (*m/z*): (EI+) calc'd for C$_{24}$H$_{28}$O$_2$ [M]$^+$: 348.2089, found: 348.2089.

5-(3-(4-(*tert*-butyl)phenyl)bicyclo[1.1.1]pentan-1-yl)-2-methylpyridine (1g)

1) *t*-BuLi (1.2 eq.), -78 °C, 1 h
2) (dppf)PdCl$_2$ (10 mol%)
Cu$_2$O (1.0 equiv.)
5-bromo-2-methylpyridine (2.0 equiv.)

THF, 65 °C, 18 h

1a

1g, 66%
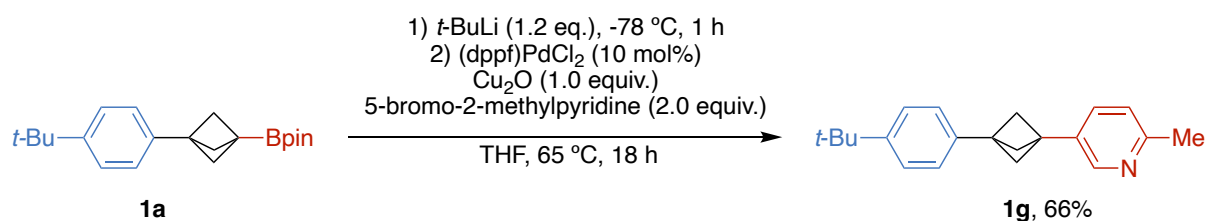
The cross-coupling was performed by modifying a published procedure.[41] A flame-dried Schlenk flask was charged with **1a** (65.3 mg, 0.200 mmol, 1.00 equiv.) and dry THF (1.0 mL). The flask was cooled to -78 °C, and 0.78 M *t*-BuLi in pentanes was added dropwise (0.316 mL, 0.240 mmol, 1.20 equiv.). The mixture was stirred at the same temperature for 1 h, and complete conversion to the corresponding borate was confirmed by ^{11}B NMR spectroscopy (~7 ppm). The septum on the Schlenk flask was firmly secured with electrical tape, and the flask brought into a nitrogen glovebox, where it was charged with (dppf)PdCl$_2$ (14.6 mg, 20.0 µmol, 0.100 equiv.), cuprous oxide (28.6 mg, 0.200 mmol, 1.00 equiv.), and 5-bromo-2-methylpyridine (68.8 mg, 0.400 mmol, 2.00 equiv.). The flask was stoppered with a glass stopper, a slight vacuum was applied to assist in maintaining the seal, and the mixture was heated in an oil bath at 65 °C for 18 h. After cooling to room temperature, the reaction mixture was diluted with ethyl acetate (10 mL) and quenched with aqueous ammonium chloride (5 mL). The mixture was filtered through a bed of MgSO$_4$ and Celite, and the solids were washed with copious amounts of ethyl acetate. The combined organic washes were concentrated and chromatographed over silica with 0 → 30% ethyl acetate in hexanes) to afford the title compound as a yellow powder (38.2 mg, 66%)

TLC: R_f = 0.48 (25% ethyl acetate in hexanes)

^{1}H NMR (500 MHz, CDCl$_3$) δ 8.43 (s, 1H), 7.48 (d, J = 7.9 Hz, 1H), 7.41 – 7.35 (m, 2H), 7.28 – 7.21 (m, 2H), 7.10 (d, J = 7.9 Hz, 1H), 2.55 (s, 3H), 2.33 (s, 6H), 1.33 (s, 9H). [See spectrum]

^{13}C NMR (126 MHz, CDCl$_3$) δ 156.5, 149.7, 147.3, 137.7, 134.4, 133.3, 126.0, 125.3, 122.7, 54.2, 41.3, 38.8, 34.6, 31.5, 24.2. [See spectrum]

HRMS (*m/z*): (ESI+) calc'd for C$_{21}$H$_{26}$N [M+H]$^+$: 292.2060, found: 292.2056.

1-(methylsulfonyl)-3-vinylbicyclo[1.1.1]pentane (11e)

11e
69%
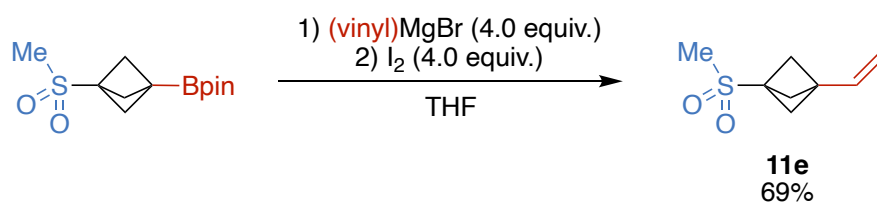
A flame-dried 25 mL round-bottom flask was charged with **11a** (68.0 mg, 0.250 mmol, 1.00 equiv.) and anhydrous THF (4 mL). The flask was cooled to -78 ºC. Vinylmagnesium bromide (1.0 M, 1.0 mmol, 1.0 mL, 4.0 equiv.) was added dropwise, and the resulting mixture was stirred at -78 ºC for 1 h. Then, I_2 (254 mg, 1.00 mmol, 4.00 equiv.) in MeOH (4.0 mL) was added dropwise, and the mixture stirred at -78 ºC for another hour. The flask was adjusted to 0 ºC, and sat. $Na_2S_2O_3$ (2 mL) was added. The mixture was diluted with water (10 mL) and extracted with ethyl acetate (30 mL x 3). The combined organic extracts were dried over $MgSO_4$, filtered, and concentrated. The crude mixture was chromatographed on SiO_2 with 30% ethyl acetate in hexanes as the eluent. Fractions containing the desired compound were collected and concentrated under vacuum to afford the title compound as an off-white solid (29.6 mg, 69%).

TLC: R_f = 0.18 (33% ethyl acetate in hexanes)

^{1}H NMR (500 MHz, CDCl$_3$) δ 5.91 (dd, J = 17.1, 10.5 Hz, 1H), 5.17 (dd, J = 10.5, 1.5 Hz, 1H), 5.12 (dd, J = 17.2, 1.5 Hz, 1H), 2.83 (s, 3H), 2.23 (s, 6H). [See spectrum]

^{13}C NMR (126 MHz, CDCl$_3$) δ 134.2, 117.7, 52.0, 50.8, 39.8, 37.6. [See spectrum]

HRMS (*m/z*): (ESI+) calc'd for $C_8H_{12}O_2NaS$ [M+Na]$^+$: 195.0450, found: 195.0449.

tert-butyl 1-(difluoromethyl)-4-vinyl-2-azabicyclo[2.1.1]hexane-2-carboxylate (30c)
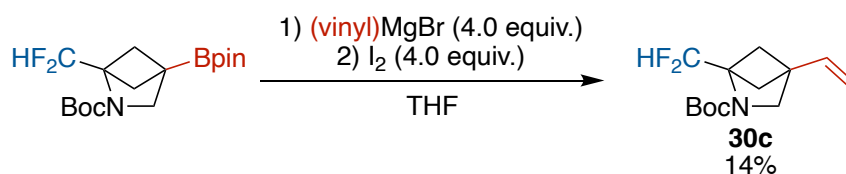
A flame-dried 25 mL round-bottom flask was charged with **30a** (36 mg, 0.10 mmol, 1.0 equiv.) and anhydrous THF (2 mL). The flask was cooled to -78 ºC. Vinylmagnesium bromide (1.0 M, 0.40 mmol, 0.40 mL, 4.0 equiv.) was added dropwise, and the resulting mixture was stirred at -78 ºC for 1 h. Then, I_2 (0.10 g, 0.40 mmol, 4.0 equiv.) in MeOH (4.0 mL) was added dropwise, and the mixture stirred at -78 ºC for another hour. The flask was adjusted to 0 ºC, and sat. $Na_2S_2O_3$ (1 mL) was added. The mixture was diluted with water (5 mL) and extracted with ethyl acetate (15 mL x 3). The combined organic extracts were dried over $MgSO_4$, filtered, and concentrated. The crude mixture was chromatographed on SiO_2 with 30% ethyl acetate in hexanes as the eluent. Fractions containing the desired compound were collected and concentrated under vacuum to afford the title compound as a colorless oil (3.6 mg, 14%). Note that the product is volatile.

TLC: N/A

^{1}H NMR (600 MHz, CDCl$_3$) δ 6.84 (t, J_{H-F} = 56.3 Hz, 1H), 6.16 (dd, J = 17.3, 10.6 Hz, 1H), 5.34 (dd, J = 10.7, 1.3 Hz, 1H), 5.30 (dd, J = 17.4, 1.4 Hz, 1H), 3.52 (s, 2H), 2.25 – 2.09 (m, 2H), 1.99 – 1.83 (m, 2H), 1.70 (s, 2H), 1.62 (s, 9H). [See spectrum]

^{13}C NMR (151 MHz, CDCl$_3$) δ 155.3, 135.4, 116.7, 112.30 (t, J_{C-F} = 237.2 Hz), 80.7, 69.18 (t, J_{C-F} = 31.2 Hz), 55.4, 47.6, 43.3, 29.8, 28.5. [See spectrum]

^{19}F NMR (565 MHz, CDCl$_3$) δ -124.4. [See spectrum]

HRMS (m/z): (ESI+) calc'd for $C_{14}H_{24}F_2NO_3$ [M+MeOH+H]$^+$: 292.1719, found: 292.1722.

1-((3-(furan-2-yl)bicyclo[1.1.1]pentan-1-yl)sulfonyl)piperidine (13c)
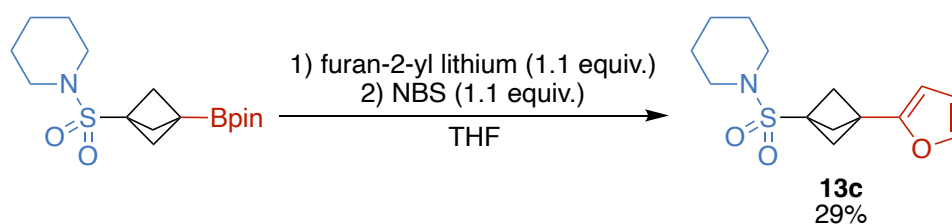
A flame-dried 10 mL RBF was charged with furan (15.0 mg, 0.220 mmol, 1.10 equiv.) and anhydrous THF (3.0 mL). *n*-BuLi in hexanes (2.5 M, 88 µL, 0.22 mmol, 1.1 equiv.) was added dropwise at –78 ºC. The mixture was warmed to ambient temperature and stirred for 1 h. A separate flame-dried 25 mL RBF was charged with **13a** (68.3 mg, 0.200 mmol, 1.00 equiv.) and anhydrous THF (3.0 mL). The solution of furan-2-yl lithium was added dropwise at -78 ºC, and the mixture stirred at -78 ºC for 1 h. Then, *N*-bromosuccinimide (39.2 mg, 0.220 mmol, 1.10 equiv.) in anhydrous THF (3.0 mL) was added, and the mixture stirred at -78 ºC for another 1 h. The flask was adjusted to 0 ºC, and sat. $Na_2S_2O_3$ (2 mL) was added. The mixture was diluted with water (10 mL) and extracted with ethyl acetate (30 mL x 3). The combined organic extracts were dried over $MgSO_4$, filtered, and concentrated. The crude mixture was chromatographed on SiO_2 with 20 → 30% ethyl acetate in hexanes as the eluent. Fractions containing the desired compound were collected and concentrated under vacuum to afford the title compound as an off-white solid (16.4 mg, 29%).

TLC: R_f = 0.35 (20% ethyl acetate in hexanes)

¹H NMR (500 MHz, CDCl₃) δ 7.32 (dd, *J* = 1.8, 0.8 Hz, 1H), 6.31 (dd, *J* = 3.2, 1.8 Hz, 1H), 6.10 (dd, *J* = 3.3, 0.9 Hz, 1H), 3.37 – 3.31 (m, 4H), 2.48 (s, 6H), 1.70 – 1.54 (m, 6H). [See spectrum]

¹³C NMR (126 MHz, CDCl₃) δ 151.6, 142.3, 110.5, 106.6, 54.0, 50.5, 47.2, 35.6, 26.2, 24.1. [See spectrum]

HRMS (*m/z*): (ESI+) calc'd for $C_{14}H_{20}O_3NS$ [M+H]⁺: 282.1158, found: 282.1160.

2-((3-(4-(*tert*-butyl)phenyl)bicyclo[1.1.1]pentan-1-yl)methyl)-4,4,5,5-tetramethyl-1,3,2-dioxaborolane (1h)
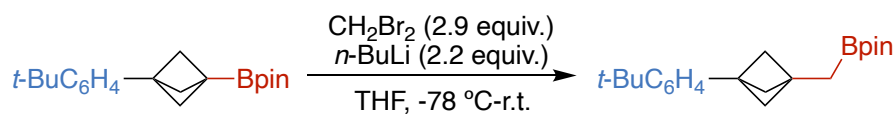
A flame-dried 50 mL flask was charged with **1a** (33.0 mg, 0.100 mmol, 1.00 equiv.), dibromomethane (20.2 µL, 0.290 mmol, 2.90 equiv.) and 1.0 mL of anhydrous THF. The reaction mixture was cooled to -78 °C under an N_2 atmosphere. Then, *n*-BuLi (2.5 M in hexanes, 0.0880 mL, 0.220 mmol, 2.20 equiv.) was added dropwise. The reaction was stirred for 1 hour at -78 °C. The reaction mixture was then warmed to room temperature and was stirred at ambient temperature for 90 min. After this time, the reaction was quenched with sat. NH_4Cl (3 mL) and extracted with ethyl acetate (10 mL x 3). The organic layers were combined and washed with brine (15 mL), dried over Na_2SO_4, and concentrated. The crude reaction mixture was eluted on SiO_2 with 0% → 20% ethyl acetate in hexanes as the eluent. Fractions containing the desired compound were collected and concentrated under vacuum to afford the title compound as a white solid (19.1 mg, 56%).

TLC: R_f = 0.65 (10% ethyl acetate in hexanes)

¹H NMR (600 MHz, CDCl₃) δ 7.32 (d, J = 8.3 Hz, 2H), 7.16 (d, J = 8.3 Hz, 2H), 1.96 (s, 6H), 1.31 (s, 10H), 1.27 (s, 13H), 1.16 (s, 2H). [See spectrum]

¹³C NMR (151 MHz, CDCl₃) δ 148.9, 138.6, 125.8, 124.9, 83.0, 54.3, 41.5, 35.9, 34.4, 31.4, 24.9. [See spectrum]

¹¹B NMR (193 MHz, CDCl₃) δ 32.9. [See spectrum]

HRMS (*m/z*): (EI+) calc'd for $C_{22}H_{33}BO_2$ [M]⁺: 340.2574, found: 340.2571.

2,2,2-trifluoro-*N*-(3-hydroxybicyclo[1.1.1]pentan-1-yl)acetamide (16d)

16a

16e, 73%
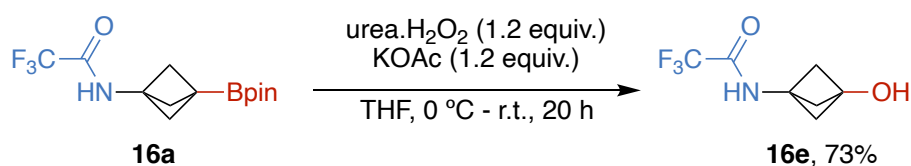
The reaction was performed by modifying a known procedure.[41] **16a** (30.5 mg, 0.100 mmol, 1.00 equiv.) was dissolved in THF (0.5 mL) in a 4 mL vial. To the solution was added urea•H_2O_2 (11.3 mg, 0.120 mmol, 1.20 equiv.) and potassium acetate (11.8 mg, 0.120 mmol, 1.20 equiv.) at 0 ºC. Then, water (0.3 mL) was also added at 0 ºC, and the mixture was stirred for 10 min. The cooling bath was removed, and the reaction mixture was stirred at room temperature for 20 h. The mixture was diluted with ethyl acetate (5 mL) and washed with saturated ammonium chloride (5 mL). The aqueous layer was extracted with ethyl acetate (5 mL x 2). The combined organic layers were dried over Na_2SO_4, filtered, and concentrated. The crude material was chromatographed on silica with 30% ethyl acetate in hexanes to afford the title compound as a white powder (14.2 mg, 73%).

TLC: R_f = 0.3 (30% ethyl acetate in hexanes)

¹H NMR (600 MHz, Acetone) δ 8.93 (bs, 1H), 5.36 (bs, 1H), 2.18 (s, 6H). [See spectrum]

¹³C NMR (151 MHz, Acetone) δ 205.2, 155.6 (q, $J_{C\text{-}F}$ = 36.5 Hz), 114.9 (q, $J_{C\text{-}F}$ = 287.9 Hz), 61.3, 54.4, 54.3, 40.0, 28.0. [See spectrum]

¹⁹F NMR (565 MHz, Acetone) δ -77.6. [See spectrum]

HRMS (*m/z*): (ESI-) calc'd for $C_7H_7F_3NO_2$ [M-H]⁻: 194.0434, found: 194.0436.

tert-butyl 4-hydroxy-2-azabicyclo[2.1.1]hexane-2-carboxylate (27c)
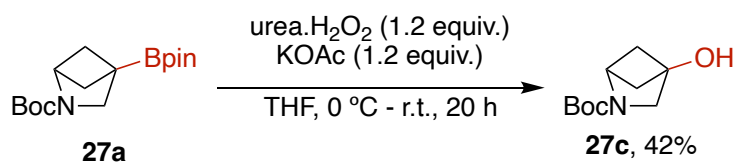
The reaction was performed by modifying a known procedure.[41] Compound **27a** (18 mg, 0.057 mmol, 1.0 equiv.) was dissolved in THF (0.25 mL) in a 4 mL vial. To the solution was added urea•H_2O_2 (6.4 mg, 0.068 mmol, 1.2 equiv.) and potassium acetate (6.7 mg, 0.12 mmol, 1.2 equiv.) at 0 ºC. Then, water (0.15 mL) was also added at 0 ºC, and the mixture was stirred for 10 min. The cooling bath was removed, and the reaction mixture was stirred at room temperature for 20 h. The mixture was diluted with ethyl acetate (4 mL) and washed with saturated ammonium chloride (4 mL). The aqueous layer was extracted with ethyl acetate (4 mL x 2). The combined organic layers were washed with saturated aqueous sodium thiosulfate (2 mL), dried over Na_2SO_4, filtered, and concentrated. The crude material was chromatographed on silica with 30% ethyl acetate in hexanes to afford the title compound as a white powder (4.8 mg, 42%).

TLC: N/A

^{1}H NMR (600 MHz, CDCl$_3$) δ 4.32 (s, 1H), 3.37 (s, 2H), 2.77 (s, 1H), 2.08 – 1.88 (m, 4H), 1.60 (s, 9H). [See spectrum]

^{13}C NMR (151 MHz, CDCl$_3$) δ 155.4, 79.7, 76.0, 52.9, 50.9, 47.2, 28.6. [See spectrum]

HRMS (m/z): (ESI+) calc'd for $C_{13}H_{26}NO_4$ [M+iPrOH+H]$^+$: 260.1851, found: 260.1862.

N-(3-(benzylamino)bicyclo[1.1.1]pentan-1-yl)-2,2,2-trifluoroacetamide (16e)

16a

16d
77%
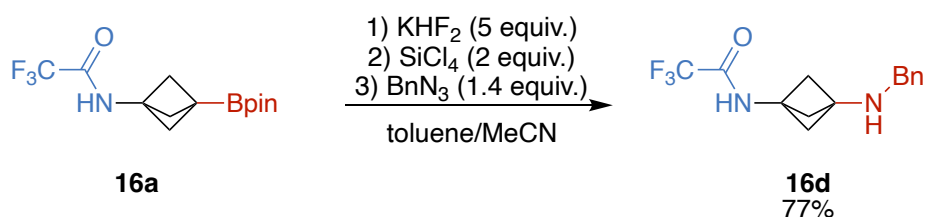
The reaction was performed by modifying a known procedure.[49] **16a** (45.8 mg, 0.150 mmol) was dissolved in a mixture of MeOH (0.4 mL) and THF (0.2 mL). Then, KHF$_2$ (58.6 mg, 0.750 mmol, 5.00 equiv.) in water (0.2 mL) was added with vigorous stirring. The resulting mixture was stirred at room temperature for 3 h. The reaction mixture was co-evaporated with 1:1 methanol:water repeatedly (1 mL x 5) to remove pinacol. The solid residue was extracted with acetone, filtered, and the filtrate concentrated. The residue was further co-evaporated with toluene (1 mL x 2) to remove residual water. The residue was dissolved in a mixture of toluene (1.5 mL) and acetonitrile (0.4 mL) in a 4 mL vial and sealed with a pressure-release septum cap. SiCl$_4$ (34.4 μL, 0.300 mmol, 2.00 equiv.) was added through the septum cap via a syringe, and the mixture was stirred for 20 min at room temperature. Then, a 0.5 M solution of benzyl azide in dichloromethane (0.42 mL, 0.21 mmol, 1.4 equiv.) was added through the septum cap. The vial was brought into a nitrogen glovebox, and the septum cap was replaced with a cap lined with a Teflon seal. The vial was heated in a 50 ºC aluminum heating block for 16 h. After the vial was cooled to room temperature, the contents were poured into water (5 mL), and the organic layer was extracted with aqueous 1 M HCl (10 mL x 5). The combined aqueous layers were basified with 2 M NaOH to pH = 9 and then extracted with ether (20 mL x 5). The ether extracts were combined, dried over MgSO$_4$, filtered, and concentrated. The crude material was chromatographed on silica gel with 100% ethyl acetate to afford the product as a white solid (33.0 mg, 77%).

TLC: R_f = 0.6 (100% ethyl acetate)

¹H NMR (500 MHz, CDCl$_3$) δ 7.33 – 7.20 (m, 5H), 6.69 (bs, 1H), 3.79 (s, 2H), 2.17 (s, 6H), 2.10 (bs, 1H). [See spectrum]

¹³C NMR (126 MHz, CDCl$_3$) δ 156.9 ($J_{C\text{-}F}$ = 37.3 Hz), 139.8, 128.5, 128.0, 127.2, 115.4 (q, $J_{C\text{-}F}$ = 288.7 Hz), 77.0, 53.5, 52.2, 50.4, 43.7. [See spectrum]

¹⁹F NMR (470 MHz, CDCl$_3$) δ -76.0. [See spectrum]

HRMS (m/z): (ESI+) calc'd for C$_{14}$H$_{16}$F$_3$N$_2$O [M+H]$^+$: 285.1210, found: 285.1209.

2.4.7 Kinetic Studies

Measurement of $^1J_{C-H}$ coupling constants.

The $^1J_{C-H}$ coupling constants were measured by *J*-resolved 2D NMR spectroscopy. 5-10 mg of the compound of interest was dissolved in CDCl$_3$, and a *J*-resolved ^{13}C-^{1}H 2D-spectrum was obtained. The peaks were assigned by comparison to the known ^{13}C NMR spectrum and the desired $^1J_{C-H}$ coupling constant was directly read from the spectrum. The case of **1b** is shown as an example below in Figure 2.12.

$^1J_{C-H} = 2783.10 - 2618.07 = 165.03$ Hz.
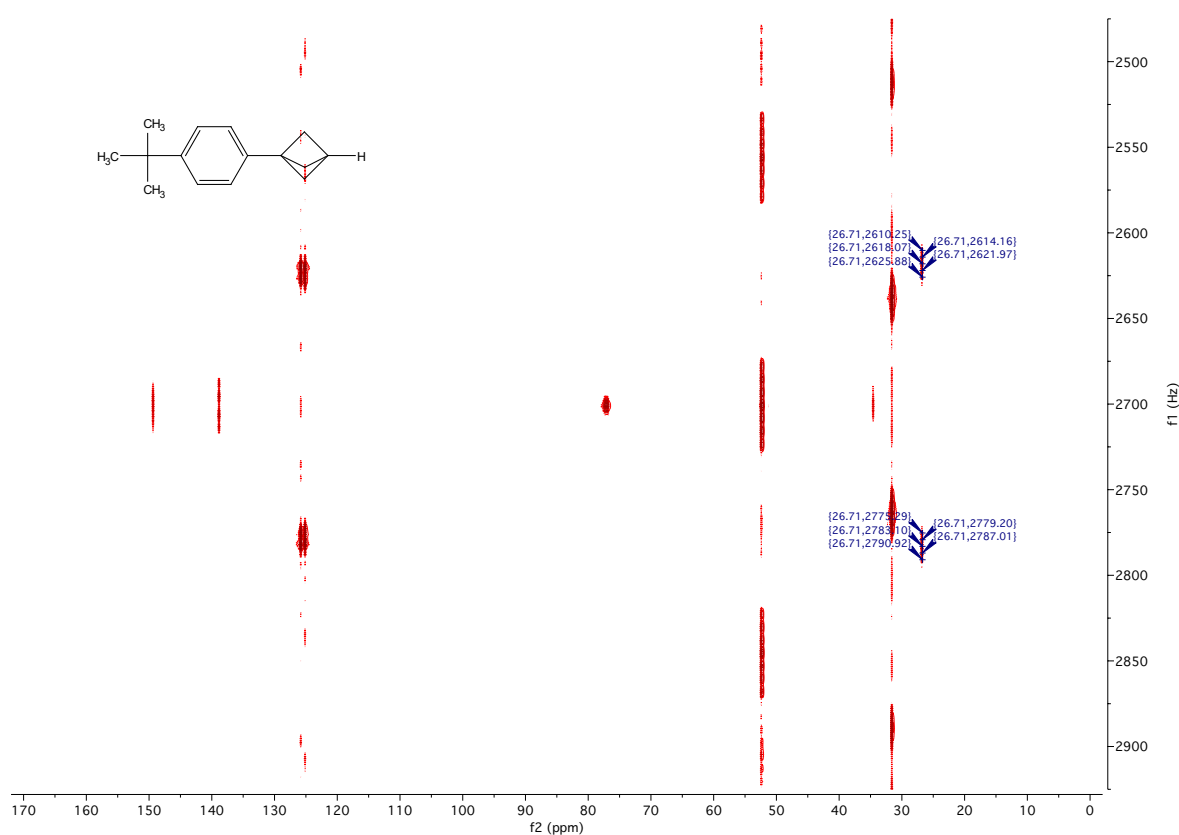
Figure 2.12. Example for the measurement of $^1J_{C-H}$ coupling constants. The example given is a *J*-resolved ^{13}C-^{1}H 2D-spectrum of **1b**.

Competition experiments.

The competition experiments with 2-mphen as ligand were run to low conversion to prevent H-D exchange from significantly affecting the ratios of products. (See Sec.) The competition experiments that were run to longer reaction times to achieve significant conversion are included for completeness.

Competition between different types of C–H bonds.

In a nitrogen glovebox, a 4 mL dram vial was charged with the appropriate ligand (25.0 µmol), [Ir(COD)(OMe)]$_2$ (8.29 mg, 12.5 µL), and B$_2$pin$_2$ (6.35 mg, 25.0 µmol). Anhydrous THF (2.5 mL) was added, after which the vial was tightly sealed with a Teflon-lined cap, removed from the glovebox, and heated in an aluminum heating block at 100 ºC for 5 min. The resultant solution was dispensed into fresh 4 mL vials (100 µL, 1.00 µmmol of catalyst), and the volatile materials were evaporated in vacuo. To the vials containing the catalyst were added B$_2$pin$_2$ (5.08 mg, 20.0 µmol), adamantane (6.81 mg, 50.0 µmol), 4-*tert*-butylphenylbicyclopentane (**1b**) (10.0 mg, 50.0 µmol), substrate (50.0 µL), cyclooctane (120 µL), and a flea stir bar. The vial was tightly sealed with a Teflon-lined cap, removed from the glovebox, and heated in an aluminum heating block at the specified temperature for the specified reaction time. After the appropriate amounts of time had elapsed, the vials were removed from the heating block, brought into the glovebox, and an aliquot removed for analysis by gas chromatography. The ratio of the products are shown in Figure 2.13 and Figure 2.14.
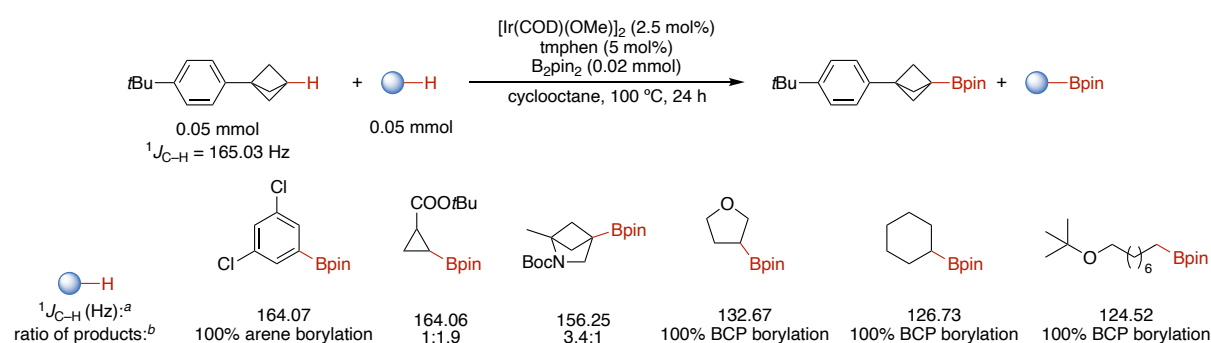
Figure 2.13. Competition experiments with substrates containing different types of C–H bonds with tmphen. Ratios of products determined with tmphen as the ligand. [a] $^1J_{C-H}$ coupling constant of the C–H bond that underwent borylation. [b] Ratio of products determined by GC analysis.
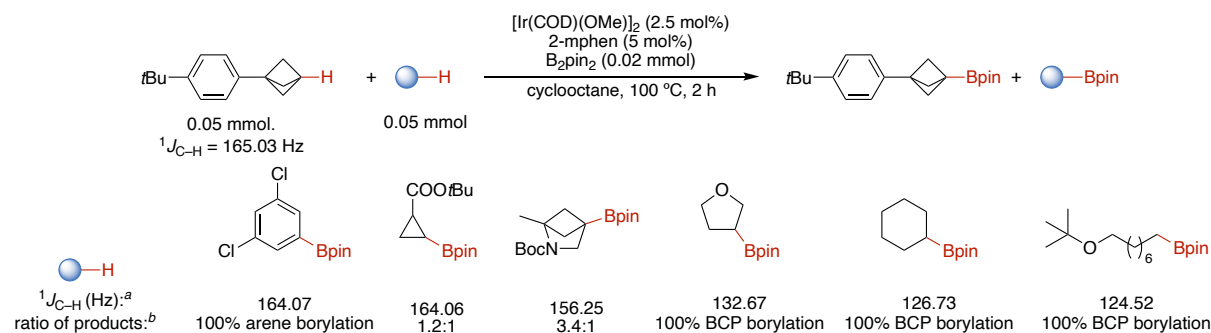
Figure 2.14. Competition experiments with substrates containing different types of C–H bonds with 2-mphen. Ratio of products determined with 2-mphen as the ligand. [a] $^1J_{C-H}$ coupling constant of the C–H bond that underwent borylation. [b] Ratio of products determined by GC analysis.

Competition between BCP substrates.

In a nitrogen glovebox, a 4 mL dram vial was charged with the appropriate ligand (25.0 µmol), [Ir(COD)(OMe)]$_2$ (8.29 mg, 12.5 µL), and B$_2$pin$_2$ (6.35 mg, 25.0 µmol). Anhydrous THF (2.5 mL) was added, after which time the vial was tightly sealed with a Teflon-lined cap, removed from the glovebox, and heated in an aluminum heating block at 100 ºC for 5 min. The resultant solution was dispensed into fresh 4 mL vials (100 µL, 1.00 µmmol of catalyst), and the volatile materials were evaporated in vacuo. To the vials containing the catalyst were added B$_2$pin$_2$ (5.08 mg, 20.0 µmol), bicyclo[1.1.1]pentan-1-yltributylstannane (**4b**) (17.9 mg, 50.0 µmol), substrate (50.0 µL), cyclooctane (120 µL), and a flea stir bar. The vial was tightly sealed with a Teflon-lined cap, removed from the glovebox, and heated in an aluminum heating block at the specified temperature for the specified reaction time. After the appropriate amounts of time had elapsed, the vials were removed from the heating block, cooled to room temperature, and CH$_2$Br$_2$ was added. An aliquot was taken and analyzed by ^{1}H NMR spectroscopy. The ratio of the products are shown in Figure 2.15 and Figure 2.16.
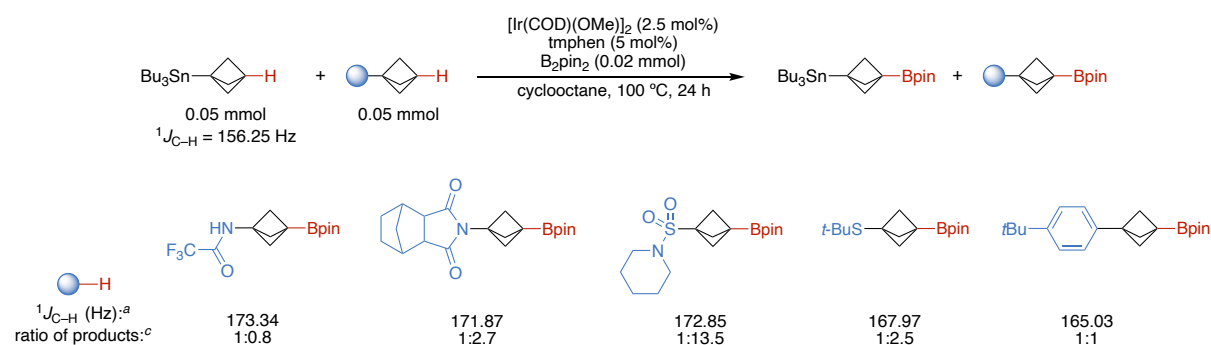
Figure 2.15. Competition experiments with different BCP substrates with tmphen. Ratios of products determined with tmphen as the ligand. [a] $^1J_{C-H}$ coupling constant of the C–H bond that underwent borylation. [c] Ratio of products determined by NMR analysis.
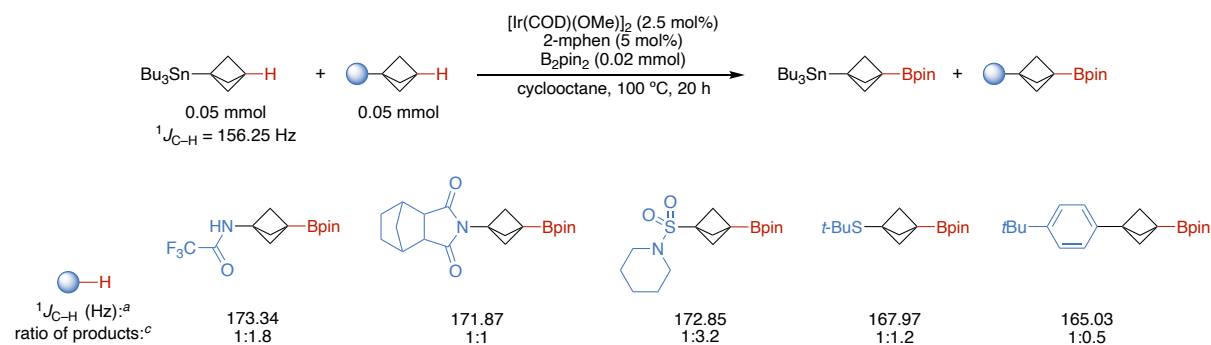
Figure 2.16 Competition experiments with different BCP substrates with 2-mphen. Ratios of products determined with 2-mphen as the ligand. [a] $^1J_{C-H}$ coupling constant of the C–H bond that underwent borylation. [c] Ratio of products determined by NMR analysis.

Measurement of kinetic isotope effects

Initial attempts to measure KIE values by performing intermolecular competition reactions with **1b** and **1b**-d_1 were hampered by several factors. Because the bridgehead position was the only one that was labelled, both substrates would react to form identical product. Thus, determination of the KIE directly would require accurate determination of the ratio of isotopomers in the remaining starting material (ideally at high conversions of the material, as in a Singleton-type experiment).[60] Unfortunately, it was found that substantial H-D scrambling occurs through protodeboronation, especially at the longer reaction times required to reach high conversion. The source of the protons is presumably adventitious water or hydroxyl groups on the walls of the glass vial, although efforts to chemically modify the glass vials did not reduce the amount of protodeboronation. We thus resorted to the double competition experiment and independent initial rates measurements presented below, both of which were run to low conversion, where H-D scrambling is expected to introduce less error into the KIE value measured. An additional hurdle was the presence of substantial induction period during reactions catalyzed by complexes of both the 2-mphen and 2,9-dmphen systems, as shown below in Figure 2.17. We observed no obvious induction period with tmphen as ligand.

Time courses showing the presence of induction periods for 2-mphen and 2,9-dmphen

In a nitrogen glovebox, a 4 mL vial was charged with 4-*tert*-butylphenylbicyclopentane (**1b**, 50.1 mg, 0.250 mmol), B_2pin_2 (95.2 mg, 0.375 mmol), (mesitylene)Ir(Bpin)$_3$ (8.67 mg, 0.0125 mmol), ligand, (2.95 mg, 0.0125 mmol), adamantane (17.0 mg, 0.125 mmol), and cyclooctane (200 μL). A stir bar was added to the mixture, and the vial tightly capped with a Teflon-lined cap. The vial was removed from the glovebox and heated in a preheated aluminum heating block at 100 °C. Aliquots were removed at appropriate timepoints and analyzed by GC analysis.
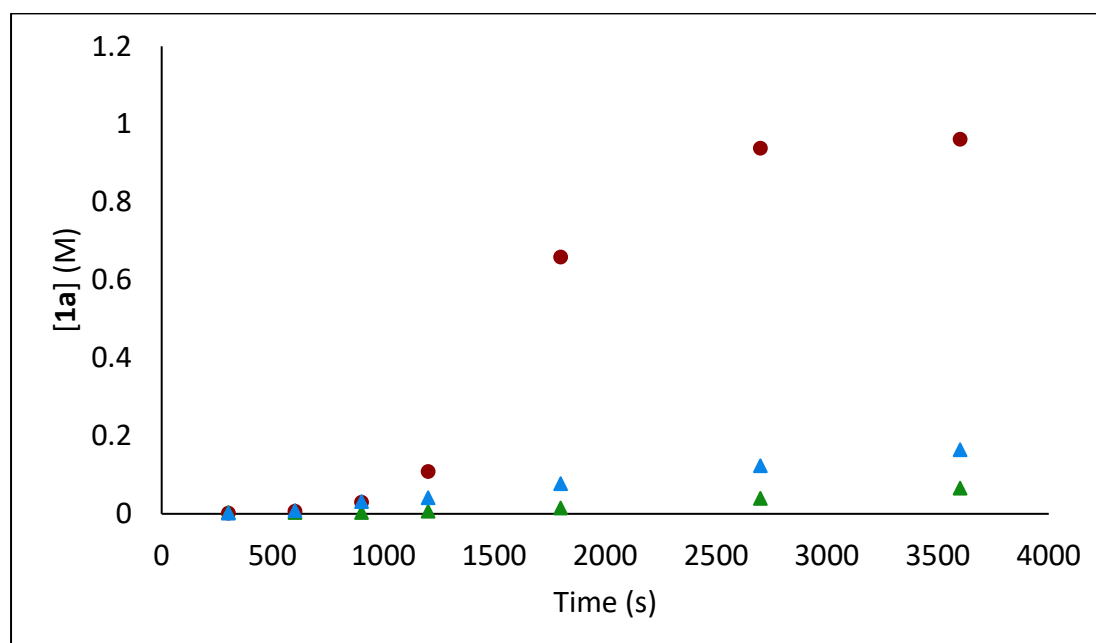
Double competition experiment for the determination of the kinetic isotope effect

In a nitrogen glovebox, a 4 mL vial was charged with 3,5-di(*tert*-butyl)phenylbicyclopentane (**2b**, 32.1 mg, 0.125 mmol) and either 4-*tert*-butylphenylbicyclopentane (**1b**, 25.0 mg, 0.125 mmol) or 4-*tert*-butylphenylbicyclopentane-d_1 (**1b-d_1**, 25.0 mg, 0.125 mmol). Then, B$_2$pin$_2$ (7.94 mg, 0.0312 mmol), [Ir(COD)OMe]$_2$ (1.04 mg, 2.50 mol%), 2-mphen (0.61 mg, 5.0 mol%), and cyclooctane (100 µL) were added. A stir bar was added to the mixture, and the vial tightly capped with a Teflon-lined cap. The vial was removed from the glovebox and heated in a preheated aluminum heating block at 100 ºC for 2 h. Then, an aliquot was taken and analyzed by GC analysis. The relative integrations for the borylated products **1a** and **2a** were recorded, and the KIE value obtained by dividing the ratios obtained from reactions done with **1b** over those obtained with **1b-d_1**. The experiment was conducted in triplicate.

KIE = (**2a**-H/**1a**-H)/(**2a**-D/**1a**-D) = 1.8 ± 0.1
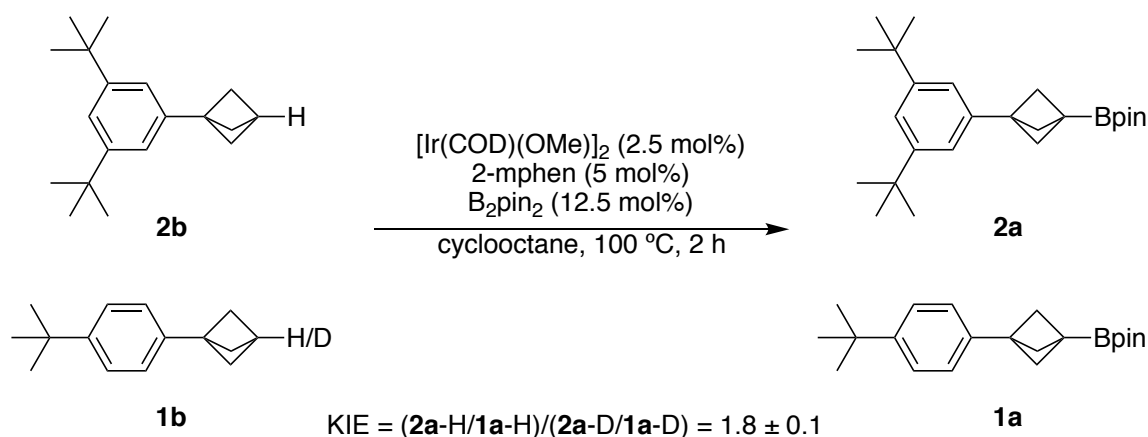
Figure 2.18. The setup for the double competition experiment. Equivalent to Figure 2.6a of the main text.

Run 1: 1.90

Run 2: 1.90

Run 3: 1.68

KIE = 1.8 ± 0.1

An analogous reaction was initiated with only **1b-d_1** under the reaction conditions. The extent of H-D scrambling in the starting material was < 5% as judged by NMR analysis. Thus, we do not anticipate large errors arising from protodeboronation.

Measurement of the KIE by the method of initial rates

In a nitrogen glovebox, a 4 mL vial was charged with either 4-*tert*-butylphenylbicyclopentane (**1b**, 50.1 mg, 0.250 mmol) or 4-*tert*-butylphenylbicyclopentane-d_1 (**1b-d_1**, 50.3 mg, 0.250 mmol). Then, B$_2$pin$_2$ (95.2 mg, 0.375 mmol), (mesitylene)Ir(Bpin)$_3$ (8.67 mg, 0.0125 mmol), tmphen (2.95 mg, 0.0125 mmol), adamantane (17.0 mg, 0.125 mmol), and cyclooctane (200 µL) were added. A stir bar was added to the mixture, and the vial tightly capped with a Teflon-lined cap. The vial was removed from the glovebox and heated in a preheated aluminum heating block at 100 ºC. Aliquots were removed at appropriate timepoints and analyzed by GC. The experiment was conducted in triplicate. The concentration of product **1a** was measured and plotted versus time to obtain the initial rates of the formation of **1a**.

With **1b**

[1a] = 0.006261 t + 0.014796
R² = 0.997

With **1b-d_1**

[1a] = 0.003393 t + 0.011778
R² = 0.997
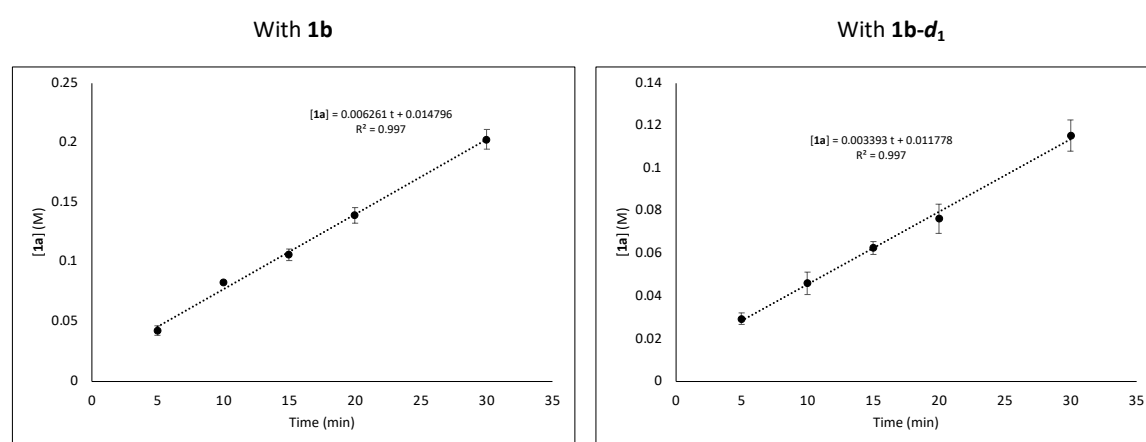
Figure 2.19. Formation of borylated product 1a vs time with either 1b or 1b-d_1.

KIE = 0.0063/0.0034 = 1.8 ± 0.1

Determination of the rate law of the catalytic reaction by the method of initial rates

Order in substrate.

In a nitrogen glovebox, adamantane (45.4 mg, 0.333 mmol) and B_2pin_2 (254 mg, 1.00 mmol) were dissolved in dry THF in a 2.0 mL volumetric flask. The resulting solution was dispensed into four 1-dram vials equipped with flea stir bars, (375 µL, 0.0625 mmol of adamantane, 0.188 mmol of B_2pin_2). In a 2.0 mL volumetric flask, 4-*tert*-butylphenylbicyclopentane (**1b**) (250 mg, 1.25 mmol) was dissolved in dry THF to make a 0.625 M solution. The solution was dispensed into the four 1-dram vials (100 µL, 0.0625 mmol; 200 µL, 0.125 mmol; 300 µL, 0.188 mmol; 400 µL, 0.250 mmol; respectively). In a 1-dram vial tmphen (11.8 mg, 0.0500 mmol), (mesitylene)Ir(Bpin)$_3$ (34.7 mg, 0.0500 mmol), and B_2pin_2 (12.7 mg, 0.0500 mmol) were dissolved in 1.00 mL dry THF. The vial was tightly sealed with a Teflon-lined cap and removed from the glovebox. The vial was heated in an aluminum heating block at 100 ºC for 5 min, resulting in a homogenous, deep red-brown solution. The vial was cooled to room temperature and returned to the glovebox. The solution was dispensed into the four 1-dram vials (125 µL, 6.25 µmmol of catalyst). All volatile materials were carefully evaporated from the four 1-dram vials in vacuo. Then, dry cyclooctane (400 µL) was added, the vials tightly sealed with Teflon-lined caps, and the vials removed from the glovebox. The vials were heated in an aluminum heating block at 100 ºC. At the appropriate timepoints, the vials were removed from the heating block, brought into the glovebox, and an aliquot removed for analysis by gas chromatography. The concentration of product **1a** was measured and plotted versus time to obtain the initial rates of the formation of **1a**.

Table 2.1. Initial concentrations of [1b], [catalyst], and [B$_2$pin$_2$] (varying [1b]), and the corresponding initial rates of formation of 1a.

[**1b**] (M)	[catalyst] (mM)	[B$_2$pin$_2$] (M)	Initial Rate of Formation of **1a** (mM.min^{-1})
0.156	15.6	0.469	0.101 ± 0.003
0.312	15.6	0.469	0.214 ± 0.004
0.469	15.6	0.469	0.359 ± 0.010
0.625	15.6	0.469	0.480 ± 0.014
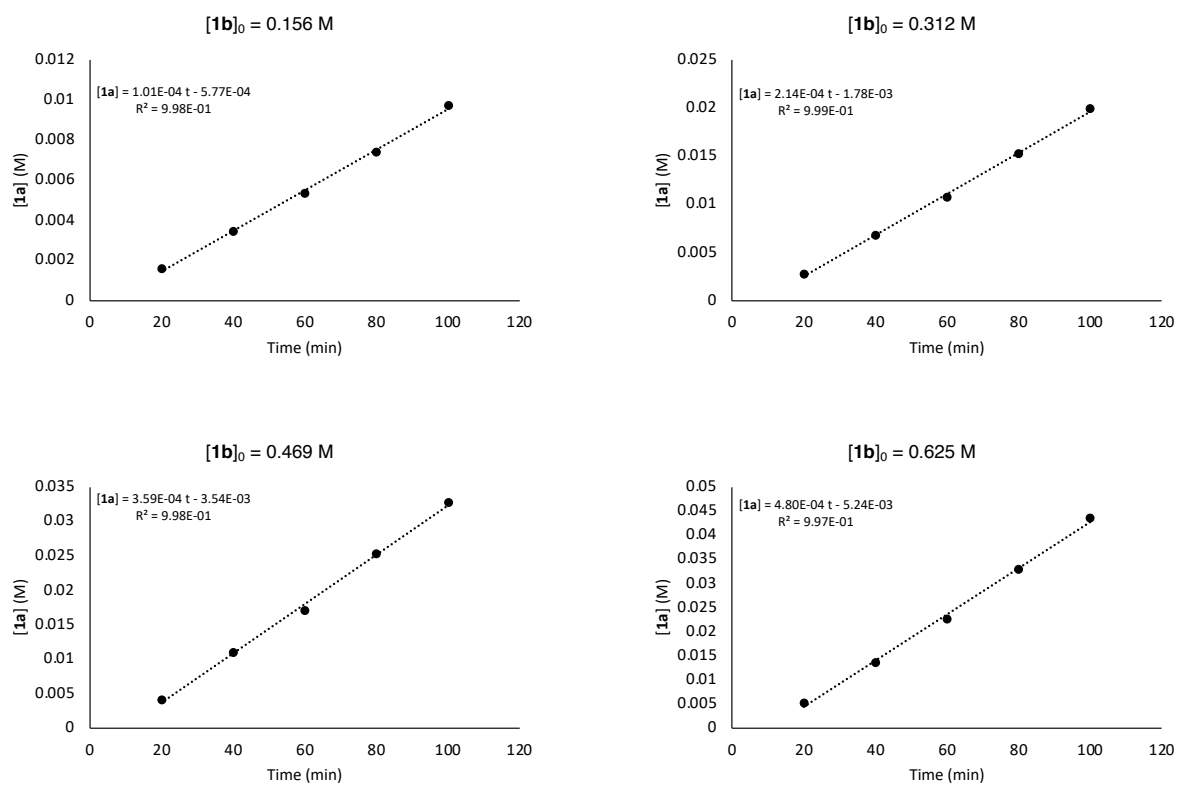
Figure 2.20. Formation of borylated product **1a** *vs* time varying initial concentration of substrate **1b**.
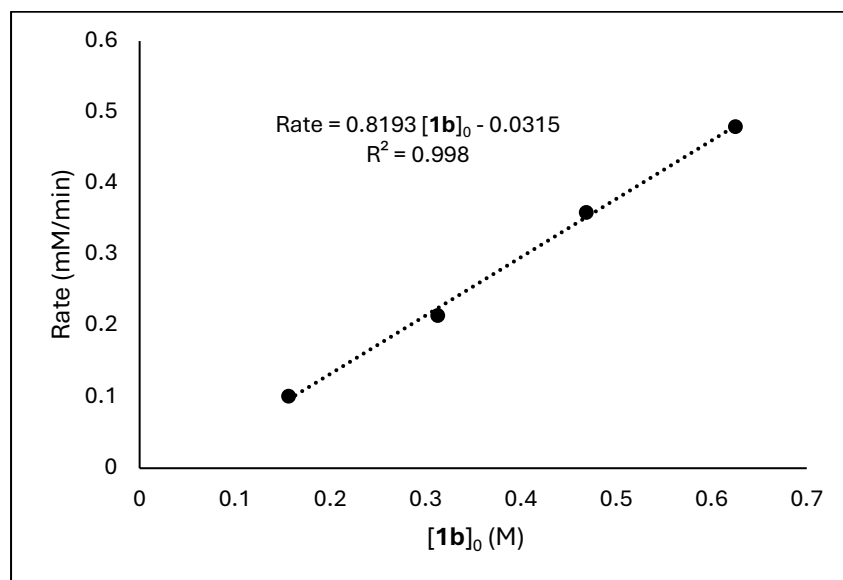
Figure 2.21. Plot of the initial rate of the formation of **1a** varying the initial concentration of substrate **1b**. Reproduced in Figure 2.6c.

Order in catalyst.

In a nitrogen glovebox, B_2pin_2 (254 mg, 1.00 mmol) was dissolved in dry THF in a 2.0 mL volumetric flask. The resulting solution was dispensed into four 1-dram vials equipped with flea stir bars, (375 µL, 0.188 mmol of B_2pin_2). In a 1.0 mL volumetric flask, 4-*tert*-butylphenylbicyclopentane (**1b**) (125 mg, 0.625 mmol) and adamantane (42.6 mg, 0.313 mmol) were dissolved in dry THF. The solution was dispensed into the four 1-dram vials (200 µL, 0.125 mmol of **1b**, 0.0625 mmol of adamantane). In a 1-dram vial tmphen (11.8 mg, 0.0500 mmol), (mesitylene)Ir(Bpin)$_3$ (34.7 mg, 0.0500 mmol), and B_2pin_2 (12.7 mg, 0.0500 mmol) were dissolved in 1.00 mL dry THF. The vial was tightly sealed with a Teflon-lined cap and removed from the glovebox. The vial was heated in an aluminum heating block at 100 ºC for 5 min, resulting in a homogenous, deep red-brown solution. The vial was cooled to room temperature and returned to the glovebox. The solution was dispensed into the four 1-dram vials (62.5 µL, 3.13 µmol; 125 µL, 6.25 µmmol; 188 µL, 9.38 µmol; 250 µL, 12.5 µmol; respectively). All volatile materials were carefully removed from the four 1-dram vials in vacuo. Then, dry cyclooctane (400 µL) was added, the vials tightly sealed with Teflon-lined caps, and the vials removed from the glovebox. The vials were heated in an aluminum heating block at 100 ºC. At the appropriate timepoints, the vials were removed from the heating block, brought into the glovebox, and an aliquot taken for gas chromatography analysis. The concentration of product **1a** was measured and plotted versus time to obtain the initial rates of the formation of **1a**.

Table 2.2. Initial concentrations of [**1b**], [catalyst], and [B_2pin_2] (varying [catalyst]), and the corresponding initial rates of formation of **1a**.

[**1b**] (M)	[catalyst] (mM)	[B_2pin_2] (M)	Initial Rate of Formation of **1a** (mM.min^{-1})
0.312	7.81	0.469	0.172 ± 0.008
0.312	15.6	0.469	0.324 ± 0.006
0.312	23.4	0.469	0.564 ± 0.014
0.312	31.2	0.469	0.713 ± 0.006
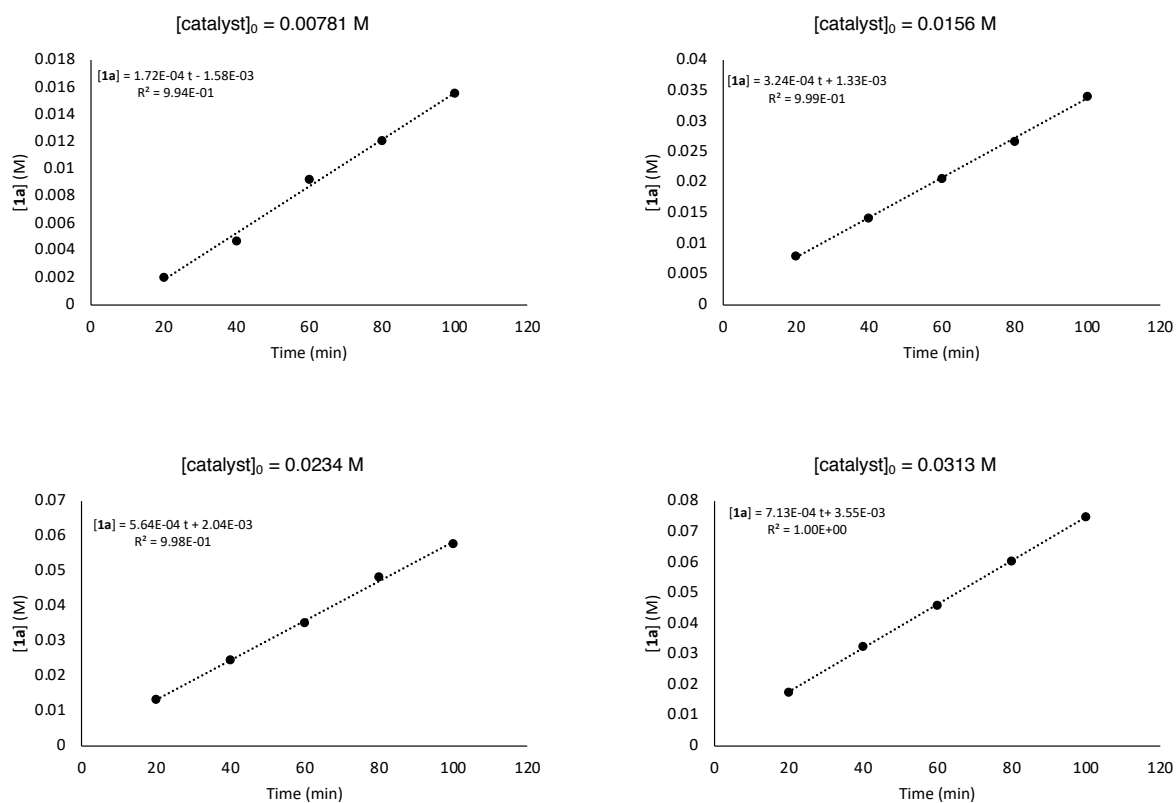
Figure 2.22. Formation of borylated product **1a** *vs* time varying loading of catalyst.
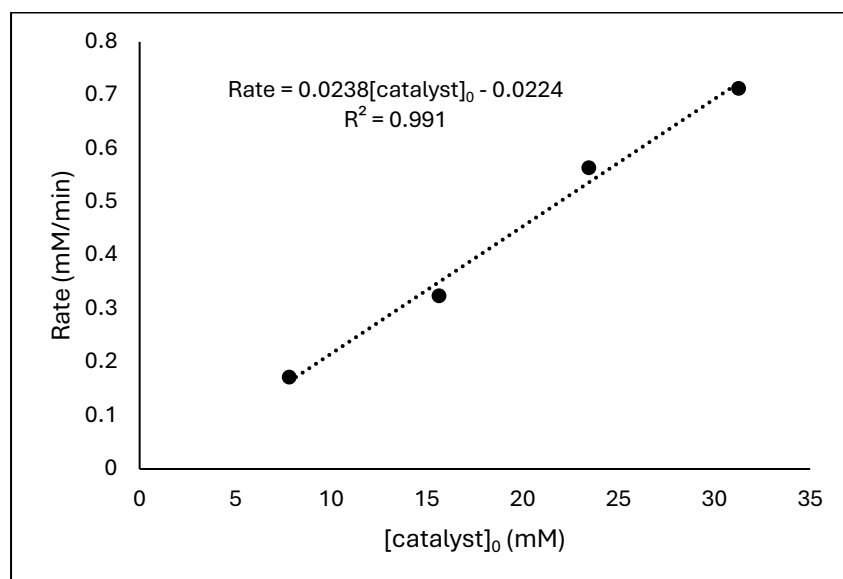
Figure 2.23. Plot of the initial rate of the formation of **1a** varying the initial concentration of catalyst. Reproduced in Figure 2.6c.

Order in B$_2$pin$_2$.

In a nitrogen glovebox, B$_2$pin$_2$ (254 mg, 1.00 mmol) was dissolved in dry THF in a 2.0 mL volumetric flask. The resulting solution was dispensed into four 1-dram vials equipped with flea stir bars, (188 µL, 0.0938 mmol; 375 µL, 0.188 mmol; 563 µL, 0.281 mmol; 750 µL, 0.375 mmol; respectively). In a 1.0 mL volumetric flask, 4-*tert*-butylphenylbicyclopentane (**1b**) (125 mg, 0.625 mmol) and adamantane (42.6 mg, 0.313 mmol) were dissolved in dry THF. The solution was dispensed into the four 1-dram vials (200 µL, 0.125 mmol of **1b**, 0.0625 mmol of adamantane). In a 1-dram vial tmphen (11.8 mg, 0.0500 mmol), (mesitylene)Ir(Bpin)$_3$ (34.7 mg, 0.0500 mmol), and B$_2$pin$_2$ (12.7 mg, 0.0500 mmol) were dissolved in 1.00 mL dry THF. The vial was tightly sealed with a Teflon-lined cap and removed from the glovebox. The vial was heated in an aluminum heating block at 100 ºC for 5 min, resulting in a homogenous, deep red-brown solution. The vial was cooled to room temperature and returned to the glovebox. The solution was dispensed into the four 1-dram vials (125 µL, 6.25 µmmol of catalyst). All volatile materials were carefully removed from the four 1-dram vials in vacuo. Then, dry cyclooctane (400 µL) was added, the vials tightly sealed with Teflon-lined caps, and the vials removed from the glovebox. The vials were heated in an aluminum heating block at 100 ºC. At the appropriate timepoints, the vials were removed from the heating block, brought into the glovebox, and an aliquot taken for gas chromatography analysis. The concentration of product **1a** was measured and plotted versus time to obtain the initial rates of the formation of **1a**.

Table 2.3. Initial concentrations of [**1b**], [catalyst], and [B$_2$pin$_2$] (varying [B$_2$pin$_2$]), and the corresponding initial rates of formation of **1a**.

[**1b**] (M)	[(tmphen)Ir(Bpin)$_3$] (mM)	[B$_2$pin$_2$] (M)	Initial Rate of Formation of **1a** (mM.min^{-1})
0.312	15.6	0.234	0.238 ± 0.012
0.312	15.6	0.469	0.240 ± 0.008
0.312	15.6	0.703	0.240 ± 0.008
0.312	15.6	0.938	0.240 ± 0.010
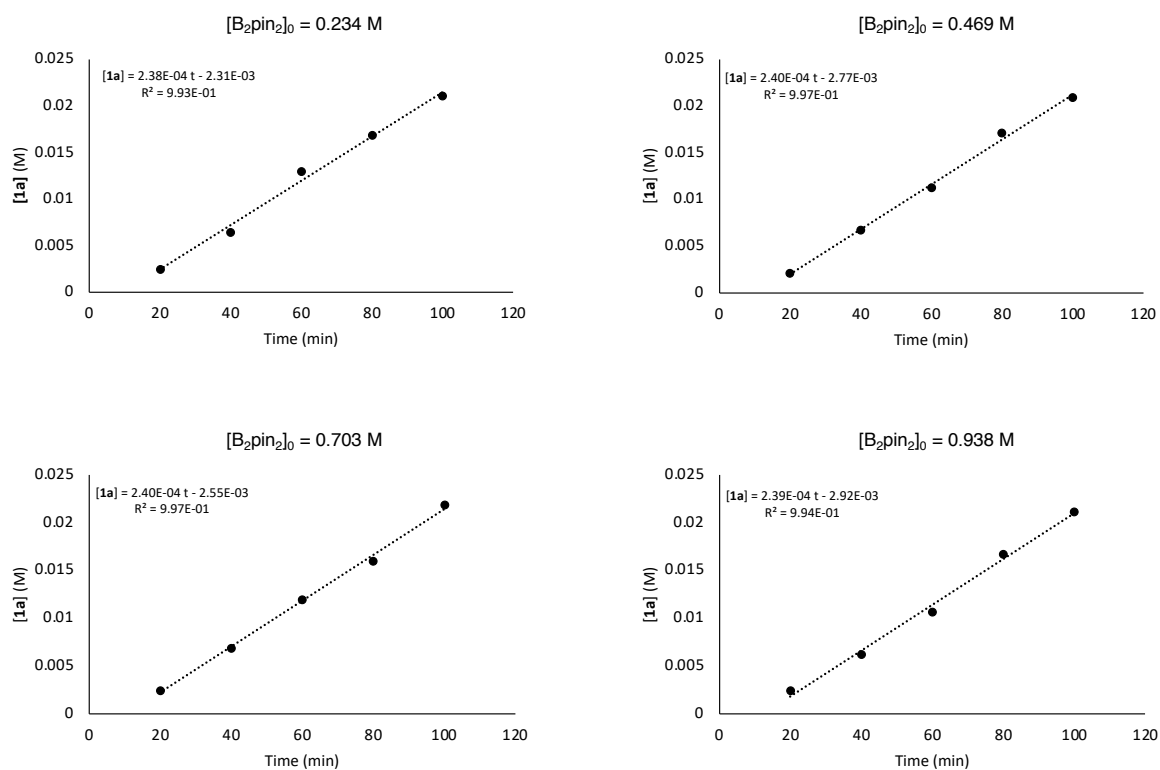
Figure 2.24. Formation of borylated product **1a** *vs* time varying the initial concentration of B_2pin_2.
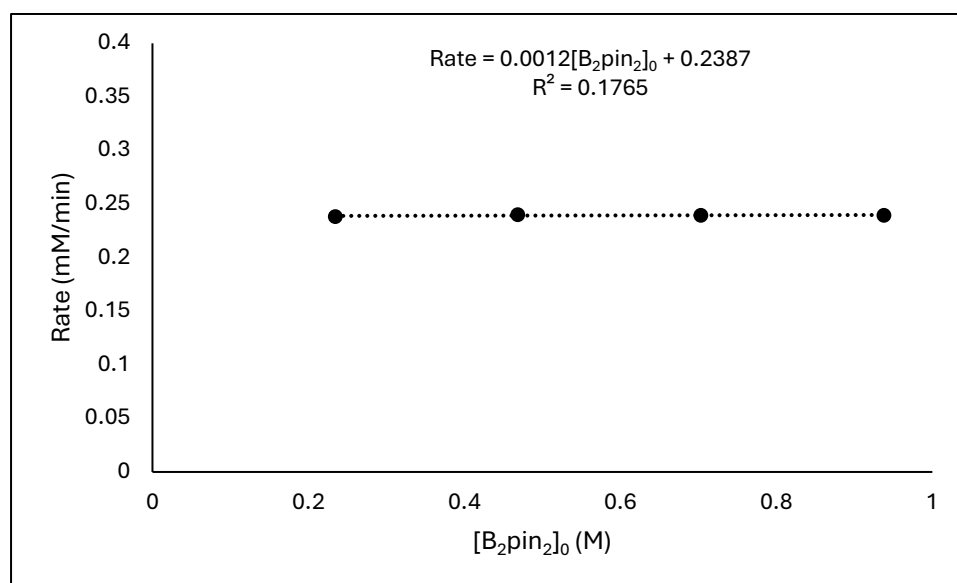
Figure 2.25. Plot of the initial rate of the formation of **1a** varying the initial concentration of B_2pin_2. Reproduced in Figure 2.6c.

2.4.8 Computational Studies

General Considerations

DFT calculations were conducted at the Molecular Graphics and Computation Facility (MGCF) at the University of California, Berkeley using the Gaussian 16 software package.[61] Initial geometries were constructed in GaussView 6 and optimized to stationary points (either minima or first-order saddle points) using the PBE0 functional (the hybrid functional based on the Perdew-Burke-Ernzerhof functional [PBE][62, 63] as described by Adamo[64]) with Grimme's D3 dispersion correction with Becke-Johnson damping (GD3-BJ)[65] and the basis sets def2-TZVP (with effective core potential) for Ir and def2-SVP for all light atoms (**BS1**). The nature of each stationary point was verified by accompanying frequency calculations (all positive eigenvalues for minima and exactly one negative eigenvalue for transition states). For each ground state and transition state, several isomeric geometries about the iridium center and conformers resulting from rotations of the boryl group about the Ir–B bond were considered. Their geometries and energies were optimized in Gaussian, and only those lowest in energy or relevant to the reaction coordinate are presented here. Connectivity of transition states to ground-state minima was established by following the intrinsic reaction coordinate (IRC). Frequencies were evaluated at 1 atm at 373.15 K (100 °C). Further single point energy (SPE) calculations were performed on the optimized geometries with the larger def2-QZVPD basis set[66] (with ECP)[67] on Ir and the def2-TZVPD basis set[66] on all light atoms (obtained through the Basis Set Exchange, accessed September 2021)[68-70] (**BS2**). The SPE calculations were performed in cyclohexane solvent using the SMD solvent continuum reported by Truhlar and co-workers.[71] In all cases, Gibbs free energies for calculations using **BS2** were approximated by summing the internal energy calculated with **BS2** and the thermal correction from the frequency calculation on the same structure with **BS1**.

Discussion of Alternate pathways

To investigate the possibility of a Ir(I)-Ir(III) cycle, the free energies of **[Ir](Bpin)**, B_2pin_2, and **[Ir](Bpin)$_3$** were calculated and compared. Formation of **[Ir](Bpin)$_3$** from **[Ir](Bpin)** and B_2pin_2 is exergonic by 50.9 kcal/mol. Thus, reactivity through Ir(I) species in the presence of large excesses of B_2pin_2 is unlikely. In contrast, the energy of **[Ir](Bpin)$_5$** is calculated to be only 3.1 kcal/mol above that of **[Ir](Bpin)$_3$** and B_2pin_2 Therefore, **[Ir](Bpin)$_5$** could be present in small quantities.

The isomerization process that we present here is analogous to that proposed for the borylation of chlorosilanes by Himo[54] and the borylation of benzylic C–H bonds by our own group.[53] The isomerization occurs through **isom-TS-[Ir](R)(H)(Bpin)$_3$,** which adopts a pentagonal-bipyramidal configuration in which the hydride is nearly coplanar with the phenanthroline ligand and two boryl groups.

Sakaki has proposed an alternative isomerization pathway prior to the reductive elimination to form the C–B bond during the borylation of tetrahydrofuran.[52] This process involves the repositioning of the two boryl groups that are located below the phenanthroline plane. We were unable to find a transition state structure for such a potential isomerization mechanism for the Ir(V)-bicyclopentyl complex. When we performed IRC calculations and fully followed **RE-**

TS-[Ir](Bpin)₃(R)(H) along its path to revert to the starting materials during an optimization calculation, we found that the structure of one of the steps resembled the transition state for isomerization reported by Sakaki. (See center structure in Figure 2.27) Therefore, it appears that reductive elimination from the bicyclopentyl complex occurs in a continuous manner with no discrete transition state for isomerization during this process.
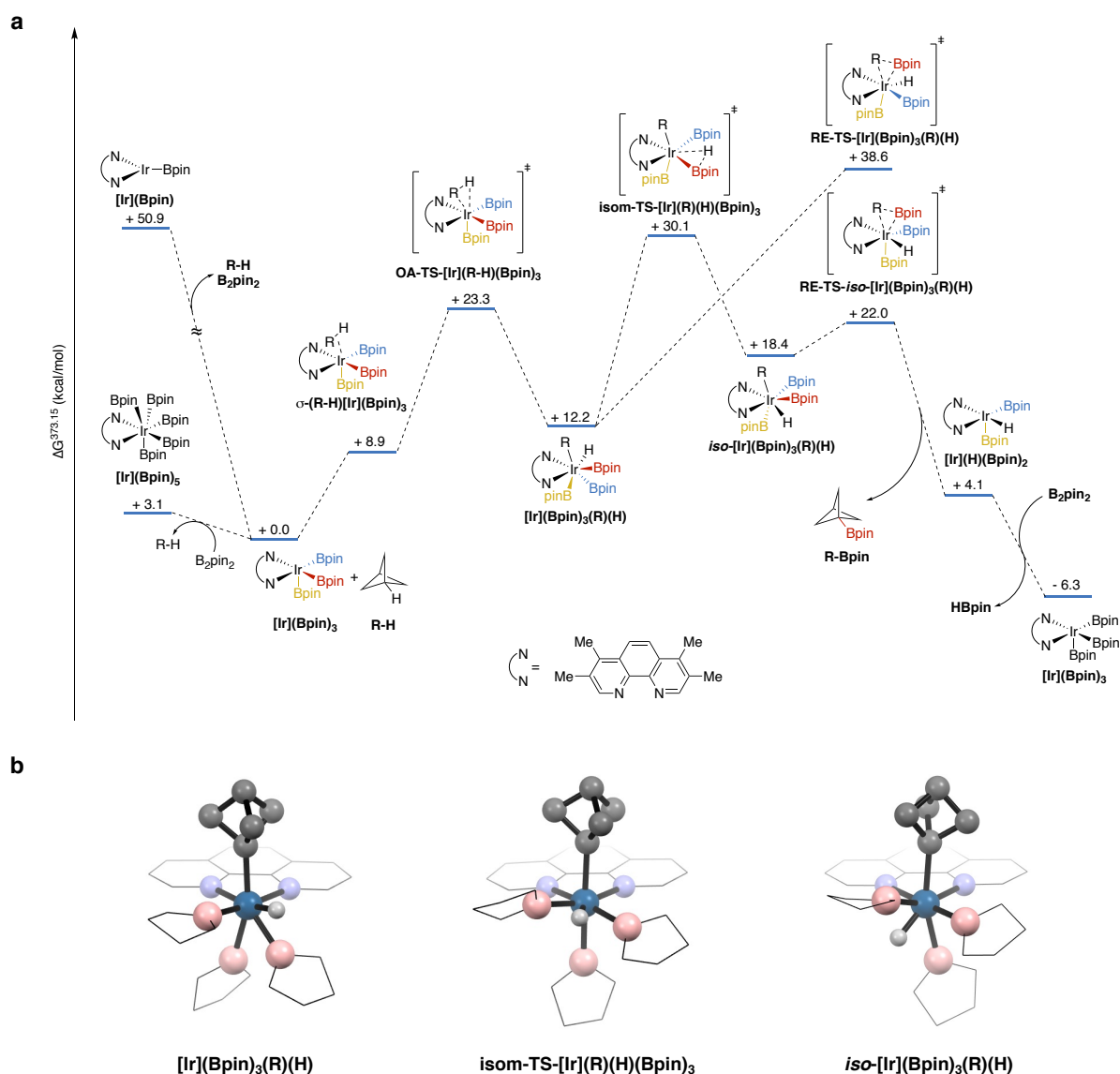
Figure 2.26. Energy Diagram obtained via DFT calculations. Equivalent to Figure 2.7.
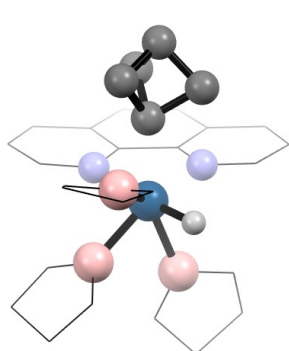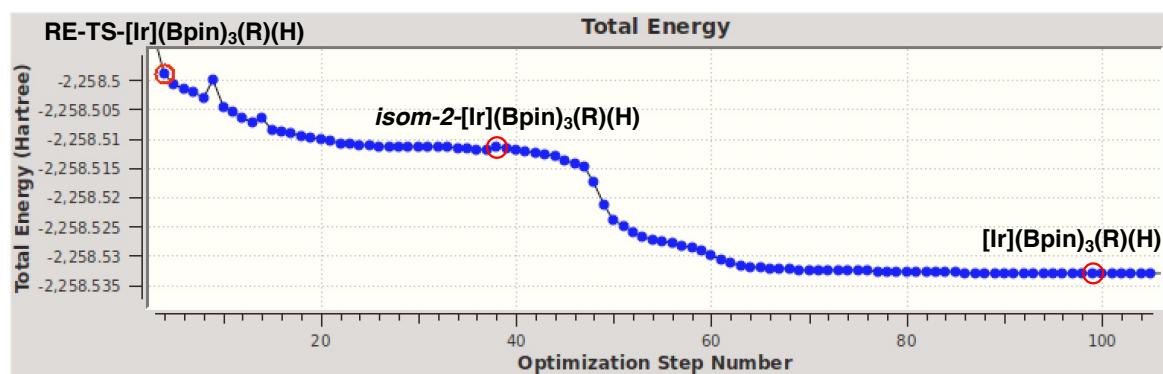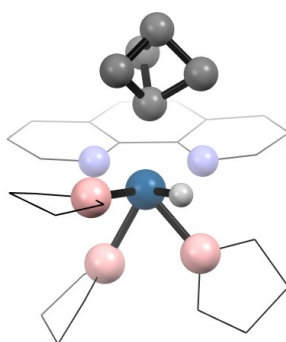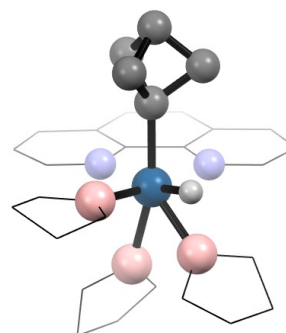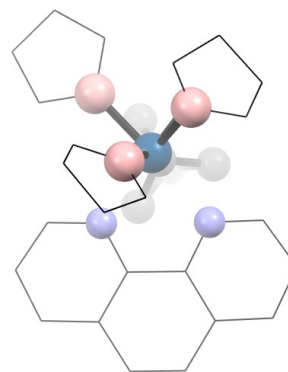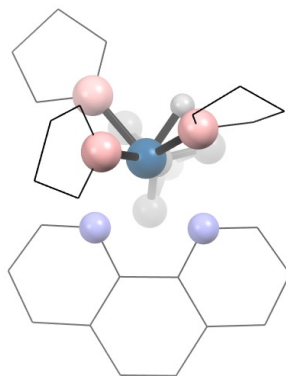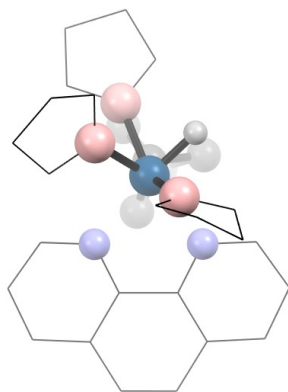
Figure 2.27. Plot of energy *versus* step number for the structure changes along the reaction coordinate from RE-TS-[Ir](Bpin)₃(R)(H) to [Ir](Bpin)₃(R)(H) and selected structures.

200

Calculated KIE value

Zero-point energies (ZPEs) were calculated assuming harmonic potentials for bicyclo-[1.1.1]-pentane, bicyclo-[1.1.1]-pentane-d_1, Isom-TS-[Ir](R)(H)(Bpin)$_3$, and Isom-TS-[Ir](R)(H)(Bpin)$_3$-d_1. The KIE value was obtained by applying the Eyring equation to the differences in ZPEs.

Species	ZPE-H (Hartree)	ZPE-D (Hartree)	ZPE-diff (Hartree)	ZPE-diff (kcal/mol)
bicyclopentane	0.117665	0.114414	0.003251	2.040
Isom-TS-[Ir](R)(H)(Bpin)$_3$	0.947681	0.945266	0.002415	1.515

KIE = exp((2.040-1.154)/0.741529) = 2.03

2.4.9 NMR spectra

Sodium bicyclo[1.1.1]pentanesulfinate [Experimental]

^{1}H NMR (600 MHz, D$_2$O)

7.26 CDCl3
3.40 MeOH
2.76
1.96

1.00
6.31

f1 (ppm)

^{13}C NMR (151 MHz, D$_2$O)

77.16 CDCl3
69.52 MeOH
57.42
47.38
37.63
26.01 MeOH

f1 (ppm)

2-methylphenanthroline

[Experimental]

¹H NMR (300 MHz, CDCl₃)

¹³C NMR (126 MHz, CDCl₃)

203
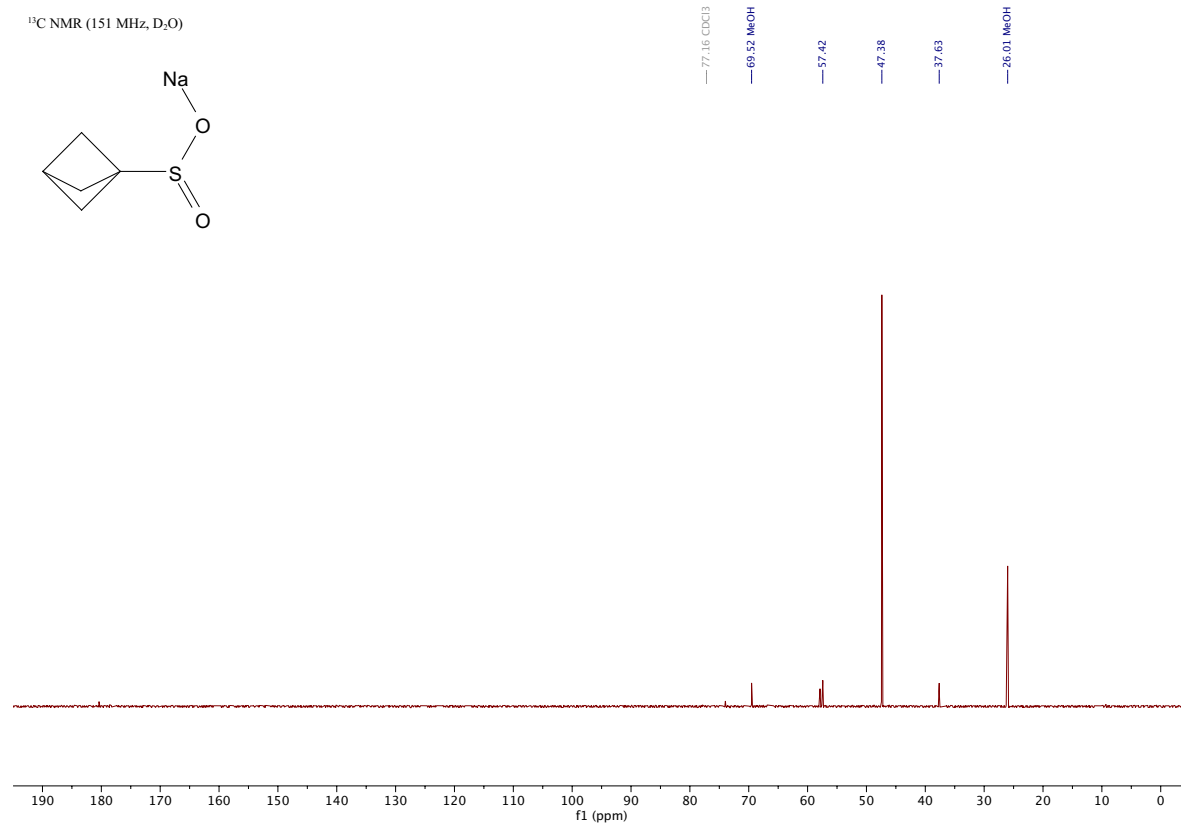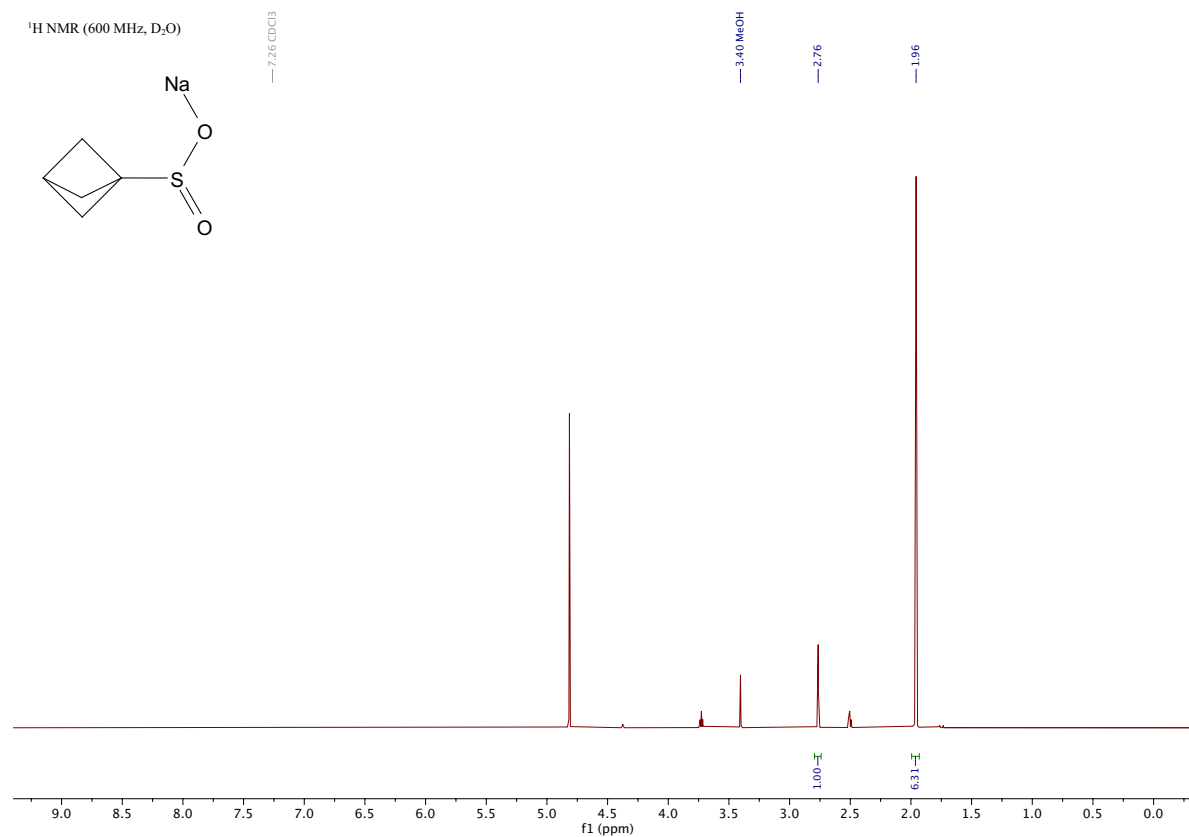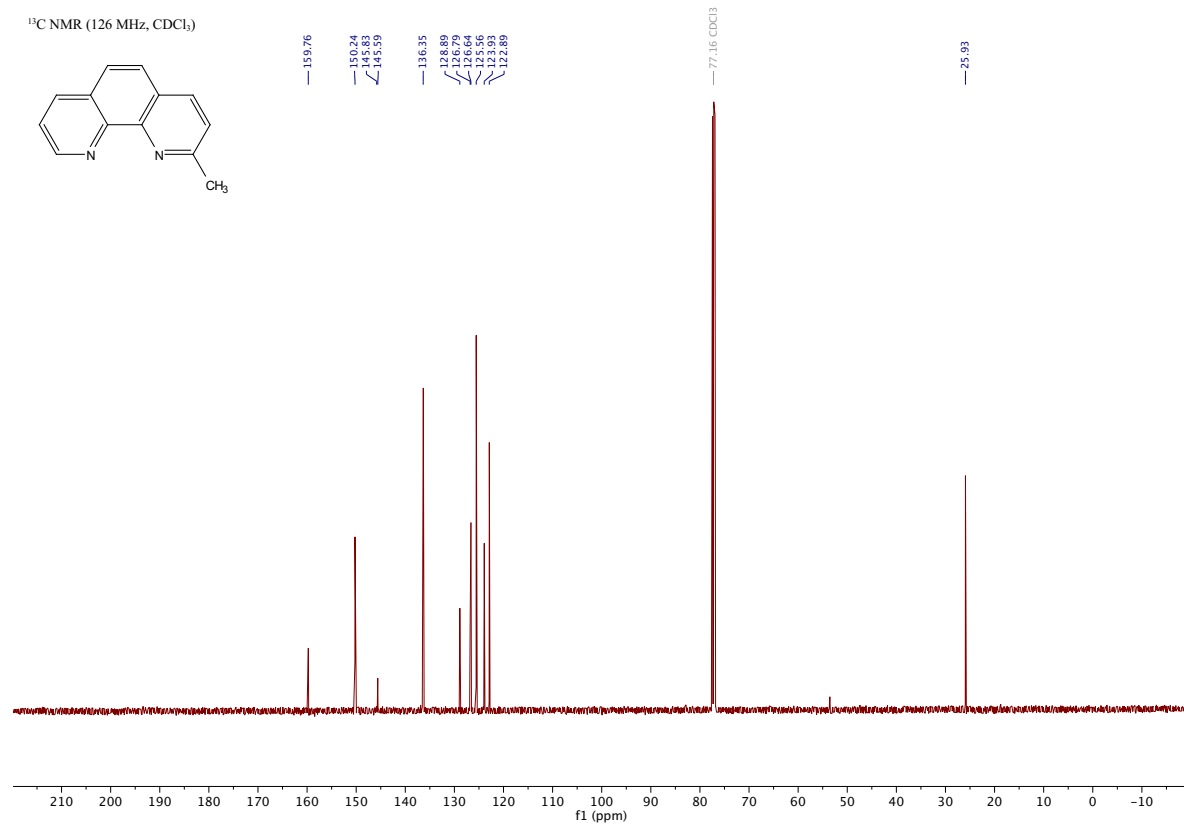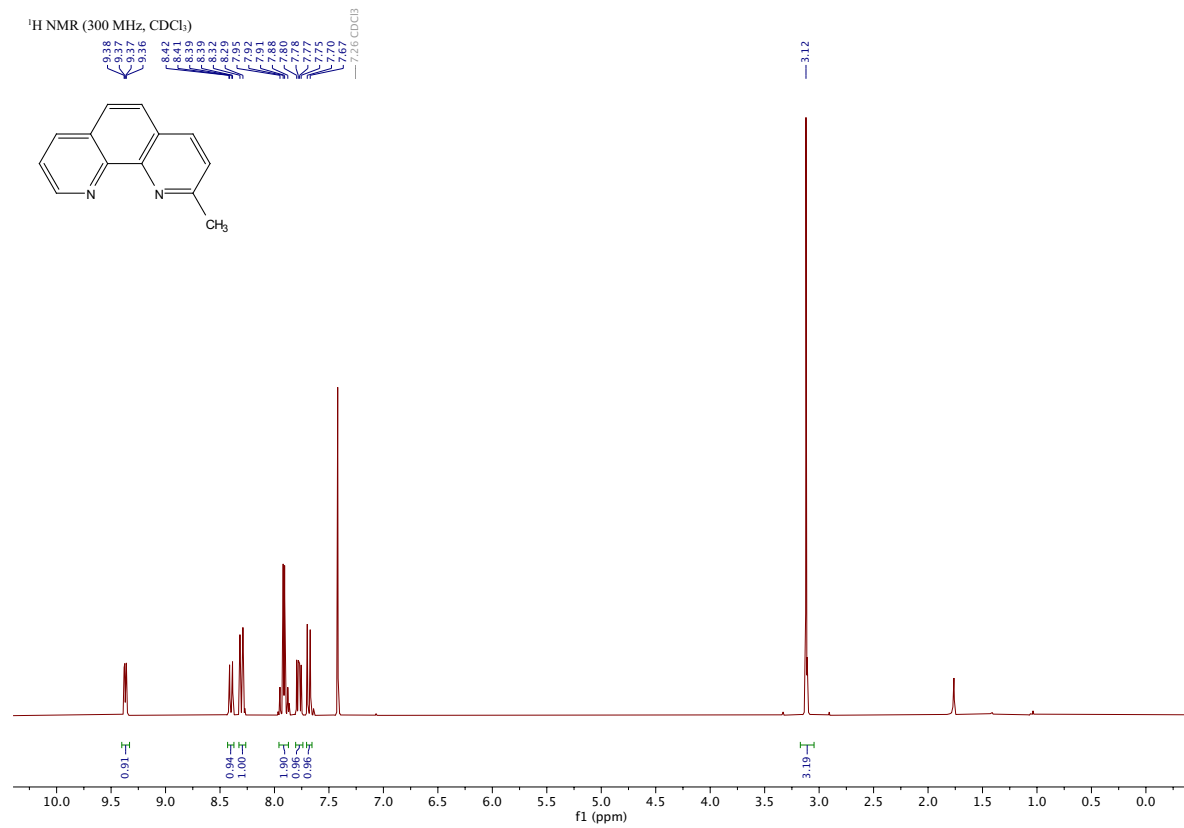
L3

2,2'-((3-fluorophenyl)methylene)dipyridine [Experimental]

¹H NMR (600 MHz, CDCl₃)

¹³C NMR (151 MHz, CDCl₃)

163.87
162.24
161.64
149.68
144.39
144.34
136.77
130.05
129.99
125.19
125.17
124.14
121.92
116.53
116.38
113.92
113.78
61.48

200 190 180 170 160 150 140 130 120 110 100 90 80 70 60 50 40 30 20 10 0
f1 (ppm)

¹⁹F NMR (565 MHz, CDCl₃) δ -112.97 (q, *J* = 8.7 Hz).

-112.95
-112.97
-112.98
-112.99

0 -5 -10 -15 -20 -25 -30 -35 -40 -45 -50 -55 -60 -65 -70 -75 -80 -85 -90 -95 -100 -105 -110 -115 -120 -125 -130 -135 -140
f1 (ppm)
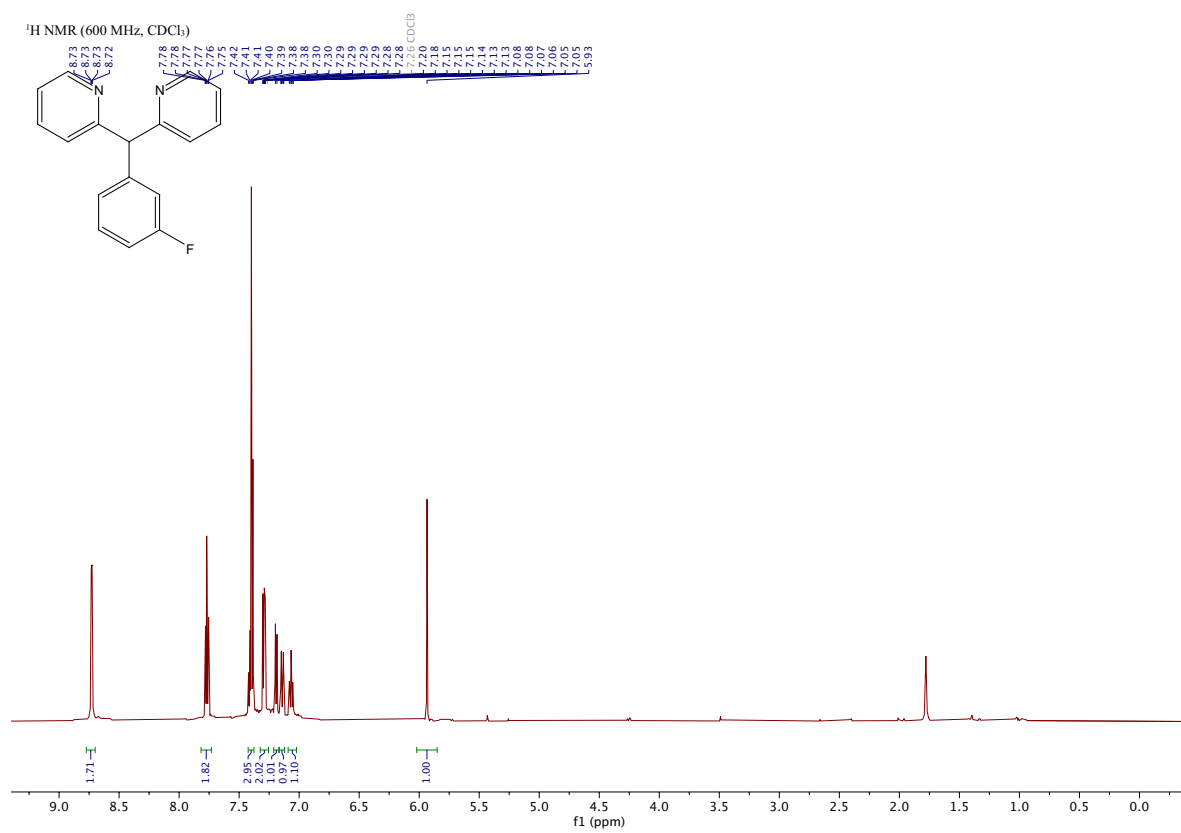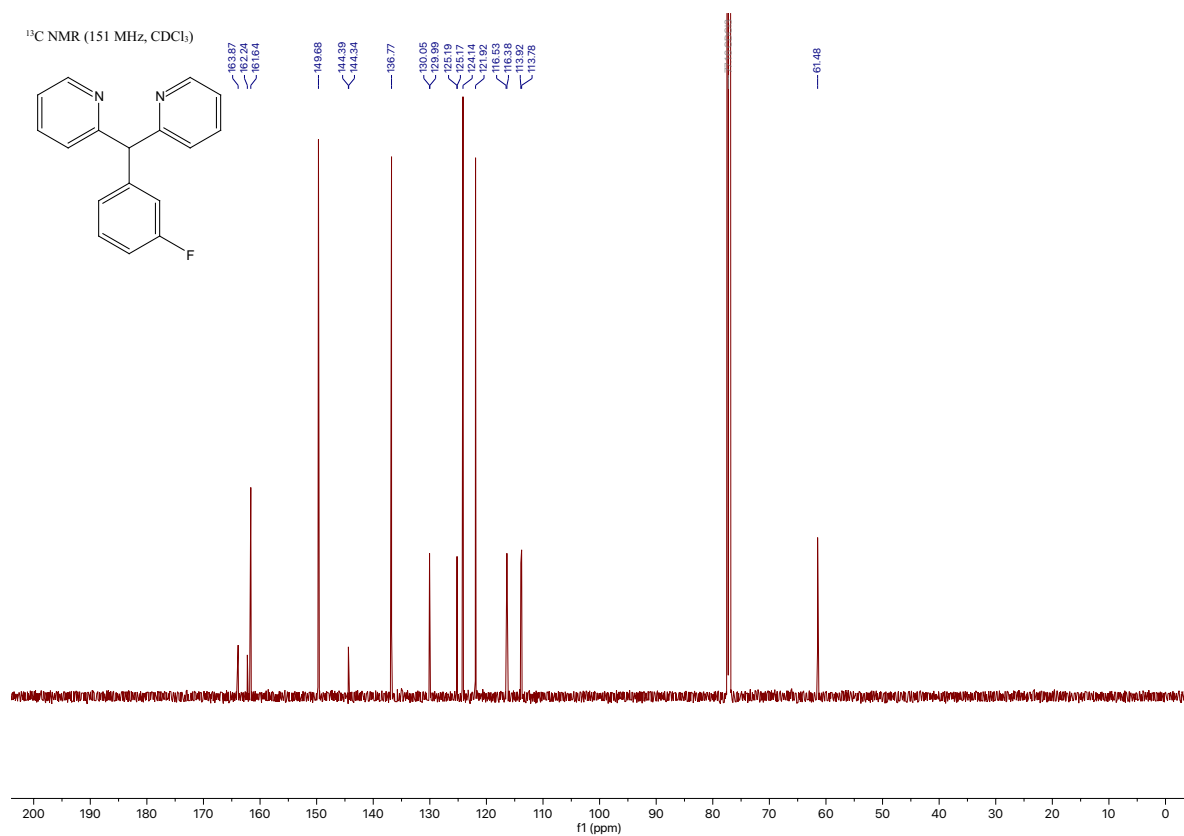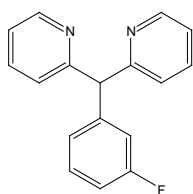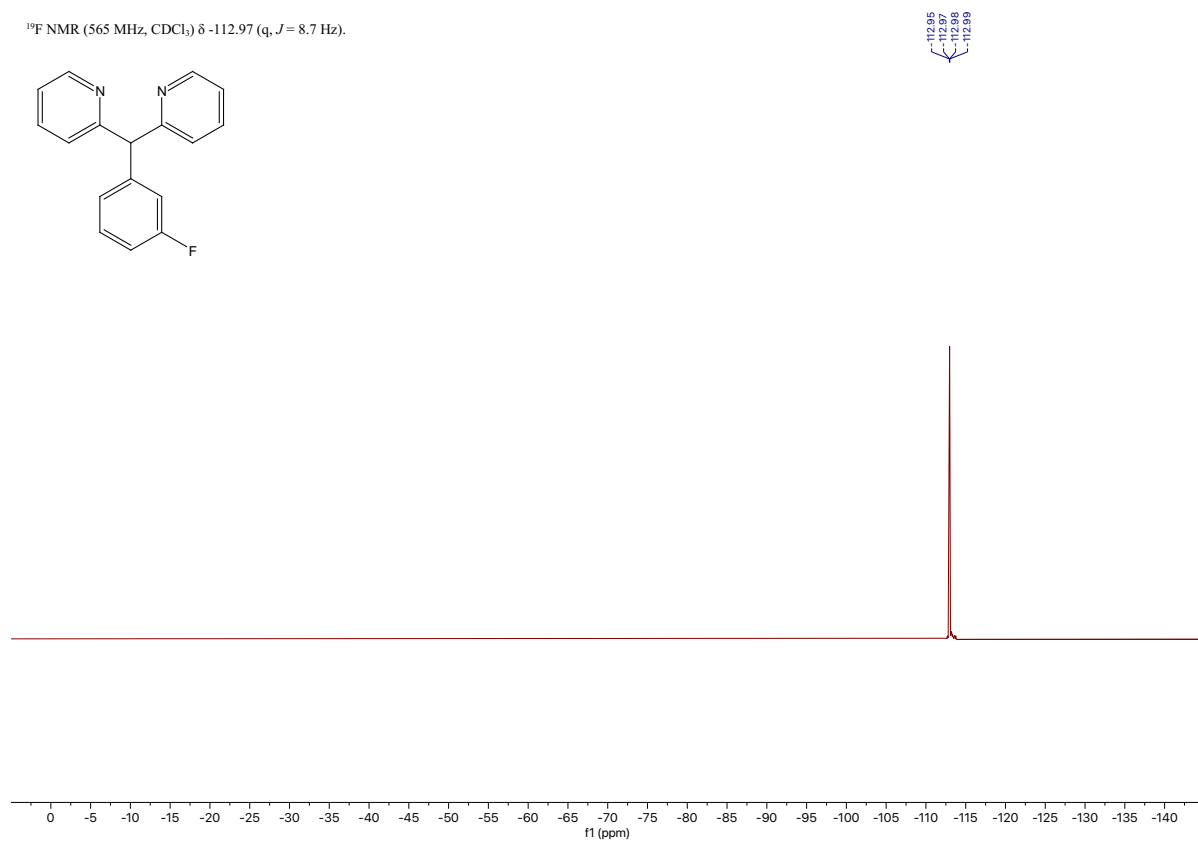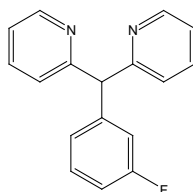
L4

5-methyl-2-(thiophen-3-yl)pyridine [Experimental]

¹H NMR (600 MHz, CDCl₃)

¹³C NMR (151 MHz, CDCl₃)
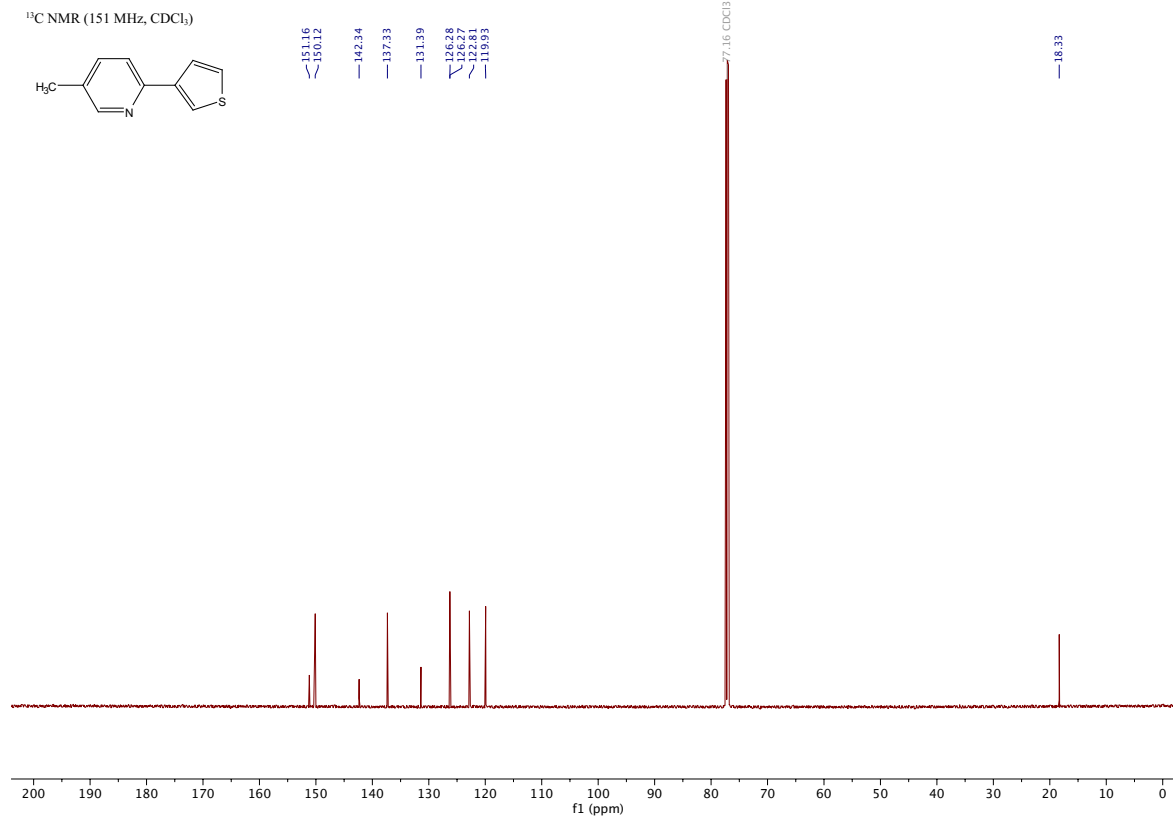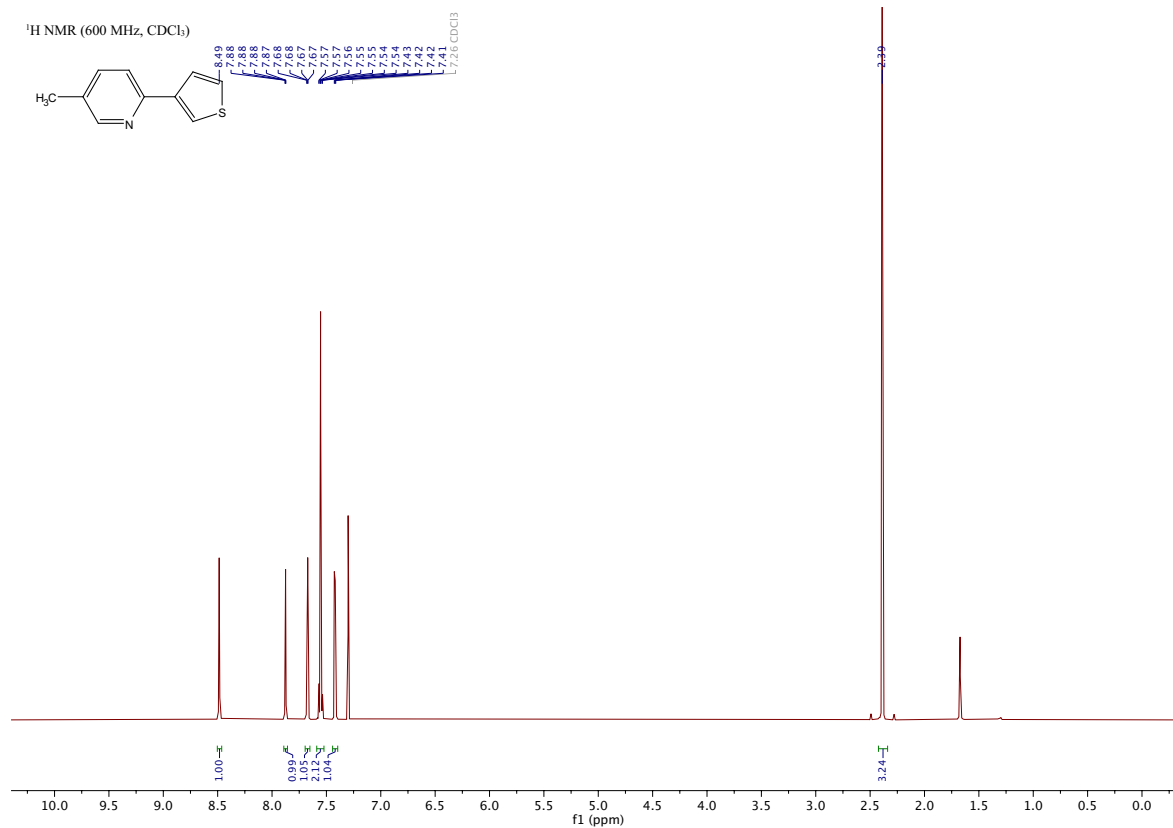
Compound 1b

1-(4-(*tert*-butyl)phenyl)bicyclo[1.1.1]pentane [Experimental]

^{1}H NMR (500 MHz, CDCl$_3$)

^{13}C NMR (126 MHz, CDCl$_3$)
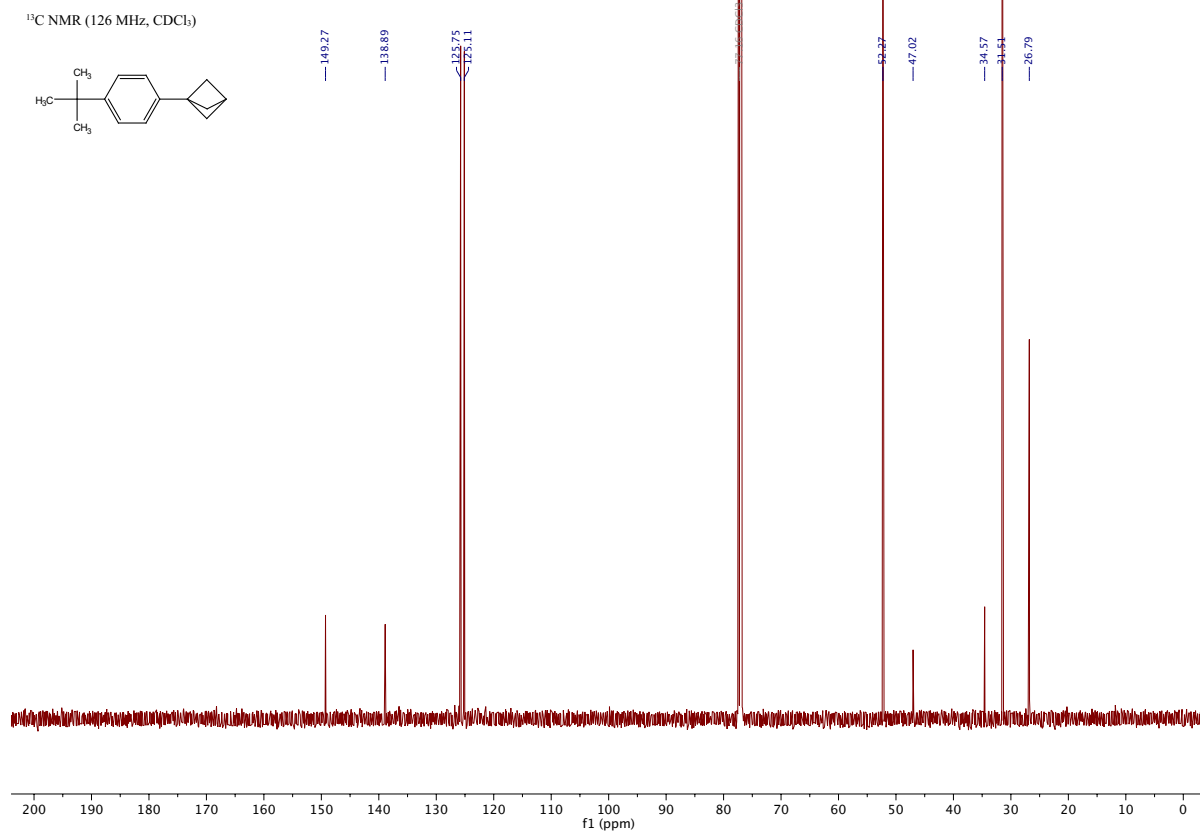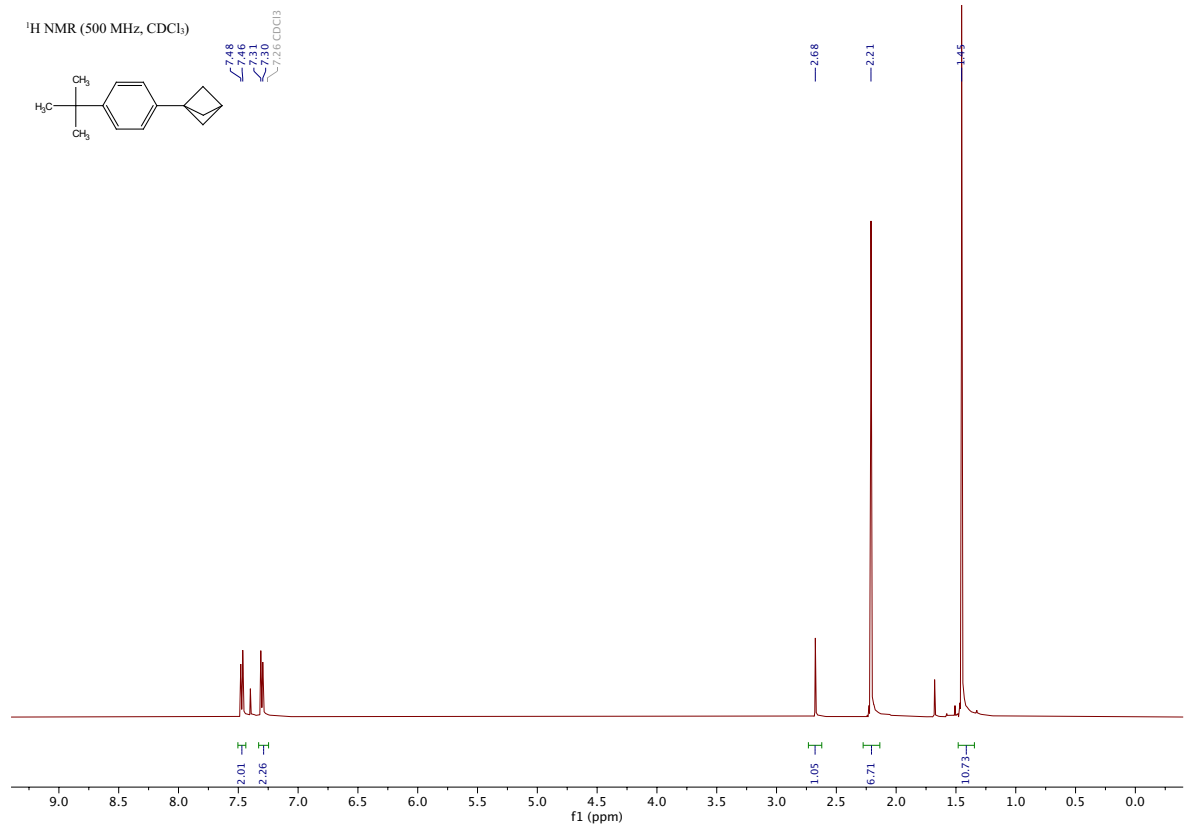
Compound 2b

1-(3,5-di-*tert*-butylphenyl)bicyclo[1.1.1]pentane [Experimental]
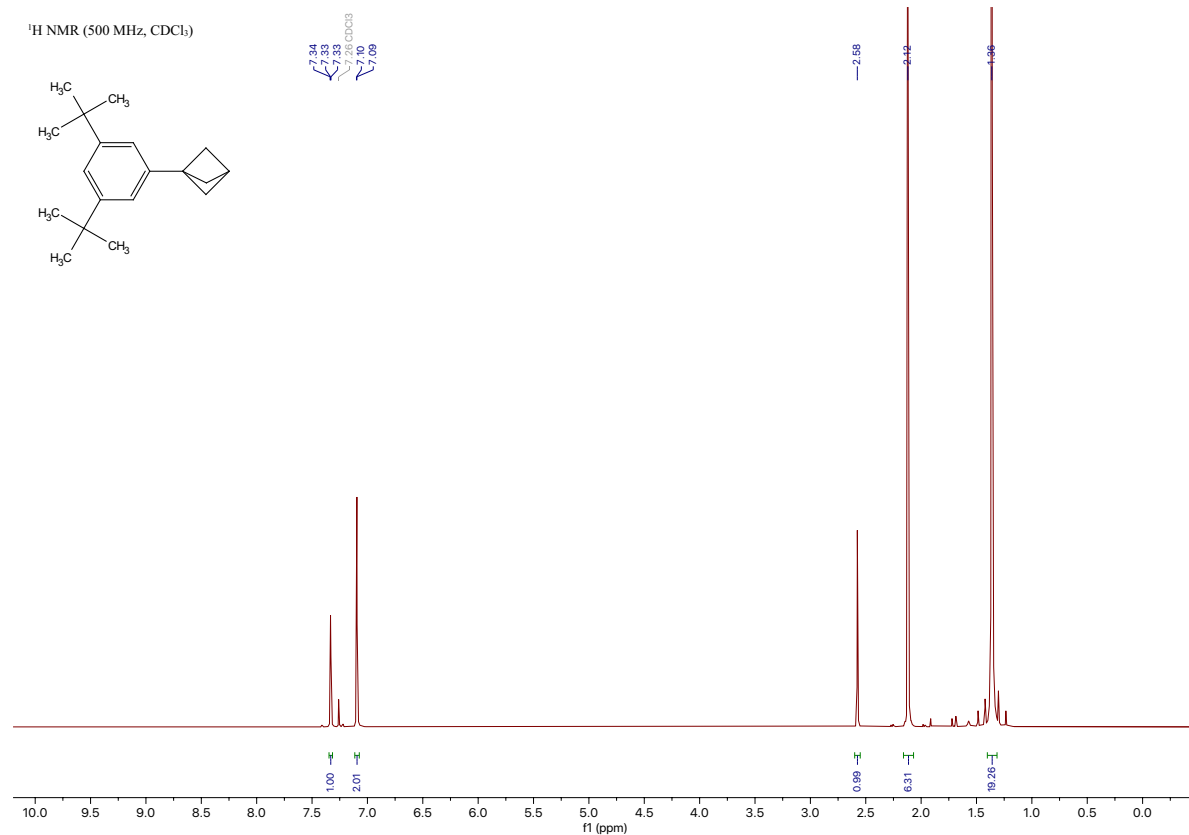
¹H NMR (500 MHz, CDCl₃)

¹³C NMR (126 MHz, CDCl₃)
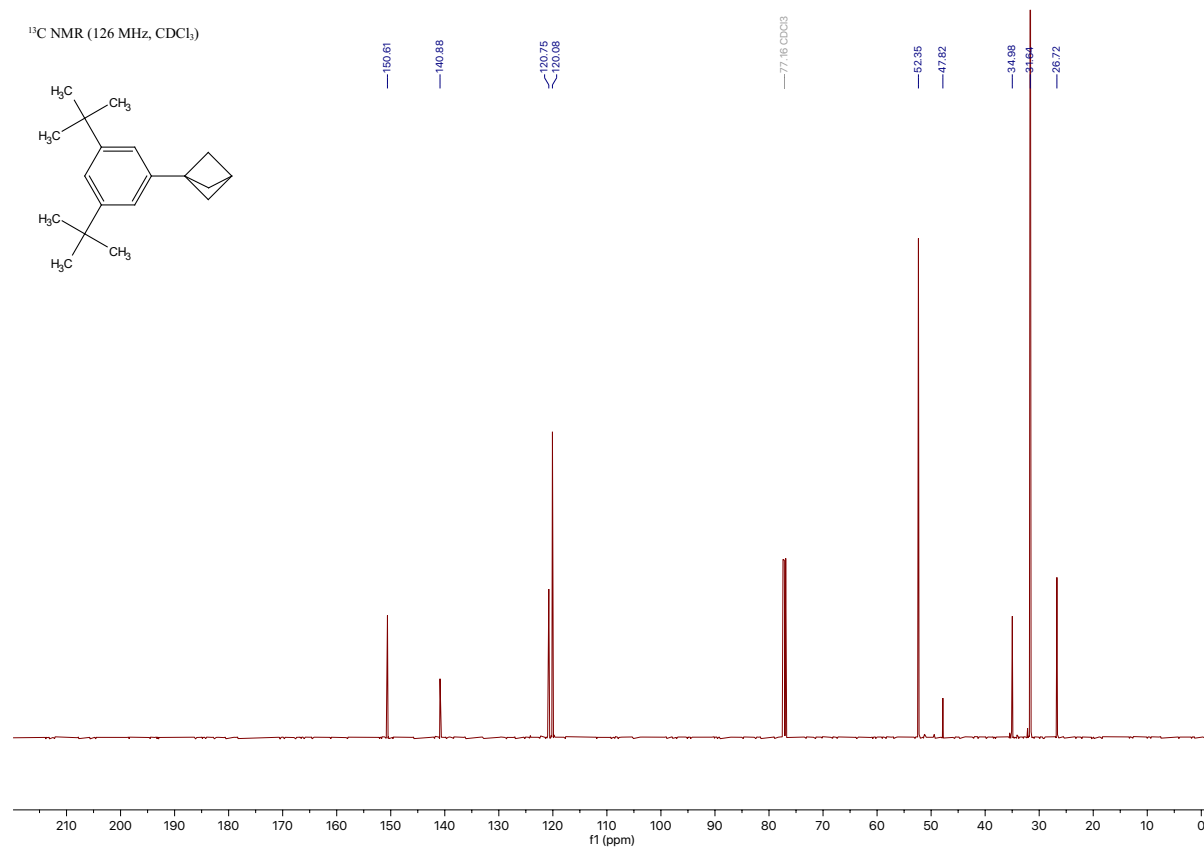
Compound 3b

bicyclo[1.1.1]pentan-1-yl(*tert*-butyl)sulfane [Experimental]

¹H NMR (500 MHz, CDCl₃)

¹³C NMR (126 MHz, CDCl₃)
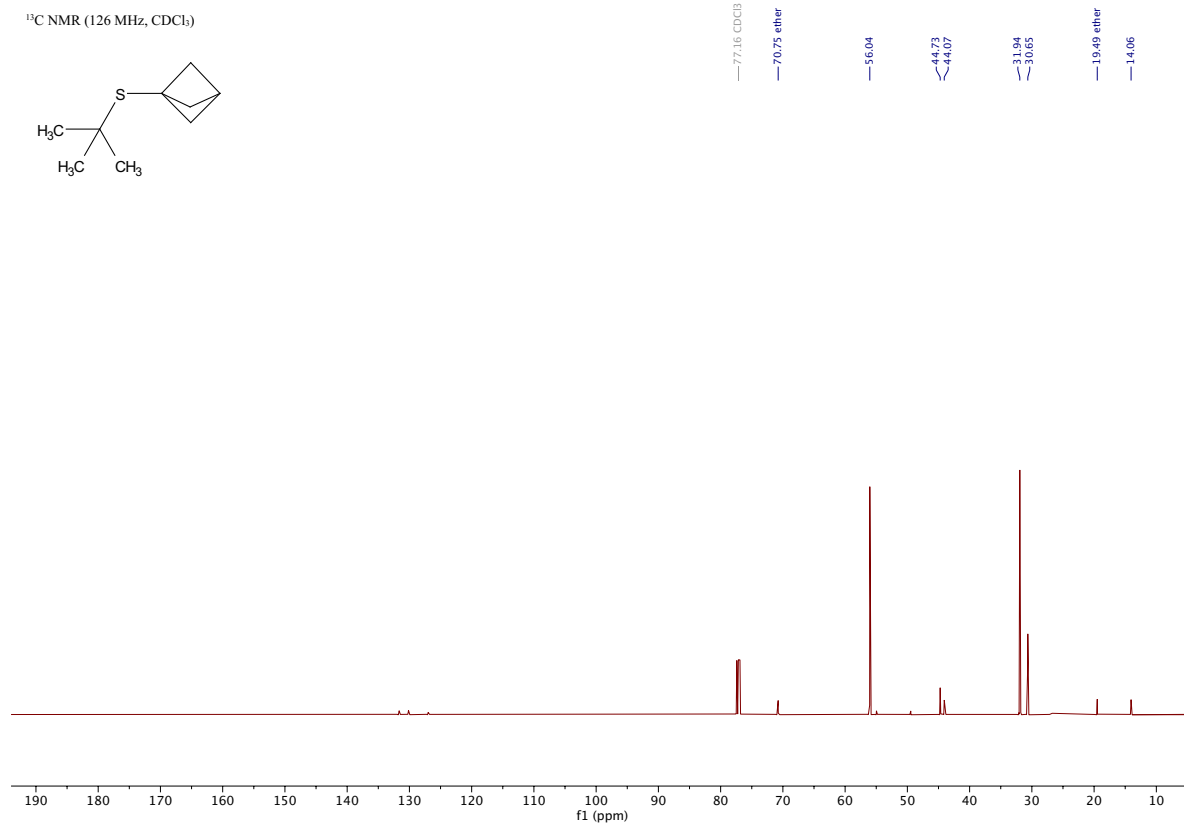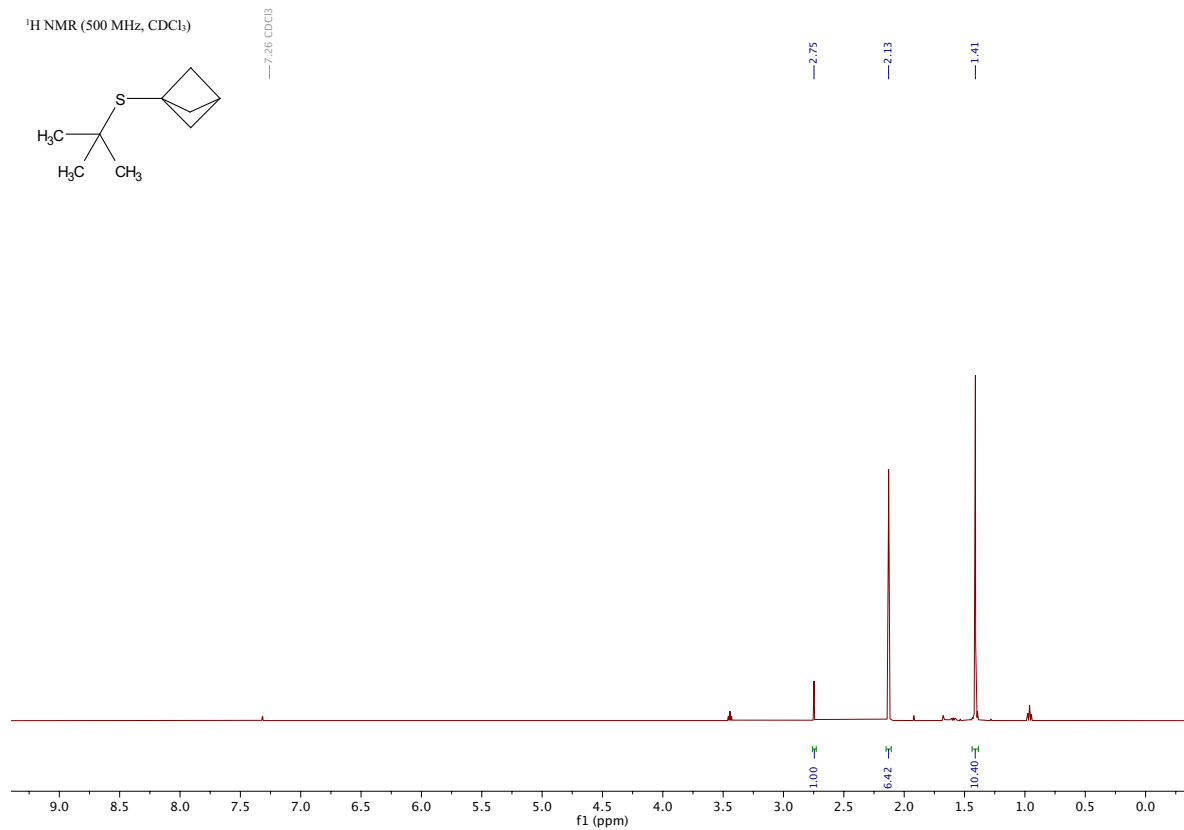
Compound 4b

bicyclo[1.1.1]pentan-1-yltributylstannane [Experimental]

¹H NMR (500 MHz, CDCl₃)

7.26 CDCl3
2.92
2.01
1.57
1.55
1.54
1.53
1.52
1.51
1.51
1.50
1.49
1.37
1.35
1.34
1.32
1.31
1.29
0.95
0.93
0.92
0.86
0.84
0.82

0.99
6.00
6.23
6.21
9.55
5.98

¹³C NMR (126 MHz, CDCl₃)

77.16 CDCl3
56.19
39.70
39.68
39.22
38.77
38.75
37.18
29.47
29.39
29.31
27.72
27.52
27.32
13.87
10.23
10.17
8.98
7.78
7.73

210
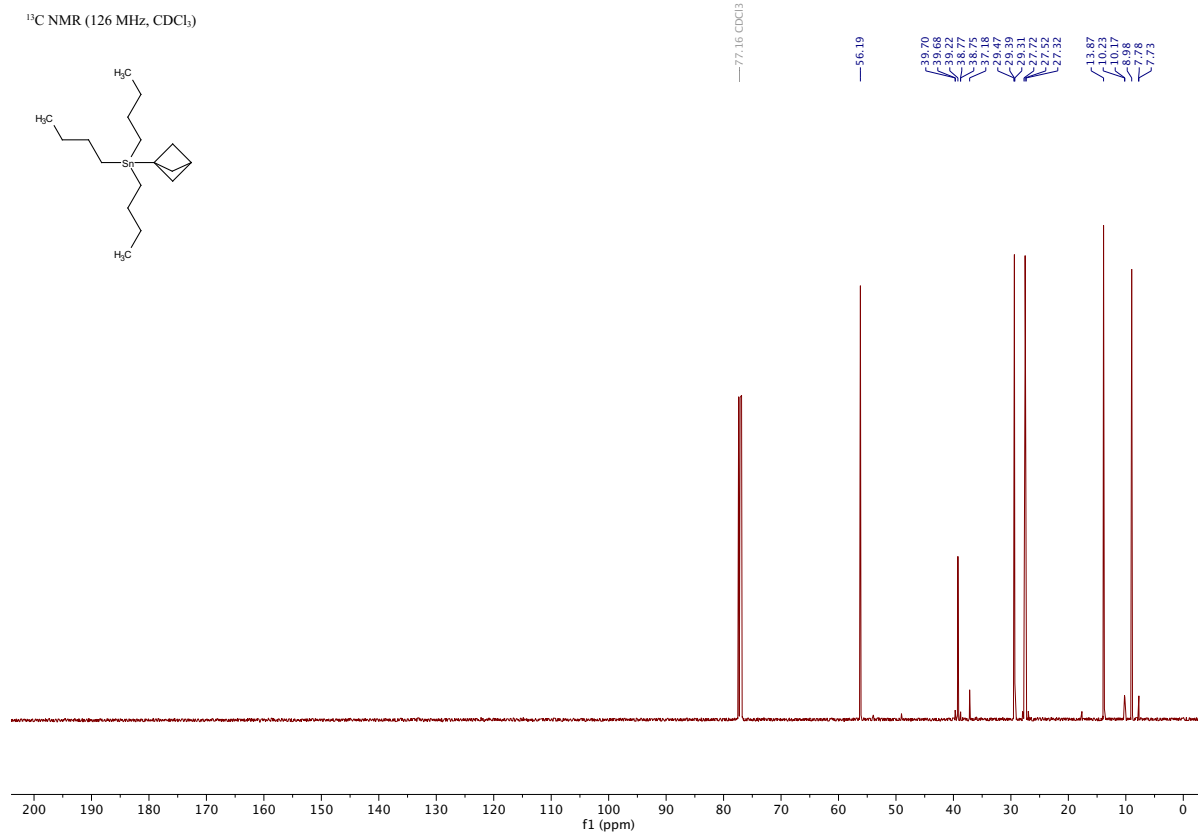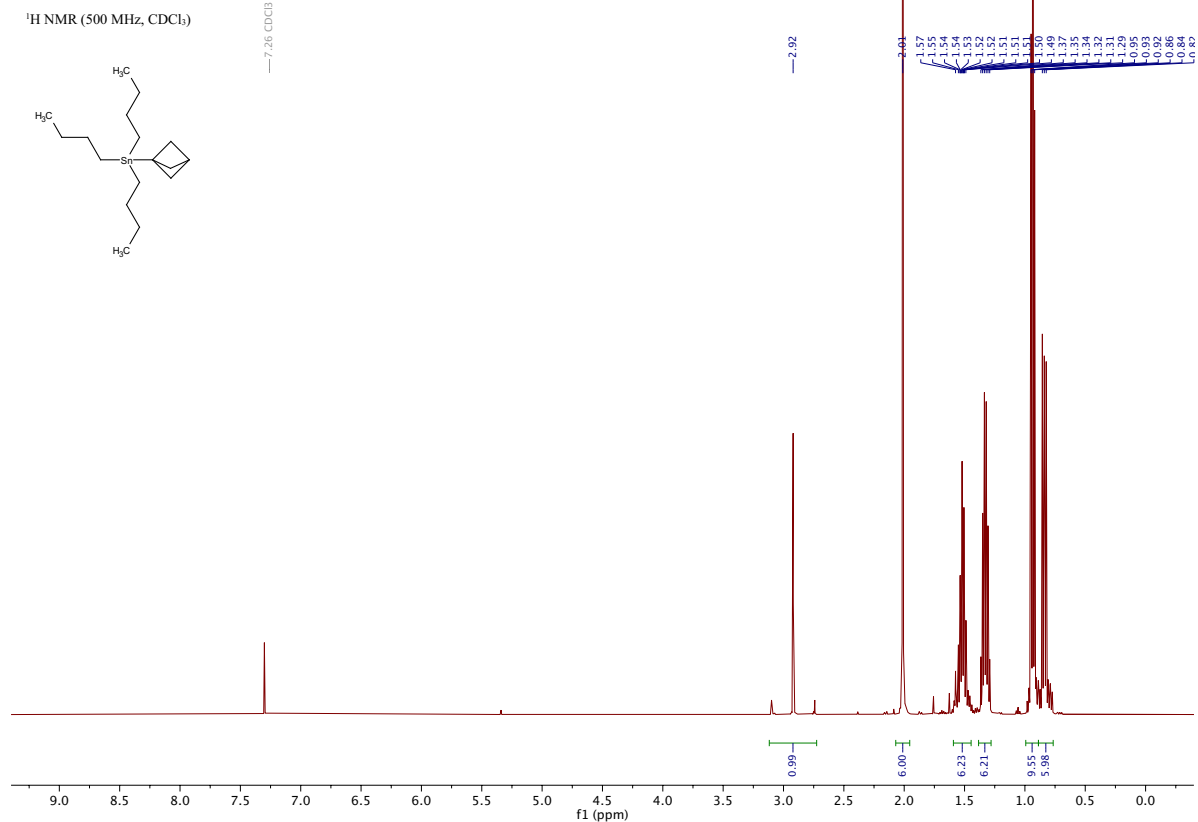
Compound 11b

1-(methylsulfonyl)bicyclo[1.1.1]pentane [Experimental]
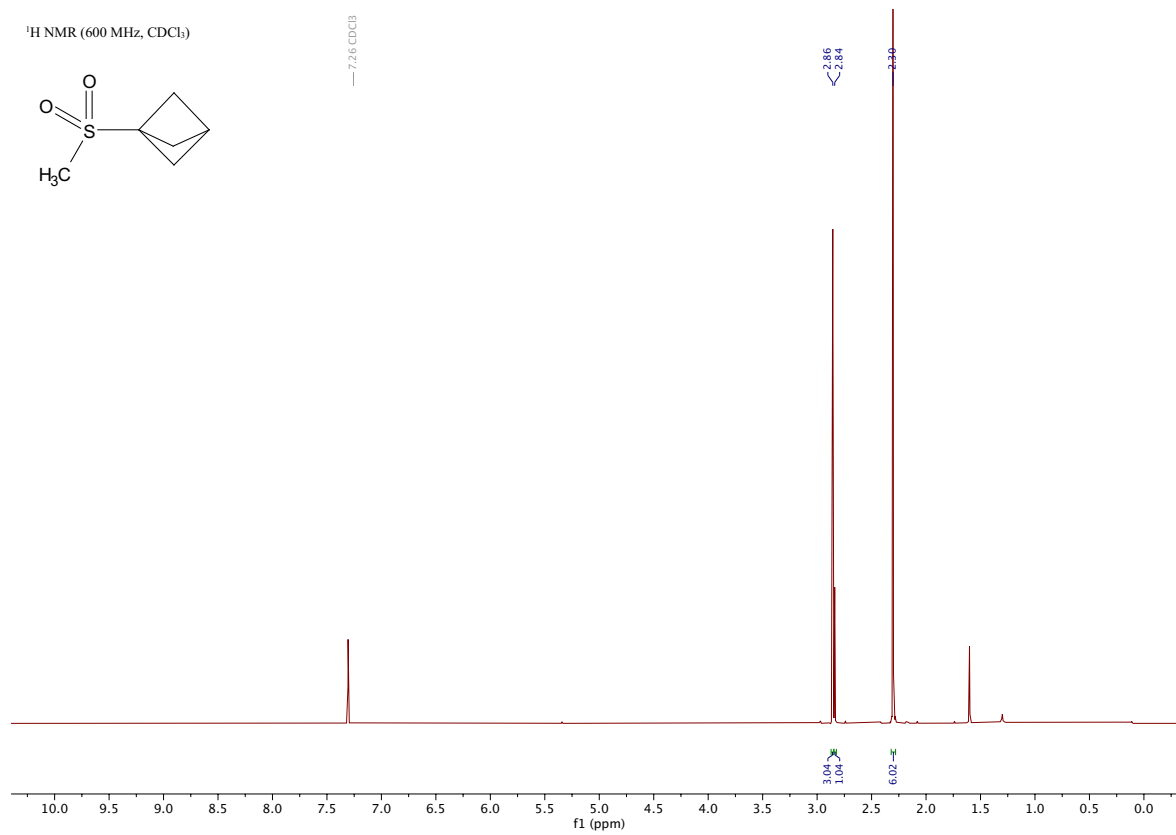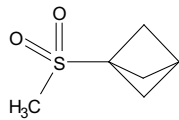
¹H NMR (600 MHz, CDCl₃)

¹³C NMR (151 MHz, CDCl₃)
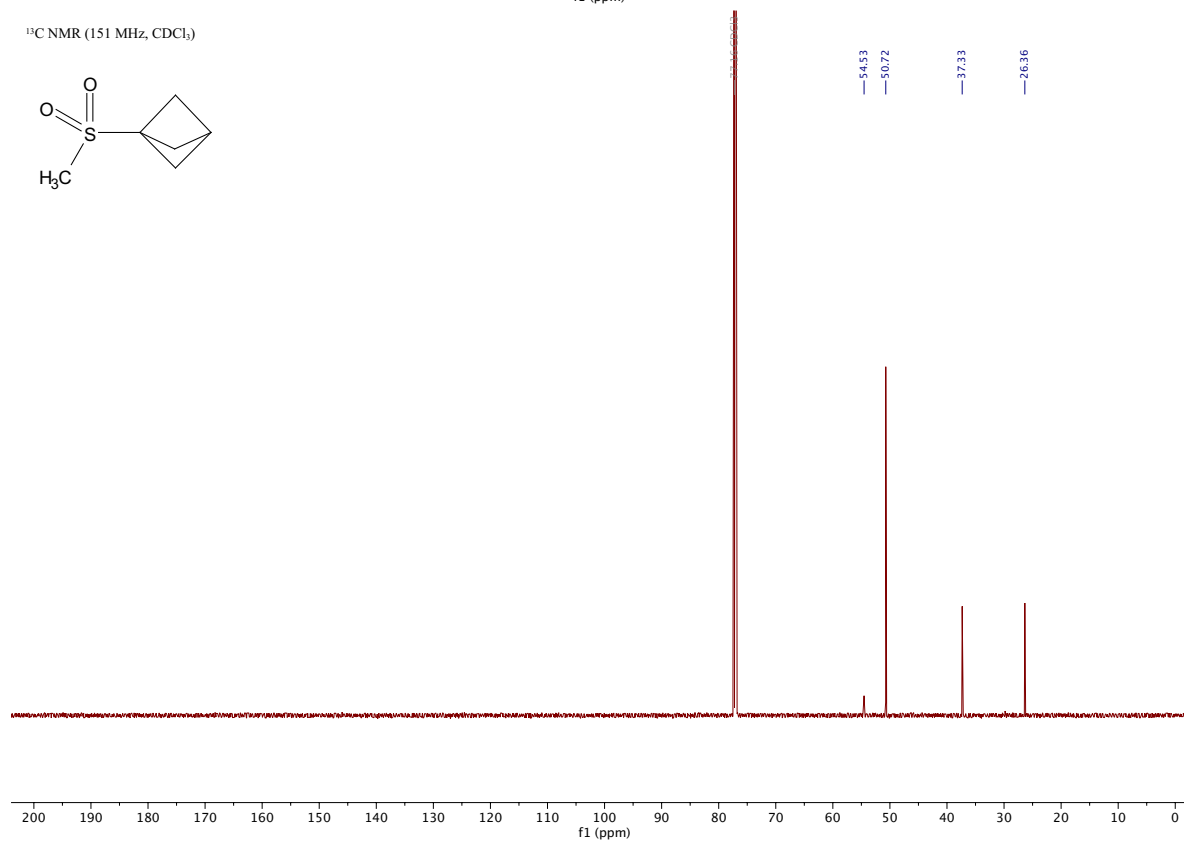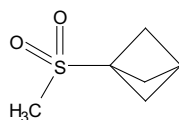
Compound 12b

bicyclo[1.1.1]pentane-1-sulfonamide [Experimental]

¹H NMR (700 MHz, Acetone)

— 7.26 CDCl3
— 6.16
— 2.80
— 2.25

2.36
1.04
6.14

¹³C NMR (176 MHz, Acetone)

— 77.16 CDCl3
— 54.75
— 50.40
— 25.52
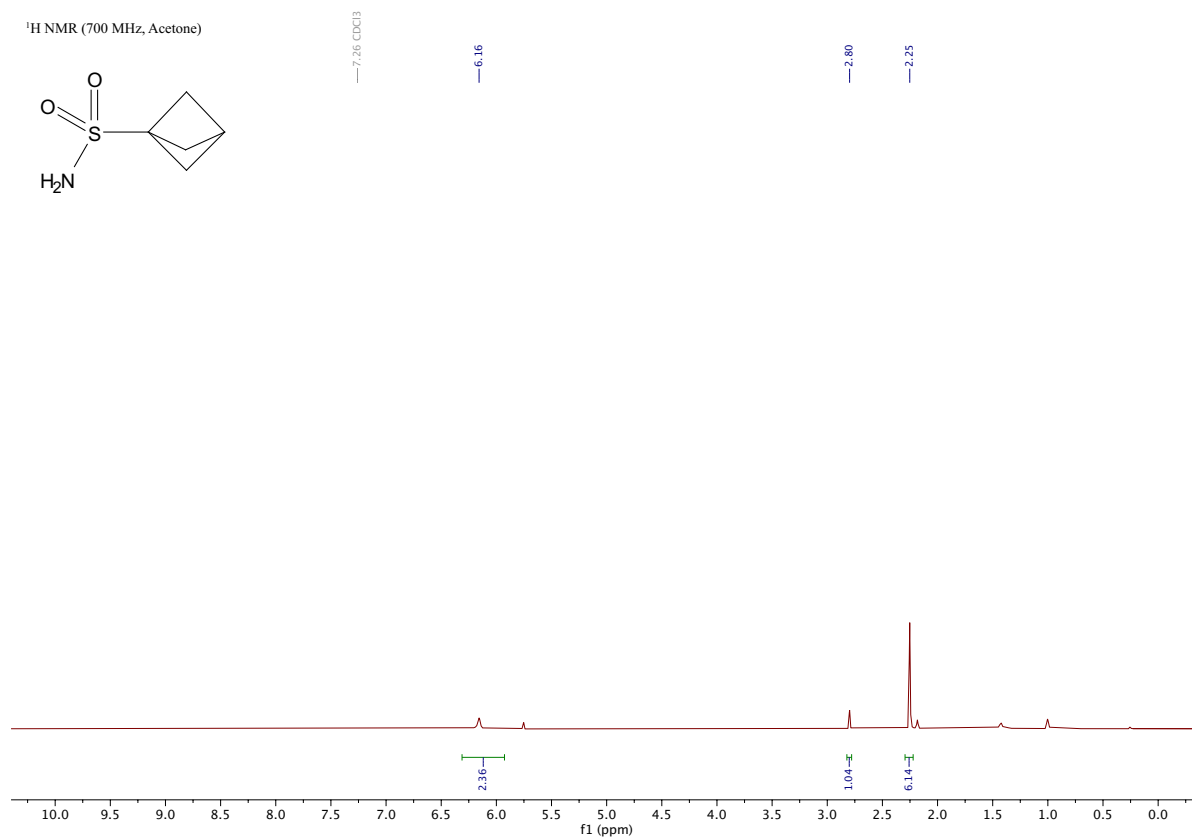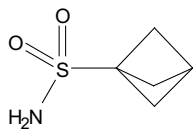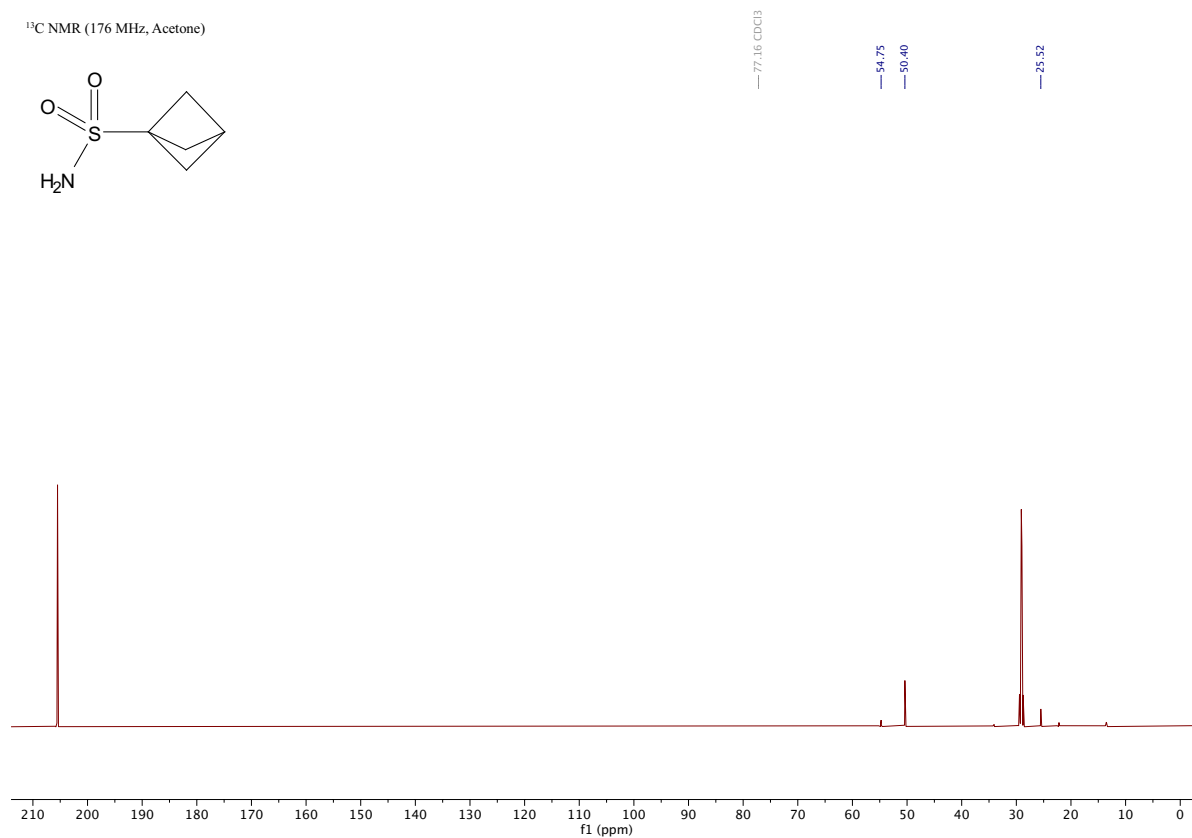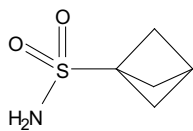
Compound 13b

1-(bicyclo[1.1.1]pentan-1-ylsulfonyl)piperidine [Experimental]

¹H NMR (500 MHz, CDCl₃)

¹³C NMR (126 MHz, CDCl₃)
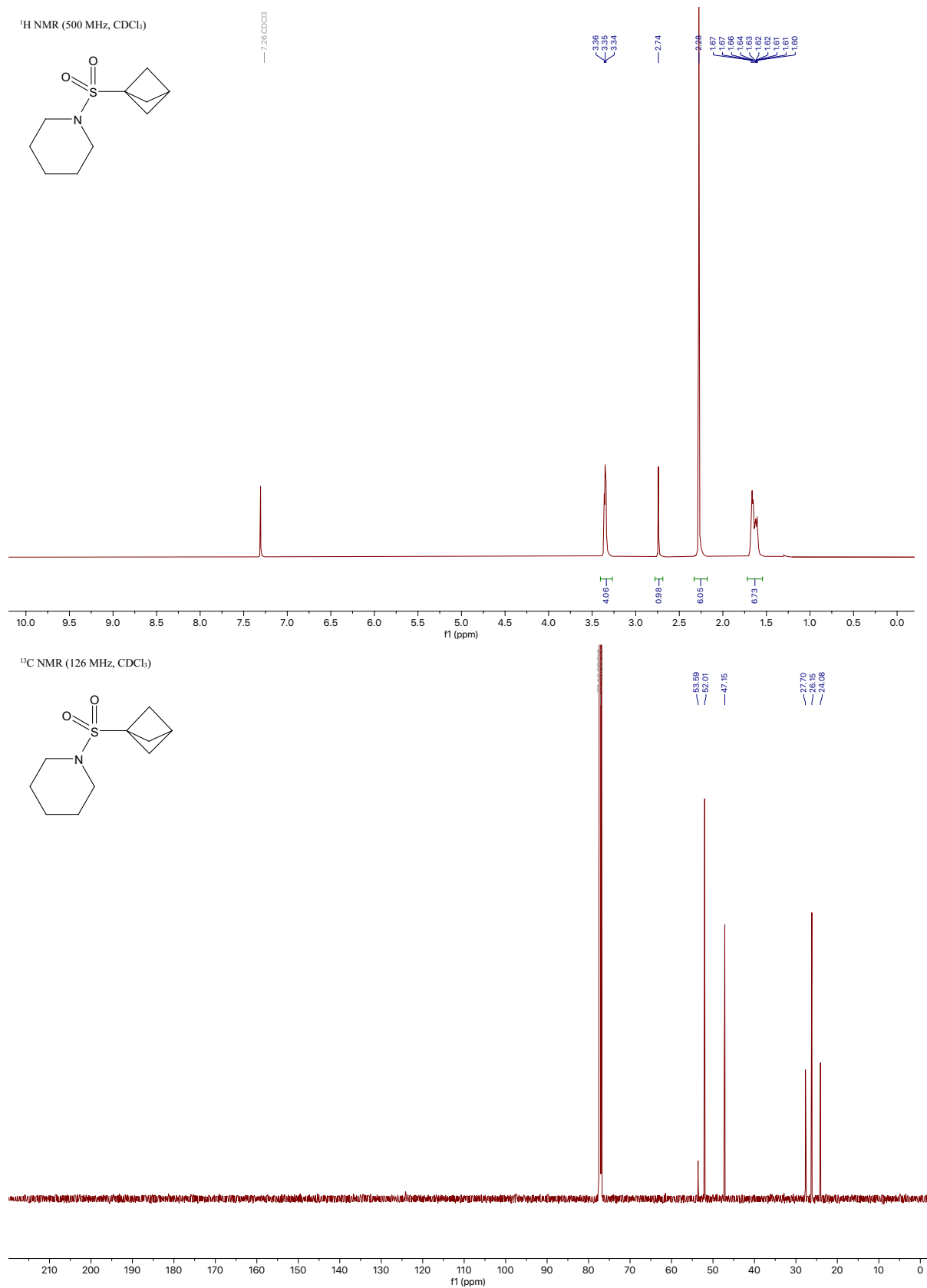
Compound 14b

4-(bicyclo[1.1.1]pentan-1-ylsulfonyl)morpholine [Experimental]
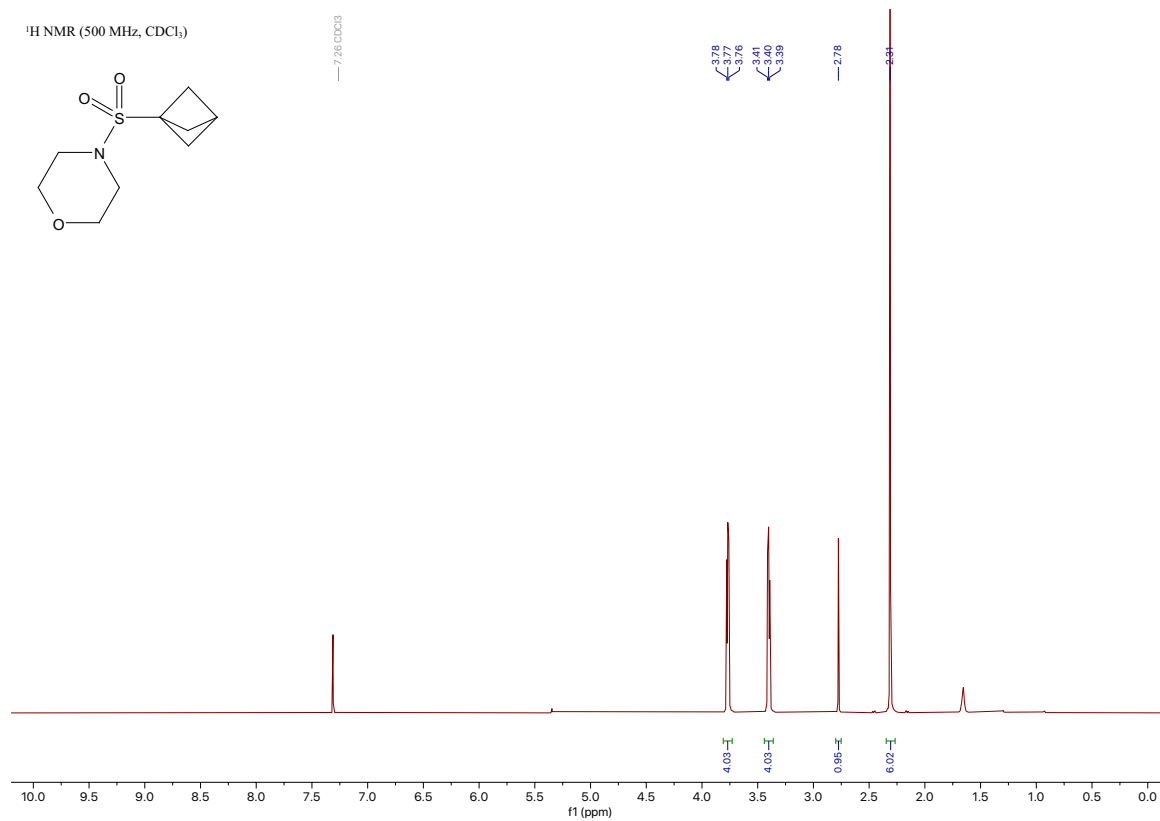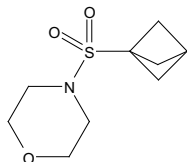
¹H NMR (500 MHz, CDCl₃)

¹³C NMR (126 MHz, CDCl₃)
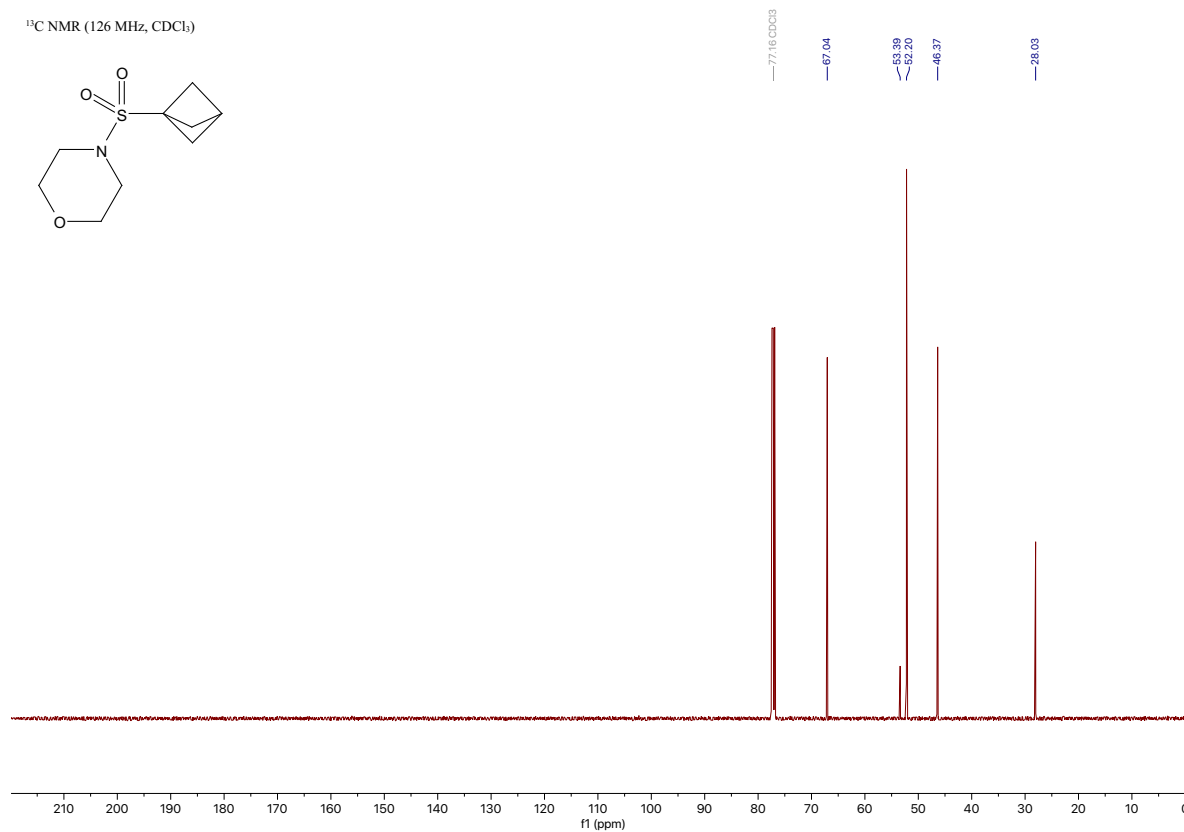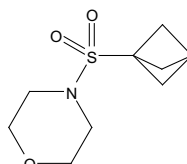
Compound 16b

N-(bicyclo[1.1.1]pentan-1-yl)-2,2,2-trifluoroacetamide [Experimental]
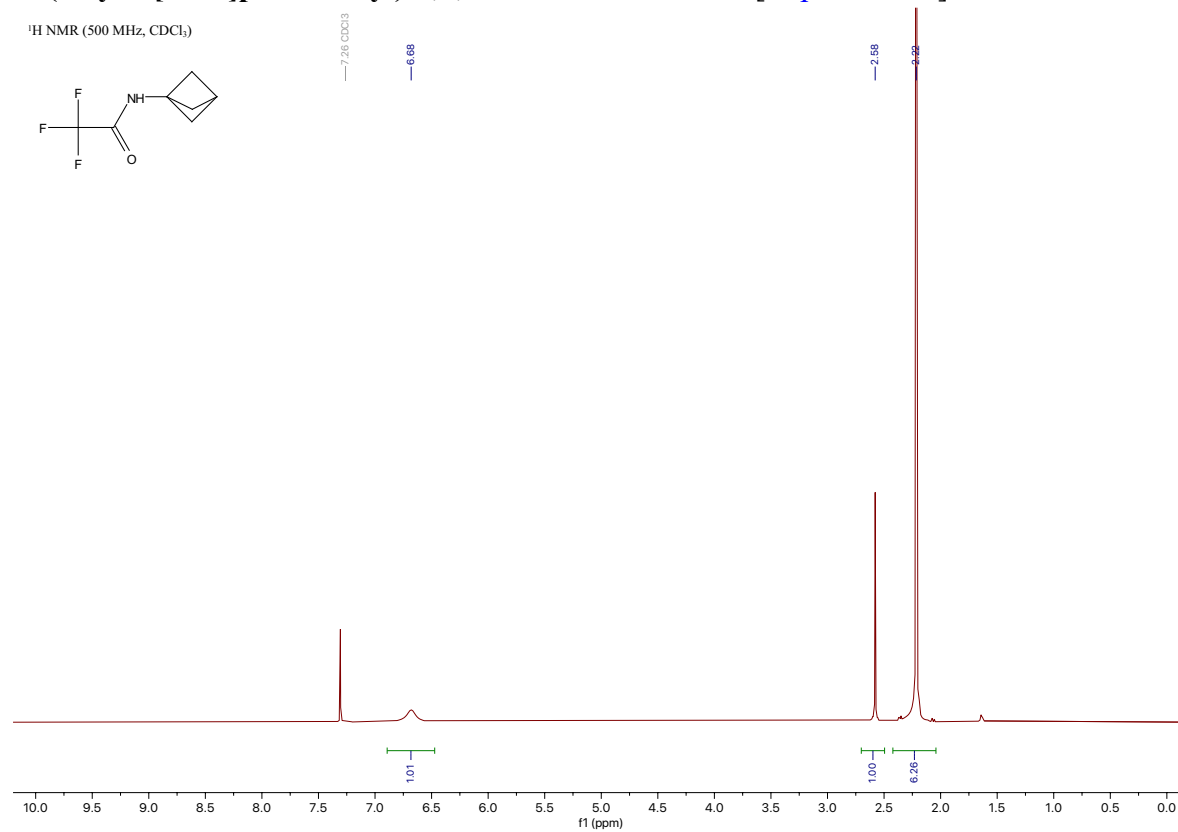
¹H NMR (500 MHz, CDCl₃)
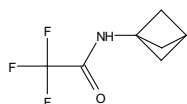
157.37
157.08
156.79
156.49

119.08
116.78
114.48
112.19

52.79
47.99

24.97

f1 (ppm)

-76.27

f1 (ppm)
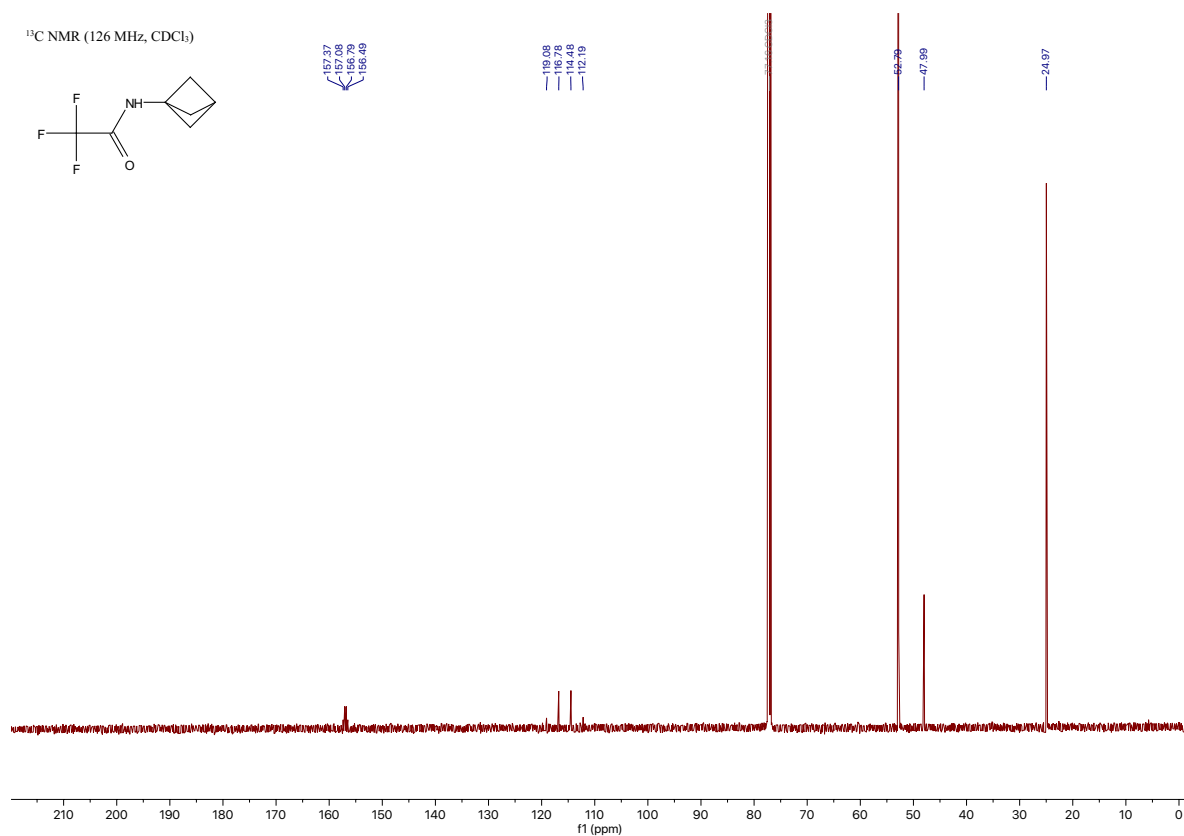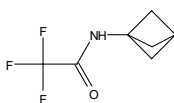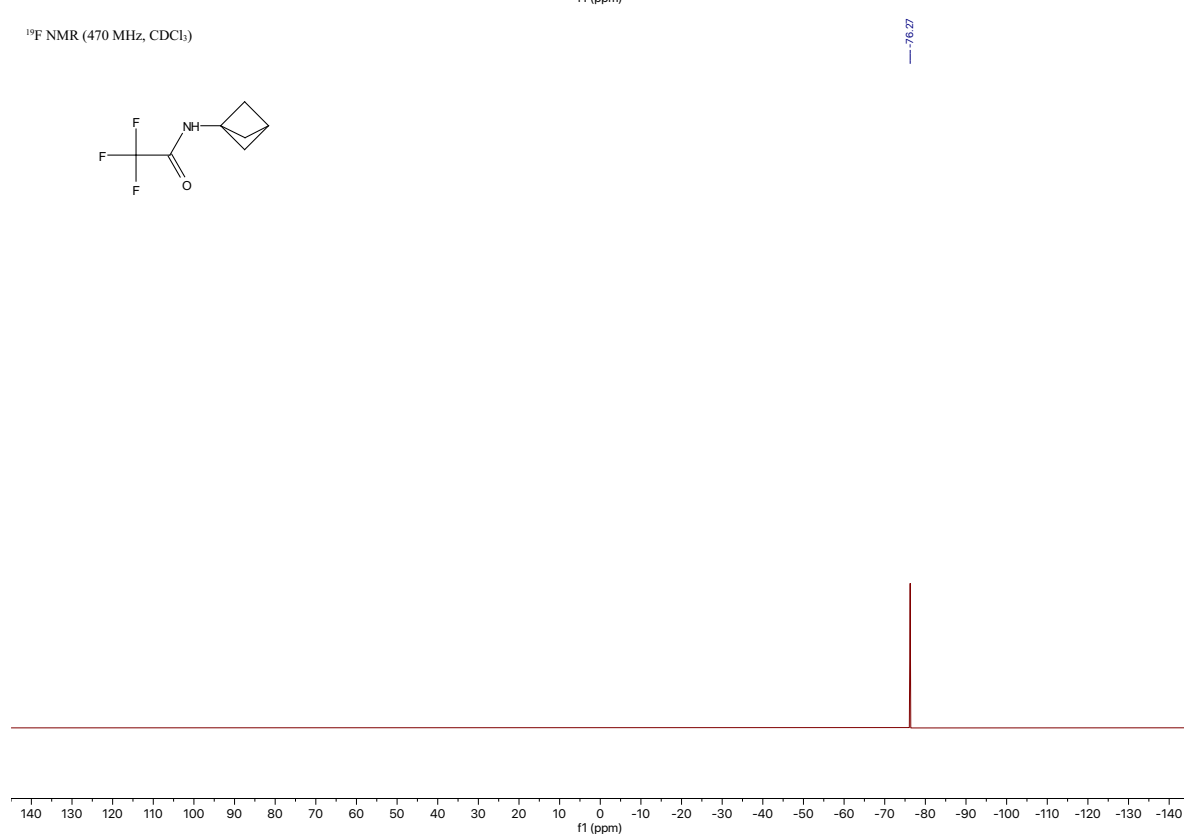
Compound 19b

1-(3-methoxyphenyl)bicyclo[1.1.1]pentane [Experimental]

¹H NMR (400 MHz, CDCl₃)

¹³C NMR (126 MHz, CDCl₃)
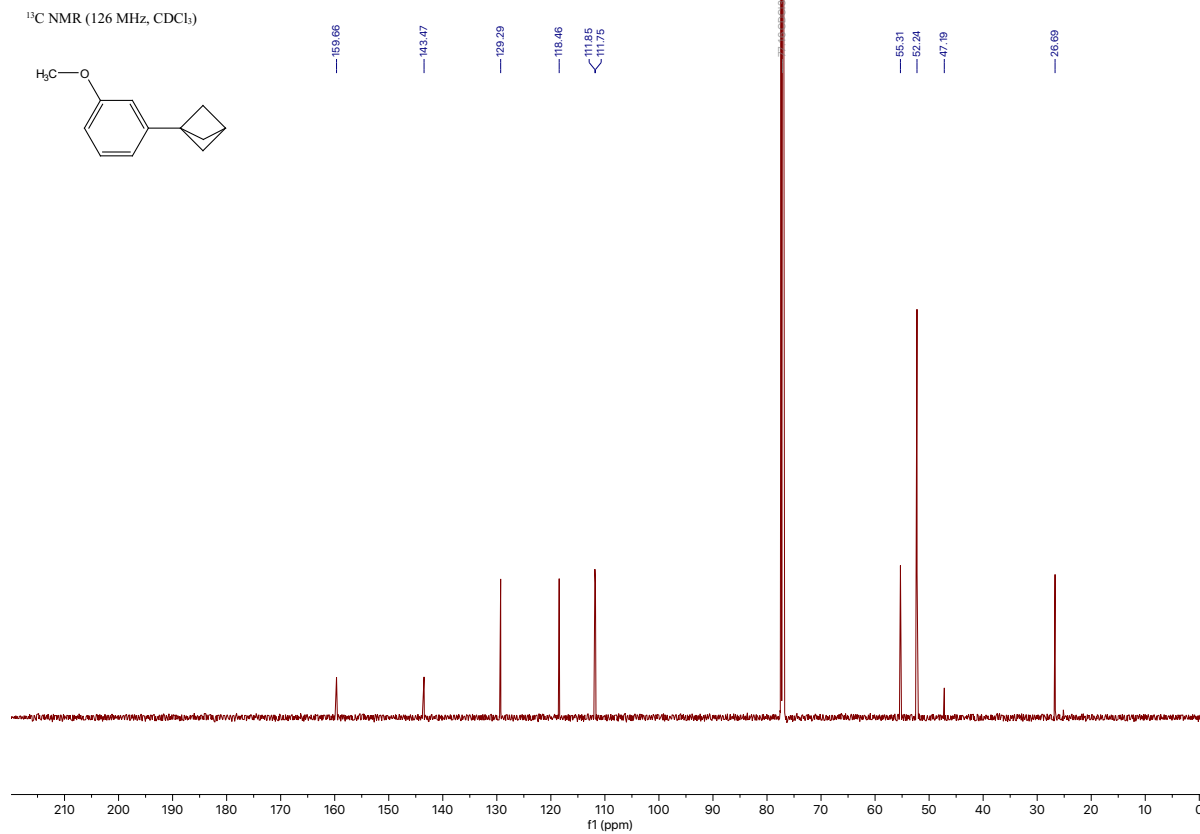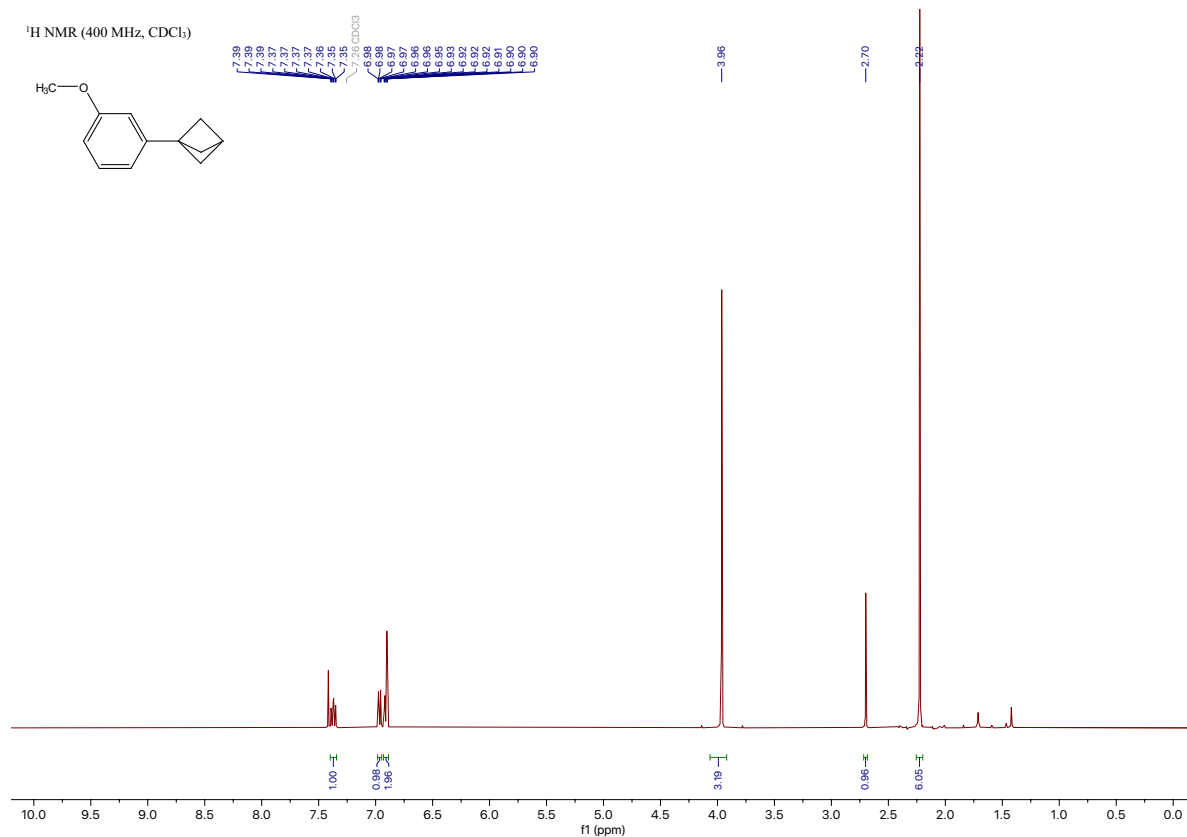
Compound 20b

N-(bicyclo[1.1.1]pentan-1-yl)-2-propylpentanamide [Experimental]

CHLOROFORM-d

8 — 176.39

12,14,15 — 52.74
11 — 47.77

2,3 — 35.21

4,6 — 20.85
1 — 24.74

5,7 — 14.15

77.00

Chemical Shift (ppm)

0.46

2.33 0.85   2.20   0.911.74 1.54

13
12, 14, 15
1
4, 6
5, 7

2.43, 24.35 (?, 1)(13, ?)
0.89, 14.03 (?, 5)(?, 7)
0.89, 20.72 (?, 4)(?, 6)(5, ?)(7, ?)
1.57, 20.79 (?, 4)(?, 6)
1.29, 20.78 (4, 4)(6, 6)
1.57, 35.16 (?, 2)(?, 3)
1.91, 47.74 (1, ?)
2.09, 52.59 (12, 12)(14, 14)(15, 15)

F2 Chemical Shift (ppm)
F1 Chemical Shift (ppm)

5, 7
4, 6
1
2, 3
12, 14, 15

219
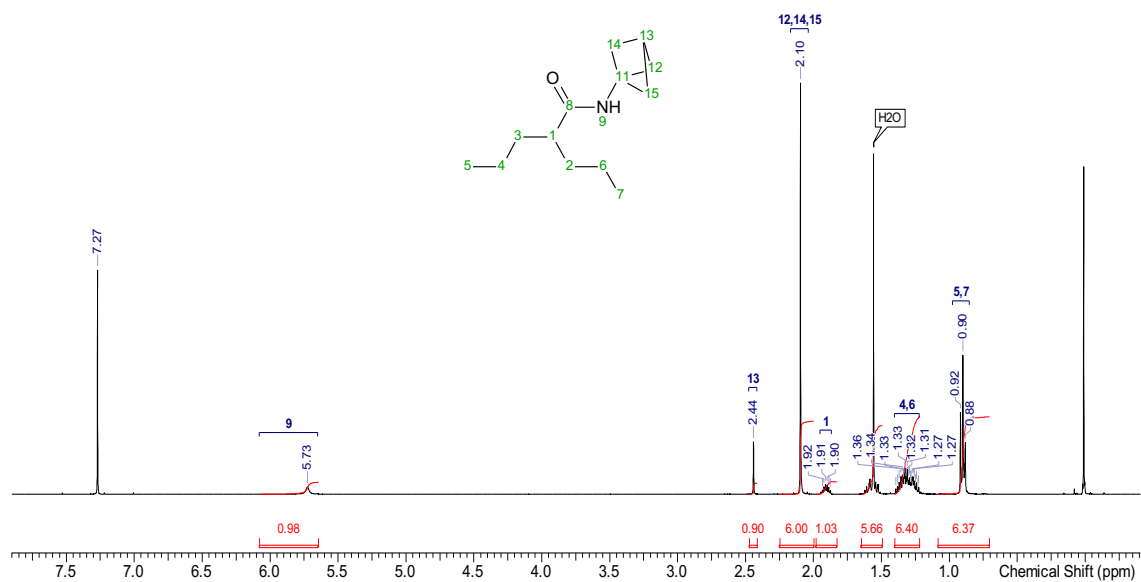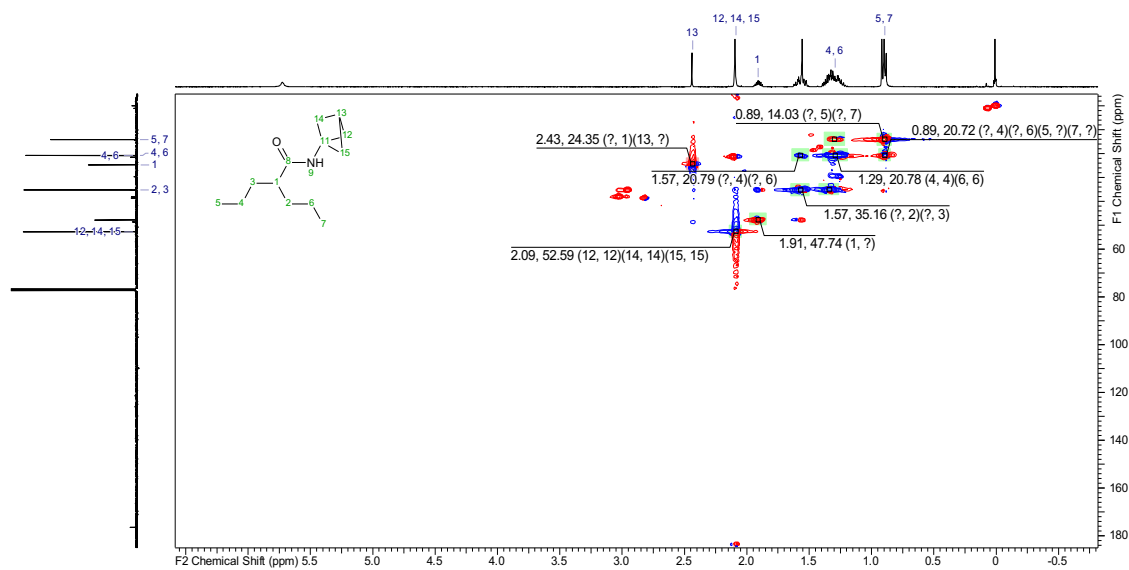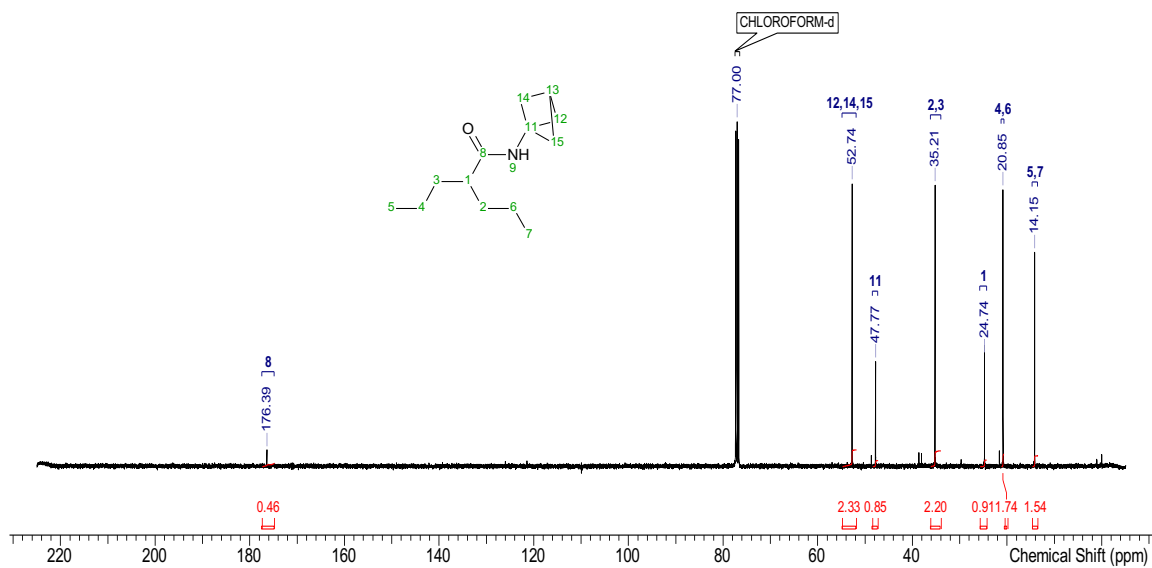
Compound 21b

(1*R*,4a*R*,4b*R*,10a*R*)-*N*-(bicyclo[1.1.1]pentan-1-yl)-7-isopropyl-1,4a-dimethyl-1,2,3,4,4a,4b,5,6,10,10a-decahydrophenanthrene-1-carboxamide [Experimental]
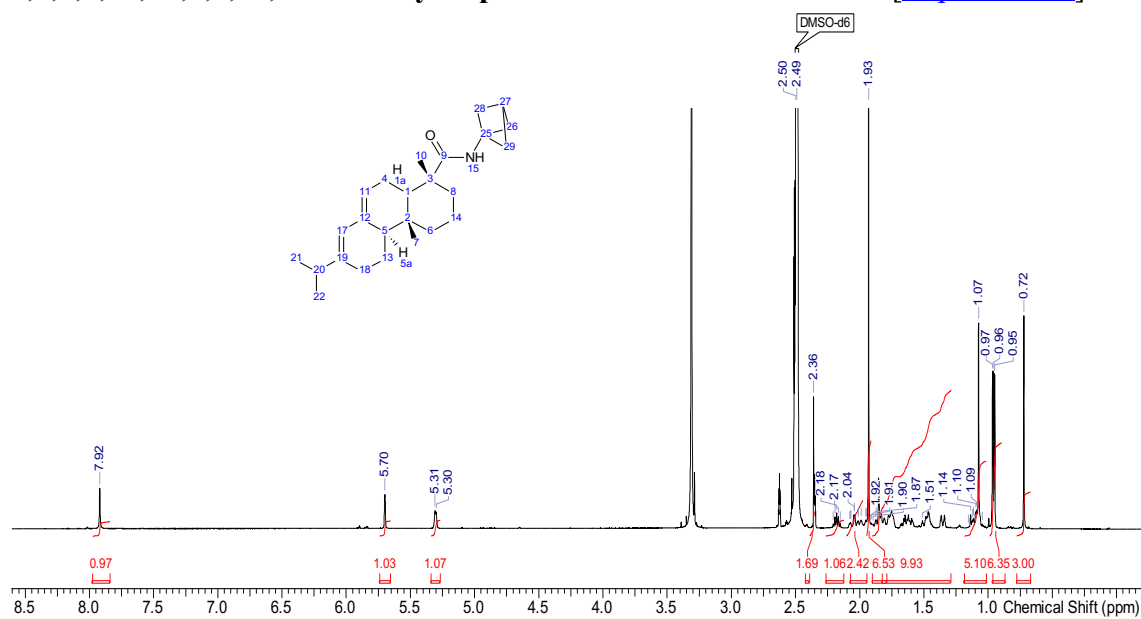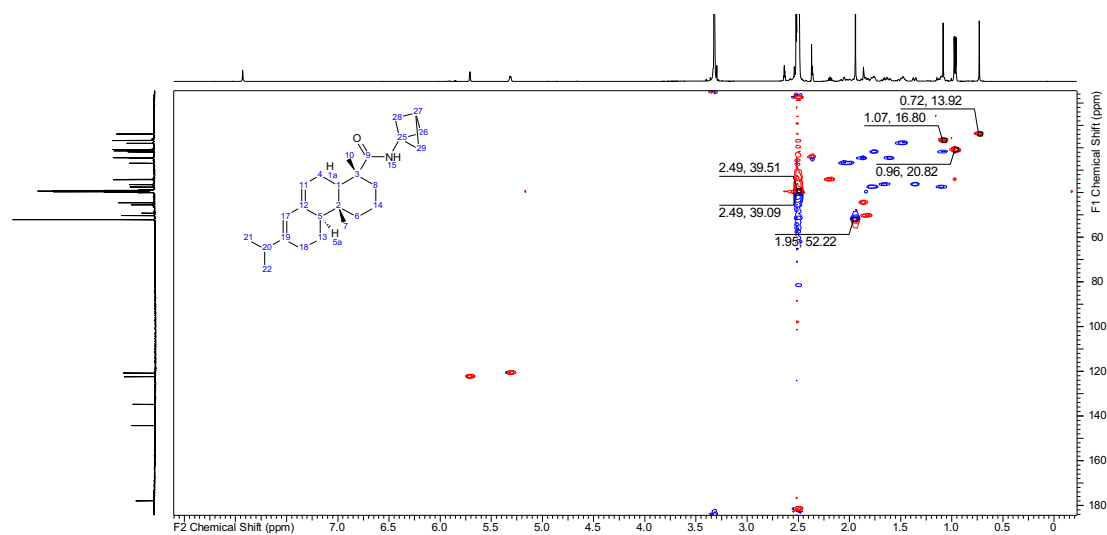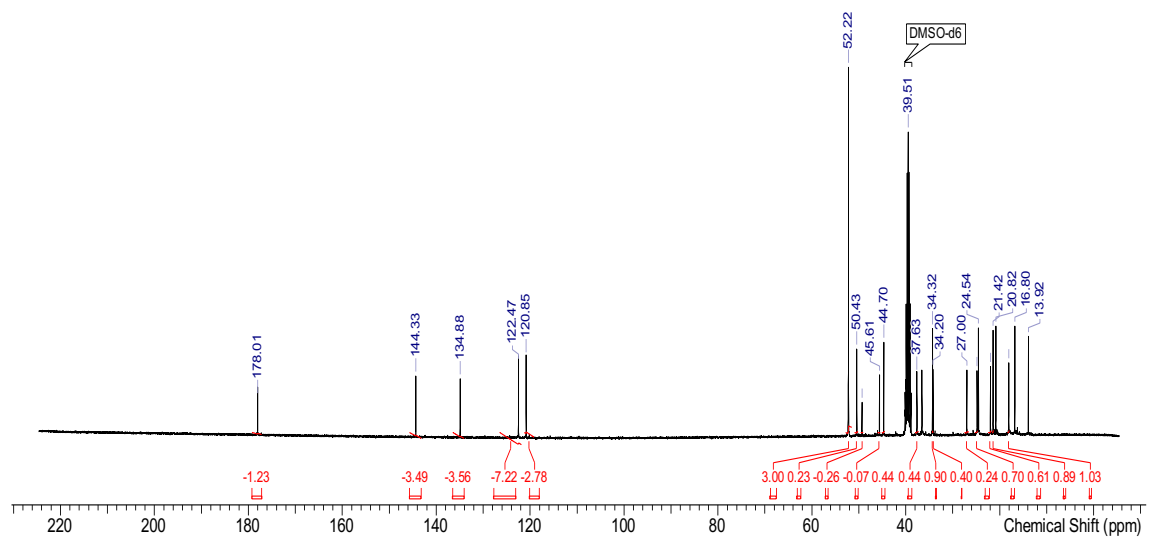
Compound 34b

tert-butyl 4-((triisopropylsilyl)ethynyl)-2-azabicyclo[2.1.1]hexane-2-carboxylate
[Experimental]
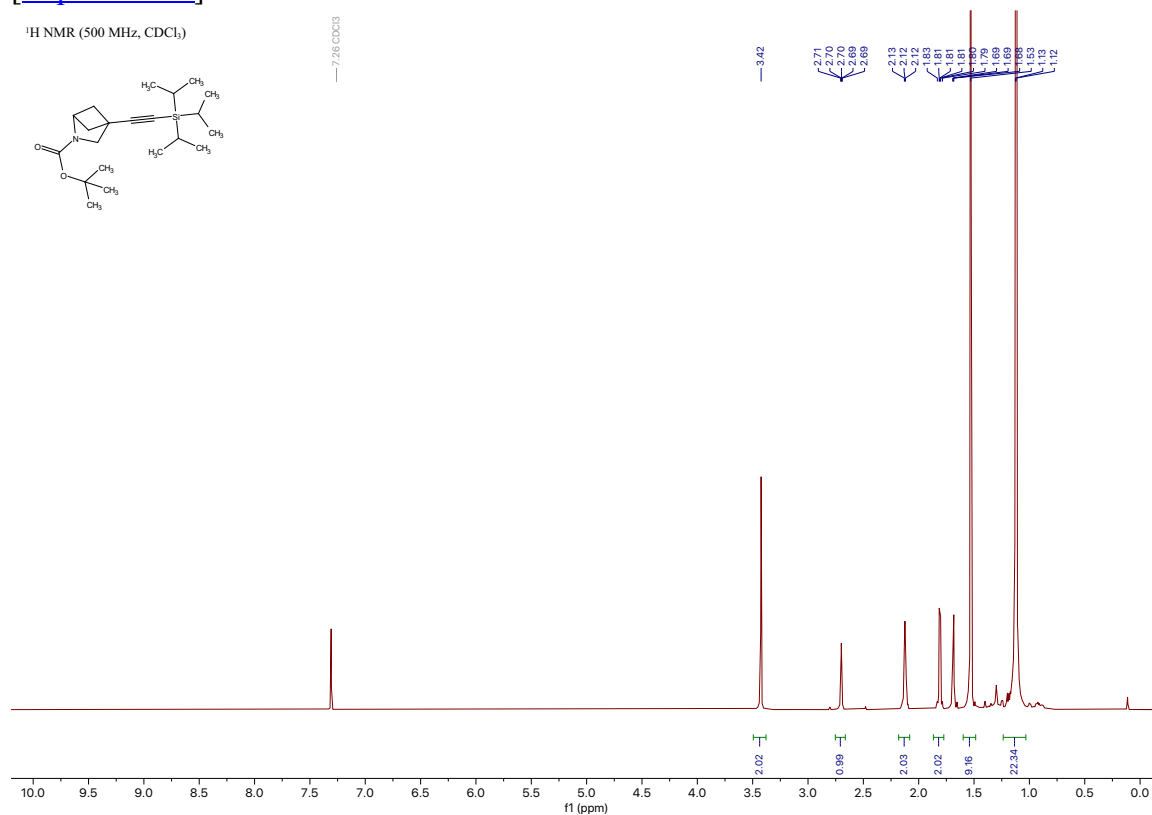
¹H NMR (500 MHz, CDCl₃)

¹³C NMR (126 MHz, CDCl₃)
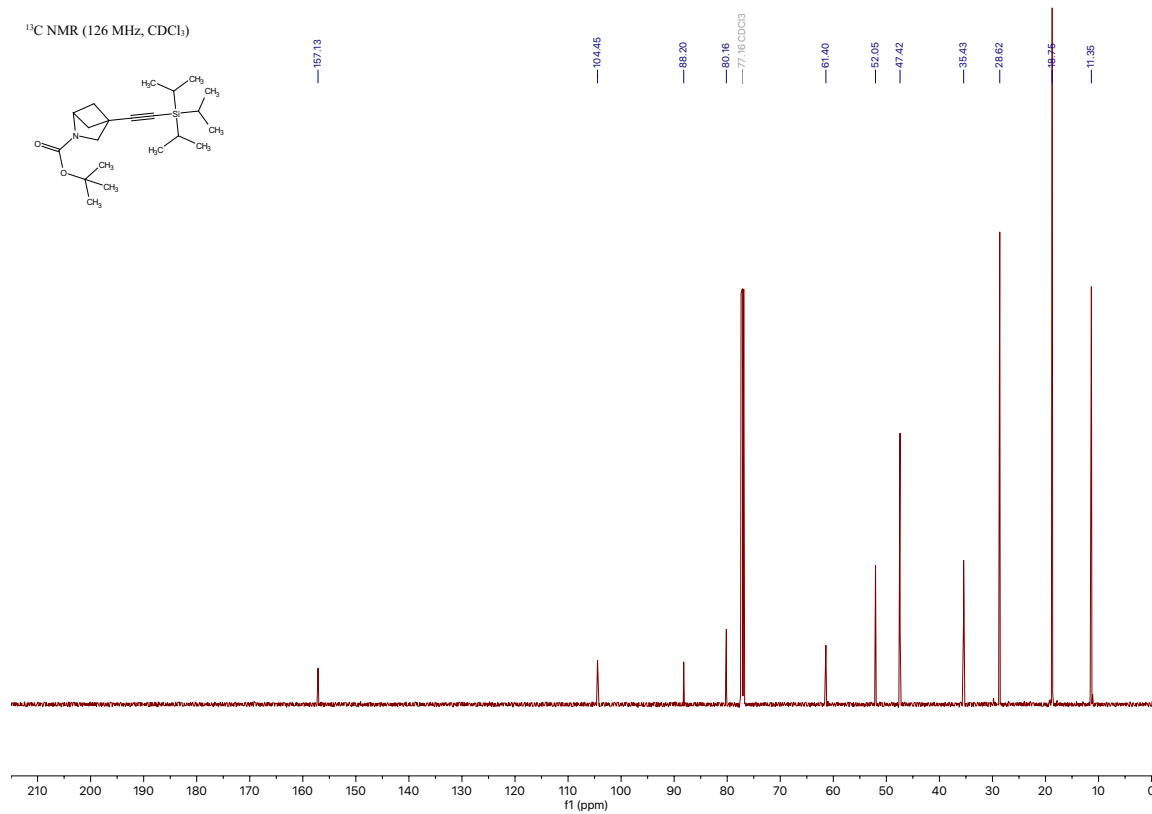
bicyclo[1.1.0]butane-1-carboxylic acid, *tert*-butyl ester

[Experimental]

¹H NMR (600 MHz, CDCl₃)
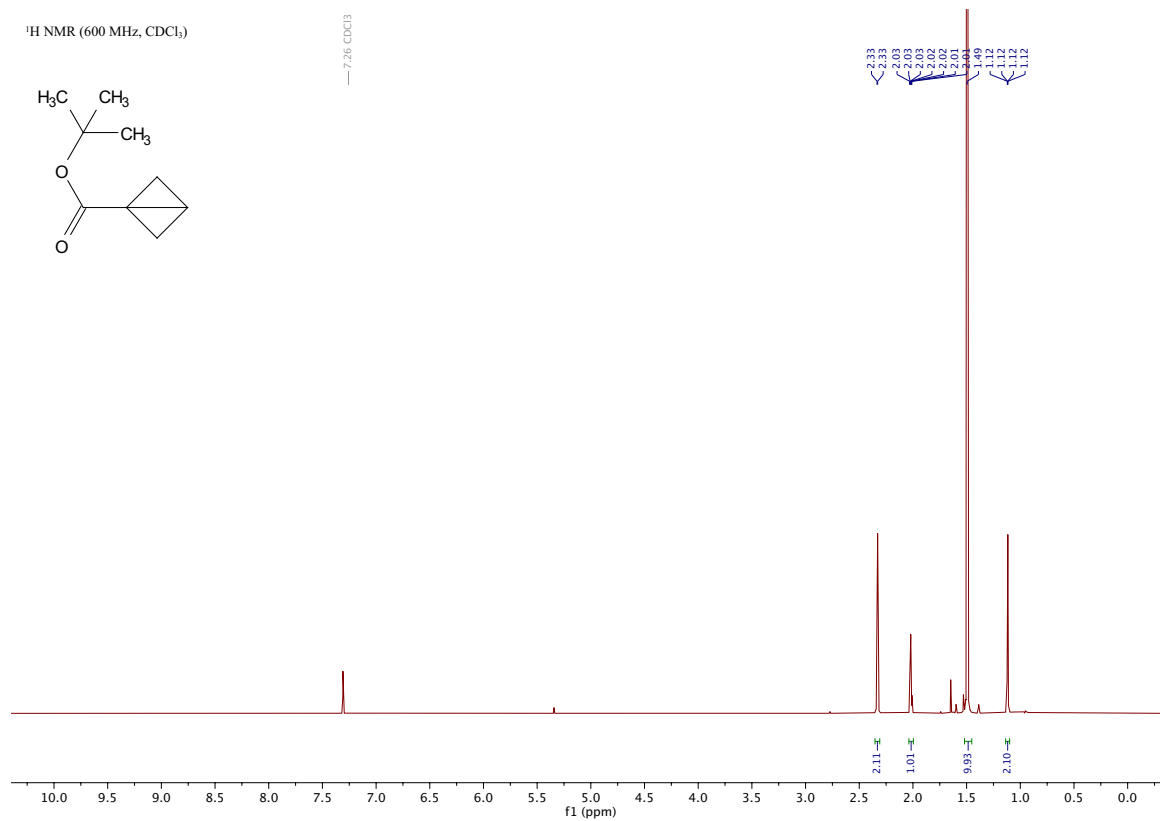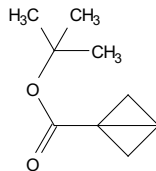
¹³C NMR (151 MHz, CDCl₃) δ 172.49, 80.41, 35.46, 28.23, 15.85, 10.15.
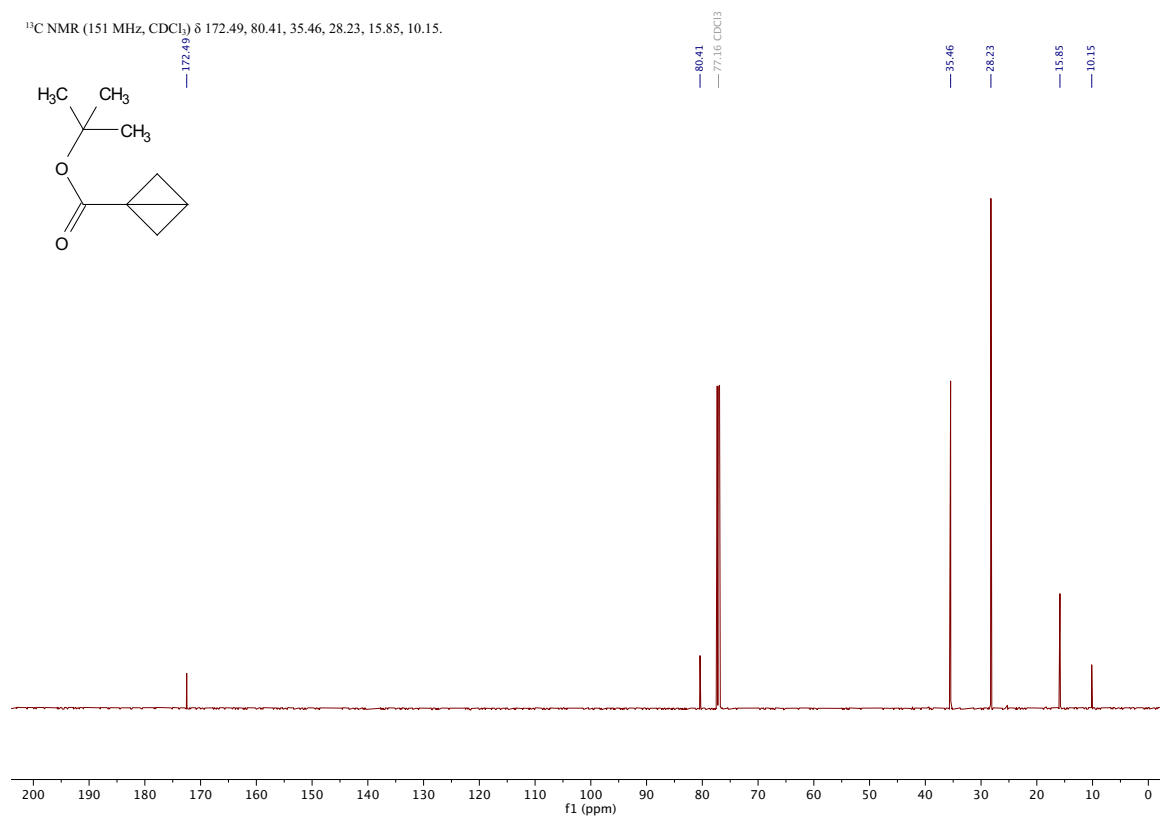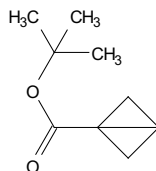
Compound 1a

2-(3-(4-(*tert*-butyl)phenyl)bicyclo[1.1.1]pentan-1-yl)-4,4,5,5-tetramethyl-1,3,2-dioxaborolane [Experimental]

¹H NMR (500 MHz, CDCl₃)
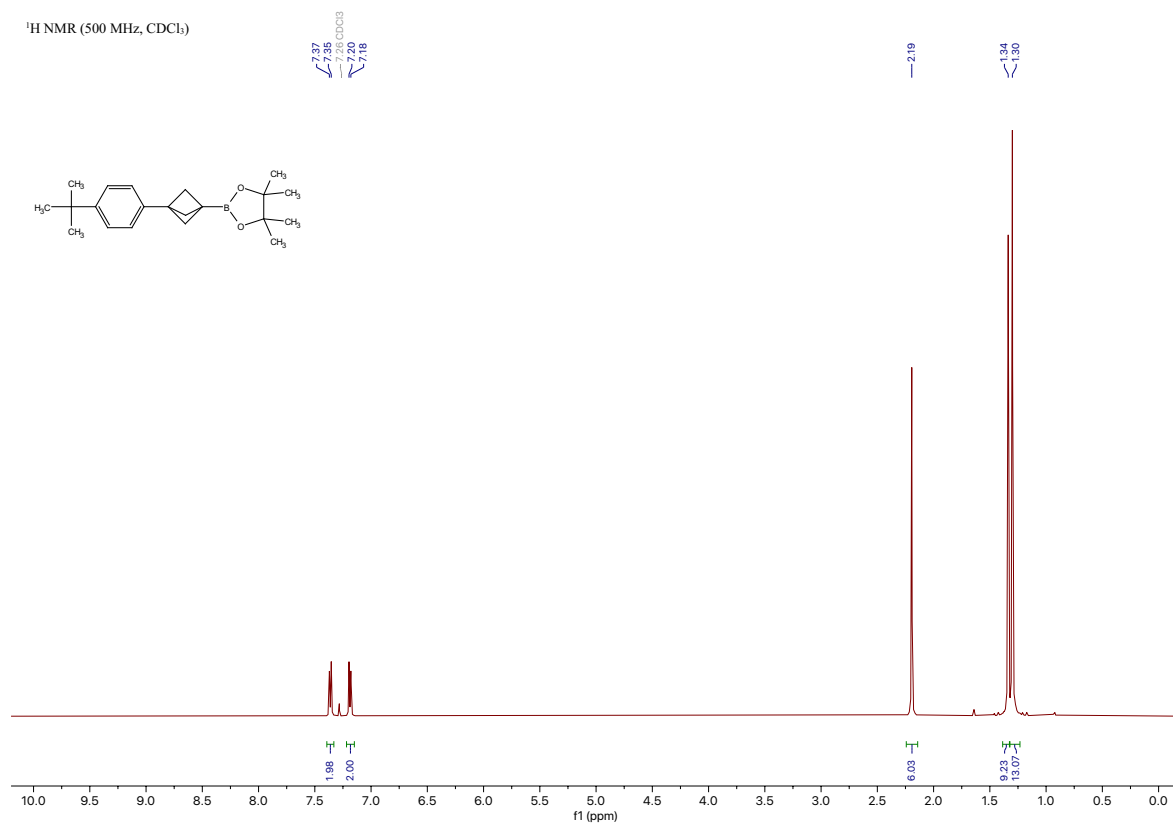
^{13}C NMR (126 MHz, CDCl$_3$)
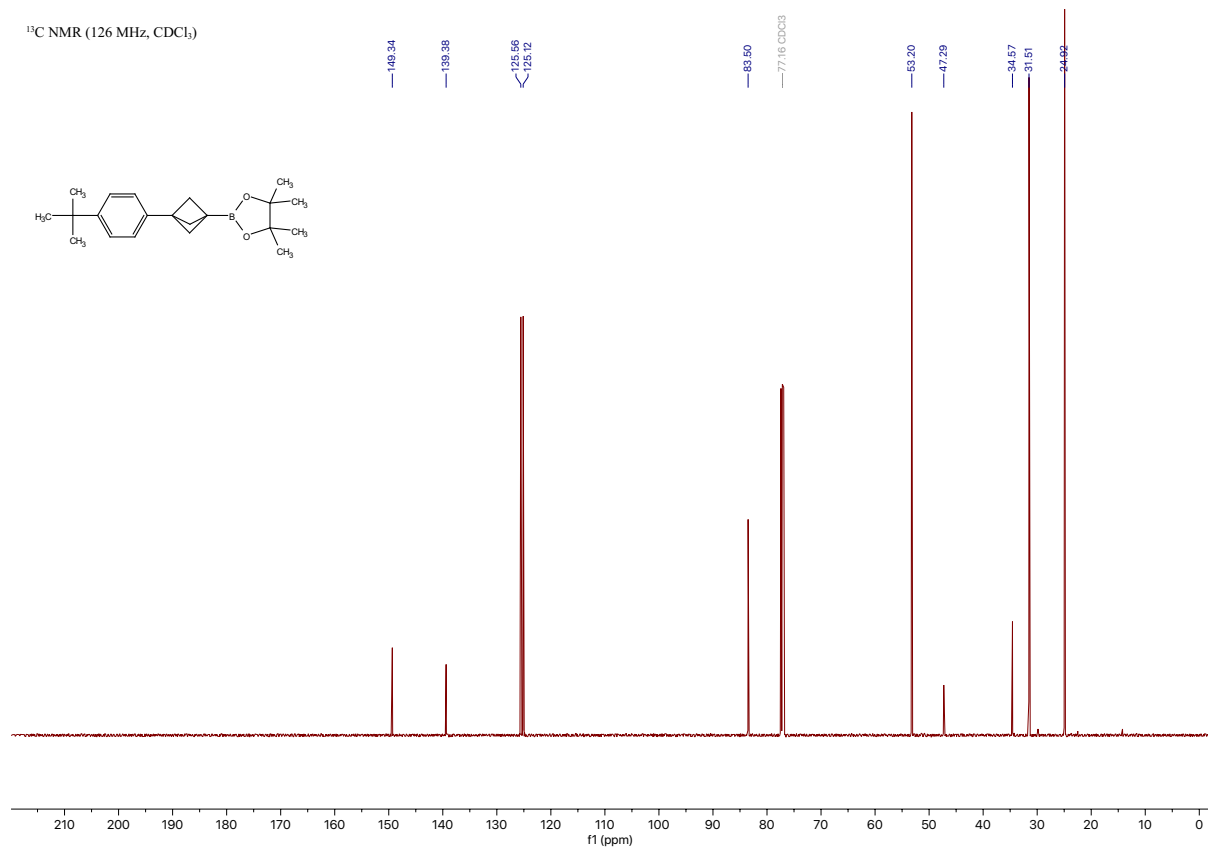
^{11}B NMR (160 MHz, CDCl$_3$)
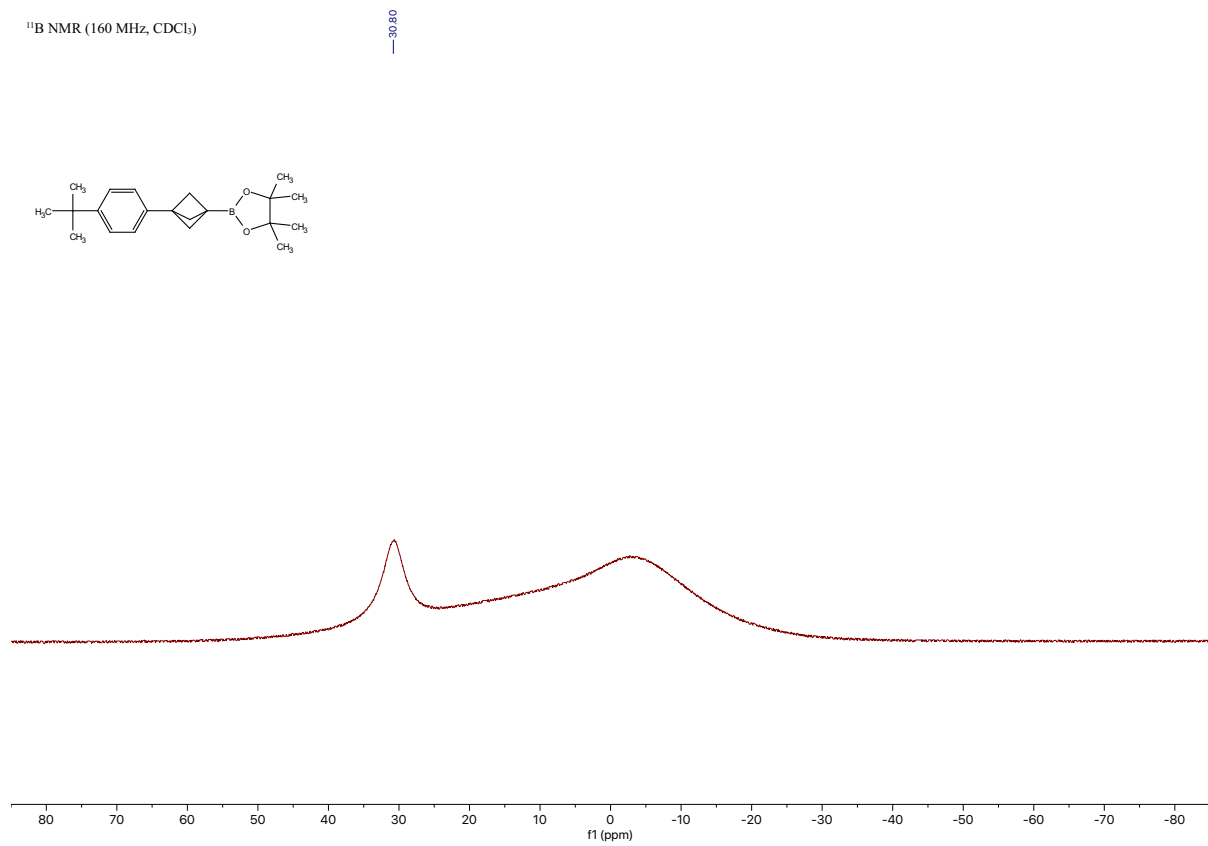
Compound 2a

2-(3-(3,5-di-*tert*-butylphenyl)bicyclo[1.1.1]pentan-1-yl)-4,4,5,5-tetramethyl-1,3,2-dioxaborolane [Experimental]

¹H NMR (600 MHz, CDCl₃)

¹³C NMR (151 MHz, CDCl₃)

¹¹B NMR (193 MHz, CDCl₃)

227
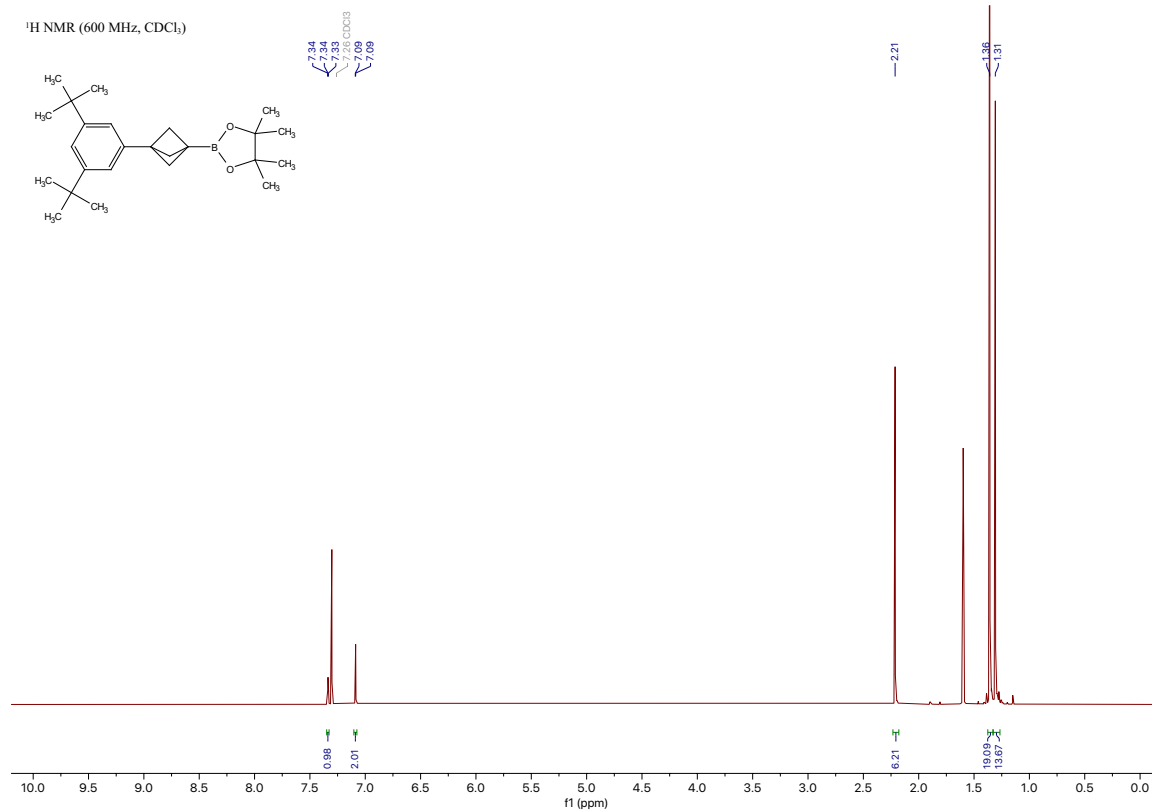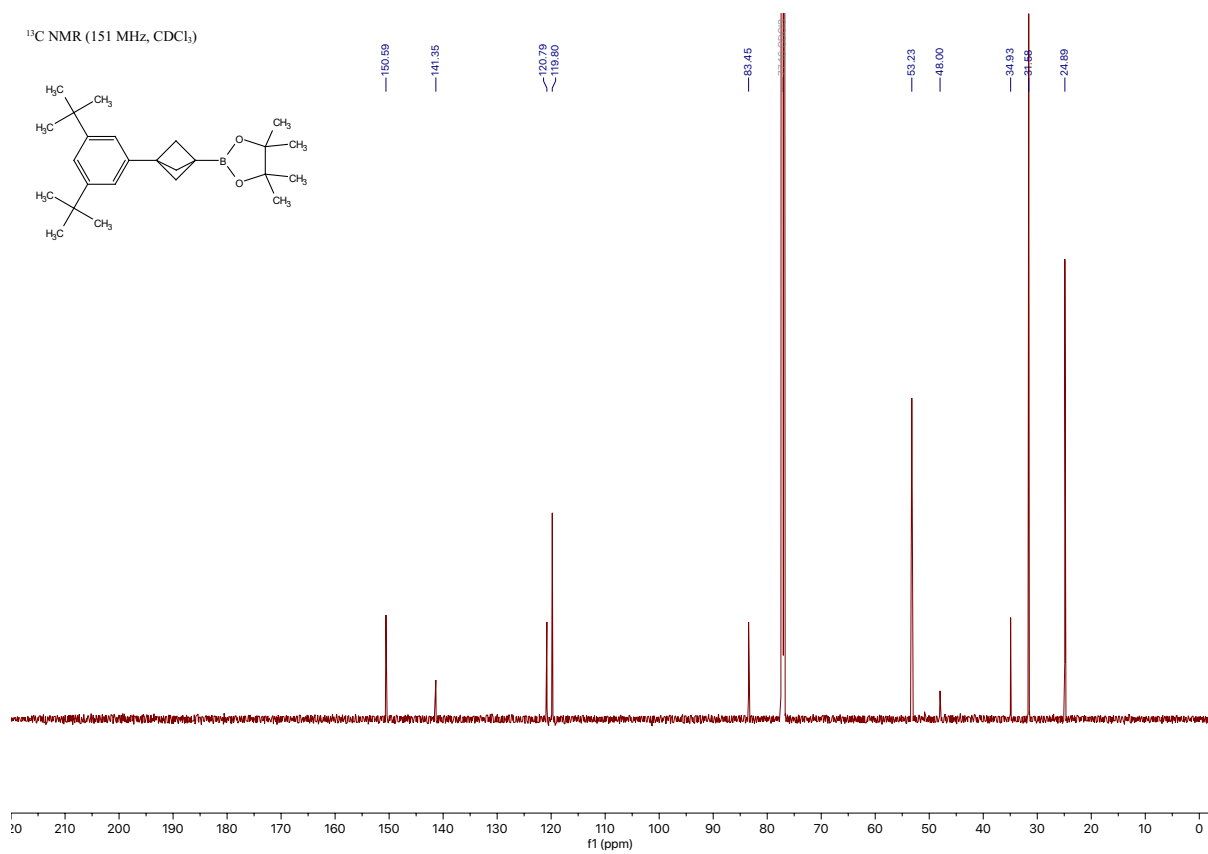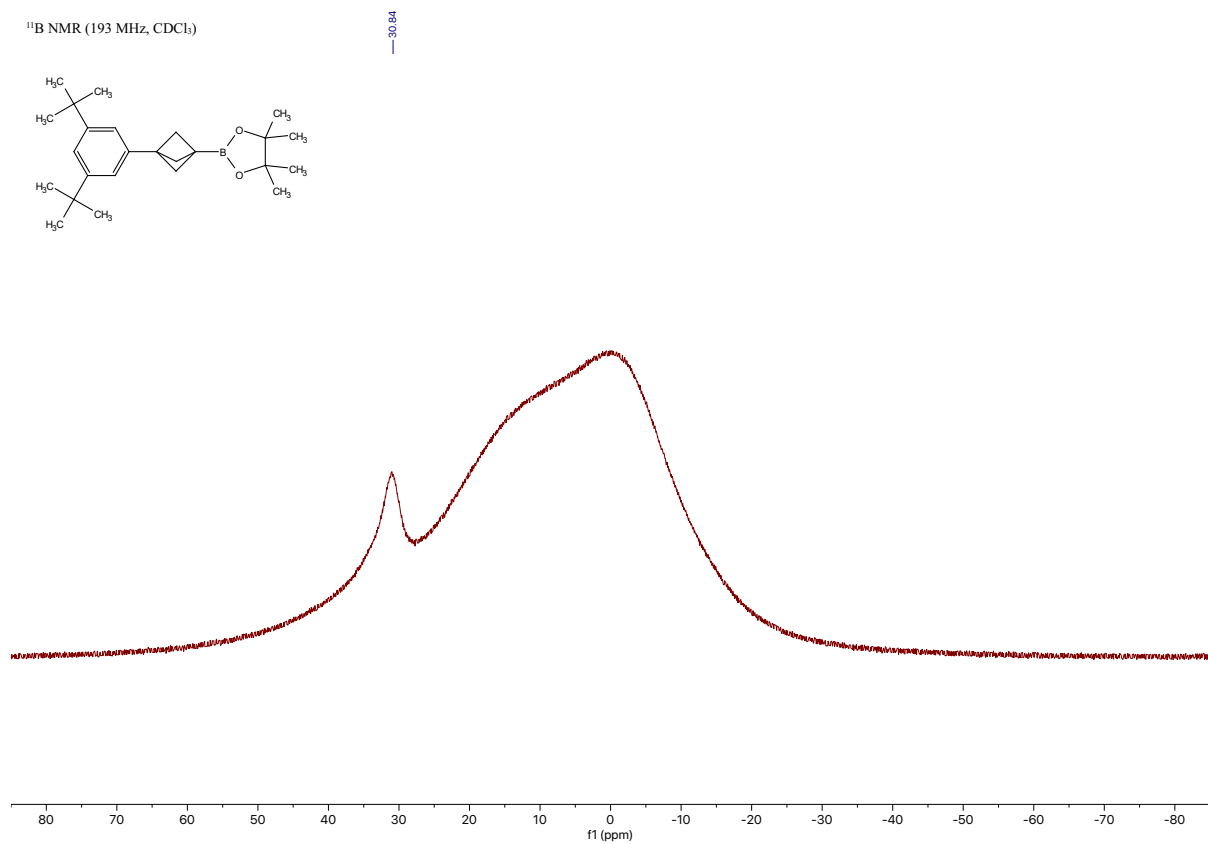
Compound 3a

2-(3-(*tert*-butylthio)bicyclo[1.1.1]pentan-1-yl)-4,4,5,5-tetramethyl-1,3,2-dioxaborolane

[Experimental]

¹³C NMR (126 MHz, CDCl₃)
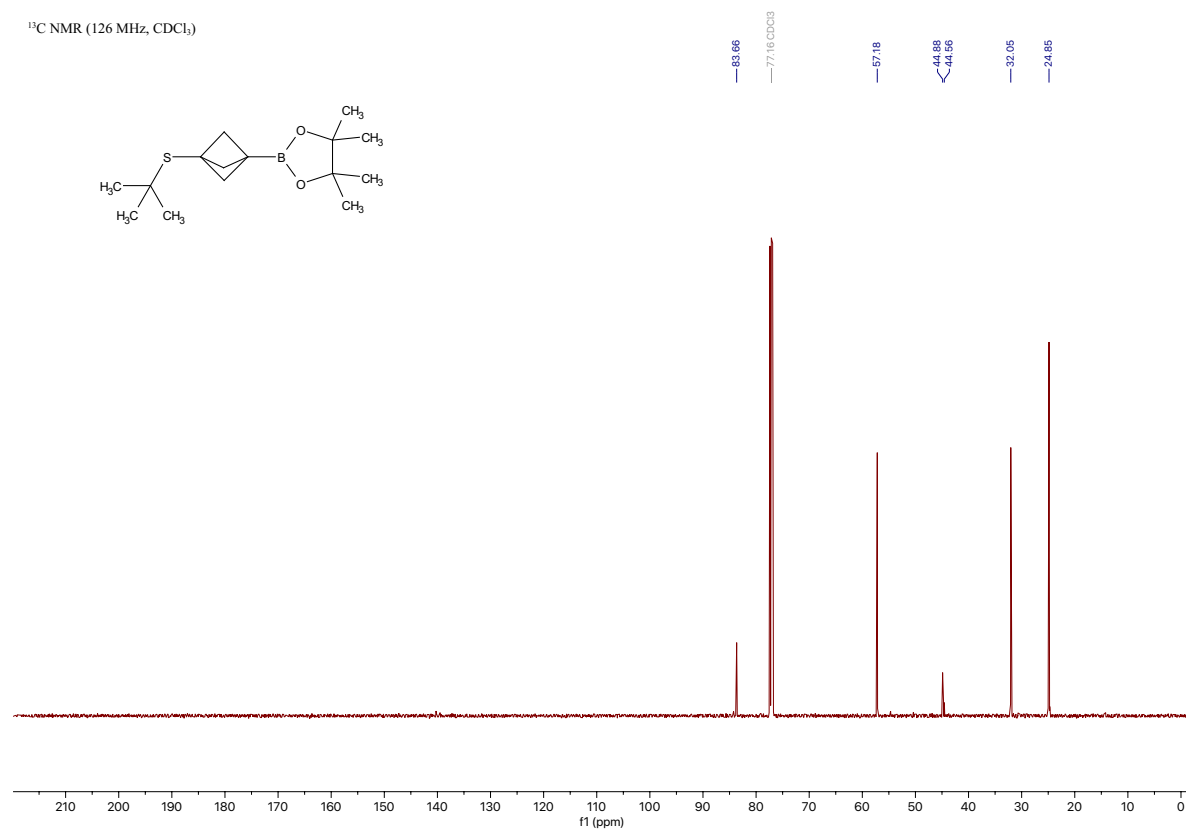
¹H NMR (500 MHz, CDCl₃)

¹¹B NMR (160 MHz, CDCl₃)

229
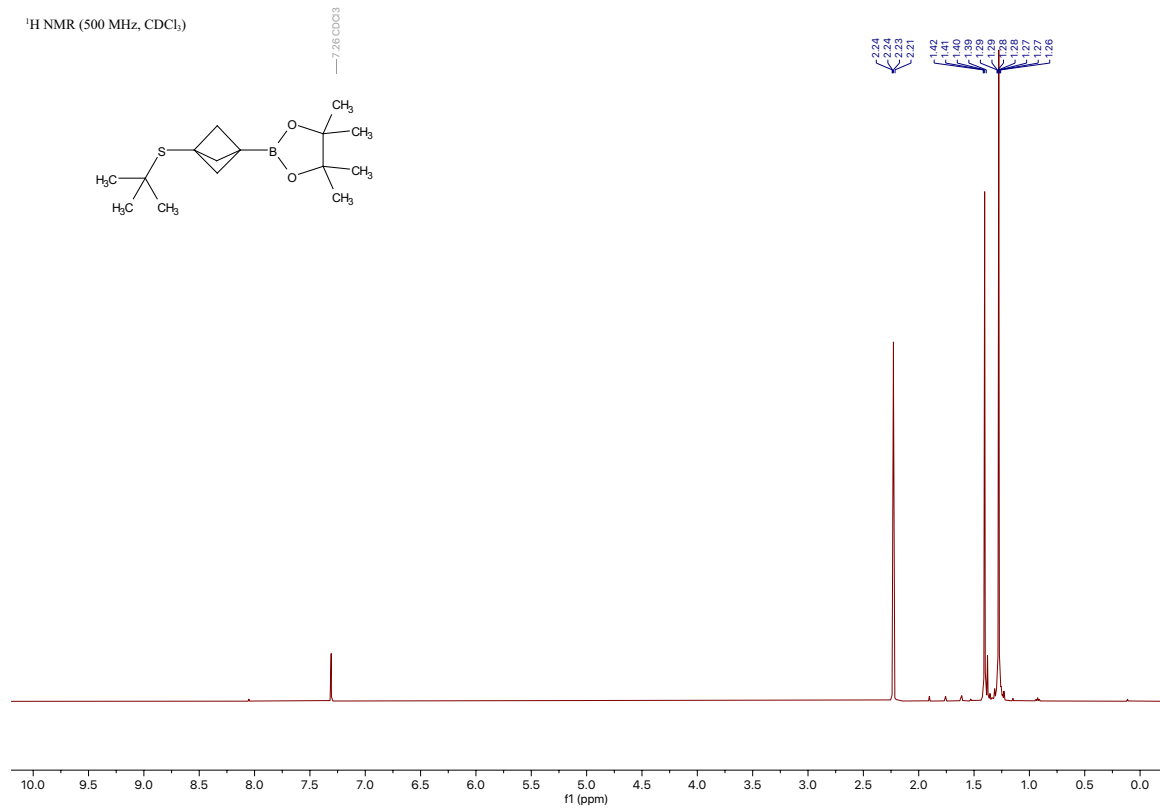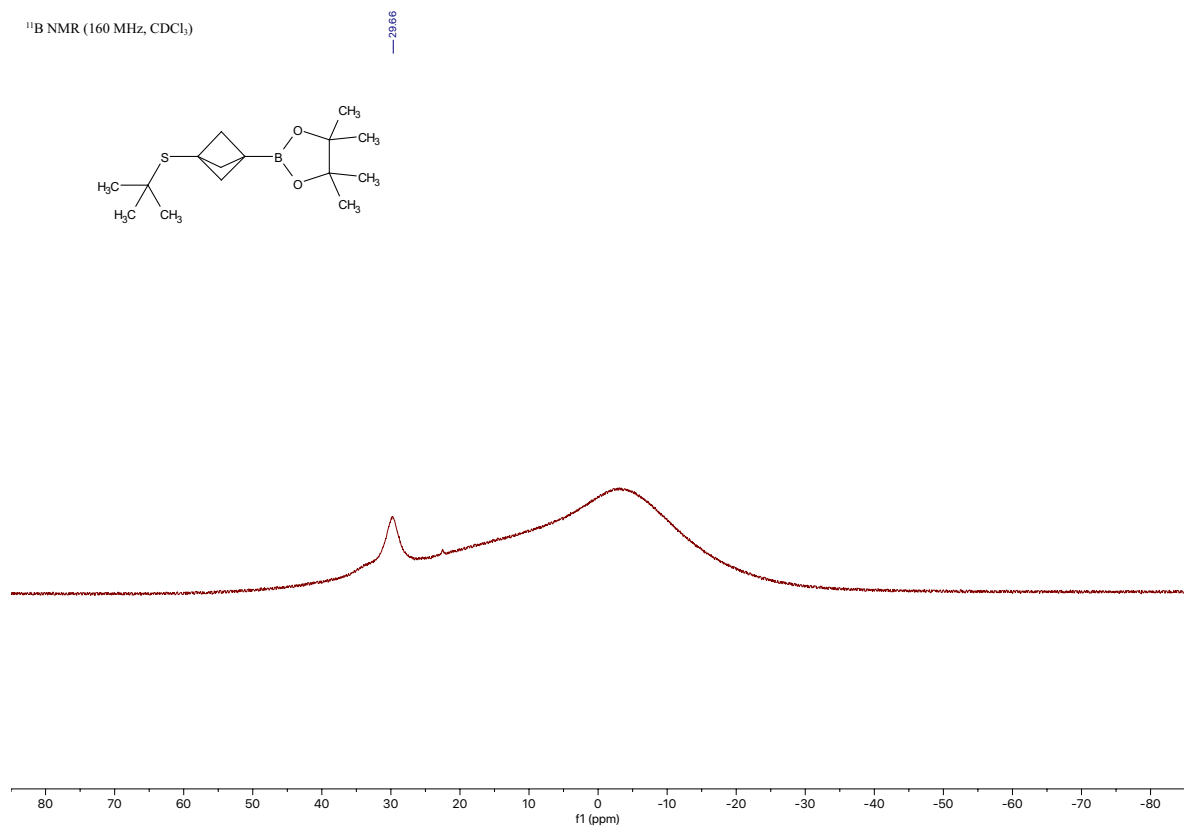
Compound 4a

tributyl(3-(4,4,5,5-tetramethyl-1,3,2-dioxaborolan-2-yl)bicyclo[1.1.1]pentan-1-yl)stannane [Experimental]

^{1}H NMR (600 MHz, CDCl$_3$)

^{13}C NMR (151 MHz, CDCl$_3$)
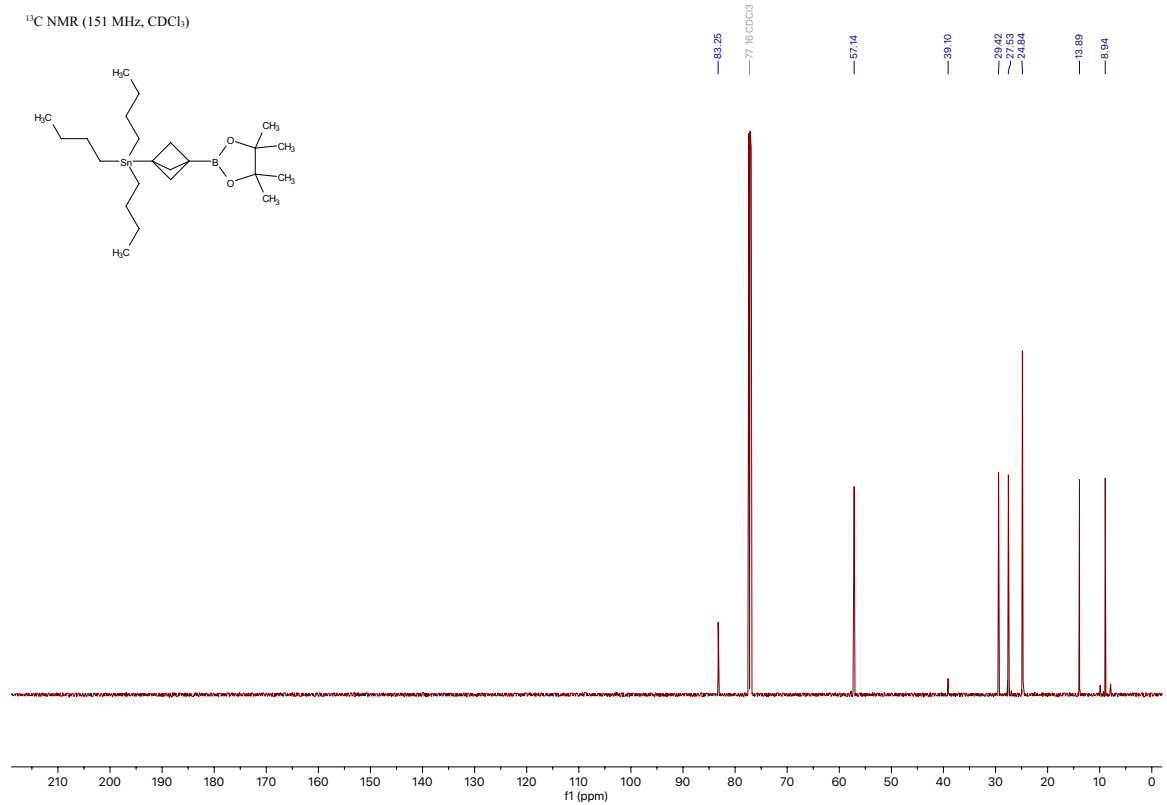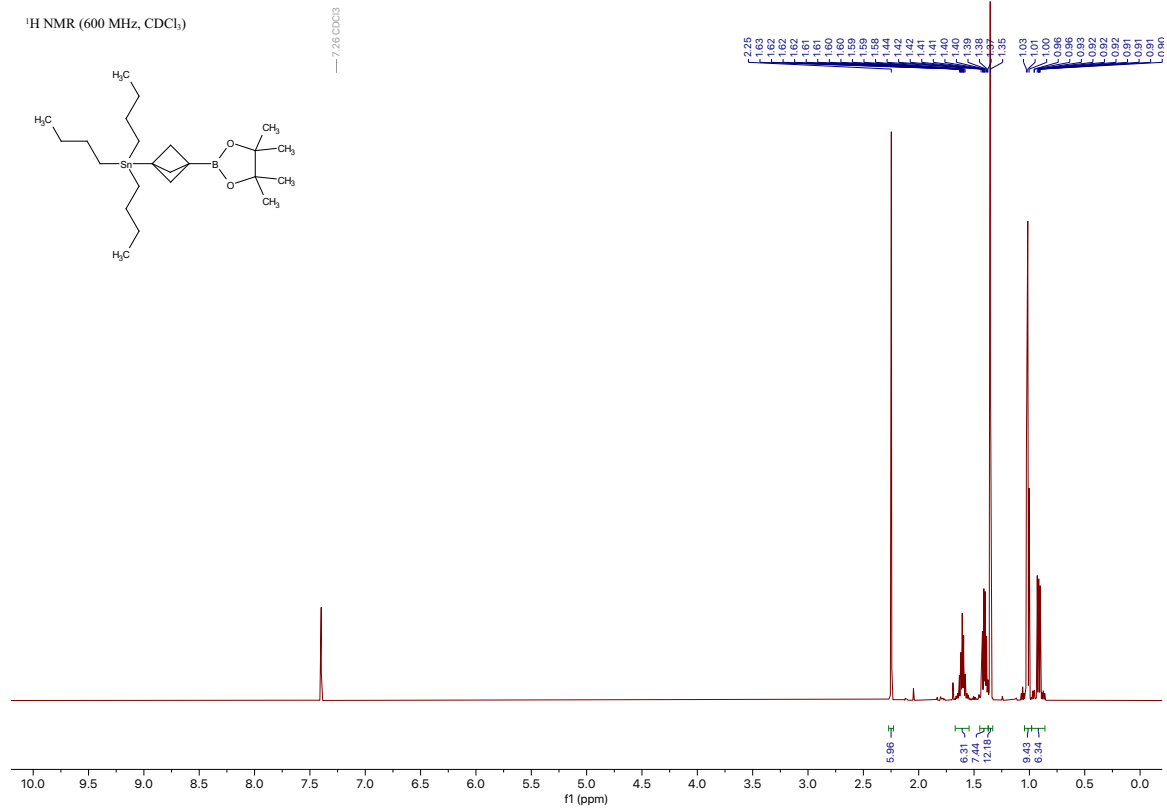
^{11}B NMR (160 MHz, CDCl$_3$)

—27.57
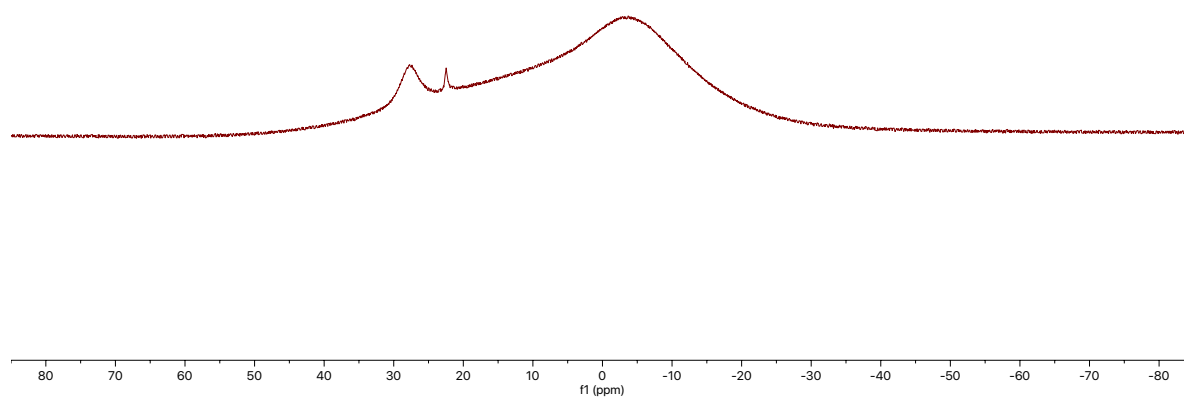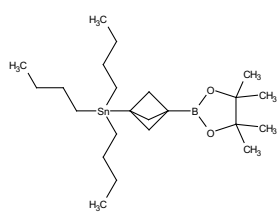
^{119}Sn NMR (224 MHz, CDCl$_3$)

—-71.27
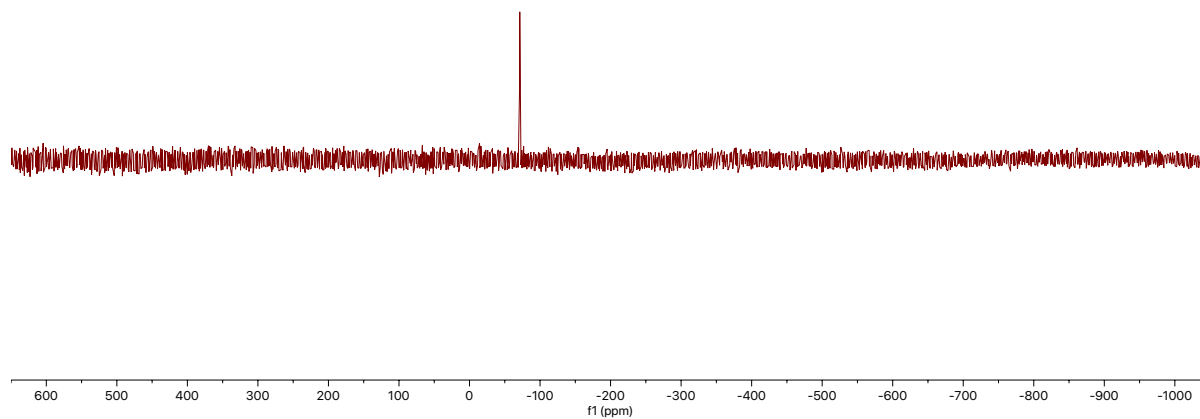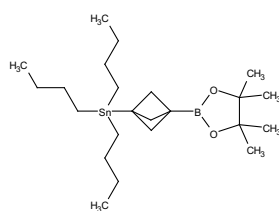
Compound 5a

2-(3-(bromomethyl)bicyclo[1.1.1]pentan-1-yl)-4,4,5,5-tetramethyl-1,3,2-dioxaborolane
[Experimental]

^{1}H NMR (500 MHz, CDCl$_3$)
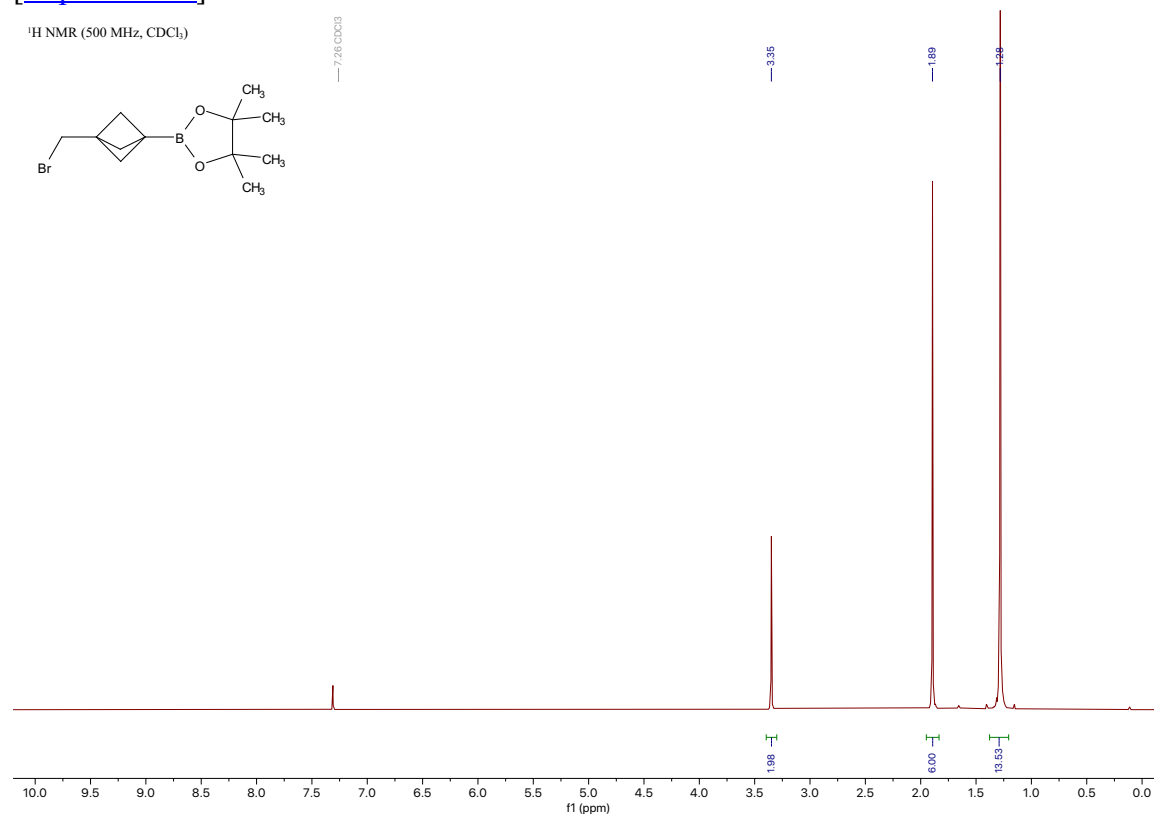
¹³C NMR (126 MHz, CDCl₃)
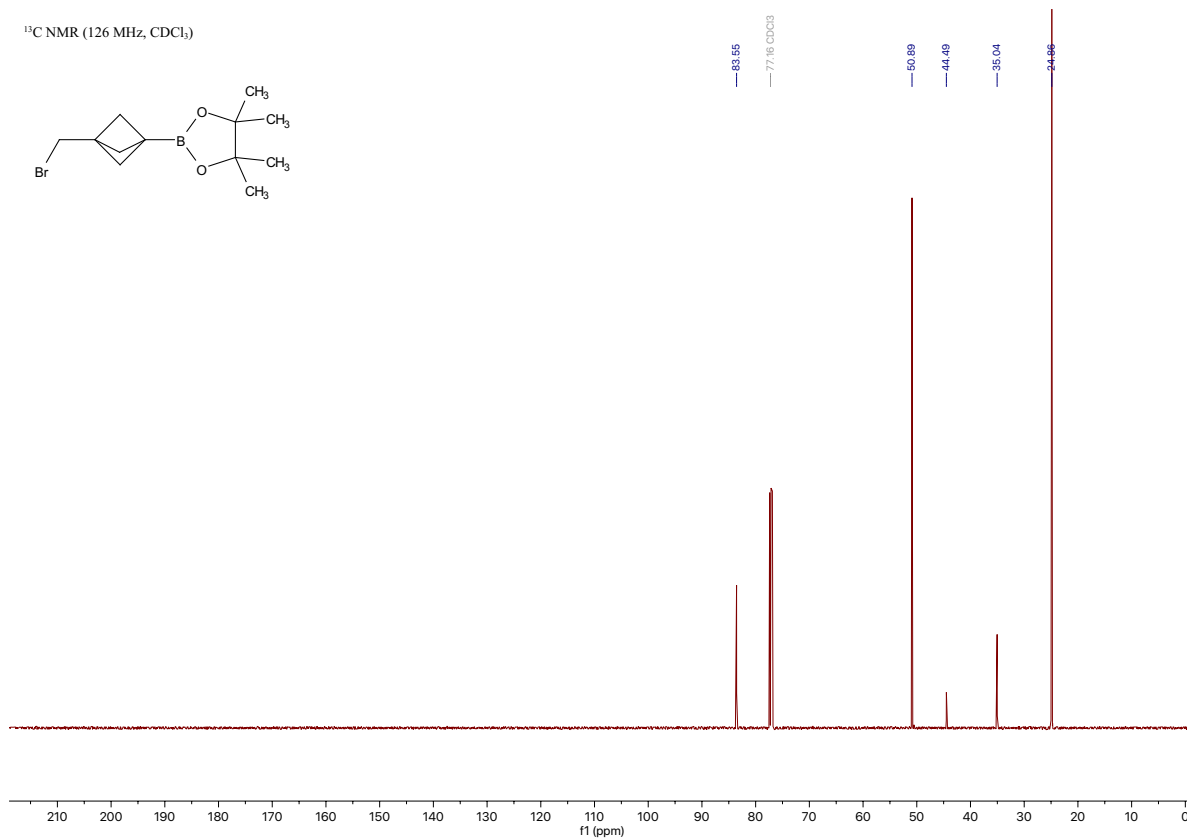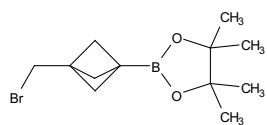
¹¹B NMR (160 MHz, CDCl₃)

233
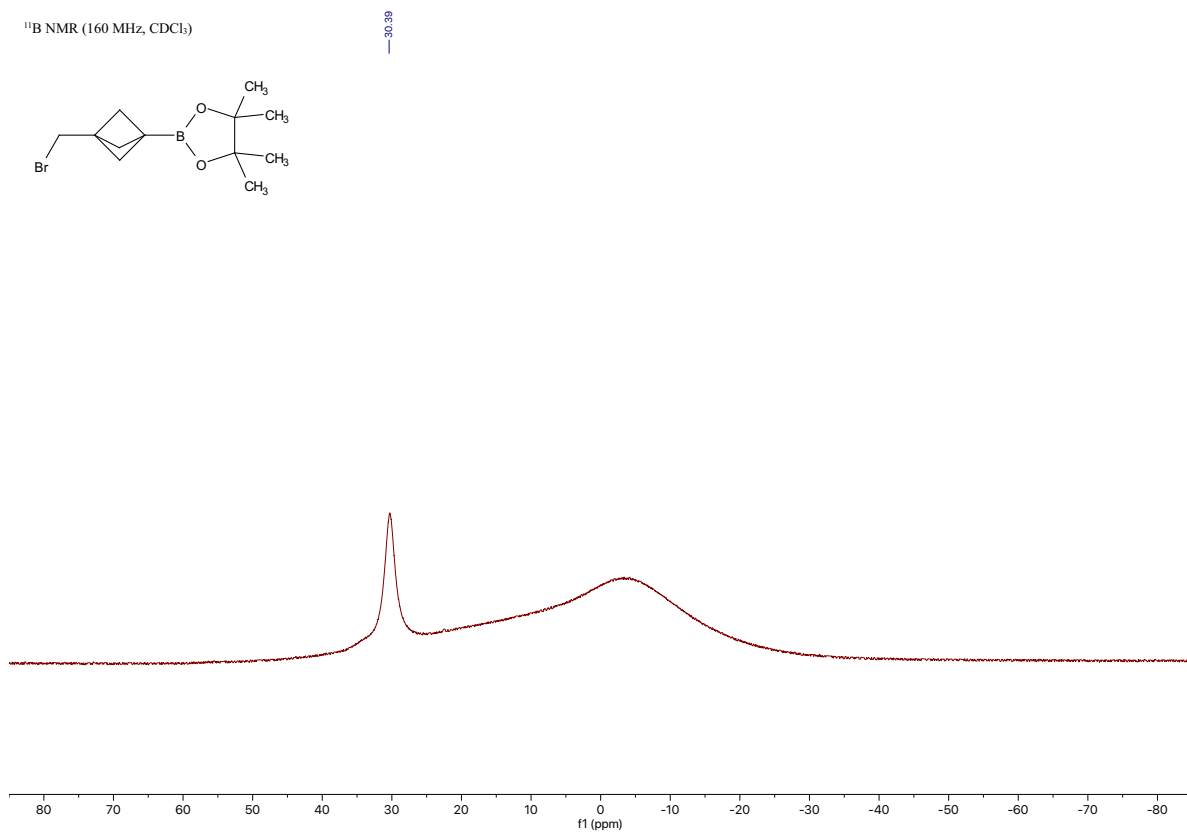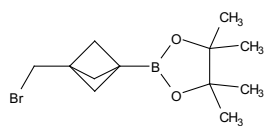
Compound 6a

(3-(4,4,5,5-tetramethyl-1,3,2-dioxaborolan-2-yl)bicyclo[1.1.1]pentan-1-yl)methanol
[Experimental]

¹H NMR (500 MHz, CDCl₃)

^{1}H NMR (500 MHz, CDCl$_3$)

¹³C NMR (126 MHz, CDCl₃)

¹¹B NMR (160 MHz, CDCl₃)

235
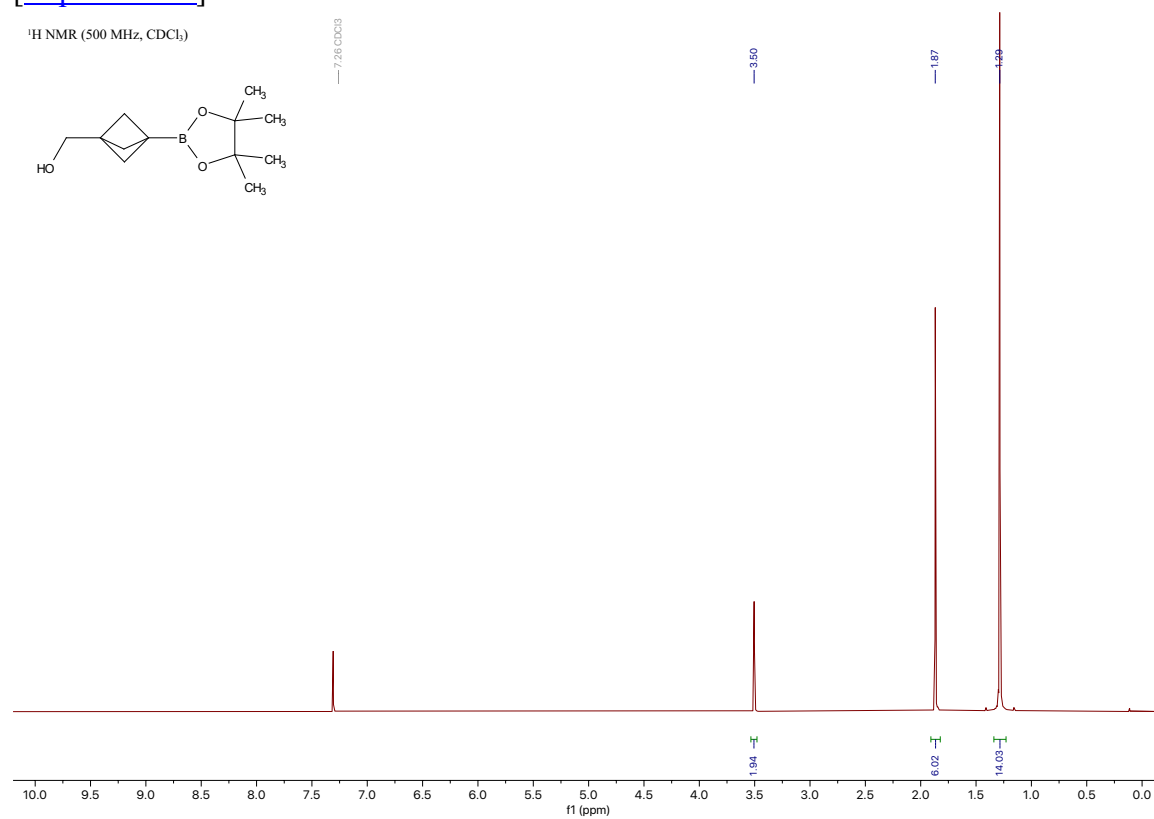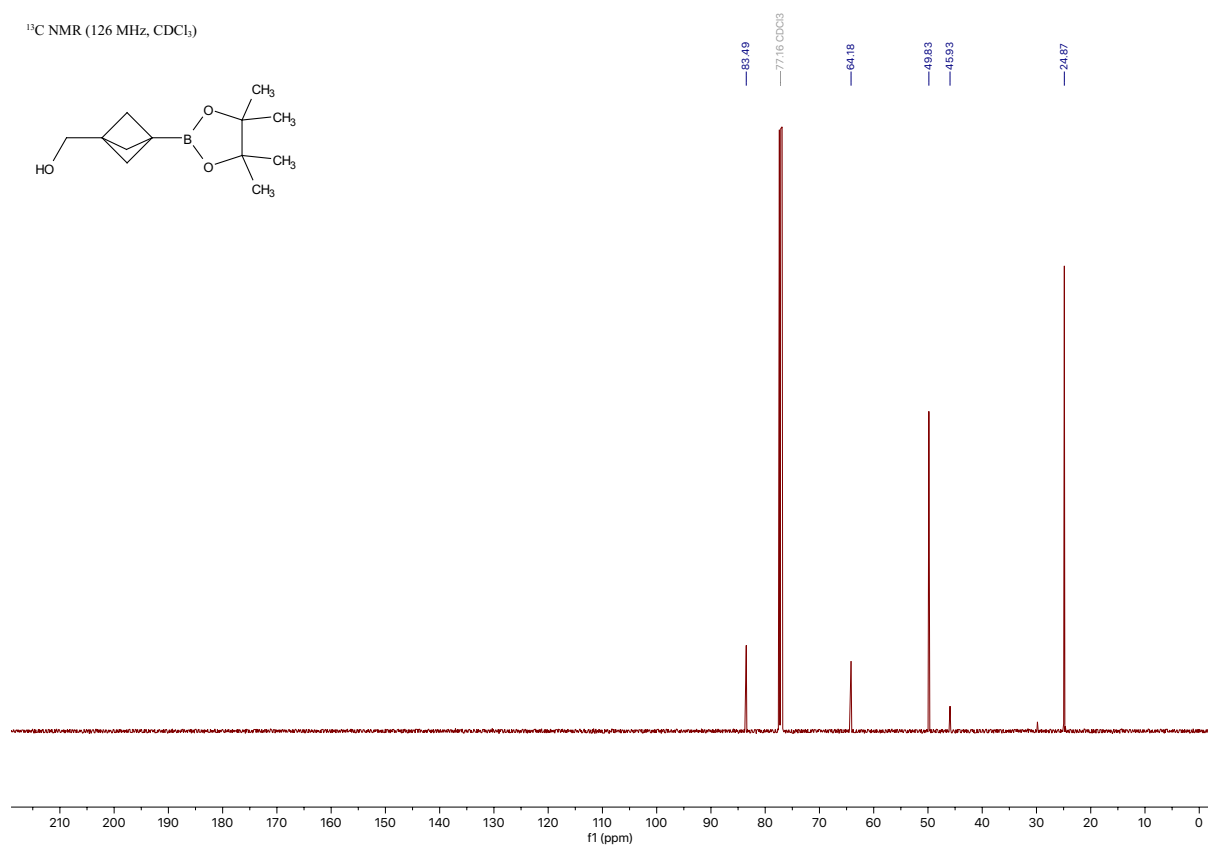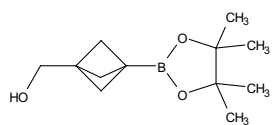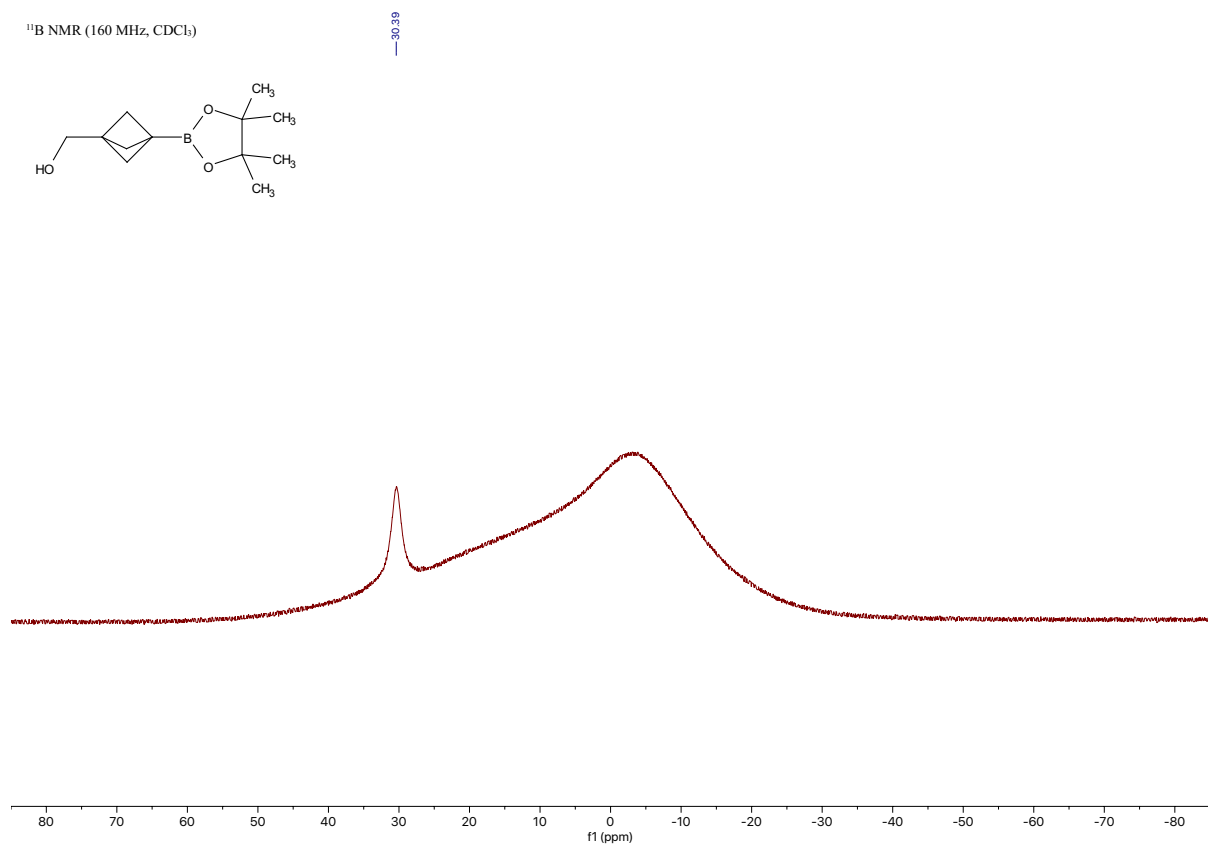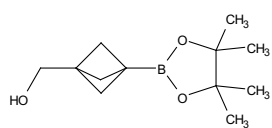
Compound 7a

2-(3-(4,4,5,5-tetramethyl-1,3,2-dioxaborolan-2-yl)bicyclo[1.1.1]pentan-1-yl)ethan-1-ol)
[Experimental]

¹H NMR (600 MHz, CDCl₃)

¹³C NMR (151 MHz, CDCl₃)

¹³C NMR (151 MHz, CDCl₃)

83.37
61.14
52.12
43.86
36.21
24.84

f1 (ppm)

¹¹B NMR (193 MHz, CDCl₃)

30.50

f1 (ppm)
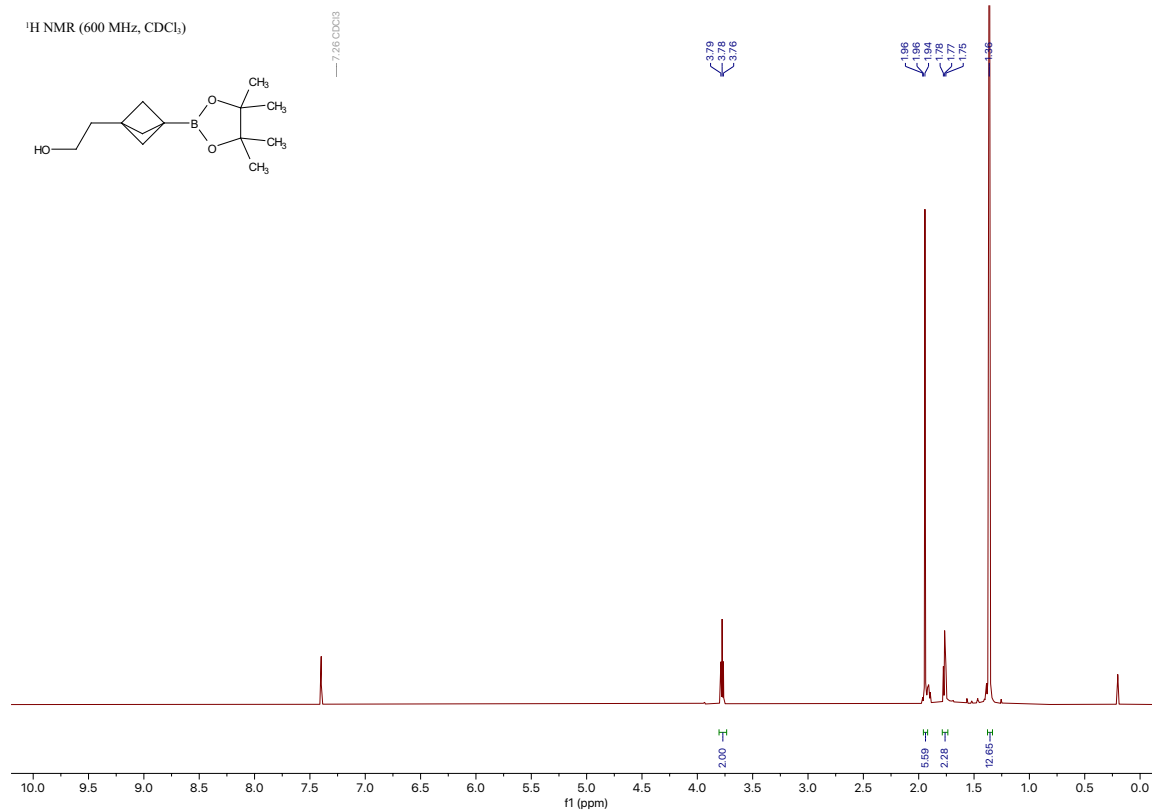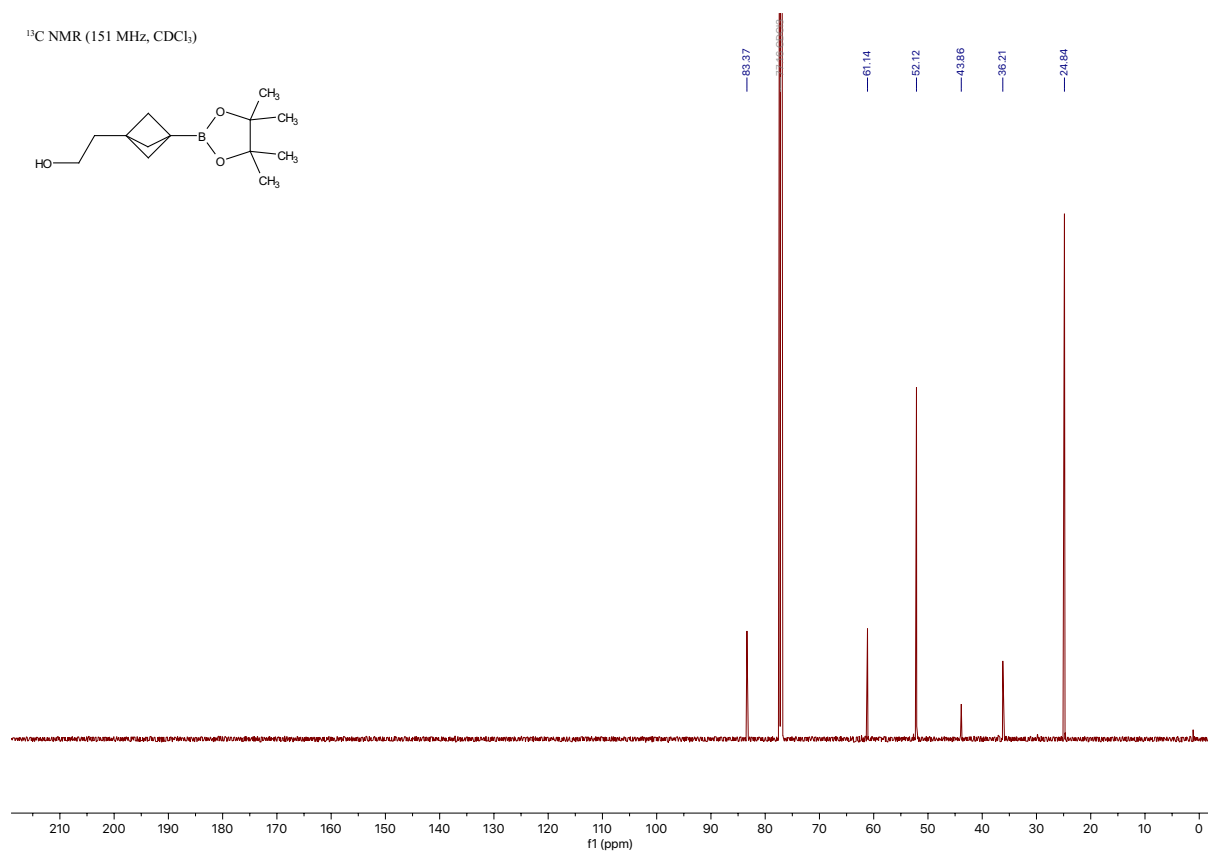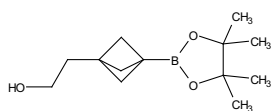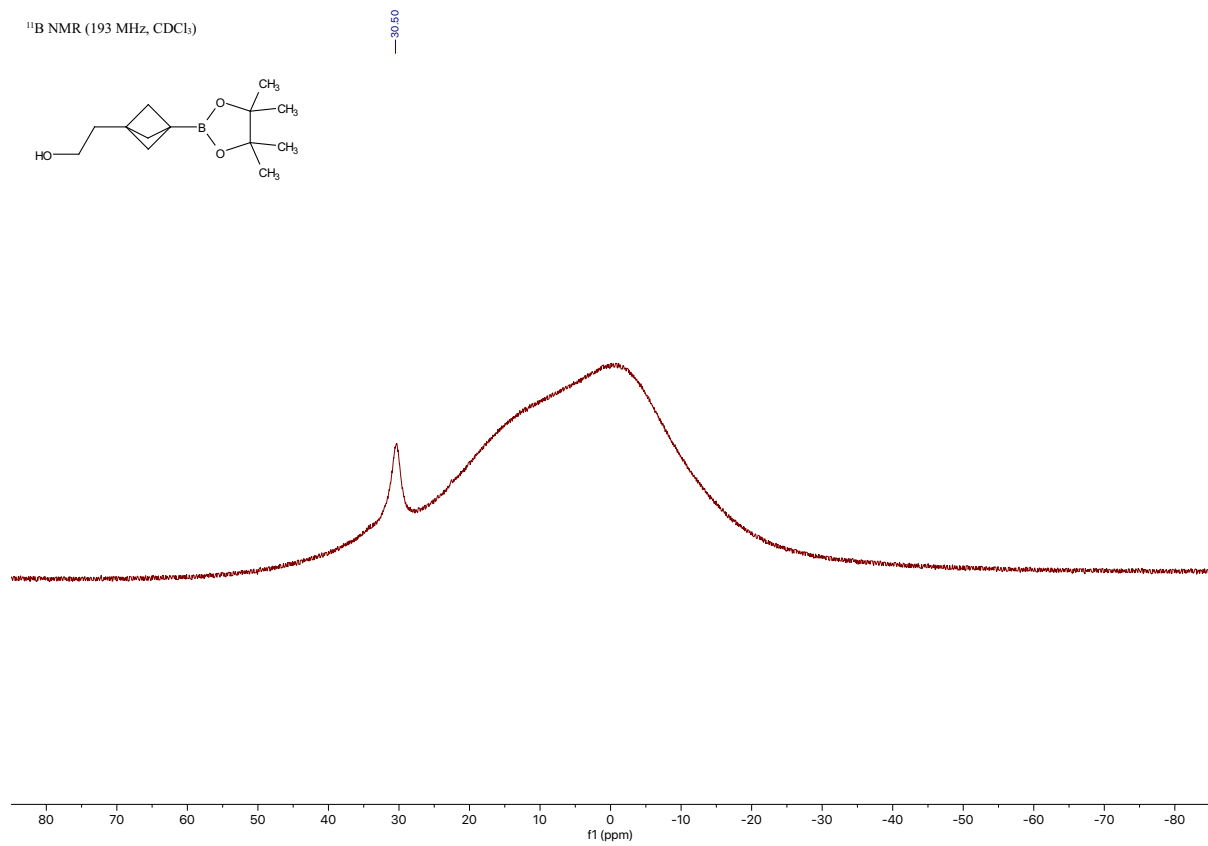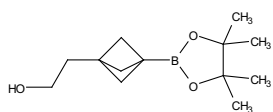
Compound 8a

tert-butyl 3-(4,4,5,5-tetramethyl-1,3,2-dioxaborolan-2-yl)bicyclo[1.1.1]pentane-1-carboxylate) [Experimental]

¹H NMR (600 MHz, CDCl₃)

¹³C NMR (151 MHz, CDCl₃)

¹¹B NMR (193 MHz, CDCl₃)

239
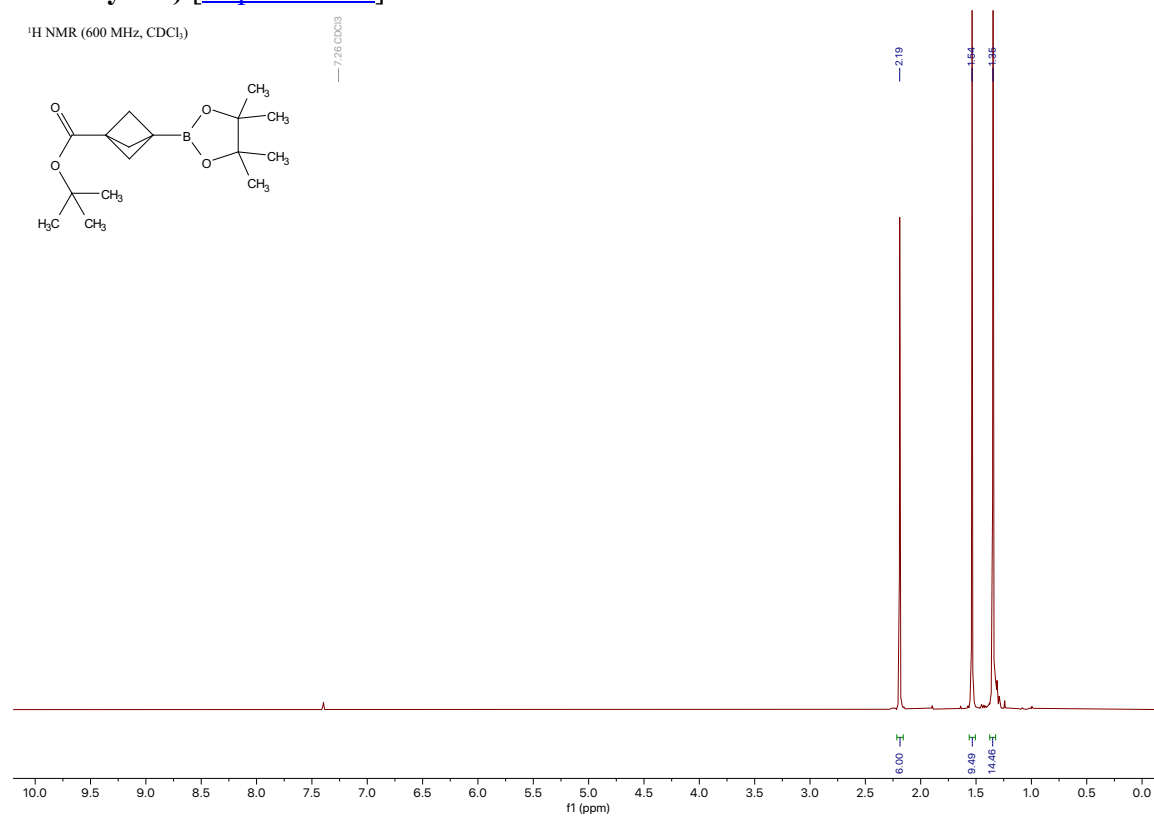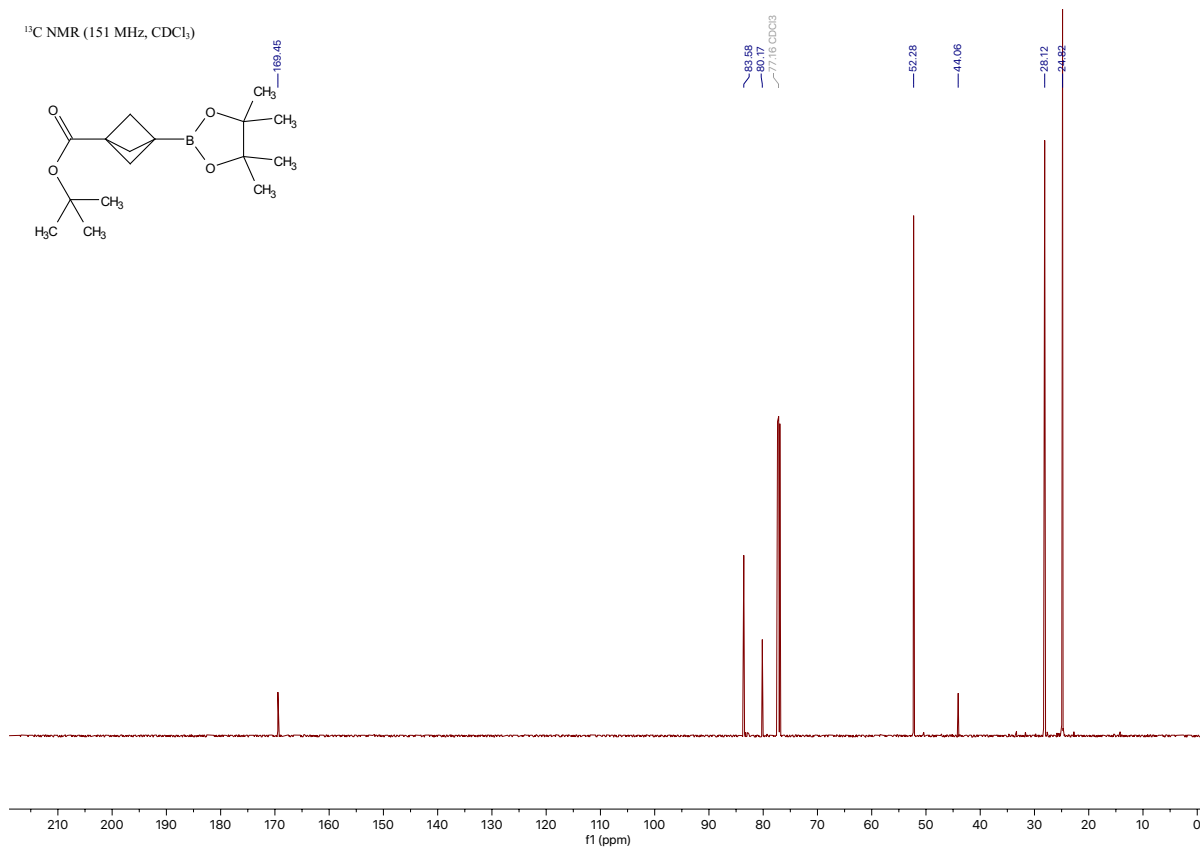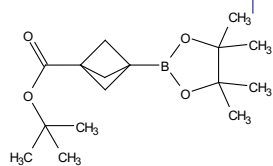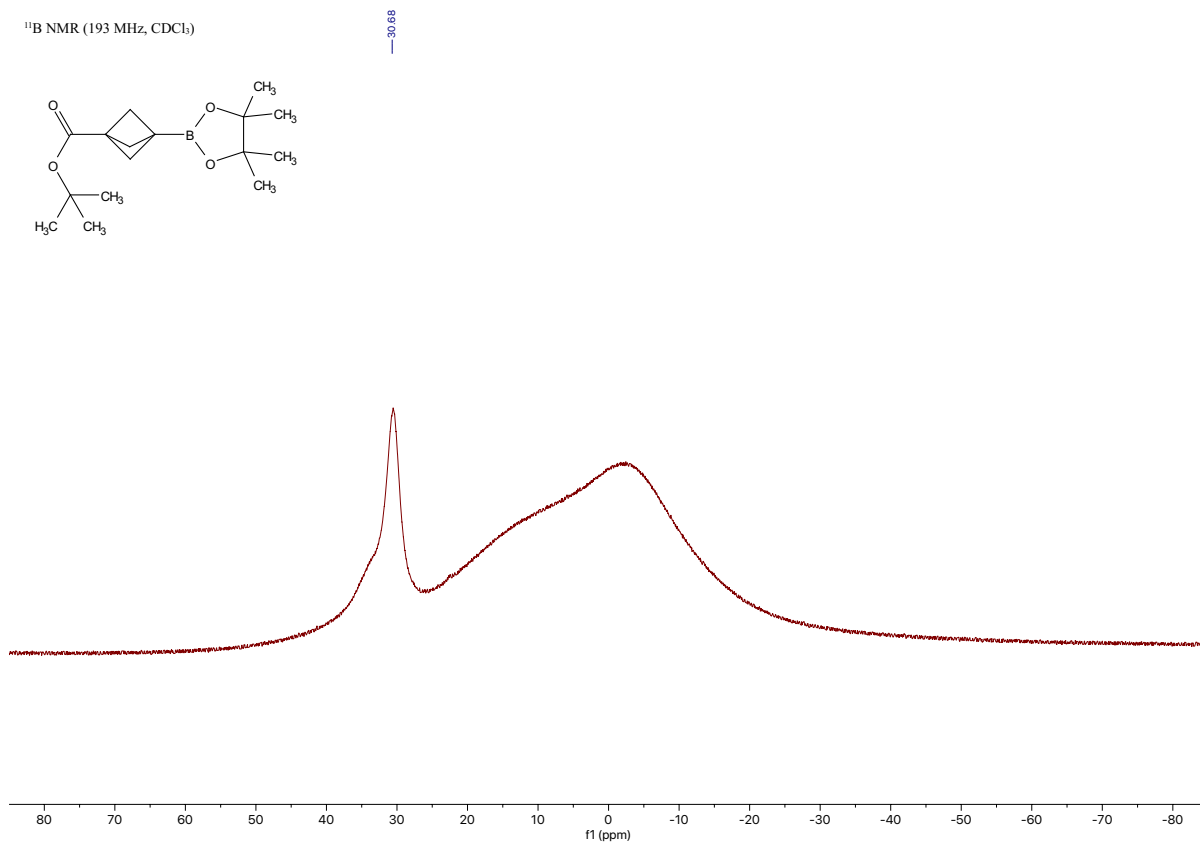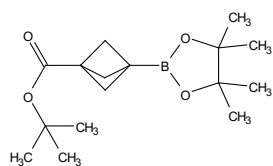
Compound 9a

tert-butyl 2-(3-(4,4,5,5-tetramethyl-1,3,2-dioxaborolan-2-yl)bicyclo[1.1.1]pentan-1-yl)acetate [Experimental]

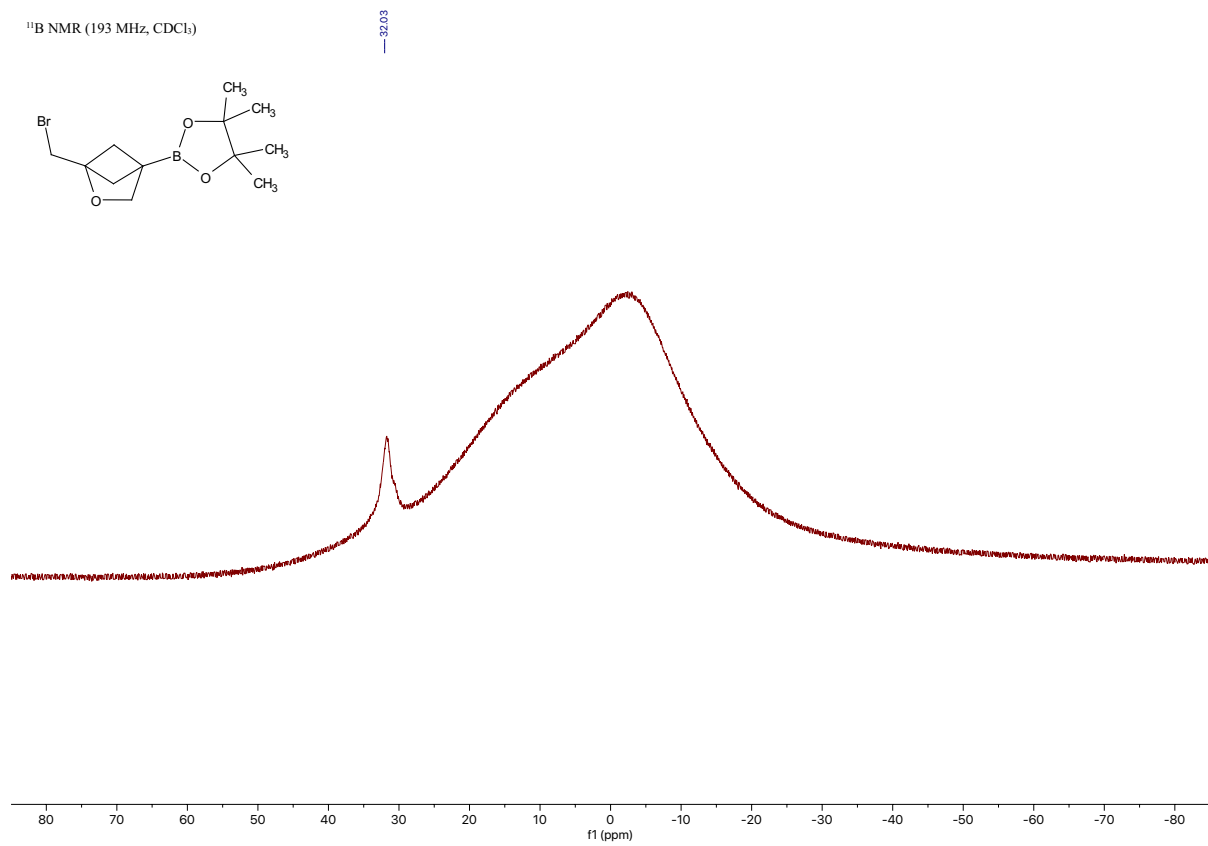
¹H NMR (500 MHz, CDCl₃)

¹³C NMR (126 MHz, CDCl₃)

13C NMR (126 MHz, CDCl3)

11B NMR (160 MHz, CDCl3)

241
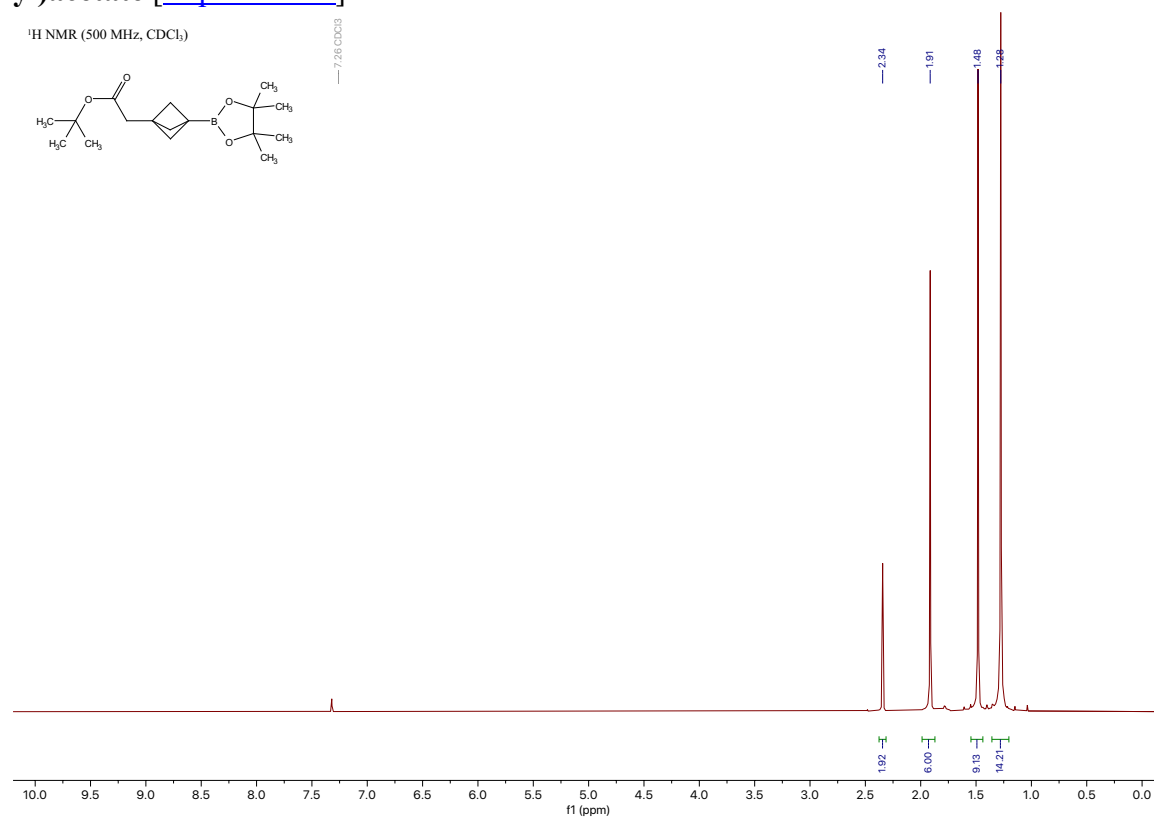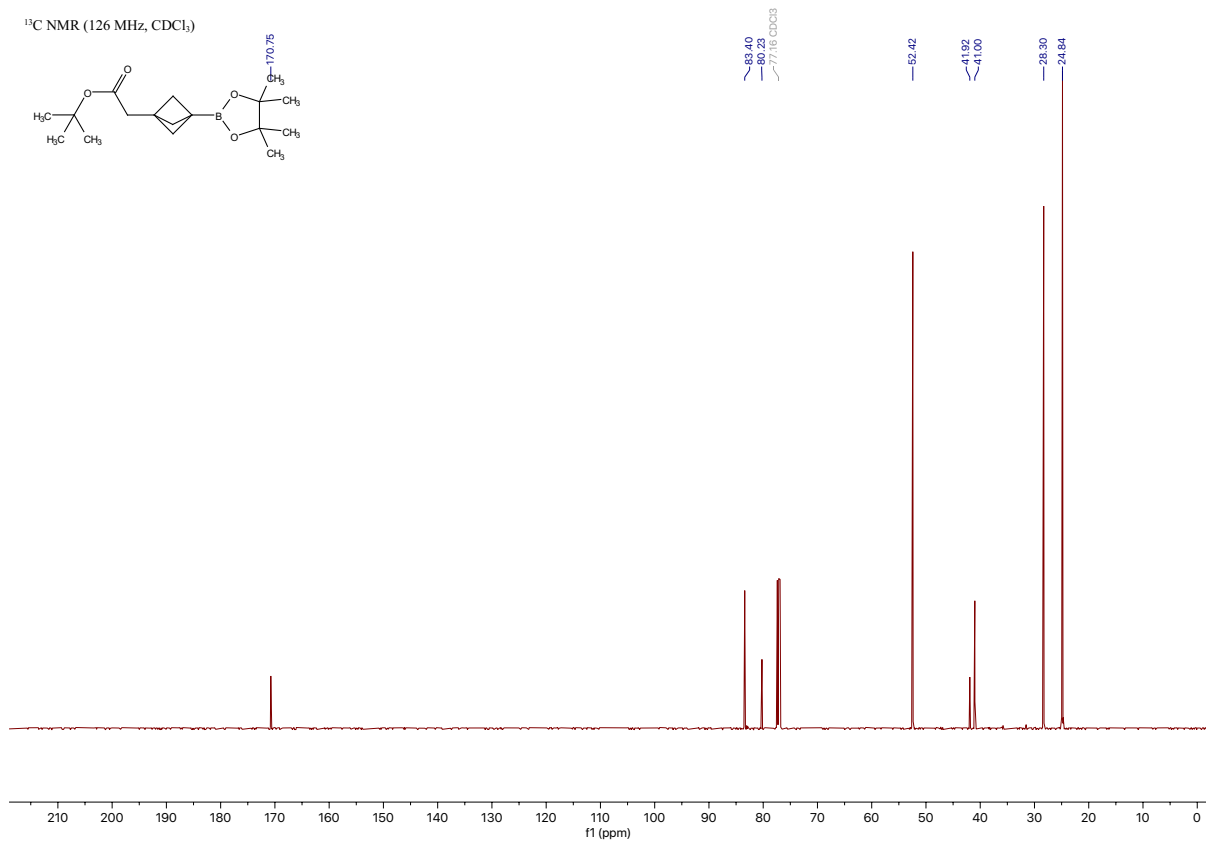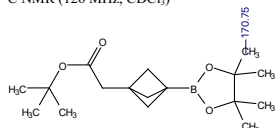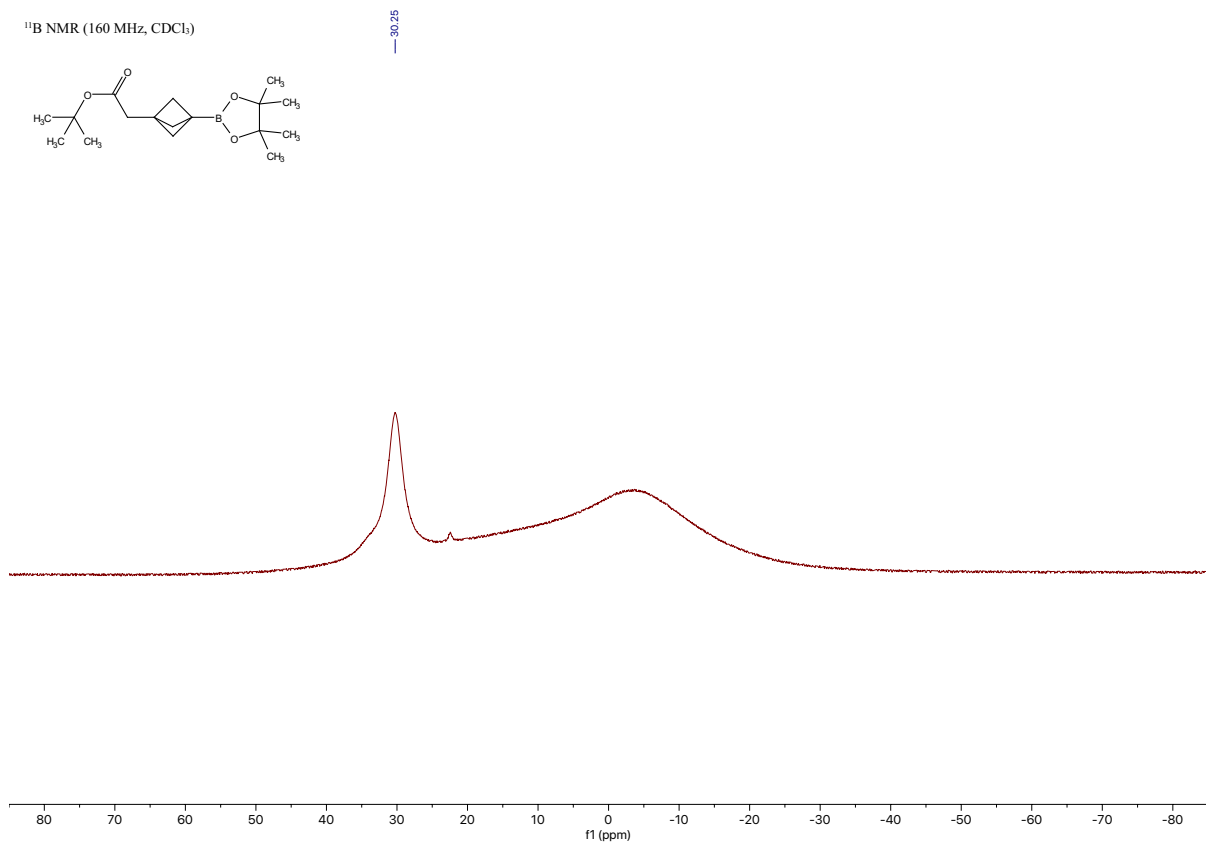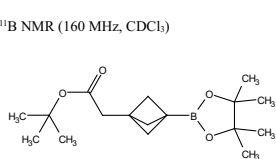
Compound 10a

tert-butyl 2,2-difluoro-2-(3-(4,4,5,5-tetramethyl-1,3,2-dioxaborolan-2-yl)bicyclo[1.1.1]pentan-1-yl)acetate [Experimental]
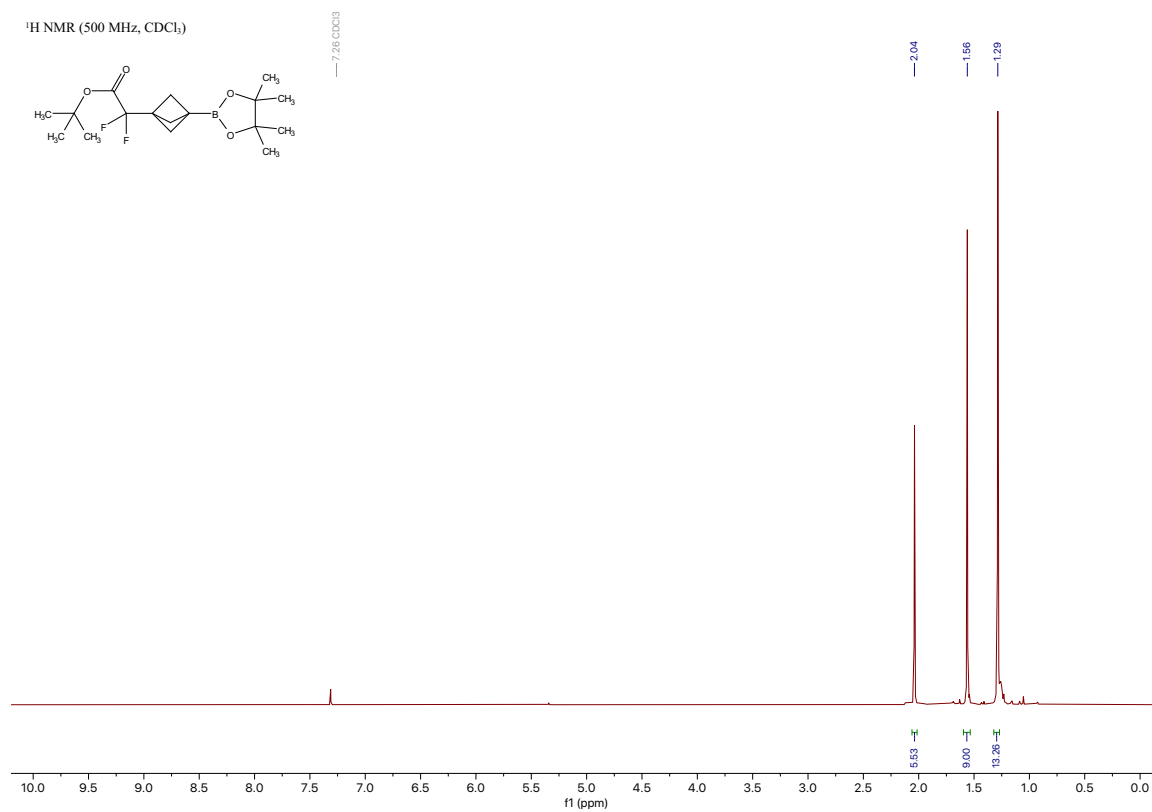
¹H NMR (500 MHz, CDCl₃)

¹³C NMR (126 MHz, CDCl₃)
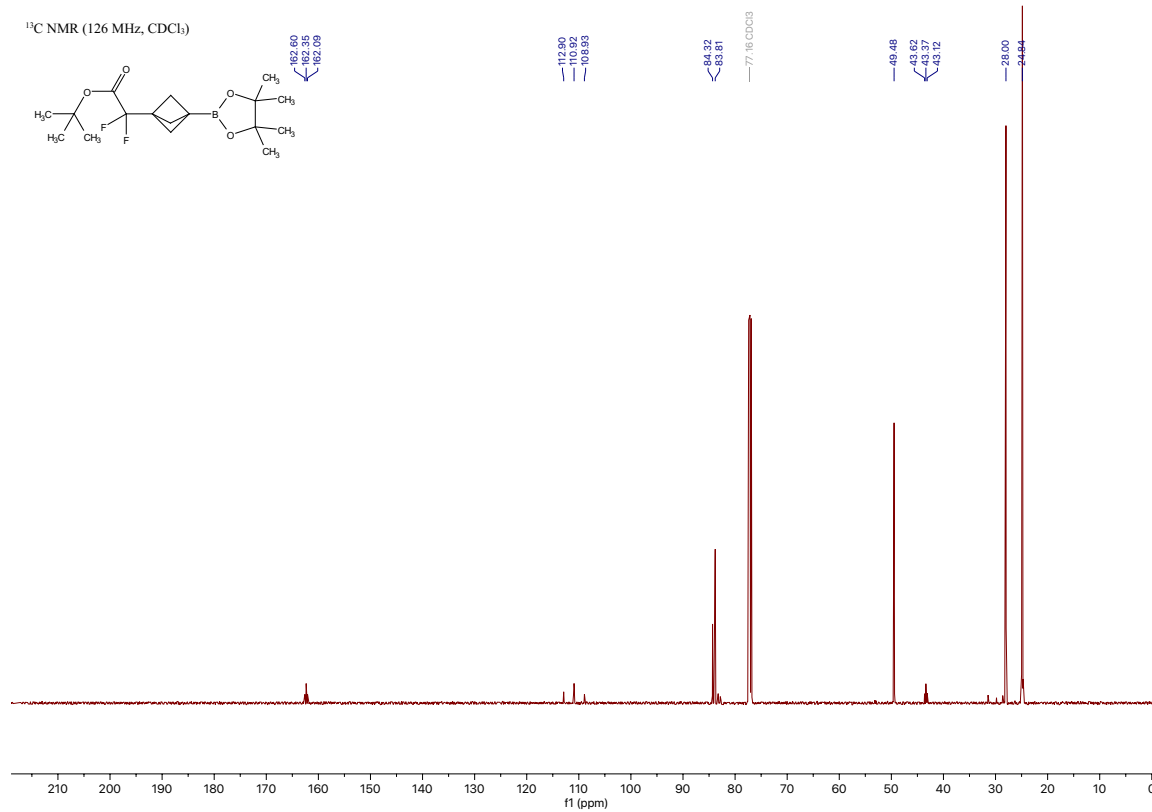
^{11}B NMR (160 MHz, CDCl$_3$)
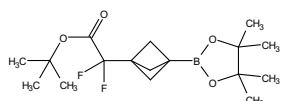
30.33
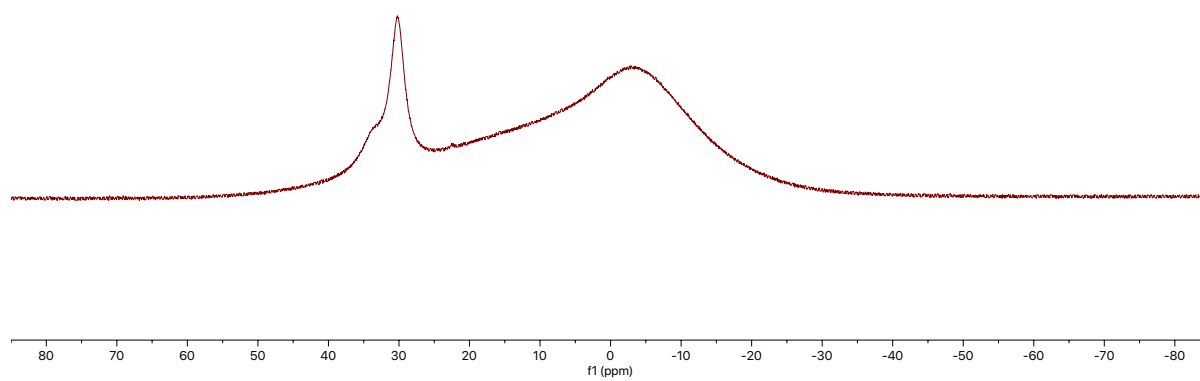
^{19}F NMR (470 MHz, CDCl$_3$)

-113.44

243
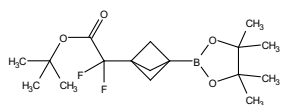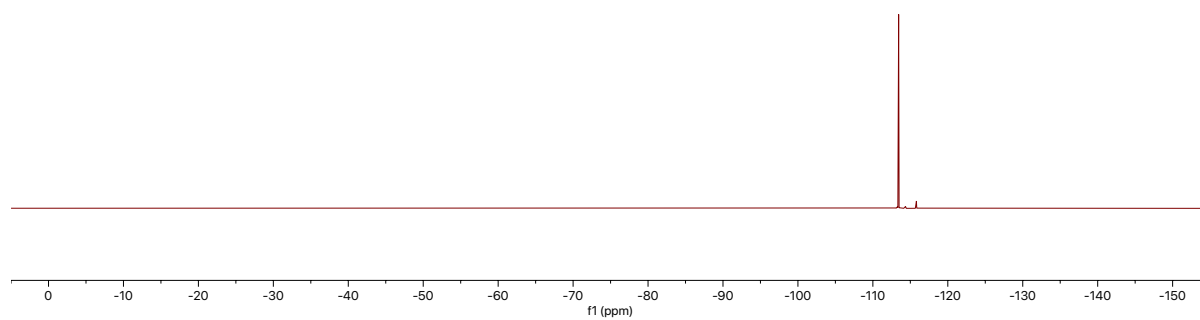
Compound 11a

4,4,5,5-tetramethyl-2-(3-(methylsulfonyl)bicyclo[1.1.1]pentan-1-yl)-1,3,2-dioxaborolane
[Experimental]
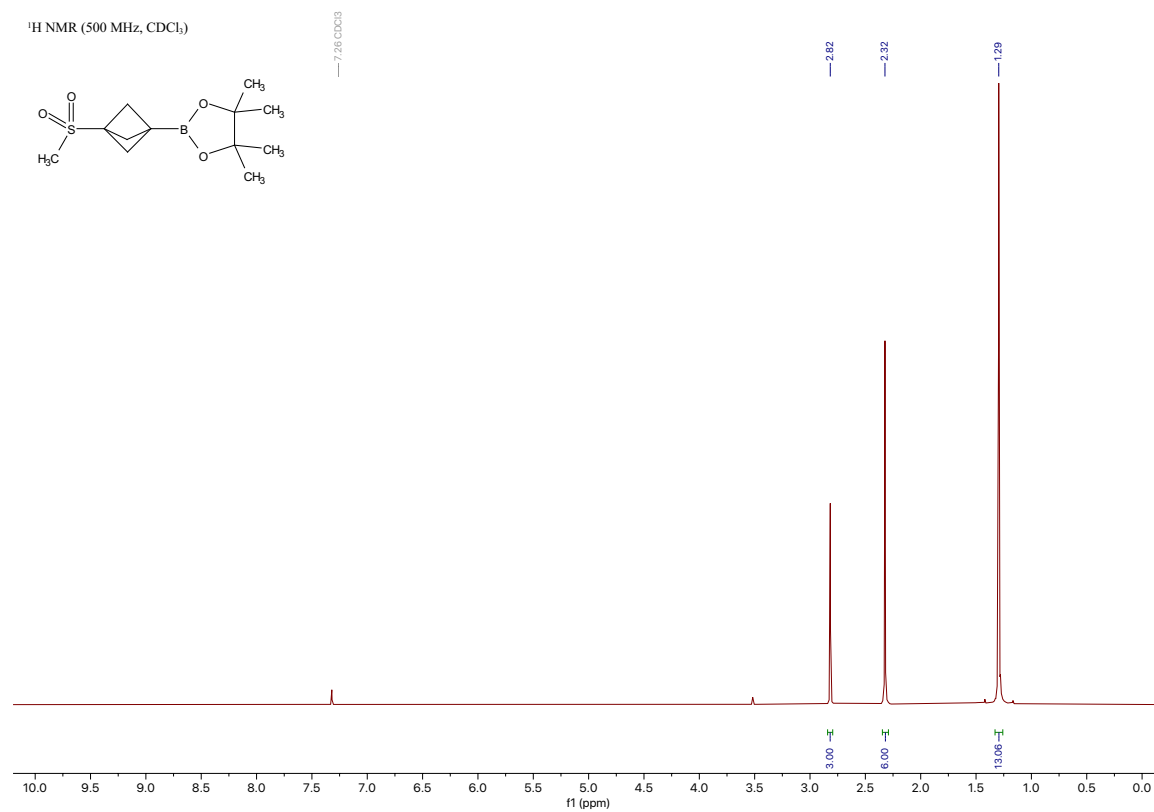
¹H NMR (500 MHz, CDCl₃)

¹³C NMR (126 MHz, CDCl₃)
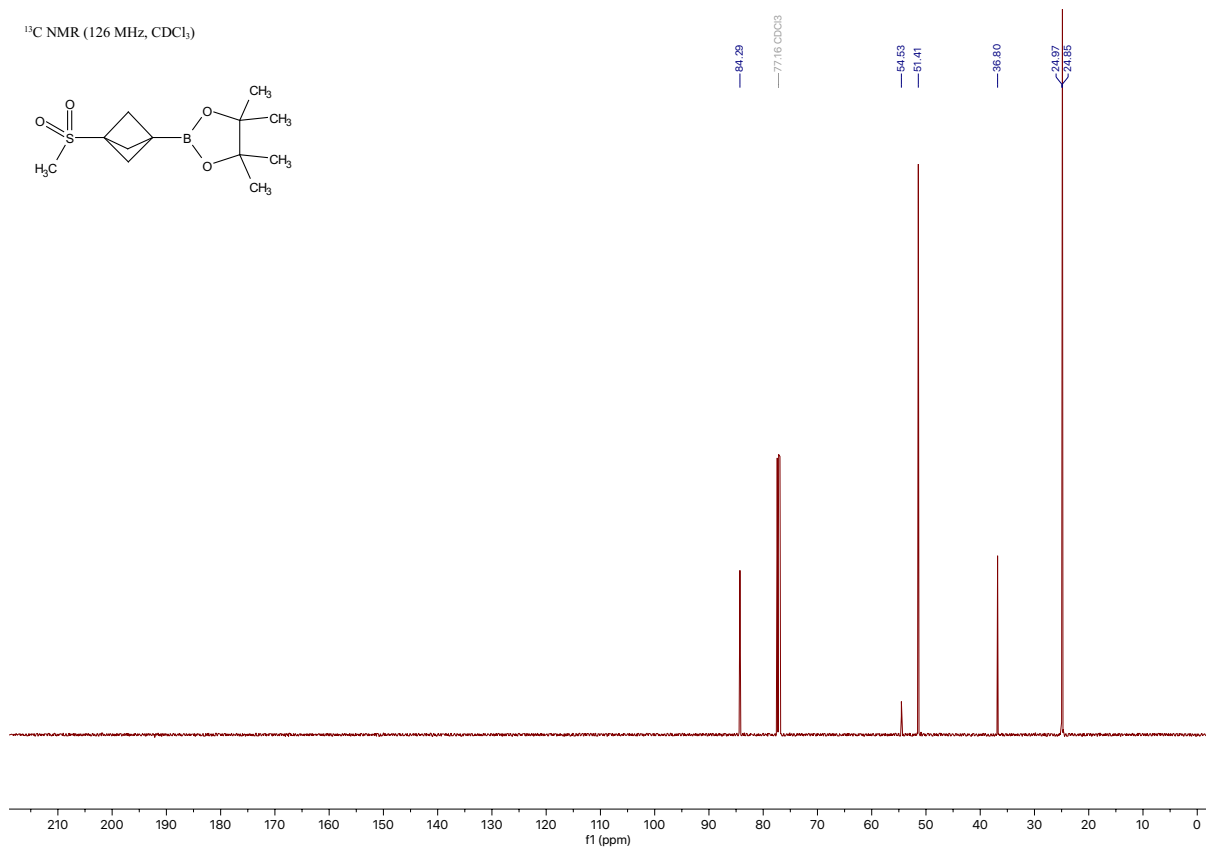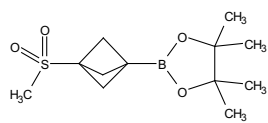
¹¹B NMR (160 MHz, CDCl₃)
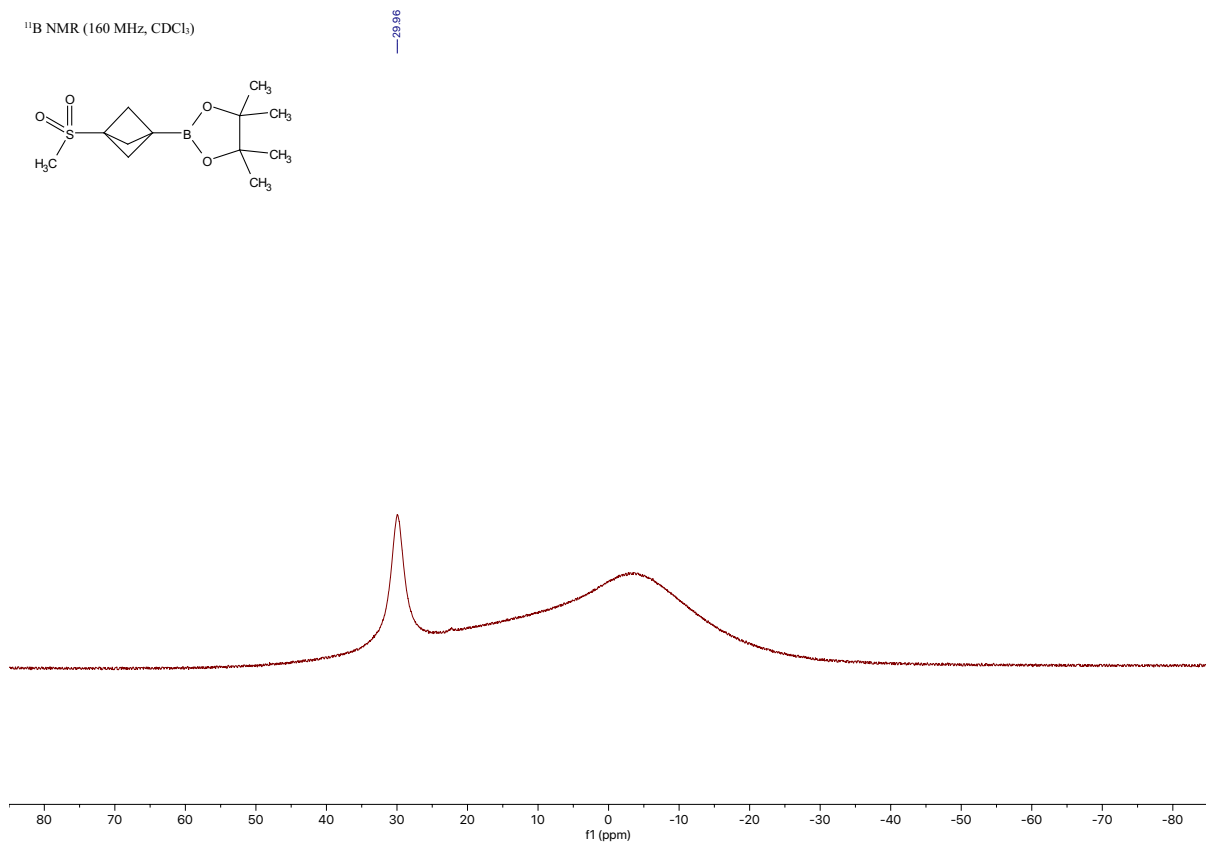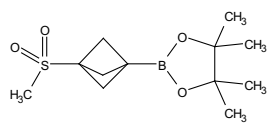
Compound 12a

3-(4,4,5,5-tetramethyl-1,3,2-dioxaborolan-2-yl)bicyclo[1.1.1]pentane-1-sulfonamide

[Experimental]

¹H NMR (500 MHz, DMSO)
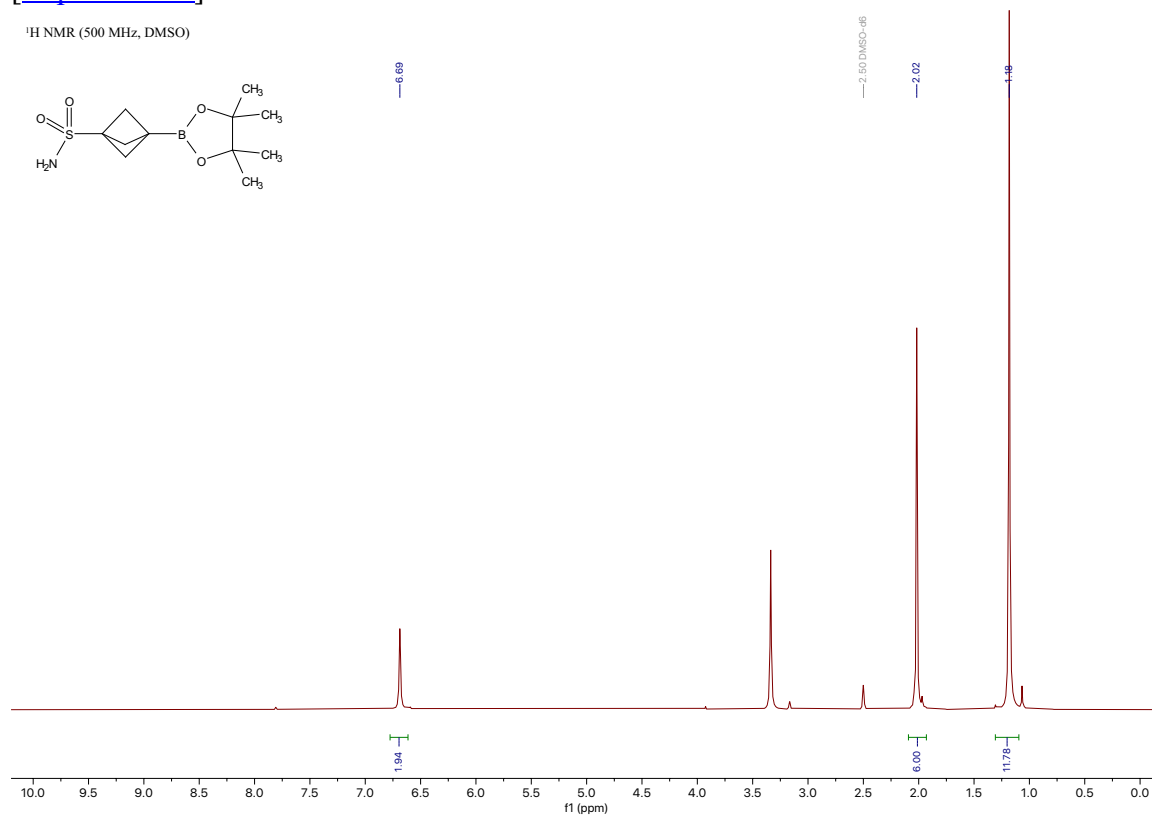
¹³C NMR (126 MHz, DMSO)

¹¹B NMR (160 MHz, DMSO)

247
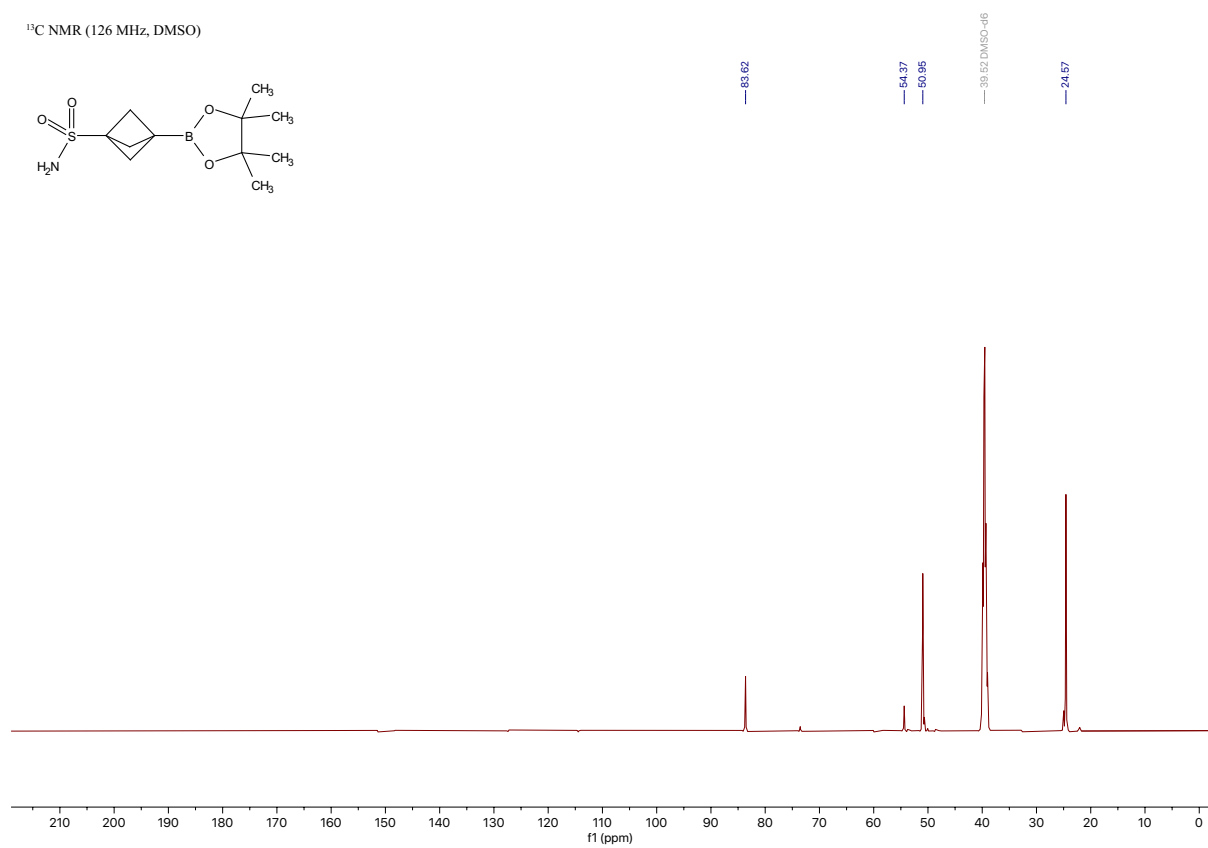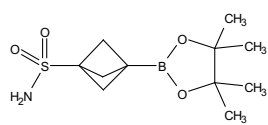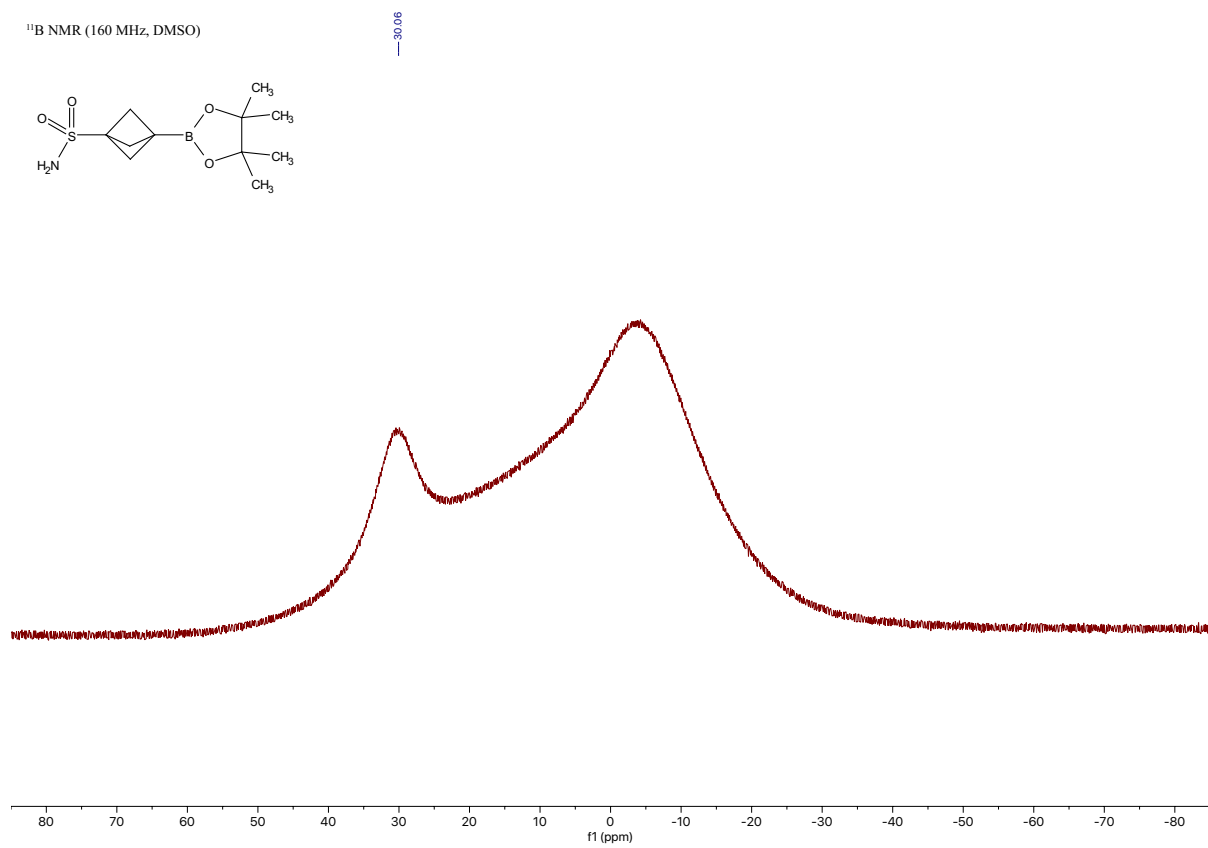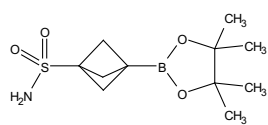
Compound 13a

1-((3-(4,4,5,5-tetramethyl-1,3,2-dioxaborolan-2-yl)bicyclo[1.1.1]pentan-1-yl)sulfonyl)piperidine [Experimental]

¹H NMR (500 MHz, CDCl₃)

¹³C NMR (126 MHz, CDCl₃)

¹¹B NMR (160 MHz, CDCl₃)

249
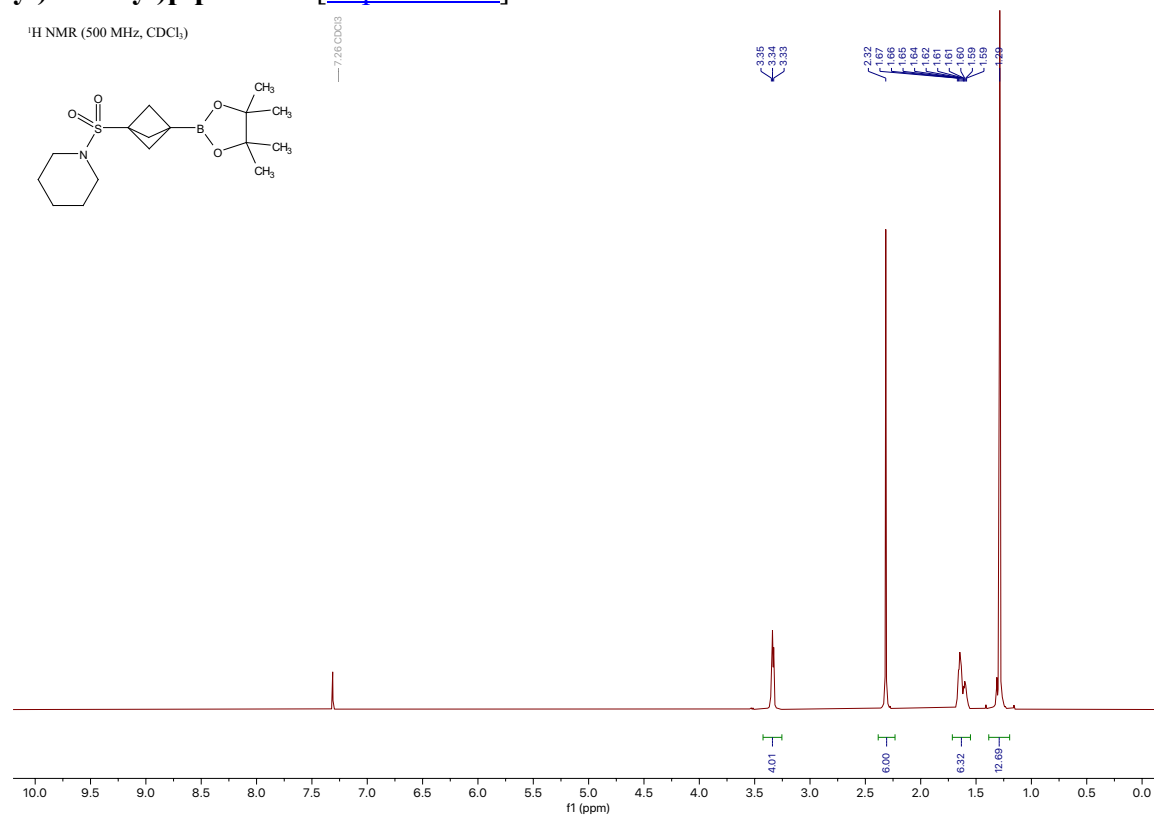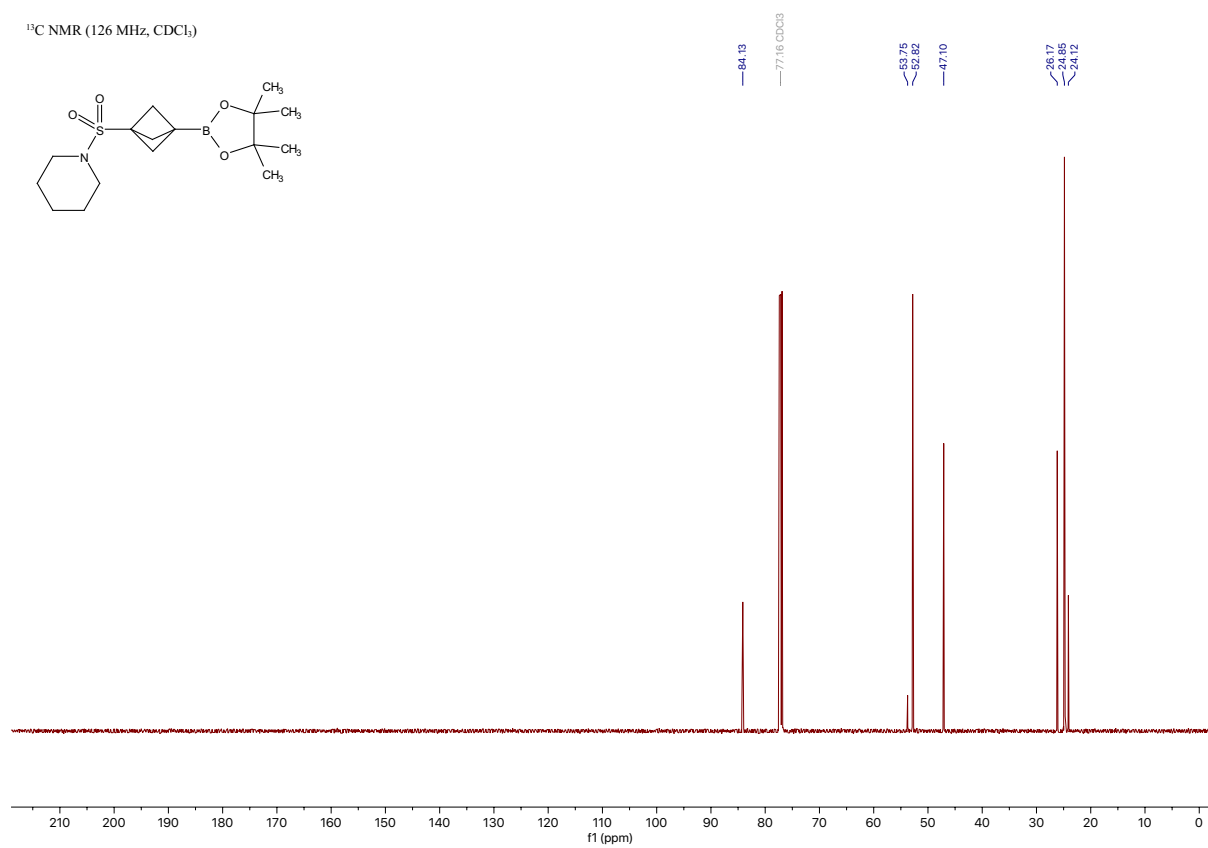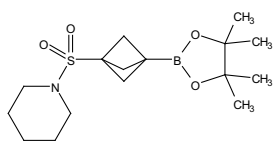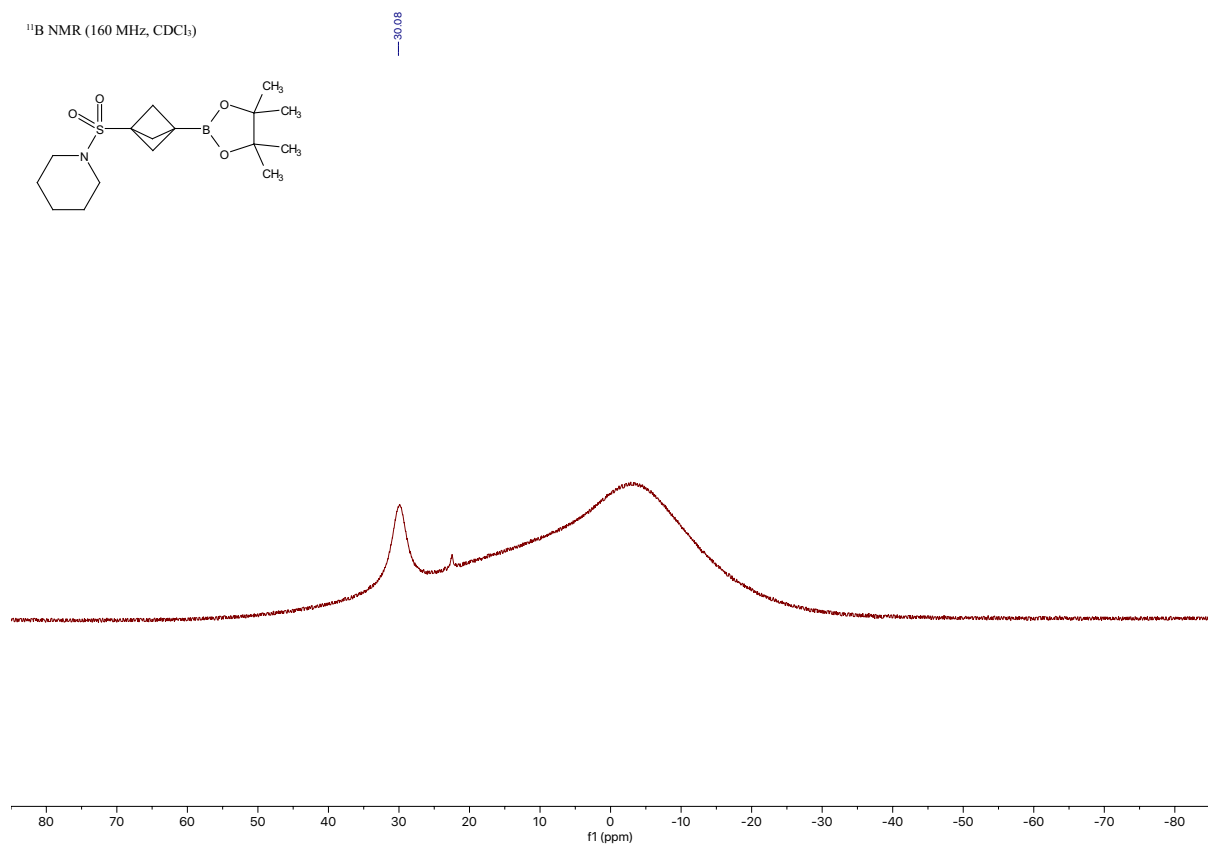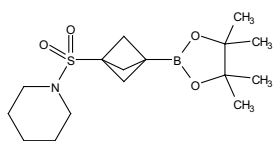
Compound 14a

4-((3-(4,4,5,5-tetramethyl-1,3,2-dioxaborolan-2-yl)bicyclo[1.1.1]pentan-1-yl)sulfonyl)morpholine [Experimental]
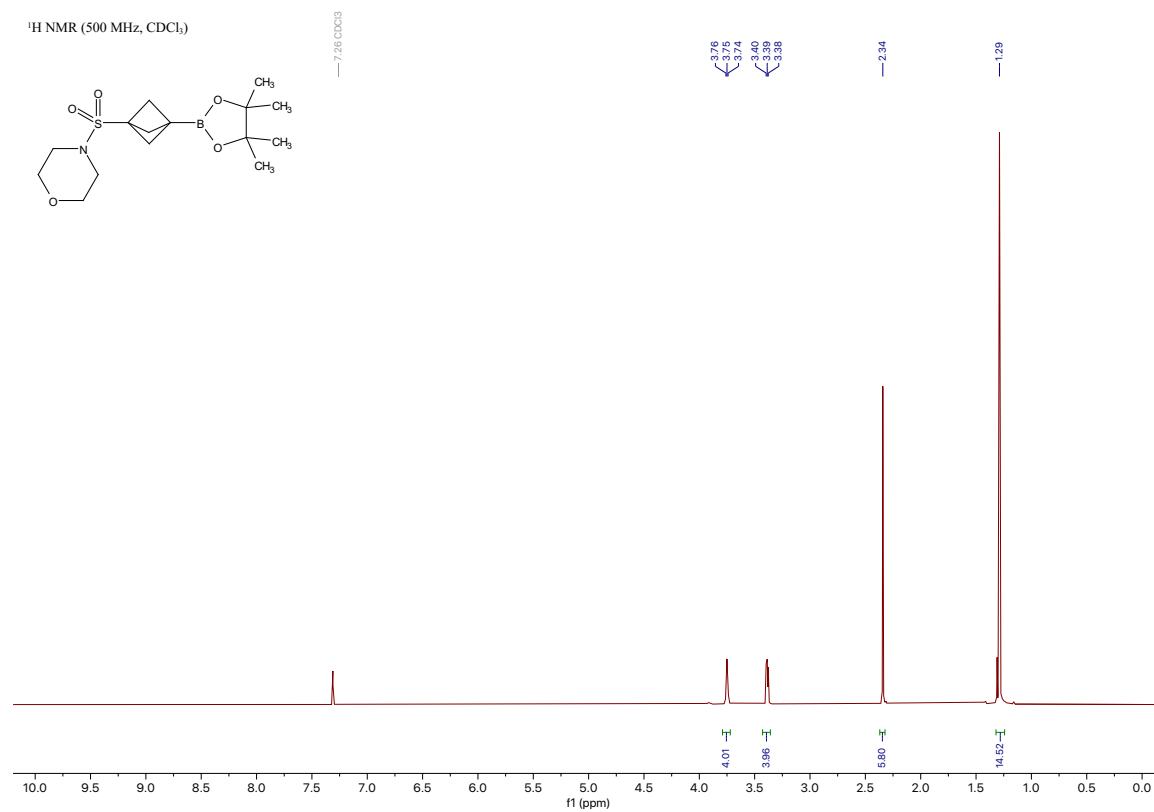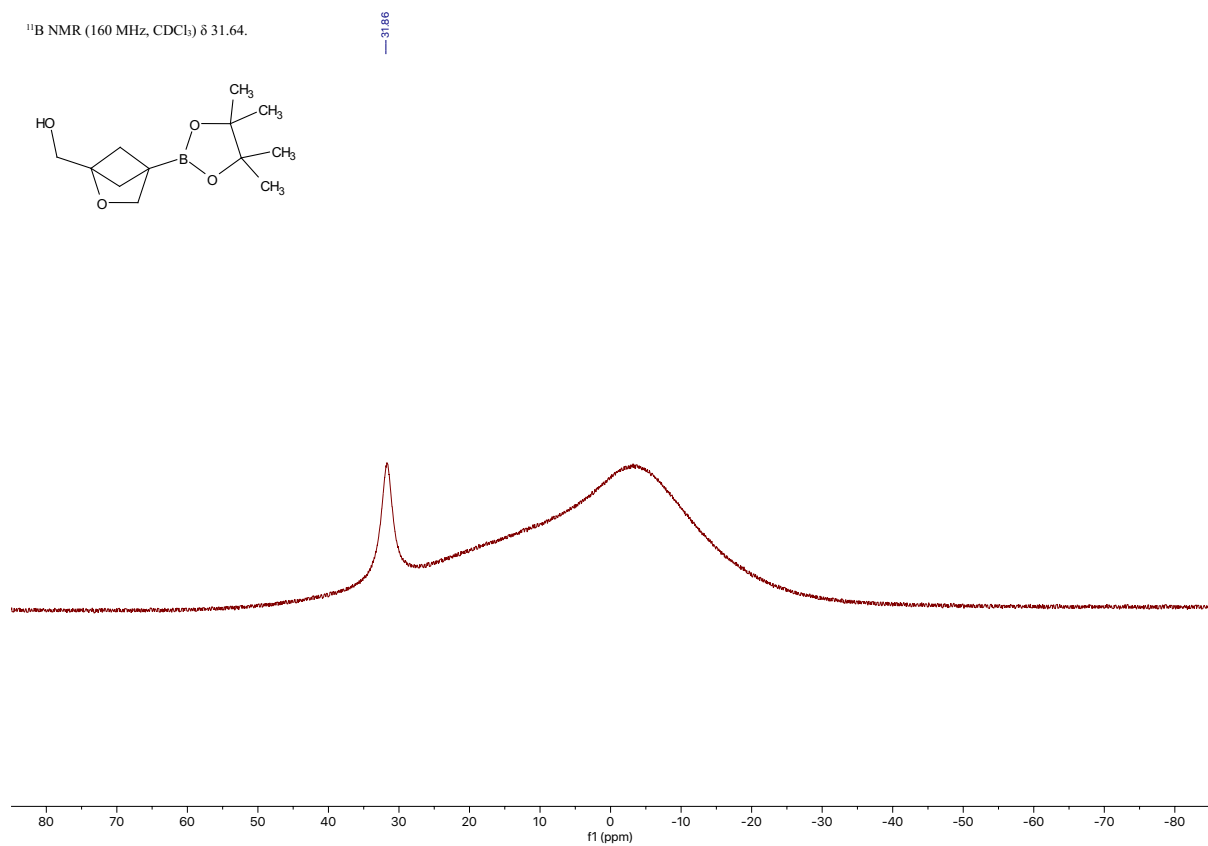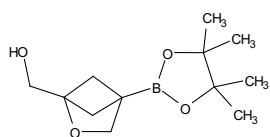
¹H NMR (500 MHz, CDCl₃)

^{13}C NMR (126 MHz, CDCl$_3$)
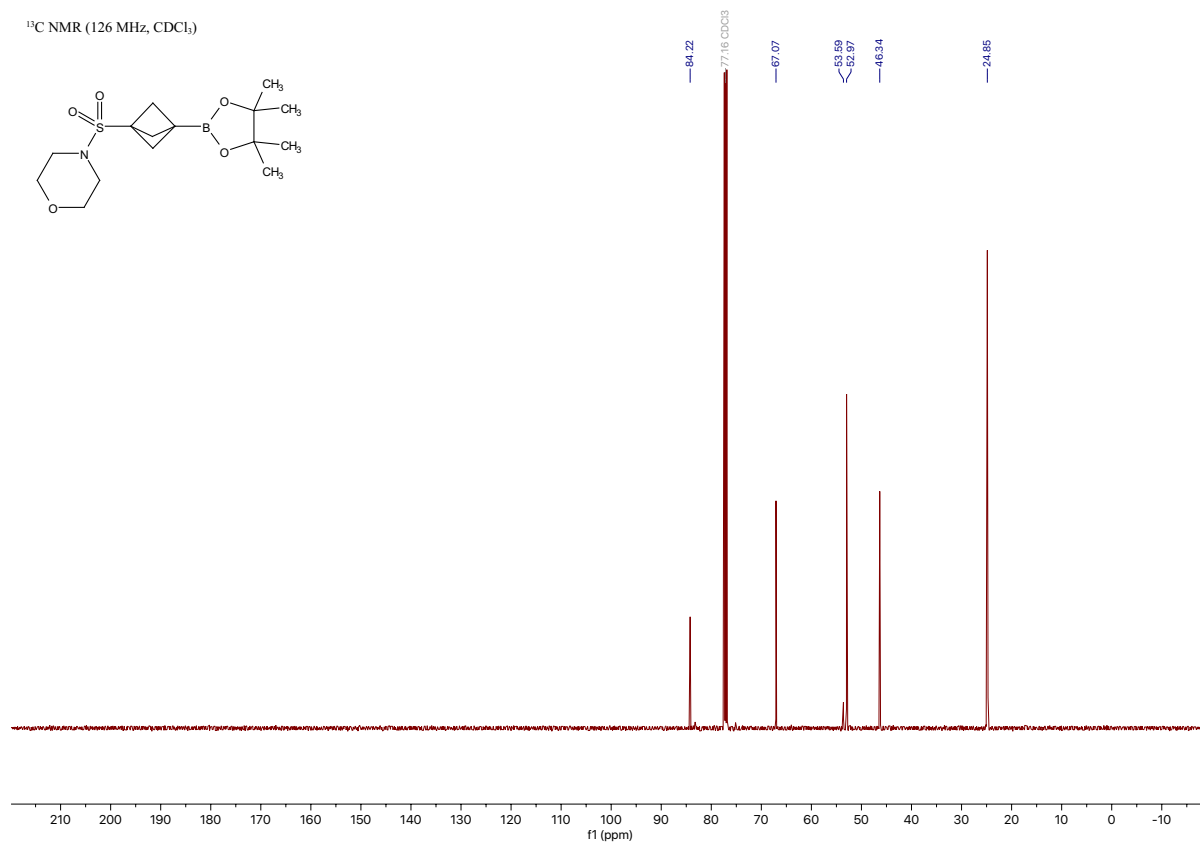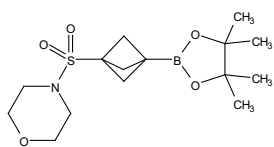
^{11}B NMR (160 MHz, CDCl$_3$)
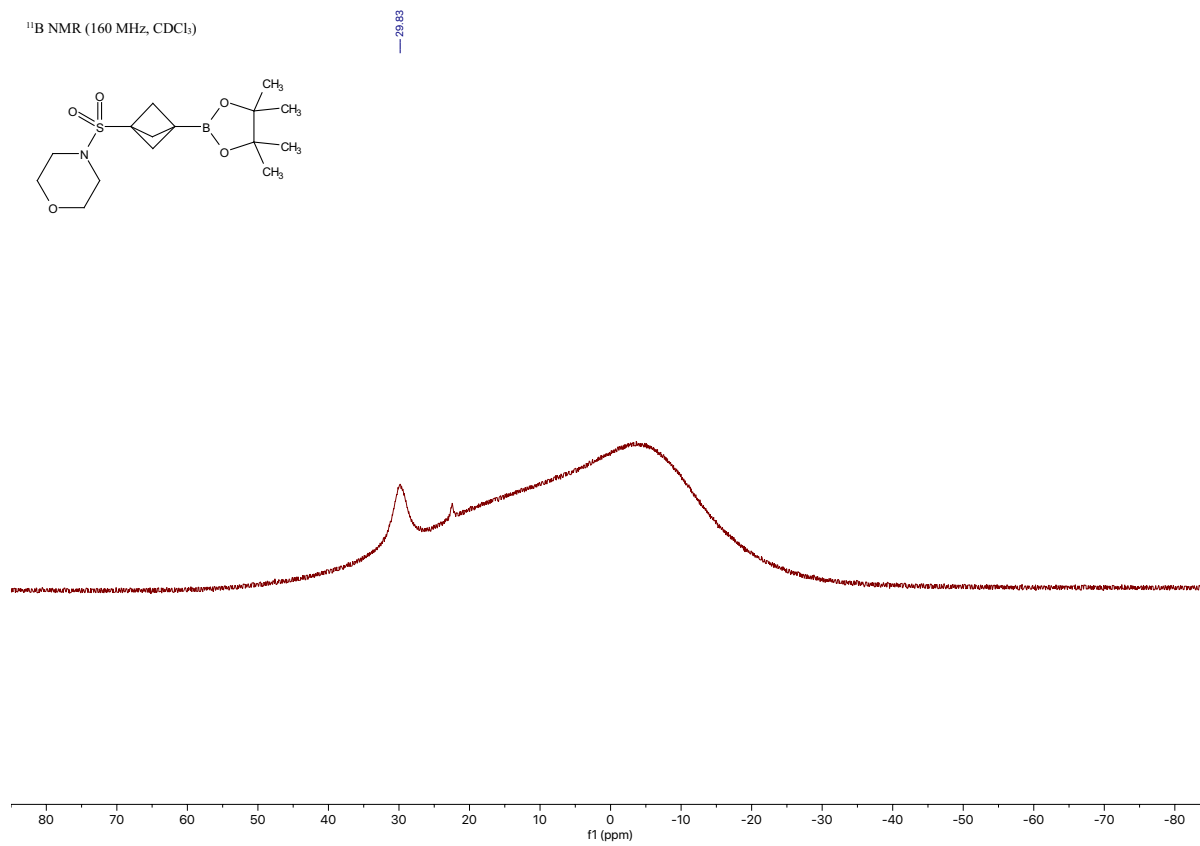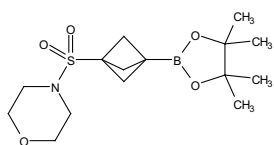
Compound 15a

2-(3-(4,4,5,5-tetramethyl-1,3,2-dioxaborolan-2-yl)bicyclo[1.1.1]pentan-1-yl)hexahydro-1*H*-4,7-methanoisoindole-1,3(2*H*)-dione [Experimental]

¹H NMR (500 MHz, CDCl₃)

^{13}C NMR (126 MHz, CDCl$_3$)

178.67

83.71
77.16 CDCl3
54.61
48.83
47.54
42.00
39.49
24.84
24.81

^{11}B NMR (160 MHz, CDCl$_3$)

30.61
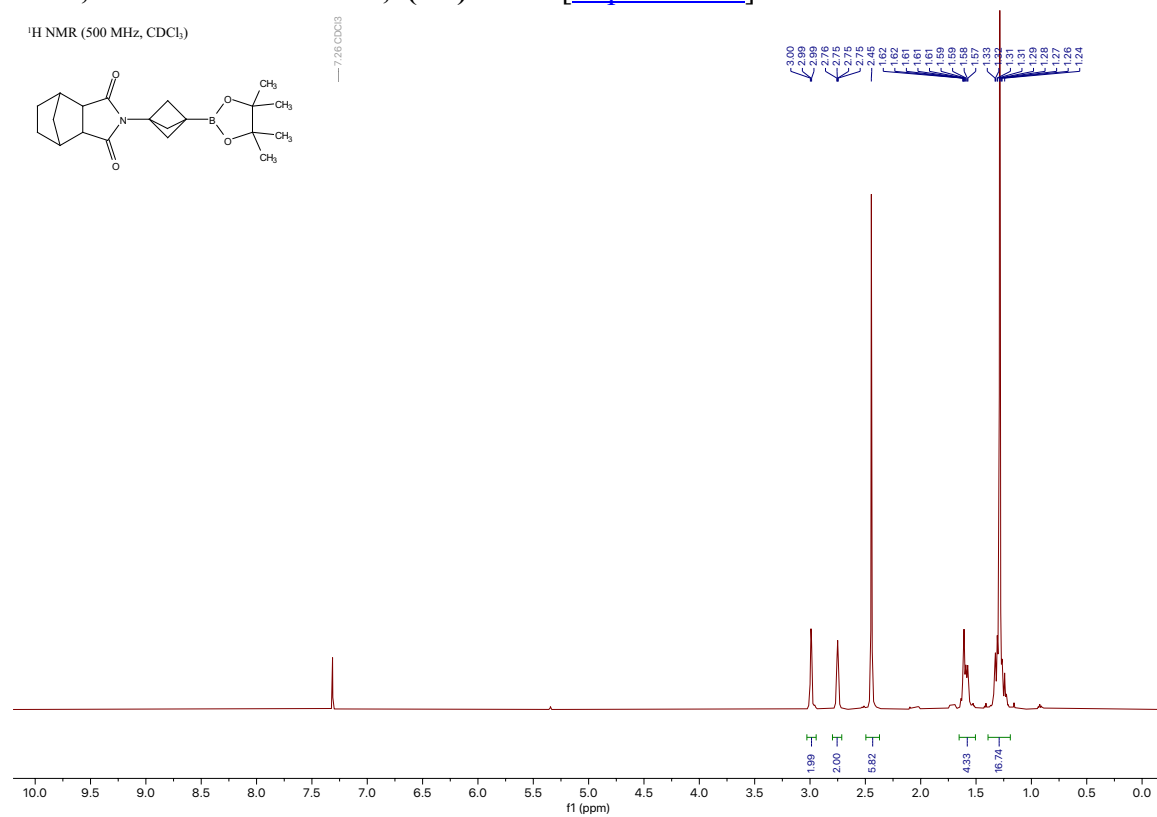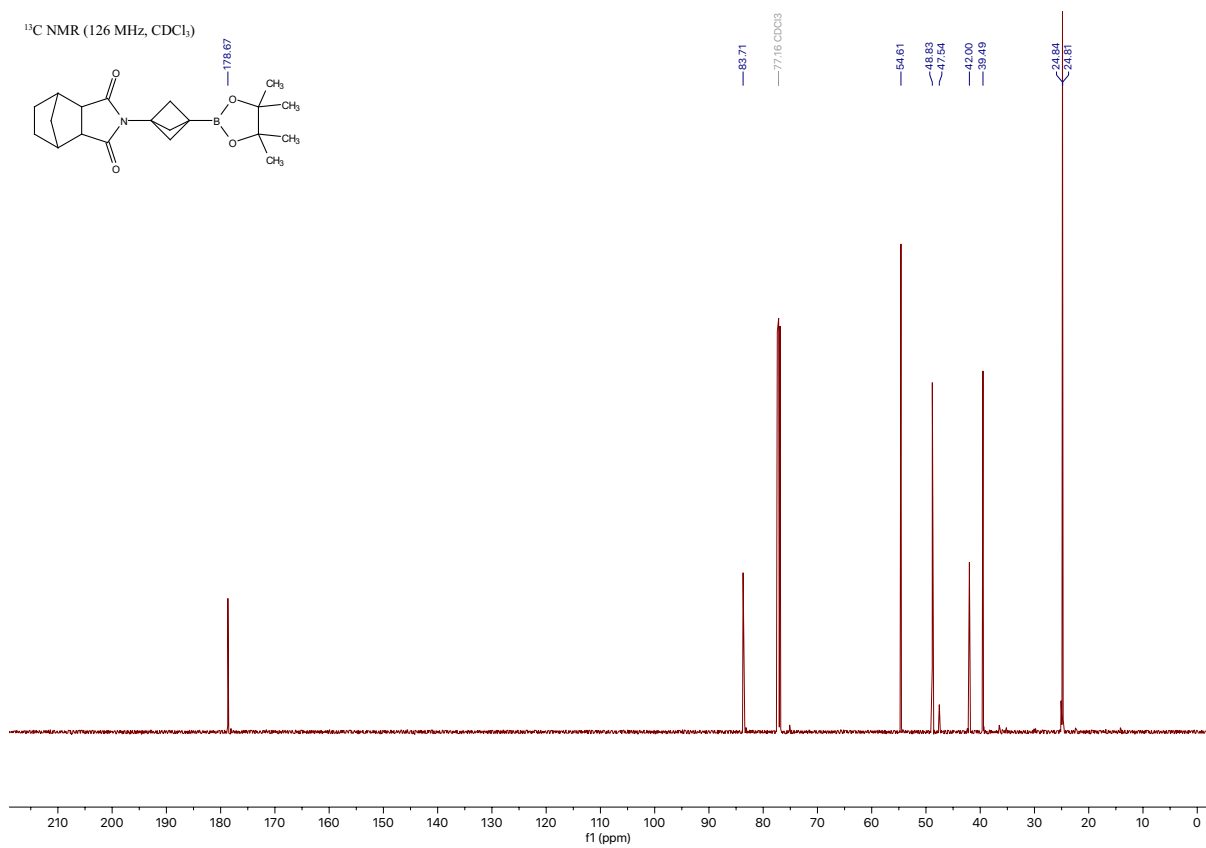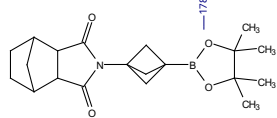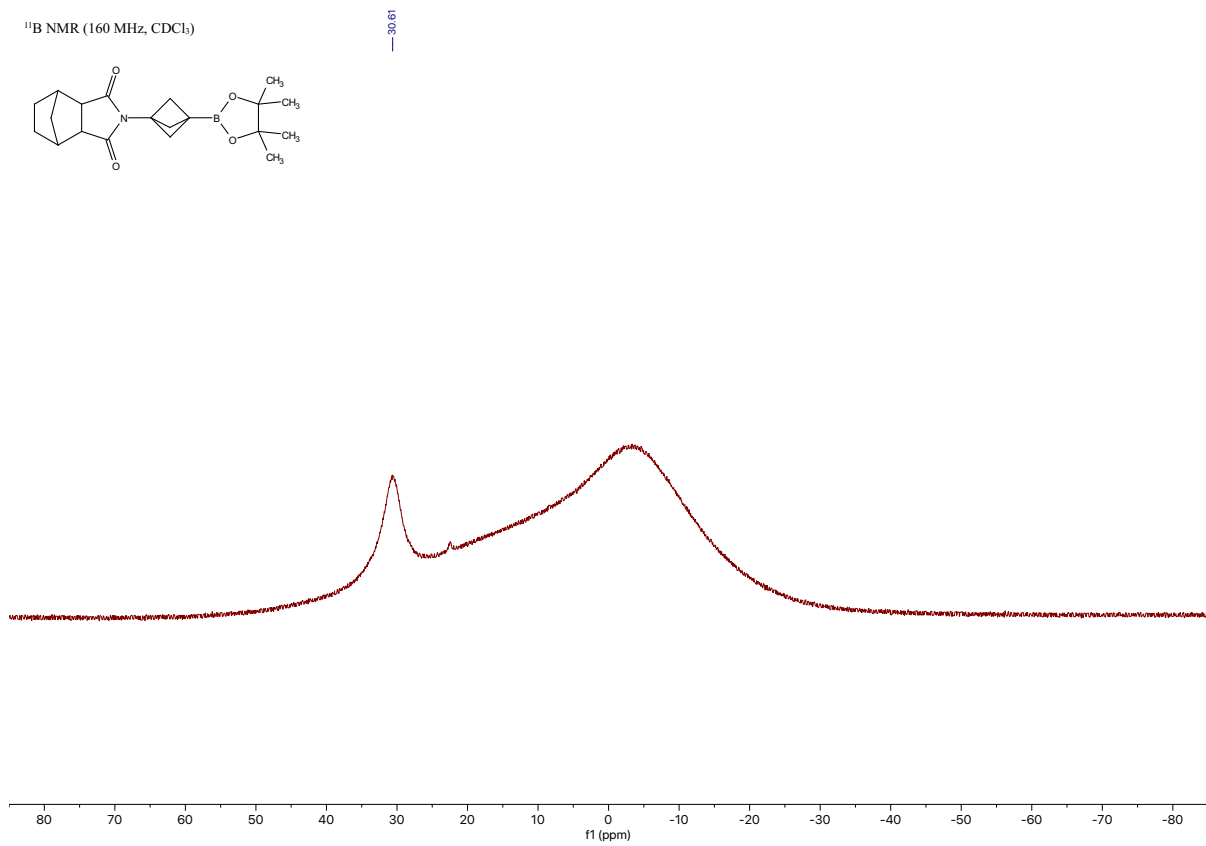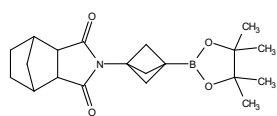
Compound 16a

2,2,2-trifluoro-*N*-(3-(4,4,5,5-tetramethyl-1,3,2-dioxaborolan-2-yl)bicyclo[1.1.1]pentan-1-yl)acetamide [Experimental]

¹H NMR (500 MHz, CDCl₃)

¹³C NMR (151 MHz, CDCl₃)

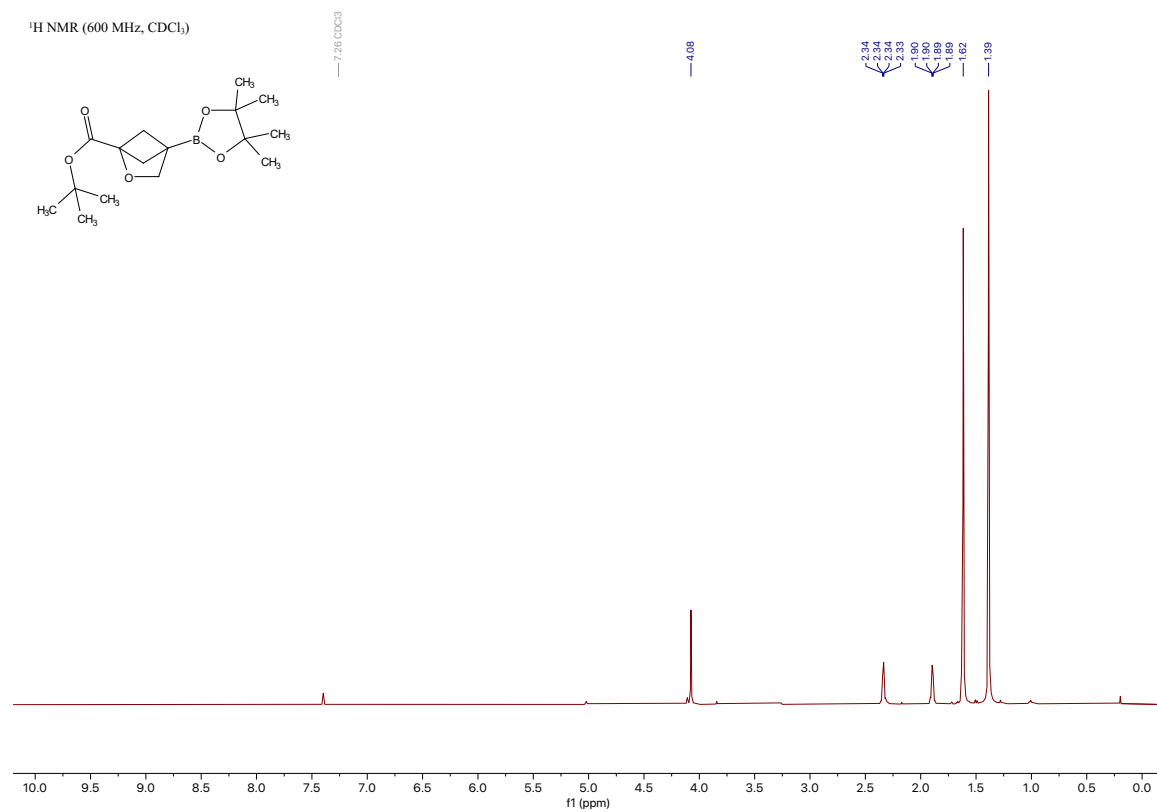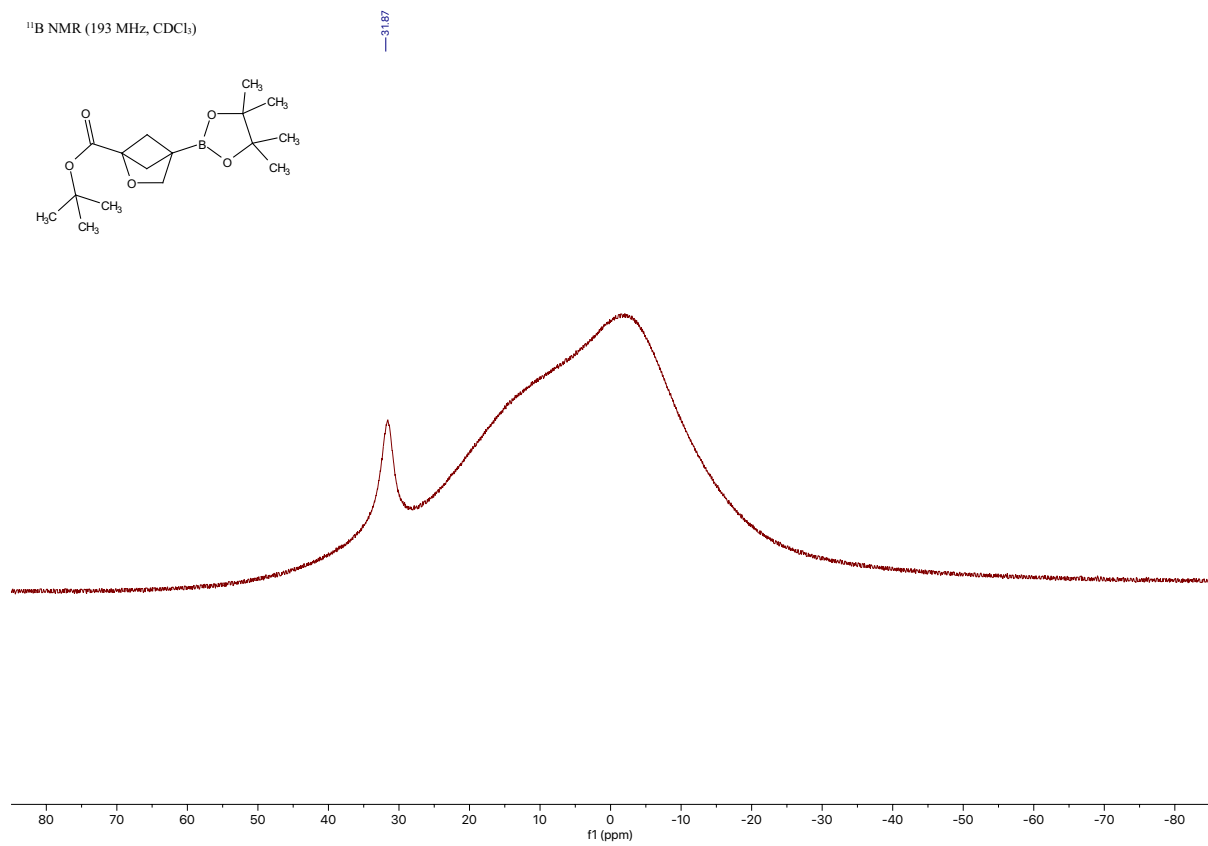¹¹B NMR (160 MHz, CDCl₃)

—30.66

f1 (ppm)
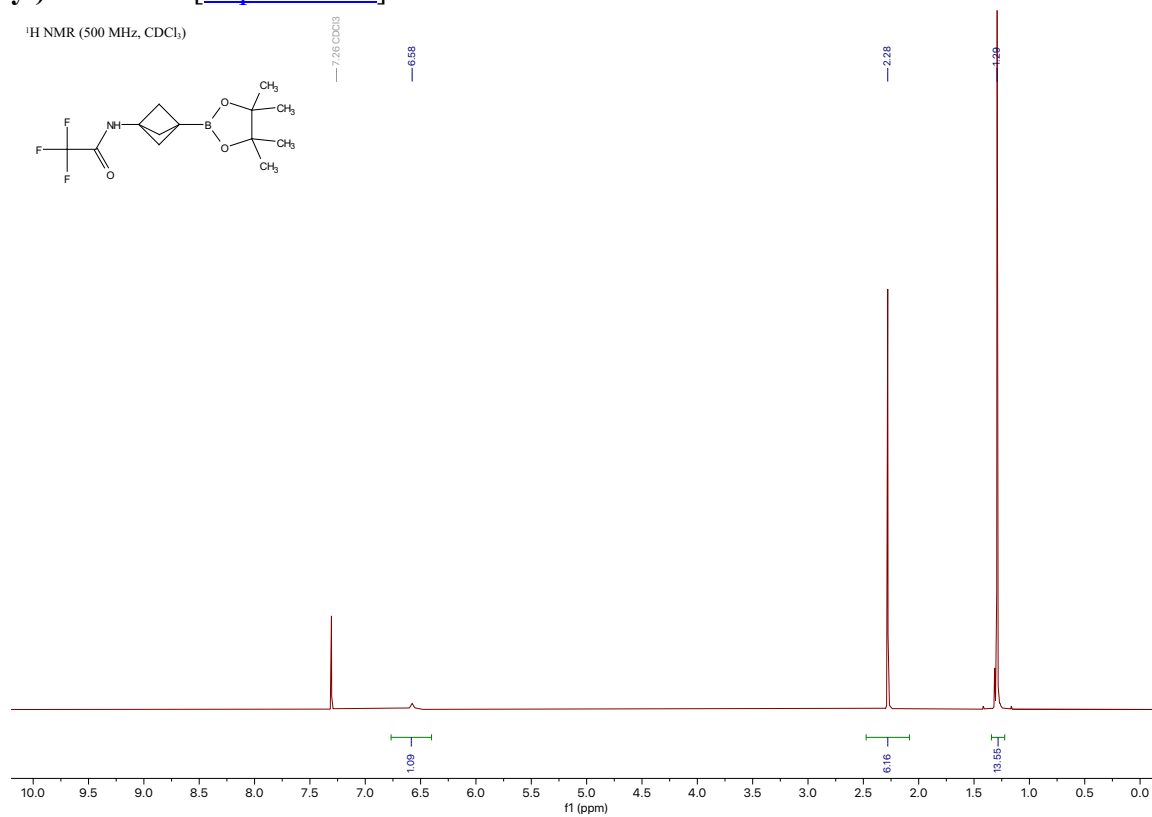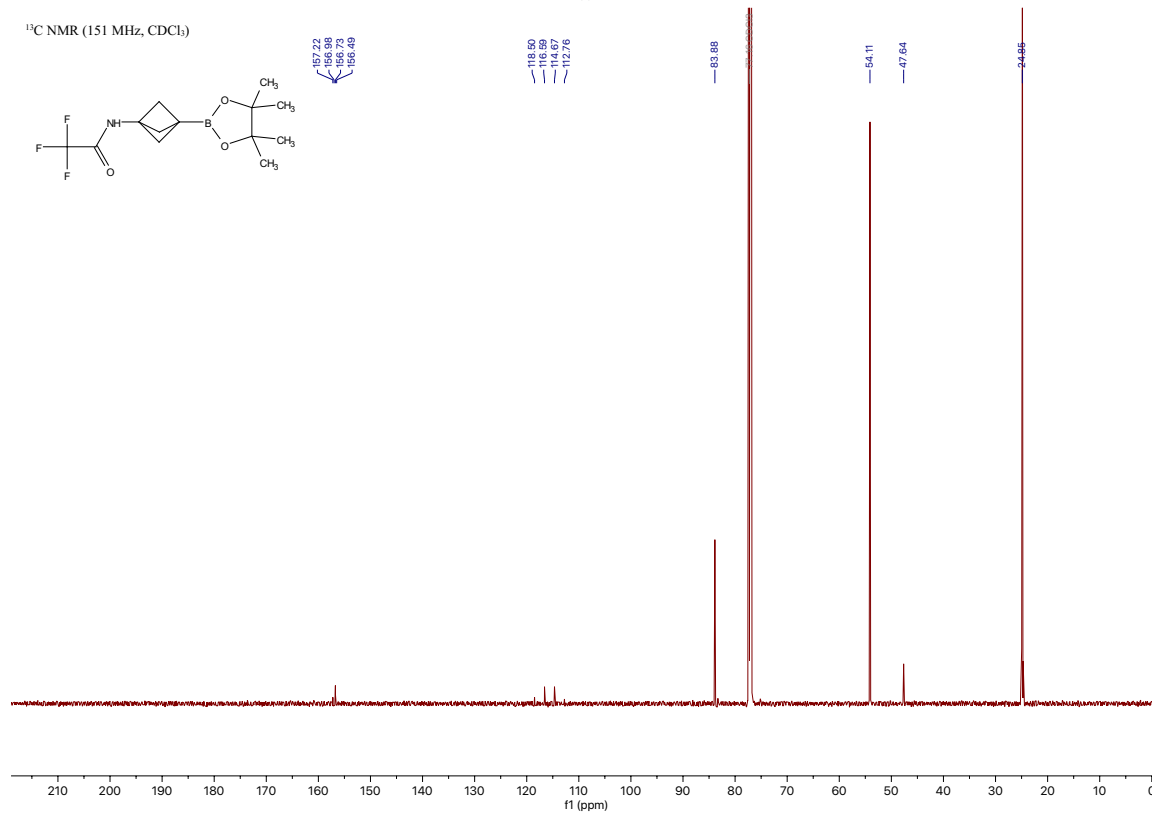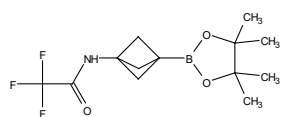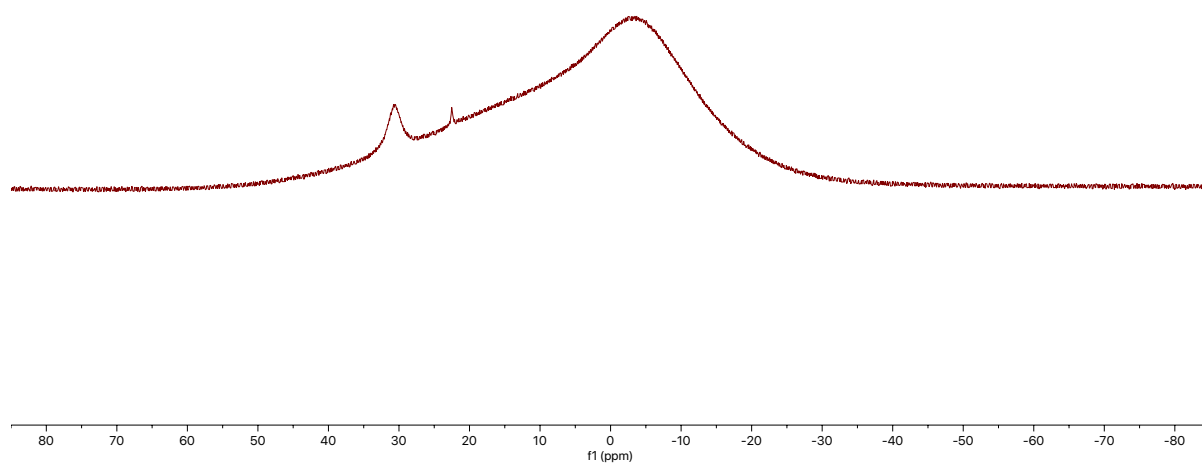
¹⁹F NMR (470 MHz, CDCl₃)

—-76.27

f1 (ppm)
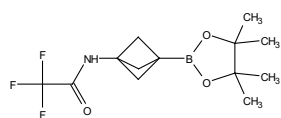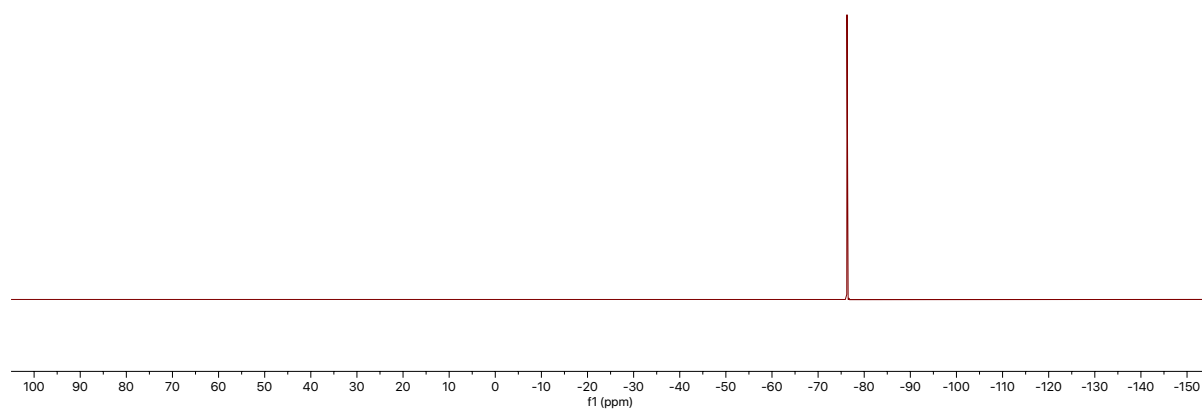
Compound 17a

***tert*-butyl 3-((3-(4,4,5,5-tetramethyl-1,3,2-dioxaborolan-2-yl)bicyclo[1.1.1]pentan-1-yl)methyl)azetidine-1-carboxylate** [Experimental]

¹H NMR (500 MHz, CDCl₃)

156.48

83.40
79.22
77.16 CDCl₃

54.96
51.79
49.99
44.65
37.88
28.53
26.82
24.85

f1 (ppm)

¹¹B NMR (160 MHz, CDCl₃)

30.33

f1 (ppm)
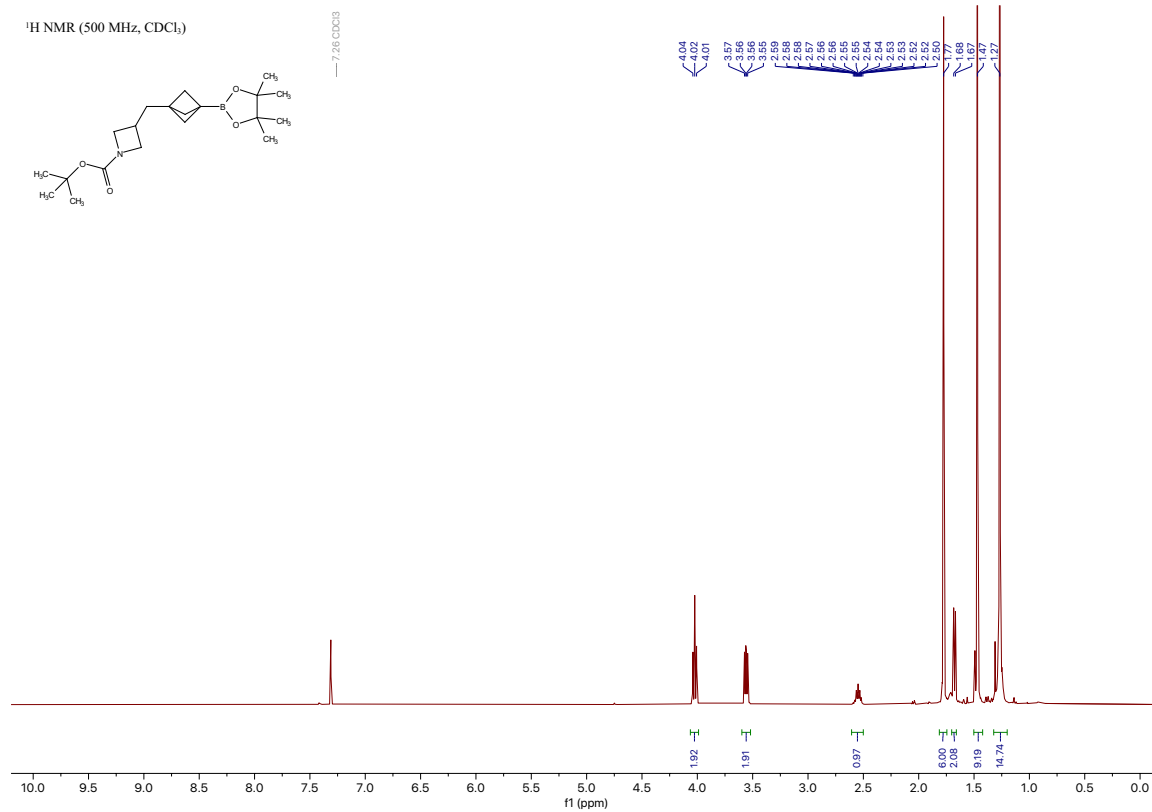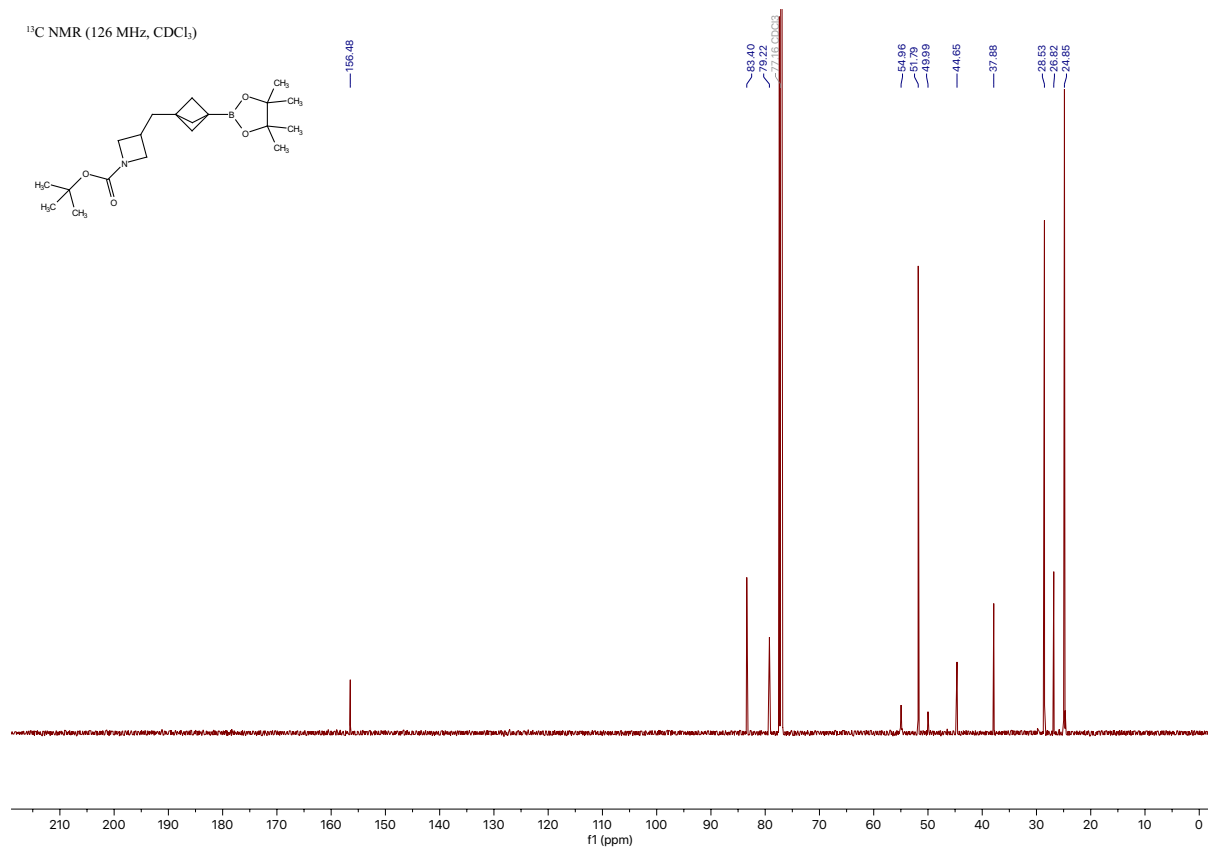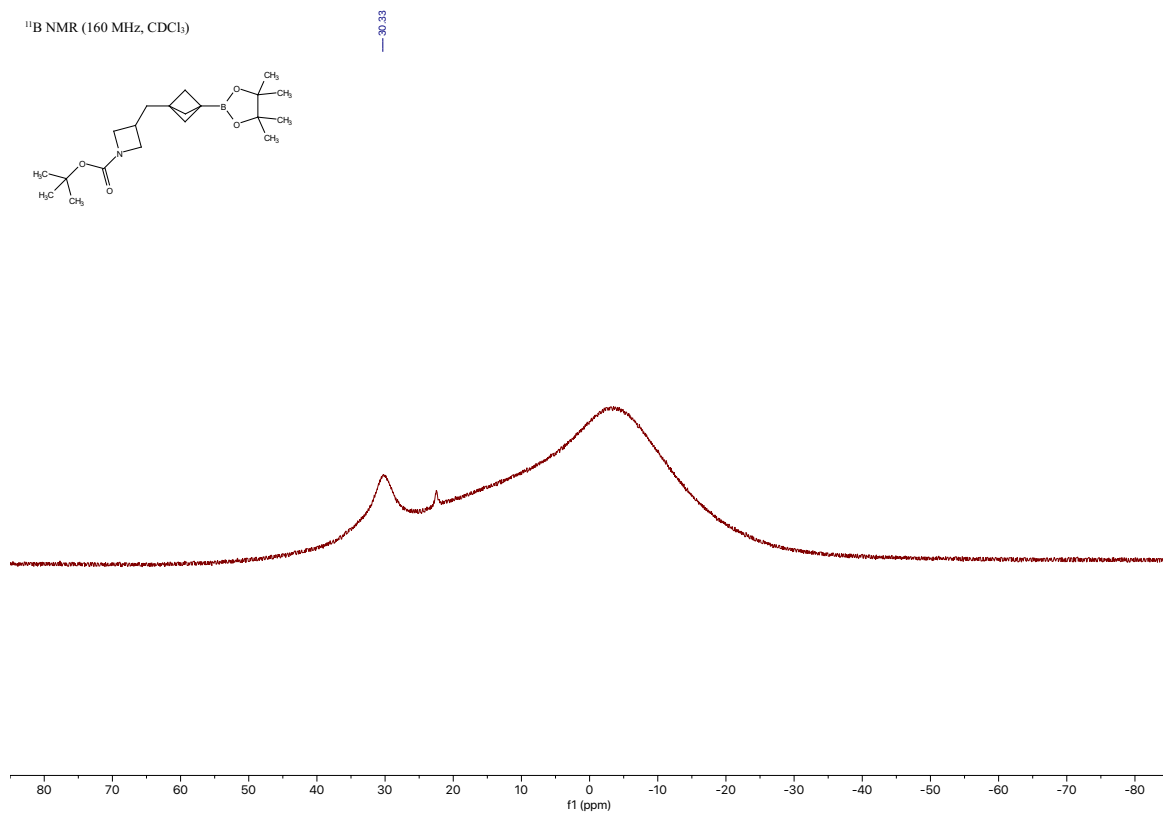
Compound 18a

tert-butyl 3-(3-(4,4,5,5-tetramethyl-1,3,2-dioxaborolan-2-yl)bicyclo[1.1.1]pentan-1-yl)pyrrolidine-1-carboxylate [Experimental]

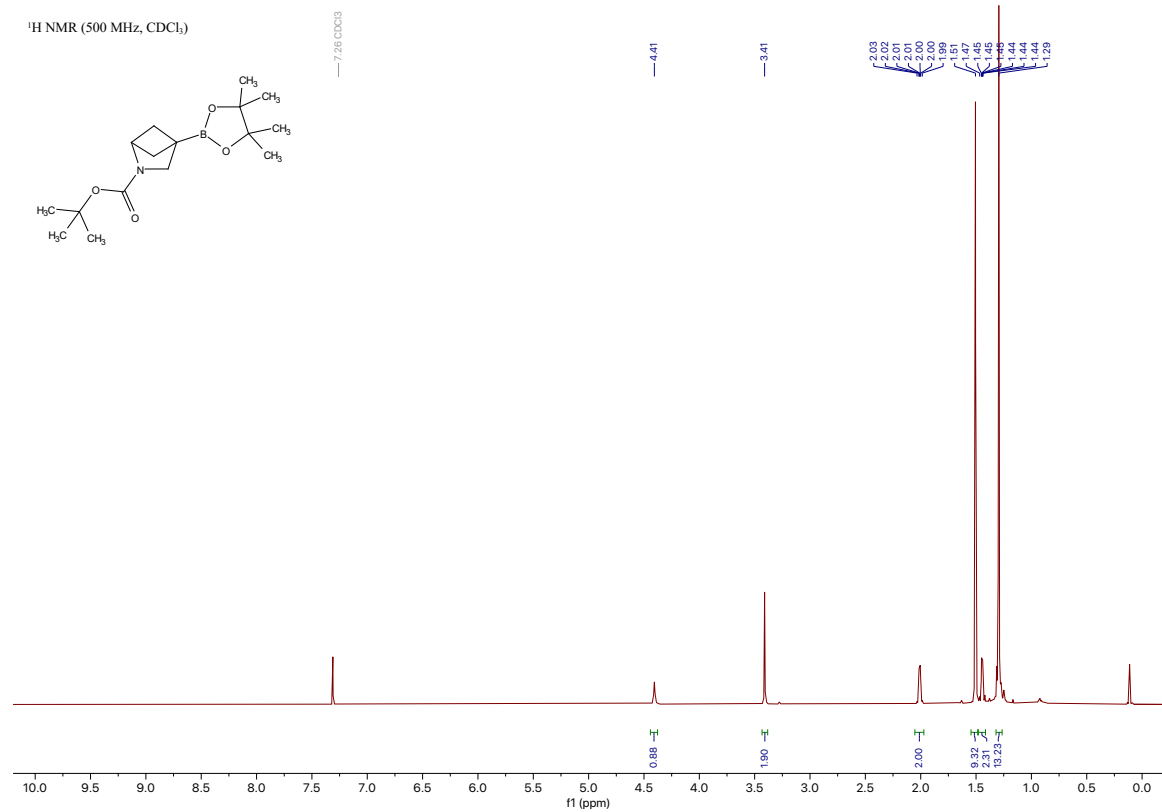¹H NMR (700 MHz, CDCl₃)
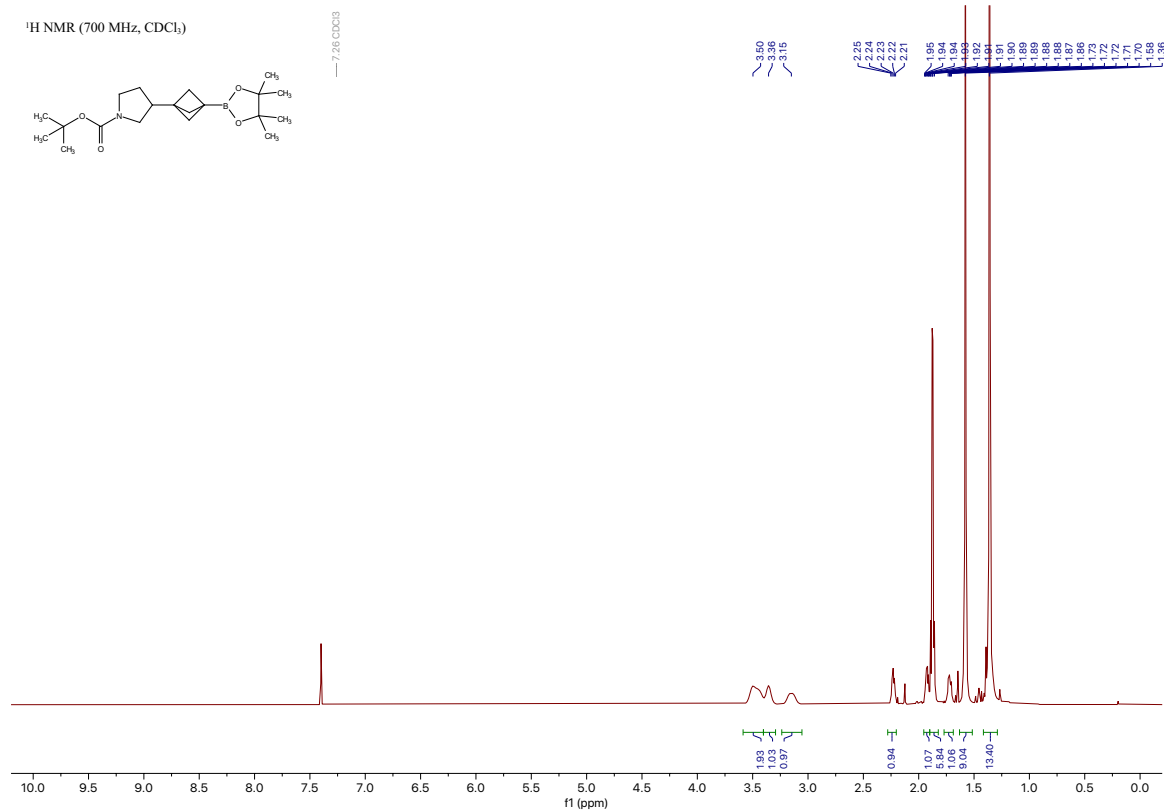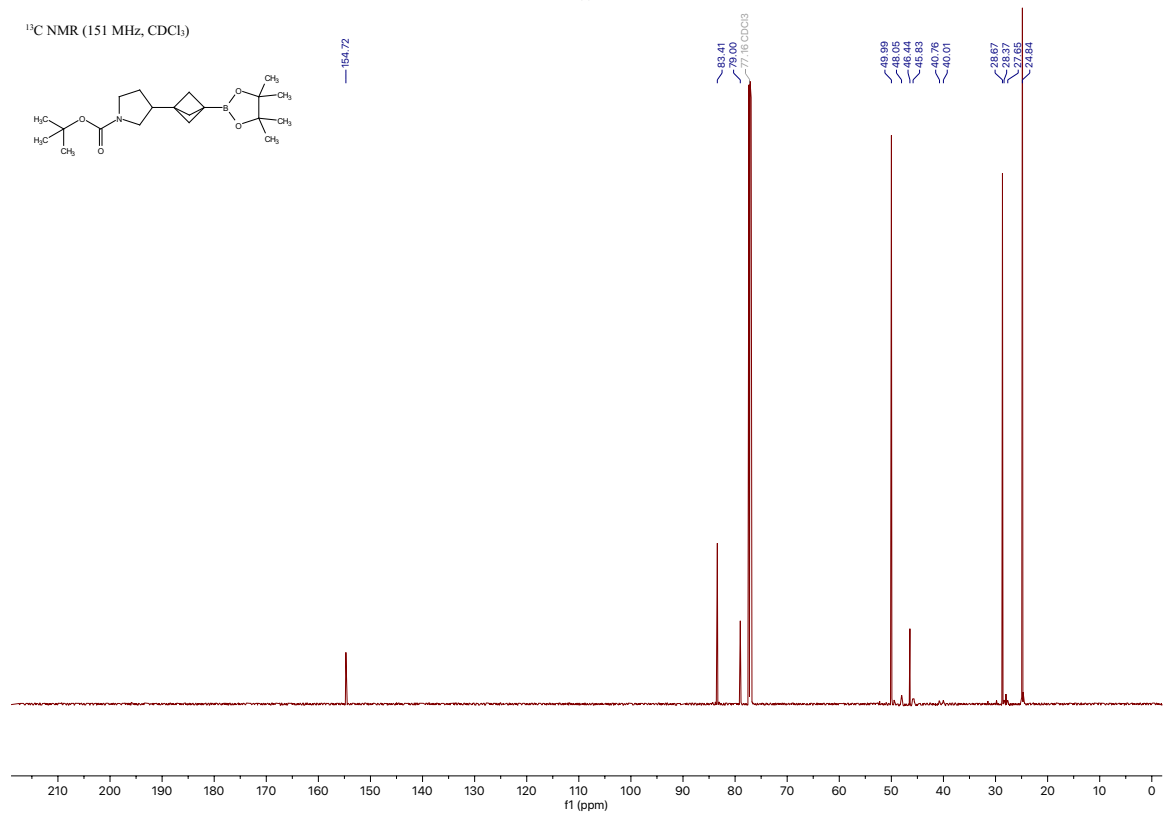
¹³C NMR (151 MHz, CDCl₃)
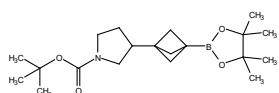
—30.78
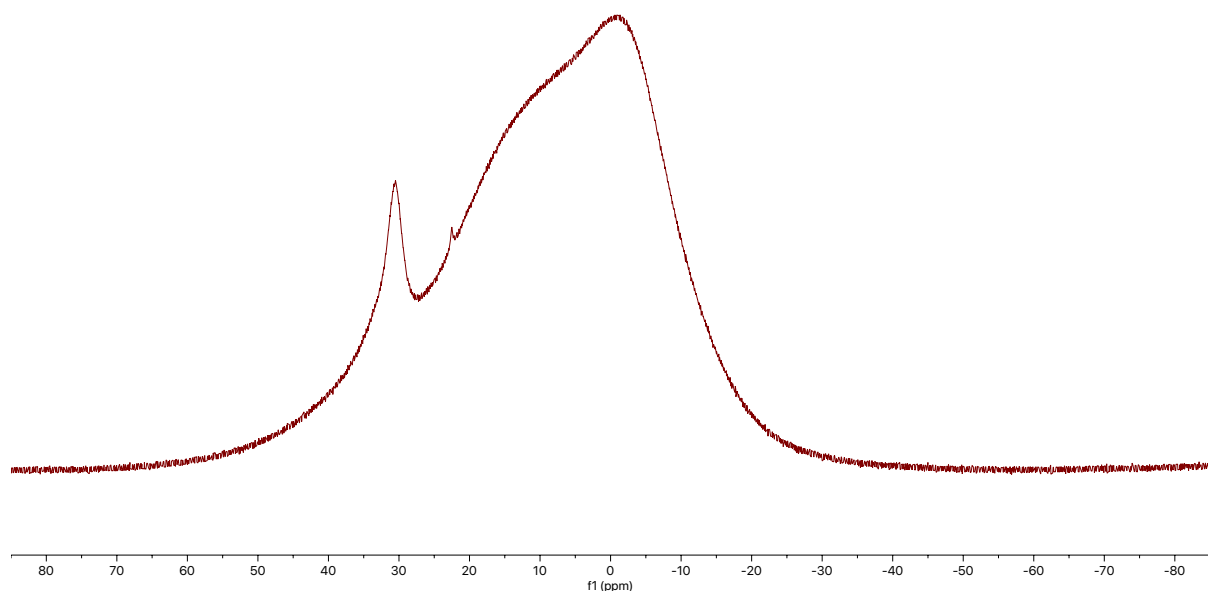
Parameter	Value
1 Experiment	HSQC
2 Spectrometer Frequency (600.13, 150.91)	

{0.83,20.59}

{1.22,24.77}

{1.58,27.99} {1.44,28.64}

{1.78,27.99}

{2.10,40.23}

{3.22,45.70}

{3.32,47.96} {3.36,45.70} {3.02,47.96}

{1.99,49.56} {1.74,49.89}

f1 (ppm)

f2 (ppm)
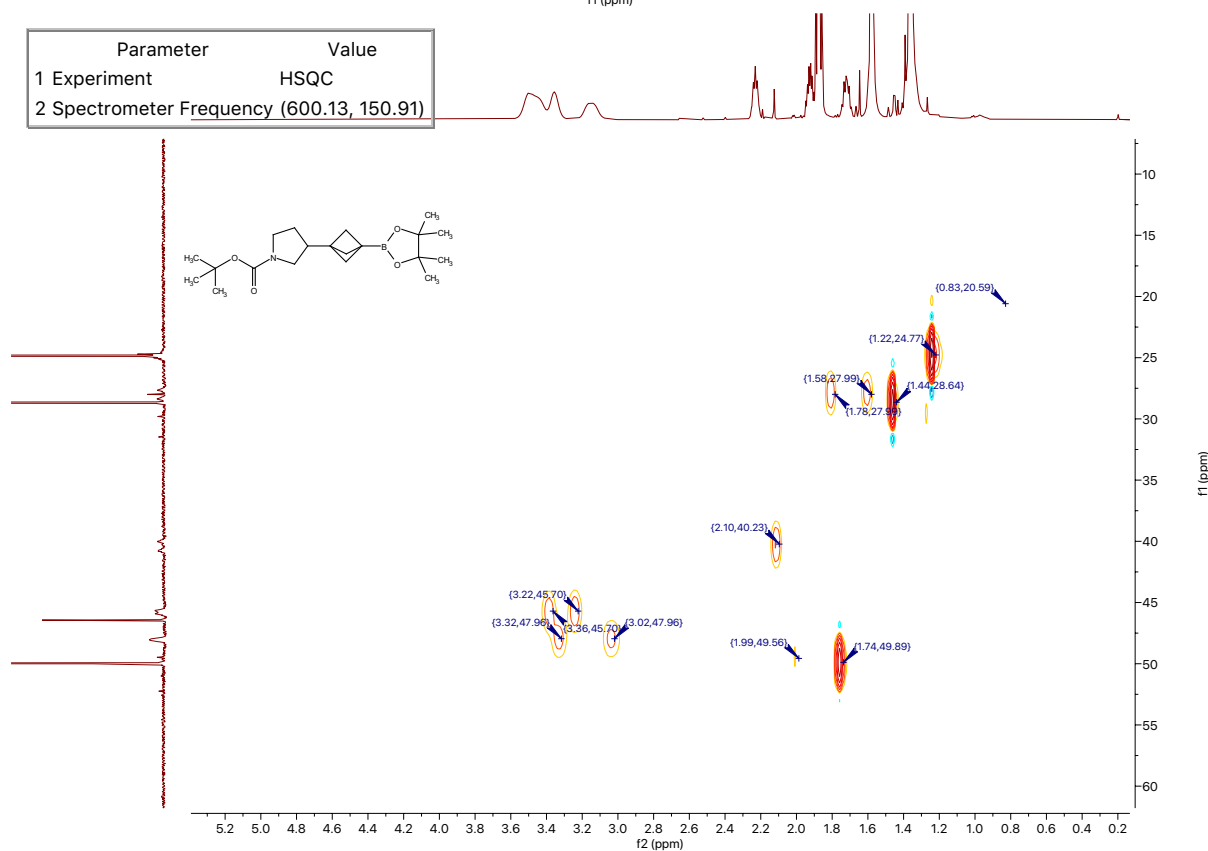
Compound 19a

2-(3-methoxy-5-(3-(4,4,5,5-tetramethyl-1,3,2-dioxaborolan-2-yl)bicyclo[1.1.1]pentan-1-yl)phenyl)-4,4,5,5-tetramethyl-1,3,2-dioxaborolane [Experimental]

¹H NMR (600 MHz, CDCl₃)

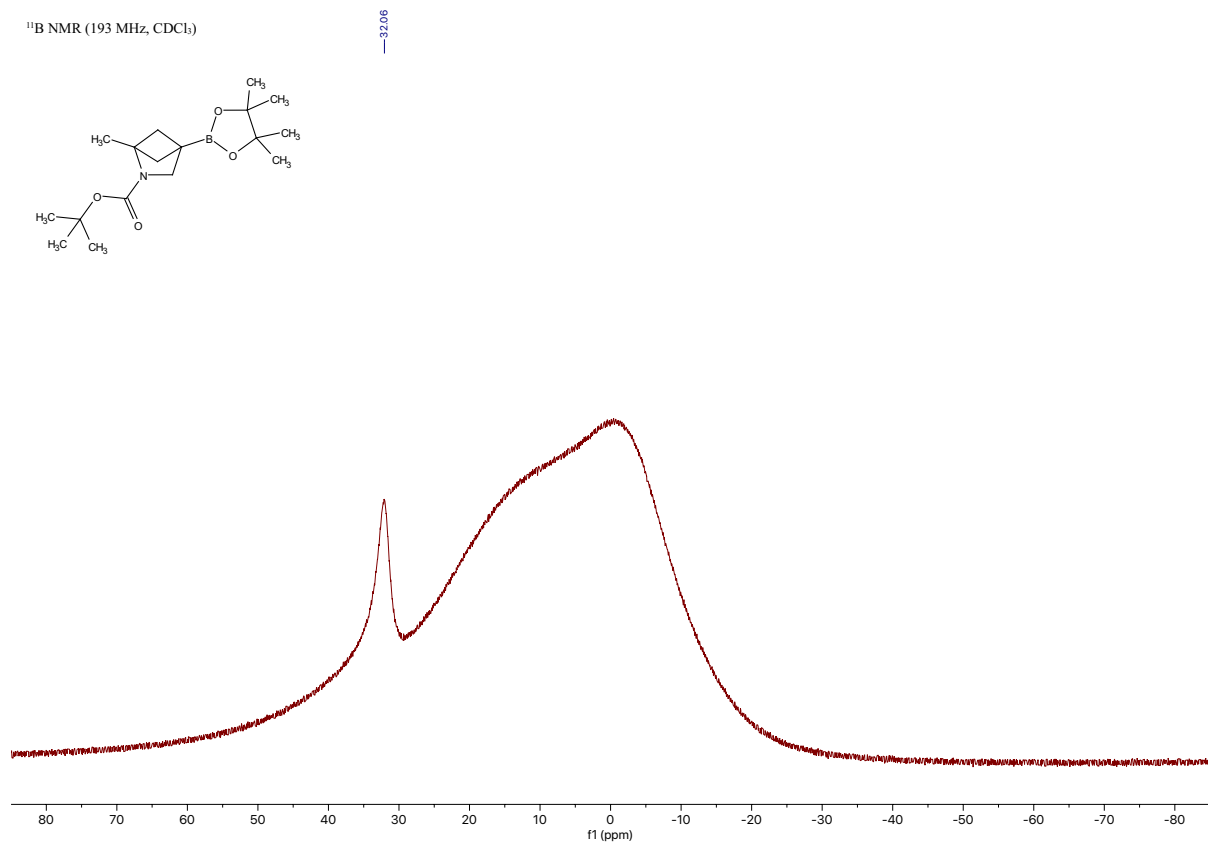¹³C NMR (151 MHz, CDCl₃)

¹¹B NMR (193 MHz, CDCl₃)

261
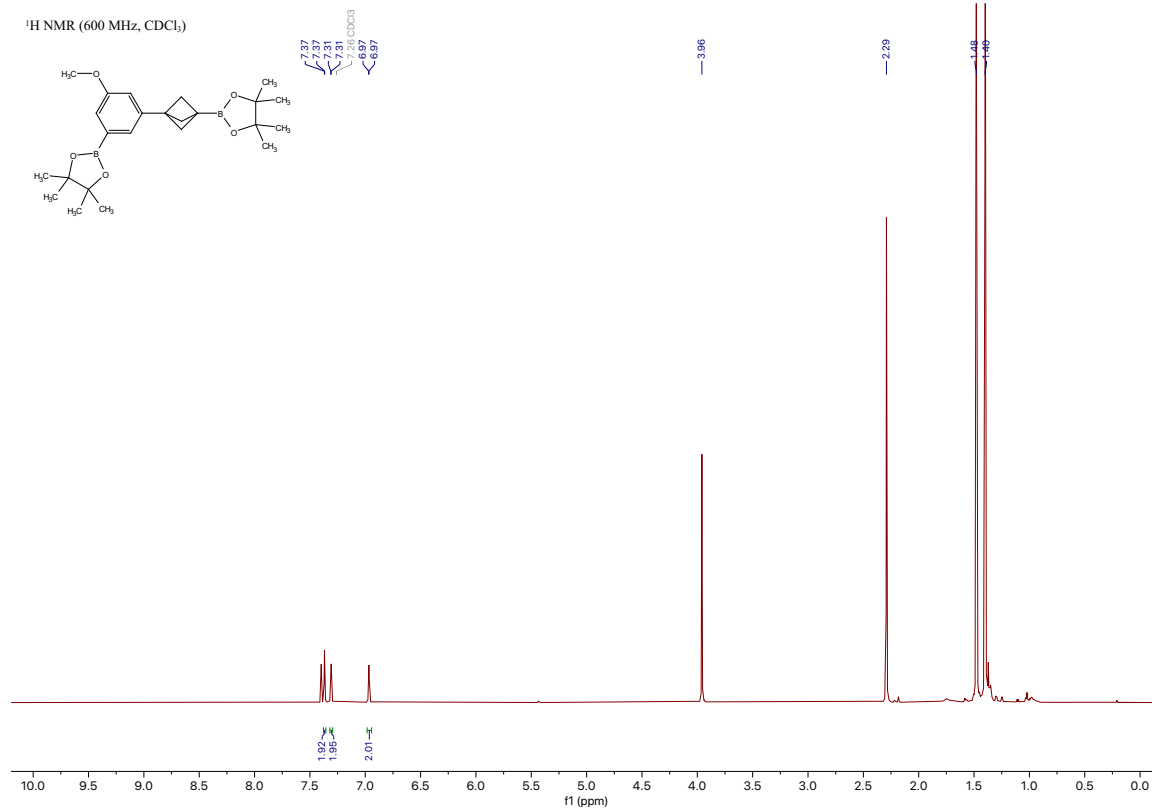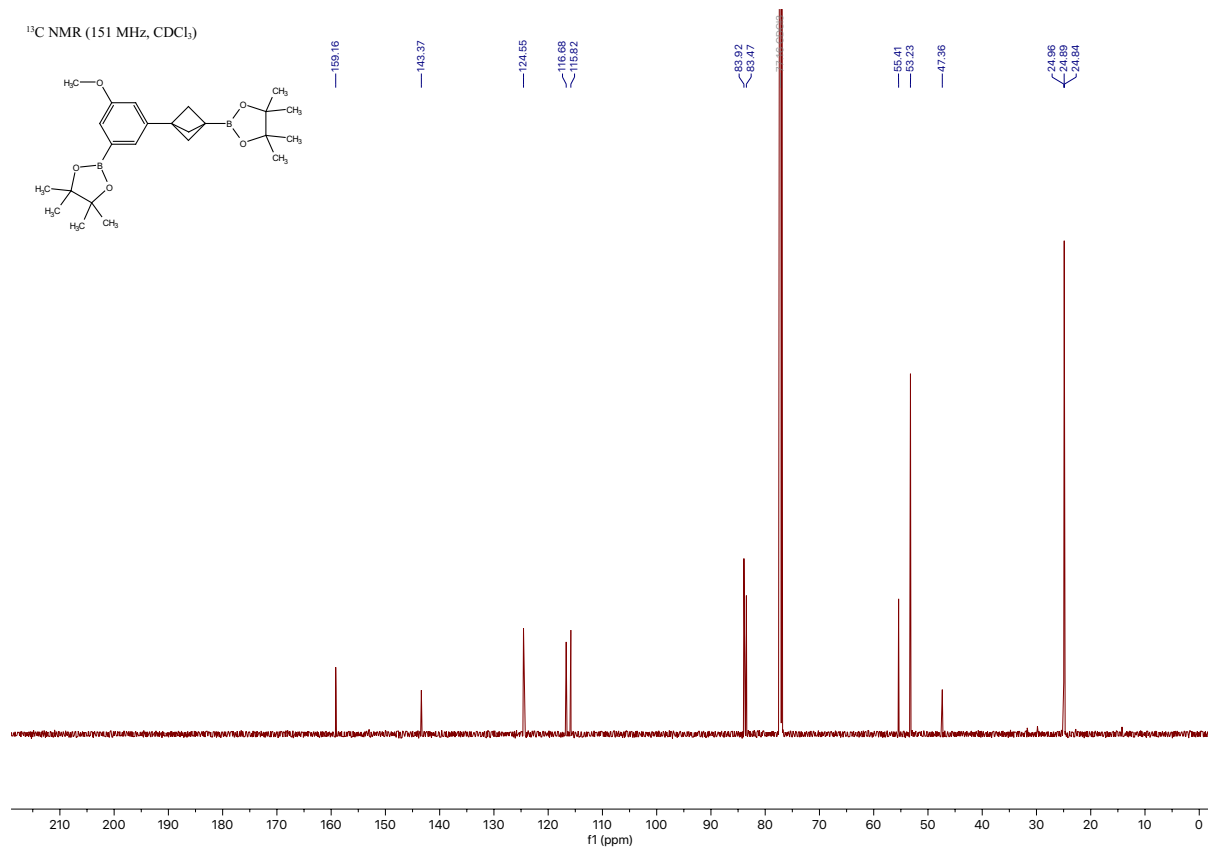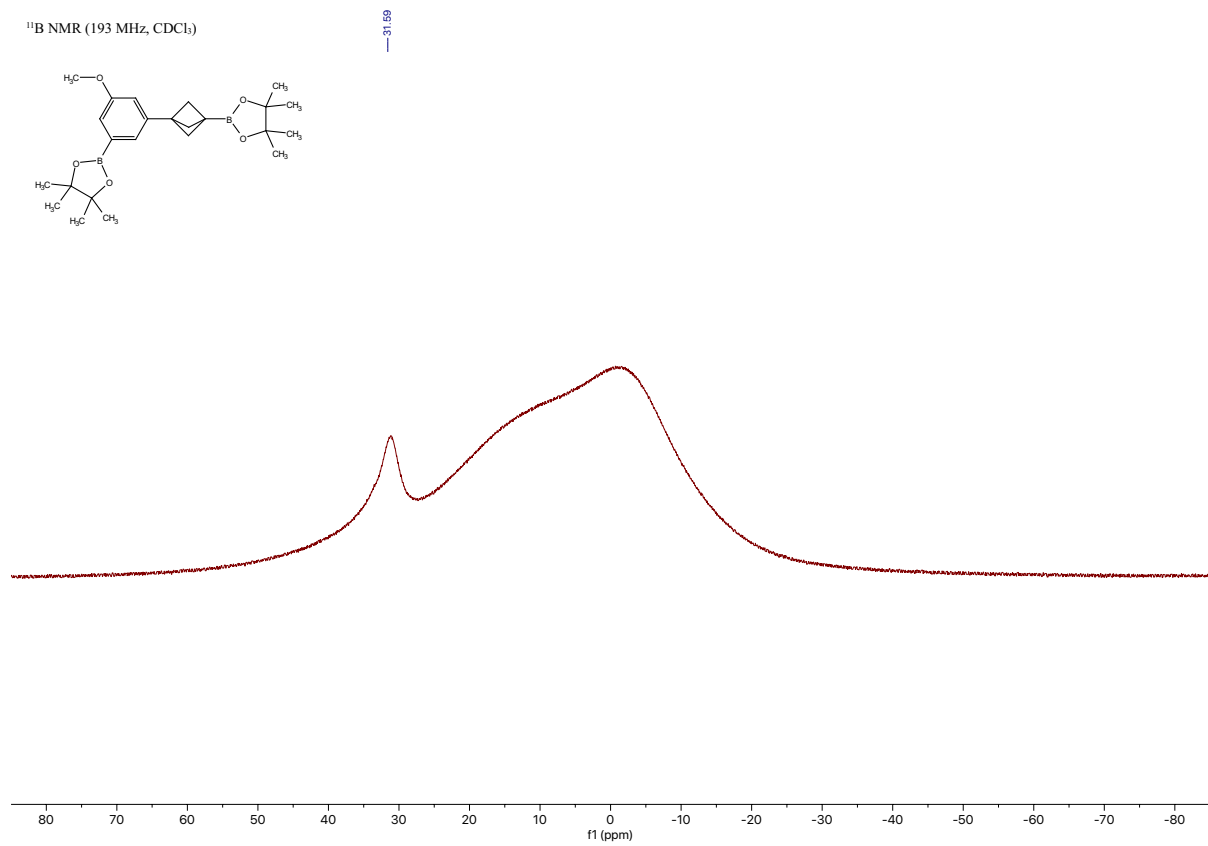
Compound 20a

2-propyl-*N*-(3-(4,4,5,5-tetramethyl-1,3,2-dioxaborolan-2-yl)bicyclo[1.1.1]pentan-1-yl)pentanamide [Experimental]

263
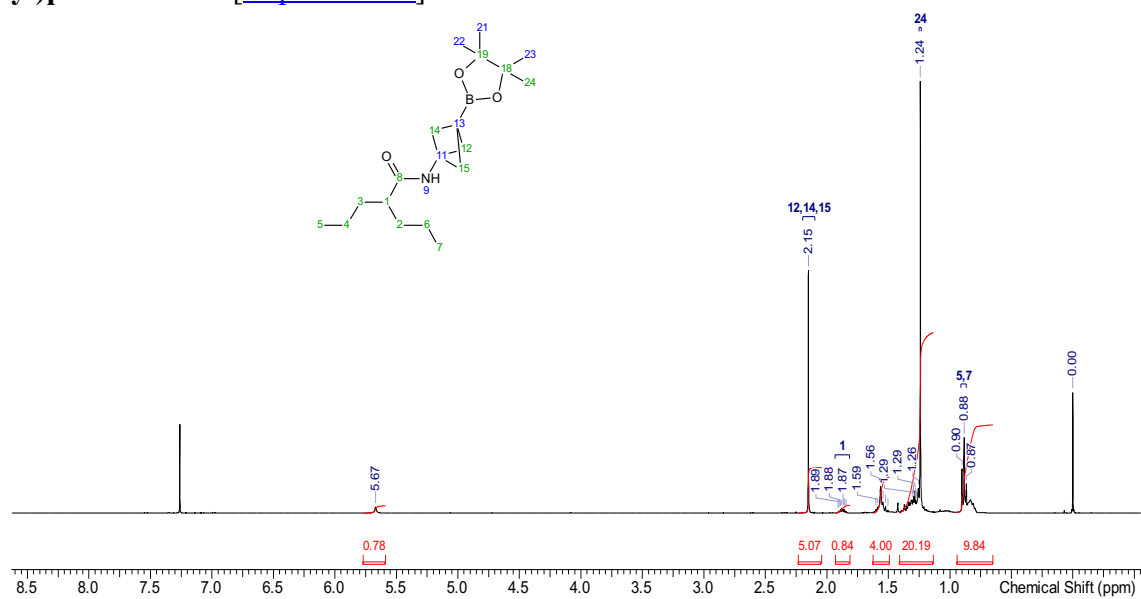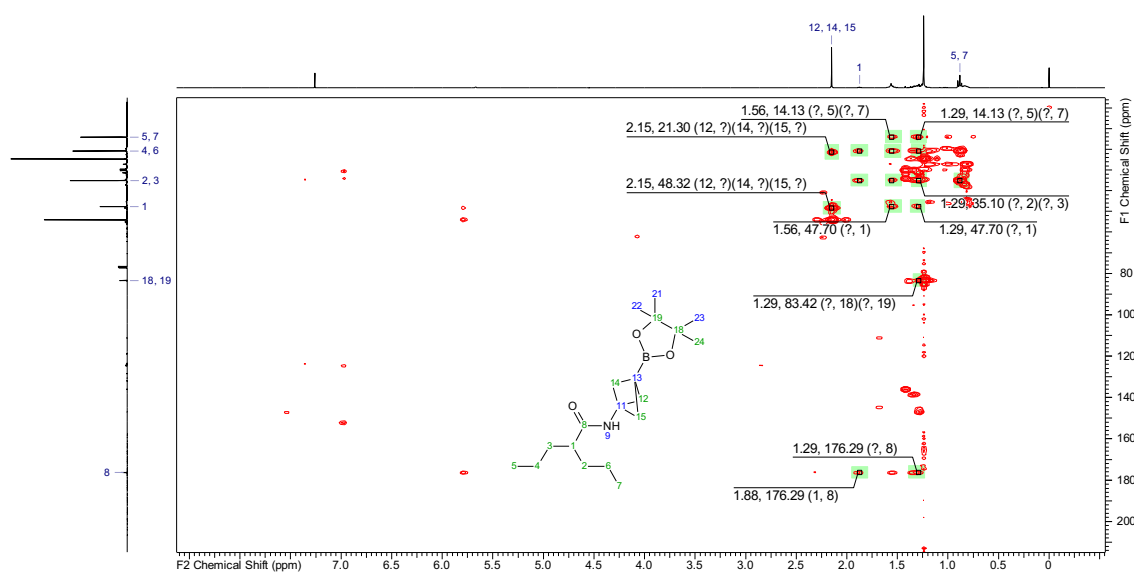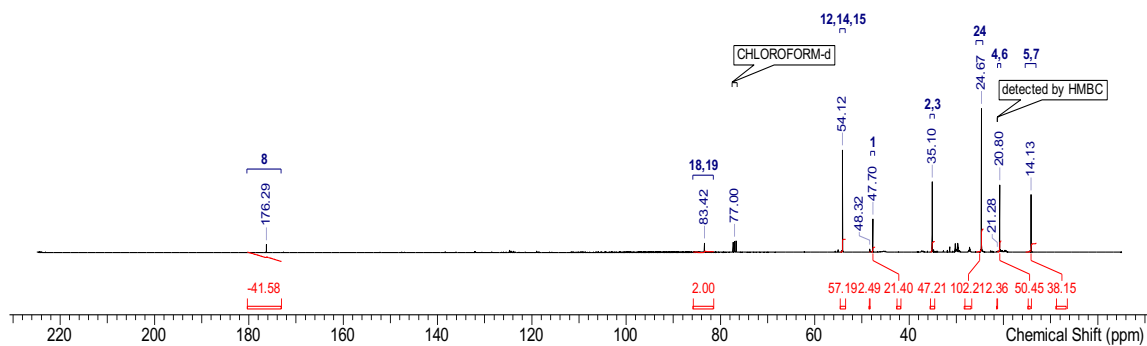
Compound 21a

(3-((1*R*,4a*R*,4b*R*,10a*R*)-7-isopropyl-1,4a-dimethyl-1,2,3,4,4a,4b,5,6,10,10a-decahydrophenanthrene-1-carboxamido)bicyclo[1.1.1]pentan-1-yl)boronic acid
[Experimental]
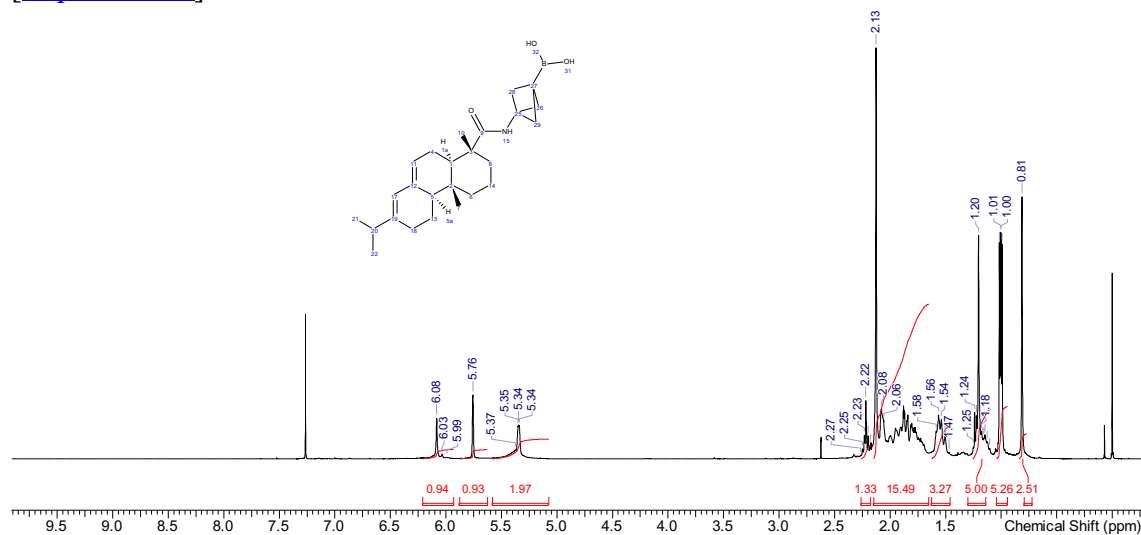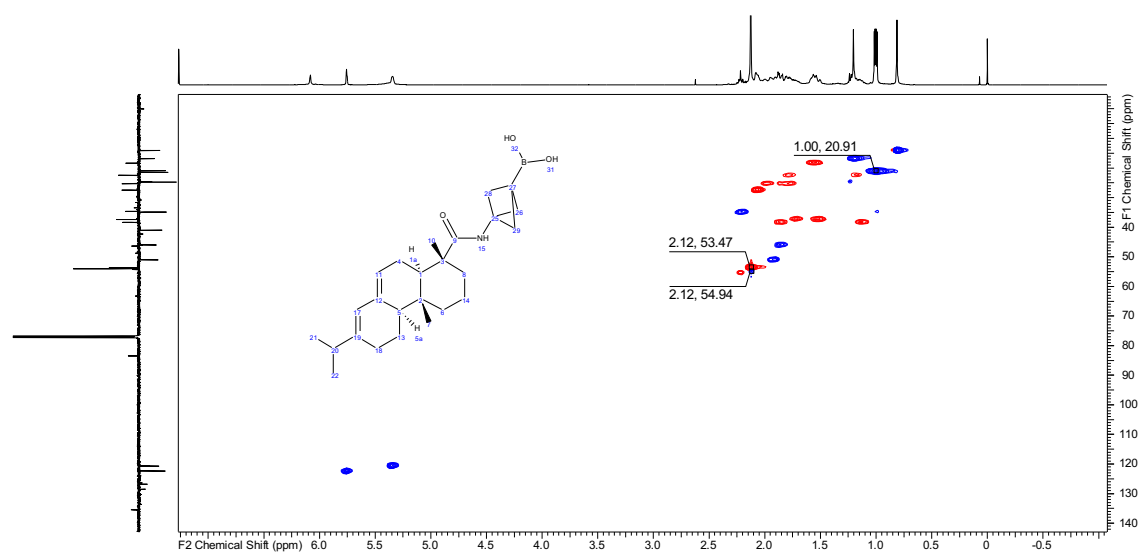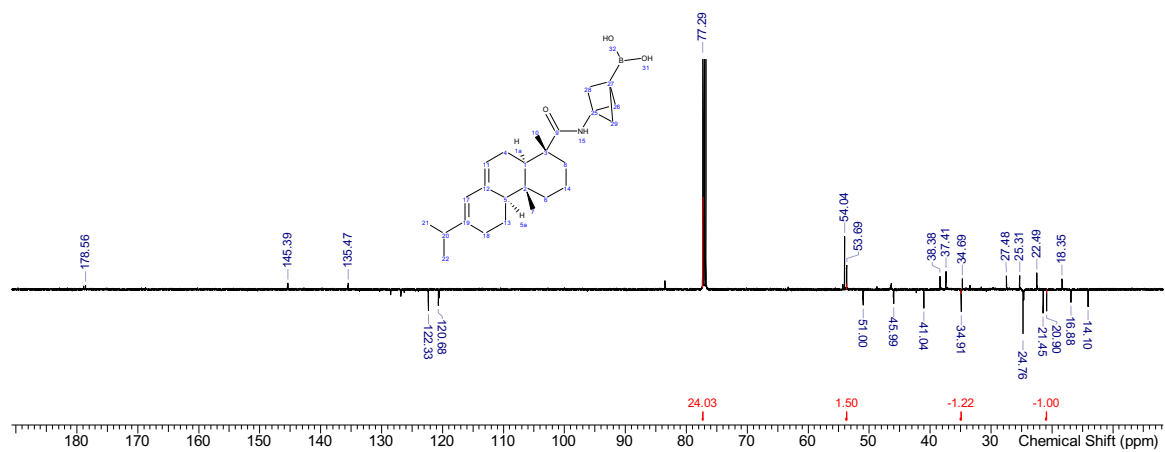
Compound 22a

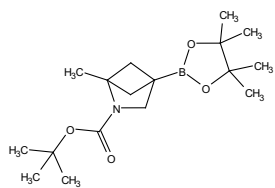***tert*-butyl 4-(4,4,5,5-tetramethyl-1,3,2-dioxaborolan-2-yl)bicyclo[2.1.1]hexane-1-carboxylate** [Experimental]

¹H NMR (500 MHz, CDCl₃)

173.55
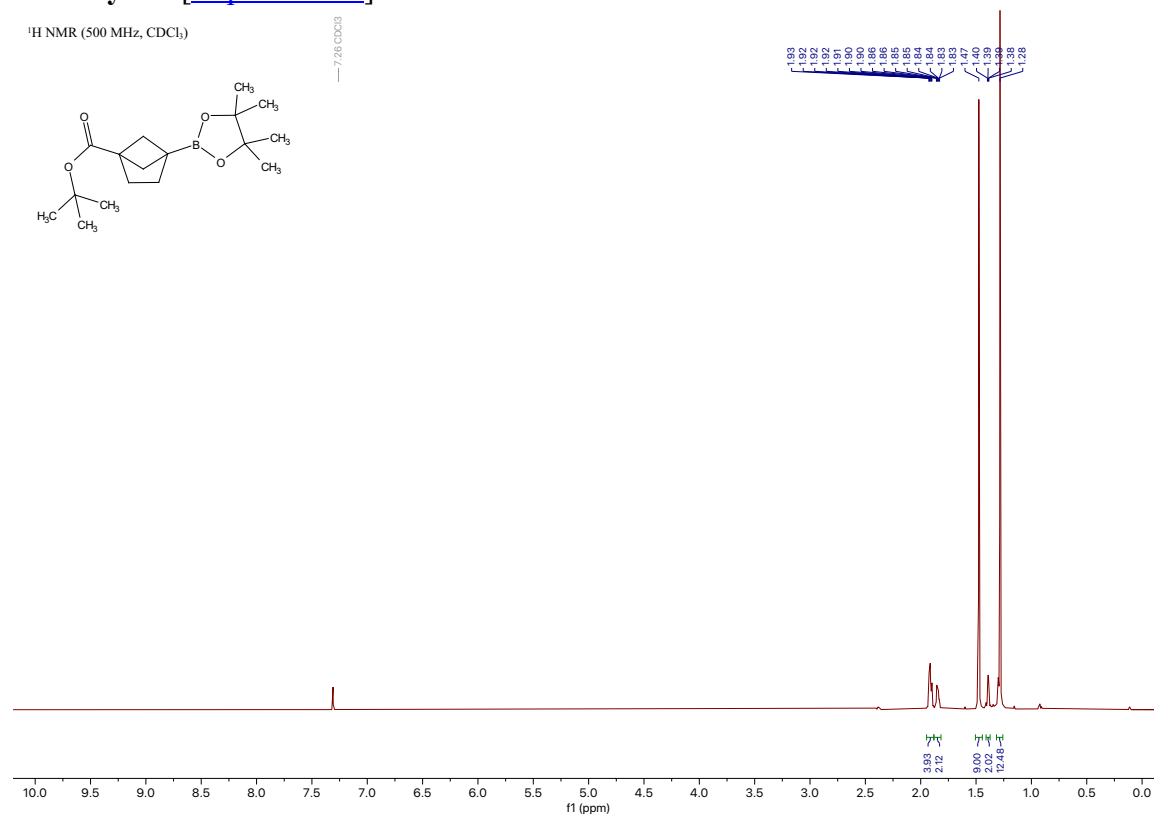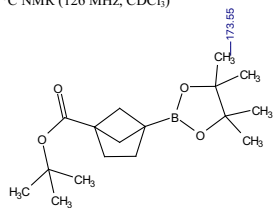
83.27
79.80
77.16 CDCl3

54.67

43.65

30.17
29.99
28.22
24.85

f1 (ppm)

32.27

f1 (ppm)
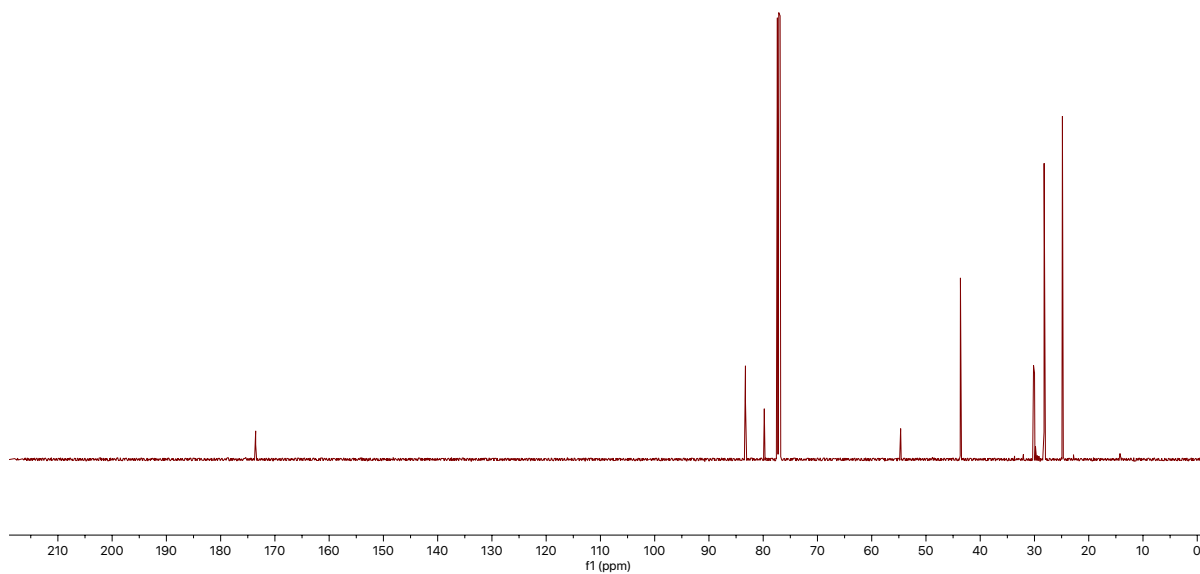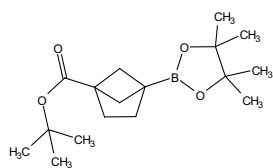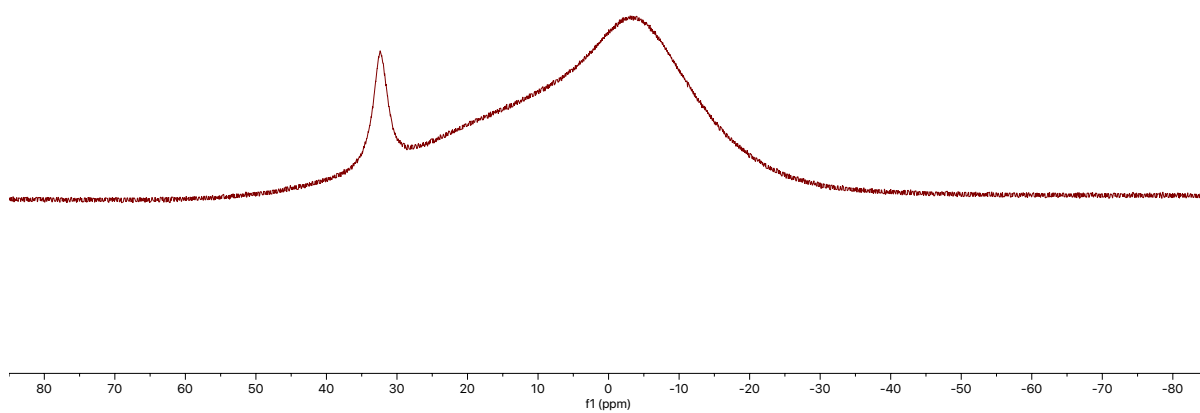
Compound 23a

tert-butyl 4-((4-(trifluoro-λ4-boraneyl)-2-oxabicyclo[2.1.1]hexan-1-yl)methyl)piperazine-1-carboxylate, potassium salt [Experimental]

¹H NMR (600 MHz, Acetone)
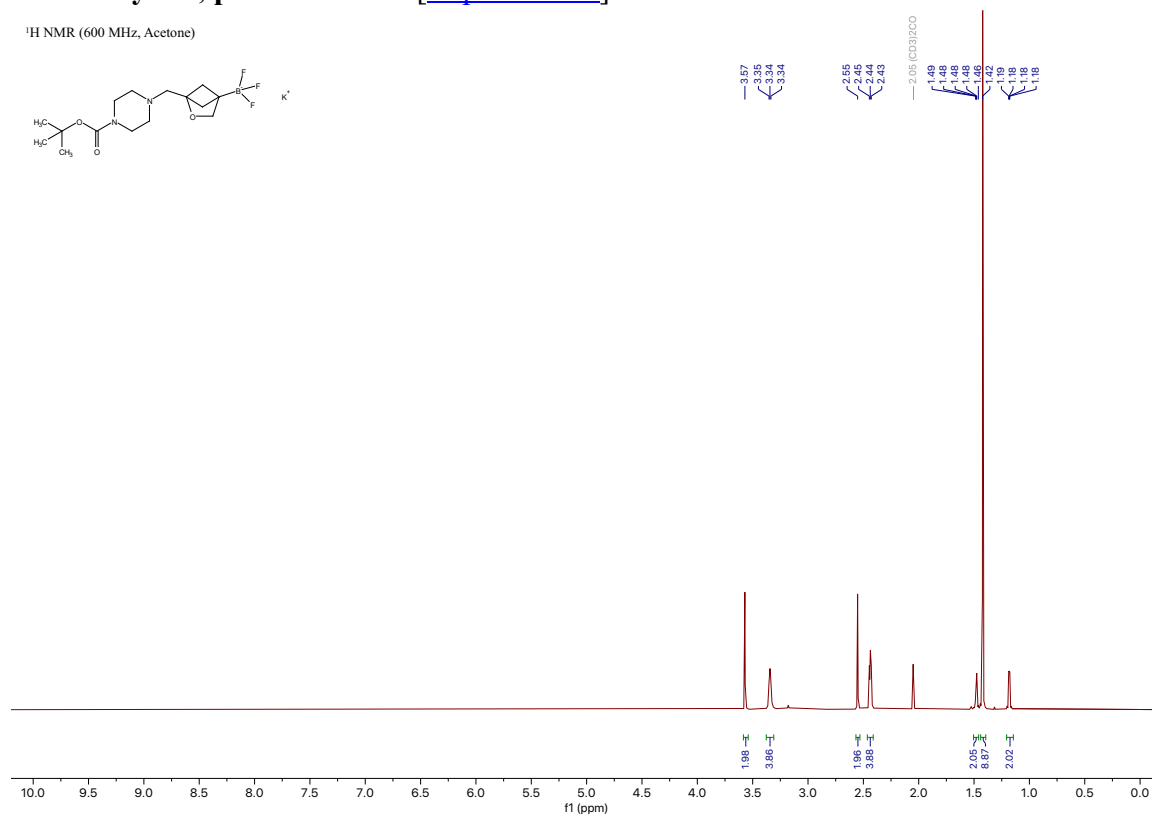
¹³C NMR (151 MHz, Acetone)
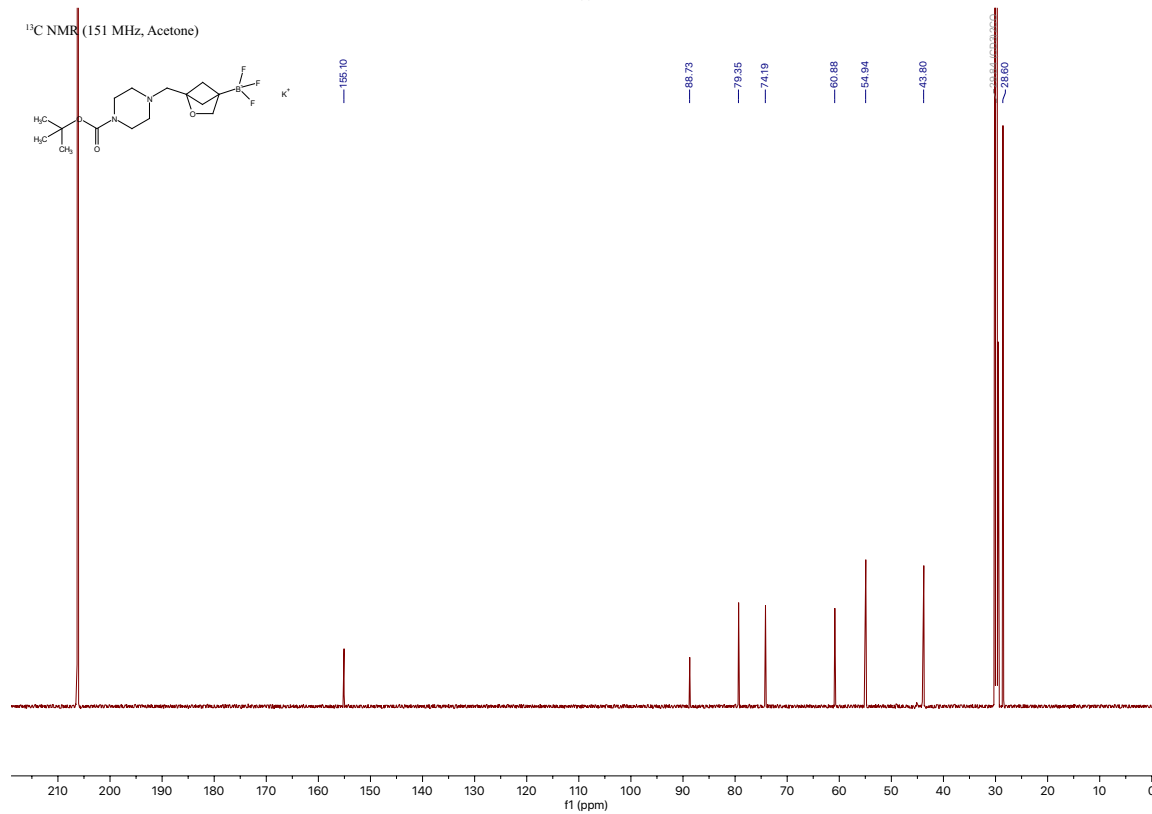
¹¹B NMR (193 MHz, Acetone)
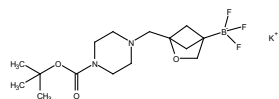
—2.56
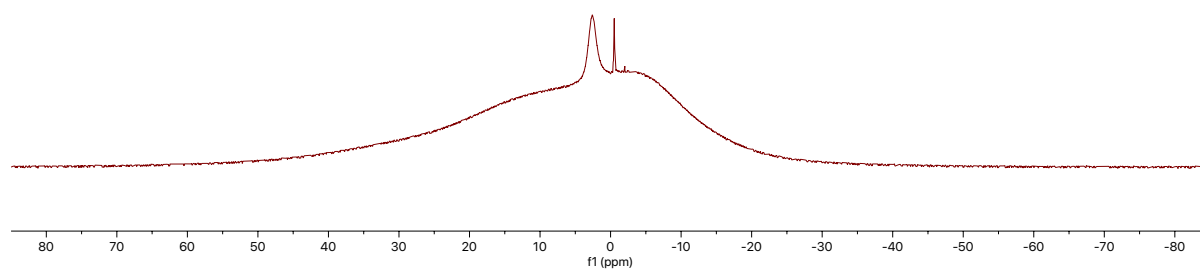
¹⁹F NMR (565 MHz, Acetone)
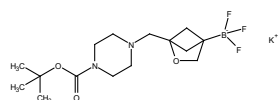
—-146.86
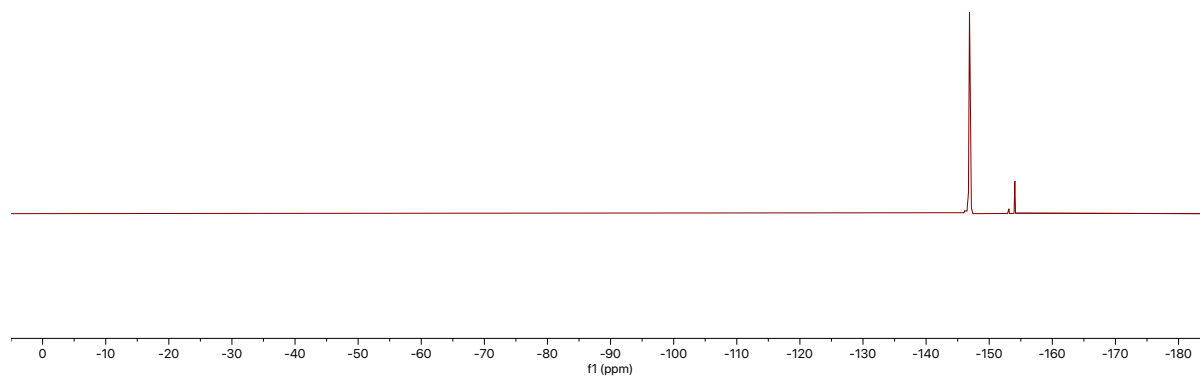
Compound 24a

2-(1-(bromomethyl)-2-oxabicyclo[2.1.1]hexan-4-yl)-4,4,5,5-tetramethyl-1,3,2-dioxaborolane [Experimental]
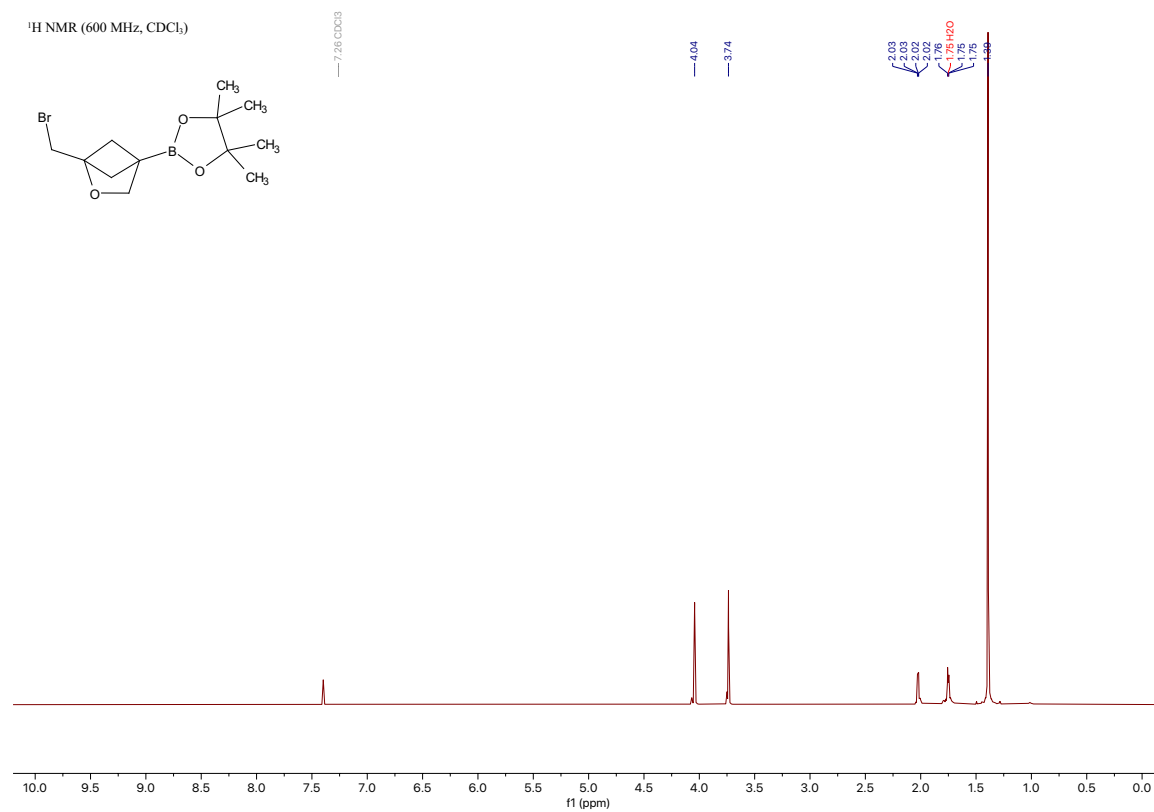
¹H NMR (600 MHz, CDCl₃)

¹³C NMR (151 MHz, CDCl₃)
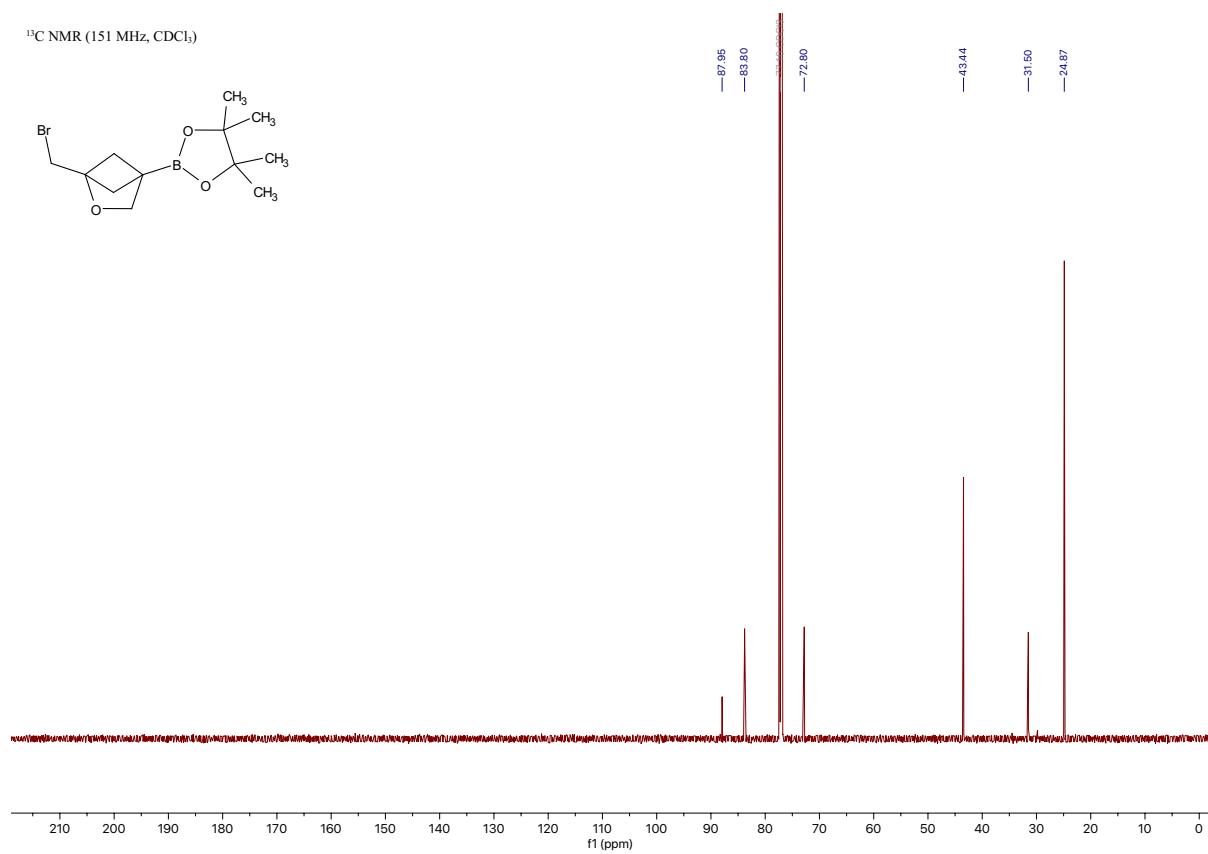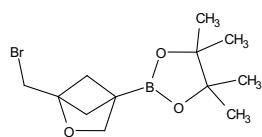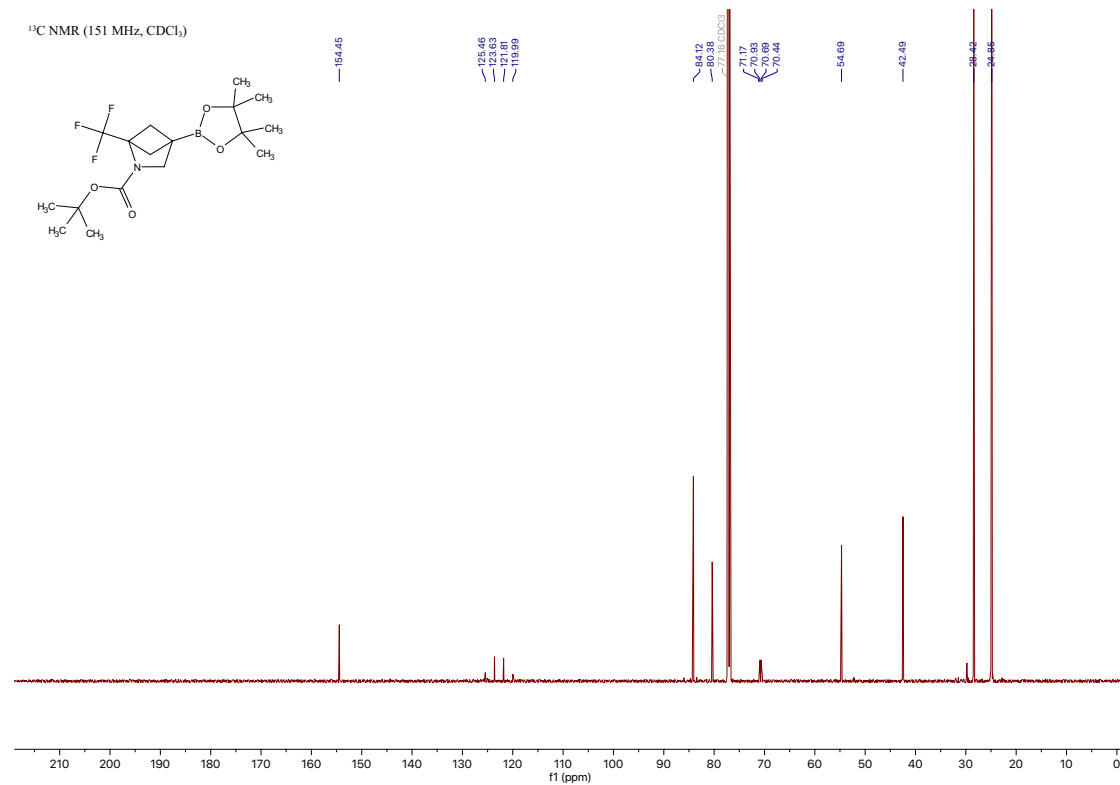

¹¹B NMR (193 MHz, CDCl₃)
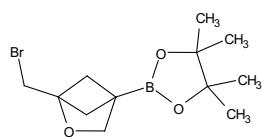
Compound 25a

(4-(4,4,5,5-tetramethyl-1,3,2-dioxaborolan-2-yl)-2-oxabicyclo[2.1.1]hexan-1-yl)methanol

[Experimental]

^{1}H NMR (500 MHz, CDCl$_3$)

¹³C NMR (126 MHz, CDCl₃)

^{13}C NMR (126 MHz, CDCl$_3$)

^{11}B NMR (160 MHz, CDCl$_3$) δ 31.64.

273
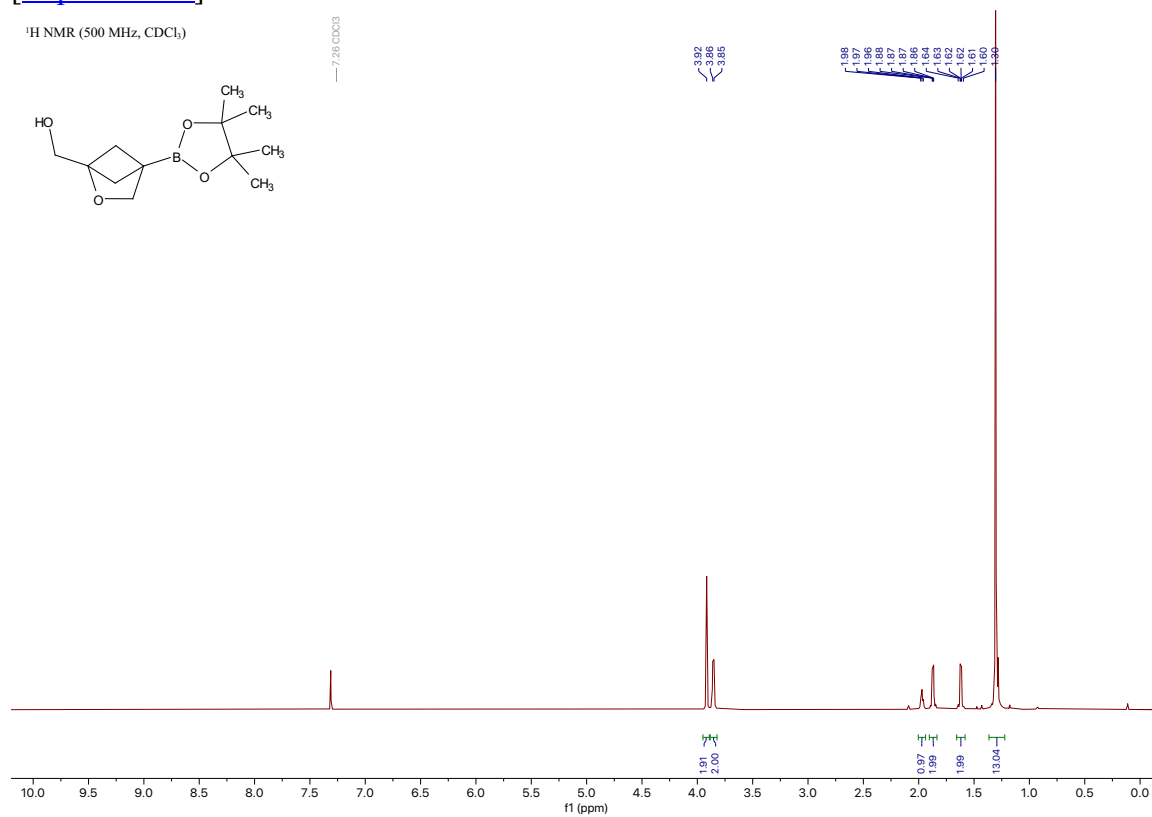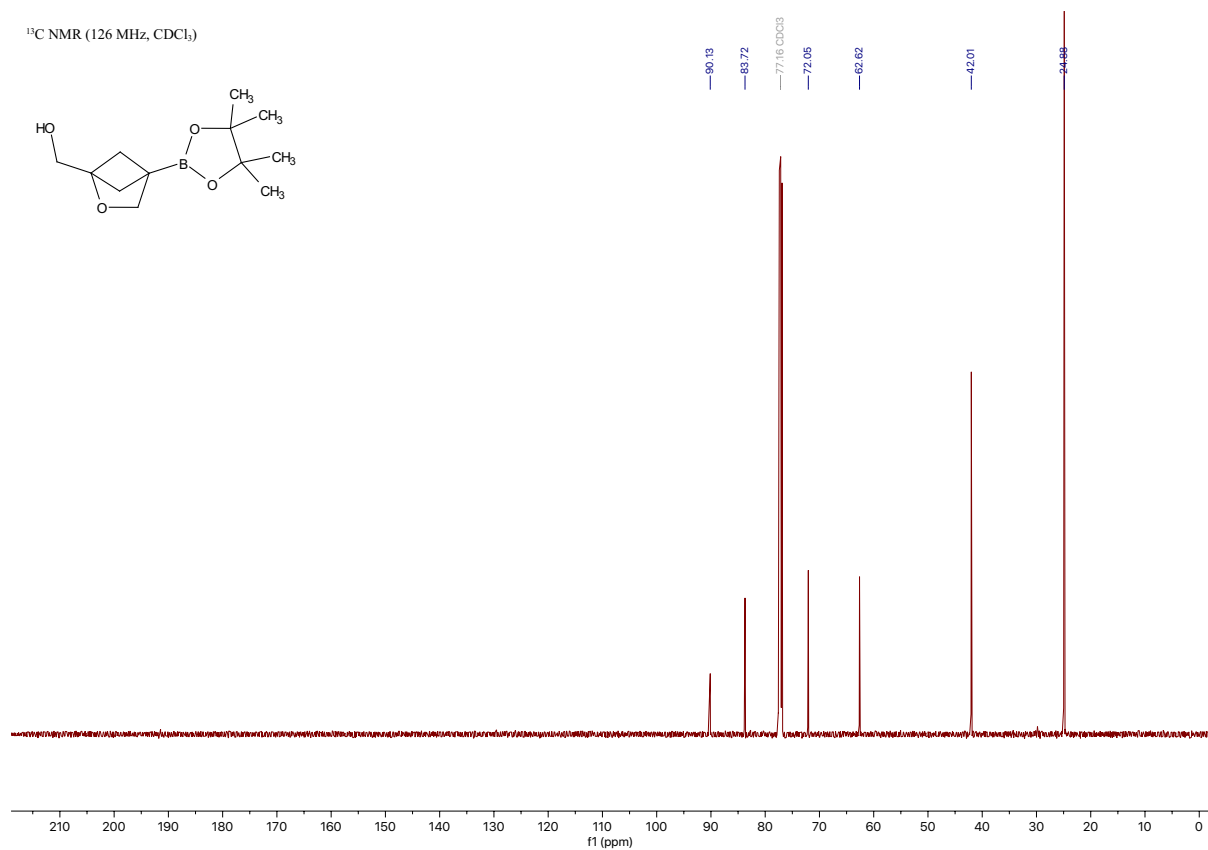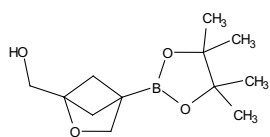
Compound 26a

tert-butyl 4-(4,4,5,5-tetramethyl-1,3,2-dioxaborolan-2-yl)-2-oxabicyclo[2.1.1]hexane-1-carboxylate [Experimental]

¹H NMR (600 MHz, CDCl₃)

¹³C NMR (151 MHz, CDCl₃)

167.68

87.13
83.88
81.91
77.16 CDC3
72.45

44.44

28.14
28.11
28.01
24.86

f1 (ppm)

¹¹B NMR (193 MHz, CDCl₃)

31.87

f1 (ppm)
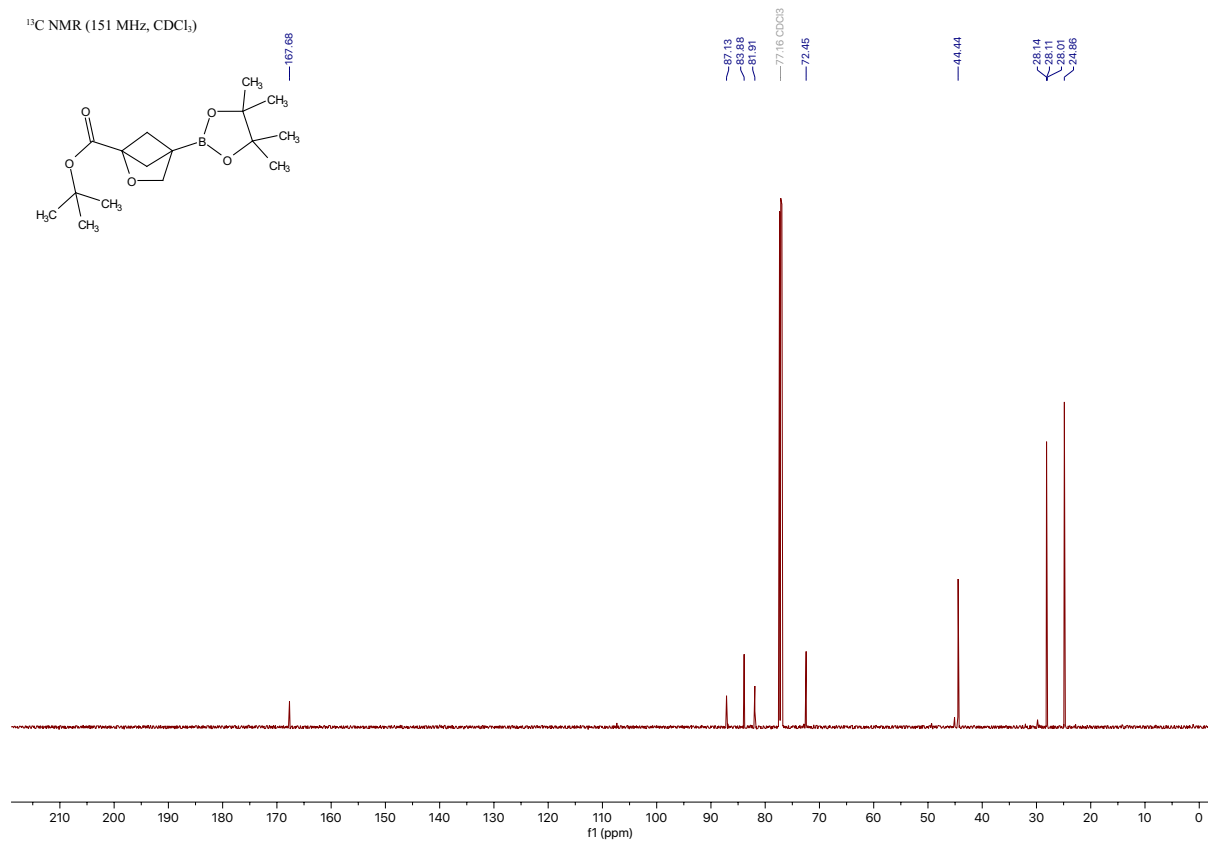
Compound 27a

***tert*-butyl 4-(4,4,5,5-tetramethyl-1,3,2-dioxaborolan-2-yl)-2-azabicyclo[2.1.1]hexane-2-carboxylate** [Experimental]

¹H NMR (500 MHz, CDCl₃)

¹³C NMR (126 MHz, CDCl₃)

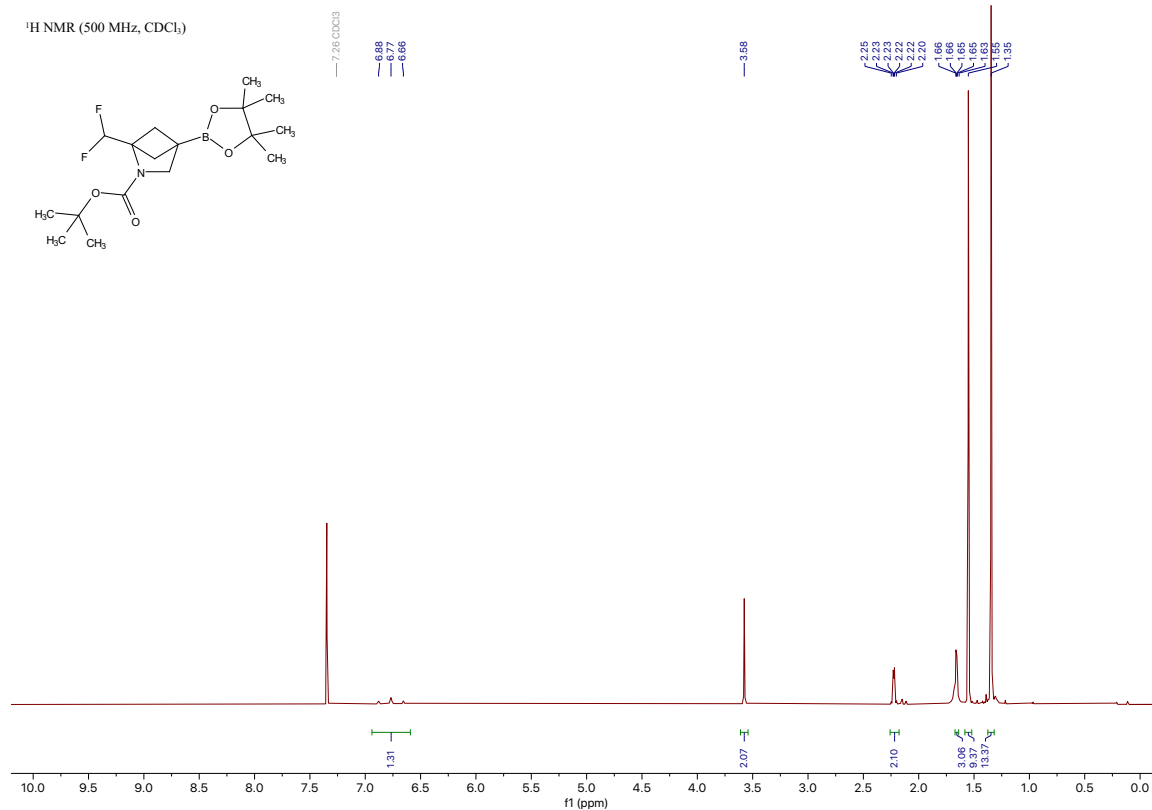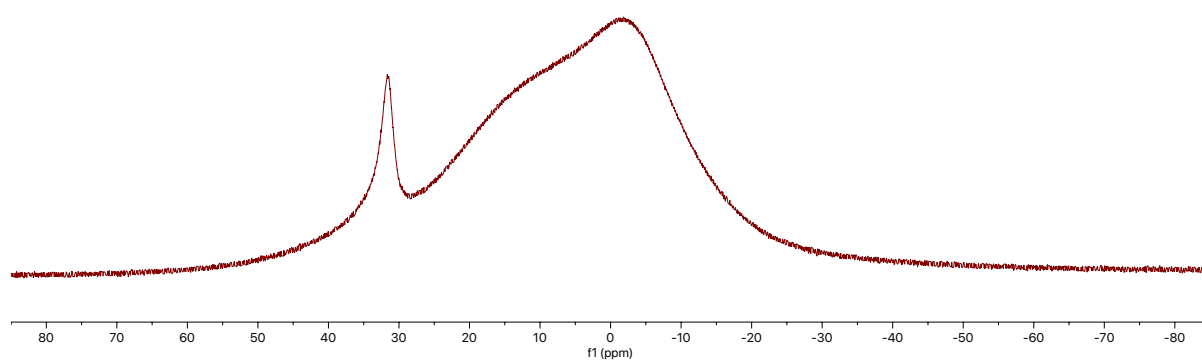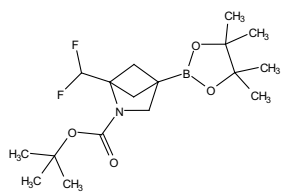¹¹B NMR (160 MHz, CDCl₃)

277
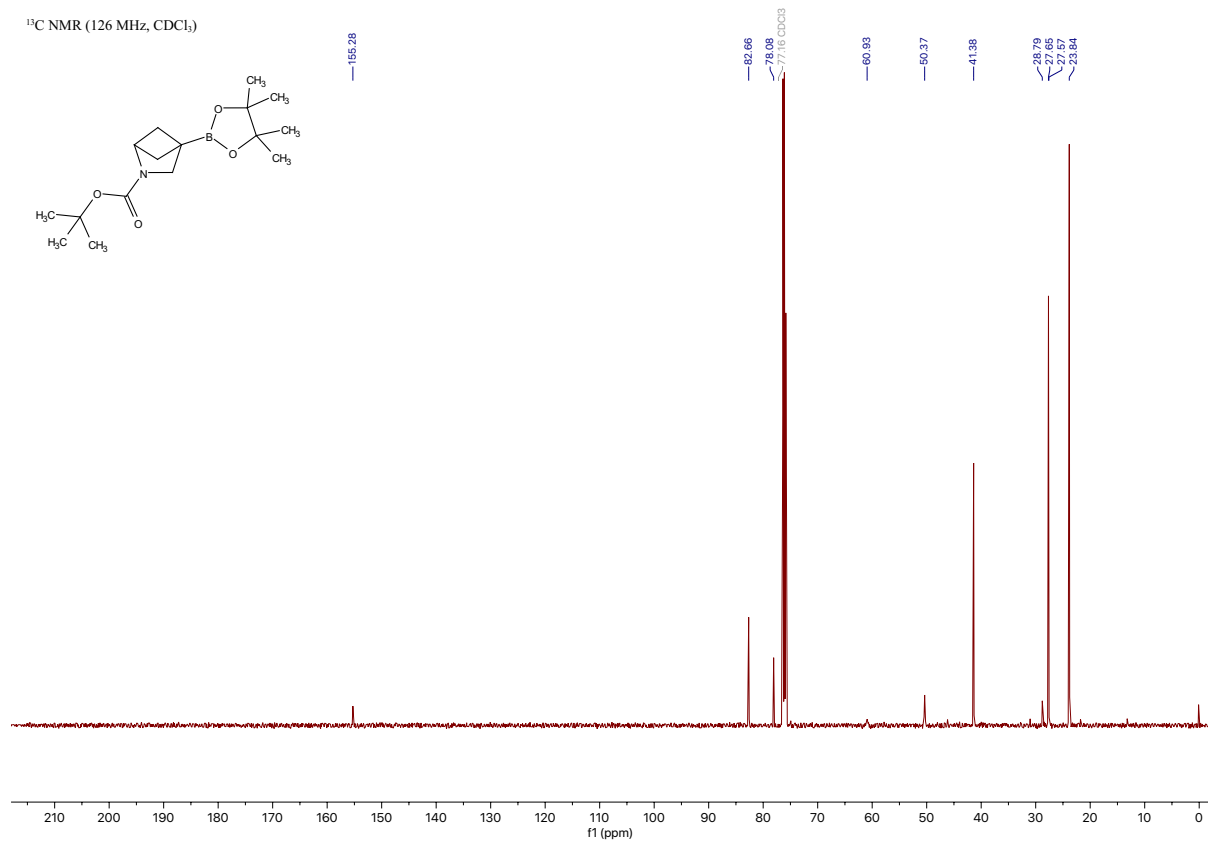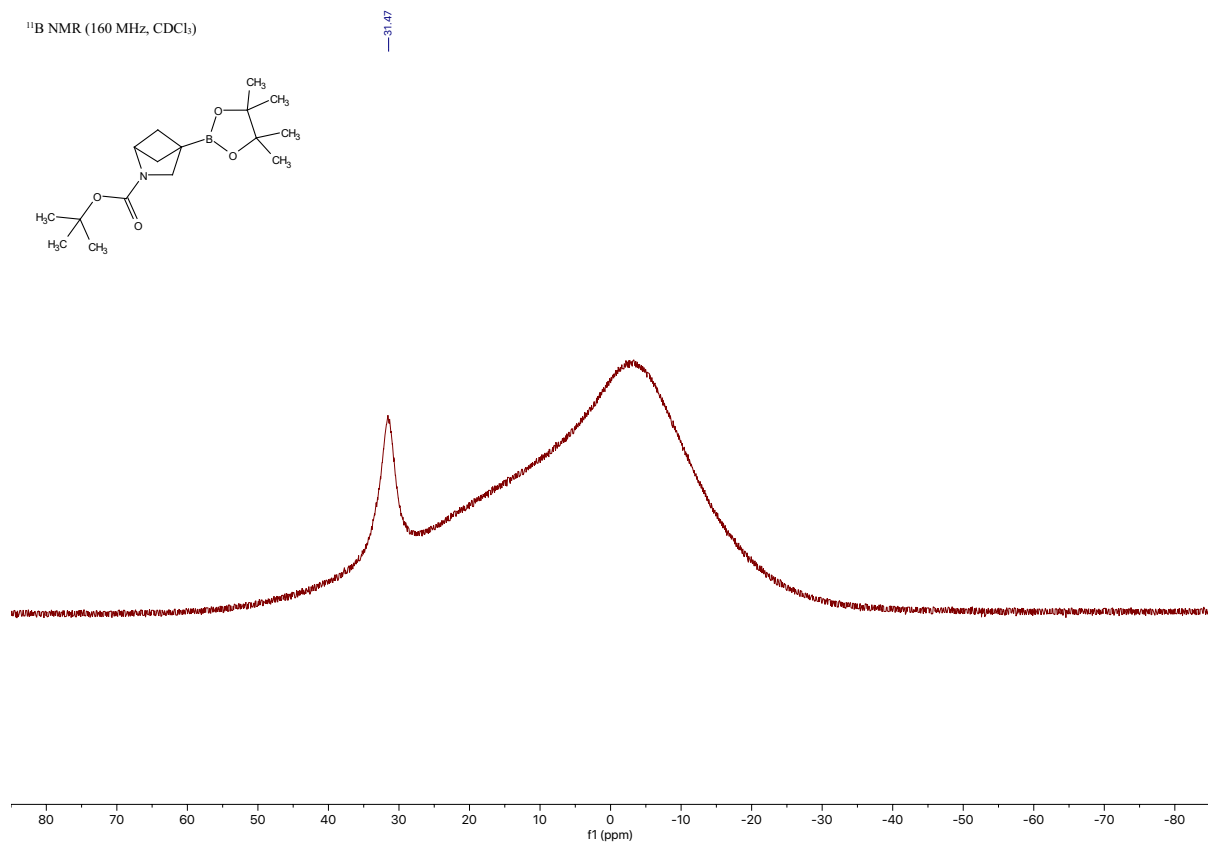
Compound 28a

tert-butyl 1-methyl-4-(4,4,5,5-tetramethyl-1,3,2-dioxaborolan-2-yl)-2-azabicyclo[2.1.1]hexane-2-carboxylate [Experimental]

¹H NMR (600 MHz, CDCl₃)

¹³C NMR (151 MHz, CDCl₃)

156.09

83.59
78.77
71.63
54.69
46.68
28.76
24.85
19.43

f1 (ppm)

¹¹B NMR (193 MHz, CDCl₃)

32.06

f1 (ppm)
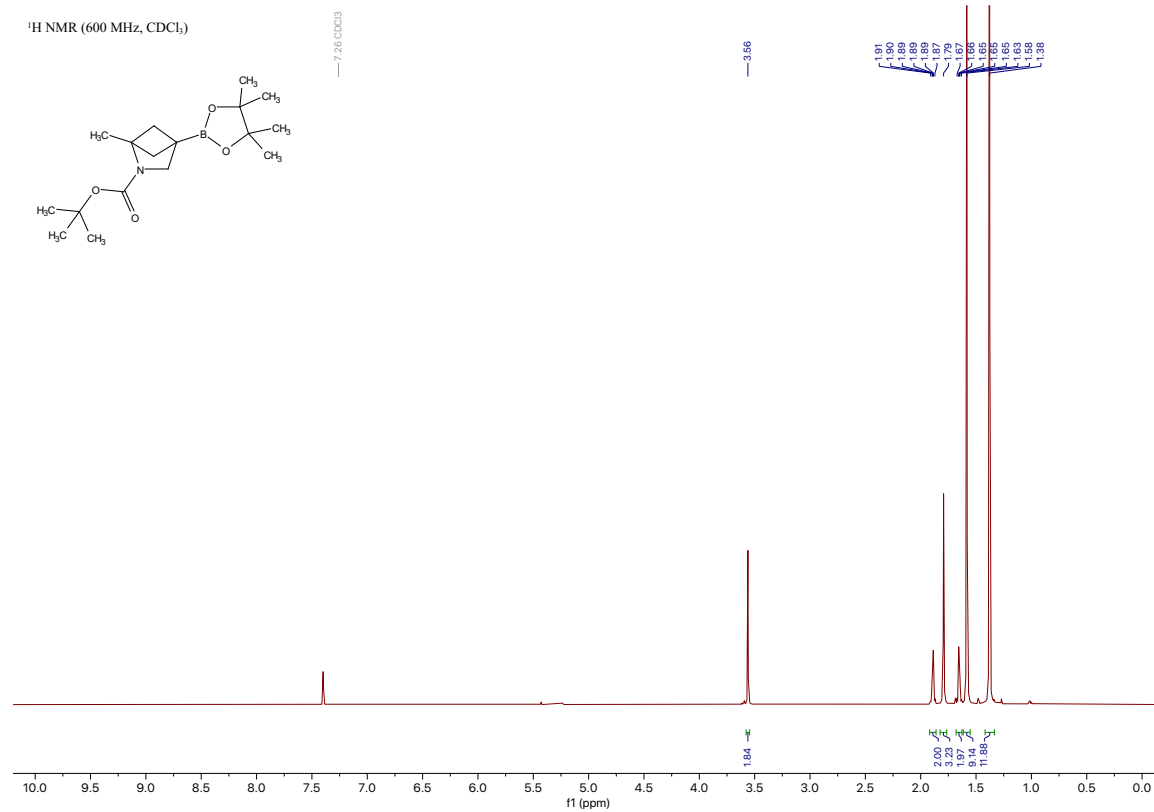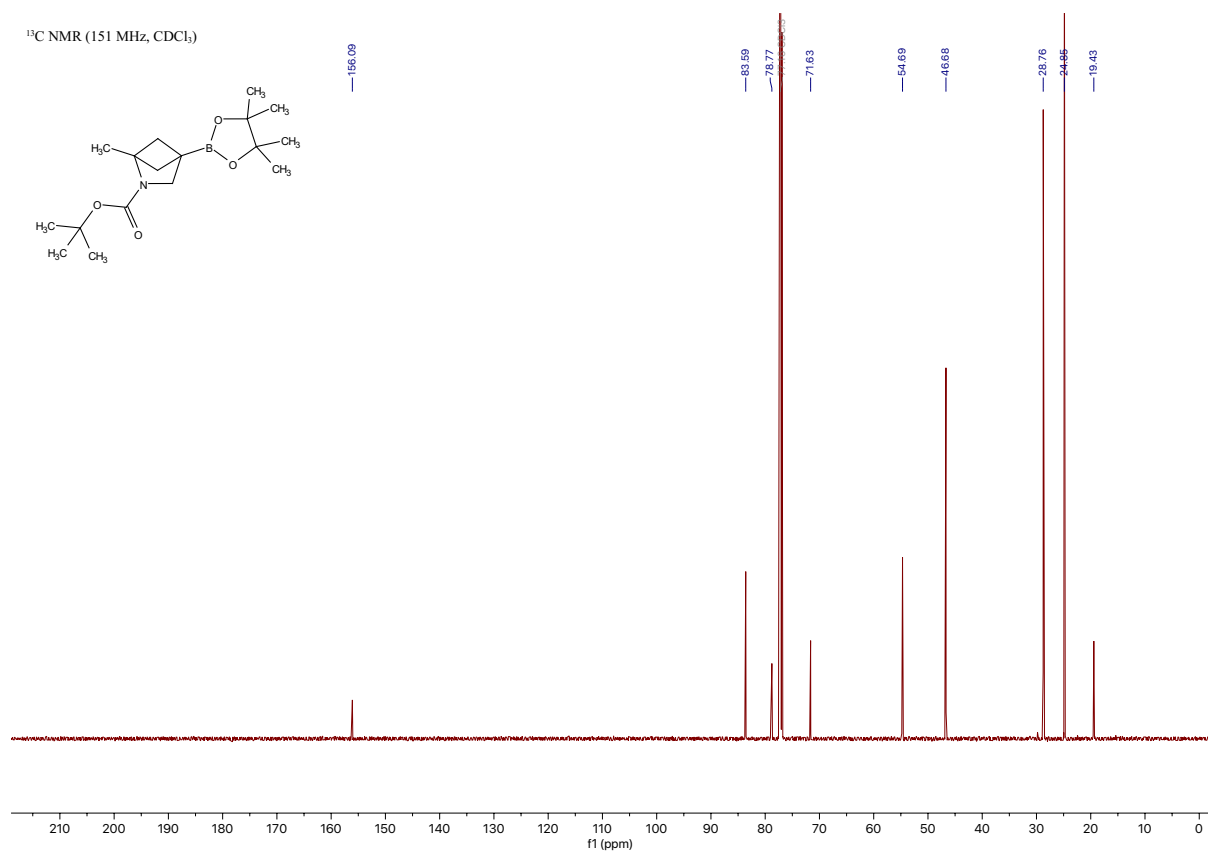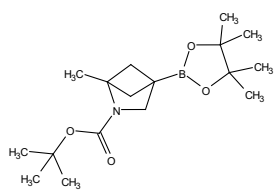
Compound 29a

tert-butyl 4-(4,4,5,5-tetramethyl-1,3,2-dioxaborolan-2-yl)-1-(trifluoromethyl)-2-azabicyclo[2.1.1]hexane-2-carboxylate [Experimental]

¹H NMR (600 MHz, CDCl₃)
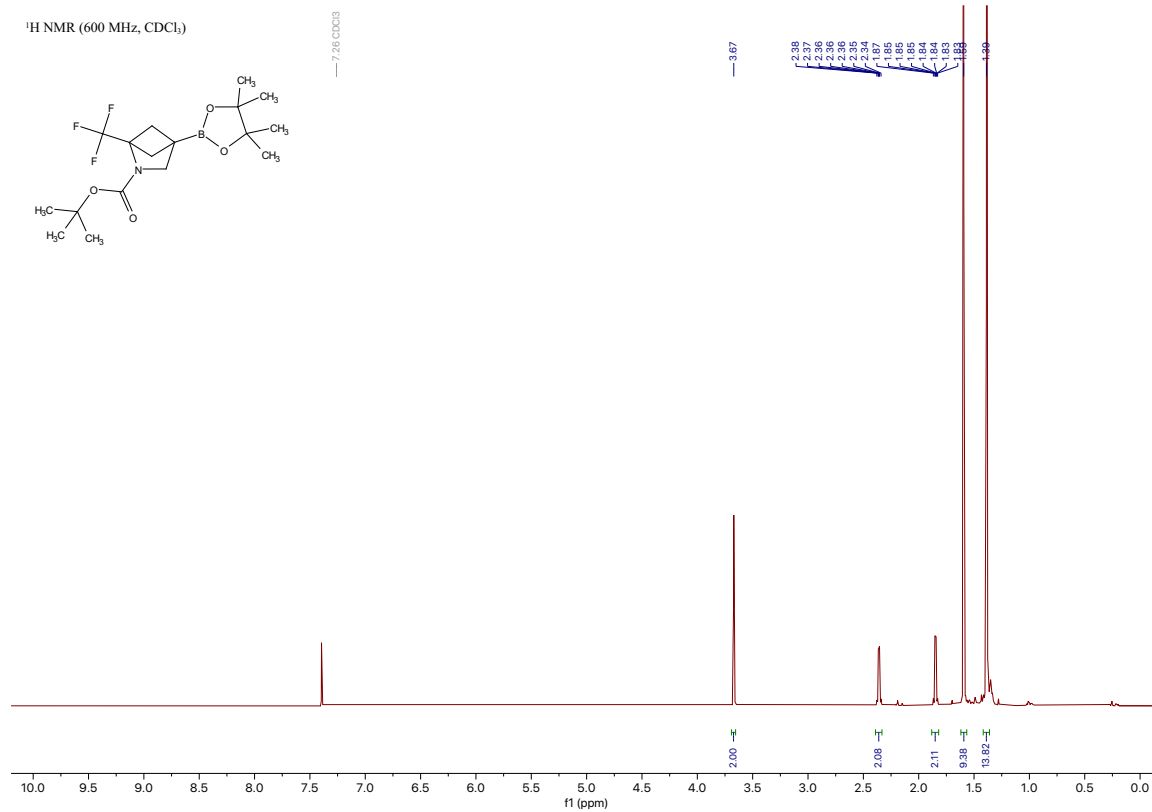
¹³C NMR (151 MHz, CDCl₃)

¹¹B NMR (193 MHz, CDCl₃)

31.49

f1 (ppm)
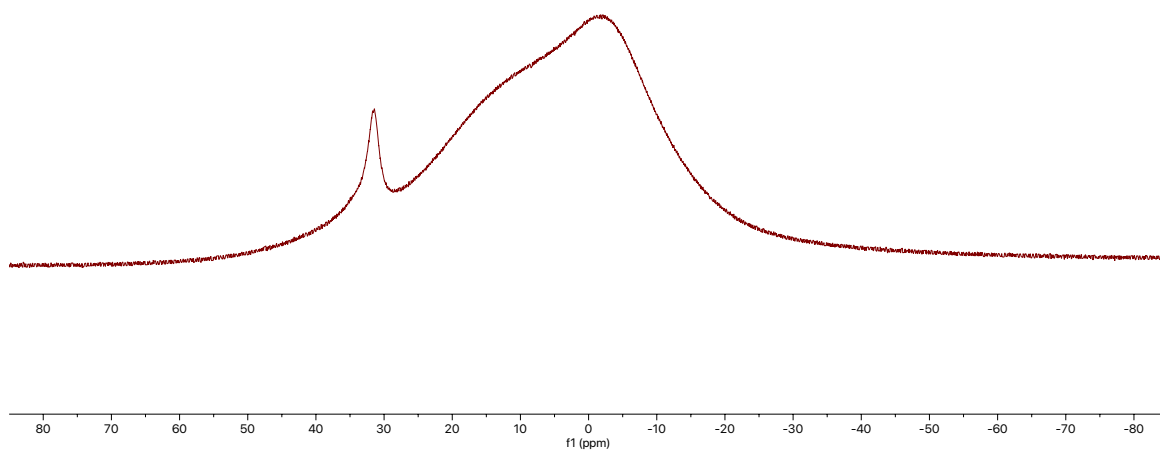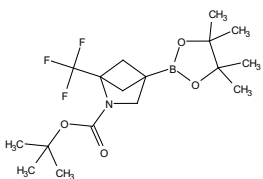
¹⁹F NMR (565 MHz, CDCl₃)

−68.46

f1 (ppm)
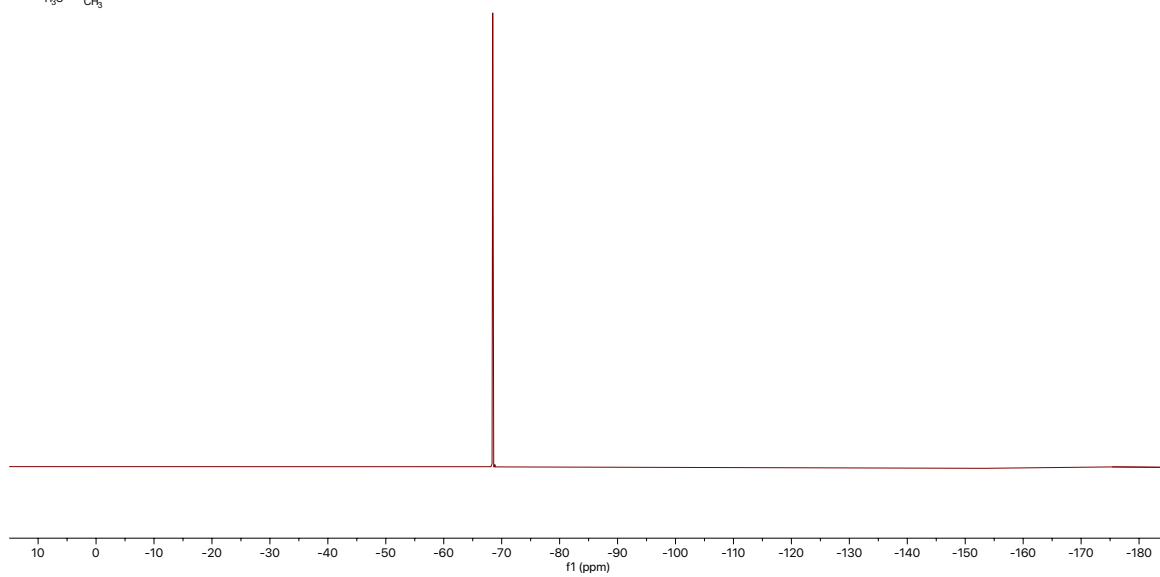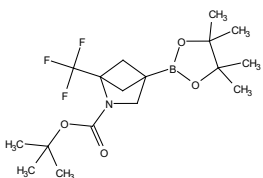
Compound 30a

tert-butyl 1-(difluoromethyl)-4-(4,4,5,5-tetramethyl-1,3,2-dioxaborolan-2-yl)-2-azabicyclo[2.1.1]hexane-2-carboxylate [Experimental]
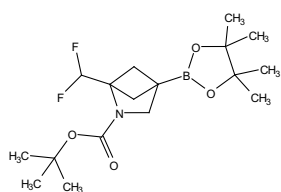
¹H NMR (500 MHz, CDCl₃)

¹³C NMR (151 MHz, CDCl₃)

—31.76

—-124.84

283
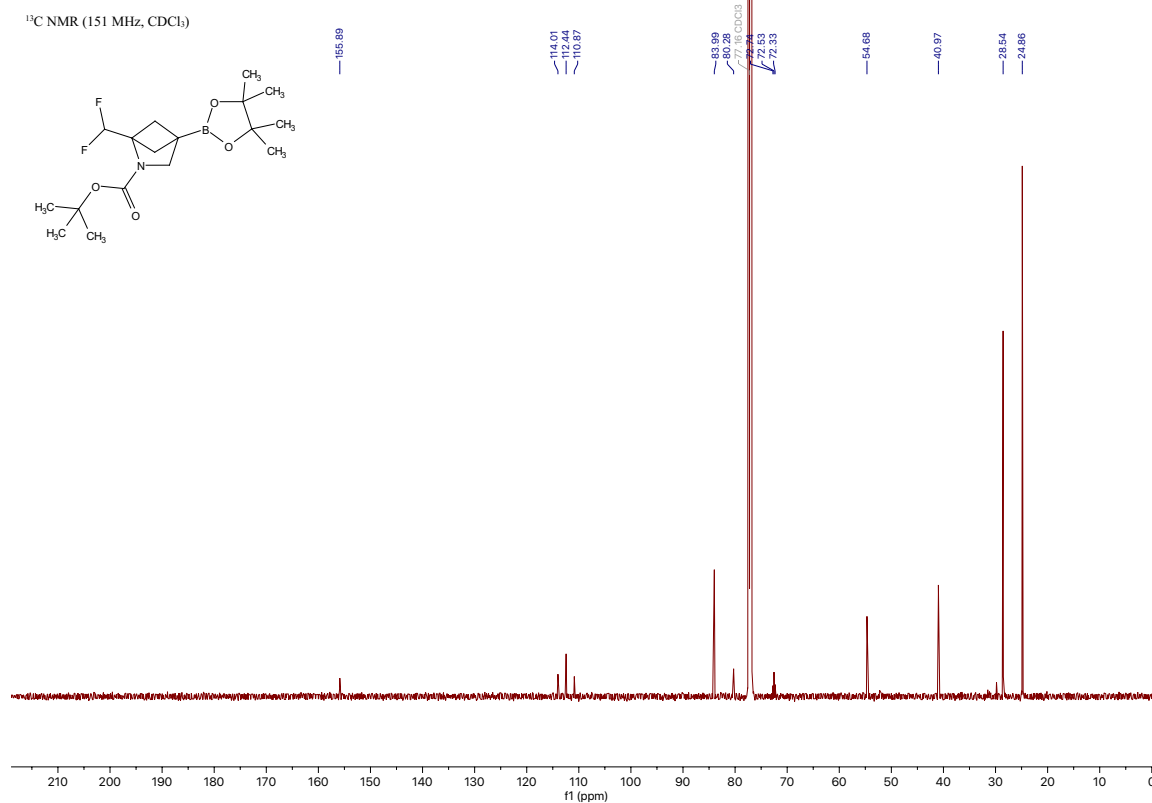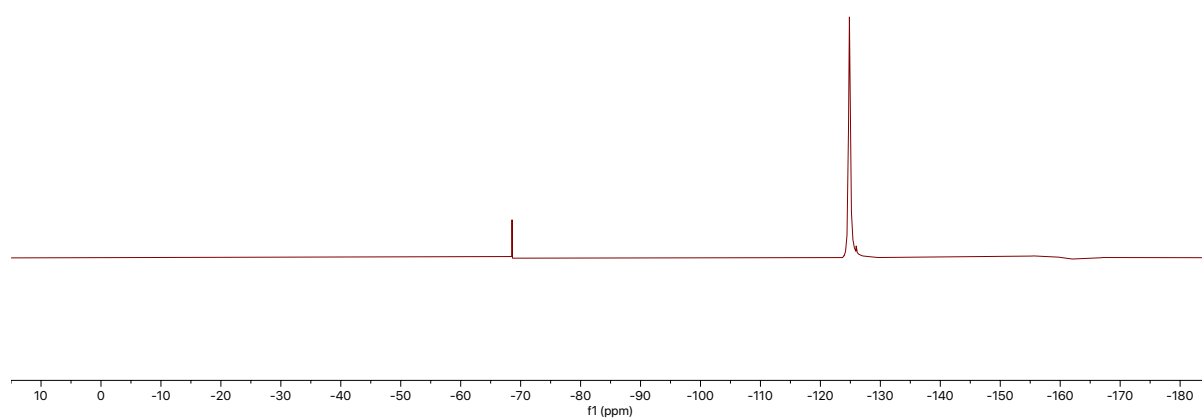
Compound 31a

tert-butyl 1-(fluoromethyl)-4-(4,4,5,5-tetramethyl-1,3,2-dioxaborolan-2-yl)-2-azabicyclo[2.1.1]hexane-2-carboxylate [Experimental]
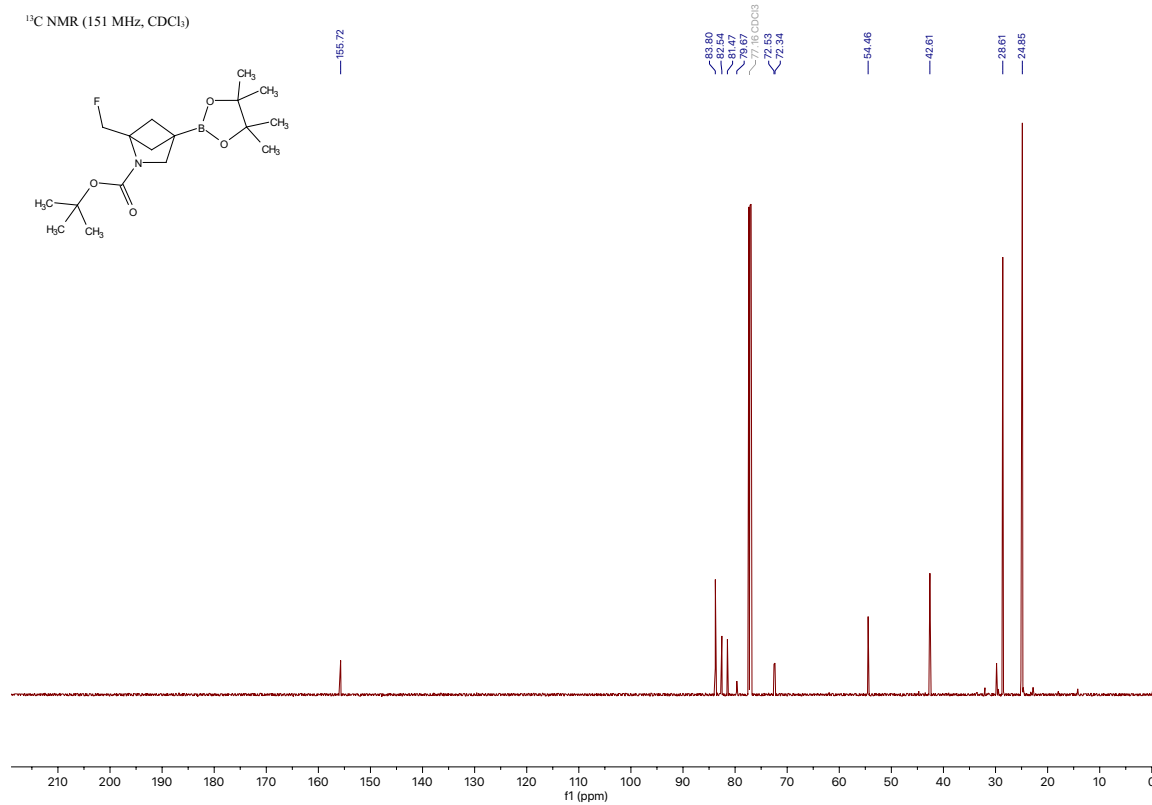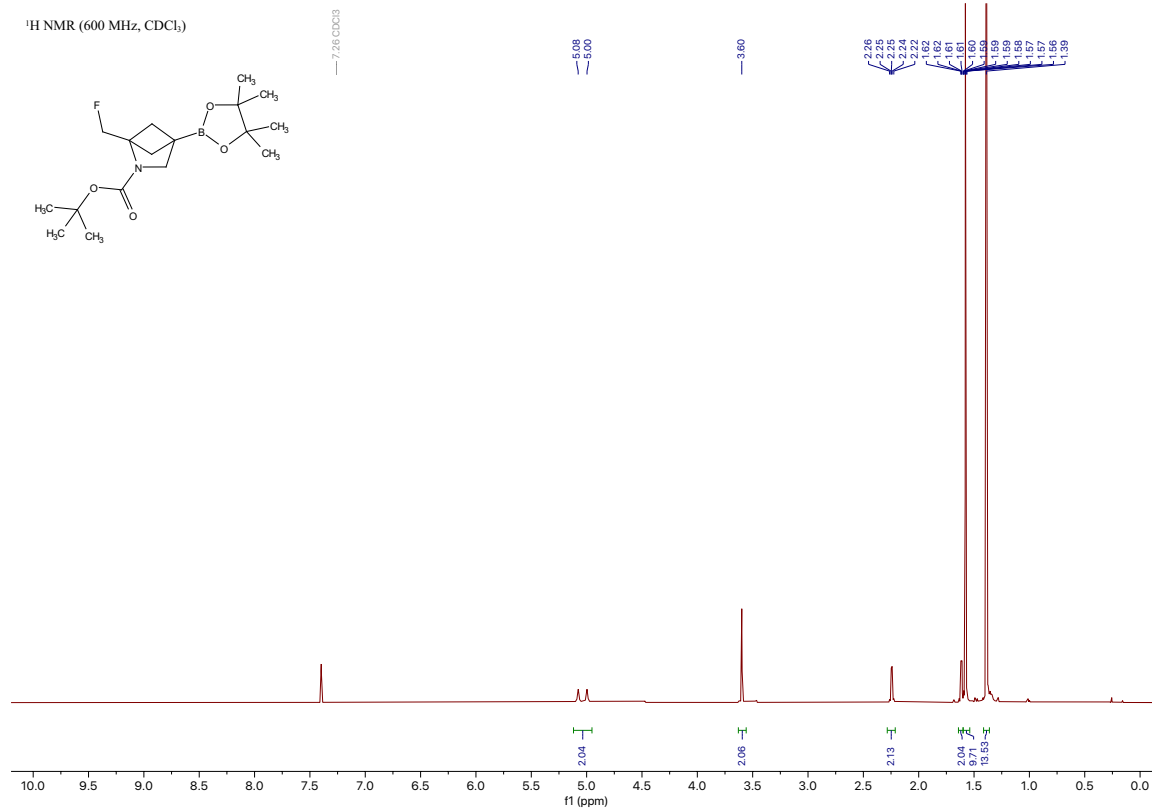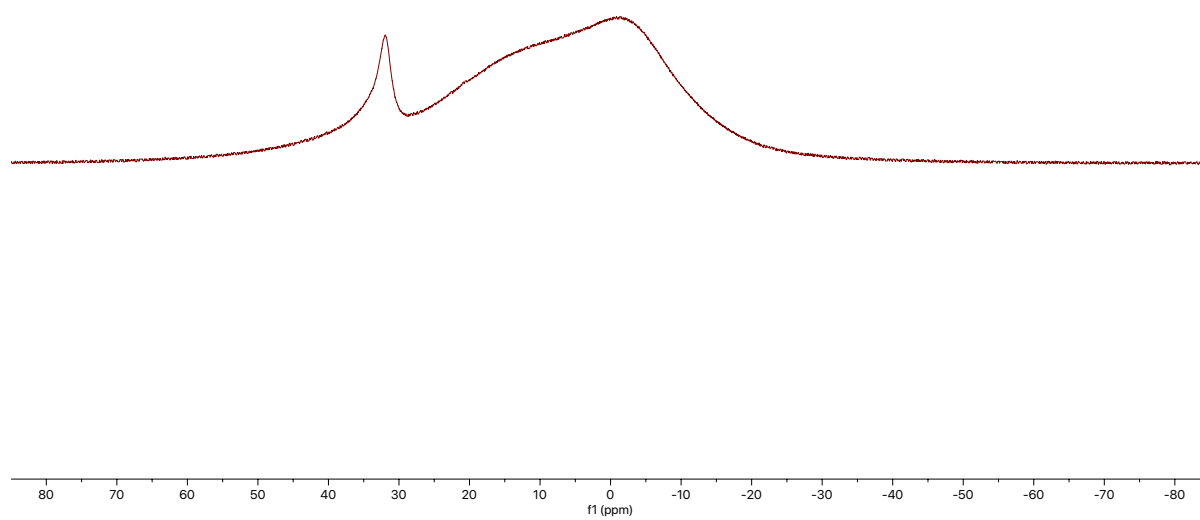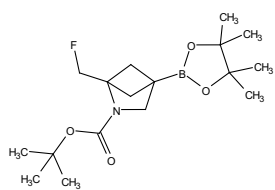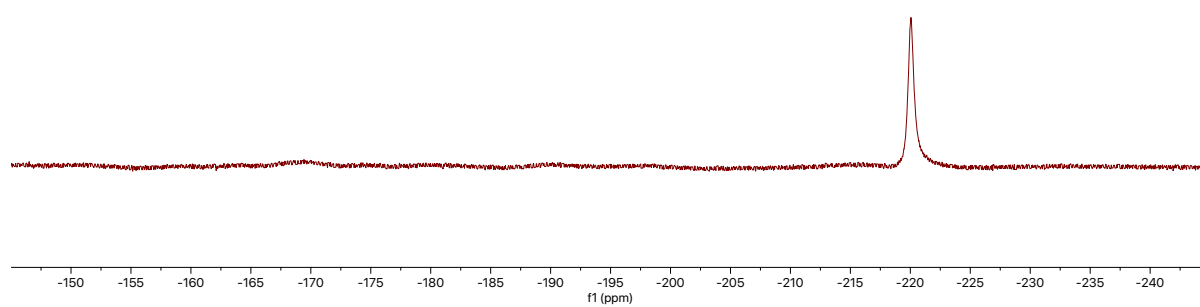
¹H NMR (600 MHz, CDCl₃)

¹³C NMR (151 MHz, CDCl₃)

¹¹B NMR (193 MHz, CDCl₃)

31.93

f1 (ppm)

¹⁹F NMR (565 MHz, CDCl₃)

-219.93

f1 (ppm)

Compound 32a

tert-butyl 1-((dimethylamino)methyl)-4-(4,4,5,5-tetramethyl-1,3,2-dioxaborolan-2-yl)-2-azabicyclo[2.1.1]hexane-2-carboxylate [Experimental]
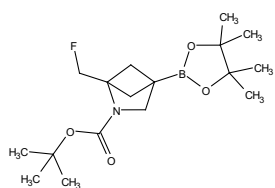
¹H NMR (600 MHz, CDCl₃)
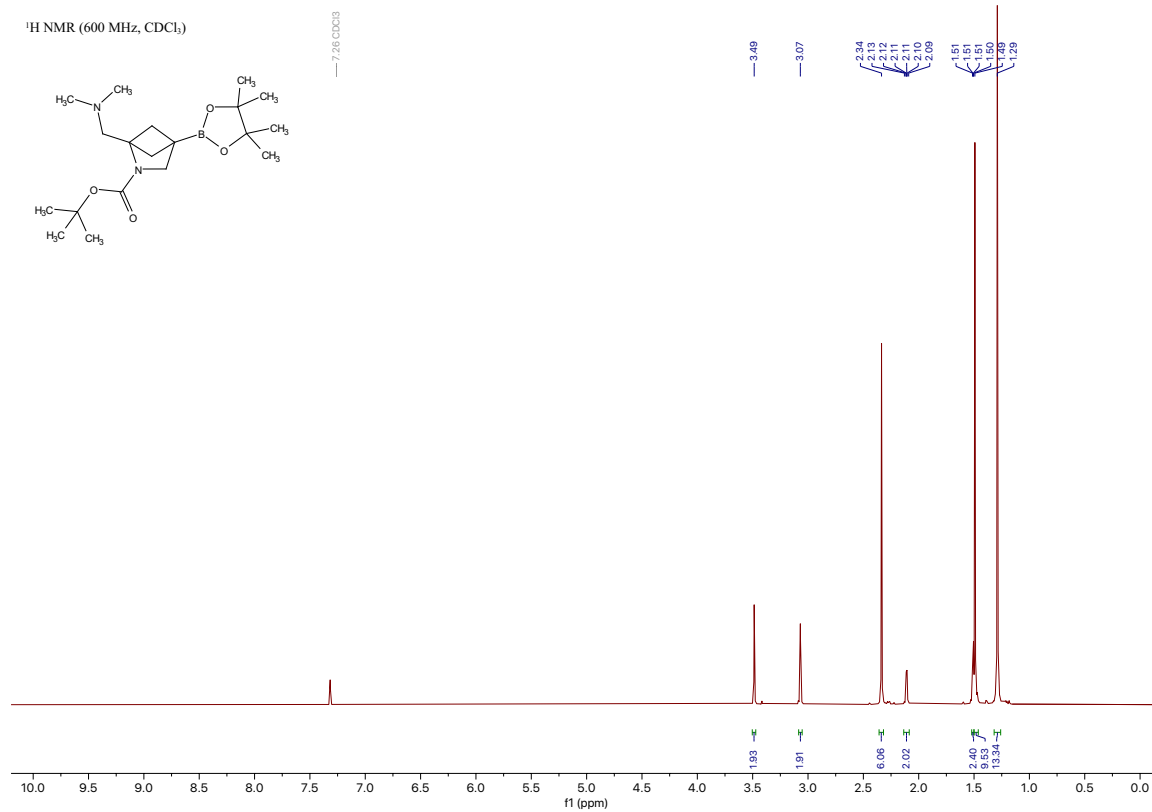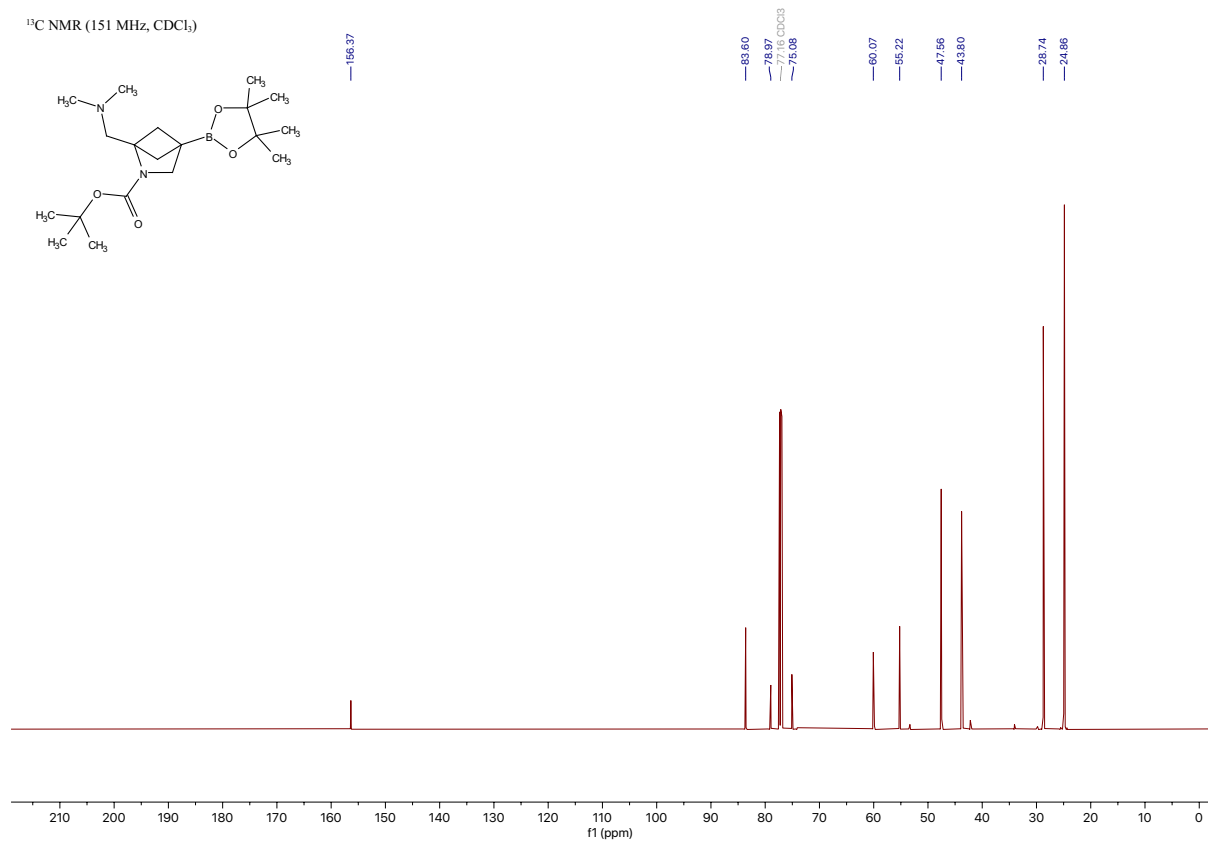
¹³C NMR (151 MHz, CDCl₃)

156.37

83.60
78.97
77.16 CDCl3
75.08
60.07
55.22
47.56
43.80
28.74
24.86

¹¹B NMR (193 MHz, CDCl₃)

32.09

287

Compound 33a

tert-butyl 1-(((_tert_-butoxycarbonyl)amino)methyl)-4-(trifluoro-λ4-boraneyl)-2-azabicyclo[2.1.1]hexane-2-carboxylate, potassium salt [Experimental]

¹H NMR (500 MHz, Acetone)

¹³C NMR (126 MHz, Acetone)

¹¹B NMR (160 MHz, Acetone)

—3.52

80   70   60   50   40   30   20   10   0   -10   -20   -30   -40   -50   -60   -70   -80
f1 (ppm)

¹⁹F NMR (470 MHz, Acetone)

—-147.72

-90   -95   -100   -105   -110   -115   -120   -125   -130   -135   -140   -145   -150   -155   -160   -165   -170
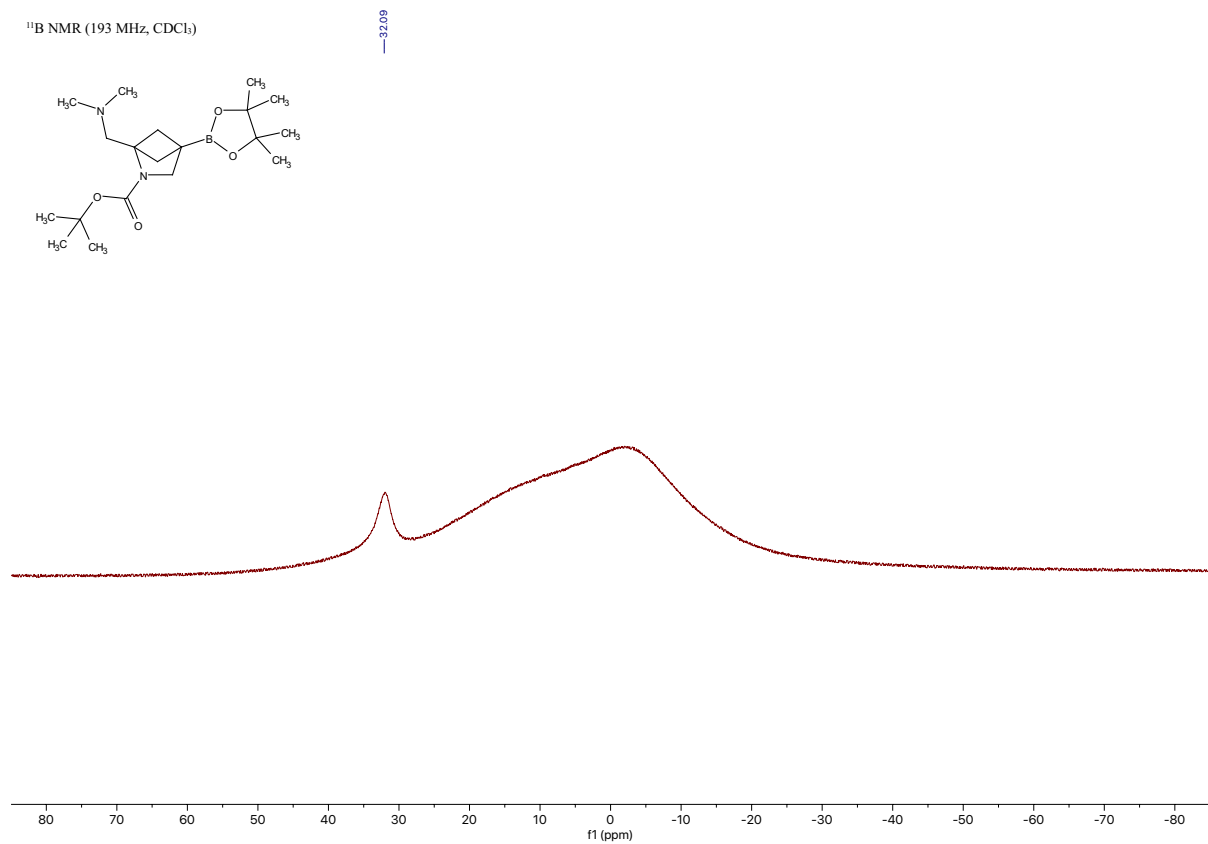f1 (ppm)
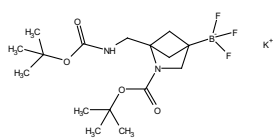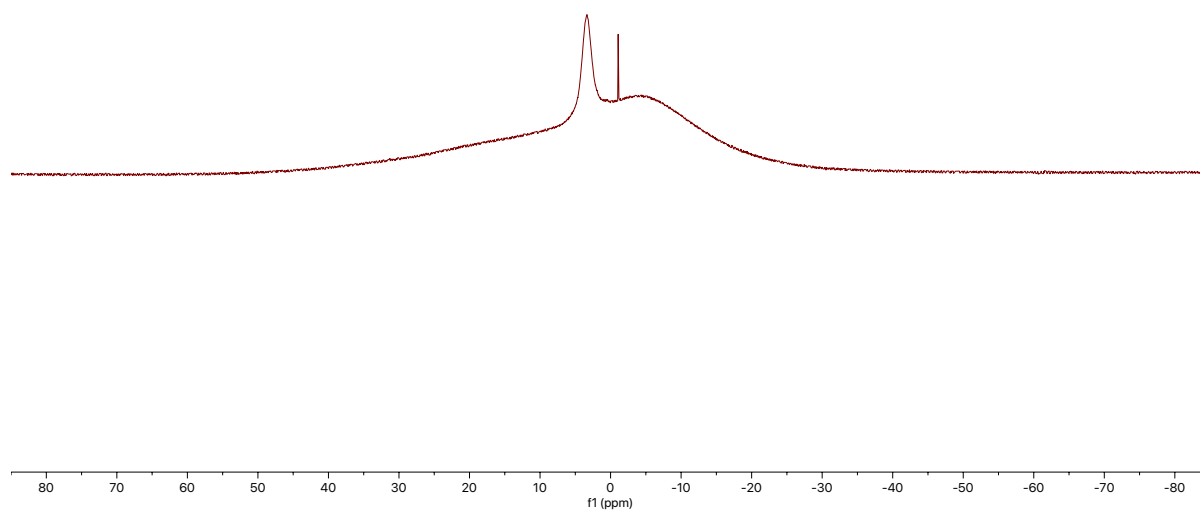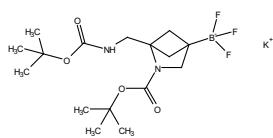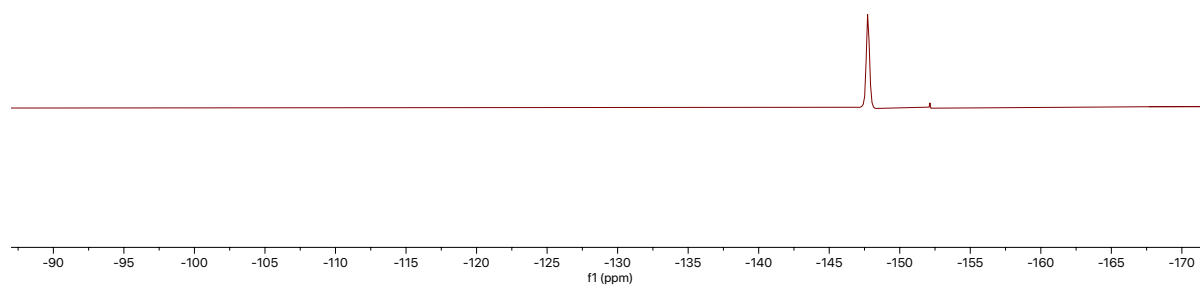
Compound 34a

tert-butyl 1-carbamoyl-4-(4,4,5,5-tetramethyl-1,3,2-dioxaborolan-2-yl)-2-azabicyclo[2.1.1]hexane-2-carboxylate [Experimental]
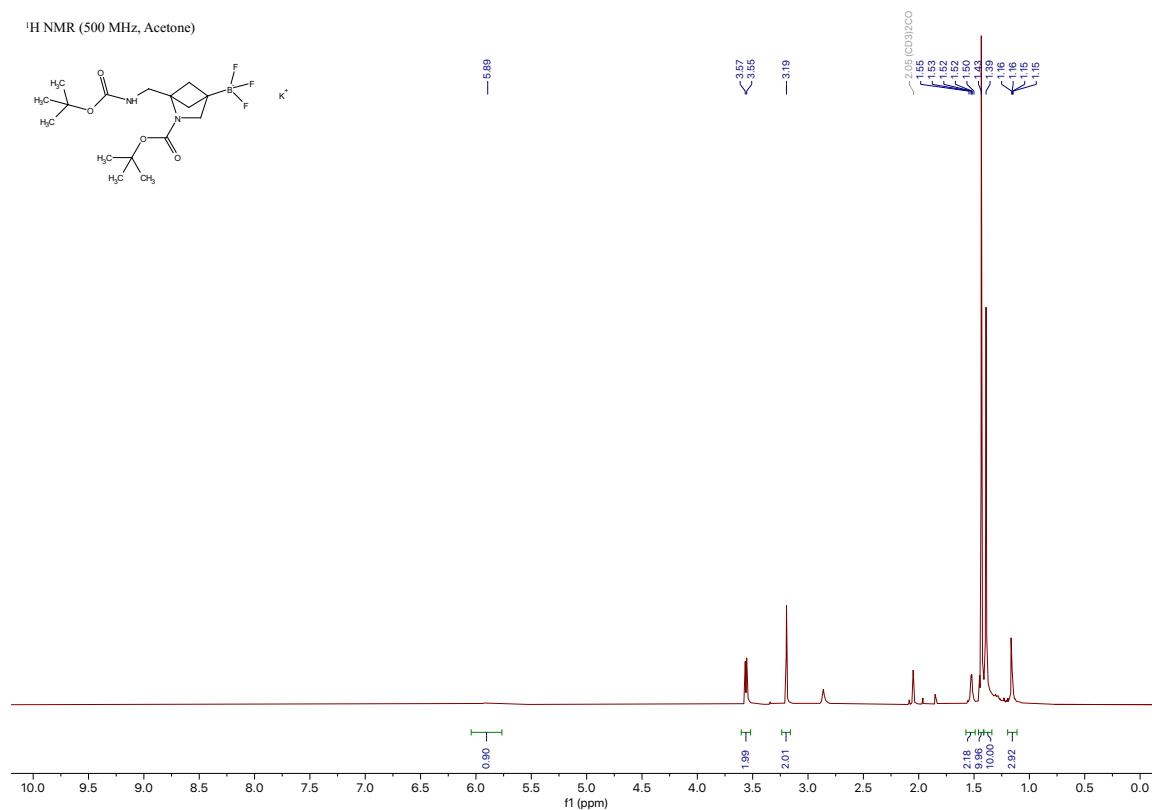
¹H NMR (600 MHz, CDCl₃)
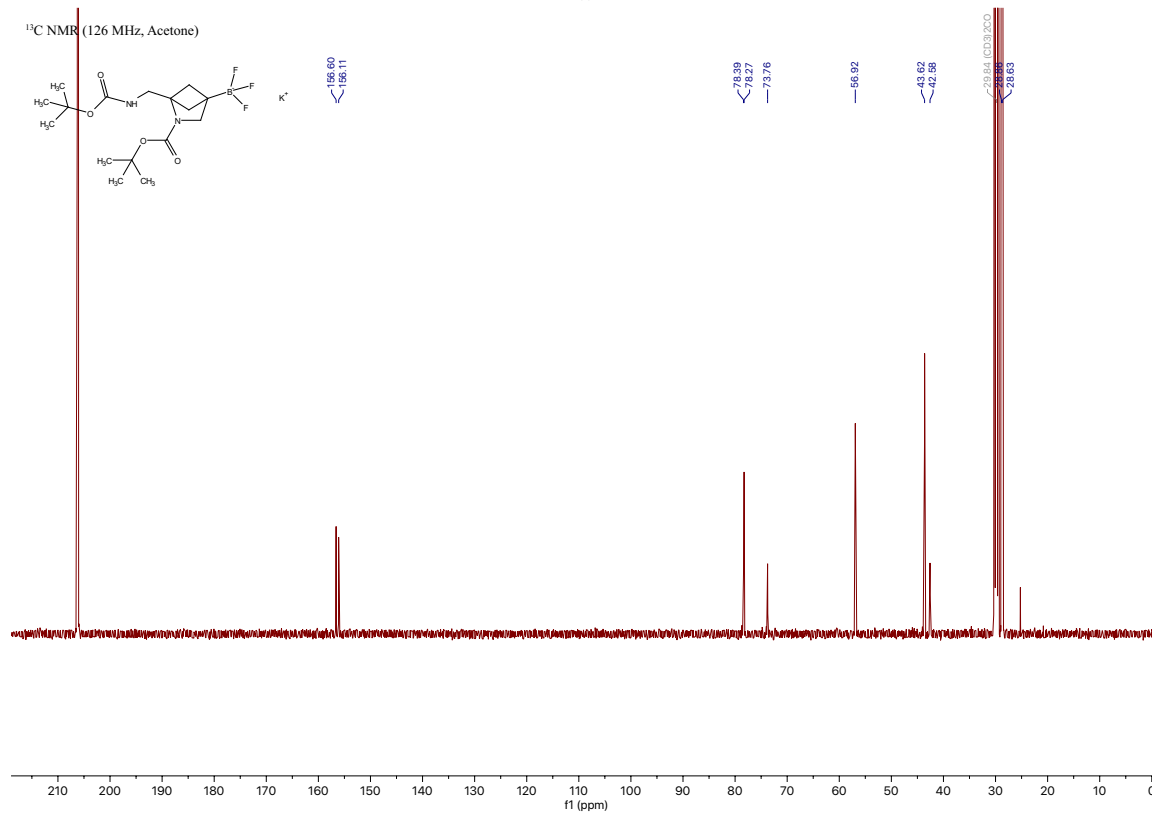
^{13}C NMR (151 MHz, CDCl$_3$)

171.38
158.30
84.00
81.06
72.94
55.62
44.22
28.34
24.85

^{11}B NMR (193 MHz, CDCl$_3$)

31.87

291

Compound 35a

***tert*-butyl 4-(4,4,5,5-tetramethyl-1,3,2-dioxaborolan-2-yl)-1-((triisopropylsilyl)ethynyl)-2-azabicyclo[2.1.1]hexane-2-carboxylate** [Experimental]

¹H NMR (600 MHz, CDCl₃)

¹³C NMR (151 MHz, CDCl₃)
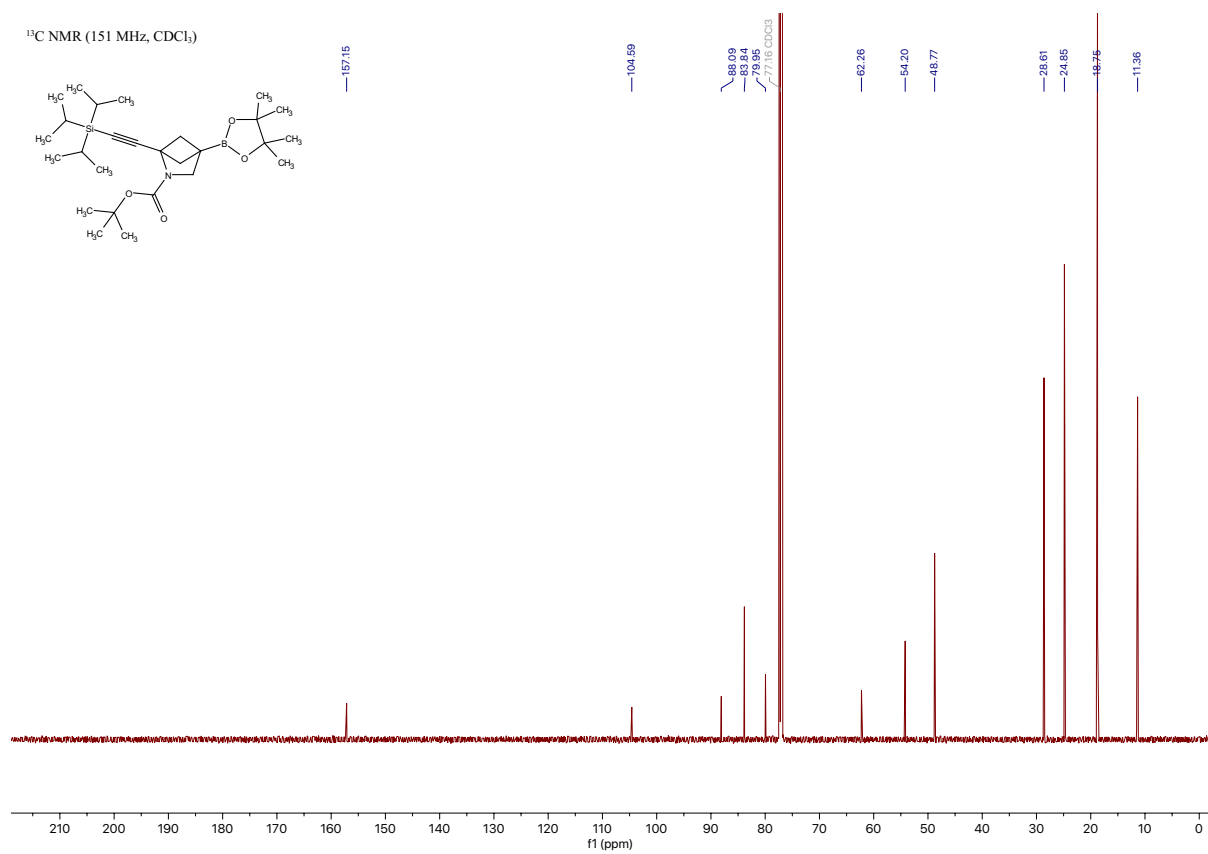
¹¹B NMR (193 MHz, CDCl₃)
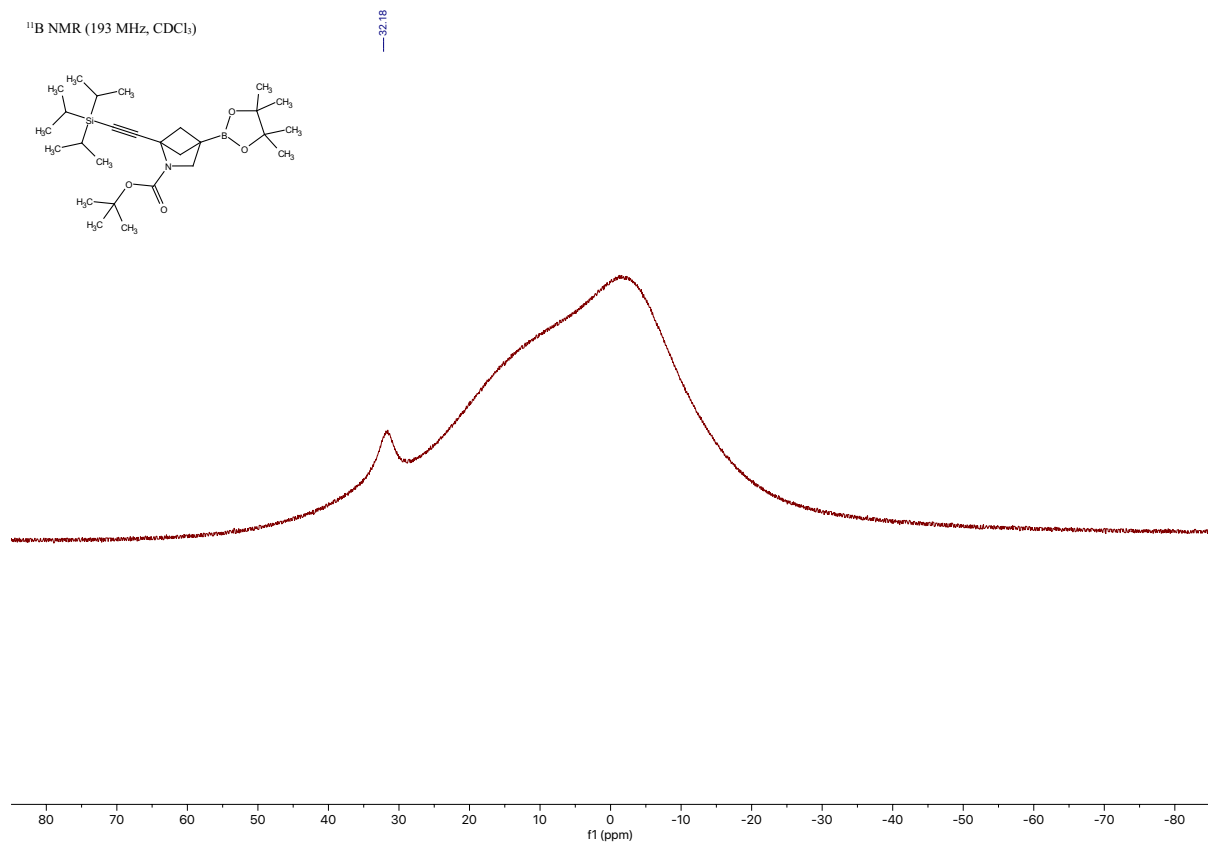
Compound 36a

tert-butyl 1-(hydroxymethyl)-4-(4,4,5,5-tetramethyl-1,3,2-dioxaborolan-2-yl)-2-azabicyclo[2.1.1]hexane-2-carboxylate [Experimental]

¹H NMR (600 MHz, CDCl₃)

¹³C NMR (151 MHz, CDCl₃)

155.82

83.81
79.91
77.16 CDCl3
75.23
61.86
54.33
43.44
28.70
24.87

210 200 190 180 170 160 150 140 130 120 110 100 90 80 70 60 50 40 30 20 10 0
f1 (ppm)

¹¹B NMR (193 MHz, CDCl₃)

32.02

80 70 60 50 40 30 20 10 0 -10 -20 -30 -40 -50 -60 -70 -80
f1 (ppm)

295
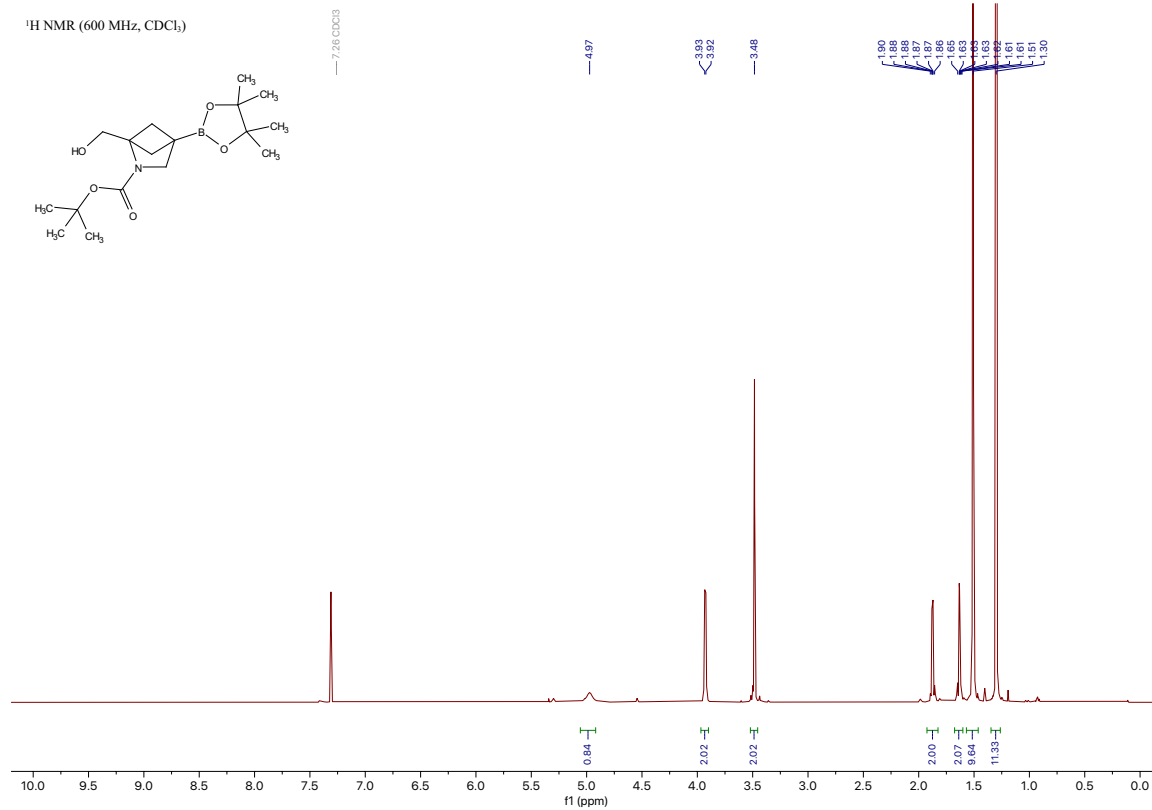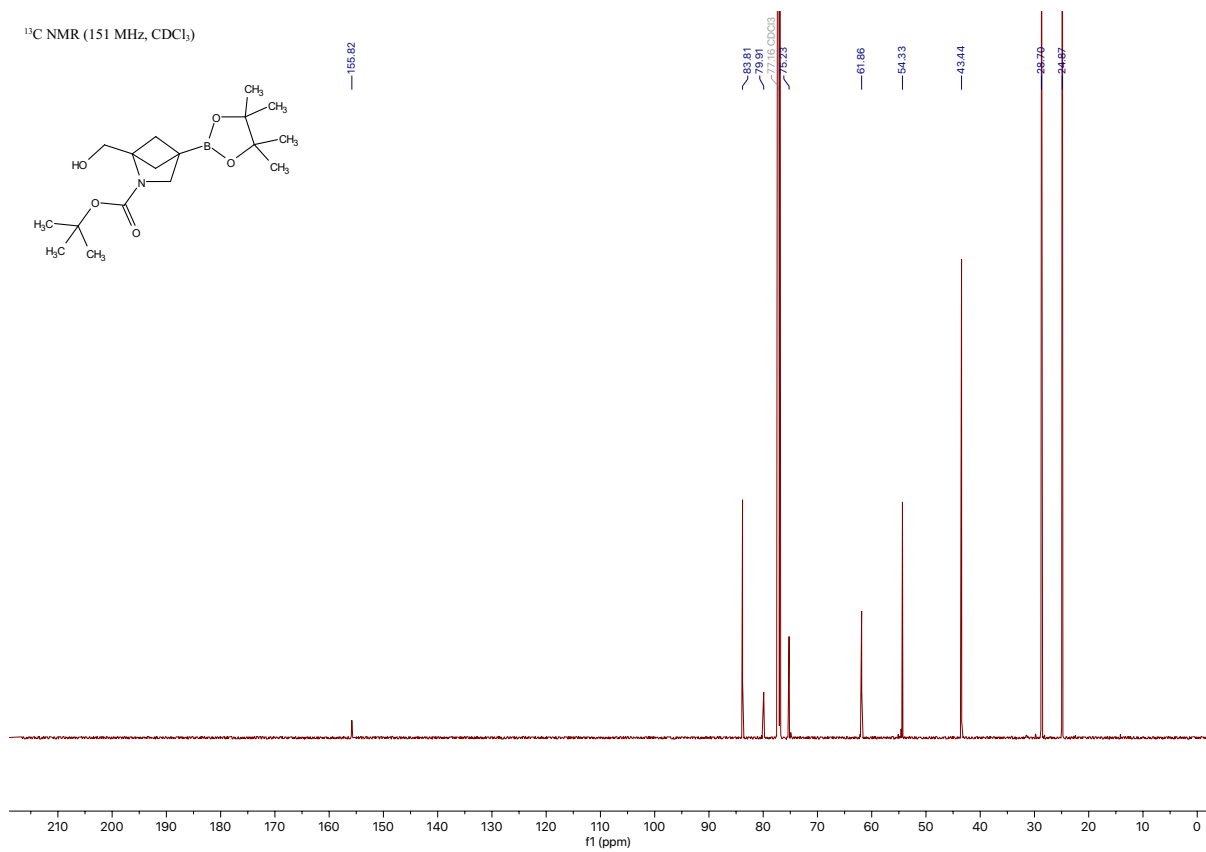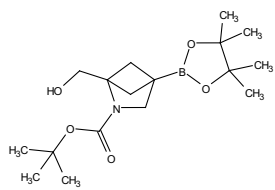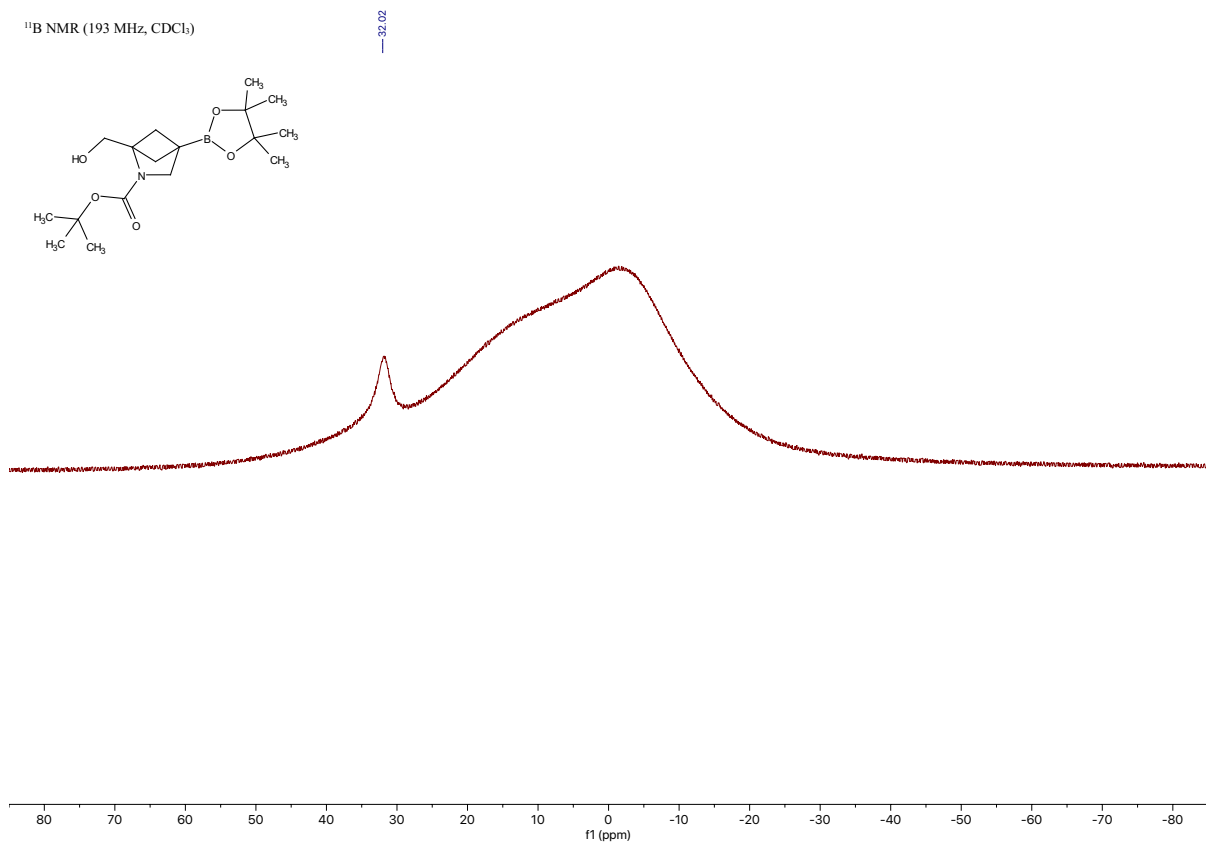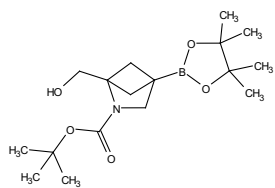
Compound 37a

(7-(4,4,5,5-tetramethyl-1,3,2-dioxaborolan-2-yl)tetrahydro-1*H*,6*H*-7,8a-methanopyrrolo[2,1-*c*][1,4]oxazin-3-yl)methanol [Experimental]

¹H NMR (500 MHz, CDCl₃)

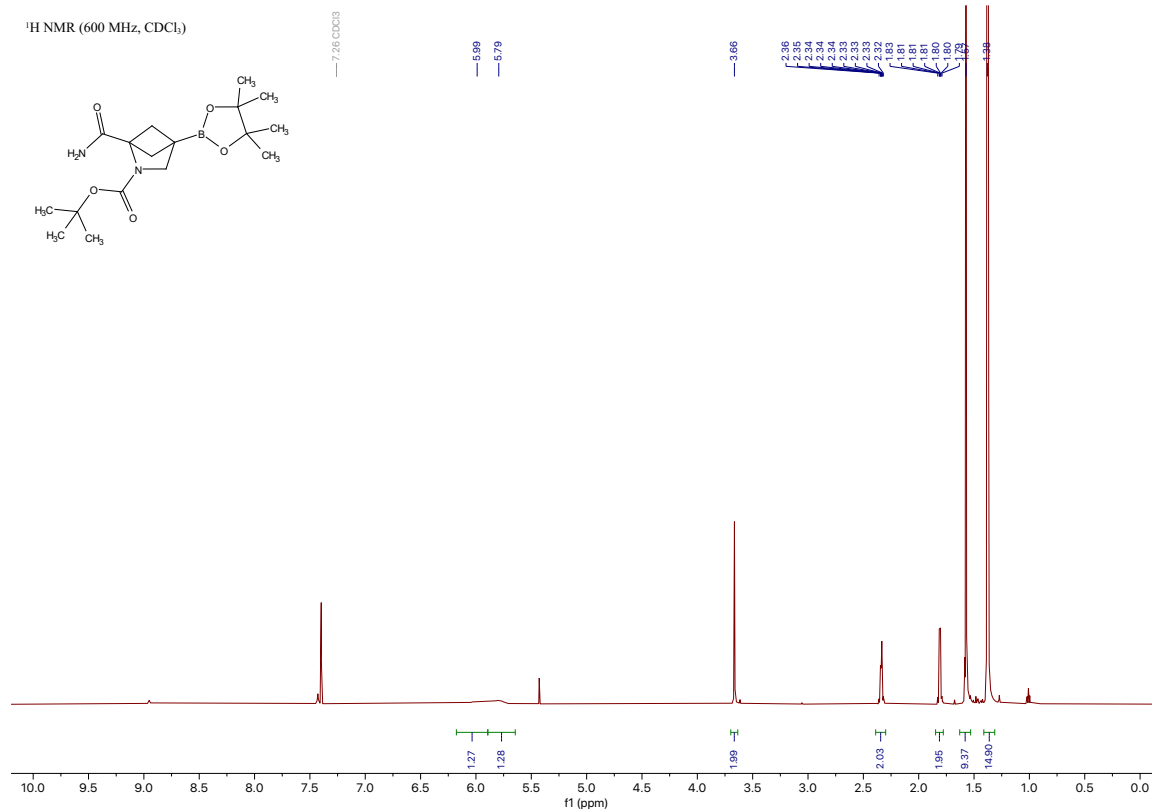¹³C NMR (126 MHz, CDCl₃)
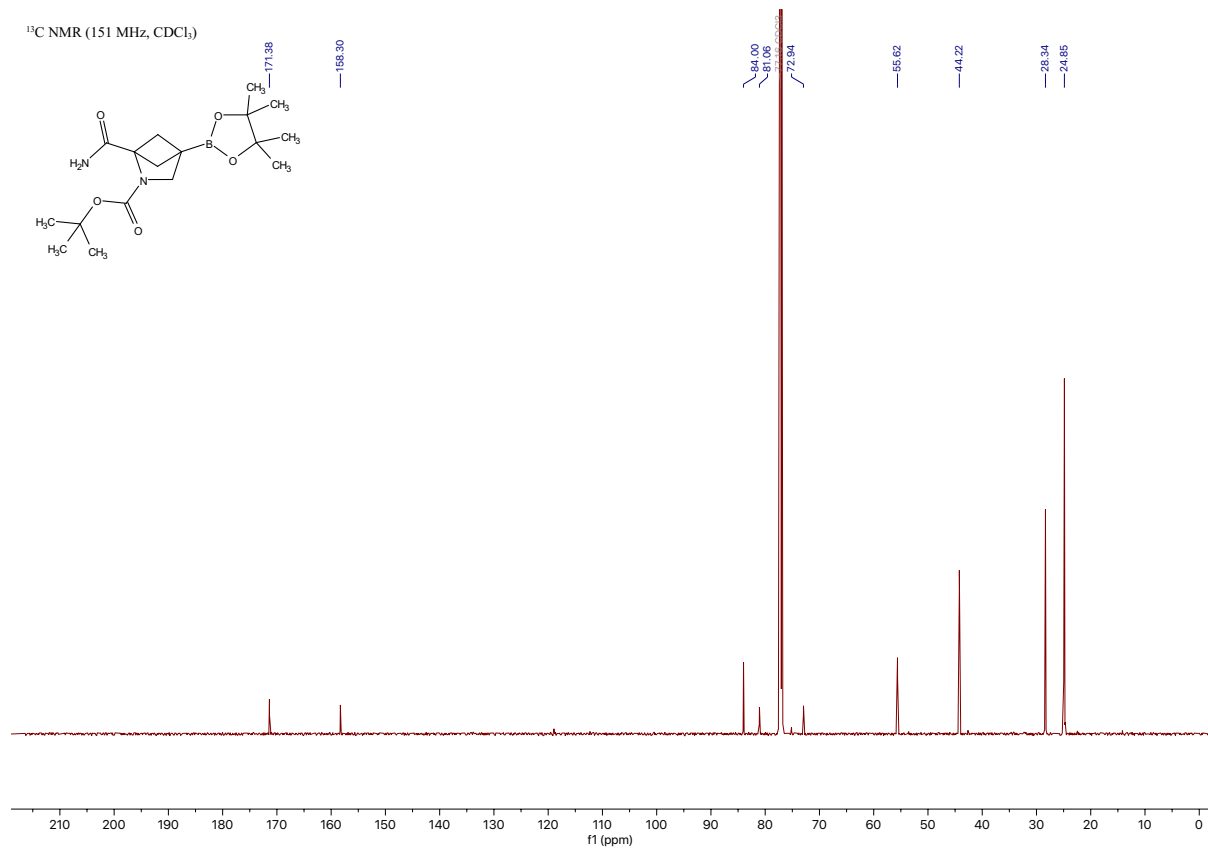

¹¹B NMR (160 MHz, CDCl₃)

297
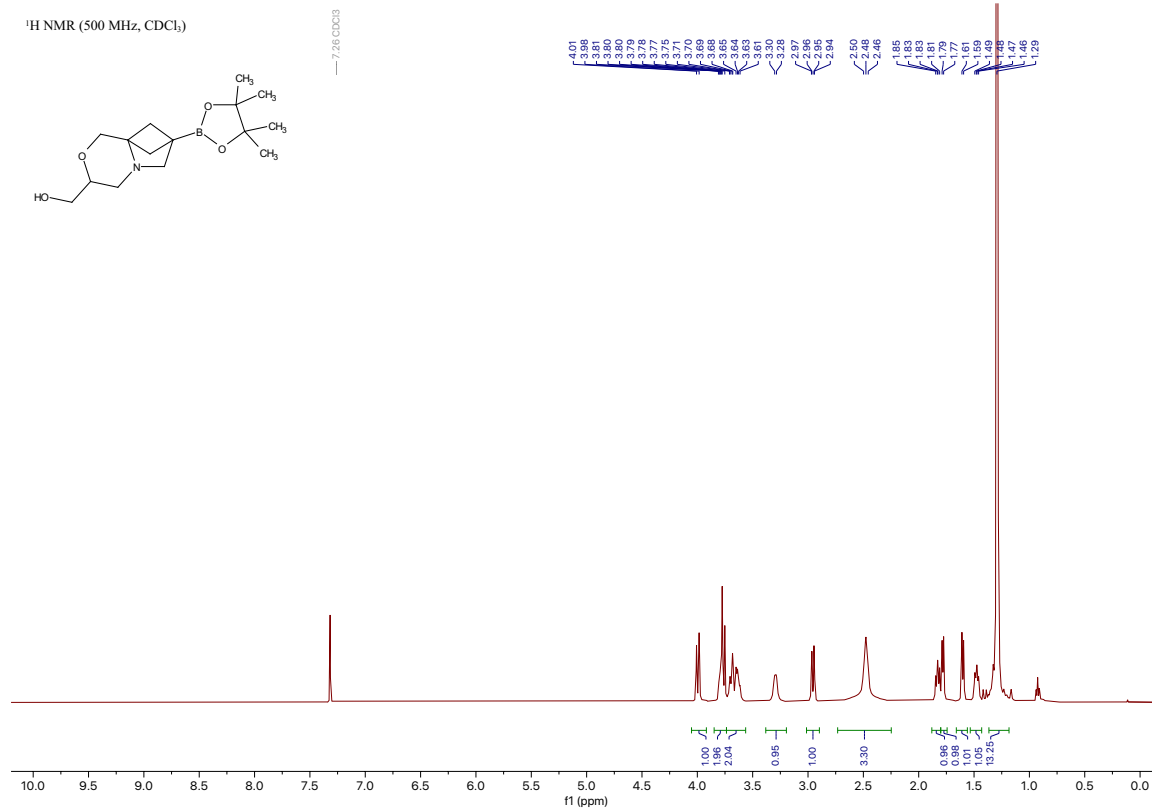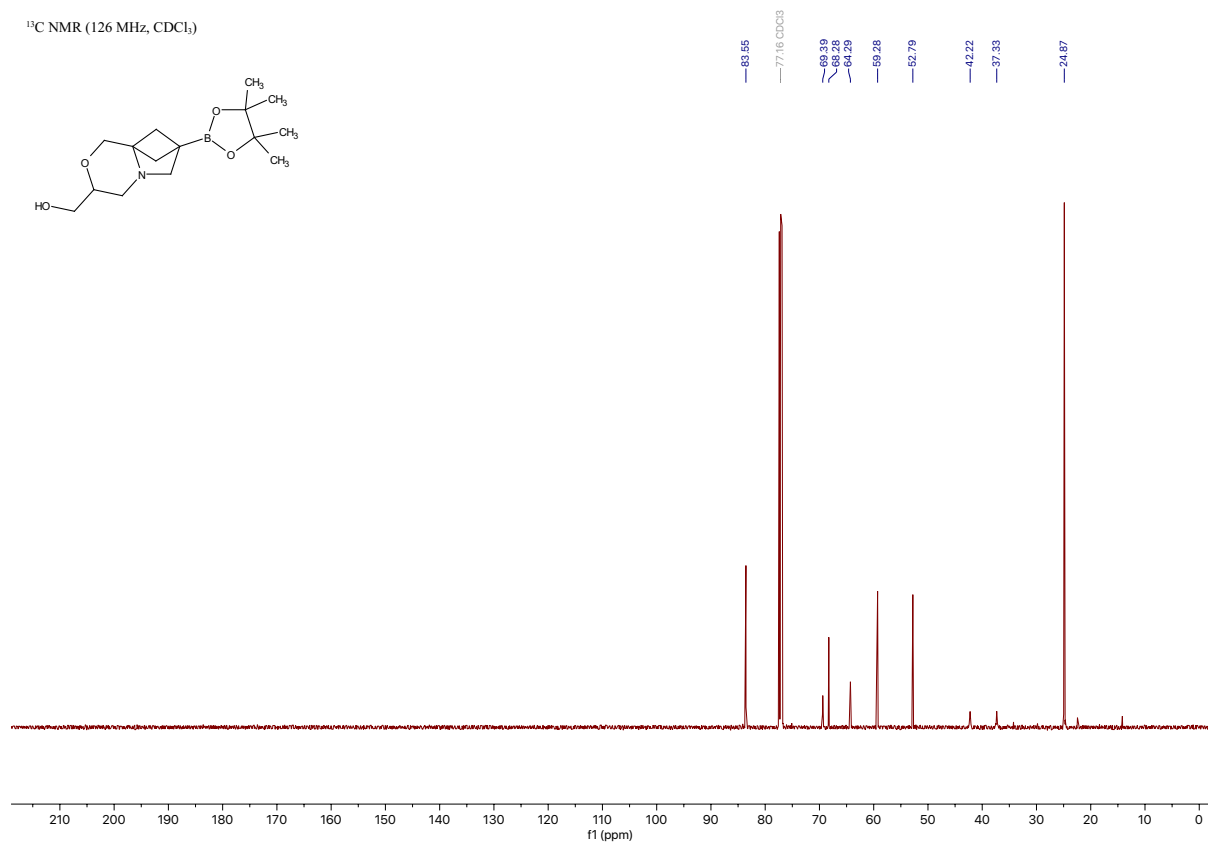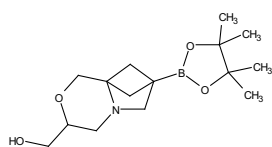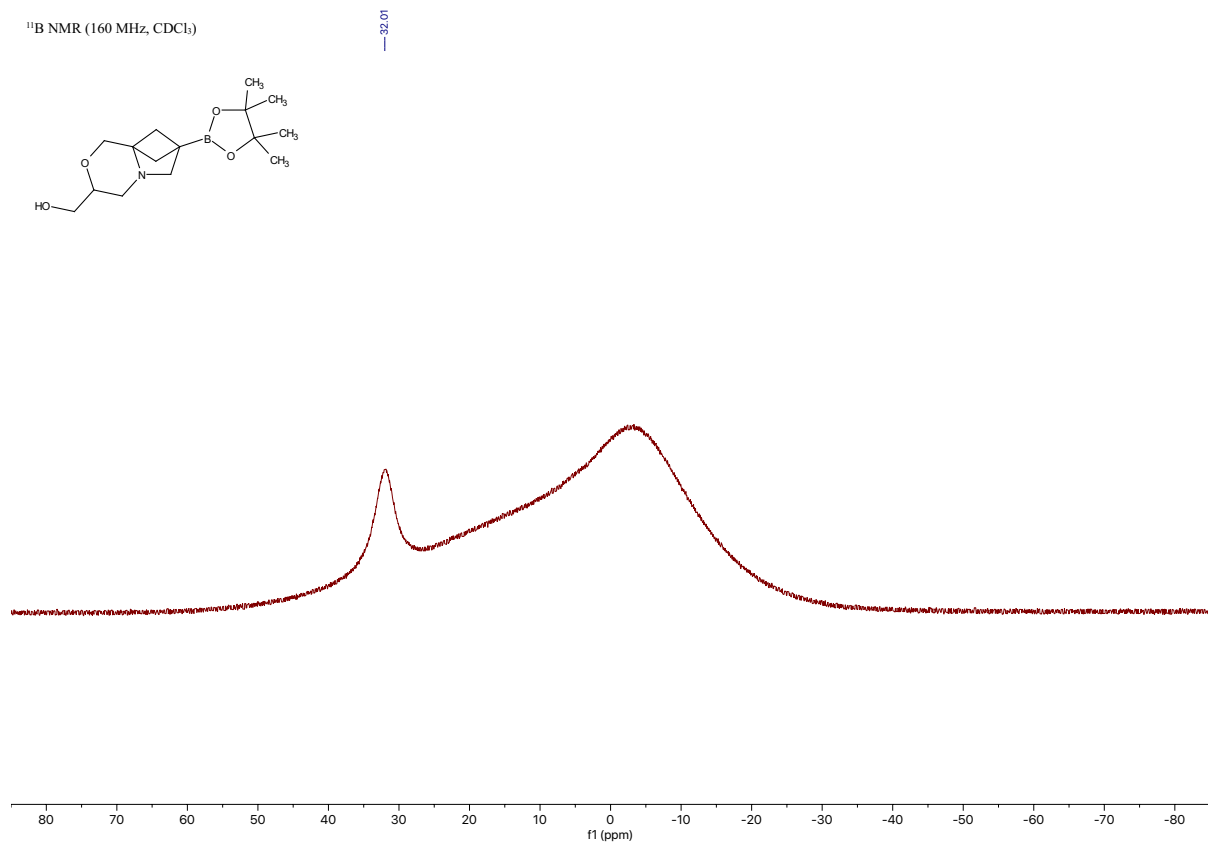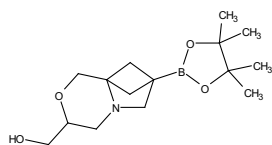
Compound 38a

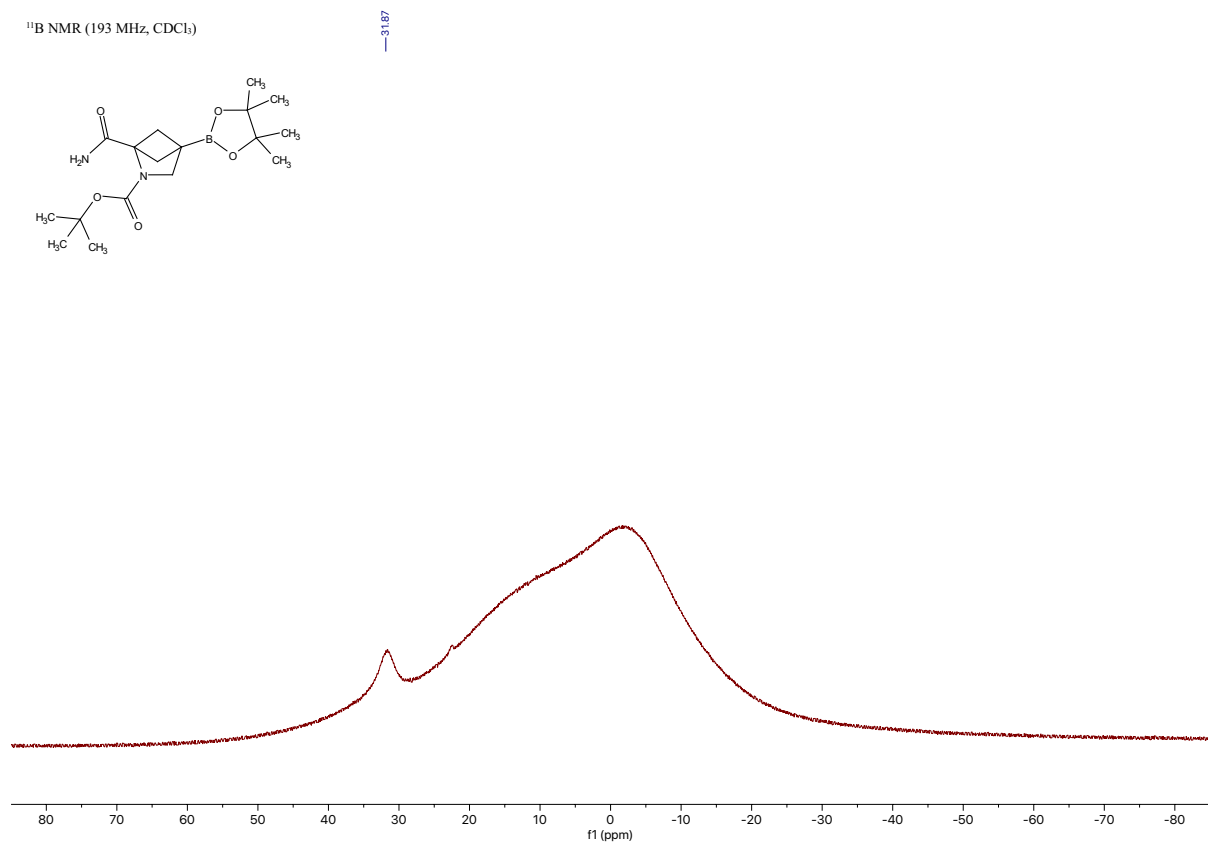## di-*tert*-butyl 4-(4,4,5,5-tetramethyl-1,3,2-dioxaborolan-2-yl)-2-azabicyclo[2.1.1]hexane-1,2-dicarboxylate [Experimental]

¹H NMR (600 MHz, CDCl₃)

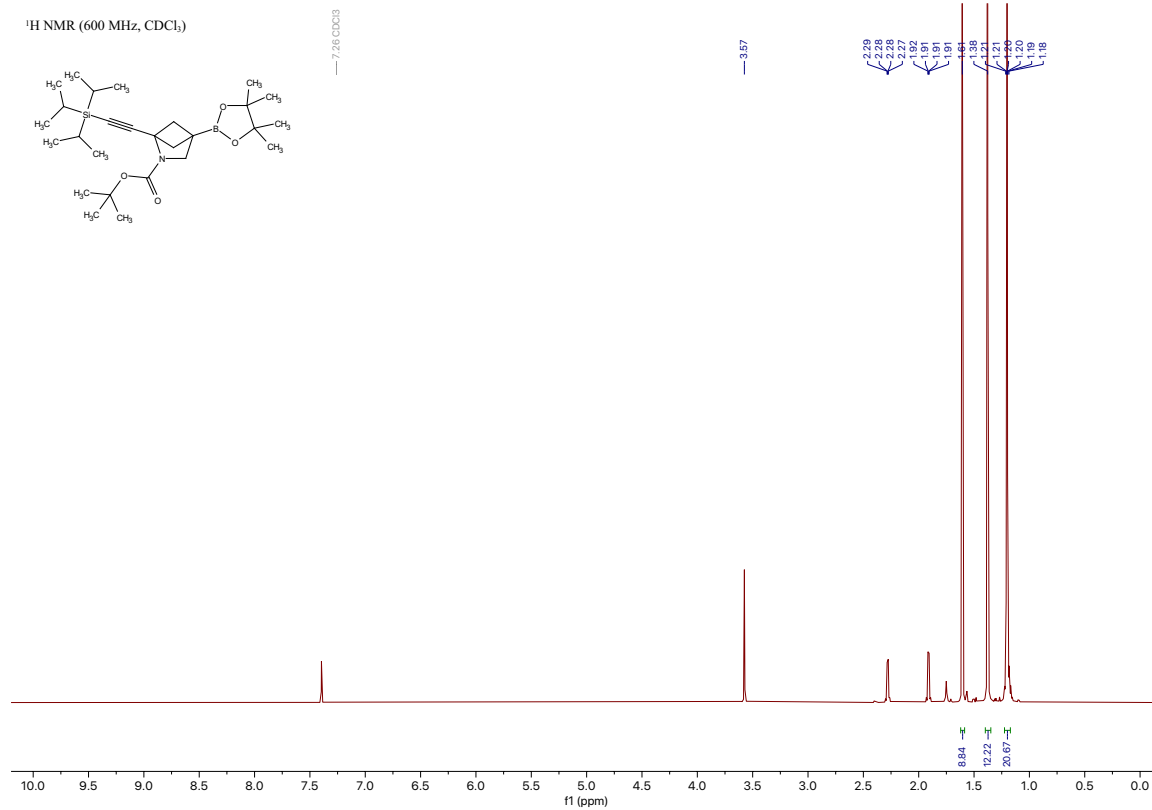¹³C NMR (151 MHz, CDCl₃)

¹¹B NMR (193 MHz, CDCl₃)

299
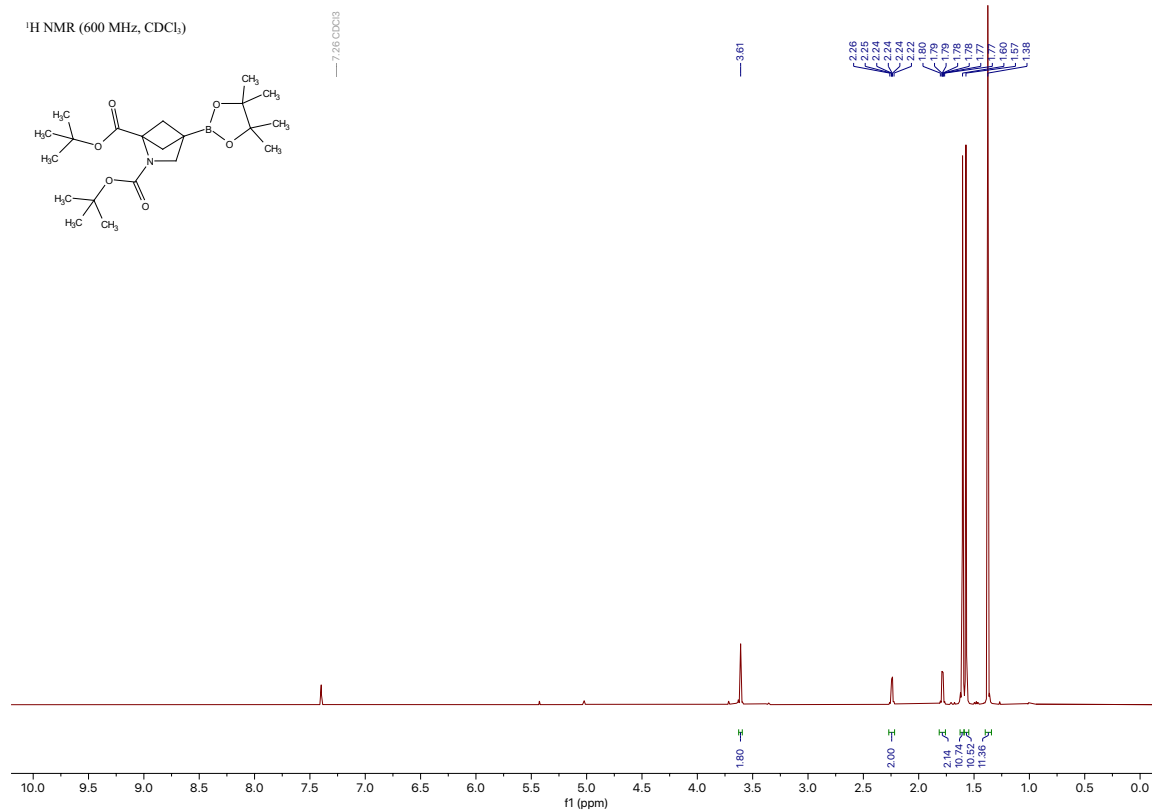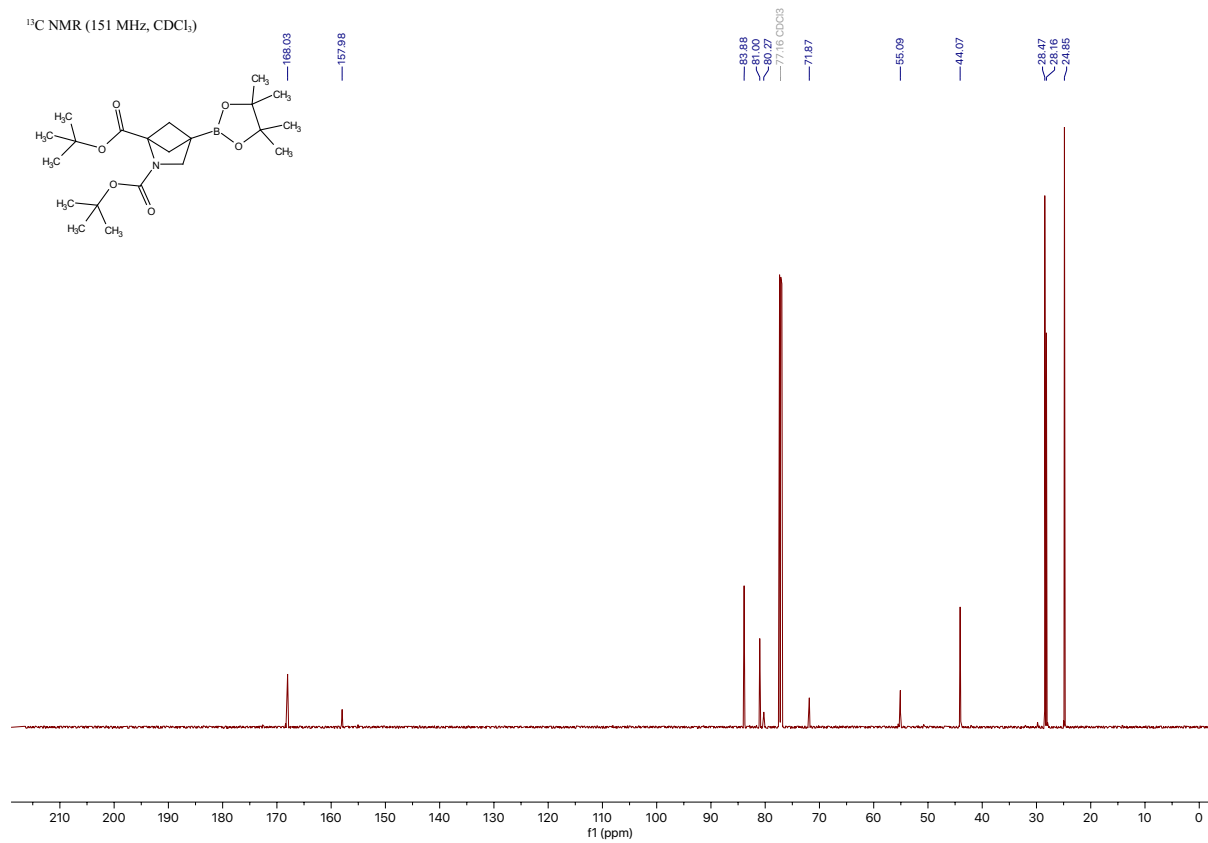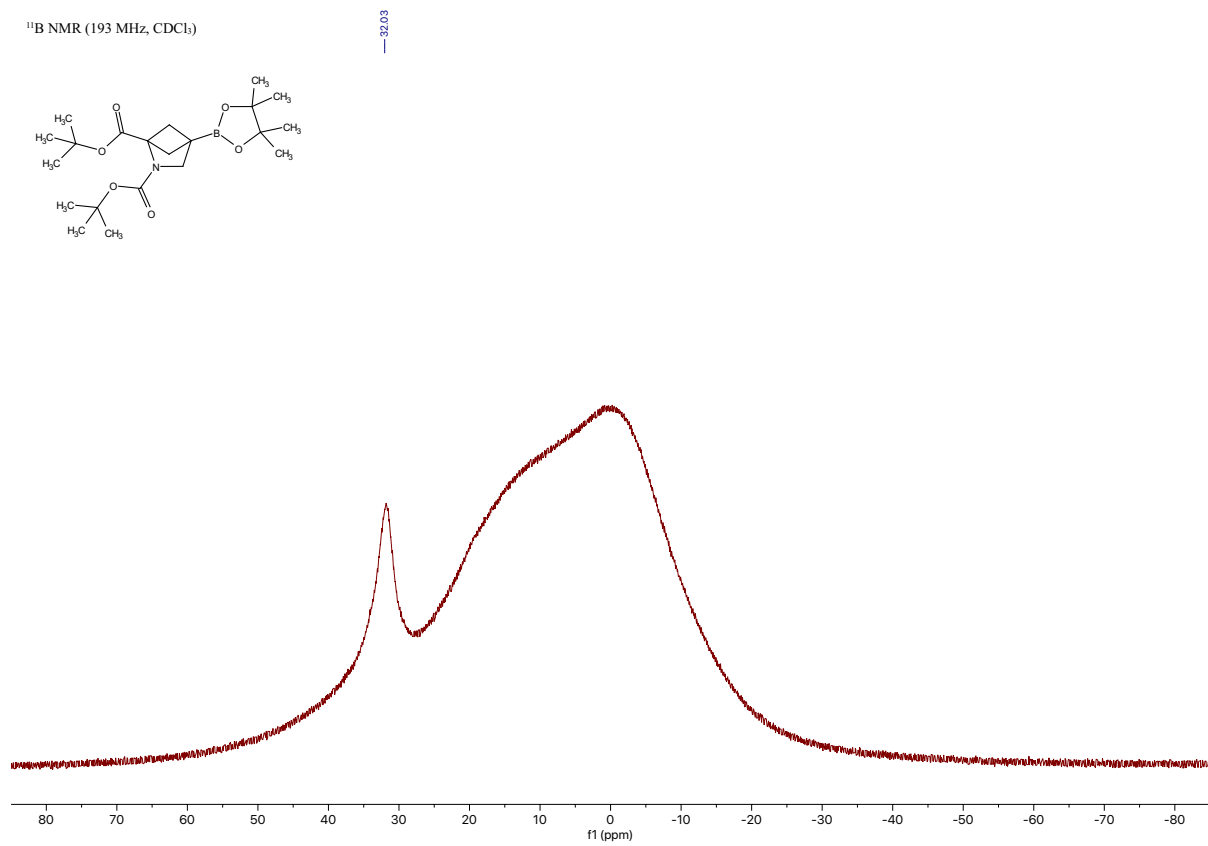
Compound 1c

(3-(4-(*tert*-butyl)phenyl)bicyclo[1.1.1]pentan-1-yl)trifluoro-λ⁴-borane, potassium salt

[Experimental]

¹H NMR (600 MHz, Acetone)

¹³C NMR (151 MHz, Acetone)

— 1.57

f1 (ppm)

— 147.57

f1 (ppm)
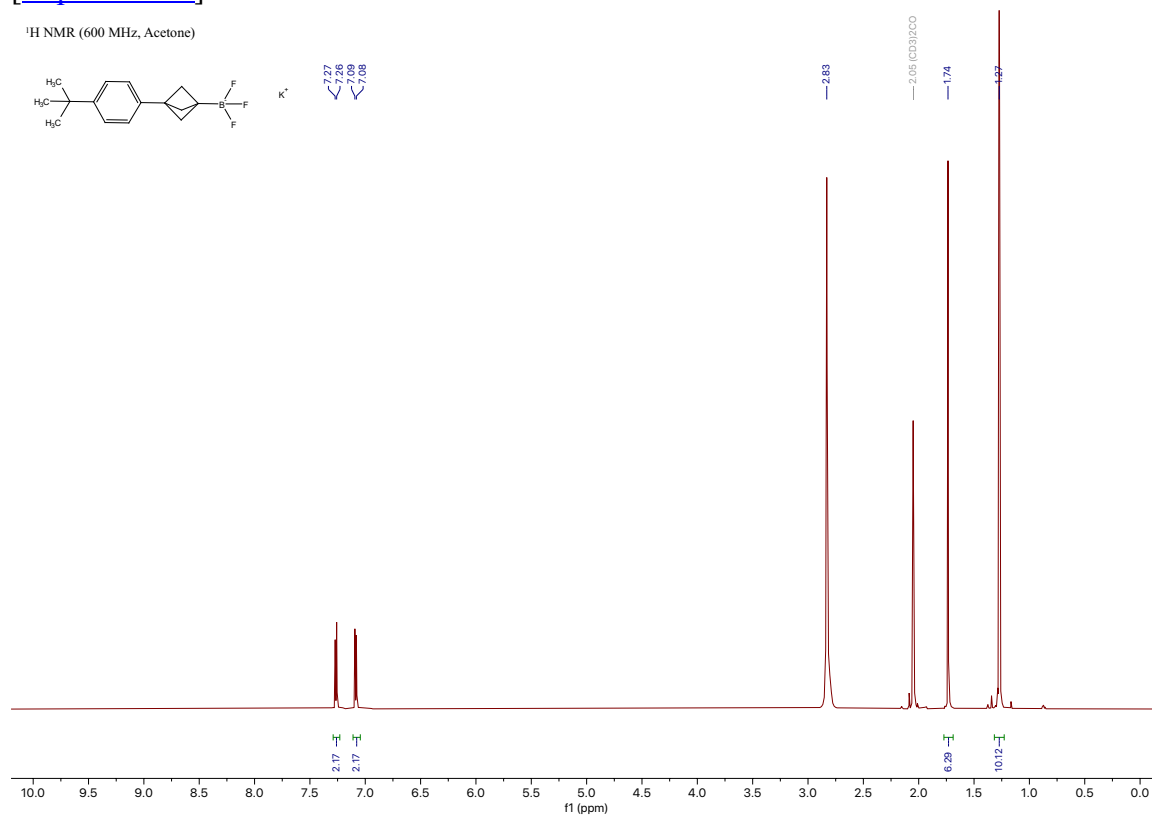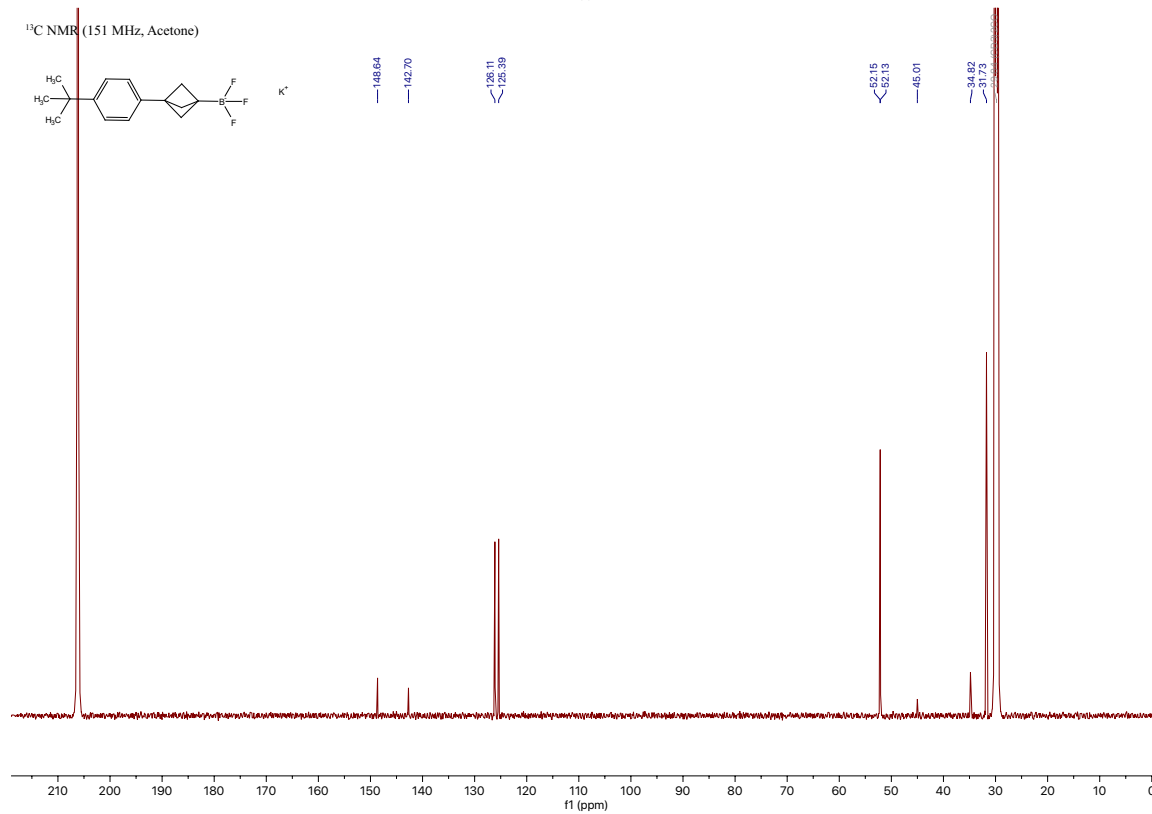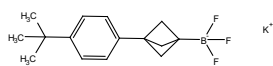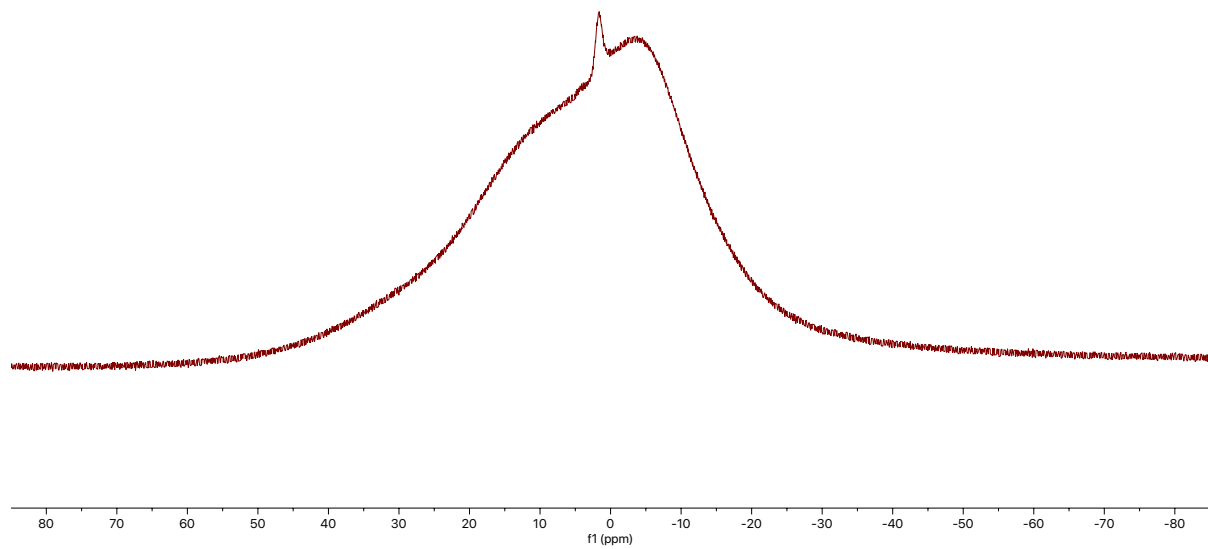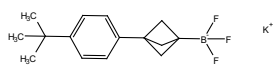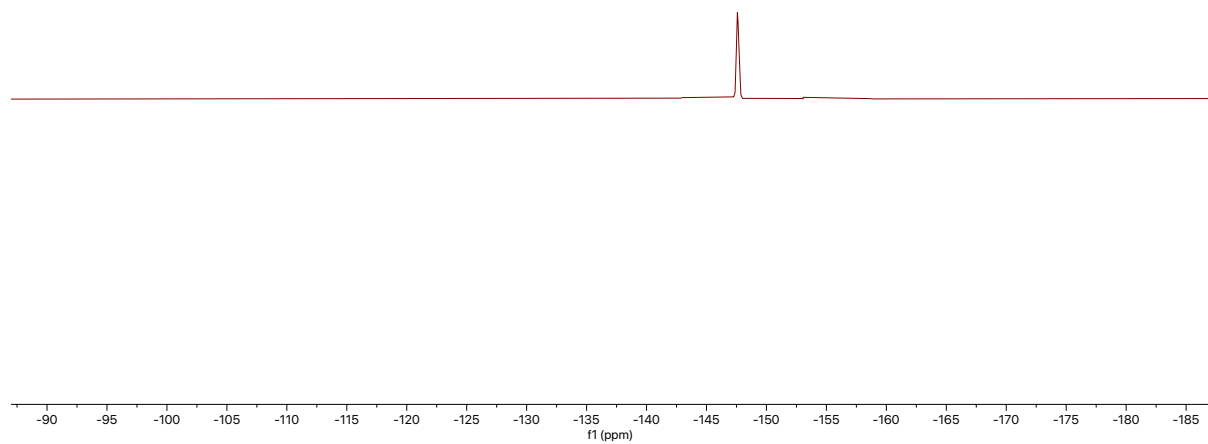
Compound 11c

(3-(methylsulfonyl)bicyclo[1.1.1]pentan-1-yl)trifluoro-λ^4-borane, tetrabutylammonium salt [Experimental]

¹H NMR (500 MHz, CDCl₃)

¹³C NMR (126 MHz, CDCl₃)

^{11}B NMR (160 MHz, CDCl$_3$)

— 2.34

^{19}F NMR (470 MHz, CDCl$_3$)

— -147.05
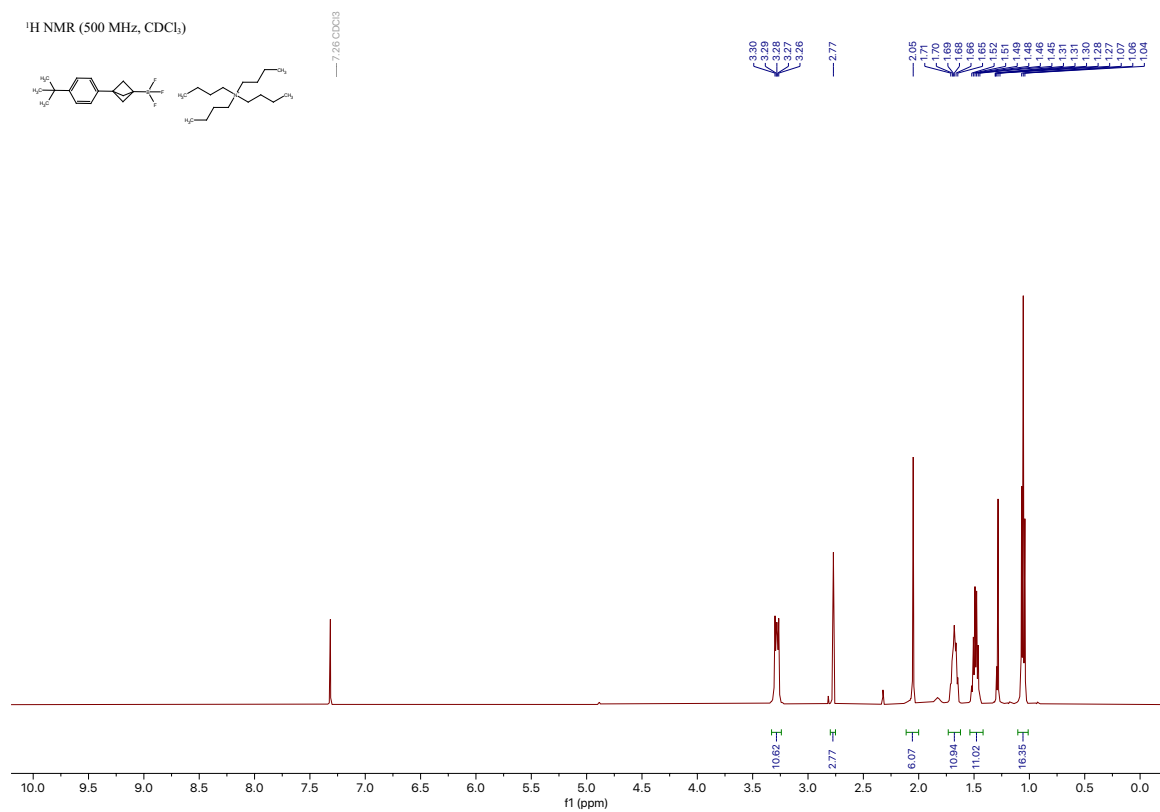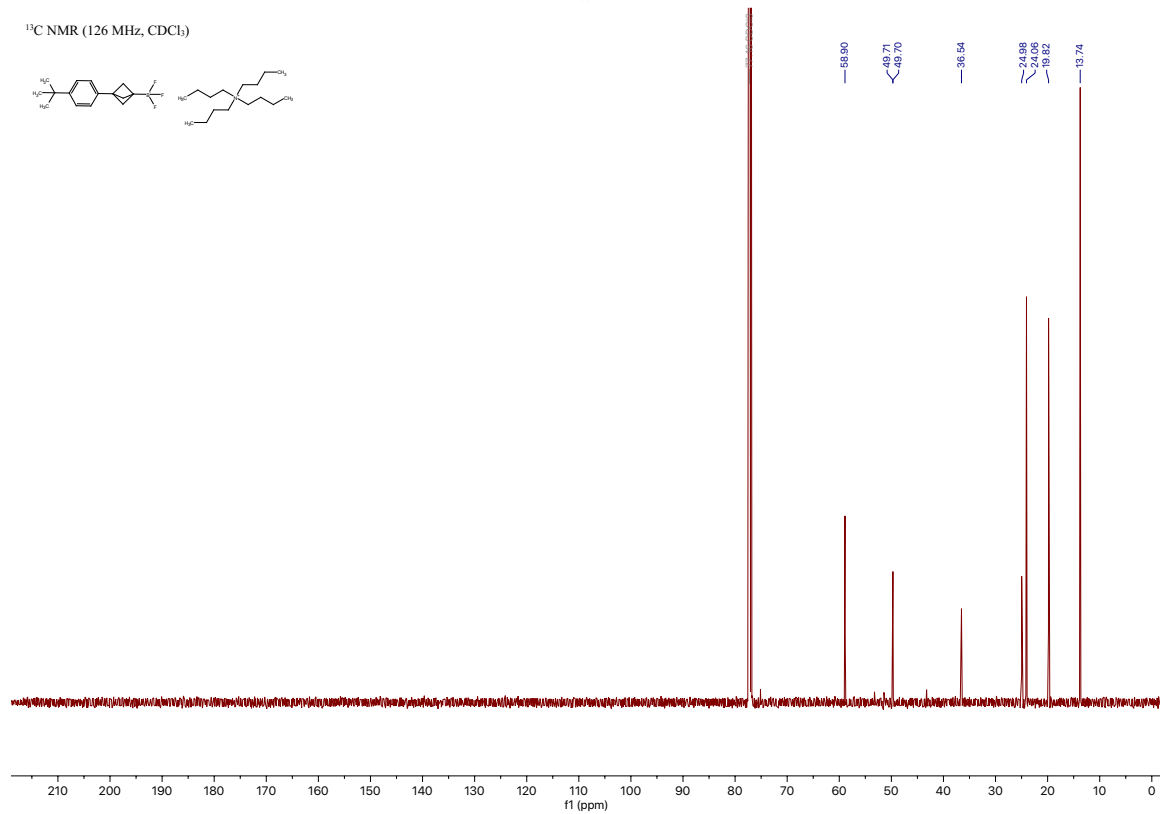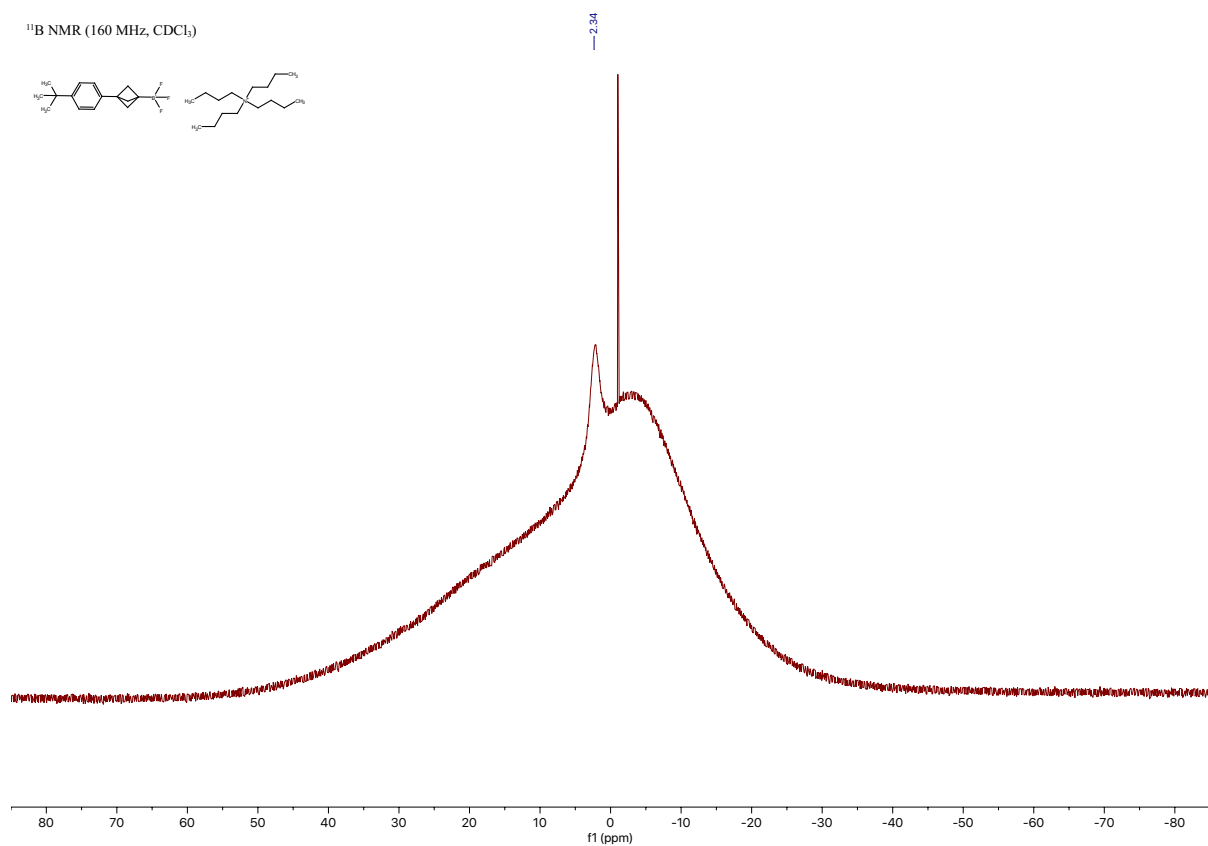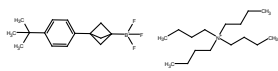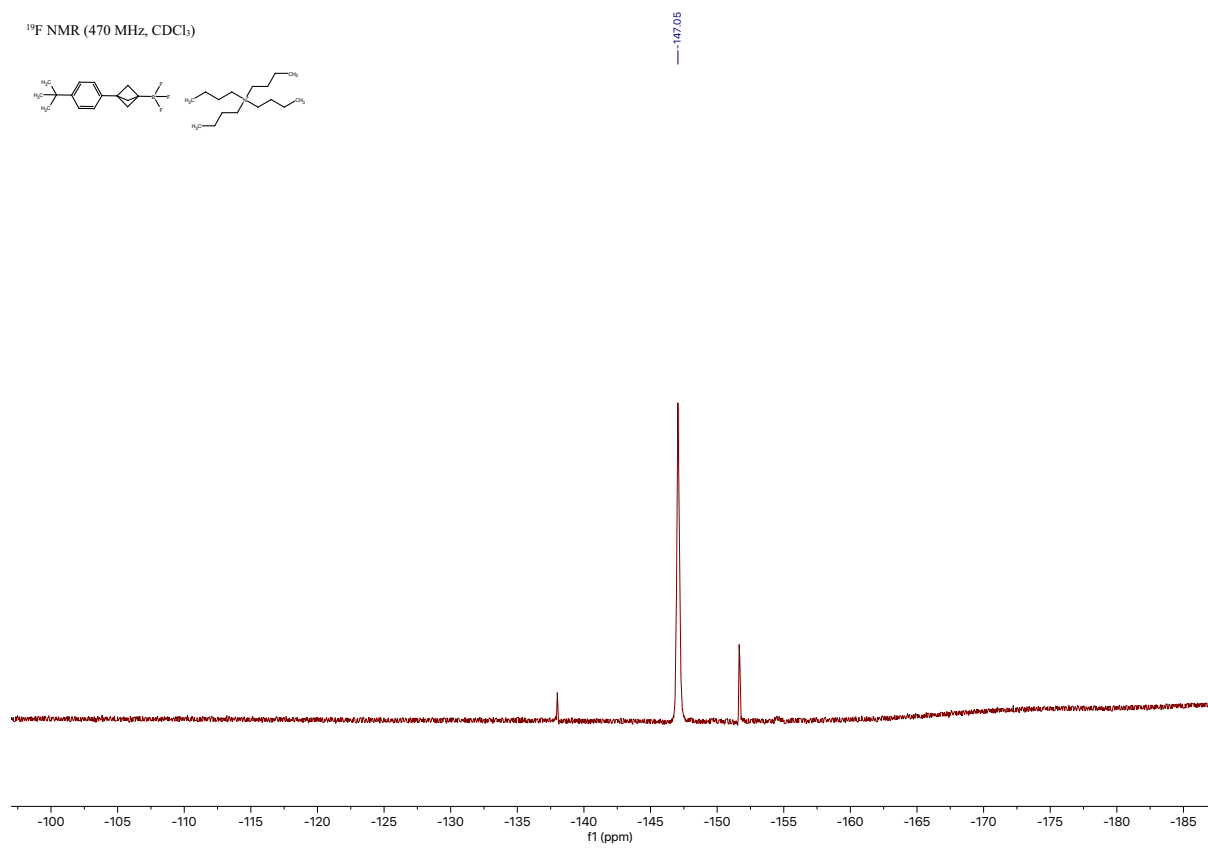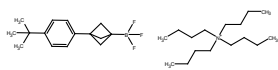
Compound 16c

2,2,2-trifluoro-*N*-(3-(trifluoro-λ^4-boraneyl)bicyclo[1.1.1]pentan-1-yl)acetamide, potassium salt [Experimental]
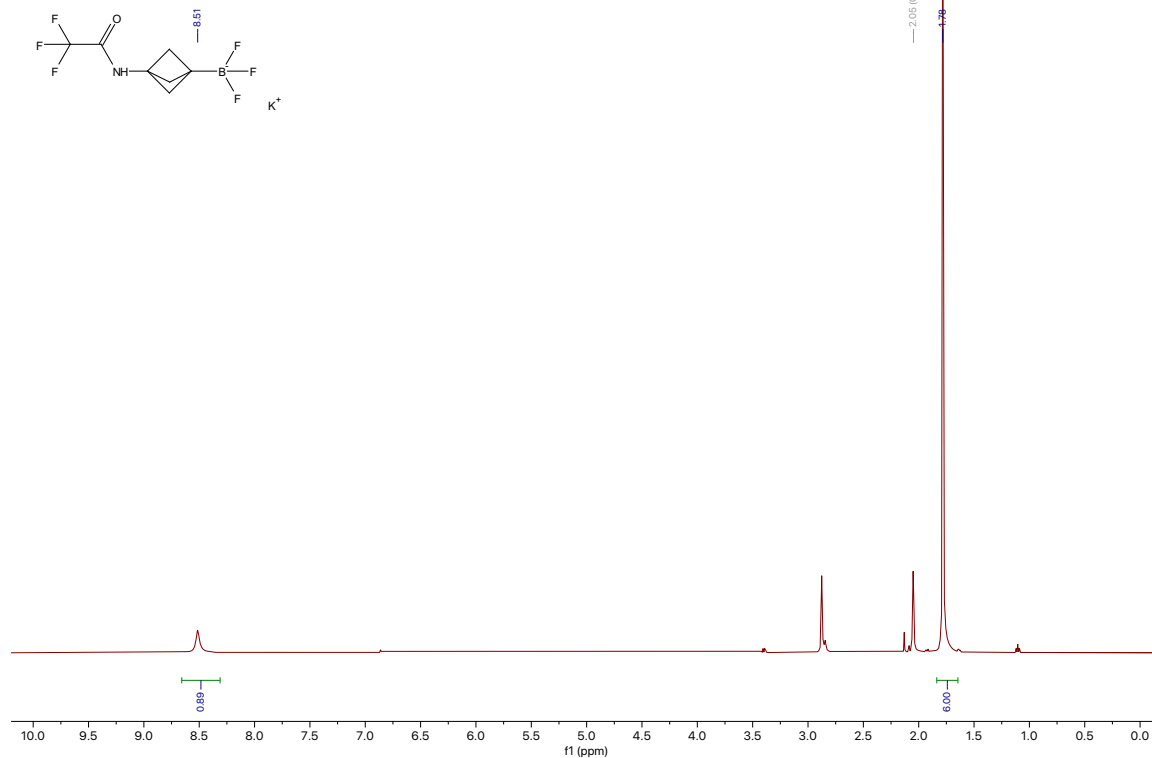
¹H NMR (500 MHz, Acetone)

¹³C NMR (151 MHz, Acetone)z
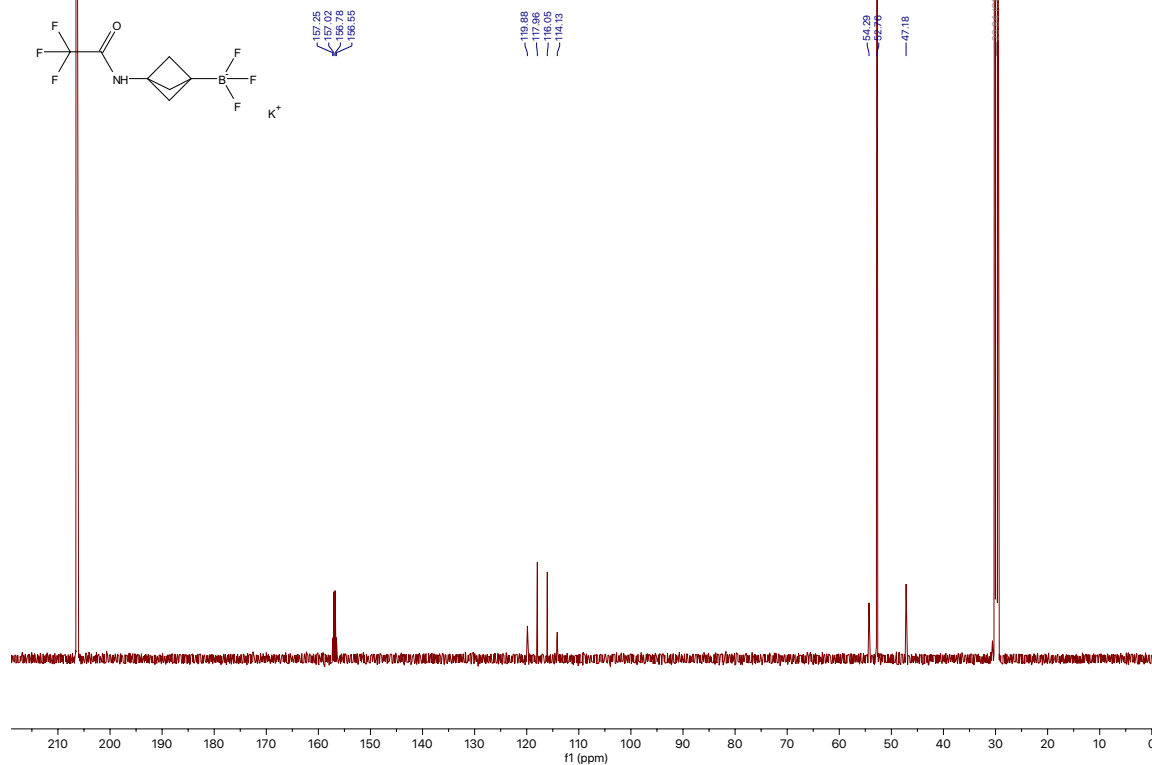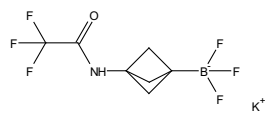
— 2.87
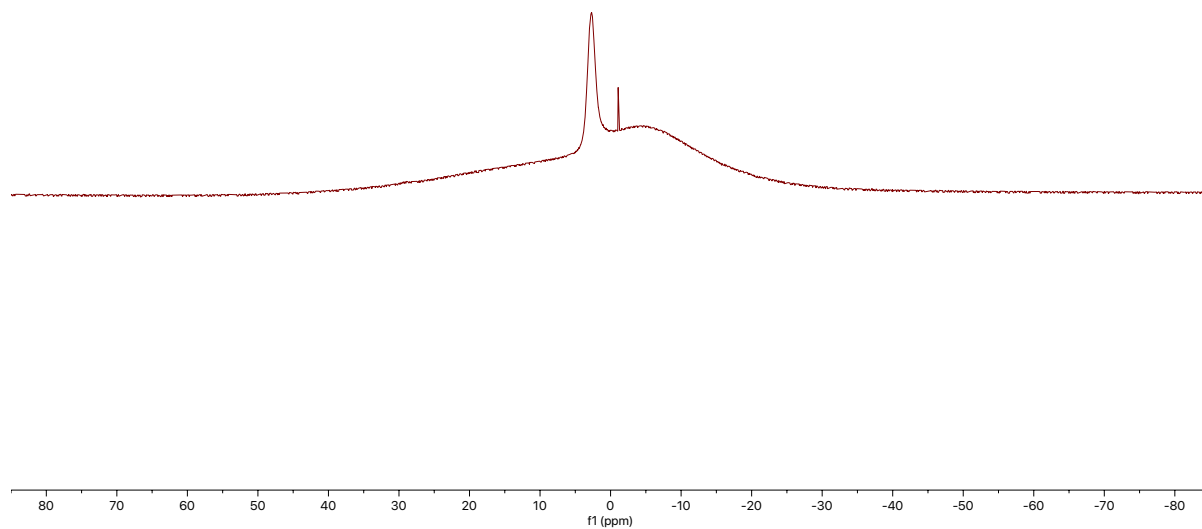
^{19}F NMR (470 MHz, Acetone)

— -146.91

305
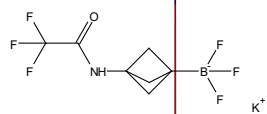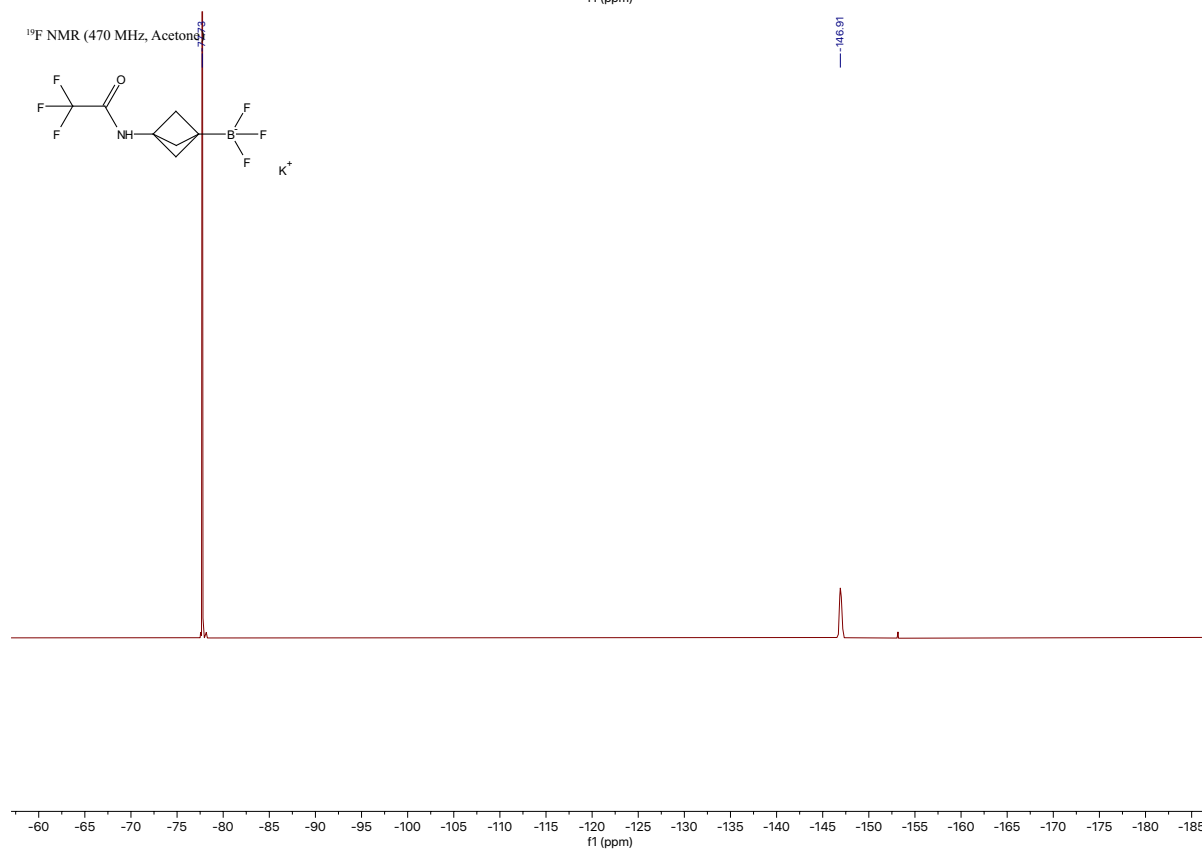
Compound 1d

(3-(4-(*tert*-butyl)phenyl)bicyclo[1.1.1]pentan-1-yl)boronic acid [Experimental]

¹H NMR (600 MHz, Acetone)

¹³C NMR (151 MHz, Acetone)

149.65
140.53
126.13
125.69
53.40
46.71
34.91
31.67

f1 (ppm)

¹¹B NMR (193 MHz, Acetone)

28.41

f1 (ppm)
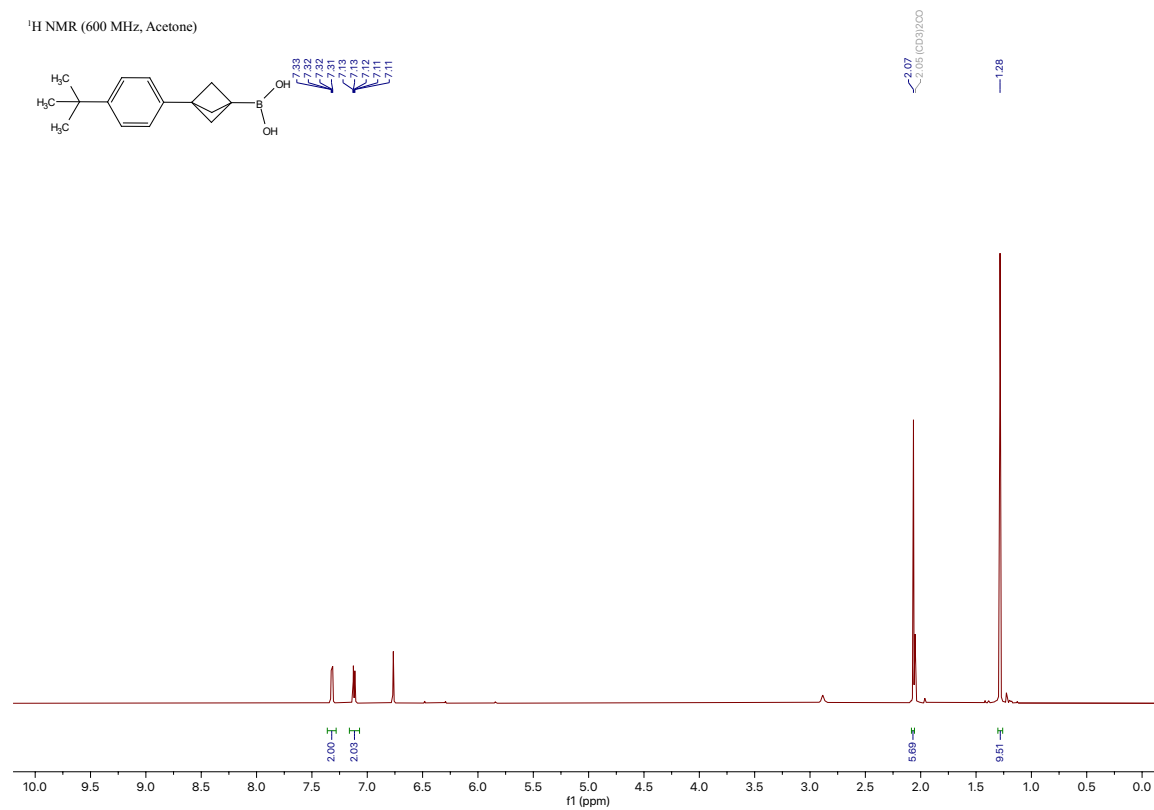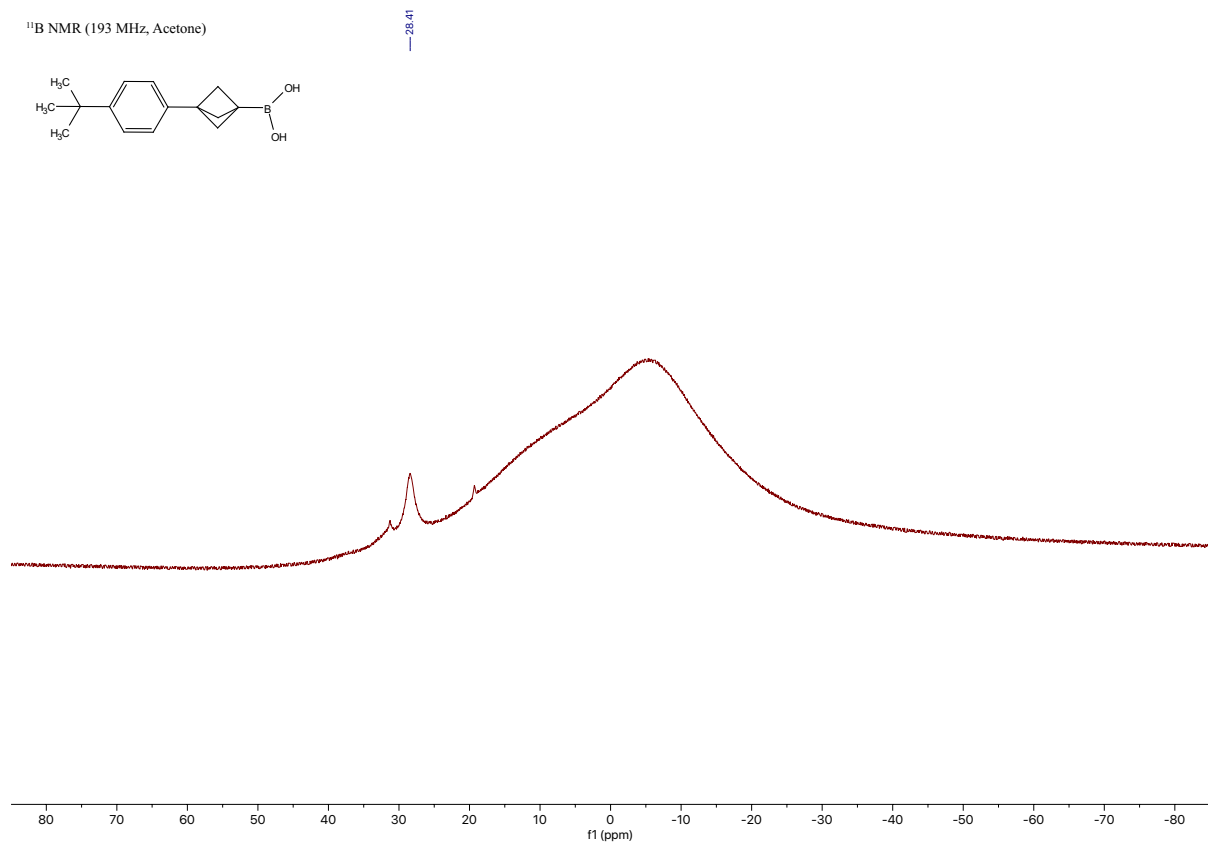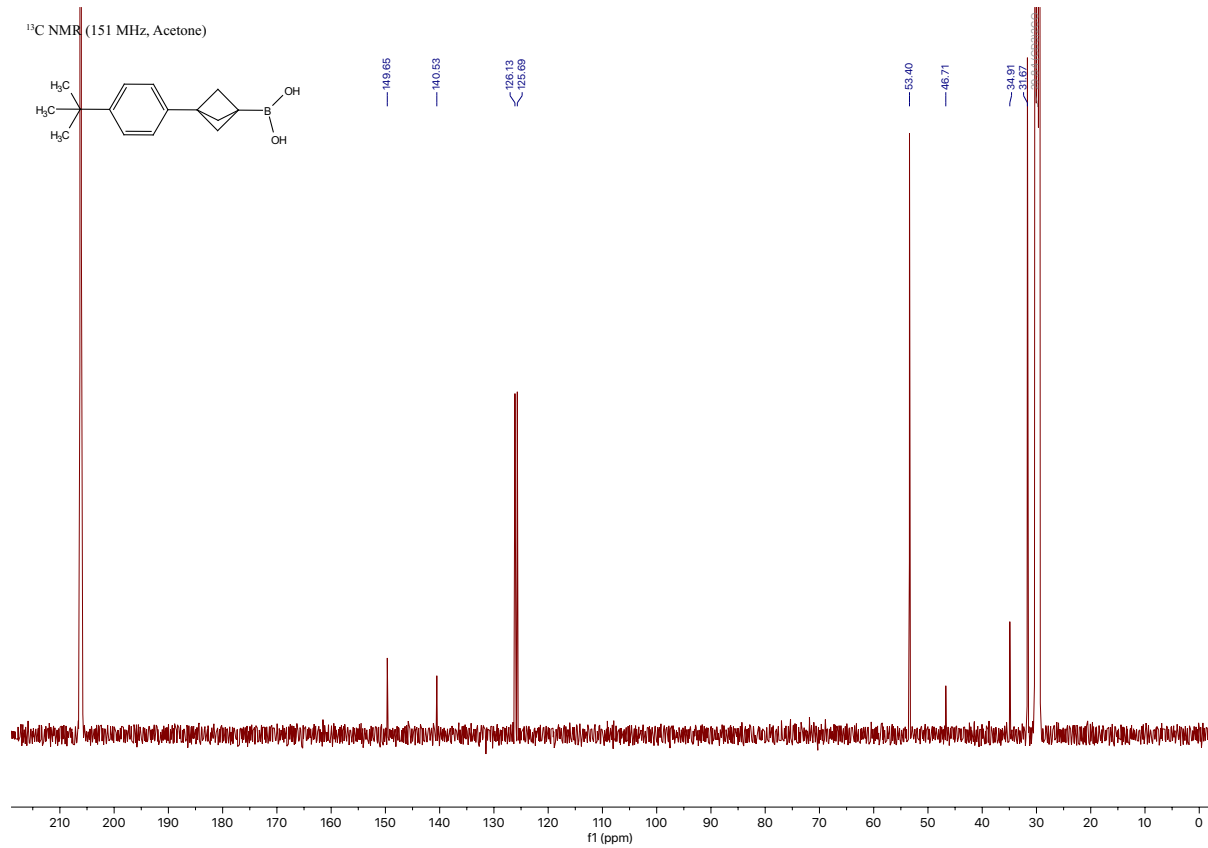
Compound 11d

(3-(methylsulfonyl)bicyclo[1.1.1]pentan-1-yl)boronic acid [Experimental]

—54.49
—51.41
—36.93

f1 (ppm)

—28.66

f1 (ppm)

309
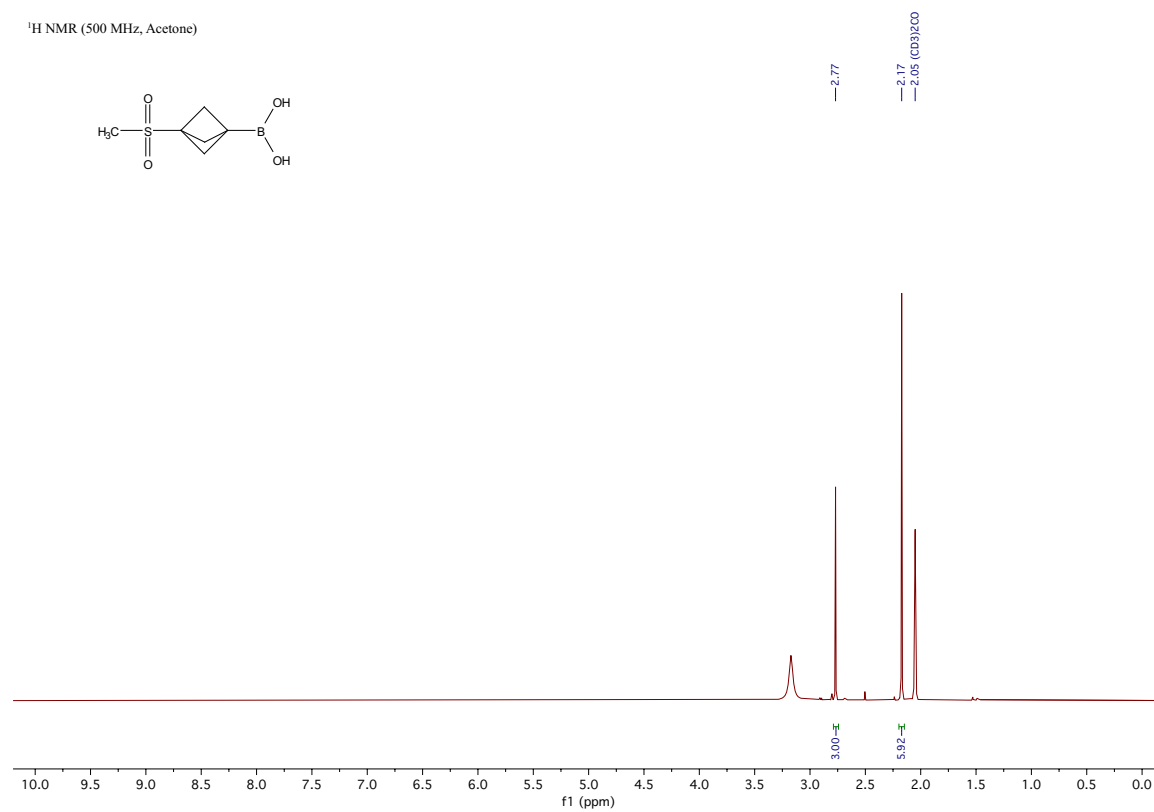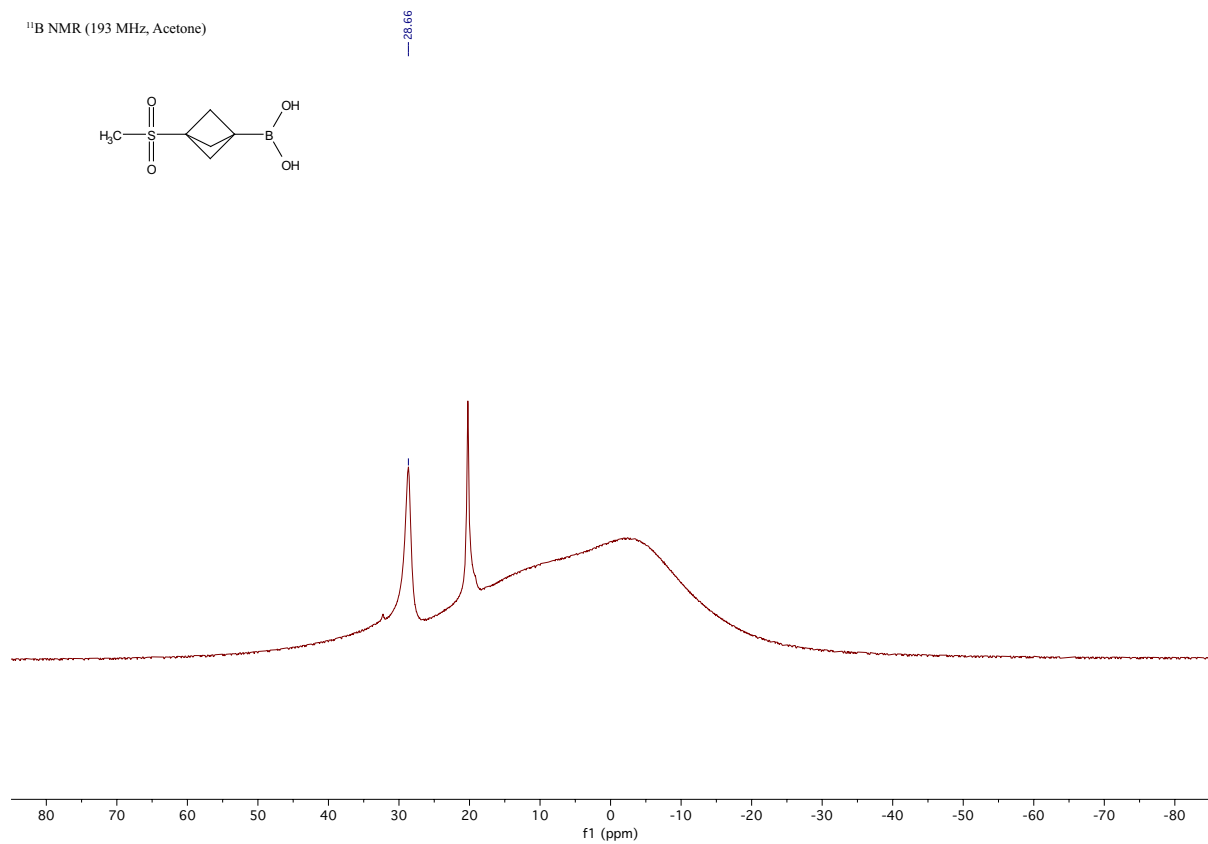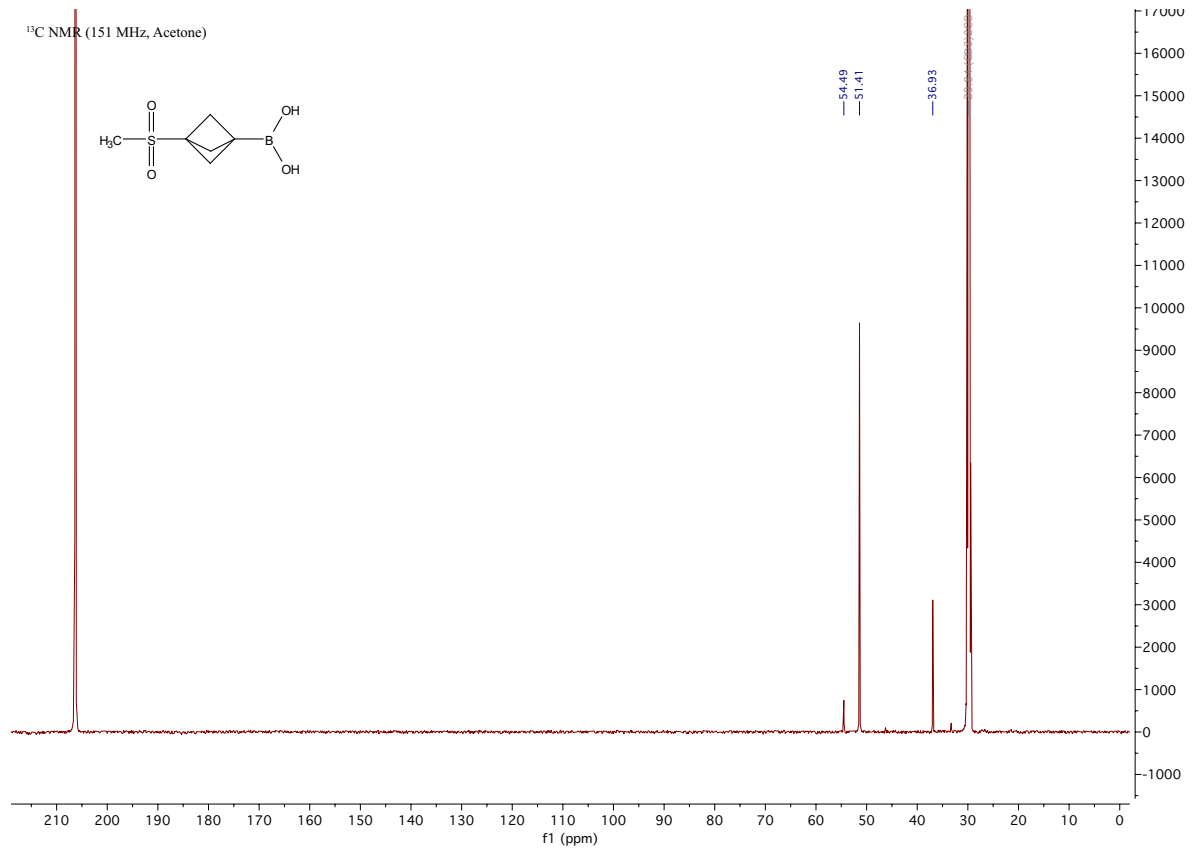
Compound 28c

(1-methyl-2-azabicyclo[2.1.1]hexan-4-yl)boronic acid [Experimental]

¹H NMR (600 MHz, Acetone)

^{13}C NMR (151 MHz, Acetone)

—72.25
—52.38
—43.91
—16.47

f1 (ppm)

^{11}B NMR (193 MHz, Acetone)

—28.50
—19.20

f1 (ppm)

311
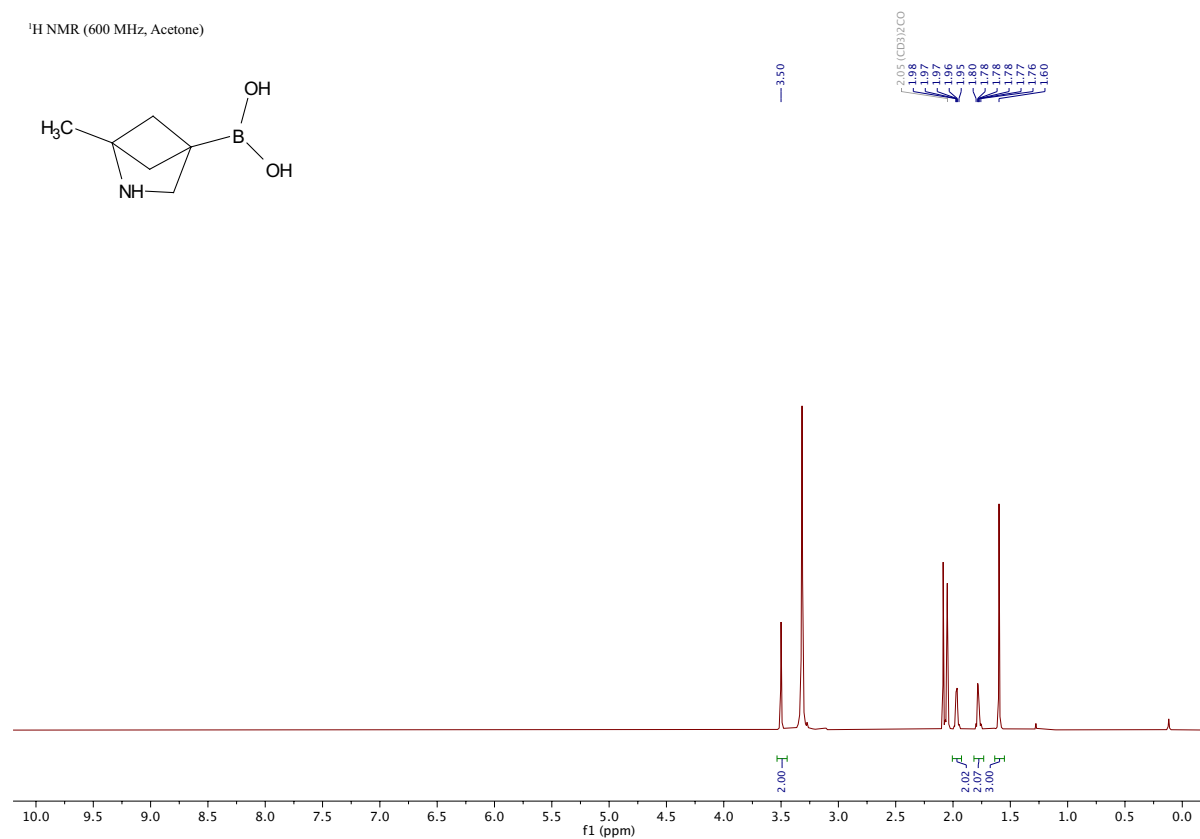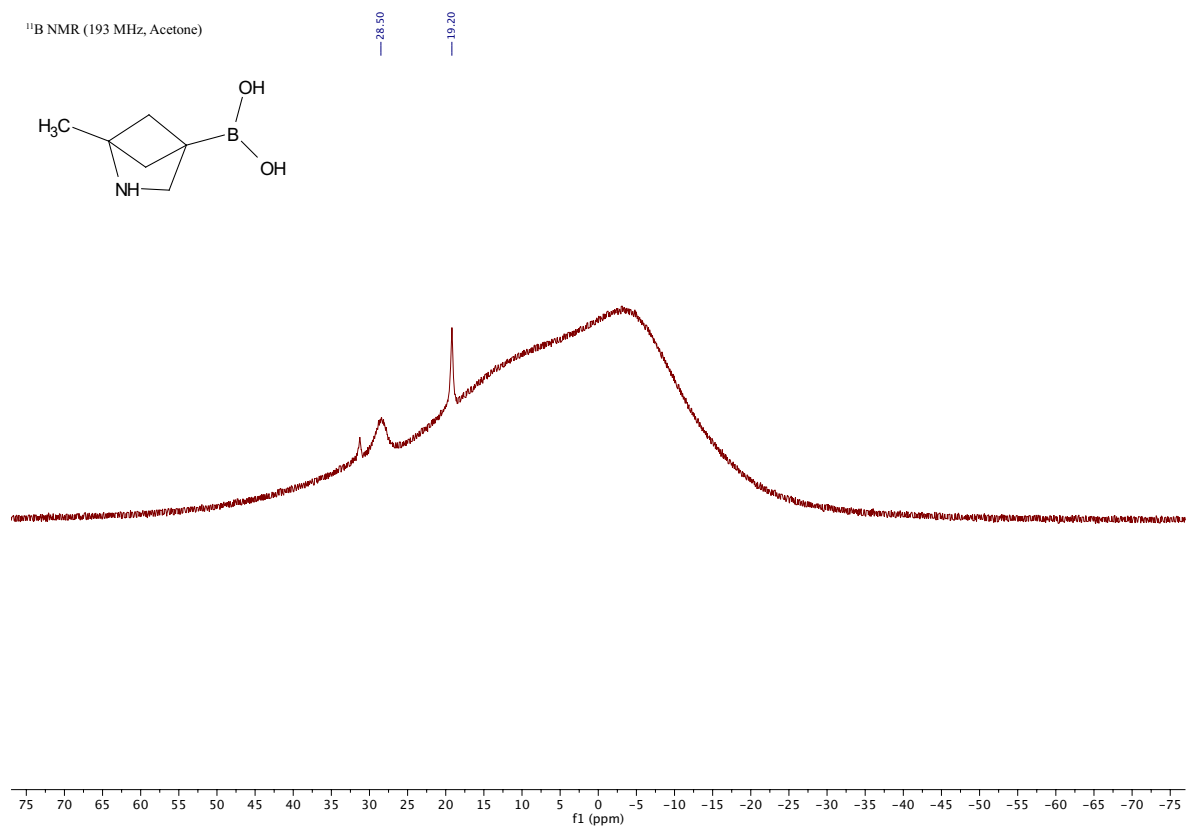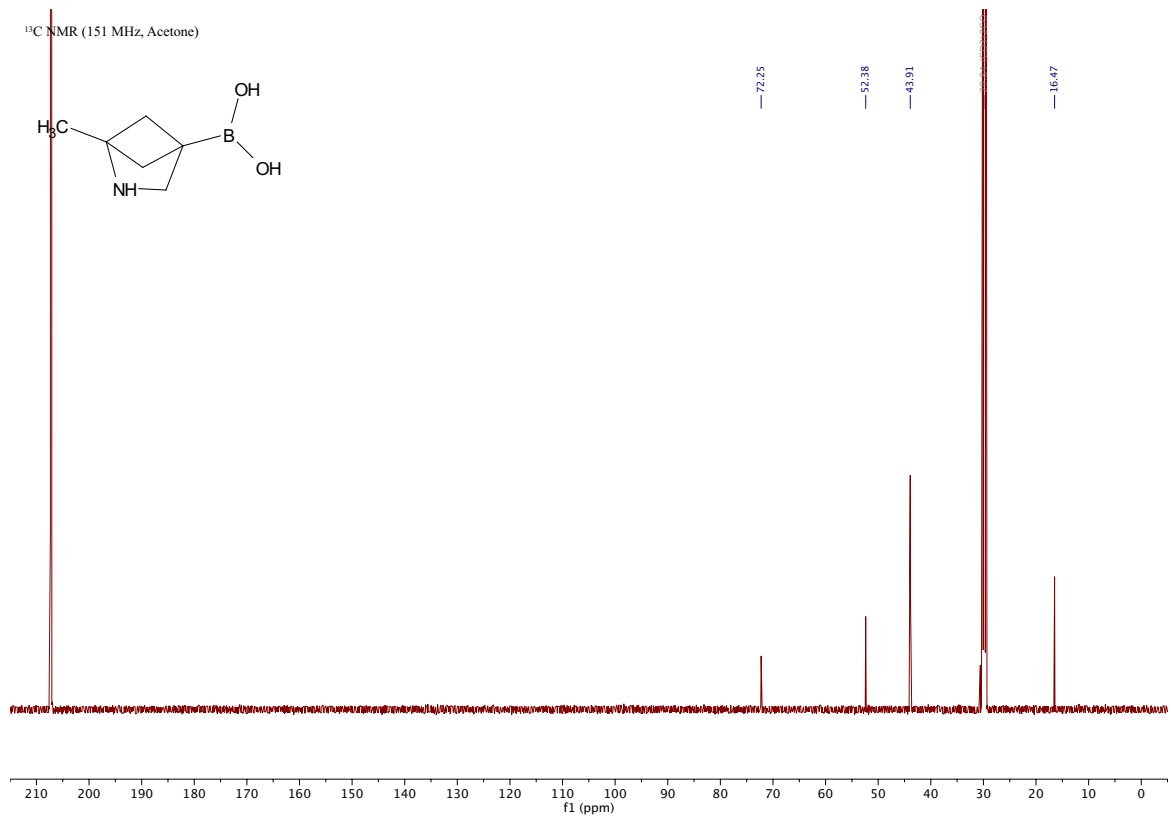
Compound 1e

2-(2-(3-(4-(*tert*-butyl)phenyl)bicyclo[1.1.1]pentan-1-yl)-4-(4-methoxyphenyl)butan-2-yl)-4,4,5,5-tetramethyl-1,3,2-dioxaborolane [Experimental]

¹H NMR (600 MHz, CDCl₃)

¹³C NMR (151 MHz, CDCl₃)

157.73
149.10
138.93
135.96
129.36
125.87
125.09
113.85
83.34
55.40
49.97
44.52
40.38
38.91
34.54
32.71
31.50
25.28
25.07
17.94

210 200 190 180 170 160 150 140 130 120 110 100 90 80 70 60 50 40 30 20 10 0
f1 (ppm)

¹¹B NMR (193 MHz, CDCl₃)

34.67

80 70 60 50 40 30 20 10 0 -10 -20 -30 -40 -50 -60 -70 -80
f1 (ppm)
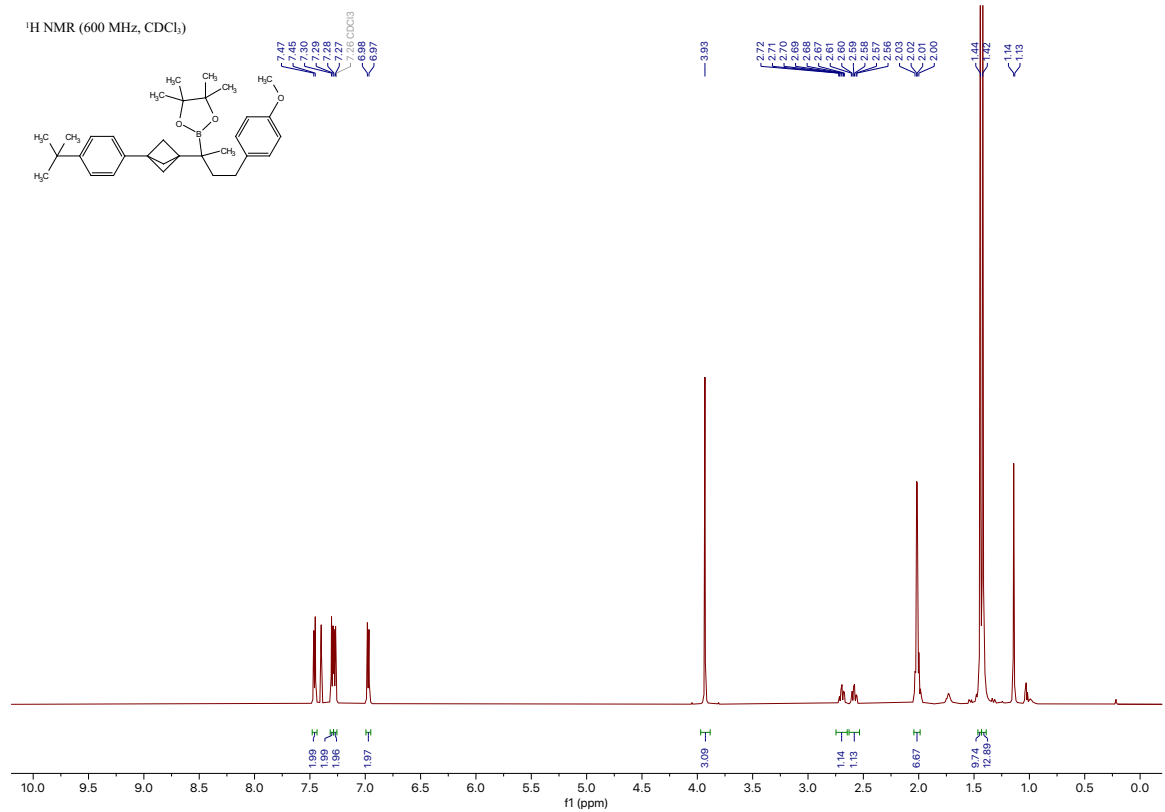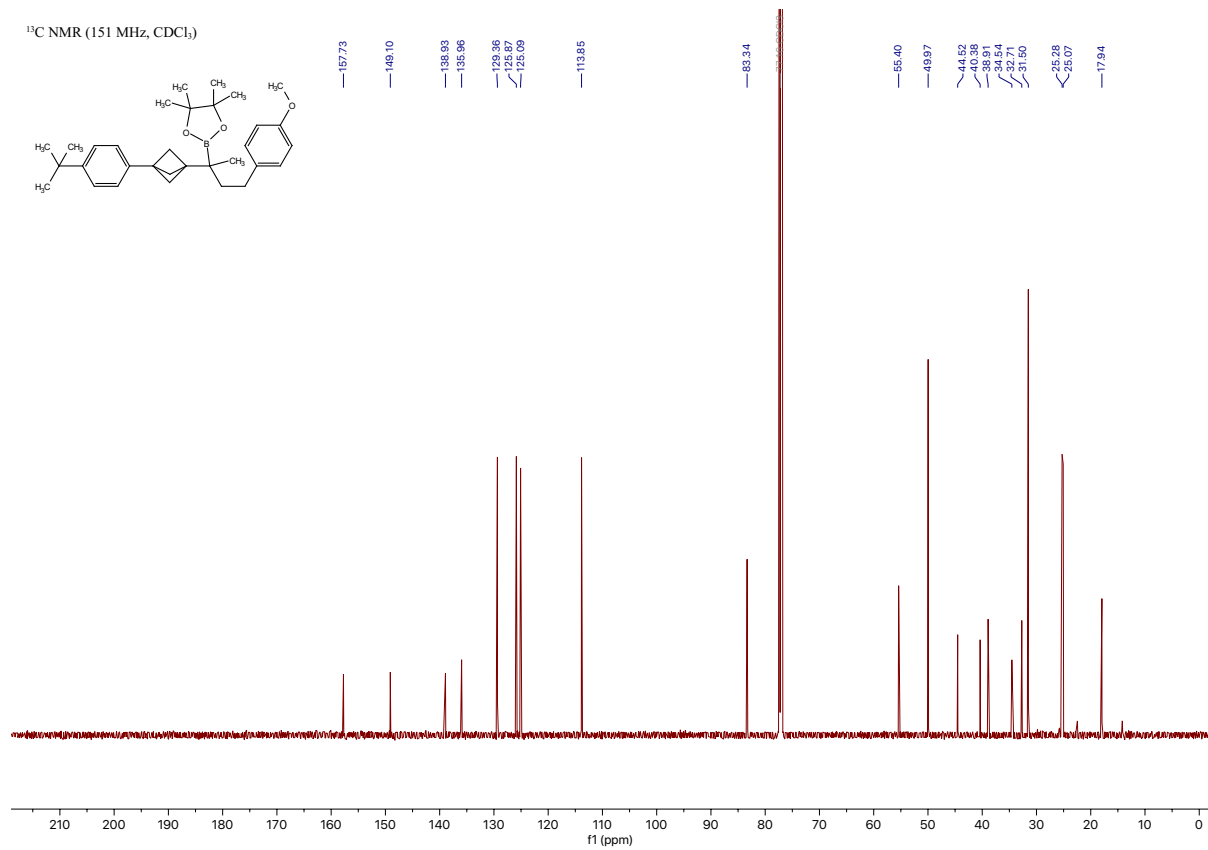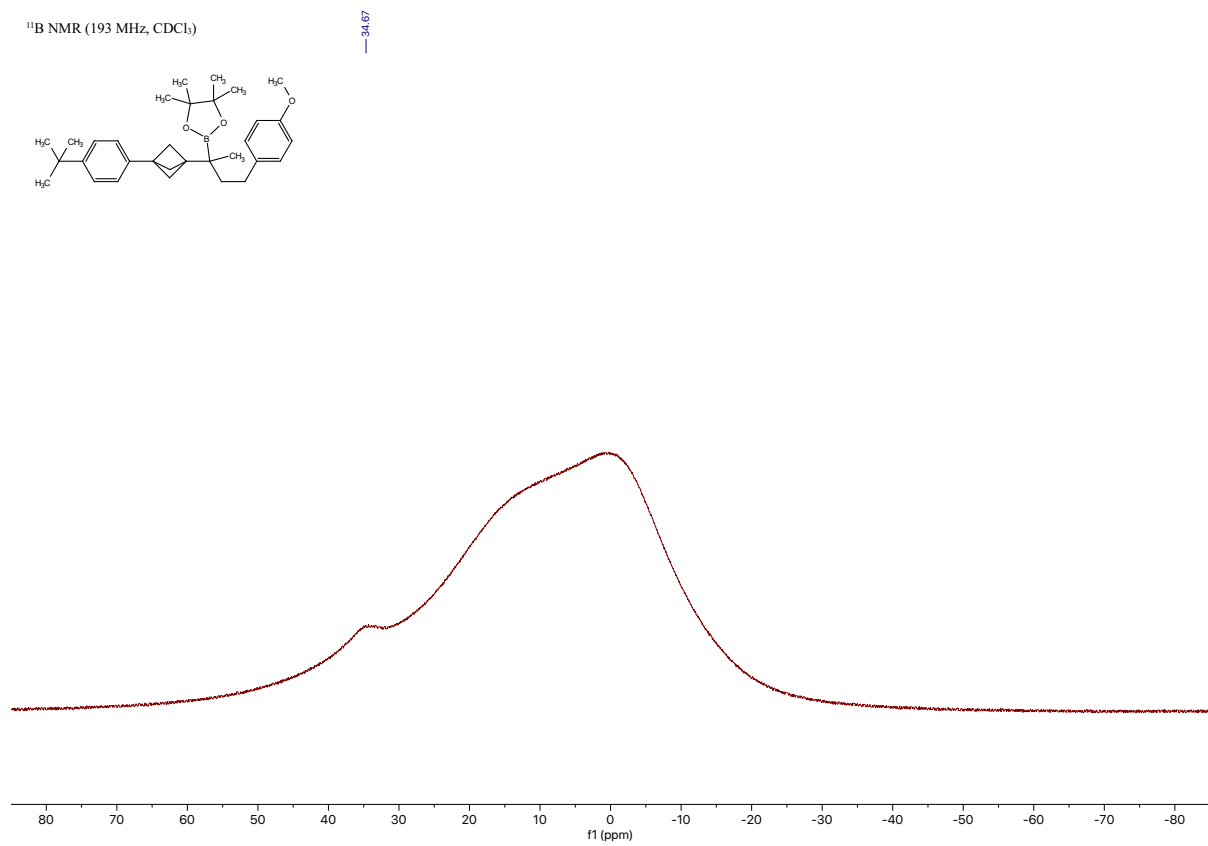
Compound 1f

ethyl 4-(3-(4-(*tert*-butyl)phenyl)bicyclo[1.1.1]pentan-1-yl)benzoate [Experimental]

¹H NMR (600 MHz, CDCl₃)

¹³C NMR (151 MHz, CDCl₃)
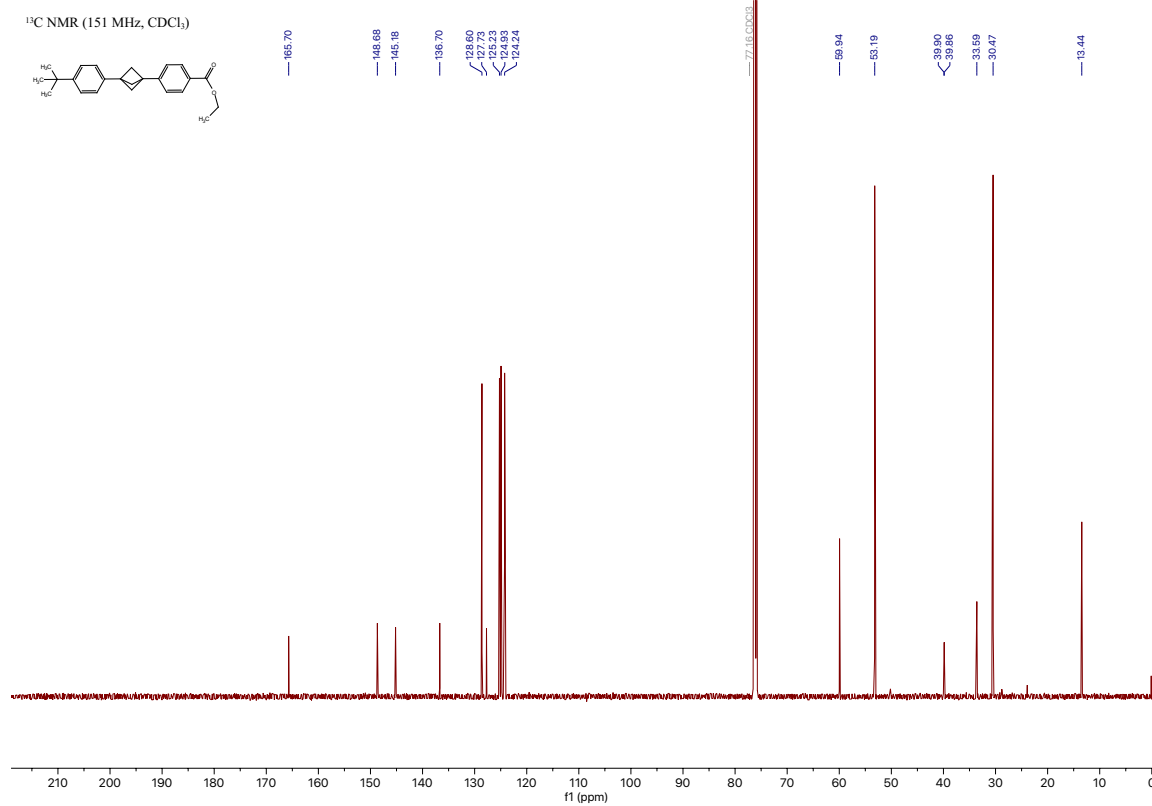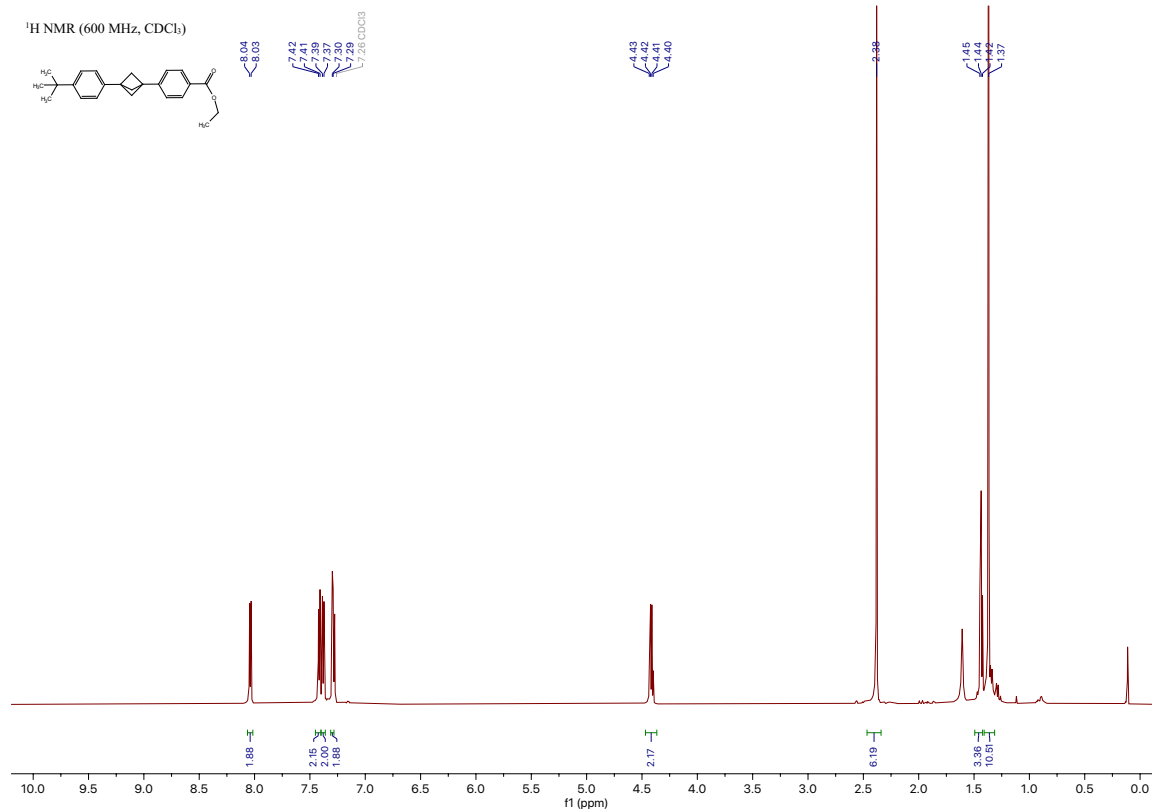
Compound 1g

5-(3-(4-(*tert*-butyl)phenyl)bicyclo[1.1.1]pentan-1-yl)-2-methylpyridine [Experimental]

¹H NMR (500 MHz, CDCl₃)

¹³C NMR (126 MHz, CDCl₃)
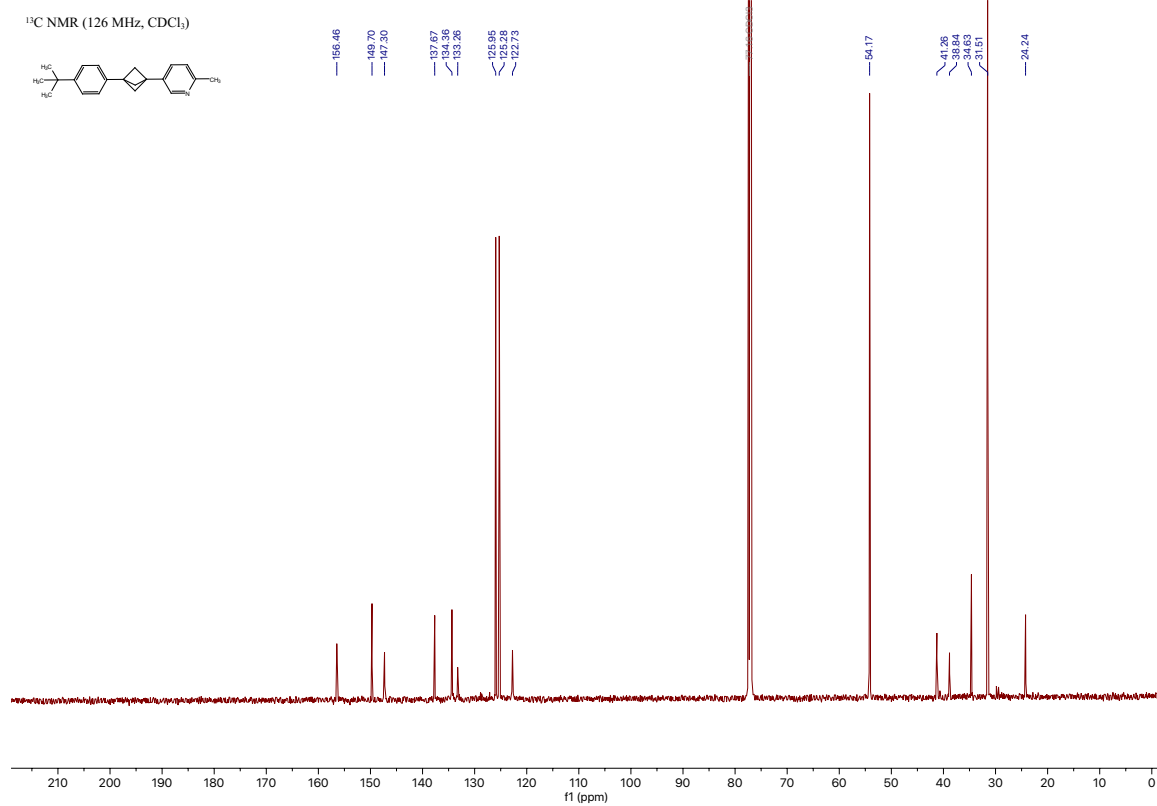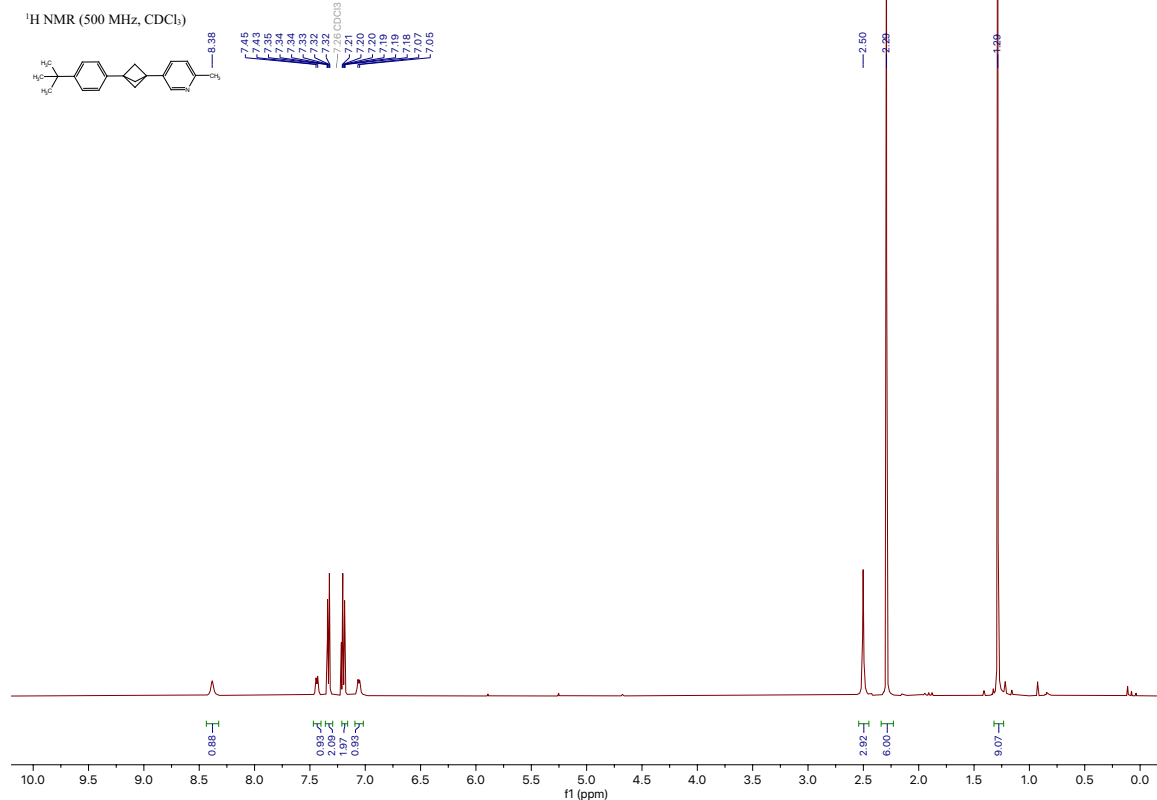
Compound 11e

1-(methylsulfonyl)-3-vinylbicyclo[1.1.1]pentane [Experimental]

¹H NMR (500 MHz, CDCl₃)
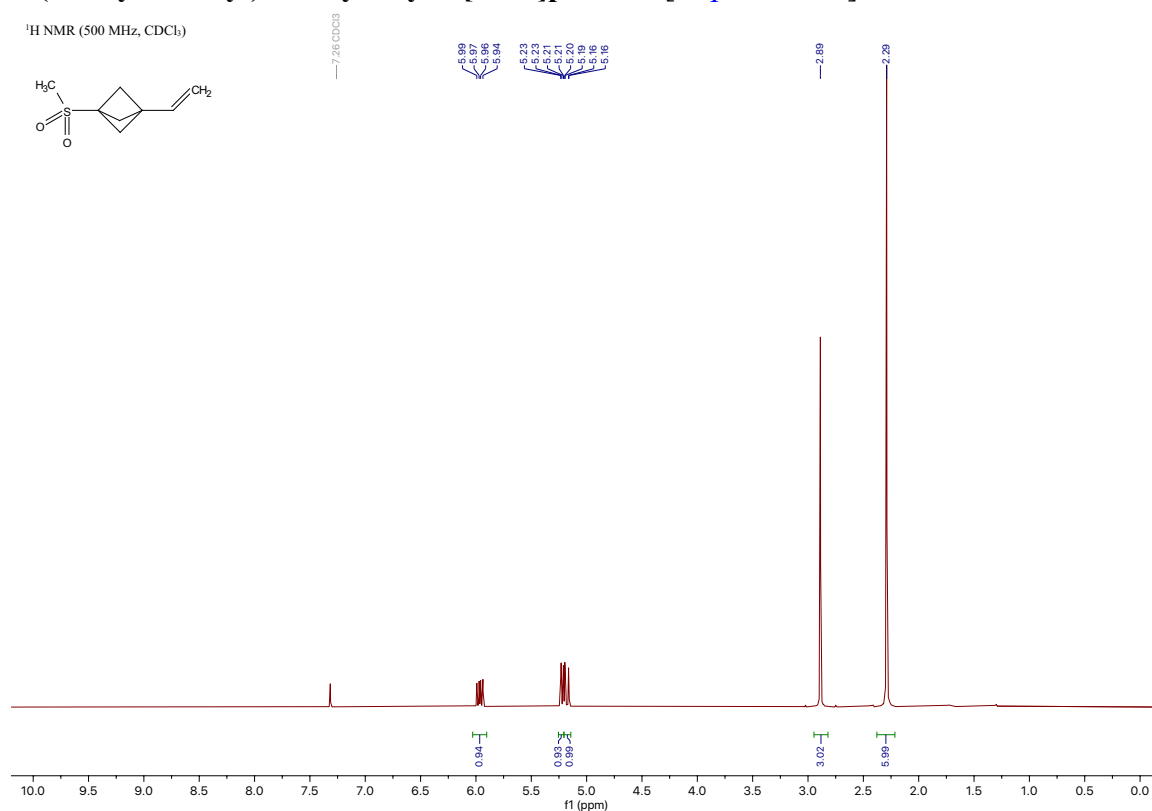
¹³C NMR (126 MHz, CDCl₃)
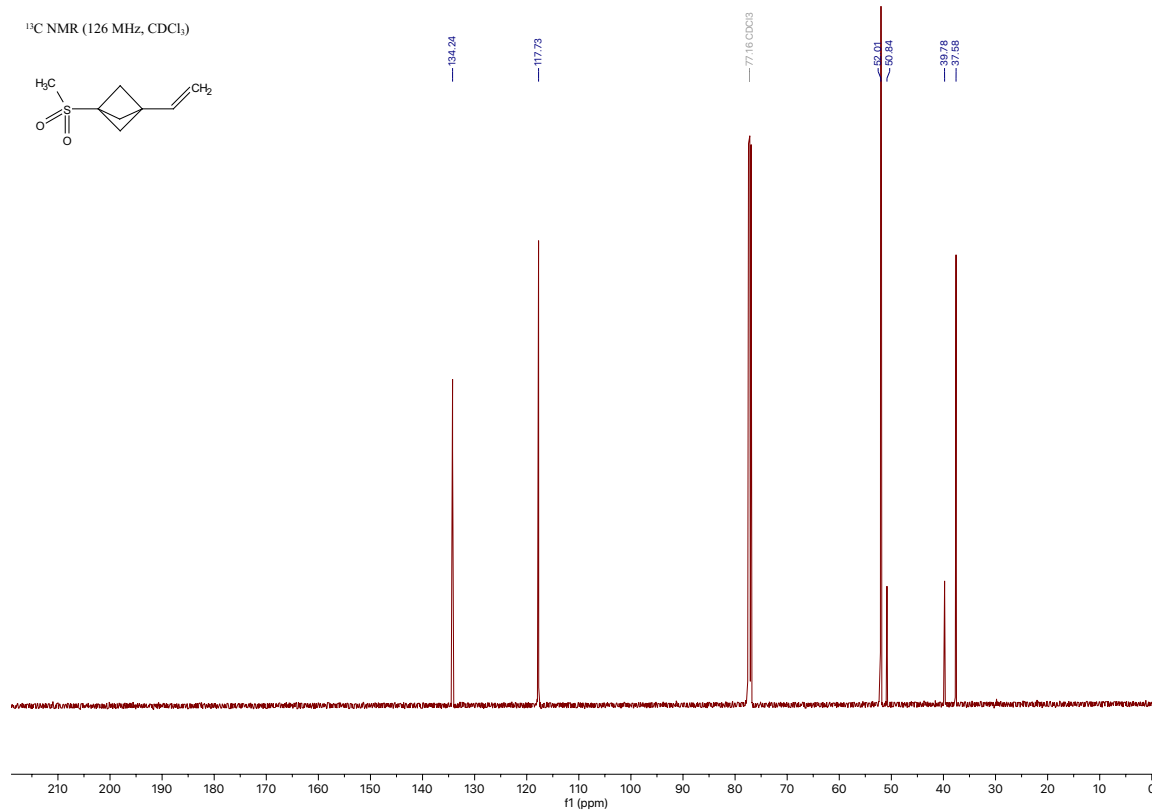
Compound 30c

tert-butyl 1-(difluoromethyl)-4-vinyl-2-azabicyclo[2.1.1]hexane-2-carboxylate

[Experimental]

¹H NMR (600 MHz, CDCl₃)

¹³C NMR (151 MHz, CDCl₃)

155.30
135.39
116.74
113.88
112.30
110.73
80.68
69.39
69.18
68.98
55.38
47.65
43.29
29.81
28.50

f1 (ppm)

¹⁹F NMR (565 MHz, CDCl₃)

-124.42

f1 (ppm)
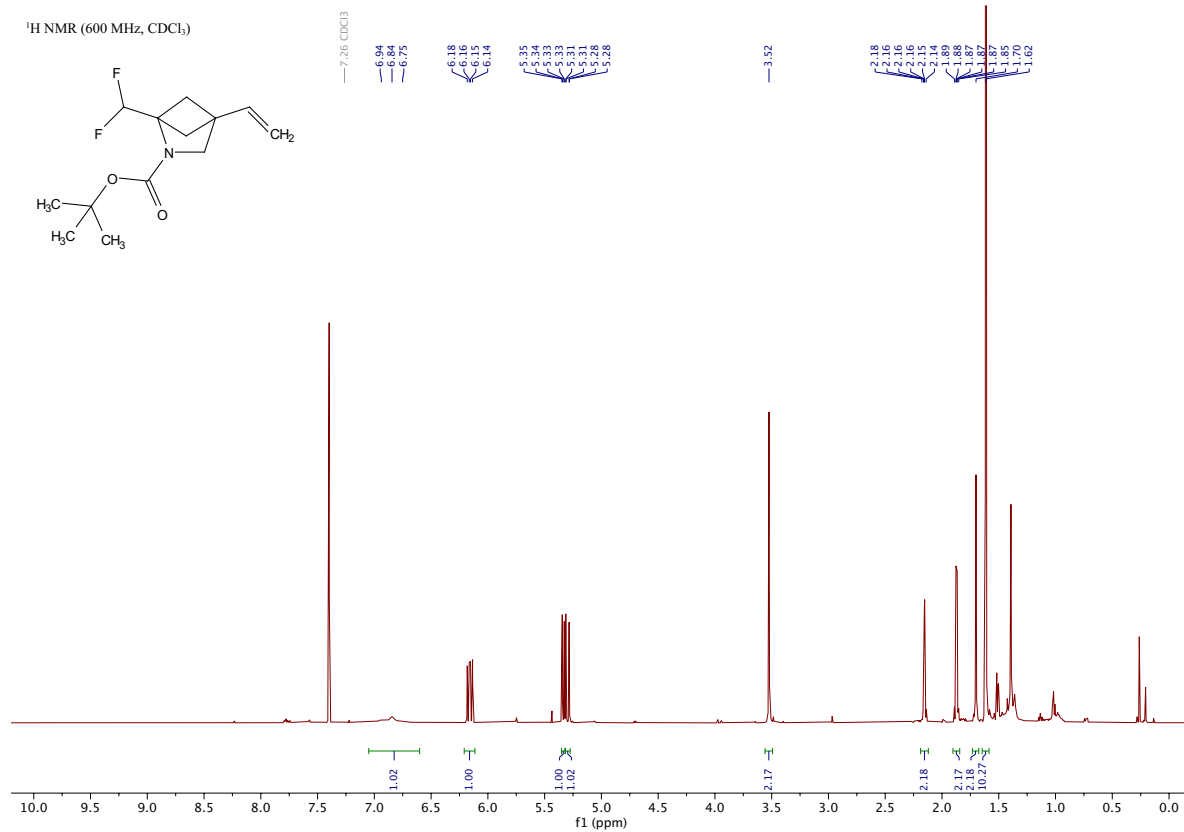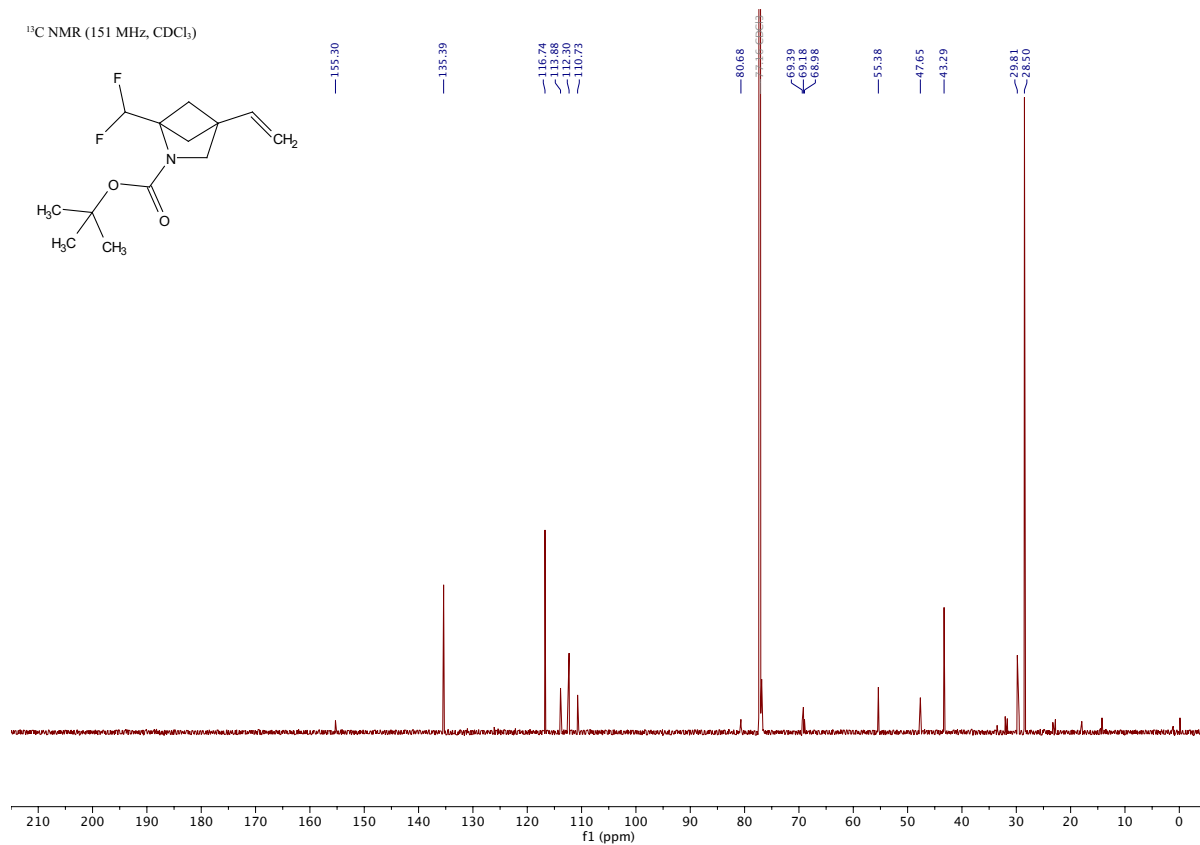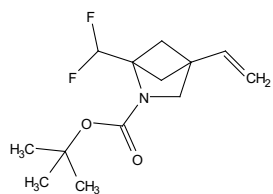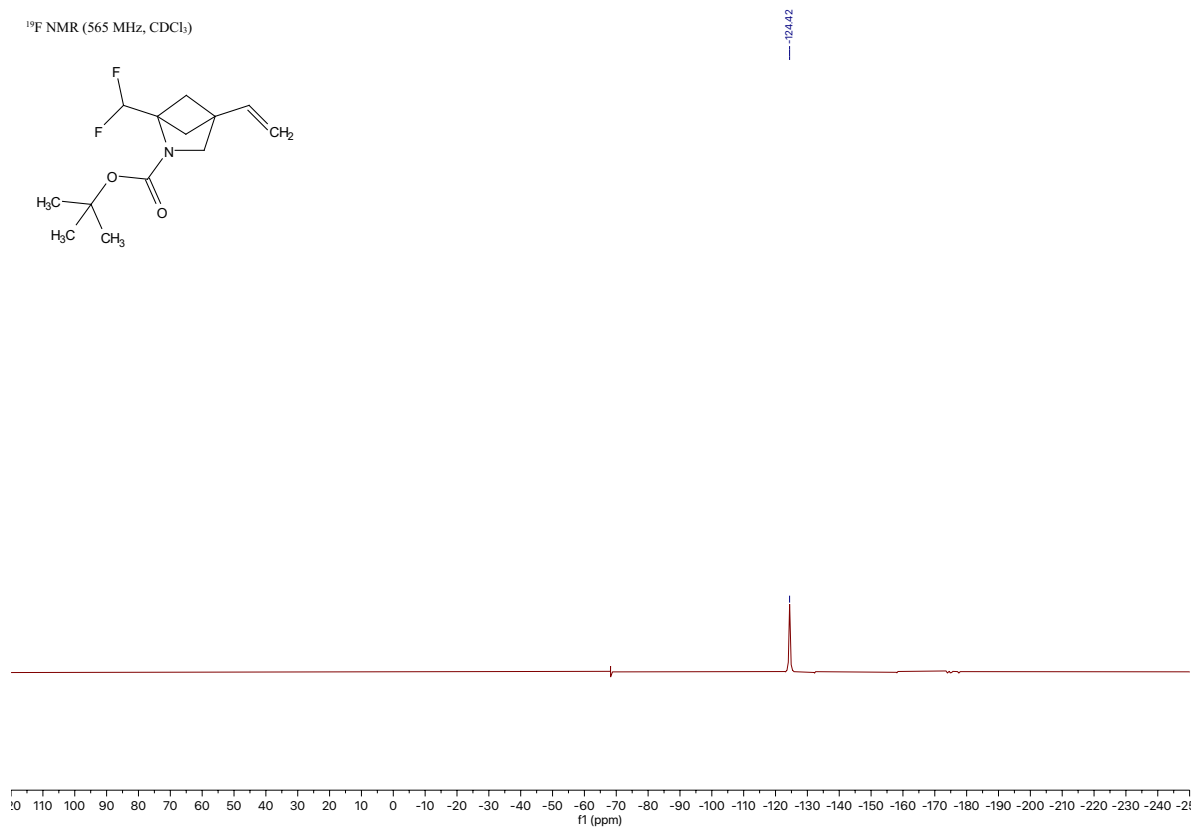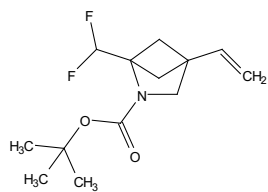
Compound 13c

1-((3-(furan-2-yl)bicyclo[1.1.1]pentan-1-yl)sulfonyl)piperidine [Experimental]
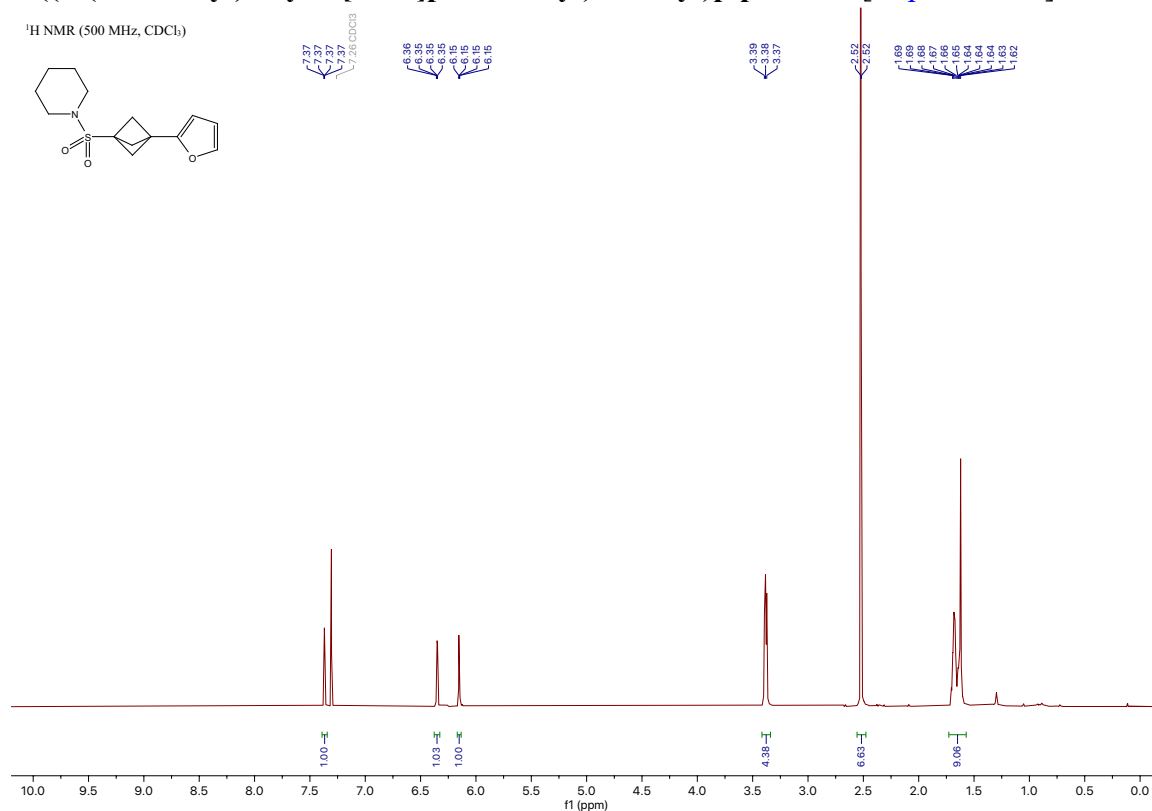
¹H NMR (500 MHz, CDCl₃)

¹³C NMR (126 MHz, CDCl₃)
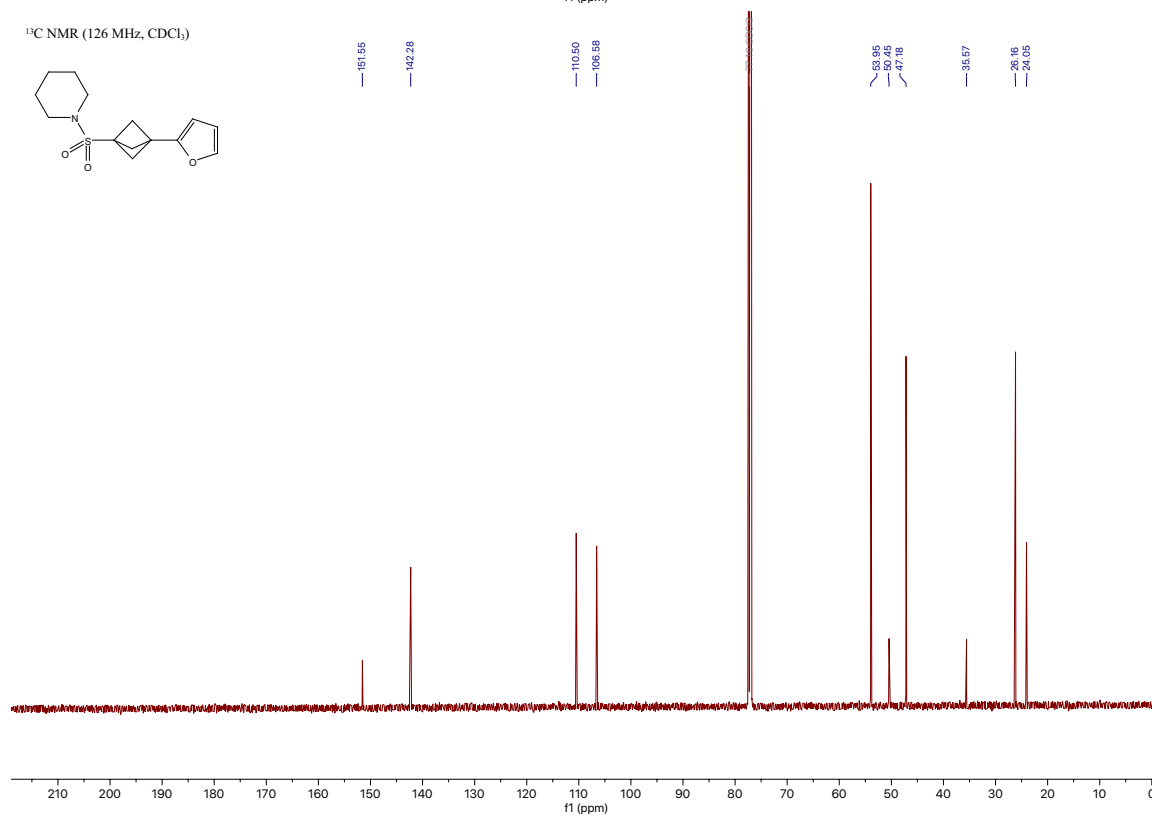
Compound 1h

2-((3-(4-(*tert*-butyl)phenyl)bicyclo[1.1.1]pentan-1-yl)methyl)-4,4,5,5-tetramethyl-1,3,2-dioxaborolane [Experimental]

¹H NMR (600 MHz, CDCl₃)

¹³C NMR (151 MHz, CDCl₃)

149.02
138.75
125.87
125.05
83.15
77.16 CDCl3
54.38
41.65
35.97
34.52
31.50
25.05

210 200 190 180 170 160 150 140 130 120 110 100 90 80 70 60 50 40 30 20 10 0
f1 (ppm)

¹¹B NMR (193 MHz, CDCl₃)

32.91

80 70 60 50 40 30 20 10 0 -10 -20 -30 -40 -50 -60 -70 -80
f1 (ppm)

321
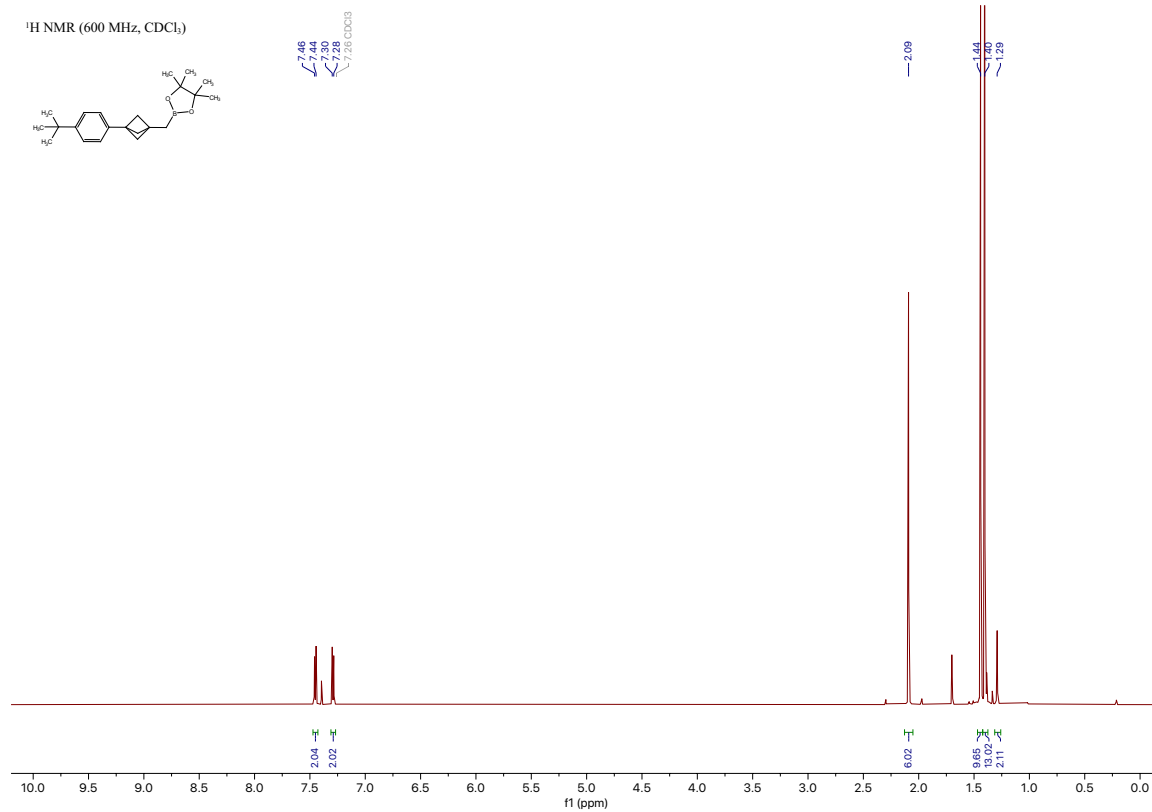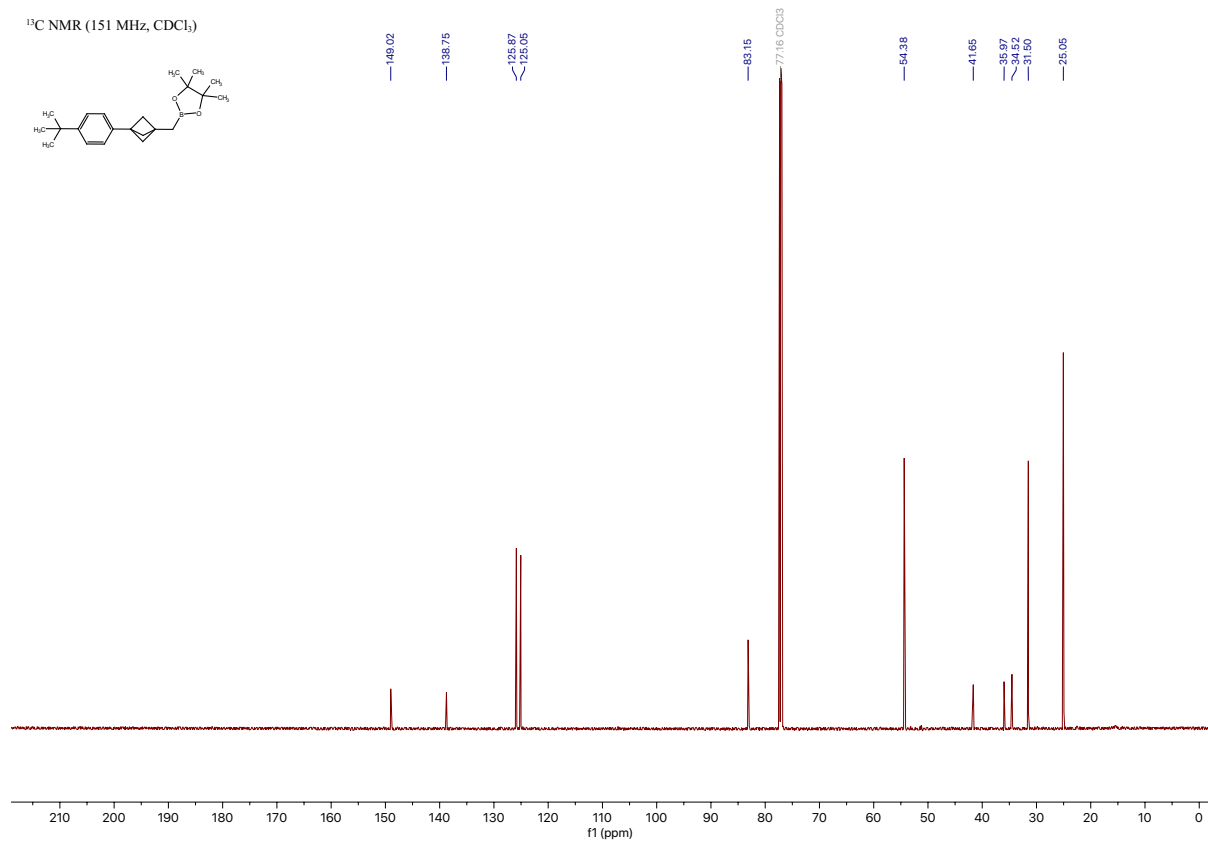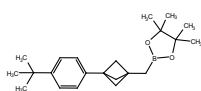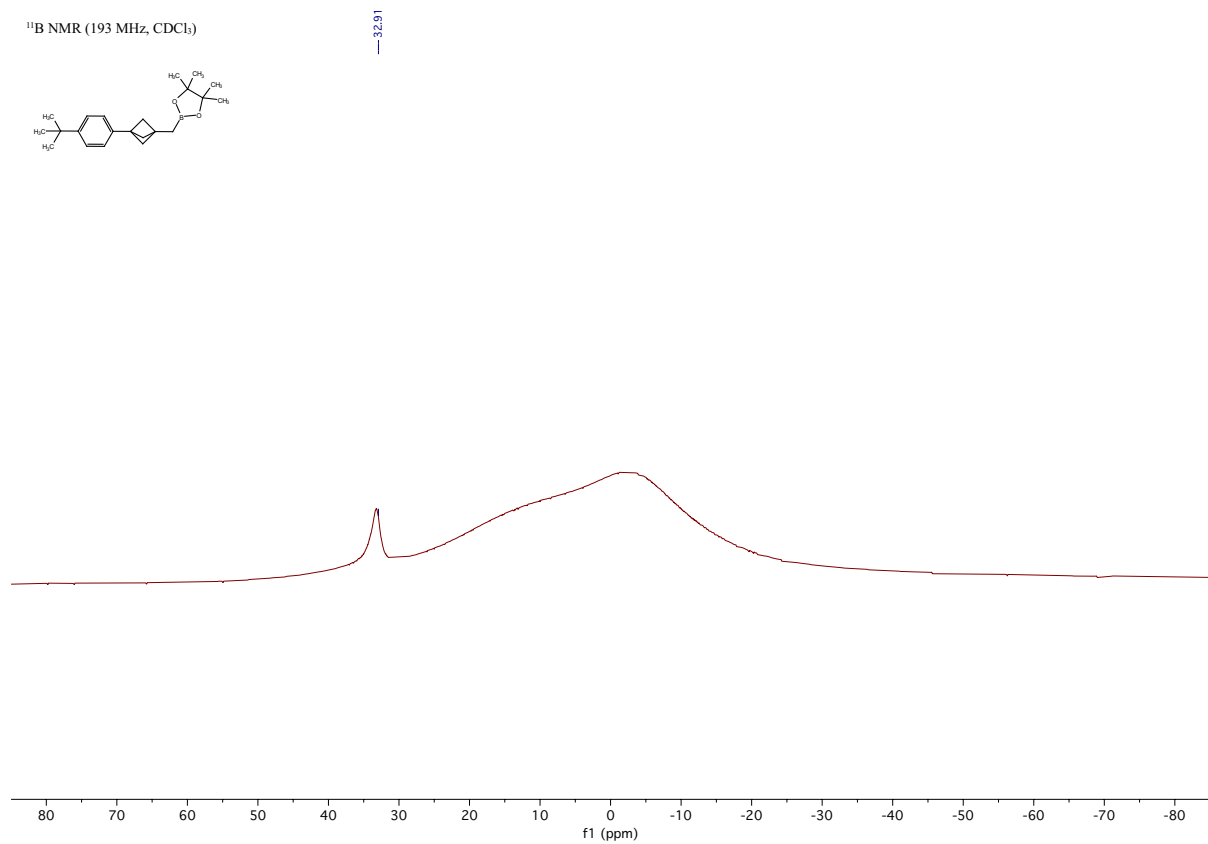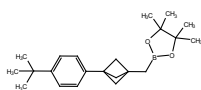
Compound 16d

2,2,2-trifluoro-*N*-(3-hydroxybicyclo[1.1.1]pentan-1-yl)acetamide [Experimental]

¹H NMR (600 MHz, Acetone)

¹³C NMR (151 MHz, Acetone)

157.92
157.68
157.44
157.20

119.75
117.84
115.93
114.02

77.16 CDCl3

63.34

56.38
56.34

42.01

f1 (ppm)

¹⁹F NMR (565 MHz, Acetone)

-77.65

f1 (ppm)
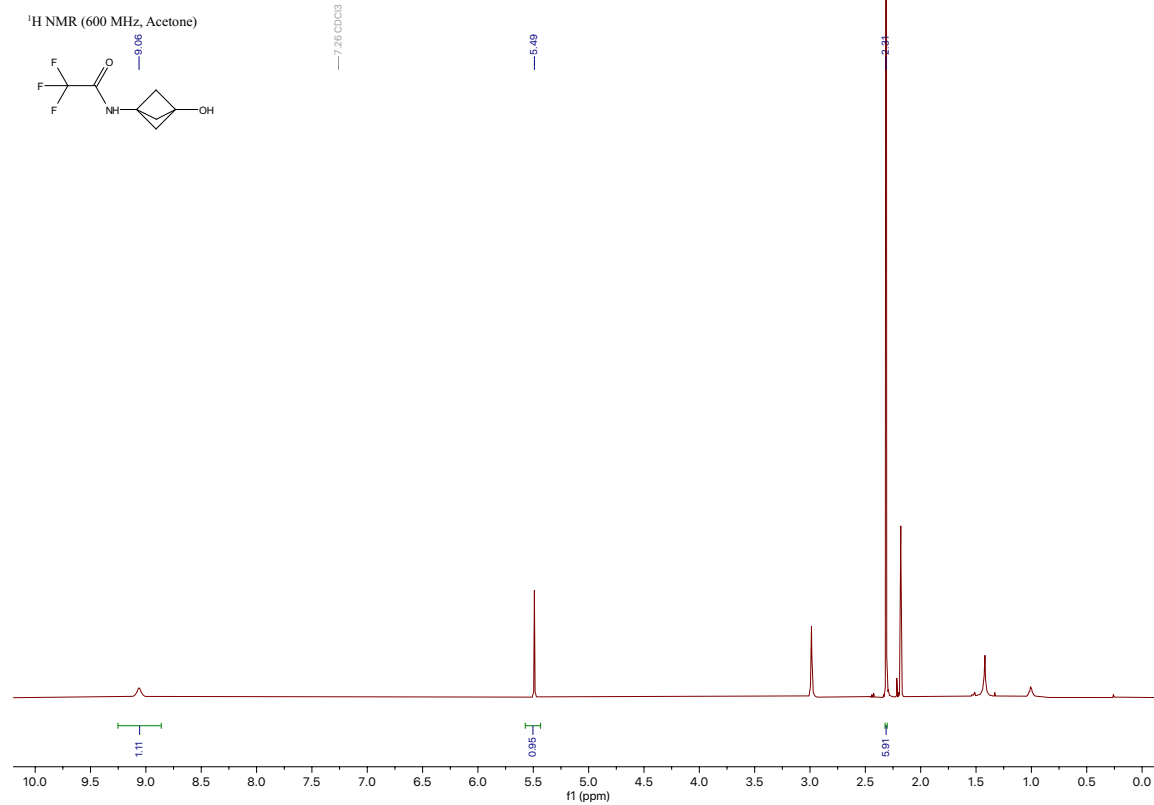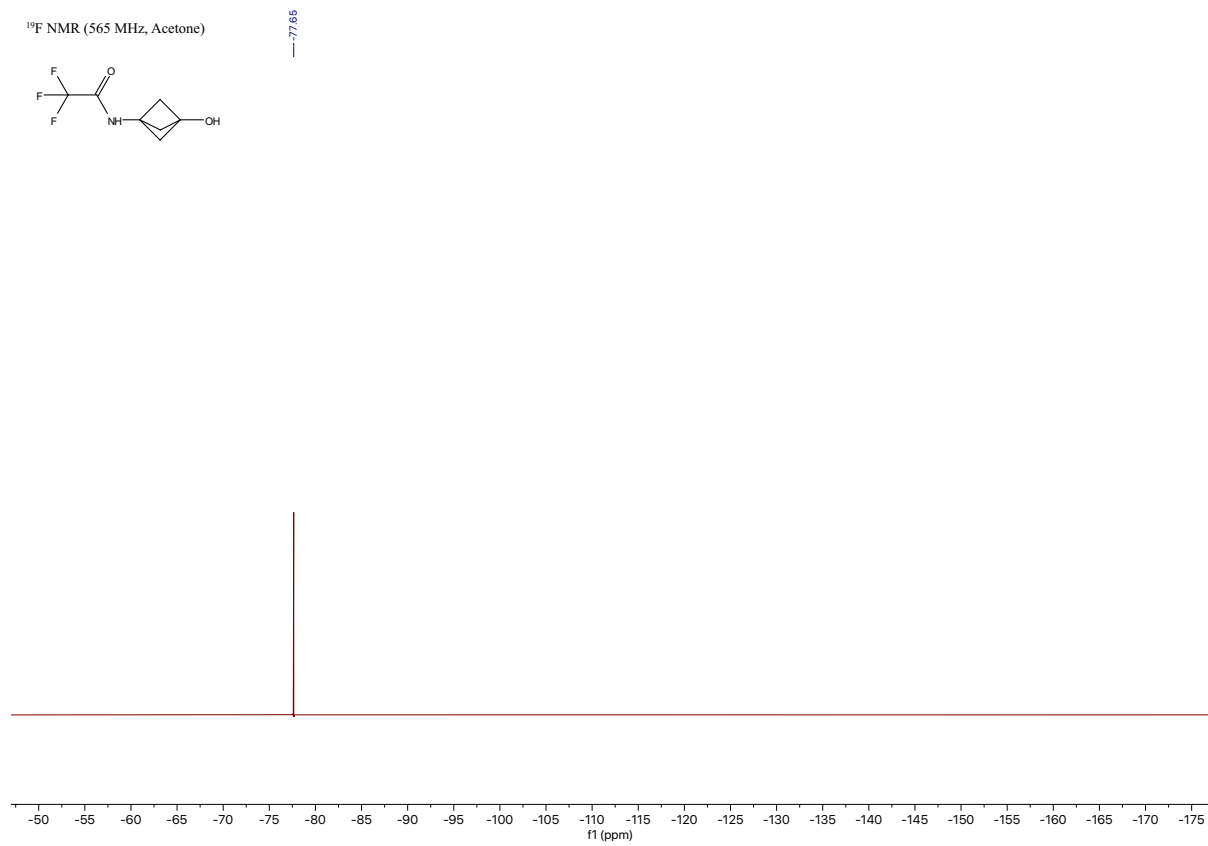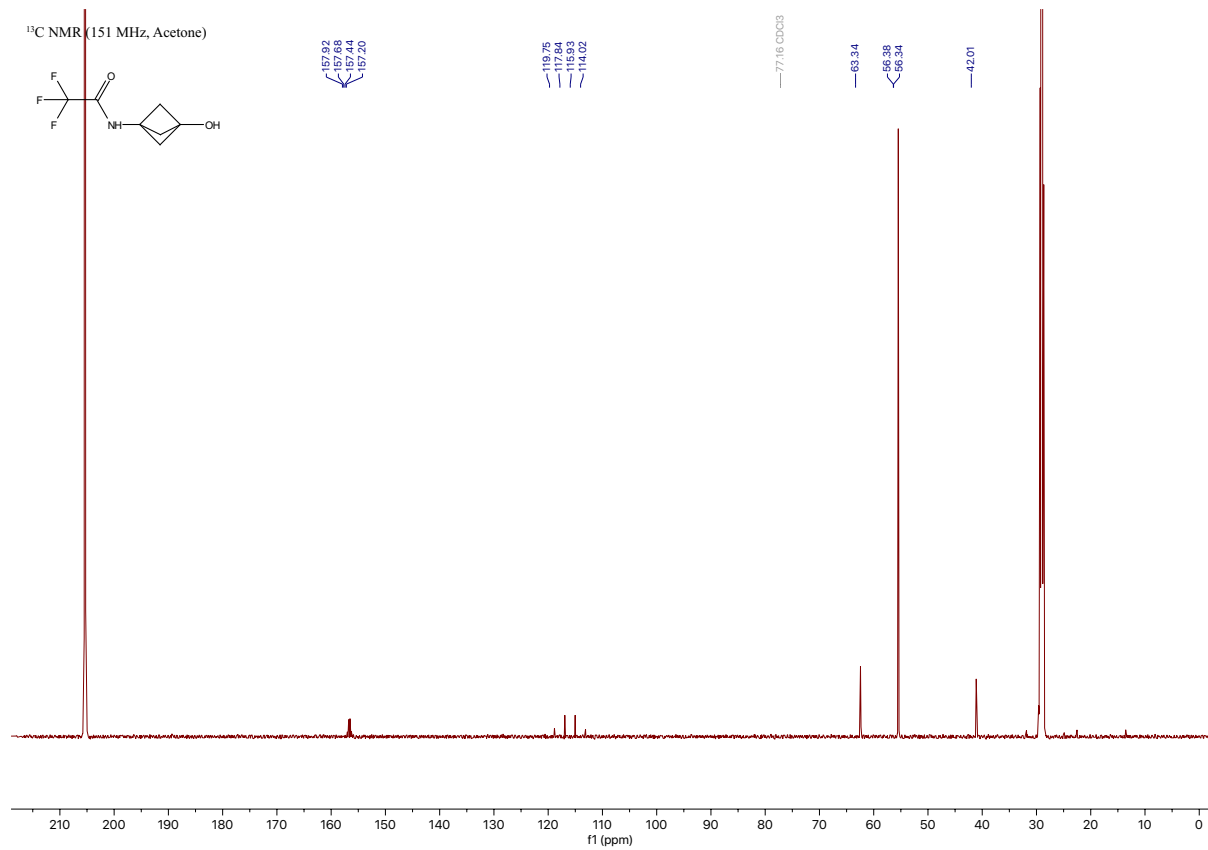
Compound 27c

tert-butyl 4-hydroxy-2-azabicyclo[2.1.1]hexane-2-carboxylate [Experimental]

¹H NMR (600 MHz, CDCl₃)

¹³C NMR (151 MHz, CDCl₃)

155.39

79.68
77.16 CDCl₃
76.00

50.94
47.23

28.59

HSQC:
¹³C NMR (126 MHz, CDCl₃)
¹H NMR (500 MHz, CDCl₃)

{1.47,28.33}

{1.86,47.02}   {1.83,47.02}
{4.19,52.02}   {4.18,51.70}   {3.24,50.89}

{7.26,77.16}CDCl₃

325
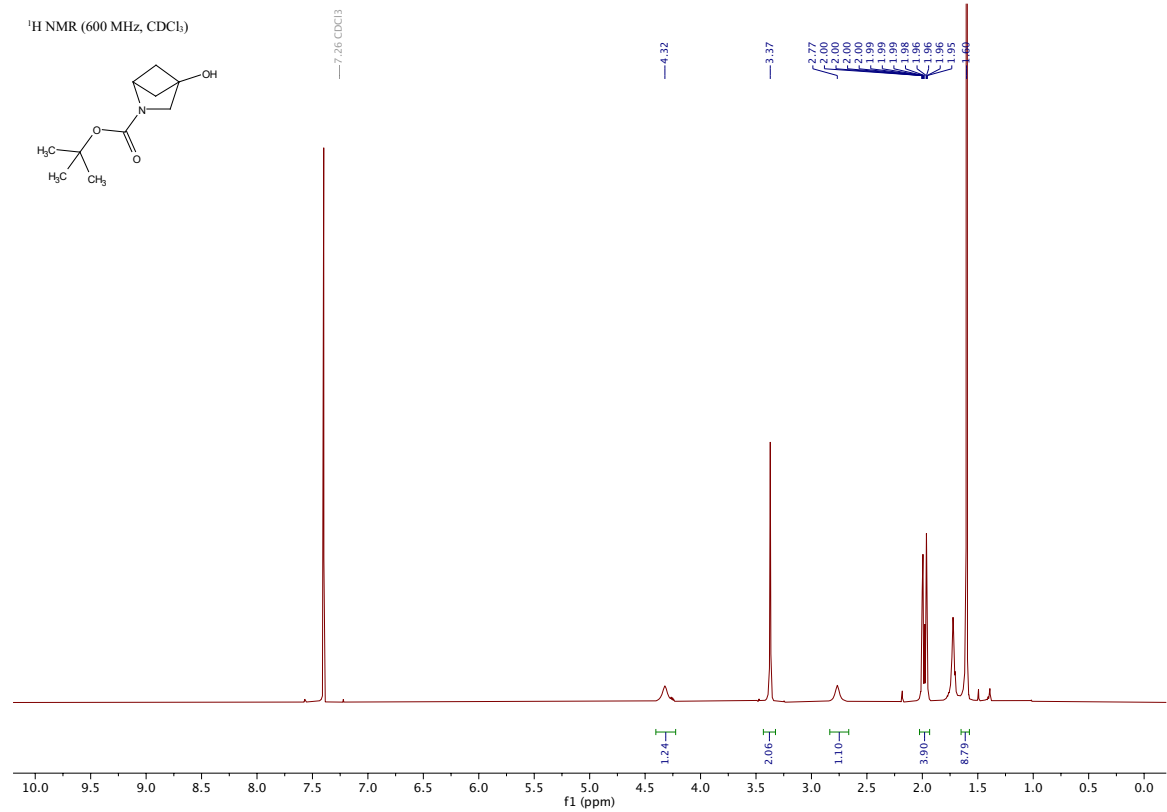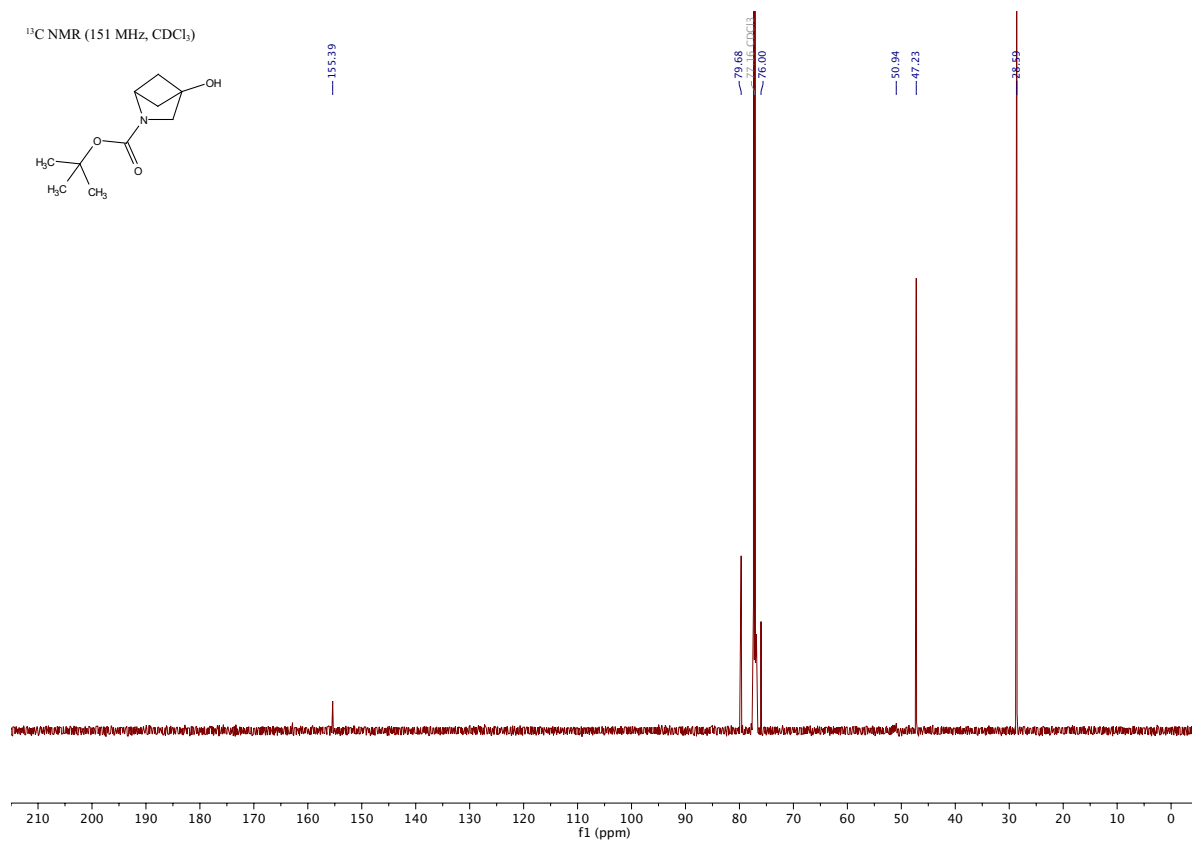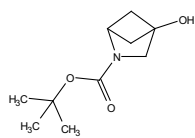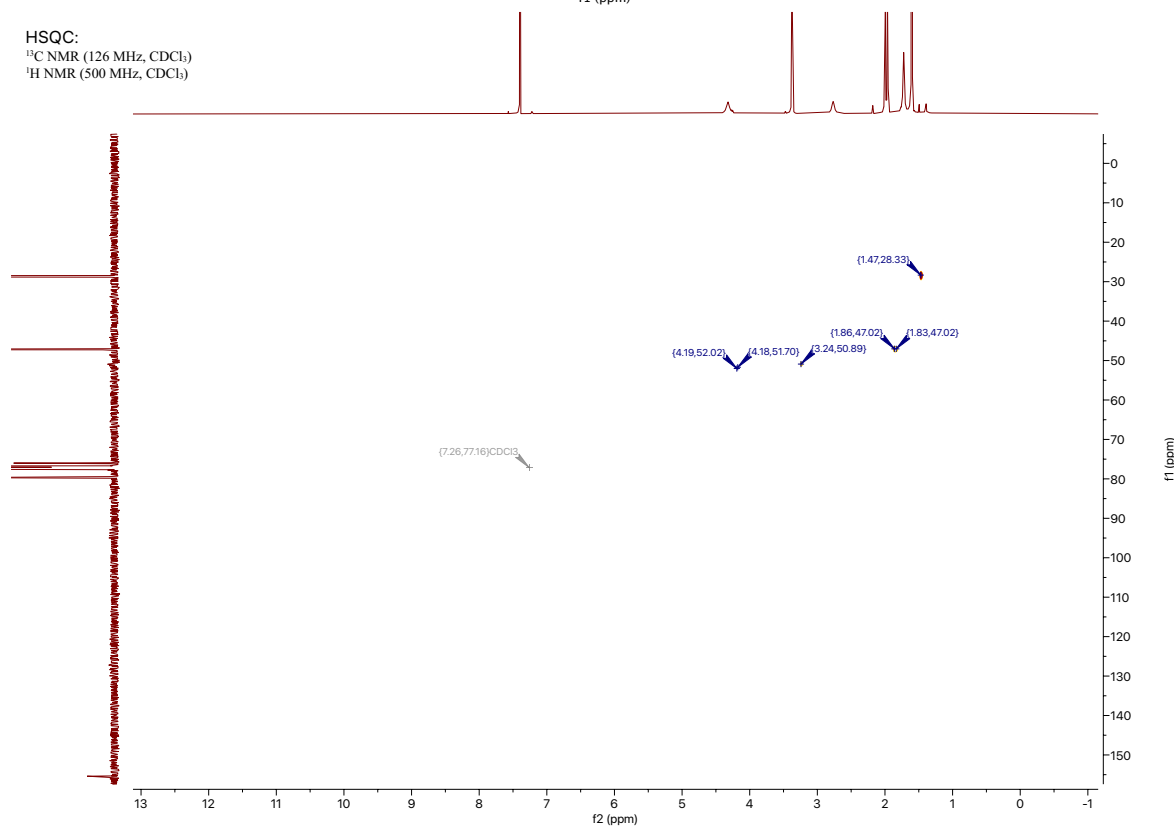
Compound 16e

N-(3-(benzylamino)bicyclo[1.1.1]pentan-1-yl)-2,2,2-trifluoroacetamide [Experimental]

^{1}H NMR (500 MHz, CDCl$_3$)

¹³C NMR (126 MHz, CDCl₃)

157.45
157.16
156.87
139.91
128.67
128.09
127.37
119.02
116.73
114.43
112.14
53.65
52.33
50.63
43.84

| 210 | 200 | 190 | 180 | 170 | 160 | 150 | 140 | 130 | 120 | 110 | 100 | 90 | 80 | 70 | 60 | 50 | 40 | 30 | 20 | 10 | 0 |

f1 (ppm)

¹⁹F NMR (470 MHz, CDCl₃)

−76.04

| −30 | −35 | −40 | −45 | −50 | −55 | −60 | −65 | −70 | −75 | −80 | −85 | −90 | −95 | −100 | −105 | −110 | −115 | −120 | −125 | −130 | −135 | −140 | −145 |

f1 (ppm)
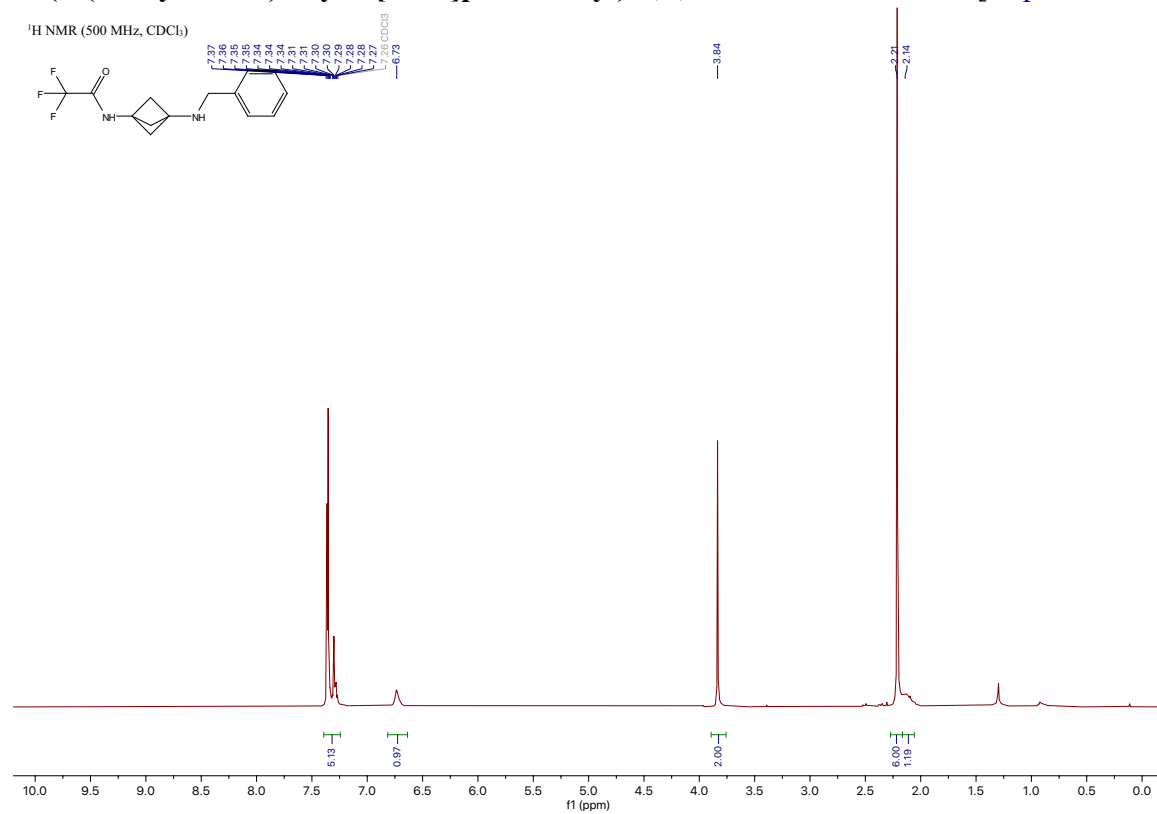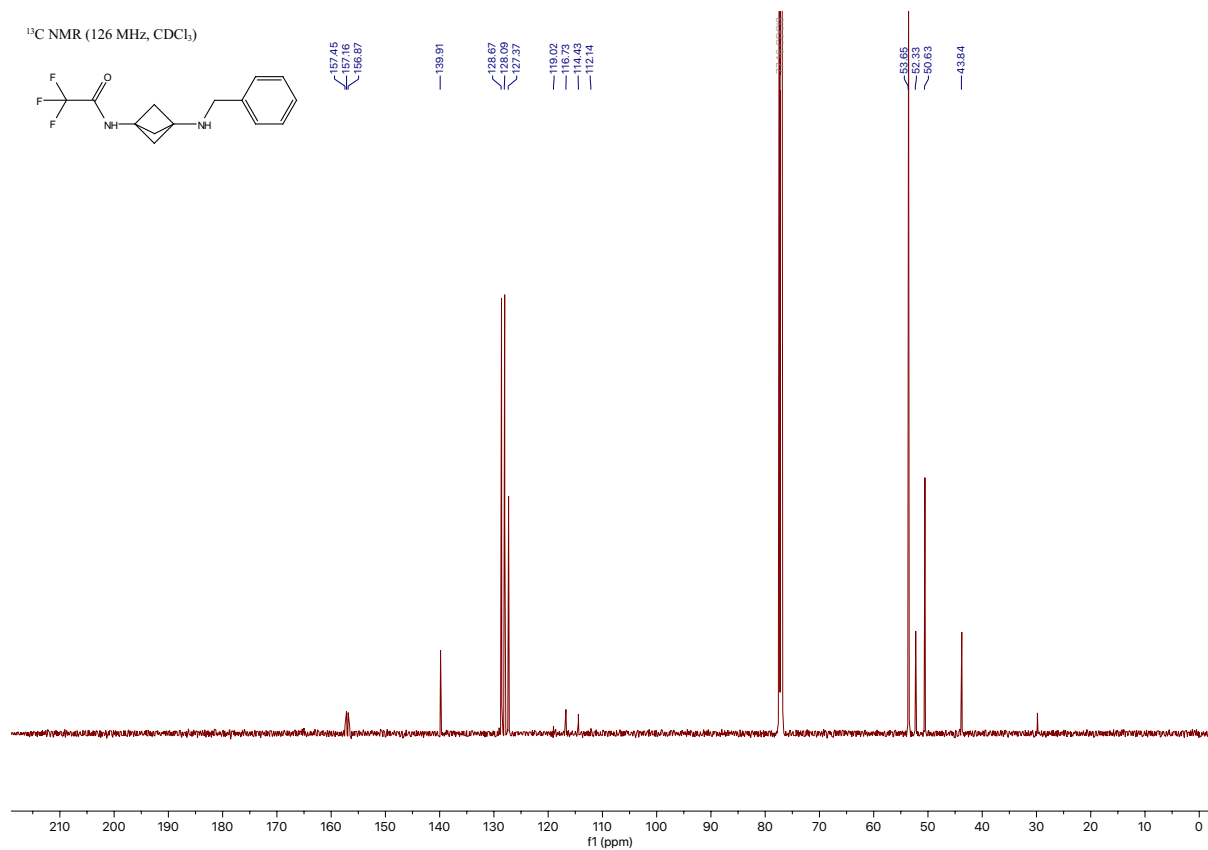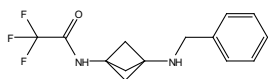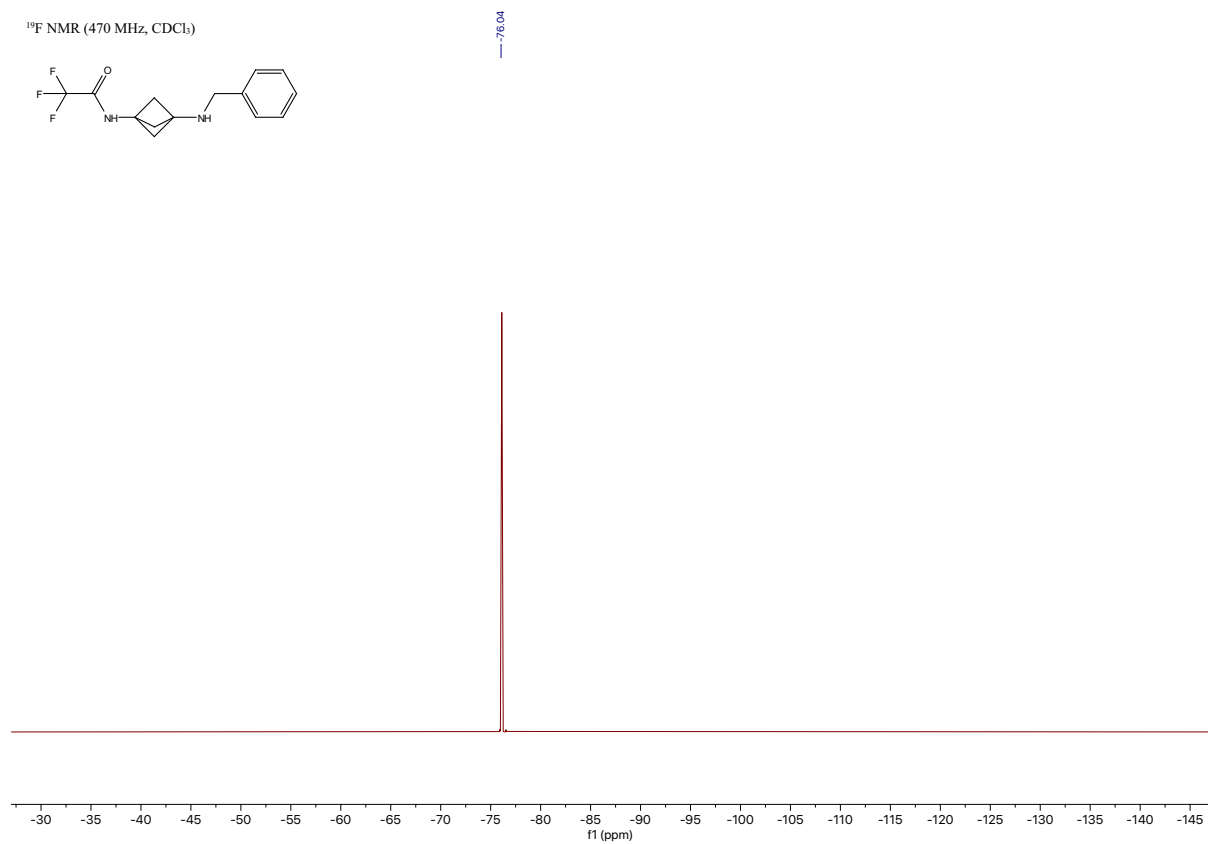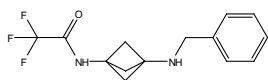
2.5 References

Parts of this chapter were reprinted with permission from:

"Catalytic Undirected Borylation of Tertiary C–H Bonds in Bicyclo[1.1.1]pentanes and Bicyclohexanes"

Yu, I.F.; Manske, J.M.; Diéguez-Vázquez, A.; Misale, A.; Pashenko, A.E.; Mykhailiuk, P.K.; Ryabukhin, S.V.; Volochnyuk, D.M.; Hartwig, J.F. *Nat. Chem.* **2023**, *15*, 685–693.

1.   Liskey, C. W.; Hartwig, J. F., Iridium-Catalyzed Borylation of Secondary C–H Bonds in Cyclic Ethers. *J. Am. Chem. Soc.* **2012,** *134*, 12422-12425.
2.   Liskey, C. W.; Hartwig, J. F., Iridium-Catalyzed C–H Borylation of Cyclopropanes. *J. Am. Chem. Soc.* **2013,** *135*, 3375-3378.
3.   Li, Q.; Liskey, C. W.; Hartwig, J. F., Regioselective Borylation of the C–H Bonds in Alkylamines and Alkyl Ethers. Observation and Origin of High Reactivity of Primary C–H Bonds Beta to Nitrogen and Oxygen. *J. Am. Chem. Soc.* **2014,** *136*, 8755-8765.
4.   Jones, M. R.; Fast, C. D.; Schley, N. D., Iridium-Catalyzed sp^3 C–H Borylation in Hydrocarbon Solvent Enabled by 2,2'-Dipyridylarylmethane Ligands. *J. Am. Chem. Soc.* **2020,** *142*, 6488-6492.
5.   Oeschger, R.; Su, B.; Yu, I.; Ehinger, C.; Romero, E.; He, S.; Hartwig, J., Diverse functionalization of strong alkyl C–H bonds by undirected borylation. *Science* **2020,** *368*, 736.
6.   Kawazu, R.; Torigoe, T.; Kuninobu, Y., Iridium-Catalyzed C(sp^3)−H Borylation Using Silyl-Bipyridine Pincer Ligands. *Angew. Chem. Int. Ed. n/a*, e202202327.
7.   Shu, C.; Noble, A.; Aggarwal, V. K., Metal-free photoinduced C(sp^3)–H borylation of alkanes. *Nature* **2020,** *586*, 714-719.
8.   Lovering, F.; Bikker, J.; Humblet, C., Escape from Flatland: Increasing Saturation as an Approach to Improving Clinical Success. *J. Med. Chem.* **2009,** *52*, 6752-6756.
9.   Stepan, A. F.; Subramanyam, C.; Efremov, I. V.; Dutra, J. K.; O'Sullivan, T. J.; DiRico, K. J.; McDonald, W. S.; Won, A.; Dorff, P. H.; Nolan, C. E.; Becker, S. L.; Pustilnik, L. R.; Riddell, D. R.; Kauffman, G. W.; Kormos, B. L.; Zhang, L.; Lu, Y.; Capetta, S. H.; Green, M. E.; Karki, K.; Sibley, E.; Atchison, K. P.; Hallgren, A. J.; Oborski, C. E.; Robshaw, A. E.; Sneed, B.; O'Donnell, C. J., Application of the Bicyclo[1.1.1]pentane Motif as a Nonclassical Phenyl Ring Bioisostere in the Design of a Potent and Orally Active γ-Secretase Inhibitor. *J. Med. Chem.* **2012,** *55*, 3414-3424.
10.   Measom, N. D.; Down, K. D.; Hirst, D. J.; Jamieson, C.; Manas, E. S.; Patel, V. K.; Somers, D. O., Investigation of a Bicyclo[1.1.1]pentane as a Phenyl Replacement within an LpPLA2 Inhibitor. *ACS Med. Chem. Lett.* **2017,** *8*, 43-48.
11.   Auberson, Y. P.; Brocklehurst, C.; Furegati, M.; Fessard, T. C.; Koch, G.; Decker, A.; La Vecchia, L.; Briard, E., Improving Nonspecific Binding and Solubility: Bicycloalkyl Groups and Cubanes as para-Phenyl Bioisosteres. *ChemMedChem* **2017,** *12*, 590-598.
12.   Pu, Q.; Zhang, H.; Guo, L.; Cheng, M.; Doty, A. C.; Ferguson, H.; Fradera, X.; Lesburg, C. A.; McGowan, M. A.; Miller, J. R.; Geda, P.; Song, X.; Otte, K.; Sciammetta, N.; Solban, N.; Yu, W.; Sloman, D. L.; Zhou, H.; Lammens, A.; Neumann, L.; Bennett, D. J.; Pasternak, A.; Han, Y., Discovery of Potent and Orally Available Bicyclo[1.1.1]pentane-Derived Indoleamine-2,3-dioxygenase 1 (IDO1) Inhibitors. *ACS Med. Chem. Lett.* **2020,** *11*, 1548-1554.

13.   Makarov, I. S.; Brocklehurst, C. E.; Karaghiosoff, K.; Koch, G.; Knochel, P., Synthesis of Bicyclo[1.1.1]pentane Bioisosteres of Internal Alkynes and para-Disubstituted Benzenes from [1.1.1]Propellane. *Angew. Chem. Int. Ed.* **2017,** *56,* 12774-12777.

14.   Barbachyn, M. R.; Hutchinson, D. K.; Toops, D. S.; Reid, R. J.; Zurenko, G. E.; Yagi, B. H.; Schaadt, R. D.; Allison, J. W., U-87947E, a protein quinolone antibacterial agent incorporating a bicyclo[1.1.1]pent-1-yl (BCP) subunit. *Bioorganic Med. Chem. Lett.* **1993,** *3,* 671-676.

15.   Westphal, M. V.; Wolfstädter, B. T.; Plancher, J.-M.; Gatfield, J.; Carreira, E. M., Evaluation of tert-Butyl Isosteres: Case Studies of Physicochemical and Pharmacokinetic Properties, Efficacies, and Activities. *ChemMedChem* **2015,** *10,* 461-469.

16.   Denisenko, A.; Garbuz, P.; Shishkina, S. V.; Voloshchuk, N. M.; Mykhailiuk, P. K., Saturated Bioisosteres of ortho-Substituted Benzenes. *Angew. Chem. Int. Ed.* **2020,** *59,* 20515-20521.

17.   Levterov, V. V.; Panasyuk, Y.; Pivnytska, V. O.; Mykhailiuk, P. K., Water-Soluble Non-Classical Benzene Mimetics. *Angew. Chem. Int. Ed.* **2020,** *59,* 7161-7167.

18.   Levterov, V. V.; Michurin, O.; Borysko, P. O.; Zozulya, S.; Sadkova, I. V.; Tolmachev, A. A.; Mykhailiuk, P. K., Photochemical In-Flow Synthesis of 2,4-Methanopyrrolidines: Pyrrolidine Analogues with Improved Water Solubility and Reduced Lipophilicity. *J. Org. Chem.* **2018,** *83,* 14350-14361.

19.   Homon, A. A.; Hryshchuk, O. V.; Mykhailenko, O. V.; Vashchenko, B. V.; Melnykov, K. P.; Michurin, O. M.; Daniliuc, C. G.; Gerus, I. I.; Kovtunenko, V. O.; Kondratov, I. S.; Grygorenko, O. O., 4-(Di-/Trifluoromethyl)-2-heterabicyclo[2.1.1]hexanes: Advanced Fluorinated Phenyl Isosteres and Proline analogues. *Eur. J. Org. Chem.* **2021,** *2021,* 6580-6590.

20.   Wiberg, K. B.; Waddell, S. T.; Laidig, K., [1.1.1]Propellane: Reaction with free radicals. *Tet. Lett.* **1986,** *27,* 1553-1556.

21.   Kaszynski, P.; Michl, J., A practical photochemical synthesis of bicyclo [1.1.1] pentane-1, 3-dicarboxylic acid. *J. Org. Chem.* **1988,** *53,* 4593-4594.

22.   Wiberg, K. B.; Waddell, S. T., Reactions of [1.1.1] propellane. *J. Am. Chem. Soc.* **1990,** *112,* 2194-2216.

23.   Bunker, K. D.; Sach, N. W.; Huang, Q.; Richardson, P. F., Scalable Synthesis of 1-Bicyclo[1.1.1]pentylamine via a Hydrohydrazination Reaction. *Org. Lett.* **2011,** *13,* 4746-4748.

24.   Kanazawa, J.; Maeda, K.; Uchiyama, M., Radical Multicomponent Carboamination of [1.1.1]Propellane. *J. Am. Chem. Soc.* **2017,** *139,* 17791-17794.

25.   Caputo, D. F. J.; Arroniz, C.; Dürr, A. B.; Mousseau, J. J.; Stepan, A. F.; Mansfield, S. J.; Anderson, E. A., Synthesis and applications of highly functionalized 1-halo-3-substituted bicyclo[1.1.1]pentanes. *Chem. Sci.* **2018,** *9,* 5295-5300.

26.   Bär, R. M.; Kirschner, S.; Nieger, M.; Bräse, S., Alkyl and Aryl Thiol Addition to [1.1.1]Propellane: Scope and Limitations of a Fast Conjugation Reaction. *Chem. Eur. J.* **2018,** *24,* 1373-1382.

27.   Nugent, J.; Arroniz, C.; Shire, B. R.; Sterling, A. J.; Pickford, H. D.; Wong, M. L. J.; Mansfield, S. J.; Caputo, D. F. J.; Owen, B.; Mousseau, J. J.; Duarte, F.; Anderson, E. A., A General Route to Bicyclo[1.1.1]pentanes through Photoredox Catalysis. *ACS Catal.* **2019,** *9,* 9568-9574.

28.   Zhang, X.; Smith, R. T.; Le, C.; McCarver, S. J.; Shireman, B. T.; Carruthers, N. I.; MacMillan, D. W. C., Copper-mediated synthesis of drug-like bicyclopentanes. *Nature* **2020,** *580,* 220-226.

29.   Kim, J. H.; Ruffoni, A.; Al-Faiyz, Y. S. S.; Sheikh, N. S.; Leonori, D., Divergent Strain-Release Amino-Functionalization of [1.1.1]Propellane with Electrophilic Nitrogen-Radicals. *Angew. Chem. Int. Ed.* **2020,** *59*, 8225-8231.

30.   Shin, S.; Lee, S.; Choi, W.; Kim, N.; Hong, S., Visible-Light-Induced 1,3-Aminopyridylation of [1.1.1]Propellane with N-Aminopyridinium Salts. *Angew. Chem. Int. Ed.* **2021,** *60*, 7873-7879.

31.   Gianatassio, R.; Lopchuk, J. M.; Wang, J.; Pan, C.-M.; Malins, L. R.; Prieto, L.; Brandt, T. A.; Collins, M. R.; Gallego, G. M.; Sach, N. W.; Spangler, J. E.; Zhu, H.; Zhu, J.; Baran, P. S., Strain-release amination. *Science* **2016,** *351*, 241-246.

32.   Lopchuk, J. M.; Fjelbye, K.; Kawamata, Y.; Malins, L. R.; Pan, C.-M.; Gianatassio, R.; Wang, J.; Prieto, L.; Bradow, J.; Brandt, T. A.; Collins, M. R.; Elleraas, J.; Ewanicki, J.; Farrell, W.; Fadeyi, O. O.; Gallego, G. M.; Mousseau, J. J.; Oliver, R.; Sach, N. W.; Smith, J. K.; Spangler, J. E.; Zhu, H.; Zhu, J.; Baran, P. S., Strain-Release Heteroatom Functionalization: Development, Scope, and Stereospecificity. *J. Am. Chem. Soc.* **2017,** *139*, 3209-3226.

33.   Shelp, R. A.; Walsh, P. J., Synthesis of BCP Benzylamines From 2-Azaallyl Anions and [1.1.1]Propellane. *Angew. Chem. Int. Ed.* **2018,** *57*, 15857-15861.

34.   Hughes, J. M. E.; Scarlata, D. A.; Chen, A. C. Y.; Burch, J. D.; Gleason, J. L., Aminoalkylation of [1.1.1]Propellane Enables Direct Access to High-Value 3-Alkylbicyclo[1.1.1]pentan-1-amines. *Org. Lett.* **2019,** *21*, 6800-6804.

35.   Trongsiriwat, N.; Pu, Y.; Nieves-Quinones, Y.; Shelp, R. A.; Kozlowski, M. C.; Walsh, P. J., Reactions of 2-Aryl-1,3-Dithianes and [1.1.1]Propellane. *Angew. Chem. Int. Ed.* **2019,** *58*, 13416-13420.

36.   Yu, S.; Jing, C.; Noble, A.; Aggarwal, V. K., 1,3-Difunctionalizations of [1.1.1]Propellane via 1,2-Metallate Rearrangements of Boronate Complexes. *Angew. Chem. Int. Ed.* **2020,** *59*, 3917-3921.

37.   Schwärzer, K.; Zipse, H.; Karaghiosoff, K.; Knochel, P., Highly Regioselective Addition of Allylic Zinc Halides and Various Zinc Enolates to [1.1.1]Propellane. *Angew. Chem. Int. Ed.* **2020,** *59*, 20235-20241.

38.   Garlets, Z. J.; Sanders, J. N.; Malik, H.; Gampe, C.; Houk, K. N.; Davies, H. M. L., Enantioselective C–H functionalization of bicyclo[1.1.1]pentanes. *Nat. Catal.* **2020,** *3*, 351-357.

39.   Fawcett, A.; Pradeilles, J.; Wang, Y.; Mutsuga, T.; Myers, E. L.; Aggarwal, V. K., Photoinduced decarboxylative borylation of carboxylic acids. *Science* **2017,** *357*, 283-286.

40.   VanHeyst, M. D.; Qi, J.; Roecker, A. J.; Hughes, J. M. E.; Cheng, L.; Zhao, Z.; Yin, J., Continuous Flow-Enabled Synthesis of Bench-Stable Bicyclo[1.1.1]pentane Trifluoroborate Salts and Their Utilization in Metallaphotoredox Cross-Couplings. *Org. Lett.* **2020,** *22*, 1648-1654.

41.   Kondo, M.; Kanazawa, J.; Ichikawa, T.; Shimokawa, T.; Nagashima, Y.; Miyamoto, K.; Uchiyama, M., Silaboration of [1.1.1]Propellane: A Storable Feedstock for Bicyclo[1.1.1]pentane Derivatives. *Angew. Chem. Int. Ed.* **2020,** *59*, 1970-1974.

42.   Yang, Y.; Tsien, J.; Hughes, J. M. E.; Peters, B. K.; Merchant, R. R.; Qin, T., An intramolecular coupling approach to alkyl bioisosteres for the synthesis of multisubstituted bicycloalkyl boronates. *Nat. Chem.* **2021,** *13*, 950-955.

43.   Shelp, R. A.; Ciro, A.; Pu, Y.; Merchant, R. R.; Hughes, J. M. E.; Walsh, P. J., Strain-release 2-azaallyl anion addition/borylation of [1.1.1]propellane: synthesis and functionalization of benzylamine bicyclo[1.1.1]pentyl boronates. *Chem. Sci.* **2021,** *12*, 7066-7072.

44.	Yu, S.; Ai, Y.; Hu, L.; Lu, G.; Duan, C.; Ma, Y., Palladium-Catalyzed Stagewise Strain-Release-Driven C-C Activation of Bicyclo[1.1.1]pentanyl Alcohols. *Angew. Chem. Int. Ed. n/a*.

45.	Hoque, M. E.; Hassan, M. M. M.; Chattopadhyay, B., Remarkably Efficient Iridium Catalysts for Directed C(sp^2)–H and C(sp^3)–H Borylation of Diverse Classes of Substrates. *J. Am. Chem. Soc.* **2021,** *143*, 5022-5037.

46.	Ishiyama, T.; Takagi, J.; Ishida, K.; Miyaura, N.; Anastasi, N. R.; Hartwig, J. F., Mild Iridium-Catalyzed Borylation of Arenes. High Turnover Numbers, Room Temperature Reactions, and Isolation of a Potential Intermediate. *J. Am. Chem. Soc.* **2002,** *124*, 390-391.

47.	Hinkes, S. P. A.; Klein, C. D. P., Virtues of Volatility: A Facile Transesterification Approach to Boronic Acids. *Org. Lett.* **2019,** *21*, 3048-3052.

48.	Yang, Y.; Tsien, J.; Ben David, A.; Hughes, J. M. E.; Merchant, R. R.; Qin, T., Practical and Modular Construction of C(sp^3)-Rich Alkyl Boron Compounds. *J. Am. Chem. Soc.* **2021,** *143*, 471-480.

49.	Matteson, D. S.; Kim, G. Y., Asymmetric Alkyldifluoroboranes and Their Use in Secondary Amine Synthesis. *Org. Lett.* **2002,** *4*, 2153-2155.

50.	Tian, Z.; Kass, S. R., Carbanions in the Gas Phase. *Chem. Rev.* **2013,** *113*, 6986-7010.

51.	Boller, T. M.; Murphy, J. M.; Hapke, M.; Ishiyama, T.; Miyaura, N.; Hartwig, J. F., Mechanism of the Mild Functionalization of Arenes by Diboron Reagents Catalyzed by Iridium Complexes. Intermediacy and Chemistry of Bipyridine-Ligated Iridium Trisboryl Complexes. *J. Am. Chem. Soc.* **2005,** *127*, 14263-14278.

52.	Zhong, R.-L.; Sakaki, S., sp^3 C–H Borylation Catalyzed by Iridium(III) Triboryl Complex: Comprehensive Theoretical Study of Reactivity, Regioselectivity, and Prediction of Excellent Ligand. *J. Am. Chem. Soc.* **2019,** *141*, 9854-9866.

53.	Larsen, M. A.; Wilson, C. V.; Hartwig, J. F., Iridium-Catalyzed Borylation of Primary Benzylic C–H Bonds without a Directing Group: Scope, Mechanism, and Origins of Selectivity. *J. Am. Chem. Soc.* **2015,** *137*, 8633-8643.

54.	Huang, G.; Kalek, M.; Liao, R.-Z.; Himo, F., Mechanism, reactivity, and selectivity of the iridium-catalyzed C(sp^3)-H borylation of chlorosilanes. *Chem. Sci.* **2015,** *6*, 1735-1746.

55.	Bär, R. M.; Gross, P. J.; Nieger, M.; Bräse, S., Sodium Bicyclo[1.1.1]pentanesulfinate: A Bench-Stable Precursor for Bicyclo[1.1.1]pentylsulfones and Bicyclo-[1.1.1]pentanesulfonamides. *Chem. Eur. J.* **2020,** *26*, 4242-4245.

56.	Cheng, C.; Hartwig, J. F., Iridium-Catalyzed Silylation of Aryl C–H Bonds. *J. Am. Chem. Soc.* **2015,** *137*, 592-595.

57.	Della, E. W.; Lochert, I. J.; Peruchena, N. M.; Aucar, G. A.; Contreras, R. H., Experimental and theoretical study of substituent effects on 3J(13C1-1H) coupling constants in 1-X-bicyclo[1.1.1]pentanes. *J. Phys. Org. Chem.* **1996,** *9*, 168-178.

58.	McNamee, R. E.; Haugland, M. M.; Nugent, J.; Chan, R.; Christensen, K. E.; Anderson, E. A., Synthesis of 1,3-disubstituted bicyclo[1.1.0]butanes via directed bridgehead functionalization. *Chemical Science* **2021,** *12*, 7480-7485.

59.	Bunker, K. D.; Guo, C.; Grier, M. C.; Hopkins, C. D.; Pinchman, J. R.; Slee, D. H.; Huang, Q.; Kahraman, M. Preparation of bicyclic compounds as analgesics. US20160075654, 2016.

60.	Singleton, D. A.; Thomas, A. A., High-Precision Simultaneous Determination of Multiple Small Kinetic Isotope Effects at Natural Abundance. *J. Am. Chem. Soc.* **1995,** *117*, 9357-9358.

61.	Frisch, M. J.; Trucks, G. W.; Schlegel, H. B.; Scuseria, G. E.; Robb, M. A.; Cheeseman, J. R.; Scalmani, G.; Barone, V.; Petersson, G. A.; Nakatsuji, H.; Li, X.; Caricato, M.; Marenich, A. V.; Bloino, J.; Janesko, B. G.; Gomperts, R.; Mennucci, B.; Hratchian, H. P.; Ortiz, J. V.; Izmaylov, A. F.; Sonnenberg, J. L.; Williams; Ding, F.;

Lipparini, F.; Egidi, F.; Goings, J.; Peng, B.; Petrone, A.; Henderson, T.; Ranasinghe, D.; Zakrzewski, V. G.; Gao, J.; Rega, N.; Zheng, G.; Liang, W.; Hada, M.; Ehara, M.; Toyota, K.; Fukuda, R.; Hasegawa, J.; Ishida, M.; Nakajima, T.; Honda, Y.; Kitao, O.; Nakai, H.; Vreven, T.; Throssell, K.; Montgomery Jr., J. A.; Peralta, J. E.; Ogliaro, F.; Bearpark, M. J.; Heyd, J. J.; Brothers, E. N.; Kudin, K. N.; Staroverov, V. N.; Keith, T. A.; Kobayashi, R.; Normand, J.; Raghavachari, K.; Rendell, A. P.; Burant, J. C.; Iyengar, S. S.; Tomasi, J.; Cossi, M.; Millam, J. M.; Klene, M.; Adamo, C.; Cammi, R.; Ochterski, J. W.; Martin, R. L.; Morokuma, K.; Farkas, O.; Foresman, J. B.; Fox, D. J. *Gaussian 16 Rev. A.03*, Wallingford, CT, 2016.

62. Perdew, J. P.; Burke, K.; Ernzerhof, M., Generalized Gradient Approximation Made Simple. *Phys. Rev. Lett.* **1996,** *77*, 3865-3868.

63. Perdew, J. P.; Burke, K.; Ernzerhof, M., Generalized Gradient Approximation Made Simple [Phys. Rev. Lett. 77, 3865 (1996)]. *Phys. Rev. Lett.* **1997,** *78*, 1396-1396.

64. Adamo, C.; Barone, V., Toward reliable density functional methods without adjustable parameters: The PBE0 model. *J. Chem. Phys.* **1999,** *110*, 6158-6170.

65. Grimme, S.; Ehrlich, S.; Goerigk, L., Effect of the damping function in dispersion corrected density functional theory. *J. Comput. Chem* **2011,** *32*, 1456-1465.

66. Weigend, F.; Ahlrichs, R., Balanced basis sets of split valence, triple zeta valence and quadruple zeta valence quality for H to Rn: Design and assessment of accuracy. *Phys. Chem. Chem. Phys.* **2005,** *7*, 3297-3305.

67. Andrae, D.; Häußermann, U.; Dolg, M.; Stoll, H.; Preuß, H., Energy-adjusted ab initio pseudopotentials for the second and third row transition elements. *Theor. Chim. Acta* **1990,** *77*, 123-141.

68. Schuchardt, K. L.; Didier, B. T.; Elsethagen, T.; Sun, L.; Gurumoorthi, V.; Chase, J.; Li, J.; Windus, T. L., Basis Set Exchange: A Community Database for Computational Sciences. *J. Chem. Inf. Model.* **2007,** *47*, 1045-1052.

69. Pritchard, B. P.; Altarawy, D.; Didier, B.; Gibson, T. D.; Windus, T. L., New Basis Set Exchange: An Open, Up-to-Date Resource for the Molecular Sciences Community. *J. Chem. Inf. Model.* **2019,** *59*, 4814-4820.

70. Feller, D., The role of databases in support of computational chemistry calculations. *J. Comput. Chem* **1996,** *17*, 1571-1586.

71. Marenich, A. V.; Cramer, C. J.; Truhlar, D. G., Universal Solvation Model Based on Solute Electron Density and on a Continuum Model of the Solvent Defined by the Bulk Dielectric Constant and Atomic Surface Tensions. *J. Phys. Chem. B* **2009,** *113*, 6378-6396.

CHAPTER 3 2-Aminophenanthroline Ligands Enable Mild, Undirected, Iridium-Catalyzed Borylation of Alkyl C–H Bonds

3.1 Introduction

The functionalization of C–H bonds creates the potential to modify hydrocarbon chemical feedstocks and conduct late-stage diversification of complex molecules.[1-3] The borylation of C–H bonds is particularly valuable because the boronic ester products are precursors to a wide range of functional groups.[4] Such borylations of aryl C–H bonds catalyzed by iridium complexes with nitrogen-based ligands have been studied intensively because of the mild reaction conditions and high tolerance for auxiliary functional groups. Thus, borylations of C–H bonds have been used for applications from medicine to materials.[5] In contrast, the borylation of unactivated alkyl C–H bonds with iridium catalysts remains under development. Such reactions have required higher temperatures and super-stoichiometric quantities of substrate,[6-12] except for reactions of activated alkyl C–H bonds in cyclopropanes,[13] in methylarenes,[14] or nearby a directing group.[15-29] The photochemical and electrochemical borylations of alkyl C–H bonds occur at mild temperatures but have required high loadings of the substrate or metal.[30-33] These limitations have prevented the widespread adoption of alkyl C–H borylation by synthetic chemists.

334
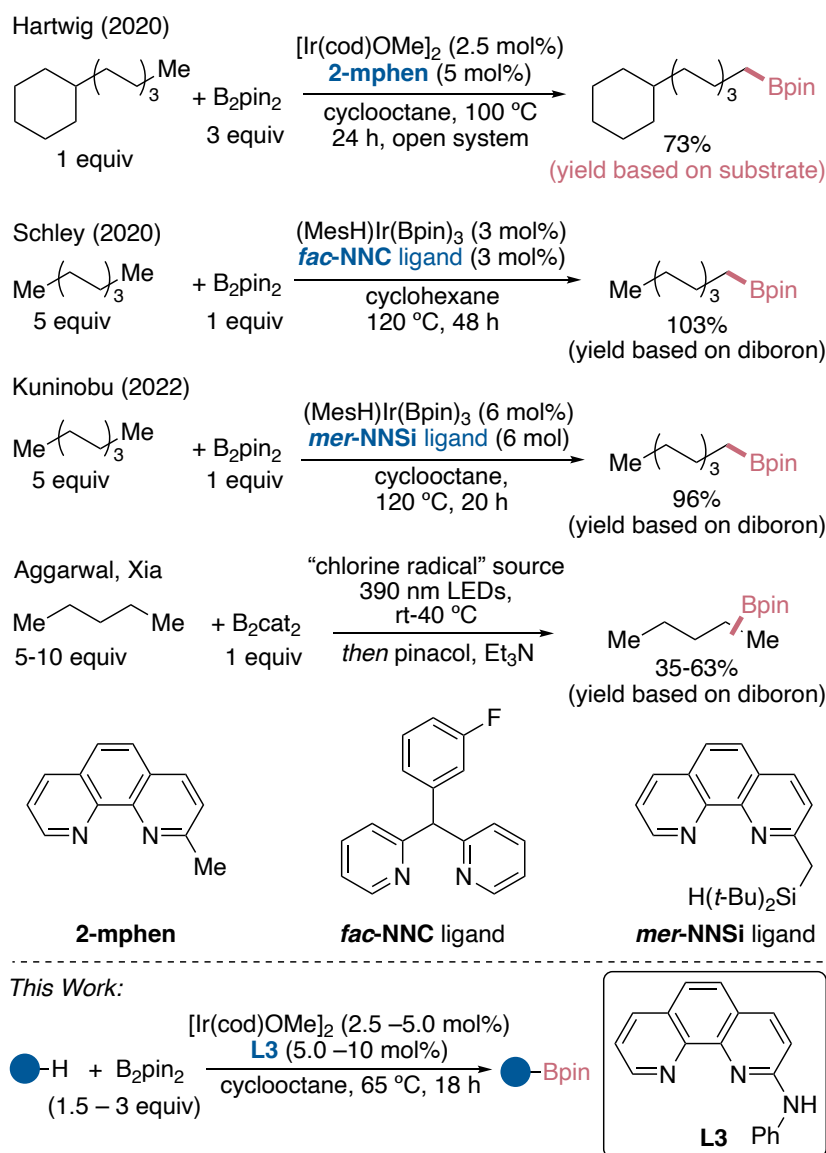
Figure 3.1 Prior reports of undirected borylation of alkyl C–H bonds with limiting or near-limiting quantities of substrate and this work on milder reactions and facile activation with aminophenanthroline ligands.

Recent developments have begun to transform the catalytic undirected borylation of alkyl C–H bonds into an increasingly practical method to access alkyl boronic esters (Figure 3.1). Schley and Kuninobu reported ligands that form complexes that catalyze the borylation of alkyl C–H bonds with higher turnover numbers than were observed previously,[34, 35] but these reactions still occur at relatively high temperatures ($\geq$100 °C) and require super-stoichiometric amounts of substrate.

In parallel, our group discovered that iridium complexes formed from 2-methylphenanthroline (2-mphen) catalyze the borylation of alkyl C–H bonds with higher rates than those observed with phenanthrolines, such as 3,4,7,8-tetramethylphenanthroline (tmphen), used previously for these reactions. The use of 2-mphen enabled the borylations of alkyl C–H bonds to occur with the substrate as the limiting reagent, albeit at 100 °C.[36, 37] A substantial induction period in these reactions was observed and necessitated higher reaction temperatures than are needed for the catalytic cycle and limiting the total amount of active catalyst. Mechanistic experiments implied that slow modification of the 2-methyl substituent, presumably by borylation of one or more C–H bonds, leads to the active catalytic species. We report that the combination of 2-aminophenanthrolines with iridium leads to facile activation of the catalyst at reduced temperature, thus enabling the borylation of alkyl C–H bonds to occur at temperatures below those of any previous catalyst and to occur even at room temperature.
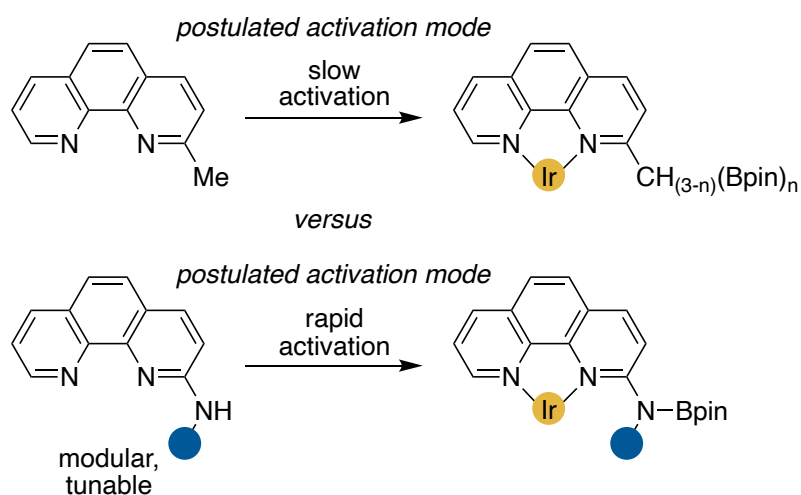
Figure 3.2. Illustration of a possible mode for activation of catalysts containing 2-mphen and design of modular and tunable ligands for more rapid activation.

3.2 Results and Discussion

3.2.1 Reaction Development of the Mild Borylation of Alkyl C–H Bonds

To identify ligands that generate the active catalyst for the borylation of alkyl C–H bonds without an extensive induction period, we studied phenanthrolines containing an amino group in place of a 2-methyl group. This change would enhance modification of the substituent at the 2-position because catalyzed or uncatalyzed borylations of N–H bonds are more rapid than

those of C–H bonds.[38] In addition, 2-aminophenanthrolines are more readily prepared by a modular synthesis than 2-alkylphenanthrolines (Figure 3.2).
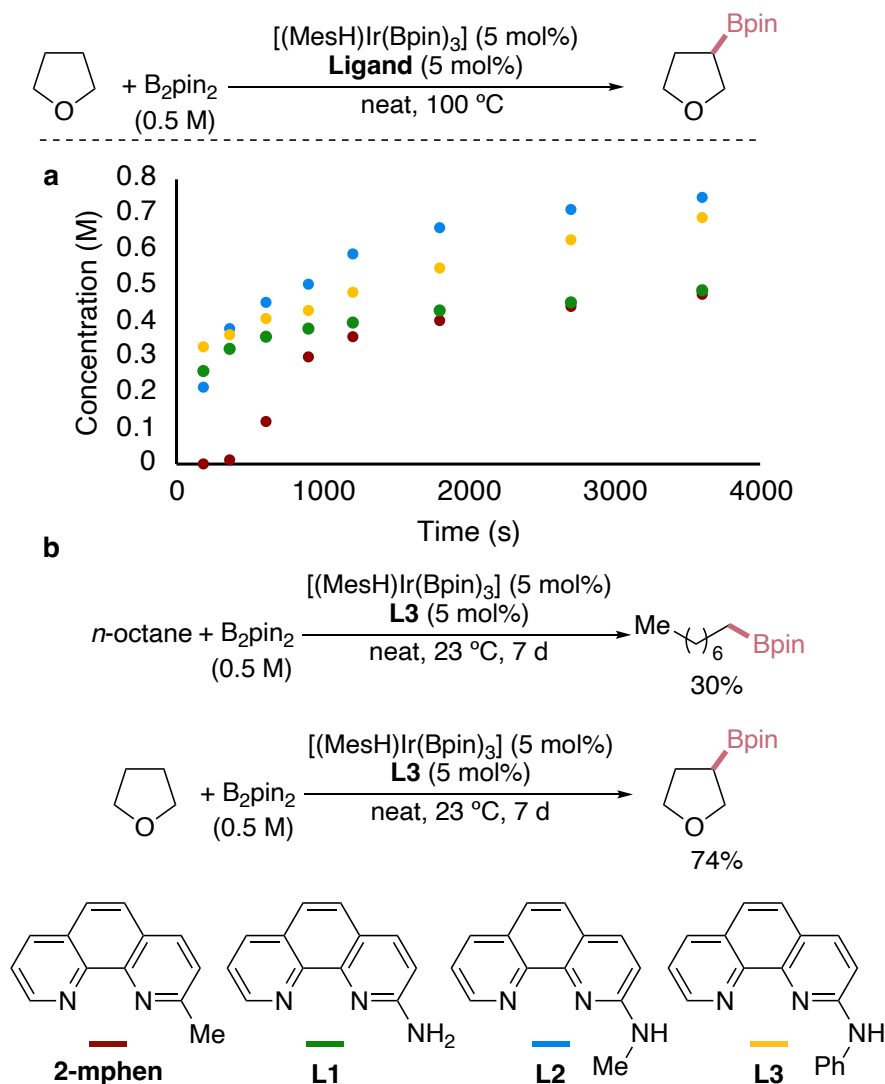
Figure 3.3. Evaluation of the reactivity of 2-aminophenthrolines. Timecourses of the borylation of tetrahydrofuran with either 2-mphen or a variety of 2-aminophenanthrolines at 100 °C.

Thus, we prepared a variety of 2-aminophenanthrolines and tested them for the borylation of neat tetrahydrofuran at 100 °C. In contrast to the borylation of THF catalyzed by Ir complexes of 2-methylphenantholine, the borylations catalyzed by Ir complexes of 2-aminophenanthrolines occurred with little to no induction period (Figure 3.3). The yields of the alkylboronic ester product even exceeded 100%, indicating partial reaction of the HBpin byproduct with THF to form the same 3-boryl-THF.

With the facile generation of the active catalyst, reactions catalyzed by Ir and 2-aminophenanthrolines occurred at lower temperatures. Reactions with limiting quantities of *tert*-butyloctyl ether **1b** as a model substrate in the presence of a series of ligands and metal precatalysts at 65 °C are shown in Table 3.1.

Table 3.1 Reaction development for the catalytic borylation of alkyl C–H bonds under limiting substrate conditions.
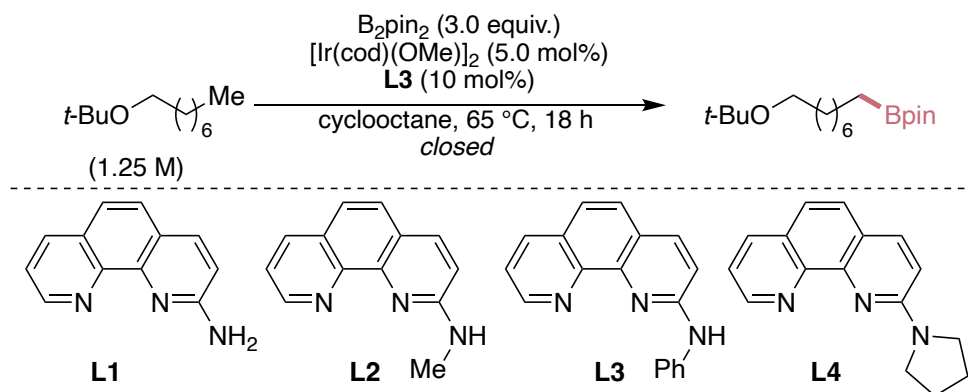
entry	precatalyst (mol%)	variation	yield[a]
1	[Ir(cod)OMe]$_2$ (5)	none	52%
2	[Ir(cod)OMe]$_2$ (2.5)	5 mol% of **L3**, 1.5 equiv of B$_2$pin$_2$	24%
3	[Ir(cod)OMe]$_2$ (5)	100 ºC	39%
4	[Ir(cod)OMe]$_2$ (5)	2-mphen instead of L3	0%
5	[Ir(cod)OMe]$_2$ (5)	**L1** instead of **L3**	6%
6	[Ir(cod)OMe]$_2$ (5)	**L2** instead of **L3**	10%
7	[Ir(cod)OMe]$_2$ (5)	**L4** instead of **L3**	0%
8	none	none	0%
9	[Ir(cod)OMe]$_2$ (5)	no ligand added	0%
10	(MesH)Ir(Bpin)$_3$ (10)	none	53%
11	[Ir(cod)Cl]$_2$ (5)	none	35%
12	[Rh(cod)Cl]$_2$ (5)	none	0%
13	[Ir(cod)OMe]$_2$ (5)	HBpin instead of B$_2$pin$_2$	0%
14	[Ir(cod)OMe]$_2$ (5)	Et$_3$SiBpin instead of B$_2$pin$_2$	0%

[a]Determined by ^{1}H NMR spectroscopy with dibromomethane as the internal standard. MesH = 1,3,5-trimethylbenzene.

These studies showed that the iridium system formed from 2-anilinyl-1,10-phenanthroline (**L3**) and [Ir(cod)OMe]$_2$ catalyzed the borylation of **1b** to form **1a** in good yield with the substrate as the limiting reagent. Varying the metal precursor, boron reagent, or substituent on the amino group did not lead to significant increases in yield (see Figure 3.7-Figure 3.10 for details on the reaction development). In contrast, the reaction with 2-mphen as the ligand gave no product after 18 h at 65 °C. Low yields of the boronic ester were observed from reactions with the parent 2-aminophenanthroline **L1** as ligand. Higher yields, but still lower than with **L3** as ligand, were observed with **L2** as ligand, and no yield was obtained from reactions with the dialkylaminophenanthroline **L4**. Control experiments showed that both **L3** and the iridium precursor were necessary to form the product. Yields for reactions conducted with (MesH)Ir(Bpin)$_3$ as the iridium source were similar to those conducted with the commercially available [Ir(cod)OMe]$_2$.

Under the conditions for the borylation of model substrate **1b**, we explored the scope of the undirected borylation of alkyl C–H bonds (Figure 3.4). The borylations of a variety of substrates occurred smoothly; most occurred with 5 mol% loading of the catalyst with **L3** and 1.5 equivalents of the diboron reagent. Common protecting groups or those with minor modifications to prevent borylation of an aryl C–H bond in the protecting group were tolerated. Alkyl ether **1b** and *N*-methyl amine **2b** underwent borylation at their primary C–H bond. Cyclopropane **3b** and cyclobutane **4b** underwent borylation at secondary C–H bonds within the strained carbocycle, and epoxide **5b** and azetidine **6b** underwent borylation at the most accessible secondary C–H bond on the strained saturated heterocyclic ring. Spirocyclic cyclobutanes, such as **7b** and **8b**, also underwent borylation cleanly, albeit requiring higher catalyst loading and affording lower yields of the product than monosubstituted cyclobutanes, presumably because of steric hinderance. Less strained saturated heterocycles also underwent borylation at the position *β*- to the heteroatom (**9b-12b**). Highly strained bicyclopentane **13b** underwent selective borylation of the bridgehead, tertiary C–H bond.

The mild reaction conditions were conducive to the borylation of complex substrates containing many C–H bonds and functional groups. The fenchol derivative **14b** underwent borylation of the cyclobutane moiety. The cholesterol derivative **15b** underwent borylation of the bicyclopentane moiety. Primary C–H bonds in 6-deoxysugars, such as *L*-fucose (**16b**, **17b**), underwent borylation cleanly and was applied to the synthesis of the corresponding rare *L*-galactose **17c**.[39, 40]

The yields of reactions conducted with **L3** at 65 °C were generally higher than those with 2-mphen at 100 °C in closed vials, which are most easily run on mmol scale. Broadly speaking, these higher yields can be attributed to either improved functional group tolerance, due to the mild conditions, or improved catalyst activity. (See Section 4.1 of the SI for discussions on mass balance of the 2-mphen reactions.) For example, we see less decomposition of the boryl epoxide product in the case of **5a**, and we only see the desired product with **L3** in the cases of **7a** and **8a**. In the case of amide **11a**, we see reduction of the amide to the corresponding amine by the HBpin byproduct when the reaction was run with 2-mphen at 100 ºC.

The high activity and rapid activation of the iridium catalyst containing **L3** was further exemplified by observing the borylation of neat substrates at room temperature (Figure 3.5). To avoid an induction period observed for the borylation of THF at room temperature with [Ir(cod)(OMe)]$_2$ as precursor (Fig. S8), (MesH)Ir(Bpin)$_3$ was used as the Ir source. With this modification, a variety of acyclic and cyclic ethers, amines, and alkanes underwent borylation at room temperature. While long reaction times did maximize conversion to product **9a** a majority of the product formed within 48 hours (62% of the 74% formed after 7 days, see Fig. S8).
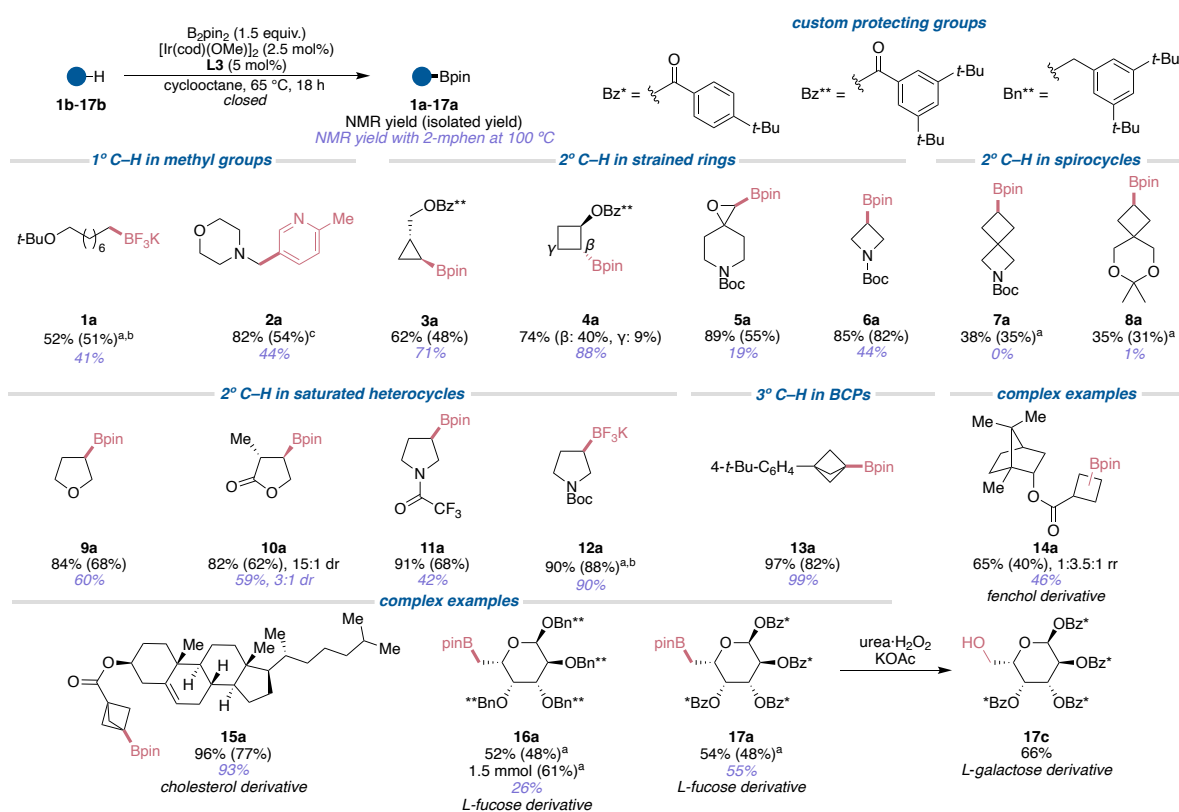
Figure 3.4. Scope of the Borylation of Alkyl C–H Bonds with Limiting Substrate. [a]10 mol% catalyst, 3.0 equiv. B$_2$pin$_2$. [b]Treatment with KF and tartaric acid. [c]One-pot cross-coupling with ArBr in the presence of Pd$_2$(dba)$_3$, QPhos, and CsF.

All these substrates previously required temperatures of 100 °C or higher with Ir catalysts under similar conditions. Other iridium catalysts reported for undirected borylation of alkyl C–H bonds, including those with 3,4,7,8-tetramethyl, 2-silylmethyl and 2-methyl-substituted phenanthroline ligands, as well as 2,2'-dipyridylarylmethane ligands,[9, 34-36] gave 0-1% yields of tetrahydrofuryl product **9a** at room temperature (Fig. S5).
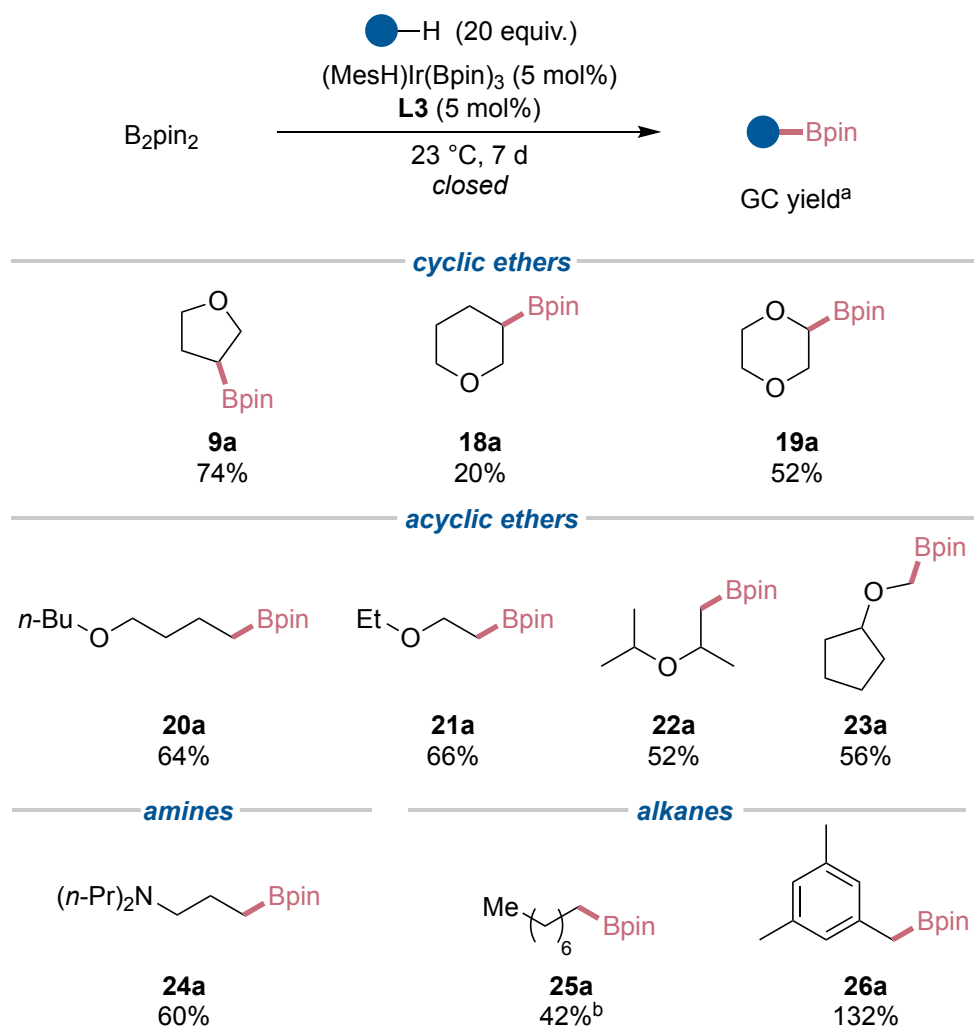
Figure 3.5 Borylation of Alkyl C–H Bonds at Room Temperature. [a] Determined by GC-FID with adamantane as the internal standard. [b] 10 mol% catalyst.

3.2.2 Preliminary Investigation of the Mechanism of the Iridium-Catalyzed Borylation of Alkyl C–H Bonds with Aminophenanthroline Ligands

Preliminary mechanistic insight was gained from a kinetic isotope effect (KIE). The lack of an induction period with **L3** as the ligand allowed an accurate KIE value to be obtained from the initial rates of separate reactions with THF or THF-d_8. A primary KIE of 3.2 ± 0.2 was observed (Fig. 4a, S9), which is consistent with irreversible, rate-limiting cleavage of the C–H bond by the active catalyst.

Initial information on the origin of the high activity of the catalyst generated from **L3** has been obtained. The requirement for an unsubstituted N–H bond in the ligand for reactivity at 65 °C implies that functionalization of the N–H bond occurs under the reaction conditions. The

combination of **L3** and (MesH)Ir(Bpin)$_3$ in the presence of B$_2$pin$_2$ generated a complicated mixture, and clean formation of iridium complexes was hampered by low solubility of **L3** and borylation of the ligand at aryl C–H bonds of the phenanthroline unit, in addition to the N–H bond (Fig. S11). However, reactions with the more soluble **L1** generated an iridium complex that we assigned as (**L5**)Ir(Bpin)$_3$ (see below, Fig. S12), resulting from borylation of the amino group. At 65 °C, the temperature at which the catalytic reaction occurs within hours, this single species evolved into additional complexes, likely resulting from multiple non-selective borylation events on the ligand, that we have not identified (Fig. S13).

The borylation of **L1** with HBpin at room temperature occurred at the N–H moiety in the presence of 1 mol% of (MesH)Ir(Bpin)$_3$ to form the borylamino ligand **L5** (Fig. 4b), whereas the analogous reactions with 2-mphen formed products predominantly from borylation at the 8-position (Fig. S10).

The combination of **L5** and (MesH)Ir(Bpin)$_3$ in the presence of B$_2$pin$_2$ formed a clean iridium species that we assigned as (**L5**)Ir(Bpin)$_3$ on the basis of the ^{1}H NMR spectrum (Fig. 4c, S14). The addition of triphenylphosphite to this complex formed (**L5**)Ir(Bpin)$_3$(P(OPh)$_3$), which was characterized by X-ray diffraction. Complex (**L5**)Ir(Bpin)$_3$ generated *in situ* is competent as a precatalyst for the borylation of neat THF, but with a short induction period (Fig. 4d, S15). Furthermore, the stoichiometric reaction of this complex with THF did not form 3-boryl THF. Thus, more detailed studies are needed to determine how (**L5**)Ir(Bpin)$_3$ converts to the active catalyst, but we suggest that a second borylation occurs to make a ligand more similar in structure to that resulting from the borylation of **L3.** We hypothesize that the phenanthroline ligand in the active catalyst formed from **L3** bears a trisubstituted nitrogen atom with at least one Bpin group, and that this boryl substituent accelerates the oxidative addition of the C–H bond of the substrate, which is the rate-limiting step according to parallel KIE experiments with both ligands that contain and lack a 2-substituent.[9] Detailed studies of the role of this boryl substituent in the oxidative addition step are underway that combine DFT calculations in conjunction with designed ligands that form a discrete active catalyst, and our findings will be reported in due course.
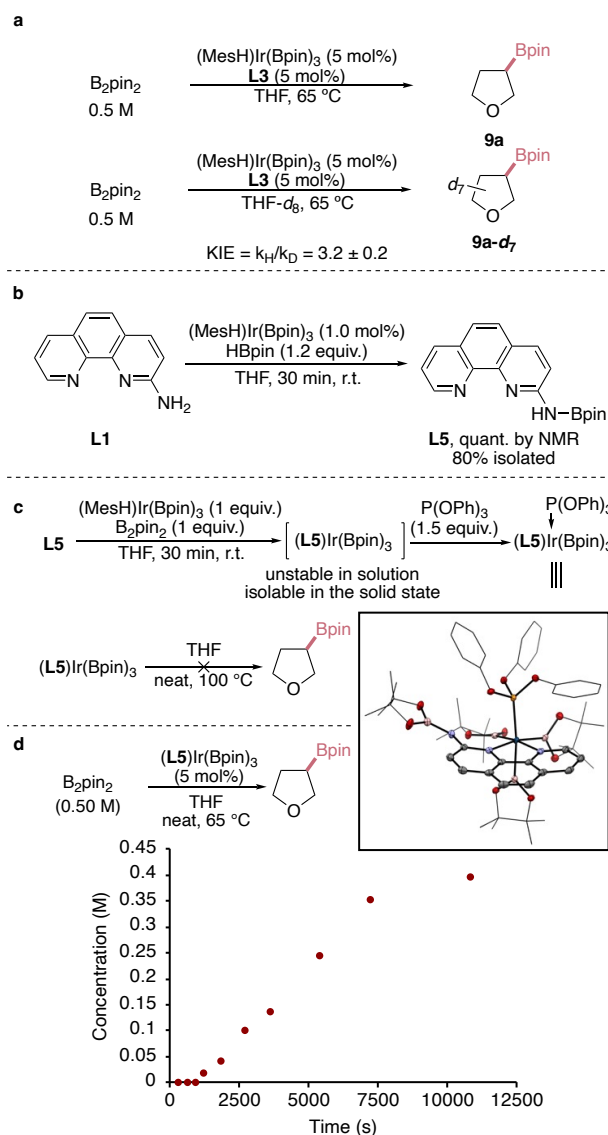
Figure 3.6. Mechanistic Experiments. a) KIE for the borylation of THF. b) Synthesis of *N*-borylated 2-aminophenanthroline **L5**. c) Synthesis of an iridium trisboryl complex containing **L5**. d) Catalytic reactivity of (**L5**)Ir(Bpin)₃.

3.3 Conclusion

In summary, the iridium catalyst containing the 2-anilinophenanthroline **L3** enables the borylation of alkyl C–H bonds under mild conditions with little induction period and with the substrate as the limiting reagent, thereby enhancing the scope and stereoselectivity of the borylation of diverse substrates. Modification of the 2-amino substituent initiates catalytic activity, and many 2-aminophenanthrolines led to Ir catalysts for the borylation of alkyl C–H bonds. This class of tunable ligands puts practical borylation of alkyl C–H bonds within reach. Ongoing efforts seek to understand the identity of the active catalyst and to apply this 2-aminophenanthroline motif to the site-selective borylation of alkyl C–H bonds in synthetic applications.

3.4 Experimental

3.4.1 General Information

Reagents and Solvents

All catalytic reactions were assembled under inert atmosphere in a nitrogen-filled glovebox equipped with an oxygen sensor (working level ≤ 1.0 ppm) and a low temperature refrigeration unit (–35 °C), unless otherwise noted. All other reactions were assembled under inert atmosphere with a Schlenk manifold or a nitrogen glovebox, unless otherwise noted. All reagents and solvents were purchased from commercial sources and used as received, unless otherwise noted. All glassware was flame-dried or dried overnight at 120 °C, allowed to cool under vacuum, and stored in a N_2-atomsphere drybox until use unless otherwise noted. Tetrahydrofuran, toluene, and diethyl ether were purified by passing the degassed solvents (N_2) through a column of activated alumina (solvent purification system purchased from Innovative Technologies, Newburyport, MA). Cyclooctane was degassed by three freeze-pump-thaw cycles and further dried over activated 4 Å molecular sieves. Deuterated solvents were purchased from Cambridge Isotope Laboratories and used as received. See section 2 for the synthesis of ligands and substrates.

Chromatography and Data Analysis

Flash column chromatography was conducted on a Teledyne ISCO Combiflash Rf or Rf+ system, with prepacked RediSep Gold silica gel and C18 columns. All reactions were followed by thin-layer chromatography (TLC) when practical, using Merck Kieselgel 60 F_{254} fluorescent treated silica, which was visualized under UV light when practical, or by staining with a solution of anisaldehyde or phosphomolybdic acid followed by heating.

^{1}H, ^{11}B, ^{13}C, and ^{19}F NMR spectra were recorded on AVQ-400, JEOL-400, AVB-400, AV-500, AV-600, NEO-500, and AV-700 spectrometers. Chemical shifts (δ) are reported in parts per million (ppm), relative to the residual solvent signal. Coupling constants (J) are given in Hertz (Hz), rounded to the nearest 0.1 Hz. The ^{1}H NMR spectra are reported as follows: ppm (multiplicity, coupling constants, number of protons). Abbreviations are as follows: s (singlet), d (doublet), t (triplet), q (quartet), m (multiplet), br (broad). The carbon attached to boron is usually not observed.

High-resolution mass spectral (HRMS) data were obtained from the QB3/Chemistry Mass Spectrometry Facility or the LBNL Catalysis Facility.

Gas Chromatography (GC) was performed on an HP 6890 GC system with an Agilent HP-5 column (25 m × 0.200 mm, 0.33 micron).

Elemental Analyses were conducted at the microanalytical facility at the College of Chemistry at UC Berkeley.

Naming of Compounds

Compound names were generated by ChemDraw 20.0 software (PerkinElmer), following the IUPAC nomenclature.

3.4.2 Synthesis of Ligands and Substrates

The ligands and substrates were obtained from commercial vendors, prepared according to literature procedures, or independently synthesized (see below).

tert-butyloctyl ether (**1b**),[41]   *tert*-butyl azetidine-1-carboxylate (**6b**),[42] *tert*-butyl 2-azaspiro[3.3]heptane-2-carboxylate (**7b**),[43] and 1-(4-(*tert*-butyl)phenyl)bicyclo[1.1.1]pentane (**13b**)[44] were synthesized according to literature precedent. The spectral data of the known compounds were identical to those reported in the literature. All other chemicals were purchased from commercial vendors and used as received, unless otherwise noted.

General Procedure A: Synthesis of 2-Aminophenanthrolines

On the bench, a 4 mL vial was charged with 2-chloro-1,10-phenanthroline (107 mg, 0.500 mmol, 1.00 equiv) and amine (1.50 mmol, 3.00 equiv). A magnetic stir bar and 1 mL of *N*-methyl-2-pyrrolidone (NMP) were added to the vial, and the vial was tightly sealed with a Teflon lined cap. The vial was heated at 120 ºC in a preheated aluminum heating block for 24 h. After cooling to ambient temperature, the mixture was diluted with DCM (5 mL), and 5 mL of 2 M NaOH was added. The layers were separated, and the aqueous layer was extracted with DCM (5 mL x2). The combined organic layers were dried over MgSO$_4$, filtered, and concentrated in vacuo. The crude residue was purified by flash column chromatography to afford the aminophenanthroline product.

General Procedure B: Synthesis of Amides and Esters[45]

On the bench, a 20 mL vial was charged with the carboxylic acid (2.00 mmol, 1.00 equiv), the alcohol or amine (2.00 mmol, 1.00 equiv), and *N*-methylimidazole (345 mg, 4.20 mmol, 2.10 equiv). The mixture was diluted with DCM (4 mL), and a stirbar was added to the solution. The solution was stirred vigorously, and chloro-*N,N,N′,N′*-tetramethylformamidinium hexafluorophosphate (TCFH) (617 mg, 2.20 mmol, 1.10 equiv) was added in one portion. The vial was sealed with a Teflon-lined cap and stirred at room temperature for 24 h. The mixture was diluted with water (10 mL) and DCM (10 mL). The layers were separated, and the aqueous layer was further extracted with DCM (10 mL*2). The combined organic layers were dried over MgSO$_4$, filtered, and concentrated in vacuo. The crude residue was purified by flash column chromatography to afford the amide or ester product.

1,10-phenanthrolin-2-amine (L1)
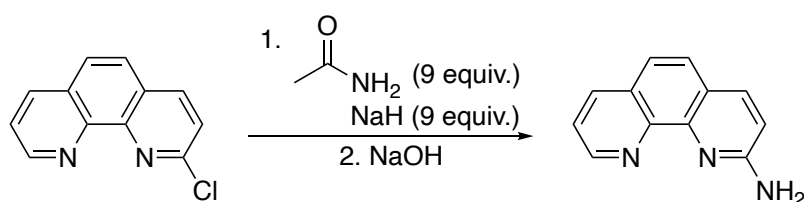
Adapted from literature procedures.[46] A suspension of sodium hydride (2.16 g, 9.00 equiv, 90.0 mmol) (washed with hexanes, powder form) in dry xylene (50 mL) was prepared in a 100 mL round bottom flask in the glovebox. The flask was capped and brought out of the glovebox. Acetamide (5.32 g, 9.00 equiv, 90.0 mmol) was added to the grey suspension, and the flask was fitted with a condenser. The mixture was then carefully heated at 100 °C for 1 h to form a white sludge.

*** Caution *** Gas evolution! Equip the top of the condenser with a well-vented nitrogen inlet.

Then, 2-chloro-1,10-phenanthroline (2.15 g, 1.00 equiv, 10.0 mmol) was added as a solid. The resulting yellow mixture was stirred at 140 °C for 16 h. The reaction mixture was cooled to 100 ºC, then solid sodium hydroxide (6.00 g, 15.0 equiv, 150 mmol), water (20 mL), and MeOH (60 mL) were added to the resulting sludge, and the mixture heated at 100 °C for 24 h. The reaction mixture was cooled to room temperature, and the contents of the flask was transferred to a 250 mL round bottom flask with MeOH. Volatile materials were evaporated in vacuo, and the residue was dry loaded onto silica. The crude material was purified by chromatography on silica gel with 0% → 25% (30% aq. ammonia in MeOH) in ethyl acetate as eluent to afford the title product (1.42 g, 73%) as a faint yellow powder.

1H NMR (600 MHz, CDCl$_3$) δ 9.21 (d, J = 4.2 Hz, 1H), 8.29 (d, J = 8.1 Hz, 1H), 8.09 (d, J = 8.6 Hz, 1H), 7.76 (d, J = 8.6 Hz, 1H), 7.68 – 7.62 (m, 2H), 7.03 (d, J = 8.6 Hz, 1H), 5.39 (bs, 2H). [See spectrum]

13C NMR (151 MHz, CDCl$_3$) δ 157.8, 149.6, 145.6, 145.0, 138.2, 136.0, 129.3, 126.5, 122.8, 122.5, 122.0, 112.1. [See spectrum]

N-methyl-1,10-phenanthrolin-2-amine (L2)

A suspension of sodium hydride (324 mg, 9.00 equiv, 13.5 mmol) (washed with hexanes, powder form) in dry xylene (5 mL) was prepared in a 20 mL flask in the glovebox. The flask was capped and brought out of the glovebox. *N*-methylacetamide (987 mg, 9.00 equiv, 13.5 mmol) was added to the grey suspension and the flask fitted with a condenser. The mixture was then carefully heated at 100 °C for 1 h to form a white sludge.
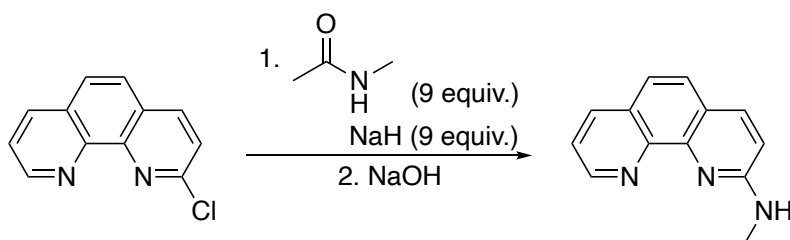
*** Caution *** Gas evolution! Equip the top of the condenser with a well-vented nitrogen inlet.

Then 2-chloro-1,10-phenanthroline (322 mg, 1.00 equiv, 1.50 mmol) was added as a solid. The resulting yellow mixture was stirred at 140 °C for 16 h. The reaction mixture was cooled to 100 °C, then solid sodium hydroxide (900 mg, 15.0 equiv, 22.5 mmol), water (2 mL), and MeOH (6 mL) were added to the resulting sludge, and the mixture heated at 100 °C for 24 h. The reaction mixture was cooled to room temperature, and the contents of the flask was transferred to a 50 mL round bottom flask with MeOH. Volatile materials were evaporated in vacuo, and the residue was dry loaded onto silica. The crude material was purified by chromatography on silica gel with 0% → 25% (30% aq. ammonia in MeOH) in ethyl acetate as eluent to afford the product *N*-methyl-1,10-phenanthrolin-2-amine (100 mg, 30%) as a faint yellow powder.

^{1}H NMR (600 MHz, CDCl$_3$) δ 9.22 (dd, J = 4.3, 1.8 Hz, 1H), 8.29 (dd, J = 8.0, 1.8 Hz, 1H), 8.13 (d, J = 8.7 Hz, 1H), 7.76 (d, J = 8.6 Hz, 1H), 7.65 (dd, J = 8.0, 4.3 Hz, 1H), 7.59 (d, J = 8.6 Hz, 1H), 6.99 (d, J = 8.7 Hz, 1H), 5.56 (bs, 1H), 3.25 (d, J = 4.4 Hz, 3H). [See spectrum]

^{13}C NMR (151 MHz, CDCl$_3$) δ 159.1, 149.4, 146.1, 145.2, 138.1, 136.0, 129.5, 126.7, 122.4, 122.4, 121.2, 108.8, 29.6. [See spectrum]

HRMS (*m/z*): (ESI+) calc'd for C$_{13}$H$_{12}$N$_3$ [M+H]$^+$: 210.1026, found: 210.1027.

N-phenyl-1,10-phenanthrolin-2-amine (L3)
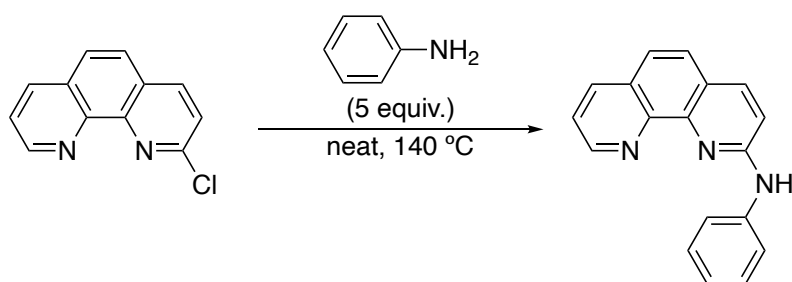
To a 20 mL vial equipped with a stirbar was added 2-chloro-1,10-phenanthroline (1.07 g, 1.00 equiv, 5.00 mmol) and aniline (2.33 g, 5.00 equiv, 25.0 mmol). The vial was capped tightly with a Teflon-lined cap, and the mixture was heated at 140 ºC for 48 h. The reaction mixture was cooled to room temperature, diluted with DCM (50 mL), and 2 M NaOH (50 mL) was added. The layers were separated, and the aqueous layer was extracted with DCM (100 mL x3), and the combined organic layers were dried over MgSO$_4$, filtered, and concentrated in vacuo. The crude material was purified by chromatography on silica gel with 0% → 30% (30% aq. ammonia in MeOH) in ethyl acetate as eluent to afford the title product (901 mg, 67%) as an off-white powder.

^{1}H NMR (600 MHz, CDCl$_3$) δ 9.17 (dd, J = 4.3, 1.7 Hz, 1H), 8.24 (dd, J = 8.1, 1.8 Hz, 1H), 8.07 (d, J = 8.8 Hz, 1H), 7.72 (d, J = 8.6 Hz, 1H), 7.64 – 7.58 (m, 2H), 7.54 (bs, 1H), 7.47 – 7.37 (m, 5H), 7.19 (tt, J = 7.1, 1.3 Hz, 1H). [See spectrum]

^{13}C NMR (151 MHz, CDCl$_3$) δ 155.8, 149.7, 146.1, 145.2, 140.1, 138.2, 136.2, 129.7, 129.4, 126.5, 124.1, 123.6, 122.8, 122.4, 121.8, 110.3. [See spectrum]

HRMS (*m/z*): (ESI+) calc'd for C$_{18}$H$_{14}$N$_3$ [M+H]$^+$: 272.1182, found: 272.1183.

2-(pyrrolidin-1-yl)-1,10-phenanthroline (L4)
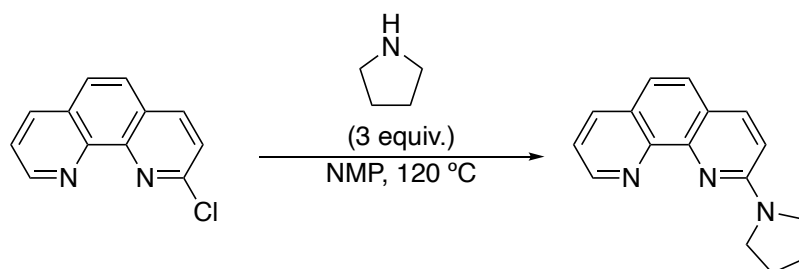
Prepared according to General Procedure A.

(901 mg, 67%) as an off-white powder.

¹H NMR (500 MHz, CDCl$_3$) δ 9.14 (dd, J = 4.3, 1.8 Hz, 1H), 8.18 (d, J = 8.1 Hz, 1H), 7.97 (d, J = 8.9 Hz, 1H), 7.65 (d, J = 8.6 Hz, 1H), 7.54 (dd, J = 8.1, 4.3 Hz, 1H), 7.46 (d, J = 8.6 Hz, 1H), 6.87 (d, J = 8.8 Hz, 1H), 3.82 (bs, 4H), 2.11 (bs, 4H). [See spectrum]

¹³C NMR (101 MHz, CDCl$_3$) δ 156.6, 149.3, 146.3, 145.4, 137.4, 136.2, 129.6, 126.9, 122.2, 121.6, 120.5, 110.4, 47.3, 29.9, 25.8. [See spectrum]

HRMS (*m/z*): (ESI+) calc'd for C$_{16}$H$_{16}$N$_3$ [M+H]$^+$: 250.1339, found: 250.1341.

N-(4,4,5,5-tetramethyl-1,3,2-dioxaborolan-2-yl)-1,10-phenanthrolin-2-amine (L5)
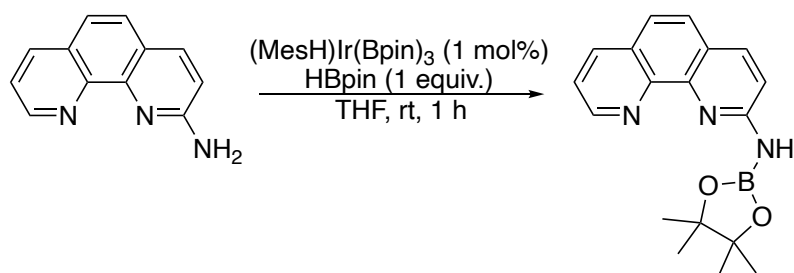
(MesH)Ir(Bpin)$_3$ (6.93 mg, 1.00 mol%, 10.0 µmol) and 1,10-phenanthrolin-2-amine (195 mg, 1.00 equiv, 1.00 mmol) were weighed into a 20 mL vial in the glovebox. Then, THF (2 mL) and HBpin (128 mg, 1.00 equiv, 500 µmol) were added. A stirbar was introduced, and the mixture was stirred vigorously, with the slurry quickly becoming homogenous. The reaction was stirred for 1 h at room temperature. All volatile materials were evaporated, and the residue was resuspended in diethyl ether with stirring for 10 min. The mixture was filtered over a fine frit and washed with pentanes to afford the title compound (258 mg, 80%) as a beige powder.

¹H NMR (500 MHz, CDCl$_3$) δ 9.26 (dd, J = 4.3, 1.7 Hz, 1H), 8.33 (dd, J = 8.1, 1.8 Hz, 1H), 8.20 (d, J = 8.7 Hz, 1H), 7.98 (d, J = 8.7 Hz, 1H), 7.83 (d, J = 8.7 Hz, 1H), 7.74 – 7.66 (m, 2H), 6.41 (s, 1H), 1.47 (s, 12H). [See spectrum]

¹³C NMR (126 MHz, CDCl$_3$) δ 156.5, 149.7, 145.4, 145.3, 138.1, 136.1, 129.2, 126.5, 124.2, 123.0, 122.6, 114.4, 83.5, 24.8. [See spectrum]

¹¹B NMR (160 MHz, CDCl$_3$) δ 24.4. [See spectrum]

HRMS (m/z): (ESI+) calc'd for C$_{18}$H$_{21}$O$_2$N$_3$B [M+H]$^+$: 322.1721, found: 322.1721.

N-cyclohexyl-1,10-phenanthrolin-2-amine (L6)
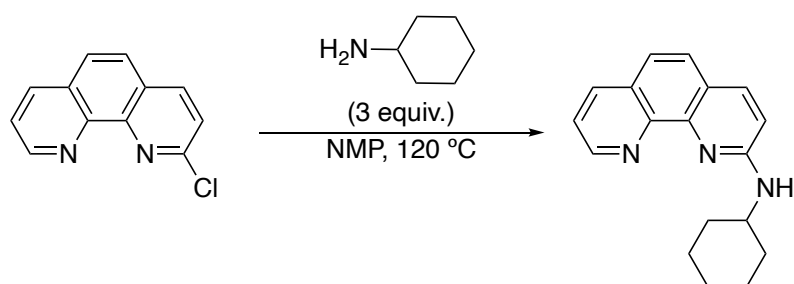
Prepared according to General Procedure A on a 0.50 mmol scale. The crude material was purified by chromatography on silica gel with 0% → 30% (30% aq. ammonia in MeOH) in ethyl acetate as eluent to afford the title product (96 mg, 69%) as an faintly orange powder.

^{1}H NMR (600 MHz, CDCl$_3$) δ 9.12 (dd, J = 4.3, 1.8 Hz, 1H), 8.19 (dd, J = 8.1, 1.8 Hz, 1H), 8.02 (d, J = 8.8 Hz, 1H), 7.65 (d, J = 8.6 Hz, 1H), 7.56 (dd, J = 8.0, 4.3 Hz, 1H), 7.49 (d, J = 8.6 Hz, 1H), 6.91 (d, J = 8.8 Hz, 1H), 5.60 (s, 1H), 3.60 (dtd, J = 13.5, 9.3, 3.8 Hz, 1H), 2.14 (dd, J = 13.1, 4.0 Hz, 2H), 1.86 (dt, J = 13.4, 4.1 Hz, 2H), 1.71 (dt, J = 13.1, 3.9 Hz, 1H), 1.52 – 1.43 (m, 2H), 1.43 – 1.28 (m, 4H). [See spectrum]

^{13}C NMR (151 MHz, CDCl$_3$) δ 157.6, 149.4, 146.4, 145.1, 138.1, 136.0, 129.4, 126.6, 122.4, 122.2, 120.9, 108.7, 51.0, 33.5, 25.8, 24.9. [See spectrum]

HRMS (*m/z*): (ESI+) calc'd for C$_{18}$H$_{20}$N$_3$ [M+H]$^+$: 278.1652, found: 278.1650.

N-(cyclopropylmethyl)-1,10-phenanthrolin-2-amine (L7)

Prepared according to General Procedure A on 0.50 mmol scale. The crude material was purified by chromatography on silica gel with 0% → 30% (30% aq. ammonia in MeOH) in ethyl acetate as eluent to afford the title product (90 mg, 72%) as an off-white powder.

^{1}H NMR (500 MHz, CDCl$_3$) δ 9.23 (dd, J = 4.3, 1.8 Hz, 1H), 8.29 (dd, J = 8.1, 1.8 Hz, 1H), 8.12 (d, J = 8.8 Hz, 1H), 7.75 (d, J = 8.7 Hz, 1H), 7.66 (dd, J = 8.1, 4.3 Hz, 1H), 7.60 (d, J = 8.6 Hz, 1H), 6.99 (d, J = 8.8 Hz, 1H), 5.75 (s, 1H), 3.44 (dd, J = 7.0, 5.3 Hz, 2H), 1.35 – 1.24 (m, 1H), 0.76 – 0.67 (m, 2H), 0.45 (dt, J = 5.9, 4.6 Hz, 2H). [See spectrum]

^{13}C NMR (126 MHz, CDCl$_3$) δ 158.2, 149.4, 146.1, 145.2, 138.2, 136.0, 129.5, 126.7, 122.4, 122.4, 121.1, 108.9, 47.6, 11.0, 3.6. [See spectrum]

HRMS (*m/z*): (ESI+) calc'd for C$_{16}$H$_{16}$N$_3$ [M+H]$^+$: 250.1339, found: 250.1341.
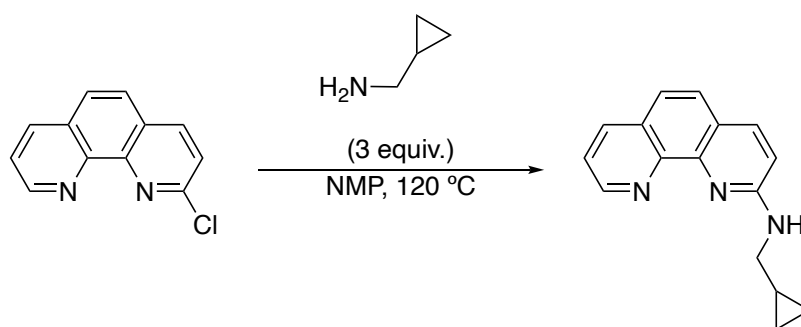
_N_-isobutyl-1,10-phenanthrolin-2-amine (L8)

Prepared according to General Procedure A on 0.50 mmol scale. The crude material was purified by chromatography on silica gel with 0% → 30% (30% aq. ammonia in MeOH) in ethyl acetate as eluent to afford the title product (89 mg, 71%) as an off-white powder.

¹H NMR (500 MHz, CDCl₃) δ 9.13 (dd, J = 4.3, 1.8 Hz, 1H), 8.20 (dd, J = 8.0, 1.8 Hz, 1H), 8.03 (d, J = 8.8 Hz, 1H), 7.66 (d, J = 8.6 Hz, 1H), 7.56 (dd, J = 8.1, 4.3 Hz, 1H), 7.50 (d, J = 8.6 Hz, 1H), 6.91 (d, J = 8.8 Hz, 1H), 5.62 (bs, 1H), 3.27 (t, J = 6.3 Hz, 2H), 2.01 (dp, J = 13.4, 6.7 Hz, 1H), 1.10 (d, J = 6.7 Hz, 6H). [See spectrum]

¹³C NMR (126 MHz, CDCl₃) δ 158.6, 149.4, 146.2, 145.1, 138.2, 136.0, 129.5, 126.7, 122.4, 122.3, 121.0, 108.5, 50.6, 28.8, 20.6. [See spectrum]

HRMS (_m/z_): (ESI+) calc'd for $C_{16}H_{18}N_3$ [M+H]⁺: 252.1495, found: 252.1497.
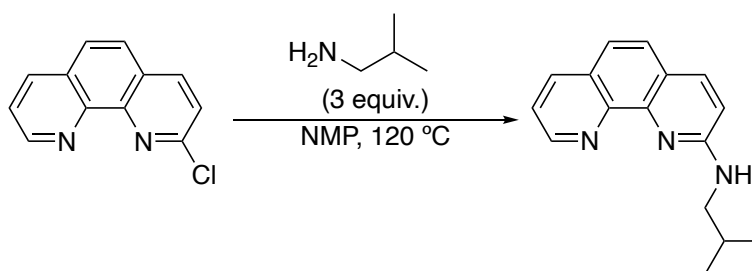
N-isopentyl-1,10-phenanthrolin-2-amine (L9)

Prepared according to General Procedure A on 0.50 mmol scale. The crude material was purified by chromatography on silica gel with 0% → 30% (30% aq. ammonia in MeOH) in ethyl acetate as eluent to afford the title product (85 mg, 64%) as an off-white powder.

^{1}H NMR (500 MHz, CDCl$_3$) δ 9.13 (dd, J = 4.3, 1.7 Hz, 1H), 8.20 (dd, J = 8.1, 1.7 Hz, 1H), 8.04 (d, J = 8.7 Hz, 1H), 7.66 (d, J = 8.6 Hz, 1H), 7.56 (dd, J = 8.1, 4.3 Hz, 1H), 7.50 (d, J = 8.5 Hz, 1H), 6.91 (d, J = 8.7 Hz, 1H), 5.49 (s, 1H), 3.49 – 3.42 (m, 2H), 1.84 (dp, J = 13.4, 6.7 Hz, 1H), 1.64 (q, J = 7.1 Hz, 2H), 1.02 (d, J = 6.6 Hz, 6H). [See spectrum]

^{13}C NMR (126 MHz, CDCl$_3$) δ 158.4, 149.4, 146.2, 145.1, 138.2, 136.0, 129.5, 126.7, 122.4, 122.5, 121.1, 108.6, 41.0, 38.7, 25.9, 22.7. [See spectrum]

HRMS (*m/z*): (ESI+) calc'd for C$_{17}$H$_{20}$N$_3$ [M+H]$^+$: 266.1652, found: 266.1653.

N-benzyl-1,10-phenanthrolin-2-amine (L10)

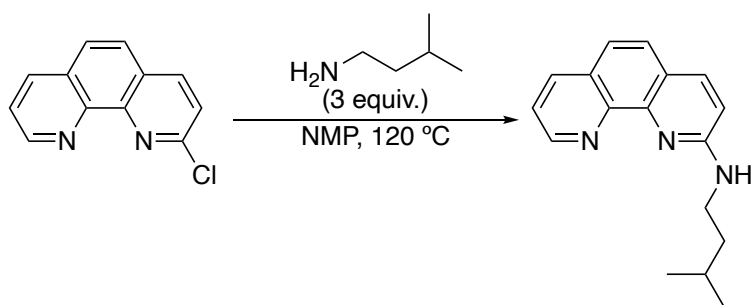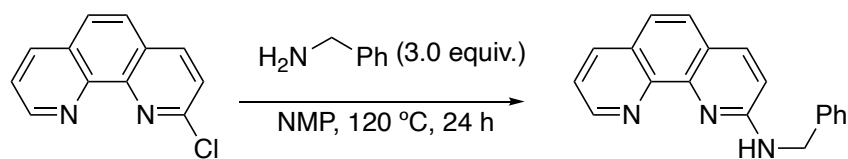Prepared according to General Procedure A on 0.50 mmol scale. The crude material was purified by chromatography on silica gel with 0% → 25% (30% aq. ammonia in MeOH) in ethyl acetate as eluent to afford the title product (102 mg, 72%) as an off-white powder.

¹H NMR (600 MHz, CDCl₃) δ 9.24 (dd, J = 4.3, 1.8 Hz, 1H), 8.30 (dd, J = 8.1, 1.8 Hz, 1H), 8.09 (d, J = 8.7 Hz, 1H), 7.75 (d, J = 8.6 Hz, 1H), 7.67 (dd, J = 8.1, 4.3 Hz, 1H), 7.61 (d, J = 8.6 Hz, 1H), 7.56 (d, J = 6.9 Hz, 2H), 7.48 (t, J = 7.6 Hz, 2H), 7.42 (d, J = 7.4 Hz, 1H), 6.00 (bs, 1H), 4.83 (d, J = 5.9 Hz, 2H). [See spectrum]

¹³C NMR (151 MHz, CDCl₃) δ 158.2, 149.5, 146.1, 145.2, 138.7, 138.2, 136.0, 129.5, 128.8, 127.5, 127.4, 126.7, 122.7, 122.5, 121.4, 109.1, 46.9. [See spectrum]

HRMS (m/z): (ESI+) calc'd for $C_{19}H_{16}N_3$ [M+H]⁺: 286.1339, found: 286.1340.

N-(4-methoxybenzyl)-1,10-phenanthrolin-2-amine (L11)

Prepared according to General Procedure A on 0.50 mmol scale. The crude material was purified by chromatography on silica gel with 0% → 30% (30% aq. ammonia in MeOH) in ethyl acetate as eluent to afford the title product (55 mg, 35%) as an off-white powder.

¹H NMR (500 MHz, CDCl₃) δ 9.24 (dd, J = 4.3, 1.8 Hz, 1H), 8.31 (dd, J = 8.1, 1.8 Hz, 1H), 8.10 (d, J = 8.7 Hz, 1H), 7.76 (d, J = 8.6 Hz, 1H), 7.67 (dd, J = 8.1, 4.3 Hz, 1H), 7.62 (d, J = 8.6 Hz, 1H), 7.48 (d, J = 8.6 Hz, 2H), 7.02 (d, J = 8.7 Hz, 2H), 6.97 (d, J = 8.8 Hz, 1H), 5.99 (s, 1H), 4.76 (d, J = 5.7 Hz, 2H), 3.94 (s, 3H). [See spectrum]

¹³C NMR (126 MHz, CDCl₃) δ 159.1, 158.1, 149.5, 145.1, 138.2, 136.0, 130.6, 129.5, 128.7, 126.7, 122.6, 122.5, 121.4, 114.2, 109.2, 55.4, 46.4. [See spectrum]

HRMS (m/z): (ESI+) calc'd for $C_{20}H_{18}N_3O$ [M+H]⁺: 316.1444, found: 316.1442.
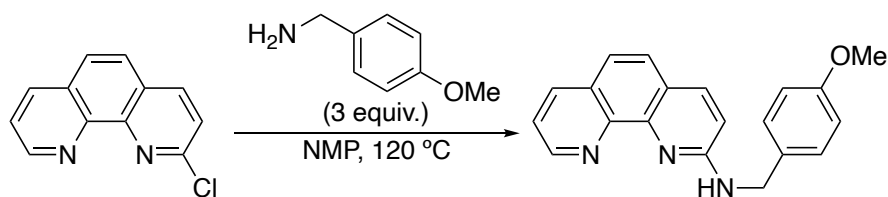
N-phenethyl-1,10-phenanthrolin-2-amine (L12)

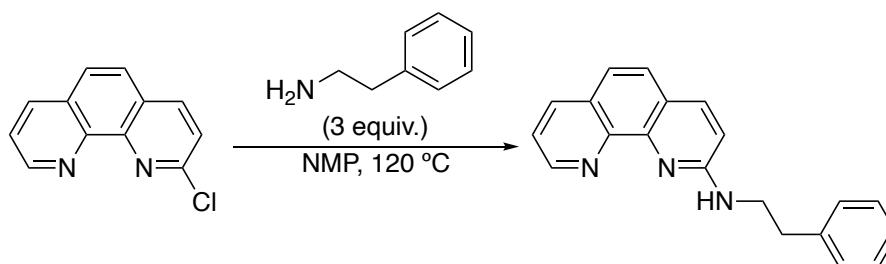
Prepared according to General Procedure A on 0.50 mmol scale. The crude material was purified by chromatography on silica gel with 0% → 30% (30% aq. ammonia in MeOH) in ethyl acetate as eluent to afford the title product (128 mg, 86%) as an off-white powder.

¹H NMR (500 MHz, CDCl$_3$) δ 9.12 (dd, J = 4.3, 1.7 Hz, 1H), 8.18 (dd, J = 8.1, 1.8 Hz, 1H), 8.01 (d, J = 8.7 Hz, 1H), 7.65 (d, J = 8.6 Hz, 1H), 7.55 (dd, J = 8.1, 4.3 Hz, 1H), 7.49 (d, J = 8.6 Hz, 1H), 7.39 – 7.24 (m, 5H), 6.88 (d, J = 8.7 Hz, 1H), 5.51 (s, 1H), 3.78 (q, J = 6.7 Hz, 2H), 3.04 (t, J = 7.1 Hz, 2H). [See spectrum]

¹³C NMR (126 MHz, CDCl$_3$) δ 158.1, 149.5, 146.1, 145.2, 138.9, 138.2, 136.0, 129.5, 129.0, 128.8, 126.7, 126.7, 122.5, 122.4, 121.3, 109.0, 44.0, 36.1. [See spectrum]

HRMS (m/z): (ESI+) calc'd for C$_{20}$H$_{18}$N$_3$ [M+H]$^+$: 300.1495, found: 300.1498.

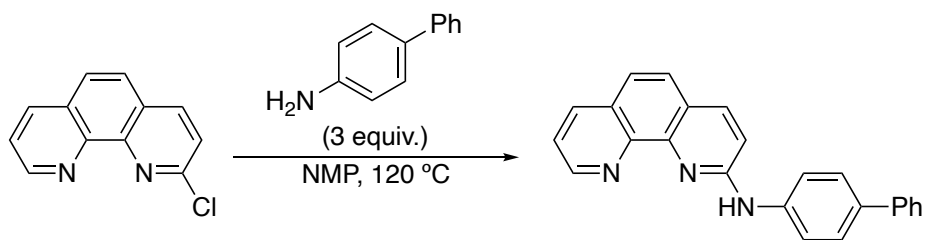**N-([1,1'-biphenyl]-4-yl)-1,10-phenanthrolin-2-amine (L13)**

Prepared according to General Procedure A on 0.50 mmol scale. The crude material was purified by chromatography on silica gel with 0% → 30% (30% aq. ammonia in MeOH) in ethyl acetate as eluent to afford the title product (96 mg, 55%) as an off-white powder.

^{1}H NMR (600 MHz, CDCl$_3$) δ 9.19 (dd, J = 4.3, 1.8 Hz, 1H), 8.26 (dd, J = 8.1, 1.8 Hz, 1H), 8.11 (d, J = 8.8 Hz, 1H), 7.73 (d, J = 8.6 Hz, 1H), 7.70 – 7.57 (m, 7H), 7.52 – 7.45 (m, 5H), 7.39 (t, J = 7.4 Hz, 1H). [See spectrum]

^{13}C NMR (151 MHz, CDCl$_3$) δ 155.5, 149.8, 145.9, 145.1, 140.7, 139.4, 138.4, 136.9, 136.1, 129.5, 128.9, 128.3, 127.2, 126.9, 126.5, 123.7, 122.8, 122.6, 121.7, 110.6. [See spectrum]

HRMS (*m/z*): (ESI+) calc'd for C$_{24}$H$_{18}$N$_3$ [M+H]$^+$: 348.1495, found: 348.1497.
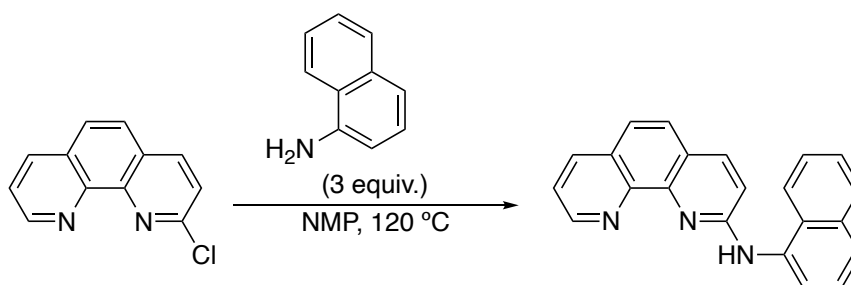
_N_-(naphthalen-1-yl)-1,10-phenanthrolin-2-amine (L14)

Prepared according to General Procedure A on 0.50 mmol scale. The crude material was purified by chromatography on silica gel with 0% → 30% (30% aq. ammonia in MeOH) in ethyl acetate as eluent to afford the title product (118 mg, 73%) as a brown powder.

^{1}H NMR (600 MHz, CDCl$_3$) δ 9.21 (dd, J = 4.3, 1.7 Hz, 1H), 8.26 (dd, J = 8.1, 1.8 Hz, 1H), 8.23 (d, J = 7.4 Hz, 1H), 7.97 (t, J = 9.3 Hz, 1H), 7.83 (d, J = 8.2 Hz, 1H), 7.70 (d, J = 8.6 Hz, 1H), 7.66 – 7.51 (m, 7H), 7.04 (d, J = 8.8 Hz, 1H). [See spectrum]

^{13}C NMR (151 MHz, CDCl$_3$) δ 157.4, 149.8, 146.0, 145.2, 138.2, 136.2, 135.8, 134.9, 130.0, 129.5, 128.6, 126.7, 126.6, 126.4, 126.0, 123.5, 122.8, 122.7, 122.3, 121.6, 110.6. [See spectrum]

HRMS (_m/z_): (ESI+) calc'd for C$_{22}$H$_{16}$N$_3$ [M+H]$^+$: 322.1339, found: 322.1335.
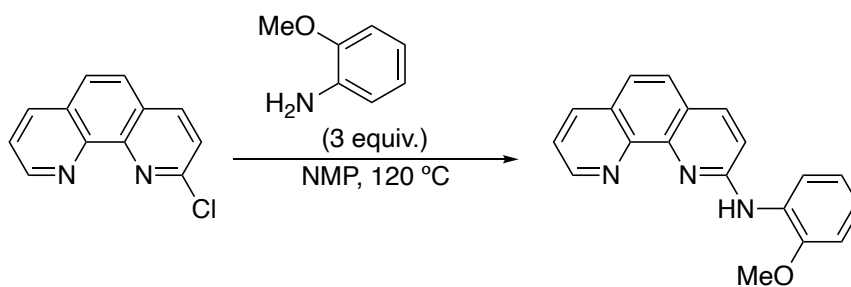
N-(2-methoxyphenyl)-1,10-phenanthrolin-2-amine (L15)

Prepared according to General Procedure A on 0.50 mmol scale. The crude material was purified by chromatography on silica gel with 0% → 30% (30% aq. ammonia in MeOH) in ethyl acetate as eluent to afford the title product (74 mg, 49%) as an off-white powder.

^{1}H NMR (600 MHz, CDCl$_3$) δ 9.19 (dd, J = 4.3, 1.7 Hz, 1H), 8.24 (dd, J = 8.1, 1.8 Hz, 1H), 8.07 (d, J = 8.8 Hz, 1H), 7.74 – 7.69 (m, 2H), 7.63 – 7.57 (m, 2H), 7.43 (d, J = 8.7 Hz, 1H), 7.11 (td, J = 7.7, 1.7 Hz, 1H), 7.07 (td, J = 7.6, 1.6 Hz, 1H), 7.00 (dd, J = 7.9, 1.6 Hz, 1H), 3.93 (s, 3H). [See spectrum]

^{13}C NMR (151 MHz, CDCl$_3$) δ 155.2, 150.3, 149.8, 146.1, 145.4, 138.0, 136.1, 129.8, 129.4, 126.5, 123.6, 123.2, 122.6, 122.4, 121.0, 119.5, 111.3, 111.0, 55.7. [See spectrum]

HRMS (m/z): (ESI+) calc'd for C$_{19}$H$_{16}$N$_3$O [M+H]$^+$: 302.1288, found: 302.1289.
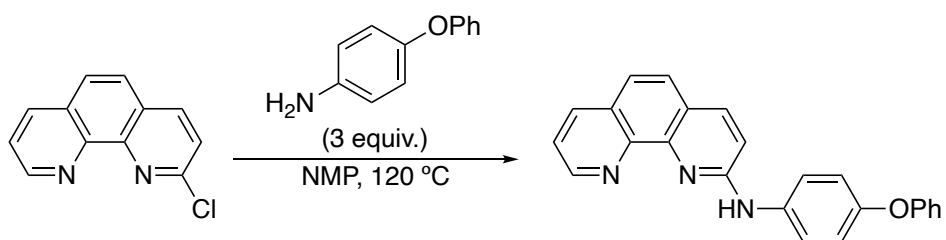
N-(4-phenoxyphenyl)-1,10-phenanthrolin-2-amine (L16)

Prepared according to General Procedure A on 0.50 mmol scale. The crude material was purified by chromatography on silica gel with 0% → 30% (30% aq. ammonia in MeOH) in ethyl acetate as eluent to afford the title product (137 mg, 75%) as a brown powder.

^{1}H NMR (600 MHz, CDCl$_3$) δ 9.16 (dd, J = 4.3, 1.7 Hz, 1H), 8.23 (dd, J = 8.1, 1.7 Hz, 1H), 8.05 (d, J = 8.8 Hz, 1H), 7.70 (d, J = 8.6 Hz, 1H), 7.62 – 7.56 (m, 2H), 7.45 (s, 1H), 7.41 – 7.35 (m, 4H), 7.28 (d, J = 8.8 Hz, 1H), 7.14 (t, J = 7.4 Hz, 1H), 7.09 (td, J = 8.7, 1.7 Hz, 4H). [See spectrum]

^{13}C NMR (151 MHz, CDCl$_3$) δ 157.6, 156.2, 153.9, 149.7, 146.0, 145.2, 138.3, 136.1, 135.5, 129.9, 129.5, 126.5, 124.2, 123.5, 123.3, 122.7, 122.3, 120.3, 118.7, 110.1. [See spectrum]

HRMS (m/z): (ESI+) calc'd for C$_{24}$H$_{18}$N$_3$O [M+H]$^+$: 364.1444, found: 364.1446.
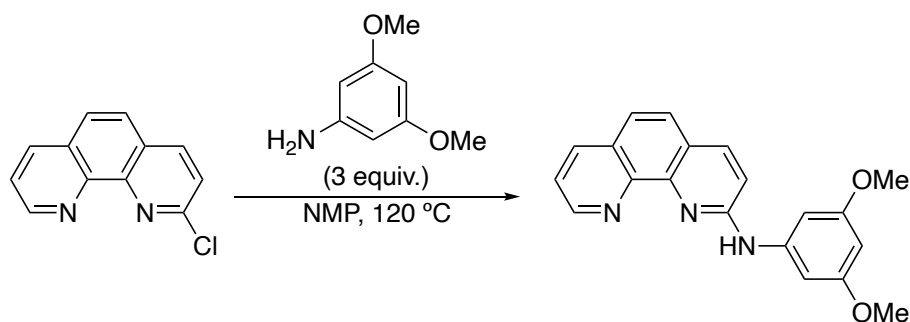
N-(3,5-dimethoxyphenyl)-1,10-phenanthrolin-2-amine (L17)

Prepared according to General Procedure A on 0.50 mmol scale. The crude material was purified by chromatography on silica gel with 0% → 30% (30% aq. ammonia in MeOH) in ethyl acetate as eluent to afford the title product (103 mg, 61%) as a white powder.

^{1}H NMR (600 MHz, CDCl$_3$) δ 9.22 (dd, J = 4.4, 1.7 Hz, 1H), 8.32 (dd, J = 8.1, 1.8 Hz, 1H), 8.15 (d, J = 8.7 Hz, 1H), 7.79 (d, J = 8.6 Hz, 1H), 7.74 – 7.56 (m, 3H), 7.53 (d, J = 8.8 Hz, 1H), 6.80 (d, J = 2.2 Hz, 2H), 6.38 (s, 1H), 3.96 (s, 6H). [See spectrum]

^{13}C NMR (151 MHz, CDCl$_3$) δ 161.7, 155.3, 149.7, 145.9, 145.3, 142.2, 138.1, 136.1, 129.4, 126.5, 123.7, 122.7, 122.6, 111.3, 99.3, 95.8, 55.5. [See spectrum]

HRMS (m/z): (ESI+) calc'd for C$_{20}$H$_{18}$N$_3$O$_2$ [M+H]$^+$: 332.1394, found: 332.1395.

N^1,N^1-dimethyl-N^4-(1,10-phenanthrolin-2-yl)benzene-1,4-diamine (L18)

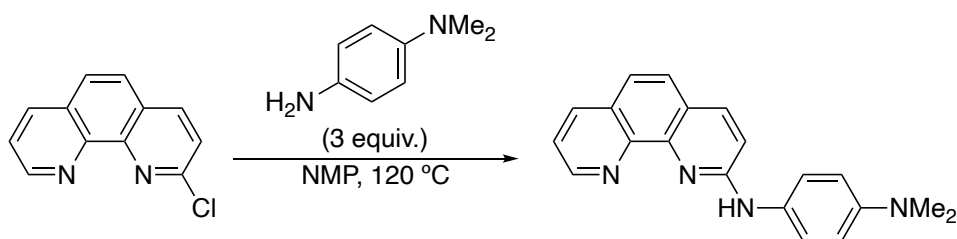

Prepared according to General Procedure A on 0.50 mmol scale. The crude material was purified by chromatography on silica gel with 0% → 30% (30% aq. ammonia in MeOH) in ethyl acetate as eluent to afford the title product (95 mg, 60%) as yellow powder.

^{1}H NMR (500 MHz, CDCl$_3$) δ 9.25 (d, J = 4.3 Hz, 1H), 8.32 (d, J = 8.2 Hz, 1H), 8.10 – 8.04 (m, 1H), 7.80 – 7.74 (m, 1H), 7.72 – 7.66 (m, 1H), 7.64 (d, J = 8.5 Hz, 1H), 7.38 – 7.33 (m, 3H), 7.22 (d, J = 8.8 Hz, 1H), 6.92 (d, J = 8.3 Hz, 2H), 3.11 (s, 6H). [See spectrum]

^{13}C NMR (126 MHz, CDCl$_3$) δ 157.8, 149.5, 148.8, 146.1, 145.2, 138.0, 136.1, 129.4, 129.0, 126.6, 126.1, 123.0, 122.6, 121.6, 113.6, 109.7, 41.0. [See spectrum]

HRMS (*m/z*): (ESI+) calc'd for C$_{20}$H$_{19}$N$_4$ [M+H]$^+$: 315.1604, found: 315.1605.

N-(3,5-bis(trifluoromethyl)phenyl)-1,10-phenanthrolin-2-amine (L19)
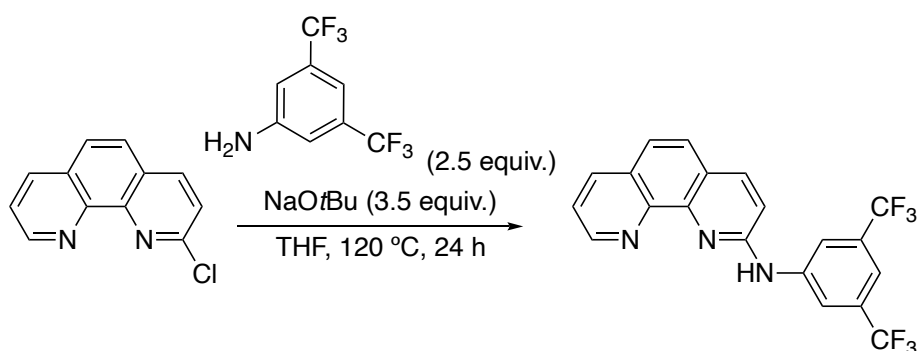
In a glovebox, a 20 mL vial was charged with 2-chloro-1,10-phenanthroline (215 mg, 1.00 equiv, 1.00 mmol), 3,5-bis(trifluoromethyl)aniline (537 mg, 2.50 equiv, 2.50 mmol), and sodium *tert*-butoxide (336 mg, 3.50 equiv, 3.50 mmol). THF (2 mL) and a stirbar were added to the vial, and the vial was tightly sealed with a Teflon cap. The vial was taken out of the glovebox and the reaction mixture heated at 120 ºC for 24 h. The crude material was purified by chromatography on silica gel with 0% → 30% (30% aq. ammonia in MeOH) in ethyl acetate as eluent to afford the title product (357 mg, 88%) as yellow powder.

^{1}H NMR (500 MHz, CDCl$_3$) δ 9.18 (dd, J = 4.3, 1.7 Hz, 1H), 8.30 – 8.24 (m, 3H), 8.18 (d, J = 8.7 Hz, 1H), 7.76 (d, J = 8.6 Hz, 1H), 7.69 (d, J = 8.7 Hz, 1H), 7.65 (dd, J = 8.1, 4.3 Hz, 1H), 7.57 (s, 1H), 7.32 (d, J = 8.7 Hz, 1H). [See spectrum]

^{13}C NMR (126 MHz, CDCl$_3$) δ 153.4, 150.1, 145.3, 145.0, 142.2, 138.7, 136.2, 132.8 (q, J = 33.3 Hz), 129.4, 126.2, 124.2, 123.9, 123.4 (q, J = 272.9 Hz), 123.1, 118.9, 118.9, 115.7, 111.9. [See spectrum]

^{19}F NMR (470 MHz, CDCl$_3$) δ -63.0. [See spectrum]

HRMS (*m/z*): (ESI+) calc'd for C$_{20}$H$_{12}$N$_3$F$_6$ [M+H]$^+$: 408.0930, found: 408.0928.

**N-(3,5-di-tert-butylphenyl)-1,10-phenanthrolin-2-amine (L20)**
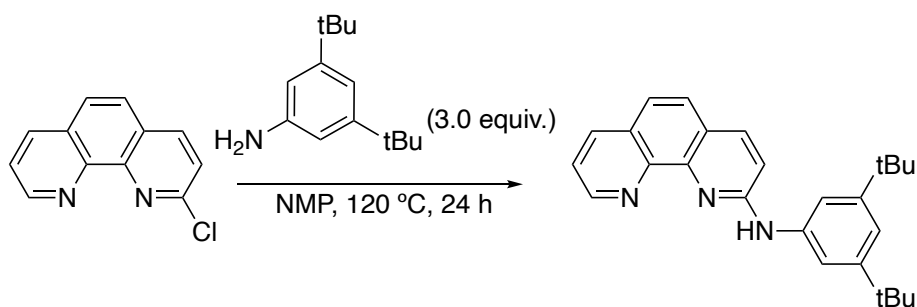
Prepared according to General Procedure A on 0.50 mmol scale. The crude material was purified by chromatography on silica gel with 0% → 50% ethyl acetate in (1% NEt$_3$ in hexane) to afford the title product (173 mg, 90%) as yellow powder.

**^{1}H NMR** (600 MHz, CDCl$_3$) δ 9.26 (dd, J = 4.3, 1.8 Hz, 1H), 8.33 (dd, J = 8.1, 1.8 Hz, 1H), 8.14 (d, J = 8.8 Hz, 1H), 7.80 (d, J = 8.6 Hz, 1H), 7.70 (dd, J = 8.1, 4.3 Hz, 1H), 7.67 (d, J = 8.6 Hz, 1H), 7.55 (bs, 1H), 7.44 (d, J = 8.8 Hz, 1H), 7.38 – 7.37 (m, 1H), 7.36 (d, J = 1.6 Hz, 2H), 1.49 (s, 18H). [See spectrum]

^{13}C NMR (151 MHz, CDCl$_3$) δ 156.5, 152.4, 149.6, 146.2, 145.3, 139.4, 138.1, 136.0, 129.4, 126.5, 123.4, 122.6, 122.1, 118.6, 117.0, 110.3, 35.1, 31.6. [See spectrum]

HRMS (*m/z*): (ESI+) calc'd for C$_{26}$H$_{30}$N$_3$ [M+H]$^+$: 384.2434, found: 384.2436.

cyclopropylmethyl 3,5-di-*tert*-butylbenzoate (3b)
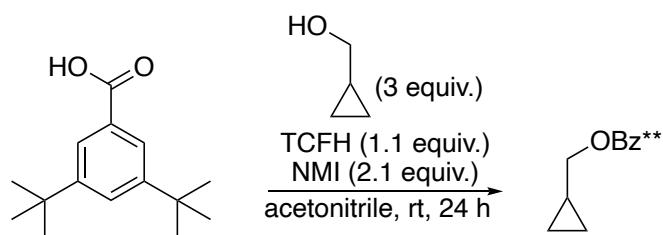
Synthesized according to General Conditions B on 2.00 mmol scale with the following modifications: The reaction was conducted in acetonitrile and with a threefold excess of the alcohol.

The crude material was purified by chromatography on silica gel with 0→40% ethyl acetate in hexanes as eluent to afford the title compound as a clear oil (570 mg, 99%).

^{1}H NMR (500 MHz, CDCl$_3$) δ 7.95 (d, J = 1.9 Hz, 2H), 7.66 (t, J = 1.9 Hz, 1H), 4.20 (d, J = 7.2 Hz, 2H), 1.40 (s, 18H), 1.38 – 1.27 (m, 1H), 0.71 – 0.58 (m, 2H), 0.42 (dt, J = 6.1, 4.6 Hz, 2H). [See spectrum]

^{13}C NMR (126 MHz, CDCl$_3$) δ 167.6, 151.1, 130.1, 127.1, 123.9, 69.6, 35.1, 31.5, 10.2, 3.4. [See spectrum]

HRMS (*m/z*): (ESI+) calc'd for C$_{19}$H$_{29}$O$_2$ [M+H]$^+$: 289.2162, found: 289.2160.

tert-butyl 1-oxa-6-azaspiro[2.5]octane-6-carboxylate (5b)
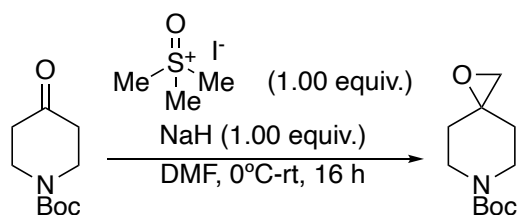
In a glovebox, a 100 mL round bottom flask was charged with sodium hydride (pre-washed with hexanes, 120 mg, 5.00 mmol, 1.00 equiv) and DMF (10 mL). A stir bar was added to the flask, and the flask was sealed with a rubber septum. The flask was brought out of the glove box, and a nitrogen inlet was inserted through the septum. The suspension was cooled to 0 ºC, and trimethylsulfoxonium iodide (1.10 g, 5.00 mmol, 1.00 equiv) added in one portion. The mixture was stirred for 1 h, then *tert*-butyl 4-oxopiperidine-1-carboxylate (996 mg, 5.00 mmol, 1.00 equiv) was added. The mixture was allowed to warm to room temperature overnight. The solution was diluted with ethyl acetate (50 mL) and washed with water (3*20 mL). The organic layer was dried over MgSO$_4$, 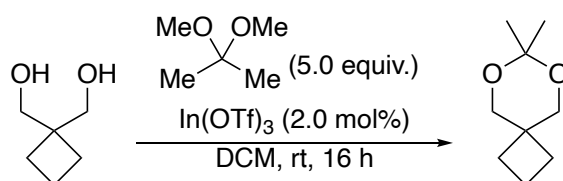filtered, and concentrated in vacuo. The crude material was purified by chromatography on silica gel with 0→50% ethyl acetate in hexanes as eluent to afford the title compound as a clear oil (578 mg, 54%).

¹H NMR (400 MHz, CDCl$_3$) δ 3.84 (d, J = 13.5 Hz, 2H), 3.54 (ddd, J = 13.3, 9.5, 3.7 Hz, 2H), 2.81 (s, 2H), 1.92 (ddd, J = 13.8, 9.6, 4.5 Hz, 2H), 1.63 – 1.53 (m, 11H). [See spectrum]

¹³C NMR (126 MHz, CDCl$_3$) δ 154.9, 79.9, 57.3, 53.9, 42.6, 33.1, 28.6. [See spectrum]

HRMS (*m/z*): (ESI+) calc'd for C$_{11}$H$_{20}$O$_3$N [M+H]$^+$: 214.1438, found: 214.1440.

**7,7-dimethyl-6,8-dioxaspiro[3.5]nonane (8b)**

Adapted from a literature procedure.[47] In a glovebox, a 20 mL vial was charged with In(OTf)$_3$ (56 mg, 0.10 mmol, 2.0 mol%), cyclobutane-1,1-diyldimethanol (580 mg, 5.0 mmol, 1.0 equiv), and 2,2-dimethoxypropane (2.6 g, 25 mmol, 5.0 equiv). DCM (10 mL) and a stir bar were added, and the vial was sealed with a Teflon-lined cap. The mixture was stirred at room temperature overnight. The solution was diluted with DCM (20 mL), and the layers were separated. The aqueous layer was further extracted with DCM (20 mL x2), dried over MgSO$_4$, filtered, and concentrated in vacuo. The crude material was purified by chromatography on silica gel with 0→50% ethyl acetate in hexanes as eluent to afford the title compound as a clear oil (580 mg, 74%).

^{1}H NMR (600 MHz, CDCl$_3$) δ 3.85 (s, 4H), 2.07 – 1.98 (m, 2H), 1.97 – 1.90 (m, 4H), 1.51 (s, 6H). [See spectrum]

^{13}C NMR (151 MHz, CDCl$_3$) δ 97.7, 69.2, 36.8, 28.0, 23.9, 15.6. [See spectrum]

HRMS (*m/z*): (ESI+) calc'd for C$_9$H$_{17}$O$_2$ [M+H]$^+$: 157.1229, found: 157.1228.

1,7,7-trimethylbicyclo[2.2.1]heptan-2-yl cyclobutanecarboxylate (14b)
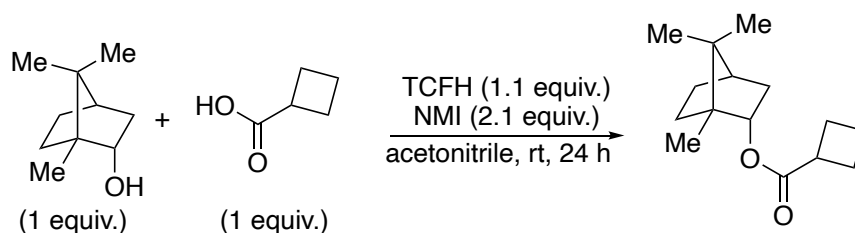
Synthesized according to General Conditions B on 3.00 mmol scale and in acetonitrile as the solvent.
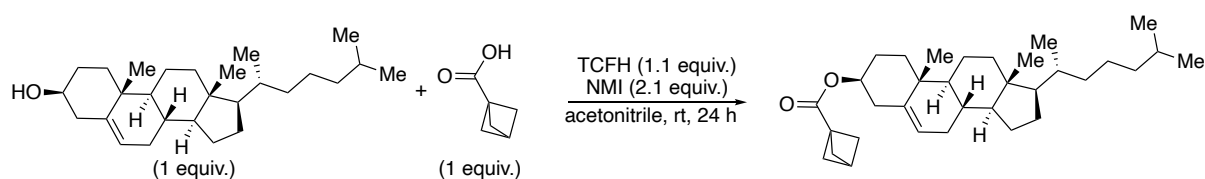
The crude material was purified by chromatography on silica gel with 0→30% ethyl acetate in hexanes as eluent to afford the title compound as a clear volatile oil (350 mg, 49%).

^{1}H NMR (600 MHz, CDCl$_3$) δ 4.48 (d, J = 2.0 Hz, 1H), 3.30 (dt, J = 16.8, 8.6 Hz, 1H), 2.48 – 2.38 (m, 2H), 2.40 – 2.30 (m, 2H), 2.16 – 1.99 (m, 2H), 1.93 – 1.79 (m, 2H), 1.71 (dd, J = 10.2, 2.2 Hz, 1H), 1.62 – 1.51 (m, 1H), 1.31 (d, J = 10.2 Hz, 1H), 1.24 (s, 3H), 1.24 – 1.17 (m, 1H), 1.17 (s, 3H), 0.90 (s, 3H). [See spectrum]

^{13}C NMR (151 MHz, CDCl$_3$) δ 176.0, 85.8, 48.5, 48.4, 41.4, 39.5, 38.6, 29.8, 26.7, 25.9, 25.6, 25.4, 20.2, 19.5, 18.7. [See spectrum]

HRMS (*m/z*): (ESI+) calc'd for C$_{15}$H$_{25}$O$_2$ [M+H]$^+$: 237.1849, found: 237.1850.

(3S,8S,9S,10R,13R,14S,17R)-10,13-dimethyl-17-((R)-6-methylheptan-2-yl)-2,3,4,7,8,9,10,11,12,13,14,15,16,17-tetradecahydro-1H-cyclopenta[a]phenanthren-3-yl bicyclo[1.1.1]pentane-1-carboxylate (15b)

Synthesized according to General Conditions B on 1.00 mmol scale and in acetonitrile as the solvent.

The crude material was purified by chromatography on silica gel with 0→30% ethyl acetate in hexanes as eluent to afford the title compound as a clear volatile oil (150 mg, 31%).

^{1}H NMR (500 MHz, CDCl$_3$) δ 5.41 (d, J = 3.9 Hz, 1H), 4.62 (dtd, J = 12.1, 8.3, 4.3 Hz, 1H), 2.45 (s, 1H), 2.34 (d, J = 7.6 Hz, 2H), 2.11 (s, 6H), 2.03 (ddt, J = 23.1, 17.4, 4.4 Hz, 2H), 1.88 (dtt, J = 15.0, 9.9, 4.8 Hz, 3H), 1.69 – 1.45 (m, 7H), 1.46 – 1.26 (m, 5H), 1.26 – 1.09 (m, 7H), 1.06 (s, 3H), 1.05 – 0.97 (m, 2H), 0.96 (d, J = 6.4 Hz, 3H), 0.93 – 0.89 (m, 6H), 0.72 (s, 3H). [See spectrum]

^{13}C NMR (126 MHz, CDCl$_3$) δ 169.4, 139.9, 122.7, 73.9, 56.8, 56.2, 51.6, 50.1, 43.1, 42.4, 39.8, 39.6, 38.2, 37.1, 36.7, 36.3, 35.9, 32.0, 32.0, 28.4, 28.1, 27.8, 27.7, 24.4, 24.0, 22.9, 22.7, 21.2, 19.5, 18.8, 12.0. [See spectrum]

HRMS (m/z): (ESI+) calc'd for C$_{33}$H$_{52}$O$_2$Na [M+Na]$^+$: 503.3860, found: 503.3854.

(2*R*,3*S*,4*R*,5*R*,6*S*)-2,3,4,5-tetrakis((3,5-di-*tert*-butylbenzyl)oxy)-6-methyltetrahydro-2*H*-pyran (16b)
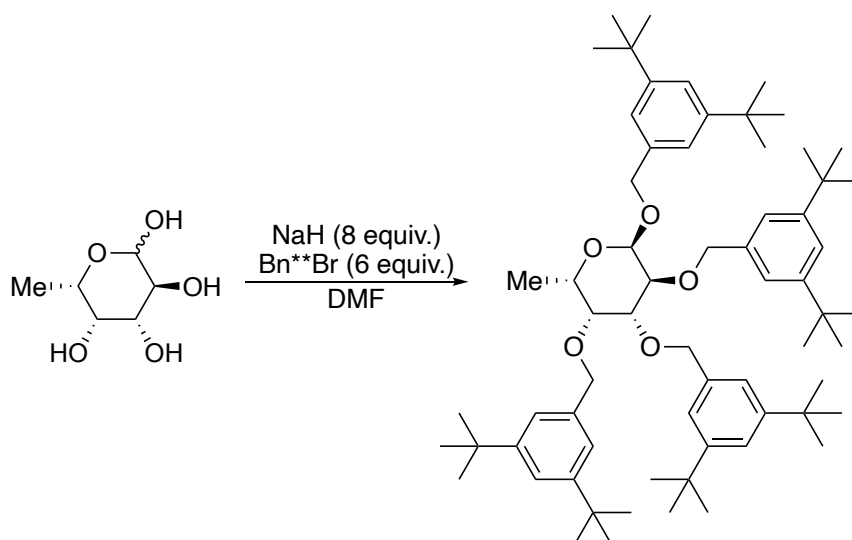
To a flame-dried, nitrogen-flushed, 250 mL, two-neck round bottom flask was added *L*-fucose (1.20 g, 7.31 mmol, 1.00 equiv) and dry DMF (30 mL). The solution was cooled to 0 ºC, and NaH (hexane washed, 1.40 g, 58.5 mmol, 8.00 equiv) was added. The suspension was stirred at 0 ºC for 30 min. 3,5-di-*tert*-butylbenzylbromide (12.4 g, 43.9 mmol, 6.00 equiv) was added. The mixture was allowed to warm to room temperature overnight. The mixture was quenched with MeOH (20 mL). Water (30 mL) and DCM (50 mL) were added, and the layers were separated. The aqueous layer was further extracted with DCM (50 mL x2), dried over MgSO$_4$, filtered, and concentrated in vacuo. The crude material was purified by chromatography on silica gel with 0→20% ethyl acetate in pentanes to afford the title compound as a white solid (3.65 g, 51%). The furanose isomer eluted after the desired pyranose isomer and was isolated as a white solid (1.69 g, 24%).

^{1}H NMR (600 MHz, CDCl$_3$) δ 7.52 (t, *J* = 1.8 Hz, 1H), 7.49 – 7.47 (m, 2H), 7.46 (t, *J* = 1.9 Hz, 1H), 7.42 – 7.38 (m, 4H), 7.30 (d, *J* = 1.8 Hz, 2H), 7.27 (d, *J* = 1.8 Hz, 2H), 5.21 (d, *J* = 4.2 Hz, 1H), 5.01 (d, *J* = 11.6 Hz, 1H), 4.97 (d, *J* = 12.3 Hz, 1H), 4.89 (d, *J* = 7.6 Hz, 1H), 4.87 (d, *J* = 7.1 Hz, 1H), 4.83 – 4.76 (m, 3H), 4.53 (d, *J* = 11.8 Hz, 1H), 4.37 (t, *J* = 6.8 Hz, 1H), 4.25 (dd, *J* = 7.1, 4.2 Hz, 1H), 4.11 (dd, *J* = 8.1, 6.5 Hz, 1H), 3.91 (p, *J* = 6.5 Hz, 1H), 1.46 (s, 18H), 1.45 (s, 18H), 1.43 (s, 18H), 1.42 (s, 18H), 1.40 (d, *J* = 6.3 Hz, 3H). [See spectrum]

^{13}C NMR (126 MHz, CDCl$_3$) δ 151.0, 150.9, 150.8, 150.8, 138.1, 137.4, 136.8, 136.6, 122.9, 122.4, 122.1, 122.0, 121.9, 121.8, 121.8, 121.8, 98.4, 84.7, 83.9, 83.2, 78.7, 72.9, 72.8, 72.4, 69.1, 34.9, 34.9, 34.9, 31.6, 31.6, 31.6, 16.2. [See spectrum]

HRMS (*m/z*): (ESI+) calc'd for C$_{66}$H$_{100}$O$_5$Na [M+Na]$^+$: 995.7463, found: 995.7448.

(2*S*,3*S*,4*R*,5*R*,6*S*)-6-methyltetrahydro-2H-pyran-2,3,4,5-tetrayl   tetrakis(4-(tert-butyl)benzoate) (17b)
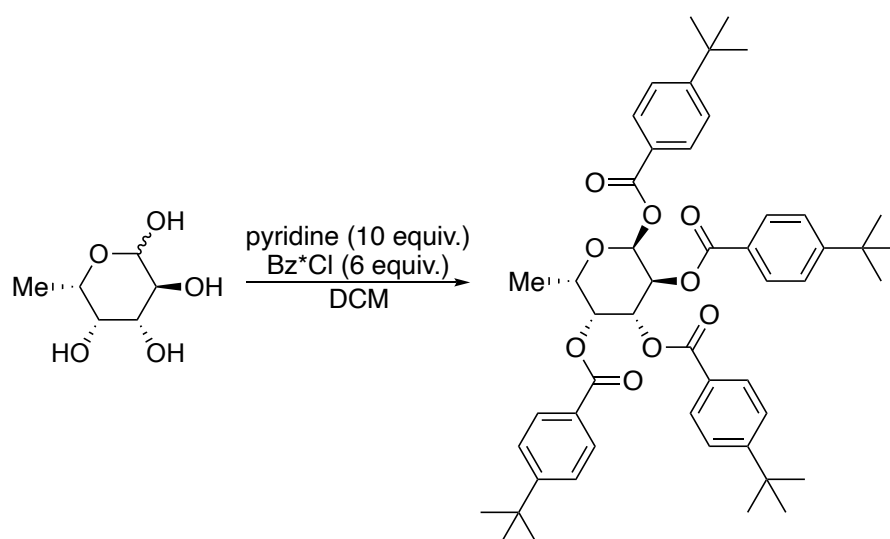
To a flame-dried, nitrogen-flushed, 100 mL, round bottom flask was added *L*-fucose (400 mg, 2.44 mmol, 1.00 equiv) and dry DCM (40 mL). The solution was cooled to 0 ºC, and pyridine (1.93 g, 24.4 mmol, 10.0 equiv) was added. Then, 4-*tert*-butylbenzoyl chloride (2.88 g, 14.6 mmol, 6 equiv) was added dropwise. The mixture was allowed to warm to room temperature and stirred overnight. MeOH (5 mL) was added, and the mixture stirred for 30 min. Then, sat. NaHCO$_3$ (50 mL) was added. The layers were separated, and the aqueous layer was further extracted with DCM (50 mL x3). The combined organic layers were dried over MgSO$_4$, filtered, and concentrated in vacuo. The crude material was purified by chromatography on silica gel with 0→50% ethyl acetate in hexanes as eluent to afford the title compound as a white solid (438 mg, 22%). The combined yield of all pyranose, furanose isomers was 66%.

^{1}H NMR (500 MHz, CDCl$_3$) δ 8.21 (d, *J* = 8.4 Hz, 4H), 7.93 (d, *J* = 8.6 Hz, 2H), 7.89 (d, *J* = 8.6 Hz, 2H), 7.69 – 7.65 (m, 4H), 7.44 (d, *J* = 8.6 Hz, 2H), 7.42 (d, *J* = 8.5 Hz, 2H), 6.96 (d, *J* = 3.6 Hz, 1H), 6.21 (dd, *J* = 10.8, 3.2 Hz, 1H), 6.10 (dd, *J* = 10.8, 3.6 Hz, 1H), 5.99 (dd, *J* = 3.3, 1.3 Hz, 1H), 4.73 (q, *J* = 6.1 Hz, 1H), 1.52 (s, 9H), 1.52 (s, 9H), 1.42 (d, *J* = 6.5 Hz, 3H), 1.39 (s, 9H), 1.38 (s, 9H). [See spectrum]

^{13}C NMR (126 MHz, CDCl$_3$) δ 166.0, 166.0, 165.7, 164.8, 157.6, 157.4, 157.1, 157.0, 130.0, 130.0, 129.8, 126.7, 126.6, 126.4, 126.3, 125.8, 125.8, 125.5, 125.4, 90.8, 71.5, 68.9, 68.0, 67.6, 35.4, 35.3, 35.2, 31.3, 31.2, 31.1, 31.1, 16.4. [See spectrum]

HRMS (*m/z*): (ESI+) calc'd for C$_{50}$H$_{60}$O$_9$Na [M+Na]$^+$: 827.4130, found: 827.4126.

3.4.3 Evaluation of Conditions for the Mild Borylation of C–H Bonds.

Evaluation of Ligands.

In a nitrogen glovebox, a 4 mL vial was sequentially charged with the ligand (10.0 µmol, 10.0 mol%), [Ir(cod)OMe]$_2$ (4.14 mg, 5.00 µmol, 10.0 mol% iridium), *tert*-butyloctyl ether (**1b**) (18.6 mg, 0.100 mmol, 1.00 equiv), and B$_2$pin$_2$ (95.2 mg, 0.300 mmol, 3.00 equiv). A magnetic stir bar and 0.1 mL of cyclooctane were added to the vial, and the vial was tightly sealed with a Teflon lined cap. The vial was removed from the glovebox and heated at 65 ºC in a preheated aluminum heating block for the specified time. After cooling to ambient temperature, the reaction mixture was diluted with CDCl$_3$, 50 µL of CH$_2$Br$_2$ (internal standard) added, and an aliquot was removed, and subjected to ^{1}H NMR analysis.
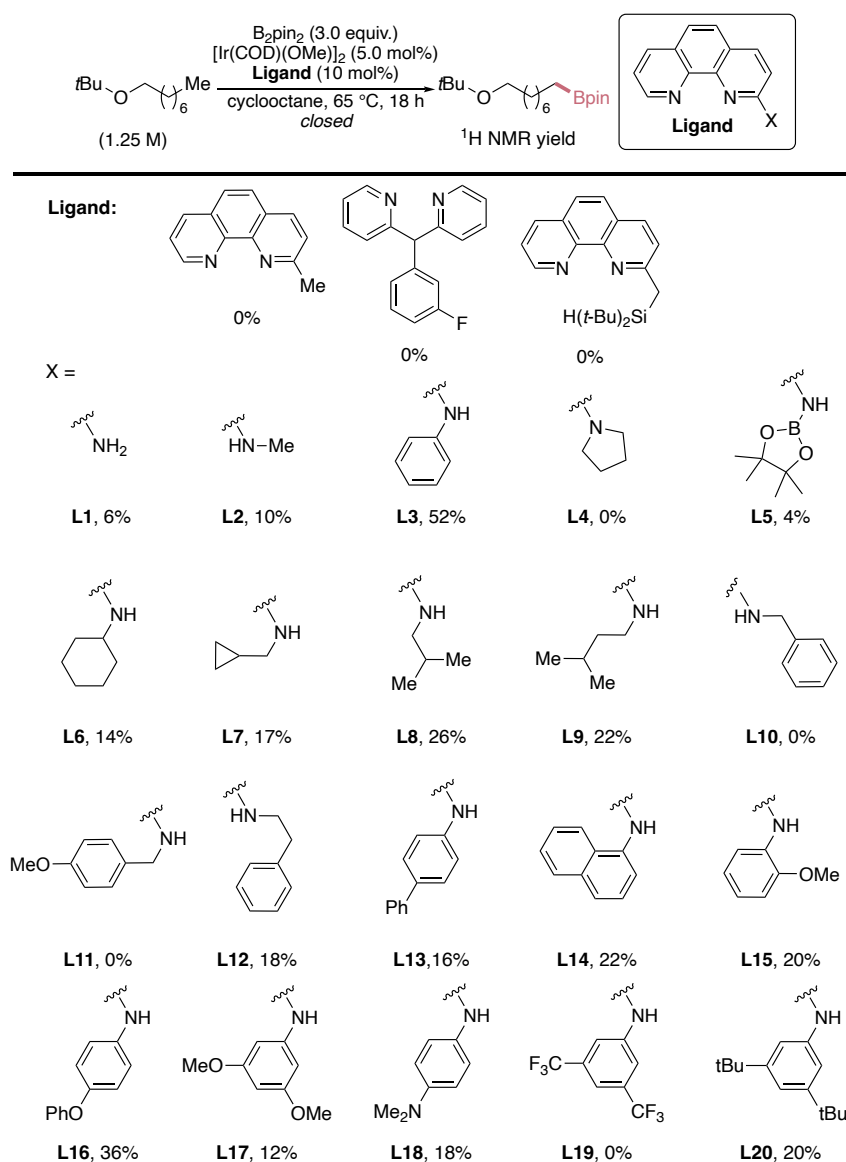

Figure 3.7. Evaluation of ligands for the borylation of alkyl C–H bonds at 65 ºC.

Timecourse experiment with various ligands at 100 ºC.

In a nitrogen glovebox, a 4 mL vial was sequentially charged with ligand (5.00 μmol, 5.00 mol%), (MesH)Ir(Bpin)₃ (3.47 mg, 5.00 μmol, 5.00 mol%), adamantane (internal standard, 13.6 mg, 0.100 mmol), B₂pin₂ (25.4 mg, 0.100 mmol, 1.00 equiv), and THF (0.2 mL). A magnetic stir bar was added to the vial, and the vial was tightly sealed with a Teflon lined cap. The vial was removed from the glovebox and heated in a pre-heated aluminum block at 100 ºC. At the specified timepoints, aliquots were taken and analyzed by GC-FID analysis.
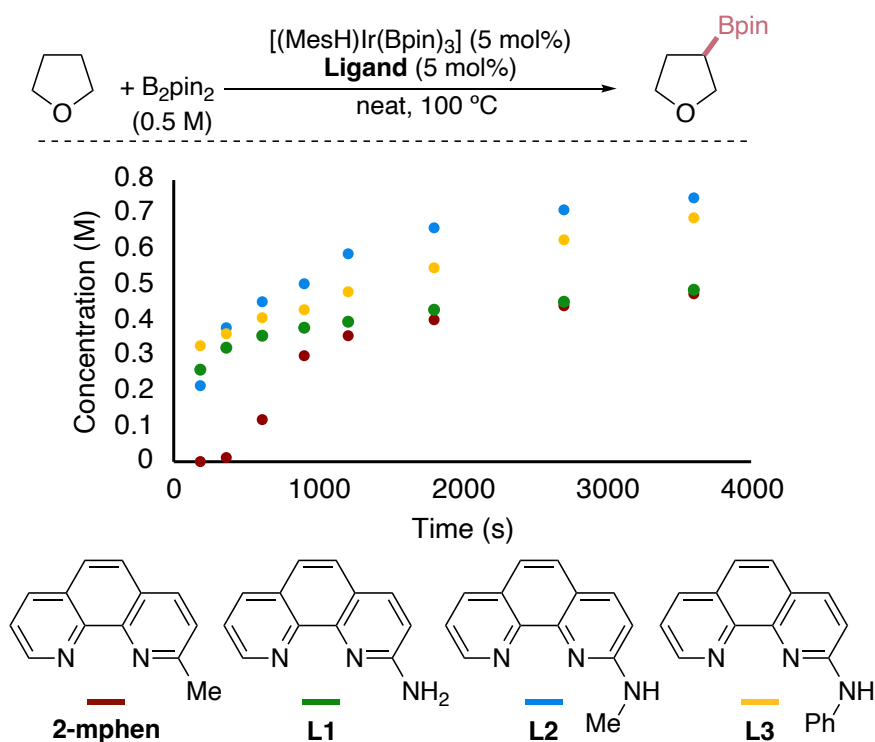

Figure 3.8. Evaluation of the reactivity of 2-aminophenthrolines. Timecourses of the borylation of tetrahydrofuran with either 2-mphen or a variety of 2-aminophenanthrolines at 100 °C. (Equivalent to Figure 3.3)

Evaluation of Metal Precursors and Diboron Reagents.

In a nitrogen glovebox, a 4 mL vial was sequentially charged with *N*-phenyl-1,10-phenanthrolin-2-amine (**L3**) (3.38 mg, 10.0 μmol, 10.0 mol%), iridium precursor (10.0 mol% iridium), *tert*-butyloctyl ether (**1b**) (18.6 mg, 0.100 mmol, 1.00 equiv), and diboron reagent (0.300 mmol, 3.00 equiv). A magnetic stir bar and 0.1 mL of cyclooctane were added to the vial, and the vial was tightly sealed with a Teflon lined cap. The vial was removed from the glovebox and heated at 65 ºC in a preheated aluminum heating block for the specified time. After cooling to ambient temperature, the reaction mixture was diluted with CDCl$_3$, 50 μL of CH$_2$Br$_2$ (internal standard) added, and an aliquot was removed, and subjected to ^{1}H NMR analysis.
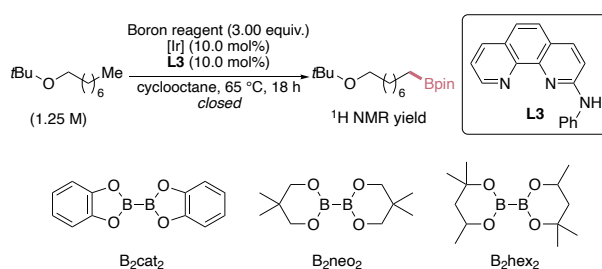
Entry	precatalyst	Boron reagent	NMR yield (%)
1	(MesH)Ir(Bpin)$_3$	B$_2$pin$_2$ (3 equiv.)	53
2	[Ir(cod)OMe]$_2$	B$_2$pin$_2$ (3 equiv.)	52
3	[Ir(cod)Cl]$_2$	B$_2$pin$_2$ (3 equiv.)	34
4	[Ir(coe)$_2$Cl]$_2$	B$_2$pin$_2$ (3 equiv.)	36
5	[Rh(cod)Cl]$_2$	B$_2$pin$_2$ (3 equiv.)	0
6	[Rh(cod)OH]$_2$	B$_2$pin$_2$ (3 equiv.)	0
7	[Rh(coe)$_2$Cl]$_2$	B$_2$pin$_2$ (3 equiv.)	0
8	[Ir(cod)(OMe)]$_2$	Et$_3$SiBpin (3 equiv.)	0
9	[Ir(cod)(OMe)]$_2$	B$_2$cat$_2$ (3 equiv.)	0
10	[Ir(cod)(OMe)]$_2$	B$_2$neo$_2$ (3 equiv.)	0
11	[Ir(cod)(OMe)]$_2$	B$_2$hex$_2$ (3 equiv.)	0
12	[Ir(cod)(OMe)]$_2$	HBpin (3 equiv.)	0

Figure 3.9. Evaluation of metal precursors and boron reagents for the borylation of alkyl C–H bonds at 65 ºC.

Evaluation of the Effect of Additives, Solvents and Reaction Temperature.

In a nitrogen glovebox, a 4 mL vial was sequentially charged with *N*-phenyl-1,10-phenanthrolin-2-amine (**L3**) (3.38 mg, 10.0 μmol, 10.0 mol%), [Ir(cod)OMe]$_2$ (4.14 mg, 5.00 μmol, 10.0 mol% iridium), *tert*-butyloctyl ether (**1b**) (18.6 mg, 0.100 mmol, 1.00 equiv), and B$_2$pin$_2$ (95.2 mg, 0.300 mmol, 3.00 equiv). A magnetic stir bar, 0.1 mL of solvent, and the specified amount of additive were added to the vial, and the vial was tightly sealed with a Teflon lined cap. The vial was removed from the glovebox and heated at the specified temperature in a preheated aluminum heating block for the specified time. After cooling to ambient temperature, an aliquot was removed and subjected to ^{1}H NMR analysis.

Entry	Deviation	NMR yield (%)
1	None	52
2	Addition of 10 μL of Hg	52
3	Addition of 2.5 mol% of KO*t*Bu	51
4	Addition of 5.0 mol% of KO*t*Bu	52
5	Addition of 10 mol% of KO*t*Bu	23
6	Perfluorodecalin as solvent	39
7	40 °C instead of 65 °C	5
8	50 °C instead of 65 °C	19
9	60 °C instead of 65 °C	51
10	80 °C instead of 65 °C	48
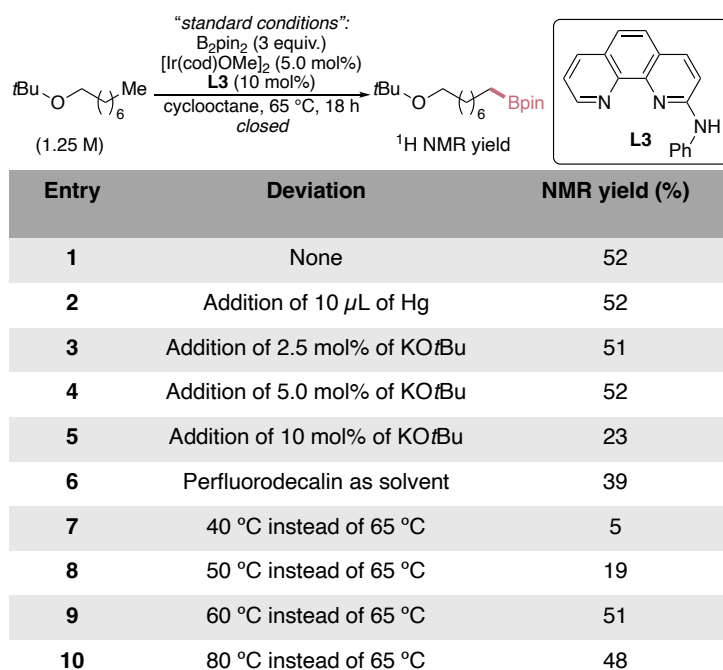
Figure 3.10 Evaluation of additives, solvents, and reaction temperatures for the borylation of alkyl C–H bonds.

Evaluation of Ligands for the Room Temperature Borylation of THF.

In a nitrogen glovebox, a 4 mL vial was sequentially charged with ligand (5.00 μmol, 5.00 mol%), (MesH)Ir(Bpin)$_3$ (3.47 mg, 5.00 μmol, 5.00 mol%), adamantane (internal standard, 13.6 mg, 0.100 mmol), B$_2$pin$_2$ (25.4 mg, 0.100 mmol, 1.00 equiv), and THF (162 μL, 2.00 mmol, 20.0 equiv). A magnetic stir bar was added to the vial, and the vial was tightly sealed with a Teflon lined cap. The vial was removed from the glovebox and stirred at 23 ºC. After 7 days, the vial was removed from the stir plate and brought into the glovebox. An aliquot of the solution was removed from the vial and analyzed by GC-FID.
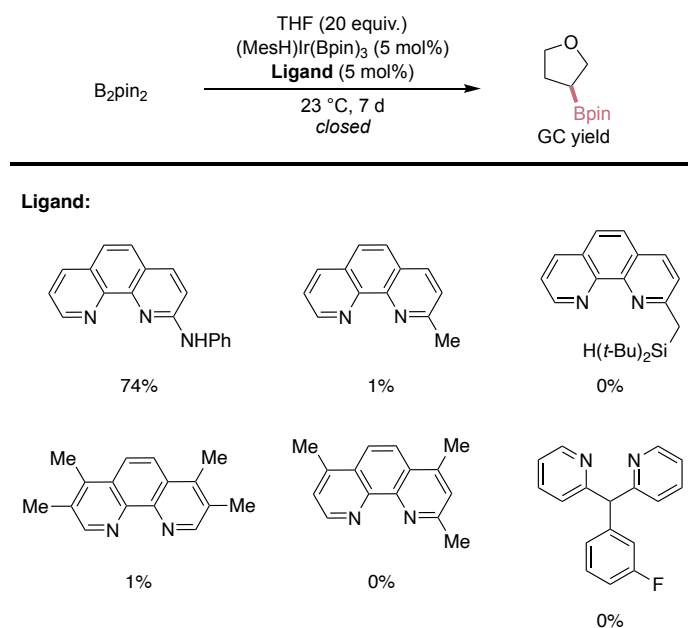
Figure 3.11. Evaluation of ligands for the borylation of THF at room temperature.

3.4.4 Scope of the Catalytic Borylation of Alkyl C–H Bonds

General Comments on Comparisons with 2-mphen and Mass Balance
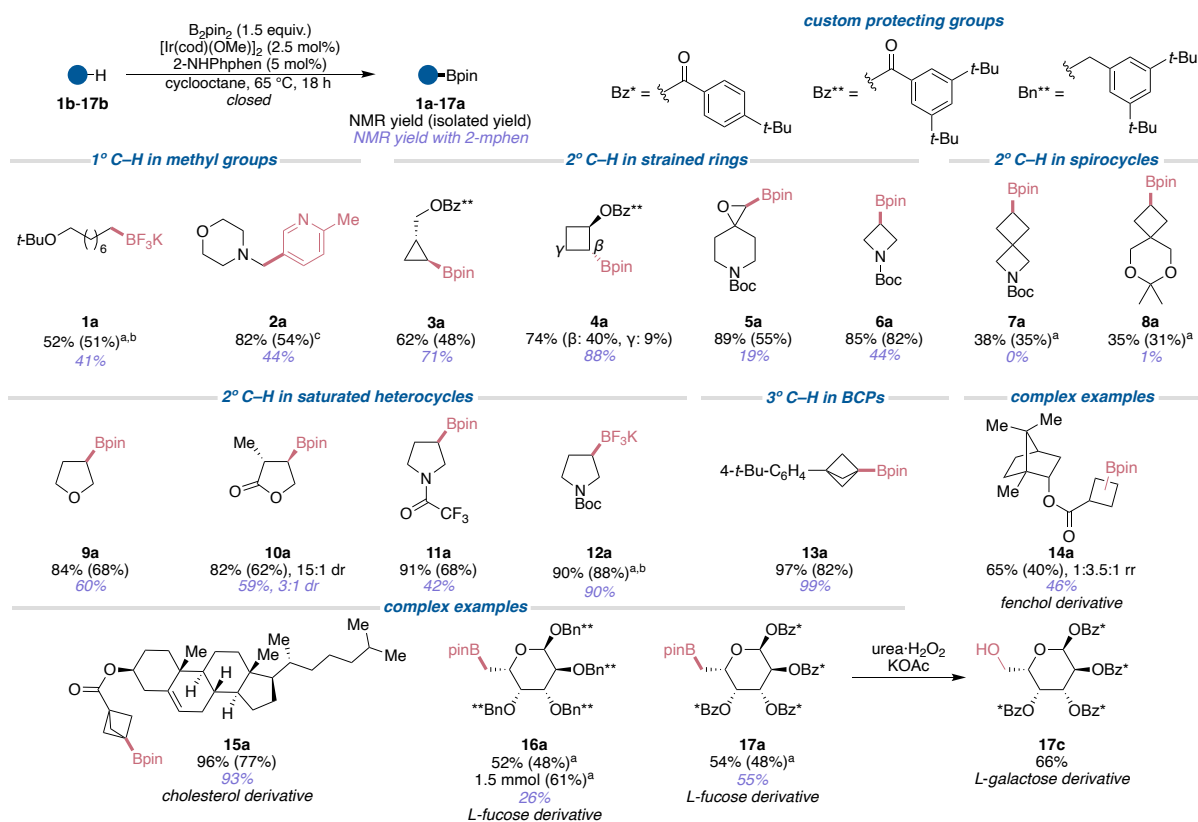
Figure 3.12. Scope of Borylation of Alkyl C–H Bonds Under Limiting Substrate Conditions (Equivalent to Figure 3.4)

The mass balance of reactions of **1a-17a** conducted with 2-NHPhphen (**L3**) was unconsumed starting material. In all these cases, the sum of products and starting material accounted for >90% of the amount of starting substrate. In comparison, reactions conducted with 2-mphen at 100 °C occurred to lower conversion (**1a-2a**, **6a-7a**, **9a-11a**, **14a**) or formed side products (**5a**, **8a**, **16a**).

Borylation of Alkyl C–H Bonds at Room Temperature
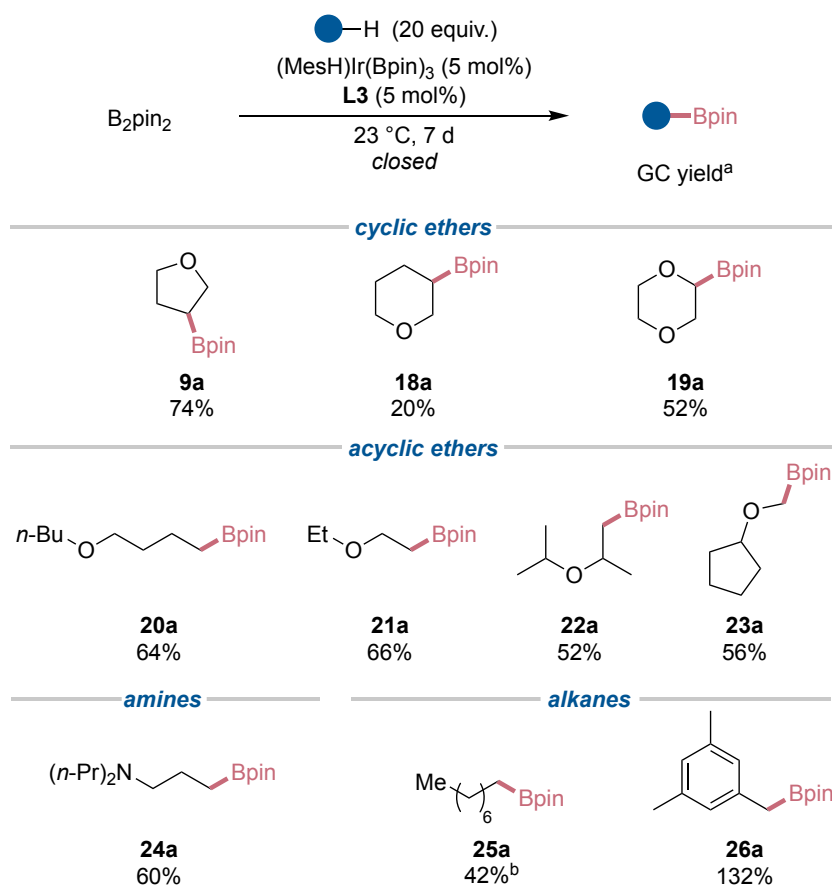
Figure 3.13. Scope of Borylation of Alkyl C–H Bonds at Room Temperature. (Equivalent to Figure 3.5) [a]Determined by GC-FID with adamantane as the internal standard. [b]10 mol% catalyst.

In a nitrogen glovebox, a 4 mL vial was sequentially charged with N-phenyl-1,10-phenanthrolin-2-amine (**L3**) (1.36 mg, 5.00 μmol, 5.00 mol%), (MesH)Ir(Bpin)₃ (3.47 mg, 5.00 μmol, 5.00 mol%), adamantane (internal standard, 13.6 mg, 0.100 mmol), B₂pin₂ (25.4 mg, 0.100 mmol, 1.00 equiv), and substrate (2.00 mmol, 20.0 equiv). A magnetic stir bar was added to the vial, and the vial was tightly sealed with a Teflon lined cap. The vial was removed from the glovebox and stirred at 23 ºC. After 7 days, an aliquot was removed and analyzed by GC-FID to quantify the yield.

Reaction Profile for Room Temperature Borylation of THF

In a nitrogen glovebox, a 4 mL vial was sequentially charged with N-phenyl-1,10-phenanthrolin-2-amine (**L3**) (1.36 mg, 5.00 μmol, 5.00 mol%), (MesH)Ir(Bpin)₃ (3.47 mg, 5.00 μmol, 5.00 mol%) or [Ir(cod)(OMe)]₂ (1.66 mg, 2.50 μmol, 2.50 mol%), adamantane (internal standard, 13.6 mg, 0.100 mmol), B₂pin₂ (25.4 mg, 0.100 mmol, 1.00 equiv), and THF (162 μL, 2.00 mmol, 20.0 equiv). A magnetic stir bar was added to the vial, and the vial was tightly sealed with a Teflon lined cap. The vial was removed from the glovebox and stirred at 23 ºC.

At various time points, the vial was removed from the stir plate and brought into the glovebox. An aliquot of the solution was removed from the vial and analyzed by GC-FID.
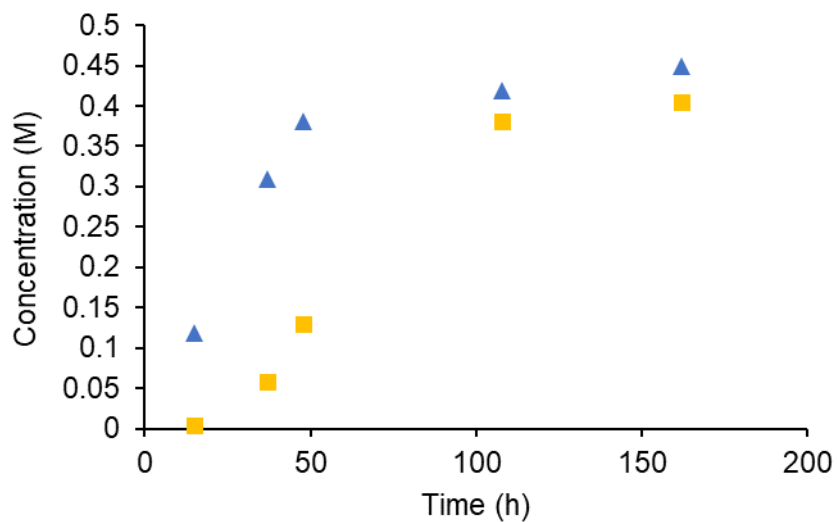

Figure 3.14. Profile of the reaction of THF and B$_2$pin$_2$ catalyzed by the combination of aminophenanthroline ligand L3 and (MesH)Ir(Bpin)$_3$ (blue triangles) or [Ir(cod)(OMe)]$_2$ (yellow squares) at room temperature.

3.4.5 Scope of the Mild Borylation of Alkyl C–H Bonds

General Procedure C: Catalytic Borylation of C–H Bonds and Isolation as the Boronic Ester.

In a nitrogen glovebox, a 4 mL vial was sequentially charged with *N*-phenyl-1,10-phenanthrolin-2-amine (**L3**) (3.38 mg, 12.5 μmol, 5.00 mol%), [Ir(cod)(OMe)]$_2$ (4.14 mg, 6.25 μmol, 2.50 mol%), substrate (0.250 mmol, 1.00 equiv), and B$_2$pin$_2$ (95.2 mg, 0.375 mmol, 1.50 equiv) (If the substrate was a liquid, it was added last). A magnetic stir bar and 0.2 mL of cyclooctane were added to the vial, and the vial was tightly sealed with a Teflon lined cap. The vial was removed from the glovebox and heated at 65 °C in a preheated aluminum heating block for the specified time. After cooling to ambient temperature, CDCl$_3$ and CH$_2$Br$_2$ (internal standard) were added to the vial, and a sample was removed and analyzed by ^{1}H NMR spectroscopy to quantify the conversion. The mixture was then co-evaporated with MeOH (5 mL) at 45 °C (Caution: vigorous gas evolution upon addition of MeOH!). The crude residue was purified by flash column chromatography on silica (0 → 50% ethyl acetate in hexanes as eluent) to give the borylated product.

General Procedure D: Catalytic Borylation of C–H Bonds and Transformation to the Trifluoroborate Salt

In a nitrogen glovebox, a 4 mL vial was sequentially charged with *N*-phenyl-1,10-phenanthrolin-2-amine (**L3**) (3.38 mg, 12.5 μmol, 5.00 mol%), [Ir(cod)(OMe)]$_2$ (4.14 mg, 6.25 μmol, 2.50 mol%), substrate (0.250 mmol, 1.00 equiv), and B$_2$pin$_2$ (95.2 mg, 0.375 mmol, 1.50 equiv) (If the substrate was a liquid, it was added last). A magnetic stir bar and 0.2 mL of cyclooctane were added to the vial, and the vial was tightly sealed with a Teflon lined cap. The vial was removed from the glovebox and heated at 65 °C in a preheated aluminum heating block for the specified time. After cooling to ambient temperature, CDCl$_3$ and CH$_2$Br$_2$ (internal standard) were added to the vial, and a sample was taken and analyzed by ^{1}H NMR spectroscopy to quantify the conversion. The trifluoroborate salt formation was adapted from a literature procedure.[48] All volatile materials were evaporated in vacuo, then MeOH (3 mL) and acetonitrile (3 mL) were added. A solution of KF (2.04 g in 3 mL of water) was added and the mixture stirred for 40 min at room temperature. Then, a solution of tartaric acid (2.7 g in 12.5 mL of THF) was added dropwise while rapidly stirring. The suspension was filtered, and the solids were further washed with acetonitrile (5 mL x3). The combined filtrate was concentrated to afford the desired product.

General Procedure E: Catalytic Borylation of C–H Bonds and One-Pot Cross-Coupling.

In a nitrogen glovebox, a 4 mL vial was sequentially charged with *N*-phenyl-1,10-phenanthrolin-2-amine (**L3**) (3.38 mg, 12.5 μmol, 5.00 mol%), [Ir(cod)(OMe)]$_2$ (4.14 mg, 6.25 μmol, 2.50 mol%), substrate (0.250 mmol, 1.00 equiv), and B$_2$pin$_2$ (95.2 mg, 0.375 mmol, 1.50 equiv) (If the substrate was a liquid, it was added last). A magnetic stir bar and 0.2 mL of cyclooctane were added to the vial, and the vial was tightly sealed with a Teflon lined cap. The vial was removed from the glovebox and heated at 65 °C in a preheated aluminum heating block for the specified time. After cooling to ambient temperature, CDCl$_3$ and CH$_2$Br$_2$ (internal standard) were added to the vial, and a sample was removed and analyzed by ^{1}H NMR

spectroscopy to quantify the conversion. All volatile materials were evaporated in vacuo, and pentaphenyl(di-tert-butylphosphino)ferrocene (QPhos, 8.88 mg, 12.5 μmol, 5.00 mol%), $Pd_2(dba)_3$ (5.72 mg, 6.25 μmol, 2.50 mol%), 5-bromo-2-methylpyridine (64.5 mg, 0.375 mmol, 1.50 equiv), and CsF (114 mg, 0.750 mmol, 3.00 equiv) were added. Dioxane (0.5 mL) and water (0.1 mL) were added, and the mixture was heated at 100 ºC for 24 h. The resulting mixture was diluted with ethyl acetate (2 mL), filtered through a pad of Celite and $MgSO_4$, and concentrated. The crude material was purified by flash column chromatography on silica (0 → 25% (premixed 30% NH_4OH in MeOH) in ethyl acetate).

(8-(*tert*-butoxy)octyl)trifluoro-λ4-borane, potassium salt (1a)
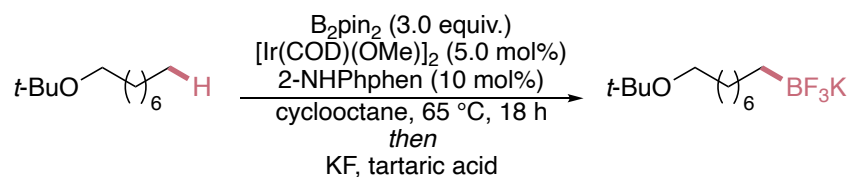
Synthesized according to General Procedure D on 0.250 mmol scale with the following modifications: The reaction was run with 10 mol% of [Ir] and 3 equiv of B_2pin_2 to afford the title compound as an off-white solid (37.8 mg, 51%).

¹H NMR (600 MHz, acetone) δ 3.44 (t, J = 6.5 Hz, 2H), 1.63 – 1.54 (m, 2H), 1.50 – 1.36 (m, 10H), 1.27 (s, 9H), 0.32 – 0.24 (m, 2H). [See spectrum]

¹³C NMR (151 MHz, acetone) δ 71.7, 61.2, 33.8, 30.9, 30.1, 29.8, 27.1, 26.5, 25.6. [See spectrum]

¹¹B NMR (193 MHz, acetone) δ 4.9. [See spectrum]

¹⁹F NMR (565 MHz, acetone) δ -141.8. [See spectrum]

HRMS (*m/z*): (ESI+) calc'd for $C_{12}H_{25}OBF_3$ [M-K]⁻: 253.1956, found: 253.1957.

4-((6-methylpyridin-3-yl)methyl)morpholine (2a)
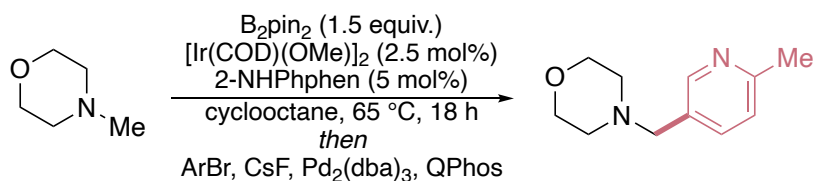
Synthesized according to General Procedure E on 0.250 mmol scale to afford the title compound as an off-white solid (37.8 mg, 51%).

^{1}H NMR (500 MHz, CDCl$_3$) δ 8.45 (d, J = 2.3 Hz, 1H), 7.61 (dd, J = 8.0, 2.3 Hz, 1H), 7.16 (d, J = 7.9 Hz, 1H), 3.74 (t, J = 4.6 Hz, 4H), 3.51 (s, 2H), 2.58 (s, 3H), 2.48 (t, J = 4.7 Hz, 4H). [See spectrum]

^{13}C NMR (126 MHz, CDCl$_3$) δ 157.5, 149.9, 137.4, 130.0, 123.1, 67.0, 60.4, 53.6, 24.2. [See spectrum]

HRMS (*m/z*): (ESI+) calc'd for C$_{11}$H$_{17}$ON$_2$ [M+H]$^+$: 193.1335, found: 193.1335.

((1*S*,2*S*)-2-(4,4,5,5-tetramethyl-1,3,2-dioxaborolan-2-yl)cyclopropyl)methyl   3,5-di-*tert*-butylbenzoate (3a)
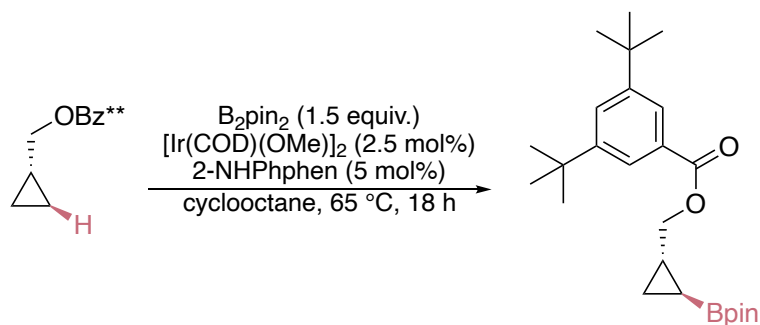
Synthesized according to General Procedure C on 0.250 mmol scale to afford the title compound as an off-white solid (49.9 mg, 48%).

**¹H NMR** (500 MHz, CDCl₃) δ 8.08 (d, J = 1.9 Hz, 2H), 7.80 (t, J = 1.9 Hz, 1H), 4.44 (dd, J = 11.3, 6.3 Hz, 1H), 4.28 (dd, J = 11.3, 7.5 Hz, 1H), 1.74 – 1.64 (m, 1H), 1.53 (s, 18H), 1.41 (s, 6H), 1.40 (s, 6H), 1.01 (td, J = 7.0, 3.7 Hz, 1H), 0.90 (ddd, J = 9.2, 5.1, 3.8 Hz, 1H), 0.14 – 0.06 (m, 1H). [See spectrum]

¹³C NMR (126 MHz, CDCl₃) δ 167.5, 151.0, 130.0, 127.1, 123.9, 83.2, 69.4, 35.0, 31.5, 24.8, 24.8, 16.6, 9.9. [See spectrum]

¹¹B NMR (160 MHz, CDCl₃) δ 33.2. [See spectrum]

HRMS (*m/z*): (ESI+) calc'd for $C_{25}H_{40}BO_4$ [M+H]⁺: 415.3014, found: 415.3015.

(1*R*,2*R*)-2-(4,4,5,5-tetramethyl-1,3,2-dioxaborolan-2-yl)cyclobutyl 3,5-di-*tert*-butylbenzoate (4a-*β*) and (1*s*,3*s*)-3-(4,4,5,5-tetramethyl-1,3,2-dioxaborolan-2-yl)cyclobutyl 3,5-di-*tert*-butylbenzoate (4a-*γ*)
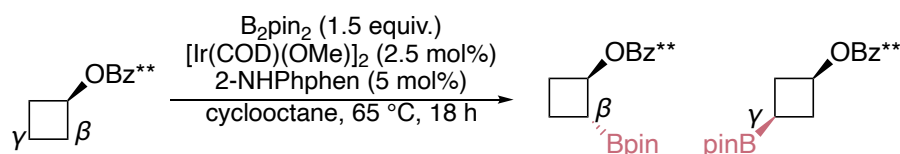
Synthesized according to General Procedure C on 0.250 mmol scale to afford the title compounds as white solids.

4a-*β*, 41.1 mg, 40%.

^{1}H NMR (500 MHz, CDCl$_3$) δ 7.90 (d, J = 1.9 Hz, 2H), 7.64 (t, J = 1.9 Hz, 1H), 5.23 (q, J = 7.5 Hz, 1H), 2.53 (ddt, J = 10.5, 7.5, 3.9 Hz, 1H), 2.38 (dtd, J = 11.4, 9.9, 7.6 Hz, 1H), 2.13 (td, J = 10.0, 7.7 Hz, 1H), 2.04 (qd, J = 10.6, 3.2 Hz, 1H), 1.78 (qd, J = 10.0, 7.9 Hz, 1H), 1.38 (s, 18H), 1.33 (s, 12H). [See spectrum]

^{13}C NMR (126 MHz, CDCl$_3$) δ 166.8, 150.9, 130.0, 127.0, 123.9, 83.5, 70.8, 35.0, 31.5, 31.1, 24.9, 24.9, 16.1. [See spectrum]

^{11}B NMR (160 MHz, CDCl$_3$) δ 32.9. [See spectrum]

HRMS (*m/z*): (ESI+) calc'd for C$_{25}$H$_{40}$BO$_4$ [M+H]$^+$: 415.3014, found: 415.3011.

4a-*γ*, 9.7 mg, 9%.

^{1}H NMR (500 MHz, CDCl$_3$) δ 7.91 (d, J = 1.9 Hz, 2H), 7.65 (t, J = 1.9 Hz, 1H), 5.33 – 5.21 (m, 1H), 2.57 (qd, J = 7.9, 2.8 Hz, 2H), 2.25 (dtd, J = 11.6, 8.7, 2.9 Hz, 2H), 1.60 – 1.49 (m, 1H), 1.39 (s, 18H), 1.30 (s, 12H). [See spectrum]

^{13}C NMR (126 MHz, CDCl$_3$) δ 166.9, 151.0, 129.9, 127.1, 123.9, 83.4, 68.8, 35.0, 32.5, 31.5, 24.9. [See spectrum]

^{11}B NMR (160 MHz, CDCl$_3$) δ 33.2. [See spectrum]

HRMS (*m/z*): (ESI+) calc'd for C$_{25}$H$_{40}$BO$_4$ [M+H]$^+$: 415.3014, found: 415.3013.

tert-butyl 2-(4,4,5,5-tetramethyl-1,3,2-dioxaborolan-2-yl)-1-oxa-6-azaspiro[2.5]octane-6-carboxylate (5a)
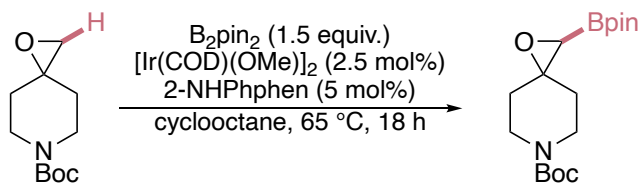
Synthesized according to General Procedure C on 0.250 mmol scale to afford the title compound as a brown oil (46.3 mg, 55%).

^{1}H NMR (500 MHz, CDCl$_3$) δ 3.85 – 3.63 (m, 2H), 3.48 (ddt, J = 13.5, 9.5, 4.0 Hz, 2H), 2.33 (s, 1H), 1.93 – 1.82 (m, 2H), 1.73 – 1.65 (m, 1H), 1.51 (s, 9H), 1.32 (s, 6H), 1.32 (s, 6H). [See spectrum]

^{13}C NMR (126 MHz, CDCl$_3$) δ 154.8, 84.7, 79.8, 61.5, 51.0, 42.6, 35.2, 28.5, 24.9, 24.8. [See spectrum]

^{11}B NMR (160 MHz, CDCl$_3$) δ 31.3. [See spectrum]

HRMS (m/z): (ESI+) calc'd for C$_{17}$H$_{30}$BO$_5$NNa [M+Na]$^+$: 362.2109, found: 362.2109.

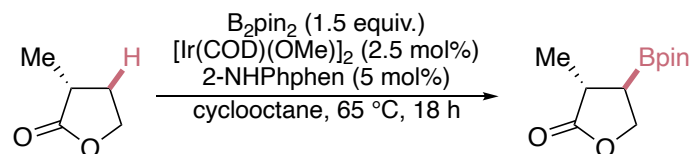**_tert_-butyl 3-(4,4,5,5-tetramethyl-1,3,2-dioxaborolan-2-yl)azetidine-1-carboxylate (6a)**
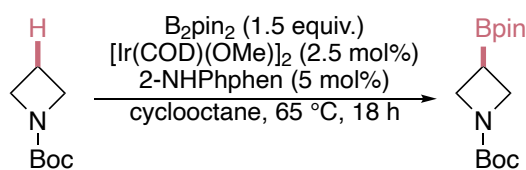
Synthesized according to General Procedure C on 0.250 mmol scale to afford the title compound as a yellow oil (57.8 mg, 82%).

¹H NMR (600 MHz, CDCl₃) δ 4.14 (dd, *J* = 10.0, 7.9 Hz, 2H), 4.05 (t, *J* = 7.5 Hz, 2H), 2.24 (tt, *J* = 10.0, 7.1 Hz, 1H), 1.56 (s, 9H), 1.40 (s, 12H). [See spectrum]

¹³C NMR (151 MHz, CDCl₃) δ 156.4, 83.8, 79.2, 51.1, 50.1, 28.5, 24.9, 11.3. [See spectrum]

¹¹B NMR (193 MHz, CDCl₃) δ 33.4. [See spectrum]

HRMS (_m/z_): (ESI+) calc'd for C₁₄H₂₇BO₄N [M+H]⁺: 284.2028, found: 284.2029.

***tert*-butyl 6-(4,4,5,5-tetramethyl-1,3,2-dioxaborolan-2-yl)-2-azaspiro[3.3]heptane-2-carboxylate (7a)**
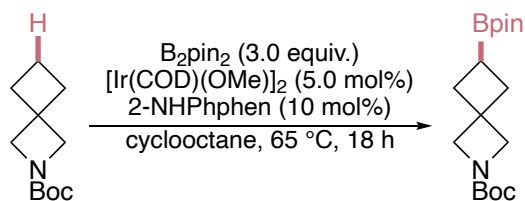
Synthesized according to General Procedure C on 0.100 mmol scale with the following modifications: The reaction was run with 10 mol% of [Ir] and 3 equiv of B_2pin_2 to afford the title compound as a colorless oil (11.2 mg, 35%).

^{1}H NMR (500 MHz, CDCl$_3$) δ 3.91 (s, 2H), 3.88 (s, 2H), 2.33 – 2.25 (m, 2H), 2.24 – 2.11 (m, 2H), 1.74 (tt, *J* = 9.5, 7.2 Hz, 1H), 1.47 (s, 9H), 1.28 (s, 12H). [See spectrum]

^{13}C NMR (126 MHz, CDCl$_3$) δ 156.4, 83.3, 79.2, 61.8, 37.8, 34.6, 28.5, 24.8, 11.7. [See spectrum]

^{11}B NMR (160 MHz, CDCl$_3$) δ 33.8. [See spectrum]

HRMS (*m/z*): (ESI+) calc'd for $C_{17}H_{30}BO_4NNa$ [M+Na]$^+$: 346.2160, found: 346.2158.

2-(7,7-dimethyl-6,8-dioxaspiro[3.5]nonan-2-yl)-4,4,5,5-tetramethyl-1,3,2-dioxaborolane (8a)
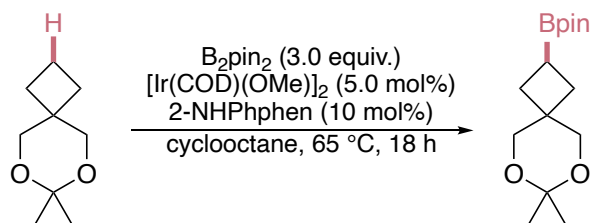
Synthesized according to General Procedure C on 0.250 mmol scale with the following modifications: The reaction was run with 10 mol% of [Ir] and 3 equiv of B$_2$pin$_2$ to afford the title compound as a colorless oil (21.9 mg, 31%).

^{1}H NMR (500 MHz, CDCl$_3$) δ 3.79 (s, 2H), 3.78 (s, 2H), 2.05 – 1.95 (m, 2H), 1.92 – 1.80 (m, 3H), 1.43 (s, 6H), 1.29 (s, 12H). [See spectrum]

^{13}C NMR (126 MHz, CDCl$_3$) δ 97.6, 83.3, 69.3, 69.1, 35.9, 29.3, 24.9, 23.9. [See spectrum]

^{11}B NMR (160 MHz, CDCl$_3$) δ 34.0. [See spectrum]

HRMS (*m/z*): (ESI+) calc'd for C$_{15}$H$_{27}$BO$_4$Na [M+Na]$^+$: 305.1895, found: 305.1895.

4,4,5,5-tetramethyl-2-(tetrahydrofuran-3-yl)-1,3,2-dioxaborolane (9a)
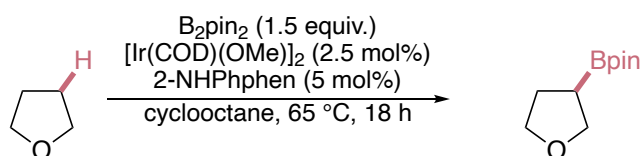
Synthesized according to General Procedure C on 0.250 mmol scale to afford the title compound as a colorless oil (33.6 mg, 68%).

¹H NMR (400 MHz, CDCl₃) δ 3.98 (t, *J* = 8.3 Hz, 1H), 3.80 (tdd, *J* = 8.2, 4.3, 1.7 Hz, 1H), 3.69 (q, *J* = 7.6 Hz, 1H), 3.61 (t, *J* = 9.3, 8.9 Hz, 1H), 2.09 – 1.96 (m, 1H), 1.81 (ddt, *J* = 12.0, 9.6, 8.2 Hz, 1H), 1.59 (p, *J* = 9.2 Hz, 1H), 1.23 (s, 12H). [See spectrum]

¹³C NMR (101 MHz, CDCl₃) δ 83.5, 70.4, 68.6, 28.9, 24.9. [See spectrum]

***rac*-(3*R*,4*R*)-3-methyl-4-(4,4,5,5-tetramethyl-1,3,2-dioxaborolan-2-yl)dihydrofuran-2(3*H*)-one (10a)**

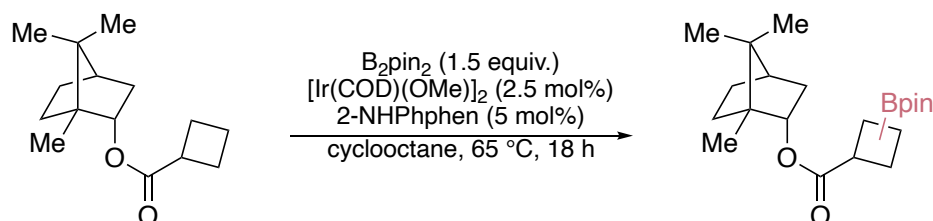
Synthesized according to General Procedure C on 0.250 mmol scale to afford the title compound as a yellow oil (35.0 mg, 62%). The diastereoselectivity was determined by analysis of the crude ^{1}H NMR spectrum.

^{1}H NMR (500 MHz, CDCl$_3$) δ 4.42 (t, *J* = 8.8 Hz, 1H), 4.16 (dd, *J* = 11.9, 9.0 Hz, 1H), 2.58 (dq, *J* = 13.9, 7.0 Hz, 1H), 1.76 (td, *J* = 12.3, 8.6 Hz, 1H), 1.32 (d, *J* = 7.0 Hz, 3H), 1.30 (s, 12H). [See spectrum]

^{13}C NMR (126 MHz, CDCl$_3$) δ 180.4, 84.2, 68.2, 37.2, 24.9, 24.8, 15.2. [See spectrum]

^{11}B NMR (160 MHz, CDCl$_3$) δ 32.6. [See spectrum]

2,2,2-trifluoro-1-(3-(4,4,5,5-tetramethyl-1,3,2-dioxaborolan-2-yl)pyrrolidin-1-yl)ethan-1-one (11a)
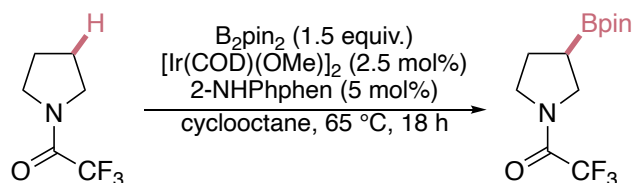
Synthesized according to General Procedure C on 0.250 mmol scale to afford the title compound as a yellow oil (50.2 mg, 68%). Mixture of rotamers.

^{1}H NMR (500 MHz, CDCl$_3$) δ 4.05 – 3.70 (m, 2H), 3.71 – 3.42 (m, 2H), 2.32 – 2.04 (m, 1H), 2.03 – 1.81 (m, 1H), 1.81 – 1.58 (m, 1H), 1.29 (s, 12H). [See spectrum]

^{13}C NMR (126 MHz, CDCl$_3$) δ 155.4 (q, J = 36.2 Hz), 116.52 (q, J = 287.6 Hz), 84.0, 84.0, 49.8, 48.8 (q, J = 3.5 Hz), 48.3, 47.4 (q, J = 3.4 Hz), 28.9, 26.1, 24.8. [See spectrum]

^{11}B NMR (160 MHz, CDCl$_3$) δ 33.1. [See spectrum]

^{19}F NMR (470 MHz, CDCl$_3$) δ -72.5, -72.6. [See spectrum]

HRMS (*m/z*): (ESI+) calc'd for C$_{12}$H$_{20}$BO$_3$NF$_3$ [M+H]$^+$: 294.1483, found: 294.1487.

tert-butyl 3-(trifluoro-λ⁴-boraneyl)pyrrolidine-1-carboxylate, potassium salt (12a)
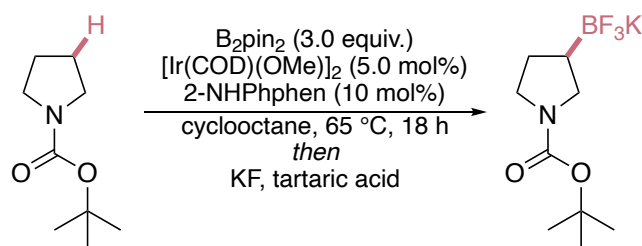
Synthesized according to General Procedure D on 0.250 mmol scale with the following modifications:

The reaction was run with 10 mol% of [Ir] and 3 equiv of B$_2$pin$_2$ to afford the title compound as an off-white solid (60.9 mg, 88%).

¹H NMR (700 MHz, Acetone) δ 3.42 (qd, J = 10.6, 4.6 Hz, 2H), 3.16 – 3.06 (m, 2H), 1.83 (tt, J = 12.7, 6.4 Hz, 1H), 1.76 – 1.63 (m, 1H), 1.54 (s, 9H), 1.16 – 1.02 (m, 1H). [See spectrum]

¹³C NMR (126 MHz, Acetone) δ 155.0, 77.8, 77.8, 50.7, 50.3, 48.4, 48.2, 28.8, 25.0. [See spectrum]

¹¹B NMR (160 MHz, Acetone) δ 4.6. [See spectrum]

HRMS (_m/z_): (ESI-) calc'd for C$_9$H$_{16}$BO$_2$NF$_3$ [M-K]⁻: 238.1232, found: 238.1234.

2-(3-(4-(*tert*-butyl)phenyl)bicyclo[1.1.1]pentan-1-yl)-4,4,5,5-tetramethyl-1,3,2-dioxaborolane (13a)
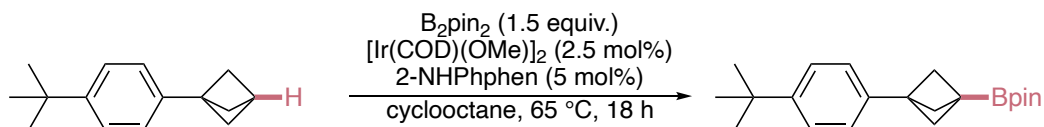
Synthesized according to General Procedure D on 0.250 mmol scale to afford the title compound as an off-white solid (67.0 mg, 82%).

1H NMR (500 MHz, CDCl$_3$) δ 7.37 (d, *J* = 8.3 Hz, 2H), 7.19 (d, *J* = 8.3 Hz, 2H), 2.20 (s, 6H), 1.34 (s, 9H), 1.31 (s, 12H). [See spectrum]

13C NMR (126 MHz, CDCl$_3$) δ 149.3, 139.4, 125.6, 125.1, 83.5, 53.2, 47.3, 34.6, 31.5, 24.9. [See spectrum]

(1S,2S,4R)-1,7,7-trimethylbicyclo[2.2.1]heptan-2-yl   cyclobutanecarboxylate-2,4,4,5,5-pentamethyl-1,3,2-dioxaborolane (14a)

Synthesized according to General Procedure C on 0.250 mmol scale to afford the title compound as a colorless oil, mixture of inseparable isomers (1:3.5:1) (36.1 mg, 40%).

^{1}H NMR (600 MHz, CDCl$_3$) δ 4.50 – 4.44 (m, 1H), 3.44 – 3.30 (m, 1H), 2.62 – 2.47 (m, 1H), 2.47 – 2.36 (m, 2H), 2.36 – 2.27 (m, 1H), 2.18 – 2.05 (m, 1H), 2.05 – 1.75 (m, 4H), 1.75 – 1.67 (m, 1H), 1.66 – 1.44 (m, 2H), 1.42 – 1.34 (m, 12H), 1.34 – 1.28 (m, 1H), 1.23 (d, J = 4.5 Hz, 3H), 1.22 – 1.11 (m, 3H), 0.93 – 0.87 (m, 3H). [See spectrum]

^{13}C NMR (151 MHz, CDCl$_3$) δ 176.1, 176.0, 175.9, 175.5, 85.8, 85.7, 85.6, 83.4, 83.3, 83.3, 48.5, 48.5, 48.5, 48.4, 48.4, 48.4, 41.4, 41.4, 39.6, 39.5, 39.5, 39.5, 38.6, 38.1, 29.8, 29.8, 29.8, 27.0, 26.8, 26.7, 26.7, 26.7, 26.6, 26.4, 25.9, 25.4, 25.2, 24.9, 24.9, 24.9, 24.8, 24.8, 20.2, 20.2, 20.2, 20.2, 19.5, 19.5. [See spectrum]

^{11}B NMR (160 MHz, CDCl$_3$) δ 33.6. [See spectrum]

HRMS (*m/z*): (ESI-) calc'd for C$_{21}$H$_{35}$BO$_4$Na [M+Na]$^+$: 385.2521, found: 385.2519.

(3*S*,8*S*,9*S*,10*R*,13*R*,14*S*,17*R*)-10,13-dimethyl-17-((*R*)-6-methylheptan-2-yl)-2,3,4,7,8,9,10,11,12,13,14,15,16,17-tetradecahydro-1*H*-cyclopenta[*a*]phenanthren-3-yl 3-(4,4,5,5-tetramethyl-1,3,2-dioxaborolan-2-yl)bicyclo[1.1.1]pentane-1-carboxylate (15a)
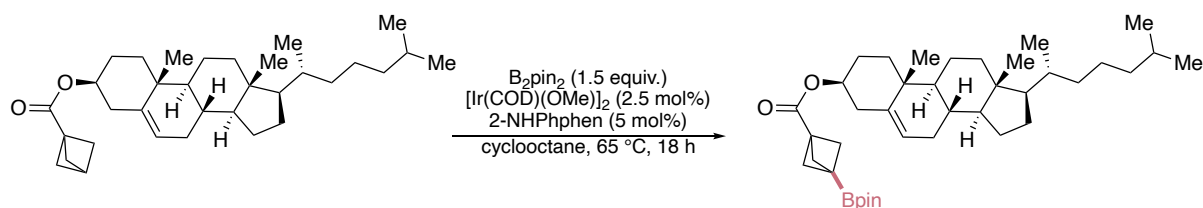
Synthesized according to General Procedure C on 0.100 mmol scale to afford the title compound as an white solid (46.5 mg, 77%).

^{1}H NMR (600 MHz, CDCl$_3$) δ 5.49 (d, *J* = 3.9 Hz, 1H), 4.69 (dtd, *J* = 11.9, 8.3, 4.3 Hz, 1H), 2.43 (d, *J* = 8.2 Hz, 2H), 2.25 (s, 6H), 2.17 – 2.06 (m, 2H), 2.01 – 1.92 (m, 3H), 1.74 – 1.54 (m, 8H), 1.54 – 1.43 (m, 3H), 1.37 (s, 12H), 1.33 – 1.17 (m, 7H), 1.16 (s, 3H), 1.14 – 1.07 (m, 3H), 1.05 (d, *J* = 6.5 Hz, 3H), 1.00 (dd, *J* = 6.6, 2.7 Hz, 6H), 0.81 (s, 3H). [See spectrum]

^{13}C NMR (151 MHz, CDCl$_3$) δ 169.4, 139.9, 122.6, 83.6, 73.9, 56.8, 56.2, 52.4, 50.1, 43.4, 42.4, 39.9, 39.6, 38.2, 37.1, 36.7, 36.3, 35.9, 32.0, 32.0, 28.3, 28.1, 27.8, 24.8, 24.4, 23.9, 22.9, 22.7, 21.2, 19.5, 18.8, 12.0. [See spectrum]

^{11}B NMR (193 MHz, CDCl$_3$) δ 30.8. [See spectrum]

HRMS (*m/z*): (ESI+) calc'd for C$_{39}$H$_{63}$BO$_4$Na [M+Na]$^+$: 629.4712, found: 629.4715.

4,4,5,5-tetramethyl-2-(((2*S*,3*R*,4*R*,5*S*,6*R*)-3,4,5,6-tetrakis((3,5-di-*tert*-butylbenzyl)oxy)tetrahydro-2*H*-pyran-2-yl)methyl)-1,3,2-dioxaborolane (16a)
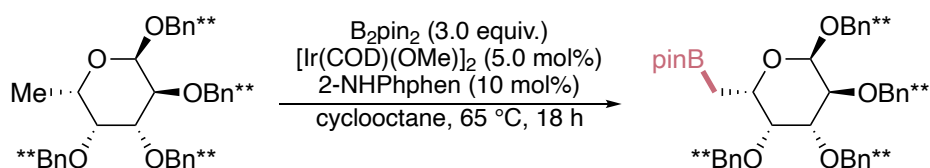
Synthesized according to General Procedure C on 0.100 mmol scale with the following modifications: The reaction was run with 10 mol% of [Ir] and 3 equiv of B_2pin_2 to afford the title compound as a colorless syrup that crystallized slowly (52.8 mg, 48%).

^{1}H NMR (600 MHz, CDCl$_3$) δ 7.45 (t, *J* = 1.9 Hz, 1H), 7.43 (q, *J* = 2.1 Hz, 2H), 7.41 (d, *J* = 1.9 Hz, 3H), 7.39 (d, *J* = 1.8 Hz, 2H), 7.36 (d, *J* = 1.8 Hz, 2H), 7.33 (d, *J* = 1.9 Hz, 2H), 5.25 (d, *J* = 11.0 Hz, 1H), 5.20 (d, *J* = 11.0 Hz, 1H), 5.16 (d, *J* = 12.2 Hz, 1H), 5.12 (d, *J* = 11.8 Hz, 1H), 4.97 (d, *J* = 8.6 Hz, 1H), 4.95 (d, *J* = 9.7 Hz, 1H), 4.78 (d, *J* = 11.0 Hz, 1H), 4.73 (d, *J* = 11.8 Hz, 1H), 4.64 (d, *J* = 7.7 Hz, 1H), 4.11 (dd, *J* = 9.7, 7.7 Hz, 1H), 3.86 (d, *J* = 3.0 Hz, 1H), 3.82 – 3.73 (m, 2H), 1.59 – 1.50 (m, 2H), 1.44 (s, 18H), 1.41 (s, 18H), 1.41 (s, 18H), 1.36 (s, 18H), 1.36 (s, 6H), 1.35 (s, 6H). [See spectrum]

^{13}C NMR (151 MHz, CDCl$_3$) δ 150.8, 150.6, 150.5, 150.4, 138.5, 138.4, 138.3, 137.3, 123.0, 122.1, 121.8, 121.5, 121.4, 121.3, 121.3, 121.2, 103.2, 83.2, 83.1, 80.1, 78.4, 76.3, 75.8, 74.4, 72.1, 71.3, 34.9, 34.9, 34.8, 31.6, 31.6, 31.6, 31.6, 25.0, 25.0. [See spectrum]

^{11}B NMR (193 MHz, CDCl$_3$) δ 33.6. [See spectrum]

HRMS (*m/z*): (ESI-) calc'd for $C_{72}H_{111}BO_7Na$ [M+Na]$^+$: 1121.8315, found: 1121.8333.

4,4,5,5-tetramethyl-2-(((2S,3R,4R,5S,6R)-3,4,5,6-tetrakis((3,5-di-*tert*-butylbenzyl)oxy)tetrahydro-2*H*-pyran-2-yl)methyl)-1,3,2-dioxaborolane (17a)
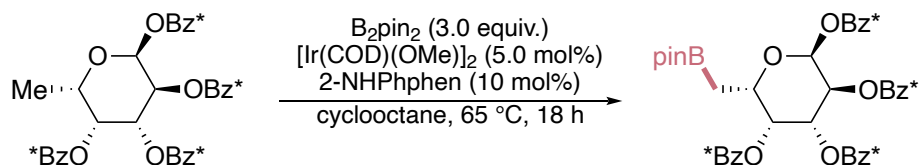
Synthesized according to General Procedure C on 0.100 mmol scale with the following modifications: The reaction was run with 10 mol% of [Ir] and 3 equiv of B_2pin_2 to afford the title compound as a colorless syrup that crystallized slowly (44.2 mg, 48%).

^{1}H NMR (600 MHz, CDCl$_3$) δ 8.23 (d, J = 8.2 Hz, 2H), 8.20 (d, J = 8.1 Hz, 2H), 7.94 (d, J = 8.4 Hz, 2H), 7.89 (d, J = 8.4 Hz, 2H), 7.68 (d, J = 8.2 Hz, 2H), 7.65 (d, J = 8.1 Hz, 2H), 7.44 (d, J = 8.3 Hz, 2H), 7.41 (d, J = 8.3 Hz, 2H), 6.94 (d, J = 3.8 Hz, 1H), 6.26 (dd, J = 10.7, 3.4 Hz, 1H), 6.09 – 6.02 (m, 2H), 4.84 (t, J = 7.6 Hz, 1H), 1.55–1.49 (m, 11H), 1.40 (s, 9H), 1.38 (s, 9H), 1.38 (s, 9H), 1.31 (s, 6H), 1.28 (s, 6H). [See spectrum]

^{13}C NMR (151 MHz, CDCl$_3$) δ 166.0, 165.8, 165.7, 164.9, 157.4, 157.2, 157.0, 156.8, 130.0, 130.0, 129.8, 126.9, 126.8, 126.6, 126.4, 125.7, 125.7, 125.4, 125.4, 90.7, 83.7, 83.6, 71.6, 69.9, 68.9, 67.8, 35.3, 35.3, 35.1, 35.1, 31.3, 31.2, 31.1, 31.1, 25.2, 24.8, 24.8. [See spectrum]

^{11}B NMR (193 MHz, CDCl$_3$) δ 30.8. [See spectrum]

HRMS (*m/z*): (ESI-) calc'd for $C_{56}H_{61}BO_{11}Na$ [M+Na]$^+$: 953.4982, found: 953.4995.

(2*S*,3*S*,4*R*,5*R*,6*S*)-6-(hydroxymethyl)tetrahydro-2*H*-pyran-2,3,4,5-tetrayl tetrakis(4-(*tert*-butyl)benzoate) (17c)
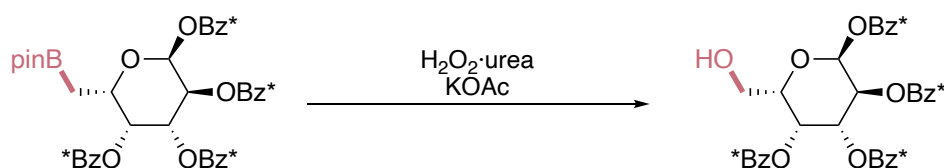
A 20 mL vial was charged with 4,4,5,5-tetramethyl-2-(((2*S*,3*R*,4*R*,5*S*,6*R*)-3,4,5,6-tetrakis((3,5-di-tert-butylbenzyl)oxy)tetrahydro-2*H*-pyran-2-yl)methyl)-1,3,2-dioxaborolane (**17a**, 23.3 mg, 25.0 µmol, 1.00 equiv), and THF (0.125 mL) was added and the solution cooled with an ice bath. H_2O_2·urea (2.82 mg, 30.0 µmol, 1.20 equiv) and KOAc (2.94 mg, 30.0 µmol, 1.20 equiv) were added, and water was added (75 µL). The cooling bath was removed, and the mixture stirred for 24 h. The mixture was diluted with DCM (5 mL) and sat. aq. $NaHCO_3$ (5 mL) was added. The layers were separated, and the aqueous layer further extracted with DCM (5 mL x3). The combined organic layers were dried over $MgSO_4$, filtered, and concentrated. The crude material was purified by column chromatography on silica (0→50% ethyl acetate in pentane) to afford the title compound as a white powder (13.5 mg, 66%).

^{1}H NMR (600 MHz, CDCl$_3$) δ 8.22 (d, *J* = 6.6 Hz, 2H), 8.21 (d, *J* = 6.4 Hz, 2H), 7.95 (d, *J* = 8.3 Hz, 2H), 7.92 (d, *J* = 8.3 Hz, 2H), 7.69 (dd, *J* = 8.4, 4.0 Hz, 4H), 7.45 (d, *J* = 8.4 Hz, 2H), 7.42 (d, *J* = 8.3 Hz, 2H), 6.98 (d, *J* = 3.4 Hz, 1H), 6.21 (qd, *J* = 10.8, 3.2 Hz, 2H), 6.10 (d, *J* = 3.0 Hz, 1H), 4.65 (t, *J* = 6.8 Hz, 1H), 3.91 (dt, *J* = 13.5, 6.8 Hz, 1H), 3.74 (dt, *J* = 11.8, 6.9 Hz, 1H), 2.68 (t, *J* = 7.2 Hz, 1H), 1.52 (s, 18H), 1.39 (s, 9H), 1.38 (s, 9H). [See spectrum]

^{13}C NMR (151 MHz, CDCl$_3$) δ 166.9, 165.8, 164.7, 157.9, 157.8, 157.2, 157.2, 130.2, 130.0, 129.8, 129.8, 126.4, 126.3, 126.2, 126.1, 125.9, 125.5, 125.5, 90.6, 72.1, 69.5, 68.6, 67.8, 60.6, 35.4, 35.4, 35.2, 35.2, 31.2, 31.1. [See spectrum]

HRMS (*m/z*): (ESI-) calc'd for $C_{50}H_{60}O_{10}Na$ [M+Na]$^+$: 843.4079, found: 843.4073.

3.4.6 Mechanistic Studies

Kinetic Isotope Effects

In a nitrogen glovebox, a 4 mL vial was sequentially charged with *N*-phenyl-1,10-phenanthrolin-2-amine (**L3**) (2.71 mg, 10.0 μmol, 5.00 mol%), (MesH)Ir(Bpin)$_3$ (6.93 mg, 10.00 μmol, 5.00 mol%), adamantane (internal standard, 13.6 mg, 0.100 mmol), B$_2$pin$_2$ (50.8 mg, 0.200 mmol, 1.00 equiv), and either THF or THF-*d*$_8$ (4.80 mmol, 24.0 equiv). A magnetic stir bar was added to the vial, and the vial was tightly sealed with a Teflon-lined cap. The vial was removed from the glovebox and stirred at 65 ºC. At the various time points, the vial was removed from the heating block and brought into the glovebox. An aliquot of the solution was removed from the vial and analyzed by GC.
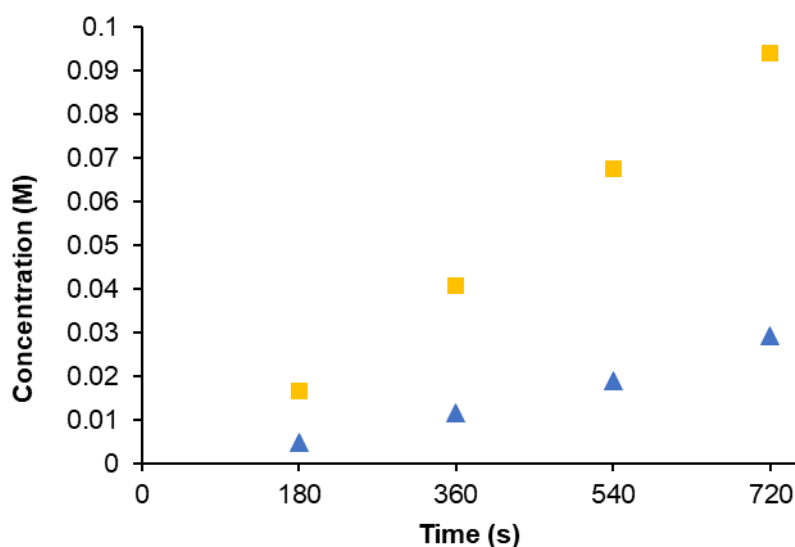
Figure 3.15. Initial rate plots for determination of the KIE. Profile of the reaction of THF (yellow squares) or THF-*d*$_8$ (blue triangles) and B$_2$pin$_2$ catalyzed by the combination of (MesH)Ir(Bpin)$_3$ and aminophenanthroline ligand L3. Average of two runs shown. The average values of the slopes for the reaction of THF and THF-*d*$_8$ were $8.6 \times 10^{-3} \pm 2.7 \times 10^{-4}$ and $2.7 \times 10^{-3} \pm 1.5 \times 10^{-4}$, respectively.

Borylation of Ligands

Borylation of 2-mphen
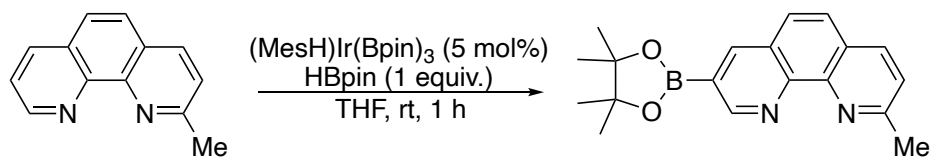
(MesH)Ir(Bpin)$_3$ (3.47 mg, 5.00 mol%, 5.00 μmol) and 2-methyl-1,10-phenanthroline (19.4 mg, 1.00 equiv, 0.100 mmol) were weighed into a 4 mL vial in the glovebox. Then THF-d_8 (0.5 mL) and HBpin (12.8 mg, 1.00 equiv, 100 μmol) were added. A stirbar was introduced, and the mixture was stirred vigorously, with the slurry quickly becoming homogenous. The reaction was stirred for 1 h at room temperature. The orange solution was transferred to an NMR tube for characterization. Borylation occurs predominately at the 8-position of the phenanthroline backbone.
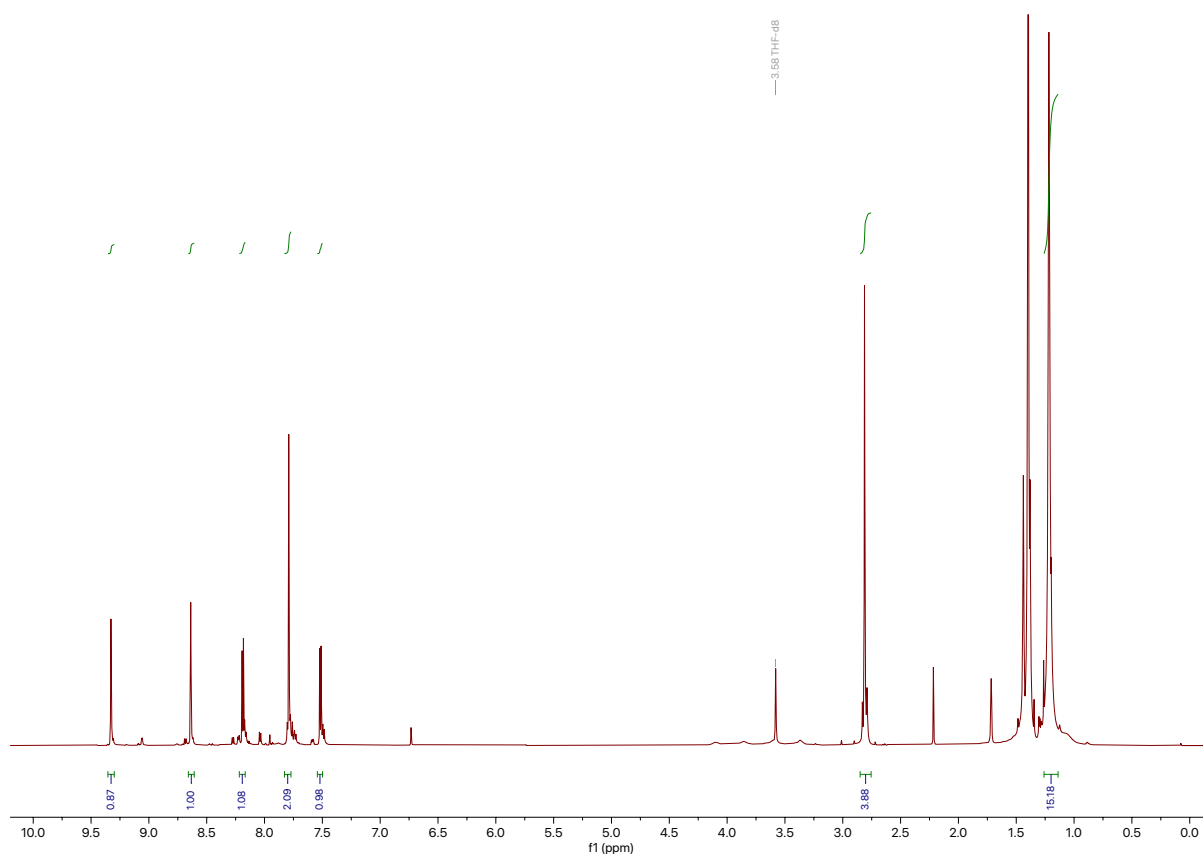
Figure 3.16. ^{1}H NMR spectrum of borylated 2-mphen.

Borylation of 1,10-phenanthrolin-2-amine (L1)

See synthesis of L5 for borylation of L1. Borylation occurs cleanly at the N–H.

Synthesis and Reactivity of Iridium Complexes

Attempted Formation of an Ir(III) trisboryl complex ligated by L3

In a nitrogen glovebox, a 4 mL vial was sequentially charged with *N*-phenyl-1,10-phenanthrolin-2-amine (**L3**, 6.78 mg, 25.0 μmol, 1.00 equiv), (MesH)Ir(Bpin)₃ (17.3 mg, 25.0 μmol, 1.00 equiv), and B₂pin₂ (9.52 mg, 37.5 μmol, 1.50 equiv). A magnetic stirbar was added to the vial. THF-*d₈* (0.5 mL) was introduced to the vial under vigorous stirring, and the vial was sealed with a Teflon cap. The heterogenous solution was stirred at rt for 1 h and transferred to an NMR tube for characterization.

We were unable to assign the identities of the components of the complex mixture observed. This spectrum is in stark contrast to that obtained with **L5**.
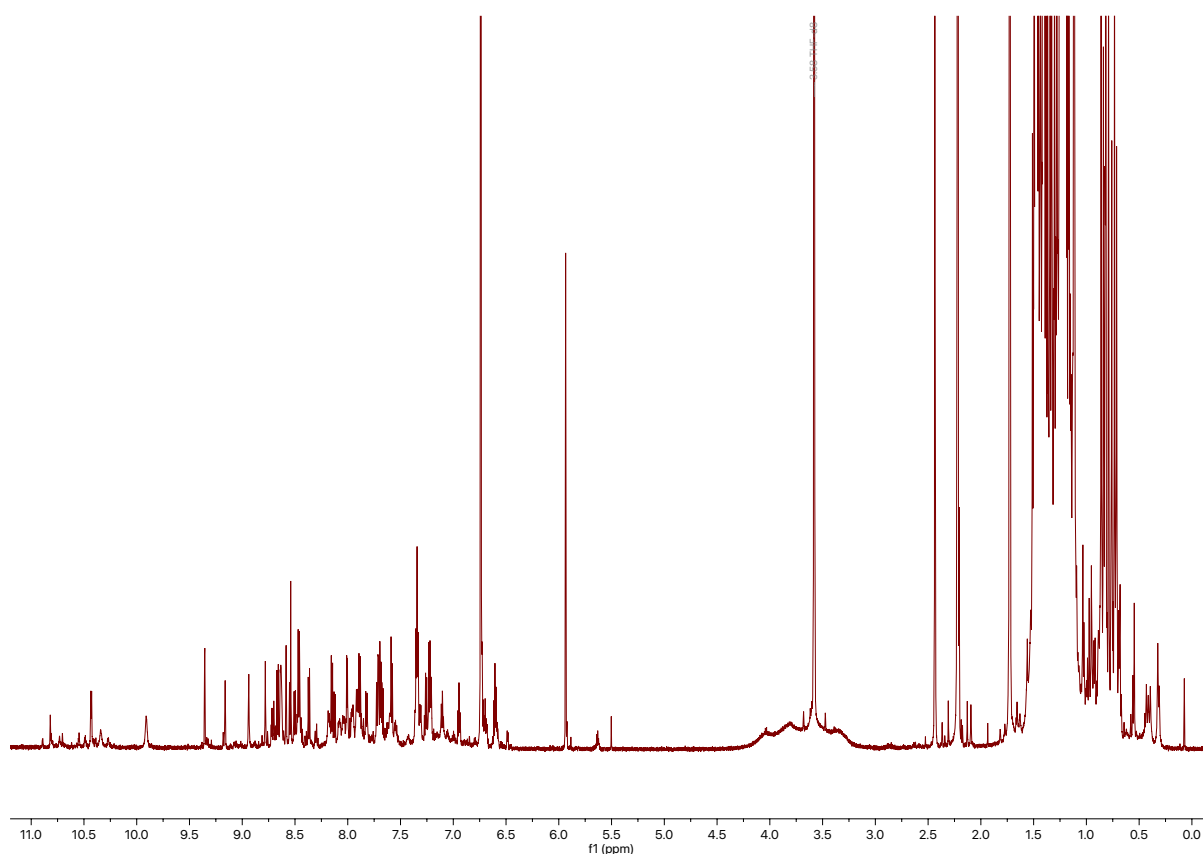
Figure 3.17. ¹H NMR spectrum of attempted complexation of L3 with (MesH)Ir(Bpin)₃.

Generation of (L5)Ir(Bpin)₃ from L1
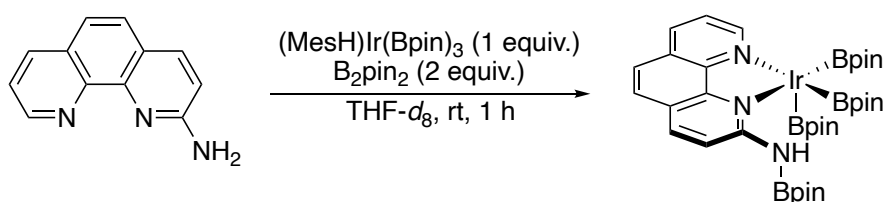
In a nitrogen glovebox, a 4 mL vial was sequentially charged with 1,10-phenanthroline-2-amine (**L1**, 4.88 mg, 25.0 μmol, 1.00 equiv), (MesH)Ir(Bpin)₃ (17.3 mg, 25.0 μmol, 1.00 equiv), and B₂pin₂ (12.7 mg, 50.0 μmol, 2.00 equiv). A magnetic stirbar was added to the vial, THF-d_8 (0.5 mL) was introduced to the vial under vigorous stirring, and the vial was sealed with a Teflon cap. The orange solution was stirred at rt for 1 h and transferred to an NMR tube for characterization. No iridium-hydride species were detected. The major species was assigned to be (**L5**)Ir(Bpin)₃. <u>See below</u> for direct generation of (**L5**)Ir(Bpin)₃ from **L5**.

Note: If no B₂pin₂ is added to the reaction, then immediate precipitation of iridium black occurs upon mixing **L1** and (MesH)Ir(Bpin)₃.

¹H NMR (600 MHz, THF) δ 9.88 (d, J = 4.9 Hz, 1H), 8.43 (s, 1H), 8.06 (t, J = 8.3 Hz, 2H), 7.89 (d, J = 8.8 Hz, 1H), 7.71 (d, J = 8.5 Hz, 2H), 7.49 (d, J = 8.4 Hz, 1H), 7.27 (dd, J = 8.0, 4.9 Hz, 1H).

¹¹B NMR (193 MHz, THF) δ 30.5, 28.2, 27.3.
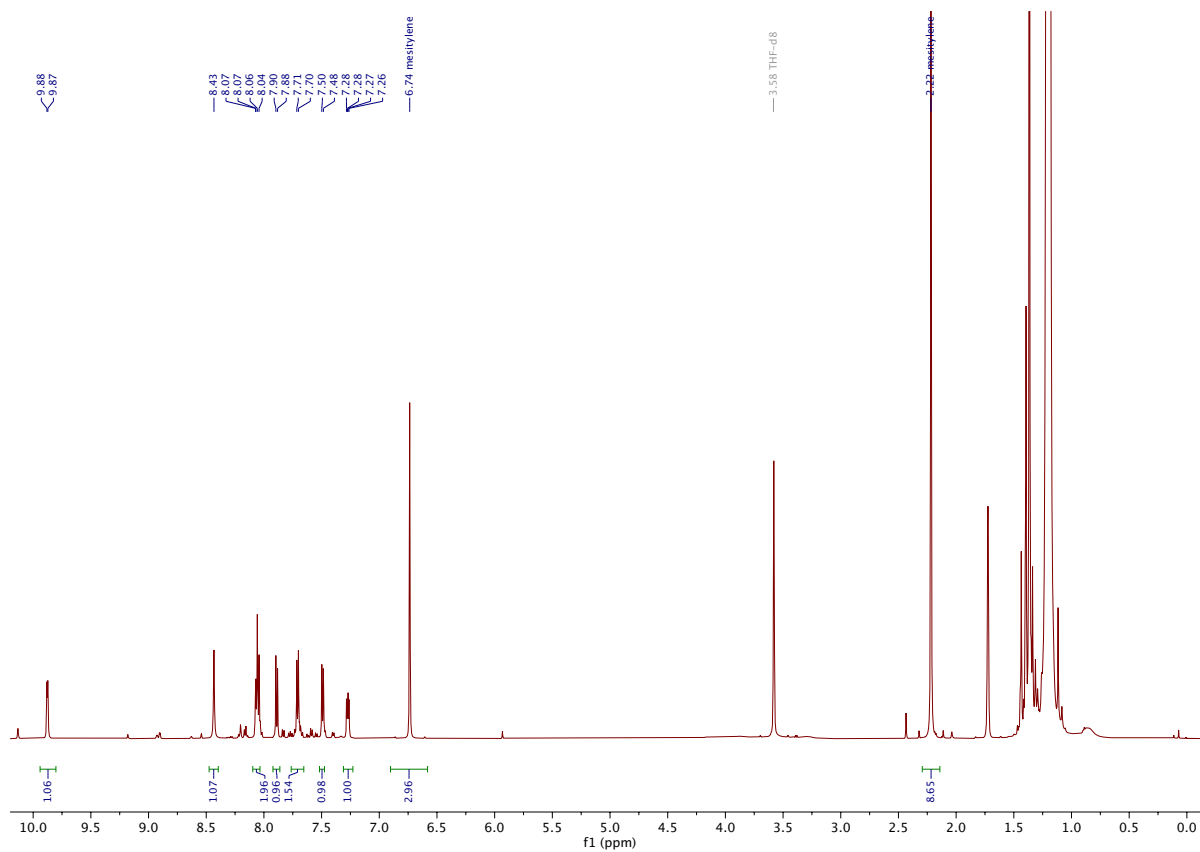
Figure 3.18. ¹H NMR spectrum of (L5)Ir(Bpin)₃ generated in situ by the complexation of L1.

NMR study of Iridium Complexes formed from L1 and (MesH)Ir(Bpin)₃

In a nitrogen glovebox, a 4 mL vial was sequentially charged with 1,10-phenanthroline-2-amine (**L1**, 4.88 mg, 25.0 µmol, 1.00 equiv), (MesH)Ir(Bpin)₃ (17.3 mg, 25.0 µmol, 1.00 equiv), and B₂pin₂ (63.5 mg, 0.250 mmol, 10.0 equiv). A magnetic stirbar was added to the vial. THF-d_8 (0.5 mL) was introduced to the vial under vigorous stirring, and the vial was sealed with a Teflon cap. The orange solution was stirred at rt for 1 h and transferred to an NMR tube. The mixture was heated in an aluminum heating block at 65 ºC for 30 min, and the resulting mixture was analyzed by ^{1}H NMR spectroscopy.

Multiple iridium species were formed in the reaction mixture, including several iridium hydride species (see inset). We have not been able to assign the structure of the iridium species formed.
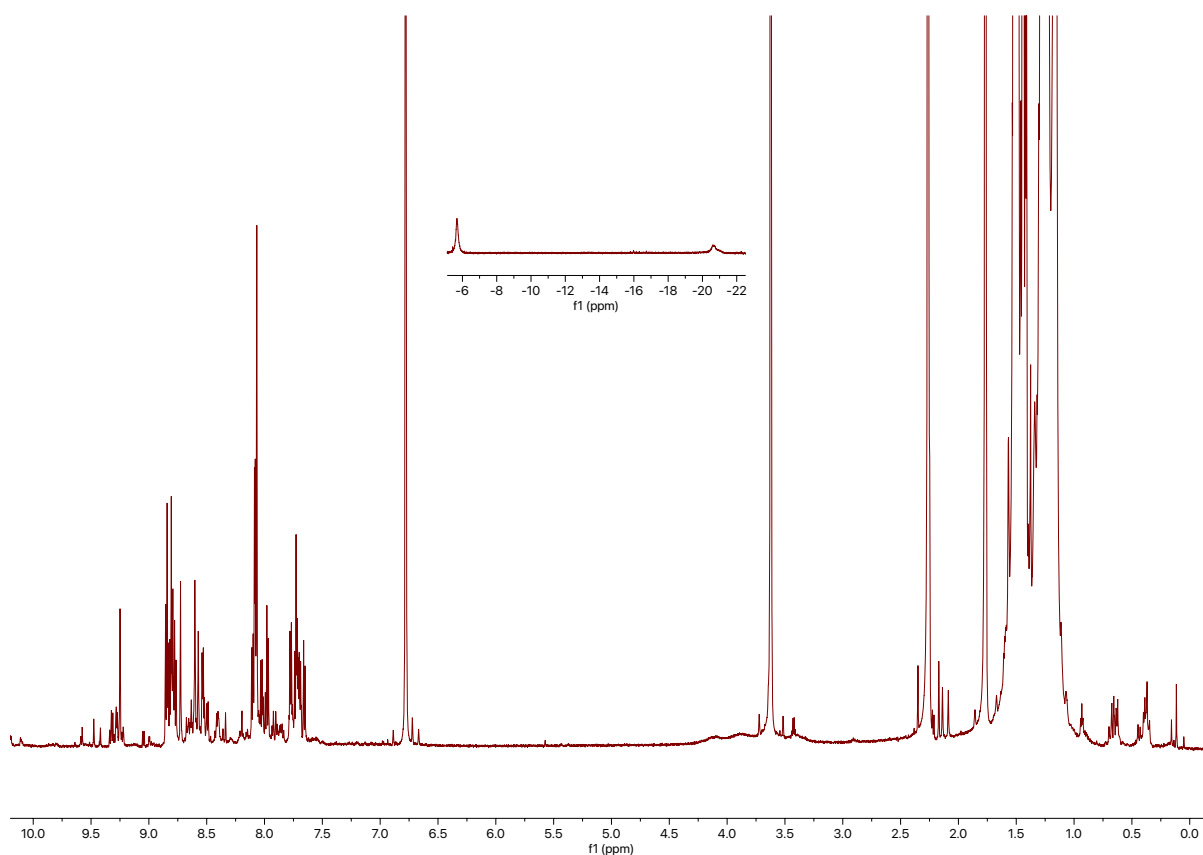
Figure 3.19: ^{1}H NMR spectrum of the reaction mixture of L1, (MesH)Ir(Bpin)₃, B₂pin₂, and THF after heating at 65 ºC for 30 min.

Synthesis of (L1)Ir(Bpin)₃(P(OPh)₃)
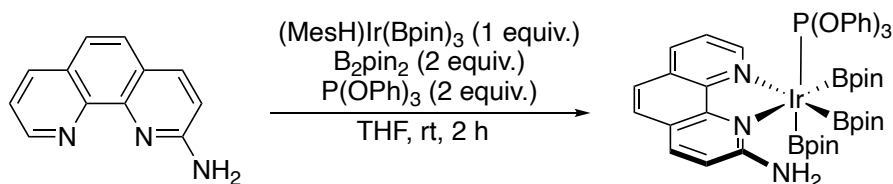
In a nitrogen glovebox, a 20 mL vial was sequentially charged with 1,10-phenanthroline-2-amine (**L1**, 14.1 mg, 72.1 μmol, 1.00 equiv), (MesH)Ir(Bpin)₃ (50.0 mg, 72.1 μmol, 1.00 equiv), and B₂pin₂ (36.6 mg, 144 μmol, 2.00 equiv). A magnetic stirbar was added to the vial, THF (2 mL) was introduced to the vial under vigorous stirring, and the vial was sealed with a Teflon cap. Triphenylphosphite (44.7 mg, 144 μmol, 2.00 equiv) was added. The solution turned a deep yellow color and was further stirred at rt for 2 h. All volatile materials were evaporated in vacuo, and 2 mL of pentane added to the residue. The mixture was stirred vigorously for 1 h, during which a fine yellow powder precipitated. The crude material was collected by filtration, and recrystallized from THF/pentane at -35 ºC to afford the title compound as deep yellow crystals (50 mg, 64%). Single crystals suitable for X-ray crystallography were grown by slow diffusion of pentane into a THF/ether solution of the compound.

¹H NMR (600 MHz, THF) δ 10.01 (d, J = 5.0 Hz, 1H), 8.01 (d, J = 8.0 Hz, 1H), 7.77 (d, J = 8.7 Hz, 1H), 7.58 (d, J = 8.4 Hz, 1H), 7.42 (d, J = 8.5 Hz, 1H), 7.35 (bs, 2H), 7.16 (dd, J = 8.0, 5.0 Hz, 1H), 6.86 – 6.78 (m, 12H), 6.74 (t, J = 7.0 Hz, 3H), 6.68 (d, J = 8.7 Hz, 1H), 1.30 (s, 6H), 1.28 (s, 6H), 1.26 (s, 6H), 1.25 (s, 6H), 0.57 (s, 6H), 0.51 (s, 6H). [See spectrum]

¹³C NMR (151 MHz, THF) δ 162.3, 155.0, 154.6 (d, $J_{P–C}$ = 9.9 Hz), 149.8, 149.6, 136.6, 134.8, 131.6, 129.3, 127.3, 124.3, 123.5, 123.4, 122.5 (d, $J_{P–C}$ = 3.9 Hz), 121.4, 114.1, 81.5, 81.2, 80.3, 80.2, 26.6, 26.5, 26.4, 26.4, 25.3, 25.3. [See spectrum]

¹¹B NMR (193 MHz, THF) δ 42.6, 31.8. [See spectrum]

³¹P NMR (243 MHz, THF) δ 107.4. [See spectrum]

Elemental Analysis: Anal. Calcd for C₄₈H₆₀B₃IrN₃O₉P: C, 53.45; H, 5.61; N, 3.90. Found: C, 53.64; H, 5.62; N, 3.76.

In Situ Generation of (L5)Ir(Bpin)₃
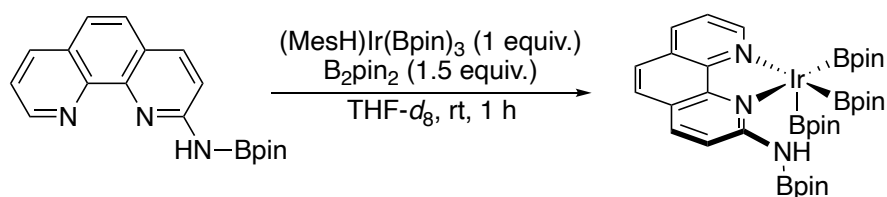
In a nitrogen glovebox, a 4 mL vial was sequentially charged with *N*-(4,4,5,5-tetramethyl-1,3,2-dioxaborolan-2-yl)-1,10-phenanthrolin-2-amine (**L5**, 8.03 mg, 25.0 µmol, 1.00 equiv), (MesH)Ir(Bpin)₃ (17.3 mg, 25.0 µmol, 1.00 equiv), and B₂pin₂ (9.52 mg, 37.5 µmol, 1.50 equiv). A magnetic stirbar was added to the vial. THF-d_8 (0.5 mL) was introduced to the vial under vigorous stirring, and the vial was sealed with a Teflon cap. The orange solution was stirred at rt for 1 h and transferred to an NMR tube for characterization. No iridium hydride species were detected. The resonances of the major species match those observed from the complexation of **L1** with (MesH)Ir(Bpin)₃ in the presence of excess B₂pin₂ (see above).

Note: If no B₂pin₂ is added to the reaction, then immediate precipitation of iridium black occurs upon mixing **L5** and (MesH)Ir(Bpin)₃.

¹H NMR (700 MHz, THF) δ 10.06 (d, *J* = 4.8 Hz, 1H), 8.59 (s, 1H), 8.22 (dd, *J* = 8.7, 4.2 Hz, 2H), 8.06 (d, *J* = 8.8 Hz, 1H), 7.86 (d, *J* = 8.5 Hz, 1H), 7.63 (d, *J* = 8.4 Hz, 1H), 7.44 (dd, *J* = 8.0, 5.0 Hz, 1H), 6.89 (s, 3H), 2.37 (s, 9H).
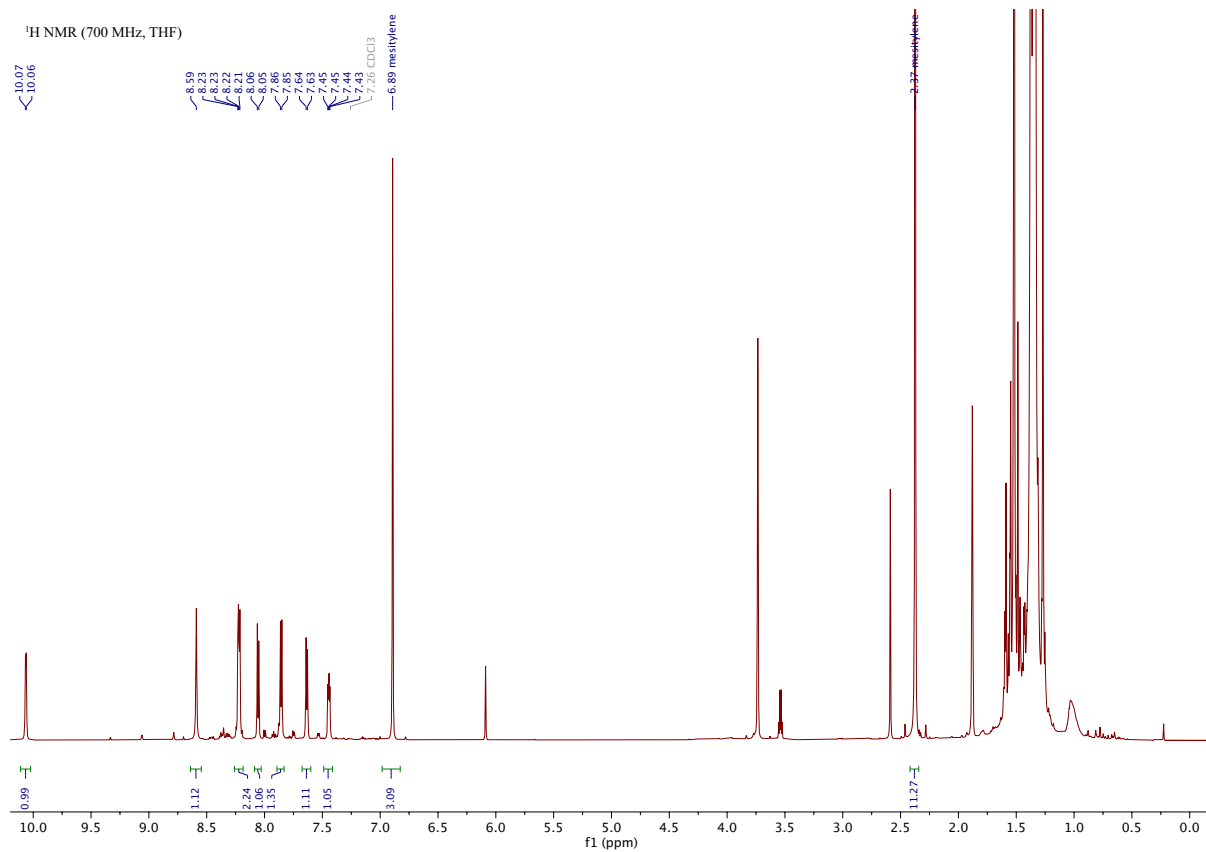
Figure 3.20: ^{1}H NMR spectrum of in situ generated (L5)Ir(Bpin)$_3$.

Isolation of (L5)Ir(Bpin)₃
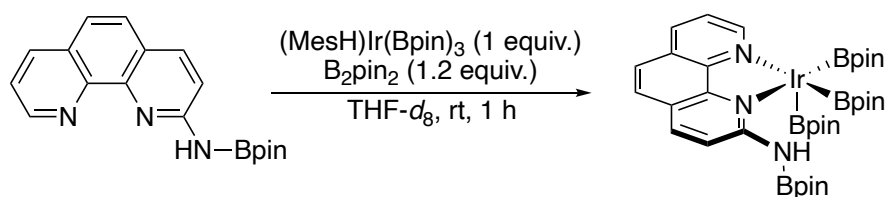
In a nitrogen glovebox, a 4 mL vial was sequentially charged with *N*-(4,4,5,5-tetramethyl-1,3,2-dioxaborolan-2-yl)-1,10-phenanthrolin-2-amine (**L5**, 60.0 mg, 187 μmol, 1.00 equiv), (MesH)Ir(Bpin)₃ (130 mg, 187 μmol, 1.00 equiv), and B₂pin₂ (56.9 mg, 224 μmol, 1.20 equiv). A magnetic stirbar was added to the vial. THF (1 mL) was introduced to the vial under vigorous stirring, and the vial was sealed with a Teflon cap. The orange solution was stirred at rt for 40 min, after which time all volatile materials were evaporated in vacuo. Pentane (2 mL) was added to the residue. The mixture was stirred for 30 min, and a dark orange solid precipitated. The solid was collected by filtration to afford (**L5**)Ir(Bpin)₃ (44.5 mg, 26%). The solid could be stored in the freezer at -35 ºC under an inert atmosphere. Redissolving the solid in THF or DCM led to decomposition within 10 min, which precluded the collection of ¹³C NMR spectra.

¹H NMR (600 MHz, THF) δ 10.05 (s, 1H), 8.56 (s, 1H), 8.09 (d, *J* = 8.9 Hz, 1H), 8.04 (d, *J* = 7.7 Hz, 1H), 7.98 (d, *J* = 8.8 Hz, 1H), 7.68 (d, *J* = 8.4 Hz, 1H), 7.38 (d, *J* = 8.1 Hz, 1H), 7.30 (t, *J* = 6.7 Hz, 1H), 1.36 (s, 12H), 1.18 (s, 36H). [See spectrum]

¹¹B NMR (193 MHz, THF) δ 29.8, 26.0, 21.0. [See spectrum]

Stoichiometric Reactivity of (L5)Ir(Bpin)₃ with 1,3-Dichlorobenzene
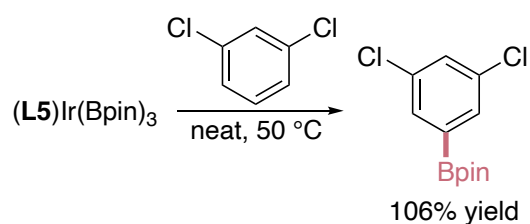
106% yield

In a nitrogen glovebox, a 4 mL vial was charged with (**L5**)Ir(Bpin)₃ (4.6 mg, 5.0 µmol) and adamantane (6.8 mg, 50 µmol), and a magnetic stirbar was added, followed by 1,3-dichlorobenzene (0.2 mL). The vial was sealed with a Teflon-lined cap, and the vial was removed from the glovebox and heated at 50 ºC in a preheated aluminum heating block for 1 h. An aliquot of the reaction mixture was removed and analyzed by GC-FID analysis. The yield of 2-(3,5-dichlorophenyl)-4,4,5,5-tetramethyl-1,3,2-dioxaborolane was determined to be 106% based on the starting iridium complex.

Stoichiometric Reactivity of (L5)Ir(Bpin)₃ with THF
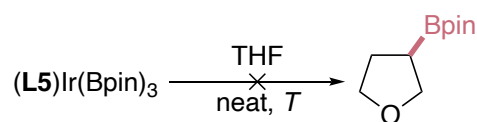
In a nitrogen glovebox, a 4 mL vial was charged with (**L5**)Ir(Bpin)₃ (4.6 mg, 5.0 µmol) and adamantane (6.8 mg, 50 µmol), and a magnetic stirbar was added, followed by THF (0.2 mL). The vial was sealed with a Teflon-lined cap, and the vial was removed from the glovebox and heated at either 65 ºC or 100 ºC in a preheated aluminum heating block for 1 h. An aliquot of the reaction mixture was removed and analyzed by GC-FID analysis. The yield of 4,4,5,5-tetramethyl-2-(tetrahydrofuran-3-yl)-1,3,2-dioxaborolane was determined to be 0% in both cases.

Catalytic Reactivity of (L5)Ir(Bpin)₃ with THF
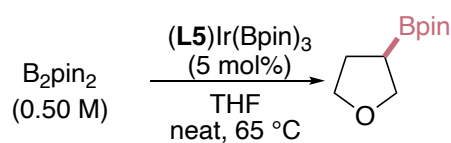
In a nitrogen glovebox, a 4 mL vial was charged with (**L5**)Ir(Bpin)₃ (5.6 mg, 6.2 µmol, 5.0 mol%), B₂pin₂ (31.7 mg, 125 µmol, 1.00 equiv), and adamantane (8.5 mg, 62 µmol, 0.50 equiv). A magnetic stirbar was added, followed by THF (0.25 mL). The vial was sealed with a Teflon-lined cap, and the vial was removed from the glovebox and heated at 65 °C in a preheated aluminum heating block. At the specified timepoints, the vial was cooled to rt, returned to the glovebox, and an aliquot was removed for GC-FID analysis.
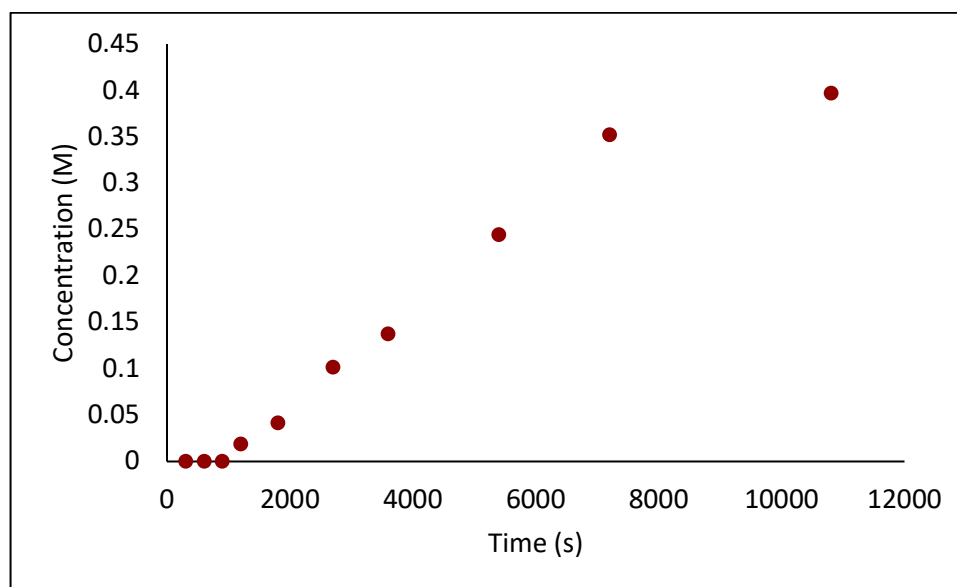
Figure 3.21: Timecourse of the borylation of THF catalyzed by (L5)Ir(Bpin)₃.

Synthesis of (L5)Ir(Bpin)₃(P(OPh)₃)
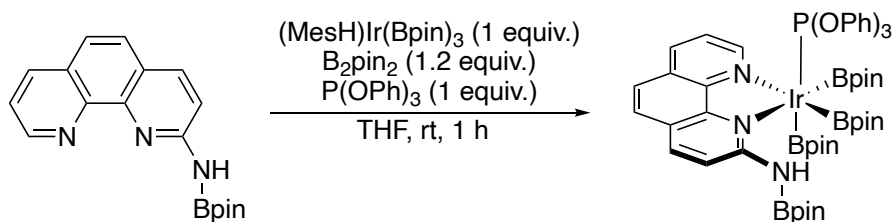
In a nitrogen glovebox, a 20 mL vial was sequentially charged with *N*-(4,4,5,5-tetramethyl-1,3,2-dioxaborolan-2-yl)-1,10-phenanthrolin-2-amine (**L5**, 40.0 mg, 0.125 mmol), (MesH)Ir(Bpin)₃ (86.3 mg, 0.125 mmol, 1.00 equiv), and B₂pin₂ (37.9 mg, 0.125 mmol, 1.20 equiv). A magnetic stirbar was added to the vial. THF (1 mL) was introduced to the vial under vigorous stirring, and the vial was sealed with a Teflon cap. After 10 min, triphenylphosphite (38.6 mg, 125 µmol, 1.00 equiv) was added. The solution turned a deep orange color and was further stirred at room temperature for 1 h. All volatile materials were evaporated in vacuo, and 2 mL of pentane was added to the residue. The mixture was stirred vigorously for 30 min, during which time small amounts of orange powder precipitated. The mixture was filtered, the filtrate was diluted with hexamethyl disiloxane (HMDSO) (4 mL), and the solution stored at -35 ºC. The brown-yellow solids that formed were collected by filtration and washed with cold HMDSO to afford the title compound as deep yellow crystals (62 mg, 56%). Single crystals suitable for X-ray crystallography were grown by slow diffusion of TMS into an ether solution of the compound containing a drop of THF.

¹H NMR δ 9.98 (d, *J* = 5.2 Hz, 1H), 8.87 (bs, 1H), 8.10 (d, *J* = 8.0 Hz, 1H), 7.97 (d, *J* = 8.9 Hz, 1H), 7.92 (d, *J* = 8.9 Hz, 1H), 7.69 (d, *J* = 8.5 Hz, 1H), 7.58 (d, *J* = 8.6 Hz, 1H), 7.28 (dd, *J* = 8.0, 5.1 Hz, 1H), 6.85 – 6.81 (m, 6H), 6.81 – 6.75 (m, 6H), 6.71 – 6.66 (m, 3H), 1.37 (s, 6H), 1.34 (s, 6H), 1.29 (s, 6H), 1.29 (s, 6H), 1.28 (s, 12H), 0.47 (s, 6H), 0.43 (s, 6H). [See spectrum]

¹³C NMR (151 MHz, THF) δ 160.4, 154.8, 154.4 (d, *J*$_{P-C}$ = 10.4 Hz), 150.2, 149.1, 136.9, 134.7, 131.4, 129.0, 129.0, 127.0, 126.1, 123.4, 123.4, 123.2, 122.5 (d, *J*$_{P-C}$ = 4.1 Hz), 115.8, 84.0, 81.8, 81.2, 80.0, 80.0, 26.5, 26.2, 26.1, 26.0, 25.8, 25.0, 25.0. [See spectrum]

¹¹B NMR (193 MHz, THF) δ 42.0, 31.8, 24.1. [See spectrum]

³¹P NMR (243 MHz, THF) δ 108.2. [See spectrum]

Elemental Analysis: Anal. Calcd for C₅₄H₇₁B₄IrN₃O₁₁P: C, 53.84; H, 5.94; N, 3.49. Found: C, 54.22; H, 6.28; N, 3.12.

Crystallographic Data

(L1)Ir(Bpin)₃(P(OPh)₃)

A clear yellow block 0.177 x 0.125 x 0.081 mm in size was mounted on a Cryoloop with Paratone oil. Data were collected on a ROD, Synergy Custom DW system, Pilatus 200K diffractometer in a nitrogen gas stream at 100.00(10) K during data collection using omega scans. Crystal-to-detector distance was 30.23 mm and exposure time was 1.00 seconds per frame using a scan width of 0.5°. Data collection was 99.9% complete to 26.3° in θ. A total of 51159 reflections were collected covering the indices -13≤h≤13, -14≤k≤15, - 23≤l≤23. 9741 reflections were founded to be symmetry independent, with an Rint of 0.0573. Indexing and unit cell refinement indicated a primitive, triclinic lattice. The space group was found to be P - 1 (No. 2). The data were integrated using the CrysAlisPro 1.171.39.46e software program and scaled using the SCALE3 ABSPACK scaling algorithm. Solution by intrinsic phasing (SHELXT-2015) produced a heavy-atom phasing model consistent with the proposed structure. All non-hydrogen atoms were refined anisotropically by full-matrix least-squares (SHELXL2014). All hydrogen atoms were placed using a riding model. Their positions were constrained relative to their parent atom using the appropriate HFIX command in SHELXL-2014.

(L1)Ir(Bpin)₃(P(OPh)₃)

Table 3.2

Crystal data and structure refinement for (L1)Ir(Bpin)₃(P(OPh)₃)

Empirical formula	$C_{48}H_{60}B_3IrN_3O_9P$
Formula weight	1078.59
Temperature/K	100.0
Crystal system	triclinic
Space group	P-1
a/Å	10.81663(19)
b/Å	12.44516(20)
c/Å	18.5000(3)
α/°	94.2696(12)
β/°	100.7164(13)
γ/°	101.8595(14)
Volume/Å³	2378.21(7)
Z	2
ρ_{calc}g/cm³	1.506
μ/mm⁻¹	2.899
F(000)	1096.0
Crystal size/mm³	0.177 × 0.125 × 0.081
Radiation	Mo Kα (λ = 0.71073)
2Θ range for data collection/°	5.722 to 52.742
Index ranges	-13 ≤ h ≤ 13, -14 ≤ k ≤ 15, -23 ≤ l ≤ 23
Reflections collected	51159
Independent reflections	9741 [R_{int} = 0.0573, R_{sigma} = 0.0385]
Data/restraints/parameters	9741/188/818

Goodness-of-fit on F^2 1.041

Final R indexes [I>=2σ (I)] $R_1 = 0.0213$, $wR_2 = 0.0490$

Final R indexes [all data] $R_1 = 0.0249$, $wR_2 = 0.0500$

Largest diff. peak/hole / e Å^{-3} 0.64/-0.56

(L5)Ir(Bpin)₃(P(OPh)₃)

A clear light yellow block 0.386 x 0.304 x 0.245 mm in size was mounted on a Cryoloop with Paratone oil. Data were collected on a ROD, Synergy Custom DW system, Pilatus 200K diffractometer in a nitrogen gas stream at 100.00(10) K during data collection using omega scans. Crystal-to-detector distance was 30.23 mm and exposure time was 0.50 seconds per frame using a scan width of 0.5°. Data collection was 99.8% complete to 25.25° in θ. A total of 67995 reflections were collected covering the indices -15≤h≤15, -16≤k≤15, - 31≤l≤31. 15669 reflections were founded to be symmetry independent, with an Rint of 0.0338. Indexing and unit cell refinement indicated a primitive, triclinic lattice. The space group was found to be P -1 (No. 2). The data were integrated using the CrysAlisPro 1.171.39.46e software program and scaled using the SCALE3 ABSPACK scaling algorithm. Solution by intrinsic phasing (SHELXT-2015) produced a heavy-atom phasing model consistent with the proposed structure. All non-hydrogen atoms were refined anisotropically by full-matrix least-squares (SHELXL2014). All hydrogen atoms were placed using a riding model. Their positions were constrained relative to their parent atom using the appropriate HFIX command in SHELXL-2014.

(L5)Ir(Bpin)₃(P(OPh)₃)

Table 3.3

Crystal data and structure refinement for (L5)Ir(Bpin)₃(P(OPh)₃)

Empirical formula	$C_{54}H_{71}B_4IrN_3O_{11}P$
Formula weight	1204.54
Temperature/K	100.0
Crystal system	triclinic
Space group	P-1
a/Å	11.0800(2)
b/Å	11.2036(2)
c/Å	22.4960(4)
α/°	97.497(2)
β/°	93.217(2)
γ/°	96.767(2)
Volume/Å³	2742.14(9)
Z	2
ρ_{calc}g/cm³	1.459
μ/mm⁻¹	2.525
F(000)	1232.0
Crystal size/mm³	0.386 × 0.304 × 0.245
Radiation	Mo Kα (λ = 0.71073)
2Θ range for data collection/°	5.97 to 61.012
Index ranges	-15 ≤ h ≤ 15, -16 ≤ k ≤ 15, -31 ≤ l ≤ 31
Reflections collected	67995
Independent reflections	15669 [R_{int} = 0.0338, R_{sigma} = 0.0256]
Data/restraints/parameters	15669/0/687
Goodness-of-fit on F²	1.024

Final R indexes [I>=2σ (I)] $R_1 = 0.0193$, $wR_2 = 0.0454$

Final R indexes [all data] $R_1 = 0.0215$, $wR_2 = 0.0460$

Largest diff. peak/hole / e Å^{-3} 0.82/-0.76

3.4.7 NMR Spectra

Ligand L1

1,10-phenanthrolin-2-amine   [**Experimental**]

¹H NMR (600 MHz, CDCl₃)

¹³C NMR (151 MHz, CDCl₃)
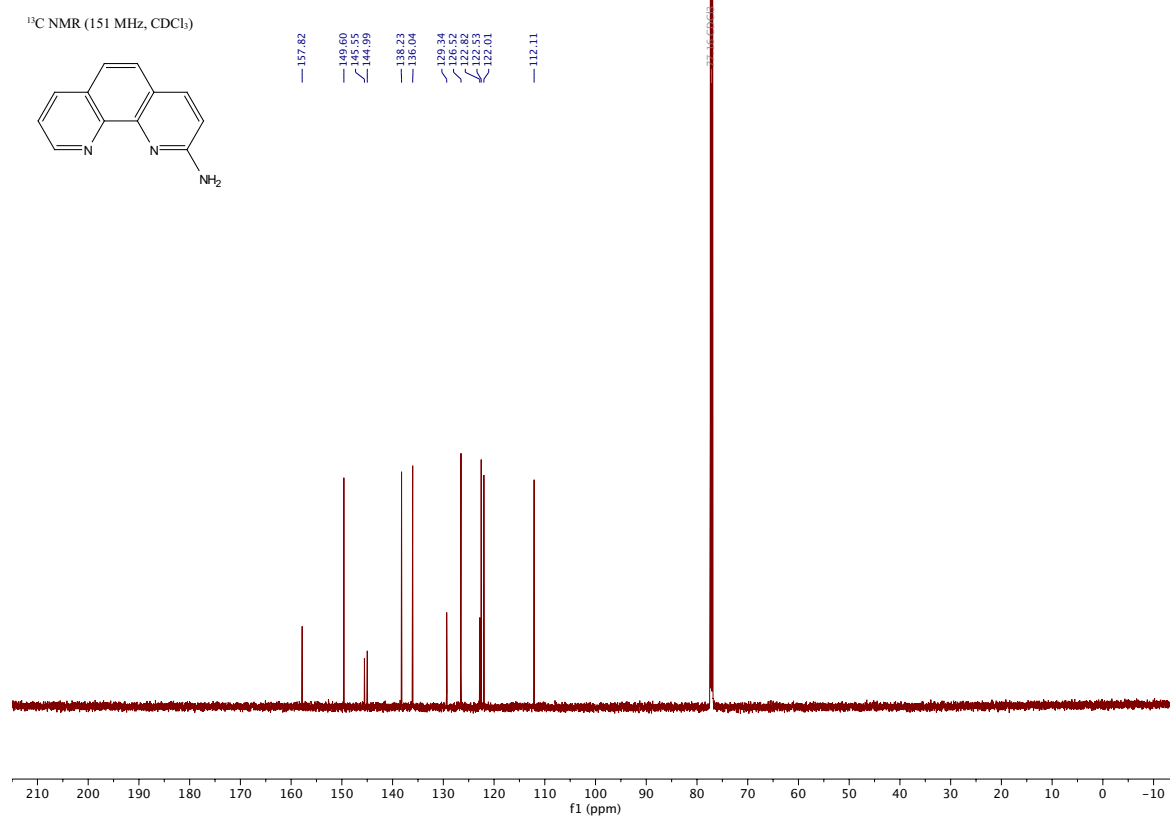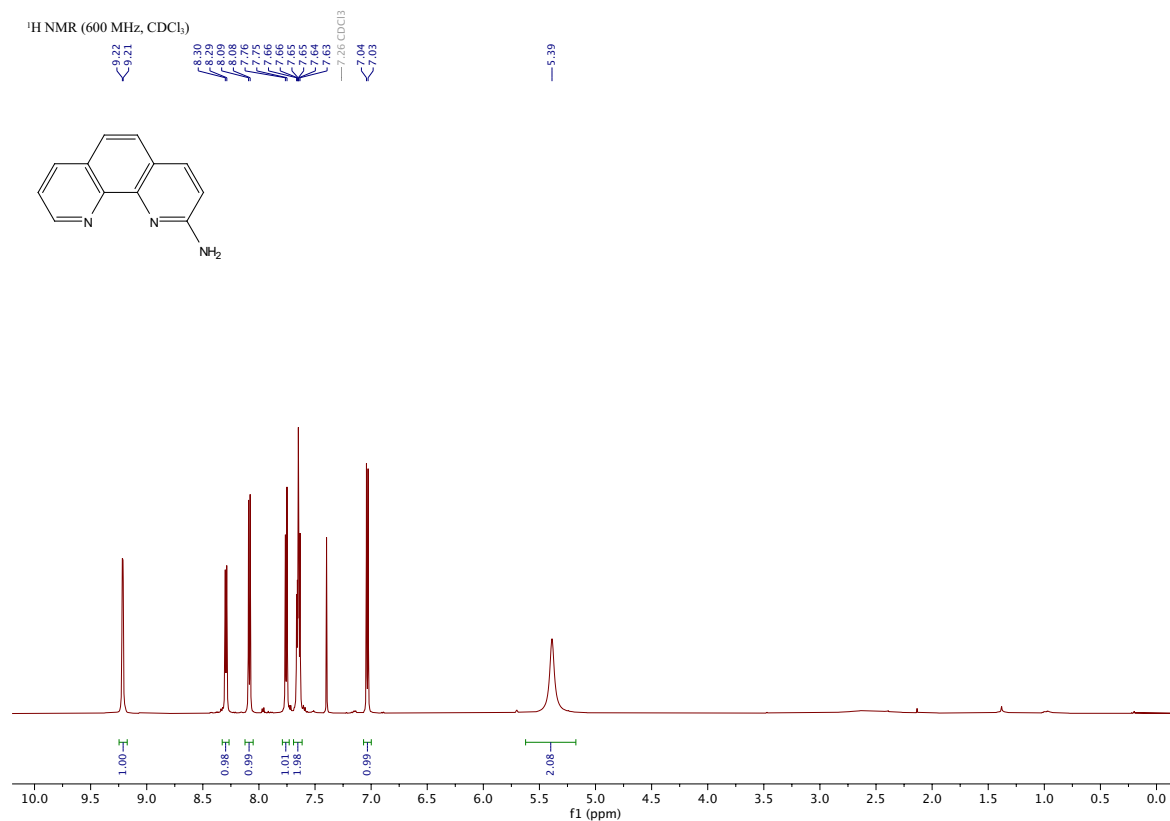
Ligand L2
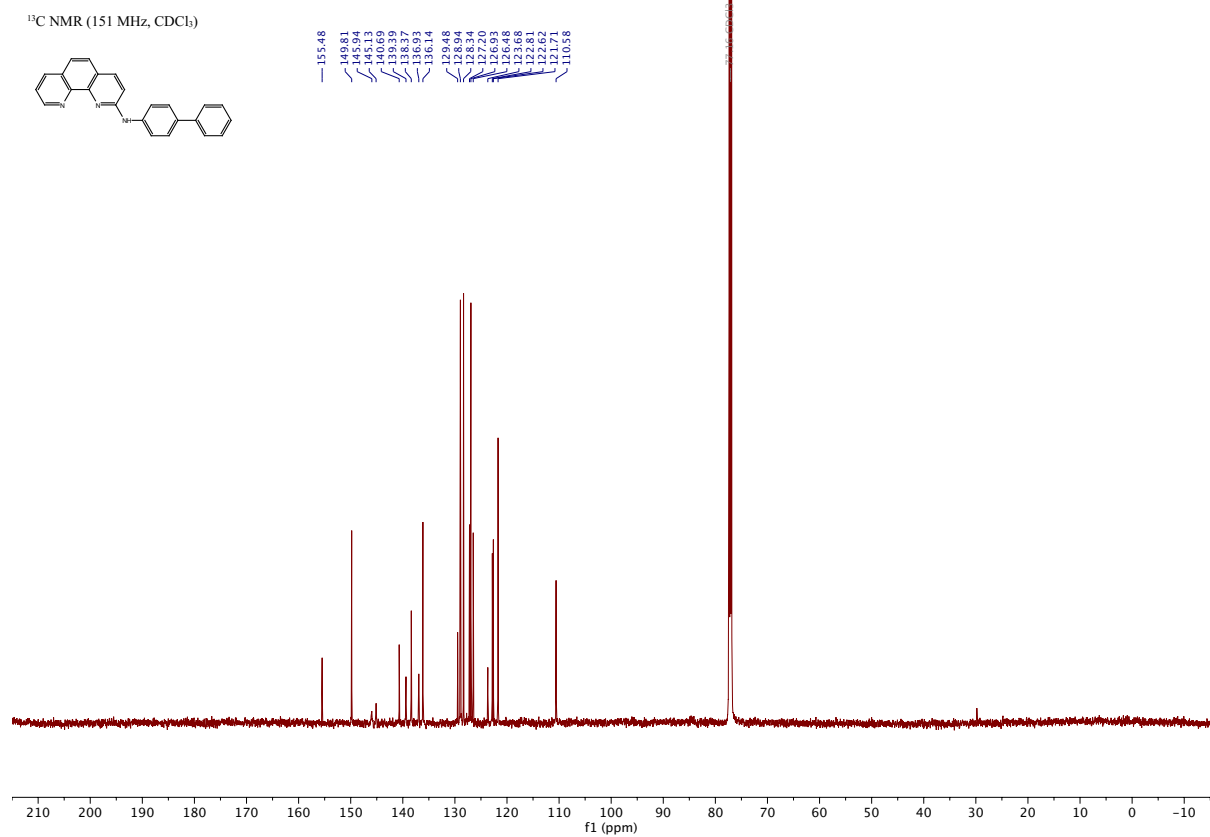
N-methyl-1,10-phenanthrolin-2-amine [Experimental]
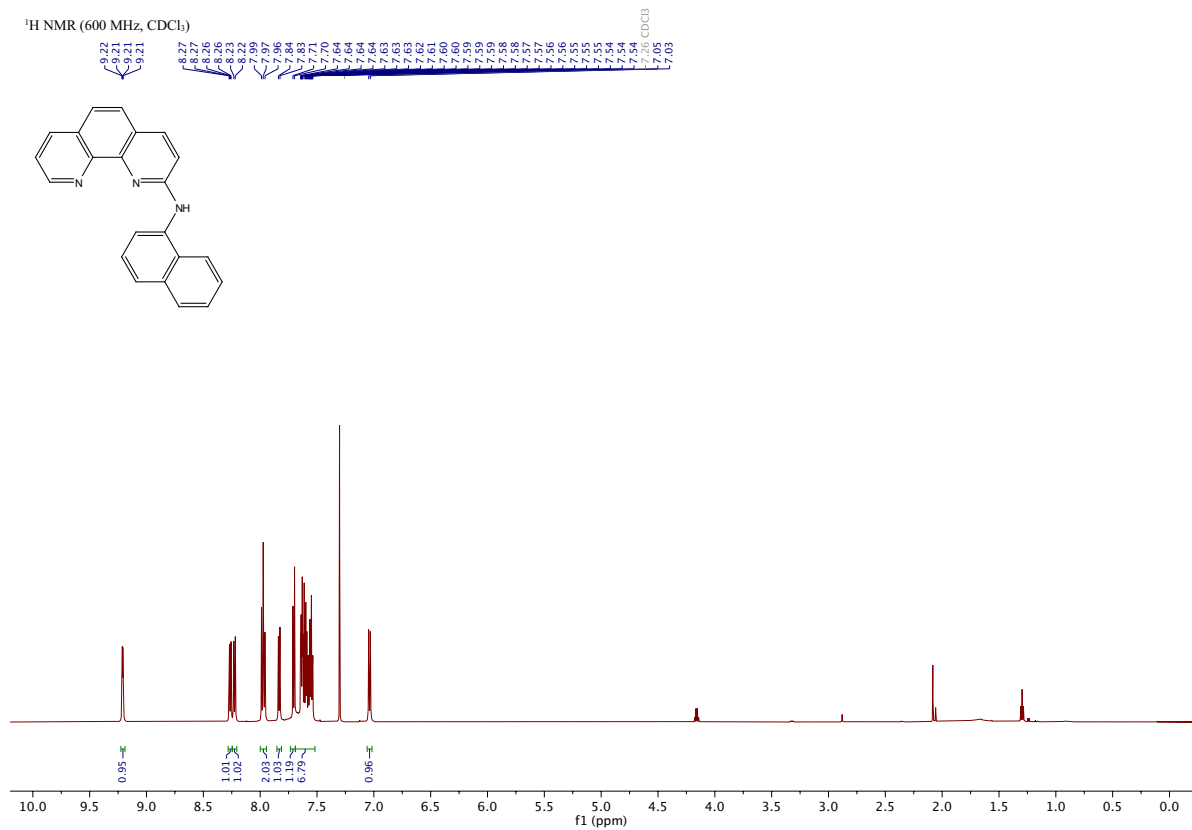
^{1}H NMR (600 MHz, CDCl$_3$)

^{13}C NMR (151 MHz, CDCl$_3$)
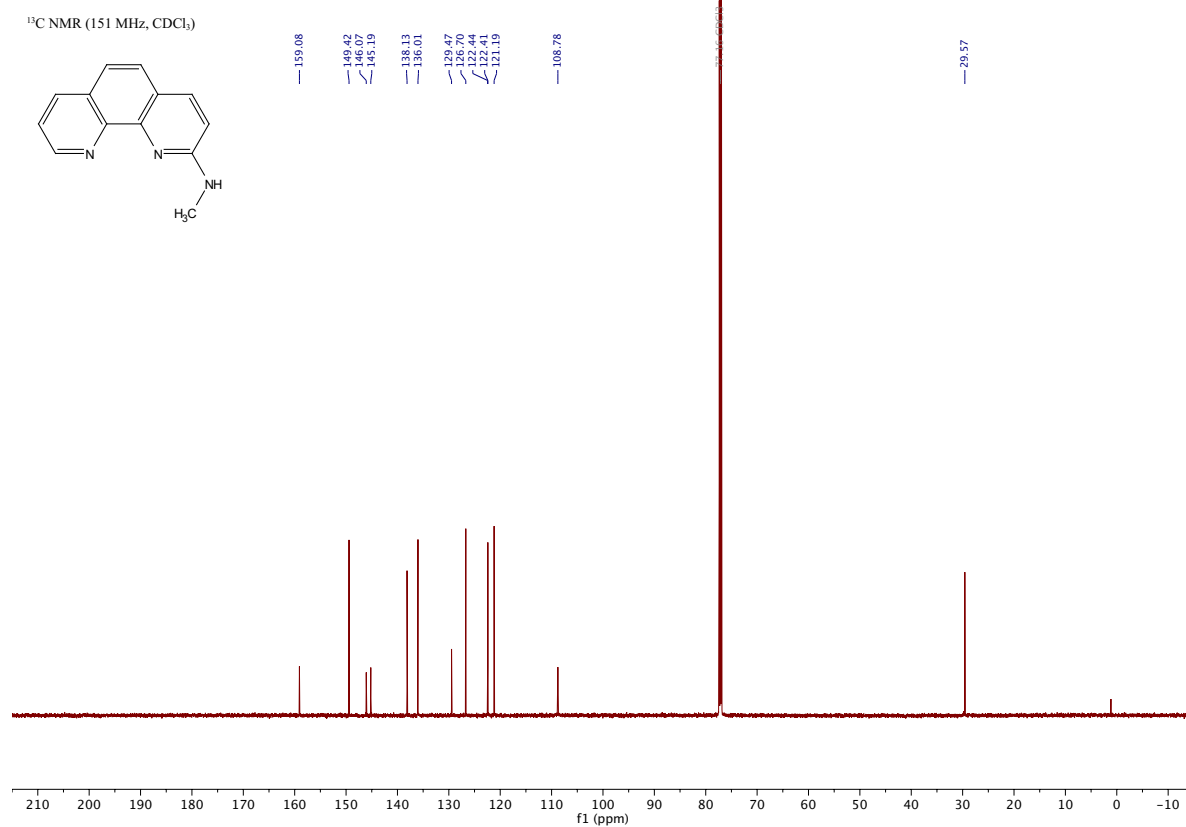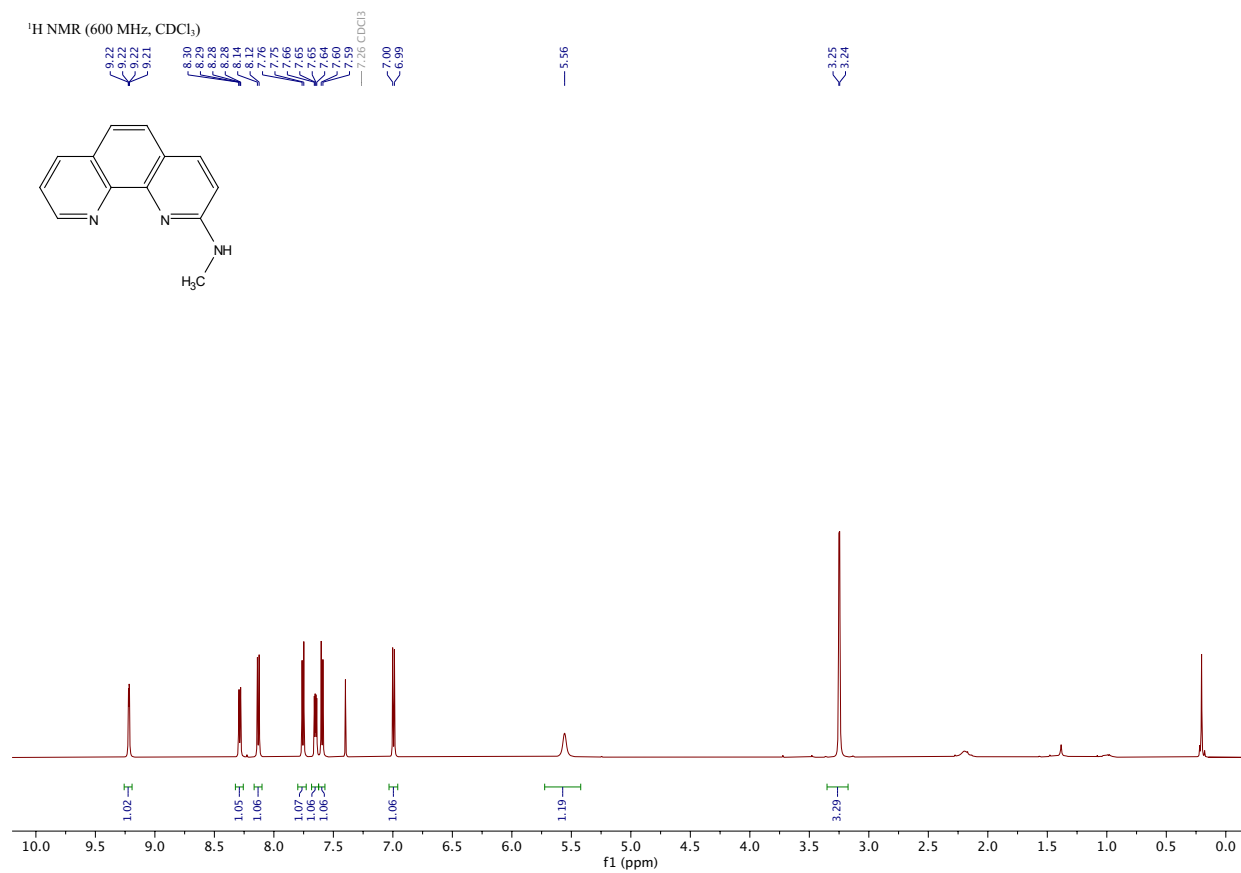
Ligand L3

N-phenyl-1,10-phenanthrolin-2-amine [Experimental]

¹H NMR (600 MHz, CDCl₃)

¹³C NMR (151 MHz, CDCl₃)
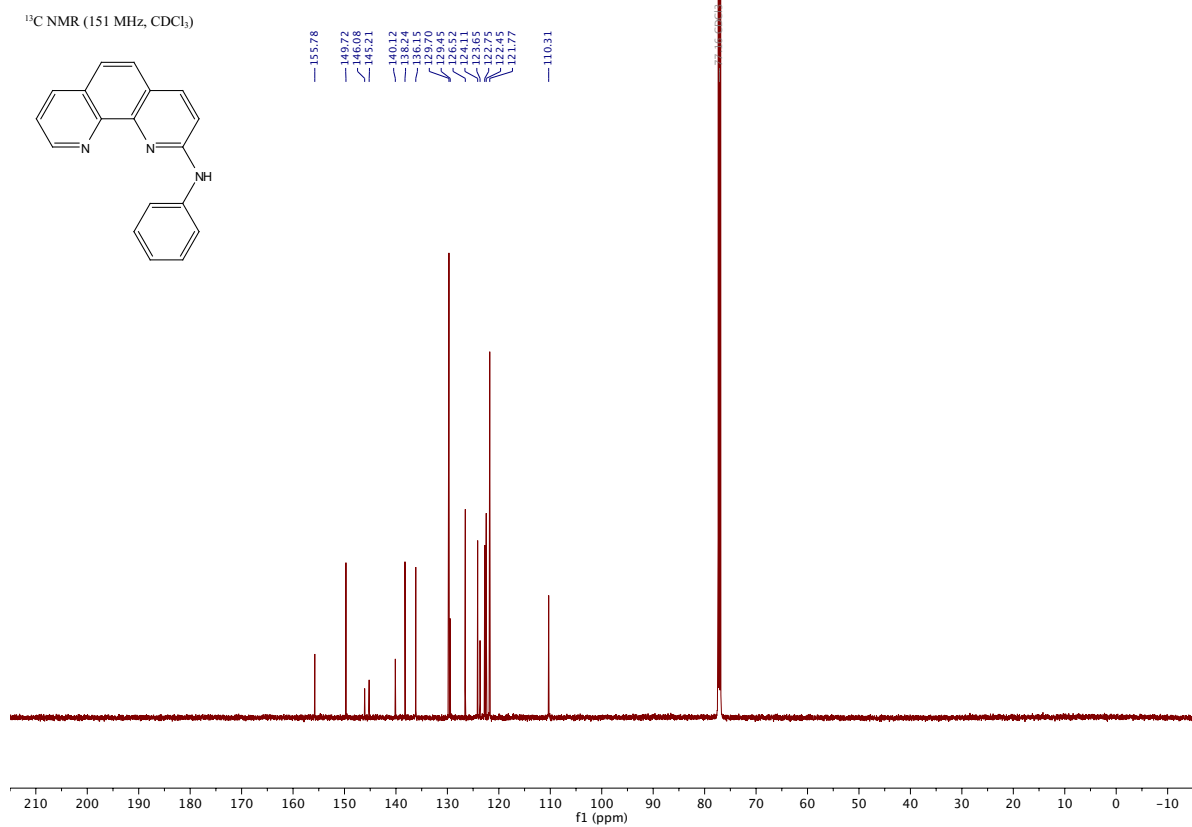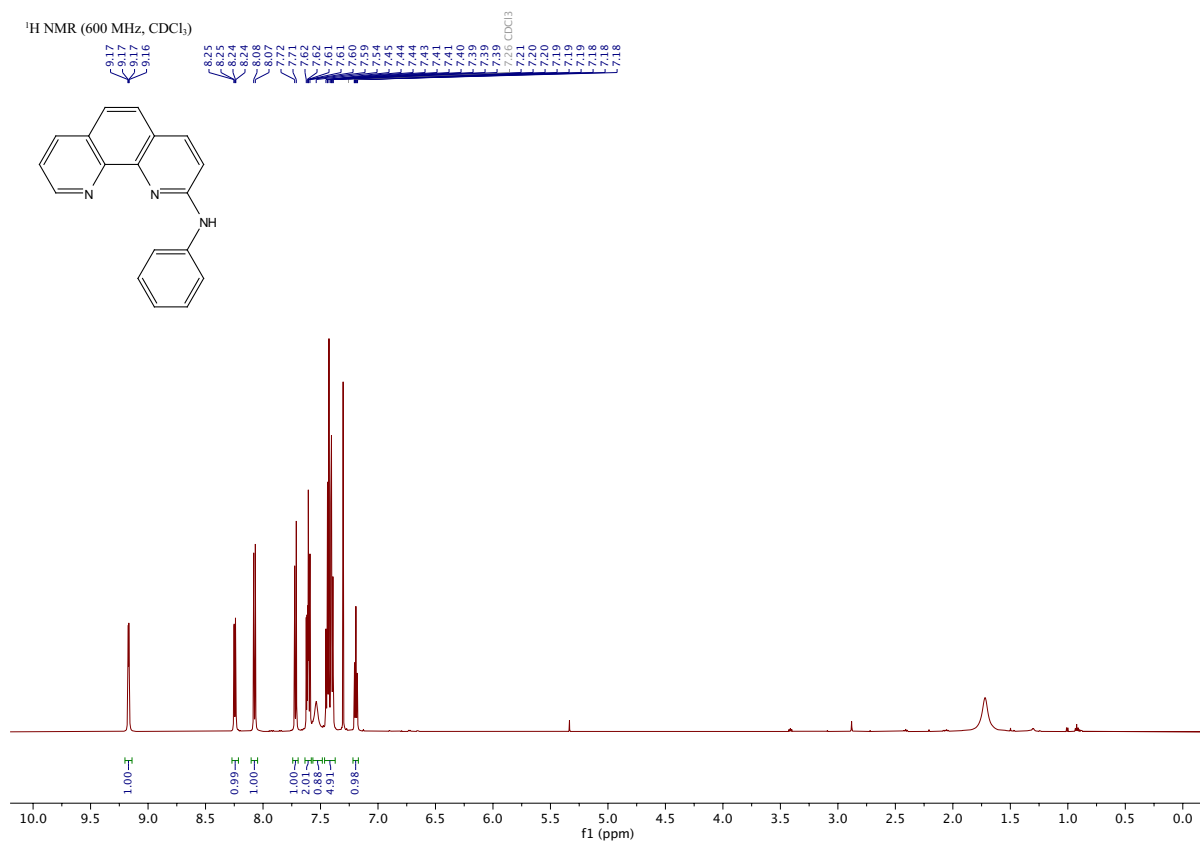
Ligand L4

2-(pyrrolidin-1-yl)-1,10-phenanthroline [Experimental]

^{1}H NMR (500 MHz, CDCl$_3$)

^{13}C NMR (101 MHz, CHLOROFORM-D)

Ligand L5

N-(4,4,5,5-tetramethyl-1,3,2-dioxaborolan-2-yl)-1,10-phenanthrolin-2-amine [Experimental]

¹³C NMR (126 MHz, CDCl₃)
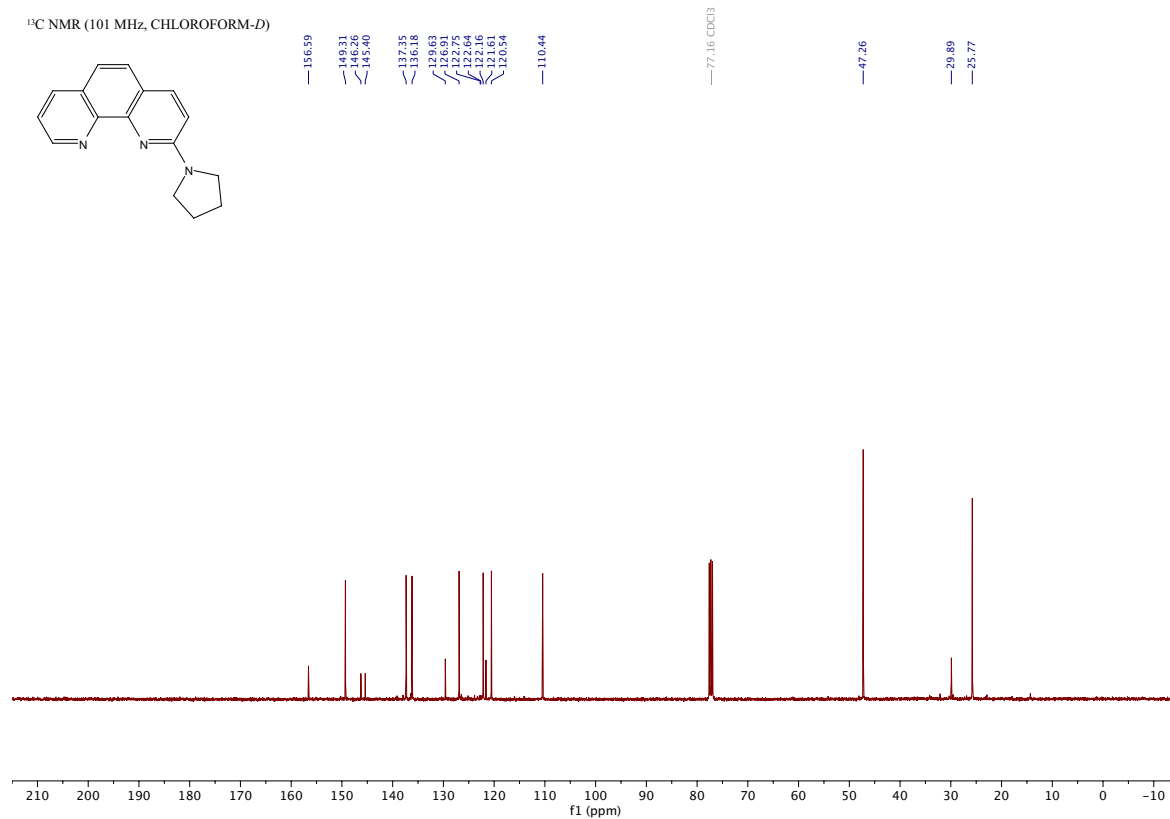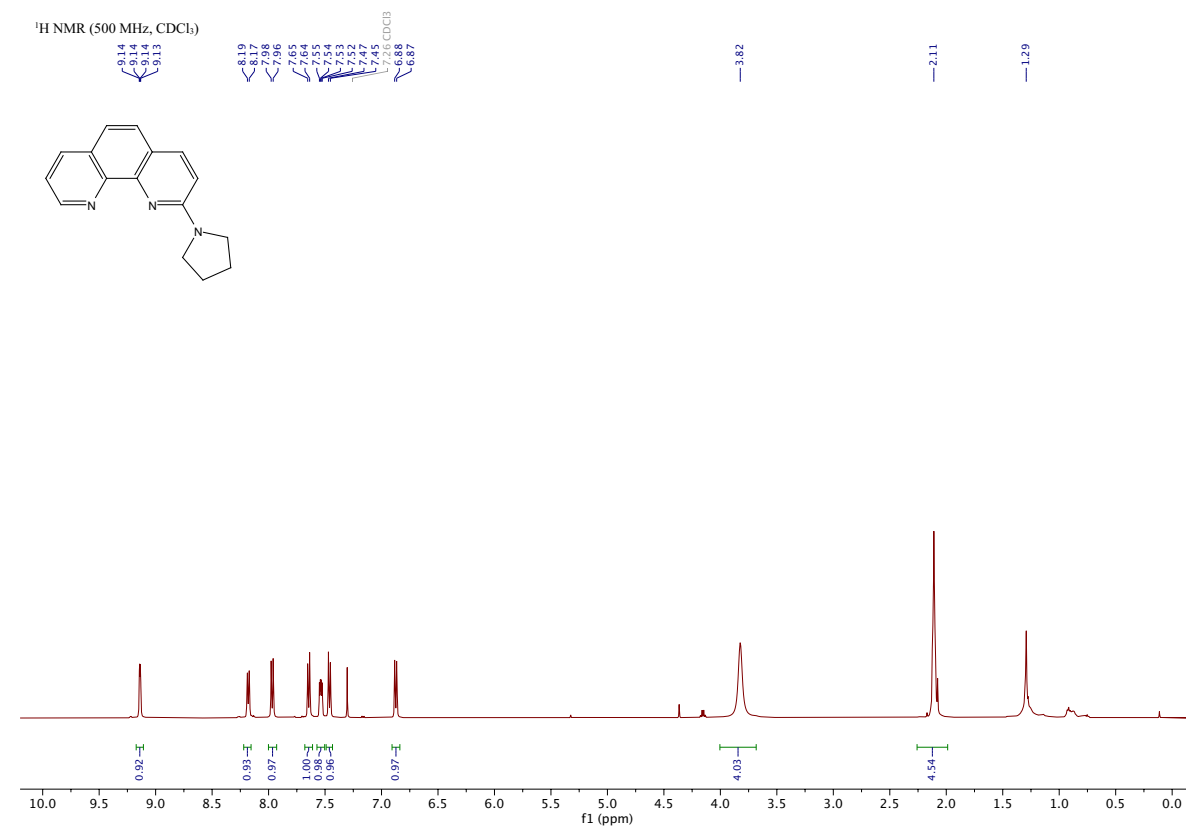
¹³C NMR (126 MHz, CDCl₃)
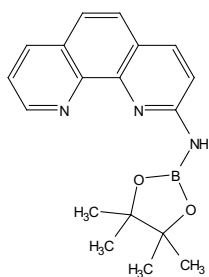
156.52
149.74
145.41
145.31
138.06
136.11
129.15
126.52
124.20
122.97
122.56
114.35
83.46
77.16 CDCl3
24.76
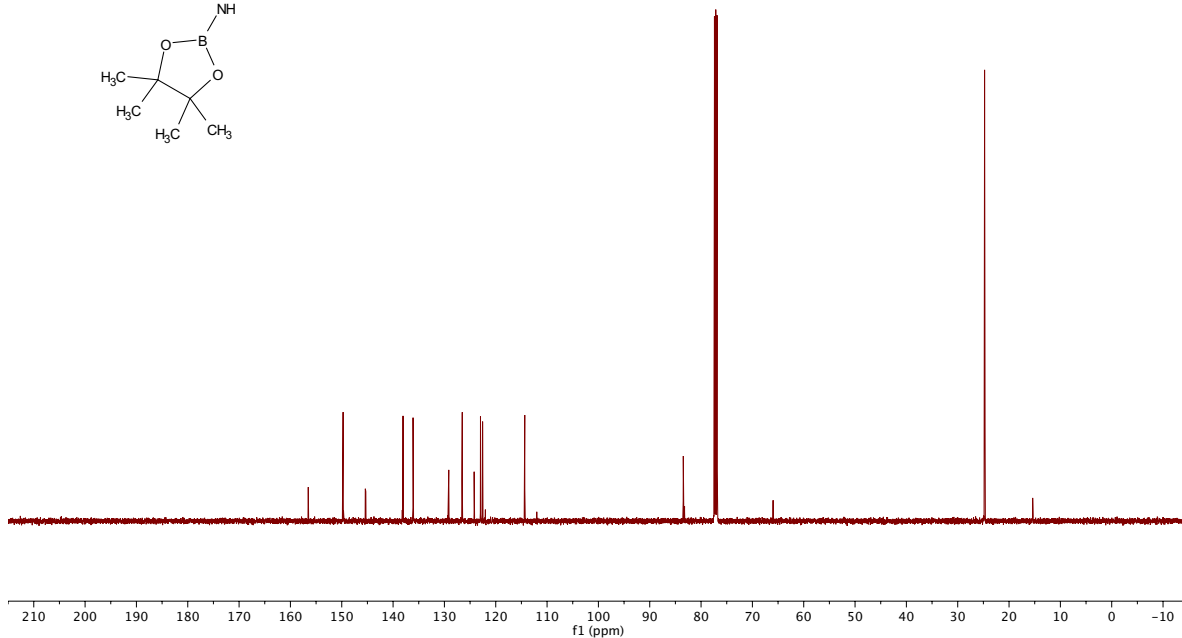
¹¹B NMR (160 MHz, CDCl₃)

24.39

425
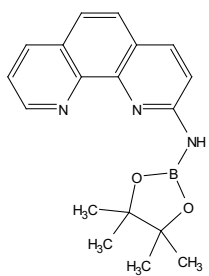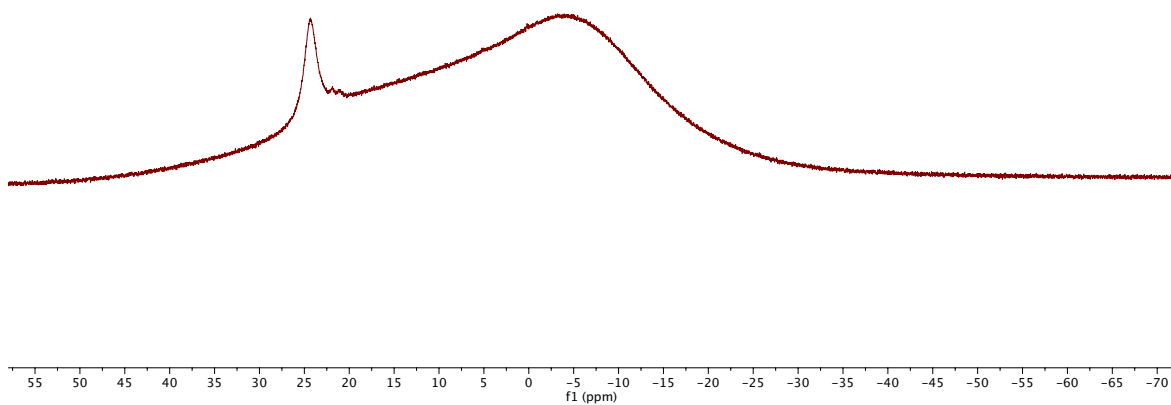
Ligand L6

N-cyclohexyl-1,10-phenanthrolin-2-amine   [Experimental]

¹H NMR (600 MHz, CDCl₃)

¹³C NMR (151 MHz, CDCl₃)
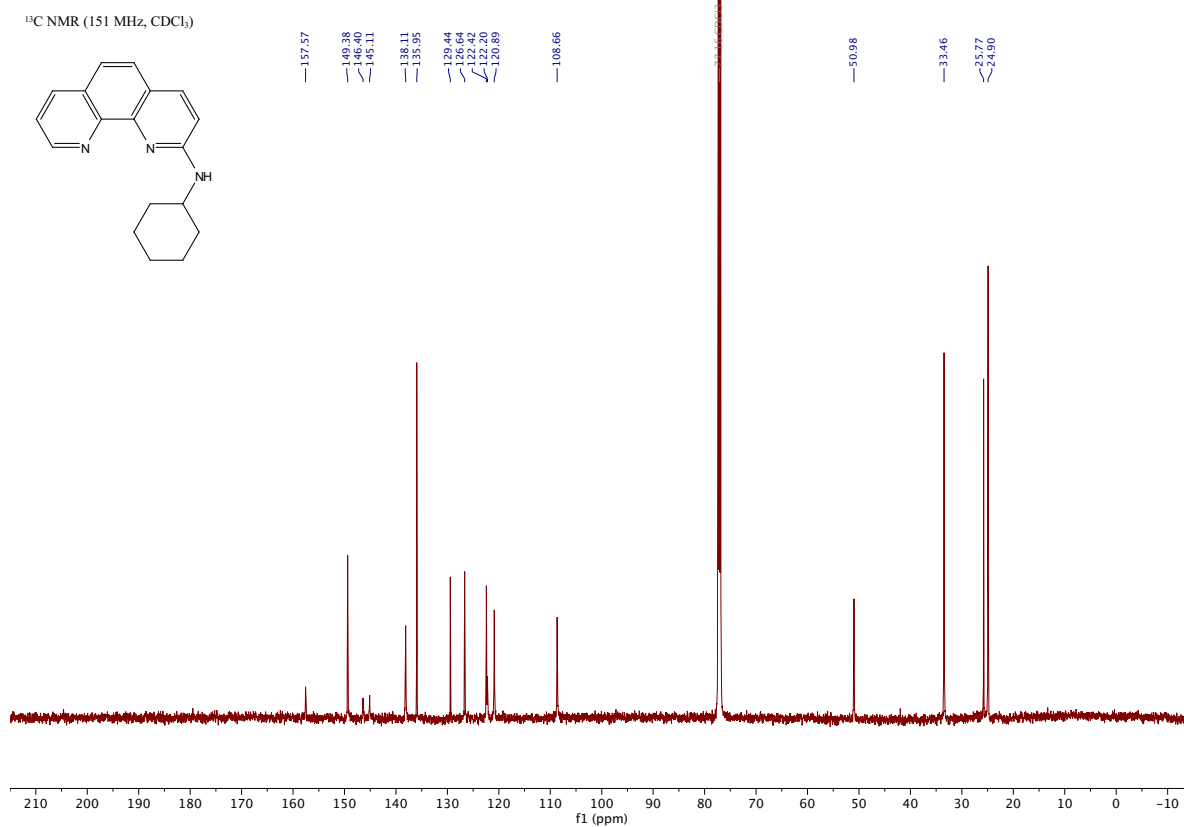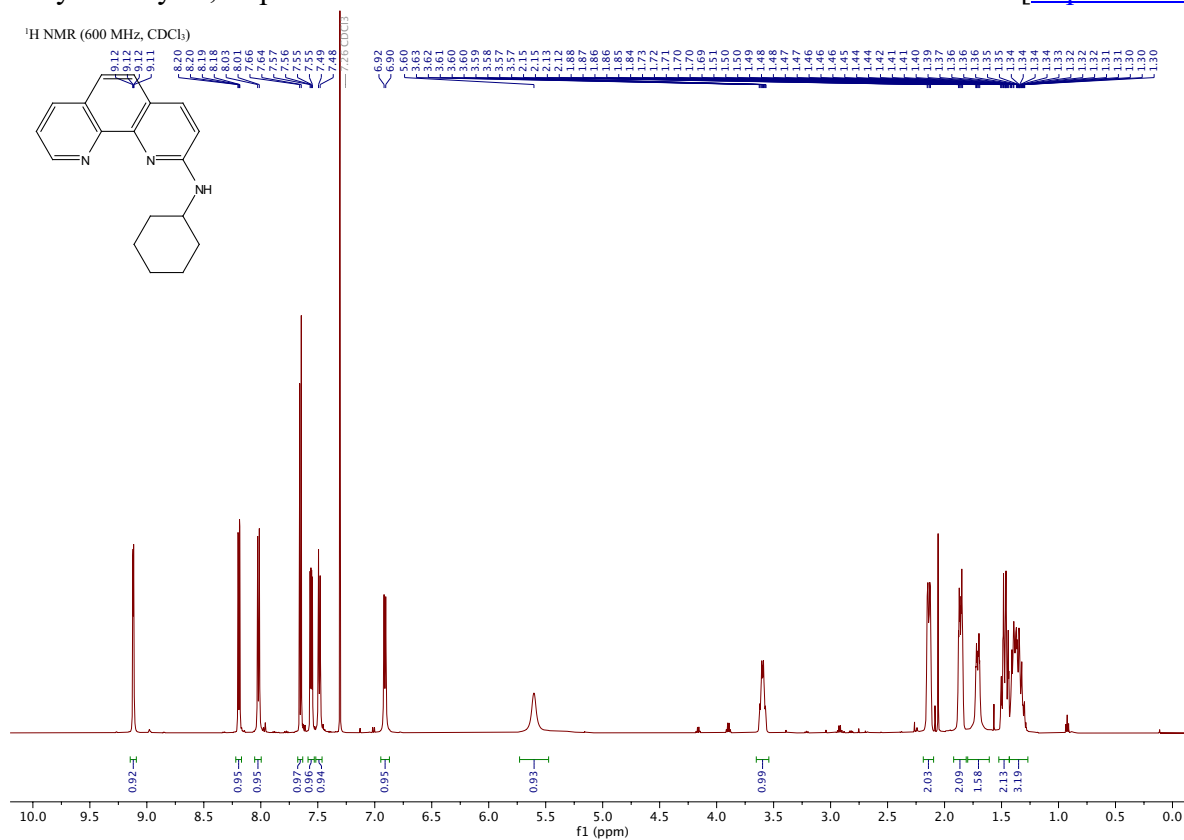
Ligand L7

N-(cyclopropylmethyl)-1,10-phenanthrolin-2-amine [Experimental]
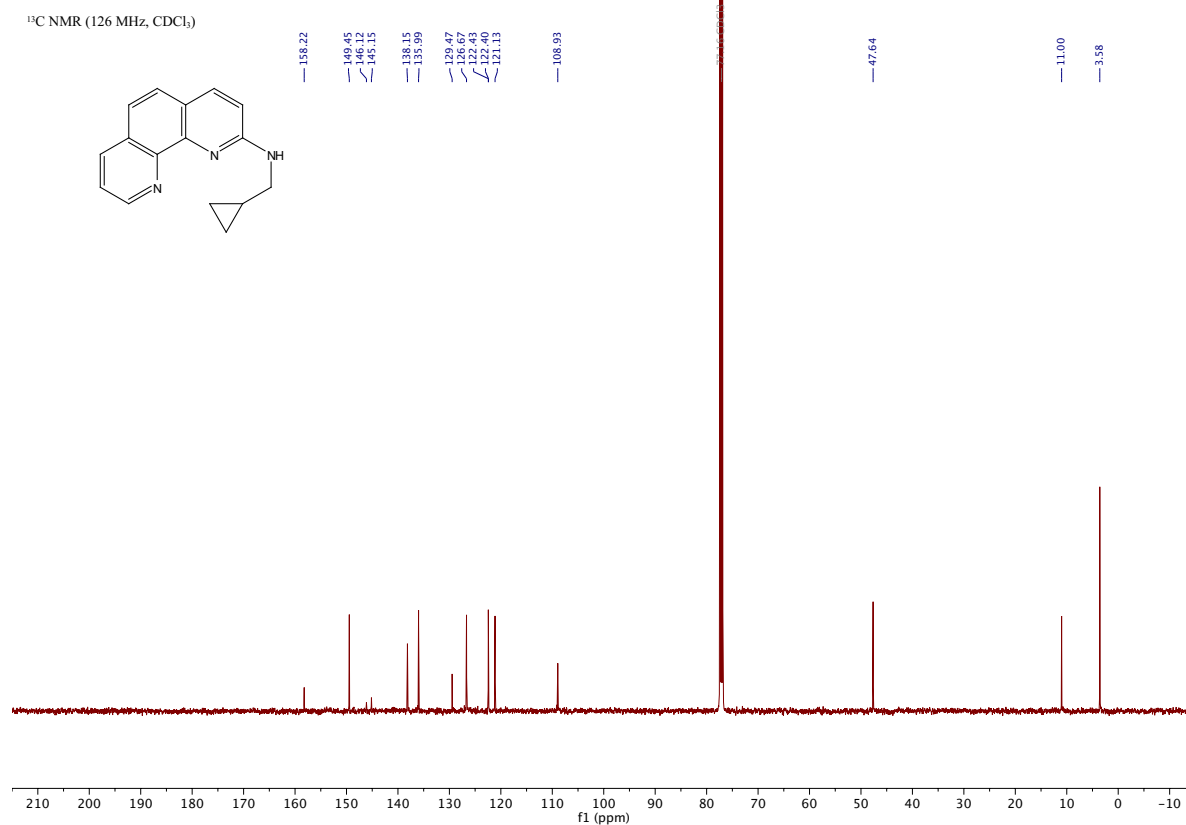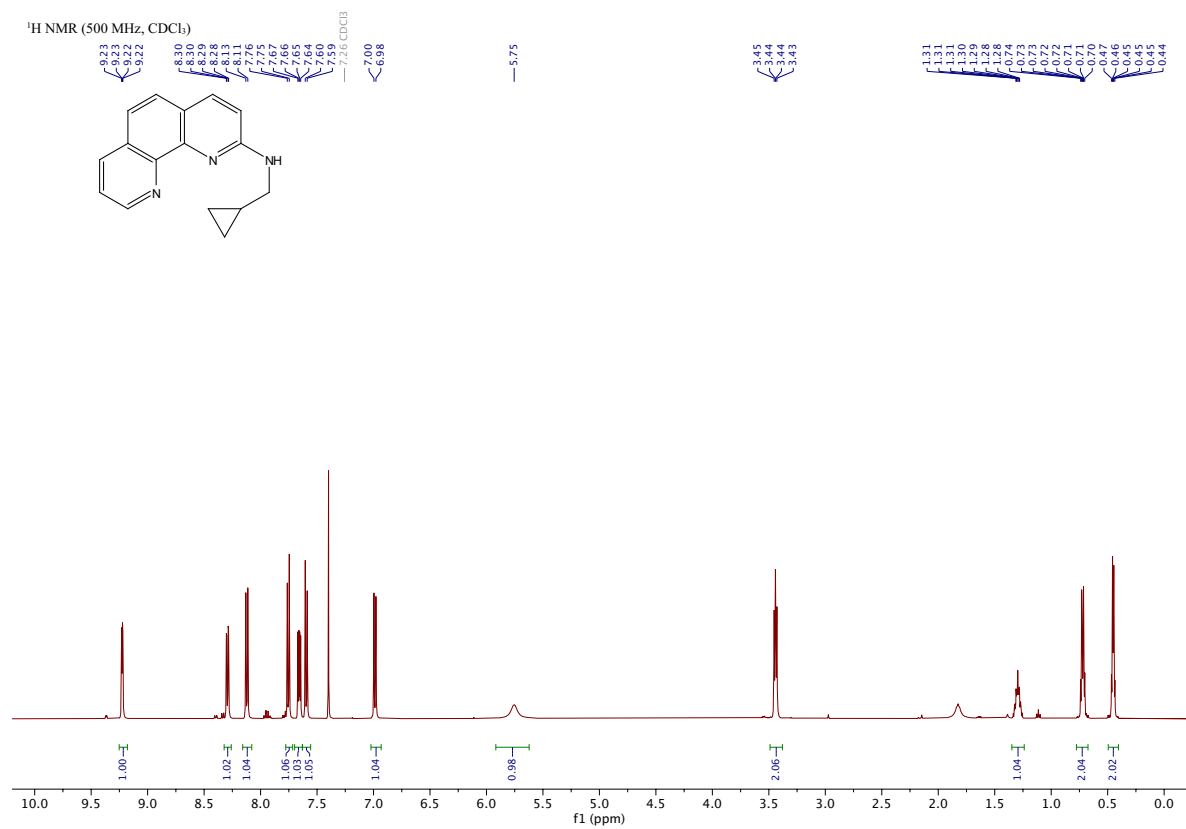
Ligand L8

N-isobutyl-1,10-phenanthrolin-2-amine [Experimental]

^{1}H NMR (500 MHz, CDCl$_3$)

^{13}C NMR (126 MHz, CDCl$_3$)
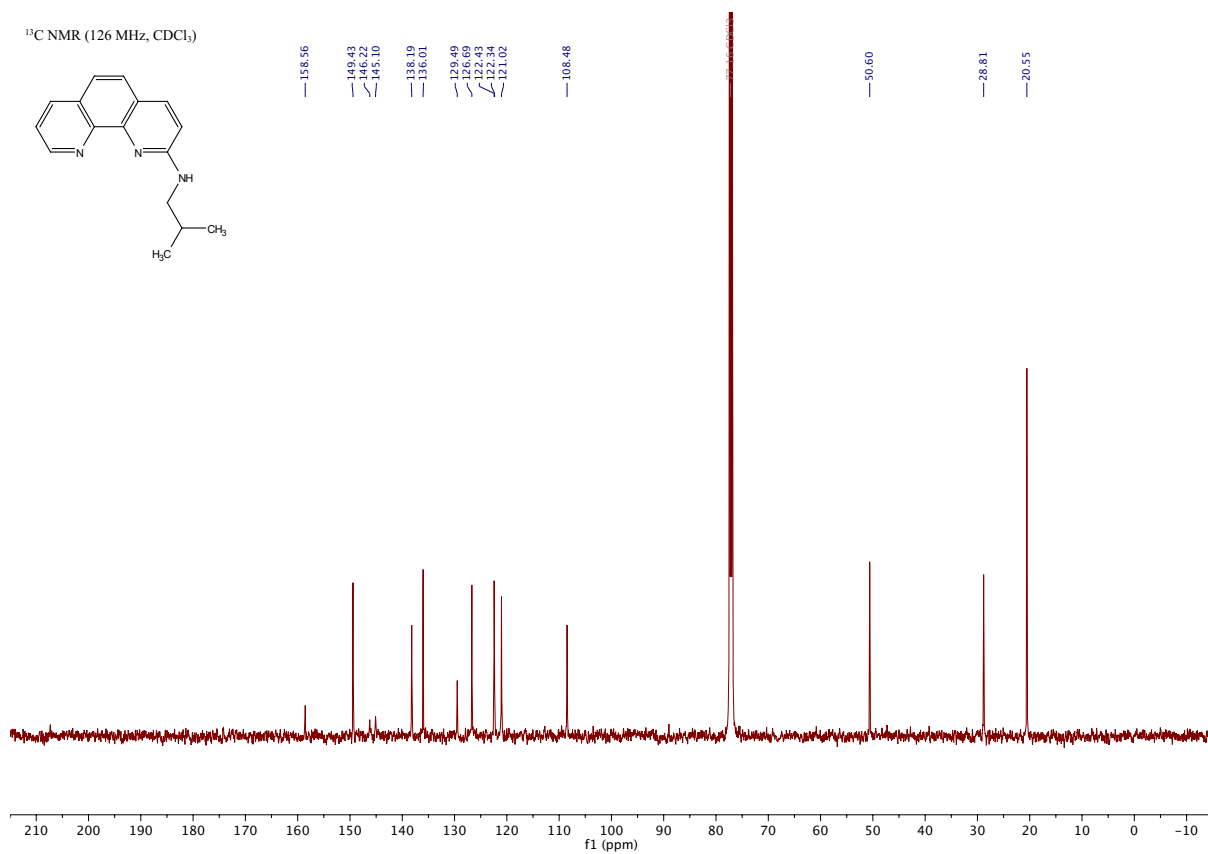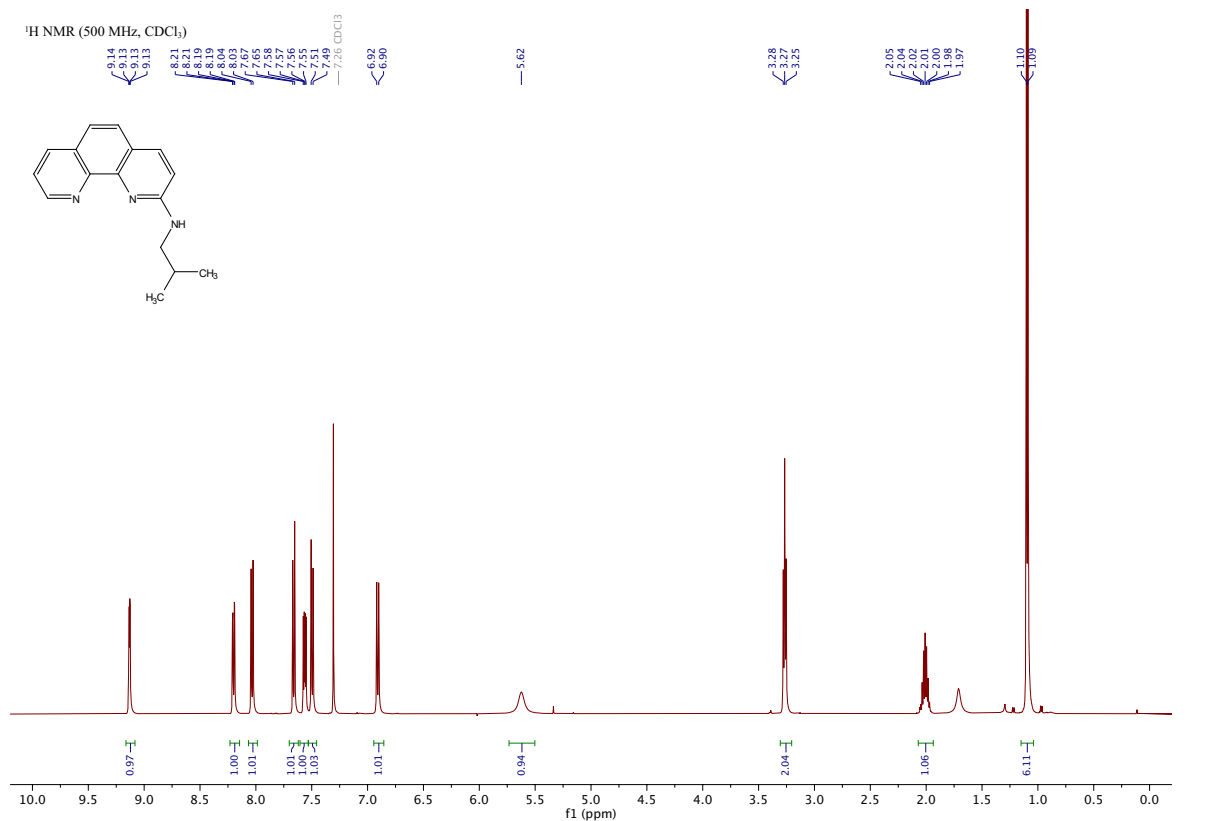
Ligand L9

N-isopentyl-1,10-phenanthrolin-2-amine [Experimental]

¹H NMR (500 MHz, CDCl₃)

¹³C NMR (126 MHz, CDCl₃)
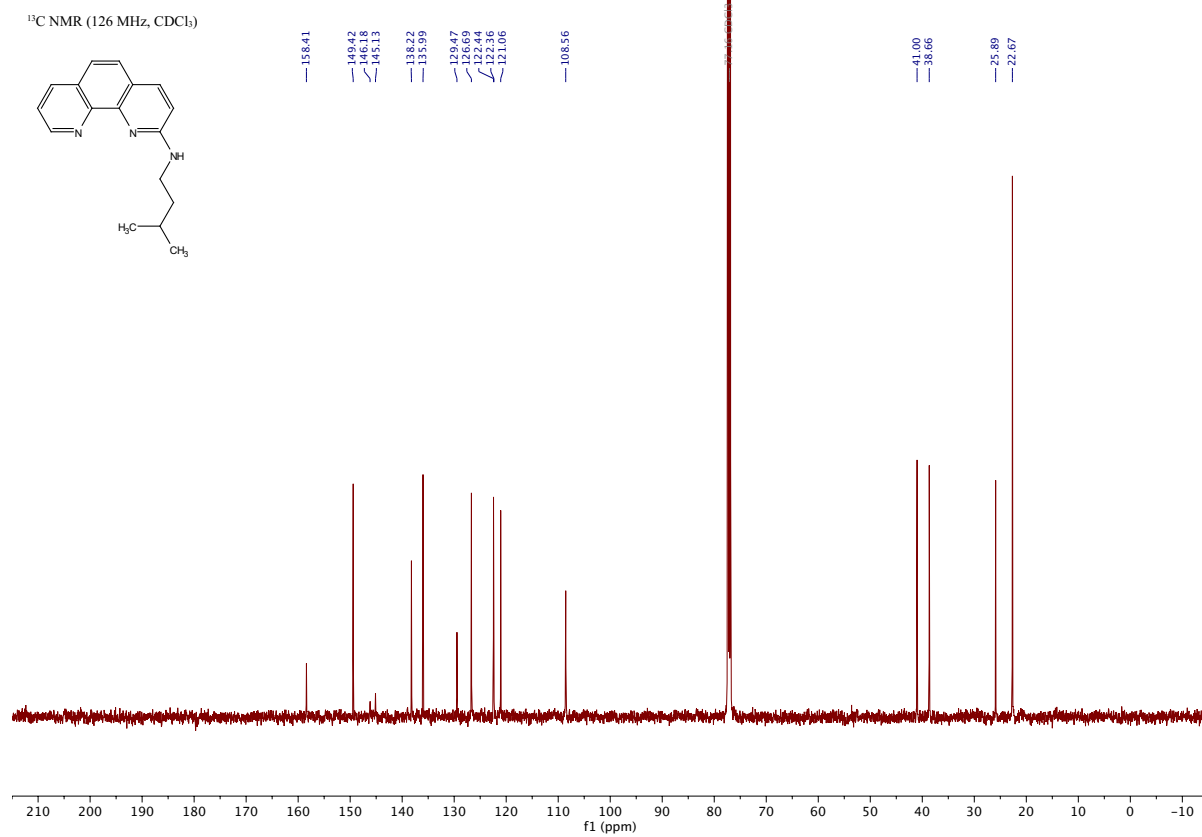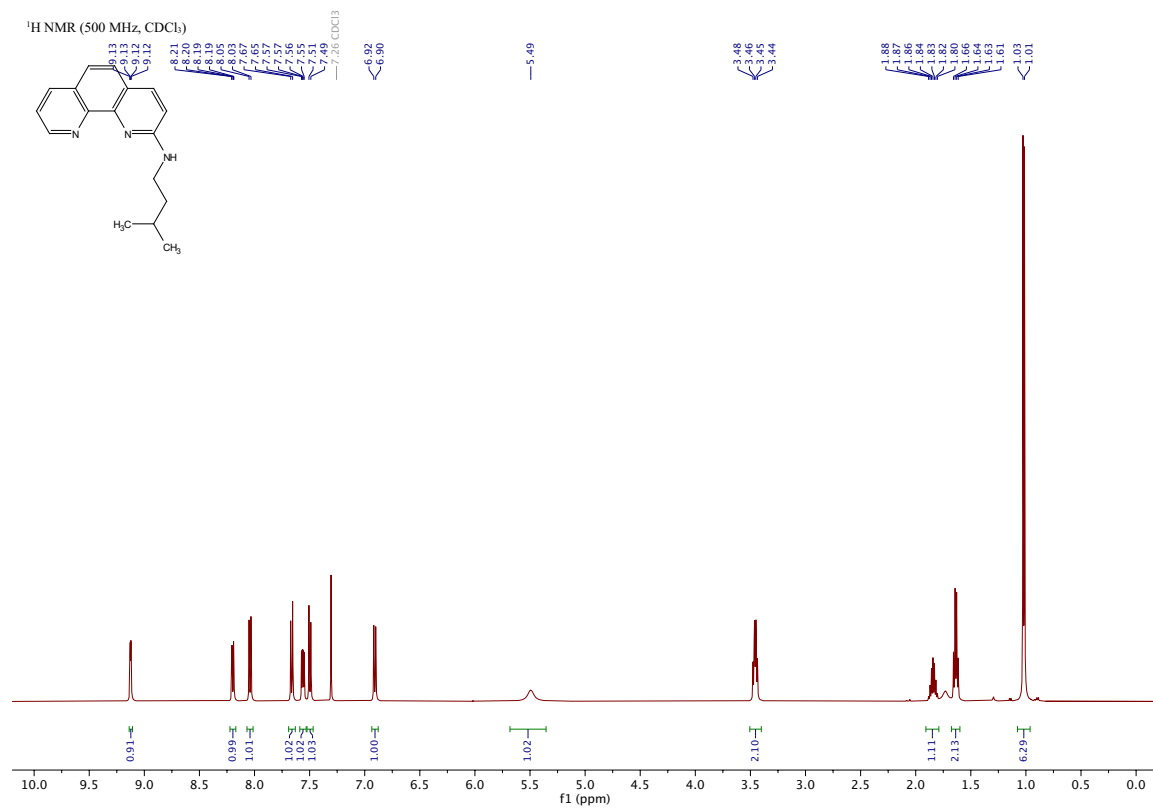
Ligand L10

N-benzyl-1,10-phenanthrolin-2-amine [Experimental]

¹H NMR (600 MHz, CDCl₃)

¹³C NMR (151 MHz, CDCl₃)
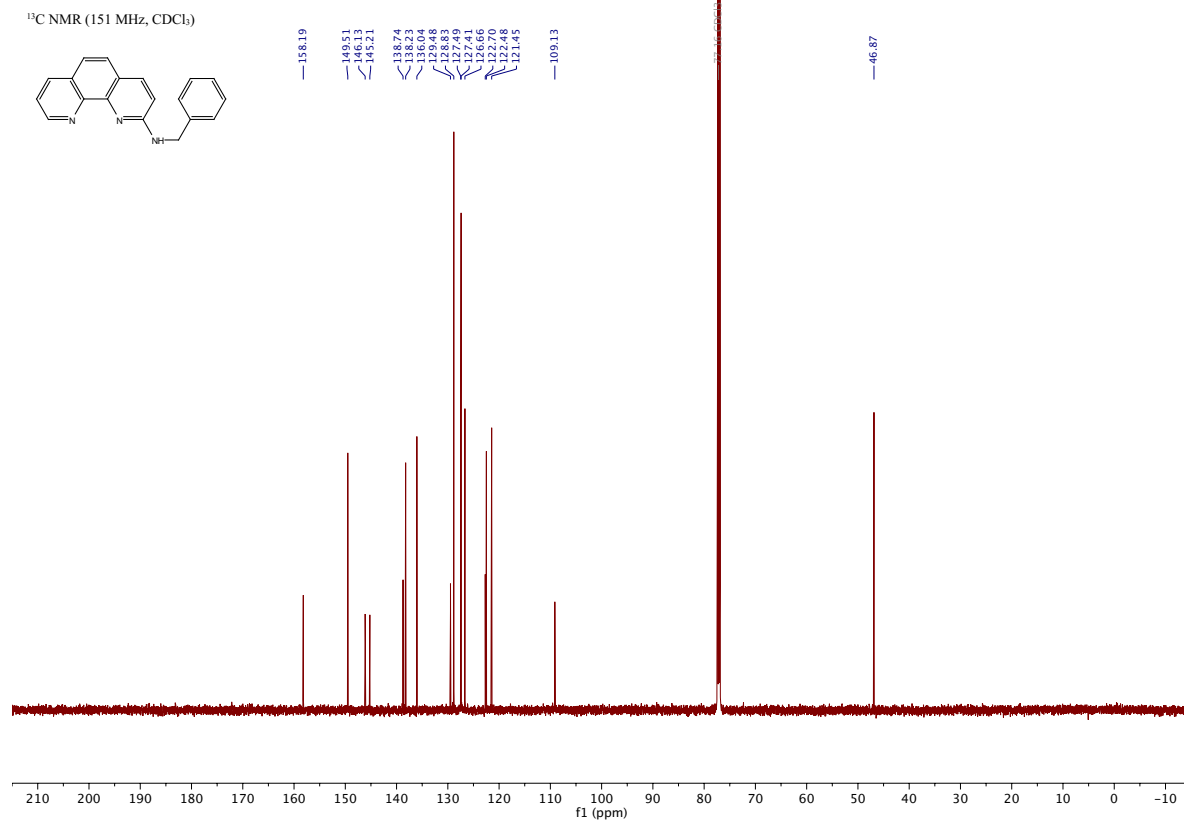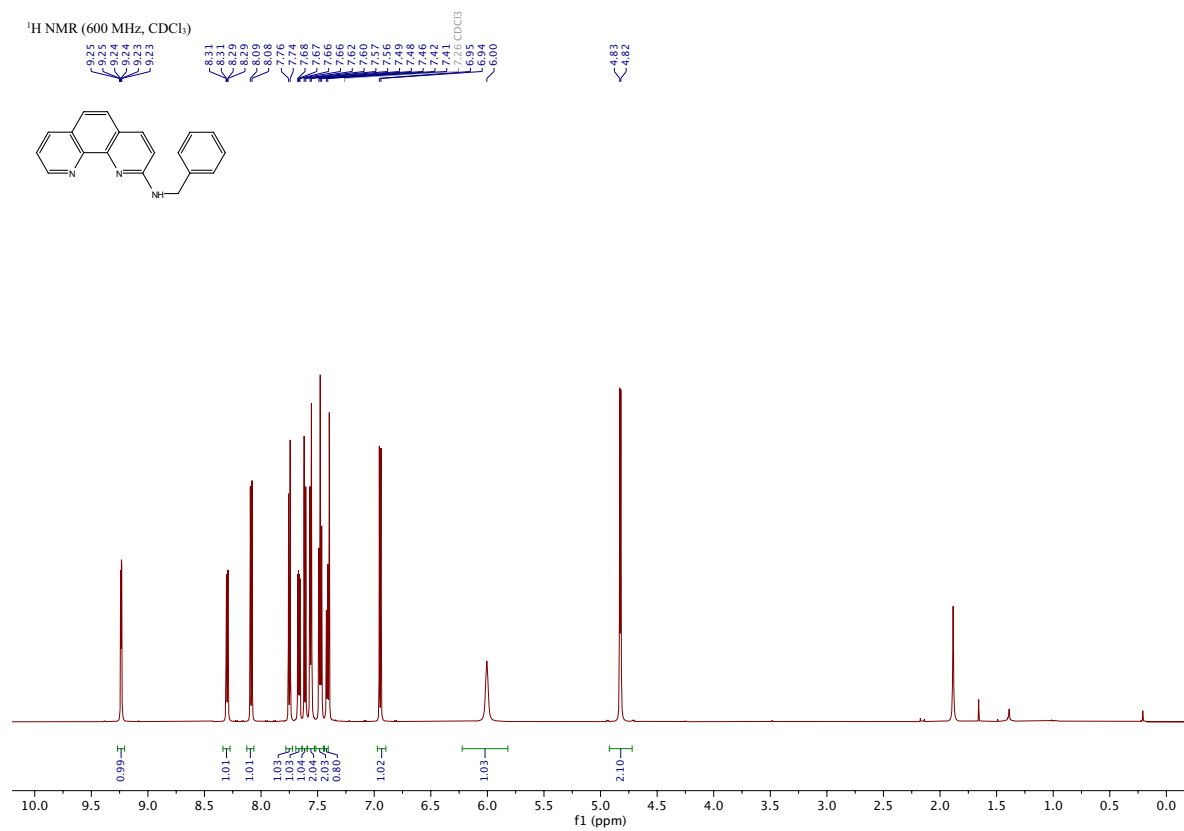
Ligand L11

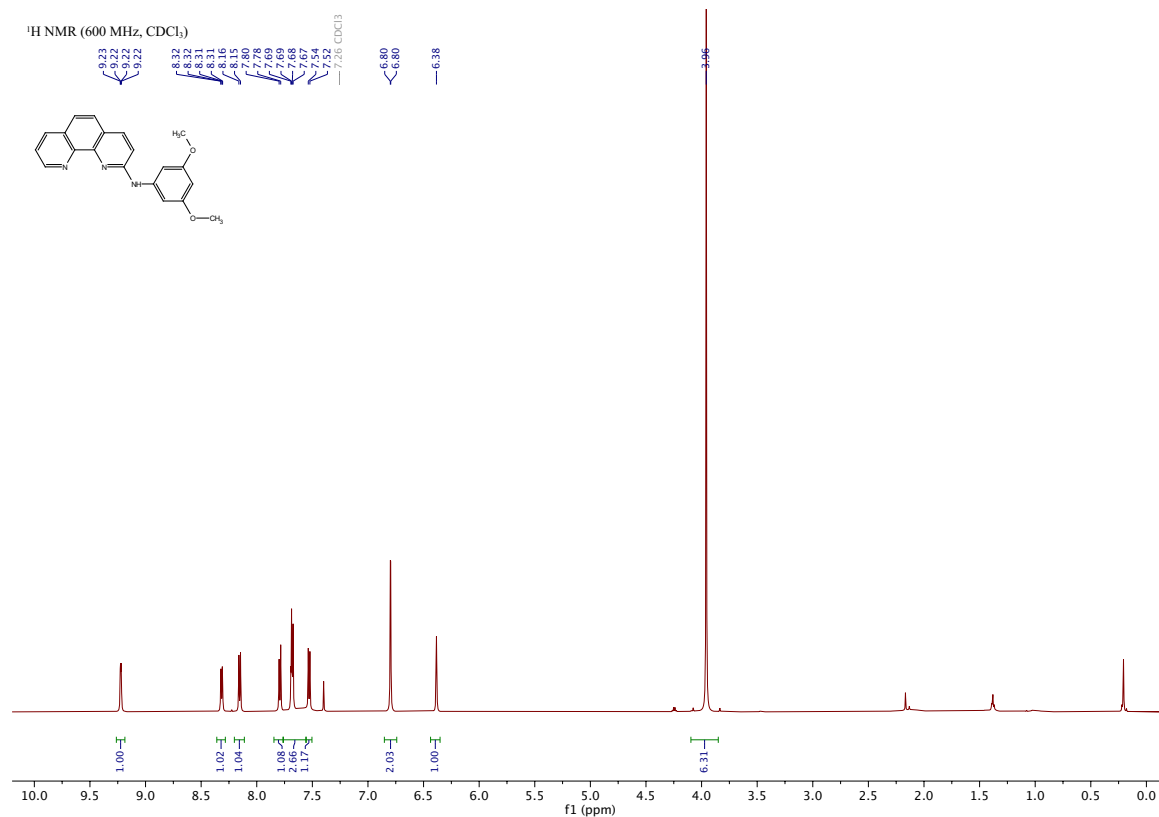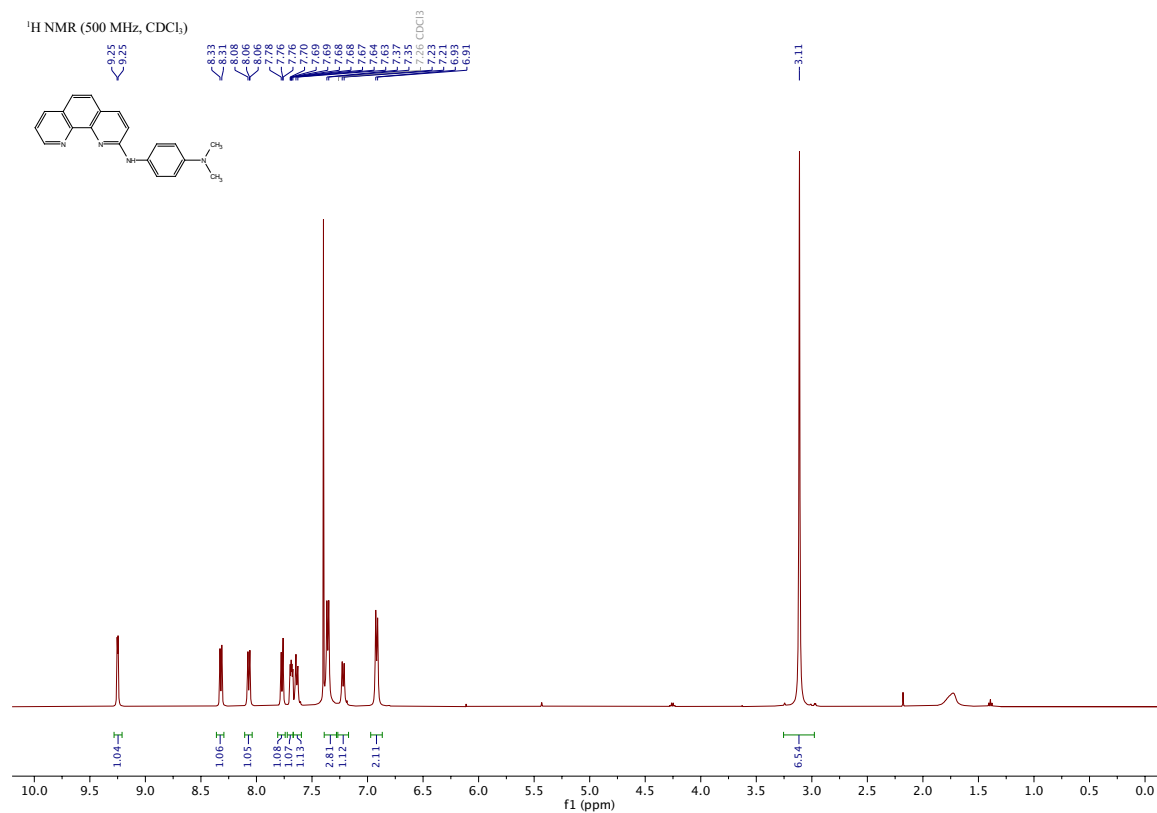*N*-(4-methoxybenzyl)-1,10-phenanthrolin-2-amine [Experimental]

¹H NMR (500 MHz, CDCl₃)

¹³C NMR (126 MHz, CDCl₃)
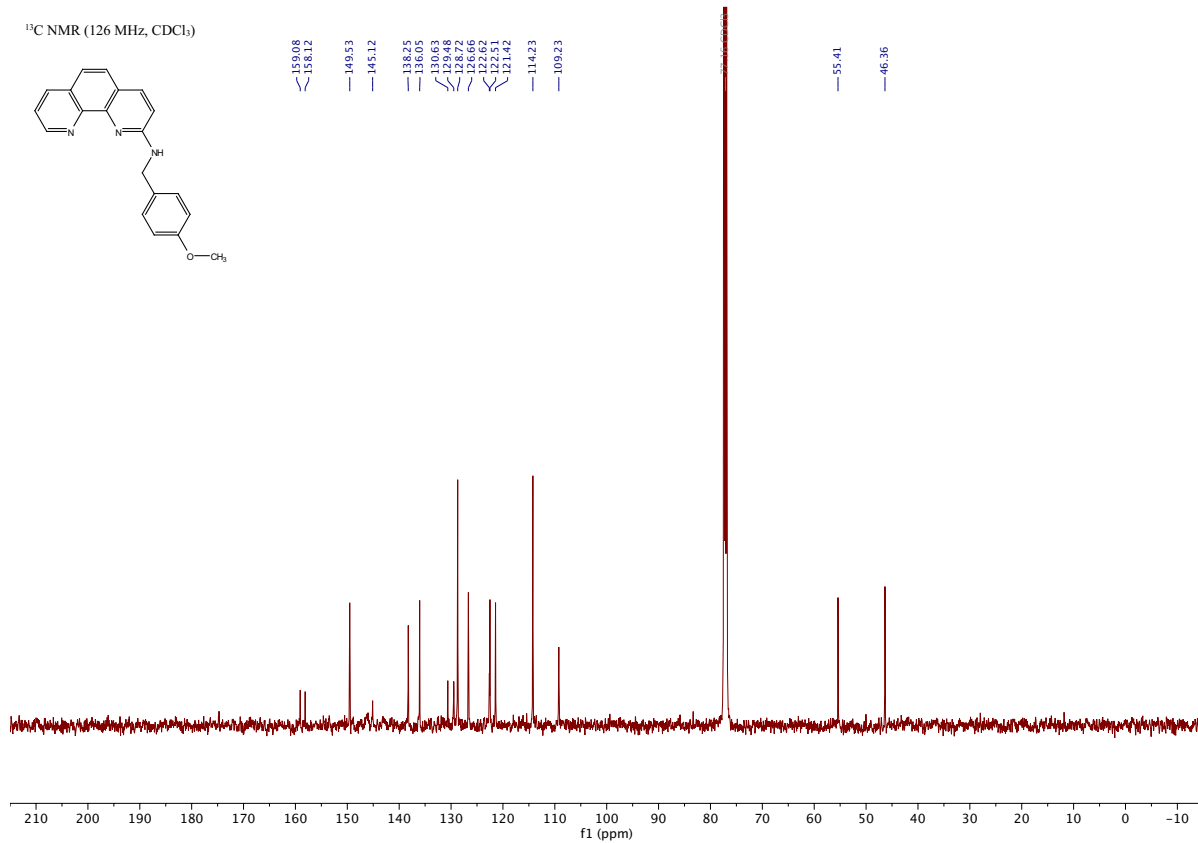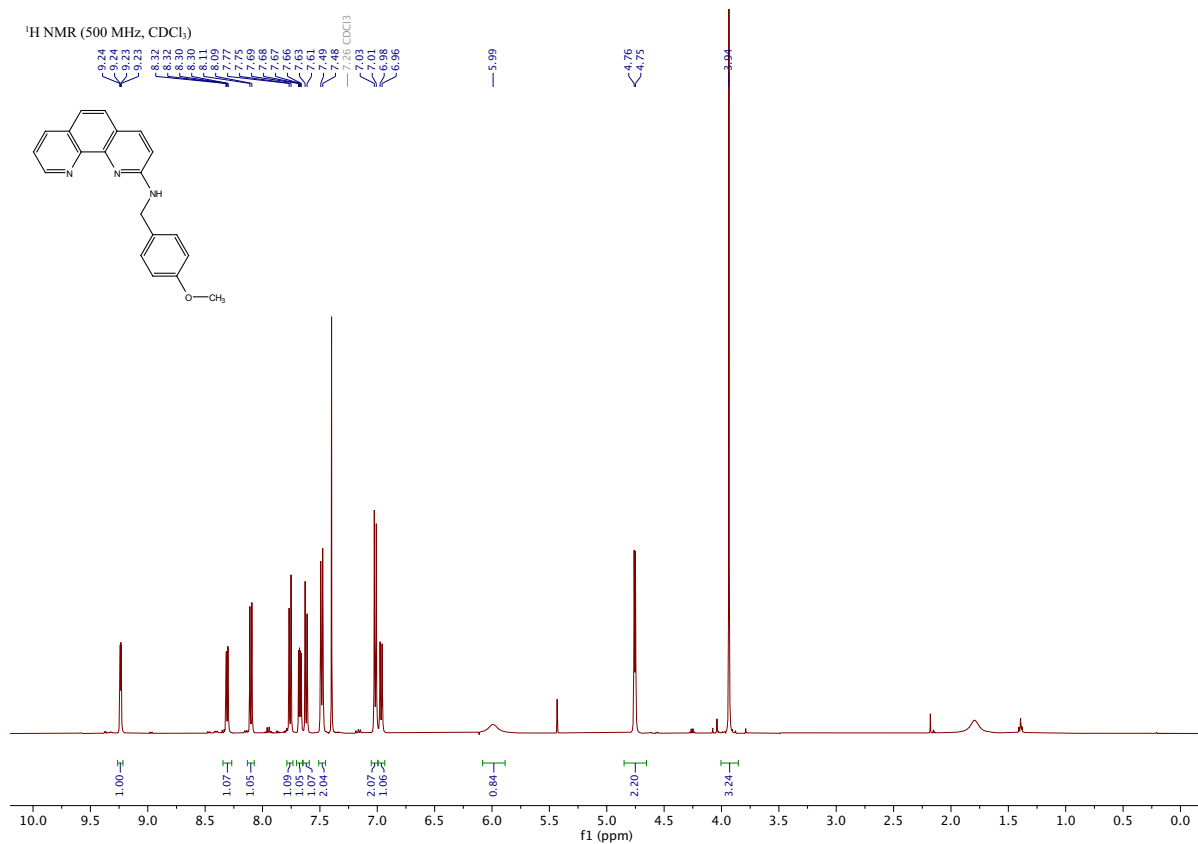
Ligand L12

N-phenethyl-1,10-phenanthrolin-2-amine [Experimental]

¹H NMR (500 MHz, CDCl₃)

¹³C NMR (126 MHz, CDCl₃)
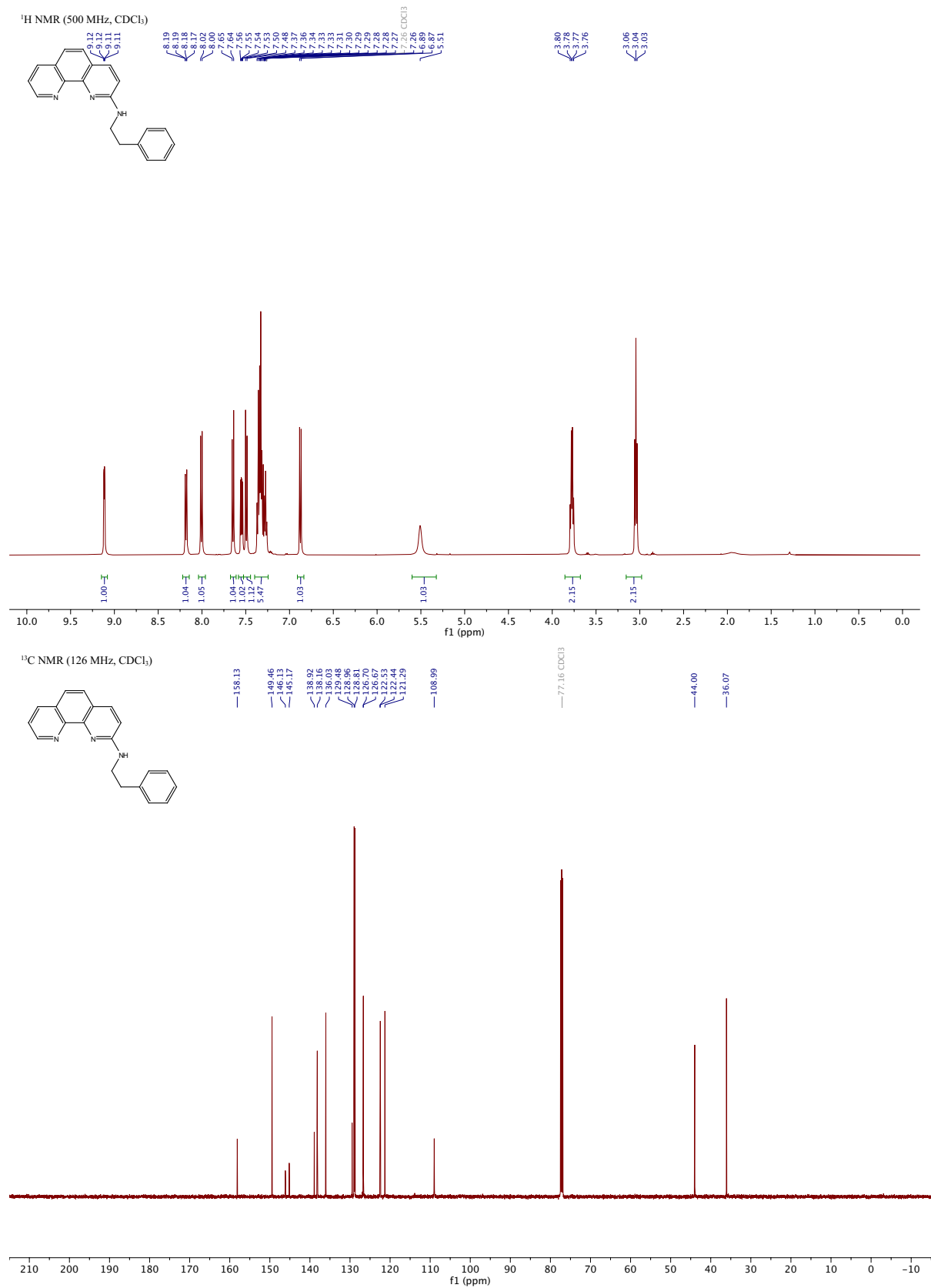
Ligand L13

N-([1,1'-biphenyl]-4-yl)-1,10-phenanthrolin-2-amine [Experimental]

^{1}H NMR (600 MHz, CDCl$_3$)

^{13}C NMR (151 MHz, CDCl$_3$)
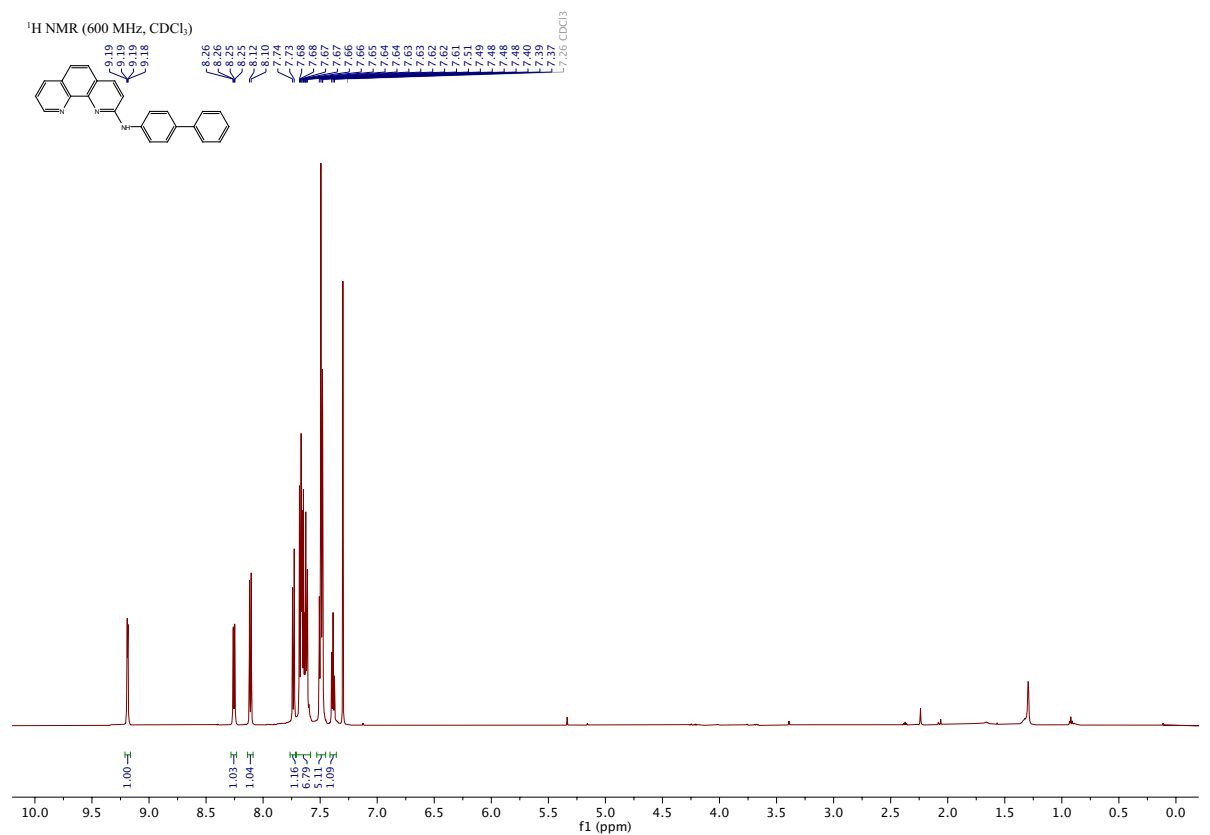
Ligand L14

N-(naphthalen-1-yl)-1,10-phenanthrolin-2-amine [Experimental]

¹H NMR (600 MHz, CDCl₃)

¹³C NMR (151 MHz, CDCl₃)
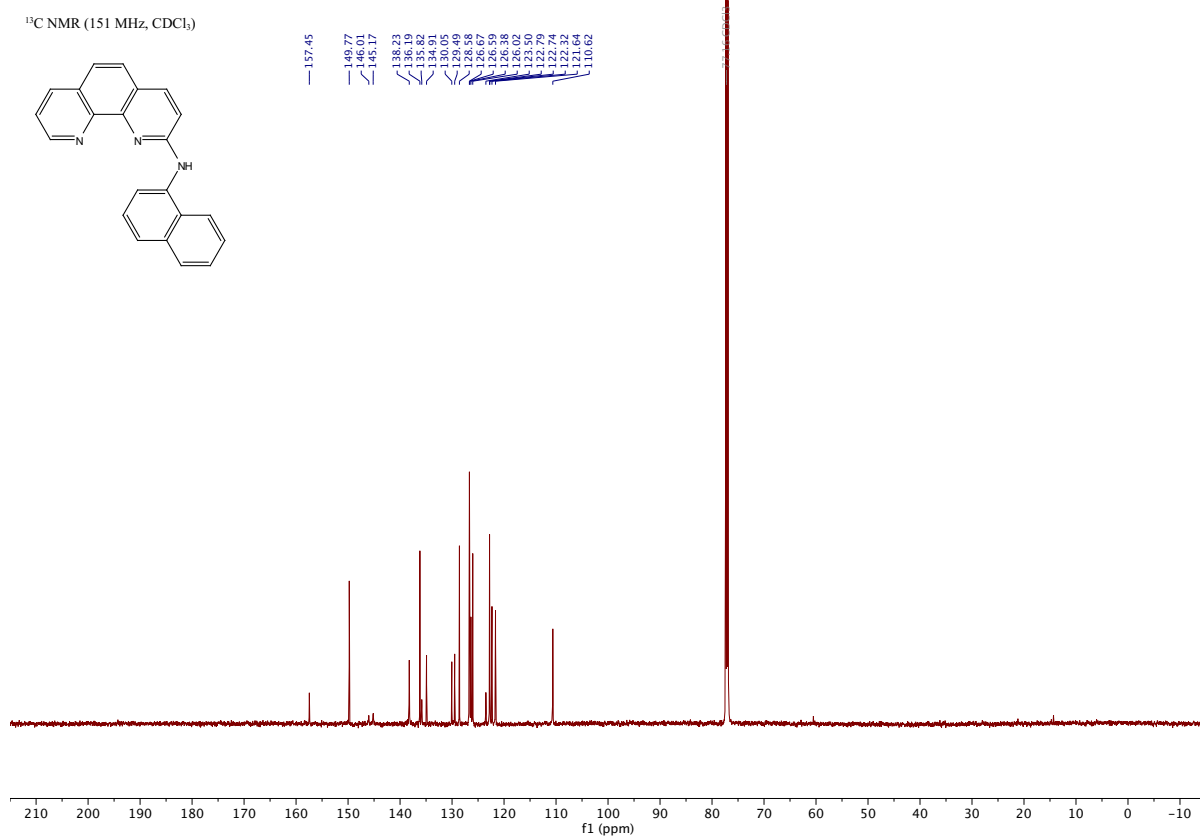
Ligand L15

N-(2-methoxyphenyl)-1,10-phenanthrolin-2-amine [Experimental]

¹H NMR (600 MHz, CDCl₃)

¹³C NMR (151 MHz, CDCl₃)
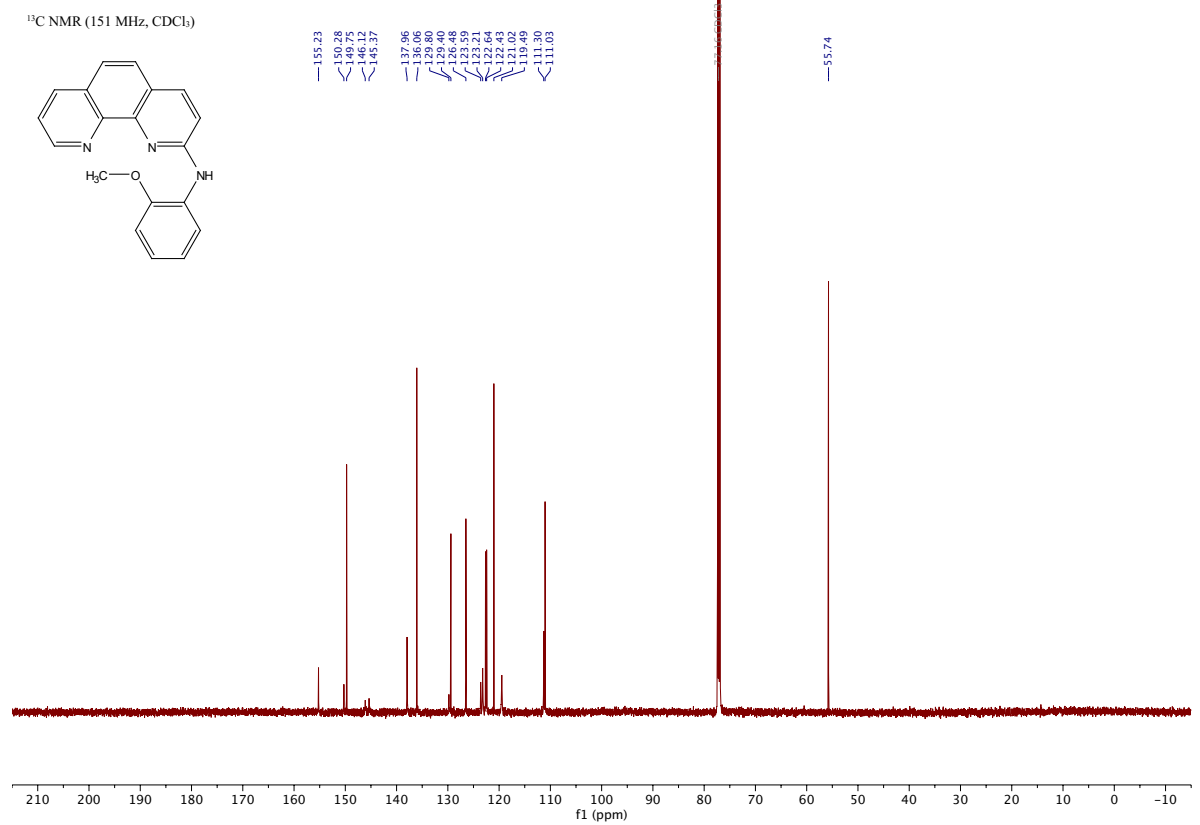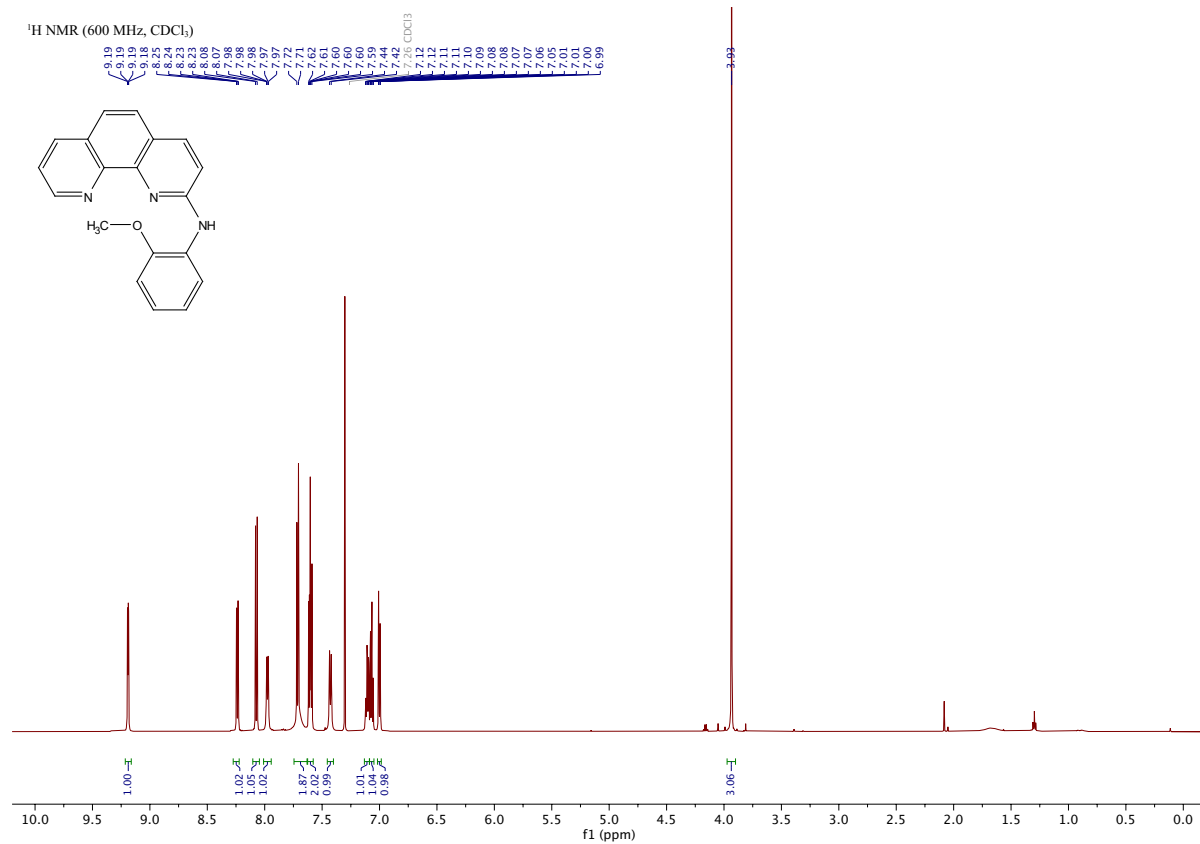
Ligand L16

N-(4-phenoxyphenyl)-1,10-phenanthrolin-2-amine [Experimental]

¹H NMR (600 MHz, CDCl₃)

¹³C NMR (151 MHz, CDCl₃)
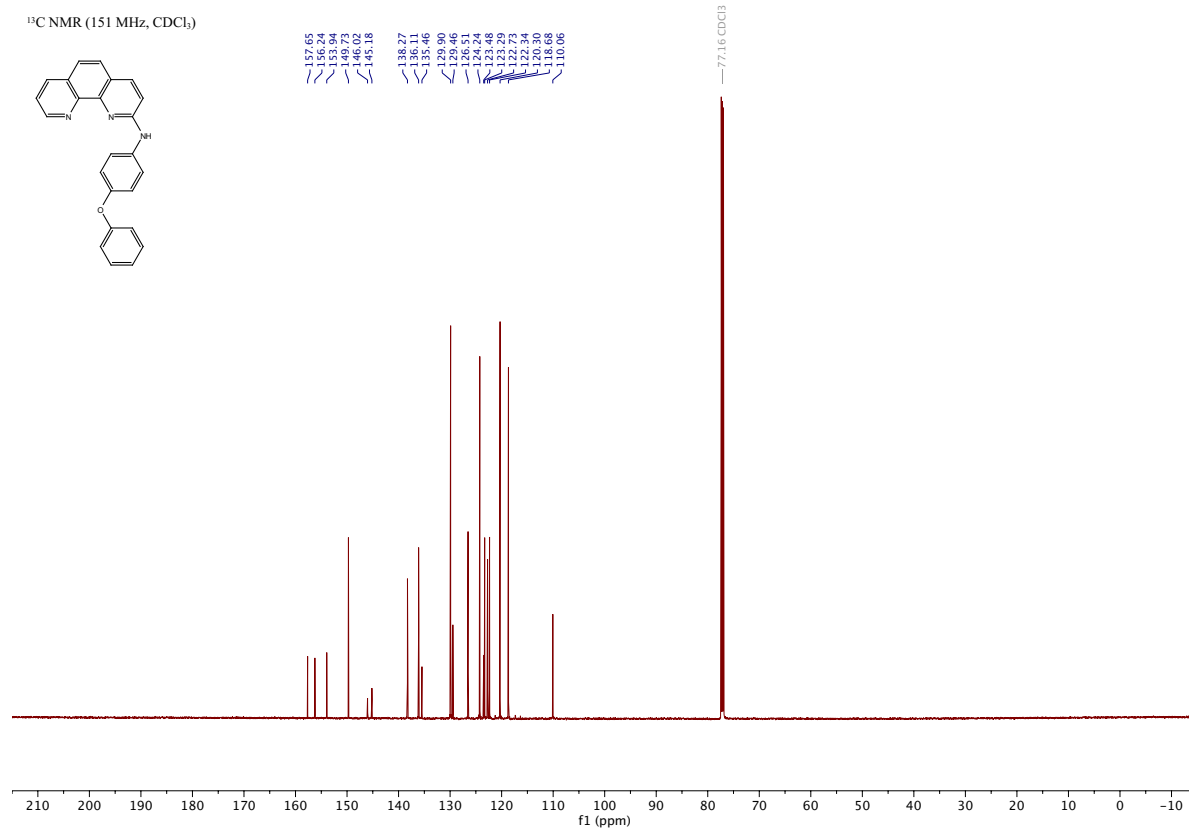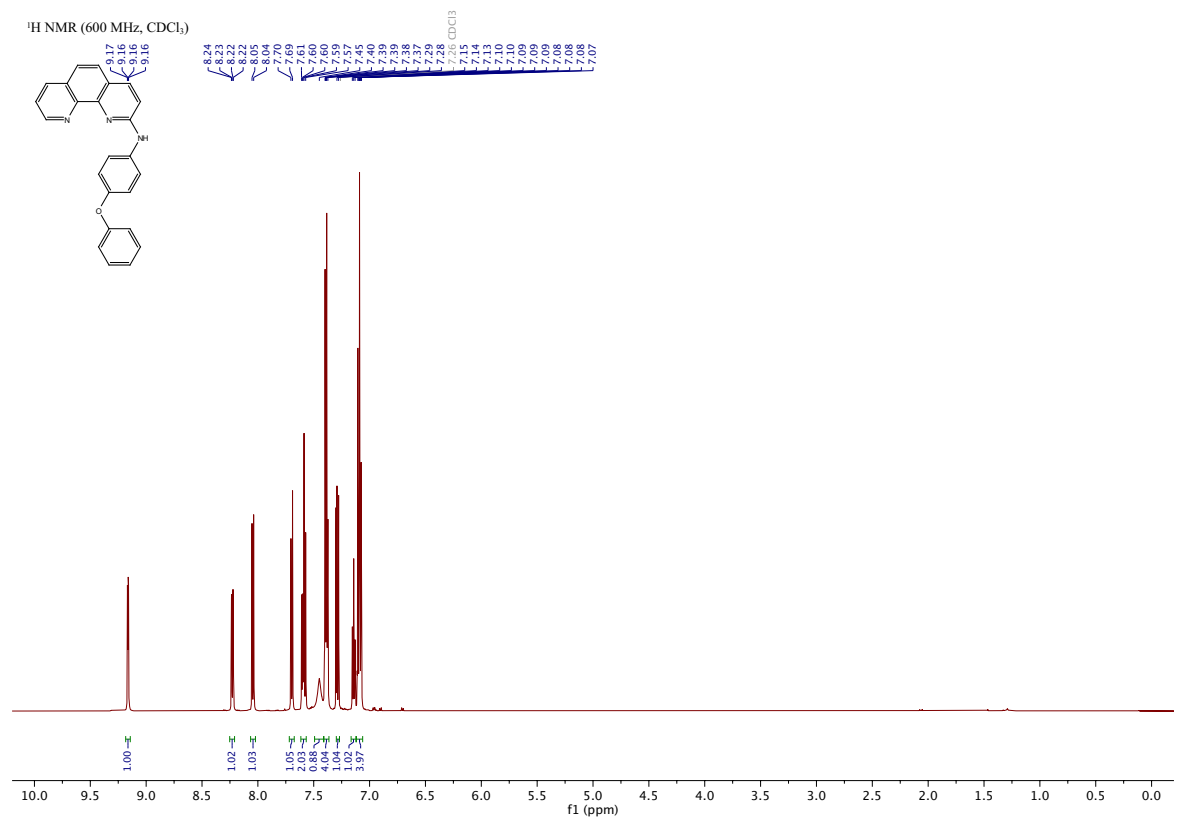
Ligand L17

N-(3,5-dimethoxyphenyl)-1,10-phenanthrolin-2-amine [Experimental]

¹H NMR (600 MHz, CDCl₃)

¹³C NMR (151 MHz, CDCl₃)
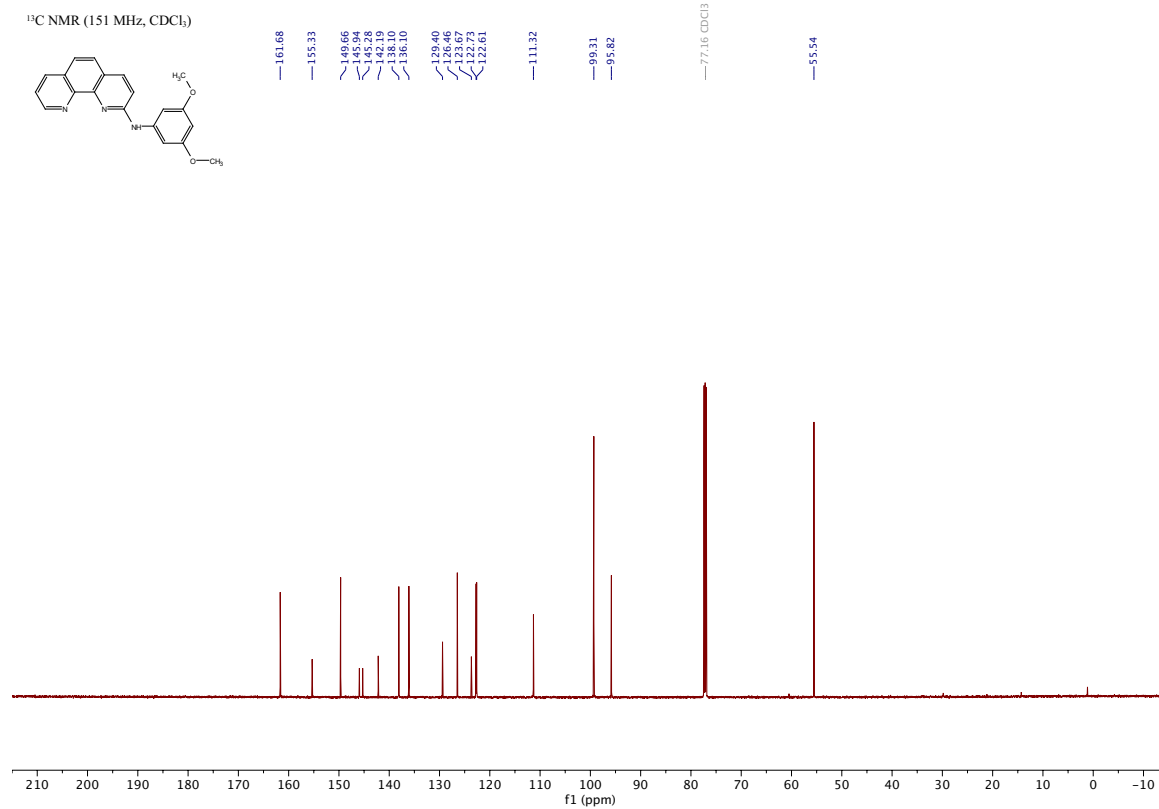
Ligand L18

*N*¹,*N*¹-dimethyl-*N*⁴-(1,10-phenanthrolin-2-yl)benzene-1,4-diamine [Experimental]

¹H NMR (500 MHz, CDCl₃)

¹³C NMR (126 MHz, CDCl₃)
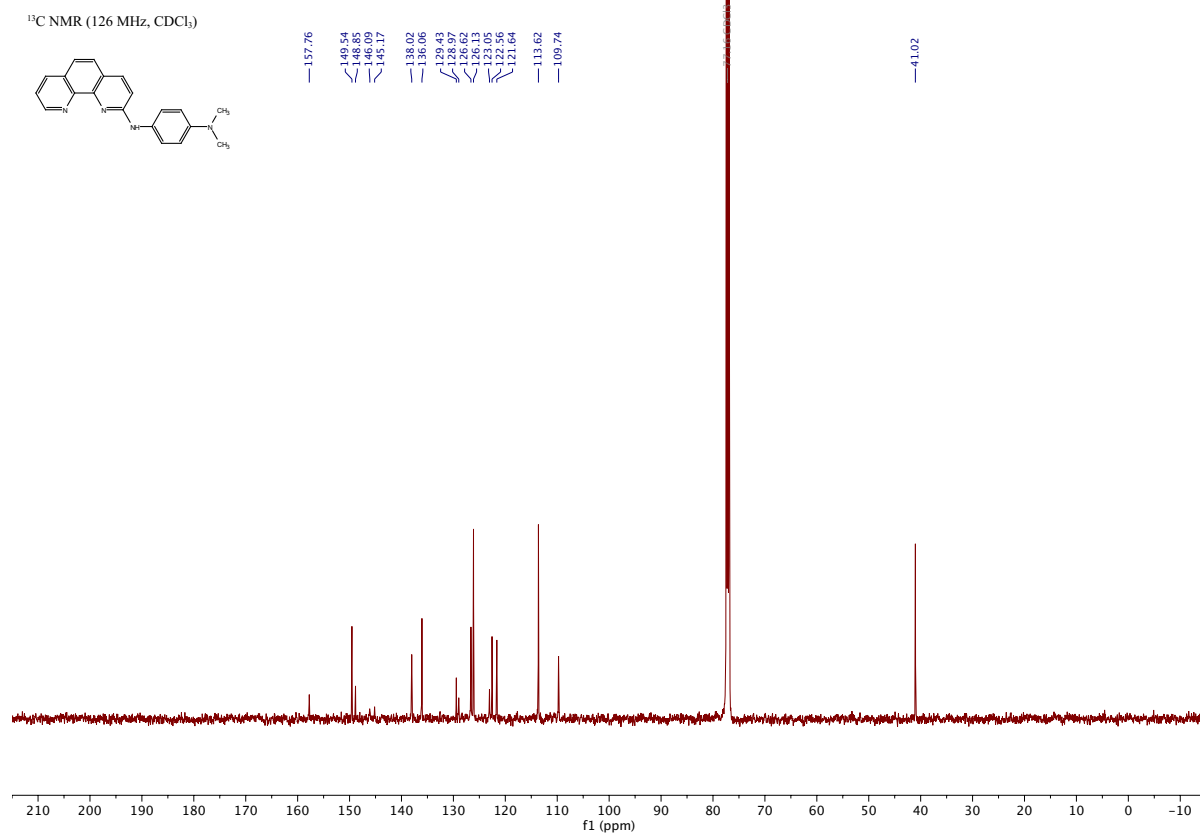
Ligand L19

N-(3,5-bis(trifluoromethyl)phenyl)-1,10-phenanthrolin-2-amine   [Experimental]

¹H NMR (500 MHz, CDCl₃)
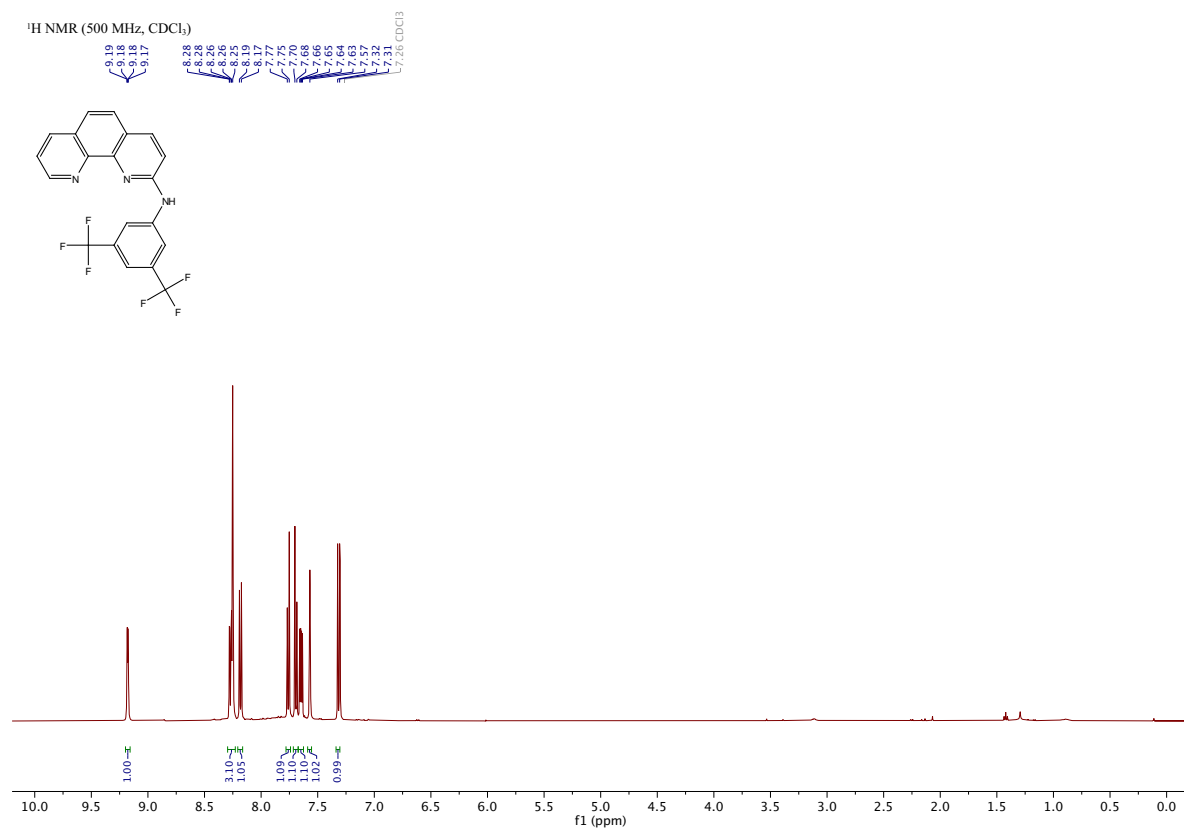
¹³C NMR (126 MHz, CDCl₃)
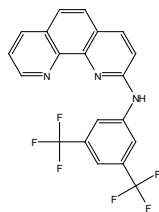
153.43
150.11
145.29
145.04
142.20
138.71
136.16
133.16
132.89
132.63
132.36
129.44
126.70
126.17
124.53
124.16
123.87
123.14
122.36
120.19
118.92
115.74
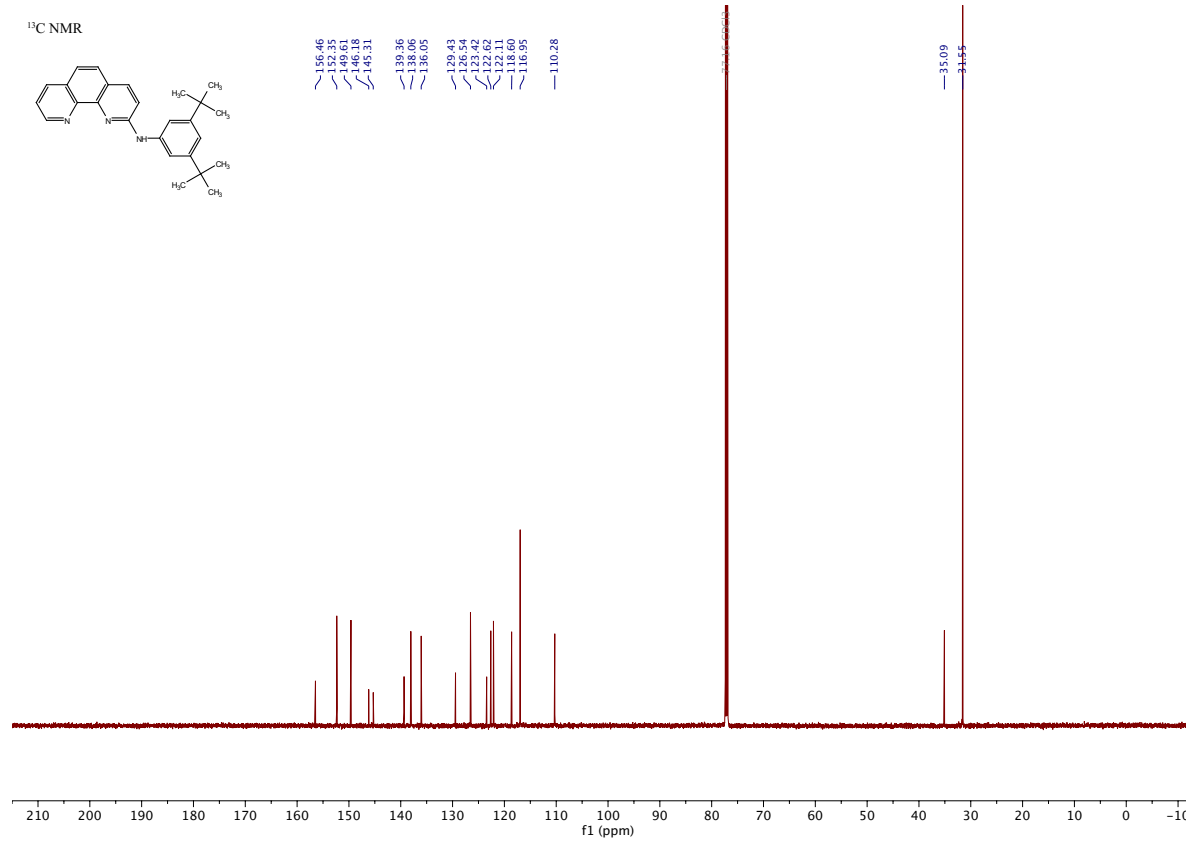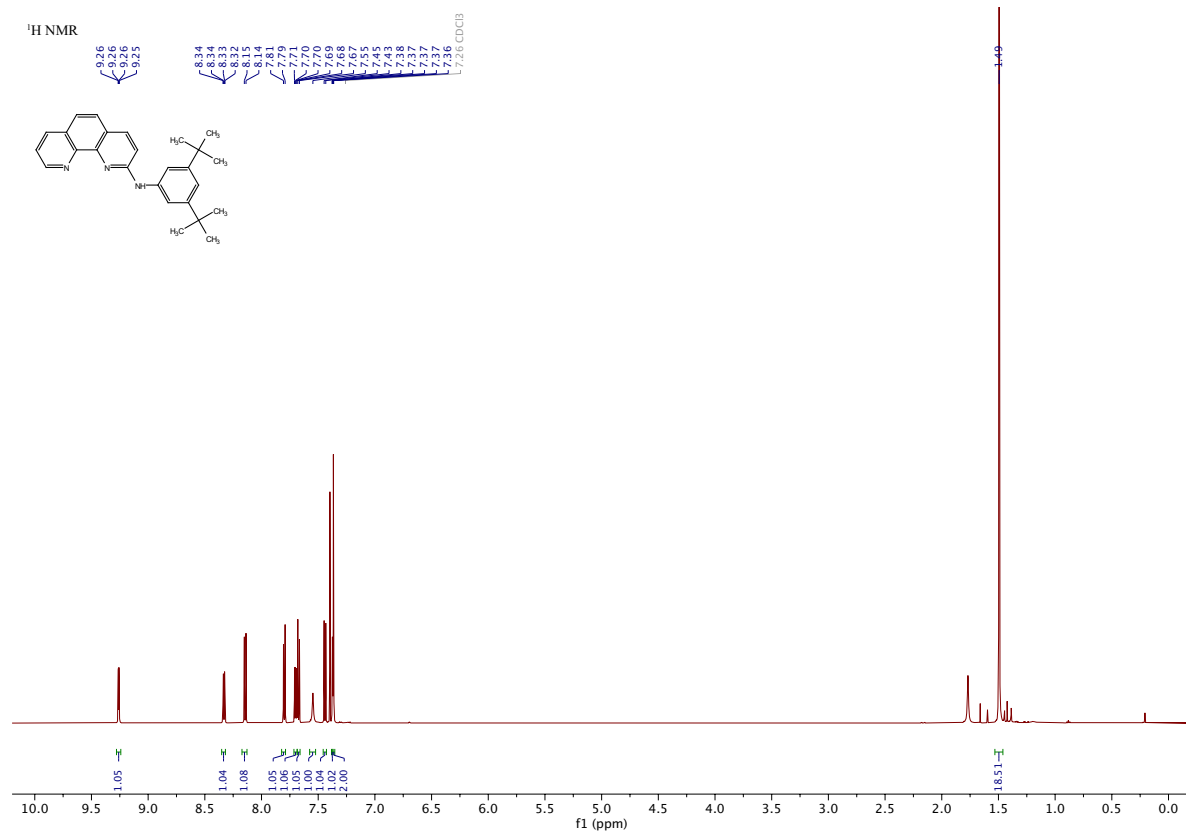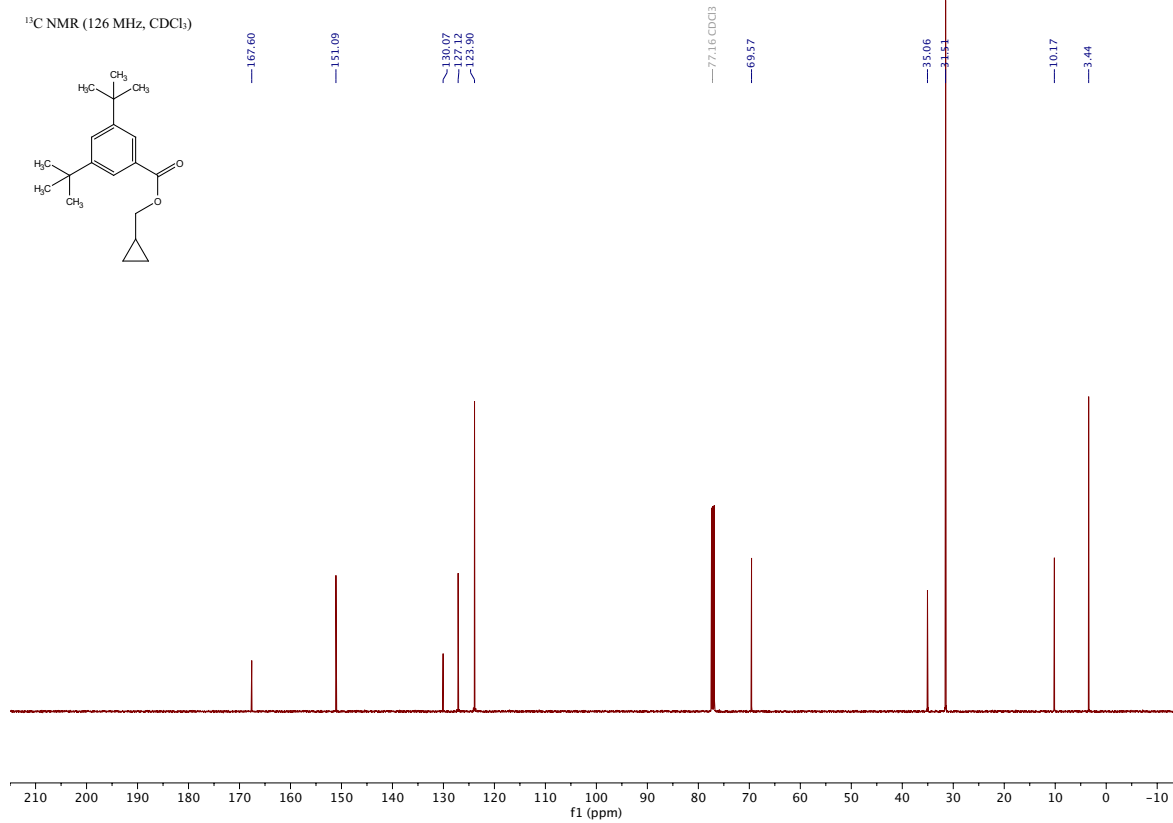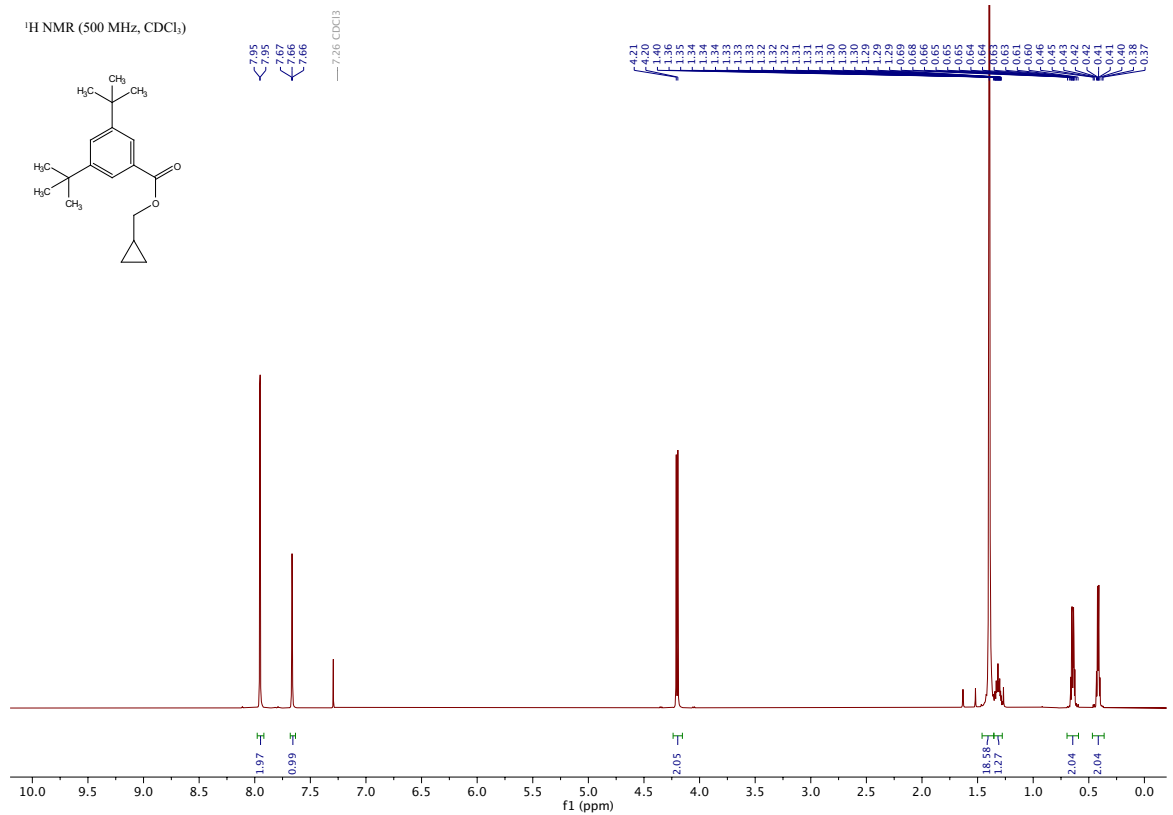111.93
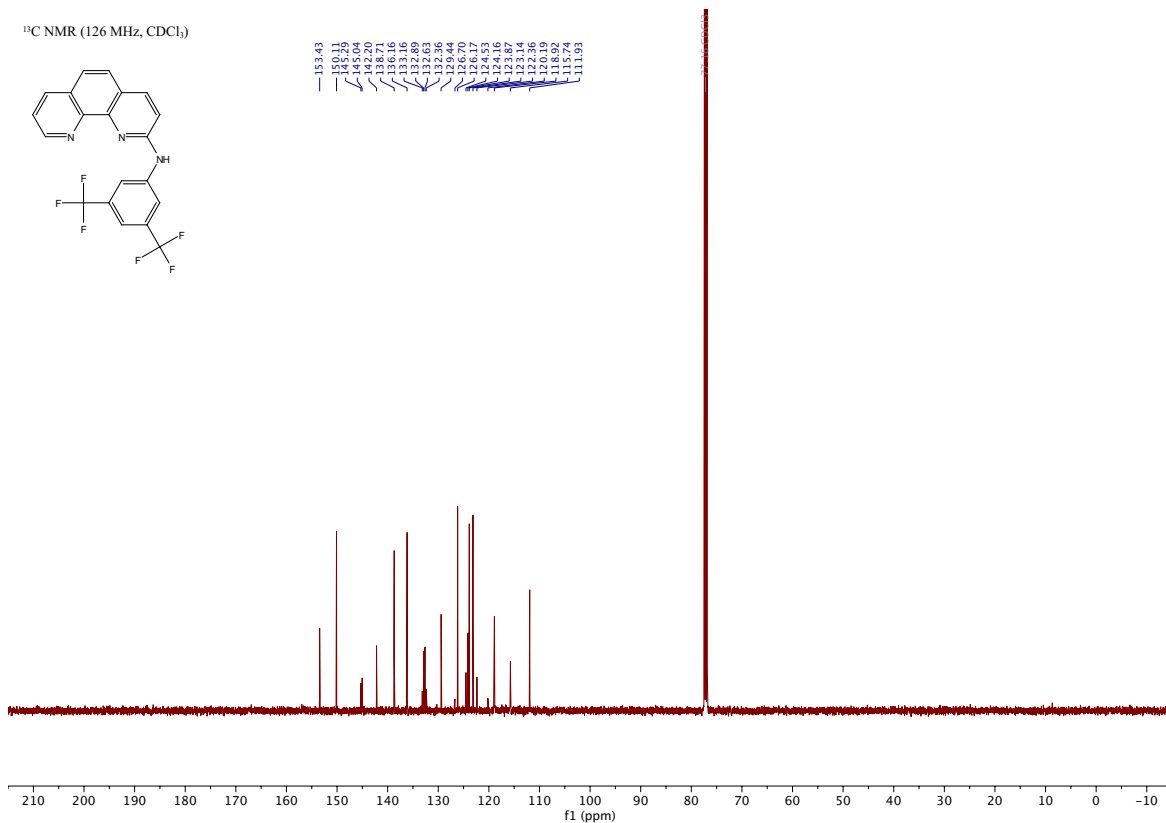
¹⁹F NMR (470 MHz, CDCl₃)
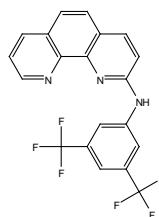
−62.96
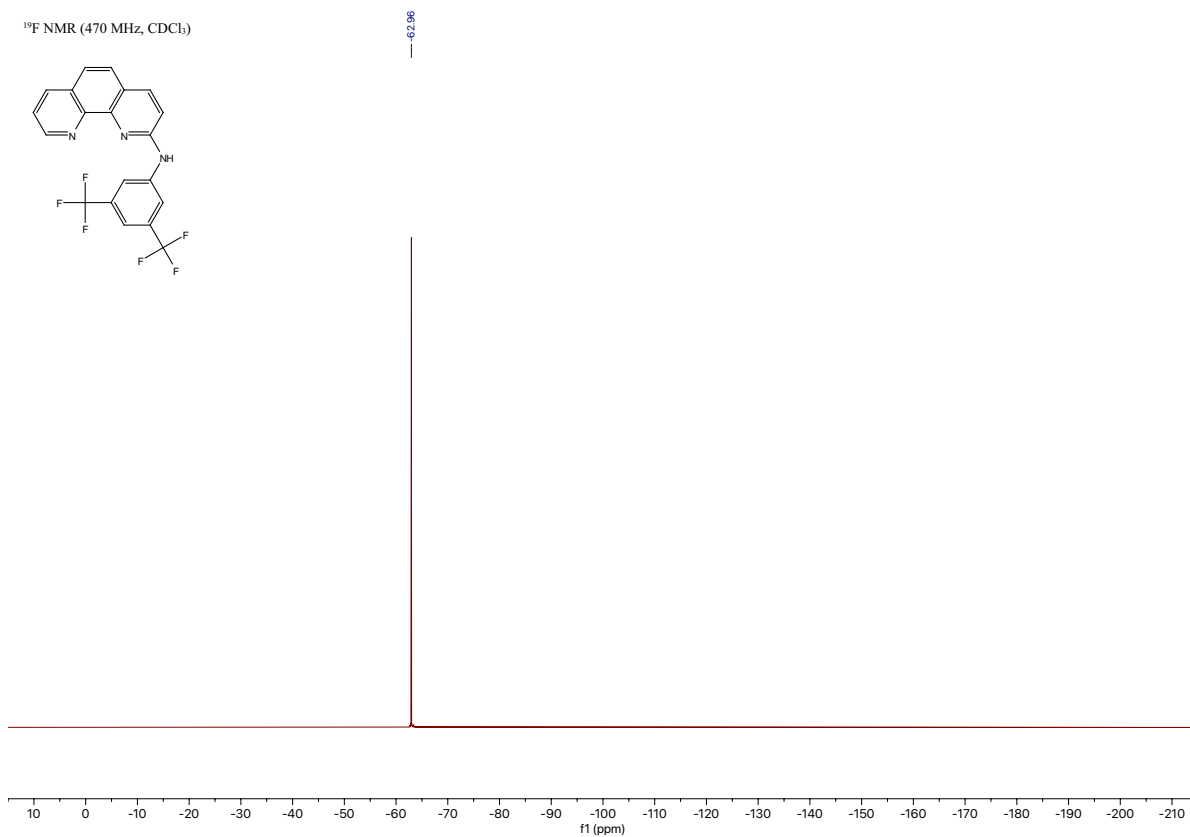
Ligand L20

N-(3,5-di-tert-butylphenyl)-1,10-phenanthrolin-2-amine [Experimental]

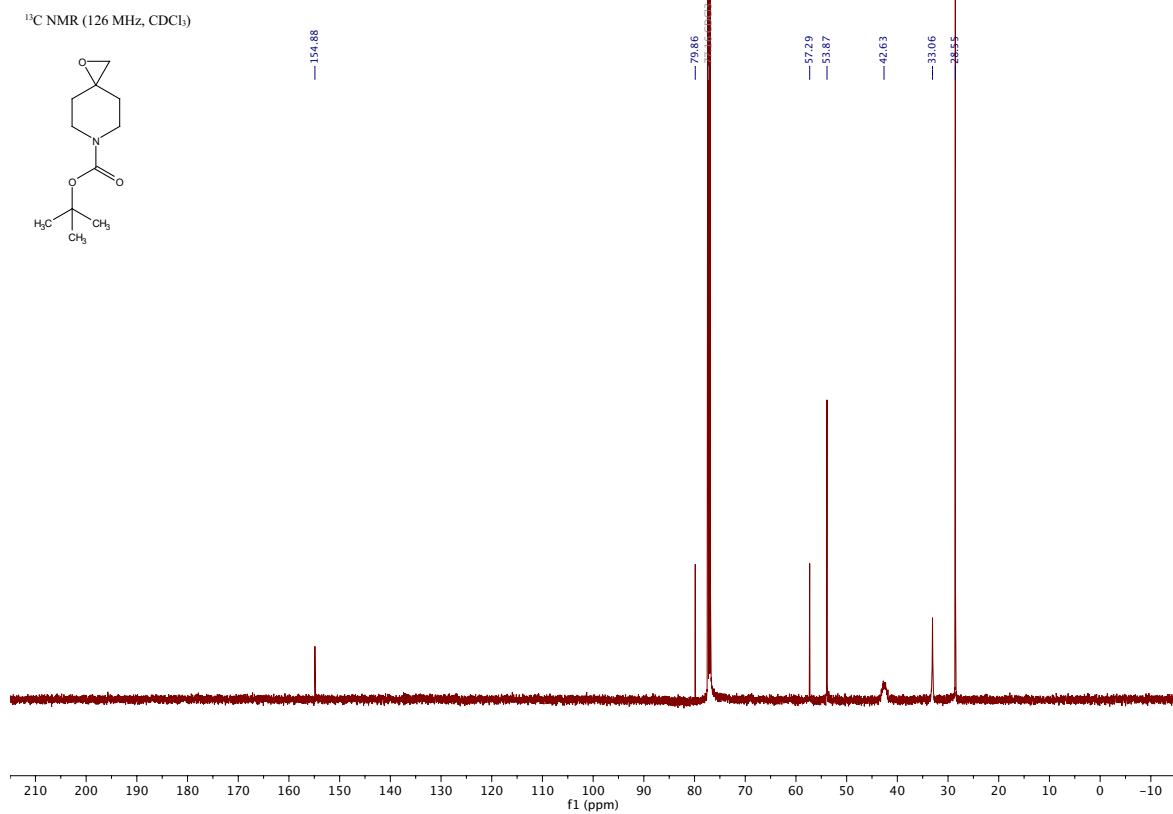## Substrate 3b

cyclopropylmethyl 3,5-di-*tert*-butylbenzoate [Experimental]

¹H NMR (500 MHz, CDCl₃)

¹³C NMR (126 MHz, CDCl₃)

Substrate 5b

tert-butyl 1-oxa-6-azaspiro[2.5]octane-6-carboxylate [Experimental]

¹H NMR (400 MHz, CDCl₃)

¹³C NMR (126 MHz, CDCl₃)
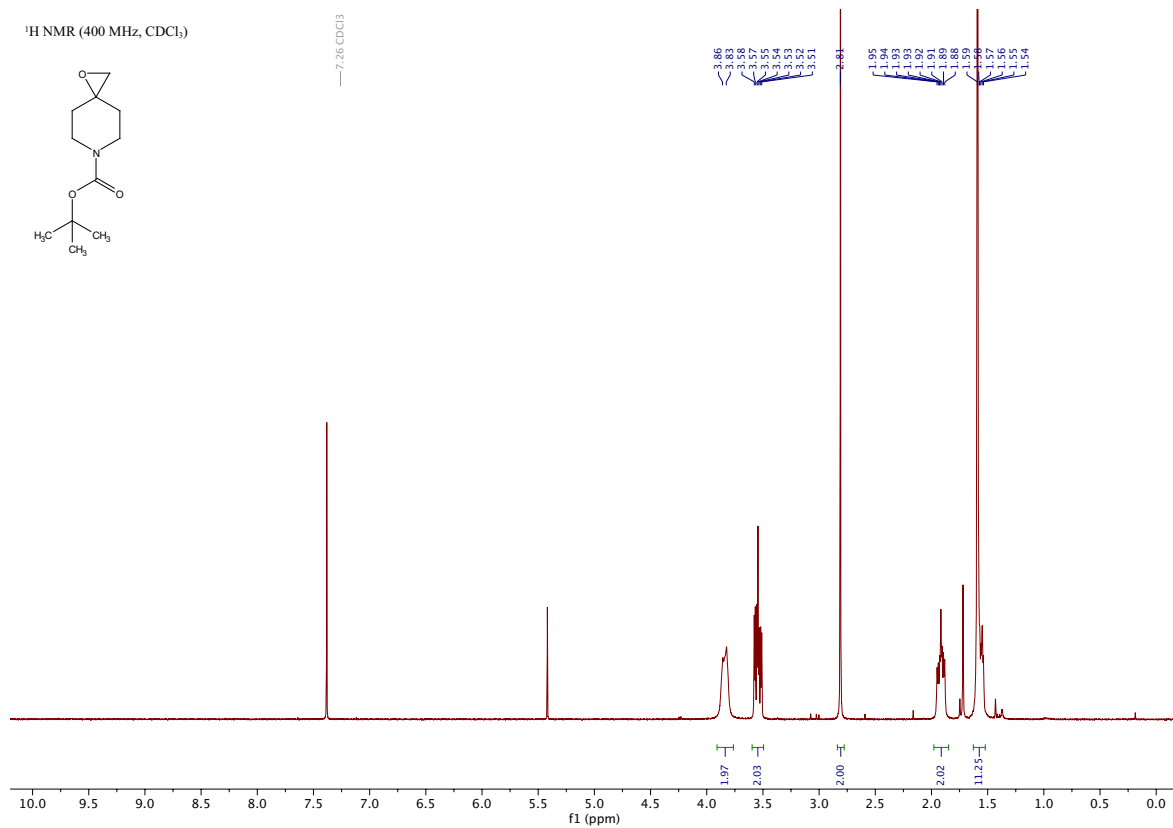
Substrate 8b

7,7-dimethyl-6,8-dioxaspiro[3.5]nonane [Experimental]

¹H NMR (600 MHz, CDCl₃)

¹³C NMR (151 MHz, CDCl₃)
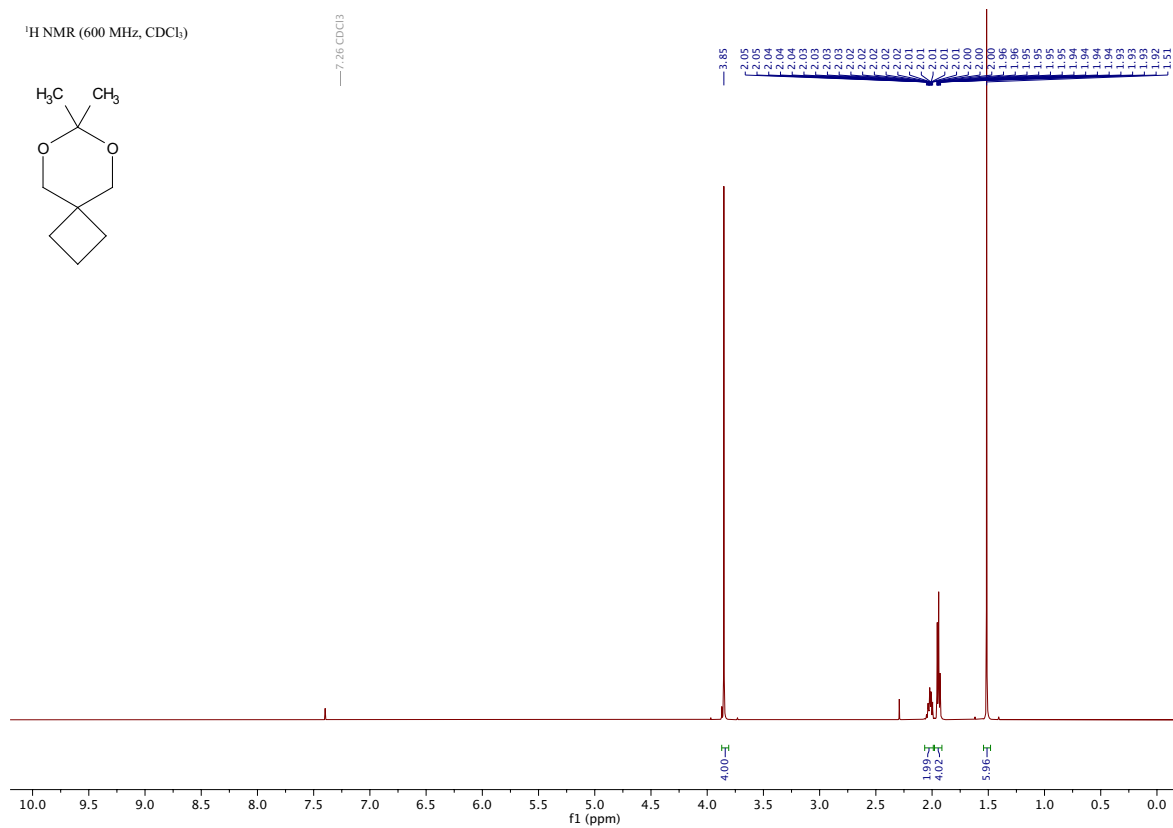
Substrate 14b

1,7,7-trimethylbicyclo[2.2.1]heptan-2-yl cyclobutanecarboxylate [Experimental]

¹H NMR (600 MHz, CDCl₃)
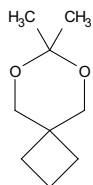
¹³C NMR (151 MHz, CDCl₃)
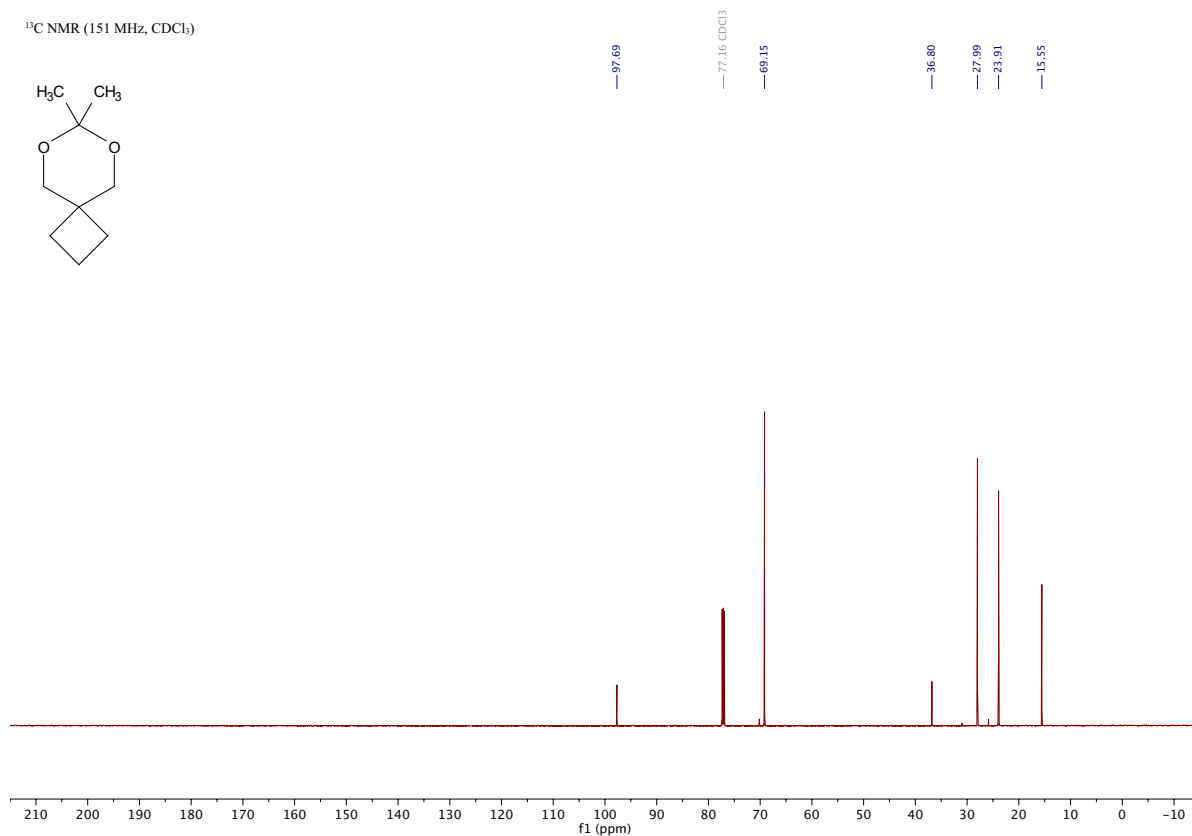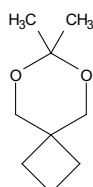
Substrate 15b

(3*S*,8*S*,9*S*,10*R*,13*R*,14*S*,17*R*)-10,13-dimethyl-17-((*R*)-6-methylheptan-2-yl)-2,3,4,7,8,9,10,11,12,13,14,15,16,17-tetradecahydro-1H-cyclopenta[*a*]phenanthren-3-yl bicyclo[1.1.1]pentane-1-carboxylate [Experimental]

¹H NMR (500 MHz, CDCl₃)

¹³C NMR (126 MHz, CDCl₃)
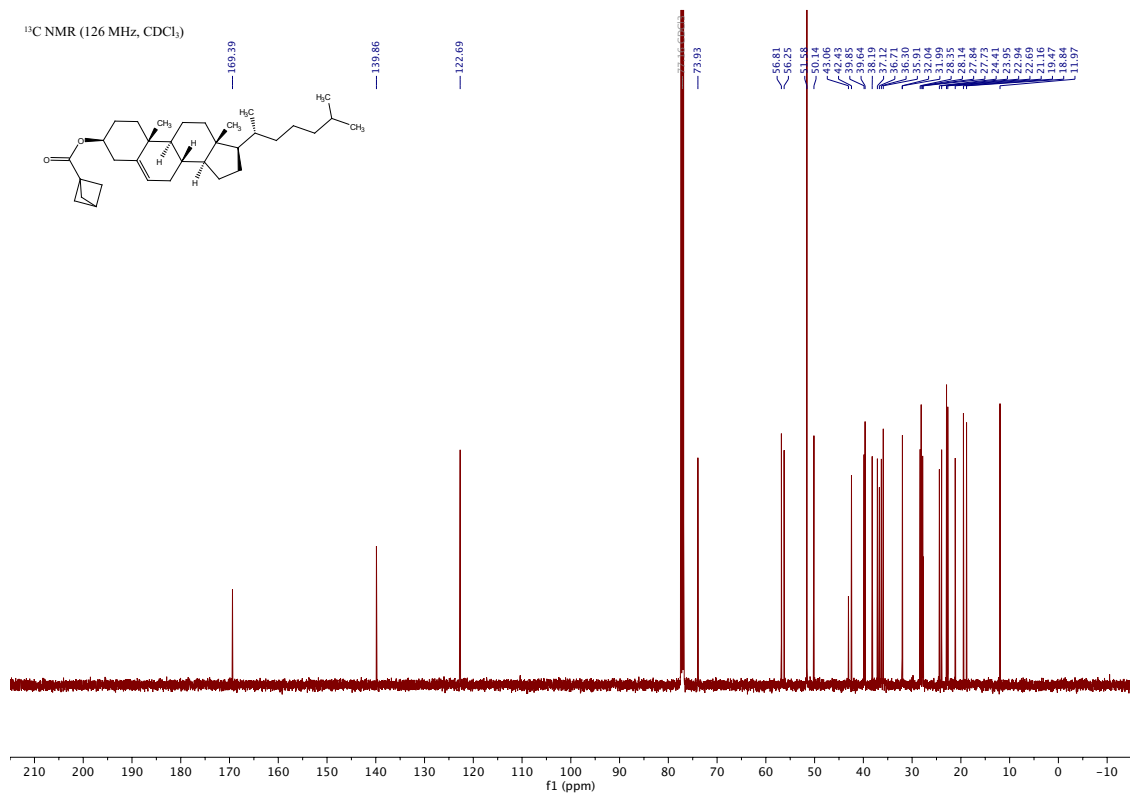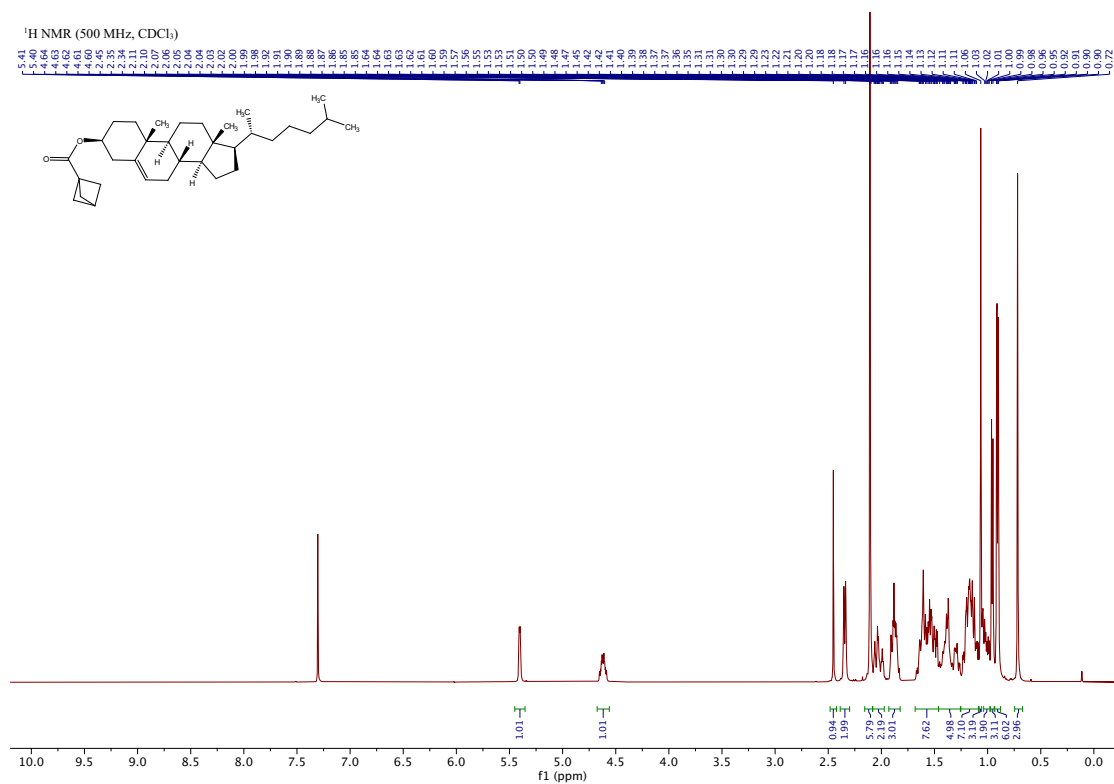
Substrate 16b

(2*R*,3*S*,4*R*,5*R*,6*S*)-2,3,4,5-tetrakis((3,5-di-*tert*-butylbenzyl)oxy)-6-methyltetrahydro-2*H*-pyran
[Experimental]

¹H NMR (600 MHz, CDCl₃)
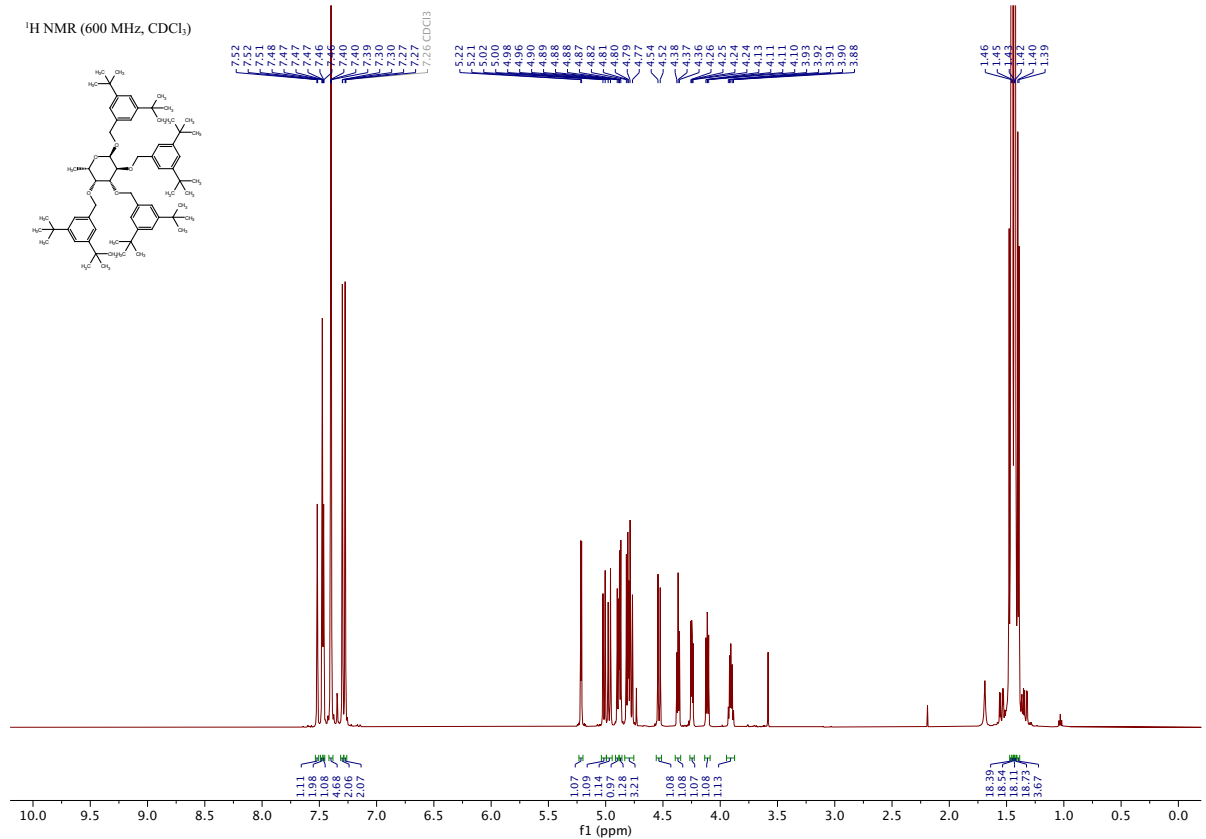
¹³C NMR (126 MHz, CDCl₃)
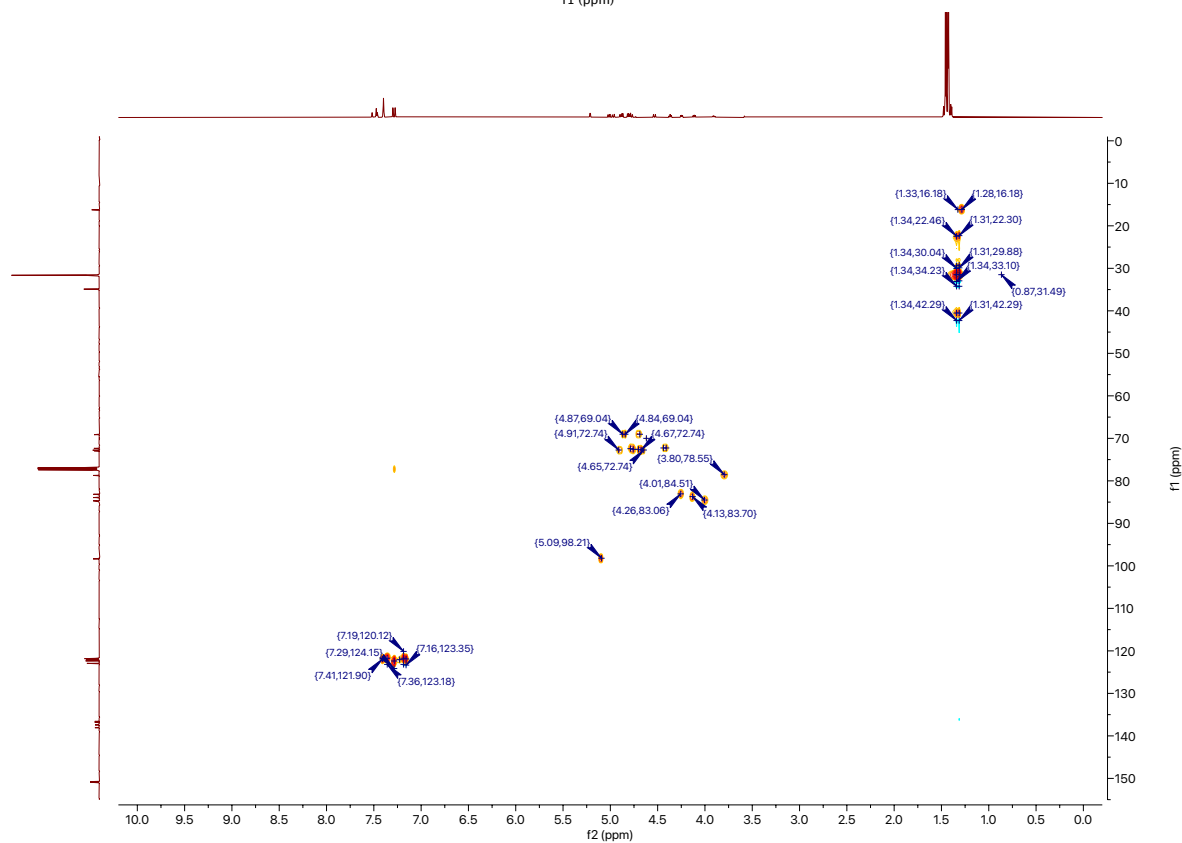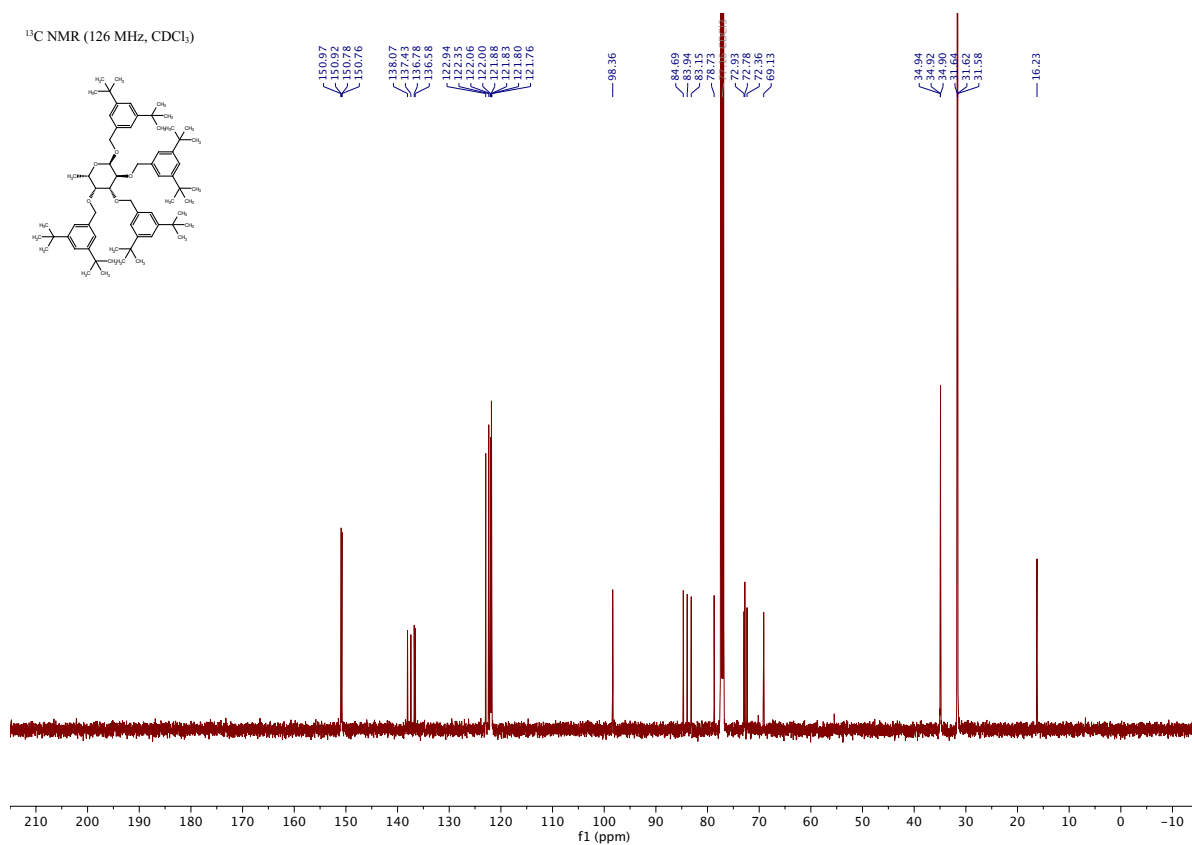
Substrate 17b

(2*S*,3*S*,4*R*,5*R*,6*S*)-6-methyltetrahydro-2H-pyran-2,3,4,5-tetrayl tetrakis(4-(tert-butyl)benzoate)
[Experimental]

¹H NMR (500 MHz, CDCl₃)

¹³C NMR (126 MHz, CDCl₃)

450
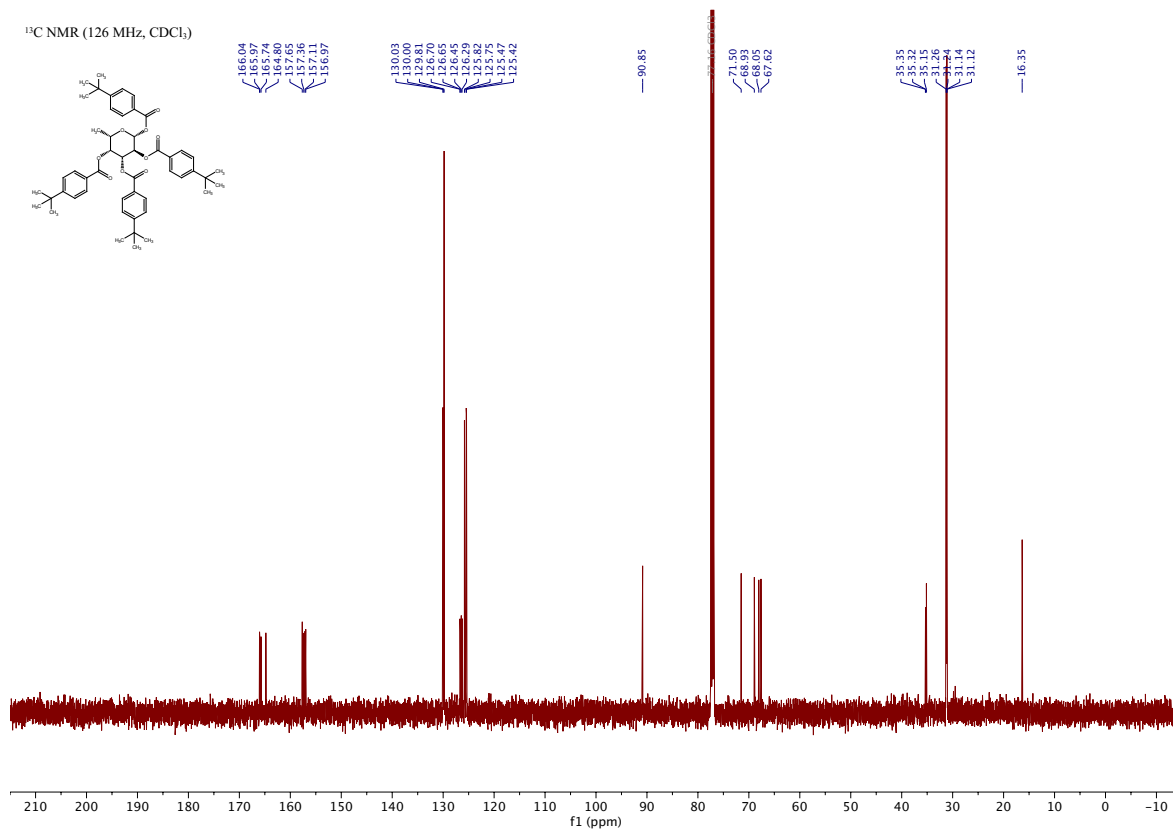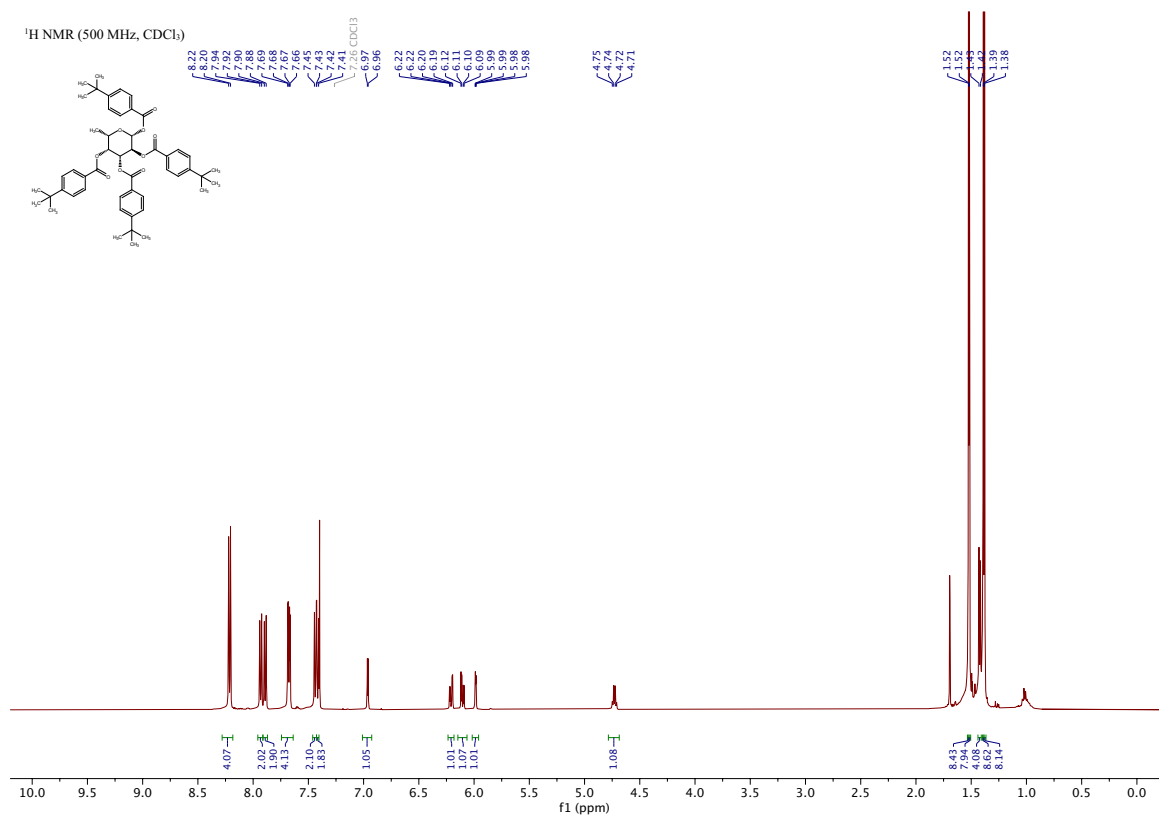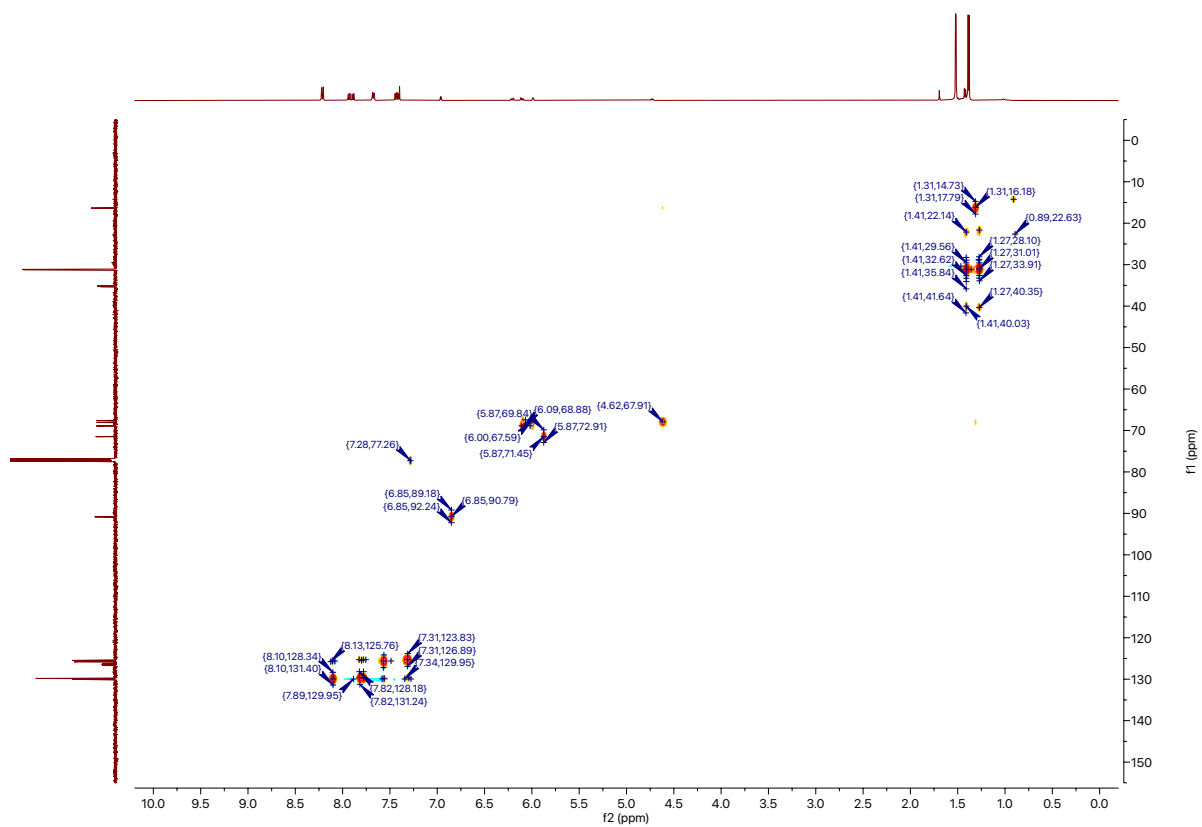
Product 1a

(8-(*tert*-butoxy)octyl)trifluoro-λ⁴-borane, potassium salt [Experimental]

¹H NMR (600 MHz, Acetone)

¹³C NMR (151 MHz, Acetone)

451

—4.90

f1 (ppm)

—-141.80

f1 (ppm)
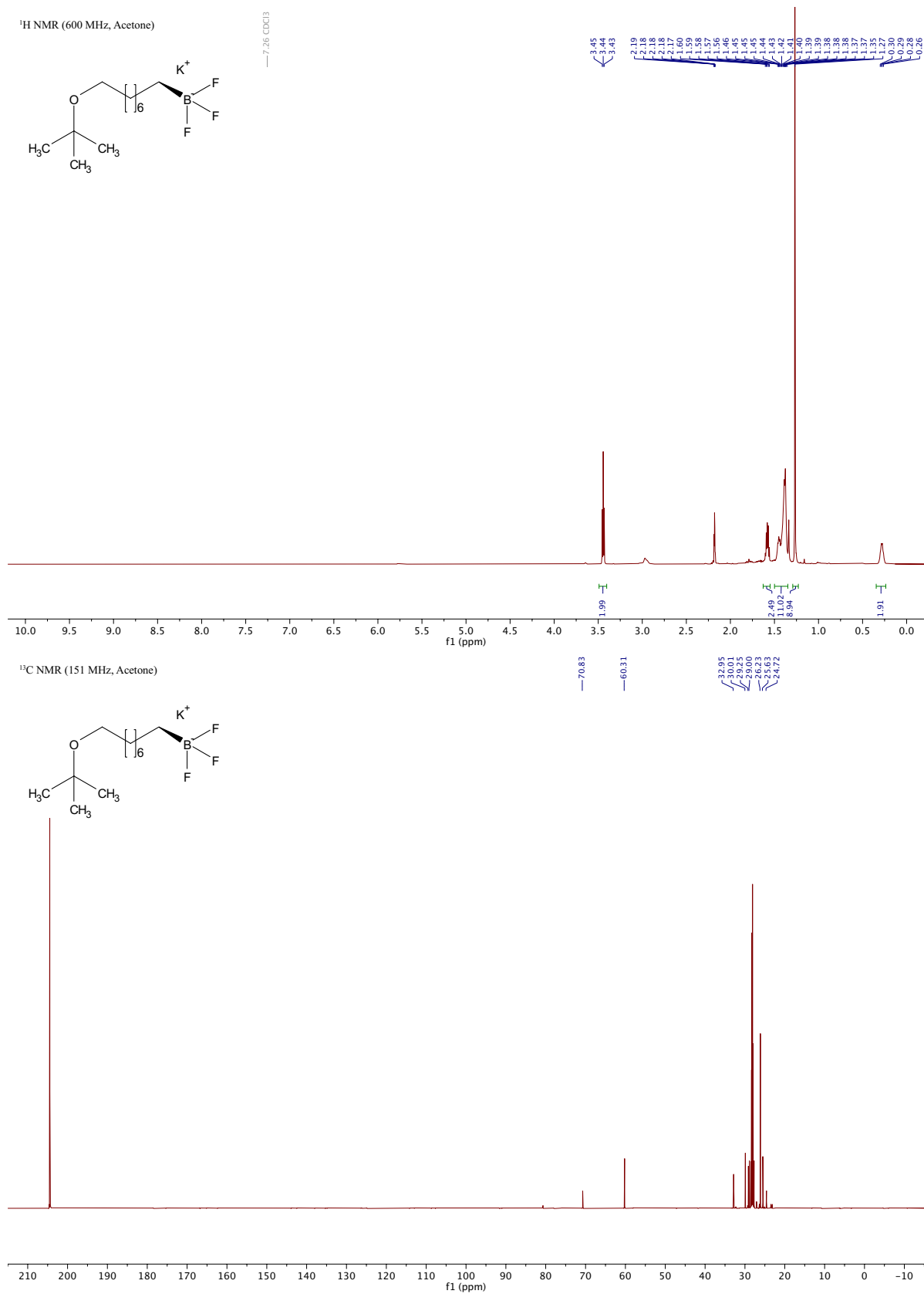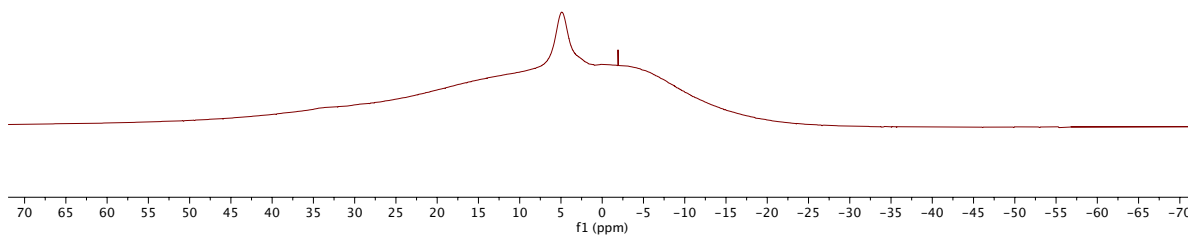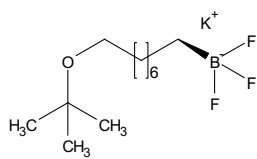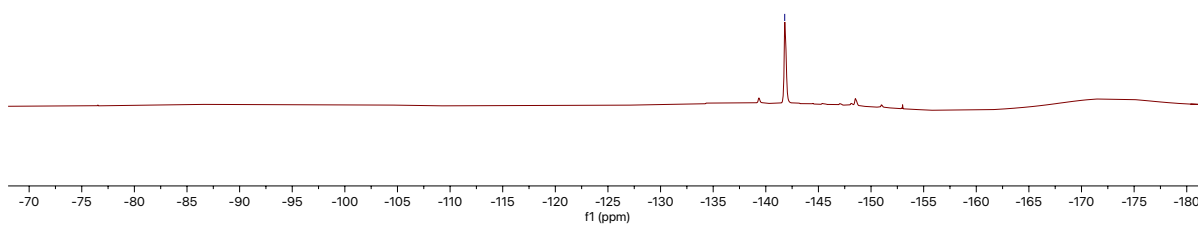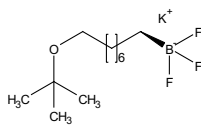
Product 2a

4-((6-methylpyridin-3-yl)methyl)morpholine [Experimental]

¹H NMR (500 MHz, CDCl₃)

¹³C NMR (126 MHz, CDCl₃)
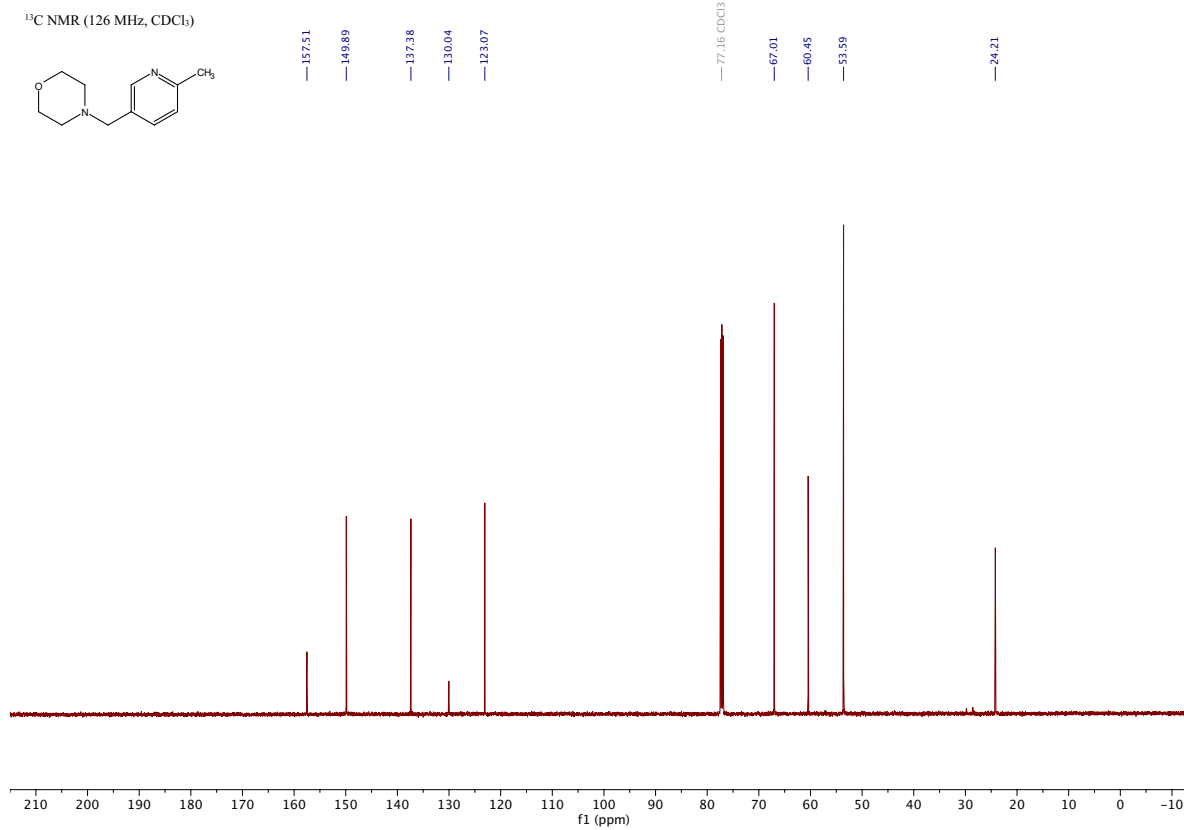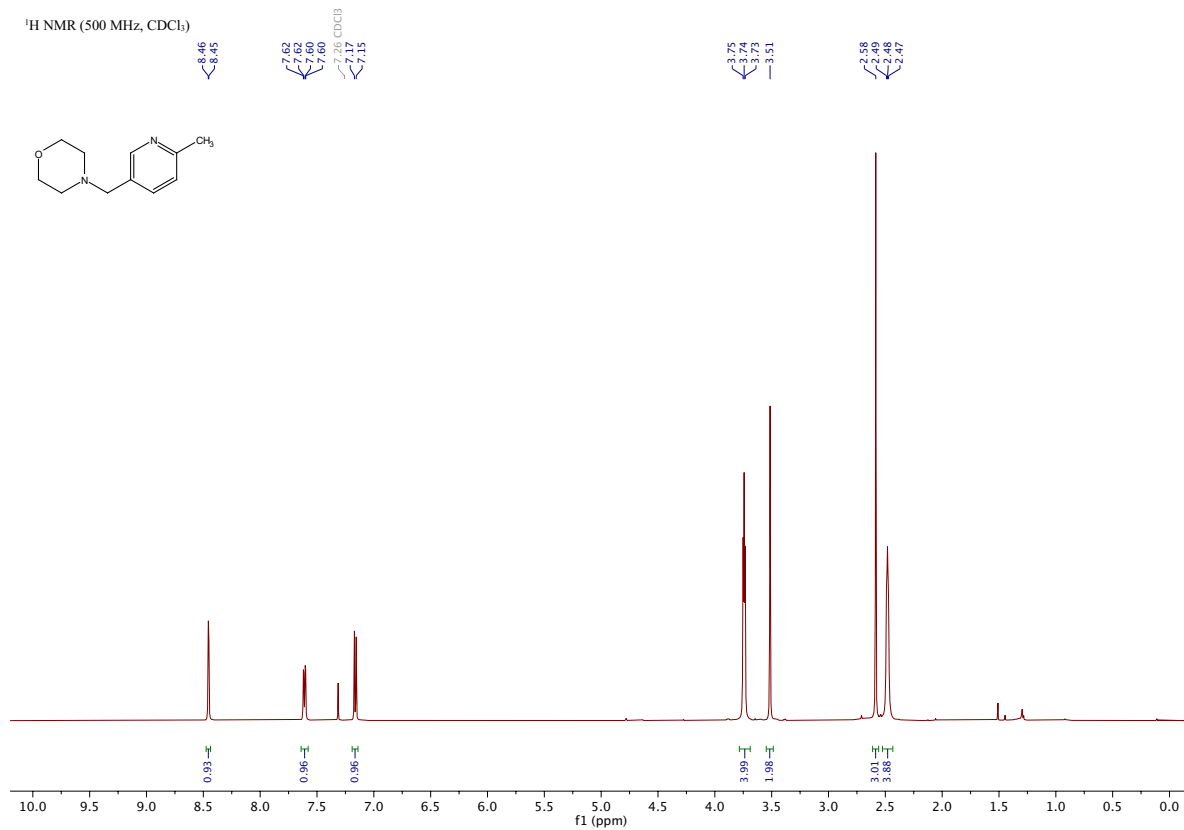
Product 3a

rac-((1*S*,2*S*)-2-(4,4,5,5-tetramethyl-1,3,2-dioxaborolan-2-yl)cyclopropyl)methyl   3,5-di-*tert*-butylbenzoate   [Experimental]

¹H NMR (500 MHz, CDCl₃)

¹³C NMR (126 MHz, CDCl₃)

167.46
151.05
129.99
127.10
123.92
83.24
77.16 CDCl3
69.45
35.04
31.50
24.81
24.79
16.65
9.91

f1 (ppm)

¹¹B NMR (160 MHz, CDCl₃)

33.21

f1 (ppm)

455

Product 4a-*β*

(1*R*,2*R*)-2-(4,4,5,5-tetramethyl-1,3,2-dioxaborolan-2-yl)cyclobutyl   3,5-di-*tert*-butylbenzoate
[Experimental]

¹H NMR (500 MHz, CDCl₃)

^{13}C NMR (126 MHz, CDCl$_3$)

166.75
150.93
130.03
126.96
123.89
83.46
77.16 CDCl3
70.84
35.03
31.51
31.10
24.93
24.91
16.06

^{11}B NMR (160 MHz, CDCl$_3$)

32.92

457

Product 4a-*γ*

(1*s*,3*s*)-3-(4,4,5,5-tetramethyl-1,3,2-dioxaborolan-2-yl)cyclobutyl   3,5-di-*tert*-butylbenzoate
[Experimental]

¹H NMR (500 MHz, CDCl₃)

459
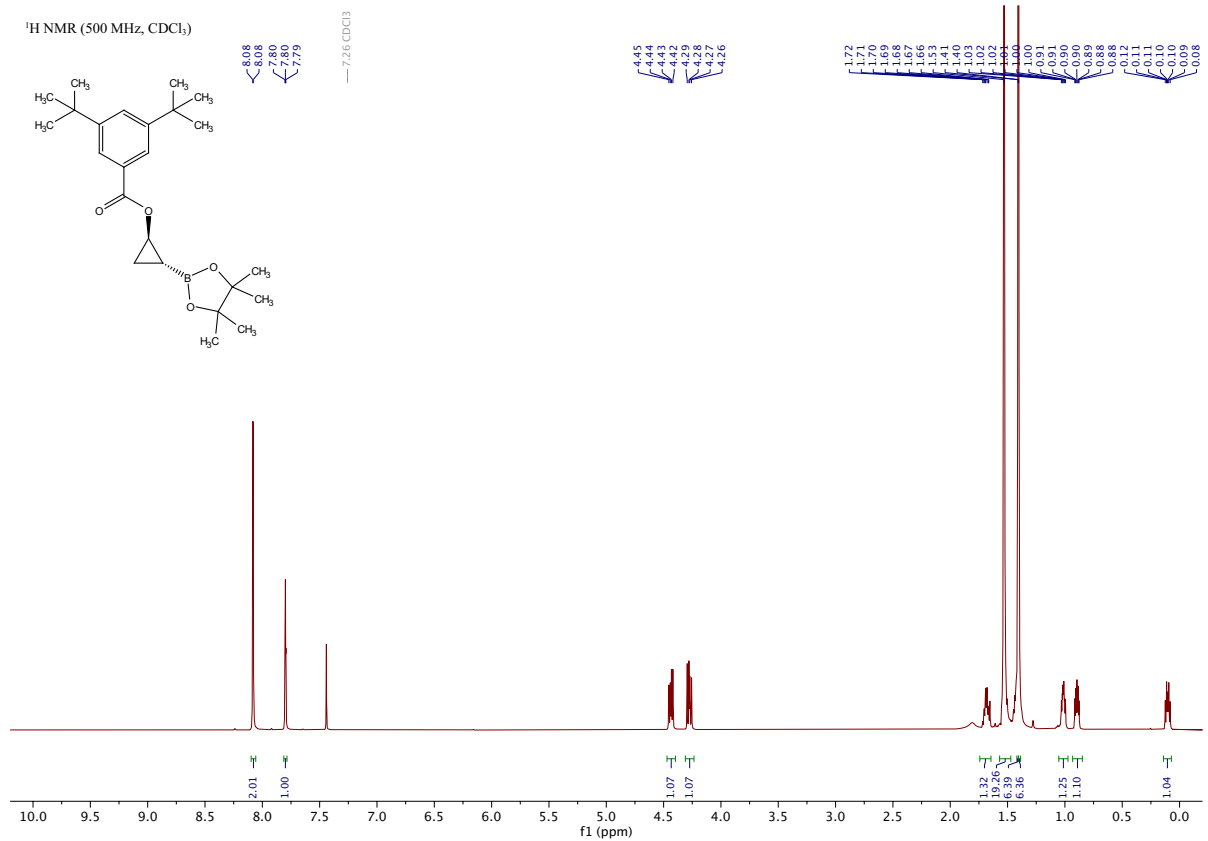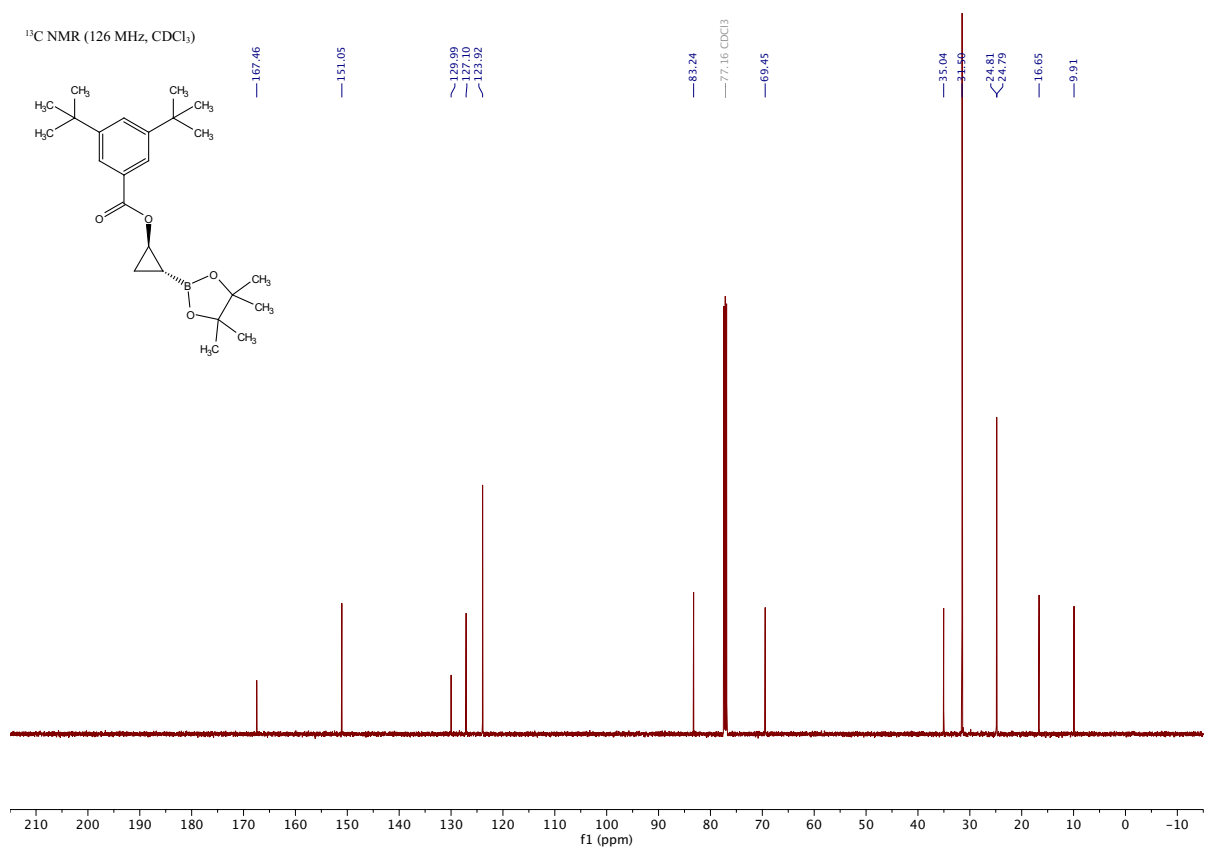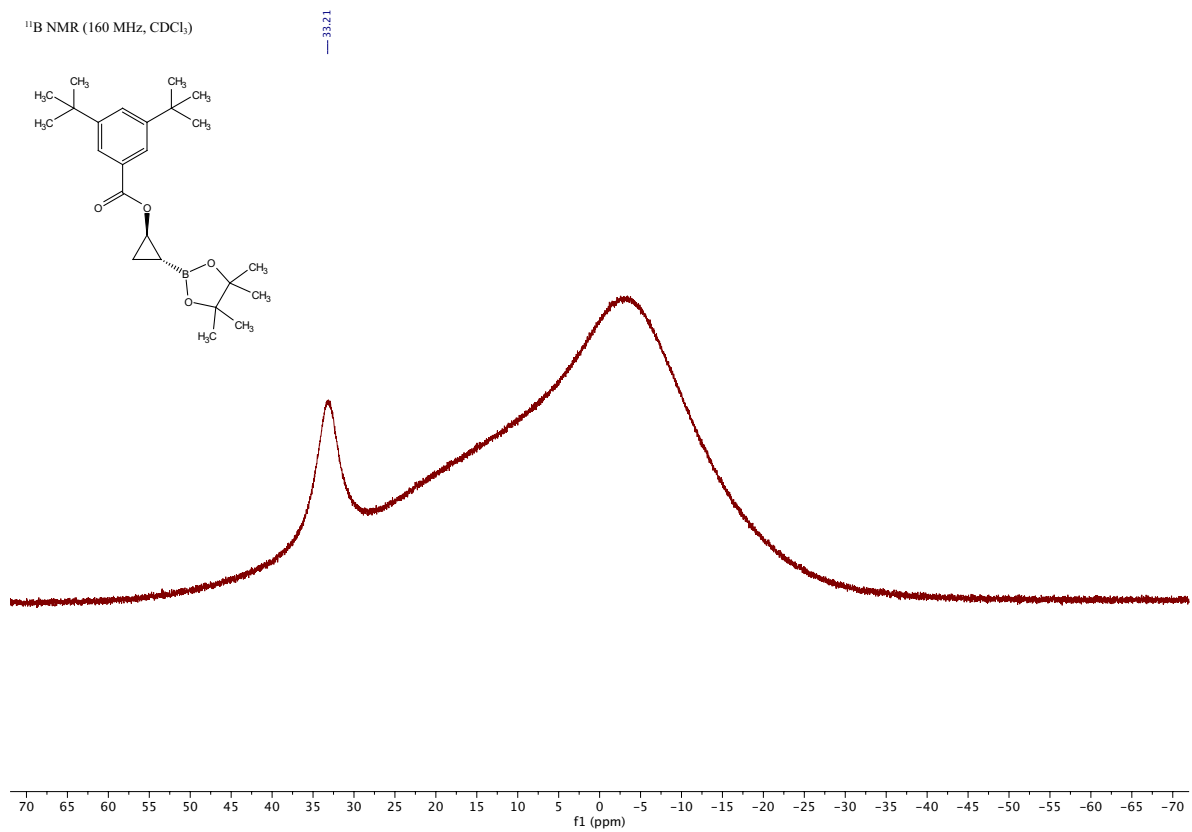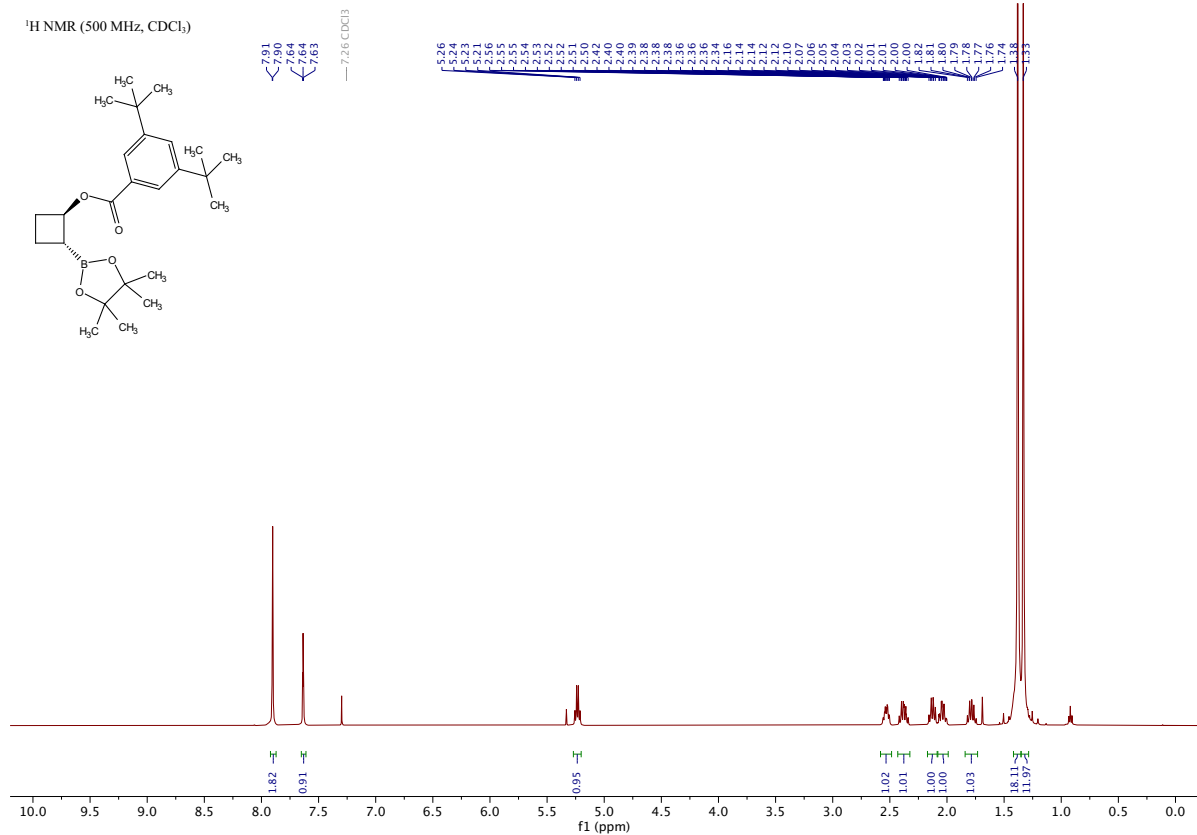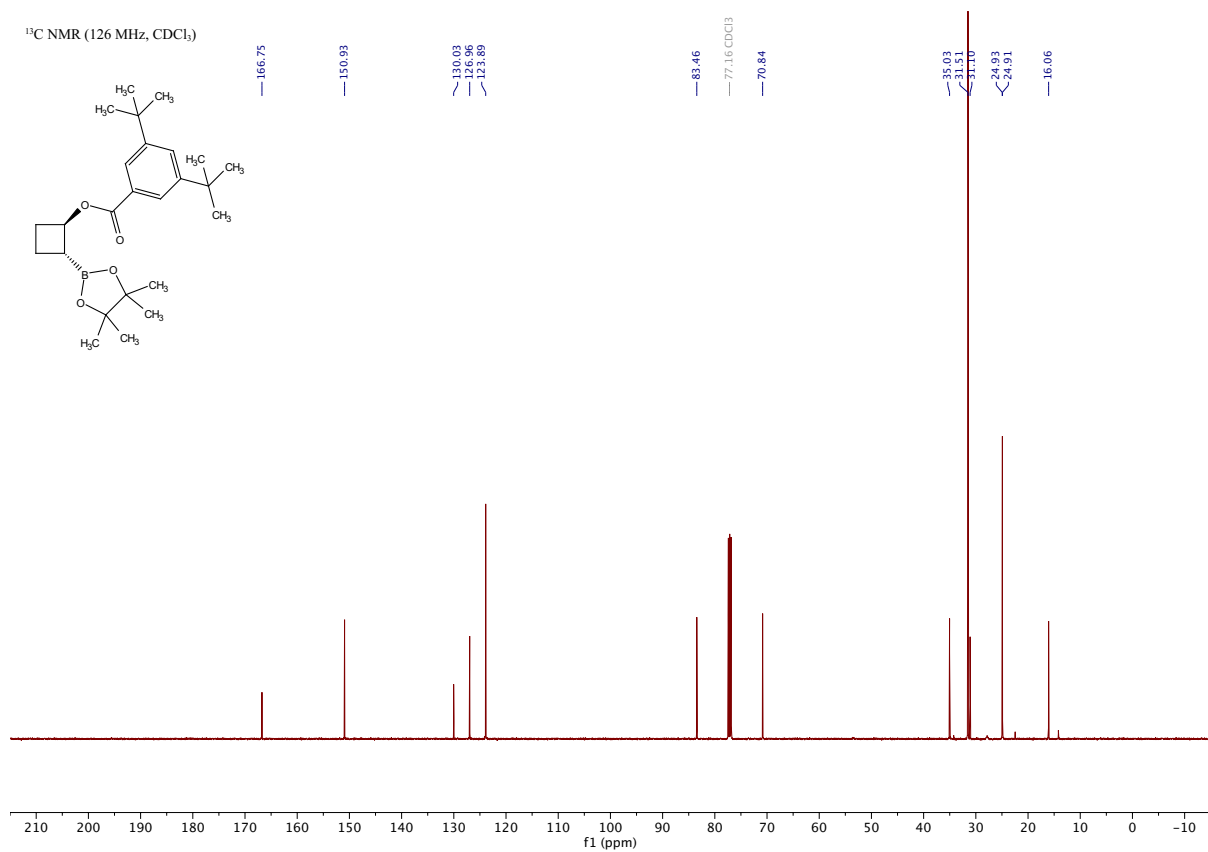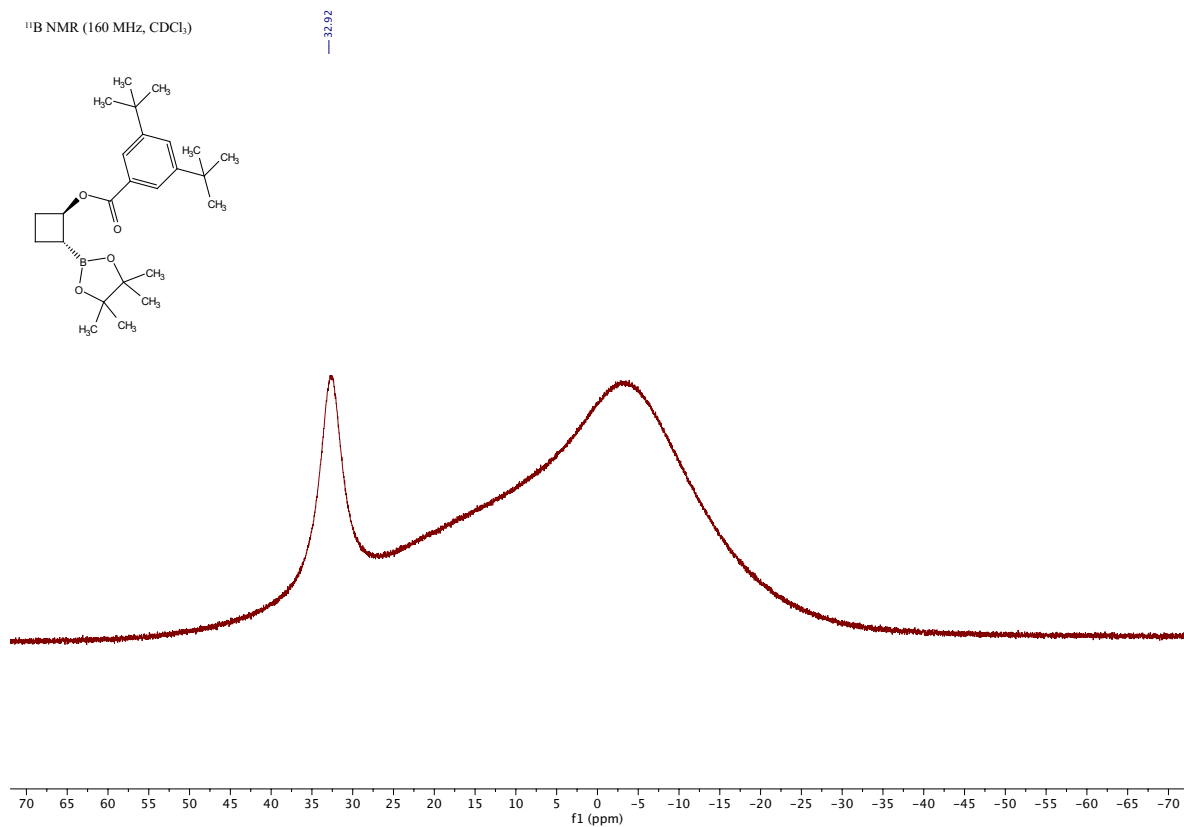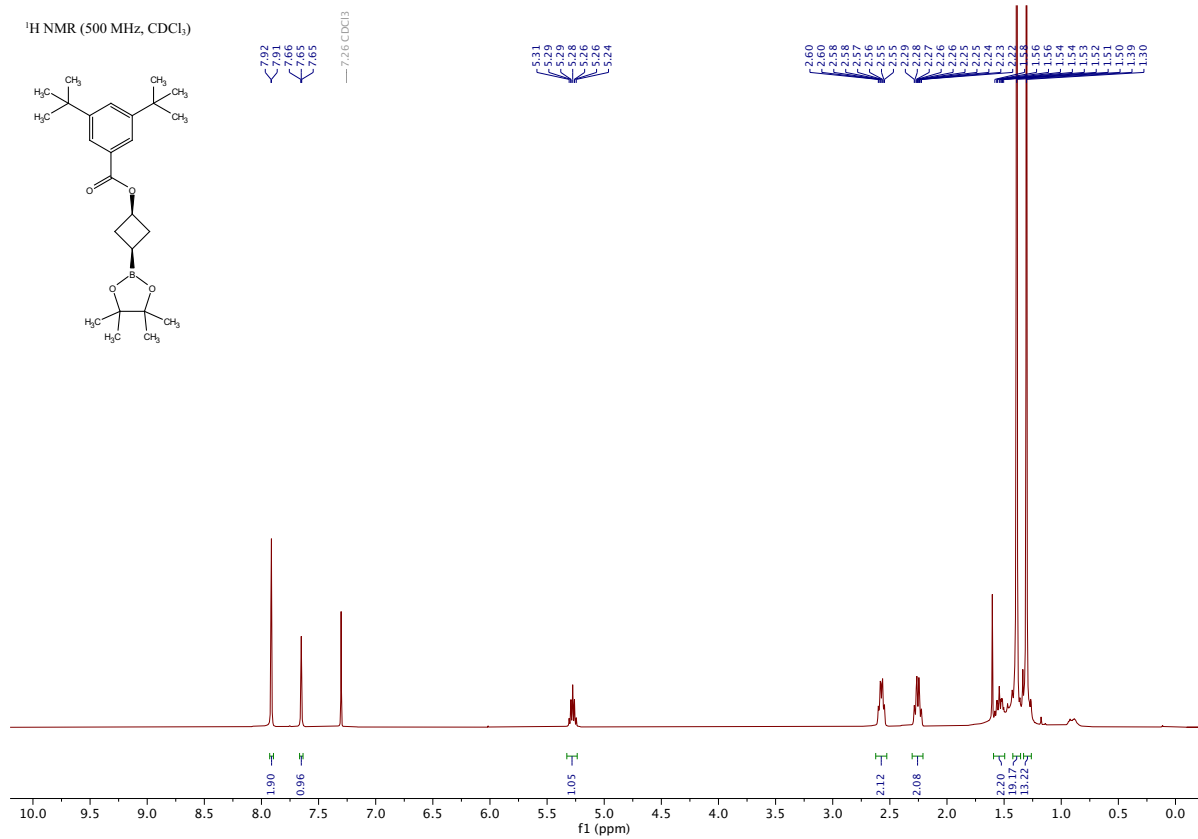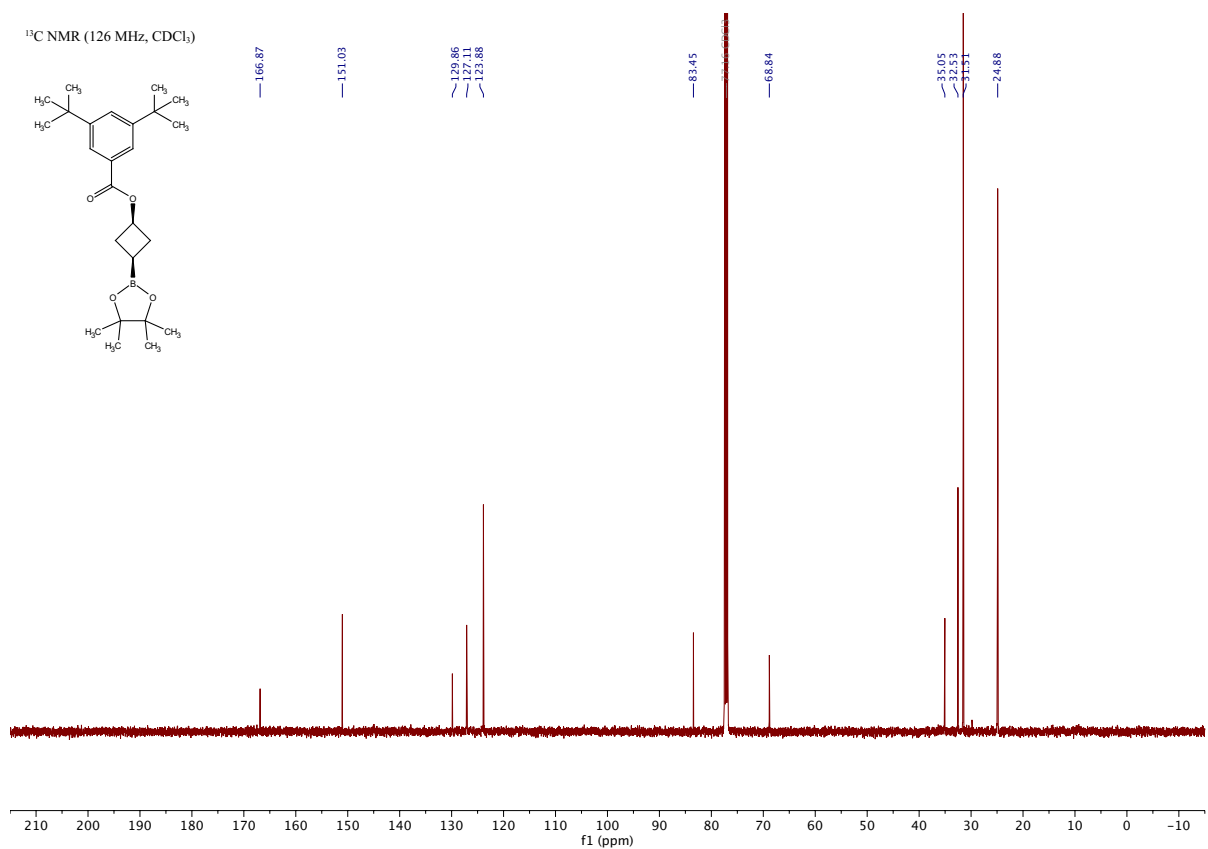
Product 5a

tert-butyl 2-(4,4,5,5-tetramethyl-1,3,2-dioxaborolan-2-yl)-1-oxa-6-azaspiro[2.5]octane-6-carboxylate [Experimental]

¹H NMR (500 MHz, CDCl₃)

¹³C NMR (126 MHz, CDCl₃)

¹¹B NMR (160 MHz, CDCl₃)

461

Product 6a

tert-butyl 3-(4,4,5,5-tetramethyl-1,3,2-dioxaborolan-2-yl)azetidine-1-carboxylate
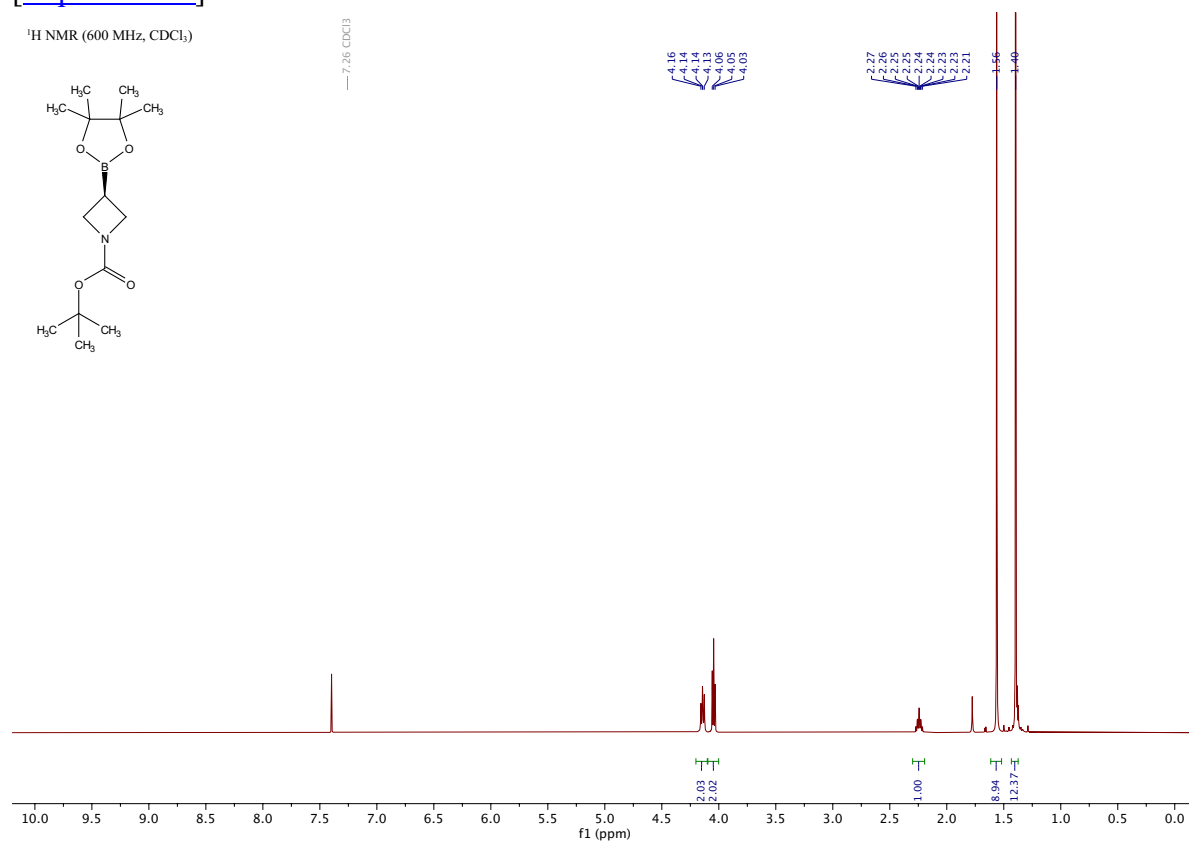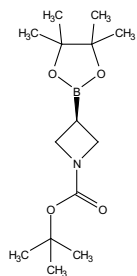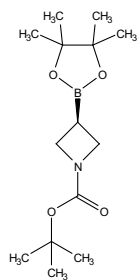
[Experimental]

¹H NMR (600 MHz, CDCl₃)

^13^C NMR (151 MHz, CDCl₃)

— 156.50
— 83.97
— 79.31
— 51.21
— 50.26
— 28.65
— 25.00
— 11.46

^11^B NMR (193 MHz, CDCl₃)

— 33.45

463

Product 7a

tert-butyl 6-(4,4,5,5-tetramethyl-1,3,2-dioxaborolan-2-yl)-2-azaspiro[3.3]heptane-2-carboxylate [Experimental]

¹H NMR (500 MHz, CDCl₃)

^{13}C NMR (126 MHz, CDCl$_3$)

156.45
83.33
79.21
77.16 CDCl$_3$
61.81
37.75
34.55
28.53
24.85
11.73
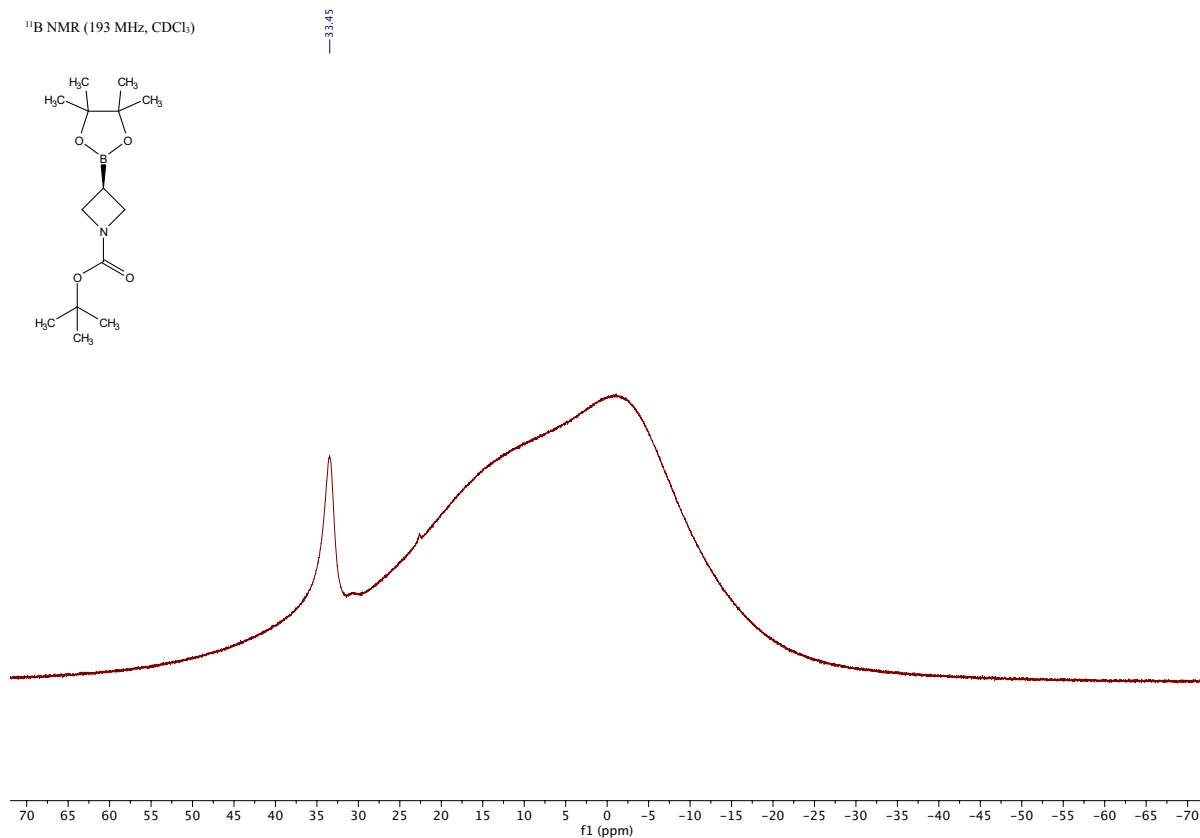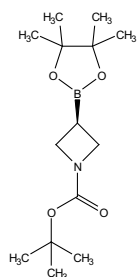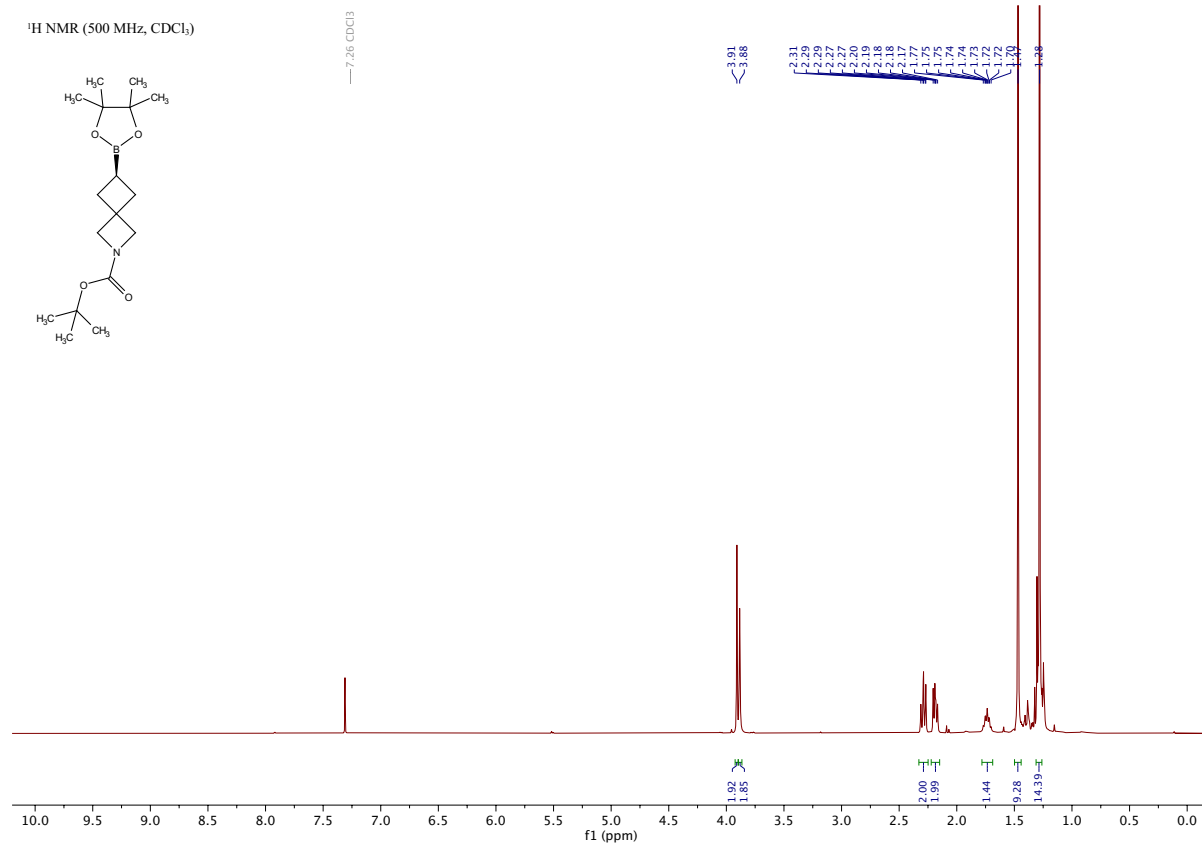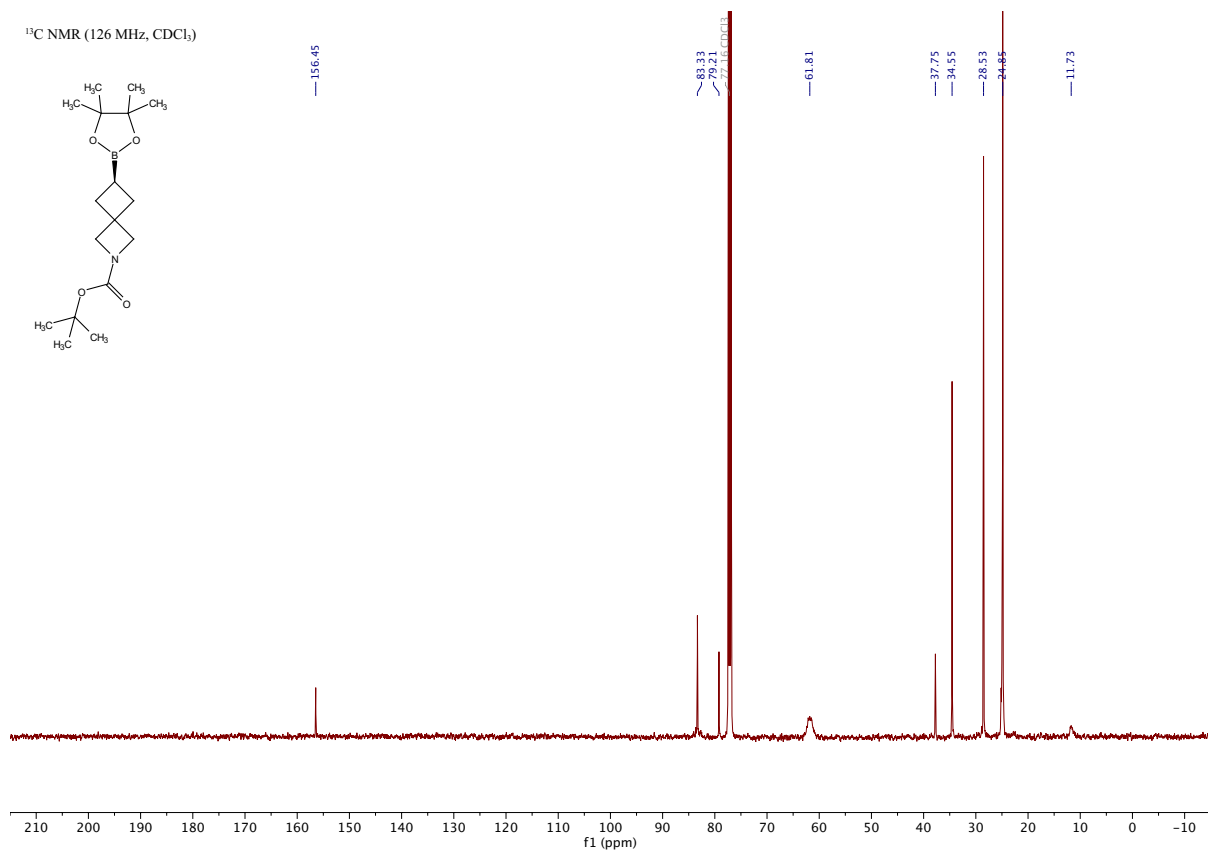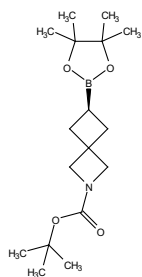
^{11}B NMR (160 MHz, CDCl$_3$)

33.83

Product 8a

2-(7,7-dimethyl-6,8-dioxaspiro[3.5]nonan-2-yl)-4,4,5,5-tetramethyl-1,3,2-dioxaborolane
[Experimental]

¹H NMR (500 MHz, CDCl₃)

¹³C NMR (126 MHz, CDCl₃)

97.61
83.30
77.16 CDCl3
69.26
69.08
35.94
29.29
24.86
23.92

210 200 190 180 170 160 150 140 130 120 110 100 90 80 70 60 50 40 30 20 10 0 −10
f1 (ppm)

¹¹B NMR (160 MHz, CDCl₃)

34.02

70 65 60 55 50 45 40 35 30 25 20 15 10 5 0 −5 −10 −15 −20 −25 −30 −35 −40 −45 −50 −55 −60 −65 −70
f1 (ppm)
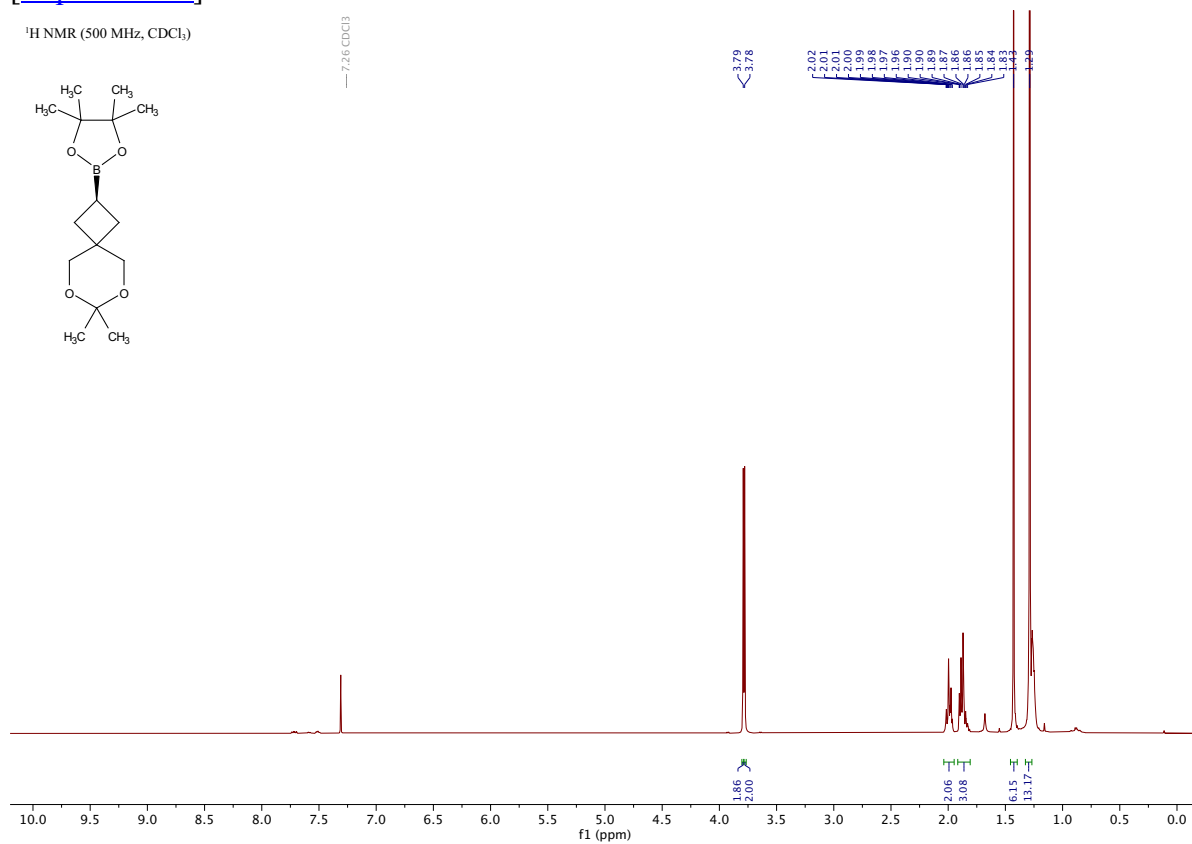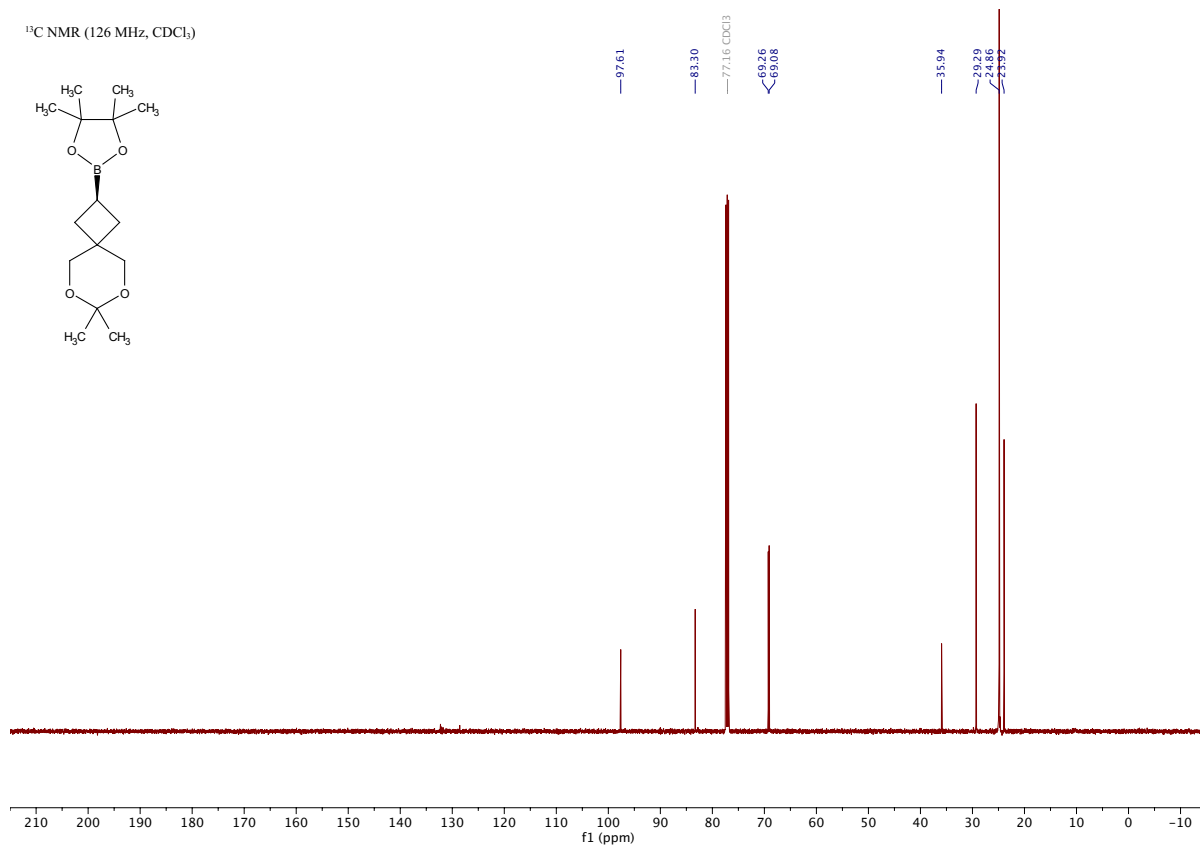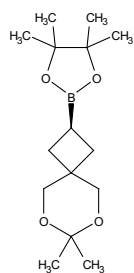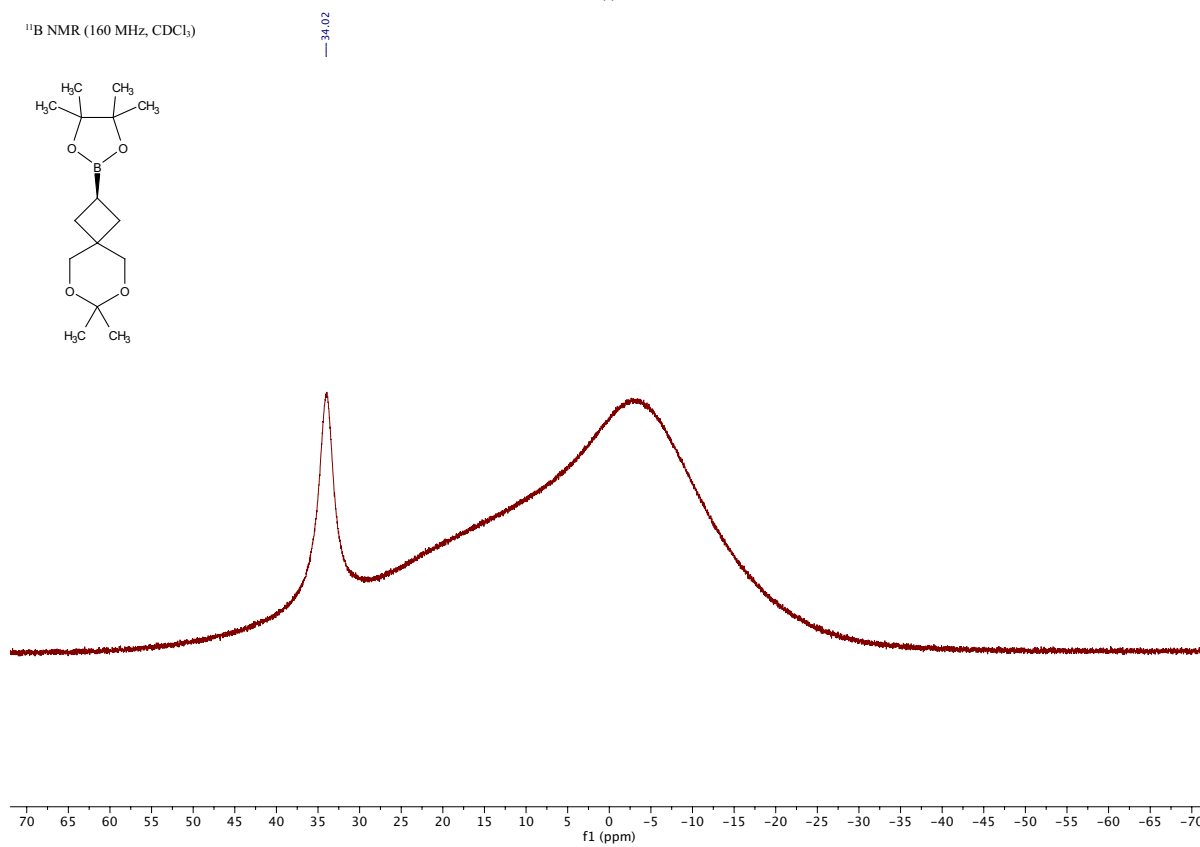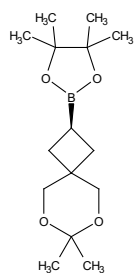
Product 9a

4,4,5,5-tetramethyl-2-(tetrahydrofuran-3-yl)-1,3,2-dioxaborolane [Experimental]

¹H NMR (400 MHz, CHLOROFORM-*D*)
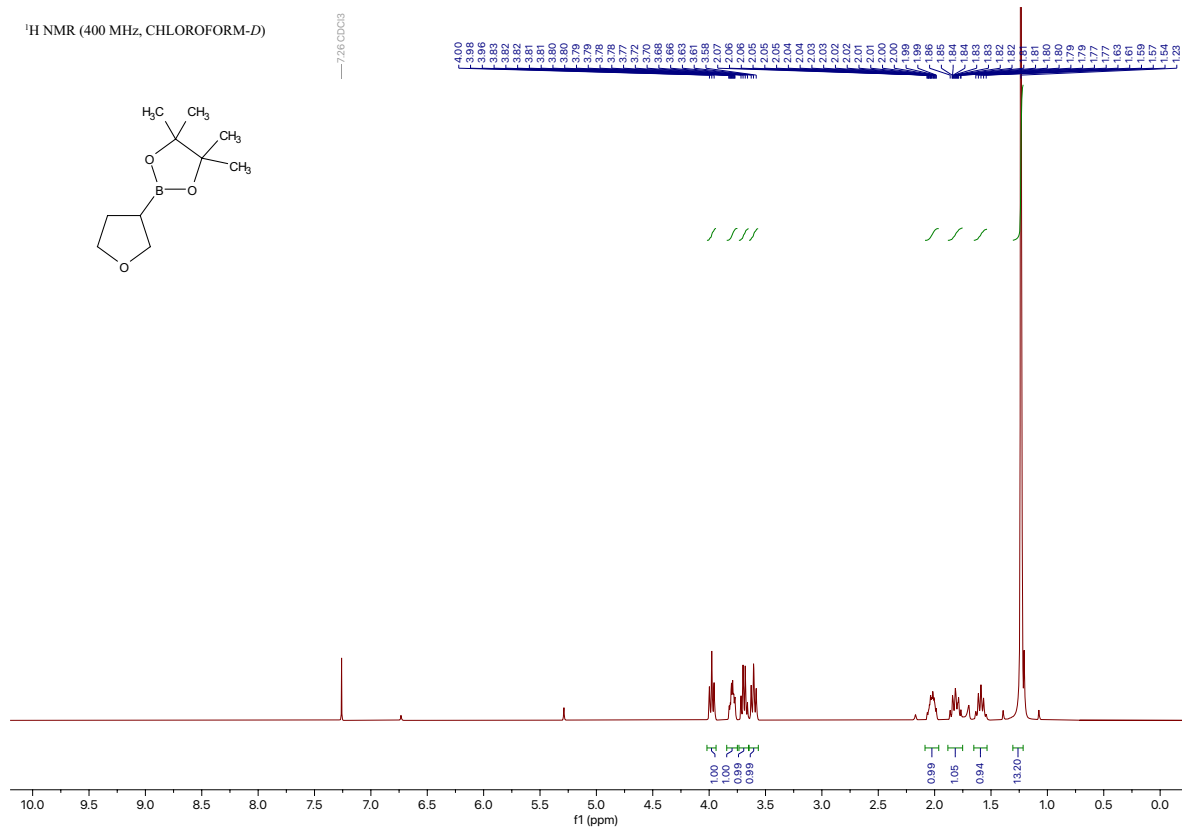
¹³C NMR (101 MHz, CHLOROFORM-*D*)
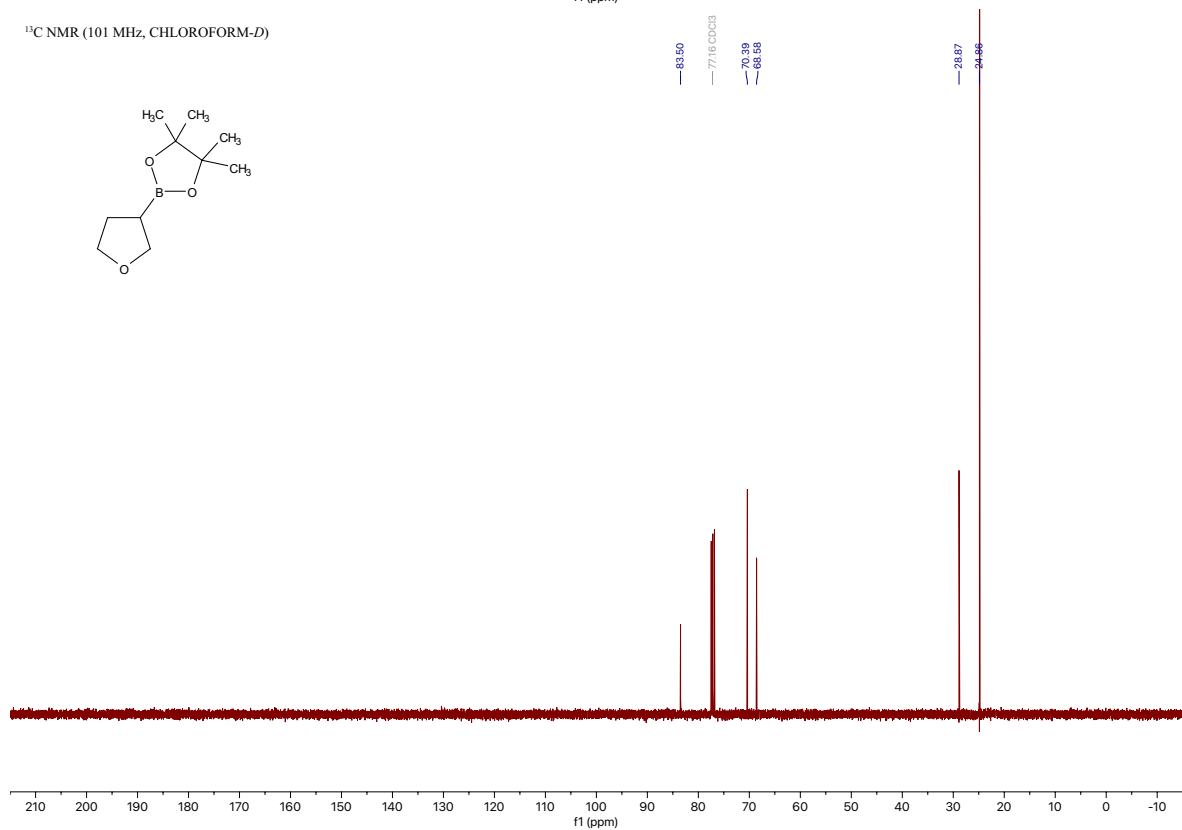
Product 10a

rac-(3*R*,4*R*)-3-methyl-4-(4,4,5,5-tetramethyl-1,3,2-dioxaborolan-2-yl)dihydrofuran-2(3*H*)-one [Experimental]

¹H NMR (500 MHz, CDCl₃)

¹³C NMR (126 MHz, CDCl₃)

¹¹B NMR (160 MHz, CDCl₃)

470
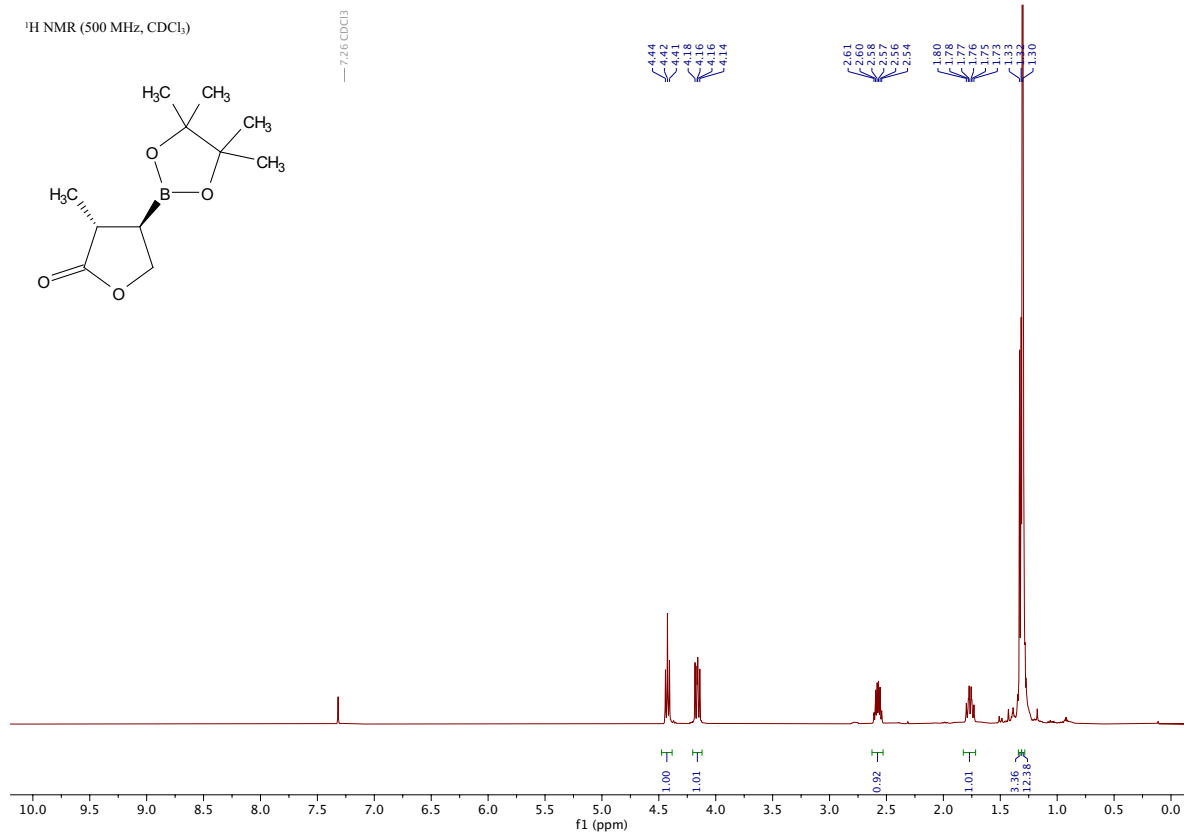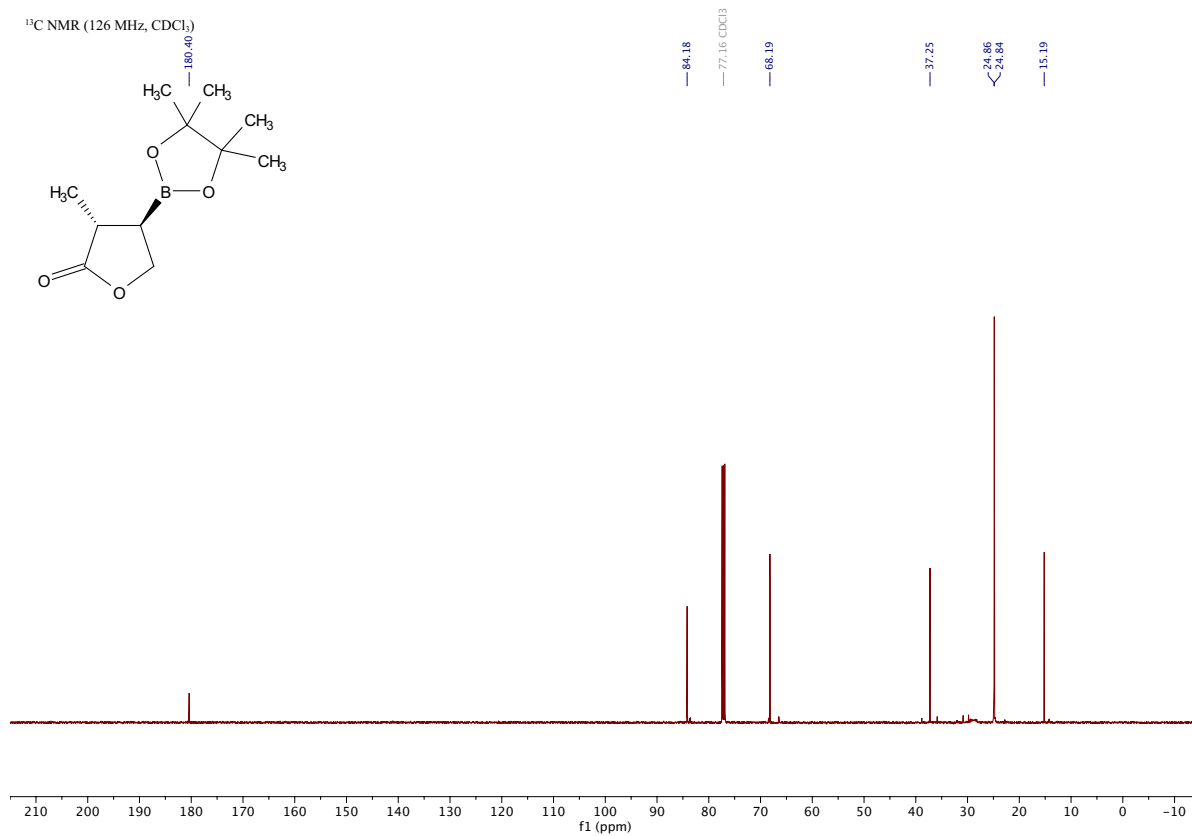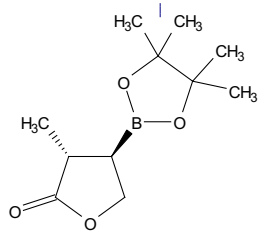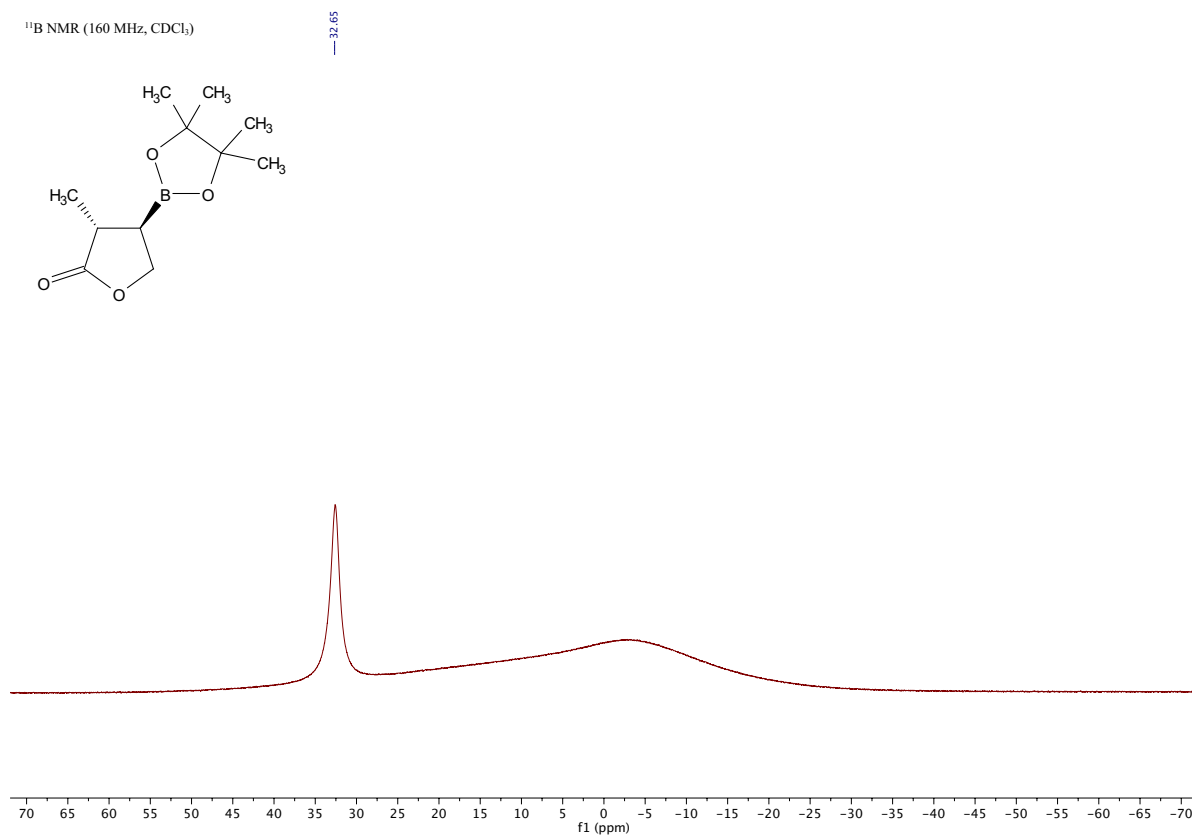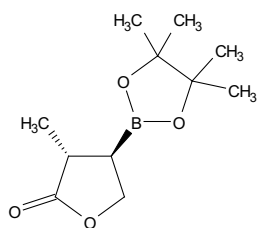
Product 11a

2,2,2-trifluoro-1-(3-(4,4,5,5-tetramethyl-1,3,2-dioxaborolan-2-yl)pyrrolidin-1-yl)ethan-1-one [Experimental]

^{1}H NMR (500 MHz, CDCl$_3$)

^{13}C NMR (126 MHz, CDCl$_3$)
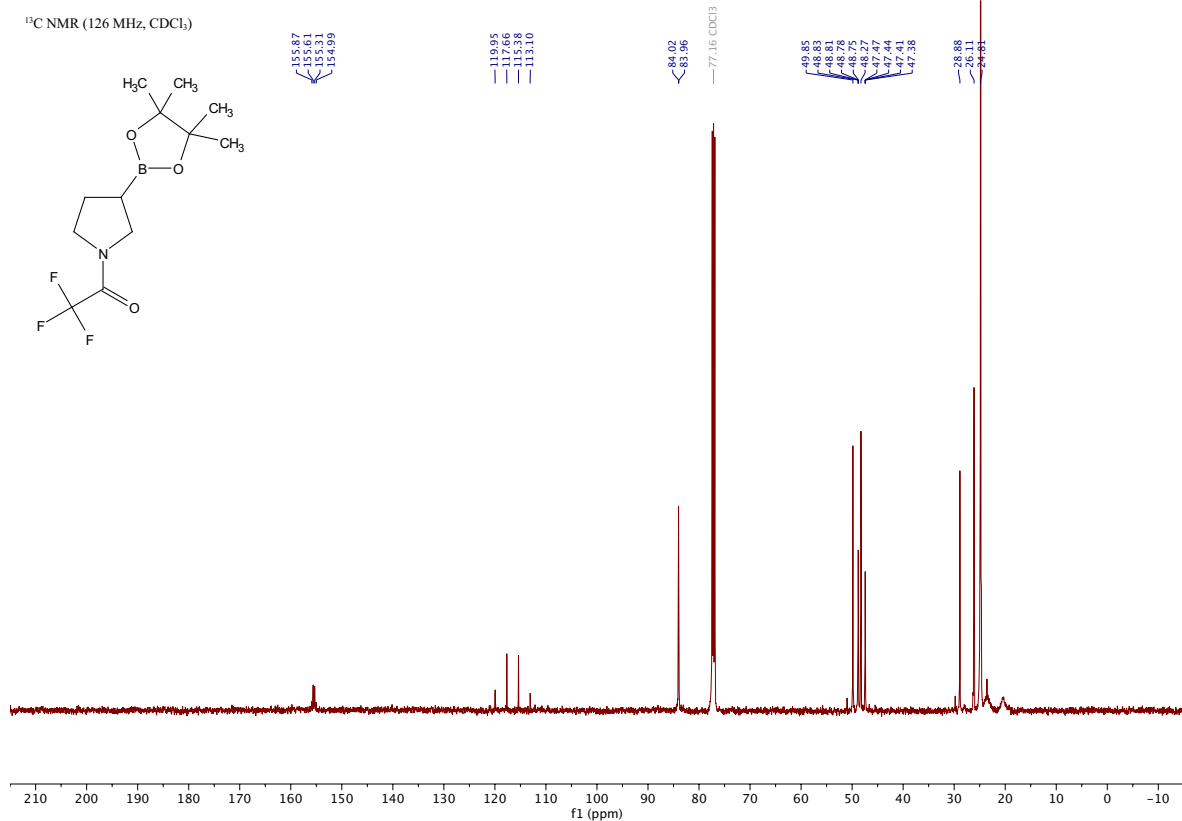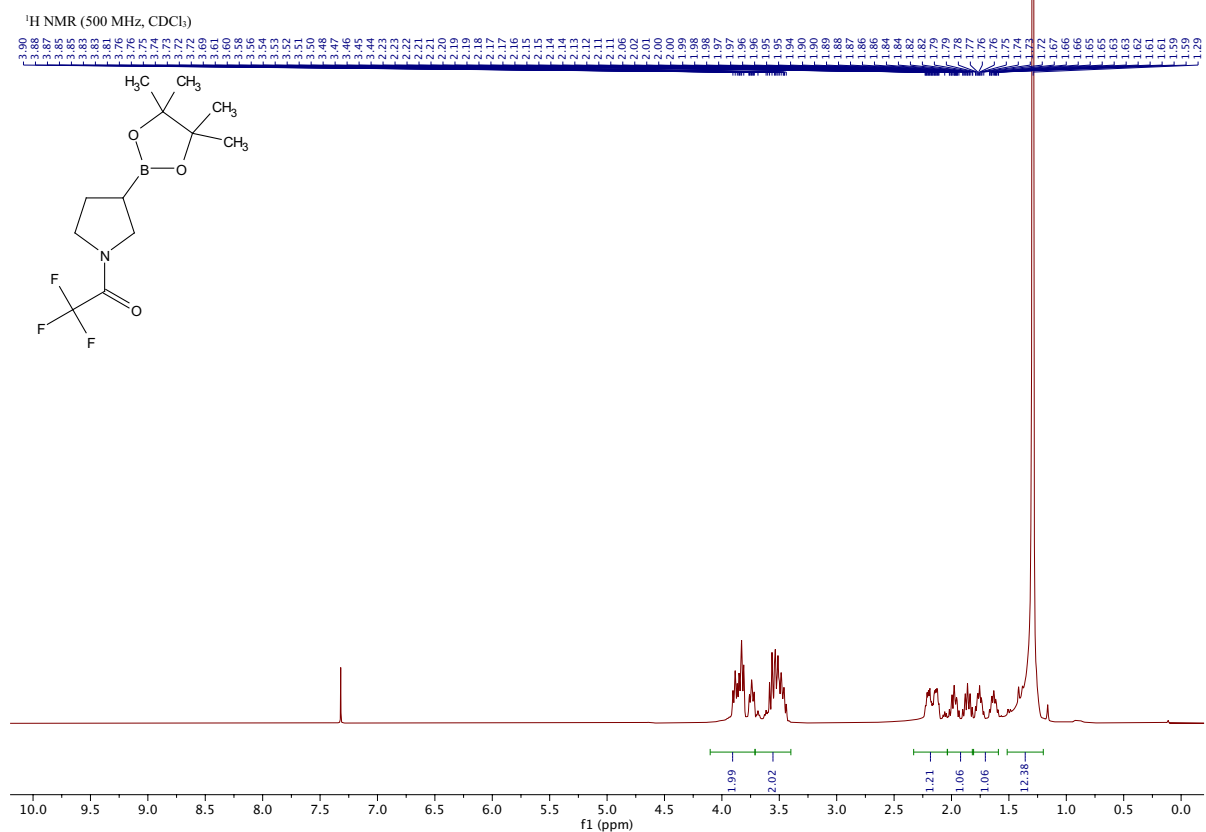
¹¹B NMR (160 MHz, CDCl₃)

33.11
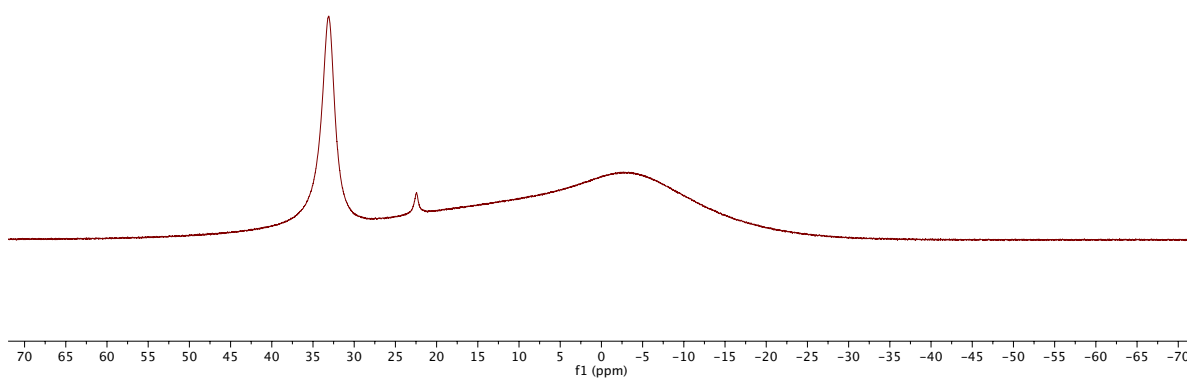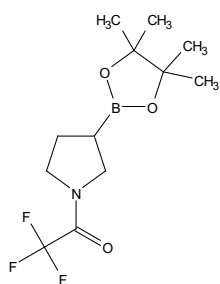
¹⁹F NMR (470 MHz, CDCl₃) δ -72.47, -72.65.

-72.47
-72.65

472
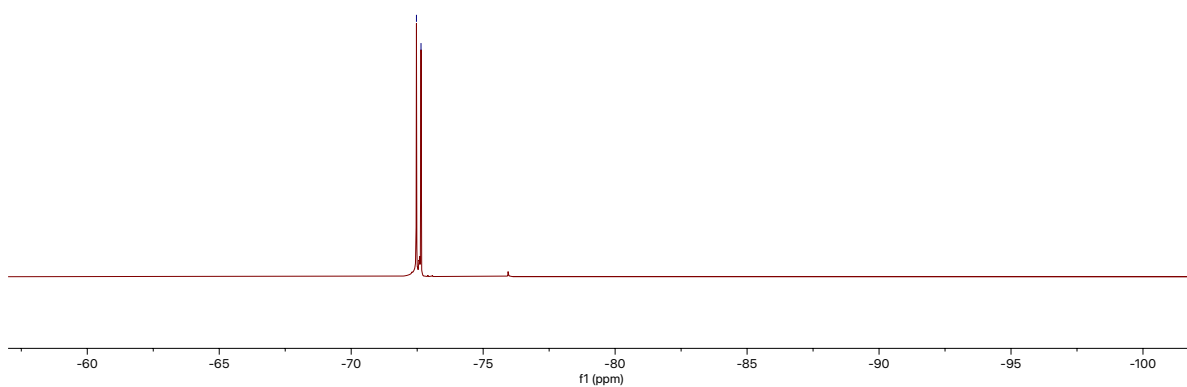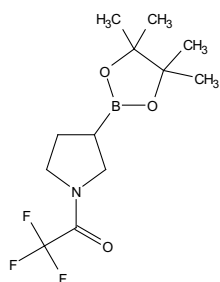
Product 12a

tert-butyl 3-(trifluoro-λ4-boraneyl)pyrrolidine-1-carboxylate, potassium salt [Experimental]

¹H NMR (700 MHz, Acetone)

¹³C NMR (126 MHz, Acetone)

154.97
77.83
77.77
50.72
50.29
48.42
48.16
28.85
25.04

f1 (ppm)

¹¹B NMR (160 MHz, Acetone) δ 4.63.

4.63

f1 (ppm)

474
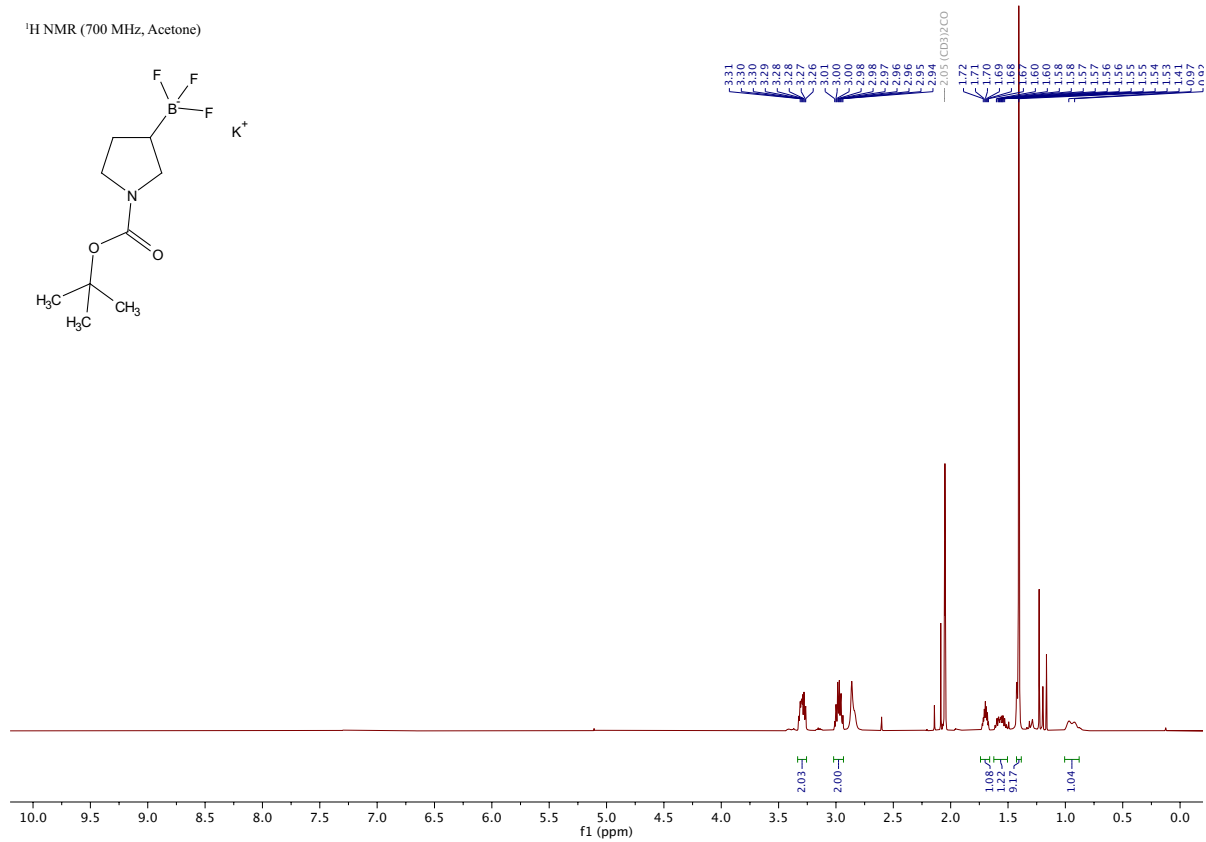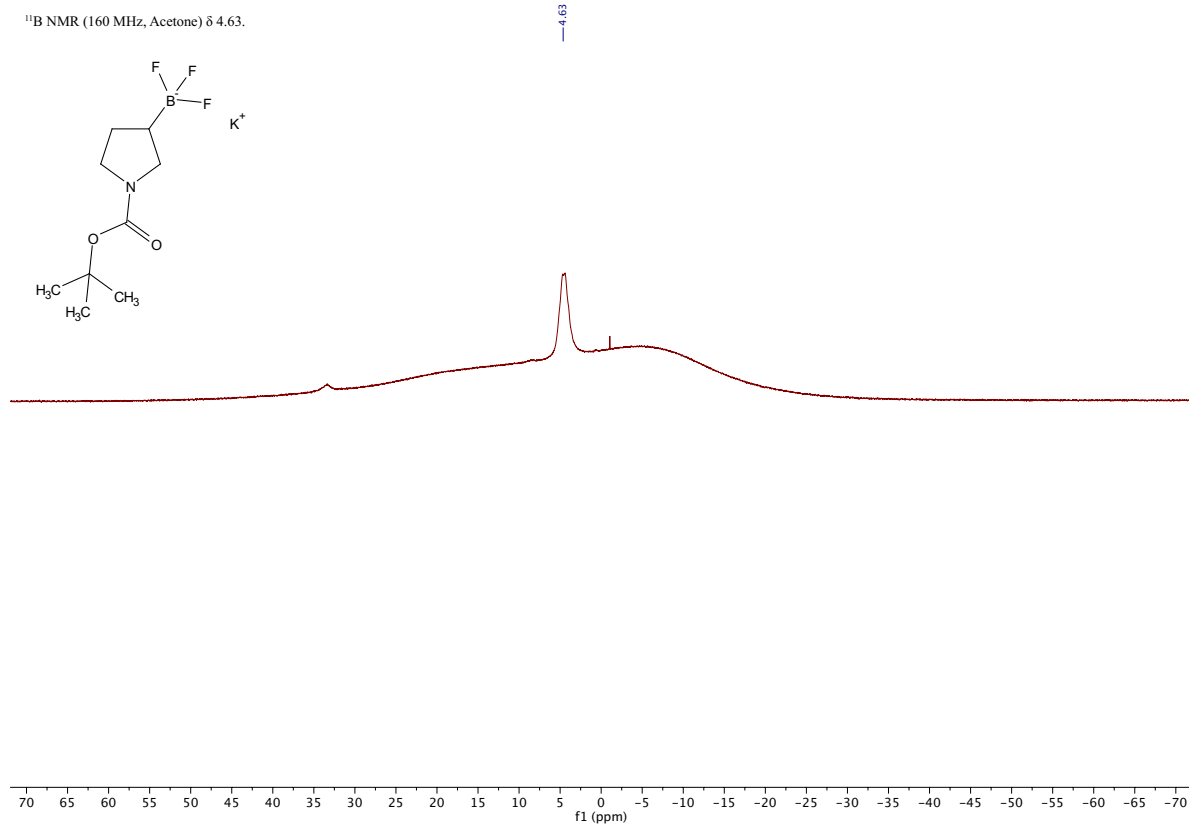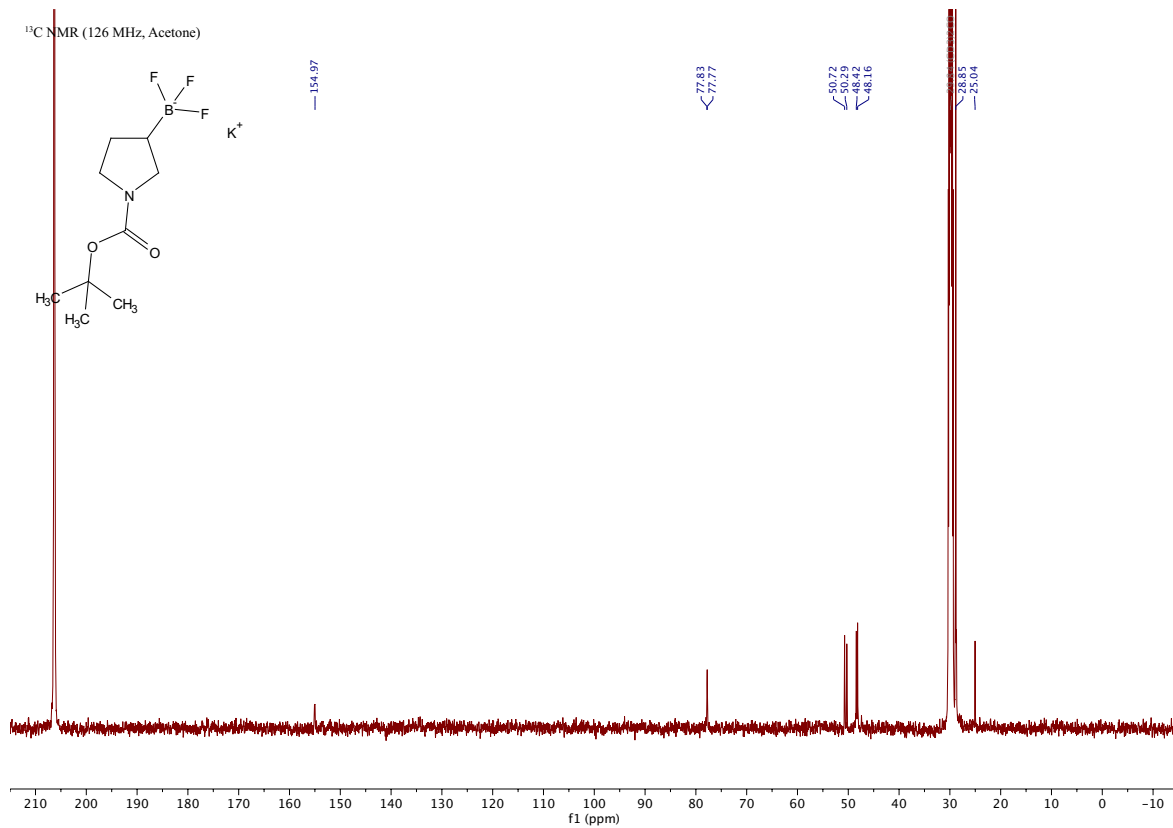
Product 13a

2-(3-(4-(*tert*-butyl)phenyl)bicyclo[1.1.1]pentan-1-yl)-4,4,5,5-tetramethyl-1,3,2-dioxaborolane
[Experimental]

¹H NMR (500 MHz, CDCl₃)

¹³C NMR (126 MHz, CDCl₃)
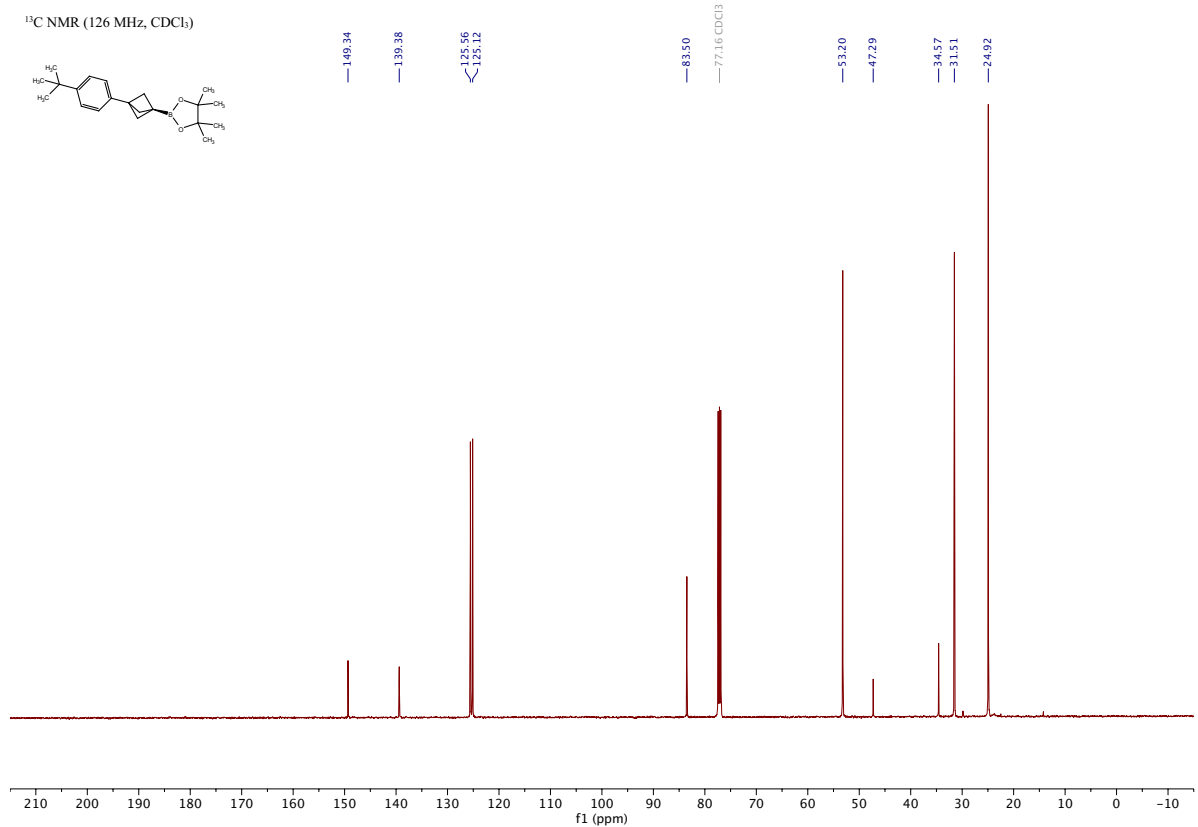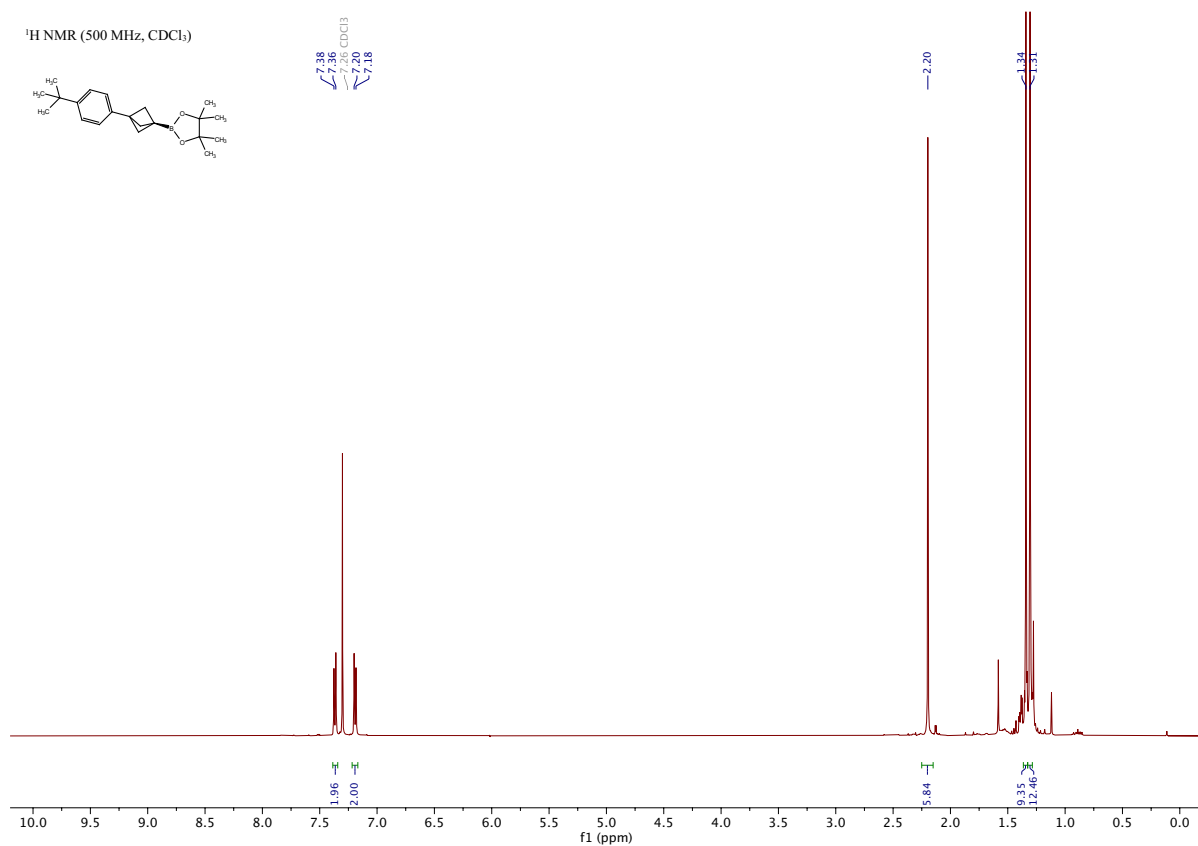
Product 14a

(1S,2S,4R)-1,7,7-trimethylbicyclo[2.2.1]heptan-2-yl   cyclobutanecarboxylate-2,4,4,5,5-pentamethyl-1,3,2-dioxaborolane [Experimental]

^{1}H NMR (600 MHz, CDCl$_3$)

174.37
176.18
176.16
175.73

85.99
85.92
85.83
83.58
83.55
83.51

48.76
48.72
48.70
48.67
48.65
48.64
41.67
41.64
39.79
39.75
39.74
39.72
38.83
38.35

30.03
30.02
27.18
27.02
26.95
26.94
26.92
26.82
26.68
25.63
25.48
25.15
25.13
25.09
25.06
25.03
20.47
20.46
20.44
20.42
19.73

210 200 190 180 170 160 150 140 130 120 110 100 90 80 70 60 50 40 30 20 10 0 −10
f1 (ppm)

^{11}B NMR (193 MHz, CDCl$_3$) δ 33.57.

33.57

70 65 60 55 50 45 40 35 30 25 20 15 10 5 0 −5 −10 −15 −20 −25 −30 −35 −40 −45 −50 −55 −60 −65 −70
f1 (ppm)
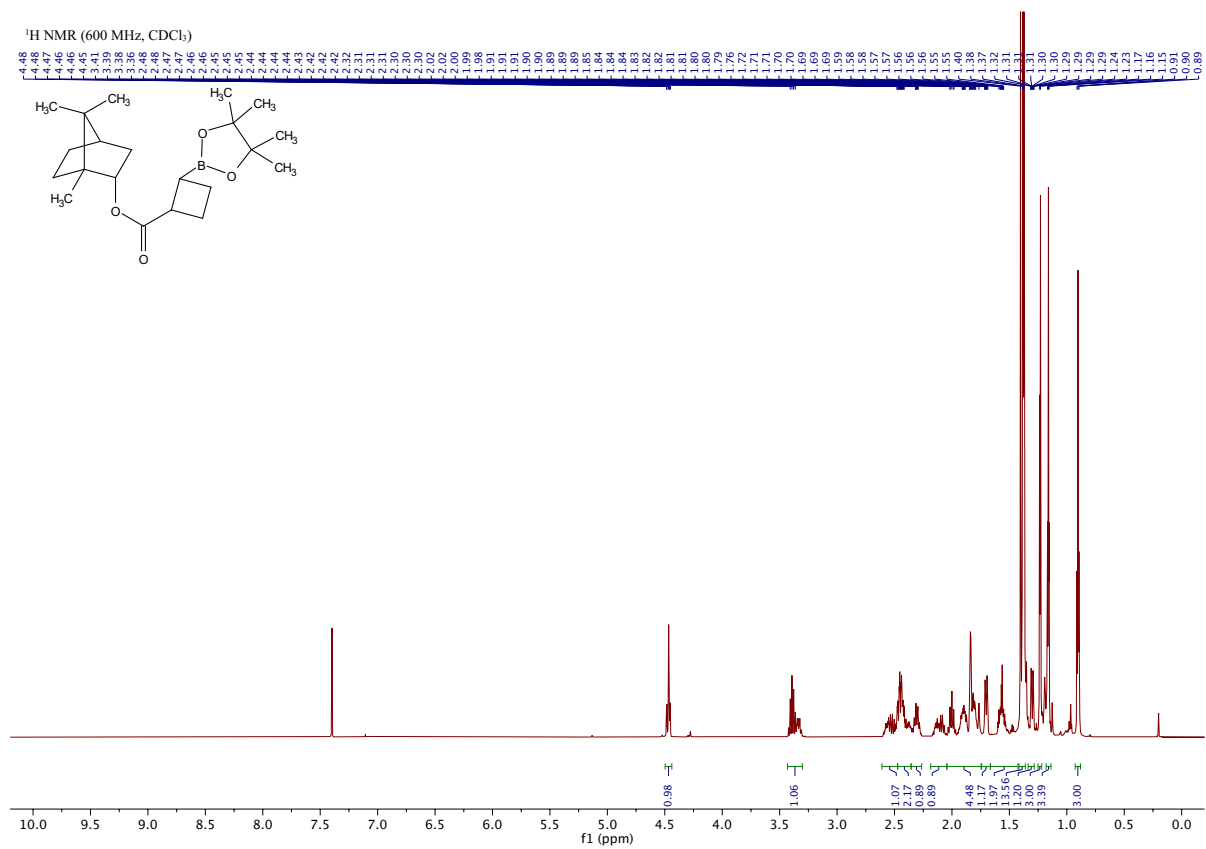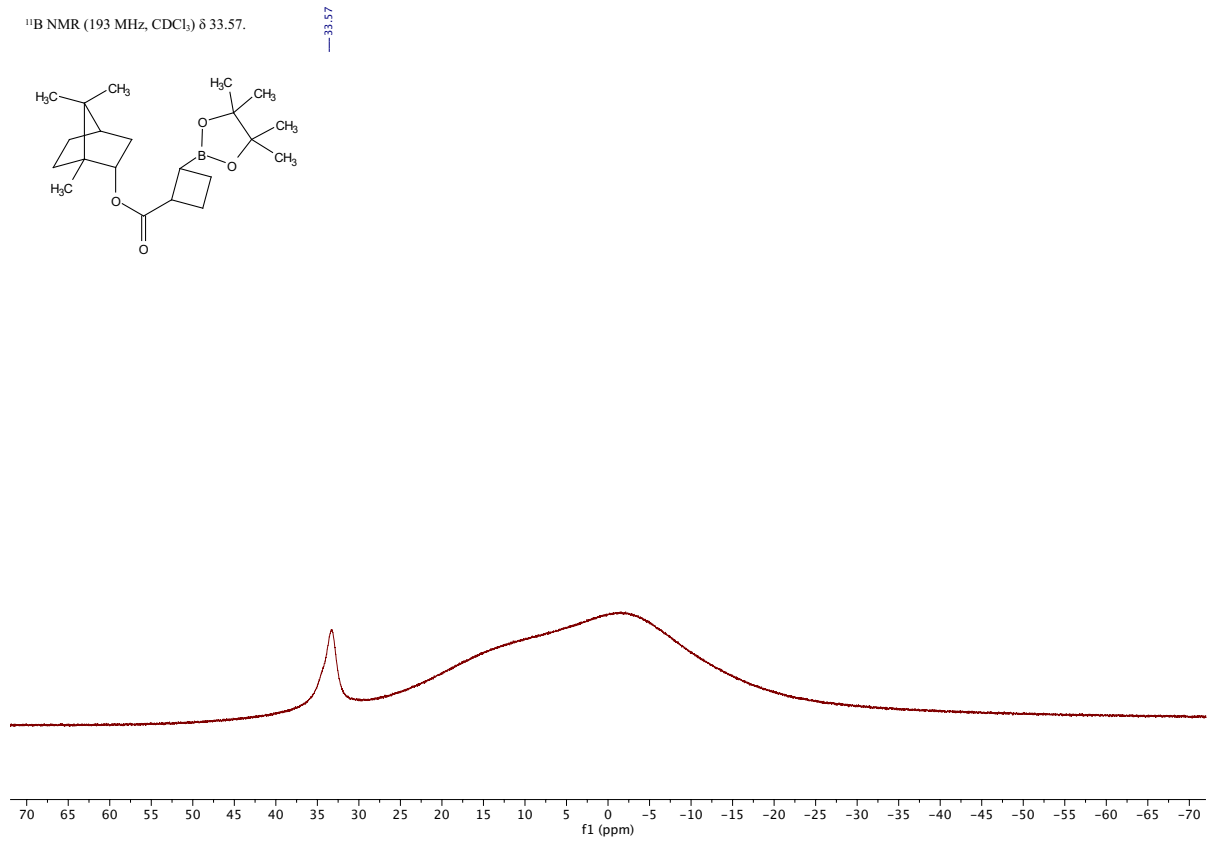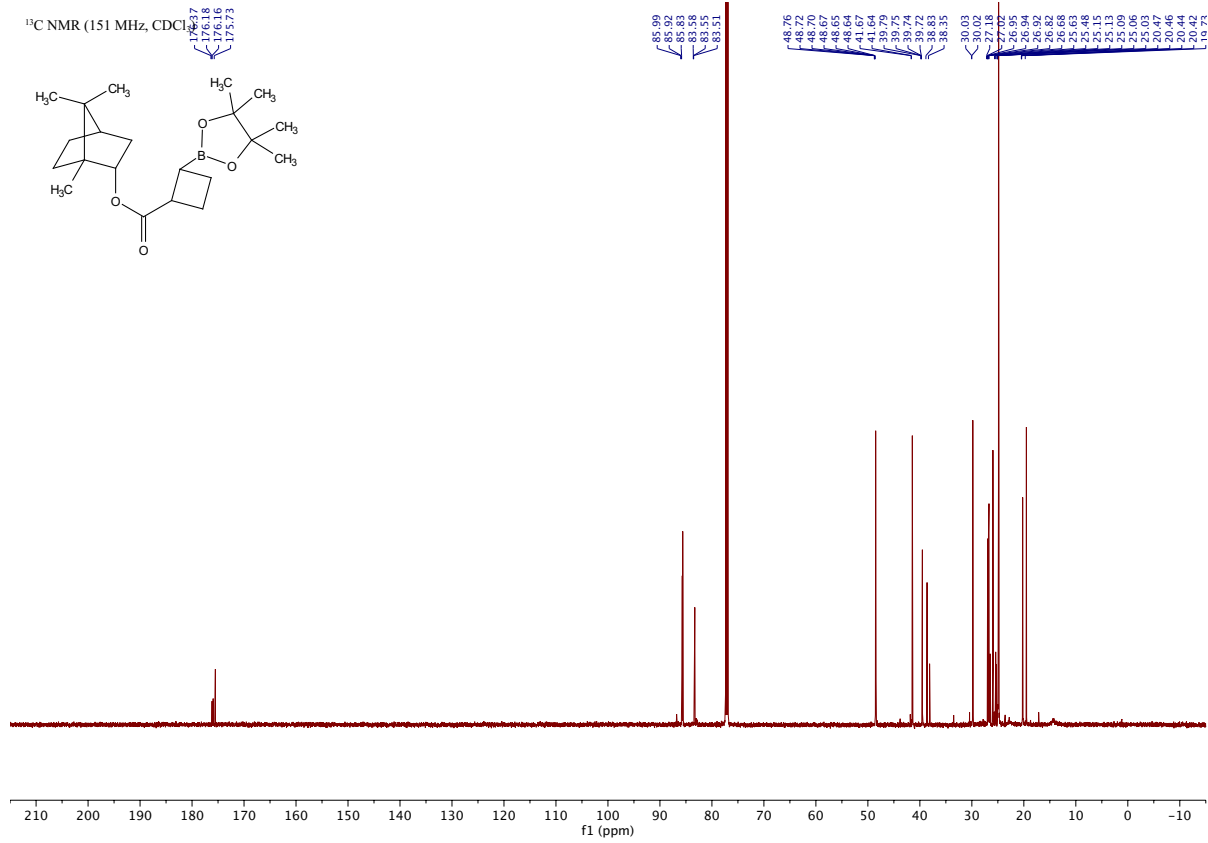
Product 15a

(3*S*,8*S*,9*S*,10*R*,13*R*,14*S*,17*R*)-10,13-dimethyl-17-((*R*)-6-methylheptan-2-yl)-2,3,4,7,8,9,10,11,12,13,14,15,16,17-tetradecahydro-1*H*-cyclopenta[*a*]phenanthren-3-yl   3-(4,4,5,5-tetramethyl-1,3,2-dioxaborolan-2-yl)bicyclo[1.1.1]pentane-1-carboxylate
[Experimental]

¹H NMR (600 MHz, CDCl₃)

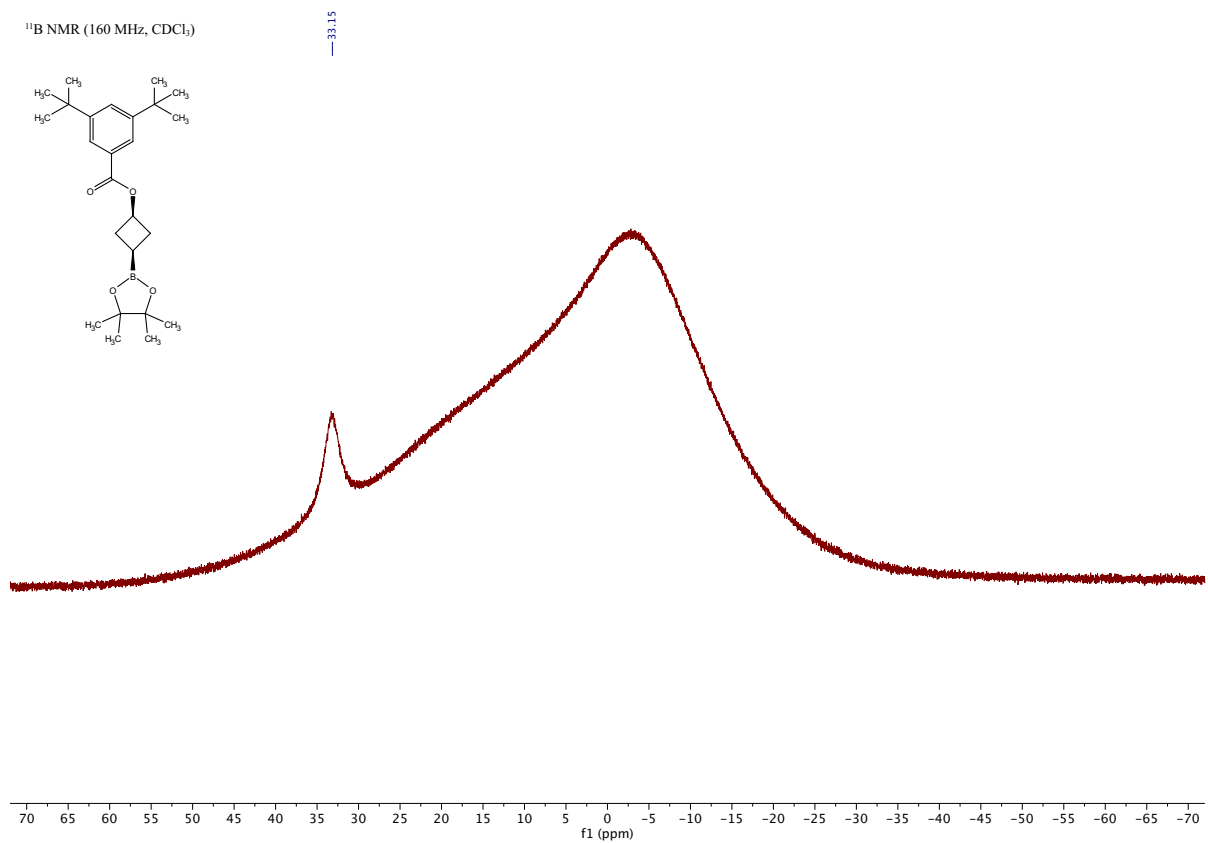^{13}C NMR (151 MHz, CDCl$_3$)

169.46
140.03
122.74
83.77
74.00
56.93
56.37
52.50
50.26
43.55
43.49
39.98
39.75
38.29
37.24
36.82
36.42
36.02
32.15
32.10
28.46
28.24
27.94
24.96
24.52
24.06
23.05
22.79
21.27
19.59
18.95
12.08

^{11}B NMR (193 MHz, CDCl$_3$) δ 30.84.

30.84
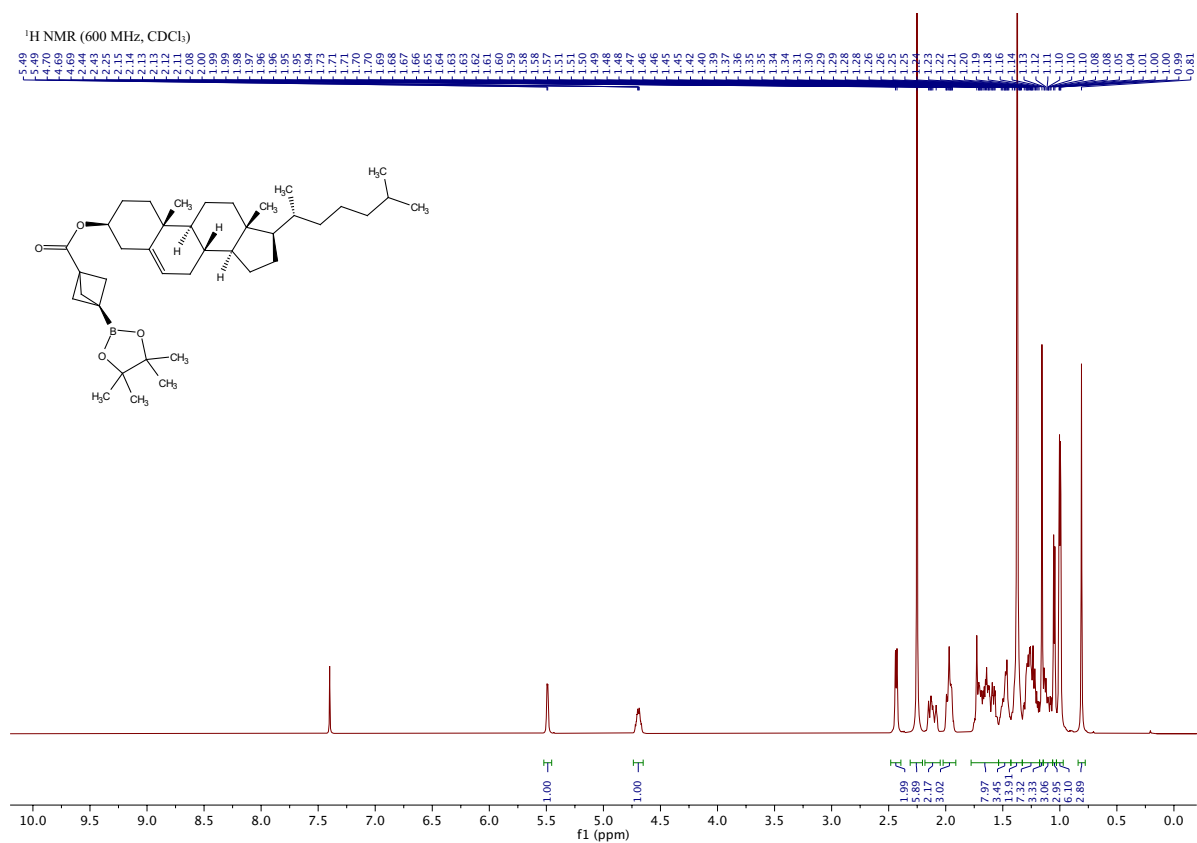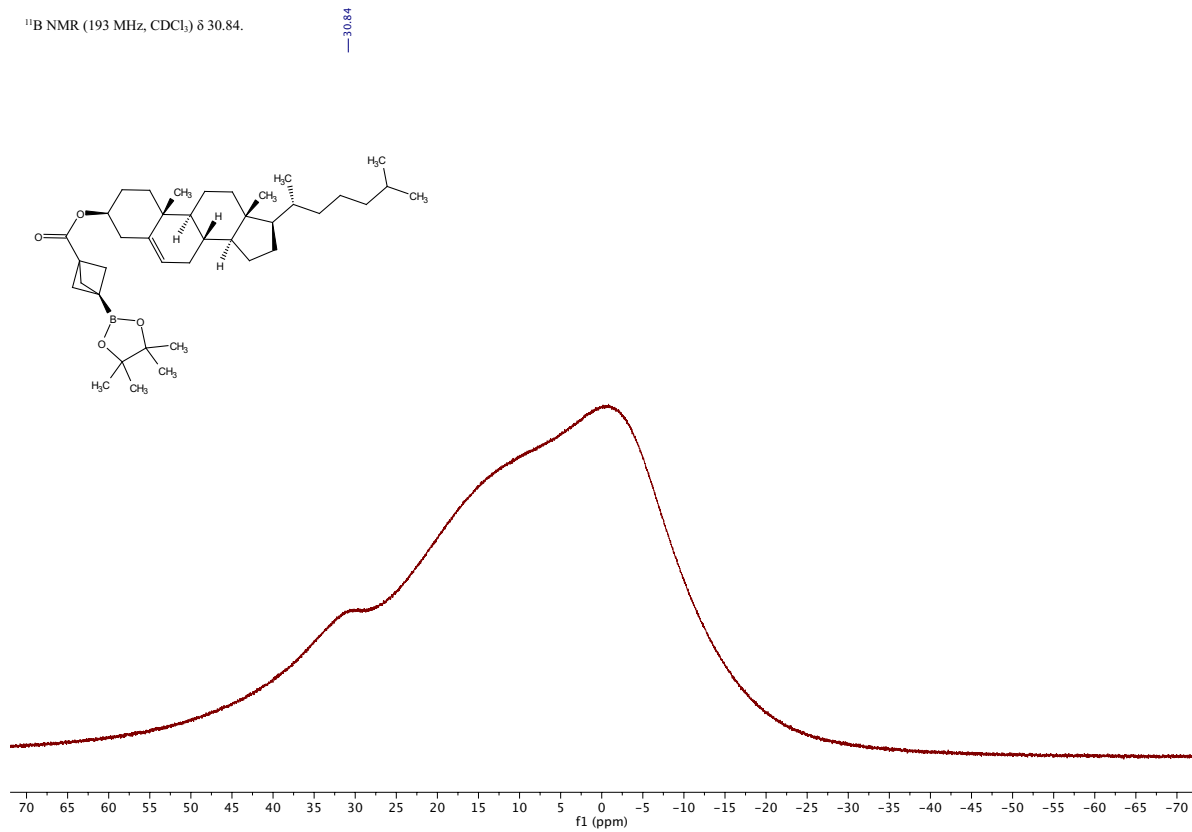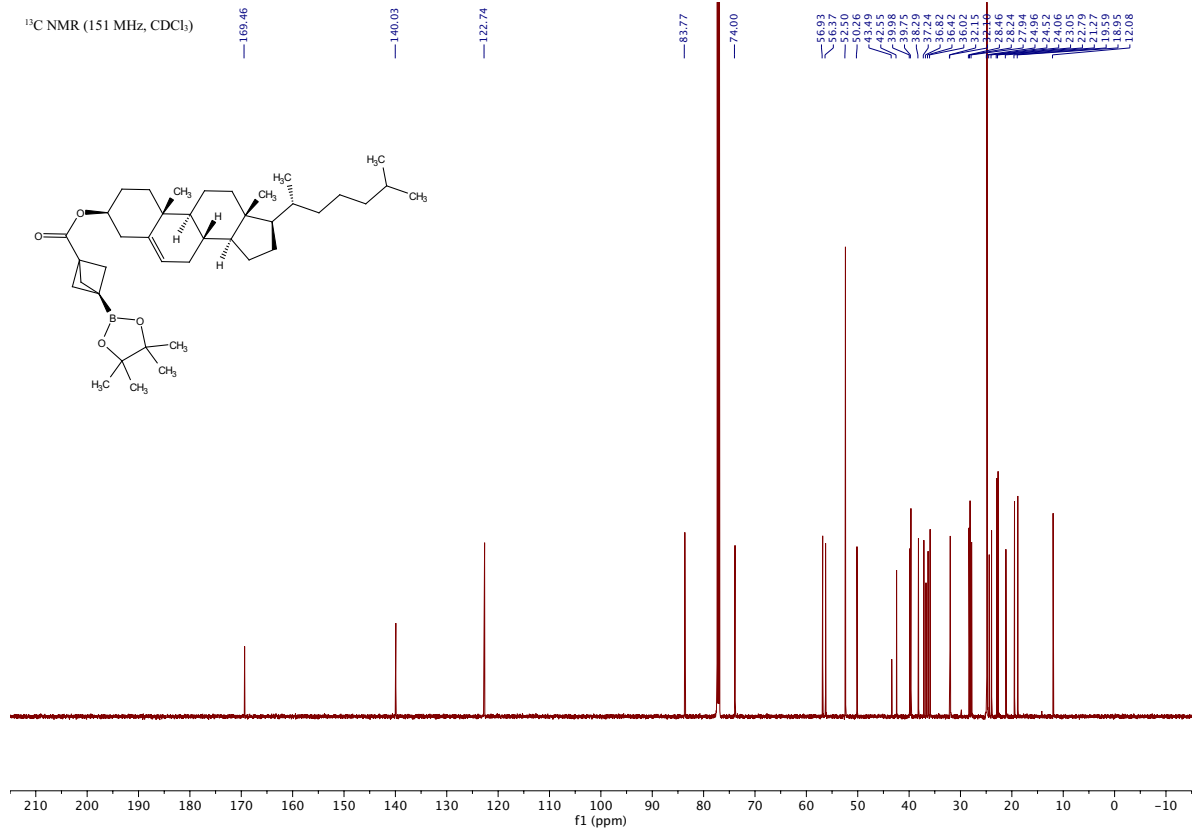
Product 16a

4,4,5,5-tetramethyl-2-(((2*S*,3*R*,4*R*,5*S*,6*R*)-3,4,5,6-tetrakis((3,5-di-*tert*-butylbenzyl)oxy)tetrahydro-2*H*-pyran-2-yl)methyl)-1,3,2-dioxaborolane   [Experimental]

¹H NMR (600 MHz, CDCl₃)

Product 17a

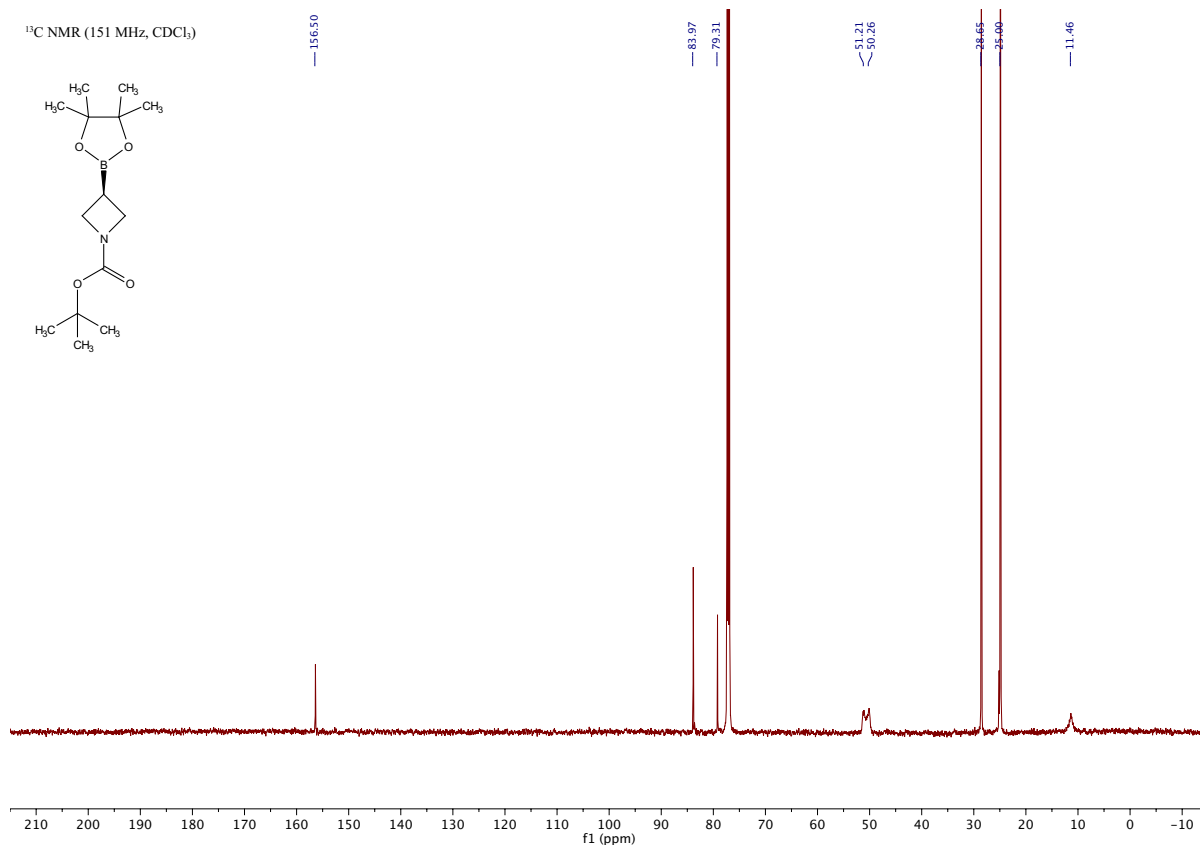4,4,5,5-tetramethyl-2-(((2S,3R,4R,5S,6R)-3,4,5,6-tetrakis((3,5-di-*tert*-butylbenzyl)oxy)tetrahydro-2*H*-pyran-2-yl)methyl)-1,3,2-dioxaborolane   [Experimental]

¹H NMR (600 MHz, CDCl₃)

¹³C NMR (151 MHz, CDCl₃)

166.07
165.96
165.85
164.99
157.56
157.27
157.13
156.95

130.17
130.15
129.93
127.04
126.94
126.70
126.50
125.84
125.77
125.56
125.49

90.84

83.85
83.73

71.75
70.01
69.02
67.90

35.43
35.40
35.25
35.23
31.38
31.36
31.25
31.23
25.26
24.91
24.88

210 200 190 180 170 160 150 140 130 120 110 100 90 80 70 60 50 40 30 20 10 0 −10
f1 (ppm)

¹¹B NMR (193 MHz, CDCl₃)

30.77

70 65 60 55 50 45 40 35 30 25 20 15 10 5 0 −5 −10 −15 −20 −25 −30 −35 −40 −45 −50 −55 −60 −65 −70
f1 (ppm)

Product 17c

(2*S*,3*S*,4*R*,5*R*,6*S*)-6-(hydroxymethyl)tetrahydro-2*H*-pyran-2,3,4,5-tetrayl   tetrakis(4-(*tert*-butyl)benzoate) [Experimental]

¹H NMR (600 MHz, CDCl₃)

¹³C NMR (151 MHz, CDCl₃)

(L1)Ir(Bpin)₃(P(OPh)₃)

[Experimental]

¹H NMR (600 MHz, THF)

¹³C NMR (151 MHz, THF)

—42.60

—31.85

f1 (ppm)

—107.42

f1 (ppm)
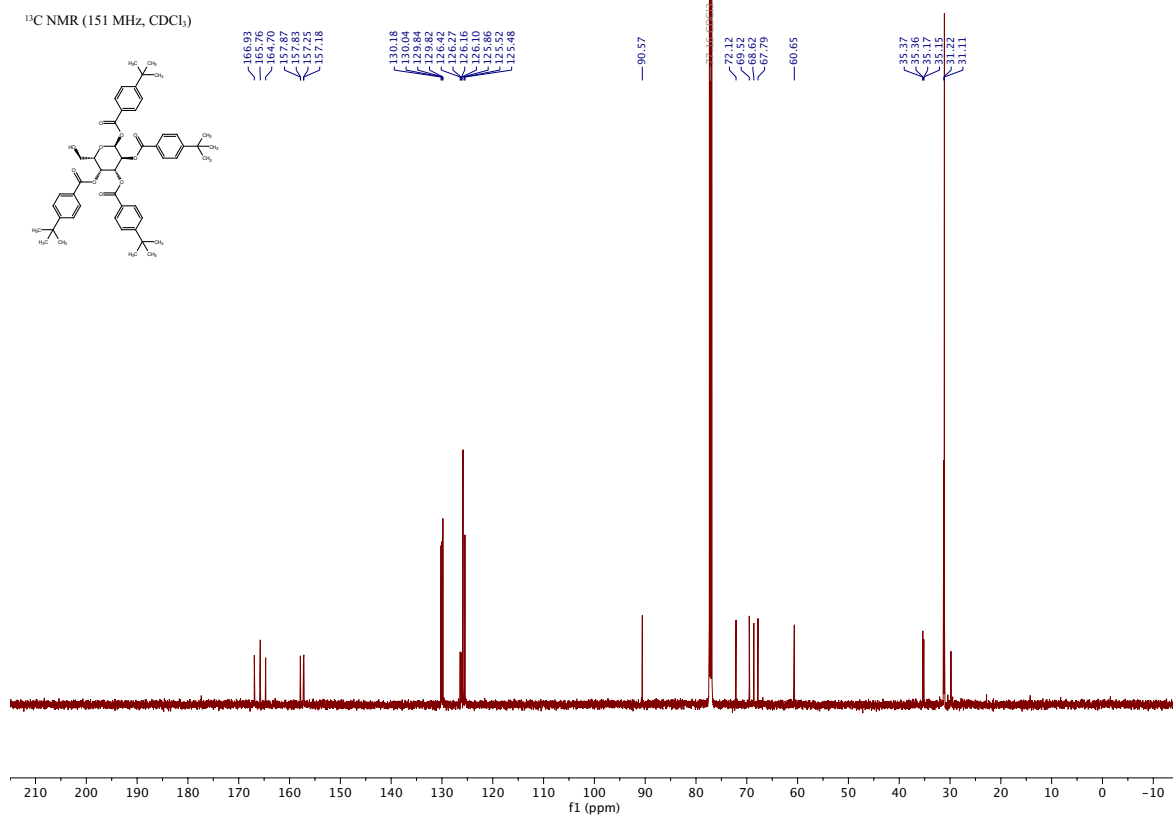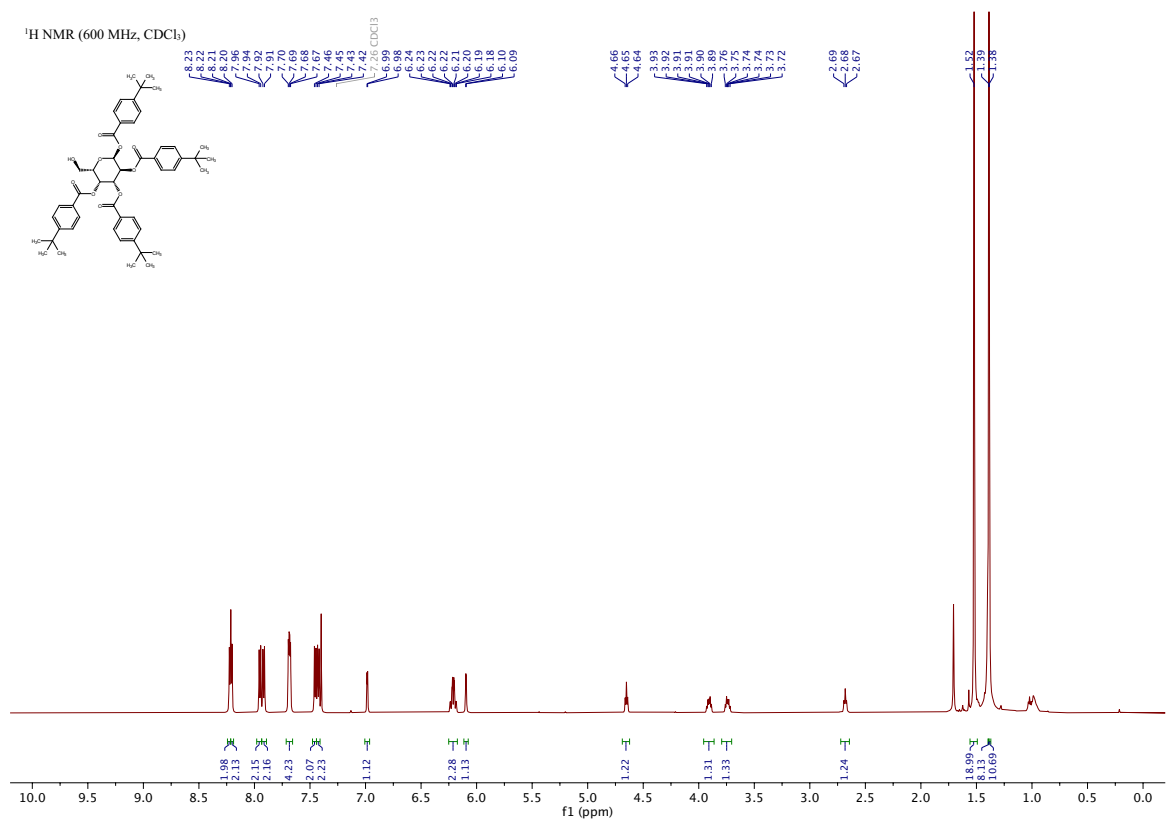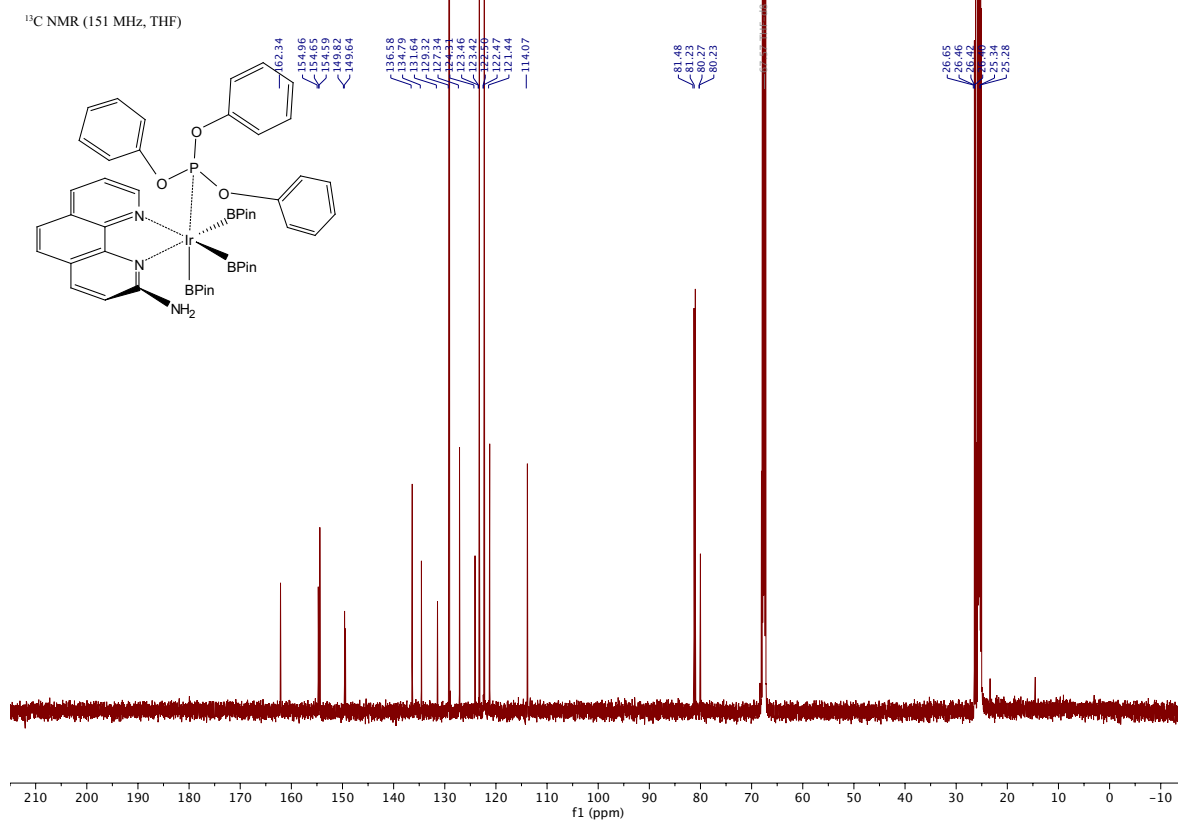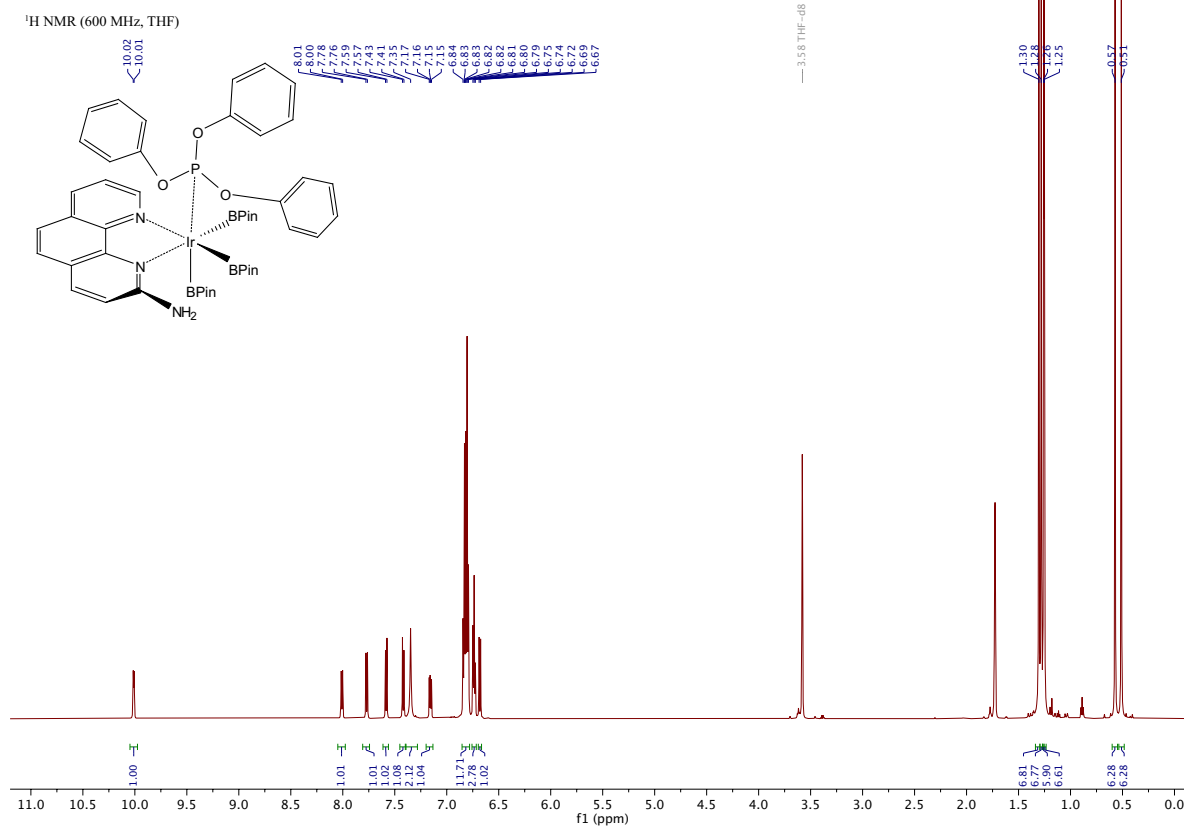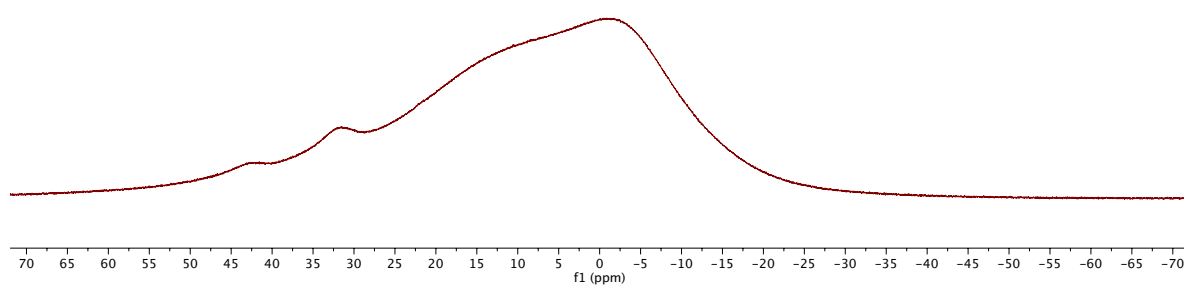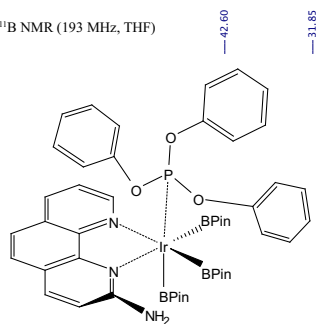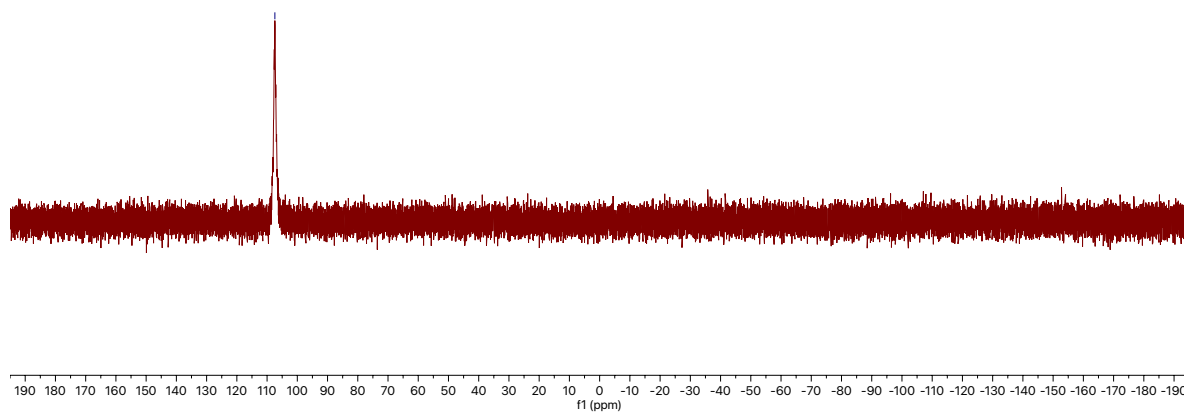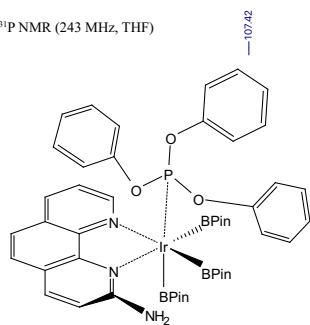
(L5)Ir(Bpin)₃

[Experimental]
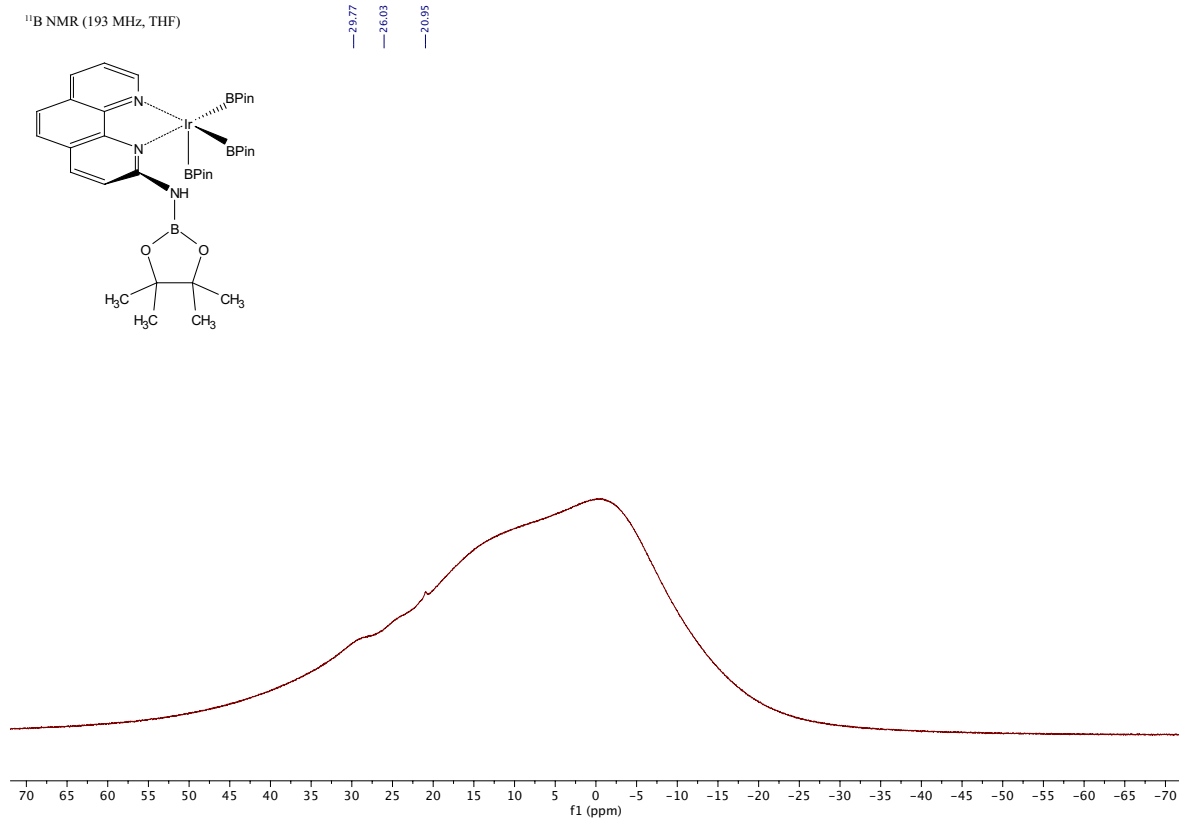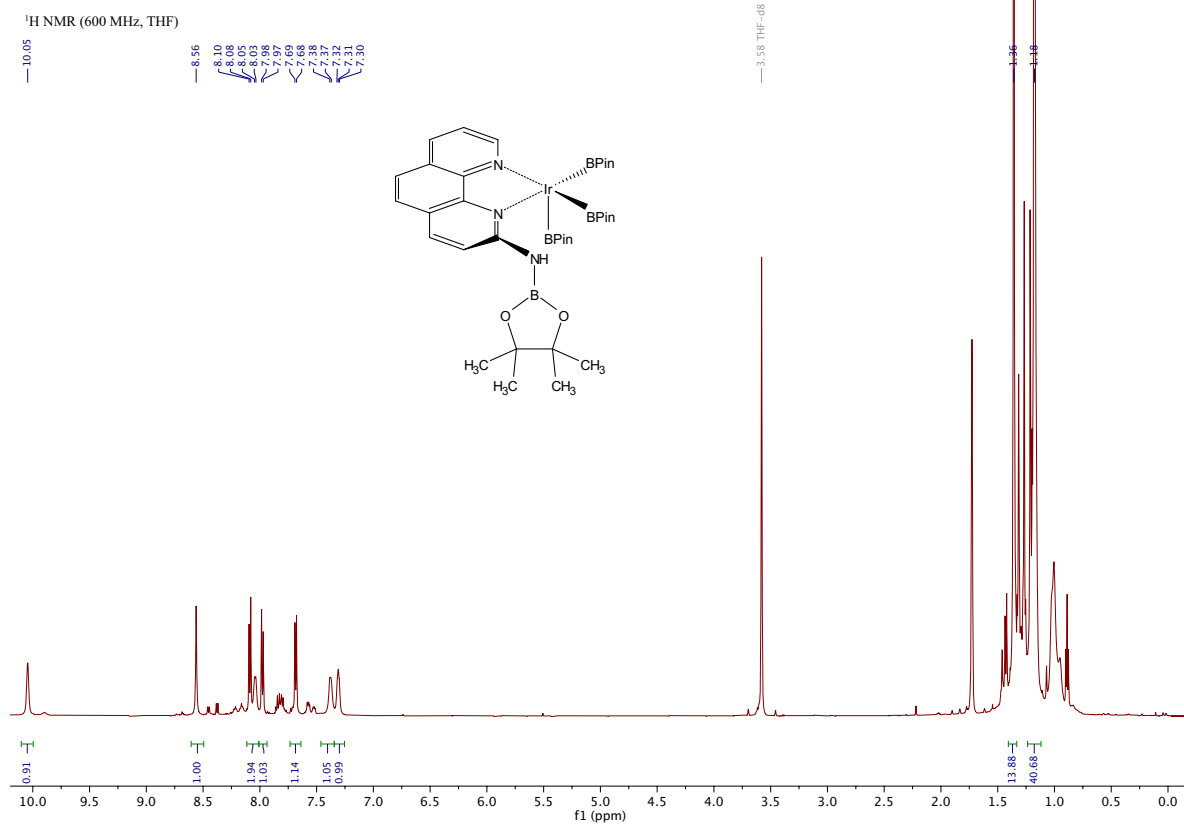
¹H NMR (600 MHz, THF)

¹¹B NMR (193 MHz, THF)

487

(L5)Ir(Bpin)₃(P(OPh)₃)

[Experimental]

¹H NMR (600 MHz, THF)

¹³C NMR (151 MHz, THF)

—42.04

—31.85

—24.13

70 65 60 55 50 45 40 35 30 25 20 15 10 5 0 −5 −10 −15 −20 −25 −30 −35 −40 −45 −50 −55 −60 −65 −70
f1 (ppm)

^{31}P NMR (243 MHz, THF)

—108.19

140 130 120 110 100 90 80 70 60 50 40 30 20 10 0 −10 −20 −30
f1 (ppm)
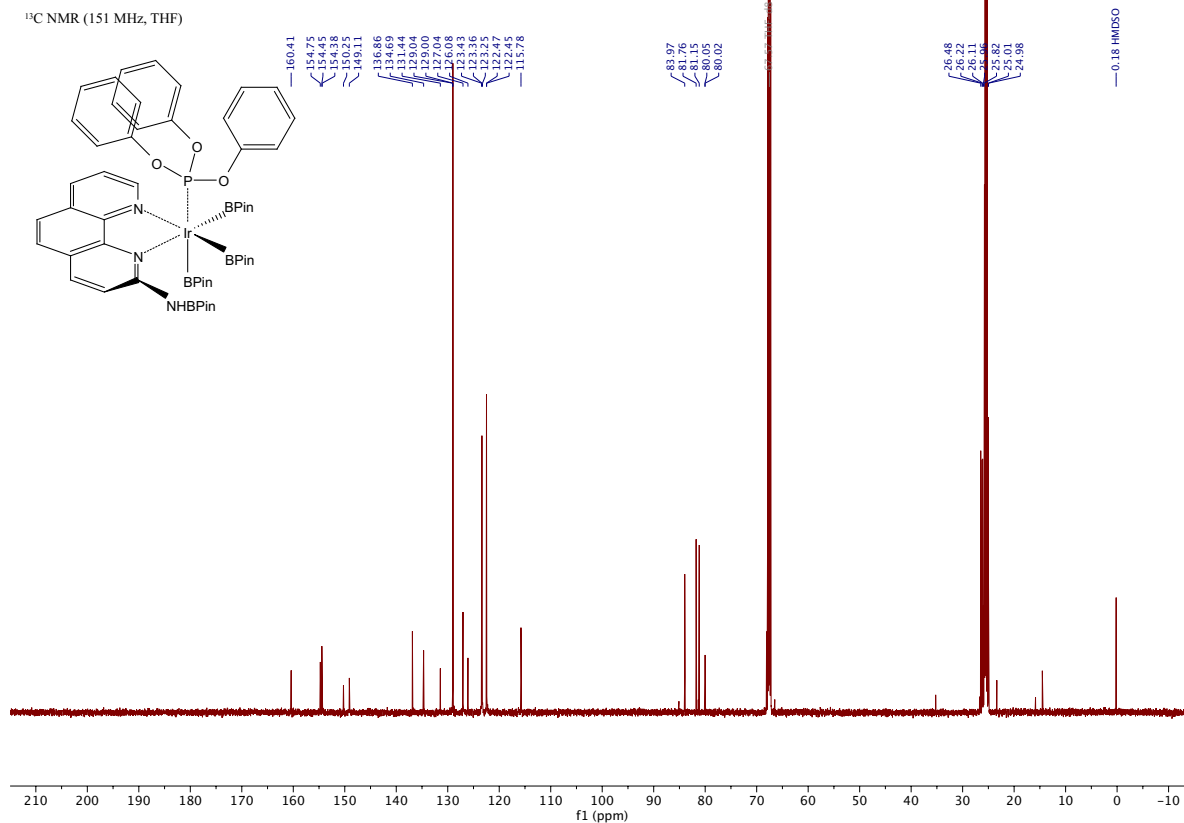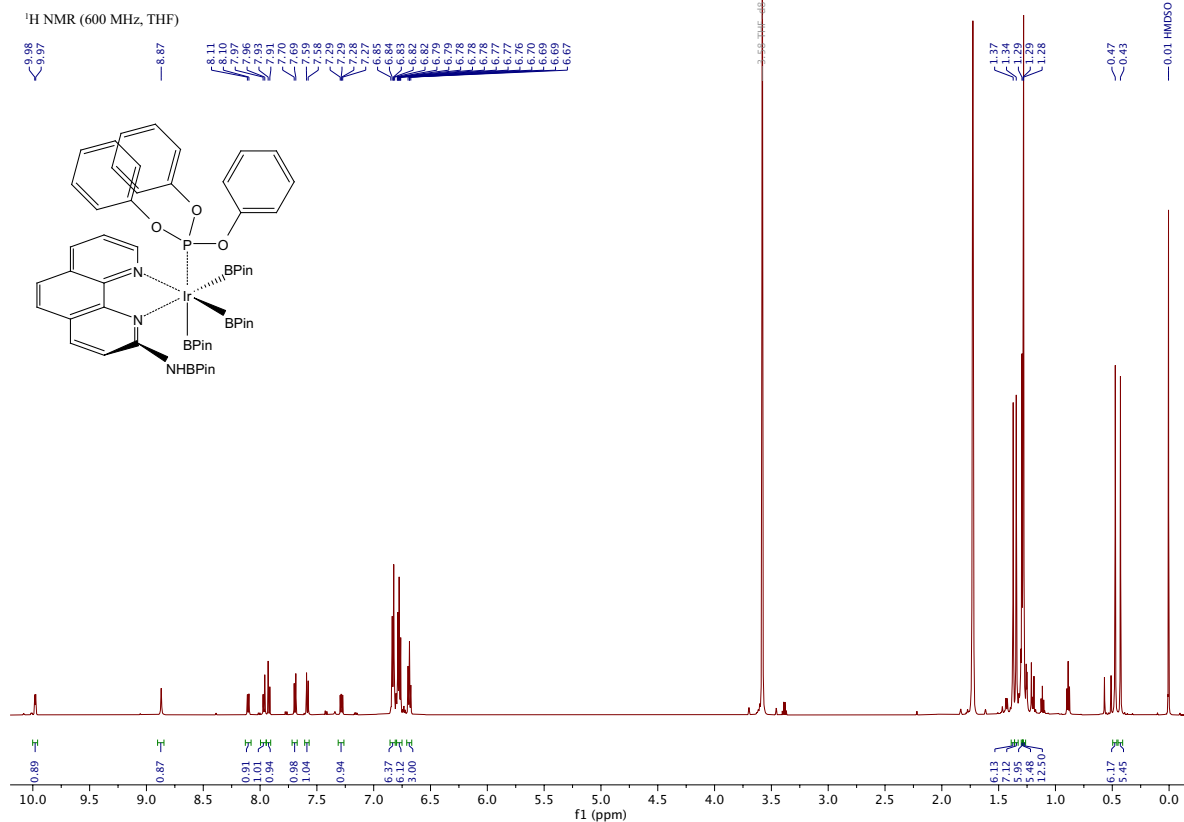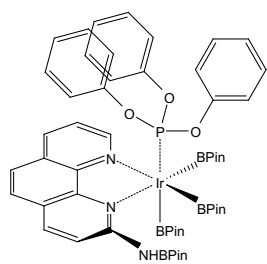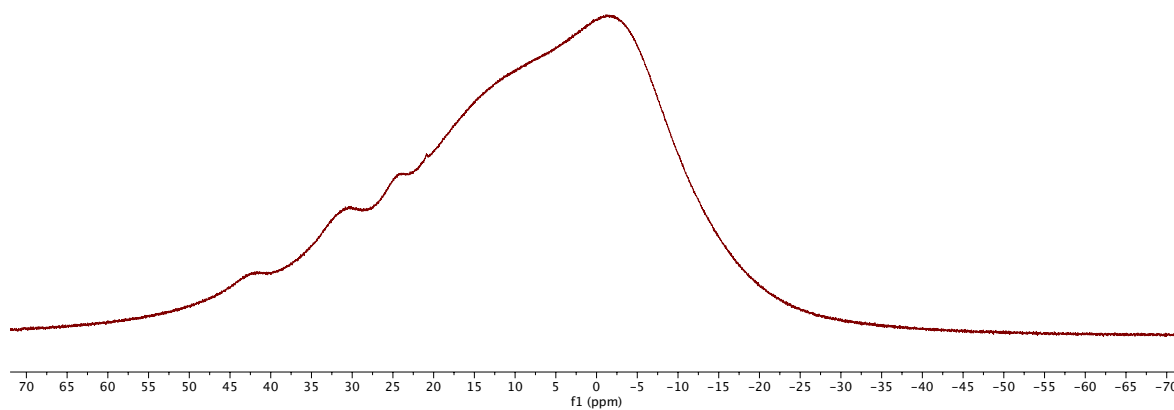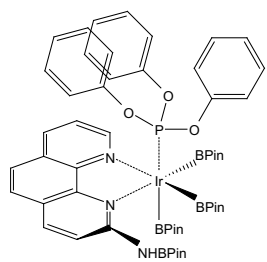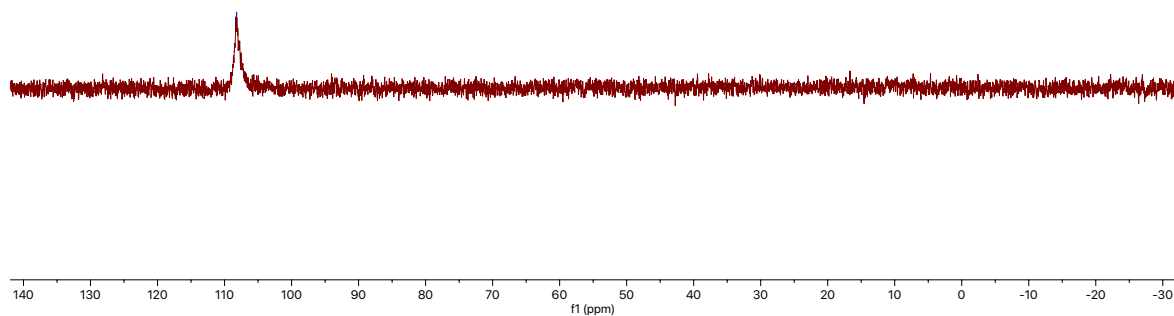
3.5 References

Parts of this chapter were reprinted with permission from:

"2-Aminophenanthroline Ligands Enable Mild, Undirected, Iridium-Catalyzed Borylation of Alkyl C–H Bonds"

Yu, I.F.; D'Angelo, K.A.; Hernandez-Mejías, Á,D.; Cheng, N.; Hartwig, J.F. *J. Am. Chem. Soc.* **2024**, *146*, 7124–7129.

1.   Wencel-Delord, J.; Glorius, F., C–H bond activation enables the rapid construction and late-stage diversification of functional molecules. *Nat. Chem.* **2013,** *5*, 369–375.

2.   Goldberg, K. I.; Goldman, A. S., Large-Scale Selective Functionalization of Alkanes. *Acc. Chem. Res.* **2017,** *50*, 620–626.

3.   Guillemard, L.; Kaplaneris, N.; Ackermann, L.; Johansson, M. J., Late-stage C–H functionalization offers new opportunities in drug discovery. *Nat. Rev. Chem.* **2021,** *5*, 522–545.

4.   Hartwig, J. F., Borylation and Silylation of C–H Bonds: A Platform for Diverse C–H Bond Functionalizations. *Acc. Chem. Res.* **2012,** *45*, 864–873.

5.   Yu, I. F.; Wilson, J. W.; Hartwig, J. F., Transition-Metal-Catalyzed Silylation and Borylation of C–H Bonds for the Synthesis and Functionalization of Complex Molecules. *Chem. Rev.* **2023,** *123*, 11619–11663.

6.   Chen, H.; Schlecht, S.; Semple, T. C.; Hartwig, J. F., Thermal, Catalytic, Regiospecific Functionalization of Alkanes. *Science* **2000,** *287*, 1995.

7.   Lawrence, J. D.;   Takahashi, M.;   Bae, C.; Hartwig, J. F., Regiospecific Functionalization of Methyl C−H Bonds of Alkyl Groups in Reagents with Heteroatom Functionality. *J. Am. Chem. Soc.* **2004,** *126*, 15334–15335.

8.   Ohmura, T.; Torigoe, T.; Suginome, M., Catalytic Functionalization of Methyl Group on Silicon: Iridium-Catalyzed C(sp^3)–H Borylation of Methylchlorosilanes. *J. Am. Chem. Soc.* **2012,** *134*, 17416–17419.

9.   Liskey, C. W.; Hartwig, J. F., Iridium-Catalyzed Borylation of Secondary C–H Bonds in Cyclic Ethers. *J. Am. Chem. Soc.* **2012,** *134*, 12422–12425.

10.   Ohmura, T.; Torigoe, T.; Suginome, M., Functionalization of Tetraorganosilanes and Permethyloligosilanes at a Methyl Group on Silicon via Iridium-Catalyzed C(sp^3)–H Borylation. *Organometallics* **2013,** *32*, 6170–6173.

11.   Li, Q.; Liskey, C. W.; Hartwig, J. F., Regioselective Borylation of the C–H Bonds in Alkylamines and Alkyl Ethers. Observation and Origin of High Reactivity of Primary C–H Bonds Beta to Nitrogen and Oxygen. *J. Am. Chem. Soc.* **2014,** *136*, 8755–8765.

12.   Ohmura, T.; Torigoe, T.; Suginome, M., Iridium-catalysed borylation of sterically hindered C(sp^3)–H bonds: remarkable rate acceleration by a catalytic amount of potassium tert-butoxide. *Chem. Commun.* **2014,** *50*, 6333–6336.

13.   Liskey, C. W.; Hartwig, J. F., Iridium-Catalyzed C–H Borylation of Cyclopropanes. *J. Am. Chem. Soc.* **2013,** *135*, 3375–3378.

14.   Larsen, M. A.; Wilson, C. V.; Hartwig, J. F., Iridium-Catalyzed Borylation of Primary Benzylic C–H Bonds without a Directing Group: Scope, Mechanism, and Origins of Selectivity. *J. Am. Chem. Soc.* **2015,** *137*, 8633–8643.

15.   Mita, T.; Ikeda, Y.; Michigami, K.; Sato, Y., Iridium-catalyzed triple C(sp^3)–H borylations: construction of triborylated sp3-carbon centers. *Chem. Commun.* **2013,** *49*, 5601–5603.

16.   Kawamorita, S.; Murakami, R.; Iwai, T.; Sawamura, M., Synthesis of Primary and Secondary Alkylboronates through Site-Selective C(sp^3)–H Activation with Silica-Supported Monophosphine–Ir Catalysts. *J. Am. Chem. Soc.* **2013,** *135*, 2947–2950.

17.   Larsen, M. A.; Cho, S. H.; Hartwig, J., Iridium-Catalyzed, Hydrosilyl-Directed Borylation of Unactivated Alkyl C–H Bonds. *J. Am. Chem. Soc.* **2016,** *138*, 762–765.

18.   Shi, Y.; Gao, Q.; Xu, S., Chiral Bidentate Boryl Ligand Enabled Iridium-Catalyzed Enantioselective C(sp^3)–H Borylation of Cyclopropanes. *J. Am. Chem. Soc.* **2019,** *141*, 10599–10604.

19.   Yamamoto, T.; Ishibashi, A.; Suginome, M., Boryl-Directed, Ir-Catalyzed C(sp^3)–H Borylation of Alkylboronic Acids Leading to Site-Selective Synthesis of Polyborylalkanes. *Org. Lett.* **2019,** *21*, 6235–6240.

20.   Chen, L.; Yang, Y.; Liu, L.; Gao, Q.; Xu, S., Iridium-Catalyzed Enantioselective α-C(sp^3)–H Borylation of Azacycles. *J. Am. Chem. Soc.* **2020,** *142*, 12062–12068.

21.   Chen, X.; Chen, L.; Zhao, H.; Gao, Q.; Shen, Z.; Xu, S., Iridium-Catalyzed Enantioselective C(sp^3)–H Borylation of Cyclobutanes. *Chin. J. Chem.* **2020,** *38*, 1533–1537.

22.   Du, R.; Liu, L.; Xu, S., Iridium-Catalyzed Regio- and Enantioselective Borylation of Unbiased Methylene C(sp^3)−H Bonds at the Position β to a Nitrogen Center. *Angew. Chem. Int. Ed.* **2021,** *60*, 5843–5847.

23.   Yang, Y.; Chen, L.; Xu, S., Iridium-Catalyzed Enantioselective Unbiased Methylene C(sp^3)–H Borylation of Acyclic Amides. *Angew. Chem. Int. Ed.* **2021,** *60*, 3524–3528.

24.   Luhua Liu, R. D., Senmiao Xu, Ligand-Free Iridium-Catalyzed Borylation of Secondary Benzylic C–H Bonds. *Chin. J. Org. Chem.* **2021,** *41*, 1572–1581.

25.   Shi, Y.; Yang, Y.; Xu, S., Iridium-Catalyzed Enantioselective C(sp^3)−H Borylation of Aminocyclopropanes. *Angew. Chem. Int. Ed.* **2022,** *61*, e202201463.

26.   Zou, X.; Li, Y.; Ke, Z.; Xu, S., Chiral Bidentate Boryl Ligand-Enabled Iridium-Catalyzed Enantioselective Dual C–H Borylation of Ferrocenes: Reaction Development and Mechanistic Insights. *ACS Catal.* **2022,** *12*, 1830–1840.

27.   Wenqi Liu, Z. S., Senmiao Xu, Synthesis of 1,1-Diboron Alkanes via Diborylation of Unactivated Primary Csp^3–H Bonds Enabled by AsPh$_3$/Iridium Catalysis. *Chin. J. Org. Chem.* **2022,** *42*, 1101–1110.

28.   Xie, T.; Chen, L.; Shen, Z.; Xu, S., Simple Ether-Directed Enantioselective C(sp^3)−H Borylation of Cyclopropanes Enabled by Iridium Catalysis. *Angew. Chem. Int. Ed.* **2023,** *62*, e202300199.

29.   Gao, Q.; Xu, S., Site- and Stereoselective C(sp^3)−H Borylation of Strained (Hetero)Cycloalkanols Enabled by Iridium Catalysis. *Angew. Chem. Int. Ed.* **2023,** *62*, e202218025.

30.   Shu, C.; Noble, A.; Aggarwal, V. K., Metal-free photoinduced C(sp^3)–H borylation of alkanes. *Nature* **2020,** *586*, 714–719.

31.   Sang, R.; Han, W.; Zhang, H.; Saunders, C. M.; Noble, A.; Aggarwal, V. K., Copper-Mediated Dehydrogenative C(sp^3)–H Borylation of Alkanes. *J. Am. Chem. Soc.* **2023,** *145*, 15207–15217.

32.   Tu, J. L.; Hu, A. M.; Guo, L.; Xia, W., Iron-Catalyzed C(Sp(3))-H Borylation, Thiolation, and Sulfinylation Enabled by Photoinduced Ligand-to-Metal Charge Transfer. *J Am Chem Soc* **2023,** *145*, 7600-7611.

33.   Zhong, P.-F.; Tu, J.-L.; Zhao, Y.; Zhong, N.; Yang, C.; Guo, L.; Xia, W., Photoelectrochemical oxidative C(sp^3)−H borylation of unactivated hydrocarbons. *Nat. Commun.* **2023,** *14*, 6530.

34.   Jones, M. R.; Fast, C. D.; Schley, N. D., Iridium-Catalyzed sp^3 C–H Borylation in Hydrocarbon Solvent Enabled by 2,2'-Dipyridylarylmethane Ligands. *J. Am. Chem. Soc.* **2020,** *142*, 6488–6492.

35.   Kawazu, R.; Torigoe, T.; Kuninobu, Y., Iridium-Catalyzed C(sp^3)–H Borylation Using Silyl-Bipyridine Pincer Ligands. *Angew Chem Int Ed Engl* **2022,** *61*, e202202327.

36.   Oeschger, R.; Su, B.; Yu, I.; Ehinger, C.; Romero, E.; He, S.; Hartwig, J., Diverse functionalization of strong alkyl C–H bonds by undirected borylation. *Science* **2020,** *368*, 736.

37.   Yu, I. F.; Manske, J. L.; Diéguez-Vázquez, A.; Misale, A.; Pashenko, A. E.; Mykhailiuk, P. K.; Ryabukhin, S. V.; Volochnyuk, D. M.; Hartwig, J. F., Catalytic undirected borylation of tertiary C–H bonds in bicyclo[1.1.1]pentanes and bicyclo[2.1.1]hexanes. *Nat. Chem.* **2023,** *15*, 685–693.

38.   Irvine, G. J.; Lesley, M. J. G.; Marder, T. B.; Norman, N. C.; Rice, C. R.; Robins, E. G.; Roper, W. R.; Whittell, G. R.; Wright, L. J., Transition Metal−Boryl Compounds: Synthesis, Reactivity, and Structure. *Chem. Rev.* **1998,** *98*, 2685–2722.

39.   Frihed, T. G.; Heuckendorff, M.; Pedersen, C. M.; Bols, M., Easy Access to L-Mannosides and L-Galactosides by Using C–H Activation of the Corresponding 6-Deoxysugars. *Angew. Chem. Int. Ed.* **2012,** *51*, 12285–12288.

40.   Frihed, T. G.; Pedersen, C. M.; Bols, M., Synthesis of All Eight L-Glycopyranosyl Donors Using C–H Activation. *Angew. Chem. Int. Ed.* **2014,** *53*, 13889–13893.

41.   Mallesha, N.; Prahlada Rao, S.; Suhas, R.; Channe Gowda, D., An efficient synthesis of tert-butyl ethers/esters of alcohols/amino acids using methyl tert-butyl ether. *Tet. Lett.* **2012,** *53*, 641–645.

42.   Tian, H.; Xia, Q.; Wang, Q.; Dong, J.; Liu, Y.; Wang, Q., Direct α-Monofluoroalkenylation of Heteroatomic Alkanes via a Combination of Photoredox Catalysis and Hydrogen-Atom-Transfer Catalysis. *Org. Lett.* **2019,** *21*, 4585–4589.

43.   Xu, H.; Liu, H. Method for mildly preparing 2-azaspiro [3.3] heptane hydrochloride. CN202110228426A, 2021.

44.   Garlets, Z. J.; Sanders, J. N.; Malik, H.; Gampe, C.; Houk, K. N.; Davies, H. M. L., Enantioselective C–H functionalization of bicyclo[1.1.1]pentanes. *Nat. Catal.* **2020,** *3*, 351–357.

45.   Beutner, G. L.; Young, I. S.; Davies, M. L.; Hickey, M. R.; Park, H.; Stevens, J. M.; Ye, Q., TCFH–NMI: Direct Access to N-Acyl Imidazoliums for Challenging Amide Bond Formations. *Org. Lett.* **2018,** *20*, 4218–4222.

46.   Adam, A.; Haberhauer, G.; Wölper, C., Bio-inspired Herringbone Foldamers: Strategy for Changing the Structure of Helices. *J. Org. Chem.* **2017,** *82*, 4203–4215.

47.   Smith, B. M.; Graham, A. E., Indium triflate mediated tandem acetalisation-acetal exchange reactions under solvent-free conditions. *Tet. Lett.* **2011,** *52*, 6281–6283.

48.   Lennox, A. J. J.; Lloyd-Jones, G. C., Preparation of Organotrifluoroborate Salts: Precipitation-Driven Equilibrium under Non-Etching Conditions. *Angew. Chem. Int. Ed.* **2012,** *51*, 9385–9388.

CHAPTER 4 Mechanism of the Undirected, Iridium-Catalyzed Borylation of Alkyl C–H Bonds with Aminophenanthroline Ligands

4.1 Introduction

The functionalization of C–H bonds has been termed one of the "Holy Grails" of organic chemistry[1] and promises to shorten synthetic routes and enable late-stage functionalization.[2, 3] The borylation of C–H bonds is one such powerful reaction, primarily due to the versatility of the installed boronic ester,[4, 5] which can be transformed into a myriad of functional groups. The synthetic utility of these reactions is best demonstrated by the numerous applications in fields as diverse as medicinal chemistry, polymer chemistry, and organic materials chemistry.[6]

Interest in sp^3-rich scaffolds for applications in drug discovery has increased recently.[7] The alkyl boronic esters resulting from the borylation of alkyl C–H bonds are especially valuable in this context as building blocks because of the rapidly developing array of transformations at alkyl-boron bonds.[8] However, the borylation of alkyl C–H bonds is much slower than the borylation of aryl C–H bonds. Thus, the borylation of alkyl C–H bonds often requires large excesses of the substrate containing the alkyl C–H bond and high reaction temperatures, or the installation of a directing group. Efforts from our laboratory and many others have focused on developing catalysts[9-13] or additives[14] that cause the borylation reaction to occur with faster rates, or to design combinations of directing groups and catalysts[15-23] that will enable the borylation reactions to occur under synthetically useful conditions. Recently, our laboratory reported that iridium complexes containing 2-aminophenanthroline ligands catalyze the undirected borylation of alkyl C–H bonds to occur with high rates and, thus, with limiting quantities of substrate and at mild reaction temperatures ($\leq$ 65 ºC).[12]

Yet, the active catalysts for these reactions have not been observed directly, and connections between observed species and reaction rates has not been made. Such characterization and connections between the structures of these complexes and the reaction rates would facilitate future advances in catalysts. Two particular features of these catalysts and their reactions motivated our study of the mechanism (Figure 4.1). First, initial studies of these systems suggested that borylation of a substituent at the 2-position leads to the active species, but there is no direct evidence for the presence or precise role of the pendant boryl substituent in the active catalyst. Second, the identity of the active catalyst could not be determined because borylations of the phenanthroline occur in concert with the substituent at the 2-position, so the number of boryl or hydride groups on the catalyst could not be determined and a potential change in mechanism to one involving a different oxidation state or number of boryl groups on iridium could occur. Third, it was unclear if the substituent accelerated reactions of only sp^3 alkyl C–H bonds or if it also accelerated the reactions of sp^2 aryl C–H bonds. Finally, borylations of alkyl C–H bonds typically do not occur with HBpin as a boron source, in contrast to what is commonly observed during the borylation of aryl C–H bonds. Studies to understand these features of the catalysts and their reactions have been hindered by the presence of induction periods that can be longer than the catalytic reaction and formation of mixtures of species during this induction period that likely occur by the borylation of the aryl or benzylic C–H bonds of the phenanthroline ligands and prevent clear identification of the active catalyst.[11, 12] These factors, therefore, required a design of ancillary, nitrogen-based ligands that would enable formation of a single catalytic species required for mechanistic analysis.

495

Which Ir complexes are intermediates in the reaction?

What is the role of the 2-substituent?

Why does the use of HBpin lead to low yields
for the borylation of sp³ C–H bonds with these catalysts?

Does this catalyst also lead to higher rates for the borylation of sp² C–H bonds?
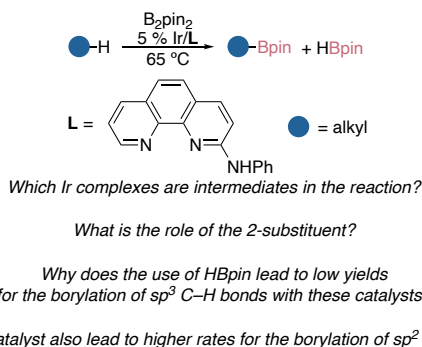
Figure 4.1. Catalytic borylation of alkyl C–H bonds and outstanding mechanistic questions.

We report a modified phenanthroline ligand and resulting iridium complex that catalyzes the borylation of alkyl C–H bonds without an induction period and with the presence of active catalytic complexes that can be clearly identified. This ligand contains hindered alkyl and aryl groups, in addition to a 2-anilino group containing large substituents on the aryl ring, to prevent modification and the identification of catalytic intermediates. We show that the *N*-borylated iridium trisboryl complex is the active species and that the corresponding iridium bisboryl hydride species does not catalyze the borylation of alkyl C–H bonds. We also show that the 2-aminophenanthroline group increases the reactivity toward both alkyl and aryl C–H bonds by 1-3 orders of magnitude, and computational models provide a rationale for the inactivity of the bisboryl hydride species with the 2-amino substituent on the phenanthroline.

4.2 Results and Discussion

To simplify catalyst speciation and facilitate assignment of the resting state of the catalyst, we initiated our studies by synthesizing 2-aminophenanthroline ligands that could be sterically protected from borylation. We chose the most active ligand in our previous study, *N*-phenyl-2-amino-1,10-phenanthroline (NHPhphen, **L1**), as our starting point for ligand design. Two main considerations were followed when designing these ligands. First, additional substitutions on the ligand backbone were carefully selected, such that the activity of the catalyst with the resulting ligand would be similar to that of the catalyst with **L1**. Second, the added steric bulk needed to be sufficient to prevent borylation from occurring on the ligand at positions other than the N–H bond.

To evaluate the effect of substitutions on catalyst activity, a series of *N*-phenyl-2-aminophenananthroline ligands substituted by methyl or bromo substituents on the ligand backbone were prepared. We found that the borylation reactions of *tert*-butyl octyl ether with catalysts containing ligands containing substitution at the 3-, 7-, and 9- positions occurred in significantly lower yields than those run with catalysts containing ligands with substitution at the 5-, 6-, and 8- positions (Figure 4.2b, see Figure 4.13). Because borylation with iridium catalysts typically do not occur *ortho-* or *peri-* to large substituents, such as *tert*-butyl, trifluoromethyl, and aryl groups, we designed a phenanthroline ligand (**L2**) containing 2-(3,5-bis*tert*-butylphenyl)amino, 5-(3,5-bistrifluoromethylphenyl), and 8-*tert*-butyl substituents (Figure 4.2c).

496
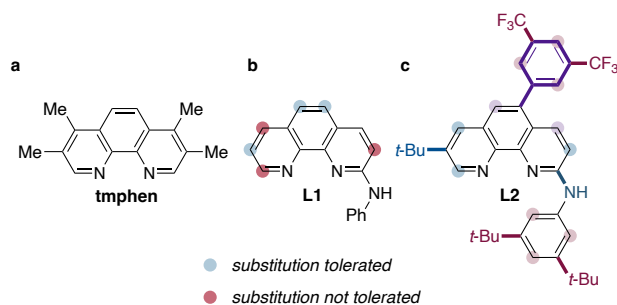
Figure 4.2. Design of the "ironclad" aminophenanthroline. (a) Structure of 3,4,7,8-tetramethylphenanthroline (tmphen), workhorse ligand for the borylation of aryl C–H bonds. (b) Effect of substitution sites (Me or Br) on catalyst activity. (c) Structure of the "ironclad" ligand **L2** showing how the substituents shield the C–H bonds of the ligand.

The iridium catalysts formed from **L2** were compared to that of the catalyst from tmphen and from that of **L1** lacking the steric protection at the backbone. Plots showing the relative reactivity of the catalyst from ligand **L2** to that of catalysts from tmphen and ligand **L1** for the reactions of an arene and of THF are provided in Figure 4.3. These data show that the catalysts from **L1** or **L2** are more active than that formed from 3,4,7,8-tetramethylphenanthroline (tmphen) for the borylation of aryl C–H bonds by about an order of magnitude (Figure 4.3a). The catalysts that contain **L1** or **L2** are also active for the borylation of the alkyl C–H bond of THF at 65 ºC, while the catalyst that contains tmphen is not (Figure 4.3b). These data show that the catalyst generated from **L2** reacts like that from **L1** we have reported and that the increased reactivity toward alkyl C–H bonds we observed previously with **L1** is also is observed for the reactions of an aryl C–H bond.
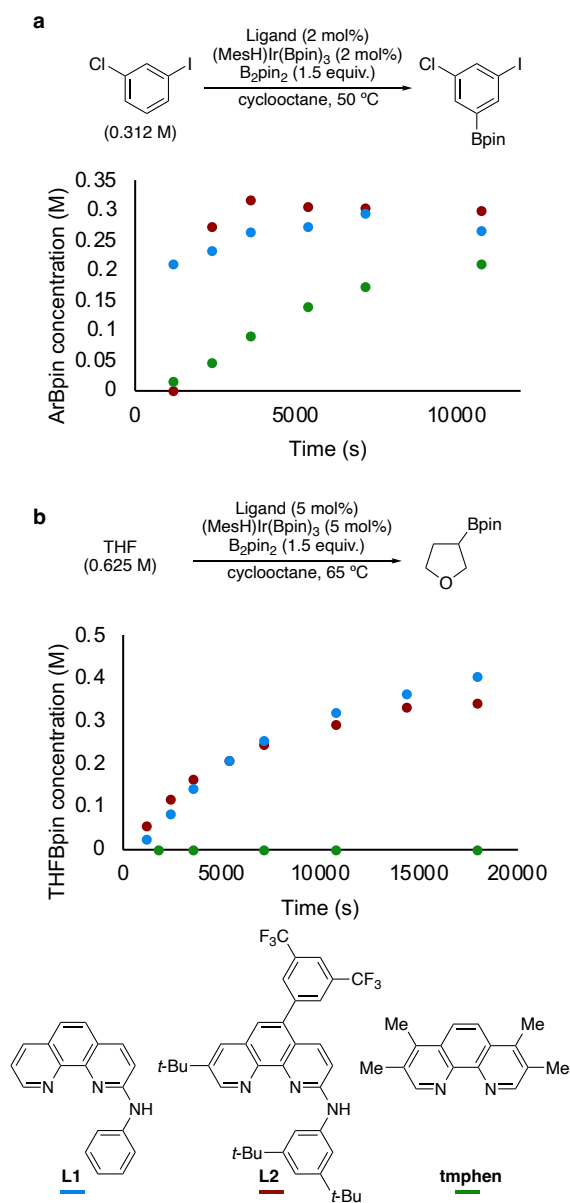
Figure 4.3. Timecourses for the borylation of C–H bonds with catalysts containing L1, L2 and tmphen. (a) Timecourses for the borylation of 1-chloro-3-iodobenzene. (b) Timecourses for the borylation of tetrahydrofuran.
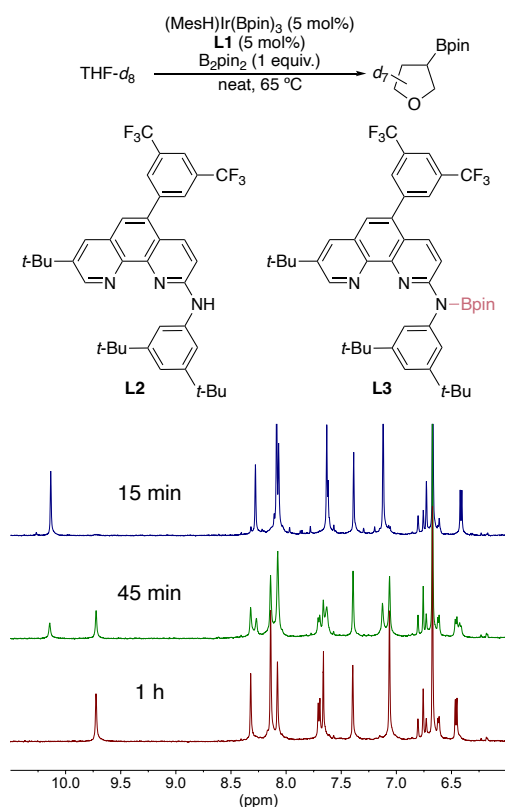
Figure 4.4. Monitoring of the borylation of THF-d_8 with iridium catalysts formed from **L2** by ^{1}H NMR spectroscopy.

The borylation of THF-d_8 with iridium catalysts formed from the combination of (MesH)Ir(Bpin)$_3$ and **L1** was monitored by ^{1}H NMR spectroscopy and resulted in a complex mixture (Figure 4.16), highlighting the need for a sterically protected ligand for spectroscopic monitoring of the catalytic reaction. The borylation of THF-d_8 with iridium catalysts formed from the combination of (MesH)Ir(Bpin)$_3$ and **L2** was also monitored by ^{1}H NMR spectroscopy. In the initial stages of the reaction, one single species was observed. This complex was assigned to be (**L3**)Ir(Bpin)$_3$ (**L3** = N-borylated **L2**) based on trapping experiments (Figure 4.4, red trace, see below). At later stages of the reaction, a second iridium species was observed. This species was assigned to be (**L3**)Ir(H)(Bpin)$_2$ based on trapping experiments (see below). This second species eventually became the sole iridium species upon completion of the borylation process (Figure 4.4, blue trace). The combination of [Ir(cod)(OMe)]$_2$ and **L2** also formed (**L3**)Ir(Bpin)$_3$ in the presence of B$_2$pin$_2$ (Figure 4.18).

To identify these species by converting them to an isolable species, we performed trapping studies with triphenylphosphite. Aliquots of the reaction of the borylation of THF were taken, an excess of P(OPh)$_3$ was added (Figure 4.5b), and the resulting solutions were analyzed by ^{31}P NMR spectroscopy. Trapping of the species formed in the initial stages of the reaction afforded a complex with a corresponding ^{31}P chemical shift of 100 ppm. At later stages of the reaction, a new phosphite-capped species predominated with a corresponding chemical shift of 106 ppm. The identity of the first complex was determined by independent synthesis to be (**L3**)Ir(Bpin)$_3$(P(OPh)$_3$). This independent synthesis was accomplished by allowing **L2** and (MesH)Ir(Bpin)$_3$ to react in the presence of B$_2$pin$_2$ at 65 °C, followed by adding B$_2$pin$_2$, and

finally trapping with P(OPh)$_3$ (Figure 4.5c). The connectivity of the complex was determined unambiguously by single crystal X-ray crystallography (Figure 4.5d). The identity of the second complex was also determined by independent synthesis, in this case to be (**L3**)Ir(H)(Bpin)$_2$(P(OPh)$_3$). In this case, the independent synthesis was accomplished by heating a mixture of **L2** with (MesH)Ir(Bpin)$_3$ in the presence of B$_2$pin$_2$ in tetrahydrofuran until all the diboron was consumed, followed by addition of P(OPh)$_3$ (Figure 4.5c). The ^{1}H NMR spectrum of (**L3**)Ir(H)(Bpin)$_2$(P(OPh)$_3$) contained an iridium hydride resonance at -13.3 ppm. The origin of the hydride is likely from the borylation of the N–H of the ligand and the tetrahydrofuran solvent.

Comparison of the timecourse of the reaction with the distribution of phosphite complexes strongly suggests that (**L3**)Ir(H)(Bpin)$_2$ becomes the dominant iridium species as the reaction progresses and is the major species in the reaction when B$_2$pin$_2$ is fully consumed. At this point, the solution contains HBpin and not B$_2$pin$_2$, as determined by ^{11}B NMR spectroscopy, but the HBpin does not react with the tetrahydrofuran solvent in the presence of the iridium catalyst formed from **L2**. Thus, the bisboryl hydride complex (**L3**)Ir(H)(Bpin)$_2$ is much less reactive toward THF than is the trisboryl complex (**L3**)Ir(Bpin)$_3$.

a

(MesH)Ir(Bpin)$_3$ (5 mol%)
L (5 mol%)
B$_2$pin$_2$ (1 equiv.)
THF
(0.5 M) → neat, 65 °C

b

P(OPh)$_3$

(**L3**)Ir(H)(Bpin)$_2$(P(OPh)$_3$)

(**L3**)Ir(Bpin)$_3$(P(OPh)$_3$)

10 min
20 min
30 min
40 min
50 min
60 min

c

L2
+ (MesH)Ir(Bpin)$_3$

1. B$_2$pin$_2$, THF, 65 °C
2. B$_2$pin$_2$, rt
3. P(OPh)$_3$

L2
+ (MesH)Ir(Bpin)$_3$
+ B$_2$pin$_2$

THF, 65 °C
then P(OPh)$_3$

d

501
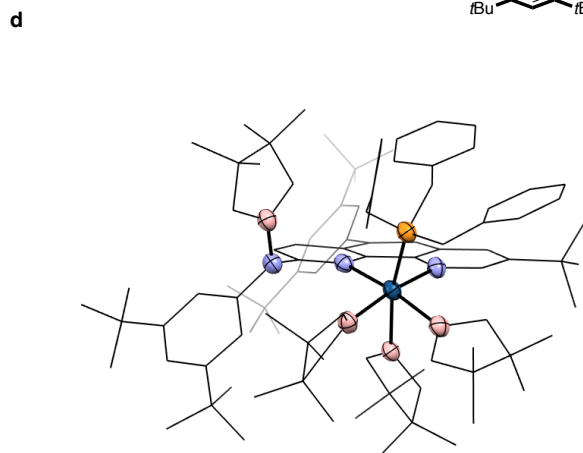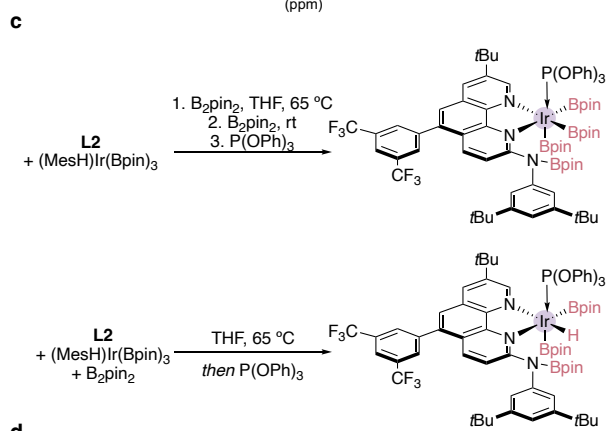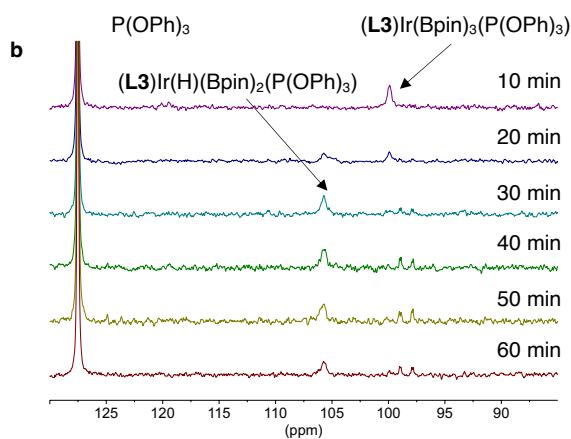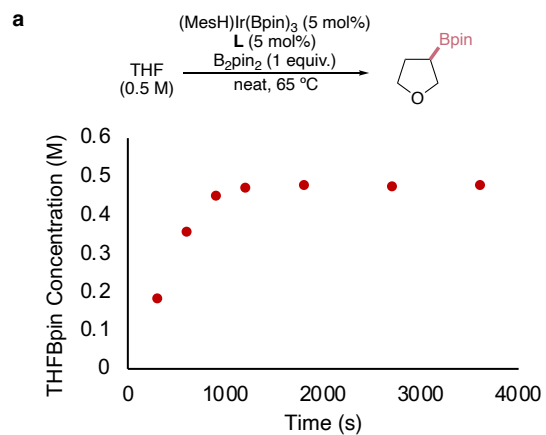
Figure 4.5. Trapping experiments and independent syntheses of phosphite capped complexes. (a) Timecourse of the borylation of THF. (b) ^{31}P NMR spectra of aliquots. (c) Independent syntheses of phosphite capped complexes. (d) Crystal structure of (**L2**)Ir(Bpin)$_3$(P(OPh)$_3$). Thermal ellipsoids are shown at 50% probability.

To gain a further understanding of the dependence of the speciation of the catalyst as a function of the composition of the catalytic reaction, we first studied how the catalyst speciation depends on the ratio of HBpin to B$_2$pin$_2$. Solutions of the catalyst (0.005 M) in the presence of boron reagents (varying ratios of HBpin : B$_2$pin$_2$, total concentration 0.5 M) were prepared, and the ratio of (**L3**)Ir(Bpin)$_3$ to (**L3**)Ir(H)(Bpin)$_2$ was measured by ^{1}H NMR spectroscopy. The equilibrium constant of the reaction of (**L3**)Ir(Bpin)$_3$ with HBpin to form (**L3**)Ir(H)(Bpin)$_2$ and B$_2$pin$_2$ is 0.14 ± 0.01 at 298 K (Figure 4.6). This value implies that the trisboryl species (**L3**)Ir(Bpin)$_3$ will be the major species in solution throughout most of the reaction.
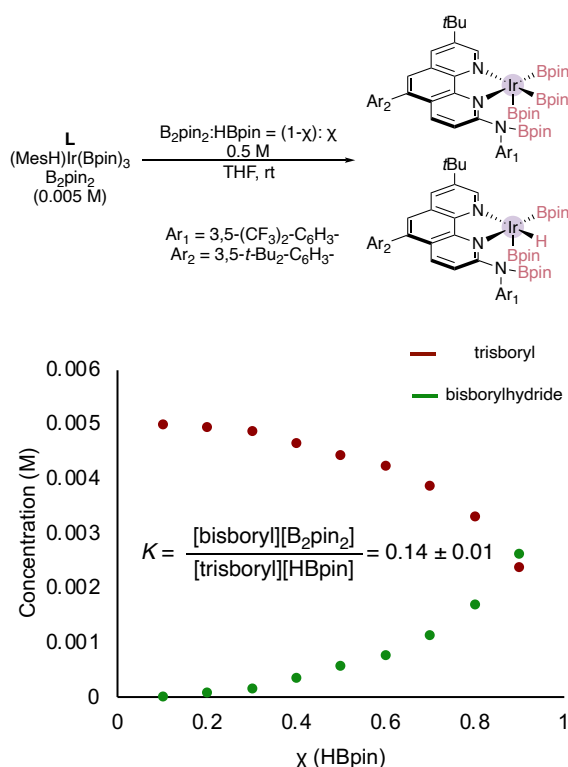
Figure 4.6. Dependence of catalyst speciation on boron reagent molar ratio.

In addition to the trapping studies, kinetic studies were performed to establish the relative stoichiometry of the resting state and the transition state of the turnover-limiting step during the initial stages of the reaction. The reaction was first order in tetrahydrofuran, indicating that this ether is not bound to the resting state and associates prior to the transition state of the turnover-limiting step of the catalytic process. The reaction was zero order in the diboron reagent, indicating that it is either present in the resting state, or that it reacts with the catalyst after the turnover-limiting step. In the absence of additives, the reaction was not first order in catalyst (Figure 4.7a), because the amount of mesitylene and HBpin formed in the catalyst activation process is proportional to the amount of catalyst. This was further supported by inverse orders observed for mesitylene (Figure 4.28) and HBpin (Figure 4.7b). When the

reaction was conducted with 1.5 equiv of HBpin to ensure that the concentration of this component does not change significantly when it is generated by activation of the catalyst, the reaction was first order in catalyst (Figure 4.7c). In combination with the measured equilibrium in Figure 4.6 which shows that the HBpin affects the speciation of the catalyst at higher HBpin to B_2pin_2 ratios, we derived the rate equations for the catalytic cycle under conditions with added HBpin as shown in eq. 1-4. Under initial rates conditions, and if the concentration of HBpin introduced by catalyst activation is held constant by holding the catalyst concentration constant, the rate equation simplifies to eq. 5, and the reaction is first order in tetrahydrofuran and zero order in diboron. With the addition of a constant concentration of HBpin, eq. 4 also predicts that the reaction is first order in catalyst. If the concentration of HBpin is varied, eq. 6 shows that the plot of 1/rate versus concentration of HBpin should be a straight line with non-negligible intercept.

$$(\textbf{L3})\mathrm{Ir}(\mathrm{Bpin})_3 = \mathrm{cat3}$$

$$(\textbf{L3})\mathrm{Ir}(\mathrm{H})(\mathrm{Bpin})_3 = \mathrm{cat2}$$
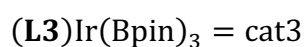
$$K = \frac{[\mathrm{cat2}][B_2pin_2]}{[\mathrm{cat3}][\mathrm{HBpin}]} \tag{1}$$

$$[\mathrm{cat}]_0 = [\mathrm{cat2}] + [\mathrm{cat3}] \tag{2}$$

$$[\mathrm{cat}]_0 = \left(\frac{K[\mathrm{HBpin}]}{[B_2pin_2]} + 1\right)[\mathrm{cat3}] \tag{3}$$

$$\mathrm{rate} = k[\mathrm{cat3}][\mathrm{THF}] = k[\mathrm{cat}]_0[\mathrm{THF}]\left(\frac{1}{1 + \frac{K[\mathrm{HBpin}]}{[B_2pin_2]}}\right) \tag{4}$$

$$\mathrm{if}\ [\mathrm{HBpin}] \ll [B_2pin_2],\ \mathrm{then}\ \frac{K[\mathrm{HBpin}]}{[B_2pin_2]} \ll 1,\ \mathrm{then\ rate} = k[\mathrm{cat}]_0[\mathrm{THF}] \tag{5}$$

$$\frac{1}{\mathrm{rate}} = \frac{1}{k[\mathrm{cat}]_0[\mathrm{THF}]}\left(1 + \frac{K[\mathrm{HBpin}]}{B_2pin_2}\right) \tag{6}$$
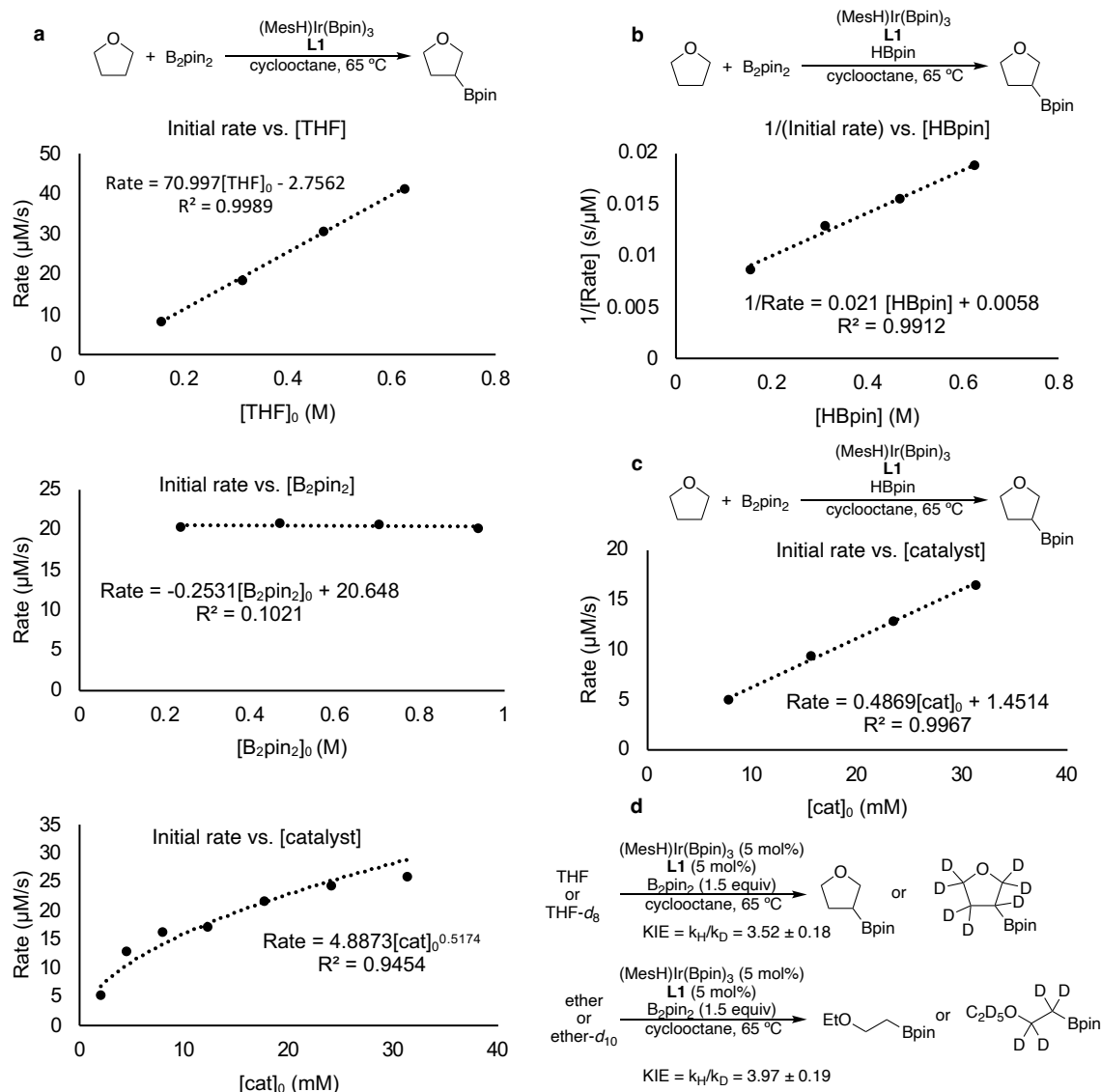
Figure 4.7. Kinetic studies. (a) Reaction orders obtained by the method of initial rates without saturation in HBpin. The reaction was 1st order in THF, 0 order in B2pin2, and half-order in catalyst. (b) Reaction order by the method of initial rates for HBpin. The reaction was inverse order in HBpin. (c) Reaction order in catalyst by the method of initial rates with saturation in HBpin. The reaction was 1st order in catalyst. (d) KIEs of THF and ether by parallel rates.

To reveal whether oxidative addition of the C–H bond is the turnover limiting step, the kinetic isotope effect of the borylation of various alkyl ethers was measured (Figure 4.7d). The KIE value obtained from the initial rates of separate reactions with THF or THF-d_8 was 3.5 ± 0.2. The KIE value obtained from the initial rates of separate reactions with diethyl ether or diethyl ether-d_{10} was 4.0 ± 0.2. These primary KIE values are consistent with irreversible, turnover-limiting cleavage of the C–H bond by the active catalyst.

To understand the origins of the increased activity with the *N*-borylated **L3** ligand and understand why the borylation of alkyl C–H bonds only proceeds with the iridium trisboryl complex and not the iridium bisboryl hydride complex, we conducted DFT studies to understand how the barriers to oxidative addition change, depending on the speciation of the

iridium complex (Figure 4.8). Calculations were conducted at the PBE0-D3BJ, def2-SVP/def2-TZVP(Ir)//PBE0-D3BJ, def2-TZVPD/def2-QZVPD(Ir), SMD(cyclohexane) level. The ligand was truncated to *N*-phenyl-*N*-Bpin-1,10-phenanthrolin-2-amine (**L4**). The computed barrier for the oxidative addition of THF to (**L4**)Ir(Bpin)$_3$ was 32.6 kcal/mol, while that for oxidative addition of THF to (**L4**)Ir(H)(Bpin)$_2$ was 35.0 kcal/mol, and a transition state for oxidative addition of THF to *iso*-(**L4**)Ir(H)(Bpin)$_2$ could not be located. In (**L4**)Ir(H)(Bpin)$_2$ the aminoboryl substituent is proximal to a boryl ligand whereas in *iso*-(**L4**)Ir(H)(Bpin)$_2$ the aminoboryl substituent is proximal to a hydride ligand, thereby minimizing the steric clash. The reaction of HBpin with (**L4**)Ir(Bpin)$_3$ to form B$_2$pin$_2$ and (**L4**)Ir(H)(Bpin)$_2$ was computed to be endothermic by 10.5 kcal/mol, and that to form *iso*-(**L4**)Ir(H)(Bpin)$_2$ was computed to be endothermic by 6.4 kcal/mol.

Although the calculated barriers are higher than those corresponding to the experimental rates, we could draw certain qualitative conclusions and rationalize the inactivity of the observed bisborylhydride species. Through the process of oxidative addition of tetrahydrofuran to (**L4**)Ir(Bpin)$_3$, the computed structure suggests that the forming hydride is close to one of the boryl groups connected to iridium (d(B–H) = 2.020 Å) and to the pendant *N*-boryl group (d(B–H) = 3.299 Å). A similar arrangement is seen in the computed transition state for the oxidative addition of tetrahydrofuran to (**L4**)Ir(H)(Bpin)$_2$. Such an arrangement is impossible during oxidative addition of tetrahydrofuran to *iso*-(**L4**)Ir(H)(Bpin)$_2$, in which the iridium hydride lies adjacent to the bulky sidearm of the phenanthroline ligand.
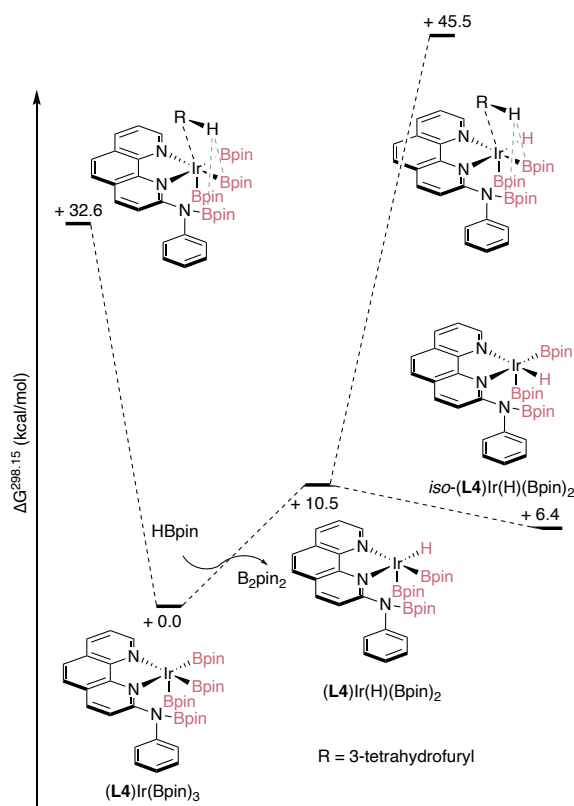
Figure 4.8. DFT calculations for the barriers to oxidative addition of THF to various iridium complexes.

Based on our experimental and computational data, we propose that the borylation of alkyl C–H bonds with iridium catalysts formed from aminophenanthroline ligands occurs by the mechanism in Figure 4.9. Rapid borylation of the *N*-H of the aminophenanthroline ligand occurs to form (**L4**)Ir(Bpin)$_3$. Turnover-limiting oxidative addition of the C–H bond of the substrate occurs to (**L4**)Ir(Bpin)$_3$ and is assisted by the *N*-boryl to generate a 7-coordinate Ir(V) species. Isomerization of this intermediate is followed by reductive elimination to form (**L4**)Ir(H)(Bpin)$_2$ and the borylated product.
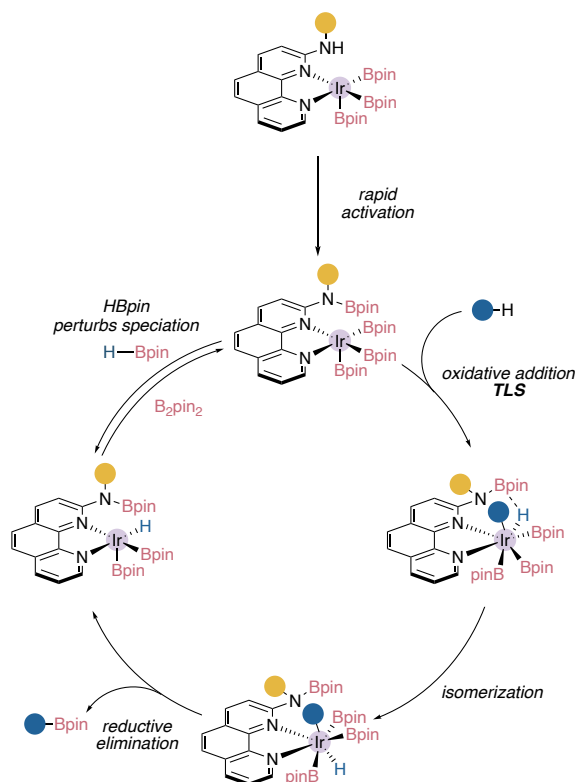
Figure 4.9. Proposed mechanism based on the experimental and computational data.

4.3 Conclusions

In conclusion, the *N*-borylated aminophenanthroline iridium trisboryl complex is the active catalyst in the borylation of alkyl C–H bonds. This assignment is supported by in situ detection and trapping of the active species and the connectivity of the complex supported by X-ray crystallography. In contrast, the *N*-borylated, aminophenanthroline-iridium bisboryl hydride complex is inactive for the borylation of alkyl C–H bonds. Kinetic studies have revealed that the reaction rate depends on the concentration of catalyst and substrate but not the diboron reagent. Inverse orders in the hydroborane byproduct led us to investigate the effects of HBpin have on catalyst speciation, demonstrating that the catalyst speciation gradually shifts towards the inactive bisboryl hydride as the proportion of HBpin to B$_2$pin$_2$ increases. This observation also explains why the use of superstoichiometric B$_2$pin$_2$ (1.5 equiv to 3.0 equiv) is often required for good conversion of the substrate and why borylation of alkyl substrates typically require the use of B$_2$pin$_2$ and cannot be run effectively with HBpin as the boron source. The measured KIEs indicate that C–H oxidative addition is the turnover-limiting step. Finally,

increased activity for the activation of C–H bonds with the catalyst generated from aminophenanthroline is observed for both the borylation of alkyl and aryl C–H bonds.

We speculate that the increased activity for the activation of C–H bonds is due to the synergistic effect of both the *N*-boryl substituent and one of the boryl ligands on the C–H oxidative addition. Further efforts to isolate a phosphite-capped *N*-boryl iridium trisboryl complex that contains a phosphite that does not undergo borylation and to test the stoichiometric reactivity of such a complex are underway, as are efforts to obtain detailed computational understanding of how the pendant boryl group lowers the barrier to C–H oxidative addition.

4.4 Experimental

4.4.1 General Information

Reagents and Solvents

All catalytic reactions were assembled under inert atmosphere in a nitrogen-filled glovebox equipped with an oxygen sensor (working level ≤ 1.0 ppm) and a low temperature refrigeration unit (–35 °C) unless otherwise noted. All other reactions were assembled under inert atmosphere with a Schlenk manifold or a nitrogen glovebox unless otherwise noted. All reagents and solvents were purchased from commercial sources and used as received, unless otherwise noted. All glassware was flame-dried or dried overnight at 120 °C, allowed to cool under vacuum, and stored in a N_2-atomsphere drybox until use unless otherwise noted. Tetrahydrofuran, toluene, and diethyl ether were purified by passing the degassed solvents (N_2) through a column of activated alumina (solvent purification system purchased from Innovative Technologies, Newburyport, MA). The tetrahydrofuran and tetrahydrofuran-d_8 used for the synthesis of complexes were dried over Na/K overnight and filtered before use. Cyclooctane was degassed by three freeze-pump-thaw cycles and further dried over activated 4 Å molecular sieves. Deuterated solvents were purchased from Cambridge Isotope Laboratories and used as received. See section 2 for synthesis of ligands and substrates.

Chromatography and Data Analysis

Flash column chromatography was conducted on a Teledyne ISCO Combiflash Rf or Rf+ system, with prepacked RediSep Gold silica gel and C18 columns. All reactions were followed by thin-layer chromatography (TLC) when practical, using Merck Kieselgel 60 F_{254} fluorescent treated silica, which was visualized under UV light when practical, or by staining with a solution of anisaldehyde or phosphomolybdic acid followed by heating.

^{1}H, ^{11}B, ^{13}C, and ^{19}F NMR spectra were recorded on AVQ-400, JEOL-400, AVB-400, AV-500, AV-600, NEO-500, and AV-700 spectrometers. Chemical shifts (*d*) reported given in parts per million (ppm) relative to the residual solvent signal. Coupling constants (*J*) are given in Hertz (Hz), rounded to the nearest 0.1 Hz. The ^{1}H NMR spectra are reported as follows: ppm (multiplicity, coupling constants, number of protons). Abbreviations are as follows: s (singlet), d (doublet), t (triplet), q (quartet), m (multiplet), br (broad). The carbon attached to boron is usually not observed.

High-resolution mass spectral (HRMS) data were obtained from the QB3/Chemistry Mass Spectrometry Facility or the Catalysis Center at UC Berkeley.

Gas Chromatography (GC) was performed on an HP 6890 GC system with an Agilent HP-5 column (25 m × 0.200 mm, 0.33 micron).

Naming of Compounds

Compound names were generated by ChemDraw 20.0 software (PerkinElmer), following the IUPAC nomenclature.

4.4.2 Synthesis of Ligands and Materials

The ligands and materials were obtained from commercial vendors, prepared according to literature procedures, or independently synthesized (see below). *N*-phenyl-1,10-phenanthroline-2-amine[12], *tert*-butyl octyl ether[24] were synthesized according to literature precedent. The spectral data of the known compounds were identical to those reported in the literature. All other chemicals were purchased from commercial vendors and used as received unless otherwise noted.

5-bromo-2-chloroquinolin-8-amine
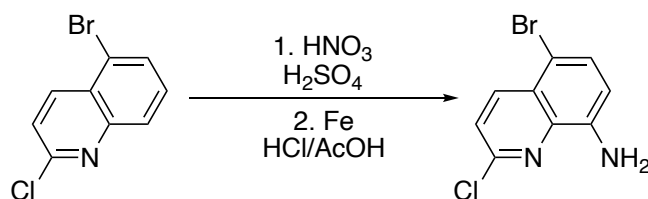
5-Bromo-2-chloro-quinoline (5.0 g, 15 mmol, 1.0 equiv) was added to a 100 mL round bottom flask equipped with a magnetic stir bar. Concentrated sulfuric acid (20 mL) was added, and the mixture stirred until the solids dissolved. Then the flask was cooled to 0 °C in an ice bath, and concentrated nitric acid (2.1 mL, 45 mmol, 3.0 equiv) was added dropwise. The mixture was allowed to warm to room temperature overnight. The mixture was poured carefully into a stirred beaker containing ice mixed with 2 M NaOH (~200 mL total volume), and the pH was adjusted with 2 M NaOH until pH > 10. DCM (100 mL) was added, and the layers were separated. The aqueous layer was further extracted with DCM (50 mL • 3) and the combined organic layers were dried over MgSO$_4$, filtered, and concentrated to dryness in a 250 mL round bottom flask. To this flask was added a magnetic stir bar, concentrated hydrochloric acid (15 mL) and acetic acid (15 mL). The suspension was heated to 45 °C, and iron dust (2.6 g, 45 mmol, 3.0 equiv) was added. The mixture was stirred overnight. The mixture was poured carefully into a stirred beaker containing ice mixed with 2 M NaOH (~200 mL total volume), and the pH was adjusted with 2 M NaOH until pH > 10. DCM (200 mL) and MeOH (100 mL) were added, and the green-black suspension was filtered over a pad of Celite. The Celite layer was washed with DCM/MeOH (2:1, 1 L) until the filtrate was a very light-yellow color. The combined filtrate was transferred to a separatory funnel, the layers separated, and the aqueous layer further extracted with DCM/MeOH (2:1, 200 mL•5). The combined organic layers were dried over MgSO$_4$, filtered, and concentrated to afford the title compound as yellow-brown flakes (3.3 g, 83%) The material was judged to be of sufficient purity to be used in the next step.

^{1}H NMR (500 MHz, CDCl$_3$) δ 8.39 (d, J = 8.8 Hz, 1H), 7.59 (d, J = 8.2 Hz, 1H), 7.46 (d, J = 8.8 Hz, 1H), 6.84 (d, J = 8.2 Hz, 1H), 4.98 (bs, 2H).

^{13}C NMR (126 MHz, CDCl$_3$) δ 148.8, 143.3, 138.7, 138.3, 131.3, 126.7, 123.7, 111.6, 107.1.

HRMS (*m/z*): (ESI+) calc'd for C$_9$H$_7$N$_2$BrCl [M+H]$^+$: 256.9476, found: 256.9477.

5-bromo-8-(*tert*-butyl)-2-chloro-1,10-phenanthroline
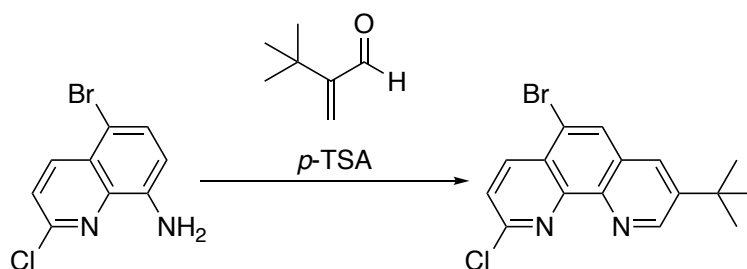
To a 20 mL vial was added 5-bromo-2-chloroquinolin-8-amine (258 mg, 1.00 mmol, 1.00 equiv), *p*-toluenesulfonic acid monohydrate (19.0 mg, 0.100 mmol, 0.100 equiv), and 3,3-dimethyl-2-methylenebutanal (168 mg, 1.50 mmol, 1.50 equiv). A magnetic stir bar and toluene (4 mL) were added to the vial, and then the vial was sealed with a Teflon-lined cap. The vial was heated at 120 ºC for 24 h. After the vial had cooled to room temperature, the mixture was diluted with DCM (20 mL), and 2 M NaOH (10 mL) was added. The layers were separated, and the aqueous layer was further extracted with DCM (20 mL•2). The combined layers were dried over MgSO$_4$, filtered, and concentrated. The crude material was chromatographed on silica with 1% NEt$_3$ and 10% DCM in hexanes as the eluent to afford the title compound as a yellow foam (240 mg, 69%).

^{1}H NMR (500 MHz, CDCl$_3$) δ 9.35 (d, *J* = 2.4 Hz, 1H), 8.59 (d, *J* = 8.6 Hz, 1H), 8.15 (s, 1H), 8.09 (d, *J* = 2.4 Hz, 1H), 7.70 (d, *J* = 8.5 Hz, 1H), 1.53 (s, 9H).

^{13}C NMR (126 MHz, CDCl$_3$) δ 152.5, 150.6, 147.0, 146.4, 142.3, 138.8, 130.5, 130.4, 129.1, 126.4, 124.7, 119.8, 34.2, 31.0.

HRMS (*m/z*): (ESI+) calc'd for C$_{16}$H$_{15}$N$_2$BrCl [M+H]$^+$: 349.0102, found: 349.0104.

5-bromo-8-(*tert*-butyl)-*N*-(3,5-di-*tert*-butylphenyl)-1,10-phenanthrolin-2-amine
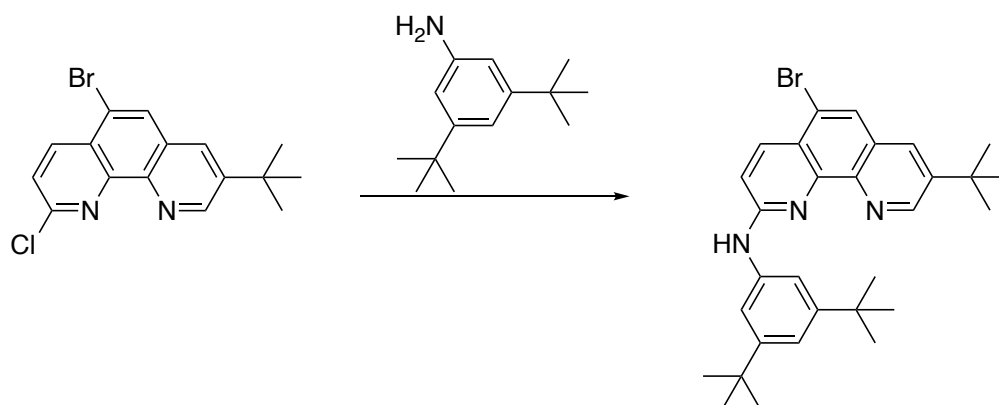
To a 20 mL vial was added 5-bromo-8-(*tert*-butyl)-2-chloro-1,10-phenanthroline (750 mg, 2.14 mmol, 1.00 equiv), 3,5-di-*tert*-butylaniline (1.32 g, 6.43 mmol, 3.00 equiv), a magnetic stir bar, and toluene (10 mL). The vial was sealed with a Teflon-lined cap and heated at 120 ºC for 24 h. The reaction was cooled to room temperature, diluted with DCM (50 mL), and 2 M NaOH was added (20 mL). The layers were separated, and the aqueous layer was further extracted with DCM (50 mL•3). The combined organic layers were dried over MgSO$_4$, filtered, and concentrated. The crude material was purified by column chromatography on silica. Eluent: 0 → 30% ethyl acetate in (1% NEt$_3$ in hexanes) to afford the title compound as an off-white foam (780 mg, 70%).

¹H NMR (600 MHz, CDCl$_3$) δ 9.34 (d, *J* = 2.4 Hz, 1H), 8.51 (d, *J* = 9.0 Hz, 1H), 8.13 (d, *J* = 2.4 Hz, 1H), 7.97 (s, 1H), 7.62 (bs, 1H), 7.45 (d, *J* = 9.0 Hz, 1H), 7.40 – 7.39 (m, 1H), 7.37 (d, *J* = 1.7 Hz, 2H), 1.62 (s, 9H), 1.50 (s, 18H).

¹³C NMR (151 MHz, CDCl$_3$) δ 156.7, 152.4, 149.2, 146.7, 145.9, 142.4, 138.9, 137.9, 130.4, 129.2, 125.3, 122.0, 120.9, 118.9, 117.1, 110.4, 35.1, 34.1, 31.6, 31.1.

HRMS (*m/z*): (ESI+) calc'd for C$_{30}$H$_{37}$N$_3$Br [M+H]$^+$: 518.2165, found: 518.2164.

5-(3,5-bis(trifluoromethyl)phenyl)-8-(*tert*-butyl)-*N*-(3,5-di-*tert*-butylphenyl)-1,10-phenanthrolin-2-amine (L2)
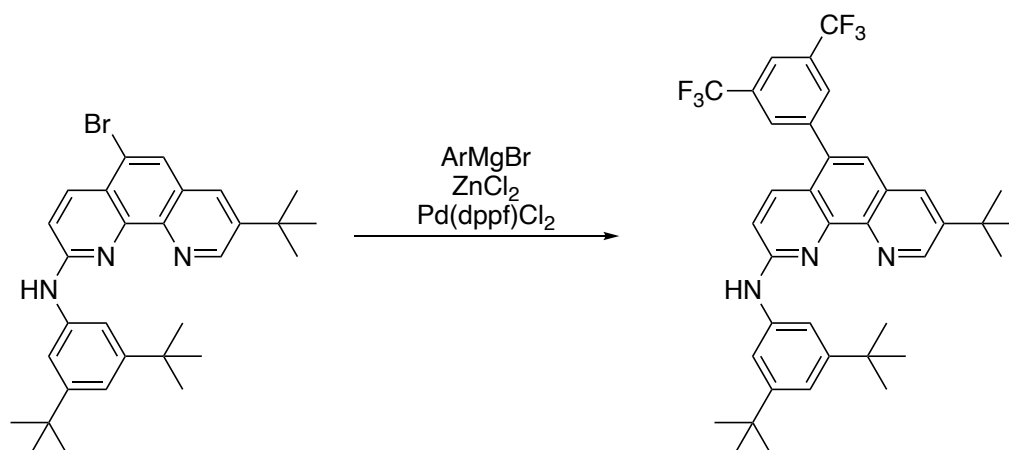
A 100 mL round bottom flask was charged with dry THF (25 mL) and zinc chloride (434 mg, 3.18 mmol, 3.00 equiv) in a glovebox and sealed with a rubber septum. The flask was brought out of the glovebox, cooled over an ice bath, and to the cloudy white mixture was dropwise added 3,5-bis(trifluoromethyl)phenyl)magnesium bromide (6.36 mL, 0.5 molar in THF, 3.18 mmol, 3.00 equiv). The resulting solution was stirred for 10 min at room temperature. The septum was secured tightly with copper wire, and the flask carefully brought back into the glovebox. 5-bromo-8-(tert-butyl)-N-(3,5-di-tert-butylphenyl)-1,10-phenanthrolin-2-amine (550 mg, 1.06 mmol, 1.00 equiv) was added, followed by (dppf)PdCl$_2$ (77.6 mg, 0.106 mmol, 10.0 mol%). The flask was brought out of the glovebox, and the solution was refluxed for 16 h. The mixture was cooled to room temperature, diluted with DCM (80 mL), and 2 M aqueous NaOH (50 mL) was added. The layers were separated, and the aqueous layer further extracted with DCM (50 mL•3). The combined organic layers were dried over MgSO$_4$, filtered, and concentrated. The crude material was purified by chromatography on silica, eluting with 0 → 30% of ethyl acetate in (1% NEt$_3$ in hexanes) to afford the title compound as a brown solid (642 mg, 93%).

¹H NMR (600 MHz, CDCl$_3$) δ 9.41 (d, *J* = 2.4 Hz, 1H), 8.26 (d, *J* = 2.4 Hz, 1H), 8.12 (s, 3H), 7.94 (d, *J* = 9.1 Hz, 1H), 7.63 (s, 2H), 7.40 – 7.38 (m, 2H), 7.36 (d, *J* = 1.7 Hz, 2H), 1.65 (s, 9H), 1.48 (s, 18H).

¹³C NMR (151 MHz, CDCl$_3$) δ 156.6, 152.6, 149.8, 146.7, 146.0, 143.0, 142.3, 139.1, 135.8, 135.5, 132.2 (q, *J* = 33.2 Hz), 131.6, 130.2, 128.3, 123.6, 123.5 (q, *J* = 272.9 Hz) 121.8, 121.1, 119.1, 117.3, 110.0, 35.2, 34.2, 31.7, 31.2.

¹⁹F NMR (565 MHz, CDCl$_3$) δ -62.7.

HRMS (*m/z*): (ESI+) calc'd for C$_{38}$H$_{40}$N$_3$F$_6$ [M+H]$^+$: 652.3121, found: 652.3129.

tris(4-bromophenyl) phosphite (L5)
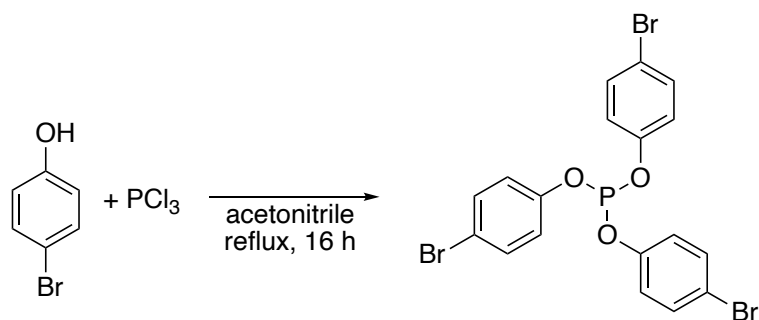
A flame-dried 250 mL round bottom flask was charged with 4-bromophenol (5.0 g, 29 mmol, 3.0 equiv) under nitrogen. The solid phenol was dissolved in dry acetonitrile (100 mL). Then phosphorous trichloride (0.93 mL, 11 mmol, 1.1 equiv) was added dropwise via syringe. The solution was stirred at room temperature for 10 min, then a nitrogen-flushed reflux condenser equipped with a nitrogen outlet was attached to the round bottom flask, and the solution refluxed for 16 h. The reflux condenser was removed, and all volatile materials were evaporated in vacuo. The flask was brought into a nitrogen glovebox, and the residue was washed with pentane. The solids were redissolved in dichloromethane and diethyl ether (1:4), layered with pentane, and stored at -35 ºC overnight. The title compound crystallized as white needles (4.2 g, 80%)

^{1}H NMR (500 MHz, C_6D_6) δ 7.18 (d, J = 8.9 Hz, 6H), 6.79 (d, J = 8.8 Hz, 6H).

^{13}C NMR (126 MHz, CDCl$_3$) δ 150.4, 132.8, 122.4(J_{C-P} = 6.6 Hz), 117.5.

^{31}P NMR (202 MHz, C_6D_6) δ 126.7.

HRMS (*m/z*): (ESI+) calc'd for $C_{18}H_{13}Br_3O_3P$ [M+H]$^+$: 546.8126, found: 546.8131.

9-methyl-*N*-phenyl-1,10-phenanthrolin-2-amine
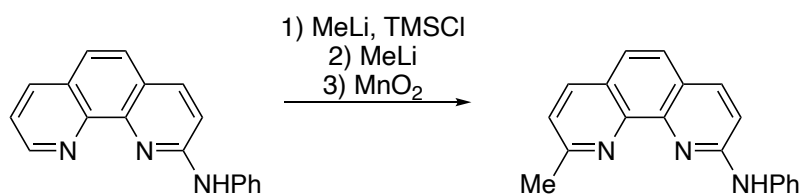
A 100 mL Schlenk tube was charged with *N*-phenyl-1,10-phenanthrolin-2-amine (240 mg, 885 µmol, 1.00 equiv) and dry THF (50 mL). MeLi (1.60 M, 829 µL, 1.33 mmol, 1.50 equiv) was added at room temperature, followed by TMSCl (168 µL, 1.33 mmol, 1.50 equiv). The mixture was stirred for 30 min. MeLi (1.60 M, 829 µL, 1.33 mmol, 1.50 equiv) was then added, the Schlenk sealed, and the mixture heated at 80 ºC for 16 hours. The reaction mixture was quenched with water (5 mL), the layers were separated, and the aqueous layer extracted with DCM (50 mL•3). The combined organic layers were dried over MgSO$_4$. To the resulting deep yellow solution was added activated MnO$_2$ (500 mg), and the mixture was stirred at room temperature for 16 h. The solution was filtered through Celite, concentrated, and purified by column chromatography (0-100% ethyl acetate in (1% NEt$_3$ in hexanes)) to afford the title compound as a yellow foam (155 mg, 61%).

^{1}H NMR (500 MHz, CDCl$_3$) δ 8.13 (d, *J* = 8.2 Hz, 1H), 8.05 (d, *J* = 8.8 Hz, 1H), 7.65 (d, *J* = 8.6 Hz, 1H), 7.57 (d, *J* = 8.6 Hz, 1H), 7.50 (d, *J* = 8.2 Hz, 1H), 7.47 – 7.39 (m, 4H), 7.36 (d, *J* = 8.9 Hz, 1H), 7.18 (tt, *J* = 6.5, 2.1 Hz, 1H), 2.97 (s, 3H).

^{13}C NMR (126 MHz, CDCl$_3$) δ 158.8, 155.5, 145.4, 144.4, 140.2, 138.3, 136.4, 129.6, 127.4, 125.5, 124.0, 123.7, 123.5, 122.5, 121.6, 110.5, 26.0.

HRMS (*m/z*): (ESI+) calc'd for C$_{19}$H$_{16}$N$_3$ [M+H]$^+$: 286.1339, found: 286.1335.

8-methyl-*N*-phenyl-1,10-phenanthrolin-2-amine

To a 4 mL vial was added 2-chloro-8-methyl-1,10-phenanthroline (57.2 mg, 0.250 mmol, 1.00 equiv), aniline (69.8 mg, 0.750 mmol, 3.00 equiv), a magnetic stirbar, and toluene (1 mL). The vial was sealed with a Teflon-lined cap and heated at 140 ºC for 24 h. The reaction was cooled to room temperature, diluted with DCM (10 mL), poured into 2 M NaOH added (10 mL), and the layers separated. The aqueous layer was further extracted with DCM (10 mL•2). The combined organic layers were dried over MgSO$_4$, filtered, and concentrated. The crude material was purified by column chromatography on silica. Eluent: 0 → 20% (30% NH$_4$OH in methanol) in ethyl acetate to afford the title compound as a brown powder (26.9 mg, 38%).

¹H NMR (500 MHz, CDCl$_3$) δ 9.01 (d, *J* = 2.3 Hz, 1H), 8.06 (d, *J* = 8.8 Hz, 1H), 8.01 (dd, *J* = 2.2, 1.1 Hz, 1H), 7.68 (d, *J* = 8.6 Hz, 1H), 7.54 (d, *J* = 8.7 Hz, 1H), 7.48 – 7.36 (m, 6H), 7.19 (tt, *J* = 7.2, 1.3 Hz, 1H), 2.62 (s, 3H).

¹³C NMR (151 MHz, CDCl$_3$) δ 155.5, 151.4, 145.7, 143.0, 140.0, 138.4, 135.3, 132.5, 129.7, 129.3, 126.4, 124.2, 123.1, 122.3, 121.8, 110.0, 18.9.

HRMS (*m/z*): (ESI+) calc'd for C$_{19}$H$_{16}$N$_3$ [M+H]$^+$: 286.1339, found: 286.1337.

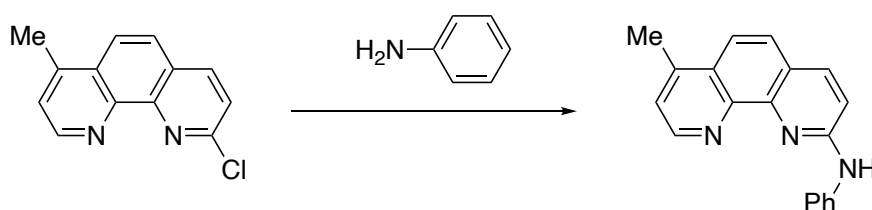## 7-methyl-*N*-phenyl-1,10-phenanthrolin-2-amine

To a 4 mL vial was added 2-chloro-8-methyl-1,10-phenanthroline (57.2 mg, 0.250 mmol, 1.00 equiv), aniline (69.8 mg, 0.750 mmol, 3.00 equiv), a magnetic stirbar, and toluene (1 mL). The vial was sealed with a Teflon-lined cap and heated at 140 ºC for 24 h. The reaction was cooled to room temperature, diluted with DCM (10 mL), poured into 2 M NaOH added (10 mL), and the layers separated. The aqueous layer was further extracted with DCM (10 mL•2). The combined organic layers were dried over MgSO₄, filtered, and concentrated. The crude material was purified by column chromatography on silica. Eluent: 0 → 20% (30% NH₄OH in methanol) in ethyl acetate to afford the title compound as a brown powder (27.6 mg, 39%).

¹H NMR (500 MHz, CDCl₃) δ 9.04 (d, *J* = 4.4 Hz, 1H), 8.09 (d, *J* = 8.8 Hz, 1H), 7.83 (d, *J* = 9.2 Hz, 1H), 7.75 (d, *J* = 8.9 Hz, 1H), 7.49 – 7.36 (m, 6H), 7.21 (d, *J* = 6.6 Hz, 1H), 2.82 (s, 3H).

¹³C NMR (126 MHz, CDCl₃) δ 155.4, 149.4, 144.4, 139.8, 138.6, 129.8, 129.1, 125.9, 124.4, 124.0, 123.0, 122.0, 118.7, 110.5, 19.4.

HRMS (*m/z*): (ESI+) calc'd for C₁₉H₁₆N₃ [M+H]⁺: 286.1339, found: 286.1334.

5,6-dibromo-*N*-phenyl-1,10-phenanthrolin-2-amine
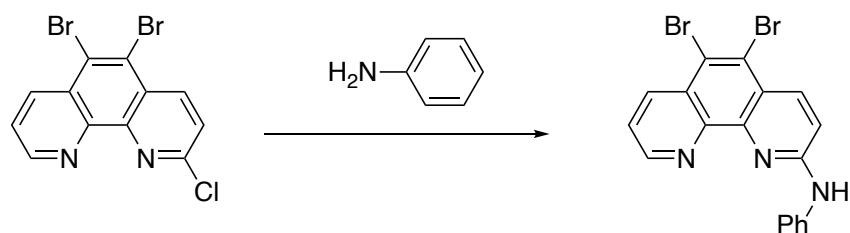
To a 20 mL vial was added 5,6-dibromo-2-chloro-1,10-phenanthroline (372 mg, 1.00 mmol, 1.00 equiv), aniline (279 mg, 3.00 mmol, 3.00 equiv), a magnetic stir bar, and toluene (2 mL). The vial was sealed with a Teflon-lined cap and heated at 140 ºC for 24 h. The reaction was cooled to room temperature, diluted with DCM (10 mL), and poured into 2 M NaOH (20 mL). The layers were separated, and the aqueous layer was further extracted with DCM (10 mL•3). The combined organic layers were dried over MgSO$_4$, filtered, and concentrated. The crude material was purified by column chromatography on silica. Eluent: 0 → 80% ethyl acetate in (1% NEt$_3$ and 10% DCM in hexanes) to afford the title compound as a grey solid (131 mg, 30%).

*NMR peaks were very broad, reported as observed.

^{1}H NMR (600 MHz, CDCl$_3$) δ 9.31 (s, 1H), 8.87 (d, *J* = 8.2 Hz, 1H), 8.67 (d, *J* = 9.1 Hz, 1H), 7.88 (s, 1H), 7.59 – 7.54 (m, 3H), 7.53 (d, *J* = 7.6 Hz, 2H), 7.36 (t, *J* = 7.3 Hz, 1H).

^{13}C NMR (151 MHz, CDCl$_3$) δ 139.8, 138.9, 137.1, 129.9, 125.2, 122.5.

HRMS (*m/z*): (ESI+) calc'd for C$_{18}$H$_{12}$N$_3$Br$_2$ [M+H]$^+$: 427.9392, found: 427.9387.

### 3,8-dimethyl-*N*-phenyl-1,10-phenanthrolin-2-amine
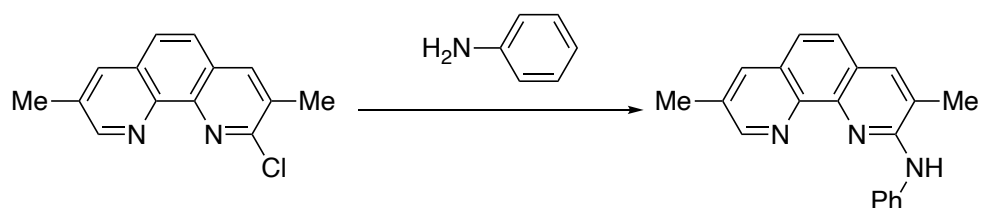
To a 4 mL vial was added 2-chloro-3,8-dimethyl-1,10-phenanthroline (60.7 mg, 0.250 mmol, 1.00 equiv), aniline (69.8 mg, 0.750 mmol, 3.00 equiv), a magnetic stir bar, and toluene (2 mL). The vial was sealed with a Teflon-lined cap and heated at 140 ºC for 24 h. The reaction was cooled to room temperature, diluted with DCM (10 mL), and poured into 2 M NaOH (20 mL). The layers were separated, and the aqueous layer was further extracted with DCM (10 mL•3). The combined organic layers were dried over MgSO$_4$, filtered, and concentrated. The crude material was purified by column chromatography on silica. Eluent: 0 → 80% ethyl acetate in (1% NEt$_3$ and 10% DCM in hexanes) to afford the title compound as a brown solid (38.2 mg, 51%).

¹H NMR (500 MHz, CDCl$_3$) δ 9.01 (s, 1H), 7.99 (d, *J* = 13.3 Hz, 2H), 7.95 (d, *J* = 15.1 Hz, 2H), 7.68 (d, *J* = 8.7 Hz, 1H), 7.58 (d, *J* = 8.6 Hz, 1H), 7.47 (t, *J* = 7.7 Hz, 2H), 7.13 (t, *J* = 7.4 Hz, 1H), 2.62 (s, 3H), 2.52 (s, 3H).

¹³C NMR (126 MHz, CDCl$_3$) δ 153.2, 151.6, 143.0, 141.0, 137.7, 135.1, 132.0, 129.4, 128.6, 125.8, 123.4, 122.9, 122.6, 121.8, 119.5, 18.89, 18.3.

HRMS (*m/z*): (ESI+) calc'd for C$_{20}$H$_{18}$N$_3$ [M+H]$^+$: 300.1495, found: 300.1490.

2-chloro-8-methyl-1,10-phenanthroline
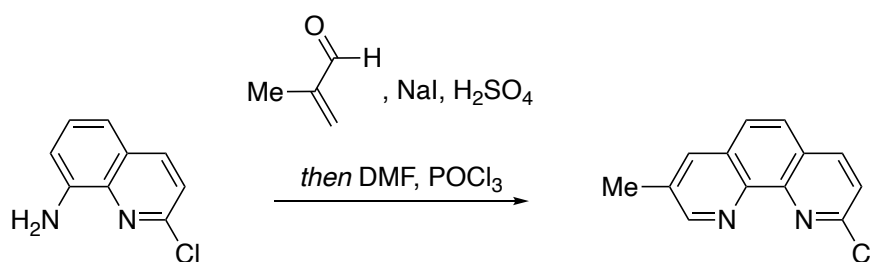
A 20 mL septum vial was charged with 2-chloroquinolin-8-amine (893 mg, 5.00 mmol, 1.00 equiv), sodium iodide (7.49 mg, 0.0500 mmol, 1.00 mol%), a magnetic stir bar, and concentrated sulfuric acid (18 M, 1.52 mL, 20.0 mmol, 4.00 equiv). The vial was sealed with the septum cap and heated at 110 °C. Methacrylaldehyde (691 µL, 8.35 mmol, 1.67 equiv) was added via syringe over 3 h. The reaction mixture was cooled to room temperature and poured into 2 M NaOH (10 mL). The layers were separated, and the aqueous layer was further extracted with DCM (10 mL•3). The combined organic layers were dried over MgSO$_4$ and filtered. ^{1}H NMR analysis revealed that partial hydrolysis of the chloride had occurred. To the filtrate was added DMF (96.8 µL, 1.25 mmol, 0.250 equiv) and POCl$_3$ (350 µL, 3.75 mmol, 0.75 equiv). The mixture was stirred overnight. The reaction mixture was poured into 2 M NaOH (10 mL). The layers were separated, and the aqueous layer was further extracted with DCM (10 mL•3). The combined organic layers were dried over MgSO$_4$, filtered, and concentrated. The crude material was purified by column chromatography on silica. Eluent: 0 → 80% ethyl acetate in DCM to afford the title compound as an off-white powder (407 mg, 36%).

^{1}**H NMR** (600 MHz, CDCl$_3$) δ 9.16 (d, J = 2.2 Hz, 1H), 8.26 (d, J = 8.3 Hz, 1H), 8.11 (dd, J = 2.2, 1.1 Hz, 1H), 7.84 (s, 2H), 7.69 (d, J = 8.3 Hz, 1H), 2.71 (s, 3H).

^{13}**C NMR** (151 MHz, CDCl$_3$) δ 152.5, 151.4, 146.3, 143.2, 138.8, 135.3, 133.5, 129.0, 126.9, 126.8, 125.8, 124.0, 19.0.

HRMS (*m/z*): (ESI+) calc'd for C$_{13}$H$_{10}$N$_2$Cl [M+H]$^+$: 229.0527, found: 229.0525.
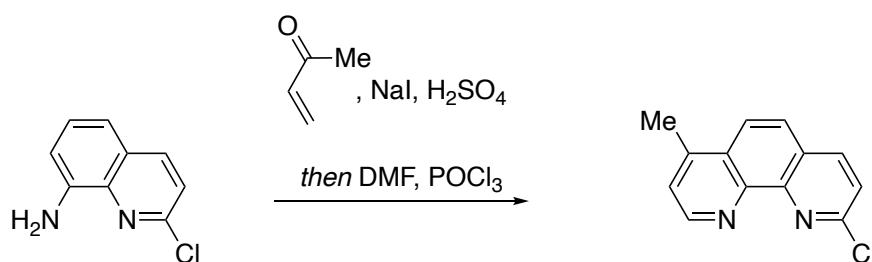
2-chloro-7-methyl-1,10-phenanthroline

A 20 mL septum vial was charged with 2-chloroquinolin-8-amine (893 mg, 5.00 mmol, 1.00 equiv), sodium iodide (7.49 mg, 0.0500 mmol, 1.00 mol%), a magnetic stir bar, and concentrated sulfuric acid (18 M, 1.52 mL, 20.0 mmol, 4.00 equiv). The vial was sealed with the septum cap and heated at 110 °C. But-3-en-2-one (696 µL, 8.35 mmol, 1.67 equiv) was added via syringe over 3 h. The reaction mixture was cooled to room temperature and poured into 2 M NaOH (10 mL). The layers were separated, and the aqueous layer was further extracted with DCM (10 mL•3). The combined organic layers were dried over MgSO$_4$ and filtered. ^{1}H NMR analysis revealed that partial hydrolysis of the chloride had occurred. To the filtrate was added DMF (96.8 µL, 1.25 mmol, 0.250 equiv) and POCl$_3$ (350 µL, 3.75 mmol, 0.75 equiv). The mixture was stirred overnight. The reaction mixture was poured into 2 M NaOH (10 mL). The layers were separated, and the aqueous layer was further extracted with DCM (10 mL•3). The combined organic layers were dried over MgSO$_4$, filtered, and concentrated. The crude material was purified by column chromatography on silica. Eluent: 0 → 80% ethyl acetate in DCM to afford the title compound as an off-white powder (338 mg, 30%).

^{1}H NMR (600 MHz, CDCl$_3$) δ 9.20 (d, J = 4.5 Hz, 1H), 8.32 (d, J = 8.4 Hz, 1H), 8.15 (d, J = 9.0 Hz, 1H), 7.93 (d, J = 9.0 Hz, 1H), 7.74 (d, J = 8.3 Hz, 1H), 7.61 (dd, J = 4.4, 0.9 Hz, 1H), 2.92 (s, 3H).

^{13}C NMR (151 MHz, CDCl$_3$) δ 151.6, 150.5, 146.5, 144.9, 144.6, 138.8, 128.8, 127.0, 125.4, 124.7, 124.4, 123.1, 19.3.

HRMS (*m/z*): (ESI+) calc'd for C$_{13}$H$_{10}$N$_2$Cl [M+H]$^+$: 229.0527, found: 229.0527.

5,6-dibromo-2-chloro-1,10-phenanthroline
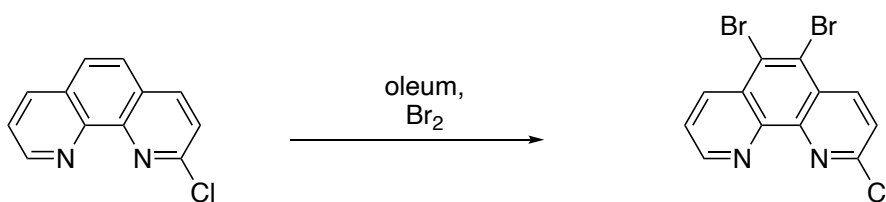
2-chlorophenanthroline (1.0 g, 5.0 mmol, 1.0 equiv) was placed in a heavy-walled glass reaction tube with a Teflon screw top fitted with a Viton O-ring. The reaction vessel was placed in an ice bath, and 3 mL of oleum (15%) and 0.1 mL (3.0 mmol, 0.60 equiv) of bromine were added. The reaction tube was placed in a silicon oil bath, and the temperature was slowly raised to 135 °C. After 24 h, the reaction mixture was cooled to room temperature, poured over ice, and neutralized with NH₄OH. The mixture was extracted with chloroform (10 mL•3). The extracts were stirred with charcoal and then dried over Na₂SO₄. The crude reaction mixture contained about 5% unreacted phenanthroline as judged by 1H NMR spectroscopy. The crude material was purified by column chromatography on silica. Eluent: 0 → 80% ethyl acetate in DCM to afford the title compound as an off-white powder (180 mg, 10%).

¹H NMR (600 MHz, CDCl₃) δ 9.34 (dd, J = 4.3, 1.6 Hz, 1H), 8.82 (dd, J = 8.4, 1.6 Hz, 1H), 8.77 (d, J = 8.6 Hz, 1H), 7.84 (dd, J = 8.4, 4.3 Hz, 1H), 7.79 (d, J = 8.7 Hz, 1H).

¹³C NMR (151 MHz, CDCl₃) δ 152.8, 151.6, 145.5, 144.5, 140.1, 137.3, 129.1, 127.5, 125.8, 125.6, 125.0, 124.4.

HRMS (*m/z*): (ESI+) calc'd for $C_{12}H_6N_2Br_2Cl$ [M+H]⁺: 370.8581, found: 370.8580.

2-chloro-3,8-dimethyl-1,10-phenanthroline
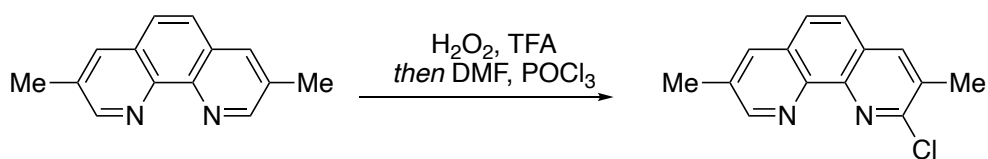
A 50 mL round bottom flask was charged with 3,8-dimethyl-1,10-phenanthroline (385 mg, 1.85 mmol, 1.00 equiv), trifluoroacetic acid (1.42 mL), and 30% hydrogen peroxide (283 µL). The mixture was heated at 65 ºC for 16 h. The solution was cooled to room temperature, and 2 M NaOH was added until the pH > 13. The mixture was extracted with DCM (10 mL •5). The combined organic layers were dried over MgSO$_4$ and filtered. Then DMF (1 mL) and POCl$_3$ (5 mL) were added. The mixture was stirred at room temperature for another 16 h. The mixture was poured into 40% NaOH solution, filtered through a bed of Celite, and extracted with chloroform (10 mL•3). The combined organic layers were dried over MgSO$_4$, filtered, and concentrated. The crude material was purified by column chromatography on silica. Eluent: 0 → 30% ethyl acetate in (1% NEt$_3$ and 10% DCM in hexanes) to afford the title compound as an off-white powder (243 mg, 54%).

^{1}H NMR (500 MHz, CDCl$_3$) δ 9.08 (d, J = 2.2 Hz, 1H), 8.09 (s, 1H), 8.05 (d, J = 1.2 Hz, 1H), 7.79 – 7.71 (m, 2H), 2.65 (s, 3H), 2.64 (s, 3H).

^{13}C NMR (126 MHz, CDCl$_3$) δ 152.5, 152.3, 144.5, 143.3, 138.2, 135.4, 133.0, 132.2, 128.5, 127.6, 126.7, 125.6, 20.3, 18.9.

HRMS (*m/z*): (ESI+) calc'd for C$_{14}$H$_{12}$N$_2$Cl [M+H]$^+$: 243.0684, found: 243.0682.

4.4.3 Determination of Gas Chromatography Response factors

In a 4 mL vial, known quantities (5-20 mg) of the aryl or alkyl boronic ester were mixed with known quantities (5-20 mg) of the adamantane internal standard. The mixture was dissolved in ethyl acetate, and an aliquot analyzed by GC-FID. The known mol ratios of the materials were plotted against the ratios of the integrated GC signals.
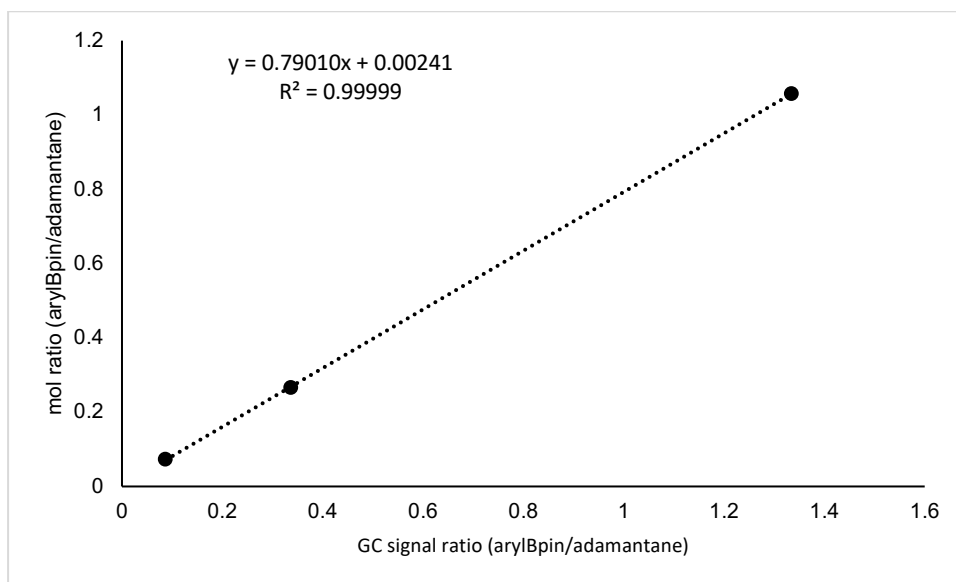

Figure 4.10. Determination of the response factor for (3-chloro-5-iodophenyl)-4,4,5,5-tetramethyl-1,3,2-dioxaborolane.
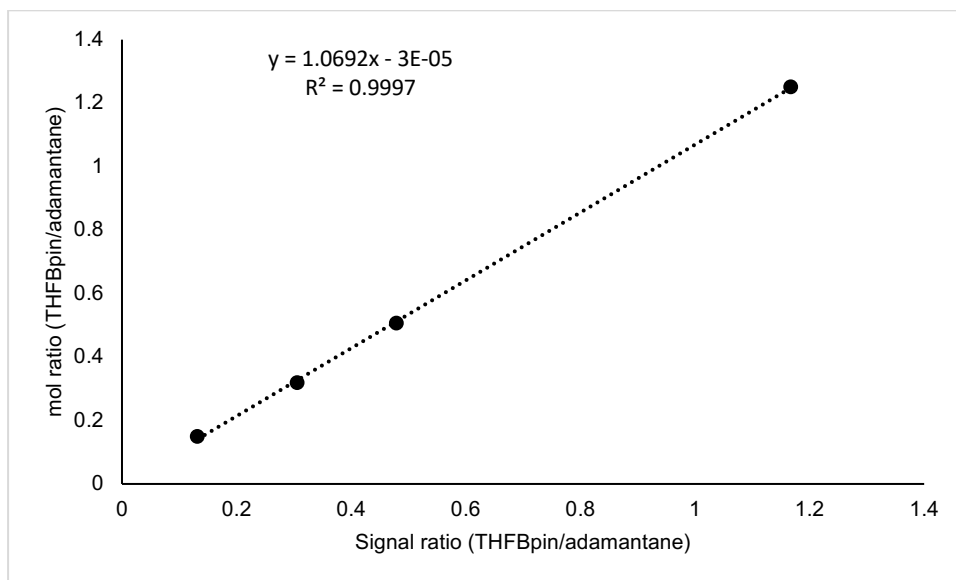

Figure 4.11. Determination of the response factor for 4,4,5,5-tetramethyl-2-(tetrahydrofuran-3-yl)-1,3,2-dioxaborolane.
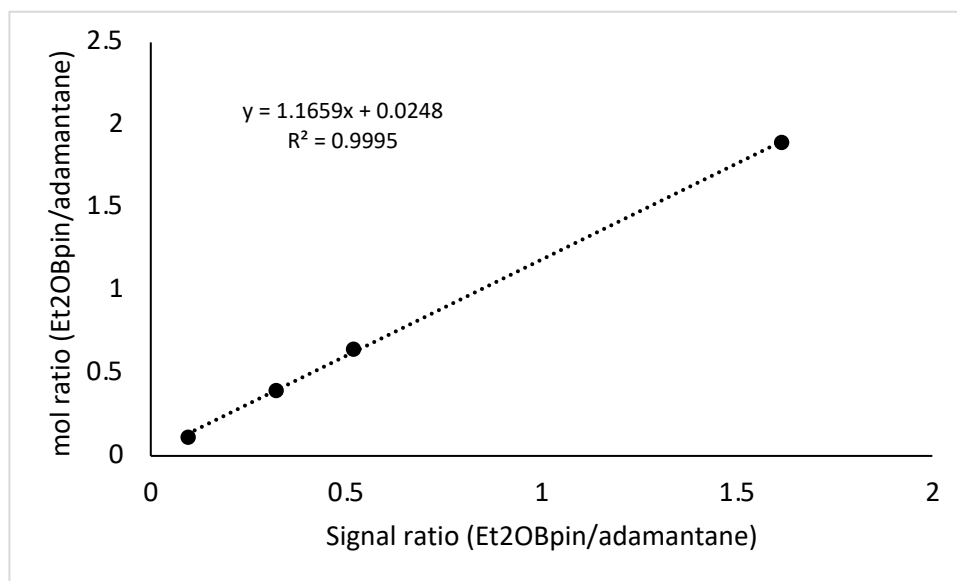
Figure 4.12. Determination of the response factor for 2-(2-ethoxyethyl)-4,4,5,5-tetramethyl-1,3,2-dioxaborolane.

4.4.4 Design and Evaluation of "Ironclad" Ligand

Evaluation of the effect of substitution.

In a nitrogen glovebox, a 4 mL vial was charged with ligand (0.010 mmol, 10 mol%), [Ir(cod)(OMe)]$_2$ (3.3 mg, 0.0050 mmol, 5.0 mol%), B$_2$pin$_2$ (76 mg, 0.30 mmol, 3.0 equiv), and *tert*-butyl octyl ether (19 mg, 0.10 mmol, 1.0 equiv). A stir bar and cyclooctane (100 µL) were added to the vial, the vial was capped with a Teflon-lined cap, and the vial was heated at 65 ºC in a preheated aluminum block. At the end of the reaction, the reaction mixture was diluted with CDCl$_3$, CH$_2$Br$_2$ (internal standard) was added, and the solution was analyzed by ^{1}H NMR spectroscopy to determine the yield of the borylated ether. We found that substitution at the 3-, 7-, and 9- positions lead to more than two-fold reduction in the yield of the borylated product, while substitution at the 5-, 6-, and 8- positions do not lead to such drastic reductions in the yield of the borylated product.
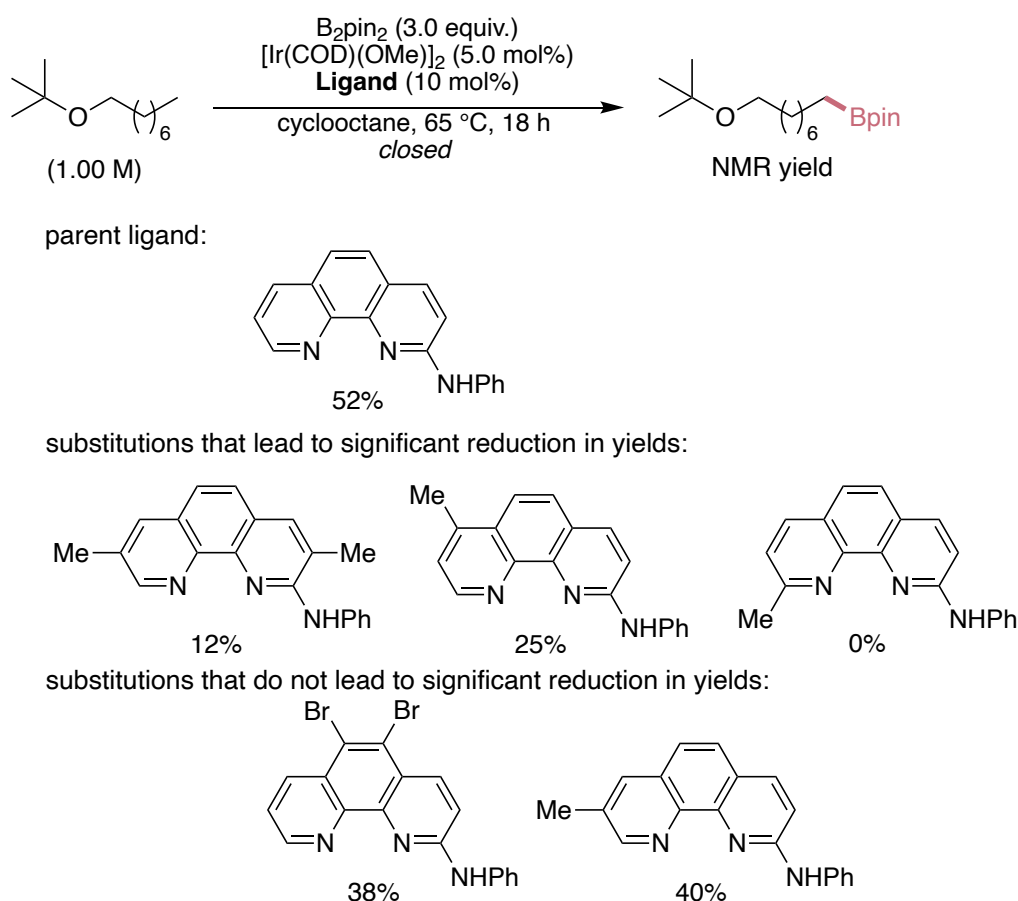

Figure 4.13 Evaluation of 2-aminophenanthrolines for the borylation of *tert*-butyl octyl ether.

Timecourses for the borylation of 1-chloro-3-iodobenzene.

In a nitrogen glovebox, a 4 mL vial was sequentially charged with ligand (5.00 μmol, 2.00 mol%), (MesH)Ir(Bpin)₃ (3.47 mg, 5.00 μmol, 2.00 mol%), adamantane (internal standard, 17.0 mg, 0.125 mmol, 0.5 equiv), B₂pin₂ (95.2 mg, 0.375 mmol, 1.50 equiv), and 1-chloro-3-iodobenzene (59.6 mg, 0.250 mmol, 1.00 equiv). A magnetic stir bar and cyclooctane (0.8 mL) were added to the vial, and the vial was tightly sealed with a Teflon-lined cap. The vial was removed from the glovebox and stirred at 50 ºC. At the various time points, the vial was removed from the heating block and brought into the glovebox. An aliquot of the solution was removed from the vial and analyzed by GC.
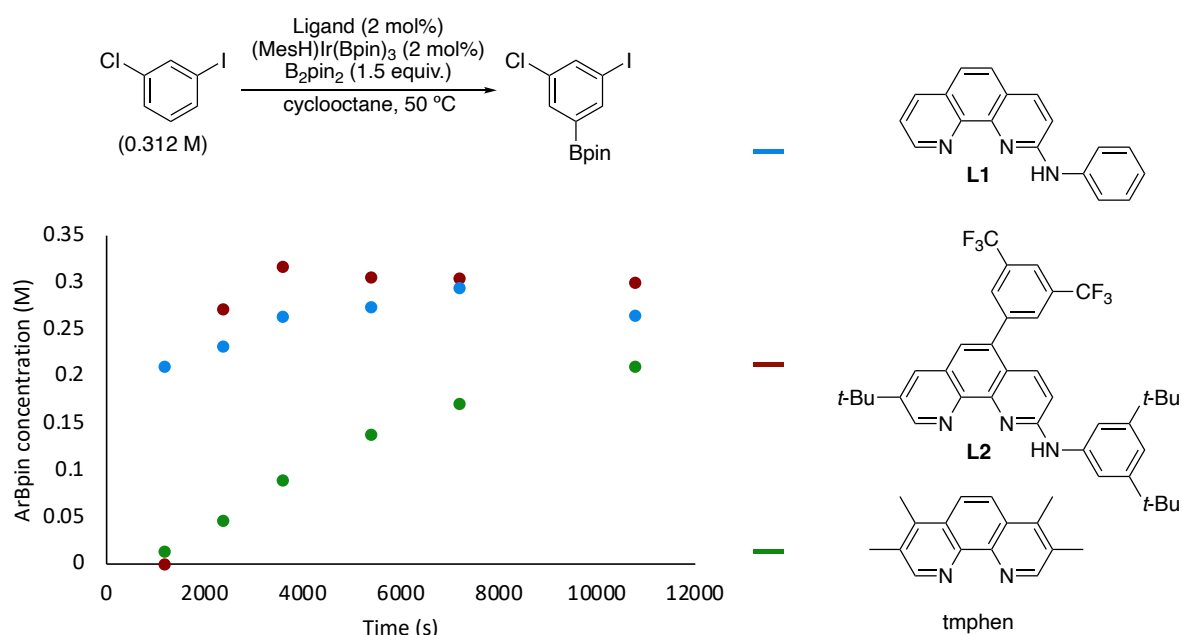

Figure 4.14. Timecourses of the borylation of 1-chloro-3-iodobenzene with parent *N*-phenyl-2-aminophenanthroline (L1, blue), designer 2-aminophenanthroline (L2, red), and tmphen (green).

Timecourses for the borylation of tetrahydrofuran.

In a nitrogen glovebox, a 4 mL vial was sequentially charged with ligand (12.5 μmol, 5.00 mol%), (MesH)Ir(Bpin)$_3$ (8.67 mg, 12.5 μmol, 5.00 mol%), adamantane (internal standard, 17.0 mg, 0.125 mmol, 0.5 equiv), B$_2$pin$_2$ (95.2 mg, 0.375 mmol, 1.50 equiv), and tetrahydrofuran (18.0 mg, 0.250 mmol, 1.00 equiv). A magnetic stir bar and cyclooctane (0.4 mL) were added to the vial, and the vial was tightly sealed with a Teflon-lined cap. The vial was removed from the glovebox and stirred at 65 °C. At the various time points, the vial was removed from the heating block and brought into the glovebox. An aliquot of the solution was removed from the vial and analyzed by GC.
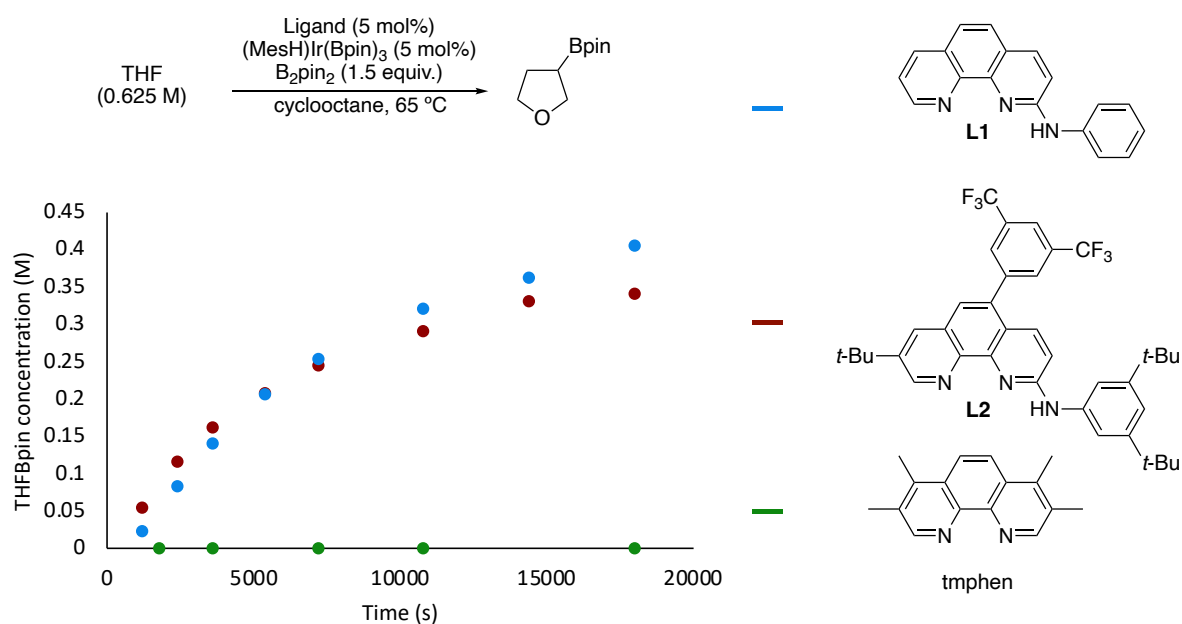
Figure 4.15. Timecourses of the borylation of tetrahydrofuran with parent *N*-phenyl-2-aminophenanthroline (L1, blue), designer 2-aminophenanthroline (L2, red), and tmphen (green).

4.4.5 NMR Spectroscopy Studies

Study of the species generated from L1 and (MesH)Ir(Bpin)₃ under catalytic conditions
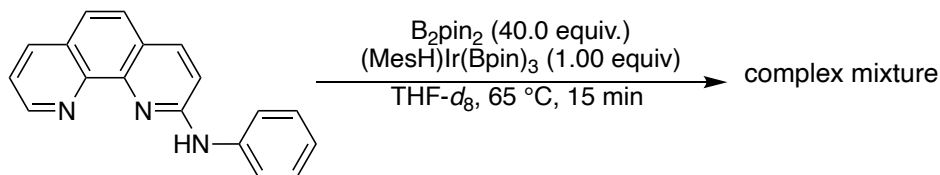
In a nitrogen glovebox, a 4 mL vial was sequentially charged with *N*-phenyl-1,10-phenanthrolin-2-amine (**L1**, 3.39 mg, 12.5 μmol, 1.00 equiv), (MesH)Ir(Bpin)₃ (8.67 mg, 12.5 μmol, 1.00 equiv), and B₂pin₂ (127 mg, 500 μmol, 40.0 equiv). A magnetic stirbar was added to the vial. THF-d_8 (0.5 mL) was introduced to the vial under vigorous stirring, and the vial was sealed with a Teflon cap. The vial was heated at 65 ºC for 15 min, and the solution was analyzed by ¹H NMR spectroscopy.
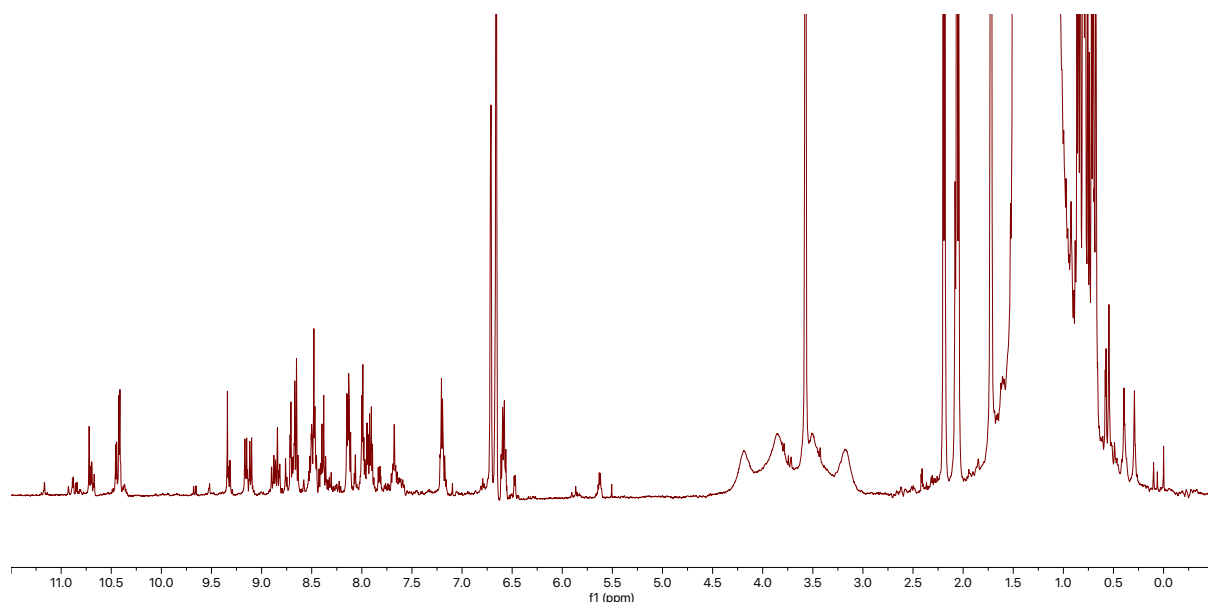
Figure 4.16. ¹H NMR spectrum of a catalytic reaction run with L1 and (MesH)Ir(Bpin)₃.

Study of the species generated from L2 and (MesH)Ir(Bpin)₃ under catalytic conditions
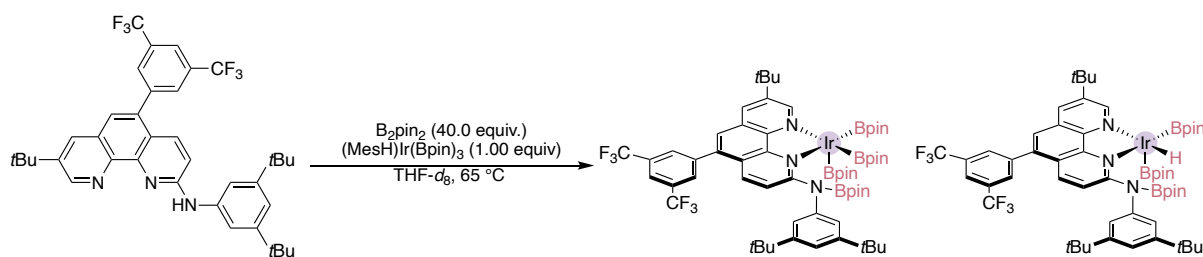
In a nitrogen glovebox, a 4 mL vial was sequentially charged with 5-(3,5-bis(trifluoromethyl)phenyl)-8-(*tert*-butyl)-*N*-(3,5-di-*tert*-butylphenyl)-1,10-phenanthrolin-2-amine (**L2**, 8.15 mg, 12.5 µmol, 1.00 equiv), (MesH)Ir(Bpin)₃ (8.67 mg, 12.5 µmol, 1.00 equiv) and B₂pin₂ (127 mg, 500 µmol, 40.0 equiv). A magnetic stirbar was added to the vial. THF-d_8 (0.5 mL) was introduced to the vial under vigorous stirring, and the contents of the vial were transferred to a J Young tube. ¹H NMR spectra were measured in an NMR spectrometer at 5 min intervals with the probe temperature held at 65 °C.
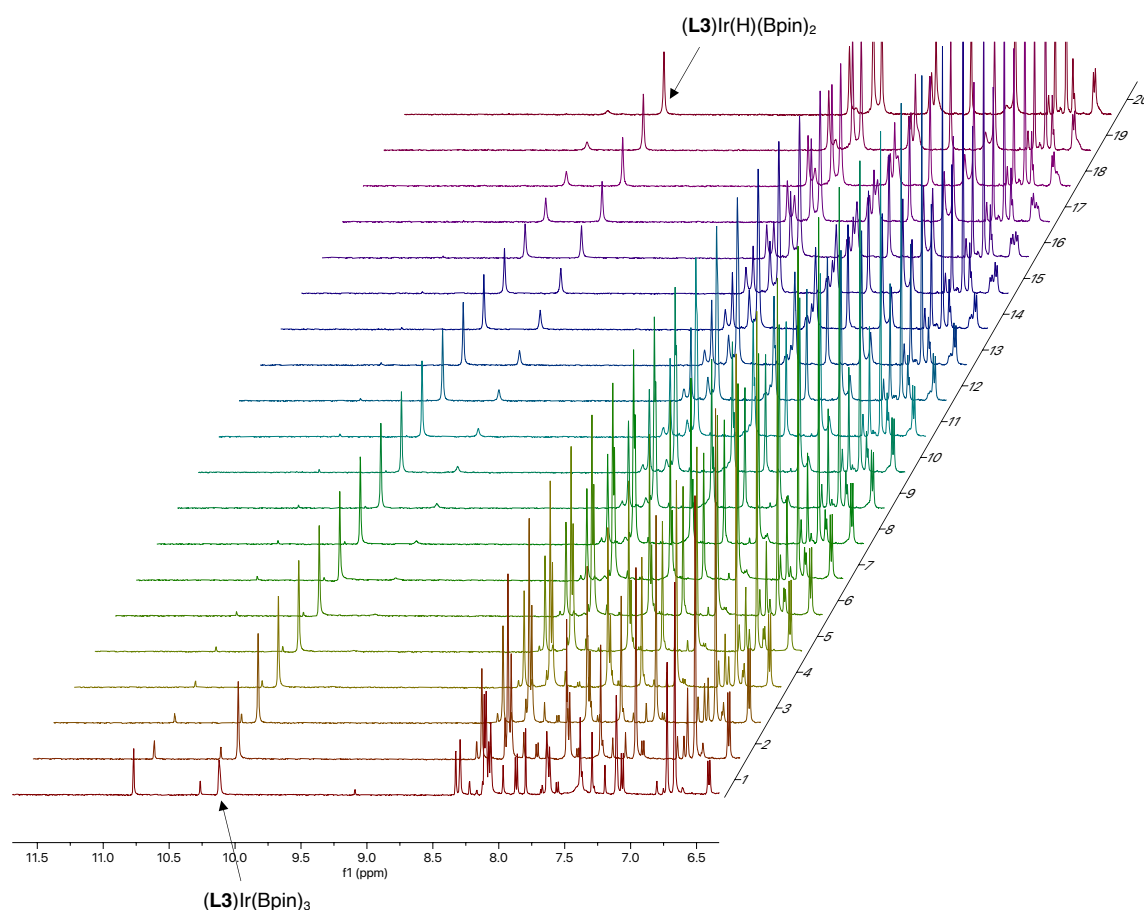
Figure 4.17. ¹H NMR spectra of a catalytic reaction run with L2 and (MesH)Ir(Bpin)₃.

Study of the species generated from L2 and [Ir(cod)(OMe)]₂ under catalytic conditions
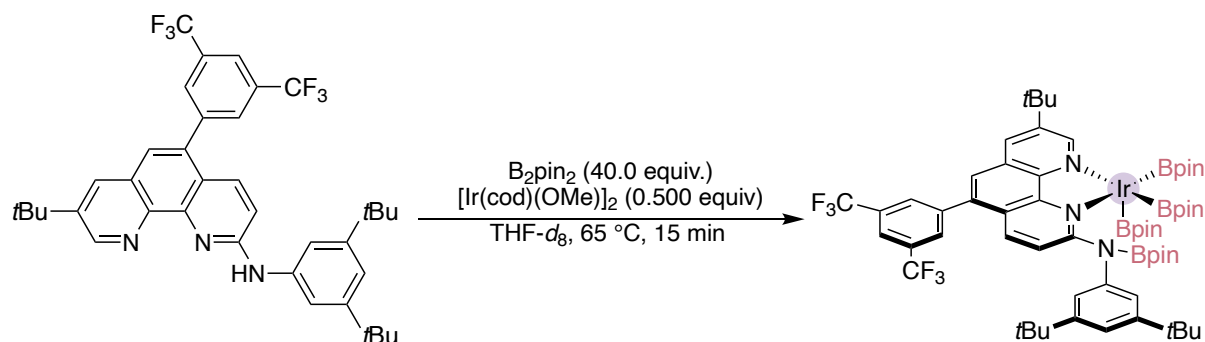
In a nitrogen glovebox, a 4 mL vial was sequentially charged with 5-(3,5-bis(trifluoromethyl)phenyl)-8-(*tert*-butyl)-*N*-(3,5-di-*tert*-butylphenyl)-1,10-phenanthrolin-2-amine (**L2**, 8.15 mg, 12.5 µmol, 1.00 equiv), [Ir(cod)(OMe)]₂ (4.14 mg, 6.25 µmol, 0.500 equiv), and B₂pin₂ (127 mg, 500 µmol, 40.0 equiv). A magnetic stirbar was added to the vial. THF-*d₈* (0.5 mL) was introduced to the vial under vigorous stirring, and the vial was sealed with a Teflon cap. The vial was heated at 65 ºC for 15 min, and the solution was analyzed by ¹H NMR spectroscopy. The aryl resonances of the spectrum match those observed in the spectrum obtained from the combination of **L2** and (MesH)Ir(Bpin)₃ (apart from mesitylene-derived resonances).

Figure 4.18. Comparison of ¹H NMR spectra of catalytic reactions run with L2 and either [Ir(cod)(OMe)]₂ (red trace) or (MesH)Ir(Bpin)₃ (blue trace).

Investigation of catalyst speciation via trapping by phosphite

In a nitrogen glovebox, a 4 mL vial was charged with 5-(3,5-bis(trifluoromethyl)phenyl)-8-(*tert*-butyl)-*N*-(3,5-di-*tert*-butylphenyl)-1,10-phenanthrolin-2-amine (**L2**, 32.6 mg, 50.0 µmol, 1.00 equiv), (MesH)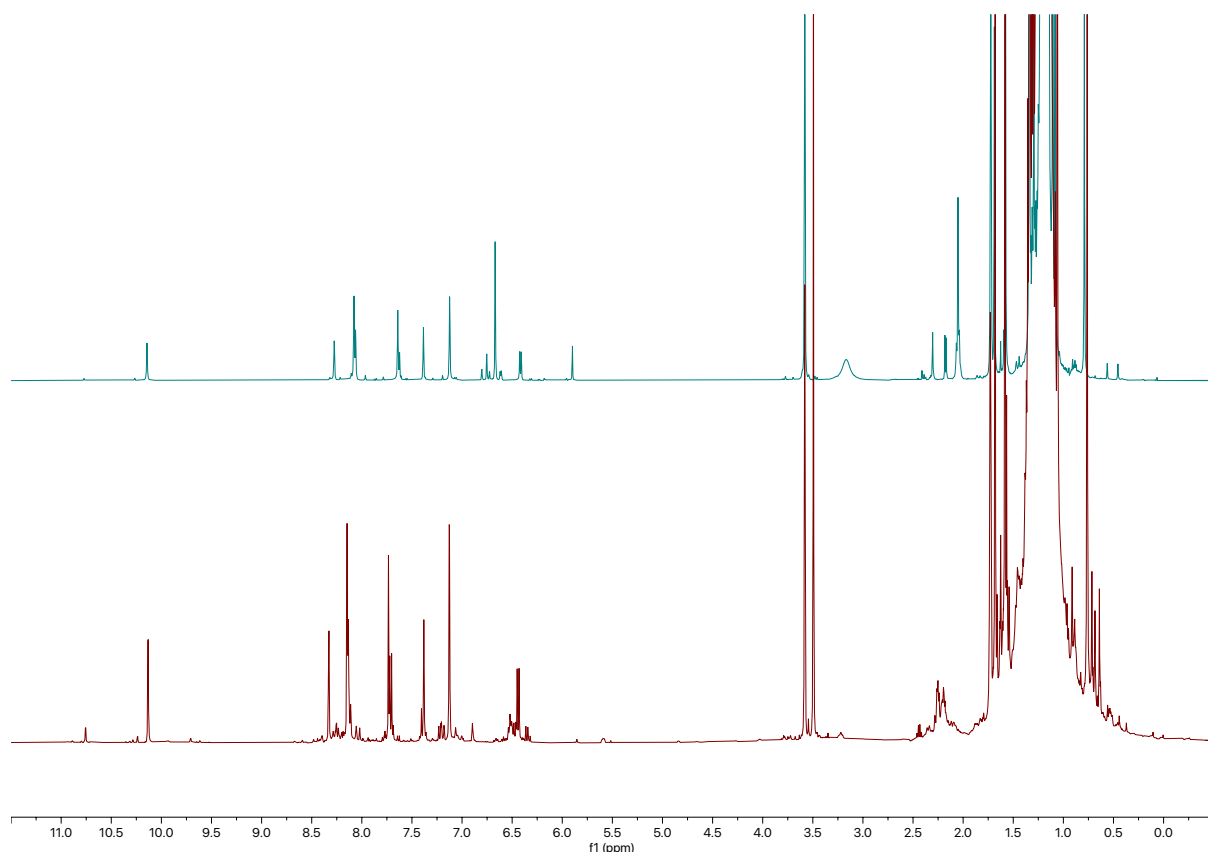Ir(Bpin)$_3$ (34.7 mg, 50.0 µmol, 1.00 equiv) and B$_2$pin$_2$ (12.7 mg, 50.0 µmol, 1.00 equiv). A magnetic stirbar and THF-d_8 (1 mL) were added, and vial was sealed with a Teflon-lined cap. The vial was brought out of the glovebox and heated in a preheated aluminum block at 65 ºC for 30 min. A 0.50 M stock solution of B$_2$pin$_2$ (solution A) was prepared by dissolving B$_2$pin$_2$ (635 mg, 2.50 mmol) in THF-d_8 in a 5 mL volumetric flask. A 0.50 M stock solution of Hpin (solution B) was prepared by dissolving HBpin (320 mg, 2.50 mmol) in THF-d_8 in a 5 mL volumetric flask. In a series of NMR tubes were added the solutions as follows: Tube 1: 45 µL A, 405 µL B; Tube 2: 90 µL A, 360 µL B; Tube 3: 135 µL A, 315 µL B; Tube 4: 180 µ A, 270 µL B; Tube 5: 225 µL A, 225 µL B; Tube 6: 270 µL A, 180 µL B; Tube 7: 315 µL A, 135 µL B; Tube 8: 360 µL A, 90 µL B, Tube 9: 405 µL A, 45 µL B. To each tube was added 50 µL of the iridium solution. The tubes were tightly capped and sealed with electrical tape, and the ^{1}H NMR spectra were observed. The resonances corresponding to the 9-positions of the bound ligands in (**L3**)Ir(Bpin)$_3$ and in (**L3**)Ir(H)(Bpin)$_2$ were integrated.
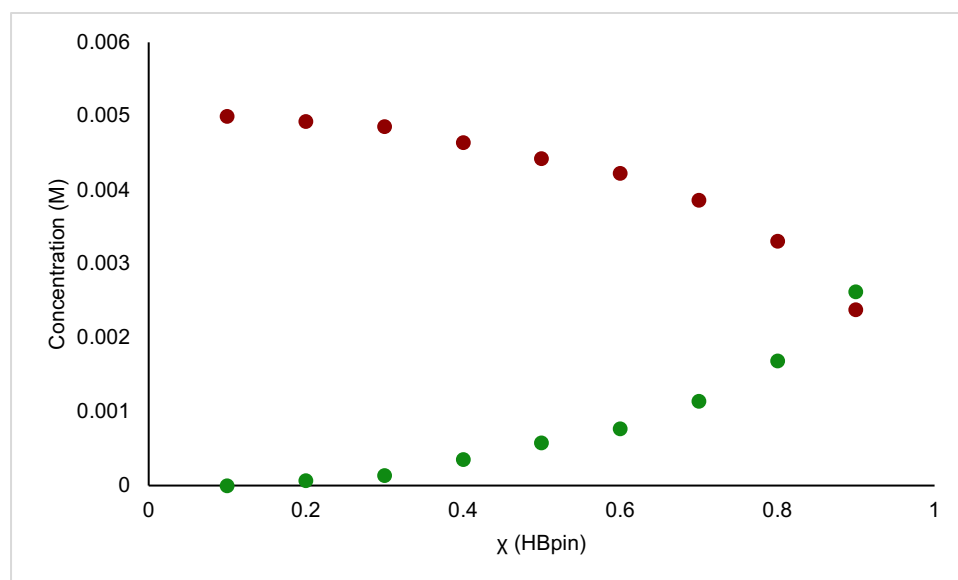
Figure 4.19. Dependence of catalyst speciation on B$_2$pin$_2$:HBpin molar ratio. Red: (**L3**)Ir(Bpin)$_3$, green: (**L3**)Ir(H)(Bpin)$_2$.
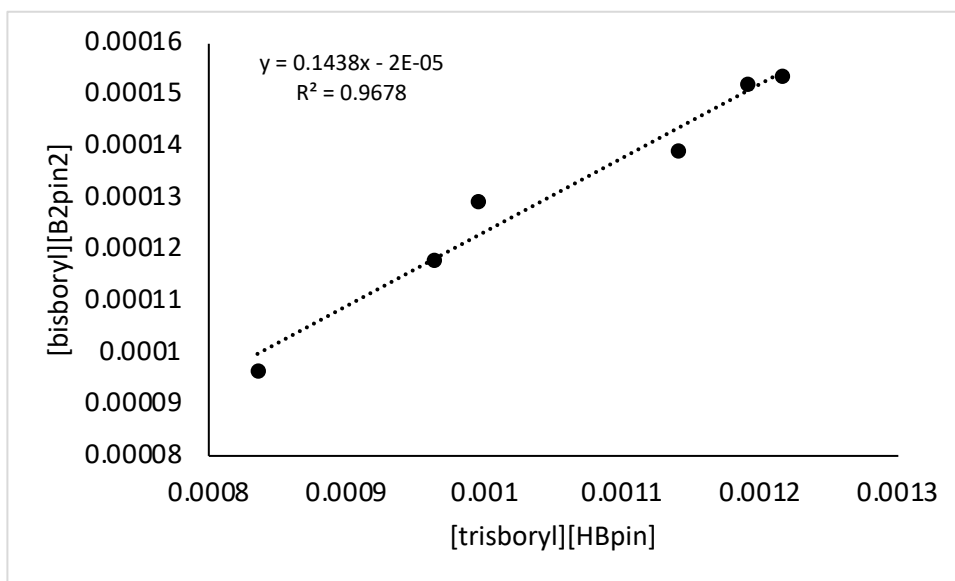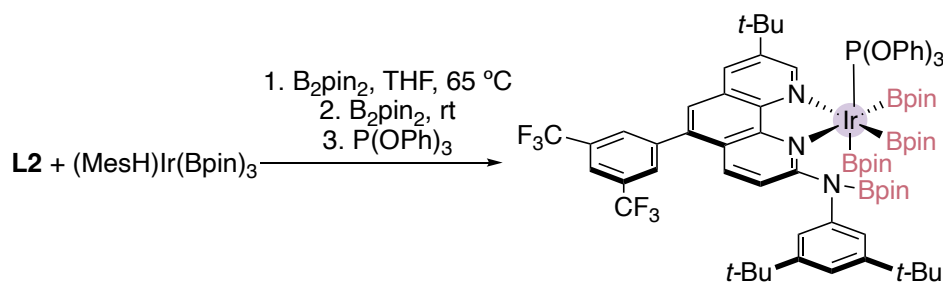
Figure 4.20. Fitting to obtain equilibrium constant. The first three points with large uncertainties in the integration of (**L3**)Ir(H)(Bpin)$_2$ were not included.

$$K = \frac{[\text{bisboryl}][\text{B}_2\text{pin}_2]}{[\text{trisboryl}][\text{HBpin}]} = 0.14 \pm 0.01$$

4.4.6 Independent Generation of Iridium Complexes

(L3)Ir(Bpin)₃(P(OPh)₃)

In a nitrogen glovebox, a 4 mL vial was sequentially charged with 5-(3,5-bis(trifluoromethyl)phenyl)-8-(*tert*-butyl)-*N*-(3,5-di-*tert*-butylphenyl)-1,10-phenanthrolin-2-amine (**L2**, 16.3 mg, 25.0 µmol, 1.00 equiv), (MesH)Ir(Bpin)₃ (17.3 mg, 25.0 µmol, 1.00 equiv) and B₂pin₂ (6.35 mg, 25.0 µmol, 1.00 equiv). THF-d_8 (0.5 mL) was introduced to the vial, the vial was sealed tightly with a Teflon-lined cap and brought out of the glovebox, and the vial was heated at 65 ºC in a preheated aluminum heating block for 10 min. The vial was cooled to room temperature and returned to the glovebox. To the vial was added B₂pin₂ (25.4 mg, 100 µmol, 4.00 equiv). The mixture was allowed to react for 5 min. P(OPh)₃ (7.76 mg, 25.0 µmol, 1.00 equiv) was then added. The solution was analyzed by NMR spectroscopy. The NMR spectra reported below contain resonances arising from impurities such as HBpin, borylated mesitylene, and B₂pin₃. Separation of the impurities from the desired complex was difficult due to the solubility of the material even in highly non-polar solvents such as pentane, hexamethyldisiloxane, and tetramethyl silane.

Crystals suitable for X-ray crystallography were prepared as follows: volatile materials were evaporated in vacuo, tetramethylsilane (1 mL) was added to the residue, and the mixture became slightly turbid. After allowing the solution to stand for 10 min, the solution was filtered through a PTFE filter (20 µm). The filtrate was stored at -40 ºC overnight to afford crystals suitable for X-ray crystallography.

¹H NMR (500 MHz, THF-d_8) δ 10.59 (s, 1H), 8.21 (s, 2H), 8.19 – 8.13 (m, 2H), 7.61 (d, *J* = 9.2 Hz, 1H), 7.58 (s, 1H), 7.40 (t, *J* = 1.9 Hz, 1H), 7.15 (t, *J* = 1.8 Hz, 1H), 7.04 (t, *J* = 1.8 Hz, 1H), 6.88 – 6.83 (m, 6H), 6.79 (d, *J* = 7.5 Hz, 6H), 6.73 (d, *J* = 7.0 Hz, 3H), 6.23 (d, *J* = 9.2 Hz, 1H), 2.22 (s, 3H), 1.93 (s, 3H), 1.61 (s, 9H), 1.38 (s, 9H), 1.35 (s, 6H), 1.32 (s, 6H), 1.30 (s, 9H), 1.21 (s, 6H), 1.20 (s, 6H), 1.05 (s, 3H), 0.62 (s, 6H), 0.56 (s, 3H), 0.51 (s, 6H).

¹³C NMR (as observed) (126 MHz, THF-d_8) δ 161.6, 161.6, 154.5, 153.1, 153.0, 151.9, 151.8, 147.1, 146.9, 146.2, 144.4, 141.8, 138.6, 138.2, 137.2, 136.9, 136.6, 135.4, 132.2, 132.0, 131.7, 131.6, 131.4, 130.2, 129.6, 129.4, 129.0, 128.5, 128.3, 126.8, 126.7, 126.2, 126.1, 124.8, 124.0, 123.3, 122.6, 122.5, 120.9, 120.9, 120.0, 119.5, 109.7, 83.0, 82.9, 82.9, 82.8, 82.5, 82.5, 81.5, 81.1, 81.0, 80.4, 80.1, 79.4, 79.4, 79.0, 34.8, 34.7, 34.5, 31.2, 31.1, 30.8, 25.7, 25.0, 24.8, 22.9, 22.6, 22.2, 22.0, 21.5, 20.6, 20.5.

¹¹B NMR (160 MHz, THF-d_8) δ 32.9, 30.7, 28.0.

¹⁹F NMR (471 MHz, THF-d_8) δ -63.4.

³¹P NMR (202 MHz, THF-*d*₈) δ 100.5.

(L3)Ir(H)(Bpin)₂(P(OPh)₃)

In a nitrogen glovebox, a 4 mL vial was sequentially charged with 5-(3,5-bis(trifluoromethyl)phenyl)-8-(*tert*-butyl)-*N*-(3,5-di-*tert*-butylphenyl)-1,10-phenanthrolin-2-amine (**L2**, 16.3 mg, 25.0 µmol, 1.00 equiv), (MesH)Ir(Bpin)₃ (17.3 mg, 25.0 µmol, 1.00 equiv) and B₂pin₂ (6.35 mg, 25.0 µmol, 1.00 equiv). THF-d_8 (0.5 mL) was introduced to the vial, the vial was sealed tightly with a Teflon-lined cap and brought out of the glovebox, and the vial was heated at 65 ºC in a preheated aluminum heating block for 10 min. The vial was cooled to room temperature and returned to the glovebox. P(OPh)₃ (7.76 mg, 25.0 µmol, 1.00 equiv) was then added. The solution was analyzed by NMR spectroscopy. The NMR spectra reported below contain resonances arising from impurities such as HBpin, borylated mesitylene, and B₂pin₃. Separation of the impurities from the desired complex was difficult due to the solubility of the material even in highly non-polar solvents such as pentane, hexamethyldisiloxane, and tetramethyl silane.

¹H NMR (600 MHz, THF-d_8) δ 9.29 (s, 1H), 8.37 (s, 2H), 8.33 (d, *J* = 9.5 Hz, 2H), 7.84 (d, *J* = 9.1 Hz, 1H), 7.68 (s, 1H), 7.59 (s, 1H), 7.40 (s, 1H), 7.21 (s, 1H), 7.18 (d, *J* = 7.6 Hz, 6H), 7.15 – 7.09 (m, 6H), 6.95 (t, *J* = 7.3 Hz, 3H), 6.68 (d, *J* = 9.1 Hz, 1H), 1.96 (s, 3H), 1.74 (s, 3H), 1.68 (s, 9H), 1.53 (s, 9H), 1.46 (s, 12H), 1.34 (s, 9H), 1.09 (s, 3H), 0.91 (s, 3H), 0.68 (s, 6H), 0.63 (s, 6H), -13.24 (d, *J* = 25.3 Hz, 1H).

¹³C NMR (as observed) (151 MHz, THF-d_8) δ 161.8, 153.3, 152.8, 152.8, 152.0, 151.8, 147.5, 147.1, 147.0, 143.3, 141.7, 138.5, 137.2, 136.9, 135.9, 132.2, 132.0, 131.8, 131.6, 131.2, 130.0, 129.7, 129.4, 128.5, 128.0, 126.8, 126.7, 126.1, 124.6, 123.3, 123.2, 122.6, 122.1, 121.7, 120.6, 120.6, 120.0, 120.0, 109.4, 82.9, 82.9, 81.5, 81.1, 79.8, 79.5, 79.3, 79.3, 34.7, 34.7, 34.0, 31.1, 31.0, 30.6, 23.3, 23.1, 22.4, 22.2, 22.2, 20.5, 20.4.

¹¹B NMR (193 MHz, THF-d_8) δ 33.8, 33.3, 28.2.

¹⁹F NMR (565 MHz, THF-d_8) δ -63.4.

³¹P NMR (243 MHz, THF-d_8) δ 106.4.
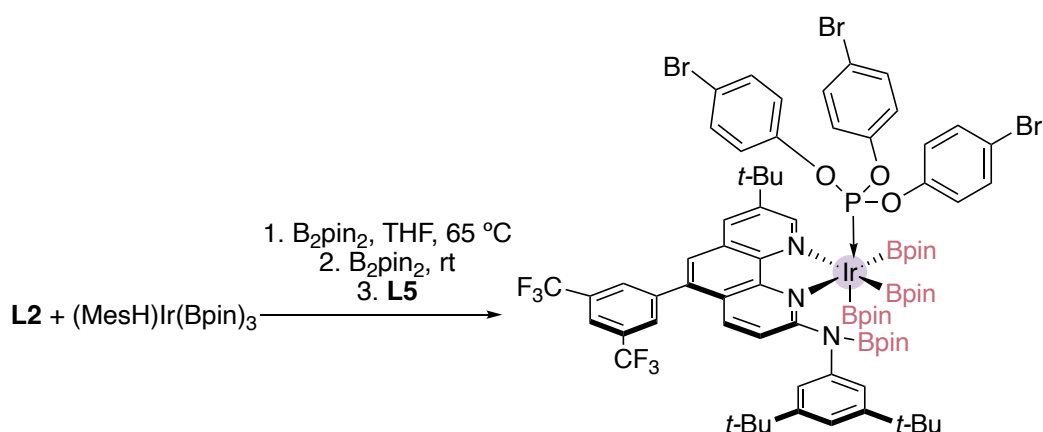
(L3)Ir(Bpin)₃(L5)

In a nitrogen glovebox, a 20 mL vial was sequentially charged with 5-(3,5-bis(trifluoromethyl)phenyl)-8-(*tert*-butyl)-*N*-(3,5-di-*tert*-butylphenyl)-1,10-phenanthrolin-2-amine (**L2**, 97.8 mg, 150 µmol, 1.00 equiv), (MesH)Ir(Bpin)₃ (104 mg, 150 µmol, 1.00 equiv) and B₂pin₂ (38.1 mg, 150 µmol, 1.00 equiv). THF-*d*₈ (5 mL) was introduced to the vial, the vial was sealed tightly with a Teflon-lined cap and brought out of the glovebox, and the vial was heated at 65 °C in a preheated aluminum heating block for 10 min. The vial was cooled to room temperature and returned to the glovebox. To the vial was added B₂pin₂ (152 mg, 600 µmol, 4.00 equiv). The mixture was allowed to react for 5 min. Tri(4-bromophenyl)phosphite (82.0 mg, 150 µmol, 1.00 equiv) was then added. Volatile materials were evaporated in vacuo, then tetramethylsilane (4 mL) was added to the residue, and the mixture became slightly turbid. After allowing the solution to stand for 10 min, the solution was filtered through a PTFE filter (20 µm).

4.4.7 Kinetic Studies

Reaction Orders by the Method of Initial Rates

Order in the THF substrate

In a nitrogen glovebox, adamantane (272 mg, 2.00 mmol) was dissolved in dry DCM in a 10 mL volumetric flask (0.20 M). B_2pin_2 (762 mg, 3.00 mmol) was dissolved in dry DCM in a 5.0 mL volumetric flask (0.60 M). 5-(3,5-bis(trifluoromethyl)phenyl)-8-(tert-butyl)-N-(3,5-di-tert-butylphenyl)-1,10-phenanthrolin-2-amine (**L2**) (130 mg, 200 µmol) was dissolved in dry DCM in a 2.0 mL volumetric flask (0.10 M). The resulting solutions were dispensed into four 1-dram vials equipped with flea stir bars, (312 µL of the adamantane solution, 62.5 µmol; 312.5 µL of the B_2pin_2 solution, 188 µmol; 62.5 µL of the ligand solution, 6.25 µmol). All volatile materials were carefully evaporated from the four 1-dram vials in vacuo.

(MesH)Ir(Bpin)$_3$ (139 mg, 200 µmol) was dissolved in dry cyclooctane in a 2.0 mL volumetric flask (0.10 M) and 62.5 µL of the resulting solution was added to each vial (6.25 µmol). THF (324 µL, 4.00 mmol) was dissolved in dry cyclooctane in a 5.0 mL volumetric flask (0.80 M), and the resulting solution dispensed to the vials as follows: (vial A: 78.1 µL (62.5 µmol); vial B: 156 µL (125 µmol); vial C: 234 µL (188 µmol); vial D: 312 µL (250 µmol). Dry cyclooctane was then added to make the total volume of the solutions in each vial 400 µL, the vials were tightly sealed with Teflon-lined caps, and the vials were removed from the glovebox. The vials were heated in an aluminum heating block at 65 ºC. At the appropriate timepoints, the vials were removed from the heating block, brought into the glovebox, and an aliquot removed for analysis by gas chromatography. The concentration of product 4,4,5,5-tetramethyl-2-(tetrahydrofuran-3-yl)-1,3,2-dioxaborolane was measured and plotted versus time to obtain the initial rates of the formation of 4,4,5,5-tetramethyl-2-(tetrahydrofuran-3-yl)-1,3,2-dioxaborolane.

Table 4.1. Initial concentrations of [THF], [catalyst], and [B_2pin_2] (varying [THF]), and the corresponding initial rates of formation of 4,4,5,5-tetramethyl-2-(tetrahydrofuran-3-yl)-1,3,2-dioxaborolane.

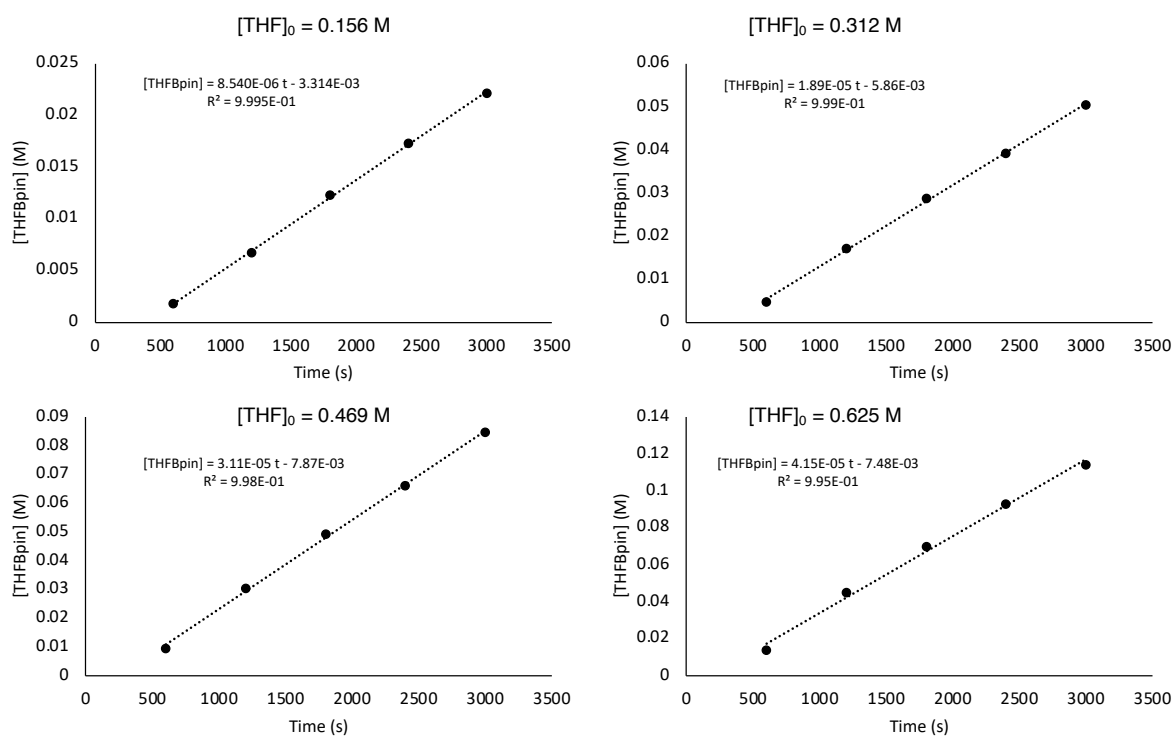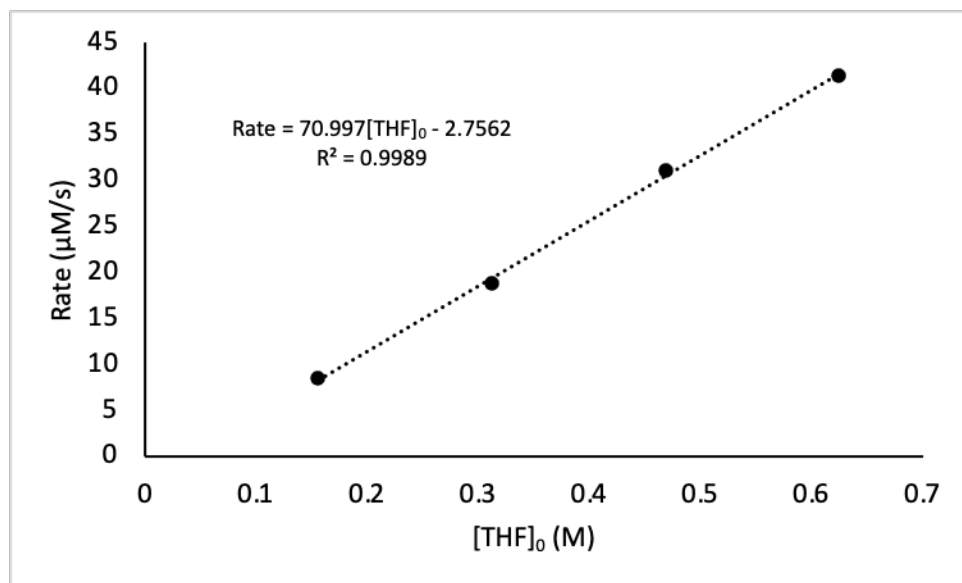| [THF] (M)	[catalyst] (mM)	[B_2pin_2] (M)	Initial Rate of Formation of THFBpin (μM.s^{-1})
0.156	15.6	0.469	8.54 ± 0.11
0.312	15.6	0.469	18.9 ± 0.3
0.469	15.6	0.469	31.1 ± 0.7
0.625	15.6	0.469	41.5 ± 1.7

Figure 4.21. Formation of borylated product THF *vs* time varying initial concentration of THF.

Order in B_2pin_2

In a nitrogen glovebox, adamantane (272 mg, 2.00 mmol) was dissolved in dry DCM in a 10 mL volumetric flask (0.20 M). 5-(3,5-bis(trifluoromethyl)phenyl)-8-(tert-butyl)-*N*-(3,5-di-tert-butylphenyl)-1,10-phenanthrolin-2-amine (**L2**) (130 mg, 200 µmol) was dissolved in dry DCM in a 2.0 mL volumetric flask (0.10 M). The resulting solutions were dispensed into four 1-dram vials equipped with flea stir bars, (312 µL of the adamantane solution, 62.5 µmol; 62.5 µL of the ligand solution, 6.25 µmol). B_2pin_2 (762 mg, 3.00 mmol) was dissolved in dry DCM in a 5.0 mL volumetric flask (0.60 M). The resulting solution was dispensed into the vials as follows: (vial A: 156 µL (93.6 µmol); vial B: 312 µL (187 µmol); vial C: 469 µL (281 µmol); vial D: 625 µL (375 µmol). All volatile materials were carefully evaporated from the four 1-dram vials in vacuo.

(MesH)Ir(Bpin)$_3$ (139 mg, 200 µmol) was dissolved in dry cyclooctane in a 2.0 mL volumetric flask (0.10 M) and 62.5 µL of the resulting solution was added to each vial (6.25 µmol). THF (324 µL, 4.00 mmol) was dissolved in dry cyclooctane in a 5.0 mL volumetric flask (0.80 M), and 156 µL of the resulting solution was dispensed to the vials (125 µmol). Dry cyclooctane was then added to make the total volume of the solutions in each vial 400 µL, the vials tightly sealed with Teflon-lined caps, and the vials removed from the glovebox. The vials were heated in an aluminum heating block at 65 ºC. At the appropriate timepoints, the vials were removed from the heating block, brought into the glovebox, and an aliquot removed for analysis by gas chromatography. The concentration of product 4,4,5,5-tetramethyl-2-(tetrahydrofuran-3-yl)-1,3,2-dioxaborolane was measured and plotted versus time to obtain the initial rates of the formation of 4,4,5,5-tetramethyl-2-(tetrahydrofuran-3-yl)-1,3,2-dioxaborolane.

Table 4.2. Initial concentrations of [THF], [catalyst], and [B_2pin_2] (varying [B_2pin_2]), and the corresponding initial rates of formation of 4,4,5,5-tetramethyl-2-(tetrahydrofuran-3-yl)-1,3,2-dioxaborolane.

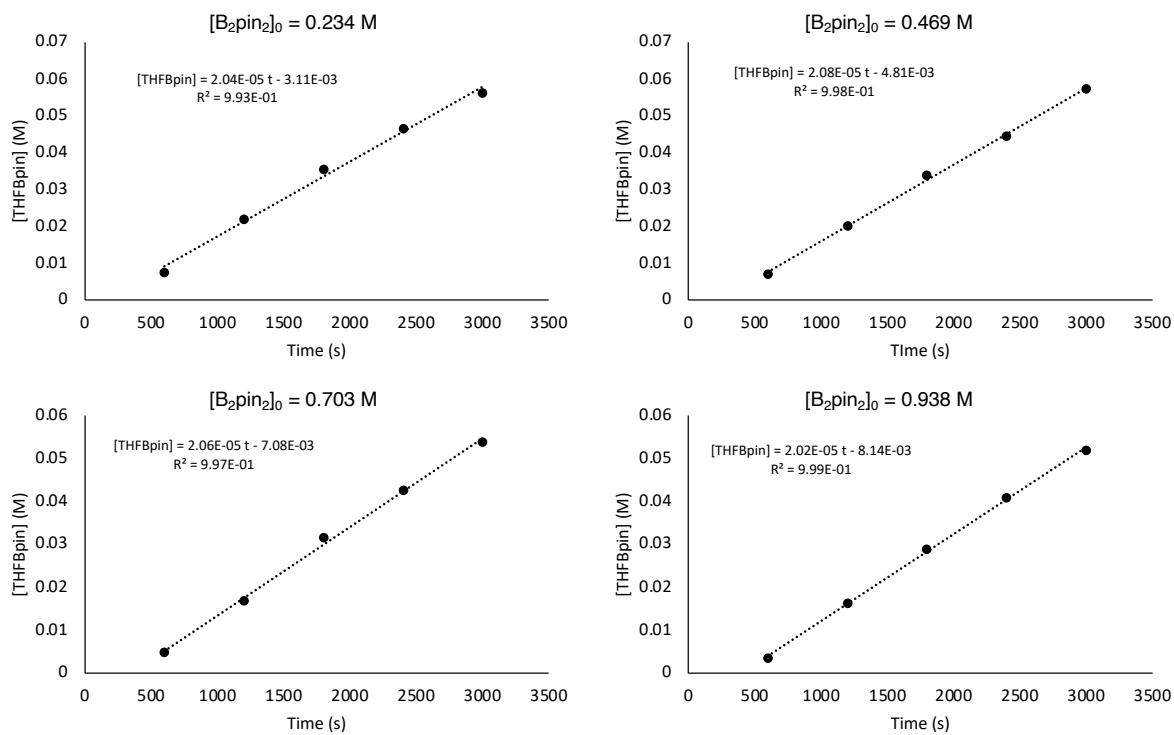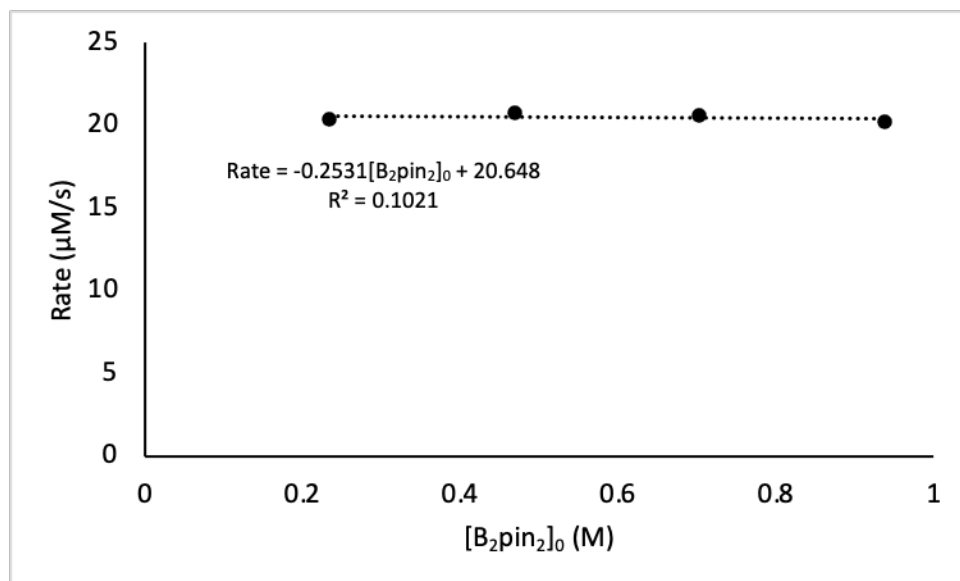| [THF] (M)	[catalyst] (mM)	[B_2pin_2] (M)	Initial Rate of Formation of THFBpin ($\mu M.s^{-1}$)
0.312	15.6	0.234	20.4 ± 1.0
0.312	15.6	0.469	20.8 ± 0.5
0.312	15.6	0.703	20.6 ± 0.6
0.312	15.6	0.938	20.2 ± 0.3

Figure 4.22. Formation of borylated product THF *vs* time varying initial concentration of diboron reagent.

Order in Catalyst, no Saturation in HBpin

In a nitrogen glovebox, adamantane (272 mg, 2.00 mmol) was dissolved in dry DCM in a 10 mL volumetric flask (0.20 M). B_2pin_2 (762 mg, 3.00 mmol) was dissolved in dry DCM in a 5.0 mL volumetric flask (0.60 M). The resulting solutions were dispensed into seven 1-dram vials equipped with flea stir bars, (312 µL of the adamantane solution, 62.5 µmol; 312.5 µL of the B_2pin_2 solution, 188 µmol). 5-(3,5-bis(trifluoromethyl)phenyl)-8-(tert-butyl)-*N*-(3,5-di-tert-butylphenyl)-1,10-phenanthrolin-2-amine (**L2**) (130 mg, 200 µmol) was dissolved in dry DCM in a 2.0 mL volumetric flask (0.10 M). The resultant solution was dispensed as follows: (vial A: 7.81 µL (0.781 µmol); vial B: 17.6 µL (1.76 µmol); vial C: 31.2 µL (3.12 µmol); vial D: 48.8 µL (4.88 µmol); vial E: 70.3 µL (7.03 µmol); vial F: 95.7 µL (9.57 µmol); vial G 125 µL (12.5 µmol). All volatile materials were carefully evaporated from the seven 1-dram vials in vacuo.

(MesH)Ir(Bpin)$_3$ (139 mg, 200 µmol) was dissolved in dry cyclooctane in a 2.0 mL volumetric flask (0.10 M), and the resulting solution was dispensed as follows: (vial A: 7.81 µL (0.781 µmol); vial B: 17.6 µL (1.76 µmol); vial C: 31.2 µL (3.12 µmol); vial D: 48.8 µL (4.88 µmol); vial E: 70.3 µL (7.03 µmol); vial F: 95.7 µL (9.57 µmol); vial G 125 µL (12.5 µmol).

THF (324 µL, 4.00 mmol) was dissolved in dry cyclooctane in a 5.0 mL volumetric flask (0.80 M), and 156 µL of the resulting solution was dispensed to the vials (125 µmol). Dry cyclooctane was then added to make the total volume of the solutions in each vial 400 µL, the vials tightly sealed with Teflon-lined caps, and the vials removed from the glovebox. The vials were heated in an aluminum heating block at 65 ºC. At the appropriate timepoints, the vials were removed from the heating block, brought into the glovebox, and an aliquot removed for analysis by gas chromatography. The concentration of product 4,4,5,5-tetramethyl-2-(tetrahydrofuran-3-yl)-1,3,2-dioxaborolane was measured and plotted versus time to obtain the initial rates of the formation of 4,4,5,5-tetramethyl-2-(tetrahydrofuran-3-yl)-1,3,2-dioxaborolane.

Table 4.3. Initial concentrations of [THF], [catalyst], and [B_2pin_2] (varying [cat]), and the corresponding initial rates of formation of 4,4,5,5-tetramethyl-2-(tetrahydrofuran-3-yl)-1,3,2-dioxaborolane.

[THF] (M)	[catalyst] (mM)	[B_2pin_2] (M)	Initial Rate of Formation of THFBpin ($\mu M.s^{-1}$)
0.312	1.95	0.469	5.55 ± 0.42
0.312	4.39	0.469	13.1 ± 0.6
0.312	7.81	0.469	16.4 ± 0.6
0.312	12.2	0.469	17.4 ± 0.4
0.312	17.6	0.469	21.8 ± 1.1

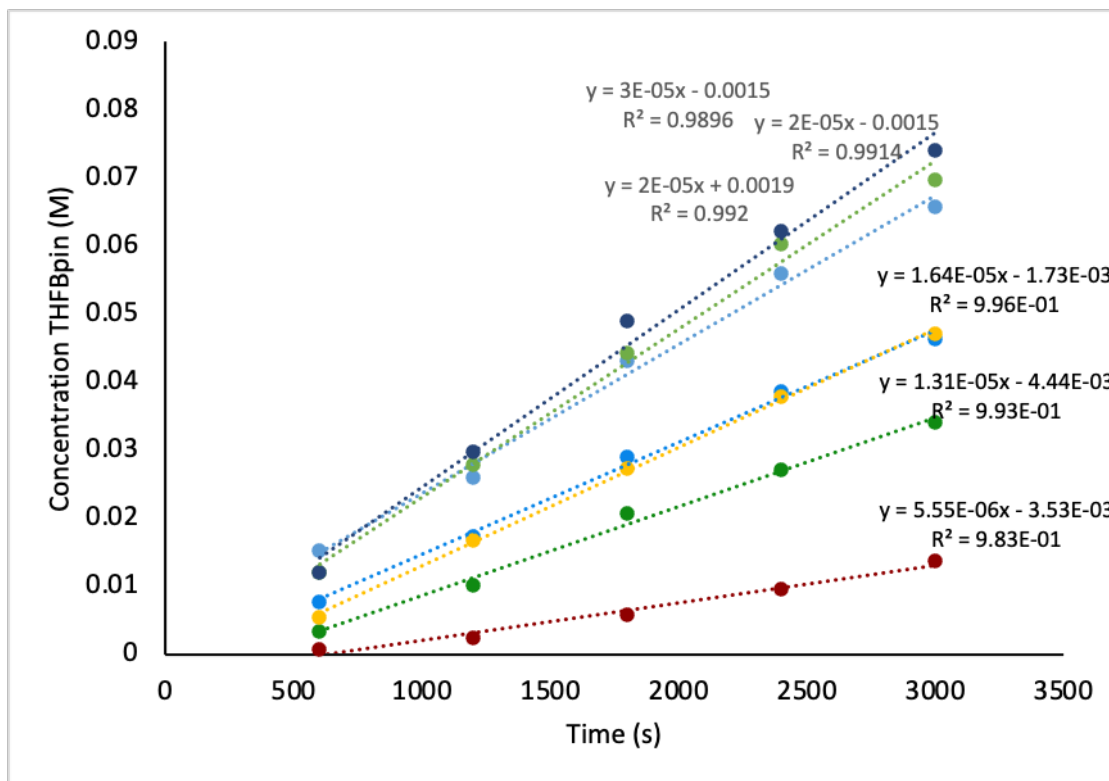| 0.312 | 23.9 | 0.469 | 24.7 ± 1.3 |
| 0.312 | 31.2 | 0.469 | 26.0 ± 1.5 |

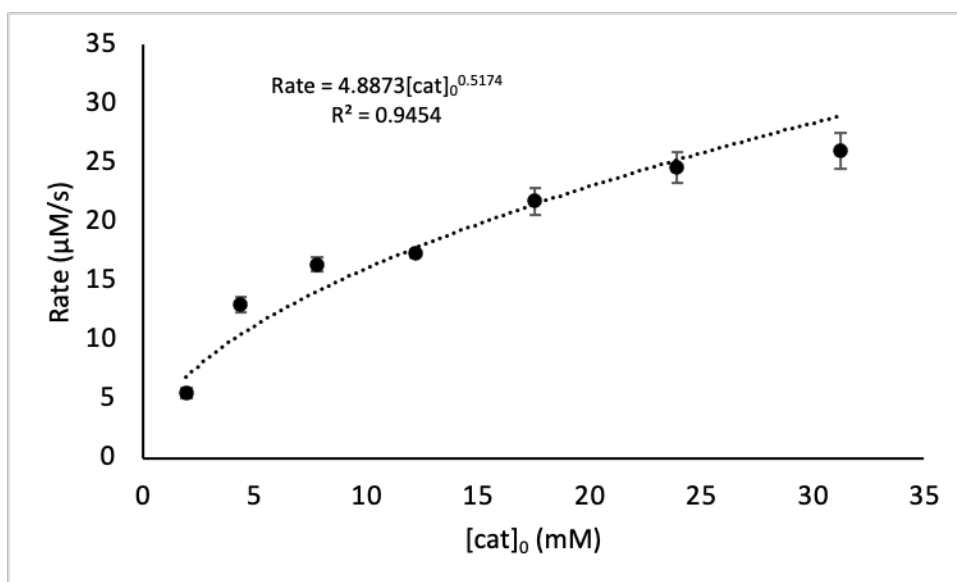**Figure 4.23.** Formation of borylated product THF *vs* time varying initial concentration of catalyst.

Figure 4.24. Rate of reaction vs concentration of catalyst. Fitting with a power law indicates an approximate half-order in catalyst.

Order in Catalyst, Saturation in HBpin

In a nitrogen glovebox, adamantane (272 mg, 2.00 mmol) was dissolved in dry DCM in a 10 mL volumetric flask (0.20 M). B_2pin_2 (762 mg, 3.00 mmol) was dissolved in dry DCM in a 5.0 mL volumetric flask (0.60 M). The resulting solutions were dispensed into four 1-dram vials equipped with flea stir bars, (312 µL of the adamantane solution, 62.5 µmol; 312.5 µL of the B_2pin_2 solution, 188 µmol). 5-(3,5-bis(trifluoromethyl)phenyl)-8-(tert-butyl)-*N*-(3,5-di-tert-butylphenyl)-1,10-phenanthrolin-2-amine (**L2**) (130 mg, 200 µmol) was dissolved in dry DCM in a 2.0 mL volumetric flask (0.10 M). The resultant solution was dispensed as follows: (vial A: 31.2 µL (3.12 µmol); vial B: 62.5 µL (6.25 µmol); vial C: 93.8 µL (9.38 µmol); vial D: 125 µL (12.5 µmol). All volatile materials were carefully evaporated from the four 1-dram vials in vacuo.

(MesH)Ir(Bpin)$_3$ (139 mg, 200 µmol) was dissolved in dry cyclooctane in a 2.0 mL volumetric flask (0.10 M), and the resulting solution was dispensed as follows: (vial A: 31.2 µL (3.12 µmol); vial B: 62.5 µL (6.25 µmol); vial C: 93.8 µL (9.38 µmol); vial D: 125 µL (12.5 µmol).

THF (324 µL, 4.00 mmol) was dissolved in dry cyclooctane in a 5.0 mL volumetric flask (0.80 M), and 156 µL of the resulting solution was dispensed to the vials (125 µmol). HBpin (512 mg, 4.00 mmol) was dissolved in dry cyclooctane in a 2.0 mL volumetric flask (2.0 M) and 93.8 µL of the resulting solution was dispensed to the vials (188 µmol, equimolar to the B_2pin_2). Dry cyclooctane was then added to make the total volume of the solutions in each vial 400 µL, the vials tightly sealed with Teflon-lined caps, and the vials removed from the glovebox. The vials were heated in an aluminum heating block at 65 ºC. At the appropriate timepoints, the vials were removed from the heating block, brought into the glovebox, and an aliquot removed for analysis by gas chromatography. The concentration of product 4,4,5,5-tetramethyl-2-(tetrahydrofuran-3-yl)-1,3,2-dioxaborolane was measured and plotted versus time to obtain the initial rates of the formation of 4,4,5,5-tetramethyl-2-(tetrahydrofuran-3-yl)-1,3,2-dioxaborolane.

Table 4.4. Initial concentrations of [THF], [catalyst], and [B_2pin_2] (varying [cat]), and the corresponding initial rates of formation of 4,4,5,5-tetramethyl-2-(tetrahydrofuran-3-yl)-1,3,2-dioxaborolane.

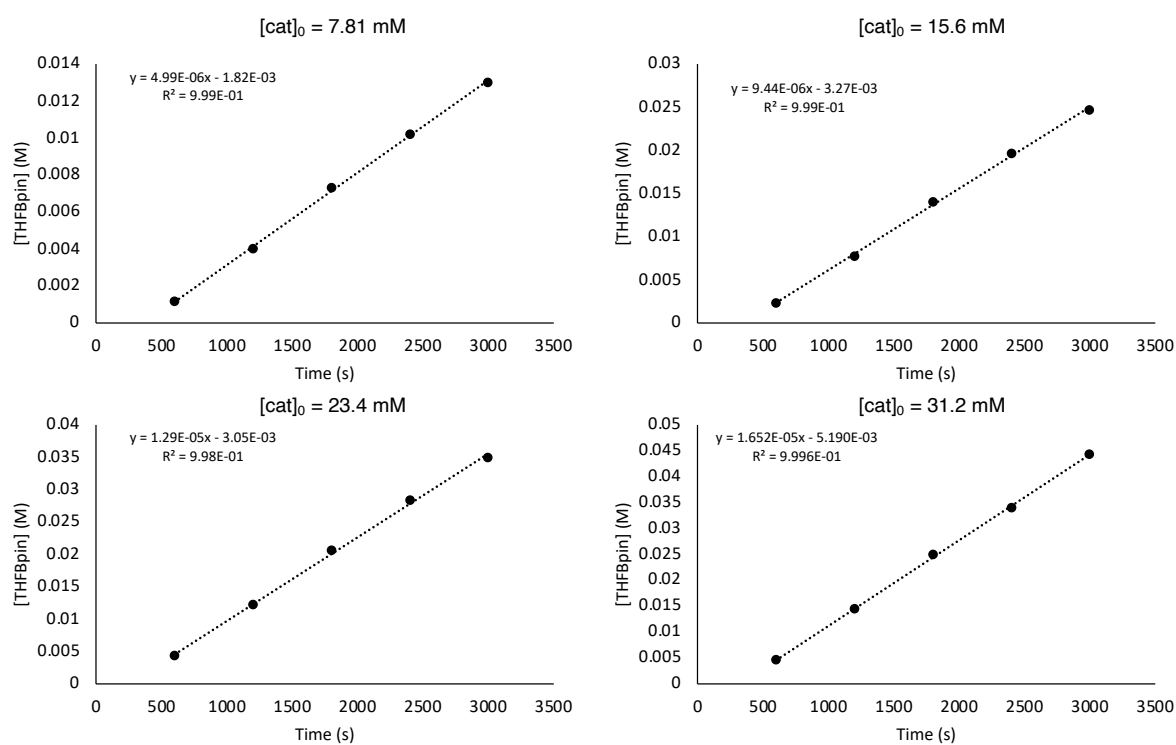| [THF] (M)	[catalyst] (mM)	[B_2pin_2] (M)	Initial Rate of Formation of THFBpin ($\mu M.s^{-1}$)
0.312	7.81	0.469	4.99 ± 0.08
0.312	15.6	0.469	9.44 ± 0.19
0.312	23.4	0.469	12.9 ± 0.3
0.312	12.2	0.469	16.5 ± 0.2

Figure 4.25. Formation of borylated product THF *vs* time varying initial concentration of catalyst.
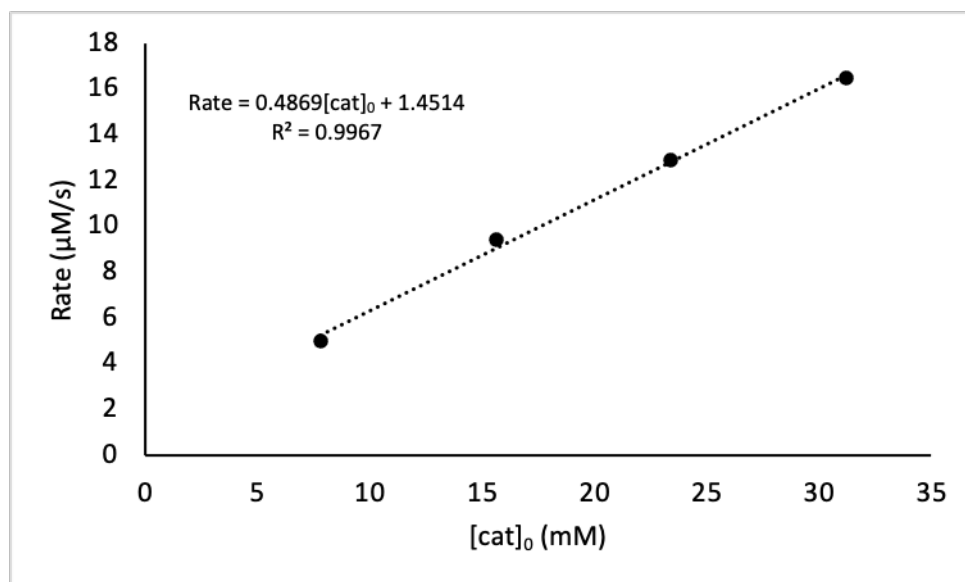

Figure 4.26. Rate of reaction vs concentration of catalyst.

Order in Mesitylene

In a nitrogen glovebox, adamantane (272 mg, 2.00 mmol) was dissolved in dry DCM in a 10 mL volumetric flask (0.20 M). B_2pin_2 (762 mg, 3.00 mmol) was dissolved in dry DCM in a 5.0 mL volumetric flask (0.60 M). 5-(3,5-bis(trifluoromethyl)phenyl)-8-(tert-butyl)-*N*-(3,5-di-tert-butylphenyl)-1,10-phenanthrolin-2-amine (**L2**) (130 mg, 200 µmol) was dissolved in dry DCM in a 2.0 mL volumetric flask (0.10 M). The resulting solutions were dispensed into four 1-dram vials equipped with flea stir bars, (312 µL of the adamantane solution, 62.5 µmol; 312.5 µL of the B_2pin_2 solution, 188 µmol; 62.5 µL of the ligand solution, 6.25 µmol). All volatile materials were carefully evaporated from the four 1-dram vials in vacuo.

$(MesH)Ir(Bpin)_3$ (139 mg, 200 µmol) was dissolved in dry cyclooctane in a 2.0 mL volumetric flask (0.10 M) and 62.5 µL of the resulting solution was added to each vial (6.25 µmol). THF (324 µL, 4.00 mmol) was dissolved in dry cyclooctane in a 5.0 mL volumetric flask (0.80 M), and 156 µL of the resulting solution was dispensed to the vials (125 µmol). Mesitylene (240 mg, 2.0 mmol) was dissolved in dry cyclooctane in a 10.0 mL volumetric flask (0.20 M) and the resulting solution was dispensed to the vials as follows to introduce additional MesH: (vial A: 0 µL (0 µmol); vial B: 31.2 µL (6.25 µmol); vial C: 93.8 µL (9.38 µmol); vial D: 125 µL (12.5 µmol). Note that for the table and plots that $[MesH]_0$ is defined as including the mesitylene from the $(MesH)Ir(Bpin)_3$ precursor. Dry cyclooctane was then added to make the total volume of the solutions in each vial 400 µL, the vials tightly sealed with Teflon-lined caps, and the vials removed from the glovebox. The vials were heated in an aluminum heating block at 65 ºC. At the appropriate timepoints, the vials were removed from the heating block, brought into the glovebox, and an aliquot removed for analysis by gas chromatography. The concentration of product 4,4,5,5-tetramethyl-2-(tetrahydrofuran-3-yl)-1,3,2-dioxaborolane was measured and plotted versus time to obtain the initial rates of the formation of 4,4,5,5-tetramethyl-2-(tetrahydrofuran-3-yl)-1,3,2-dioxaborolane.

Table 4.5. Initial concentrations of [THF], [catalyst], and $[B_2pin_2]$ (varying [cat]), and the corresponding initial rates of formation of 4,4,5,5-tetramethyl-2-(tetrahydrofuran-3-yl)-1,3,2-dioxaborolane.

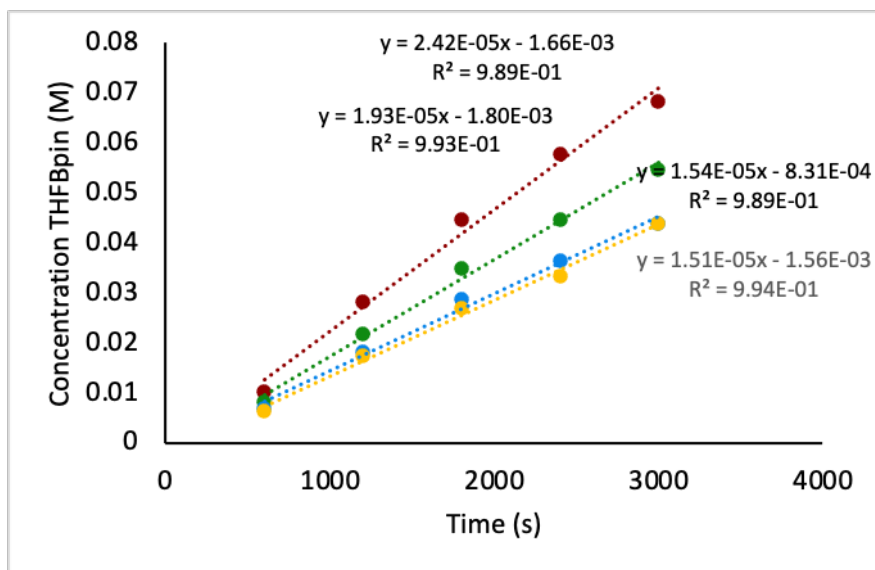| [THF] (M)	[catalyst] (mM)	$[B_2pin_2]$ (M)	[MesH] (mM)	Initial Rate of Formation of THFBpin (µM.s^{-1})
0.312	15.6	0.469	15.6	24.2 ± 1.5
0.312	15.6	0.469	31.2	19.3 ± 0.9
0.312	15.6	0.469	46.9	15.4 ± 0.9
0.312	15.6	0.469	62.5	15.1 ± 0.7

Figure 4.27. Formation of borylated product THF *vs* time varying initial concentration of mesitylene.

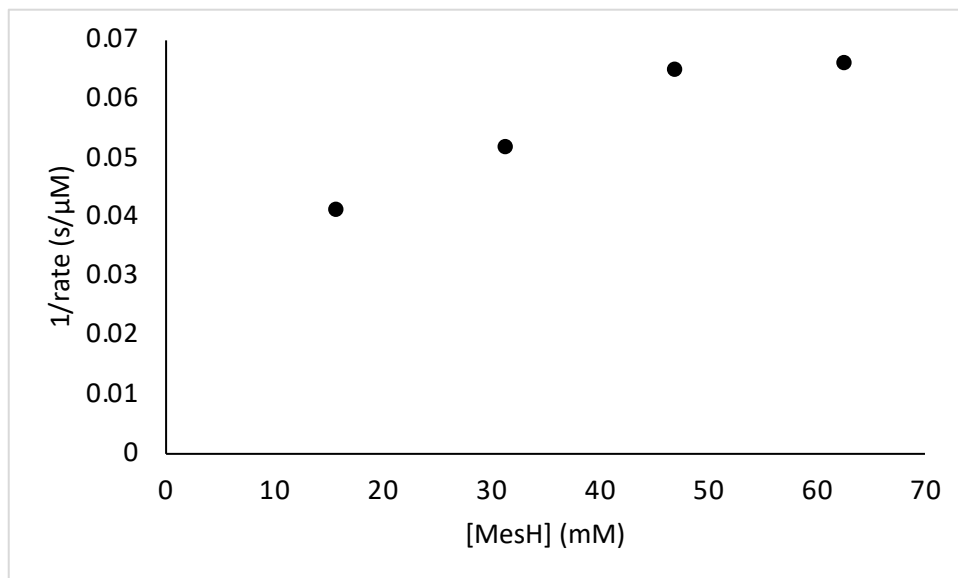**Figure 4.28.** 1/rate of reaction vs concentration of mesitylene.

Order in HBpin

In a nitrogen glovebox, adamantane (272 mg, 2.00 mmol) was dissolved in dry DCM in a 10 mL volumetric flask (0.20 M). B_2pin_2 (762 mg, 3.00 mmol) was dissolved in dry DCM in a 5.0 mL volumetric flask (0.60 M). 5-(3,5-bis(trifluoromethyl)phenyl)-8-(tert-butyl)-*N*-(3,5-di-tert-butylphenyl)-1,10-phenanthrolin-2-amine (**L2**) (130 mg, 200 µmol) was dissolved in dry DCM in a 2.0 mL volumetric flask (0.10 M). The resulting solutions were dispensed into four 1-dram vials equipped with flea stir bars, (312 µL of the adamantane solution, 62.5 µmol; 312.5 µL of the B_2pin_2 solution, 188 µmol; 62.5 µL of the ligand solution, 6.25 µmol). All volatile materials were carefully evaporated from the four 1-dram vials in vacuo.

(MesH)Ir(Bpin)$_3$ (139 mg, 200 µmol) was dissolved in dry cyclooctane in a 2.0 mL volumetric flask (0.10 M) and 62.5 µL of the resulting solution was added to each vial (6.25 µmol). THF (324 µL, 4.00 mmol) was dissolved in dry cyclooctane in a 5.0 mL volumetric flask (0.80 M), and 156 µL of the resulting solution was dispensed to the vials (125 µmol). HBpin (512 mg, 4.00 mmol) was dissolved in dry cyclooctane in a 2.0 mL volumetric flask (2.0 M) and the resulting solution was dispensed to the vials as follows: (vial A: 31.2 µL (62.5 µmol); vial B: 62.5 µL (125 µmol); vial C: 93.8 µL (188 µmol); vial D: 125 µL (250 µmol). Dry cyclooctane was then added to make the total volume of the solutions in each vial 400 µL, the vials tightly sealed with Teflon-lined caps, and the vials removed from the glovebox. The vials were heated in an aluminum heating block at 65 ºC. At the appropriate timepoints, the vials were removed from the heating block, brought into the glovebox, and an aliquot removed for analysis by gas chromatography. The concentration of product 4,4,5,5-tetramethyl-2-(tetrahydrofuran-3-yl)-1,3,2-dioxaborolane was measured and plotted versus time to obtain the initial rates of the formation of 4,4,5,5-tetramethyl-2-(tetrahydrofuran-3-yl)-1,3,2-dioxaborolane.

Table 4.6. Initial concentrations of [THF], [catalyst], [B_2pin_2], [HBpin] (varying [HBpin]), and the corresponding initial rates of formation of 4,4,5,5-tetramethyl-2-(tetrahydrofuran-3-yl)-1,3,2-dioxaborolane.

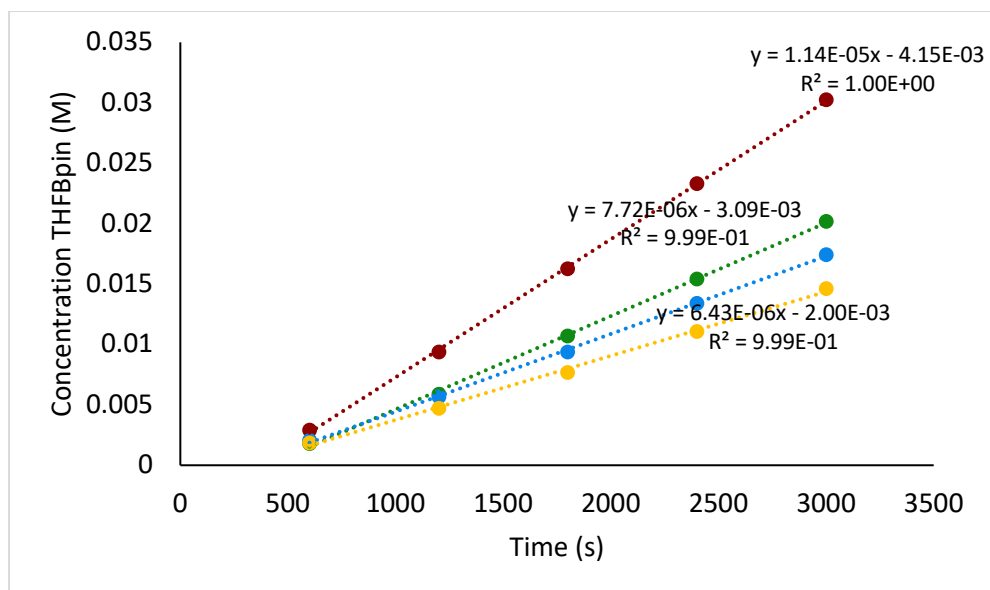| [THF] (M)	[catalyst] (mM)	[B_2pin_2] (M)	[HBpin] (mM)	Initial Rate of Formation of THFBpin ($\mu M \cdot s^{-1}$)
0.312	15.6	0.469	0.156	11.4 ± 0.1
0.312	15.6	0.469	0.312	7.72 ± 0.14
0.312	15.6	0.469	0.469	6.43 ± 0.10
0.312	15.6	0.469	0.625	5.31 ± 0.15

Figure 4.29. Formation of borylated product THF *vs* time varying initial concentration of HBpin.
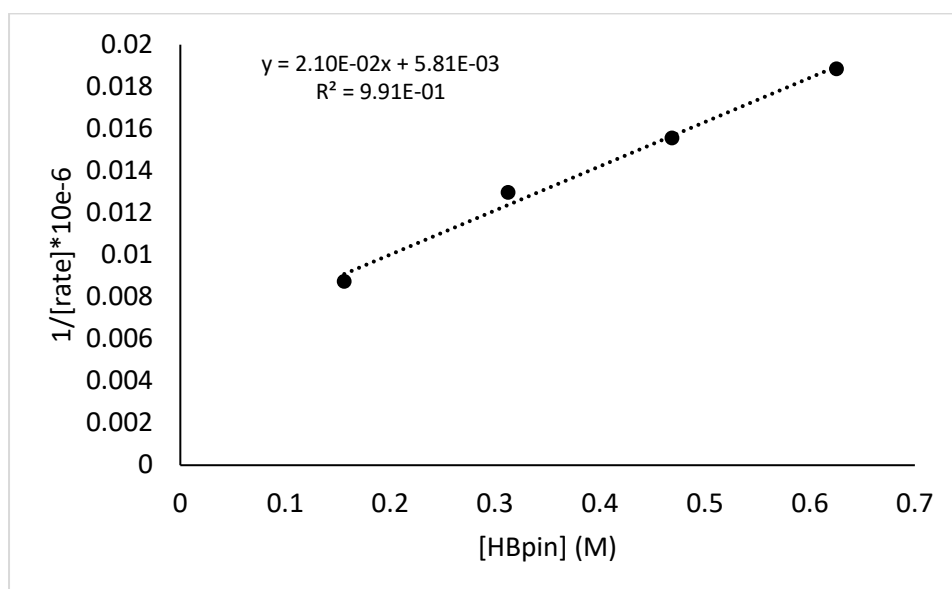

Figure 4.30. 1/rate of reaction vs concentration of HBpin.

Kinetic Isotope Effects by Parallel Reactions

KIE of THF vs THF-d_8

In a nitrogen glovebox, adamantane (272 mg, 2.00 mmol) was dissolved in dry DCM in a 10 mL volumetric flask (0.20 M). B_2pin_2 (762 mg, 3.00 mmol) was dissolved in dry DCM in a 5.0 mL volumetric flask (0.60 M). 5-(3,5-bis(trifluoromethyl)phenyl)-8-(tert-butyl)-N-(3,5-di-tert-butylphenyl)-1,10-phenanthrolin-2-amine (**L2**) (130 mg, 200 μmol) was dissolved in dry DCM in a 2.0 mL volumetric flask (0.10 M). The resulting solutions were dispensed into four 1-dram vials equipped with flea stir bars, (312 μL of the adamantane solution, 62.5 μmol; 312.5 μL of the B_2pin_2 solution, 188 μmol; 62.5 μL of the ligand solution, 6.25 μmol). All volatile materials were carefully evaporated from the four 1-dram vials in vacuo.

(MesH)Ir(Bpin)$_3$ (139 mg, 200 μmol) was dissolved in dry cyclooctane in a 2.0 mL volumetric flask (0.10 M) and 62.5 μL of the resulting solution was added to each vial (6.25 μmol). THF (324 μL, 4.00 mmol) was dissolved in dry cyclooctane in a 5.0 mL volumetric flask (0.80 M), and the resulting solution dispensed to the vials as follows: (vial A: 156 μL (125 μmol); vial B: 156 μL (125 μmol). THF-d_8 (326 μL, 4.00 mmol) was dissolved in dry cyclooctane in a 5.0 mL volumetric flask (0.80 M), and the resulting solution dispensed to the vials as follows: (vial C: 156 μL (125 μmol); vial D: 156 μL (125 μmol). Dry cyclooctane was then added to make the total volume of the solutions in each vial 400 μL, the vials tightly sealed with Teflon-lined caps, and the vials removed from the glovebox. The vials were heated in an aluminum heating block at 65 ºC. At the appropriate timepoints, the vials were removed from the heating block, brought into the glovebox, and an aliquot removed for analysis by gas chromatography. The concentration of product 4,4,5,5-tetramethyl-2-(tetrahydrofuran-3-yl)-1,3,2-dioxaborolane was measured and plotted versus time to obtain the initial rates of the formation of 4,4,5,5-tetramethyl-2-(tetrahydrofuran-3-yl)-1,3,2-dioxaborolane.
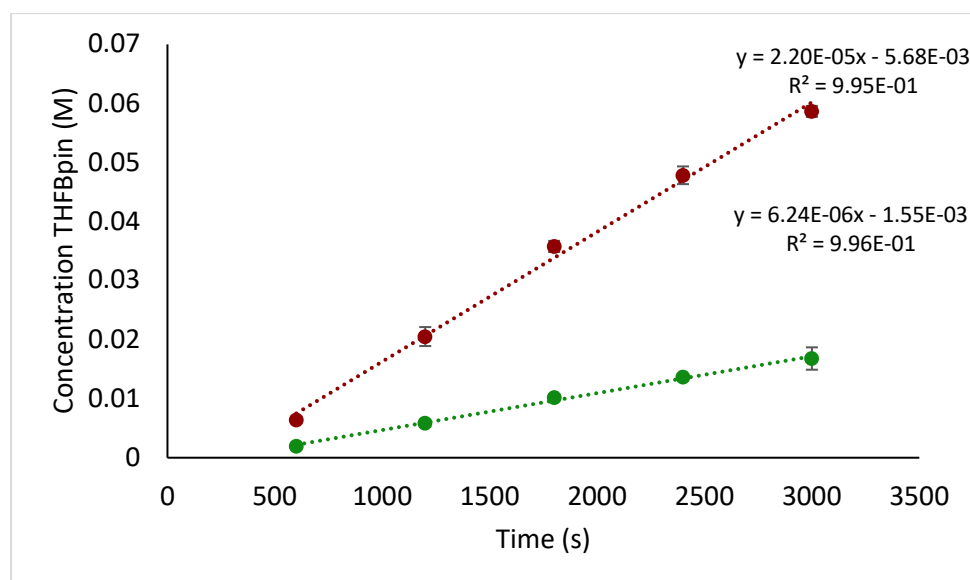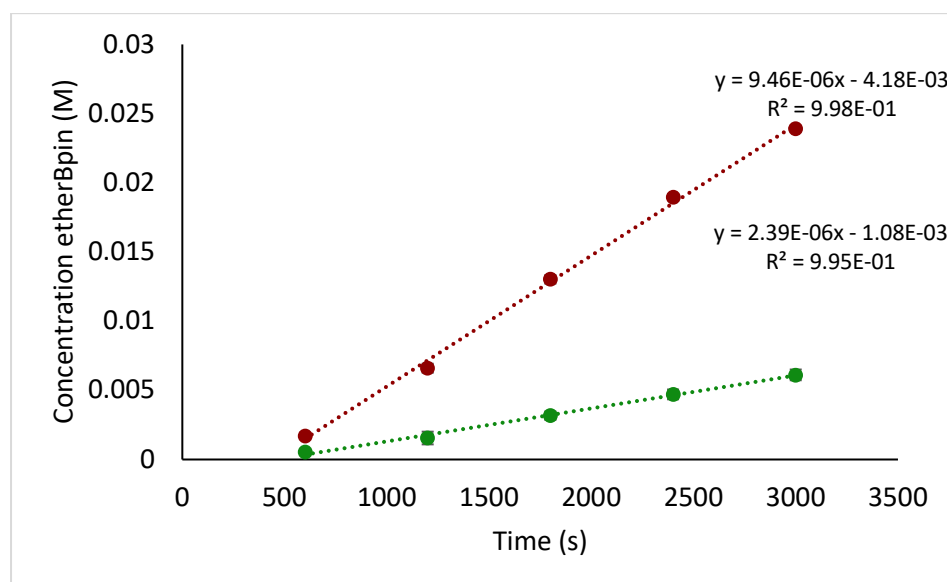

Figure 4.31. Initial rates of the formation of 4,4,5,5-tetramethyl-2-(tetrahydrofuran-3-yl)-1,3,2-dioxaborolane. Red: THF, green: THF-d_8. Average of two runs.

KIE = 3.52 ± 0.18.

KIE of ether vs ether-d_{10}

In a nitrogen glovebox, adamantane (272 mg, 2.00 mmol) was dissolved in dry DCM in a 10 mL volumetric flask (0.20 M). B$_2$pin$_2$ (762 mg, 3.00 mmol) was dissolved in dry DCM in a 5.0 mL volumetric flask (0.60 M). 5-(3,5-bis(trifluoromethyl)phenyl)-8-(tert-butyl)-N-(3,5-di-tert-butylphenyl)-1,10-phenanthrolin-2-amine (**L2**) (130 mg, 200 μmol) was dissolved in dry DCM in a 2.0 mL volumetric flask (0.10 M). The resulting solutions were dispensed into four 1-dram vials equipped with flea stir bars, (312 μL of the adamantane solution, 62.5 μmol; 312.5 μL of the B$_2$pin$_2$ solution, 188 μmol; 62.5 μL of the ligand solution, 6.25 μmol). All volatile materials were carefully evaporated from the four 1-dram vials in vacuo.

(MesH)Ir(Bpin)$_3$ (139 mg, 200 μmol) was dissolved in dry cyclooctane in a 2.0 mL volumetric flask (0.10 M) and 62.5 μL of the resulting solution was added to each vial (6.25 μmol). Ether (77.0 μL, 0.741 mmol) was dissolved in dry cyclooctane in a 2.0 mL volumetric flask (0.80 M), and the resulting solution dispensed to the vials as follows: (vial A: 338 μL (125 μmol); vial B: 338 μL (125 μmol). Ether-d_{10} (77.8 μL, 0.741 mmol) was dissolved in dry cyclooctane in a 2.0 mL volumetric flask (0.80 M), and the resulting solution dispensed to the vials as follows: (vial C: 338 μL (125 μmol); vial D: 338 μL (125 μmol). The vials tightly sealed with Teflon-lined caps, and the vials removed from the glovebox. The vials were heated in an aluminum heating block at 65 ºC. At the appropriate timepoints, the vials were removed from the heating block, brought into the glovebox, and an aliquot removed for analysis by gas chromatography. The concentration of product 2-(2-ethoxyethyl)-4,4,5,5-tetramethyl-1,3,2-dioxaborolane was measured and plotted versus time to obtain the initial rates of the formation of 2-(2-ethoxyethyl)-4,4,5,5-tetramethyl-1,3,2-dioxaborolane.

y = 9.46E-06x - 4.18E-03
R² = 9.98E-01

y = 2.39E-06x - 1.08E-03
R² = 9.95E-01

Figure 4.32. Initial rates of the formation of 2-(2-ethoxyethyl)-4,4,5,5-tetramethyl-1,3,2-dioxaborolane for the determination of the KIE. Red: ether, green: ether-d_{10}. Average of two runs.

KIE = 3.97 ± 0.19.

4.4.8 Crystallographic Data

(L3)Ir(Bpin)₃(P(OPh)₃)

A clear dark yellow block 0.39 x 0.36 x 0.33 mm in size was mounted on a Cryoloop with Paratone oil. Data were collected on a ROD, Synergy Custom DW system, Pilatus 200K diffractometer in a nitrogen gas stream at 100.00(10) K during data collection using omega scans. Crystal-to-detector distance was 30.23 mm and exposure time was 0.5 seconds per frame using a scan width of 0.5°. Data collection was 99.8% complete to 25.25° in θ. A total of 390730 reflections were collected covering the indices -25<=h<=25, -22<=k<=22, -33<=l<=33. 19388 reflections were founded to be symmetry independent, with an Rint of 0.1272. Indexing and unit cell refinement indicated a primitive, monoclinic lattice. The space group was found to be P 21/n (No. 14). The data were integrated using the CrysAlisPro 1.171.39.46e software program and scaled using the SCALE3 ABSPACK scaling algorithm. Solution by intrinsic phasing (SHELXT-2015) produced a heavy-atom phasing model consistent with the proposed structure. All non-hydrogen atoms were refined anisotropically by full-matrix least-squares (SHELXL2014). All hydrogen atoms were placed using a riding model. Their positions were constrained relative to their parent atom using the appropriate HFIX command in SHELXL-2014.

Table 4.7. Crystal data and structure refinement for (L3)Ir(Bpin)₃(P(OPh)₃)

Empirical formula	$C_{90}H_{125}B_4F_6IrN_3O_{12}PSi_2$
Formula weight	1877.51
Temperature/K	100(0)
Crystal system	monoclinic
Space group	$P2_1/n$
a/Å	20.5375(4)
b/Å	18.0275(3)
c/Å	26.4784(4)
α/°	90
β/°	104.221(2)
γ/°	90
Volume/Å³	9502.9(3)
Z	4
ρ_{calc}g/cm³	1.312

μ/mm^{-1}	1.516
F(000)	3904.0
Crystal size/mm^3	0.39 × 0.36 × 0.33
Radiation	Mo Kα (λ = 0.71073)
2Θ range for data collection/°	5.912 to 52.744
Index ranges	-25 ≤ h ≤ 25, -22 ≤ k ≤ 22, -33 ≤ l ≤ 33
Reflections collected	390730
Independent reflections	19388 [R_{int} = 0.1272, R_{sigma} = 0.0362]
Data/restraints/parameters	19388/63/1193
Goodness-of-fit on F^2	1.044
Final R indexes [I>=2σ (I)]	R_1 = 0.0492, wR_2 = 0.1316
Final R indexes [all data]	R_1 = 0.0553, wR_2 = 0.1383
Largest diff. peak/hole / e Å^{-3}	2.59/-2.39

4.4.9 Density Functional Theory Calculations

DFT calculations were conducted at the Molecular Graphics and Computation Facility (MGCF) at the University of California, Berkeley using the Gaussian 16 software package.[25] Initial geometries were constructed in GaussView 6 and optimized to stationary points (either minima or first-order saddle points) using the PBE0 functional (the hybrid functional based on the Perdew-Burke-Ernzerhof functional [PBE][26, 27] as described by Adamo[28]) with Grimme's D3 dispersion correction with Becke-Johnson damping (GD3-BJ)[29] and the basis sets def2-TZVP (with effective core potential) for Ir and def2-SVP for all light atoms (**BS1**). The nature of each stationary point was verified by accompanying frequency calculations (all positive eigenvalues for minima and exactly one negative eigenvalue for transition states). For each ground state and transition state, several isomeric geometries about the iridium center and conformers resulting from rotations of the boryl group about the Ir–B bond were considered. Their geometries and energies were optimized in Gaussian, and only those lowest in energy or relevant to the reaction coordinate are presented here. Connectivity of transition states to ground-state minima was established by following the intrinsic reaction coordinate (IRC). Frequencies were evaluated at 1 atm at 298 K. Further single point energy (SPE) calculations were performed on the optimized geometries with the larger def2-QZVPD basis set[30] (with ECP)[31] on Ir and the def2-TZVPD basis set[30] on all light atoms (obtained through the Basis Set Exchange, accessed September 2021)[32-34] (**BS2**). The SPE calculations were performed in cyclohexane solvent using the SMD solvent continuum reported by Truhlar and co-workers.[35] In all cases, Gibbs free energies for calculations using **BS2** were approximated by summing the internal energy calculated with **BS2** and the thermal correction from the frequency calculation on the same structure with **BS1**. Coordinates for optimized geometries are given as a multi-structure XYZ file.
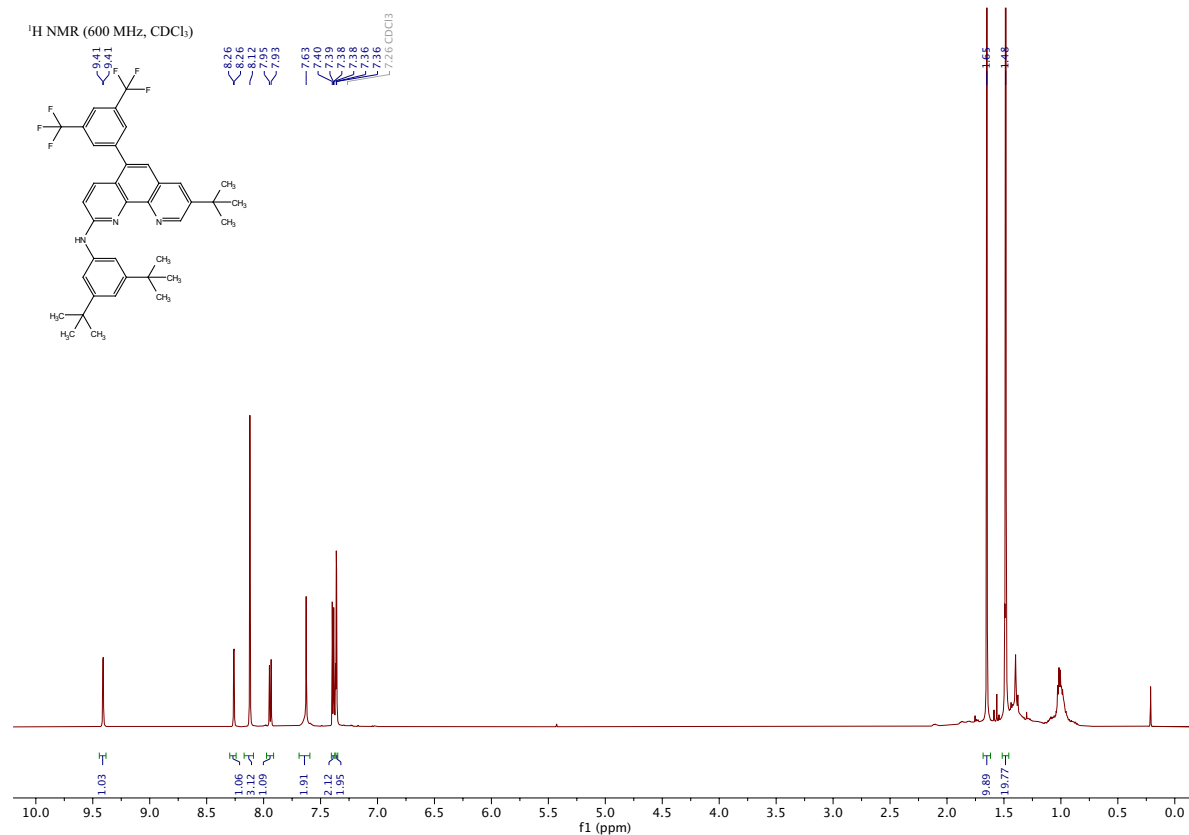
4.4.10 NMR Spectra

5-bromo-2-chloroquinolin-8-amine
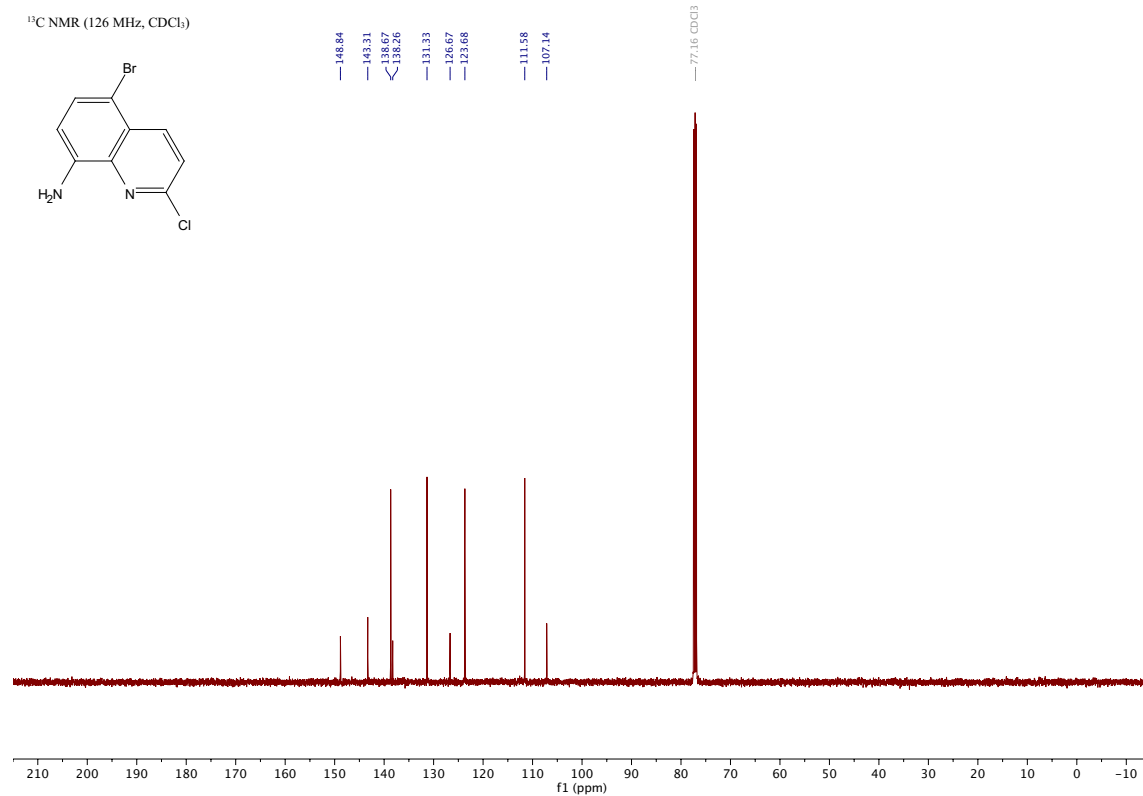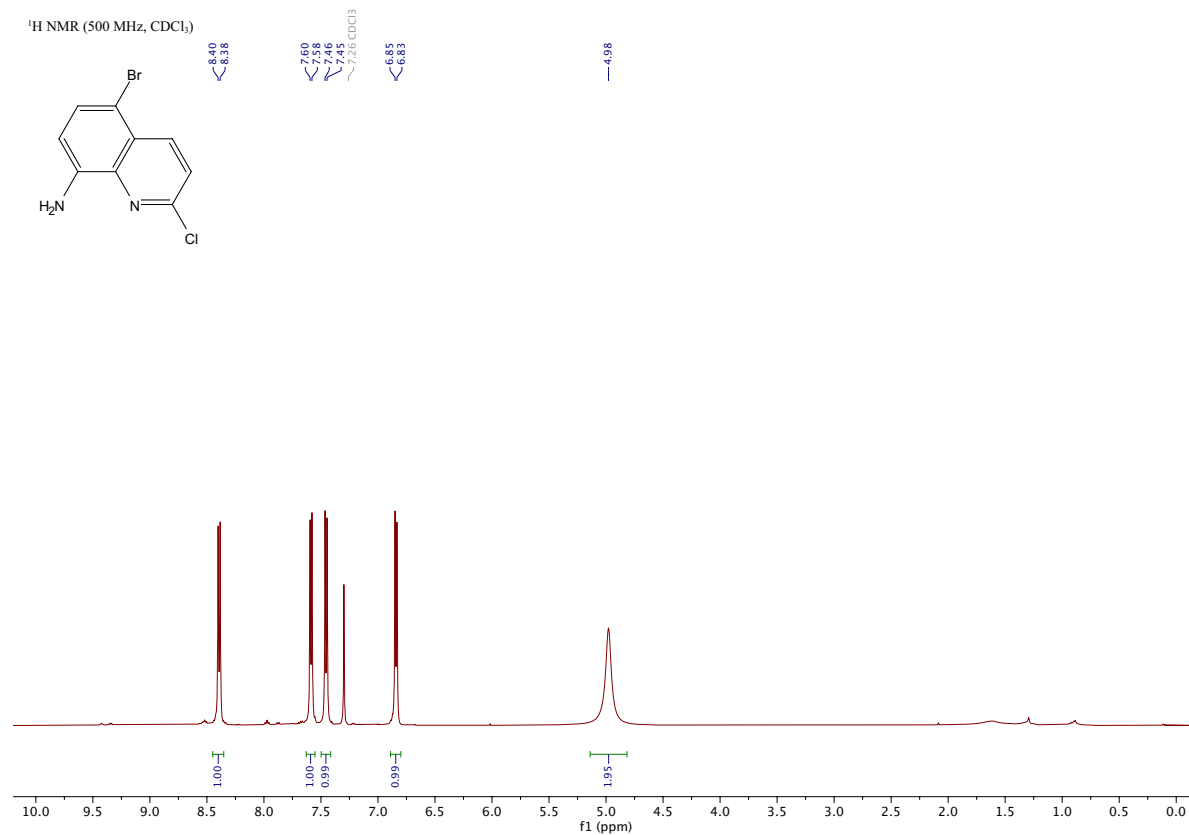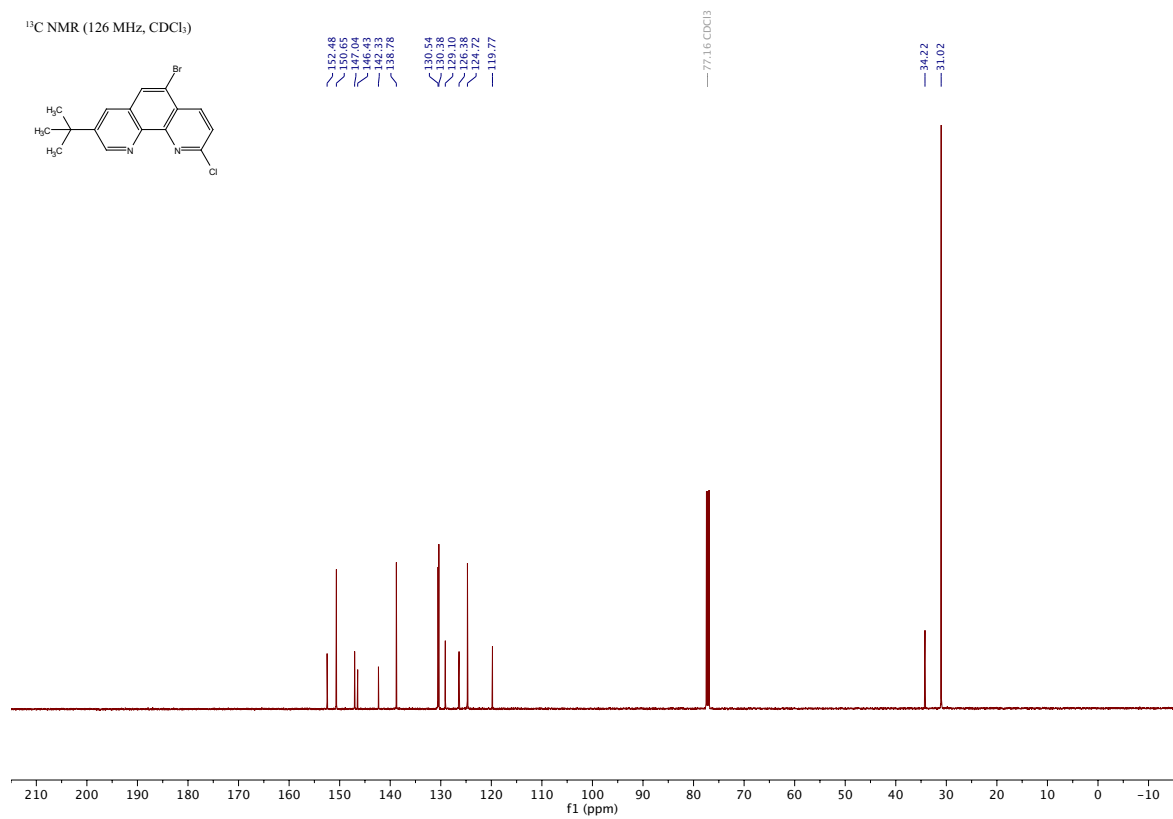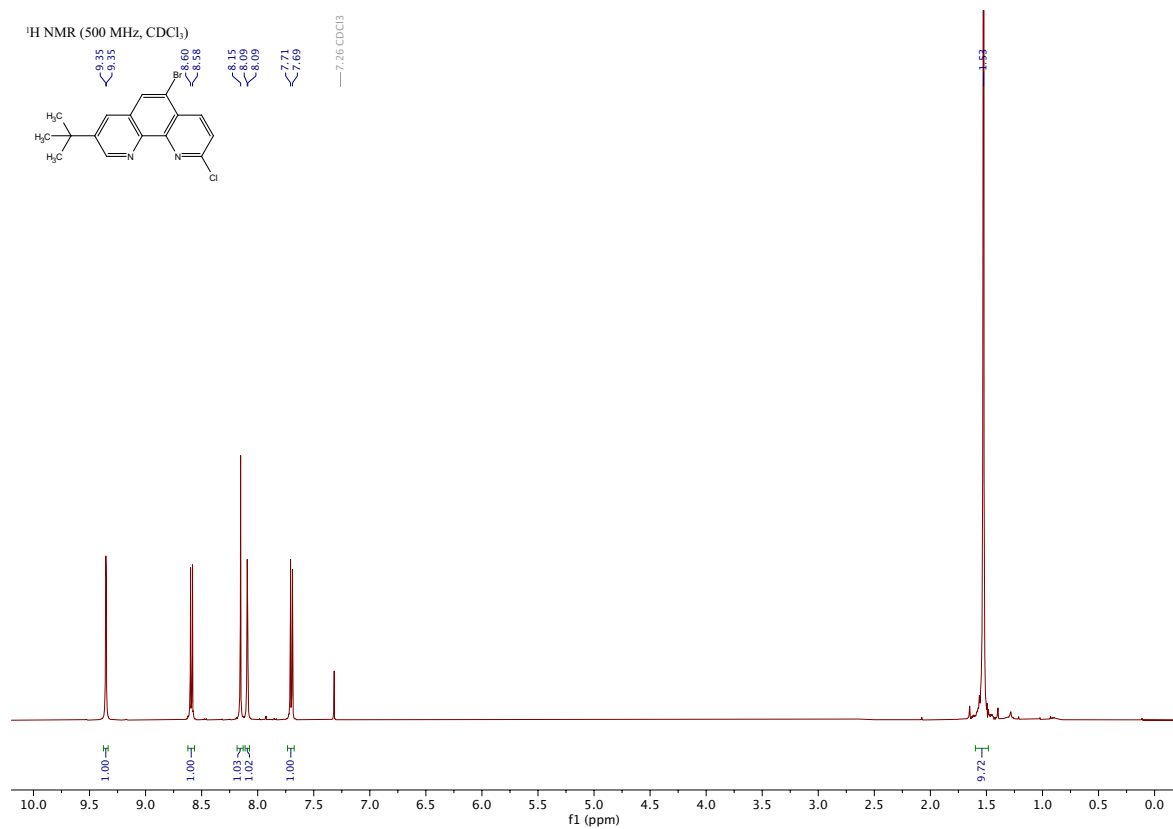
¹H NMR (500 MHz, CDCl₃)

¹³C NMR (126 MHz, CDCl₃)

5-bromo-8-(*tert*-butyl)-2-chloro-1,10-phenanthroline
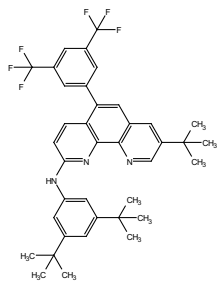
¹H NMR (500 MHz, CDCl₃)

¹³C NMR (126 MHz, CDCl₃)

5-bromo-8-(*tert*-butyl)-*N*-(3,5-di-*tert*-butylphenyl)-1,10-phenanthrolin-2-amine

¹H NMR (600 MHz, CDCl₃)

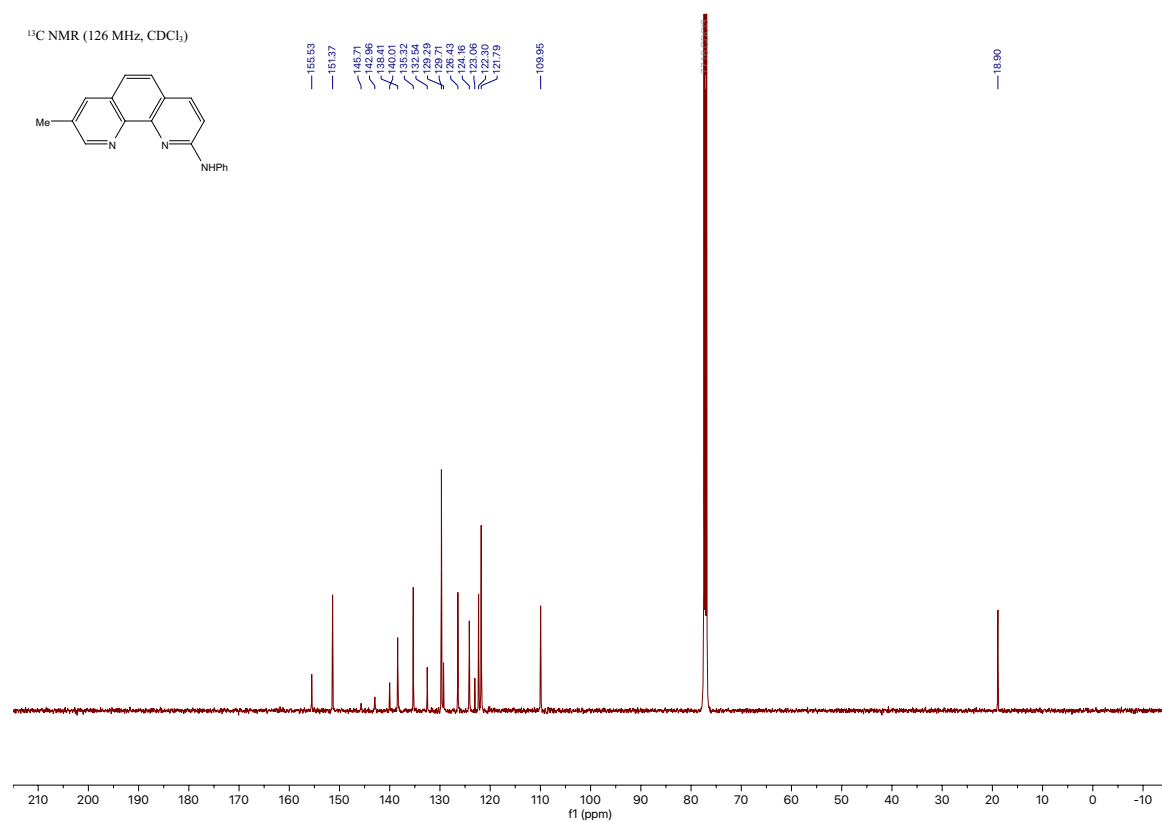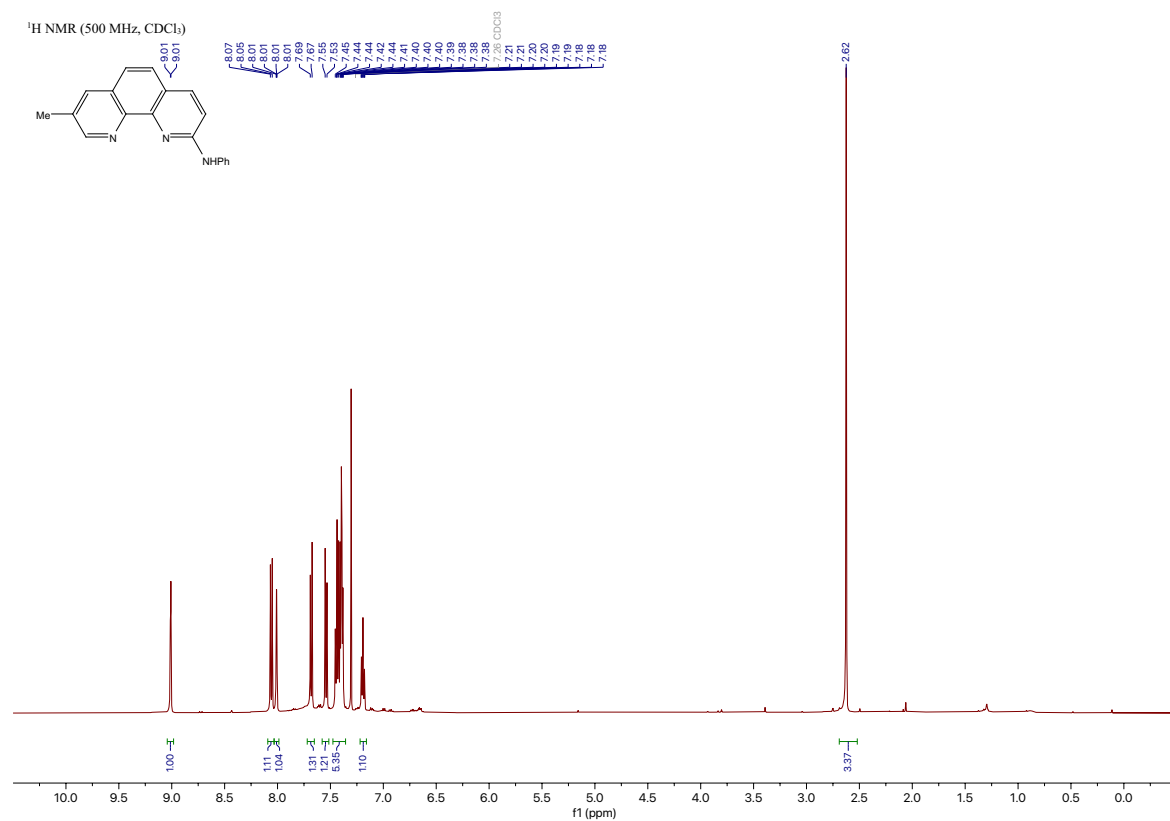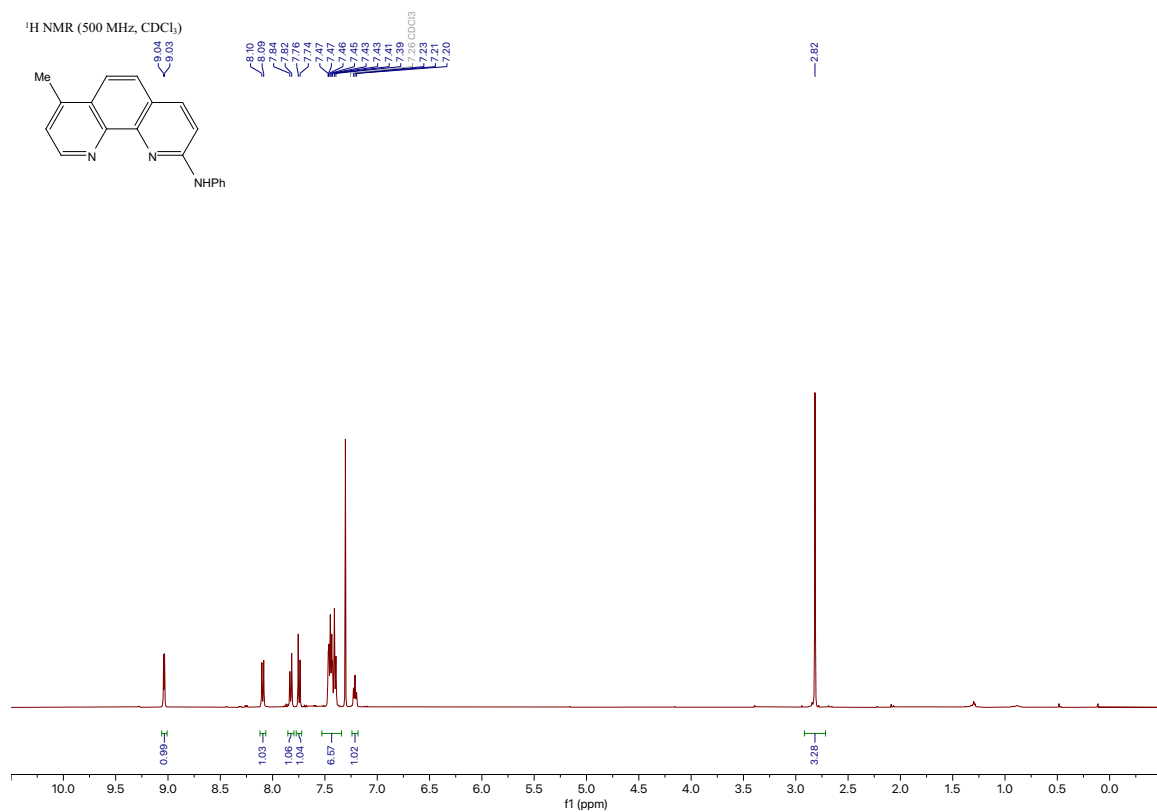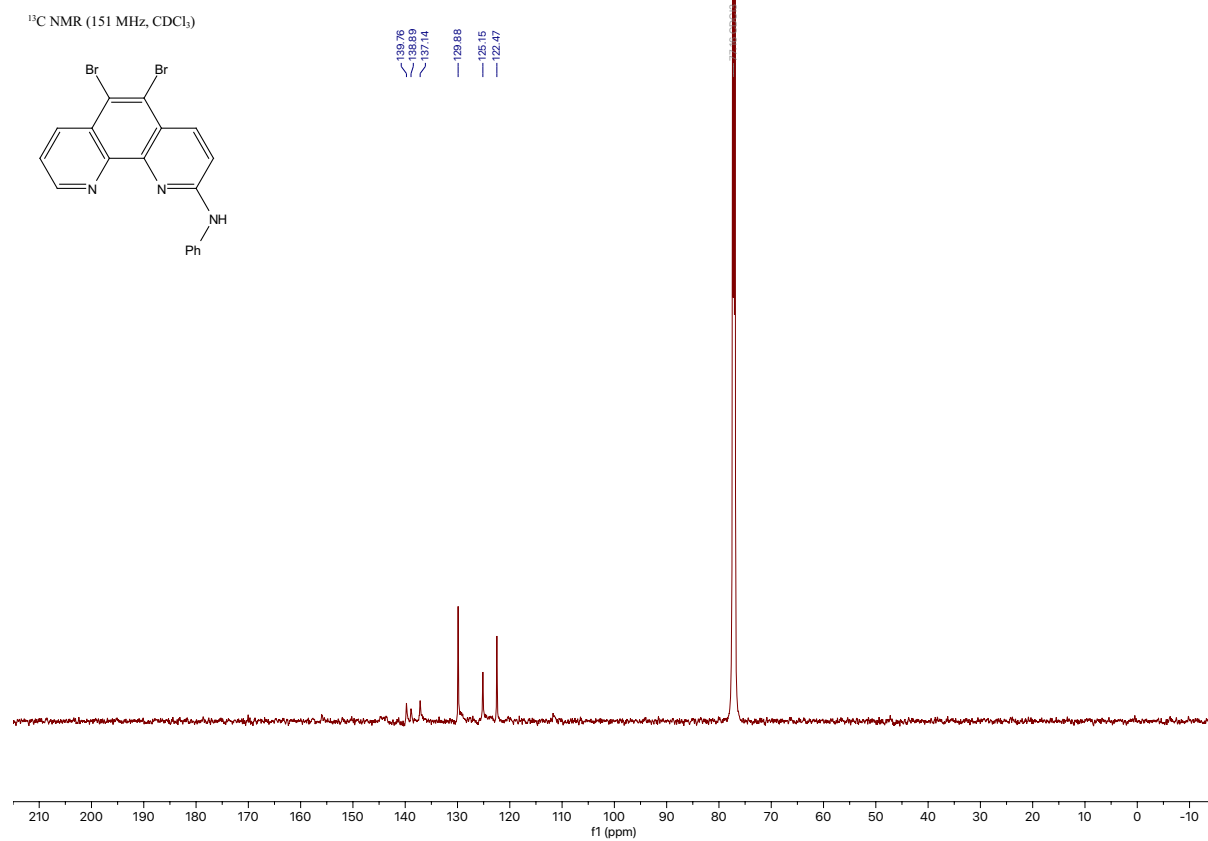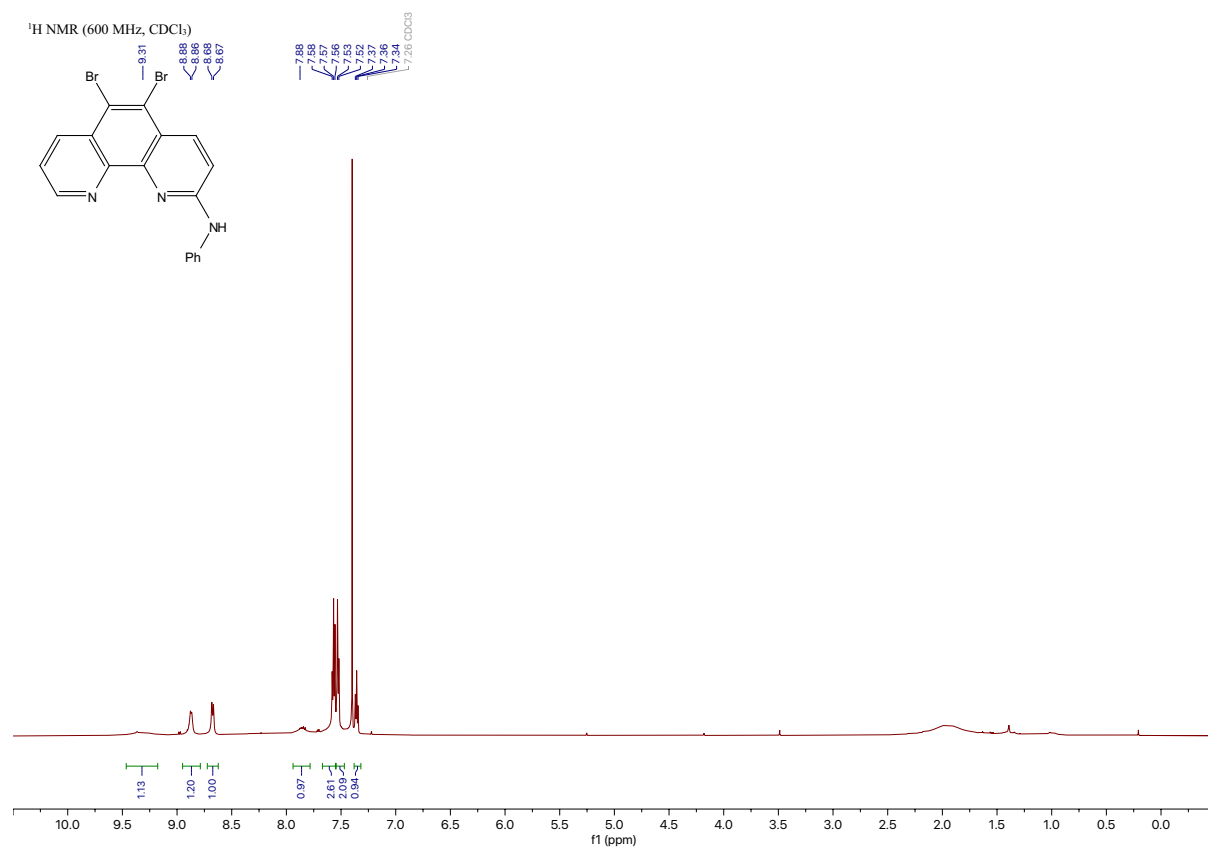¹³C NMR (151 MHz, CDCl₃)

5-(3,5-bis(trifluoromethyl)phenyl)-8-(*tert*-butyl)-*N*-(3,5-di-*tert*-butylphenyl)-1,10-phenanthrolin-2-amine

¹H NMR (600 MHz, CDCl₃)

¹³C NMR (151 MHz, CDCl₃)

^{19}F NMR (565 MHz, CDCl$_3$)

—-62.73

-43 -44 -45 -46 -47 -48 -49 -50 -51 -52 -53 -54 -55 -56 -57 -58 -59 -60 -61 -62 -63 -64 -65 -66 -67 -68 -69 -70 -71 -72 -73 -74 -75 -76 -77 -78 -79 -80 -81 -8
f1 (ppm)
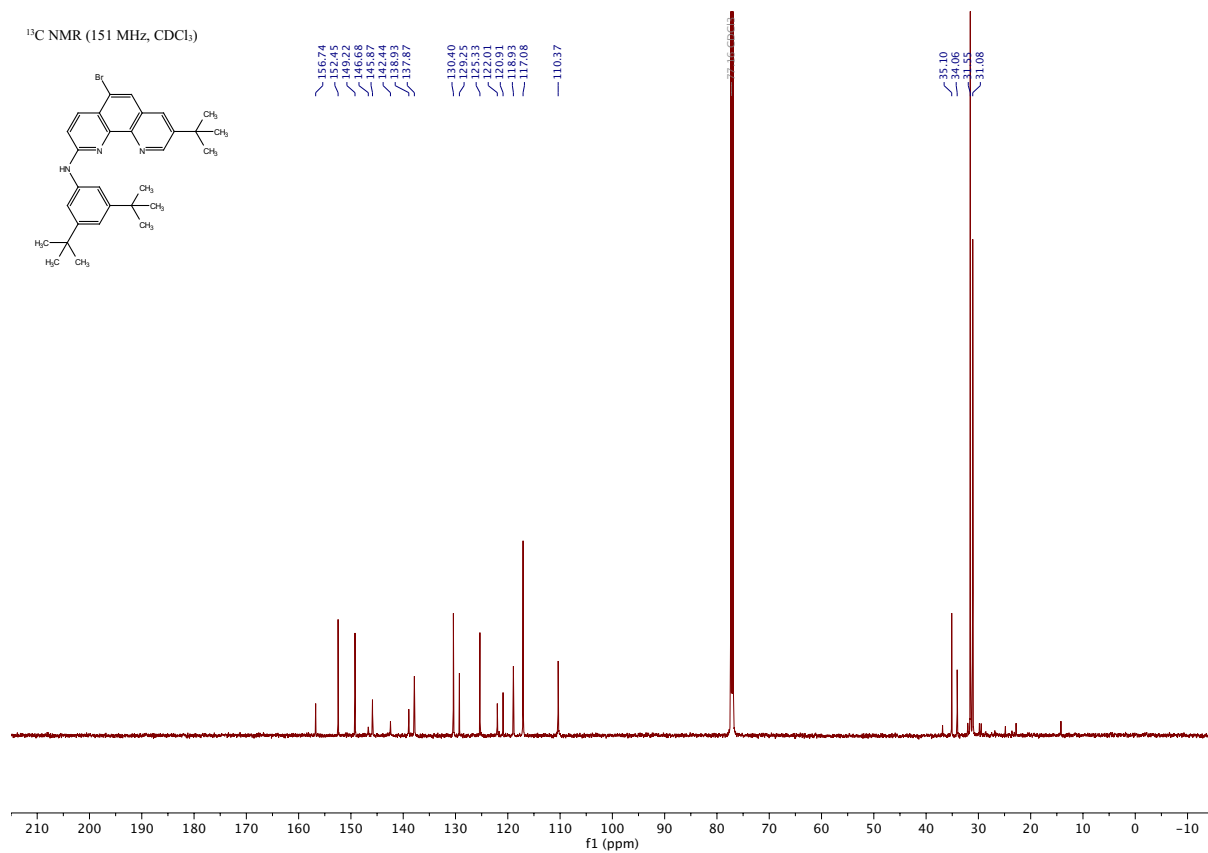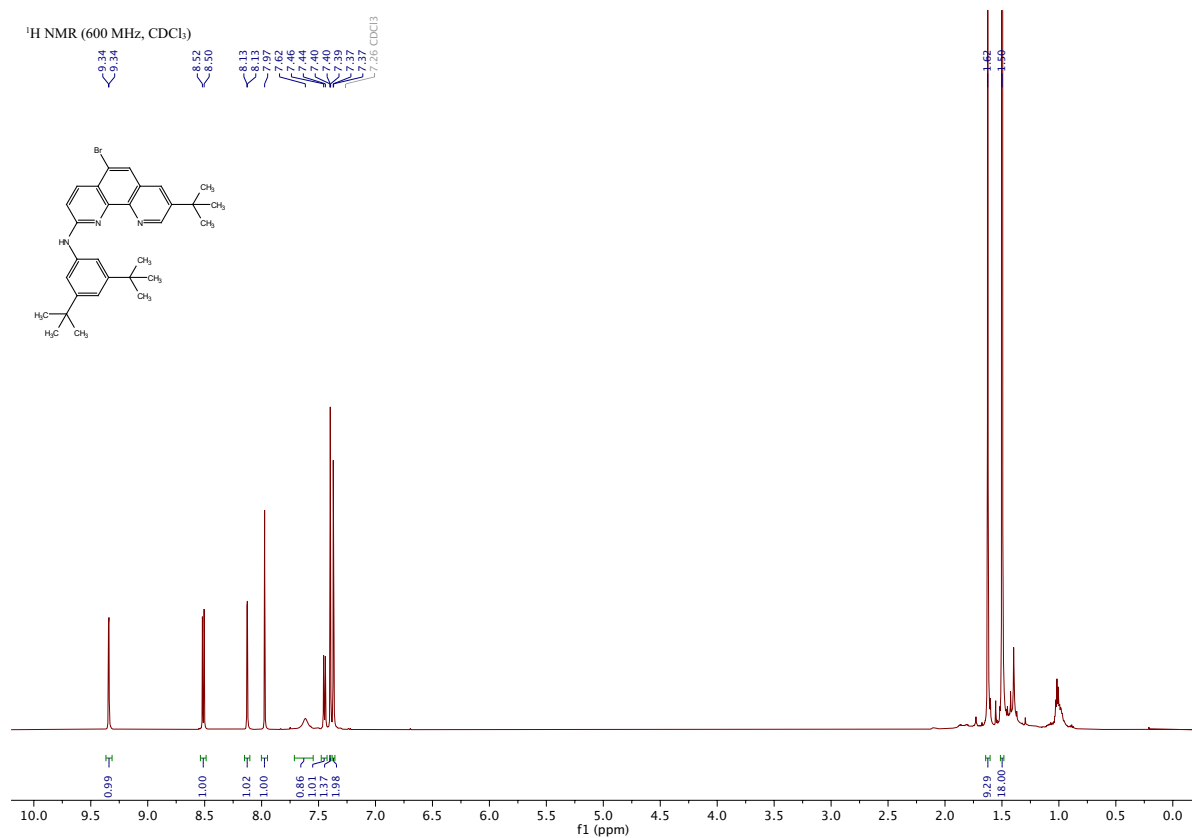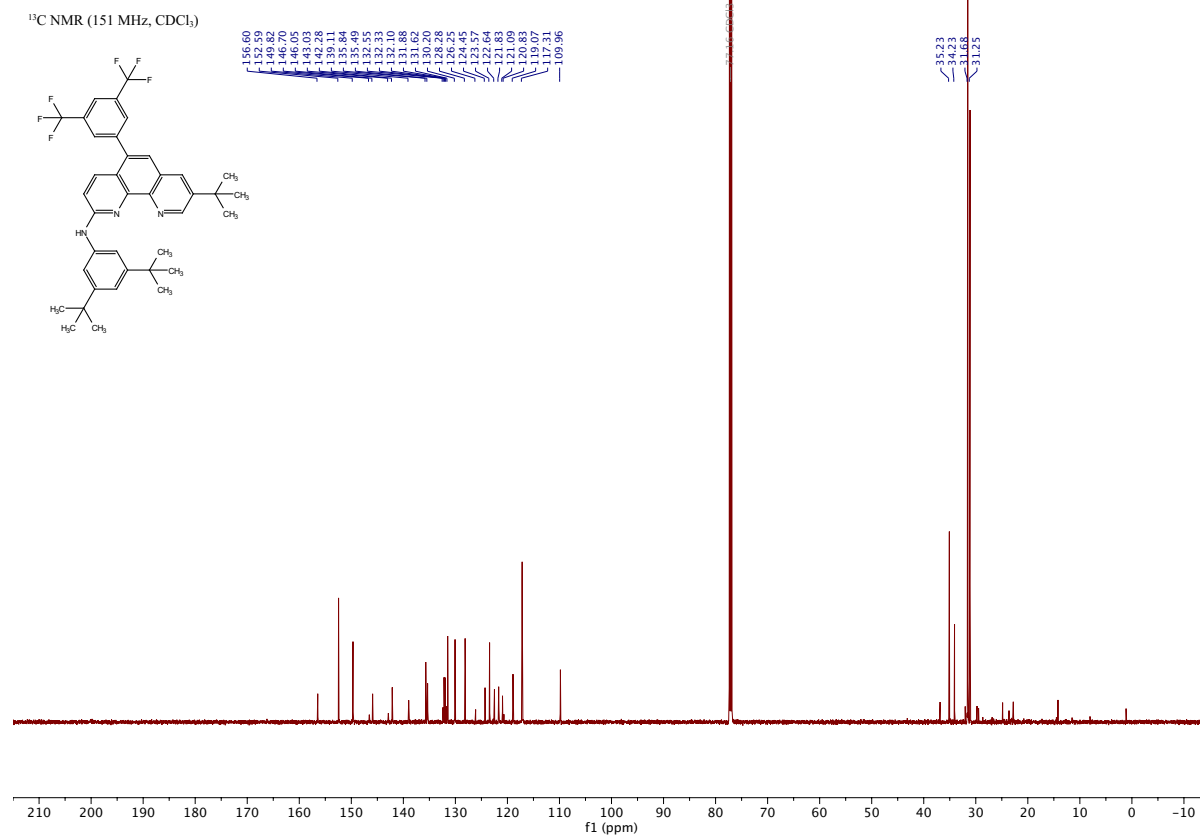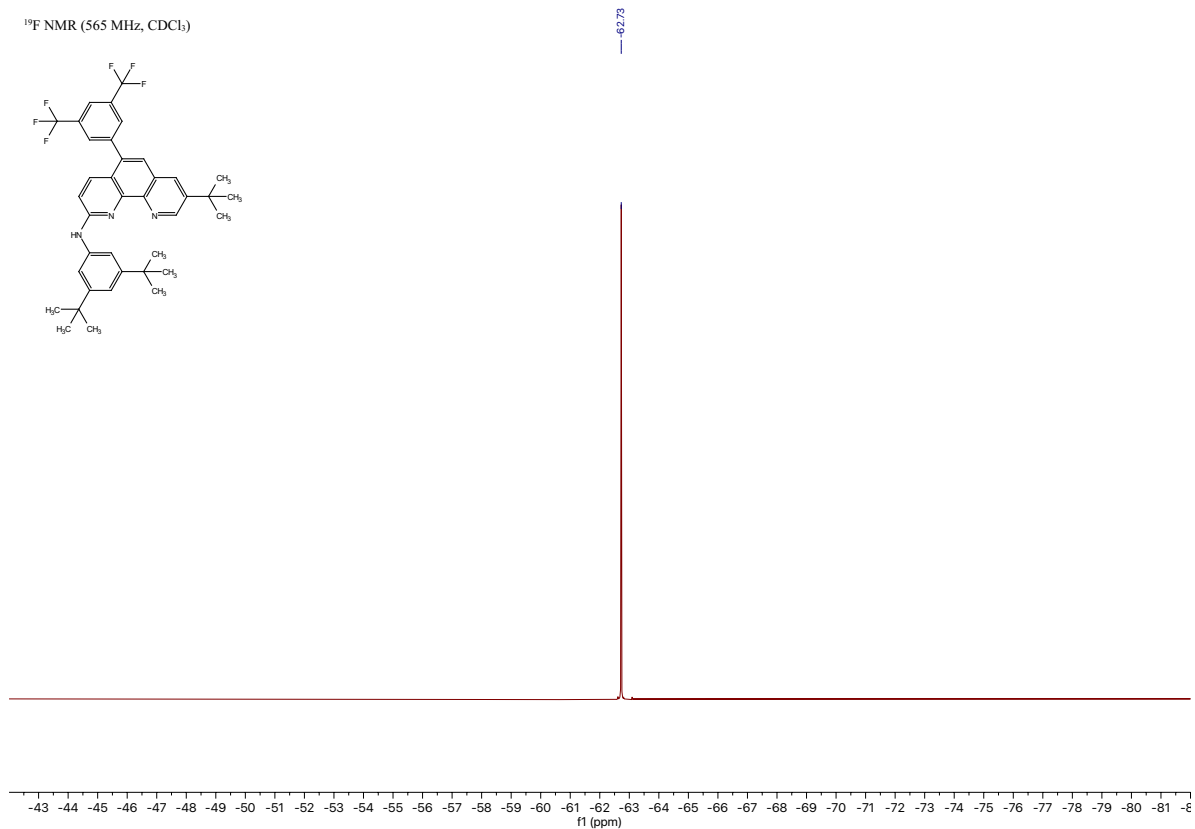
tris(4-bromophenyl) phosphite (L5)

¹H NMR (500 MHz, C₆D₆)
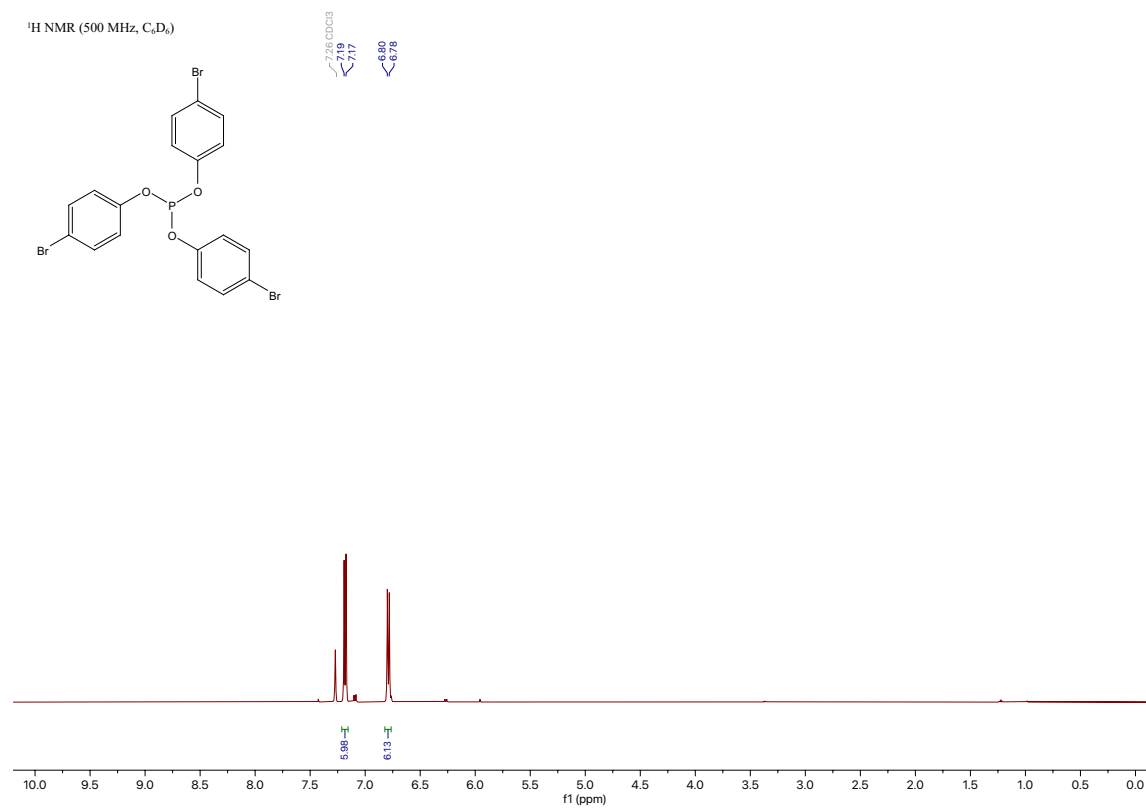
¹³C NMR (126 MHz, C₆D₆)
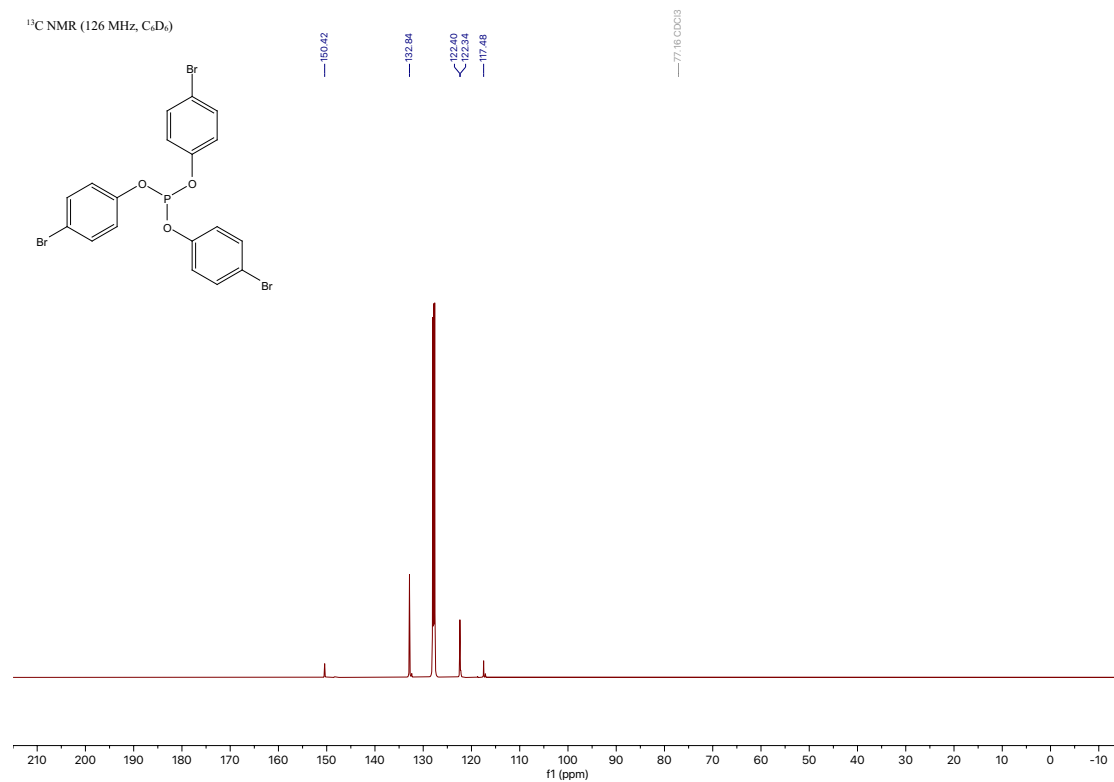
³¹P NMR (202 MHz, C₆D₆) δ 126.66.

561
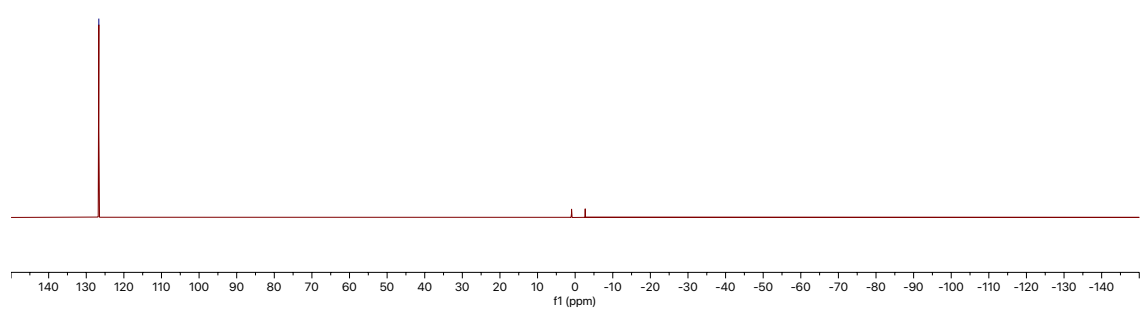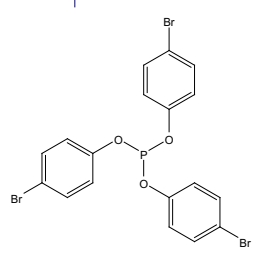
9-methyl-*N*-phenyl-1,10-phenanthrolin-2-amine

¹H NMR (500 MHz, CDCl₃)
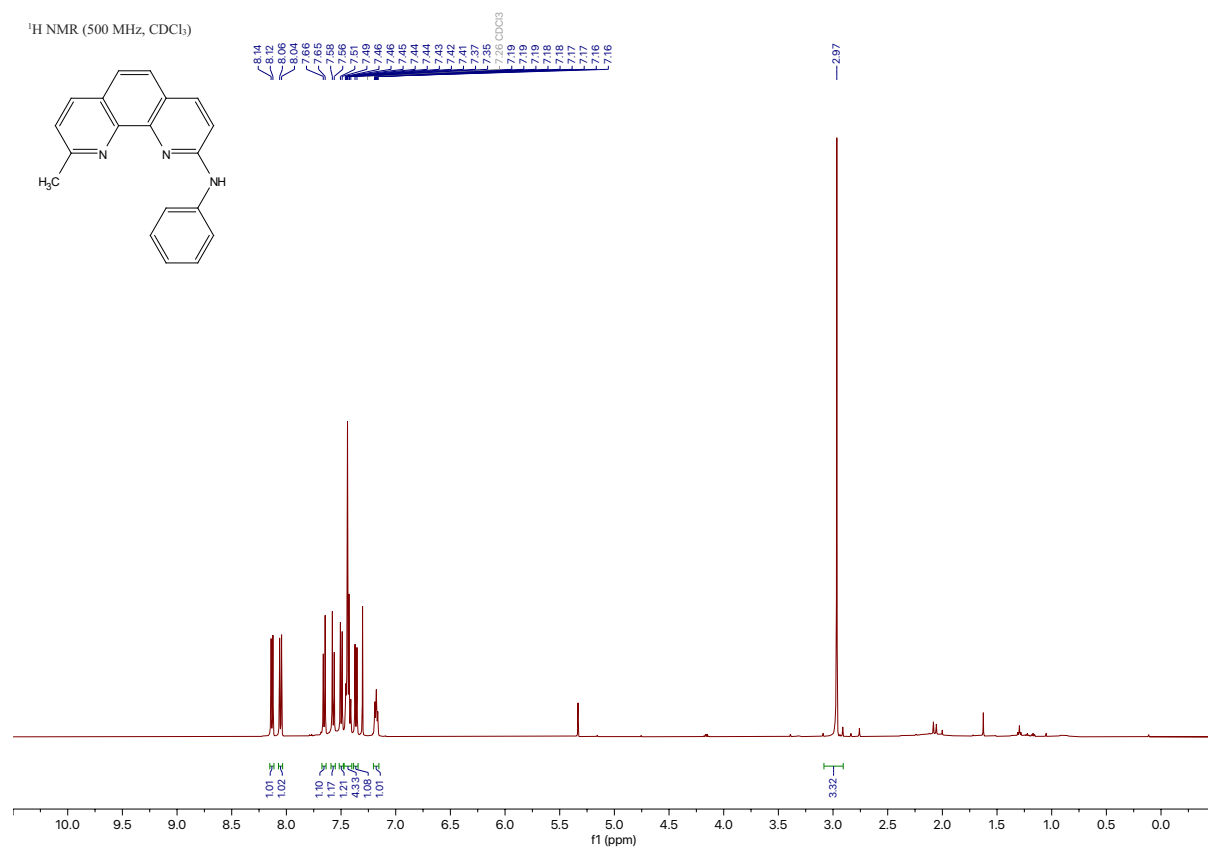
¹³C NMR (126 MHz, CDCl₃)
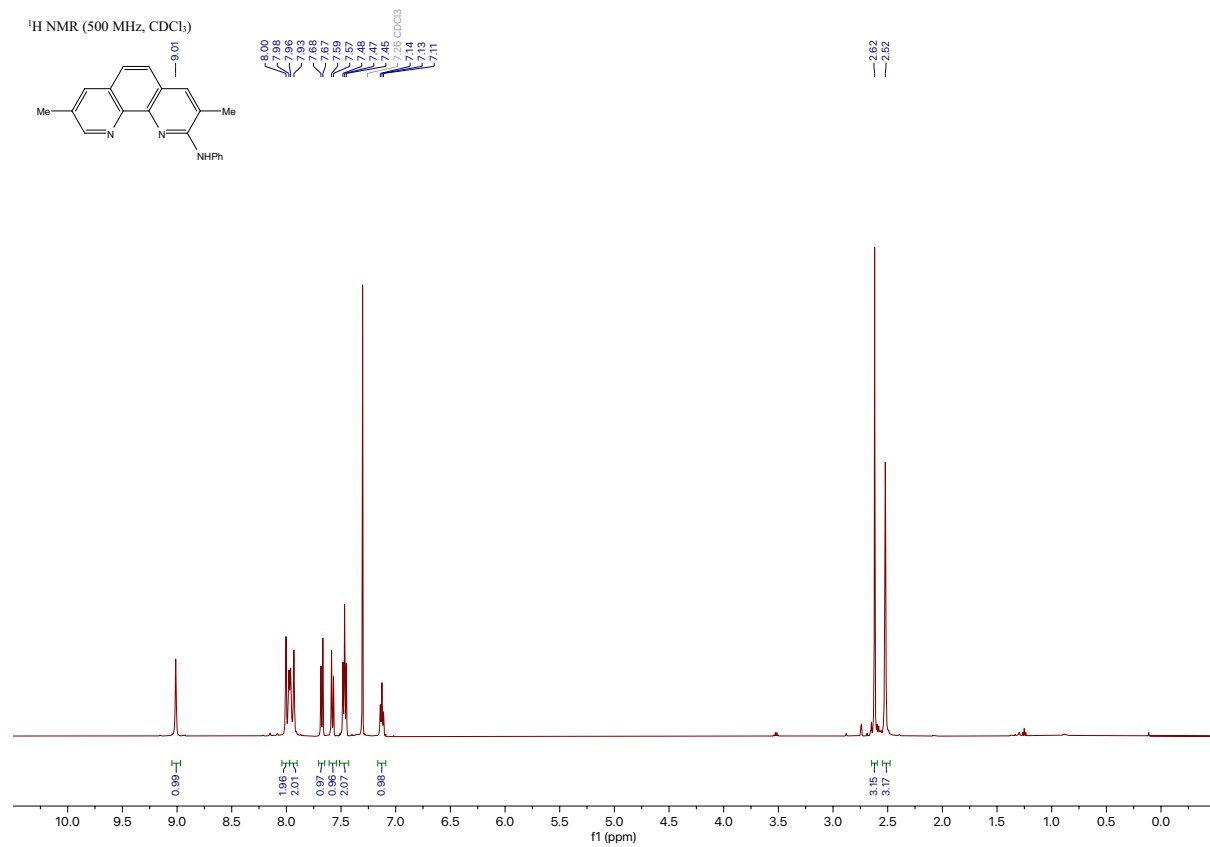
8-methyl-*N*-phenyl-1,10-phenanthrolin-2-amine

¹H NMR (500 MHz, CDCl₃)

¹³C NMR (126 MHz, CDCl₃)

563

7-methyl-*N*-phenyl-1,10-phenanthrolin-2-amine

¹H NMR (500 MHz, CDCl₃)

9.04
9.03

8.10
8.09
7.84
7.82
7.76
7.74
7.47
7.47
7.46
7.45
7.43
7.43
7.41
7.39
7.26 CDCl3
7.23
7.21
7.20

2.82

0.99

1.03
1.06
1.04
6.57
1.02

3.28

10.0　9.5　9.0　8.5　8.0　7.5　7.0　6.5　6.0　5.5　5.0　4.5　4.0　3.5　3.0　2.5　2.0　1.5　1.0　0.5　0.0
f1 (ppm)

¹³C NMR (126 MHz, CDCl₃)

155.44
149.41
144.45
139.76
138.57
129.75
129.69
125.92
124.41
123.02
124.02
122.02
118.66
110.50
19.35

210　200　190　180　170　160　150　140　130　120　110　100　90　80　70　60　50　40　30　20　10　0　-10
f1 (ppm)

5,6-dibromo-*N*-phenyl-1,10-phenanthrolin-2-amine

¹H NMR (600 MHz, CDCl₃)

¹³C NMR (151 MHz, CDCl₃)

3,8-dimethyl-*N*-phenyl-1,10-phenanthrolin-2-amine

¹H NMR (500 MHz, CDCl₃)

¹³C NMR (126 MHz, CDCl₃)

2-chloro-8-methyl-1,10-phenanthroline

¹H NMR (600 MHz, CDCl₃)

¹³C NMR (151 MHz, CDCl₃)

2-chloro-7-methyl-1,10-phenanthroline

¹H NMR (600 MHz, CDCl₃)

^{1}H NMR (600 MHz, CDCl$_3$)

¹³C NMR (151 MHz, CDCl₃)

^{13}C NMR (151 MHz, CDCl$_3$)

5,6-dibromo-2-chloro-1,10-phenanthroline

^{1}H NMR (600 MHz, CDCl$_3$)

^{13}C NMR (151 MHz, CDCl$_3$)

2-chloro-3,8-dimethyl-1,10-phenanthroline

¹H NMR (500 MHz, CDCl₃)
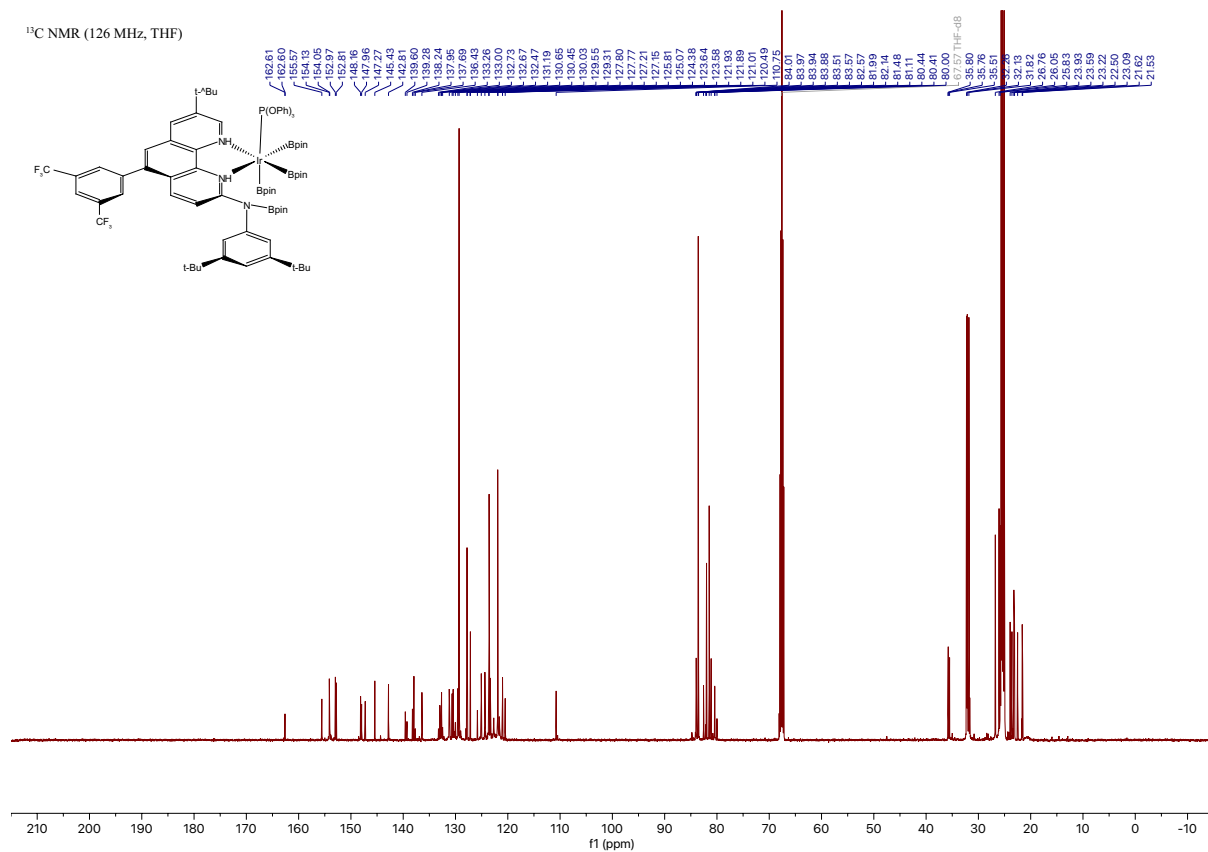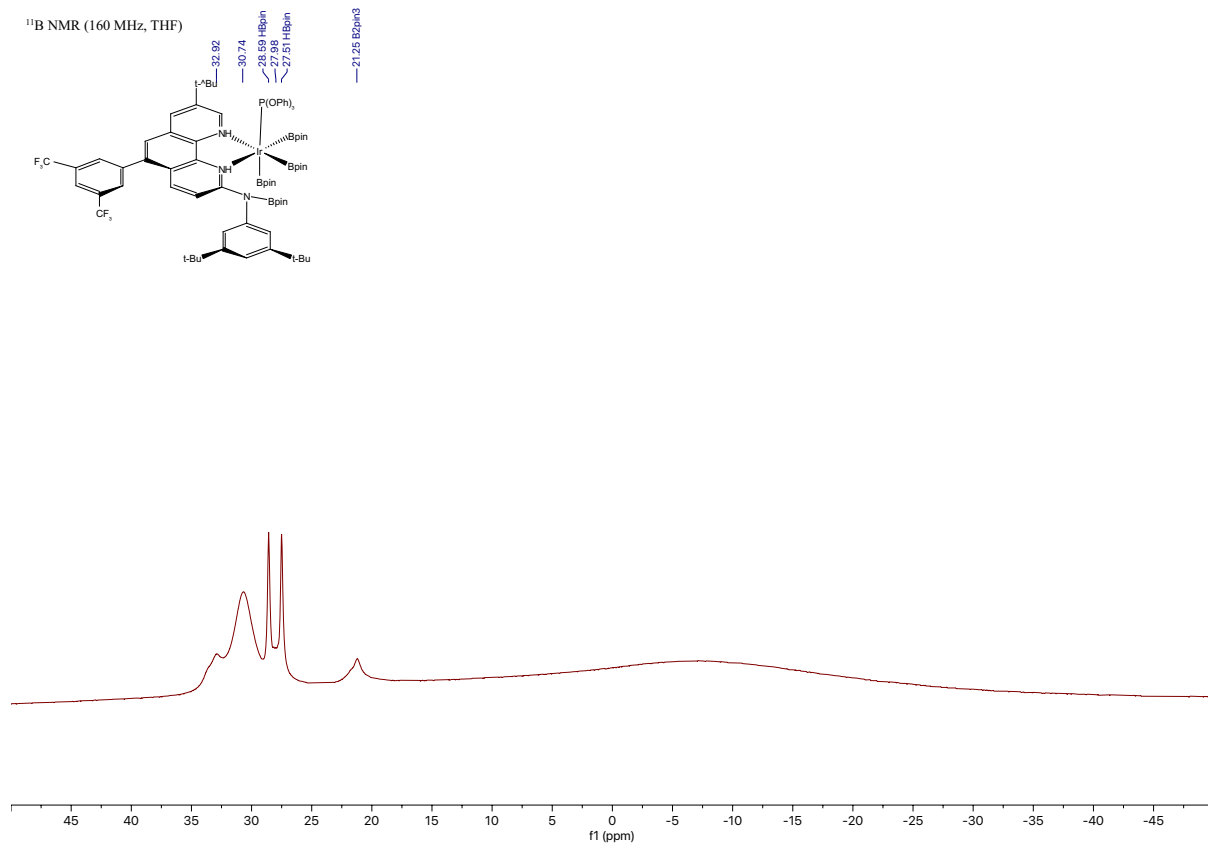

¹³C NMR (126 MHz, CDCl₃)
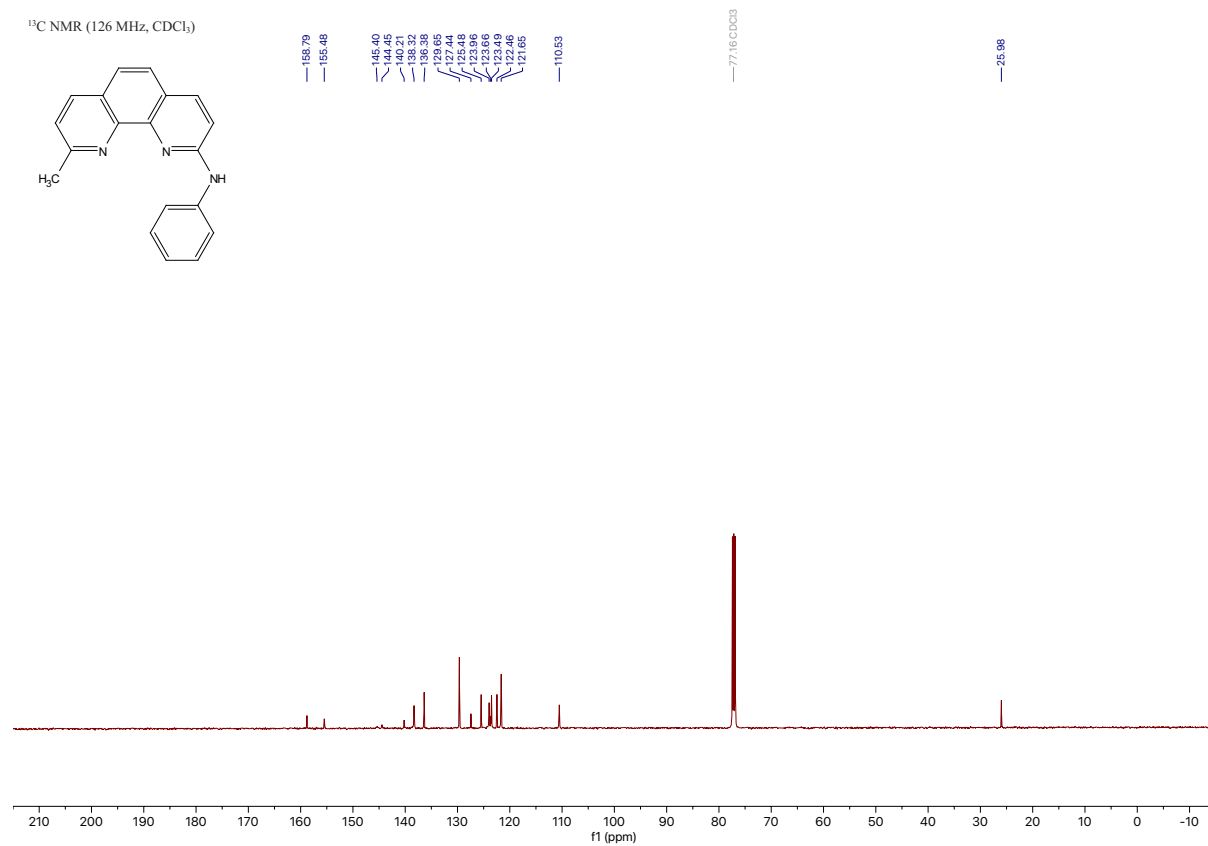
(L3) Ir(Bpin)₃(P(OPh)₃)

¹H NMR (500 MHz, THF)
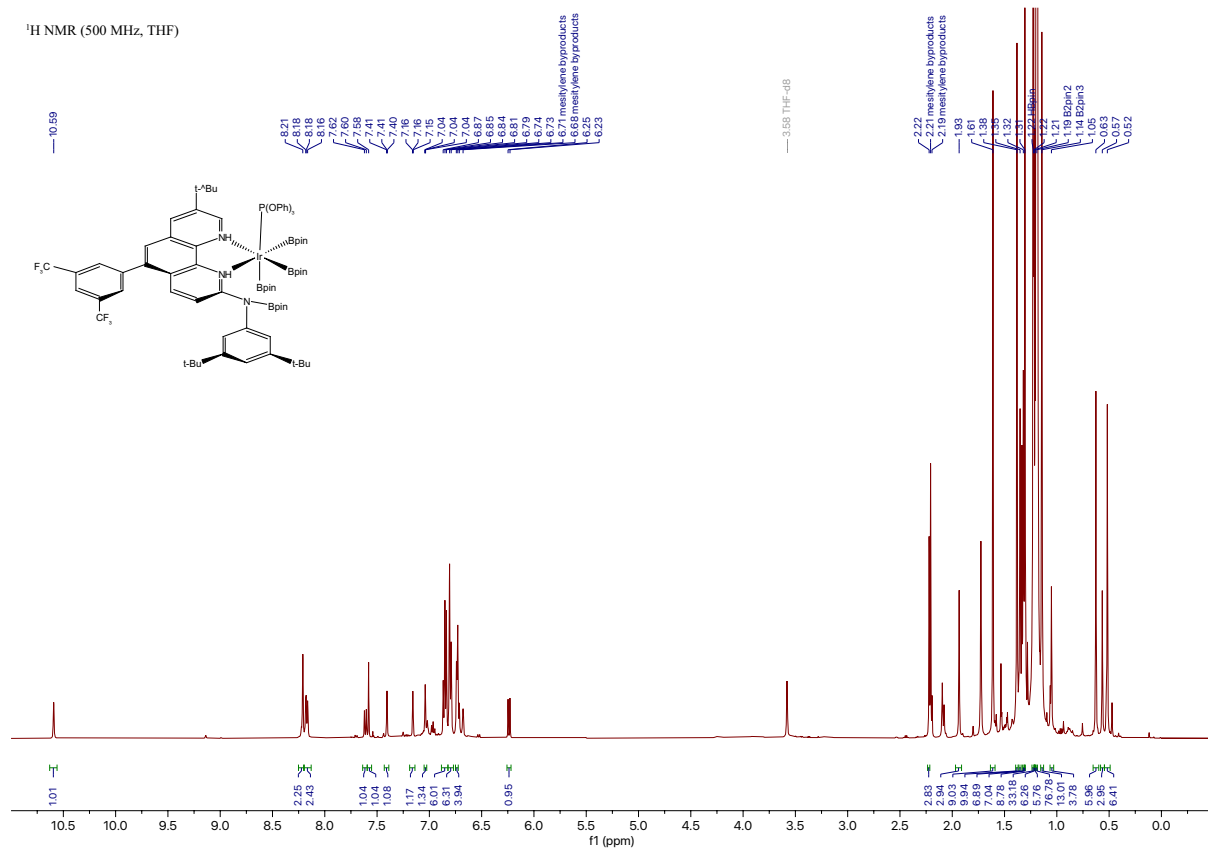
¹³C NMR (126 MHz, THF)

^{11}B NMR (160 MHz, THF)

^{19}F NMR (471 MHz, THF)
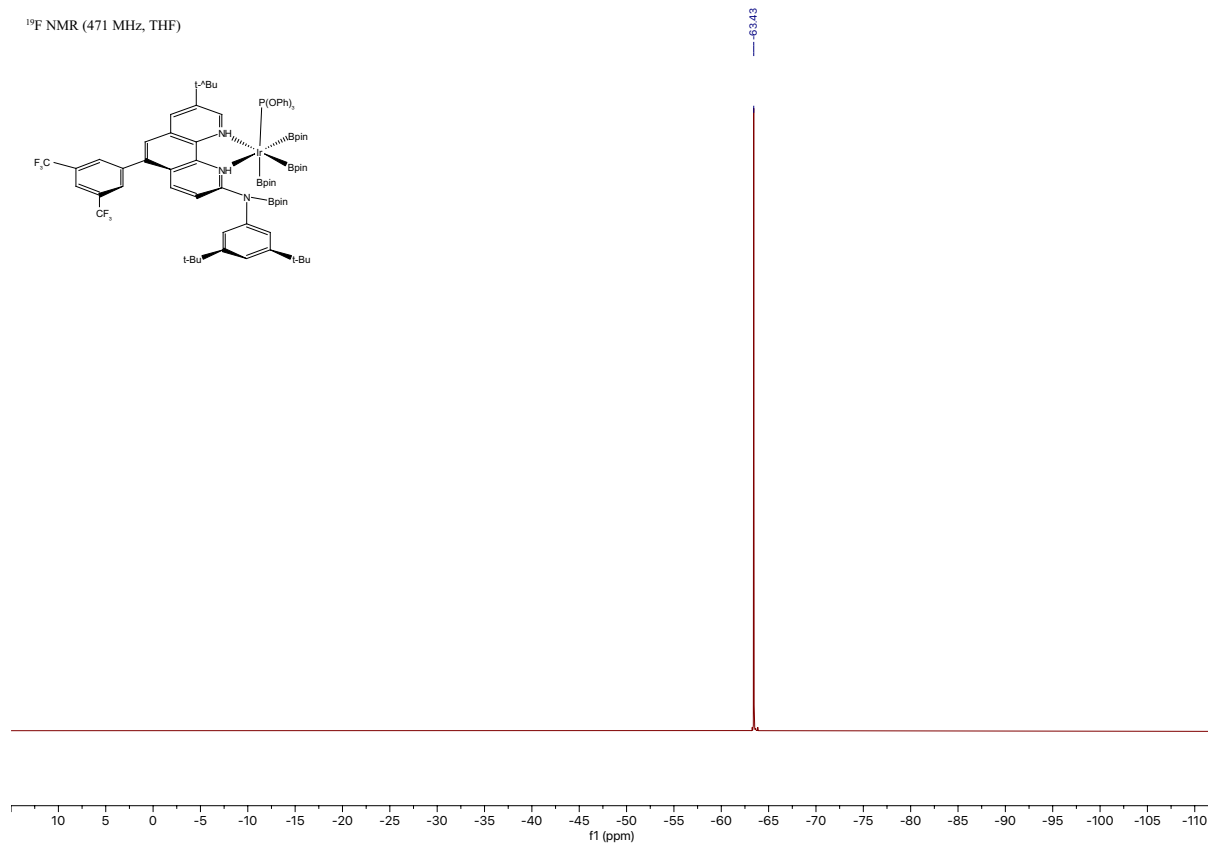
³¹P NMR (202 MHz, THF)
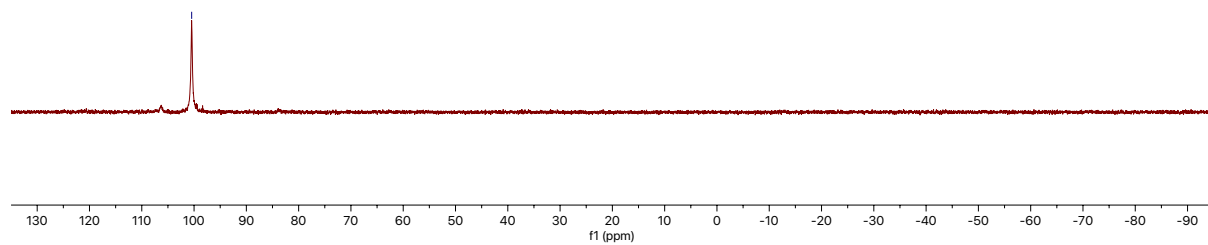
(**L3**)Ir(H)(Bpin)₂(P(OPh)₃)

¹H NMR (600 MHz, THF)

¹³C NMR (151 MHz, THF)
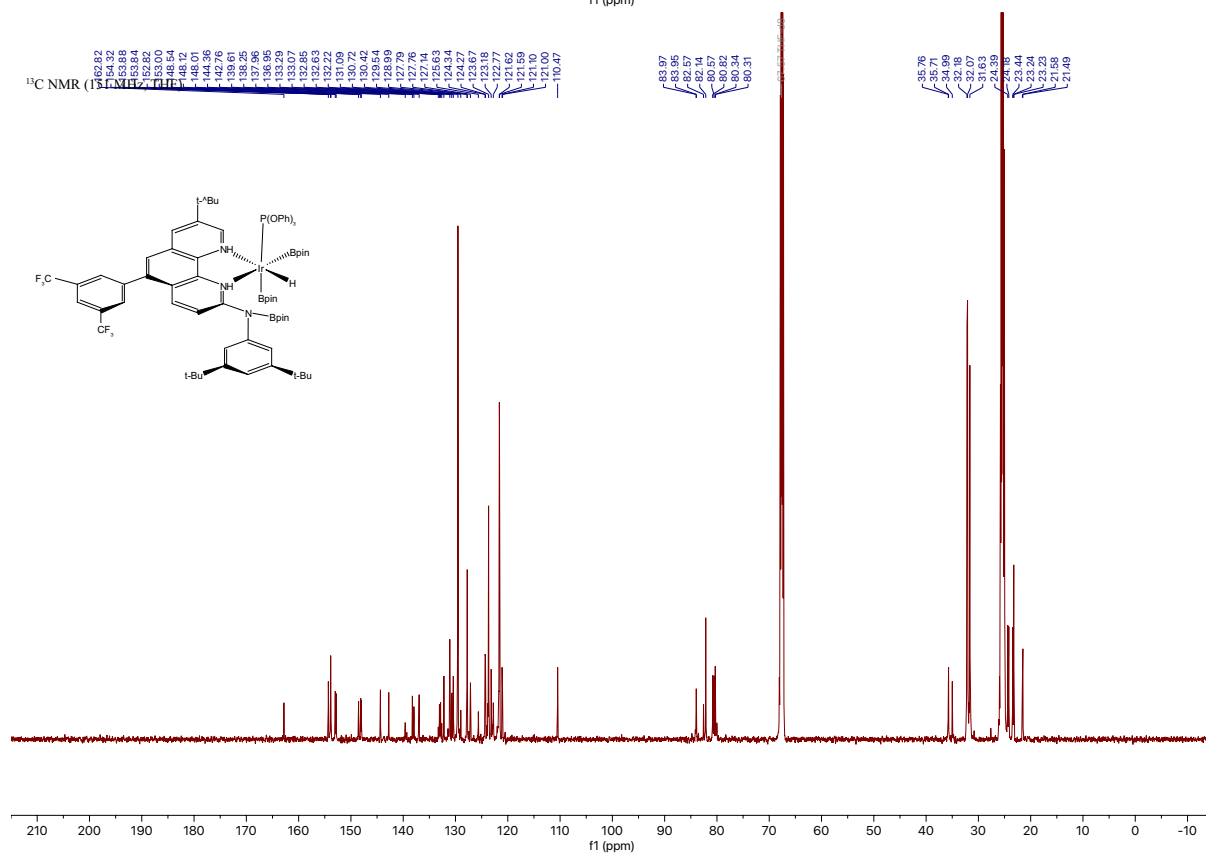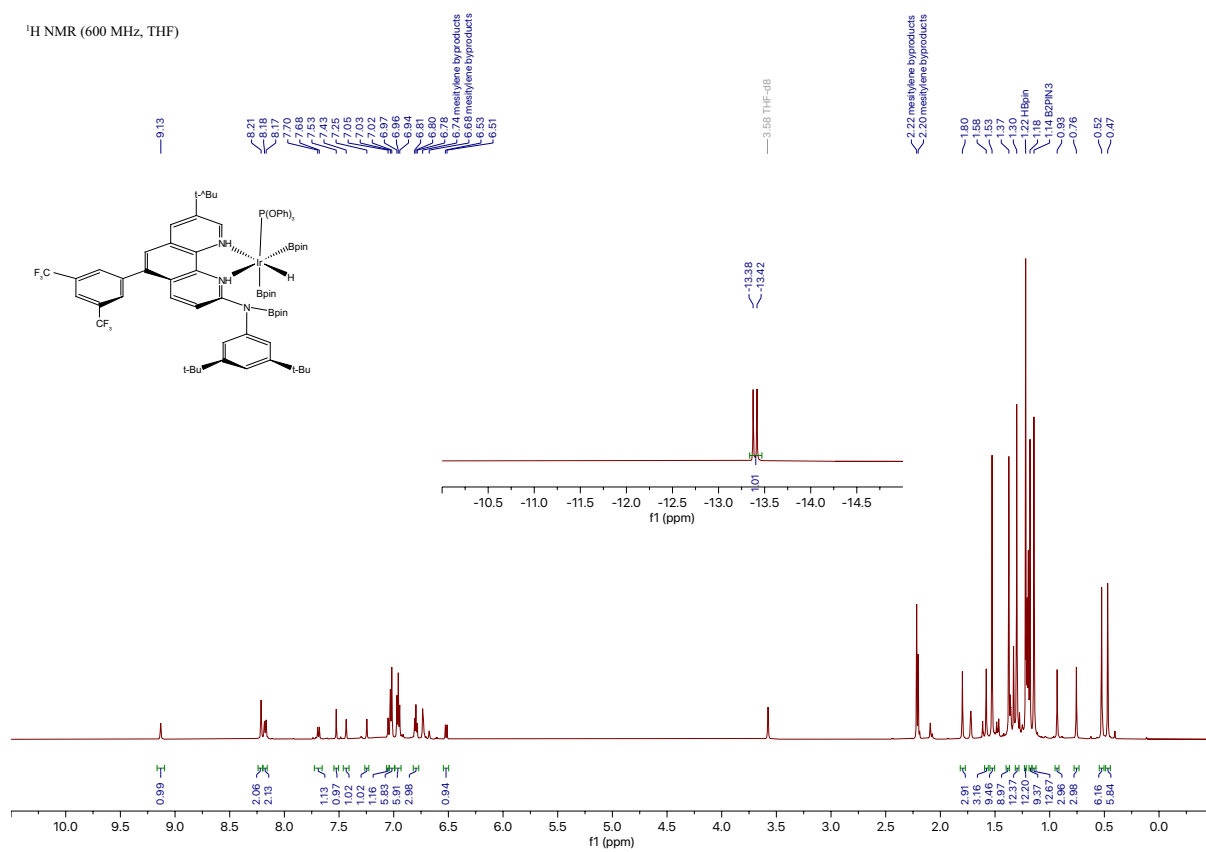
^{11}B NMR (193 MHz, THF)

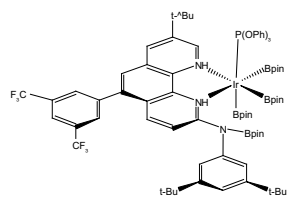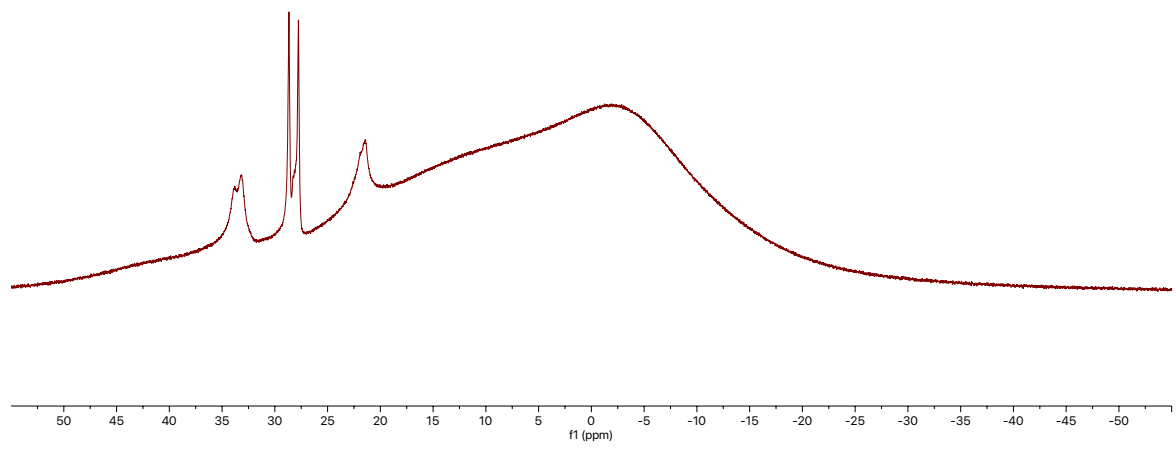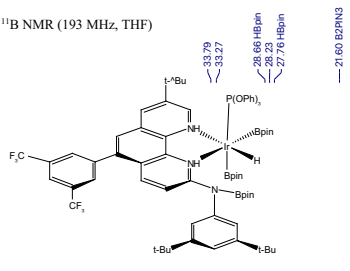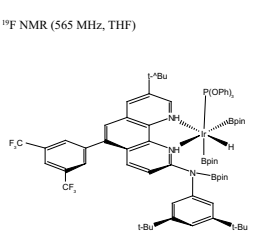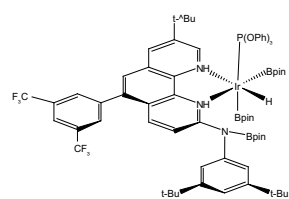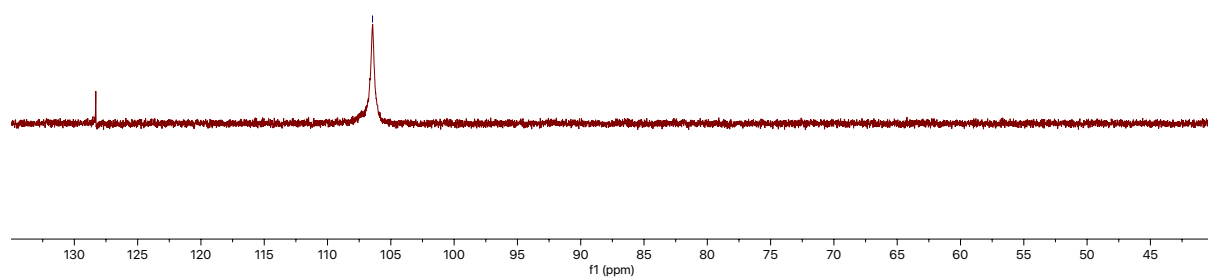^{19}F NMR (565 MHz, THF)
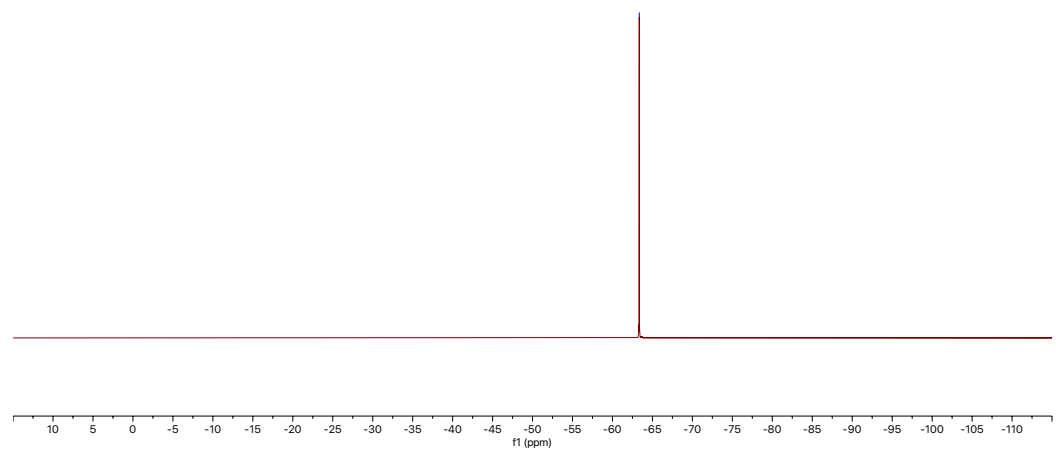
^{31}P NMR (243 MHz, THF)

— 106.45

4.5 References

1.   Arndtsen, B. A.; Bergman, R. G.; Mobley, T. A.; Peterson, T. H., Selective Intermolecular Carbon-Hydrogen Bond Activation by Synthetic Metal Complexes in Homogeneous Solution. *Acc. Chem. Res.* **1995,** *28*, 154–162.

2.   Wencel-Delord, J.; Glorius, F., C–H bond activation enables the rapid construction and late-stage diversification of functional molecules. *Nat. Chem.* **2013,** *5*, 369–375.

3.   Hong, B.; Luo, T.; Lei, X., Late-Stage Diversification of Natural Products. *ACS Cent. Sci.* **2020,** *6*, 622–635.

4.   Hall, D. G., *Boronic Acids: Preparation and Applications in Organic Synthesis, Medicine and Materials, 1&2, Second Edition*. Wiley-VCH GmbH & Co. KGaA: 2011.

5.   Hall, D. G., Structure, Properties, and Preparation of Boronic Acid Derivatives. In *Boronic Acids*, 2011; pp 1–133.

6.   Yu, I. F.; Wilson, J. W.; Hartwig, J. F., Transition-Metal-Catalyzed Silylation and Borylation of C–H Bonds for the Synthesis and Functionalization of Complex Molecules. *Chem. Rev.* **2023,** *123*, 11619–11663.

7.   Lovering, F.; Bikker, J.; Humblet, C., Escape from Flatland: Increasing Saturation as an Approach to Improving Clinical Success. *J. Med. Chem.* **2009,** *52*, 6752–6756.

8.   Volochnyuk, D. M.; Gorlova, A. O.; Grygorenko, O. O., Saturated Boronic Acids, Boronates, and Trifluoroborates: An Update on Their Synthetic and Medicinal Chemistry. *Chem. Eur. J.* **2021,** *27*, 15277-15326.

9.   Jones, M. R.; Fast, C. D.; Schley, N. D., Iridium-Catalyzed sp³ C–H Borylation in Hydrocarbon Solvent Enabled by 2,2'-Dipyridylarylmethane Ligands. *J. Am. Chem. Soc.* **2020,** *142*, 6488–6492.

10.   Kawazu, R.; Torigoe, T.; Kuninobu, Y., Iridium-Catalyzed C(sp³)–H Borylation Using Silyl-Bipyridine Pincer Ligands. *Angew Chem Int Ed Engl* **2022,** *61*, e202202327.

11.   Oeschger, R.; Su, B.; Yu, I.; Ehinger, C.; Romero, E.; He, S.; Hartwig, J., Diverse functionalization of strong alkyl C–H bonds by undirected borylation. *Science* **2020,** *368*, 736.

12.   Yu, I. F.; D'Angelo, K. A.; Hernandez-Mejías, Á. D.; Cheng, N.; Hartwig, J. F., 2-Aminophenanthroline Ligands Enable Mild, Undirected, Iridium-Catalyzed Borylation of Alkyl C–H Bonds. *J. Am. Chem. Soc.* **2024,** *146*, 7124-7129.

13.   Yu, I. F.; Manske, J. L.; Diéguez-Vázquez, A.; Misale, A.; Pashenko, A. E.; Mykhailiuk, P. K.; Ryabukhin, S. V.; Volochnyuk, D. M.; Hartwig, J. F., Catalytic undirected borylation of tertiary C–H bonds in bicyclo[1.1.1]pentanes and bicyclo[2.1.1]hexanes. *Nat. Chem.* **2023,** *15*, 685–693.

14.   Kuroda, Y.; Park, K.; Shimazaki, Y.; Zhong, R.-L.; Sakaki, S.; Nakao, Y., An Iridium/Aluminum Cooperative Strategy for the β-C(sp3)-H Borylation of Saturated Cyclic Amines. *Angew. Chem. Int. Ed.* **2023,** *62*, e202300704.

15.   Shi, Y.; Gao, Q.; Xu, S., Chiral Bidentate Boryl Ligand Enabled Iridium-Catalyzed Enantioselective C(sp³)–H Borylation of Cyclopropanes. *J. Am. Chem. Soc.* **2019,** *141*, 10599–10604.

16.   Chen, L.; Yang, Y.; Liu, L.; Gao, Q.; Xu, S., Iridium-Catalyzed Enantioselective α-C(sp³)–H Borylation of Azacycles. *J. Am. Chem. Soc.* **2020,** *142*, 12062–12068.

17.   Chen, X.; Chen, L.; Zhao, H.; Gao, Q.; Shen, Z.; Xu, S., Iridium-Catalyzed Enantioselective C(sp³)–H Borylation of Cyclobutanes. *Chin. J. Chem.* **2020,** *38*, 1533–1537.

18.   Du, R.; Liu, L.; Xu, S., Iridium-Catalyzed Regio- and Enantioselective Borylation of Unbiased Methylene C(sp³)−H Bonds at the Position β to a Nitrogen Center. *Angew. Chem. Int. Ed.* **2021,** *60*, 5843–5847.

19.   Yang, Y.; Chen, L.; Xu, S., Iridium-Catalyzed Enantioselective Unbiased Methylene C(sp³)–H Borylation of Acyclic Amides. *Angew. Chem. Int. Ed.* **2021,** *60*, 3524–3528.

20.   Shi, Y.; Yang, Y.; Xu, S., Iridium-Catalyzed Enantioselective C(sp^3)−H Borylation of Aminocyclopropanes. *Angew. Chem. Int. Ed.* **2022,** *61*, e202201463.

21.   Zou, X.; Li, Y.; Ke, Z.; Xu, S., Chiral Bidentate Boryl Ligand-Enabled Iridium-Catalyzed Enantioselective Dual C–H Borylation of Ferrocenes: Reaction Development and Mechanistic Insights. *ACS Catal.* **2022,** *12*, 1830–1840.

22.   Xie, T.; Chen, L.; Shen, Z.; Xu, S., Simple Ether-Directed Enantioselective C(sp^3)−H Borylation of Cyclopropanes Enabled by Iridium Catalysis. *Angew. Chem. Int. Ed.* **2023,** *62*, e202300199.

23.   Gao, Q.; Xu, S., Site- and Stereoselective C(sp^3)−H Borylation of Strained (Hetero)Cycloalkanols Enabled by Iridium Catalysis. *Angew. Chem. Int. Ed.* **2023,** *62*, e202218025.

24.   Mallesha, N.; Prahlada Rao, S.; Suhas, R.; Channe Gowda, D., An efficient synthesis of tert-butyl ethers/esters of alcohols/amino acids using methyl tert-butyl ether. *Tet. Lett.* **2012,** *53*, 641–645.

25.   Frisch, M. J.; Trucks, G. W.; Schlegel, H. B.; Scuseria, G. E.; Robb, M. A.; Cheeseman, J. R.; Scalmani, G.; Barone, V.; Petersson, G. A.; Nakatsuji, H.; Li, X.; Caricato, M.; Marenich, A. V.; Bloino, J.; Janesko, B. G.; Gomperts, R.; Mennucci, B.; Hratchian, H. P.; Ortiz, J. V.; Izmaylov, A. F.; Sonnenberg, J. L.; Williams; Ding, F.; Lipparini, F.; Egidi, F.; Goings, J.; Peng, B.; Petrone, A.; Henderson, T.; Ranasinghe, D.; Zakrzewski, V. G.; Gao, J.; Rega, N.; Zheng, G.; Liang, W.; Hada, M.; Ehara, M.; Toyota, K.; Fukuda, R.; Hasegawa, J.; Ishida, M.; Nakajima, T.; Honda, Y.; Kitao, O.; Nakai, H.; Vreven, T.; Throssell, K.; Montgomery Jr., J. A.; Peralta, J. E.; Ogliaro, F.; Bearpark, M. J.; Heyd, J. J.; Brothers, E. N.; Kudin, K. N.; Staroverov, V. N.; Keith, T. A.; Kobayashi, R.; Normand, J.; Raghavachari, K.; Rendell, A. P.; Burant, J. C.; Iyengar, S. S.; Tomasi, J.; Cossi, M.; Millam, J. M.; Klene, M.; Adamo, C.; Cammi, R.; Ochterski, J. W.; Martin, R. L.; Morokuma, K.; Farkas, O.; Foresman, J. B.; Fox, D. J. *Gaussian 16 Rev. A.03*, Wallingford, CT, 2016.

26.   Perdew, J. P.; Burke, K.; Ernzerhof, M., Generalized Gradient Approximation Made Simple. *Phys. Rev. Lett.* **1996,** *77*, 3865–3868.

27.   Perdew, J. P.; Burke, K.; Ernzerhof, M., Generalized Gradient Approximation Made Simple [Phys. Rev. Lett. 77, 3865 (1996)]. *Phys. Rev. Lett.* **1997,** *78*, 1396–1396.

28.   Adamo, C.; Barone, V., Toward reliable density functional methods without adjustable parameters: The PBE0 model. *J. Chem. Phys.* **1999,** *110*, 6158–6170.

29.   Grimme, S.; Ehrlich, S.; Goerigk, L., Effect of the damping function in dispersion corrected density functional theory. *J. Comput. Chem* **2011,** *32*, 1456–1465.

30.   Weigend, F.; Ahlrichs, R., Balanced basis sets of split valence, triple zeta valence and quadruple zeta valence quality for H to Rn: Design and assessment of accuracy. *Phys. Chem. Chem. Phys.* **2005,** *7*, 3297–3305.

31.   Andrae, D.; Häußermann, U.; Dolg, M.; Stoll, H.; Preuß, H., Energy-adjusted ab initio pseudopotentials for the second and third row transition elements. *Theor. Chim. Acta* **1990,** *77*, 123–141.

32.   Schuchardt, K. L.; Didier, B. T.; Elsethagen, T.; Sun, L.; Gurumoorthi, V.; Chase, J.; Li, J.; Windus, T. L., Basis Set Exchange: A Community Database for Computational Sciences. *J. Chem. Inf. Model.* **2007,** *47*, 1045–1052.

33.   Pritchard, B. P.; Altarawy, D.; Didier, B.; Gibson, T. D.; Windus, T. L., New Basis Set Exchange: An Open, Up-to-Date Resource for the Molecular Sciences Community. *J. Chem. Inf. Model.* **2019,** *59*, 4814–4820.

34.   Feller, D., The role of databases in support of computational chemistry calculations. *J. Comput. Chem* **1996,** *17*, 1571–1586.

35.   Marenich, A. V.; Cramer, C. J.; Truhlar, D. G., Universal Solvation Model Based on Solute Electron Density and on a Continuum Model of the Solvent Defined by the Bulk Dielectric Constant and Atomic Surface Tensions. *J. Phys. Chem. B* **2009,** *113*, 6378–6396.